

IN THE UNITED STATES PATENT AND TRADEMARK OFFICE

Application of: Brines *et al.*

Confirmation No.: 4194

Application No.: 10/185,841

Group Art Unit: 1647

Filed: June 26, 2002

Examiner: DeBerry, Regina M.

For: PROTECTION, RESTORATION AND  
ENHANCEMENT OF ERYTHROPOIETIN-  
RESPONSIVE CELLS, TISSUES AND ORGANS

Attorney Docket No.: 10165-015-999

SECOND DECLARATION OF MICHAEL L. BRINES, M.D., PH.D.

Sir:

I, MICHAEL L. BRINES, do hereby declare and state:

1. I am an inventor of the invention described and claimed in the above-identified patent application (hereinafter the "841 application"). I am presently Chief Scientific Officer at Warren Pharmaceuticals, Inc., licensee of the '841 application.

2. I have over thirty years of experience in biological research and clinical investigation. I am a certified member of the American Board of Internal Medicine. My academic and technical experience and honors, and a list of my publications, are set forth in my curriculum vitae, a copy of which is attached hereto as Appendix A.

3. I have read and am familiar with the '841 application, the pending claims and the outstanding Office Action. I understand that the technology of the '841 application relates to the use of erythropoietin ("EPO") and chemically modified forms of EPO for protecting, maintaining, enhancing or restoring the function or viability of cells, tissues and organs.<sup>1</sup> Such chemically modified forms of EPO can be EPO molecules that do

---

<sup>1</sup> For ease of reference, I will use the term "tissue-protection" instead of the phrase "protecting, maintaining, enhancing or restoring the function or viability of cells, tissues and organs." Likewise, the ability of a protein to protect, maintain, enhance or restore the function or viability of cells, tissues and organs will be referred to as its "tissue-protective" activity.

not increase hemoglobin concentration<sup>2</sup> but retain their tissue-protective activity. I have been informed and believe that the claims of the '841 application are subject to a rejection based on the contention that the '841 application does not provide sufficient evidence that chemically modified forms of EPO have tissue-protective effects in erythropoietin-responsive cells, tissues and organs as claimed.

4. I have been asked to provide evidence that chemically modified forms of EPO have tissue-protective effects in erythropoietin-responsive mammalian cells, tissues and organs.

5. In the following paragraphs I will present evidence that shows that chemically modified EPO molecules can provide tissue-protective activity in all tissues that coexpress the EPO receptor ("EpoR") and the common beta receptor ("cbR"). I will further present experimental data, citing a non-exhaustive list of examples from the literature, that chemically modified EPO has tissue protective effects in a wide range of different tissues.

I. THE TISSUE PROTECTIVE AND ERYTHROPOIETIC ACTIVITIES OF EPO ARE MEDIATED BY SEPARATE AND DISTINCT PATHWAYS

6. EPO provides tissue-protective activity via a separate pathway from the pathway it uses to exert its erythropoietic effects. (Brines *et al.*, 2004, PNAS 101: 14907-14912.) EPO exerts its erythropoietic effect via a classic EPO Receptor homodimer (the "classical EPO Receptor"), whereas the tissue-protective activity of EPO is due to the interaction of the molecule with a different receptor, known as the "Tissue-Protective Receptor Complex", a heteromer of the classical EPO Receptor and cbR, a signal-transducing subunit shared by the granulocyte-macrophage colony stimulating factor, and the IL-3 and IL-5 receptor. (Brines, 2004).

7. The chemically modified EPO molecules of the invention are non-erythropoietic yet retain tissue protective activity. These chemically modified EPO molecules are tissue protective because they retain their ability to interact with the Tissue-Protective Receptor Complex, but have reduced erythropoietic activity compared with native EPO, e.g., by losing its ability to interact with the classical EPO Receptor. Based on these

---

<sup>2</sup> Molecules that do not increase hemoglobin concentration in a mammal will be referred to as non-erythropoietic.



properties, the chemically modified, non-erythropoietic forms of EPO can be expected to provide tissue-protection in any tissue which has a Tissue-Protective Receptor Complex, *i.e.* any erythropoietin-receptive tissue.

8. Therefore, chemically modified forms of EPO can be expected to exert tissue-protective effects in all tissues that coexpress the EpoR and the cbR. A detailed list of tissues expressing Common Beta Receptor is attached as Appendix B. Appendix B also contains a non-exhaustive list of references that describe EpoR-expressing cells, tissues, or organs. For example, representative cell types demonstrated to express the EpoR include, but are not limited to, endothelial cells, myocytes, macrophages, retinal cells, cells of the adrenal cortex and medulla, small bowel, spleen, liver, kidney and lung, as well as cells of the central nervous system, such as neurons and glial cells, and astrocytes. Thus, I believe that the tissue protective activity of EPO, which is mediated through the Tissue-Protective Receptor Complex, may be found in all tissues.

9. In the paragraphs 10 to 23, below, I describe experiments from the literature that demonstrate that EPO and chemically modified forms of EPO, *e.g.*, carbamylated EPO ("CEPO"), showed both tissue-protective activity in a variety of tissue types.

## II. CENTRAL NERVOUS SYSTEM

10. Numerous studies have corroborated and extended the applicant's discovery that carbamylated recombinant human erythropoietin ("rhCEPO") shows tissue-protective activity in the brain. For example, Wang *et al.* (Brit. J. Pharmacol. 2007, 151: 1337-1384) have shown, using a rat model of focal cerebral ischemia, that carbamylated recombinant human EPO significantly reduced the cortical infarct volume and reduced neurological impairment. Wang *et al.* also showed in analogous experiments that also recombinant human EPO ("rhEPO") significantly reduced the cortical infarct volume and reduced neurological impairment. These data indicate that rhCEPO, as well as rhEPO, show anti-inflammatory and anti-apoptotic effects. Based on these studies, I conclude that CEPO shows tissue-protective activity in brain tissue.

11. Chemically modified forms of EPO have also been shown to provide tissue-protective activity in the spinal cord. Data presented in Savino *et al.* (J.

Neuroimmunol. 2006, 172: 27-37) showed that the EPO derivatives CEPO and asialo EPO, as well as rhEPO, are active in a chronic model of experimental autoimmune encephalomyelitis (EAE). The action of CEPO was associated with a decrease in the production of inflammatory cytokines in the spinal cord and peripheral lymphocytes. Savino *et al.* shows an anti-inflammatory effect of CEPO in spinal cord tissue. These studies clearly demonstrate that chemically modified forms of EPO provide tissue-protective activity in spinal cord tissue.

### III. PERIPHERAL NERVOUS SYSTEM

12. Chemically modified EPO has also been shown to provide tissue-protective activity in peripheral nerve tissue. Bianchi *et al.* (Clin. Canc. Res. 2006, 12: 2607-2612) evaluated EPO and CEPO in an experimental model of peripheral neurotoxicity induced by cisplatin that closely resembles cisplatin neurotoxicity in humans. Cisplatin given to Wistar rats significantly lowered their growth rate, with slower sensory nerve conduction velocity and reduced intraepidermal nerve fiber density. Coadministration of cisplatin and EPO or cisplatin and CEPO partially, but significantly, prevented the sensory nerve conduction velocity reduction. Both molecules preserved intraepidermal nerve fiber density. Based on these studies, it is clear that CEPO shows tissue-protective activity in peripheral nerve tissue.

### IV. OTHER TISSUES

13. Chemically modified EPO has also been shown to provide tissue-protective activity in heart tissue. Moon *et al.* (J. Pharmacol. Exp. Ther. 2006, 316: 999-1005) showed in an experimental model of myocardial infarction induced by permanent ligation of a coronary artery in rats that a single bolus injection of 30 ug/kg b.wt. of CEPO, similarly to EPO, immediately after coronary ligation reduced apoptosis in the myocardial area at risk, examined 24h later, by 50%. These data indicate that CEPO, as well as EPO, shows anti-apoptotic effects in heart tissue. Based on this study, both CEPO and EPO show tissue-protective activity in heart tissue.

14. Chemically modified EPO has further been shown to provide tissue-protective activity in the kidney. Kitamura *et al.* (Nephrol. Dial. Transplant. 2008, 0: 1-8) evaluated the therapeutic effects of CEPO using a rat unilateral ureteral obstruction model.

In this model, CEPO decreased tubular apoptosis and alpha-smooth muscle actin expression in the absence of polycythaemia, while the untreated obstructed kidneys exhibited increased tubular apoptosis with expanded alpha-smooth muscle actin expression. While EPO treatment similarly inhibited tubular apoptosis and alpha-smooth muscle actin expression, EPO treatment increased hemoglobin concentrations and induced a wedge-shaped infarction. These data indicate that CEPO, as well as EPO, shows anti-apoptotic effects in kidney tissue. Based on these studies, EPO and CEPO shows tissue-protective activity in kidney tissue.

15. Chemically modified EPO has also been shown to provide tissue-protective activity in skin tissue. Brines *et al.*, (WO2005/032467, at Example 5, p. 37) demonstrated the use of an ischemic wound flap model to determine the effect of CEPO on ischemic skin flap wound recovery. The rats that received CEPO had a greater percentage of the wound healed than those treated with saline for the same period. This data demonstrates that CEPO decreases wound size and accelerates healing. Thus, CEPO shows tissue-protective activity in skin tissue.

16. EPO can also provide tissue protection of the cochlea. Mammalian auditory hair cells are unable to regenerate and can be irreversibly damaged by various agents, including gentamicin. Monge *et al.* (Laryngoscope 2006, 116: 312-316) presented data that showed a dose-dependent protective effect of EPO on gentamicin-damaged hair cells *in vitro*. The authors concluded that decreased hair cell loss in EPO-treated organs of Corti that had been exposed to gentamicin provides evidence for a protective effect of EPO in aminoglycoside-induced hair cell death. As described above, since the tissue-protective effect is attributed to the interaction of EPO with the Tissue-Protective Receptor Complex, this experiment indicates the presence of functional Tissue-Protective Receptor Complex in the cochlea. Since EPO shows a tissue protective effect in this experiment, it is expected that a chemically modified, non-erythropoietic form of EPO having tissue protective activity would show the same tissue protective properties in the cochlea. Based on these studies, I can conclude that chemically modified forms of EPO can be expected to show tissue-protective activity in the cochlea.

17. EPO can also show tissue-protective activity in striated muscle tissue. Contaldo *et al.* (Am. J. Physiol. Heart Circ. Physiol. 2007, 293: H274-H283) investigated the effect of EPO in ischemia-reperfusion (I/R)-induced microcirculatory dysfunctions. The

study demonstrated that EPO effectively attenuates I/R injury by preserving nutritive perfusion, reducing leukocytic inflammation and inducing new vessel formation. The authors concluded that EPO protects the striated muscle microcirculation of the dorsal skinfold from postischemic injury in mice. Because the tissue-protective effect is attributed to the interaction of EPO with the Tissue-Protective Receptor Complex, this experiment demonstrates the presence of functional Tissue-Protective Receptor Complex in striated muscle tissue. Since EPO shows a tissue protective effect in this experiment, it is expected that a chemically modified, non-erythropoietic form of EPO having tissue protective activity would show the same tissue protective properties in striated muscle tissue. Based on these studies, I conclude that chemically modified forms of EPO can show tissue-protective activity in striated muscle tissue.

18. Chemically modified forms of EPO can show tissue-protective activity in endothelial tissue. Employing an elevated glucose model for endothelial cells, Chong *et al.* (Curr. Neurovasc. Res. 2007, 4: 194-204) illustrated that a final glucose concentration of 25nM over a 48h course leads to a significant loss in cell survival and correspondingly a significant increase in genomic DNA degradation when compared to control endothelial cells. Administration of EPO significantly enhanced endothelial cell survival during elevated glucose. EPO also blocked apoptotic DNA degradation in endothelial cells during elevated glucose similar to alternate models of oxidative stress in cardiac and vascular cell models. The authors showed that EPO protects endothelial cells from apoptosis. Since tissue-protective effect of EPO results from the interaction of EPO with the Tissue-Protective Receptor Complex. This experiment demonstrates the presence of the Tissue-Protective Receptor Complex in endothelial tissue, and thus, chemically modified, non-erythropoietic forms of EPO having tissue protective activity would be expected to show the same tissue protective properties in endothelial tissues. Based on these studies, I conclude that chemically modified forms of EPO can show tissue-protective activity in endothelial tissue.

19. EPO has also been shown to provide tissue-protective activity in hair follicles. Bodo *et al.* (FASEB J. 2007, 21: 3346-3354) used organ-cultured hair follicles to assess the effects of EPO in the presence/absence of classical apoptosis-inducing chemotherapeutic agents. Bodo *et al.* demonstrated that EPO significantly down-regulates chemotherapy-induced intrafollicular apoptosis. Based on EPO's productive interaction with the Tissue-Protective Receptor Complex in this experiment, a chemically modified, non-

erythropoietic, tissue protective form of EPO would be expected to have the same tissue-protective properties in hair follicles. Based on this study, I conclude that chemically modified forms of EPO would have tissue-protective activity in hair follicles.

20. EPO can also provide tissue-protective activity in bone tissue.

Holstein *et al.* (Life Sci. 2007: 893-900) investigated the effect of EPO treatment on bone healing in a murine closed femur fracture model. EPO-treated animals showed a higher torsional stiffness and an increased callus density when compared to vehicle-treated controls. Accordingly, the histomorphometric examination revealed an increased fraction of mineralized bone and osteoid. The authors concluded that EPO is involved in the process of early endochondral ossification, enhancing the transition of soft callus to hard callus. Since EPO shows a tissue protective effect in this experiment, it can be concluded that chemically modified, non-erythropoietic, tissue-protective forms of EPO would show the same tissue protective properties in bone tissue. Based on this reasoning, I conclude that chemically modified forms of EPO can provide tissue-protective activity in bone tissue.

21. EPO can also provide tissue-protective activity in intestinal tissue.

Guneli *et al.* (Mol. Med. 2007, 13, 509-517) investigated whether EPO could prevent intestinal tissue injury in Wistar rats induced by ischemia-reperfusion (I/R). Following histological assessment using a microscopic scoring system to evaluate the I/R injury in the intestinal tissue the authors concluded that their study established that a high single dose of rhEPO administered both before ischemia and at the onset of reperfusion protected the intestinal tissue against I/R injury. They further state that data from their study demonstrate that antiapoptotic, antioxidative and anti-inflammatory properties seem to be related to the EPO-mediated protective effect against I/R injury. Because the tissue-protective effect in this example is attributed to the interaction of EPO with the Tissue-Protective Receptor Complex and because EPO shows a tissue protective effect in this experiment, a chemically modified, non-erythropoietic, tissue protective form of EPO would also be expected to provide tissue protection in the intestine. Based on these studies, I conclude that chemically modified forms of EPO can be used to provide tissue-protective activity in intestinal tissue.

22. EPO has also been shown to provide tissue-protective activity in lung

tissue. Tascilar *et al.* (World J. Gastroenterol. 2007, 13: 6172-6182) investigated the effect of exogenous EPO administration on acute lung injury in an experimental model of sodium

taurodeoxycholate-induced acute necrotizing pancreatitis. The study shows that the mean pleural effusion volume, calculated lung/body weight ratio, serum IL-6 and lung tissue malondialdehyde levels were significantly lower in EPO groups than in ANP groups. Tascilar *et al.* concluded that histopathological evaluation confirmed the improvement in lung injury parameters after exogenous administration of EPO. Since the tissue-protective effect in this example is attributed to the interaction of EPO with the Tissue-Protective Receptor Complex, I conclude that a chemically modified, tissue-protective, non-erythropoietic form of EPO would also provide tissue protection in the lung. Based on this reasoning, I conclude that chemically modified forms of EPO can be used to provide provide tissue protection in lung tissue.

23. EPO can also provide tissue-protective activity in liver tissue. Yazihan *et al.* (Turk. J. Gastroenterol. 2007, 18: 239-244) used a human hepatocyte cell line for assays to determine whether EPO treatment decreases H<sub>2</sub>O<sub>2</sub>-induced toxicity. Yazihan *et al.* reported that EPO treatment significantly increased cell number at the 24<sup>th</sup> and 48<sup>th</sup> hour compared to the control group. H<sub>2</sub>O<sub>2</sub> application induced apoptosis and lactate dehydrogenase release from Hep3B cells and decreased cell number. EPO prevented H<sub>2</sub>O<sub>2</sub> toxicity in hepatocytes. Since tissue protection is attributed to the interaction of EPO with the Tissue-Protective Receptor Complex, a chemically modified non-erythropoietic, tissue protective form of EPO would also provide tissue protection in the liver. Based on these studies, I conclude that chemically modified forms of EPO can be used to provide tissue-protective activity in liver tissue.

## V. CONCLUSION

24. In summary, I have presented experimental data, citing a non-exhaustive list of examples from the literature, that chemically modified EPO has tissue protective effects in a wide range of mammalian tissues. Thus, there is ample evidence from the data presented in the literature that chemically modified, non-erythropoietic, tissue protective forms of EPO can exert tissue-protective activity in any erythropoietin-responsive tissue, *i.e.*, any tissues that expresses an Tissue-Protective Receptor Complex.

25. I declare further that all statements made in this Declaration of my own knowledge are true, that all statements made on information and belief are believed to be true, and further that these statements are made with the knowledge that willful false statements and the like so made are punishable by fine or imprisonment or both, under Section 1001 of Title 18 of the United States Code and that such willful false statements may jeopardize the validity of the application or any patent issuing thereon.

Respectfully submitted,

February 20, 2008  
Date

Michael L. Brines  
Michael L. Brines

**Attachments:**

Appendix A: Curriculum Vitae of Dr. Michael L. Brines, M.D., Ph.D.

Appendix B: References showing tissues that express the EpoR and/or cbR

Appendix C: Cited References

## Appendix A

Brines, page 1

### **MICHAEL L. BRINES PhD, MD**

1 Wepawaug Road, Woodbridge, CT 06525; office: 914-762-7586; email: [mbrines@kswi.org](mailto:mbrines@kswi.org)

- 2004- Co-founder, Director and Chief Scientific Officer,  
Warren Pharmaceuticals, Inc. Ossining, New York
- 1998- Senior Member,  
The Kenneth S. Warren Institute, Ossining, New York
- 1989-98 Assistant & Associate Professor, Endocrinology and Metabolism,  
Department of Internal Medicine, Yale University School of Medicine
- 1992-98 Co-Director, Molecular Core, Yale Diabetes and Endocrinology Research  
Center
- 1989-98 Co-Director, Yale Pituitary Center
- 1978-82 Research Associate & Assistant Professor,  
The Rockefeller University, New York (neuroscience)
- 1975-76 Research Associate, Department of Biology,  
City University of New York
- 1970-73 Research Assistant and Teaching Assistant  
Departments of Biology and Physics, University of Notre Dame

#### **Education and Training**

- 1986-89 Postdoctoral Fellow, Training Program in Endocrinology &  
Neuroendocrinology
- 1986-88 Postdoctoral Fellow, Training Program in Clinical Investigation  
Department of Internal Medicine, Yale University
- 1984-86 Intern and Resident, Department of Internal Medicine  
Yale-New Haven Hospital, New Haven, Connecticut
- 1983 M. D., Yale University, New Haven, Connecticut
- 1978 Ph. D., Neurobiology and Behavioral Science,  
The Rockefeller University, New York, New York
- 1973 B. S. (with highest honors), Physics and Biology,  
University of Notre Dame, Notre Dame, Indiana



## Appendix A

Brines, page 2

### **Licensure and Board Certification**

1989	American Board of Endocrinology and Metabolism
1988	American Board of Internal Medicine
1985	State of Connecticut, Physician and Surgeon

### **Professional Associations**

1993	The Pituitary Society
1991	The Endocrine Society
1976	American Optical Society
1976	Society for Neuroscience
1973	Sigma Xi

### **Honors, Awards and Visiting Professorships**

2003	11 <sup>th</sup> Richard Stow Visiting Professor, Ohio State University
1991	Andrew Mellon Fellowship Award (Yale University)
1989	Epilepsy Foundation Fellowship
1976	The Albert Cass Traveling Fellowship (Princeton University)
1973	Phi Beta Kappa
1967	Ford Future Scientist of America

### **Issued U.S. Patents**

***Tissue protection:*** 6531121: Protection and enhancement of erythropoietin-responsive cells, tissues and organs.

***Novel drug delivery systems:*** 6569152 & 7090861: Sustained release delivery systems for solutes

***Advanced glycosylation endproduct therapeutics:*** 6713050 & 6777557 & 7022721: Method and composition for rejuvenating cells, tissues, organs, hair and nails.

### **Primary Manuscripts** (\* key recent publications)

Villa P, van Beek J, Larsen AK, Gerwien J, Christensen S, Cerami A, Brines M, Leist M, Ghezzi P, Torup L. (2007) Reduced functional deficits, neuroinflammation, and secondary tissue damage after treatment of stroke by nonerythropoietic erythropoietin derivatives. *J Cereb Blood Flow Metab* 27: 552-563.

Mennini T, De Paola M, Bigini P, Mastrotto C, Fumagalli E, Barbera S, Mengozzi M, Viviani B, Corsini E, Marinovich M, Torup L, Van Beek J, Leist M, Brines M, Cerami A, Ghezzi P. (2006) Nonhematopoietic erythropoietin

## Appendix A

Brines, page 3

derivatives prevent motoneuron degeneration in vitro and in vivo. *Mol Med (Cambridge, Mass 12: 153-160.*

- Fantacci M, Bianciardi P, Caretti A, Coleman TR, Cerami A, Brines M, Samaja M. (2006) Carbamylated erythropoietin ameliorates the metabolic stress induced in vivo by severe chronic hypoxia. *Proc Natl Acad Sci U S A 103: 17531-17536.*
- Erbayraktar S, de Lanerolle N, de Lotbiniere A, Knisely JP, Erbayraktar Z, Yilmaz O, Cerami A, Coleman TR, Brines M. (2006) Carbamylated erythropoietin reduces radiosurgically-induced brain injury. *Molecular medicine (Cambridge, Mass 12: 74-80.*
- \*Coleman TR, Westenfelder C, Togel FE, Yang Y, Hu Z, Swenson L, Leuvenink HG, Ploeg RJ, d'Uscio LV, Katusic ZS, Ghezzi P, Zanetti A, Kaushansky K, Fox NE, Cerami A, Brines M. (2006) Cytoprotective doses of erythropoietin or carbamylated erythropoietin have markedly different procoagulant and vasoactive activities. *Proc Natl Acad Sci U S A 103: 5965-5970.*
- Grasso G, Sfacteria A, Erbayraktar S, Passalacqua M, Meli F, Gokmen N, Yilmaz O, La Torre D, Buemi M, Iacopino DG, Coleman T, Cerami A, Brines M, Tomasello F. (2006) Amelioration of spinal cord compressive injury by pharmacological preconditioning with erythropoietin and a nonerythropoietic erythropoietin derivative. *Journal of neurosurgery 4: 310-318.*
- Bianchi R, Brines M, Lauria G, Savino C, Gilardini A, Nicolini G, Rodriguez-Menendez V, Oggioni N, Canta A, Penza P, Lombardi R, Minoia C, Ronchi A, Cerami A, Ghezzi P, Cavaletti G. (2006) Protective effect of erythropoietin and its carbamylated derivative in experimental Cisplatin peripheral neurotoxicity. *Clin Cancer Res 12: 2607-2*
- Savino C, Pedotti R, Baggi F, Ubiali F, Gallo B, Nava S, Bigini P, Barbera S, Fumagalli E, Mennini T, Vezzani A, Rizzi M, Coleman T, Cerami A, Brines M, Ghezzi P, Bianchi R. (2006) Delayed administration of erythropoietin and its non-erythropoietic derivatives ameliorates chronic murine autoimmune encephalomyelitis. *J Neuroimmunol 172: 27-37.*
- Moon C, Krawczyk M, Paik D, Coleman T, Brines M, Juhaszova M, Sollott S, Lakatta EG, Talan MI. (2006) Erythropoietin, modified to not stimulate red blood cell production, retains its cardioprotective properties. *J Pharmacol Exp Ther. 999-1005.*
- Grasso G, Sfacteria A, Passalacqua M, Morabito A, Buemi M, Macri B, Brines M, Tomasello F. (2005) Erythropoietin and erythropoietin receptor expression

## Appendix A

Brines, page 4

after experimental spinal cord injury encourages therapy by exogenous erythropoietin. *Neurosurgery* 56: 821-827; discussion 821-827.

Gorio A, Madaschi L, Di Stefano B, Carelli S, Di Giulio AM, De Biasi S, Coleman T, Cerami A, Brines M. (2005) Methylprednisolone neutralizes the beneficial effects of erythropoietin in experimental spinal cord injury. *Proc Natl Acad Sci U S A* 102: 16379-16384.

Fiordaliso F, Chimenti S, Staszewsky L, Bai A, Carlo E, Cuccovillo I, Doni M, Mengozzi M, Tonelli R, Ghezzi P, Coleman T, Brines M, Cerami A, Latini R. (2005) A nonerythropoietic derivative of erythropoietin protects the myocardium from ischemia-reperfusion injury. *Proc Natl Acad Sci U S A* 102: 2046-2051.

\*Leist M, Ghezzi P, Grasso G, Bianchi R, Villa P, Fratelli M, Savino C, Bianchi M, Nielsen J, Gervien J, Kallunki P, Larsen AK, Helboe L, Christensen S, Pedersen LO, Nielsen M, Torup L, Sager T, Sfacteria A, Erbayraktar S, Erbayraktar Z, Gokmen N, Yilmaz O, Cerami-Hand C, Xie QW, Coleman T, Cerami A, Brines M. (2004) Derivatives of erythropoietin that are tissue protective but not erythropoietic. *Science* 305: 239-242.

Grasso G, Sfacteria A, Brines M, Tomasello F. (2004) A new computed-assisted technique for experimental sciatic nerve function analysis. *Med Sci Monit* 10: BR1-3.

Eid T, Brines M, Cerami A, Spencer DD, Kim JH, Schweitzer JS, Ottersen OP, de Lanerolle NC. (2004) Increased expression of erythropoietin receptor on blood vessels in the human epileptogenic hippocampus with sclerosis. *J Neuropathol Exp Neurol* 63: 73-83.

Ehrenreich H, Degner D, Meller J, Brines M, Behe M, Hasselblatt M, Woldt H, Falkai P, Knerlich F, Jacob S, von Ahsen N, Maier W, Bruck W, Ruther E, Cerami A, Becker W, Siren AL. (2004) Erythropoietin: a candidate compound for neuroprotection in schizophrenia. *Mol Psychiatry* 9: 42-54.

\*Brines M, Grasso G, Fiordaliso F, Sfacteria A, Ghezzi P, Fratelli M, Latini R, Xie QW, Smart J, Su-Rick CJ, Pobre E, Diaz D, Gomez D, Hand C, Coleman T, Cerami A. (2004) Erythropoietin mediates tissue protection through an erythropoietin and common beta-subunit heteroreceptor. *Proc Natl Acad Sci U S A* 101: 14907-14912.

Bianchi R, Buyukakilli B, Brines M, Savino C, Cavaletti G, Oggioni N, Lauria G, Borgna M, Lombardi R, Cimen B, Comelekoglu U, Kanik A, Tataroglu C, Cerami A, Ghezzi P. (2004) Erythropoietin both protects from and reverses experimental diabetic neuropathy. *Proc Natl Acad Sci U S A* 101: 823-828.

- Villa P, Bigini P, Mennini T, Agnello D, Laragione T, Cagnotto A, Viviani B, Marinovich M, Cerami A, Coleman TR, Brines M, Ghezzi P. (2003) Erythropoietin selectively attenuates cytokine production and inflammation in cerebral ischemia by targeting neuronal apoptosis. *J Exp Med* 198: 971-975.
- \*Erbayraktar S, Grasso G, Sfacteria A, Xie QW, Coleman T, Kreilgaard M, Torup L, Sager T, Erbayraktar Z, Gokmen N, Yilmaz O, Ghezzi P, Villa P, Fratelli M, Casagrande S, Leist M, Helboe L, Gerwein J, Christensen S, Geist MA, Pedersen LO, Cerami-Hand C, Wuerth JP, Cerami A, Brines M. (2003) Asialoerythropoietin is a nonerythropoietic cytokine with broad neuroprotective activity in vivo. *Proc Natl Acad Sci U S A* 100: 6741-6746.
- Calvillo L, Latini R, Kajstura J, Leri A, Anversa P, Ghezzi P, Salio M, Cerami A, Brines M. (2003) Recombinant human erythropoietin protects the myocardium from ischemia-reperfusion injury and promotes beneficial remodeling. *Proc Natl Acad Sci U S A* 100: 4802-4806.
- Junk AK, Mammis A, Savitz SI, Singh M, Roth S, Malhotra S, Rosenbaum PS, Cerami A, Brines M, Rosenbaum DM. (2002) Erythropoietin administration protects retinal neurons from acute ischemia-reperfusion injury. *Proc Natl Acad Sci U S A* 99: 10659-10664.
- \*Gorio A, Gokmen N, Erbayraktar S, Yilmaz O, Madaschi L, Cichetti C, Di Giulio AM, Vardar E, Cerami A, Brines M. (2002) Recombinant human erythropoietin counteracts secondary injury and markedly enhances neurological recovery from experimental spinal cord trauma. *Proc Natl Acad Sci U S A* 99: 9450-9455.
- \*Ehrenreich H, Hasselblatt M, Dembowski C, Cepek L, Lewczuk P, Stiefel M, Rustenbeck HH, Breiter N, Jacob S, Knerlich F, Bohn M, Poser W, Ruther E, Kochen M, Gefeller O, Gleiter C, Wessel TC, De Ryck M, Itri L, Prange H, Cerami A, Brines M, Siren AL. (2002) Erythropoietin therapy for acute stroke is both safe and beneficial. *Mol Med* 8: 495-505.
- Chatterjee O, Nakchbandi IA, Philbrick WM, Dreyer BE, Zhang JP, Kaczmarek LK, Brines M, Broadus AE. (2002) Endogenous parathyroid hormone-related protein functions as a neuroprotective agent. *Brain Res* 930: 58-66.
- Celik M, Gokmen N, Erbayraktar S, Akhisaroglu M, Konak S, Ulukus C, Genc S, Genc K, Sagioglu E, Cerami A, Brines M. (2002) Erythropoietin prevents motor neuron apoptosis and neurologic disability in experimental spinal cord ischemic injury. *Proc Natl Acad Sci U S A* 99: 2258-2263.

## Appendix A

Brines, page 6

- Agnello D, Bigini P, Villa P, Mennini T, Cerami A, Brines M, Ghezzi P. (2002) Erythropoietin exerts an anti-inflammatory effect on the CNS in a model of experimental autoimmune encephalomyelitis. *Brain Res* 952: 128-134.
- Vaitkevicius PV, Lane M, Spurgeon H, Ingram DK, Roth GS, Egan JJ, Vasas S, Wagle DR, Ulrich P, Brines M, Wuerth JP, Cerami A, Lakatta EG. (2001) A cross-link breaker has sustained effects on arterial and ventricular properties in older rhesus monkeys. *Proc Natl Acad Sci U S A* 98: 1171-1175.
- \*Siren AL, Fratelli M, Brines M, Goemans C, Casagrande S, Lewczuk P, Keenan S, Gleiter C, Pasquali C, Capobianco A, Mennini T, Heumann R, Cerami A, Ehrenreich H, Ghezzi P. (2001) Erythropoietin prevents neuronal apoptosis after cerebral ischemia and metabolic stress. *Proc Natl Acad Sci U S A* 98: 4044-4049.
- \*Brines M, Ghezzi P, Keenan S, Agnello D, de Lanerolle NC, Cerami C, Itri LM, Cerami A. (2000) Erythropoietin crosses the blood-brain barrier to protect against experimental brain injury. *Proc Natl Acad Sci U S A* 97: 10526-10531.
- Asif M, Egan J, Vasas S, Jyothirmayi GN, Masurekar MR, Lopez S, Williams C, Torres RL, Wagle D, Ulrich P, Cerami A, Brines M, Regan TJ. (2000) An advanced glycation endproduct cross-link breaker can reverse age-related increases in myocardial stiffness. *Proc Natl Acad Sci U S A* 97: 2809-2813.
- Brines M, Ling Z, Broadus AE. (1999) Parathyroid hormone-related protein protects against kainic acid excitotoxicity in rat cerebellar granule cells by regulating L-type channel calcium flux. *Neurosci Lett* 274: 13-16.
- Brines M, Broadus AE. (1999) Parathyroid hormone-related protein markedly potentiates depolarization-induced catecholamine release in PC12 cells via L-type voltage-sensitive Ca<sup>2+</sup> channels. *Endocrinology* 140: 646-651.
- Borg MA, Borg WP, Tamborlane WV, Brines M, Shulman GI, Sherwin RS. (1999) Chronic hypoglycemia and diabetes impair counterregulation induced by localized 2-deoxy-glucose perfusion of the ventromedial hypothalamus in rats. *Diabetes* 48: 584-587.
- Yavari R, Adida C, Bray-Ward P, Brines M, Xu T. (1998) Human metalloprotease-disintegrin Kuzbanian regulates sympathoadrenal cell fate in development and neoplasia. *Hum Mol Genet* 7: 1161-1167.
- Xie H, Brines M, de Lanerolle NC. (1998) Transcripts of the transposon mariner are present in epileptic brain. *Epilepsy Res* 32: 140-153.

## Appendix A

Brines, page 7

- de Lanerolle NC, Eid T, von Campe G, Kovacs I, Spencer DD, Brines M. (1998) Glutamate receptor subunits GluR1 and GluR2/3 distribution shows reorganization in the human epileptogenic hippocampus. *Eur J Neurosci* 10: 1687-1703.
- de Lanerolle NC, Williamson A, Meredith C, Kim JH, Tabuteau H, Spencer DD, Brines M. (1997) Dynorphin and the kappa 1 ligand [3H]U69,593 binding in the human epileptogenic hippocampus. *Epilepsy Res* 28: 189-205.
- Brines M, Sundaresan S, Spencer DD, de Lanerolle NC. (1997) Quantitative autoradiographic analysis of ionotropic glutamate receptor subtypes in human temporal lobe epilepsy: up-regulation in reorganized epileptogenic hippocampus. *Eur J Neurosci* 9: 2035-2044.
- Holt EH, Broadus AE, Brines M. (1996) Parathyroid hormone-related peptide is produced by cultured cerebellar granule cells in response to L-type voltage-sensitive Ca<sup>2+</sup> channel flux via a Ca<sup>2+</sup>/calmodulin-dependent kinase pathway. *J Biol Chem* 271: 28105-28111.
- de Lanerolle NC, Gunel M, Sundaresan S, Shen MY, Brines M, Spencer DD. (1995) Vasoactive intestinal polypeptide and its receptor changes in human temporal lobe epilepsy. *Brain Res* 686: 182-193.
- Brines M, Tabuteau H, Sundaresan S, Kim J, Spencer DD, de Lanerolle N. (1995) Regional distributions of hippocampal Na<sup>+</sup>,K<sup>+</sup>-(+)-ATPase, cytochrome oxidase, and total protein in temporal lobe epilepsy. *Epilepsia* 36: 371-383.
- Brines M, Dare AO, de Lanerolle NC. (1995) The cardiac glycoside ouabain potentiates excitotoxic injury of adult neurons in rat hippocampus. *Neurosci Lett* 191: 145-148.
- Borg WP, During MJ, Sherwin RS, Borg MA, Brines M, Shulman GI. (1994) Ventromedial hypothalamic lesions in rats suppress counterregulatory responses to hypoglycemia. *J Clin Invest* 93: 1677-1682.
- de Lanerolle NC, Brines M, Kim JH, Williamson A, Philips MF, Spencer DD. (1993) Neurochemical remodelling of the hippocampus in human temporal lobe epilepsy. In: G. Avanzini et al. (ed.) *Molecular Neurobiology of Epilepsy*, pp. 205-220.
- de Lanerolle N, Brines M, Williamson A, Kim J, Spencer D. (1993) Neurotransmitters and their receptors in human temporal lobe epilepsy. In: Ribak C, Gall C, Mody I (eds.) *The Dentate Gyrus and its role in Seizures*, pp. 235-250.

- Brines M, Robbins RJ. (1993)** Cell-type specific expression of Na<sup>+</sup>, K<sup>+</sup>-ATPase catalytic subunits in cultured neurons and glia: evidence for polarized distribution in neurons. *Brain Res* 631: 1-11.
- Brines M, Robbins RJ. (1993)** Glutamate up-regulates alpha 1 and alpha 2 subunits of the sodium pump in astrocytes of mixed telencephalic cultures but not in pure astrocyte cultures. *Brain Res* 631: 12-21.
- Zahler R, Brines M, Kashgarian M, Benz EJ, Jr., Gilmore-Hebert M. (1992)** The cardiac conduction system in the rat expresses the alpha 2 and alpha 3 isoforms of the Na<sup>+</sup>,K<sup>+</sup>-ATPase. *Proc Natl Acad Sci U S A* 89: 99-103.
- Schmauss C, Brines M, Lerner MR. (1992)** The gene encoding the small nuclear ribonucleoprotein-associated protein N is expressed at high levels in neurons. *J Biol Chem* 267: 8521-8529.
- Kolansky DM, Brines M, Gilmore-Hebert M, Benz EJ, Jr. (1992)** The A2 isoform of rat Na<sup>+</sup>,K<sup>+</sup>-adenosine triphosphatase is active and exhibits high ouabain affinity when expressed in transfected fibroblasts. *FEBS Lett* 303: 147-153.
- de Lanerolle NC, Brines M, Kim JH, Williamson A, Philips MF, Spencer DD. (1992)** Neurochemical remodelling of the hippocampus in human temporal lobe epilepsy. *Epilepsy Res Suppl* 9: 205-219; discussion 220.
- de Lanerolle NC, Brines M, Williamson A, Kim JH, Spencer DD. (1992)** Neurotransmitters and their receptors in human temporal lobe epilepsy. *Epilepsy Res Suppl* 7: 235-250.
- Brines M, Robbins RJ. (1992)** Inhibition of alpha 2/alpha 3 sodium pump isoforms potentiates glutamate neurotoxicity. *Brain Res* 591: 94-102.
- Robbins RJ, Brines M, Kim JH, Adrian T, de Lanerolle N, Welsh S, Spencer DD. (1991)** A selective loss of somatostatin in the hippocampus of patients with temporal lobe epilepsy. *Ann Neurol* 29: 325-332.
- Isales CM, Barrett PQ, Brines M, Bollag W, Rasmussen H. (1991)** Parathyroid hormone modulates angiotensin II-induced aldosterone secretion from the adrenal glomerulosa cell. *Endocrinology* 129: 489-495.
- Brines M, Gulanski BI, Gilmore-Hebert M, Greene AL, Benz EJ, Jr., Robbins RJ. (1991)** Cytoarchitectural relationships between [3H]ouabain binding and mRNA for isoforms of the sodium pump catalytic subunit in rat brain. *Brain Res Mol Brain Res* 10: 139-150.

## Appendix A

Brines, page 9

- Weir EC, Brines M, Ikeda K, Burtis WJ, Broadus AE, Robbins RJ. (1990) Parathyroid hormone-related peptide gene is expressed in the mammalian central nervous system. *Proc Natl Acad Sci U S A* 87: 108-112.
- Thiede MA, Daifotis AG, Weir EC, Brines M, Burtis WJ, Ikeda K, Dreyer BE, Garfield RE, Broadus AE. (1990) Intrauterine occupancy controls expression of the parathyroid hormone-related peptide gene in preterm rat myometrium. *Proc Natl Acad Sci U S A* 87: 6969-6973.
- Orloff JJ, Wu TL, Heath HW, Brady TG, Brines M, Stewart AF. (1989) Characterization of canine renal receptors for the parathyroid hormone-like protein associated with humoral hypercalcemia of malignancy. *J Biol Chem* 264: 6097-6103.
- Dworkin B, Miller NE, Dworkin S, Birbaumer N, Brines M, Jonas S, Schwentker EP, Graham JJ. (1985) Behavioral method for the treatment of idiopathic scoliosis. *Proc Natl Acad Sci U S A* 82: 2493-2497.
- Brines M, Gould J. (1982) Skylight polarization patterns and animal orientation. *J. Exp. Biol.* 96: 69-91.
- Gould J, Kirschvink J, Deffeyes K, Brines M. (1980) Magnetic field sensitivity: bees do not employ a permanent magnet detector. *J. Exp. Biol.* 86: 1-8.
- Brines M. (1980) Dynamic patterns of skylight polarization as clock and compass. *J Theor Biol* 86: 507-512.
- Dworkin B, Miller N, Brines M. (1979) Visceral learning and homeostasis. *Proceedings of the Joint Automatic Control Conference.*
- Brines M, Gould J. (1979) Bees have rules. *Science* 206: 571-573.
- Brines M. (1978) Skylight polarization patterns as cues for honey bee orientation: physical measurements and behavioral experiments. The Rockefeller University, New York, 378 pp.

### Invited Reviews

- Brines M, Cerami A. (2006) Discovering erythropoietin's extra-hematopoietic functions: biology and clinical promise. *Kidney Internat* 70: 246-250.
- Brines M, Cerami A. (2006) Tissue-protective cytokines in spinal cord injury: Challenges for a novel neuroprotective strategy. In: Hoke A (ed.) *Erythropoietin and the Nervous System: Novel Therapeutic Options for Neuroprotection*. Springer, New York, pp. 147-164.



- Brines M, Cerami A. (2005)** Emerging biological roles for erythropoietin in the nervous system. *Nat Rev Neurosci* 6: 484-494.
- Grasso G, Sfacteria A, Cerami A, Brines M. (2004)** Erythropoietin as a tissue-protective cytokine in brain injury: What do we know and where do we go? *The Neuroscientist* 10: 93-98.
- Grasso G, Brines M. (2004)** From erythropoiesis to a rational neuroprotective therapeutic strategy and beyond. *J. Supportive Oncol* 2: 44-45.
- Ghezzi P, Brines M. (2004)** Erythropoietin as an antiapoptotic, tissue-protective cytokine. *Cell Death Differ* 11 Suppl 1: S37-44.
- Coleman T, Brines M. (2004)** Science review: recombinant human erythropoietin in critical illness: a role beyond anemia? *Crit Care* 8: 337-341.
- Cerami A, Brines M, Cerami C. (2004)** Epoetin alfa has potential efficacy in central nervous system disorders. *Eur. J. Cancer* 2: 29-35.
- Erbayraktar S, Yilmaz O, Gokmen N, Brines M. (2003)** Erythropoietin Is a Multifunctional Tissue-protective Cytokine. *Curr Hematol Rep* 2: 465-470.
- Eid T, Brines M. (2002)** Recombinant human erythropoietin for neuroprotection: what is the evidence? *Clin Breast Cancer* 3 Suppl 3: S109-115.
- Cerami A, Brines M, Ghezzi P, Cerami C, Itri LM. (2002)** Neuroprotective properties of epoetin alfa. *Nephrol Dial Transplant* 17 Suppl 1: 8-12.
- Brines M. (2002)** What evidence supports use of erythropoietin as a novel neurotherapeutic? *Oncology (Huntingt)* 16: 79-89.
- Cerami A, Brines ML, Ghezzi P, Cerami CJ. (2001)** Effects of epoetin alfa on the central nervous system. *Semin Oncol* 28: 66-70.
- de Lanerolle NC, Kim JH, Brines ML. (1994)** Cellular and Molecular Alterations in Partial Epilepsy. *Clin. Neurosci.* 2: 64-81.
- de Lanerolle N, Magge S, Philips M, Trombley P, Spencer D, Brines M. (1994)** Adaptive changes of epileptic human temporal lobe tissue: properties of neurons and glia. In: Wolf P (ed.) *Seizures and Syndromes in Epilepsy*. J. Libby and Company Ltd., London, pp. 431-448.

## Clinical Publications

- Inzucchi S, Brines M. (1997) Pheochromocytoma. In: Gilman S, Goldstein G, Waxman S (eds.) *Neurobase*. Arbor Publishing, La Jolla, CA.
- Inzucchi S, Brines M. (1997) Syndrome of Inappropriate Antidiuresis. In: Gilman S, Goldstein G, Waxman S (eds.) *Neurobase*. Arbor Publishing, La Jolla, CA.
- Brines M. (1997) Diabetes Insipidus. In: Gilman S, Goldstein G, Waxman S (eds.) *Neurobase*. Arbor Publishing, La Jolla, CA.
- Brines M. (1997) Sheehan's Syndrome. In: Gilman S, Goldstein G, Waxman S (eds.) *Neurobase*. Arbor Publishing, La Jolla, CA.
- Wallace EA, Brines M, Kinder BK, de Lotbiniere AC. (1996) Clinical case seminar: Cushing's syndrome in an elderly woman with large thyroid and pituitary masses. *J Clin Endocrinol Metab* 81: 453-456.
- Brines M. (1995) Pituitary Apoplexy. In: Gilman S, Goldstein G, Waxman S (eds.) *Neurobase*. Arbor Publishing, La Jolla, CA.
- Brines M. (1995) Hypopituitarism. In: Gilman S, Goldstein G, Waxman S (eds.) *Neurobase*. Arbor Publishing, La Jolla, CA.
- Korn EA, Gaich G, Brines M, Carpenter TO. (1994) Thyrotropin-secreting adenoma in an adolescent girl without increased serum thyrotropin-alpha. *Horm Res* 42: 120-123.
- Bohler HC, Jr., Jones EE, Brines M. (1994) Marginally elevated prolactin levels require magnetic resonance imaging and evaluation for acromegaly. *Fertil Steril* 61: 1168-1170.

## Appendix B

1. Anagnostou et al., entitled "Erythropoietin receptor mRNA expression in human endothelial cells", *Proc. Natl. Acad. Sci.* 1994, 91:3974-3978.
2. Benyo et al., entitled "Expression of erythropoietin receptor by trophoblast cells in the human placenta", *Biol. Reproduct.* 1999, 60:861-870.
3. Juul et al., entitled "Erythropoietin and erythropoietin receptor in the developing human central nervous system", *Pediatr. Res.* 1998, 43:40-49.
4. Juul et al., entitled "Tissue distribution of erythropoietin and erythropoietin receptor in the developing human fetus", *Early Human Devel.* 1998, 52:235-249.
5. Li et al., entitled "Erythropoietin receptors are expressed in the central nervous system of mid-trimester human fetuses", *Pediatr. Res.* 1996, 40:376-380.
6. Liu et al., "Tissue Specific Expression of Human Erythropoietin Receptor in transgenic Mice", *Dev. Biol.* 1994, 166: 159-169.
7. Liu et al., entitled "Transgenic mice containing the human erythropoietin receptor gene exhibit correct hematopoietic and neural expression", *Proc. Assoc. Am. Physicians* 1996, 108:449-454.
8. Liu et al., entitled "Regulated human erythropoietin receptor expression in mouse brain", *J. Biol. Chem.* 1997, 272:32395-32400.
9. Marti et al., entitled "Erythropoietin gene expression in human, monkey and murine brain", *Eur. J. Neurosci.* 1996, 8:666-676.
10. Masuda et al., entitled "Insulin-like growth factors and insulin stimulate erythropoietin production in primary cultured astrocytes", *Brain Res.* 1997, 746:63-70.
11. Masuda et al., entitled "Functional erythropoietin receptor of the cells with neural characteristics. Comparison with receptor properties of erythroid cells", *J. Biol. Chem.* 1993, 268:11208-11216.
12. Mioni et al., entitled "Evidence for specific binding and stimulatory effects of recombinant human erythropoietin on isolated adult rat Leydig cells", *Acta Endocrinologica* 1992, 127:459-465.
13. Okada et al., entitled "Erythropoietin stimulates proliferation of rat-cultured gastric mucosal cells", *Digestion* 1996, 57:328-332.
14. Sawyer et al., entitled "Receptors for erythropoietin in mouse and human erythroid cells and placenta", *Blood* 1989, 74:103-109.
15. Westenfelder et al., entitled "Human, rat and mouse kidney cells express functional erythropoietin receptors", *Kidney Intl.* 1999, 55:808-820.

16. Williams et al., entitled "The expression and role of human erythropoietin receptor in erythroid and non erythroid cells", Ann. NY Acad. Sci. 1994, 718:232-244.
17. Yamaji et al., entitled "Brain capillary endothelial cells express two forms of erythropoietin receptor mRNA", Eur. J. Biochem. 1996 239(2):494-500.
18. Cytokine receptor common beta chain precursor expression profile obtained from [www.proteinatlas.org](http://www.proteinatlas.org) (queried: February 19, 2008)

## Erythropoietin receptor mRNA expression in human endothelial cells

ATHANASIOS ANAGNOSTOU<sup>\*†</sup>, ZIYAO LIU<sup>‡</sup>, MANFRED STEINER<sup>\*</sup>, KYUNG CHIN<sup>‡</sup>, EUN S. LEE<sup>\*</sup>, NOUBAR KESSIMIAN<sup>\*</sup>, AND CONSTANCE T. NOGUCHI<sup>‡</sup>

<sup>\*</sup>Memorial Hospital of Rhode Island and Brown University School of Medicine, Division of Hematology/Oncology and Department of Pathology, 111 Brewster Street, Pawtucket, RI 02860; and <sup>‡</sup>National Institutes of Health, Laboratory of Chemical Biology, National Institute of Diabetes and Digestive and Kidney Diseases, 9000 Rockville Pike, Building 10, Room 9N307, Bethesda, MD 02892

Communicated by Eugene P. Cronkite, January 3, 1994

**ABSTRACT** A previous report demonstrated that endothelial cells have erythropoietin receptors and respond to this hormone with enhanced proliferation. The present study demonstrates the existence of mRNA for erythropoietin receptor in human umbilical vein endothelial cells. We have reverse transcribed mRNA of endothelial cells and then used different PCR primers to amplify erythropoietin receptor target cDNA between exons 5 and 6 as well as 3-5 in addition to an internal standard DNA fragment. Correspondence of size as well as location of restriction endonuclease scission (*Ava* II) was used in comparing the amplified fragments of human endothelial cell erythropoietin receptor to those of two human erythroleukemia cell lines, OCIM1 and K562. No  $\alpha$ - or  $\gamma$ -globin mRNA was detected in endothelial cells but was readily demonstrable in OCIM1 cells. In addition, to determine whether the expression of human erythropoietin receptor on endothelial cells occurs *in vivo*, sections of umbilical cord and placenta were immunostained with antibodies against the extracellular portion of the receptor; the results showed strong positive staining of the vascular endothelium.

Erythropoietin (Epo) is a 30,400-Da polypeptide known to be the principal hormone regulating the proliferation, differentiation, and survival of erythroid cells (1). Its cell surface receptors, which belong to the hematopoietic (cytokine) receptor superfamily (2), are considered highly specific for cells of the erythroid lineage. We have previously reported a proliferative effect of recombinant human erythropoietin (rhEpo) on cultured human umbilical vein endothelial cells (HUVECs) and bovine adrenal capillary endothelial cells (3) and Carlini *et al.* (4) have described a similar mitogenic effect on bovine pulmonary artery endothelial cells. In this study we used PCR techniques to detect and quantitate human Epo receptor (hEpoR) gene transcripts in HUVECs and compared the abundance of this mRNA with that expressed in the erythroleukemia cell lines OCIM1 and K562. K562 cells express only 4-6 hEpoRs per cell on average (5), whereas OCIM1 cells exhibit about 3000 of these receptors per cell (6). As a negative control we used HeLa cells, which do not express hEpoR. In addition, we utilized a monoclonal antibody to the extracytoplasmic portion of hEpoR (37) which has recently become available to immunostain the endothelial lining of human blood vessels and demonstrated strong reactivity of the vascular endothelium.

### MATERIALS AND METHODS

**HUVEC.** HUVECs were obtained from umbilical cords from cesarean sections. The cells were cultured by standard methods in the presence of heparin and endothelial-cell

growth supplement (7). They were characterized by their homogeneous and typical cobblestone morphology, factor VIII antigen positivity, and the presence of Weibel-Palade bodies on electron microscopy. HUVECs were used for these studies after three to five passages.

For clonal culture to exclude contamination with hematopoietic stem cells, HUVECs ( $1-5 \times 10^5$  cells per ml) were plated in methylcellulose cultures as described (8), with the modification that half of the fetal bovine serum was replaced with human umbilical cord blood serum. Hematopoietic growth factors were added as follows: rhEpo, 2 units/ml; stem-cell factor, 10  $\mu$ g/ml; granulocyte/macrophage-colony-stimulating factor, 200 units/ml; interleukin 3, 200 units/ml; endothelial-cell growth factor, 20  $\mu$ g/ml.

**Preparation of mRNA.** After  $1-5 \times 10^7$  cells were harvested and washed twice with phosphate-buffered saline, RNA was extracted with guanidinium thiocyanate and lauryl sarcosinate (9). mRNA was adsorbed onto oligo(dT)-cellulose columns (Pharmacia) and, after the columns were washed with high- and low-salt solutions, was eluted with 10 mM Tris-HCl buffer containing 1 mM EDTA (pH 7.4) at 65°C. Total amount and concentration of mRNA were determined spectrophotometrically and confirmed by agarose gel electrophoresis.

**Reverse Transcription of RNA and Amplification of cDNA.** An aliquot of mRNA (0.5-1  $\mu$ g) was used for reverse transcription according to Gubler and Hoffmann (10). Synthesis of the first-strand cDNA began at the 3' end of poly(A)<sup>+</sup> mRNA by using (dT)<sub>12</sub> primer in 20  $\mu$ l of 50 mM Tris-HCl, pH 8.5/8 mM MgCl<sub>2</sub>/30 mM KCl/0.01 mM dithiothreitol containing 8 units of RNase inhibitor (Boehringer Mannheim), 1  $\mu$ M each dNTP, and 40 units of avian myeloblastoma virus reverse transcriptase (Boehringer Mannheim). The reaction was carried out at 42°C for 60 min in a DNA thermal cycler (Perkin-Elmer). After the reaction was stopped, 5-10  $\mu$ l of sample was used for PCR amplification. Synthetic oligonucleotide primers from exon 5 (sense, 5'-GCA-CCG-AGT-GTG-TGC-TGA-CGA-A-3') and exon 6 (antisense, 5'-GGT-CAG-CAG-CAC-CAG-CAT-GAC-3') were used to amplify hEpoR target cDNA, giving rise to a 197-bp fragment (38). Results from endothelial cells were compared with results from OCIM1 cells (positive control) and HeLa cells (negative control). To determine the specificity of the reaction, the product of the PCR amplification was subjected to digestion with the restriction endonuclease *Ava* II to obtain the expected 57-bp and 140-bp fragments.

**Quantitative PCR.** To quantify hEpoR mRNA, mRNA was reverse transcribed (see above) and multiple reaction mixtures were made with the resultant cDNA. Serial dilutions of

Abbreviations: (r)hEpo, (recombinant) human erythropoietin; hEpoR, human Epo receptor; HUVEC, human umbilical vein endothelial cell; vWF, von Willebrand factor.

<sup>†</sup>To whom reprint requests should be addressed at: Division of Hematology/Oncology, East Carolina University School of Medicine, 3E-127 Brody Building, Greenville, NC 27838.

The publication costs of this article were defrayed in part by page charge payment. This article must therefore be hereby marked "advertisement" in accordance with 18 U.S.C. §1734 solely to indicate this fact.

an internal standard were added to each reaction mixture and coamplified (11). The internal standard was constructed by PCR of hEpoR cDNA using the primer set 5'-GCGTCCCTCTAGAGTTTCGCGCT-3' and 5'-TGGCTCATCCGCTAGGCGTCAAG-3' and includes a 378-bp fragment extending from exon 3 to exon 5 of hEpoR (35). PCR amplification using *Taq* DNA polymerase Stoffel fragment (Perkin-Elmer) was performed in 10 mM Tris-HCl, pH 8.3/10 mM KCl/3 mM MgCl<sub>2</sub>/0.2 mM dNTPs; 0.25–0.5 µg of mRNA was used for each PCR. Standard DNA and hEpoR primers were used at concentrations varying from 20 to 50 ng for HUVEC and OCIM1 mRNA. [ $\alpha$ -<sup>32</sup>P]dCTP (2.5–3.0 µCi; 1 µCi = 37 kBq) was added. The thermal cycler program was begun with a melting step, 3 min at 94°C, followed by 30–35 cycles of 94°C for 1 min, 55°C for 2 min, and 72°C for 3 min. Final extension was at 72°C for 7 min. Products of the reaction were analyzed by electrophoresis in 2–2.4% agarose gels (SeaKem ME/NuSieve GTG, 1:2; FMC). The bands representing hEpoR and the standard fragment were cut out for scintillation counting. hEpoR was quantified based on the amount of standard added and on radioactivity of the standard and of the hEpoR cDNA-specific band.

**Immunohistochemistry.** Representative sections from fresh human placentas and umbilical cords were fixed for 6–18 hr in 96% absolute ethanol/1% glacial acetic acid/3% distilled water. The tissue was processed manually and embedded in paraffin. Sections of 5 µm were cut, heated at 55°C for 1 hr, deparaffinized in Clear-Rite-3 (Richard Allen, Richland, MI), and rehydrated in graded ethanol solutions to water. Endogenous peroxidase activity was quenched by freshly prepared 3% hydrogen peroxide for 30 min, and the slides were rinsed and placed in phosphate-buffered saline (pH 7.3). Monoclonal anti-human erythropoietin receptor antibody (mh2er/16.5.1, mouse IgG1, affinity purified on protein A) (Genetics Institute, Cambridge, MA) was added at a dilution of 1:25 and incubated for 75 min. Biotinylated anti-mouse IgG was used as secondary antibody and was recognized by streptavidin-peroxidase (labeled streptavidin-biotin kit, K-681; Dako); peroxidase activity was analyzed with 3-amino-9-ethylcarbazole (Vector Laboratories) as chromogen. The sections were counterstained with Harris hematoxylin. Similar tissue sections were stained for von Willebrand factor (vWF) with the standard Dako kit.

## RESULTS AND DISCUSSION

Since umbilical cord blood is rich in hematopoietic stem cells, we took several safeguards to assure that the target cells were indeed endothelial cells and not a small number of contaminating hematopoietic progenitor cells. We extensively washed the umbilical cords free of contaminating blood, removed repeatedly all nonadherent cells, and saw no evidence of emperipoiesis. More than 95% of the cells were positive for vWF. To avoid ingrowth of fibroblasts, we used HUVECs only at passages 3–5 from individual donors. We observed no proliferative effect of rhEpo on umbilical cord-derived fibroblasts or smooth muscle cells. Bovine adrenal capillary endothelial cells respond to rhEpo similarly to HUVECs even after 11–18 passages (3). HUVECs plated in a methylcellulose stem-cell culture system in the presence of endothelial-cell growth factor produced a homogeneous endothelial layer with typical cobblestone morphology. Addition of hematopoietic growth factors failed to give rise to any hematopoietic colonies over a period of 1–4 weeks but did stimulate "capillary tube" formation as described in other angiogenic assays.

To demonstrate the presence of hEpoR mRNA in HUVECs, RNA PCR was performed with avian myeloblastosis virus reverse transcriptase and (dT)<sub>15</sub> primer. Second-strand cDNA synthesis and amplification of cDNA were performed with primers from exon 5 (sense) and exon 6 (antisense) of hEpoR mRNA (Fig. 1). The amplified fragment was subjected to digestion with *Ava* II, which splits the 197-bp target into 140- and 57-bp fragments. HUVECs yielded the expected fragment sizes, which were identical to those of OCIM1 cells, confirmation that the amplification product represented hEpoR mRNA. mRNA extracted from HeLa cells did not exhibit any amplification product in the 197- to 57-bp range (Fig. 1A). Amplification of a different target cDNA of HUVECs corresponding to a 265-bp fragment extending from exon 1 to exon 3 of hEpoR mRNA showed results identical to those obtained with OCIM1, as well as with K562 cells (Fig. 1B and C). HeLa cells exhibited no evidence of this mRNA. The abundance of hEpoR mRNA evaluated by comparison with that of coamplified  $\beta$ -actin cDNA revealed roughly similar levels in HUVECs and K562 cells which were distinctly lower than those of OCIM1 cells. These studies were complemented by quantification of hEpoR mRNA (Fig. 2)

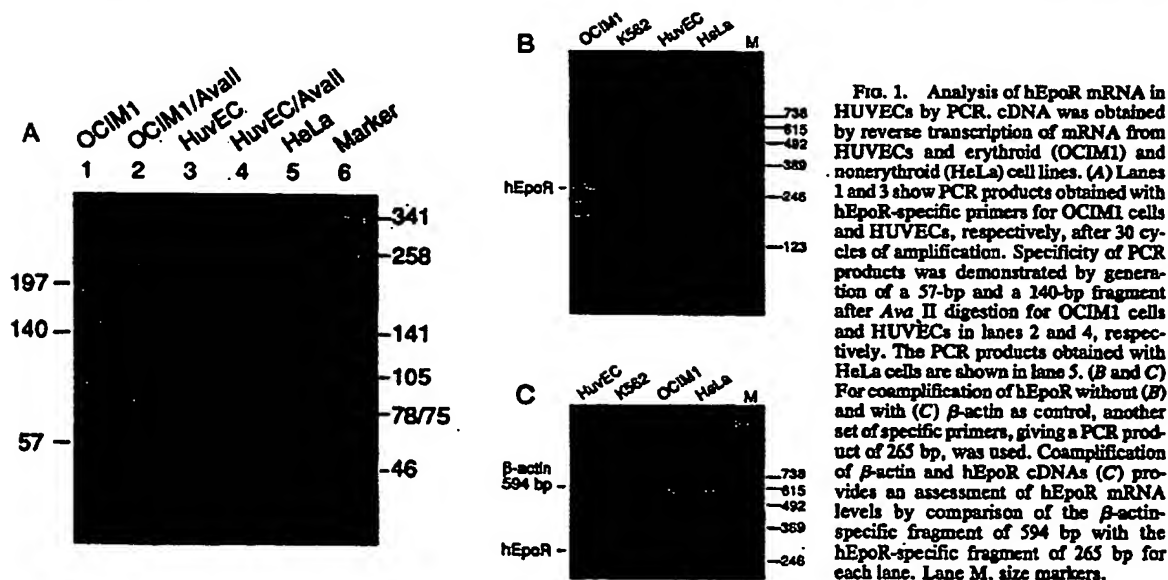


**FIG. 1.** Analysis of hEpoR mRNA in HUVECs by PCR. cDNA was obtained by reverse transcription of mRNA from HUVECs and erythroid (OCIM1) and nonerythroid (HeLa) cell lines. (A) Lanes 1 and 3 show PCR products obtained with hEpoR-specific primers for OCIM1 cells and HUVECs, respectively, after 30 cycles of amplification. Specificity of PCR products was demonstrated by generation of a 57-bp and a 140-bp fragment after *Ava* II digestion for OCIM1 cells and HUVECs in lanes 2 and 4, respectively. The PCR products obtained with HeLa cells are shown in lane 5. (B and C) For coamplification of hEpoR without (B) and with (C)  $\beta$ -actin as control, another set of specific primers, giving a PCR product of 265 bp, was used. Coamplification of  $\beta$ -actin and hEpoR cDNAs (C) provides an assessment of hEpoR mRNA levels by comparison of the  $\beta$ -actin-specific fragment of 594 bp with the hEpoR-specific fragment of 265 bp for each lane. Lane M, size markers.

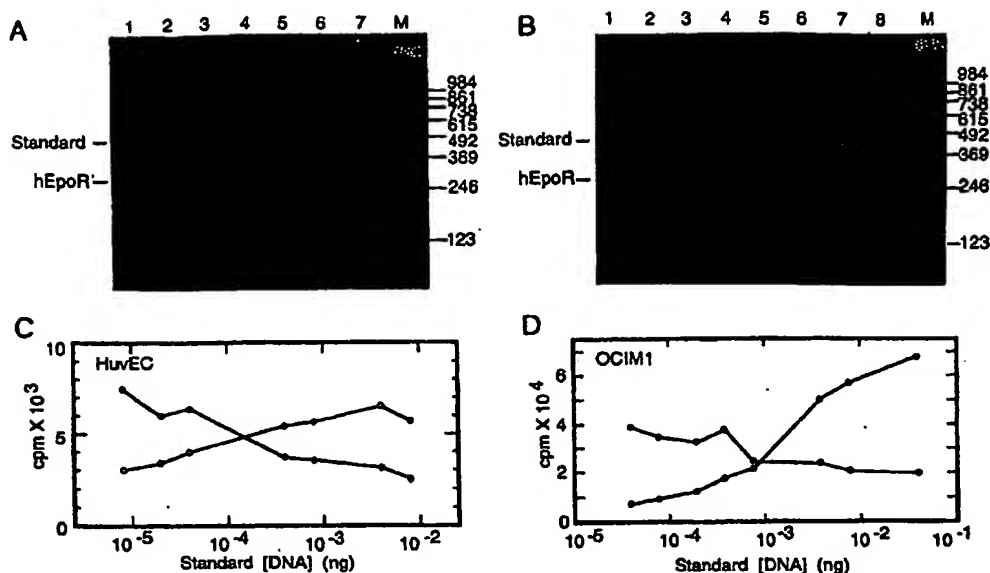


FIG. 2. Quantification of hEpoR mRNA by PCR in HUVECs and OCIM1 cells. cDNA was reverse transcribed from mRNA isolated from HUVECs (A) and OCIM1 cells (B). Multiple reactions (lanes 1–7 for HUVECs and lanes 1–8 for OCIM1 cells) for hEpoR-specific PCR amplification of cDNA were carried out with hEpoR primers. Prior to PCR amplification, increasing amounts of standard DNA were added to each reaction. At low amounts of standard the hEpoR-specific PCR product (hEpoR) was dominant. At high amounts of standard, the PCR product of 427 bp corresponding to the standard was dominant. Lane M, size markers. (C and D) To quantify the PCR products, [ $\alpha$ - $^{32}$ P]dCTP was added to each PCR mixture for HUVEC (C) and OCIM1 (D) cDNA.  $\circ$ , Internal standard;  $\bullet$ , hEpoR-specific PCR product. The amounts of radioactivity recovered in the hEpoR and standard fragments are plotted against the amount of standard added to each reaction mixture. The amount of standard corresponding to the point at which the two PCR products are equal is an indication of the amount of hEpoR cDNA present.

with an internal standard constructed from an overlapping segment of the hEpoR target sequence (12). The amount of cDNA/ $\mu$ g of mRNA of duplicate quantitative PCR experiments was  $3.0 \times 10^{-4}$  ng for HUVECs,  $4.8 \times 10^{-3}$  ng for OCIM1, and  $2.3 \times 10^{-4}$  ng for K562 cells.

To further exclude the possibility that the hEpoR mRNA detected was produced by small numbers of hematopoietic progenitors that remained undetected in our clonal cultures, we added to our standard HUVEC cultures (6) hematopoietic growth factors at concentrations similar to those of our clonal cultures, changing the supplemented medium every 3 days. After 10 days, all cells were harvested and their mRNA was extracted and analyzed by PCR for the presence of  $\alpha$ - and  $\gamma$ -globin mRNA, using reverse transcriptase (for conversion to cDNA) and primer pairs specific for each globin type (Fig. 3). PCR products corresponding to  $\alpha$ -globin and  $\gamma$ -globin transcripts were found in OCIM1 cells but not in HUVECs or HeLa cells. These results provide further confirmation of the absence of erythroid precursors in our HUVEC cultures.

Immunostaining of umbilical cord and placental vessels with antibody to vWF showed strong reactivity of the endothelium of umbilical veins and of placental blood vessels having muscle walls (Fig. 4 C and D). Staining of septal and villous thin capillaries of placental tissue was weak and inconsistent. Similar results were obtained when umbilical cord and placenta tissue sections were reacted with mouse anti-hEpoR monoclonal antibody mh2er/16.5.1. This antibody binds to the soluble version of hEpoR on several receptor-positive cell lines and inhibits binding of Epo to its receptor (13). The endothelium of umbilical veins (Fig. 4A) and of placental septal blood vessels containing muscle wall (Fig. 4B) showed strong EpoR positivity. Placental capillaries and other cells were negative (Fig. 4B). Vascular endothelial cells are remarkably heterogeneous in terms of morphology, expression of molecular markers, and biological function (14) and many capillaries are vWF negative

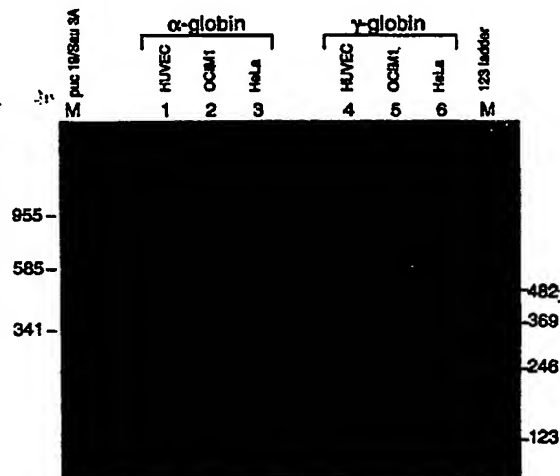


FIG. 3. PCR analysis of HUVEC mRNA for globin gene transcripts. mRNA was prepared from HUVECs, OCIM1 cells, and HeLa cells. PCR analysis for  $\alpha$ -globin and  $\gamma$ -globin transcripts was carried out using reverse transcriptase and primers specific for  $\alpha$ -globin cDNA (lanes 1–3) and  $\gamma$ -globin cDNA (lanes 4–6). The results for HUVECs are in lanes 1 and 4, for OCIM1 cells in lanes 2 and 5, and for HeLa cells in lanes 3 and 6. PCR product corresponding to  $\alpha$ -globin transcripts (372 bp) was detected in OCIM1 cells (lane 2, arrowhead) but not in HUVECs (lane 1) or HeLa cells (lane 3). The background bands in lanes 1 and 3 are nonspecific PCR products. PCR product corresponding to  $\gamma$ -globin transcripts (433 bp) was detected in OCIM1 cells (lane 5, arrowhead) but not in HUVECs (lane 4) or HeLa cells (lane 6). Lanes M, *Sau3A*-digested pUC19/plasmid (left) and a 123-bp ladder (BRL) (right).

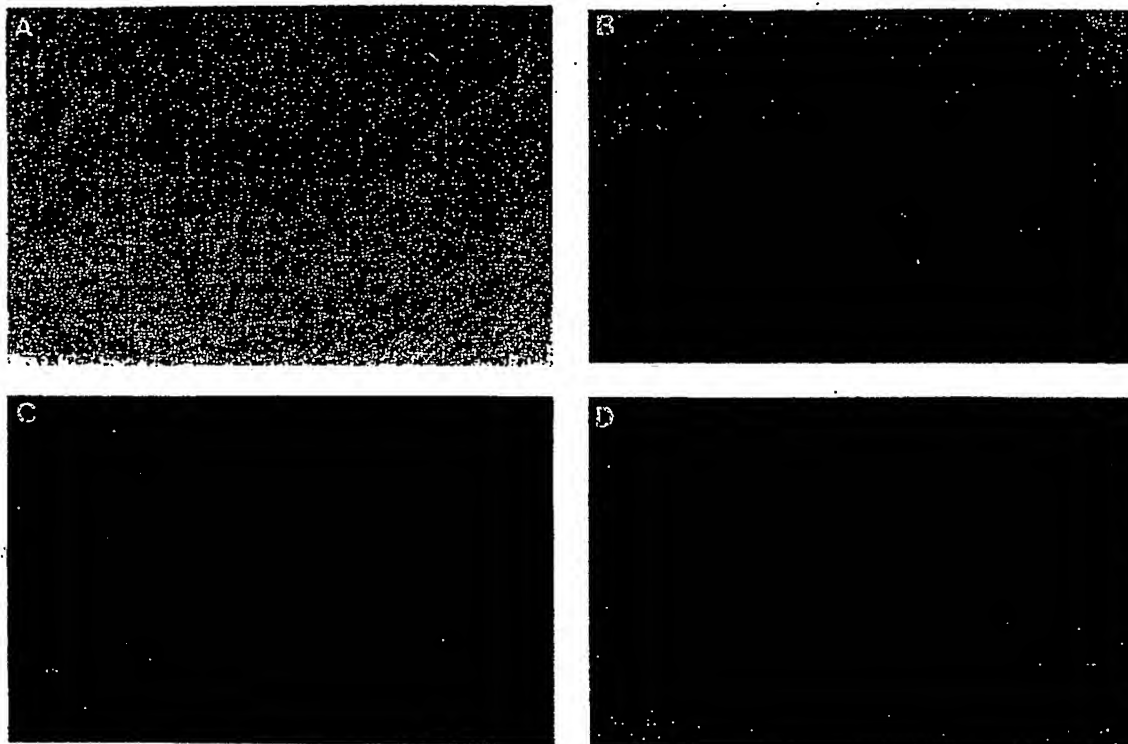


FIG. 4. Expression of vWF (C and D) and EpoR (A and B) in umbilical cord vein endothelial cells (A and C) and placenta (B and D). Acid ethanol-fixed, paraffin-embedded tissues were treated with anti-vWF or anti-EpoR antibody followed by a peroxidase-conjugated secondary antibody system. (A) Umbilical cord vein endothelial cells are strongly decorated with anti-hEpoR peroxidase (arrow). Smooth muscle of the wall is negative. ( $\times 35$ .) (B) Placental septal blood vessels with muscle wall show EpoR reactivity (filled arrow) while villous and septal capillaries are negative (open arrow). The interstitial tissue of septa and villi and the syncytiotrophoblastic cells are negative (arrowhead). ( $\times 220$ .) (C) Umbilical cord vein endothelial cells are decorated with anti-vWF peroxidase (arrow). ( $\times 35$ .) (D) Placental septal blood vessels with muscle wall are strongly positive for vWF (filled arrow) while the septal and villous thin capillaries show weak and inconsistent staining (open arrow). ( $\times 90$ .)

(15). Although the histochemical staining pattern of anti-hEpoR seems similar to that of anti-vWF, we do not yet have detailed comparative studies in other tissues to know whether this congruence extends to other vascular areas.

Our previous studies have shown that HUVECs have many more EpoRs than OCIM1 cells or other erythroid cells; however, the quantity of hEpoR mRNA in HUVECs as shown in this study is less than that in OCIM1 cells. We have no experimental evidence to explain this discrepancy, but several explanations can be suggested. In erythroid cells, the mature EpoR has an exceedingly short half-life (45–60 min), in sharp contrast to other receptors—e.g., transferrin, insulin, and asialoglycoprotein receptors, which have half-lives from 7 to 20 hr. Less than 5% of the EpoRs are found on the cell surface (16, 17). Migliaccio *et al.* (18) have proposed that it is the cellular environment in which the EpoR gene is expressed, and not simply its expression, that determines the erythroid-specific processing and function of EpoR.

The concept of strict erythroid or even hematopoietic specificity of EpoR is being challenged not only by our studies but also those of Masuda *et al.* (19), who have recently described the presence of EpoR in two rodent cell lines of neural origin. Ohneda *et al.* (20) also observed a dose-dependent mitogenic response to Epo of murine fetal liver stromal cells and detected EpoR mRNA in those cells. They hypothesized a possible involvement of Epo in the development of the fetal hematopoietic microenvironment.

Although functional high-affinity EpoR is expressed mostly at the erythroid-colony-forming unit and proerythroblast level—i.e., in erythroid cells of very late maturation stage (1)—Heberlein *et al.* (21) observed low levels of EpoR gene transcripts in embryonal or multipotential cell lines. These primitive cells had 10–100 times less EpoR mRNA than more mature stages of erythroid precursors. In fact, the EpoR gene seems to be expressed at low levels before either hematopoietic or erythroid commitment has occurred (21, 22), giving rise to speculation that EpoR in these early cells can transmit a proliferative signal either by itself or in synergy with other cytokine receptors (21).

Epo exerts primarily a mitogenic effect on early erythroid precursors and a mostly differentiating effect on later erythroid precursors (1). Erythroid cells or cell lines which respond to exogenous Epo by proliferation only (or are unresponsive) often have a single class of low-affinity receptors (23). Primitive erythroid progenitor cells (CD34<sup>+</sup>, CD71<sup>+</sup>) contain a truncated form of the receptor capable of transducing a mitogenic signal, whereas more mature erythroid cells (CD34<sup>+</sup>, CD71<sup>+</sup>) contain the full-length receptor (24). The mitogenic effect of Epo on HUVECs seems similar to that on primitive stem cells. In HUVECs, we found an Epo-induced increase in cell number and [<sup>3</sup>H]thymidine incorporation (3) and a decrease in the phosphorylation of p34<sup>cdc2</sup> (25), all in association with a high number of low-affinity hEpoRs.



Endothelial cells coexpress antigens characteristic of hematopoietic cells of various lineages (26) and produce constitutively, or after induction, hematopoietic growth factors and cytokines (27–29). Presently, they are the only human nonhematopoietic cells expressing the p55 chain of the interleukin 2 receptor (30) and, as shown by us, hEpoR. Of particular interest is their expression of markers of primitive hematopoietic cells, such as the CD34 antigen (31, 32) and GATA-2 protein (33). GATA-1 is recognized as an erythroid-specific transcription factor, but GATA-2 is also expressed in more primitive progenitor cells, possibly signaling the onset of commitment of mesoderm to form hematopoietic tissue (34).

The vascular system is the earliest to develop in embryos, to best serve the metabolic requirements of other tissues. Although the presence of hEpoR in cultured endothelial cells cannot be *a priori* equated to *in vivo* situations, it does suggest that Epo controls early mitogenic pathways for the development of the embryonic vasculature. Schmitt *et al.* (22) have also suggested that an early action of Epo may be to stimulate the development and activation of embryonic endothelial cells to produce a varied array of hematopoietic growth factors and cytokines. In fact the first recognizable hematopoietic tissue, the blood islands of the yolk sac, are composed of only endothelial cells and blood cells (35, 36). At this time, however, the *in vivo* role of endothelial hEpoR remains enigmatic.

We thank Dr. A. Schechter for his support and encouragement; Drs. M. E. Miller, A. D'Andrea, and S. Krantz for reviewing the manuscript; and Dr. S. Jones at Genetics Institute for generously providing the monoclonal anti-EpoR antibody.

- Krantz, S. B. (1991) *Blood* 77, 419–434.
- Bazan, J. F. (1989) *Biochem. Biophys. Res. Commun.* 164, 788–795.
- Anagnostou, A., Lee, E. S., Kessimian, N., Levinson, R. & Steiner, M. (1990) *Proc. Natl. Acad. Sci. USA* 87, 5978–5982.
- Carlini, R. G., Dusso, A. S., Obialo, C. I., Alvarez, U. M. & Rothstein, M. (1993) *Kidney Int.* 43, 1010–1014.
- Fraser, J. K., Lin, F. K. & Berridge, M. V. (1988) *Blood* 71, 104–109.
- Broudy, V. C., Lin, N., Egri, J., DeHaen, C., Weiss, T., Papayannopoulou, T. & Adamson, J. W. (1988) *Proc. Natl. Acad. Sci. USA* 85, 6513–6517.
- Van Hinsbergh, V. N., Mommaas-Klenhans, A. M., Weinstein, R. & Maciag, T. (1986) *Eur. J. Cell Biol.* 42, 101–110.
- Papayannopoulou, T., Brice, M., Broudy, V. C. & Zsebo, K. M. (1991) *Blood* 78, 1403–1412.
- Sambrook, J., Fritsch, E. F. & Maniatis, T. (1989) *Molecular Cloning: A Laboratory Manual* (Cold Spring Harbor Lab. Press, Plainview, NY), pp. 7.19–7.29.
- Gubler, U. & Hoffmann, B. J. (1983) *Gene* 25, 263–269.
- Gilliland, G., Perrin, S., Blanchard, K. & Bunn, H. F. (1990) *Proc. Natl. Acad. Sci. USA* 87, 2725–2729.
- Lin, J. H., Grandchamp, B. & Abraham, N. G. (1991) *Exp. Hematol.* 19, 817–822.
- D'Andrea, A. D., Rup, B. J., Fisher, M. J. & Jones, S. (1993) *Blood* 82, 46–52.
- Kuzn, I., Bicknell, I., Harris, A. L., Jones, M., Gatter, K. C. & Mason, D. Y. (1992) *J. Clin. Pathol.* 45, 143–148.
- Noden, D. M. (1990) *Ann. N.Y. Acad. Sci.* 50, 236–249.
- Yousoufian, H., Longmore, G., Neumann, D., Yoshimura, A. & Lodish, H. (1993) *Blood* 81, 2223–2236.
- Neumann, D., Wikstrom, L., Watowich, S. C. & Lodish, H. F. (1993) *J. Biol. Chem.* 268, 13639–13649.
- Migliaccio, A. R., Migliaccio, G., D'Andrea, A., Baiocchi, M., Crotta, S., Nicolis, S., Ottolenghi, S. & Adamson, J. W. (1991) *Proc. Natl. Acad. Sci. USA* 88, 11086–11090.
- Masuda, S., Nagao, M., Takahata, K., Konishi, Y., Gallyas, F., Jr., Tabira, T. & Sasaki, R. (1993) *J. Biol. Chem.* 268, 11208–11216.
- Ohneda, O., Yanai, N. & Obinata, M. (1993) *Exp. Cell Res.* 208, 327–331.
- Heberlein, C., Fischer, K.-D., Stoffel, M., Nowock, A., Ford, A., Tessmer, U. & Stocking, C. (1992) *Mol. Cell. Biol.* 12, 1815–1826.
- Schmitt, R. M., Bruyns, E. & Snodgrass, H. R. (1991) *Genes Dev.* 5, 728–740.
- D'Andrea, A. D. & Jones, S. S. (1991) *Semin. Hematol.* 28, 152–157.
- Nakamura, Y., Komatsu, N. & Nakauchi, H. (1992) *Science* 257, 1138–1141.
- Steiner, M., Lee, E. S., Noguchi, C. T. & Anagnostou, A. (1992) *Exp. Hematol.* 21, 1083 (abstr.).
- Pavaloro, E. J., Moraitis, N., Bradstock, K. & Koutts, J. (1990) *Br. J. Haematol.* 74, 385–394.
- Ascensao, J. A., Vercellotti, G. M., Jacob, H. S. & Zanjani, E. D. (1984) *Blood* 63, 553–558.
- Quisenberry, P. J. & Gimbrone, M. A. (1980) *Blood* 56, 1060–1067.
- Aye, M. T., Hashemi, S., Leclair, B., Zeibdawi, A., Trudel, E., Halpenny, M., Fuller, V. & Cheng, G. (1992) *Exp. Hematol.* 20, 523–527.
- Chen, Z. Z., Van Bockstaele, D. R., Bruyassens, N., Hendricks, D., DeMeester, I., Vanhoof, G., Scharpe, S. L., Peetermans, M. E. & Berneman, Z. N. (1991) *Leukemia* 5, 772–781.
- Delia, D., Lampugnani, M. G., Resnati, M., Dejana, E., Aiello, A., Fontanella, E., Soligo, D., Pierrotti, M. A. & Greaves, M. F. (1993) *Blood* 81, 1003–1008.
- Fina, L., Molgaard, H. V., Robertson, D., Bradley, N. J., Monaghan, P., Delia, D., Sutherland, D. R., Baker, M. A. & Greaves, M. F. (1990) *Blood* 75, 2417–2426.
- Orkin, S. H. (1992) *Blood* 80, 575–581.
- Zon, L. I., Mather, C., Burgess, S., Bolce, M. E., Harland, R. M. & Orkin, S. H. (1991) *Proc. Natl. Acad. Sci. USA* 88, 10642–10646.
- Romanoff, A. L. (1960) *The Avian Embryo* (Macmillan, New York), pp. 572–575.
- Doetschman, T. C., Eistetter, H., Katz, M., Schmidt, W. & Kemler, R. (1985) *J. Embryol. Exp. Morphol.* 87, 27–45.
- D'Andrea, A. D., Rup, B. J., Fisher, M. J. & Jones, S. (1993) *Blood* 82, 46–52.
- Noguchi, C. T., Bae, K. S., Chin, K., Wada, Y., Schechter, A. N. & Hankins, W. D. (1991) *Blood* 78, 2548–2556.

## Expression of the Erythropoietin Receptor by Trophoblast Cells in the Human Placenta<sup>1</sup>

Deborah Fairchild Benyo<sup>3</sup> and Kirk P. Conrad<sup>2,3,4</sup>

Departments of Obstetrics, Gynecology and Reproductive Sciences,<sup>3</sup> and Cell Biology and Physiology,<sup>4</sup> University of Pittsburgh and Magee-Womens Research Institute, Pittsburgh, Pennsylvania 15213

### ABSTRACT

Nonclassical sites of erythropoietin (EPO) and erythropoietin receptor (EPO-R) expression have been described that suggest new physiological roles for this hormone unrelated to erythropoiesis. The recent finding of EPO expression by trophoblast cells in the human placenta prompted us to consider whether these cells also express EPO-R. With use of immunocytochemistry, EPO-R was identified in villous and extravillous cytotrophoblast cells, as well as in the syncytiotrophoblast at all gestational ages. EPO-R was also expressed by cells within the villous core, including endothelial cells of fetoplacental blood vessels. Placental tissues and isolated and immunopurified trophoblast cells, as well as trophoblast-derived choriocarcinoma Jar cells, expressed immunoreactive EPO-R on Western blot. EPO-R mRNA was also detected in the same placental tissues and trophoblast cells by nested-primer reverse transcription-polymerase chain reaction. Finally, EPO-R was functional insofar as the receptor was phosphorylated on tyrosine residues in response to exogenous EPO treatment of cultured trophoblast or Jar cells. Thus, the present findings support the hypothesis that trophoblast cells of the human placenta express EPO-R. In view of these results, taken together with previous work demonstrating EPO expression by the same cells, an autocrine role for this hormone in the survival, proliferation, or differentiation of placental trophoblast cells is proposed.

### INTRODUCTION

Erythropoietin is a 30.4-kDa glycoprotein critical to the survival, proliferation, and differentiation of erythroid precursor cells [1–3]. The major sites of erythropoietin (EPO) production are the kidney and liver [1, 2, 4, 5]. However, other sites of EPO expression have been reported, including spleen and lung [6], bone marrow macrophages [7], early colony-forming cells [8], umbilical cord monocytes differentiated into a macrophage phenotype *in vitro* [9], and brain astrocytes [10]. Most recently, our laboratory has reported that trophoblast cells of the human placenta express EPO [11], and we have speculated that, analogous to the effects of other colony-stimulating factors produced by and acting upon trophoblast cells [12], locally derived EPO is involved in placental development. Of course, fundamental to this hypothesis would be the demonstration of EPO receptor expression by trophoblast cells.

The erythropoietin receptor (EPO-R), classically found in erythroid precursor cells [1–3], now has been described in other cell types [13–18] including endothelial cells [19–21]. These novel and nonclassical sites of EPO and EPO-

R expression raise the possibility of physiological roles for this hormone not necessarily related to erythropoiesis. The recent finding that human placental trophoblast cells express EPO prompted us to investigate whether they also express EPO-R. If so, this hormonal system may have a potentially important autocrine role in the growth and differentiation of the placenta.

### MATERIALS AND METHODS

#### Human Placentas

Human placentas were obtained from women with normal pregnancies at term immediately after cesarean section for breech presentation or repeat cesarean section. Placentas were also collected from nulliparous women with the diagnosis of preeclampsia immediately after cesarean section (in the absence of any labor). Preeclampsia was defined according to standard criteria: onset of hypertension during late pregnancy with systolic and diastolic blood pressure > 140/90 on at least two occasions and urinary protein > 2+ on dipstick or > 0.3 g/24 h [22]. First- and second-trimester placentas were obtained after elective terminations by vacuum evacuation and dilation and curettage, respectively. A total of 20 placentas were investigated. Collection of placentas was approved by the Institutional Internal Review Board of the Magee-Womens Hospital.

#### Placental Processing

Pieces of placental villi from beneath the chorionic and basal plates, as well as basal plate, were quickly dissected (approximately 0.5 g each), rinsed in Dulbecco's phosphate buffered saline (PBS), snap frozen in liquid nitrogen, and stored at –80°C for RNA and protein extraction. Small placental pieces were also fixed overnight at 4°C in 0.1 N phosphate buffer containing 4% paraformaldehyde, washed in ice-cold phosphate buffer, incubated in phosphate buffer containing 30% sucrose overnight at 4°C, embedded in OCT compound (Bayer, Elkhart, IN), snap frozen in liquid nitrogen, and stored at –80°C until cryosection. Frozen sections (12 µm) were cut and mounted on Fisher Superfrost/Plus (Pittsburgh, PA) glass slides.

#### Cell Isolation and Culture Procedures

TF-1, HeLa, and Jar cells were obtained from American Type Culture Collection (Rockville, MD). The erythroleukemic, bone marrow-derived TF-1 cells served as a positive control for EPO-R expression [23]. These nonadherent cells were seeded in 75-cm<sup>2</sup> vented tissue culture flasks and grown in RPMI-1640 medium with 1–5 ng/ml granulocyte-macrophage colony-stimulating factor (GM-CSF; Pepro Tech, Rocky Hill, NJ), 10% fetal bovine serum (FBS), L-glutamine, and penicillin/streptomycin. The Jar trophoblast-derived choriocarcinoma cells were seeded in 75-cm<sup>2</sup> vented culture flasks and grown to confluency in RPMI-1640

Accepted November 17, 1998.

Received September 25, 1998.

<sup>1</sup>Supported by NIH grants R01 HL 56410, K04 HD 01098. Portions of this work were published in abstract form: Society for Gynecologic Investigation 4:136A, 1997.

<sup>2</sup>Correspondence: Kirk P. Conrad, Magee-Womens Research Institute, 204 Craft Ave., Pittsburgh, PA 15213. FAX: 412 641 1503; e-mail: rsikpc@mail.magee.edu

medium, 10% FBS, L-glutamine, and penicillin/streptomycin; the HeLa cervical carcinoma cells were grown in Eagle's Minimum Essential Medium with nonessential amino acids, Earle's balanced salt solution, 10% FBS, L-glutamine, and penicillin/streptomycin. The HeLa cells have been reported not to express EPO-R [20] and thus served as a negative control. Another positive control cell type for EPO-R expression was fetal mouse liver cells obtained from Day 14 fetal mice and isolated immediately upon dissection by mechanical dispersion [24].

The procedure for trophoblast isolation was based on the method of Kliman et al. [25] with modifications. Briefly, the basal plate was removed, and approximately 50 g of villous tissue was harvested and teased into small fragments. Villous trophoblast cells were released by four sequential trypsin digestions (trypsin grade III; Sigma Chemical Co., St. Louis, MO). DNase I (grade II; Boehringer Mannheim, Indianapolis, IN) was used to prevent cellular aggregation. The first digestion was routinely discarded, as it contained few trophoblast cells and mainly red blood cells and leukocytes. The digests were layered over FBS and centrifuged to remove cellular debris and inactivate trypsin. The trophoblast cells were first separated from other cell types by Percoll (Pharmacia and Upjohn, Kalamazoo, MI) gradient centrifugation and then further purified using magnetic beads (PerSeptive Diagnostics, Cambridge, MA) coupled to anti-human leukocyte antigen-Class I (HLA-A,B,C) (Dako, Carpinteria, CA) for third-trimester placentas, and BioMag anti-CD45 antibody (PerSeptive Diagnostics) for first-trimester placentas. Purity was routinely > 97% as determined by immunocytochemical criteria including positive staining for cytokeratin, and viability was routinely > 95% by Trypan Blue staining. Freshly isolated cells were either snap frozen in liquid nitrogen and stored at -80°C until extraction of RNA or protein, or were immediately placed in 75-cm<sup>2</sup> tissue culture flasks (8–10 × 10<sup>6</sup> cells per flask) for a 30-min preincubation at 37°C in RPMI-1640 medium containing 0.5% BSA for analysis of EPO-R phosphorylation.

#### Immunocytochemistry

Two anti-EPO-R antibodies were used—a monoclonal antibody designated mh2er 16.5.1 from Genetics Institute (Cambridge, MA) directed against secreted recombinant human (rhu) EPO-R [26], and a sheep polyclonal antibody from Upstate Biotechnology Incorporated (Lake Placid, NY) raised against the extracellular domain of the human EPO-R. After permeabilization of the placental tissue sections or cultured cells with 0.3% Triton X-100, quenching of endogenous peroxidase with 0.6% hydrogen peroxide in methanol, and blocking with normal horse serum, the specimens were incubated with either the monoclonal or the polyclonal antibody for 1 h at room temperature. The monoclonal and polyclonal antibodies were used at concentrations of 3–30 µg/ml and 10 µg/ml, respectively, which proved to be optimal based on preliminary experiments. Negative controls were generated by substituting the same concentration of mouse IgG1κ isotype for the mouse anti-human EPO-R monoclonal antibody or sheep IgG for the sheep anti-human EPO-R polyclonal antibody. Using a Vectastain Elite ABC Kit (Vector Laboratories, Burlingame, CA) and 3,3'-diaminobenzidine peroxidase substrate solution, immunoreactive EPO-R was detected. For the sheep primary antibody, a biotinylated rabbit anti-goat secondary antibody was used (Dako). Tissue sections were not coun-

terstained so as to permit demonstration of immunoreactivity in a black-and-white photographic format. After dehydration in ethanol and xylene solutions, a coverslip was applied using Cytoseal XYL (Stephens Scientific, Riverdale, NJ).

Preabsorption experiments were conducted with the mh2er 16.5.1 antibody from Genetics Institute. For these studies, the antibody was used at a final concentration of 3 µg/ml after incubation overnight at 4°C with 3-, 10-, or 30-fold molar excess of soluble EPO-R (Genetics Institute) or of an irrelevant receptor, soluble tumor necrosis factor receptor 1 (TNF-R1) (R & D Systems, Minneapolis, MN). Because of the potential for nonspecific interaction of monoclonal antibodies with cytoskeletal proteins such as cytokeratin [27], which are abundant in the placenta, the EPO-R antibody was also incubated overnight at 4°C with a 30-fold molar excess of the most abundant cytokeratin types in the human placenta, cytokeratins 8 and 18 (Cortex Biochem, San Leandro, CA), or an equal volume of vehicle. In parallel experiments, the monoclonal antibody for cytokeratin 18 (clone CY-90; Sigma) was preabsorbed with the cytokeratin 8/18 to confirm the binding potential of the antigen.

In order to determine whether EPO-R staining was localized to the trophoblast cells, immunocytochemical procedures were performed on adjacent tissue sections using a mouse anti-human cytokeratin monoclonal antibody (1.75 µg/ml; Sigma) to identify the syncytiotrophoblast layer and underlying cytotrophoblast cells of floating villi, as well as extravillous cytotrophoblast cells in the basal plate.

#### Western Analysis

Tissue homogenates were prepared by homogenizing frozen tissues or cell pellets for 1 min on ice with a Tekmar (Cincinnati, OH) homogenizer in twice the volume of homogenizing buffer (100 mM EDTA diluted 1:2 in methanol that was combined with an equal volume of 100 mM KCl, 50 mM Tris, 50 mM NaF, 10 mM EDTA, 0.5 mM ZnCl<sub>2</sub>, 1 mM dithiothreitol, pH 6.8, and a cocktail of protease inhibitors: PMSF, antipain, leupeptin, pepstatin A, chymostatin, and soybean trypsin inhibitor). Samples were centrifuged at 4°C for 15 min at 3000 × g, and supernatants were subsequently centrifuged at 10 000 × g for another 15 min. Protein concentration was determined by the Lowry method. For SDS-PAGE, samples were combined with an equal volume of double-strength sample buffer (0.5% SDS, 5% glycerol, 5% β-mercaptoethanol, 0.005% bromophenol blue in 0.5 M Tris, pH 6.8), boiled for 4 min, and microcentrifuged briefly; then 20 µl was loaded onto either 5–20% gradient gels or single-percentage gels as appropriate and electrophoresed for 1 h at 200 V. The separated proteins were transferred onto a polyvinylidene difluoride membrane (Immobilon-P; Millipore, Bedford, MA) for 1 h at ~1 mA/cm<sup>2</sup> using a semi-dry electrophoresis transfer system.

Membranes were rehydrated for 20 min in Tris-buffered saline (TBS, 10 mM Tris, 150 mM NaCl, pH 7.4) containing 0.5% Tween 20 before blocking for 30 min in 3% non-fat dried milk diluted in TBS. Immunoblots were then incubated overnight at 4°C with monoclonal anti-human EPO-R antibody (mh2er 7.9.2; Genetics Institute) diluted 1:1000 in blocking buffer. Although this antibody was also generated against secreted rhuEPO-R, it is not neutralizing, and it recognizes a different epitope than the mh2er 16.5.1 [25]. For negative control blots, the mouse IgG<sub>1</sub> isotype

was substituted for the primary antibody. After a 5-min wash in distilled H<sub>2</sub>O and two 10-min washes with TBS plus 0.05% Tween (TBST), blots were incubated for 1 h at room temperature with alkaline phosphatase-conjugated goat anti-mouse secondary antibody (Promega, Madison, WI) diluted 1:7500 in TBST. The blots were again washed in distilled H<sub>2</sub>O and TBST; this was followed by a TBS wash and equilibration in alkaline phosphatase detection buffer (100 mM Tris, pH 9.5, 150 mM NaCl, 5 mM MgCl<sub>2</sub>) for 10 min. The chemiluminescent substrate reagent CDP-Star (Boehringer Mannheim), diluted 1:200 in alkaline phosphatase detection buffer, was reacted with the blots for 5 min, and the membrane was then exposed to X-OMAT (Eastman Kodak, Rochester, NY) film for signal detection.

Additional studies were performed to confirm the specificity of mh2er 7.9.2 binding. The first was preabsorption, for 2 h at 20°C, of the EPO-R monoclonal antibody with 100-fold molar excess of soluble EPO receptor (Genetics Institute) or nonspecific antigen (recombinant human EPO-gen; Amgen, Thousand Oaks, CA). Additionally, Western blots were probed for expression of cytokeratin to confirm that the EPO-R bands observed were not cross-reacting. The anti-cytokeratin monoclonal antibody reagent used (AE1/AE3; Dako) recognizes cytokeratins designated #1–6, 8, 10, 14–16, 19, and 20 and was incubated at 1:1000 for 2 h at room temperature with the immunoblots.

Protein molecular masses were originally estimated by visualization relative to a prestained standard (Kaliroscope broad range; Bio-Rad, Richmond, CA). More precise calculation of molecular mass was then performed by also running unstained SDS-PAGE standards (Bio-Rad), staining the blots with Coomassie blue, and then measuring the relative mobility of each stained band relative to the dye front. The molecular masses of positive EPO-R bands were then interpolated from the generated standard curve.

#### Reverse Transcription-Polymerase Chain Reaction (RT-PCR) and Restriction Enzyme Digestion

Total RNA was extracted from frozen placental tissues, isolated and immunopurified first- and third-trimester trophoblast cells, JAR trophoblast-derived choriocarcinoma cells, and freshly isolated mouse fetal liver cells by the acid phenol/guanidinium isothiocyanate extraction method [28]. RNA aliquots were stored in 2-propanol at –80°C. Precipitated RNA was redissolved in nuclease-free water and quantitated by determination of absorbency at 260 nm.

Two micrograms of RNA was annealed with 30 ng of oligo(dT)<sub>15</sub> in nuclease-free water (total volume 11 µl). Using the Perkin Elmer GeneAmp PCR System 9600 (Foster City, CA), the mixture was heated at 75°C for 10 min; the temperature was then slowly decreased to 42°C over a 20-min period, and the mixture was maintained at this temperature for 15 min. RT was performed in a total volume of 20 µl containing RT buffer (Promega), dithiothreitol (10 mM final concentration), dNTP (1.0 mM), and avian myeloblastosis virus reverse transcriptase (0.25 U/µl; Promega). Using the Perkin Elmer GeneAmp PCR System 9600, the reaction was heated at 42°C for 45 min followed by 99°C for 5 min to denature the enzyme.

Nested-primer PCR reaction was then performed. The external primers were 5'-CGA-TAT-CAC-CGT-GTC-ATC-CAC-3' and 5'-CAG-ATC-TTC-TGC-TTC-AGA-GCC-3' corresponding to base pairs (bp) 394–414 in exon 3 and bp 828–848 in exon 7, respectively, and producing a PCR product of 455 bp. The internal primers were 5'-GCA-

CCG-AGT-GTG-TGC-TGA-GCA-3' and 5'-GGT-CAG-CAG-CAC-CAG-GAT-GAC-3' corresponding to bp 605–625 in exon 5 and bp 781–801 in exon 7, respectively, and producing a PCR product of 197 bp. Although the external primer set yielded product in all tissues and cells examined, the nested-primer protocol improved both sensitivity and specificity. The external and internal primers were chosen to span several introns and exons such that amplification of any contaminating genomic DNA would produce products of 3202 and 280 bp, respectively. For the first-primer PCR, 2 µl of the RT product was amplified with Tfi Thermostable DNA Polymerase (0.01 U/µl final concentration; Epicentre Technologies, Madison, WI) in a total volume of 20 µl containing PCR buffer without magnesium (Epicentre), external primers (0.2 µM each), dNTP (0.2 mM), and magnesium chloride (1.5 mM). The first-primer PCR reaction was performed in the Perkin Elmer GeneAmp PCR System 9600 for 40 cycles of 94°C (45 sec), 54°C (30 sec), 72°C (30 sec) each. For the second amplification, 1 µl of the first PCR reaction was amplified using the same conditions as described above, except that an annealing temperature of 58°C and 30 cycles were used. For negative controls, the RT reaction was conducted without RNA or without reverse transcriptase.

The PCR products were mixed with 0.1 volume of gel-loading buffer and subjected to electrophoresis on a 2% NuSieve GTG low-melting point agarose (FMC Bioproducts, Rockland, ME) and 1% agarose (Promega) gel in single-strength Tris-borate-EDTA containing 3 µg/ml ethidium bromide.

Restriction enzyme digestion was performed using 10 µl of the nested-primer PCR reaction. One microliter of *Ava*II was added (1.0 U/µl final concentration; Promega), and the mixture was incubated for 2 h at 37°C. Both the intact material and cut material were then subjected to agarose gel electrophoresis as described above. Fragments of 140 and 57 bp were expected, if the 197-bp PCR product ultimately derived from EPO-R mRNA [20].

#### Protein Tyrosine Phosphorylation

Freshly isolated trophoblast cells from the normal term placenta or Jar cells (10 × 10<sup>6</sup> per treatment group), deprived of serum by incubation in RPMI-1640 containing only 0.5% BSA and antibiotics for 12–18 h, were used in this study. To initiate the experiments, the serum-free medium was replaced with RPMI-1640 with or without recombinant human EPO (40 U/ml; Amgen), and cells were incubated at 37°C for 2 or 5 min. Time zero controls were cells collected after preincubation in serum-free conditions. To quench experiments, flasks containing monolayer cultures of Jar cells were placed on ice, medium was aspirated, cells were rinsed with 2 ml cold PBS+0.1 mM Na<sub>3</sub>VO<sub>4</sub>, and the monolayer was then scraped into tubes and centrifuged for 1 min at 1800 × g. Trophoblast cells remained in a suspended form, and therefore the collected cells were pelleted by centrifugation for 5 min at 800 × g. Cell pellets were then resuspended in lysis buffer containing 20 mM Tris, pH 7.5, 1% Nonidet P-40, 150 mM NaCl, 2 mM EDTA, 50 mM NaF, and 1 mM Na<sub>3</sub>VO<sub>4</sub> with protease inhibitors. After incubation for 20 min at 4°C, lysates were centrifuged for 15 min at 10 000 × g, and the supernatant was stored at –80°C.

Immunoprecipitation was performed by incubating 150 µg protein from the cellular lysates with 4 µg mouse anti-EPO-R monoclonal antibody (clone mh2er 7.9.2) or sub-

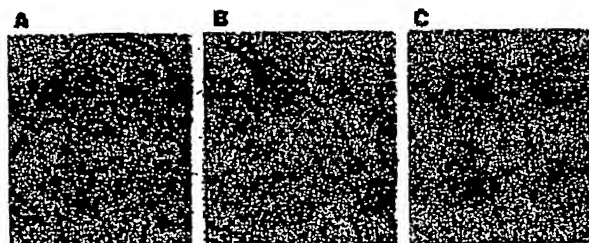


FIG. 1. Localization of immunoreactive EPO-R in first-trimester human placenta using mouse monoclonal antibody clone mh2er 16.5.1 at 10  $\mu$ g/ml. A, B) Demonstration of immunoreactivity associated with the villous cytotrophoblast (small arrowhead), syncytiotrophoblast (medium arrowhead), and the endothelium of a fetoplacental vessel (large arrowhead) within the villous core and other villous core cells. Substitution of mouse IgG1 $\kappa$  isotype for the primary antibody was used for the negative control depicted in C. See *Materials and Methods* for details. Original magnification:  $\times 400$  (reproduced at 59%).

stituted IgG1 $\kappa$  isotype (negative control for nonspecific binding) in a final volume of 0.5 ml containing immunoprecipitation buffer (10 mM Tris, pH 7.5, 1% Triton X-100, 0.5% Nonidet P-40, 150 mM NaCl, 1 mM EDTA, 0.2 mM  $\text{Na}_3\text{VO}_4$ , and protease inhibitors) for 2 h at 4°C with gentle rocking. Lysates were further incubated for 2 h after the addition of 20  $\mu$ l of Protein A/G PLUS-Agarose (Santa Cruz Biotechnology, Santa Cruz, CA) per immunoprecipitation reaction. The lysates were then centrifuged for 5 min at 10 000  $\times$  g; pellets were washed four times in immunoprecipitation buffer before final resuspension in 20  $\mu$ l of double-strength sample buffer and then boiled for separation by SDS-PAGE as described above. After transfer onto polyvinylidene difluoride membrane and blocking in 5% BSA in TBS, the blots were incubated for 2 h at room temperature with anti-phosphotyrosine antibody (Jar cell experiments: PY20 monoclonal antibody; Transduction Laboratories, Lexington, KY, and trophoblast cell experiments: PY99 monoclonal antibody; Santa Cruz Biotechnology) followed by two 10-min washes in TBST and then TBS. Blots were then incubated with secondary antibody (rabbit anti-mouse Ig, peroxidase-conjugated; Jackson Labs., West Grove, PA) diluted in 1% BSA in TBST for 1 h followed by another series of washes. Detection was performed using Renaissance Chemiluminescence Reagent

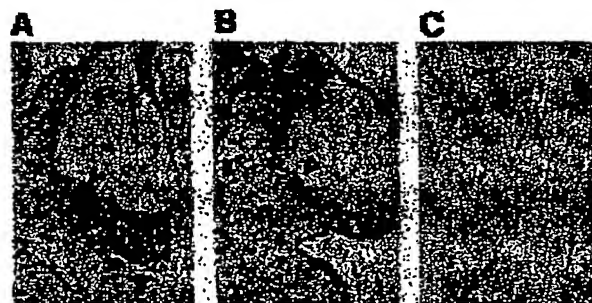


FIG. 2. Localization of immunoreactive EPO-R in second-trimester human placenta using mouse monoclonal antibody clone mh2er 16.5.1 at 30  $\mu$ g/ml. A) Cytokeratin staining identifying the cytotrophoblast cell columns (large arrowhead) emanating from an anchoring villus into the basal plate. B) EPO-R immunoreactivity in the cytotrophoblast cell columns; C) the negative control generated by substituting mouse IgG1 $\kappa$  isotype for the primary antibody. Original magnification:  $\times 200$  (reproduced at 62%).

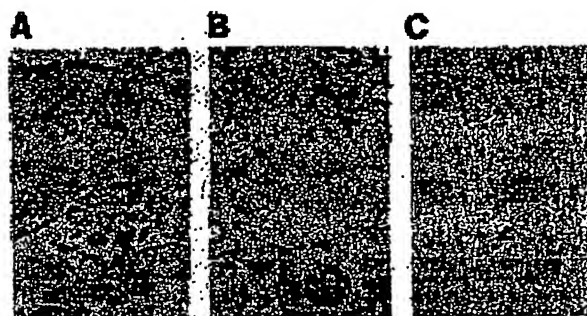


FIG. 3. Localization of immunoreactive EPO-R in third-trimester human placenta using mouse monoclonal antibody clone mh2er 16.5.1 at 30  $\mu$ g/ml. A) Cells expressing immunoreactivity within the basal plate (small arrowhead). B) EPO-R immunoreactivity associated with the endothelium of fetoplacental vessels (large arrowhead) and villous trophoblast (medium arrowhead). Substitution of mouse IgG1 $\kappa$  isotype for the primary antibody was used for the negative control depicted in C. Original magnification:  $\times 200$  (reproduced at 61%).

(NEN Life Sciences, Boston, MA) and BioMax MR film (Eastman Kodak).

## RESULTS

### Detection of EPO-R Immunoreactivity

Figures 1–3 portray the expression of immunoreactive EPO-R in the human placenta and are representative of three different placentas tested at each trimester of pregnancy. In the first-trimester placentas, immunoreactive EPO-R detected by the monoclonal antibody clone mh2er 16.5.1 was expressed by villous cytotrophoblast cells, syncytiotrophoblast, and fetoplacental vascular endothelium, as well as other cells scattered throughout the villous core (Fig. 1, A and B). The staining was particularly intense at the membrane interface between syncytiotrophoblast and underlying cytotrophoblast. Similar results were obtained with the sheep polyclonal antibody evaluated on the first-trimester placentas, although the staining was generally less intense but clearly distinguishable from the negative control (data not shown). Using the same monoclonal antibody, immunoreactive EPO-R was expressed by the syncytiotrophoblast, cytotrophoblast cell columns, and villous core cells in the second-trimester placentas (Fig. 2, A and B). Endovascular and intravascular cytotrophoblast cells were also positive for EPO-R immunoreactivity (data not shown). Immunoreactive EPO-R was also observed in the trophoblast layer and fetoplacental vascular endothelium, as well as in cells within the villous core and basal plate of third-trimester placentas using monoclonal antibody clone mh2er 16.5.1 (Fig. 3, A and B). All negative controls generated by substituting the mouse IgG1 $\kappa$  isotype for the primary antibody were virtually devoid of any staining (Figs. 1C, 2C, and 3C). In preabsorption studies, 3-, 10-, and 30-fold molar excess of soluble EPO-R markedly diminished the immunoreactive EPO-R, whereas 30-fold molar excess soluble TNF-R1 was without effect (Fig. 4, A–C). Finally, 30-fold molar excess of cytokeratin 8/18 did not affect EPO-R immunoreactivity (Fig. 4D), whereas cytokeratin staining after preabsorption was typically reduced by 50% (data not shown).

Figure 5 shows the detection of a 66-kDa band by Western analysis in the human placenta and is representative of three different placentas tested at each trimester of normal



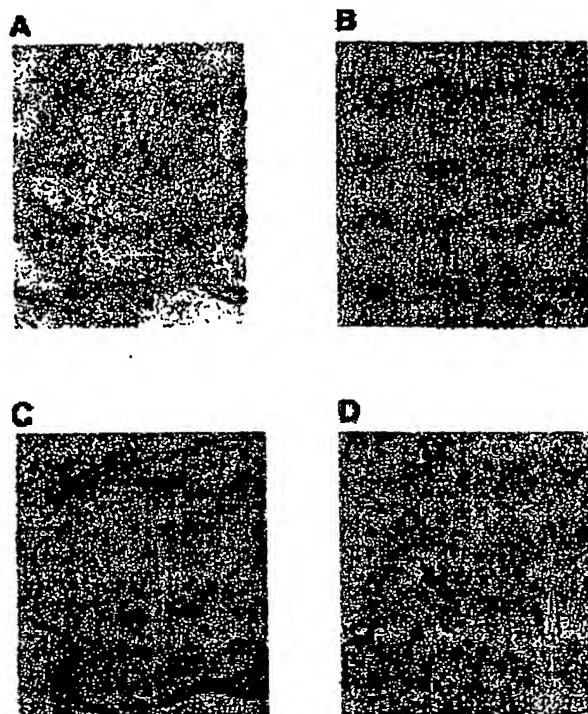


FIG. 4. Localization of immunoreactive EPO-R in the second-trimester placenta using mouse monoclonal antibody clone mh2er 16.5.1 at 3  $\mu$ g/ml. A) Prominent EPO-R immunoreactivity in the syncytiotrophoblast (medium arrowhead) and underlying villous cytotrophoblast (small arrowhead). This immunoreactivity was completely eradicated after preabsorption with a 30-fold molar excess of soluble EPO-R (B) but not with an irrelevant receptor, soluble TNF-R1 (C). Moreover, preabsorption with a 30-fold molar excess of cytokeratins 8 and 18 did not affect EPO-R immunoreactivity (D). The large, thick arrowheads in C and D identify, respectively, the endothelium of a fetoplacental vessel and cytotrophoblast cells emanating from an anchoring villus into the basal plate. Original magnification:  $\times 200$  (reproduced at 80%).

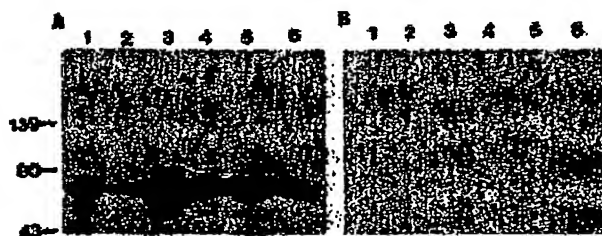


FIG. 5. Detection of EPO-R on immunoblots of human placental lysates and immunopurified trophoblast cell homogenates using mouse monoclonal antibody mh2er 7.9.2. Proteins were first separated by SDS-PAGE (see Materials and Methods for details). A) Lane 1: isolated, immunopurified first-trimester trophoblast cells; lane 2: isolated, immunopurified third-trimester trophoblast cells; lane 3: first-trimester villous placenta; lane 4: second-trimester villous placenta; lane 5: term villous placenta; lane 6: villous placenta from a woman diagnosed with preeclampsia. B) The negative control blot where the mouse IgG1k isotype was substituted for the primary antibody (lanes 1-6). Molecular weight standards  $\times 10^{-3}$  are indicated on the left.

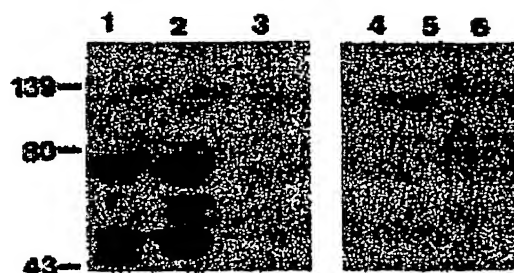


FIG. 6. Western blot analysis of EPO-R using mouse monoclonal antibody clone mh2er 7.9.2. A prominent 66-kDa band was detected in positive control cell lysates from TF-1 cells (lane 1) and in the trophoblast-derived choriocarcinoma Jar cell lysates (lane 2). No reactivity was detected in negative control HeLa cells (lane 3) or in a negative control blot where the mouse IgG1k isotype was substituted for the primary antibody (lanes 4-6). Molecular weight standards  $\times 10^{-3}$  are indicated on the left.

pregnancy and at preeclamptic pregnancy. Moreover, immunoreactive EPO-R was evident in isolated, immunopurified first- and third-trimester cytotrophoblast cells. A band of lesser intensity was observed in placental homogenates, the molecular size of which was calculated to be  $\sim 78$  kDa. Figure 6 portrays the detection of the immunoreactive 66-kDa EPO-R by Western analysis in the positive control TF-1 cells and in Jar trophoblast-derived choriocarcinoma cells, but not in the negative control HeLa cells. Negative control blots (Fig. 5B and Fig. 6, right panel) generated by substituting mouse IgG1k isotype for the primary antibody were virtually devoid of any bands. As a further control in Western blotting experiments, the 7.9.2 monoclonal antibody was also preabsorbed with soluble EPO-R (Fig. 7). The intensity of the 66-kDa band in TF-1 cells and purified trophoblast cells was considerably reduced compared to that obtained after incubation with 7.9.2 antibody alone, and the EPO-R band was eliminated altogether in placental homogenates. Band intensity was not affected when the EPO-R antibody was preabsorbed with a nonspecific antigen (rhEPO, data not shown). A larger molecular size band was also apparent ( $\sim 90$  kDa), but it was not diminished by preabsorption of the 7.9.2 monoclonal antibody with soluble EPO-R. In contrast, a lower molecular size band ( $\sim 45$  kDa, possibly the truncated EPO-R; see Discussion) was eliminated by the preabsorption protocol (data not shown). Finally, to ensure that the EPO-R monoclonal antibody was not cross-reacting with cytokeratins, simultaneous detection of EPO-R and placental cytokeratin with a pan-antibody was performed (Fig. 8, A and B). Immunoreactive EPO-R and cytokeratins bands were not overlapping. Although the pan-cytokeratin antibody does not detect cytokeratin 9, which is 64 kDa, this cytokeratin has been found exclusively in the suprabasal epidermis of the footpad [29].



FIG. 7. Detection of EPO-R in TF-1 cells (lane 1), trophoblast cells isolated and immunopurified from first-trimester placenta (lane 2), and third-trimester villous placental homogenates (lane 3). Immunoblots were detected using either anti-EPO-R monoclonal antibody 7.9.2 (A) or antibody preabsorbed with soluble EPO-R (B). C) The negative control blot where mouse IgG1k was substituted for the primary antibody. Molecular weight standard  $\times 10^{-3}$  is indicated on the left.

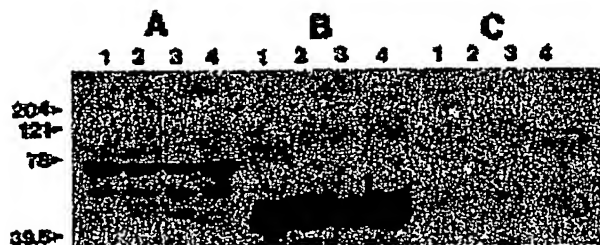


FIG. 8. Detection of EPO-R (A) and cytokeratins (B) in immunoblots of placental homogenates from lane 1, first trimester; lane 2, second trimester; lane 3, third trimester; and lane 4, preeclamptic villous placental tissues. C) The negative control blot where the mouse IgG1 $\kappa$  was substituted for primary antibody. Molecular weight standards  $\times 10^{-3}$  are indicated on the left.

#### Detection of EPO-R mRNA

By loading 20  $\mu$ g of total RNA or poly(A)<sup>+</sup> RNA from the villous placenta and from isolated first- and third-trimester trophoblast cells, we were able to detect a faint hybridization signal by Northern analysis at approximately 1.8 kilobases (data not shown). However, we used RT-PCR to verify the expression of placental EPO-R mRNA (Figs. 9 and 10). A 197-bp PCR product was amplified from reverse-transcribed RNA extracted from first- and third-trimester placentas, Jar trophoblast-derived choriocarcinoma cells, isolated and immunopurified first- and third-trimester trophoblast cells, and the positive control fetal mouse liver cells (Figs. 9A and 10A). The 197-bp product was predicted based on the internal set of primers [20]. Deletion of RNA or reverse transcriptase from the RT reaction yielded no demonstrable bands by ethidium bromide detection. As additional evidence that the amplified 197-bp PCR product was ultimately derived from EPO-R mRNA in these placental tissues and trophoblast cells, restriction enzyme di-



FIG. 9. A) Detection of EPO-R mRNA by nested-primer RT-PCR and visualization of the amplified 197-bp product by agarose gel electrophoresis in the presence of ethidium bromide. Lanes 1 and 7, size standard; lanes 2 and 8, RNA deleted from the RT reactions (negative control); lane 3, fetal mouse liver cells (positive control); lane 4, reverse transcriptase omitted from the RT reaction for RNA from fetal mouse liver cells (negative control); lane 5, Jar trophoblast-derived choriocarcinoma cells; lane 6, reverse transcriptase omitted from the RT reaction for RNA from Jar cells; lane 9, isolated, immunopurified first-trimester trophoblast cells; lane 10, reverse transcriptase omitted from the RT reaction for RNA from first-trimester trophoblast cells; lane 11, isolated, immunopurified third-trimester trophoblast cells; lane 12, reverse transcriptase omitted from the RT reaction for RNA from third-trimester trophoblast cells. B) Restriction enzyme digestion using *Ava*II and visualization of the 140- and 57-bp fragments by agarose gel electrophoresis in the presence of ethidium bromide. Lanes 1, 3, 5, and 7, size standard; lane 2, fetal mouse liver cells; lane 4, Jar trophoblast-derived choriocarcinoma cells; lane 6, isolated, immunopurified first-trimester cells; lane 8, isolated, immunopurified third-trimester cells. See Materials and Methods for details.

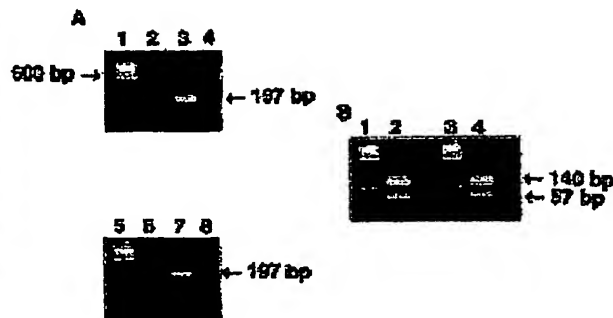


FIG. 10. A) Detection of EPO-R mRNA in placental tissues by nested-primer RT-PCR and visualization of the amplified 197-bp product by agarose gel electrophoresis in the presence of ethidium bromide. Lanes 1 and 5, size standard; lanes 2 and 6, RNA deleted from the RT reactions (negative control); lane 3, first-trimester villous placenta; lane 4, reverse transcriptase omitted from the RT reaction for RNA from first-trimester villous placenta (negative control); lane 7, third-trimester villous placenta; lane 8, reverse transcriptase omitted from the RT reaction for RNA from third-trimester villous placenta. B) Restriction enzyme digestion using *Ava*II and visualization of the 140- and 57-bp fragments by agarose gel electrophoresis in the presence of ethidium bromide. Lanes 1 and 3, size standard; lane 2, first-trimester villous placenta; lane 4, third-trimester villous placenta.

gestion was performed using *Ava*II (Figs. 9B and 10B). The predicted and observed sizes of the two restriction enzyme fragments of 140 and 57 bp were identical. These were also observed for the positive control fetal mouse liver cells.

#### Protein Tyrosine Phosphorylation

Figure 11A is representative of three different experiments showing that the EPO-R of Jar trophoblast-derived choriocarcinoma cells undergoes phosphorylation on tyrosine residues in response to treatment with exogenous rhuEPO for 2 and 5 min (40 U/ml). After immunoprecipitation of cell lysates with monoclonal anti-EPO-R antibody clone mh2er 7.9.2, and probing of the immunoblot with anti-phosphotyrosine antibody, a prominent band of  $\geq 80$  kDa was observed. Low amounts of basal tyrosine phosphorylation of the receptor were also detectable in cells prior to EPO treatment. Analysis of tyrosine phosphorylation of the EPO-R in immunopurified third-trimester placental cells was also performed (Fig. 11B). As with Jar cells, purified trophoblast cells express a phosphoprotein that can be immunoprecipitated with an anti-EPO-R antibody, and the degree of intensity is increased with exogenous EPO treatment. In this representative blot of three experiments, an intense signal was observed in the freshly isolated trophoblast cells (time zero); however, in subsequent experiments, a band of lesser intensity was detected. In addition, a higher molecular weight band was observed, but this band was also apparent when IgG1 $\kappa$  was substituted for the 7.9.2 monoclonal antibody in the immunoprecipitation procedure (data not shown). Finally, immunopurification of the EPO-R was performed with either the 7.9.2 or the 16.5.1 anti-EPO-R antibody, which recognize distinct epitopes, and a phosphotyrosine protein was found in Jar cells treated with exogenous EPO (Fig. 11C).

#### DISCUSSION

The recent report of EPO expression by trophoblast cells in the human placenta [11] prompted us to test whether the same cells also express the EPO-R. If so, then by analogy

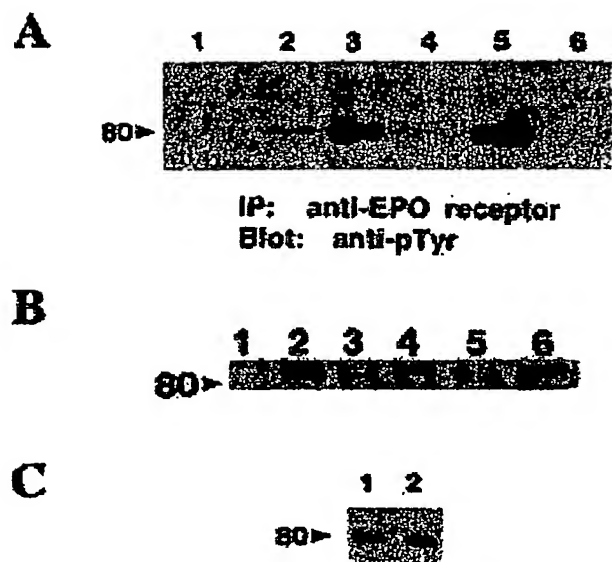


FIG. 11. A) EPO-induced tyrosine phosphorylation of the EPO-R in trophoblast-derived choriocarcinoma Jar cells. The EPO-R was immunoprecipitated with anti-EPO-R antibody (mh2er 7.9.2) from Jar cell lysates at various times after treatment with recombinant human EPO (40 U/ml) and separated on 5–20% gradient SDS-PAGE; then immunoblots were probed with anti-phosphotyrosine antibody (PY20). See *Materials and Methods* for further details. Nonstimulated Jar cells after an overnight preincubation in serum-free conditions were considered to be Time 0 (Lane 1). Lanes 2 and 3 are Jar cells after 2 min without (lane 2) or with EPO treatment (lane 3), and after 5 min without (lane 4) and with EPO treatment (lane 5). Lane 6 represents Jar cells at Time 0 that were immunoprecipitated with a mouse IgG1 $\kappa$  isotypic control. B) EPO-induced tyrosine phosphorylation of the EPO-R in freshly isolated, immunopurified trophoblast cells from the term placenta. EPO-R was immunoprecipitated with anti-EPO-R antibody (7.9.2) from cell lysates, and immunoblots were probed with an anti-phosphotyrosine antibody (PY99). Lanes 1–6 are as follows: negative control immunoprecipitation with mouse IgG1 $\kappa$ , untreated trophoblast cells at time zero, untreated trophoblast cells after 5-min incubation at 37°C, trophoblast cells incubated for 5 min with rhEPO (40 U/ml), Jar cells incubated 5 min with no treatment, Jar cells incubated 5 min with rhEPO (40 U/ml). C) EPO-induced tyrosine phosphorylation of the EPO-R in trophoblast-derived choriocarcinoma Jar cells. Cultured Jar cells were treated for 5 min with rhEPO (40 U/ml), and the EPO-R was immunoprecipitated from lysates with either monoclonal antibody mh2er 7.9.2 (lane 1) or 16.5.1 (lane 2). Immunoblots were probed with anti-phosphotyrosine antibody, PY99. Molecular weight standards  $\times 10^{-3}$  are indicated on the left.

to erythroid precursors, important functions for this hormone related to survival, proliferation, and/or differentiation of placental trophoblast cells are possible. The findings of the present work provide evidence for the expression of EPO-R by trophoblast cells: 1) villous and extravillous cytotrophoblast cells, as well as syncytiotrophoblast at all gestational stages, expressed immunoreactive EPO-R identified by immunohistochemistry; 2) placental tissues and isolated, immunopurified trophoblast cells of various gestational ages, as well as Jar trophoblast-derived choriocarcinoma cells, also expressed immunoreactive EPO-R by Western blot; 3) EPO-R mRNA was detected in the same placental tissues and trophoblast cells by RT-PCR; and 4) the EPO-R was shown to be functional, insofar as tyrosine phosphorylation of the receptor increased in response to exogenously administered EPO.

In the present investigation, we confirmed the localization of EPO-R to the endothelium of fetoplacental vessels

by immunocytochemistry as originally described by Anagnostou et al. [20] using the same m2her 16.5.1 monoclonal antibody. Indeed, this confirmation was an important "positive control" for our work. In the same term placental tissue sections, however, we also observed EPO-R immunoreactivity associated with the trophoblast layer (Fig. 3), a finding not reported by Anagnostou and coworkers. The explanation for these partly discrepant results may relate to different procedures of tissue fixation and processing, as well as to the generally lower intensity of staining in the syncytiotrophoblast as compared to the fetoplacental endothelium. There was no evaluation of placentas of earlier gestational ages or of basal plate from the term placenta in the previous report, so the observation of EPO-R expression associated with extravillous cytotrophoblast, villous cytotrophoblast, and cytotrophoblast cell columns as reported herein is also new (Figs. 1–3). Further, the present results obtained with the m2her 16.5.1 antibody were observed with a sheep polyclonal antibody. Consistent with our observation of EPO-R expression by various populations of trophoblast cells in the human placenta is the finding of EPO-R immunoreactivity associated with the trophoblast giant cells in the mouse placenta [30].

A prominent band of 66 kDa was observed on Western blot for placental tissues and trophoblast cells, confirming the immunocytochemical results demonstrating EPO-R expression by these tissues (Figs. 5 and 6). Importantly, this detection of immunoreactive EPO-R by Western blot was achieved using another monoclonal antibody that recognized a different epitope from the one employed in the immunocytochemistry [26]. Although intact placental tissues might be expected to express EPO-R by Western blot because they contain fetoplacental vascular endothelium and fetal erythroid precursors, the expression of EPO-R by Western blot was also observed in isolated and immunopurified first-trimester and term trophoblast cells, as well as in the Jar trophoblast-derived choriocarcinoma cell line.

The 66-kDa form of the EPO-R reportedly represents the Golgi form of the EPO-R and is the predominant one found in other tissues [31], including the placenta (current study). In immunoblots of placental homogenates, a less intense band of ~76–78 kDa was also observed. This protein is presumably the plasma membrane form of the receptor, which has a reported size range of 70–78 kDa [31]. The TF-1 cells, an erythroleukemic cell line known to express high levels of EPO-R [23], also demonstrated a prominent band of corresponding size, thus serving as our positive control. A recent investigation has suggested that TF-1 cells also express an abnormal transcript due to a translocation breakpoint in exon VIII, resulting in a truncated form of EPO-R (~46 kDa) [32]. Human bone marrow cells express another truncated receptor that lacks most of the cytoplasmic domain coded in exon VIII and that derives from the inclusion of the 95-bp intron VII, resulting in a premature stop codon [33]. Further, the soluble form of EPO-R of ~34 kDa lacks both the transmembrane and cytoplasmic domains and derives from the insertion of the terminal 104-bp sequence of intron IV, which contains a stop codon [34, 35]. In this regard, lower molecular mass bands were observed for the TF-1 and Jar trophoblast-derived choriocarcinoma cells on Western blot analysis (Fig. 6). Because the expression of these different forms of EPO-R, as well as of the full-length EPO-R, may vary according to the stage of erythroid differentiation, and potentially regulate the cellular action of EPO [33, 36, 37], it may be important to



determine whether the truncated and soluble forms of EPO-R are expressed by trophoblast cells.

In addition to identification of EPO-R protein, we also detected EPO-R mRNA in placental tissues and trophoblast cells using RT-PCR. Levels of EPO-R message do not seem to be very abundant; as others have reported its detection by Northern analysis in positive control TF-1 cells when 10  $\mu$ g of poly(A)<sup>+</sup> RNA was used [38]. We noted only faint hybridization signals in placental villous tissues and isolated first- and third-trimester trophoblast cells. To improve both the sensitivity and specificity of the assay, we used nested-primer RT-PCR, which revealed an intense, solitary product of 197 bp by agarose gel electrophoresis and ethidium bromide staining (Figs. 9 and 10). Using restriction enzyme digestion, we verified that the 197-bp amplicon was derived from EPO-R mRNA in the placental tissues and trophoblast cells, since the predicted and observed sizes of the two fragments generated by incubation with *Ava*II, 140 and 57 bp, were identical. The nested-primer PCR approach that we employed did not permit us to determine whether alternative splice forms of EPO-R mRNA consistent with the soluble or truncated EPO-R are present in placental tissues and trophoblast cells because the internal primers did not span the insertion sites for these alternative species. Finally, we cannot completely exclude the possibility that the EPO-R mRNA faintly detected on Northern analysis and robustly by RT-PCR was derived solely from contaminating cells in the immunopurified trophoblast preparation ( $\leq 3\%$ ). However, the presence of mRNA in the Jar trophoblast-derived choriocarcinoma cell line, as well as protein expression by trophoblast cells in placental tissues on immunocytochemistry, makes this possibility an unlikely one.

The elucidation of potential binding sites and transport of EPO across the placental barrier has clinical significance in terms of assessing safety to the fetus with rhEPO administration to anemic pregnant women (refer to [39]). In addition, measurement of circulating EPO may serve as a marker of fetal distress since increased nucleated red blood cell counts can be measured in the neonate from complicated pregnancies [40]. Previous studies have resulted in contrasting results with no demonstrable binding of radio-labeled EPO by the human placenta [41] and no transport between the maternal and fetal compartments in a model of perfused cotyledons [42]. Interestingly, in the latter study the authors measured a 50% loss of EPO from the perfusate after 5 h, suggesting that the administered rhEPO was being bound without placental transfer. Our laboratory has also attempted to identify specific EPO binding sites on isolated trophoblast cells using <sup>125</sup>I-labeled ligand without success (data not shown). However, since these cells coexpress EPO, prior occupancy of the receptors may mask binding.

A proximal event in the signal transduction of EPO in erythroid precursor cells is the phosphorylation of the EPO-R on tyrosine residues (see [43], and citations therein). Like other members of the cytokine receptor superfamily, EPO-R itself does not contain a tyrosine kinase domain. Rather, interaction with EPO results in EPO-R homodimerization and activation of the Janus tyrosine kinase, JAK 2, which is bound to the proximal cytoplasmic region of EPO-R resulting in tyrosine phosphorylation of several proteins including EPO-R itself [43]. In the present investigation, we provide evidence that the EPO-R on trophoblast cells and trophoblast-derived Jar cells is functional, insofar as it is phosphorylated on tyrosine residues in response to exogenous EPO (Fig. 11). Interestingly, some basal tyrosine

phosphorylation was also evident, perhaps reflecting the autocrine action of endogenously produced EPO, since we have previously reported that Jar trophoblast-derived choriocarcinoma cells secrete EPO [11].

The finding of EPO and EPO-R expression by the placenta adds to the growing list of hematopoietic growth factors and their receptors expressed by this organ. Various populations of placental trophoblast, villous core, and uterine decidual cells have been found to express colony-stimulating factor (CSF)-1 and its receptor, *c-fms* product [44–48], GM-CSF and GM-CSF receptor [49, 50], granulocyte-CSF and granulocyte-CSF receptor [51–53], and stem cell factor and its receptor, *c-kit* product [54], frequently in a gestational age-specific fashion. These hematopoietic growth factors are likely to exert paracrine and/or autocrine actions in the human placenta. For example, using cultured human trophoblast cells from first-trimester placenta, CSF-1 stimulated syncytiotrophoblast formation and concomitant production of hCG and human placental lactogen [55]. Similarly, spontaneous syncytial formation and production of these hormones by trophoblast cells in culture were prevented by addition of antibody directed against the CSF-1 receptor, *c-fms* product [55]. GM-CSF also possesses these differentiating effects on cultured term placental trophoblast cells [56]. It will be interesting in future studies to determine whether endogenously derived EPO has a similar role in promoting placental cell growth or differentiation. In this regard, the placentas associated with EPO<sup>−/−</sup> and EPO-R<sup>−/−</sup> knockout mice were reported to be of normal size at gestational Days 13–15 when the embryos died in utero apparently of severe anemia [57]. However, it was not reported whether the morphology and distribution of the various populations of trophoblast cells were normal. An autocrine role for EPO, whereby the hormone contributes to the survival, proliferation, and differentiation of trophoblast cells, may be analogous to its role in early colony-forming [8] and erythroleukemic cells [58], as well as human hepatocellular carcinoma cells [59].

Placental trophoblast and other cells expressed both EPO and EPO-R with the only apparent exception being the fetoplacental vascular endothelium, which expressed the receptor, but not the ligand, as assessed by immunocytochemistry ([11, 20]; present study). In addition to putative autocrine roles, another potential action of trophoblast-derived EPO is that it might interact with EPO-R on endothelium to stimulate fetoplacental and uterine vascular development, since EPO has a capacity to promote angiogenesis [19, 60]. Although the expression of EPO has been recently described in the endodermal cells of the mouse vascular yolk sac [18], possibly trophoblast-derived EPO contributes to primitive erythropoiesis and vasculogenesis in the human yolk sac or promotes the differentiation of hemangioblasts identified in the villous core [61]. Further, results of elegant studies by Dancis and colleagues [62] have suggested that perhaps the trophoblast cell has the capability to respond to erythroid differentiation signals, since reconstitution of irradiated isogeneic mice with placental cells leads to the formation of hematopoietic colonies in the spleen. Clearly, this new and nonclassical site of EPO and EPO-R expression on cells composing the human placenta opens up the possibility of physiological roles for this hormone in addition to erythropoiesis.

#### ACKNOWLEDGMENTS

We thank Theresa Miles for her expert technical assistance in the preparation of purified trophoblast cells and maintenance of cell lines, Andrea

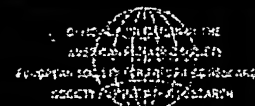
Westerhausen-Larson for invaluable technical consultation, Susan Davis for superb secretarial support, and the staff of the Magee-Womens Hospital library for their efficient service. We are also grateful to Simon Jones of the Genetics Institute in Cambridge, MA, for generously providing the EPO-R monoclonal antibodies and soluble EPO-R.

## REFERENCES

- Jelkmann W. Biology of erythropoietin. *Clin Invest* 1994; 72:S3-S10.
- Koury MJ, Bondurant MC. The molecular mechanism of erythropoietin action. *Eur J Biochem* 1992; 210:649-663.
- Yousoufian H, Longmore G, Neumann D, Yoshimura A, Lodish HF. Structure, function and activation of the erythropoietin receptor. *Blood* 1993; 81:2223-2236.
- Koury ST, Bondurant MC, Semenza GL, Koury MJ. The use of in situ hybridization to study erythropoietin gene expression in murine kidney and liver. *Microsc Res Technique* 1993; 25:29-39.
- Bachmann S, Le Hir M, Eckardt KU. Co-localization of erythropoietin mRNA and ecto-5'-nucleotidase immunoreactivity in peritubular cells of rat renal cortex indicates that fibroblasts produce erythropoietin. *J Histochem Cytochem* 1993; 41:335-341.
- Frandrey J, Bunn HF. In vivo and in vitro regulation of erythropoietin mRNA: measurement by competitive polymerase chain reaction. *Blood* 1993; 81:617-623.
- Vogt C, Pentz S, Rich IN. A role for the macrophage in normal hemopoiesis: III. In vitro and in vivo erythropoietin gene expression in macrophages detected by in situ hybridization. *Exp Hematol* 1989; 17:391-397.
- Hermine O, Beru N, Pech N, Goldwasser E. An autocrine role for erythropoietin in mouse hematopoietic cell differentiation. *Blood* 1991; 78:2253-2260.
- Ohls RK, Li Y, Trautman MS, Christensen RD. Erythropoietin production by macrophages from preterm infants: implications regarding the cause of the anemia of prematurity. *Pediatr Res* 1994; 35:169-170.
- Masuda S, Okano M, Yamagishi K, Nagao M, Ueda M, Sasaki R. A novel site of erythropoietin production. *J Biol Chem* 1994; 269:19488-19493.
- Conrad KP, Benyo DF, Westerhausen-Larsen A, Miles TM. Expression of erythropoietin by the human placenta. *FASEB J* 1996; 10:760-766.
- Guilbert L, Robertson SA, Wegmann TG. The trophoblast as an integral component of a macrophage-cytokine network. *Immunol Cell Biol* 1993; 71:49-57.
- Fraser JK, Tan AS, Lin F-K, Berridge MV. Expression of specific high-affinity binding sites for erythropoietin on rat and mouse megakaryocytes. *Exp Hematol* 1989; 17:10-16.
- Mioni R, Gottardello F, Bordon P, Montini G, Foresta C. Evidence for specific binding and stimulatory effects of recombinant human erythropoietin on isolated adult rat Leydig cells. *Acta Endocrinol* 1992; 127:459-465.
- Heberlein C, Fischer K-D, Stoffel M, Nowock J, Ford A, Tessmer U, Stocking C. The gene for erythropoietin receptor is expressed in multipotential hematopoietic and embryonal stem cells: evidence for differentiation stage-specific regulation. *Mol Cell Biol* 1992; 12:1815-1826.
- Ohneda O, Yanai N, Obinata M. Erythropoietin as a mitogen for fetal liver stromal cells which support erythropoiesis. *Exp Cell Res* 1993; 208:327-331.
- Li Y, Juul SE, Morris-Wiman JA, Calhoun DA, Christensen RD. Erythropoietin receptors are expressed in the central nervous system of mid-trimester human fetuses. *Pediatr Res* 1996; 40:376-380.
- Yasuda Y, Okano M, Nagao M, Masuda S, Konishi H, Ueda K, Matsuo T, Tsujiguchi K, Tajima S, Sasaki R, Tanimura T. Erythropoietin in mouse avascular yolk sacs is increased by retinoic acid. *Dev Dynam* 1996; 207:184-194.
- Anagnostou A, Lee ES, Kessimian N, Levinson R, Steiner M. Erythropoietin has a mitogenic and positive chemotactic effect on endothelial cells. *Proc Natl Acad Sci USA* 1990; 87:5978-5982.
- Anagnostou A, Liu Z, Steiner M, Chin K, Lee ES, Kessimian N, Noguchi CT. Erythropoietin receptor mRNA expression in human endothelial cells. *Proc Natl Acad Sci USA* 1994; 91:3974-3978.
- Yamaji R, Okada T, Moriya M, Naito M, Tsuruo T, Miyatake K, Nakano Y. Brain capillary endothelial cells express two forms of erythropoietin receptor mRNA. *Eur J Biochem* 1996; 239:494-500.
- National High Blood Pressure Education Program: Working group report on high blood pressure in pregnancy. NIH Publication No. 91-3029, 1991.
- Kitamura T, Tange T, Terasawa T, Chiba S, Kuwaki T, Miyagawa K, Piao Y-F, Miyazono K, Urabe A, Takaku F. Establishment and characterization of a unique human cell line that proliferates dependently on GM-CSF, IL-3, or erythropoietin. *J Cell Physiol* 1989; 140:323-334.
- Fukamachi H, Saito T, Tojo A, Kitamura T, Urabe A, Takaku F. Binding of erythropoietin to CFU-E derived from fetal mouse liver cells. *Exp Hematol* 1987; 15:833-837.
- Kliman JH, Nestler JE, Sermasi E, Sanger JM, Strauss JF. Purification, characterization, and in vitro differentiation of cytotrophoblasts from human term placentae. *Endocrinology* 1986; 118:1567-1582.
- D'Andrea AD, Rup BJ, Fisher MJ, Jones S. Anti-erythropoietin receptor (EPO-R) monoclonal antibodies inhibit erythropoietin binding and neutralize bioactivity. *Blood* 1993; 82:46-52.
- Harlow E, Lane D. *Antibodies: A Laboratory Manual*. New York: Cold Spring Harbor; 1988: 364-365.
- Chomczynski P, Sacchi N. Single-step method of RNA isolation by acid guanidinium thiocyanate-phenol-chloroform extraction. *Anal Biochem* 1987; 162:156-159.
- Moll R, Franke WW, Schiller DL, Gelger B, Krepler R. The catalog of human cytokeratins: patterns of expression in normal epithelia, tumors and cultured cells. *Cell* 1982; 31:11-24.
- Yasuda Y, Nagao M, Okano M, Masuda S, Sasaki R, Konishi H, Tanimura T. Localization of erythropoietin and erythropoietin-receptor in postimplantation mouse embryos. *Dev Growth Differ* 1993; 35:711-722.
- Sawyer ST, Penta K. Erythropoietin cell biology. *Hematol Oncol Clin N Am* 1994; 8:895-911.
- Winkelmann JC, Ward J, Mayeux P, Lacombe C, Schimmenti L, Jenkins RB. A translocated erythropoietin receptor gene in a human erythroleukemia cell line (TF-1) expresses an abnormal transcript and a truncated protein. *Blood* 1995; 85:179-185.
- Nakamura Y, Komatsu N, Nakauchi H. A truncated erythropoietin receptor that fails to prevent programmed cell death of erythroid cells. *Science* 1992; 257:1138-1141.
- Baynes RD, Reddy GK, Shih YJ, Skiline BS, Cook JD. Serum form of the erythropoietin receptor identified by a sequence-specific peptide antibody. *Blood* 1993; 82:2088-2095.
- Morishita E, Narita H, Nishida M, Kawashima N, Yamagishi K, Masuda S, Nagao M, Hatta H, Sasaki R. Anti-erythropoietin receptor monoclonal antibody: epitope mapping, quantification of the soluble receptor, and detection of the solubilized transmembrane receptor and the receptor-expressing cells. *Blood* 1996; 88:465-471.
- Nakamura Y, Nakauchi H. A truncated erythropoietin receptor and cell death: a reanalysis. *Science* 1994; 264:588-589.
- Nakamura Y, Tokumoto Y, Nakauchi H. Role of a truncated erythropoietin receptor for erythroid differentiation. *Biochem Biophys Res Commun* 1996; 218:205-209.
- Ward JC, Harris KW, Penny LA, Forget BG, Kitamura T, Winkelmann JC. A structurally abnormal erythropoietin receptor gene in a human erythroleukemia cell line. *Exp Hematol* 1992; 20:371-373.
- Widness JA, Schmidt RL, Sawyer ST. Erythropoietin transplacental passage—review of animal studies. *J Perinat Med* 1995; 23:61-70.
- Salafia CM, Ghidini A, Pezzullo JC, Rosenkrantz TS. Early neonatal nucleated erythrocyte counts in preterm deliveries: clinical and pathological correlations. *J Soc Gynecol Invest* 1997; 4:138-143.
- Pekonen F, Rosenlöf K, Rutanen E-M, Fyhrquist F. Erythropoietin binding sites in human foetal tissues. *Acta Endocrinol (Copenh)* 1987; 116:561-567.
- Malek A, Sager R, Eckardt K-U, Bauer C, Schneider H. Lack of transport of erythropoietin across the human placenta as studied by an in vitro perfusion system. *Pflüeg Arch Eur J Physiol* 1994; 427:157-161.
- Klingmüller U. The role of tyrosine phosphorylation in proliferation and maturation of erythroid progenitor cells. Signals emanating from the erythropoietin receptor. *Eur J Biochem* 1997; 249:637-647.
- Daier E, Pampfer S, Yeung YG, Barad D, Stanley ER, Pollard JW. Expression of colony-stimulating factor-1 in the human uterus and placenta. *J Clin Endocrinol Metab* 1992; 74:850-858.
- Kanzaki H, Yui J, Iwai M, Imai K, Kariya M, Hatayama H, Mori T, Guilbert LJ, Wegmann TG. The expression and localization of mRNA for colony-stimulating factor (CSF)-1 in human term placenta. *Hum Reprod* 1992; 7:563-567.
- Jokhi PP, Chumbley G, King A, Gardner L, Loke YW. Expression of the colony stimulating factor-1 receptor (c-fms product) by cells at the human uteroplacental interface. *Lab Invest* 1993; 68:308-320.
- Saito S, Motoyoshi K, Saito M, Kato Y, Enomoto M, Nishikawa K,

- Morii T, Ichijo M. Localization and production of human macrophage colony-stimulating factor (hM-CSF) in human placental and decidua tissues. *Lymphokine Cytokine Res* 1993; 12:101-107.
48. Jokhi PP, King A, Boocock C, Loke YW. Secretion of colony stimulating factor-1 by human first trimester placental and decidua cell populations and the effect of this cytokine on trophoblast thymidine uptake *in vitro*. *Mol Human Reprod* 1995; 10:2800-2807.
  49. Jokhi PP, King A, Jubinsky PT, Loke YW. Demonstration of the low affinity  $\alpha$  subunit of the granulocyte-macrophage colony-stimulating factor receptor (GM-CSF-R $\alpha$ ) on human trophoblast and uterine cells. *J Reprod Immunol* 1994; 26:147-164.
  50. Jokhi PP, King A, Loke YW. Production of granulocyte-macrophage colony-stimulating factor by human trophoblast cells and by decidua large granular lymphocytes. *Hum Reprod* 1994; 9:1660-1669.
  51. Saito S, Kasahara T, Kato Y, Ishihara Y, Ichijo M. Elevation of amniotic fluid interleukin 6 (IL-6), IL-8 and granulocyte colony stimulating factor (G-CSF) in term and preterm parturition. *Cytokine* 1993; 5:81-88.
  52. Saito S, Fukunaga R, Ichijo M, Nagata S. Expression of granulocyte colony-stimulating factor and its receptor at the fetomaternal interface in murine and human pregnancy. *Growth Factors* 1994; 10:135-143.
  53. McCracken S, Layton JE, Shorter SC, Starkey PM, Barlow DH, Mardon HJ. Expression of granulocyte-colony stimulating factor and its receptor is regulated during the development of the human placenta. *J Endocrinol* 1996; 149:249-258.
  54. Kauma S, Huff T, Krystal G, Ryan J, Takacs P, Turner T. The expression of stem cell factor and its receptor, *c-kit* in human endometrium and placental tissues during pregnancy. *J Clin Endocrinol Metab* 1996; 81:1261-1266.
  55. Saito S, Saito M, Enomoto M, Ito A, Motoyoshi K, Nakagawa T, Ichijo M. Human macrophage colony-stimulating factor induces the differentiation of trophoblast. *Growth Factors* 1993; 9:11-19.
  56. Garcia-Lloret MI, Morrish DW, Wegmann TG, Honore L, Turner AR, Guilbert LJ. Demonstration of functional cytokine-placental interactions: CSF-1 and GM-CSF stimulate human cytotrophoblast differentiation and peptide hormone secretion. *Exp Cell Res* 1994; 214:46-54.
  57. Wu H, Liu X, Jaenisch R, Lodish HF. Generation of committed erythroid BFU-E and CFU-E progenitors does not require erythropoietin or the erythropoietin receptor. *Cell* 1995; 83:59-67.
  58. Stage-Marroquin B, Pech N, Goldwasser E. Internal autocrine regulation by erythropoietin of erythroleukemic cell proliferation. *Exp Hematol* 1996; 24:1322-1326.
  59. Ohigashi T, Yoshioka K, Fisher JW. Autocrine regulation of erythropoietin gene expression in human hepatocellular carcinoma cells. *Life Sci* 1996; 58:421-427.
  60. Carlini RG, Reyes AA, Rotheimer M. Recombinant human erythropoietin stimulates angiogenesis. *Kidney Int* 1995; 47:740-745.
  61. Demir R, Kaufmann P, Castellucci M, Erbeni T, Kotowski A. Fetal vasculogenesis and angiogenesis in human placental villi. *Acta Anat* 1989; 136:190-203.
  62. Dancis J, Jansen V, Brown GF, Gorstein F, Balis ME. Treatment of hypoplastic anemia in mice with placental transplants. *Blood* 1977; 50:663-670.

# Pediatric Research


[Home](#) [Search](#) [Current Issue](#) [Archive](#) [Publish Ahead of Print](#)
[January 1998, 43:1 > Erythropoietin and Erythropoietin...](#)
[< Prev](#) [Feedback](#)

## ARTICLE LINKS:

[Abstract](#) | [References \(44\)](#) | [View full-size inline images](#)

Pediatric Research: Volume 43(1) January 1998 pp 40-49

## Erythropoietin and Erythropoietin Receptor in the Developing Human Central Nervous System [Regular Articles]

JUUL, SANDRA E.; ANDERSON, DOUGLAS K.; LI, YAN; CHRISTENSEN, ROBERT D.

Departments of Pediatrics [S.E.J., Y.L., R.D.C.] and Neuroscience [D.K.A.], University of Florida College of Medicine, and the Gainesville VA Medical Center [D.K.A.], Gainesville, Florida 32610-0296

Received February 7, 1997; accepted July 8, 1997.

Correspondence and reprint requests: Sandra E. Juul, M.D., Division of Neonatology, University of Florida College of Medicine, P.O. Box 100296, JHMC, Gainesville, FL 32610-0296.

Supported by Minority Clinical Associate Physician Award RR-00083, National Institutes of Health Grant HL-44951, and by grants from the Children's Miracle Network Telethon and the University of Florida Brain Institute.

### ABSTRACT TOP

We have previously shown the presence of erythropoietin (Epo) within the spinal fluid of normal preterm and term infants, and the presence of Epo receptor (Epo-R) in the spinal cords of human fetuses. It is not known, however: 1) whether cells within the fetal central nervous system (CNS) express Epo; 2) if so, whether this expression changes with development; 3) which cells within the CNS express Epo-R; 4) whether Epo-R expression within the CNS changes with development; and 5) whether Epo-R within the fetal CNS are functional. Expression of mRNA for Epo and Epo-R was sought by reverse transcription-PCR in mixed primary cultures of fetal spinal cords as well as NT2 and hNT cells, human cell lines of neuronal precursors and mature neurons, respectively. Epo was measured by ELISA in spent media from primary cell culture, and immunohistochemistry was used to identify Epo-R on neurons and glia in cell culture, and in brain sections. Developmental changes in Epo and Epo-R expression were sought in spinal cords and brains from fetuses of 7-24 wk postconception by semiquantitative PCR. To assess Epo-R function, NT2 cells were exposed to conditions which stimulate programmed cell death, and rescue from apoptosis by the addition of recombinant Epo was evaluated by nuclear matrix protein ELISA, cell counts, and by Klenow labeling of DNA fragments. Epo and Epo-R mRNA were expressed in mixed primary cultures of neural tissues and NT2 and hNT cells. Epo was detected by ELISA in media removed from mixed cell cultures, and immunohistochemical staining confirmed the presence of Epo-R on neurons and their supporting cells. Semiquantitative PCR revealed no significant change in expression of either Epo or Epo-R in spinal cords between 7 and 16 wk of gestation, with increased expression of Epo and Epo-R in brains from 8 to 24 wk of gestation. Epo mRNA expression from neurons doubled under conditions of hypoxia. Recombinant Epo decreased apoptotic cell death of neurons under conditions of hypoxia. Protein and mRNA for Epo and its receptor are expressed by human neurons and glial cells in spinal cord and brain during fetal development. These receptors appear to have a neuroprotective effect in conditions of hypoxia.

**Abbreviations:** ARA-C, cytosine  $\beta$ -D-arabino furanoside; CNS, central nervous system; DMEM, Delbecco's modified Eagle's medium; Epo, erythropoietin; Epo-R, erythropoietin receptor; rEpo, recombinant erythropoietin; FBS, fetal bovine serum; GFAP, glial fibrillary acidic protein antibody; MAP, microtubule-associated protein; RT, reverse transcription

### Article Outline

- ABSTRACT
- METHODS
- RESULTS
- DISCUSSION
- REFERENCES

### Figures/Tables

- Table 1
- Figure 1
- Figure 2
- Figure 3
- Figure 4
- Figure 5
- Figure 6
- Figure 7

Until recently, the action of Epo was considered to be restricted to erythropoiesis (1-3), but there is now evidence that certain nonerythroid cells express Epo-R which respond to rEpo *in vitro* and *in vivo*. These receptors have been demonstrated on murine cell lines of neural origin (4), in cultured murine embryonic neurons, in the developing brain and spinal cord of rodents (5-7), and in mid-trimester human fetal spinal cords (8). Regulated Epo synthesis has also been demonstrated in rodent cells of CNS origin (9, 10), and we have shown that significant concentrations of Epo are detectable in the spinal fluid of normal preterm and term human neonates, although its source is not clear (11). It is not known, however: 1) which cells within the human CNS express Epo, 2) whether this expression changes with development, 3) which cells within the CNS express Epo-R, 4) whether Epo-R expression within the CNS changes with development, and 5) whether these Epo-R are functional, and if so, what this function might be.

One mechanism by which Epo promotes erythropoiesis is by preventing the programmed cell death of erythrocyte precursors (CFU-E) via up-regulation of the bcl-2 and bcl-x<sub>L</sub> pathways (12). We propose that Epo might have similar mechanisms of action in the CNS, by decreasing apoptosis of neurons during normal brain development, or by exerting a neuroprotective effect under adverse conditions such as hypoxia.

We hypothesized that neurons and glial cells express Epo and Epo-R, that expression of this cytokine and its receptor change with advancing gestational age, and that Epo binding to Epo-R in neurons provides protection from programmed cell death. A series of studies were designed to test these hypotheses.

### METHODS TOP

**Human fetal specimens.** Spinal cords, brainstems, and brains were collected from fetuses of 5-9 wk of gestation for primary cell culture. Tissues were transported in cold DMEM (GIBCO, Gaithersburg, MD). Additional spinal cords and brains (ranging from 7 to 24 wk of gestation) were identified, washed in sterile PBS, and immediately preserved in liquid nitrogen for later RNA extraction. Only fetuses that were normal by ultrasound examination and underwent elective pregnancy termination were studied. Gestational age was determined by fetal foot and long bone length (13, 14). The members of our study group had no contact with the mothers and made no attempt to influence decisions about pregnancy termination. The studies were approved by the University of Florida Institutional Review Board.

**Mixed primary cell culture.** Spinal cord, brain stem, and brain, ranging in gestational age from 5 to 9 wk, were placed in separate 100-mm Petri dishes containing 30 mL of isotonic salt solution (125 mM NaCl, 5 mM KCl, 5 mM Na<sub>2</sub>HPO<sub>4</sub>, 1.2 mM KH<sub>2</sub>PO<sub>4</sub>, 6 mM glucose, and 60 mM sucrose), containing 100 U of penicillin, 100  $\mu$ g of streptomycin, and 0.25  $\mu$ g of Fungizone, pH 7.2. Membranes and blood vessels were stripped from the tissue surfaces, and the tissues washed twice in isotonic salt solution, before chopping into pieces of approximately 2 mm<sup>3</sup>. Tissues were then suspended in 0.25% (wt/vol) trypsin in isotonic salt solution and placed in a 37°C shaking water bath for 15 min. Sedimented tissue pieces and dissociated cells were collected and mixed with an equal volume of DMEM containing 20% FBS (Sigma Chemical Co., St. Louis, MO). Dissociated cells were pooled and treated with 160  $\mu$ g of DNase I for 5 min at 37°C, then centrifuged at 800  $\times$  g for 10 min, and washed with 40 mL of DMEM containing 10% FBS. Cells were counted by hemocytometer and plated onto poly-L-lysine-coated dishes. Three days after plating cells, the medium was removed and replaced with DMEM containing 10% FBS and 1% cytosine ARA-C. After 2 d the medium was changed to DMEM containing 10% FBS (15). Cultures medium was changed every 3 d using fresh DMEM containing 10% FBS, until approximately 3-4 wk of age. For gliat-enriched cultures, the same procedure as above was used, except the cells were incubated with DMEM containing 10% FBS without 1% ARA-C.

**NT2 and hNT cell culture.** NT2 cells are a human committed neuronal precursor cell line derived from teratocarcinoma (Stratagene, La Jolla, CA), which can be induced by retinoic acid to differentiate in

*in vitro* into postmitotic CNS neurons (hNT cells) (16, 17). In the course of the differentiation process the NT2 cells lose neuroepithelial cell markers and gain markers specific for mature neurons. We carried out experiments on NT2 cells and hNT cells (Stratagene), and also on hNT cells which we induced in our laboratory following the prescribed protocol. In brief, cells are incubated with 10  $\mu$ M retinoic acid in DMEM for 5 wk, then incubated with medium containing mitotic inhibitors (10  $\mu$ M 5-fluoro-2'-deoxyuridine, 10  $\mu$ M uridine, 1  $\mu$ M ARA-C) for 10 d, at which time they are replated using a neuron knock off technique onto plates prepared by poly-L-lysine and Matrigel® coating.

**Immunohistochemistry.** Mixed primary cultures were fixed for 1 h in 4% paraformaldehyde, then rinsed twice, for 10 min, with PBS. Two additional 10-min rinses with 1% horse serum, PBS, and 0.4% Triton X (pH 7.2) followed. Cultures were then blocked with 1:20 horse serum to PBS containing 0.4% Triton X. The primary antibody was then incubated with the cells for 2 d at 4°C. Antibodies used included: rabbit anti-MMP2 (Zymed Laboratories, San Francisco, CA) diluted 1:500 (19 dishes stained) [18], monoclonal GFAP (Sigma Chemical Co., St. Louis, Mo) diluted 1:800 (17 dishes stained) [18], monoclonal von Willebrand factor (Novocstra Laboratories, Newcastle upon Tyne NE2 4AA, UK) diluted 1:500 (10 dishes stained) [20], and polyclonal antibody to the Epo-R (Santa Cruz Biotechnology; specificity of antibody confirmed by personal communication, Dr. Renee White), diluted 1:100 (six dishes stained). Biotinylated horse anti-mouse or anti-rabbit antibodies were used as a secondary antibodies, as appropriate for each respective antibody, diluted 1:100 for 60 min. Four 10-min rinses with 1% horse serum, PBS, and 0.4% Triton followed. Vectastain ABC reagent (Vector ABC Immunokit) was applied, rinsed with PBS, and incubated in 0.05 M Tris at 5 min. Diaminobenzidine (Sigma Chemical Co.) was used as the chromogen. To control for the presence of endogenous peroxidase, sections were incubated in the absence of specific antibody. Human pulmonary artery endothelial cells (a gift from Dr. Gary Visner, University of Florida), were used as a positive control for von Willebrand antibody. Absence of the primary antibody was used as a negative control for each antibody, and in addition, for Epo-R staining, a specific blocking peptide was used (Santa Cruz). All negative controls showed absence of staining.

**Epo assay.** Epo concentrations in the conditioned media samples were assayed using the Quantikine™ IVD™ human Epo immunoassay ELISA (R&D Systems, Minneapolis, MN). Aliquots (100 µL) of conditioned medium which had been concentrated 10-fold (Centrificon, Inc. Amicon, Beverly, MA) were assayed in duplicate ( $n = 6$ ). Variability was less than 2% between duplicate samples. Sensitivity of this assay has been determined at 0.6 mU/mL. This assay has been tested for cross-reactivity with other members of its cytokine family, and the specificity of the assay is greater than 98%.

**Preparation of total RNA.** Total RNA was extracted from the washed tissues using either the guanidinium thiocyanate method (21), or using the RNeasy elution kit, a method of RNA extraction based on the selective binding of RNA to a silica membrane (Qiagen, Chatsworth, CA) (22). Total RNA was treated with RNase-free DNase I (GIBCO) before further experimentation.

**RT of RNA and amplification of cDNA.** RT of RNA and amplification of cDNA was performed using a DNA thermal cycler (Perkin-Elmer Corp., Foster City, CA). Total RNA (2.0 µg) was combined with 2.0 µM oligo(dT) primers (GIBCO), heated to 70°C for 10 min, then placed on ice. The mixture was then combined with 250 µM dNTP (GIBCO), 0.01 M DTT, 50 mM Tris, pH 8.3, 75 mM KCl, and 3 mM MgCl<sub>2</sub>. The mixture was incubated at 42°C for 7 min; 2 µL of Superscript II (GIBCO) was added, and then the mixture was incubated for an additional 50 min. The reaction was inactivated by heating to 70°C for 15 min. Amplification cycles were carried out under the following conditions: 10 mM Tris, pH 8.3, 50 mM KCl, 1.5 mM MgCl<sub>2</sub>, 2.0 mM dNTP, 0.2 µM upstream and downstream primers, 5% reverse transcriptase mix, 0.1 U/µL Ampli Taq 94°C for 1 min, 58°C for 1 min, 72°C for 2 min for 30 cycles, followed by 10-min elongation at 72°C. Primer pairs used to identify Epo, Epo-R, and β-actin are shown in Table 1 (23, 24).

**Table 1. PCR primers**

**Confirmation of Epo and Epo-R PCR products.** To confirm that the 197-bp RT-PCR product was indeed Epo-R, the PCR product derived from mRNA from primary neuronal culture was sequenced. The Taq DyeDeoxy Terminator protocol developed by Applied Biosystems (Perkin-Elmer Corp.) was used, and labeled extension products were analyzed on an Applied Biosystems model 373 DNA sequencer. The 234-bp product for Epo was likewise confirmed by direct sequencing.

**Semiquantitative PCR.** Semiquantitative PCR was performed relating synthesis of Epo and Epo-R cDNA to the internal standards  $\beta$ -actin and 18 S RNA, and to an external standard cyclophilin Compelcton™ (Ambion, Inc, Austin, TX). The PCR reaction was carried out in the presence of 2.5  $\mu$ Ci/mL of 3000 Ci/mmol  $\alpha$ - $^{32}$ PdCTP. Initial experiments to determine the optimal number of cycles required to achieve amplification in the linear range demonstrated that 30 cycles would be required (data not shown). After completion of the PCR, 30  $\mu$ L of the reaction were separated by electrophoresis through a 3% agarose gel in 0.5 $\times$  Tris-borate-EDTA buffer, and size was standardized with 100-bp DNA markers (GIBCO). Gels were photographed. The amplified products of appropriate size were then cut out of the gel, transferred to scintillation vials containing 5 mL of Cytosol, and  $^{32}$ P activity was counted. The counts for Epo and Epo-R were related to the counts for  $\beta$ -actin, 18 S RNA, or cyclophilin which were co-amplified.

**Neuroprotection assessment.** NT2 or hNT cells were grown in OptiMEM medium (GIBCO) containing 10% FBS, 2 mM L-glutamine, 100 U of penicillin, and 100 µg of streptomycin. In separate experiments, rEpo was added to quadruplicate 100-mm dishes exposed to hypoxia alone (1% oxygen, 5% carbon dioxide, 94% nitrogen) for 24, 36, or 48 h followed by 24 h of normoxic conditions. rEpo doses included 0, 0.1, 0.5, 1, 5, or 10 U/mL. A neutralizing polyclonal rabbit anti-human Epo antibody (Genzyme) was added at 1:1000 dilution to cell culture dishes containing 5 U/mL rEpo. The release of nuclear matrix protein into the media by dying cells was sought by ELISA (Calbiochem, Cambridge, MA) (25). The protein composition of the nuclear matrix determines the basic morphologic pattern of the nucleus, and as the nucleus becomes pyknotic during apoptosis, these proteins are released from the nucleus in soluble form. The amount of protein released is a function of the number of dead cells. In separate set of triplicate experiments done comparing cells cultured in the presence or absence of 5 U/mL Epo, cell viability was assessed by counting the number of live and dead cells after 36 h of hypoxia, and also after the 24 h of recovery. Cell viability was determined by trypan blue staining. The presence of apoptotic cells death was ascertained by a DNA fragmentation kit (Calbiochem, Cambridge, MA). In this assay, cells were first permeabilized with proteinase K for 5 min. Endogenous peroxidase activity was quenched with hydrogen peroxide. Klenow was then bound to exposed 3' -OH ends of cleaved DNA fragments, and biotin-labeled nucleotides were incorporated in a template-dependent manner. These nucleotides were detected using streptavidin-horse radish peroxidase conjugate. Diaminobenzidine was used as a chromogen, with methyl green as a counterstain. Incubation of cells with Dnase I was used to generate the positive controls, and water added in place of Klenow enzyme provided the negative controls. At the conclusion of triplicate experiments, the medium was removed and saved, the cell layer trypsinized, and the cells in the medium were combined with the trypsinized cells, an aliquot counted to determine cell density, and an estimated  $3.25 \times 10^5$  cells were cytopsin onto a slide and stained. Ten fields were counted per slide.

## RESULTS TOP

The first set of experiments were performed to determine whether the Epo-R mRNA detected in the fetal neuronal tissue was the result of blood contamination or meningeal endothelial cells. To exclude these possibilities, primary cultures of neuron-enriched and glial-enriched cells were grown for investigation. These cultures were characterized by immunohistochemistry and light microscopy after three weeks of culture. Figure 1a shows representative cultures exposed to 1% ARA-C to inhibit the growth of glial cells. These neuron-enriched cultures are shown stained with the monoclonal MAP2 antibody, which reacts with a specific 280-kD cytoskeletal protein, the somatodendritic MAP of neurons. This is expressed to a lesser extent in astrocytes. Although these cultures were greatly enriched for neurons, some glial cells remained. Figure 1b illustrates a typical glial-enriched culture stained with GFAP, which stains intermediate filaments of characteristic 10-nm diameter that are specific to astrocytes.

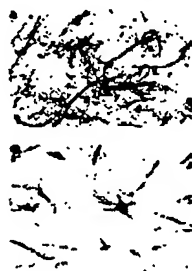


Figure 1. (A) A typical mixed cell culture identified as neuron-enriched. These cells have been stained with the monoclonal anti-MAP2 antibody. Magnification,  $\times 200$ . (B) A typical glial-enriched culture. This has been stained with the monoclonal anti-GFAP, which stains intermediate filaments specific to astrocytes. Magnification,  $\times 200$ . These mixed cell cultures contain other nondifferentiated neurons and microglia.

RT-PCR was performed on total RNA extracted from cultures that were neuron-enriched, or glial-enriched to ascertain whether these cells expressed mRNA for Epp-R and Epp. Human neuronal precursor



(NT2 cells), and their mature, differentiated counterparts (hNT cells) were also investigated, as these provided a pure growth of neuronal cells without the glial supporting cells, or possible contamination with endothelial cells. All cells tested expressed both Epo (Fig. 2A) and Epo-R (Fig. 2B) mRNA. Fig. 2C shows the  $\beta$ -actin control PCR reactions. Negative controls, done using either water or RNA, which had not been reverse transcribed, were negative.

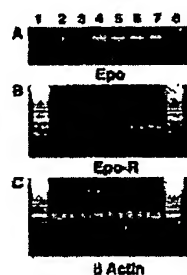


Figure 2. RT-PCR products using primers specific to human Epo(A), Epo-R (B), and  $\beta$ -actin (C) are displayed for mixed neuronal culture (lanes 2 and 3), for mixed glial-enriched cultures (lanes 4 and 5), and for NT2 and hNT cells (lanes 6 and 7). Lanes 1 and 8 contain 2  $\mu$ g of a DNA ladder marking 100-bp increments.

A rabbit polyclonal antibody specific to amino acids 489-508 of human Epo-R was used to identify cells derived from the fetal CNS that express Epo-R on their surfaces. Neurons (Fig. 3A) and astrocytes (Fig. 3B) stained positively for Epo-R. Figure 3C shows a negative control for Epo-R, incubated in the absence of primary antibody. To test endothelial cell contamination as a source of Epo-R (26, 27), cells were stained with von Willebrand factor (Fig. 3D). None of the neuron or glial-enriched cultures stained positive for von Willebrand factor, although human endothelial cells used as positive controls were positive (data not shown). All cells stained in the absence of primary antibody were negative.

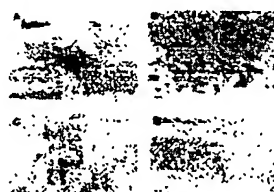


Figure 3. Polyclonal anti-Epo-R antibody 1:500 was used to identify cells expressing Epo-R. Demonstration of neuronal staining(A) and lighter staining of glial cells (B). Original magnification,  $\times 160$ . (C) A neuron-enriched culture to which no primary antibody was added (negative control). Original magnification,  $\times 400$ . (D) Lack of cell staining after incubation of a glial-enriched culture with von Willebrand antibody. Original magnification,  $\times 200$ . Bar = 9.2  $\mu$ m for C, 20  $\mu$ m for A, B, and D.

To identify which cell types show immunoreactivity to Epo-R *in vivo*, brain sections taken from a brain at 20 wk of gestation and from an adult brain were stained. Figure 4 demonstrates that *in vivo*, certain types of neurons (Cajal Retzius neurons (28) shown in Fig. 4A), astrocytes (Fig. 4B), and choroid plexus (Fig. 4C) all stained positively for Epo-R. Figure 4D shows a slice of brain adjacent to that shown in Fig. 4C, after incubation with the Epo-R-blocking peptide (negative control). Figure 4E and F shows human fetal liver at 22 wk of gestation, as a positive and negative control (with the Epo-R-blocking peptide), respectively. In adult brain, Epo-R staining was identified predominantly in astrocytes, not in neurons (data not shown).

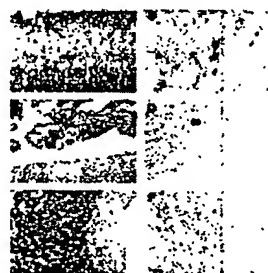


Figure 4. These photomicrographs show specific cell types within the brain that stain positively with anti-Epo-R antibody. (A) An example of Cajal Retzius neurons (arrows) in the subpial granular layer of the developing 20-wk brain. The underlying cortical plate is identified as CORT. Original magnification,  $\times 400$ . (B) Specific staining of astrocytes within the deep white matter of an adult brain. Original magnification,  $\times 400$ . An arrow identifies one astrocyte. (C) The positive staining of choroid plexus (CP) from an adult brain. Original magnification,  $\times 200$ . (D) A negative control using the specific blocking peptide for the Epo-R antibody. Original magnification,  $\times 160$ . (E) A positive control, human fetal liver from 22 wk of gestation (original magnification,  $\times 200$ ). (F) A negative control, human fetal liver from 22 wk of gestation, pretreated with blocking peptide. Original magnification,  $\times 200$ .

Epo concentrations measured in the supernatant of neuron-enriched and glial-enriched cells ranged from below the limit of detection (0.6 mU/mL) to 2 mU/mL. Unconditioned medium which had been similarly concentrated did not contain measurable Epo concentrations, ruling out cross-reactivity with the endogenous Epo in the FBS. Semiquantitative PCR of triplicate NT2 cultures showed an increase in Epo mRNA after exposure to hypoxia (mean Epo/actin value in normoxic conditions  $0.35 \pm 0.05$ ; mean  $\pm$  SEM, whereas values obtained for cells maintained in hypoxia overnight were  $0.74 \pm 0.06$ ,  $p = 0.00$  by a *t* test).

To identify changes in Epo and Epo-R mRNA expression during fetal development, spinal cords from fetuses aged 7-16 wk of gestation and brains from fetuses aged 8-24 wk of gestation were studied. RT-PCR showed that Epo and Epo-R were expressed in all samples (Fig. 5, A and B).  $\beta$ -Actin controls for each RNA sample are shown in Fig. 5C.

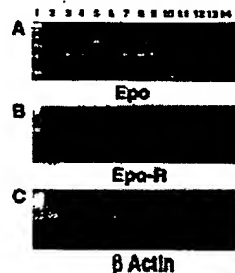


Figure 5. RT-PCR products using primers specific to human Epo(A), Epo-R (B), and  $\beta$ -actin (C) are displayed for spinal cords and brains ranging in gestational age from 7 to 24 wk. Lane 1 contains 2  $\mu$ g of DNA ladder marking 100-bp increments. Lanes 2 through 10 contain cDNA products from spinal cords of 7, 8, 9, 10, 11, 12, 13, 15, and 16 wk of gestation, respectively. Lanes 11 through 14 contain cDNA products from brains of 17, 21, 23, and 24 wk of gestation.

Semiquantitative PCR using internal and external controls revealed no significant change in spinal cord expression of Epo-R between 7 and 16 wk of gestation (Fig. 6A); however, statistical analysis using Spearman's rank correlation showed an increase ( $p = 0.007$ ,  $r_s = 0.658$ ) in expression of brain Epo-R between 8 and 24 wk of gestation. Similarly, no significant changes in spinal cord Epo mRNA expression were noted (Fig. 6B); however, like Epo-R, increased Epo expression was noted in brains between 8 and 24 wk ( $p = 0.008$ ,  $r_s = 0.838$  by Spearman's rank correlation test).

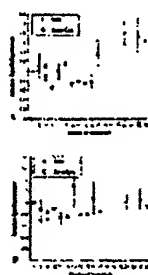


Figure 6. (A) Demonstration of relative Epo-R expression (y axis) as a function of gestational age in weeks (x axis), whereas (B) shows similar results for Epo expression. Spinal cord samples are shown by open circles, whereas brain samples are denoted by filled diamonds. Data from three semiquantitative PCR runs were combined. Results are shown  $\pm$  SEM.

To assess whether Epo might function by affecting the process of apoptosis, we cultured NT2 cells and hNT cells (in separate experiments) in 1% oxygen for 24, 36, or 48 h followed by a 24-h recovery period, conditions which we have found induce apoptotic cell death in a proportion of the cells (data not shown). Increasing concentrations of rEpo were added to quadruplicate cultures. After 24 h of hypoxia, a minority of cells underwent apoptosis. After 36 and 48 h, the number of affected cells increased. In a dose-dependent manner, rEpo decreased the effect of hypoxia on both NT2 cells and hNT cells exposed to hypoxia for 24, 36, or 48 h. After 24 h of hypoxia, 10 U/mL rEpo reduced NMP release by mature neurons by 30%. After 36 h of hypoxia, followed by 24 h of normoxia, NMP release by NT cells incubated with 0, 0.5, 5, or 10 U/mL rEpo was  $102.00 \pm 7.76$ ,  $81.44 \pm 19.72$ ,  $66.22 \pm 4.90$ , and  $57.59 \pm 7.49$ , respectively, and this effect was reversed by adding a 1:1000 dilution of Epo-neutralizing antibody to cultures containing 5 U/mL rEpo. NMP release by cells grown to 70% density in normoxic conditions are compared with these data and are shown in Figure 7.

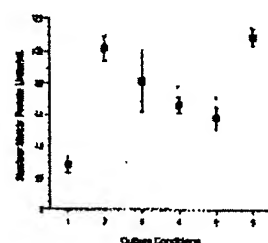


Figure 7. Nuclear matrix protein is plotted in units/mL on the y axis, whereas culture conditions are denoted on the x axis. Condition 1 is cells grown in normoxic conditions as a baseline control. Conditions 2 through 5 are: hypoxia alone (36 h of hypoxia followed by 24 h of normoxia), hypoxia plus 0.5 U rEpo/mL, hypoxia plus 5.0 U rEpo/mL, and hypoxia plus 10.0 U rEpo/mL. Condition 6 is hypoxia plus 5.0 U/mL rEpo plus 1:1,000 dilution of neutralizing anti-Epo antibody. Results are shown as mean  $\pm$  SEM. \* $p < 0.01$ .

To establish whether Epo was affecting early cell death (during the period of hypoxia) versus late cell death (during the 24 h of recovery), in separate experiments, we counted trypan blue-stained cells in the medium, and in the trypsinized cell layer, after the 36 h of hypoxia, and again after the 24-h recovery period. We found that, in both the control and rEpo-treated cells, about one-third of the cell death occurred during the hypoxia exposure (24-36.1% for control cells versus 12.5-31.1% in rEpo-treated,  $p = 0.31$ ), thus rEpo did not change the timing of cell death during the hypoxia. In separate experiments, we counted viable cells (rEpo-treated versus control) at the end of the 24-h normoxia recovery period. Cell counts from these experiments showed the rEpo-treated cells had approximately double the number of viable cells, as did the controls ( $3.13 \times 10^5 \pm 0.28 \times 10^5$  versus  $1.5 \times 10^5 \pm 0.41 \times 10^5$ , respectively,  $p < 0.05$ ), despite equal numbers of cells having been plated at the beginning of the experiment.

To detect DNA fragmentation, which typifies apoptosis, we labeled cytospun control and Epo-exposed cells with Klenow and counted 10 fields per slide. Under conditions of hypoxia followed by normoxia in the absence of added rEpo, 21.5% cells (161/750 cells counted) had no evidence of DNA fragmentation, whereas when 5 U/mL rEpo was added to the cultures, 50.5% of cells (361/715 cells counted) had no DNA fragmentation.

## DISCUSSION TOP

The action of Epo on erythroid progenitor cells has been the subject of intense investigation (1, 29-32). In contrast, the action of Epo on nonhematopoietic cells is only beginning. It is known that Epo-R exists on a wide variety of nonerythroid cell types including endothelial cells, cardiomyocytes, mesangial cells, smooth muscle cells, placental tissues, and cells of neuronal origin (4, 6, 10, 26, 33-36). Wald *et al.* (33) recently reported that addition of rEpo to cardiomyocytes results in a mitogenic and chemotactic response (like endothelial cells), and that this response is most likely mediated by  $\text{Na}^+/\text{K}^+$ -ATPase activity. Carlini *et al.* (37) reported that incubation of endothelial cells with rEpo results in an increase in endothelin release.

Although the physiologic role of Epo in the CNS is still unclear, there is increasing evidence that the Epo-Rs expressed in neural tissues are functional. Early data showed that addition of rEpo to neural cell resulted in an increase in monoamine concentrations, and an increase in intracellular calcium (4, 10, 38). Circumstantial evidence that Epo and Epo-R might serve a role in neurogenesis is provided by studies demonstrating the presence of this ligand-receptor pair in the embryonic and fetal murine brain, with evidence of developmental regulation (5, 6). Further support for developmental regulation of Epo within the CNS was provided in our previous study in which Epo concentrations were measured in spinal fluids obtained from patients ranging in age from 24 wk of gestation to adulthood. Significant concentrations (up to 32 mU/mL) were found in normal premature and term infants untreated with rEpo, but these decreased by 5 mo of age to less than 2 mU/mL (11). Epo has been shown to increase *in vivo* survival of lesioned rat cholinergic septal neurons produced by fimbria-fornix transections, and to augment choline acetyltransferase activity in cultured neurons (38, 39). There is also data to suggest that Epo might function as a neurotrophic factor, influencing neuronal development, differentiation, maintenance, and regeneration (38, 40). Most recently, Morishita *et al.* (7) has shown that, at concentrations present in the cerebrospinal fluid of normal infants, rEpo prevented glutamate-induced neuronal death if cells were preincubated for a minimum of 8 h. This suggests that at physiologically relevant concentrations Epo might be an important mechanism for neural preservation in adverse circumstances such as hypoxia.

Our first goal in the present study was to ascertain whether cells within the human fetal CNS express Epo. We observed that primary mixed cell cultures derived from first trimester spinal cords, enriched for either neurons or glial cells, synthesize Epo mRNA and protein. These cultures contained a mixture of astrocytes, microglia, neurons, undifferentiated cells, and possibly endothelial cells, thus it could not be conclusively stated which cell types were responsible for the Epo production. Although it is known that endothelial cells in the brain express Epo-R (27), it is unlikely that these cells contributed significantly to the Epo-R expression in our cultures because immunohistochemical staining with von Willebrand factor did not reveal any endothelial cells. Next we observed expression of both Epo and Epo-R in cultures of pluripotent neuronal precursors (NT2 cells) and in terminally differentiated human neurons (hNT cells), neither of which contained any endothelial cell contamination. Our primary cell cultures were derived from fetuses of 5-9 wk of gestation, and we did not exhaustively rule out the presence of endothelial cells in these cultures. Thus, we could not definitively state, based on those studies, that expression of Epo and Epo-R was from neurons or glial cells, nor that this reflected *in vivo* expression in later gestation. We therefore performed additional studies, using an immunohistochemical approach to localize Epo-R to specific cell types within the brain. In addition to the expected endothelial cell staining (27), we observed Epo-R staining of early migrating neurons (Cajal Retzius neurons in the marginal zone of a 20-wk brain) (28), of astrocytes, and of the choroid plexus. In adult brain, Epo-R staining was located predominantly in astrocytes, not in neurons. Thus at different stages of development Epo-R are present in astrocytes and neurons in human brain. In mature mouse brain, the main Epo binding sites have been localized to white matter, including the capsula interna, corpus callosum, hippocampus, and to a lesser degree, the brainstem, mesencephalon, and lateral posterior thalamic nuclei (41). The localization of Epo and Epo-R within human brain and changes with development have not been fully delineated, and are beyond the scope of the present study.

Our next goal was to determine whether expression of Epo mRNA changed during fetal development. In murine studies, the synthesis of Epo and Epo-R in brain were limited to fetal life, and decreased with fetal maturity (5, 6). We found, by semiquantitative PCR, that expression of Epo and Epo-R mRNA did not change between 7 and 16 wk of gestation in the spinal cord, but both increased between 8 and 24 wk gestation in brain. One limitation of that study is, due to the difficulty of obtaining brain specimens in early gestation fetuses, we have no data points on either Epo or Epo-R expression by the fetal brain between 10 and 16 wk of gestation. Another caveat is that expression of this cytokine-receptor pair is likely to be specific to the precise anatomic location from which the RNA was derived within the brain and this was not controlled for in our study. In addition, although statistically significant, it is unclear whether a doubling of Epo or Epo-R expression, detected by PCR, is physiologically significant.

The last goal of this study was to begin to elucidate the function of Epo-R within the developing human CNS. Murine and rodent neuronal tissues respond to hypoxic stimuli by increasing expression of Epo *in vitro* and *in vivo* (9, 41). We exposed mixed primary cell cultures to hypoxia and found an increase in Epo mRNA expression. We previously described that the concentrations of Epo in the cerebrospinal fluid of preterm infants (including those treated with rEpo) ranged from undetectable to 51 mU/mL. The Epo concentrations we measured in conditioned media from mixed cell cultures were generally much

tower than this, ranging from below the limit of detection to 2 mU/mL. It is possible that cells most responsible for contributing to cerebrospinal fluid Epo in babies 24 wk to term were not well represented in these cultures which were derived from CNS tissues of fetuses 5-9 wk of gestation, or, that the culture conditions are not representative of *in vivo* conditions. We tested whether or not Epo might have a neuroprotective effect in hypoxic conditions and found that it does. The rEpo concentrations used in these experiments were supraphysiologic, however, and these experiments must be repeated with concentrations more representative of those found in cerebrospinal fluid, perhaps with preincubation, as was published by Morishita *et al.* (7). Morishita found that when neurons were preincubated with rEpo, the effects of glutamate toxicity were counteracted. This suggests that the neuroprotection requires protein synthesis. Up-regulation of bcl-2 is an important mechanism by which neurons can be rescued from apoptotic death due to many stimuli (42-44). We speculate that Epo may rescue neurons from apoptosis via an increase in bcl-2 and bcl-x<sub>L</sub>, a mechanism by which Epo decreases programme cell death in CFU-E (12).

It is clear that Epo and its receptor have a more widespread physiologic role than was once suspected. We conclude that both Epo and Epo-R are present within the CNS of developing humans; specifically that both are present in glial cells and neurons early in development. Further studies are needed to define the change in the pattern of expression of this receptor and its ligand as development proceeds. The CNS Epo-R appears to be functional, and may serve a role in neuroprotection by inhibiting apoptotic cell death under hypoxic conditions. The physiologic importance of these issues in human fetal development require further studies.

**Acknowledgments.** The authors thank Jenny Harcum for help in obtaining specimens, Philip Joy for considerable efforts in the cell culture laboratory, Lan Chen for assistance with ELISAs and cell counting, and Anthony Yachnis for patient teaching of neurodevelopment, and guidance with immunohistochemistry.

## REFERENCES TOP

1. Ascensao JL, Bilgrami S, Zanjani ED 1991 Erythropoietin. Biology and clinical applications. *Am J Pediatr Hematol Oncol* 13:378-387  
[Medline Link] [Context Link]
2. Yousoufian H, Longmore G, Neumann D, Yoshimura AL 1993 Structure, function and activation of the erythropoietin receptor. *Blood* 81:2223-2236  
[Context Link]
3. Nisenson AR 1994 Erythropoietin overview-1993. *Blood Purif* 12:6-13  
[Context Link]
4. Masuda S, Nagao M, Takahata K, Konishi Y, Gallyas FJ, Tabira T, Sasaki R 1993 Functional erythropoietin receptor of the cells with neural characteristics. *J Biol Chem* 268:11208-11218  
[Context Link]
5. Yasuda Y, Nagao M, Okano M, Masuda S, Sasaki R, Konishi H, Tanimura T 1993 Localization of erythropoietin and erythropoietin-receptor in postimplantation mouse embryos. *Dev Growth Differ* 35:711-722  
[CrossRef] [Context Link]
6. Liu Z-Y, Chin K, Noguchi C 1994 Tissue specific expression of human erythropoietin receptor in transgenic mice. *Dev Biol* 166:159-169  
[CrossRef] [Context Link]
7. Morishita E, Masuda S, Nagao M, Yasuda Y, Sasaki R 1997 Erythropoietin receptor is expressed in rat hippocampal and cerebral cortical neurons, and erythropoietin prevents *in vitro* glutamate-induced neuronal death. *Neuroscience* 78:105-116  
[CrossRef] [Context Link]
8. Li Y, Juul SE, Morris-Wiman JA, Cathoun DA, Christensen RD 1996 Erythropoietin receptors are expressed in the central nervous system of mid-trimester human fetuses. *Pediatr Res* 40:378-380  
[Fulltext Link] [CrossRef] [Context Link]
9. Tan CC, Eckardt K-U, Firth JD, Ratcliffe PJ 1992 Feedback modulation of renal and hepatic erythropoietin mRNA in response to graded anemia and hypoxia. *Am J Physiol* 263:F474-F481  
[Context Link]
10. Masuda S, Okano M, Yamagishi K, Nagao M, Ueda M, Sasaki R 1994 A novel site of erythropoietin production. *J Biol Chem* 269:19488-19493  
[Context Link]
11. Juul SE, Li Y, Harcum J, Christensen RD 1997 Erythropoietin is present in the cerebrospinal fluid of preterm and term neonates. *J Pediatr* 130:428-430  
[Fulltext Link] [CrossRef] [Context Link]
12. Silva M, Grillot D, Benito A, Richard C, Nunez G, Fernandez-Luna J 1998 Erythropoietin can promote erythroid progenitor survival by repressing apoptosis through bcl-xL and bcl-2. *Blood* 88:1576-1582  
[Context Link]
13. Kelemen E, Janossa M, Calvo W, Flidner TM 1984 Developmental age estimated by bone-length measurement in human fetuses. *Anat Rec* 209:547-552  
[CrossRef] [Context Link]
14. Hem W 1984 Correlation of fetal age and measurements between 10 and 26 wk gestation. *Obstet Gynecol* 63:26  
[Context Link]
15. Sumners C, Phillips MI, Ratliff MK 1983 Rat brain cells in primary culture: visualization and measurement of catecholamines. *Brain Res* 264:267-275  
[CrossRef] [Context Link]
16. Lee VM-Y, Andrews PW 1986 Differentiation of NTERA-2 clonal human embryonal carcinoma cells into neurons involves the induction of all three neurofilament proteins. *J Neurosci* 6:514-521  
[Context Link]
17. Pleasure SJ, Lee VM-Y 1993 NTERA 2 cells: a human cell line which displays characteristics expected of a human committed neuronal progenitor cell. *J Neurosci Res* 35:585-602  
[CrossRef] [Context Link]
18. Trojanowski JQ, Schuck T, Schmidt ML, Lee VM 1989 Distribution of phosphate-independent MAP2 epitopes revealed with monoclonal antibodies in microwavedenatured human nervous system tissues. *J Neurosci Methods* 29:171-180  
[CrossRef] [Context Link]
19. Debus E, Weber K, Osborn M 1983 Monoclonal antibodies specific for glial fibrillary acidic (GFA) protein and for each of the neurofilament triplet polypeptides. *Differentiation* 25:193-203  
[CrossRef] [Context Link]
20. Francis SE, Joshua DE, Exner T, Kronenberg H 1985 Monoclonal antibodies to human FVIII:Ag and FVIII:C. *Pathology* 17:579-585  
[Context Link]
21. Chomczynski P, Sacchi N 1987 Single-step method of RNA isolation by acid guanidinium thiocyanate-phenol-chloroform extraction. *Anal Biochem* 162:156-159  
[CrossRef] [Context Link]
22. Martin VV, Nock S, Meyer-Gauen G, Hager K-P, Jensen U, Cerff R 1993 A method for isolation of cDNA-quality mRNA from immature seeds of a gymnosperm rich in polyphenolics. *Plant Mol Biol* 22:555-556  
[CrossRef] [Context Link]
23. Nakajima-Iijima S, Hamada H, Reddy P, Kakunaga T 1985 Molecular structure of the human cytoplasmic  $\beta$ -actin gene: interspecies homology of sequences in the introns. *Proc Natl Acad Sci USA* 82:6133-6137  
[CrossRef] [Context Link]
24. Winkelmann JC, Penny LA, Deaven LL, Forget BG, Jenkins RB 1990 The gene for the human erythropoietin receptor: analysis of the coding sequence and assignment to chromosome 19p. *Blood* 76:24-30  
[Context Link]
25. Miller T, Beausang LA, Meneghini M, Lidgard G 1993 Death-induced changes to the nuclear matrix: the use of anti-nuclear matrix antibodies to study agents of apoptosis. *Biotechniques* 15:1042-1047  
[Context Link]
26. Anagnostou A, Liu Z, Steiner M, Chin K, Lee ES, Kessimian N, Noguchi CT 1994 Erythropoietin receptor mRNA expression in human endothelial cells. *Proc Natl Acad Sci USA* 91:3974-3978  
[CrossRef] [Context Link]
27. Yamaji R, Okada T, Moriya M, Naito M, Tsuruo T, Miyatake K, Nakano Y 1996 Brain capillary endothelial cells express two forms of erythropoietin receptor mRNA. *Eur J Biochem* 239:494-500  
[Context Link]
28. Gadisseux J-F, Goffinet AM, Lyon G, Evrard P 1992 The human transient subpial granular layer: an optical, immunohistochemical, and ultrastructural analysis. *J Comp Neurol* 324:94-114  
[CrossRef] [Context Link]
29. Baru N, Goldwasser E 1989 Studies of the effect of erythropoietin on heme synthesis. *Adv Exp Med Biol* 271:87-94  
[Medline Link] [Context Link]
30. Baru N, McDonald J, Goldwasser E 1989 Activation of the erythropoietin gene due to the proximity of an expressed gene. *DNA* 8:253-259  
[Context Link]




31. Carroll M, Zhu Y, D'Andrea AD 1995 Erythropoietin-induced cellular differentiation requires prolongation of the G1 phase of the cell cycle. *Proc Natl Acad Sci USA* 92:2869-2873  
[CrossRef] [Context Link]
32. Chin K, Oda N, Shen K, Noguchi CT 1995 Regulation of transcription of the human erythropoietin receptor gene by proteins binding to GATA-1 and Sp1 motifs. *Nucleic Acids Res* 23:3041-3049  
[CrossRef] [Context Link]
33. Sawyer ST, Krantz SB, Sawada K 1989 Receptors for erythropoietin in mouse and human erythroid cells and placenta. *Blood* 74:103-109  
[Context Link]
34. Morakkabati N, Golnick F, Meyer R, Fandrey J, Jelkmann W 1996 Erythropoietin induces  $Ca^{2+}$  mobilization and contraction in rat mesangial and aortic smooth muscle cultures. *Exp Hematol* 24:392-397  
[Context Link]
35. Wald MR, Borda ES, Sterin-Borda L 1996 Mitogenic effect of erythropoietin on neonatal rat cardiomyocytes: signal transduction pathways. *J Cell Physiol* 167:461-468  
[CrossRef] [Context Link]
36. Anagnostou A, Lee ES, Kessimian N, Levinson R, Steiner M 1990 Erythropoietin has a mitogenic and positive chemotactic effect on endothelial cells. *Proc Natl Acad Sci USA* 87:5978-5982  
[CrossRef] [Context Link]
37. Carlini RG, Dusso AS, Oblato CI, Alvarez UM, Rothstein M 1993 Recombinant human erythropoietin (rHuEPO) increases endothelin-1 release by endothelial cells. *Kidney Int* 43:1010-1014  
[CrossRef] [Context Link]
38. Konishi Y, Chul D-H, Hirose H, Kunishita T, Tabira T 1993 Trophic effect of erythropoietin and other hematopoietic factors on central cholinergic neurons *in vitro* and *in vivo*. *Brain Res* 609:29-35  
[Context Link]
39. Tabira T, Konishi Y, Gallyas Jr F 1995 Neurotrophic effect of hematopoietic cytokines on cholinergic and other neurons *in vitro*. *Int J Dev Neurosci* 13:241-252  
[CrossRef] [Context Link]
40. Bikfalvi A, Han ZC 1994 Angiogenic factors are hematopoietic growth factors and vice versa. *Leukemia* 8:523-529  
[Context Link]
41. Digicayloglu M, Bichet S, Marti HH, Wenger RH, Rivas LA, Bauer C, Gassmann M 1995 Localization of specific erythropoietin binding sites in defined areas of the mouse brain. *Proc Natl Acad Sci USA* 92:3717-3720  
[CrossRef] [Context Link]
42. Zhong LT, Sarafian T, Kane DJ, Charles AC, Mah SP, Edwards RH, Bradesen DE 1993 bcl-2 inhibits death of central neural cells induced by multiple agents. *Proc Natl Acad Sci USA* 90:4533-4537  
[CrossRef] [Context Link]
43. Farlie PG, Dringen R, Rees SM, Kannourakis G, Bernard O 1995 bcl-2 transgene expression can protect neurons against developmental and induced cell death. *Proc Natl Acad Sci USA* 92:4397-4401  
[CrossRef] [Context Link]
44. Grøntund LJ, Korsmeyer SJ, Johnson Jr EM 1995 Role of BCL-2 in the survival and function of developing and mature sympathetic neurons. *Neuron* 15:649-661  
[CrossRef] [Context Link]

© International Pediatrics Research Foundation, Inc. 1998. All Rights Reserved.

**Copyright © 2007, Lippincott Williams & Wilkins. All rights reserved.**

Published monthly by Lippincott Williams and Wilkins for the International Pediatric Research Foundation and sponsored by its member societies: American Pediatric Society, European Society for Paediatric Research, Society for Pediatric Research.

[Copyright/Disclaimer Notice](#) • [Privacy Policy](#)

 [Subscribe to RSS feed](#)

VOL. 52 NO. 3

OCTOBER 1998

ISSN 0378-3782  
EHDEDN 52 (3) 199-282

# Early Human Development

AN INTERNATIONAL JOURNAL  
CONCERNED WITH THE CONTINUITY OF FETAL AND POSTNATAL LIFE

Univ. of Minn.  
Bio-Medical  
Library

10 14 98

ELSEVIER

08014

Our Home Page: <http://www.elsevier.com/locate/earlhumdev>

C00024636



Early Human Development 52 (1998) 235-249

**Early Human  
Development**

## Tissue distribution of erythropoietin and erythropoietin receptor in the developing human fetus

Sandra E. Juul<sup>a,\*</sup>, Anthony T. Yachnis<sup>b</sup>, Robert D. Christensen<sup>a</sup>

<sup>a</sup>Department of Pediatrics, University of Florida College of Medicine, P.O. Box 100296, JHMHC,  
Gainesville, FL 32610-0296, USA

<sup>b</sup>Department of Pathology, University of Florida College of Medicine, P.O. Box 100296, JHMHC,  
Gainesville, FL 32610-0296, USA

Accepted 18 March 1998

### Abstract

**Objective:** Erythropoietin receptors (Epo-R) have been demonstrated on several nonhematopoietic cell types in animal models and in cell culture. Our objective was to determine the tissue distribution and cellular specificity of erythropoietin (Epo) and its receptor in the developing human fetus. **Study design:** The expression of Epo and Epo-R mRNA was ascertained by RT-PCR for organs ranging in maturity from 5 to 24 weeks postconception. The cellular location of protein immunoreactivity was then determined using specific antiEpo and antiEpo-R antibodies. Antibody specificity was established by Western analysis. **Results:** mRNA for Epo and Epo-R was found in all organs in the first two trimesters. Immunolocalization of Epo was limited to the liver parenchymal cells, kidney interstitial cells and proximal tubules, neural retina of the eye, and adrenal cortex. As development progressed, immunoreactivity in the kidney became more prominent. In contrast, immunoreactivity for Epo-R was widespread throughout the body, in cell types including endothelial cells, myocytes, macrophages, retinal cells, cells of the adrenal cortex and medulla, as well as in small bowel, spleen, liver, kidney, and lung. **Conclusions:** The distribution of Epo and its receptor is more widespread in the developing human than was initially postulated. Epo-R is expressed on many cell types during early fetal development, leading us to speculate that Epo acts in concert with somatic growth and development factors during this period. Further investigation is required to understand the nonhematopoietic role of Epo during human development. © 1998 Elsevier Science Ireland Ltd. All rights reserved.

**Keywords:** Erythropoietin; Erythropoietin receptor; Human fetal development

\*Corresponding author. Tel.: +1 352 3924195; fax: +1 352 3924533.

## 1. Introduction

Erythropoietin (Epo) is a major determinant of tissue oxygenation, performing this function through the regulation of red blood cell production by interaction with its specific cognate receptor. Abnormalities of Epo or Epo receptor (Epo-R) regulation or function result in disease states such as polycythemia vera [1], or anemia of prematurity [2], and absence of Epo or its receptor leads to fetal death around embryonic day 13 in mouse “knock out” models [3]. In addition to their presence on cells of hematopoietic lineage, Epo-R have been demonstrated on a wide variety of nonerythroid cell types, including: liver stromal cells [4], endothelial cells [5–7], mesangial cells [8], smooth muscle cells [8], placental tissues [9,10], and cells of neuronal origin [11–15], but their specific function(s) in these nonhematopoietic sites are not fully understood. In the developing mouse embryo, the distribution of Epo and its receptor are widespread, suggesting activity as a somatic growth factor [16].

We have previously shown that Epo and its receptor are present in the developing human central nervous system (CNS), and that Epo is present in the cerebral spinal fluid (CSF) of normal preterm and term infants [15,17,18]. We believe this CNS Epo-R to be functional, because in cell culture experiments we found Epo to be neuroprotective under conditions of hypoxia [15].

Based on animal studies, cell culture experiments, and our reports of Epo and Epo-R in the fetal CNS, we hypothesized that the distribution of Epo-R and its ligand, Epo, are not limited to the hematopoietic organs and CNS of the developing human fetus. The specific objectives of this study were to determine the tissues in which mRNA for Epo and Epo-R are expressed in the first and second trimester human fetus, and, by determining the distribution of Epo and Epo-R proteins in these tissues by immunohistochemistry, to identify the cell types expressing these proteins.

## 2. Materials and methods

### 2.1. Human fetal specimens

Human fetal specimens were obtained following elective pregnancy termination, or surgical removal (tubal pregnancies). Only fetuses that were normal by ultrasound examination were studied. Termination of pregnancy was done by suction, or dilatation and curettage. Gestational age was determined by fetal foot and long bone length [19,20]. The members of our study group had no contact with the mothers and made no attempt to influence their decisions about pregnancy termination. The studies were approved by the University of Florida Institutional Review Board. Organs including brain, brainstem, spinal cord, eyes, lungs, heart, liver, spleen, kidneys, adrenal, small bowel, placenta and skin were collected from fetuses of 5 to 24 weeks postconception. Organs were identified by visual inspection using a dissecting microscope, and placed either in Bouins fixative for immunohistochemistry, or “snap frozen” for RNA extraction. Organs used for RNA studies were preserved using

liquid nitrogen within 15 to 30 min of delivery. Table 1 lists the organs used for each method, and the postconceptual age of these organs.

## 2.2. Identification of specific mRNAs

### 2.2.1. Preparation of total RNA

Total RNA was extracted from the washed tissues using the RNeasy elution kit, a method of RNA extraction based on the selective binding of RNA to a silica membrane (Qiagen, Chatsworth, CA, USA) [21]. Manufacturer directions were followed. Purity and concentration of extracted RNA was determined by measuring UV absorbance at 260 and 280 nm. Total RNA was treated with RNase-free DNase I (Gibco) prior to further experimentation.

### 2.2.2. Reverse transcription (RT) of RNA and amplification of cDNA

Reverse transcription of RNA and amplification of cDNA was performed using a DNA thermal cycler (Perkin-Elmer Cetus). Total RNA (2.0 µg) was combined with 2.0 µM oligo (dT) primers (Gibco), heated to 70°C for 10 min then placed on ice. The mixture was then combined with 250 µM dNTP (2-deoxynucleoside 5-tri-phosphates) (Gibco), 0.01 M (dithiothreitol) DTT, 50 mM Tris pH 8.3, 75 mM KCl, 3 mM MgCl<sub>2</sub>. Following a 42°C incubation for 2 min, 2 µl of Superscript II (Gibco) was added, and the mixture incubated for 50 min further. The reaction was terminated by heating to 70°C for 15 min. Amplification cycles were carried out under the following conditions: 10 mM Tris pH 8.3, 50 mM KCl, 1.5 mM MgCl<sub>2</sub>, 2.0 mM dNTP, 0.2 µM upstream and downstream primers, 5% reverse transcriptase mix, 0.1 units/µl Ampli Taq 94°C for 1 min, 56°C for 1 min, 72°C for 2 min for 30 cycles, followed by 10 min elongation at 72°C. Primer pairs used, the fragment length they identify, and location are shown in Table 2. Every sample was tested for RNA integrity by using β-actin primers. Each sample also was tested for adequacy of DNase I digestion by running a negative control Polymerase Chain Reaction (PCR) reaction using RNA which had not been reverse transcribed.

### 2.2.3. Specific Epo-R and Epo identification

Specificity of the RT-PCR products were confirmed by direct sequencing of an amplified PCR product using the Taq DyeDeoxy Terminator protocol developed by Applied Biosystems (Perkin-Elmer, Foster City, CA, USA). The labeled extension products were analyzed on an Applied Biosystems Model 373 DNA sequencer.

## 2.3. Immunohistochemistry

Tissues were fixed in Bouins solution for 6 h, removed to 70% alcohol for overnight incubation, then paraffin-embedded. Six micron sections were deparaffinized in xylene and rehydrated through a graded series of alcohols. Endogenous peroxidase was blocked with 0.3% aqueous H<sub>2</sub>O<sub>2</sub> for 5 min. The ABC<sup>®</sup> technique was performed according to an established protocol (DAKO LSAB 2 Kit, Carpinteria, CA, USA). Primary antibody reactions consisted of overnight incubations at 4°C.

Table 1  
Fetal samples tested

Fetus No.	Gest. age (weeks)	Brain	Eye	Lung	Heart	Liver	Spleen	Adrenal	Kidney	Bowel	Placenta
RT-PCR Epo/Epo-R											
1	6	+/+	+/+	±/±	±/±	±/±	±/±	±/±	±/±	±/±	±/±
2	7	+/+	+/+	±/±	±/±	±/±	±/±	±/±	±/±	±/±	±/±
3	8	+/+	+/+	±/±	±/±	±/±	±/±	±/±	±/±	±/±	±/±
4	8	+/+	+/+	±/±	±/±	±/±	±/±	±/±	±/±	±/±	±/±
5	9	+/+	+/+	±/±	±/±	±/±	±/±	±/±	±/±	±/±	±/±
6	10	+/+	+/+	±/±	±/±	±/±	±/±	±/±	±/±	±/±	±/±
7	11	+/+	+/+	±/±	±/±	±/±	±/±	±/±	±/±	±/±	±/±
8	12	+/+	+/+	±/±	±/±	±/±	±/±	±/±	±/±	±/±	±/±
9	13	+/+	+/+	±/±	±/±	±/±	±/±	±/±	±/±	±/±	±/±
10	14	+/+	+/+	±/±	±/±	±/±	±/±	±/±	±/±	±/±	±/±
11	15	+/+	+/+	±/±	±/±	±/±	±/±	±/±	±/±	±/±	±/±
12	16	+/+	+/+	±/±	±/±	±/±	±/±	±/±	±/±	±/±	±/±
13	17	+/+	+/+	±/±	±/±	±/±	±/±	±/±	±/±	±/±	±/±
14	18	+/+	+/+	±/±	±/±	±/±	±/±	±/±	±/±	±/±	±/±
15	21	+/+	+/+	±/±	±/±	±/±	±/±	±/±	±/±	±/±	±/±
16	24	+/+	+/+	±/±	±/±	±/±	±/±	±/±	±/±	±/±	±/±
Immunostaining for Epo and Epo-R											
17	5	+/+	+/+	±/±	±/±	±/±	±/±	±/±	±/±	±/±	±/±
18	6	+/+	+/+	±/±	±/±	±/±	±/±	±/±	±/±	±/±	±/±
19	6	+/+	+/+	±/±	±/±	±/±	±/±	±/±	±/±	±/±	±/±
20	8	+/+	+/+	±/±	±/±	±/±	±/±	±/±	±/±	±/±	±/±
21	9	+/+	+/+	±/±	±/±	±/±	±/±	±/±	±/±	±/±	±/±
22	10	+/+	+/+	±/±	±/±	±/±	±/±	±/±	±/±	±/±	±/±
23	11	+/+	+/+	±/±	±/±	±/±	±/±	±/±	±/±	±/±	±/±
24	16	+/+	+/+	±/±	±/±	±/±	±/±	±/±	±/±	±/±	±/±
25	18	+/+	+/+	±/±	±/±	±/±	±/±	±/±	±/±	±/±	±/±
26	22	+/+	+/+	±/±	±/±	±/±	±/±	±/±	±/±	±/±	±/±
27	24	+/+	+/+	±/±	±/±	±/±	±/±	±/±	±/±	±/±	±/±

+ Indicates presence of band on RT-PCR; immunoreactivity by immunohistochemistry.

± Indicates faint band on RT-PCR; questionable immunoreactivity.

- Indicates absence of band on RT-PCR; no immunoreactivity.

\*\* Indicates test not performed on this tissue.

Table 2  
Primers used for RT-PCR

mRNA	Primer sequence	Location on mRNA	Expected band length
Epo sense	5'-CCC-TGT-TGG-TCA-ACT-CTT-CC-3'	304 to 538	234 bp
Epo antisense	5'-GTG-TAC-AGC-TTC-AGC-TTT-CC-3'		
Epo-R sense	5'-GGC-AGT-GTG-GAC-ATA-GTG-GC-3'	1195 to 1692	497 bp
Epo-R antisense	5'-AGC-AGG-ATG-GAT-TGG-GCA-GA-3'		
B-Actin sense	5'-TGA-CGG-GGT-CAC-CCA-CAC-TGT-GCC-CAT-CTA-3'	1038 to 1876	661 bp
B-Actin antisense	5'-CTA-GAA-GCA-TTT-GCG-GTG-GAC-GAT-GGA-GGG-3'		

Phosphate buffered saline containing 0.3% Triton X-100 (PBST) with 1% bovine serum albumin was used for all antibody reactions and PBST was used for all washes. Sections were lightly counterstained with hematoxylin.

To identify Epo-immunoreactive cells, two antihuman Epo antibodies were used. The first was a mouse monoclonal antibody raised against the first 26 amino acids of human Epo (Genzyme, Cambridge, MA, USA). This antibody was used at a 1:50 dilution. Negative controls for this antibody were absence of primary antibody, and incubation with preimmune serum. A second, polyclonal, antiEpo antibody raised in goats against amino acids 35–57 of the amino terminus of the precursor form of human Epo was used at a 1:100 dilution to confirm our findings (Santa Cruz Biotechnology, Santa Cruz, CA, USA). Preincubation with a tenfold excess of specific blocking peptide (Santa Cruz) was used as a negative control for this reaction.

The antiEpo-R antibody used was an affinity purified rabbit polyclonal antibody raised against amino acids 489 to 508 of the carboxy terminus of the precursor form of human Epo-R (Santa Cruz) [22]. This antibody was used at 1:100 dilution. Preincubation with a tenfold excess of specific blocking peptide (Santa Cruz) was used as a negative control for the reaction.

Additional negative controls were done to insure the specificity of these antibody-epitope interactions: each antibody was incubated with the opposite blocking peptide, as well as with blocking peptides for the granulocyte macrophage-colony stimulating factor (GM-CSF) and GM-CSF receptor (GM-CSF-R) antibodies (Santa Cruz) to insure that the blocking peptides were, in fact, specific. Thus, the Epo antibody was preincubated with the Epo-R, GM-CSF, or GM-CSF-R blocking peptides; and the Epo-R antibody was preincubated with the Epo, GM-CSF, or GM-CSF-R blocking peptides. When using the Epo-R antibody to identify immunoreactivity in liver, we found that preincubation with the blocking peptides for GM-CSF and GM-CSF receptor did not block the immunoreactivity of the antibody, while blocking with the Epo-R peptide abolished the reaction. When using the antiEpo antibody, blocking with the Epo-R peptide, GM-CSF, or GM-CSF receptor peptide did not block the immunoreactivity, but using the specific Epo peptide did block the immunoreactivity.

KP-1 (Dako, Carpinteria, CA, USA) staining was performed to identify tissue macrophages. KP-1 is a human macrophage antigen (CD68) that corresponds to a lysosome membrane protein [23]. Slides were deparaffinized in two xylene washes and rehydrated through a graded alcohol series finishing with a tap water bath and placed in Ventana Medical Systems wash solution (solution no. 250-008). KP-1 slides were subjected to an inhibitor solution consisting of hydrogen peroxide and sodium azide (Ventana) for 4 min to block endogenous peroxidase activity. The slides were then subjected to alkaline protease (Ventana Protease 2 Reagent) prior to exposure to specific antibody in order to improve antibody binding. Optimized titers of the specific antibody were determined and then applied to the sections. KP-1 antibody was applied at a 1:100 dilution for 32 min. The slides were exposed to an avidin-horse radish peroxidase reagent for 8 min. Following this, the slides were exposed to universal biotinylated Ig secondary antibody for 8 min (Ventana). Diaminobenzidine was applied to the KP-1 slides for 8 min, and the slides were counterstained with hematoxylin.



#### 2.4. Western analysis

Specificity of the antibodies against human Epo-R (Santa Cruz) and human Epo (Genzyme) were determined by the inclusion of rhEpo 100 ng/lane (Amgen), rhG-CSF 120 pg/lane (Amgen), and human fetal liver (11 weeks postconception) as positive and negative controls. Fetal liver was lysed on ice for 20 min in 1 ml of lysis buffer, consisting of 50 mM Tris-HCl, pH 7.0, 1.5% Triton X-100, 10  $\mu$ M Pepstatin, 10  $\mu$ M Leupeptin, 10  $\mu$ M Antipain and 2 mM Phenylmethylsulfonylfluoride. Tissue samples were passed through progressively smaller gauge needles, ranging from 16 to 25 gauge, to disperse cells. Samples were spun at 12 000 g for 2 min, with supernatant removed and stored. Protein concentrations were determined by Bio-Rad Protein Assay Reagent kit (Hercules, CA, USA). Samples were denatured by heating to 98°C for 3 min and electrophoresed on 10 or 15% sodium dodecyl sulfate (SDS) polyacrylamide gel electrophoresis with 3.5% stacking gel, in 1  $\times$  Tris-glycine buffer (25 mM Tris containing 200 mM glycine, 3.5 mM SDS (pH 8.3)) in a miniprotein cell (Bio-Rad) at 60 volts in a cold room for 3 h. The separated proteins were electrotransferred to a nitrocellulose filter (Bio-Rad) using a transfer buffer (pH 8.3) containing 39 mM glycine, 48 mM Tris base, 0.037% SDS and 20% methanol in a minitransfer cell (Bio-Rad) at 200 mA in a cold room for 1 h. The filter was incubated with gentle agitation at 4°C overnight, in 20 ml of blocking buffer containing 5% dried nonfat milk, 0.01% antifoam A, 0.02% sodium azide in PBS, then probed with primary antibody for 2 h. The ABC-AP<sup>®</sup> Kit and Alkaline Phosphatase Substrate Kit (Vector Laboratories, Vectastain<sup>®</sup> ABC system) were used to detect the protein on the filter. Prestained molecular weight markers (28 400, 34 200, 48 000, 77 000, 103 000 Da) (Bio-Rad) were used to determine protein size.

#### 3. Results

The presence or absence of Epo and Epo-R mRNA was determined in organs of differing postconceptual age by RT-PCR, and these results are shown in Table 1. To demonstrate the range of findings at two points in development, Figs. 1 and 2 compare RT-PCR results from fetal organs obtained at 8 and 16 weeks postconception. At 8 weeks postconception, organs tested included brain, brainstem, spinal cord, eye, lung, heart, liver, spleen, adrenal, kidney, stomach and placenta. At 16 weeks postconception organs tested included brain, spinal cord, eye, lung, heart, liver, spleen, adrenal, kidney, stomach, small bowel and skin. At both time-points, the liver shows the most prominent band for both Epo and its receptor, however, this sensitive technique did identify the transcription of mRNA for Epo and Epo-R in most tissues. Although not quantitative, the RT-PCR was done using 30 cycles of amplification, which we have previously shown to be in the linear range (data not shown).

RT-PCR reflects all cells in a given organ, without cellular specificity. It is known that Epo-R are present on the surface of endothelial cells, cells which are present in all organs tested. The sensitivity of RT-PCR is such that the presence of these cells could be responsible for the detection of mRNA for Epo-R within the organs. To determine the cellular specificity of Epo and Epo-R immunoreactivity in fetal organs

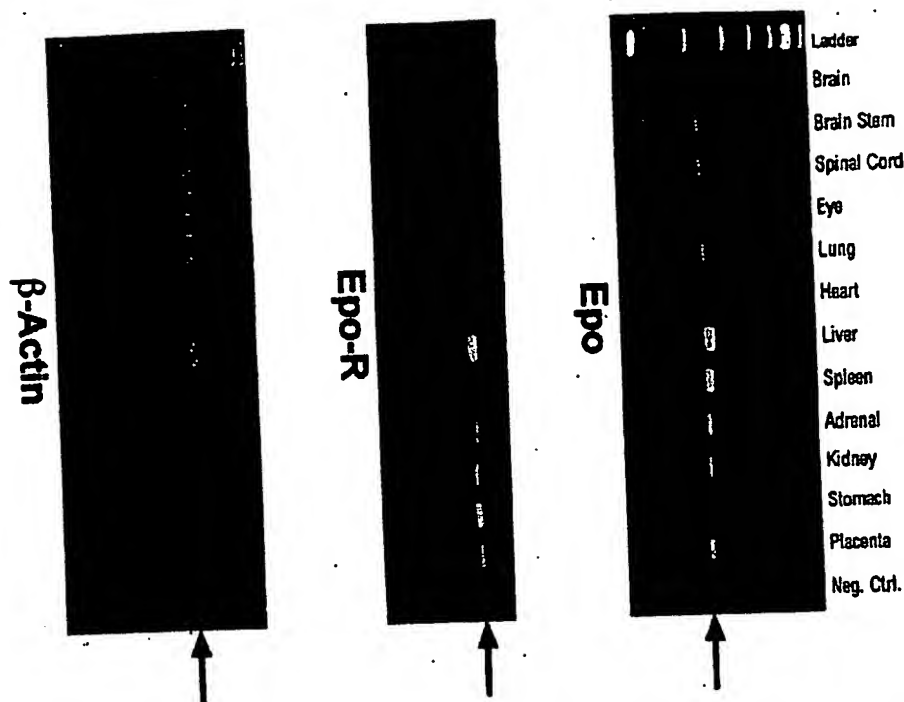


Fig. 1. Epo and Epo-R mRNA abundance in fetal tissues at 8 weeks gestation. The upper panel shows the RT-PCR products using primers specific to Epo, and the middle panel shows Epo-R products. The bottom panel shows  $\beta$ -actin controls for RNA integrity. Lane 1 contains a 100 base pair ladder for assessment of fragment size. Lanes 2–13 contain RT-PCR products from total RNA extracted from brain, brainstem, spinal cord, eye, lung, heart, liver, spleen, adrenal, kidney, stomach and placenta from 8 weeks postconception. Lane 14 contains a negative control (RNA not reverse transcribed). The expected sizes for amplified fragments for Epo, Epo-R, and  $\beta$ -actin are 234 base pairs, 497 base pairs, and 661 base pairs, respectively.

at different postconceptual ages, we used immunohistochemistry. To check for specificity of the antibody reaction used to detect Epo and Epo-R by immunohistochemistry, we performed Western analysis. Fig. 3 shows the specific banding for both antihuman Epo antibody, and antihuman Epo-R antibody.

Organs examined using immunohistochemistry are listed in Table 1, as are the results of these studies. As we have previously reported the presence of Epo and Epo-R within the developing CNS [15], only details of nonCNS organs will be given here.

Although several organs showed minor amounts of Epo staining during the first two trimesters, immunoreactivity was consistently most prominent in the liver. Fig. 4 shows representative photomicrographs of Epo immunoreactivity in the liver, lung, adrenal and kidney. The liver was the most immunoreactive organ throughout the first and second trimesters (Fig. 4A). Immunoreactivity for Epo was weak to absent in the lung parenchyma of all developmental stages investigated. There was weak to

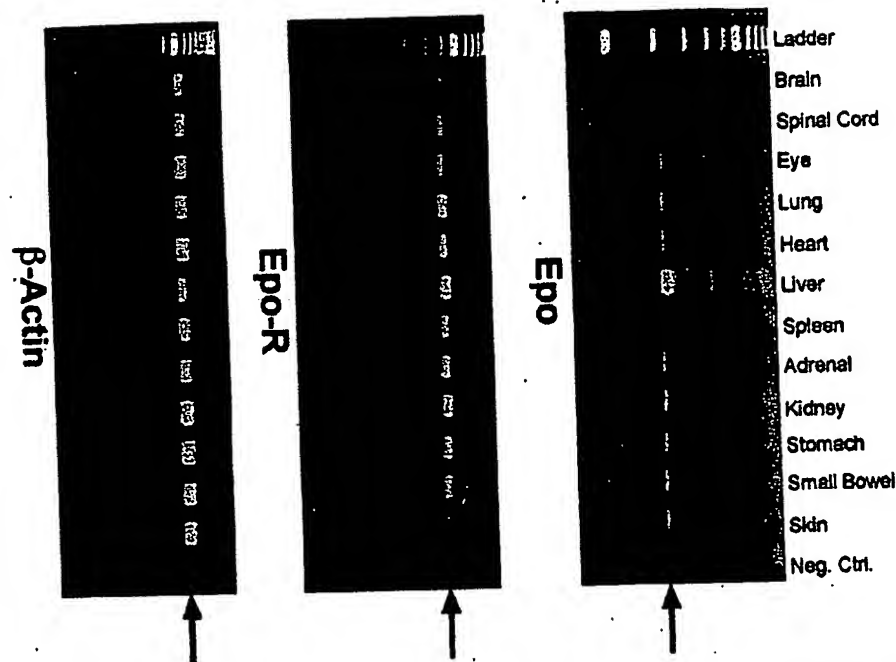


Fig. 2. Epo and Epo-R mRNA abundance in fetal tissues at 16 weeks gestation. The top panel shows the RT-PCR products using primers specific to Epo, the middle panel shows Epo-R products. Lane 1 contains a 100 base pair ladder for assessment of fragment size. Lanes 2–13 contain RT-PCR products from total RNA extracted from brain, spinal cord, eye, lung, heart, liver, spleen, adrenal, kidney, stomach, small bowel and skin from 16 weeks postconception. Lane 14 contains a negative control. The bottom panel shows the  $\beta$ -actin controls for RNA integrity.

moderate staining of what appeared to be the capillary network of the developing lung mesenchyme. The apical surface of the developing bronchi were also immunoreactive (Fig. 4B). We found moderate immunoreactivity for Epo in the developing zona fasciculata of the adrenal cortex as is shown in Panel C. In the adrenal medulla, Epo reactivity was weak to absent. Although the metanephric kidney was negative for Epo staining at 5 weeks, as was the 8 week gestation kidney, by 18 weeks postconception, weak immunoreactivity was present in the peritubular interstitial cells (Fig. 4D). By 22 weeks postconception, this immunoreactivity of the interstitial cells and of the proximal tubules was strong (Fig. 4E).

Moderate Epo staining was present in the retina of the eye, particularly in the region of active cell division. The pattern of staining in this tissue was reminiscent of that seen in the developing brain, with the most prominent staining noted in the region of active mitosis. In the heart, immunoreactivity was weak to absent throughout the time period studied. The spleen showed no notable immunoreactivity with Epo.

Thus, organs in which Epo immunoreactivity was positive during the first two trimesters were: liver, kidney, the retina of the eye, and the zona fasciculata of the

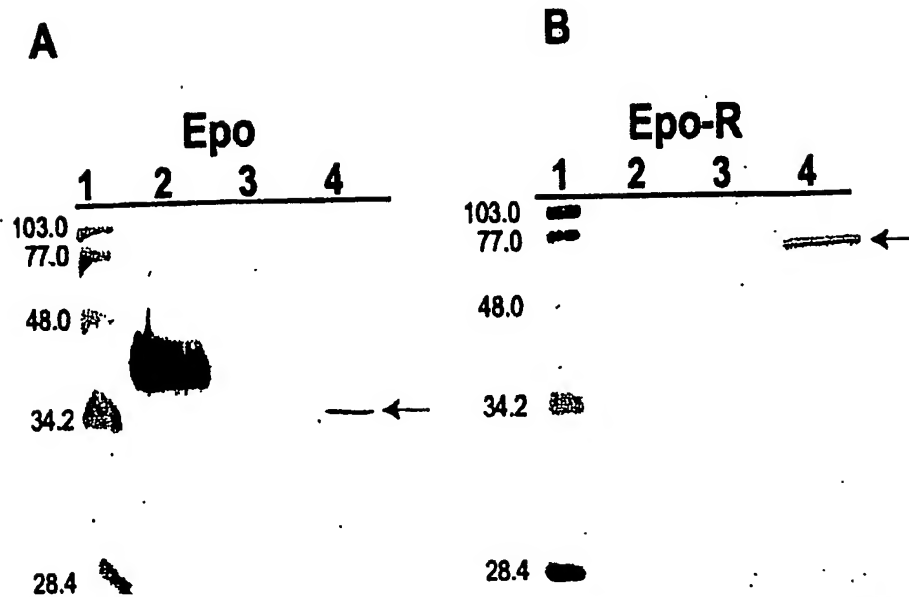


Fig. 3. Immunoblot of Epo and Epo-R. Epo reactivity is shown in panel A. Samples were electrophoresed into a 3.5% stacking gel, resolved on a 15% SDS acrylamide gel, then transferred to a nitrocellulose membrane. Lane 1 shows the molecular weight markers, identified in kDa. Lanes 2 through 4 contain: 100 ng rhEpo, 120 pg rhG-CSF and fetal liver (11 weeks postconception), respectively. The expected sizes of recombinant human Epo and endogenous Epo are 37 and 30.4 kDa, respectively. An arrow designates the expected size of Epo. Epo-R reactivity is shown in panel B. Samples were electrophoresed into a 3.5% stacking gel, resolved on a 10% SDS acrylamide gel, then transferred to a nitrocellulose membrane. Lanes 1 through 4 contain the protein markers, 100 ng rhEpo, 120 pg rhG-CSF and fetal liver (11 weeks postconception), respectively. The expected size of Epo-R is 66 kDa, and is identified by an arrow.

adrenal, and possibly, mild immunoreactivity of the apical surfaces of the bronchial epithelium. In other organs, immunoreactivity, if present, was due to vascular structures.

The pattern of immunoreactivity for the Epo-R was quite different than for its ligand. Like Epo, Epo-R reactivity was very strong in the liver parenchyma at all gestational ages studied (Fig. 5A), however, unlike Epo immunoreactivity, moderate Epo-R immunostaining was present in many other organs throughout the first two trimesters.

The myocardium became progressively more immunoreactive as gestation progressed. At 5 weeks postconception, the myocardial cells were only weakly reactive to Epo-R antibody, but by 8 and 18 weeks postconception, strong immunoreactivity was found (Fig. 5B and C). A similar increase in immunoreactivity with time was found in the lung. At 6 weeks postconception, only weak reactivity was noted, with the exception of scattered round interstitial cells. At 8 weeks postconception, the basilar surfaces of respiratory bronchi were immunoreactive, in addition to these scattered cells (Fig. 5D). By 18 weeks postconception, the epithelial cells lining the

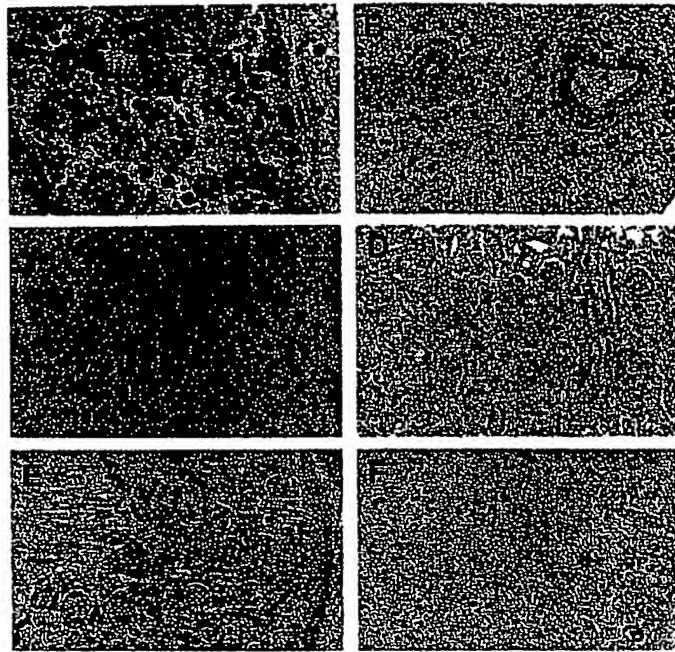


Fig. 4. Erythropoietin immunoreactivity in human fetal tissues. Panel A illustrates the strong immunoreactivity of fetal liver parenchymal cells (8 weeks postconception) as well as the nascent hematopoietic cells with antiEpo antibody ( $400\times$ ). Panel B is a photomicrograph of a lung at 5 weeks postconception (original magnification  $200\times$ ). Note the immunoreactivity of the capillary network (arrow), and the apical surfaces of the bronchial epithelium (arrow head). The zona fasciculata (ZF) of the fetal adrenal cortex (Panel C) showed moderate Epo immunoreactivity at 18 weeks postconception, but the adrenal medulla (AM) was nonreactive. Panels D and E show Epo immunoreactivity in kidney at 18, and 22 weeks gestation respectively, with panel F showing a negative control. The original magnifications of these photos were  $160\times$ , and  $100\times$ , respectively. At 18 weeks, weak immunoreactivity is present in the proximal tubules and the nearby interstitial cells (Panel D, arrow). By 22 weeks gestation, this immunoreactivity is much stronger in both the proximal tubules (arrow), and the interstitial cells (Panel E, arrow head).

bronchi as well as the scattered interstitial cells were strongly reactive for Epo-R. The smooth muscle cells of the developing bronchial arteries were also strongly immunoreactive. The mesenchymal cells of the interstitium remained negative to weakly reactive to Epo-R antibody. To determine whether the scattered cells noted within the interstitium of the developing lung might be macrophages, we stained lung at 6 weeks postconception with KP-1. We found scattered KP-1 positive cells which were morphologically similar to those identified with Epo-R (Fig. 5E).

The neural retina was immunoreactive at 6, 8, and 18 weeks postconception. The strongest immunoreactivity was present at the mitotic surface, however, the entire cell layer was moderately reactive (Fig. 5F). Unlike with Epo immunoreactivity, in the adrenal, strong immunoreactivity was present in all zones of the adrenal cortex and in the adrenal medulla (Fig. 5G). The developing kidney was immunoreactive with

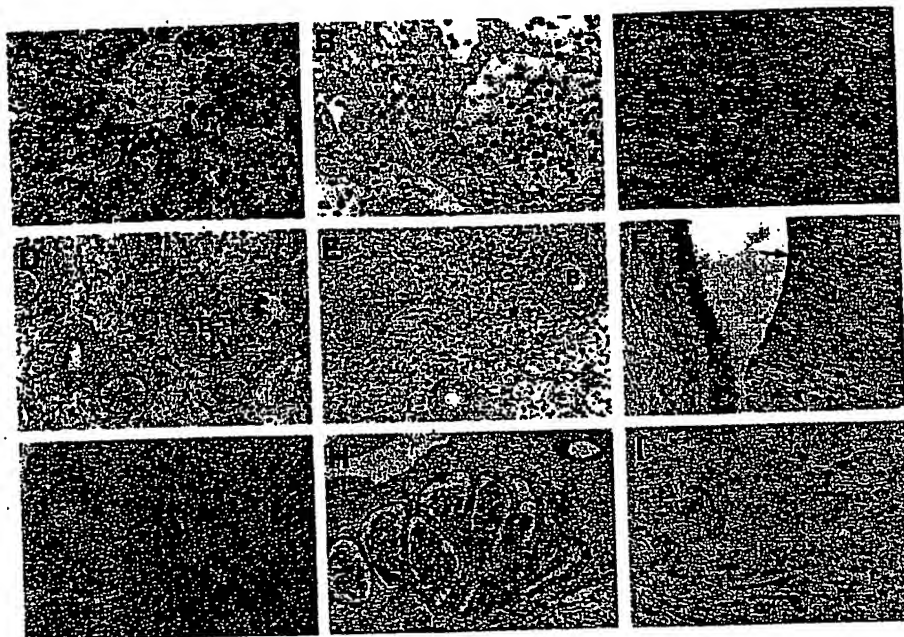


Fig. 5. Erythropoietin receptor immunoreactivity in human fetal tissues. Panel A shows an 18 week gestation liver stained with antiEpo-R antibody. Note the strong reactivity of both the liver parenchymal cells as well as the nascent hematopoietic cells (arrow). Panels B and C show immunoreactivity of the myocardium at 5 and 18 weeks postconception, respectively. At 5 weeks the myocardial cells are only weakly reactive, and this is in contrast to the circulating nucleated red blood cells (arrow) which are very well stained (original magnification  $100\times$ ). At 18 weeks postconception, the myocardium is strongly immunoreactive (original magnification  $400\times$ ). Panels D shows a lung at 8 weeks gestation stained with antiEpo-R antibody, and is compared to panel E in which a lung at 6 weeks gestation is stained with KP-1, to specifically identify macrophages. Respiratory bronchi are labeled B. Arrows identify strongly immunoreactive interstitial cells which are presumed to be macrophages (original magnification  $160\times$ ). Panel F demonstrates the immunoreactivity of the neural retina at 8 weeks gestation (original magnification  $400\times$ ). An arrow identifies a mitotic cell. Although the strongest immunoreactivity is present at the mitotic surface, the entire cell layer is moderately reactive. Panel G shows the adrenal medulla (AM), the zona fasciculata (ZF), and the zona glomerulosa (ZO) of the adrenal cortex. Note that unlike with Epo immunoreactivity, the receptor was present in all zones of the adrenal cortex and in the adrenal medulla. Panel H shows Epo-R staining of the metanephric kidney (original magnification  $100\times$ ). This is compared to the more restricted immunoreactivity noted at 22 weeks postconception seen in panel I. At this time-point, immunoreactivity is noted primarily in the proximal tubules.

Epo-R throughout the time period studied, including at the mesonephric stage (Fig. 5H). As development progressed, immunostaining became more localized to cells of the proximal tubules, as is shown in Fig. 5(Panels I).

#### 4. Discussion

Many of the hematopoietic cytokines were discovered by virtue of their growth-promoting effects on hematopoietic cell lines, or their specific immune functions.

Although it was initially assumed that effects of these cytokines were specific to the hematopoietic system, this view is now changing, as evidence of a multiplicity of functions at nonhematopoietic sites are coming to light.

Animal and *in vitro* studies have demonstrated Epo-R on liver stromal cells [4], endothelial cells [5–7,24], mesangial cells [8], smooth muscle cells [8], placental tissues [9,10], and cells of neuronal origin [11–14,25–27]. Erythropoietin has a mitogenic effect on several of these cell types *in vitro* [4,5,28], as it does in erythroid precursor cells *in vivo*. Secondary responses have also resulted from cellular stimulation with recombinant Epo (rEpo). For instance, Carlini and coworkers demonstrated a calcium-dependent increase in endothelin-1 synthesis and release by endothelial cells stimulated with rEpo [6,29]. A dose-dependent effect of rEpo on endothelial cells has been confirmed by other workers [30] and may contribute to the hypertension seen in dialysis patients treated with rEpo [31]. Another potentially important effect of rEpo on endothelial cells is that of angiogenesis [32]. Brain capillary endothelial cells express a functional membrane-bound Epo-R as well as a soluble Epo-R, and Yamaji et al. have suggested that under hypoxic conditions Epo might act as a competence factor, contributing to the growth of new capillaries in the brain [7]. In brain, available data suggests that Epo may function as a neurotrophic factor and a neuroprotective agent [12,13,15,26].

The goal of this study was to establish the distribution of Epo and its receptor within the developing human fetus. Using RT-PCR as a detection method for mRNA for Epo and Epo-R, we found messages for these proteins to be present throughout the body during the first two trimesters. The extreme sensitivity of this method, however, may be misleading, as contamination with other tissues, circulating blood elements (particularly at the earliest gestation), or gene "leakiness" may have resulted in the spurious detection of mRNA. Another limitation of this method is that although it assesses transcripts in a given organ, it does so without cellular specificity. We therefore used immunohistochemistry as a complementary technique to confirm the presence or absence of Epo and Epo-R, and to provide information as to the cellular localization of these proteins. Because Epo is a soluble protein, identification of Epo in tissues by immunoreactivity does not necessarily indicate local production, but may rather reflect ligand binding to Epo-R, thus, it will be important to establish the cellular location of synthesis by *in situ* techniques. We did, however, find a different distribution of Epo than Epo-R in our studies, suggesting that ligand binding was not the sole reason for Epo immunoreactivity in tissues.

Immunolocalization of Epo to cells other than endothelial cells was limited to the liver parenchymal cells, kidney proximal tubules and interstitial cells, neural retina of the eye, and adrenal cortex. During the first trimester, only liver and eye were found to be immunoreactive, with the exception of the developing CNS. As development progressed, immunoreactivity in the fetal kidney became more prominent.

This pattern of staining for Epo was in direct contrast to the pattern for Epo-R, which was widespread throughout the body, involving several cell types, some of which have been reported previously, (endothelial cells and myocardiocytes), and some which are previously unreported (cells of the adrenal cortex and medulla). It is interesting that cells of both the adrenal medulla, which is derived from postmitotic neural crest cells, and cells of the dorsal root ganglia, which is similarly derived,

expressed Epo-R. This widespread pattern of Epo-R distribution is consistent with findings in the developing mouse embryo [16]. Yasuda et al. identified Epo and Epo-R by a combination of RT-PCR, and immunolocalization, and after discovering the prevalence of the receptor, proposed that Epo might function as a general morphogen and inducer of neurogenesis during early development. Although we identified limited somatic immunoreactivity for Epo in the developing fetus, it has previously been shown that in addition to Epo synthesis by fetal liver, human placenta synthesizes Epo [10]. One can speculate that physiologically relevant circulating concentrations of Epo are present from early gestation, functioning in concert with other somatic growth factors to influence the growth and development of fetal organs by way of interaction with specific Epo-R.

In summary, the distribution of Epo and its receptor is more widespread in the developing human than was initially postulated. The receptor is widespread during early fetal development, leading us to speculate that Epo acts as a somatic growth or differentiation factor during this period. Although a great deal of further investigation is required to fully understand the nonhematopoietic role of Epo, it is likely that many of its mechanisms of action, which have been well worked out in hematopoiesis, might also be at work in nonhematopoietic systems.

## References

- [1] Sokol L, Luhovy M, Guan Y, Prchal JF, Semenza GL, Prchal JT. Primary familial polycythemia: a frameshift mutation in the erythropoietin receptor gene and increased sensitivity of erythroid progenitors to erythropoietin. *Blood* 1995;86:15–22.
- [2] Brown MS, Garcia JF, Phibbs RH, Dallman PR. Decreased response of plasma immunoreactive erythropoietin to "available oxygen" in anemia of prematurity. *J Pediatr* 1984;105:793.
- [3] Wu H, Liu X, Jaenisch R, Lodish HF. Generation of committed erythroid BFU-E and CFU-E progenitors does not require erythropoietin or the erythropoietin receptor. *Cell* 1995;83:59–67.
- [4] Ohneda O, Yanai N, Obinata M. Erythropoietin as a mitogen for fetal liver stromal cells which support erythropoiesis. *Exp Cell Res* 1993;208:327–31.
- [5] Anagnostou A, Lee ES, Kassamian N, Levinson R, Steiner M. Erythropoietin has a mitogenic and positive chemotactic effect on endothelial cells. *Proc Natl Acad Sci USA* 1990;87:5978–82.
- [6] Carlini RG, Dusso AS, Obialo CI, Alvarez UM, Rothstein M. Recombinant human erythropoietin (rHuEPO) increases endothelin-1 release by endothelial cells. *Kidney Int* 1993;43:1010–4.
- [7] Yamaji R, Okada T, Moriya M, Naito M, Tsuruo T, Miyatake K, Nakano Y. Brain capillary endothelial cells express two forms of erythropoietin receptor mRNA. *Eur J Biochem* 1996;239:494–500.
- [8] Morakkabati N, Gollnick F, Meyer R, Fandrey J, Jellmann W. Erythropoietin induces  $Ca^{2+}$  mobilization and contraction in rat mesangial and aortic smooth muscle cultures. *Exp Hematol* 1996;24:392–7.
- [9] Sawyer ST, Krantz SB, Sawada K. Receptors for erythropoietin in mouse and human erythroid cells and placenta. *Blood* 1989;74:103–9.
- [10] Conrad KP, Benyo DF, Westerhausen-Larsen A, Miles TM. Expression of erythropoietin by the human placenta. *FASEB J* 1996;10:760–6.
- [11] Masuda S, Nagao M, Takahata K, Konishi Y, Gallyas Jr. F, Tabira T, Sasaki R. Functional erythropoietin receptor of the cells with neural characteristics. Comparison with receptor properties of erythroid cells. *J Biol Chem* 1993;268:11208–16.



- [12] Konishi Y, Chui DH, Hirose H, Kunishita T, Tabira T. Trophic effect of erythropoietin and other hematopoietic factors on central cholinergic neurons in vitro and in vivo. *Brain Res* 1993;609:29–35.
- [13] Morishita E, Masuda S, Nagao M, Yasuda Y, Sasaki R. Erythropoietin receptor is expressed in rat hippocampal and cerebral cortical neurons, and erythropoietin prevents in vitro glutamate-induced neuronal death. *Neuroscience* 1997;76:105–16.
- [14] Marti HH, Wenger RH, Rivas LA, Straumann U, Digicaylioglu M, Henn V, Yonekawa Y, Bauer C, Gassmann M. Erythropoietin gene expression in human, monkey and murine brain. *Eur J Neurosci* 1996;8:666–76.
- [15] Juul SE, Anderson DK, Li Y, Christensen RD. Erythropoietin and erythropoietin receptor in the developing human central nervous system. *Pediatr Res* 1998;43:40–9.
- [16] Yasuda Y, Nagao M, Okano M, Masuda S, Sasaki R, Konishi H, Tanimura T. Localization of erythropoietin and erythropoietin-receptor in postimplantation mouse embryos. *Dev Growth Differ* 1993;35:711–22.
- [17] Li Y, Juul SE, Morris-Wiman JA, Calhoun DA, Christensen RD. Erythropoietin receptors are expressed in the central nervous system of mid-trimester human fetuses. *Pediatr Res* 1996;40:376–80.
- [18] Juul SE, Harcum J, Li Y, Christensen RD. Erythropoietin is present in the cerebrospinal fluid of neonates. *J Pediatr* 1997;130:428–30.
- [19] Hern W. Correlation of fetal age and measurements between 10 and 26 weeks gestation. *Obstet Gynecol* 1984;63:26.
- [20] Kelemen E, Janossa M, Calvo W, Fliedner TM. Developmental age estimated by bone-length measurement in human fetuses. *Anat Rec* 1984;209:547–52.
- [21] Martin VV, Nock S, Meyer-Ganen G, Hager K-P, Jensen U, Cerff R. A method for isolation of cDNA-quality mRNA from immature seeds of a gymnosperm rich in polyphenolics. *Plant Mol Biol* 1993;22:555–6.
- [22] Youssoufian H, Longmore G, Neumann D, Yoshimura ALH. Structure, function and activation of the erythropoietin receptor. *Blood* 1993;81:2223–36.
- [23] Holness CL, Simmons DL. Molecular cloning of CD68, a human macrophage marker related to lysosomal glycoproteins. *Blood* 1993;6:1607–13.
- [24] Anagnostou A, Liu Z, Steiner M, Chin K, Lee ES, Kessimian N, Noguchi CT. Erythropoietin receptor mRNA expression in human endothelial cells. *Proc Natl Acad Sci USA* 1994;91:3978–84.
- [25] Masuda S, Okano M, Yamagishi K, Nagao M, Ueda M, Sasaki R. A novel site of erythropoietin production. Oxygen-dependent production in cultured rat astrocytes. *J Biol Chem* 1994;269:19488–93.
- [26] Tabira T, Konishi Y, Gallyas Jr. F. Neurotrophic effect of hematopoietic cytokines on cholinergic and other neurons in vitro. *Int J Dev Neurosci* 1995;13:241–52.
- [27] Morishita E, Narita H, Nishida M, Kawashima N, Yamagishi K, Masuda S, Nagao M, Hatta H, Sasaki R. Anti-erythropoietin receptor monoclonal antibody: epitope mapping, quantification of the soluble receptor, and detection of the solubilized transmembrane receptor and the receptor-expressing cells. *Blood* 1996;88:465–71.
- [28] Wald MR, Borda ES, Sterin-Borda L. Mitogenic effect of erythropoietin on neonatal rat cardiomyocytes: signal transduction pathways. *J Cell Physiol* 1996;167:461–8.
- [29] Carlini RG, Gupta A, Liapis H, Rothstein M. Endothelin-1 release by erythropoietin involves calcium signaling in endothelial cells. *J Cardiovasc Pharmacol* 1995;26:889–92.
- [30] Nagai TAYN, Kohjiro NS, Nabeshima K, Kanamori N, Takayama K, Kinugasa E, Koshikawa S. Effects of rHuEpo on cellular proliferation and endothelin-1 production in cultured endothelial cells. *Nephrol Dial Transplant* 1995;10:1814–9.
- [31] Maschio G. Erythropoietin and systemic hypertension. *Nephrol Dial Transplant* 1995;2:74–9.
- [32] Carlini RG, Reyes AA, Rothstein M. Recombinant human erythropoietin stimulates angiogenesis in vitro. *Kidney Int* 1995;47:740–5.

# Erythropoietin Receptors Are Expressed in the Central Nervous System of Mid-Trimester Human Fetuses

YAN LI, SANDRA E. JUUL, JOYCE A. MORRIS-WIMAN, DARLENE A. CALHOUN, AND  
ROBERT D. CHRISTENSEN

From the Division of Neonatology, Department of Pediatrics, University of Florida College of Medicine [Y.L., S.E.J., D.A.C., R.D.C.], and the Department of Orthodontics, University of Florida College of Dentistry [J.M.W.], Gainesville, Florida 32610-0296

## ABSTRACT

Recombinant erythropoietin (rEpo) is an effective treatment for infants with the anemia of prematurity. rEpo was previously thought to act only on erythroid progenitor cells, but evidence now indicates that certain nonerythroid cells also express functional erythropoietin receptors (Epo-R). Such receptors have been observed on cells in the developing murine brain and spinal cord. The objective of this study was to determine whether Epo-R are expressed in the CNS of mid-trimester human fetuses. For this study, spinal cords were collected from five mid-trimester abortuses. RNA was extracted from the washed specimens, and the presence of Epo-R mRNA was sought by reverse transcription followed by polymerase chain reaction. Immunohistochemistry was then used to determine the anatomic location of the cells expressing Epo-R within the fetal spinal cord. The

results showed that all fetal spinal cords tested contained Epo-R mRNA. The cells expressing Epo-R were radiating from the ependymal canal toward the anterior and posterior median sulci. We conclude that Epo-R are expressed on cells in the developing human CNS. Further studies are needed to determine whether they are clinically relevant in the premature infant. (*Pediatr Res* 40: 376-380, 1996)

## Abbreviations

Epo, erythropoietin  
Epo-R, erythropoietin receptor  
rEpo, recombinant erythropoietin  
RT, reverse transcription  
PCR, polymerase chain reaction

Diminishing the number of transfusions administered to preterm neonates is widely maintained to be a desirable goal, as the risk of adverse reactions, or infection accompanying multiple transfusions, although small, is real. Multiple large clinical trials have shown that rEpo treatment can reduce both the number and total volume of transfusions required in this patient population (1-5). The cost of treatment with rEpo may be significantly less than the cost of transfusions, although this analysis is dependent on the costs of rEpo, and whether single or multiple doses are obtained per vial of drug (6-8). No significant adverse effects of rEpo administration to preterm infants have been identified, although an unexplained, possibly coincidental association with sudden infant death syndrome has been noted (9-11). The experience with rEpo in human infants to date is insufficient to guarantee the absence of significant toxicity, particularly for complications which occur

rarely. Additional long-term studies are needed to assess the neurodevelopmental effects of Epo administration to this population.

Epo, a 34-kD glycoprotein, was originally thought to act only on erythroid progenitor cells, stimulating their proliferation and differentiation by binding to a specific 66-kD membrane receptor (12-17). There is now growing evidence in animal models that Epo-R are also present in some nonhematopoietic tissues such as endothelial cells (18, 19) and fetal cells of neural origin (20), although the physiologic role of Epo-R at these sites is unclear. These receptors do, however, appear to be functional as assessed by *in vitro* and *in vivo* studies. We will concentrate primarily on work done in tissues of neural origin, as there is accumulating evidence that Epo may be active within the developing CNS.

Masuda *et al.* (20) first demonstrated the presence of Epo-R on two rodent cell lines of neural origin (PC12 and SN6 cells) which responded to rEpo by increasing the intracellular concentration of monoamines, and by rapidly increasing cytosolic concentrations of free calcium. The possibility that this receptor is developmentally regulated was suggested by Liu *et al.* (21) in work observing substantial expression of Epo-R within

Received November 27, 1995; accepted March 19, 1996.

Correspondence and reprint requests: Yan Li, M.D., Division of Neonatology, University of Florida College of Medicine, P.O. Box 100296, JHMHC, Gainesville, FL 32610-0296.

Supported by National Institutes of Health Grants HL-44951 and RR-00083 and by a grant from the Children's Miracle Network Telethon.

the early fetal murine brain falling to undetectable levels by gestational d 16.

A prerequisite for assigning a physiologic role to Epo-R within the fetal CNS is the presence of the ligand, Epo, within this system, either by crossing the blood-brain barrier, or by synthesis within the CNS. Yasuda *et al.* (22) provided such support for a role of Epo in neurogenesis in a study of postimplantation mouse embryos, where both Epo and Epo-R messages were identified in the primitive streak. Our own work in human infants has documented the presence of Epo within the spinal fluid of premature and term neonates, which appears to be developmentally modulated (23).

Studies directed at determining the function of Epo within the CNS have demonstrated oxygen-regulated Epo synthesis by primary cultures of astrocytes from rat cerebrum (24). The Epo produced within the brain had a different extent of sialylation, and was more active *in vitro* than was rEpo. Tan *et al.* (25), studying *in vivo* exposure of rats to hypoxic conditions (7.5% oxygen) showed an induction of Epo mRNA in brain tissue. The possibility that Epo might function as a neurotropic factor is raised by a study showing that rEpo increased survival of damaged rat cholinergic septal neurons produced by fimbria-fornix transections (26, 27).

Thus, an endogenous source of Epo within the developing CNS and the presence of functional Epo-R have been established in murine models, although their role, if any, is not clear. Our laboratory has demonstrated the presence of Epo within the spinal fluid of neonates, and we now show that Epo-R are present in the CNS of developing humans. We speculate that if functional Epo-R are expressed within the CNS of the mid-trimester fetus, as they are in developing rodents, treatment of premature infants with rEpo might have unanticipated neurodevelopmental consequences, and we echo the caveats voiced by others that, before treatment with rEpo becomes the standard of care for the treatment of anemia of prematurity, further neurodevelopmental studies to determine the physiologic relevance of this finding should be carried out.

## METHODS

**Human fetal specimens.** Spinal columns were obtained from five human abortuses at 13 to 17 wk of gestation. Only fetuses that were normal by ultrasound examination and underwent elective pregnancy termination were studied. Pregnancy terminations were carried out by suction curettage. No contact with the mother or attempt to influence her decision was made. The studies were approved by the University of Florida Institutional Review Board. The spinal cords were obtained after severing the dorsal lamina from the spinal column, blotting the spinal cord several times on sterile gauze, and extensively washing the cords in sterile minimal essential medium,  $\alpha$  modification (HyClone Laboratories, Logan, UT). The meninges were removed from some of the spinal cord samples under a dissecting microscope.

**Preparation of total RNA.** Total cellular RNA was extracted from the washed spinal cords using the guanidinium thiocyanate method (28). The spinal cord tissue and OCIM1 cells (an erythroleukemia cell line used as a positive control for Epo-R)

were homogenized in 4 M guanidinium thiocyanate, and the RNA was separated from DNA and protein by phenol/chloroform extraction, followed by isopropanol precipitation. The purity and concentration of the RNA were determined spectrophotometrically.

**RT of RNA and amplification of cDNA.** RT of RNA and amplification of cDNA were performed by using the GeneAmp RNA PCR kit (Perkin-Elmer Corp., Norwalk, CT) in a DNA thermal cycler (Perkin-Elmer Corp.). One microgram of total RNA was incubated with 50 U of reverse transcriptase for 1 h at 37°C. The reverse transcriptase was inactivated at the end of the reaction by heating to 95°C for 5 min. Amplification of first strand cDNA was carried out under the following conditions: 10 mM Tris, pH 8.3, 50 mM KCl, 2.5 mM MgCl<sub>2</sub>, 2.0 mM dNTP, 0.2  $\mu$ M upstream and downstream primers, 10% RT reaction mix, 5 U/ $\mu$ L Ampli Taq 94°C for 1 min, 57°C for 1 min, 72°C for 2 min for 35 cycles, followed by 10-min elongation at 72°C. The following oligonucleotide primers were used to amplify a 197-bp fragment from the reverse transcribed Epo-R mRNA: sense primer 5'-GCA-CCG-AGT-GTG-TGC-TGA-GCA-A, and antisense primer 5'-GGT-CAG-CAG-CAC-CAG-GAT-GAC. These primers amplified the region from nucleotide 632 to 829 of the Epo-R sequence (29). The primers used to identify  $\alpha$ -globin mRNA amplified the region from nucleotide 37 to 236 of the  $\alpha$ -globin sequence resulting in a 199-bp fragment (30) and the primers used to identify  $\beta$ -actin mRNA amplified the region between nucleotides 1038 and 1876 of the  $\beta$ -actin sequence resulting in a 661-bp fragment (31).

**Specific Epo-R mRNA identification by digestion products and sequence analysis.** To further confirm whether the 197-bp RT-PCR product was indeed Epo-R, the product was digested with the restriction endonuclease *Ava*II, according to the protocol of Anagnostou *et al.* (19). This digestion should produce two fragments, one of 57 and the other 140 bp. A positive control was obtained by digesting the RT-PCR product of the OCIM1 cell line with *Ava*II. Specificity of the RT-PCR product was additionally confirmed by direct sequencing of an amplified PCR product using the Taq DyeDeoxy Terminator protocol developed by Applied Biosystems (Perkin-Elmer Corp., Foster City, CA). The labeled extension products were analyzed on an Applied Biosystems Model 373 DNA sequencer.

**Immunofluorescent staining.** Representative sections from mid-trimester human spinal cords were fixed overnight at 4°C in 94% absolute ethanol/3% glacial acetic acid/3% distilled water. The tissue was processed manually and embedded in paraffin. Sections of 7  $\mu$ m were cut, mounted on drops of water, and heated to 37°C for 1 h. They were then deparaffinized in Clear-Rite-3 (Richard Allen, Richland, MI) and rehydrated in graded ethanol solutions to PBS. Nonspecific staining was blocked using 1% normal goat serum. Monoclonal anti-human Epo-R antibody (mh2er/16.5.1, mouse IgG1, affinity purified on protein A, Genetics Institute, Cambridge, MA) was added at a dilution of 1:50 and incubated for 3 h. After rinsing thoroughly in PBS, secondary antibody (goat anti-mouse IgG conjugated to fluorescein (Sigma Chemical Co., St. Louis, MO) was applied at a 1:50 dilution and incubated for 1 h. Sections were mounted in glycerol with anti-

quenching agent and viewed under epifluorescence with a Nikon FXA photomicroscope. In the negative control, nonimmune mouse serum was substituted for the primary anti-Epo-R antibody.

## RESULTS

The upper panel of Figure 1 shows the RT-PCR products obtained from the five mid-trimester fetal spinal cords. The single, anticipated, 197-bp band was amplified from RNA isolated from all five spinal cords. To determine whether circulating erythroid cells, which might be contaminating the spinal cord preparations were responsible for the Epo-R RNA, RT-PCR was performed with primers specific to human  $\alpha$ -globin (Fig. 1, middle panel). Only one spinal cord sample and OCIM1 cells showed the presence of  $\alpha$ -globin mRNA. RT-PCR was also performed using primers for  $\beta$ -actin, and in each case a single band of appropriate size was obtained (Fig. 1, lower panel).

To further confirm that the 197-bp product, resulting from RT-PCR with primers specific to Epo-R, was indeed Epo-R mRNA, we digested the product with the restriction endonuclease *Ava*II, which resulted in the expected restriction fragments of 57 and 140 bp (29) (Fig. 2). As the cytokine family

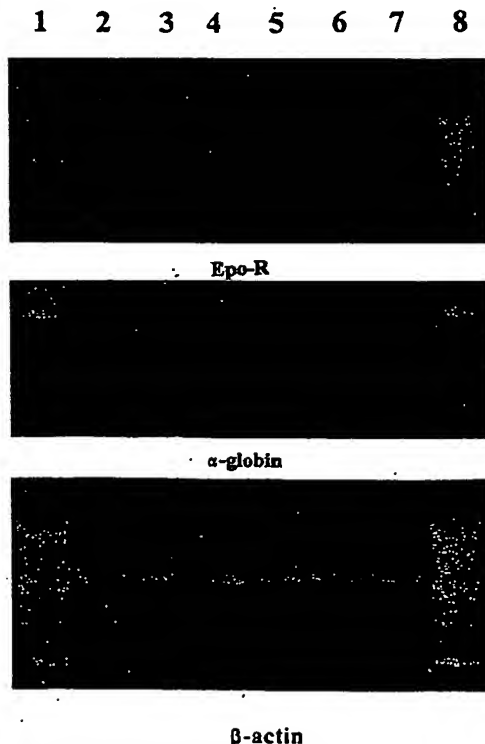


Figure 1. Lanes 1 and 8 contain 100-bp DNA markers. Lanes 2 through 6 contain RT-PCR products from 15-, 13-, 14-, 15-, and 16-wk gestation fetal spinal cords, respectively. Lane 7 contains the RT-PCR product from OCIM1 cells, as a positive control. The upper panel shows the RT-PCR products obtained using primers specific to human Epo-R (197-bp product expected). The middle panel shows the RT-PCR products resulting from primers specific to  $\alpha$ -globin (199-bp product expected), and the lower panel shows the RT-PCR products resulting from primers specific to  $\beta$ -actin (661-bp product expected).

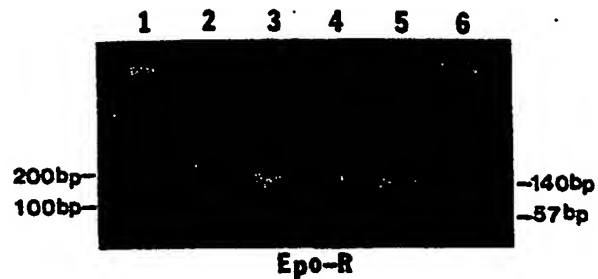


Figure 2. Specific digestion of the 197-bp Epo-R RT-PCR product with the restriction endonuclease *Ava*II, showing restriction fragments of 57 and 140 bp. Lanes 1 and 6 contain 100-bp DNA markers. Lane 2 contains the undigested RT-PCR product from human fetal spinal cord, lane 3 contains the RT-PCR product digested with *Ava*II, yielding the two smaller bands of 140 and 57 bp. Lanes 4 and 5 contain the uncut and cut products, respectively, from the positive control OCIM1 cells.

to which Epo-R belongs contains a number of sequence homologies, we obtained direct nucleotide sequence information from an amplified gene product. The results confirmed amplification between nucleotides 632 and 829 of the published Epo-R sequence (29).

Figure 3 shows the Epo-R immunostain of the fetal spinal cords. Ependymal cells enclosing the central canal express Epo-R, as demonstrated in panel A, by the red staining of these cells. The regions proximal to the anterior and posterior median sulci also are intensely immunopositive. Panel B shows the negative control.

## DISCUSSION

Approximately 8% of live births in the United States are delivered prematurely (32). These infants are at significant risk for receiving erythrocyte transfusions during their hospital stay, due initially to iatrogenic blood loss, and later to the anemia of prematurity (4, 33). Diminishing the number of transfusions to which premature infants are exposed is considered to be a worthwhile goal (33). Toward that aim, multiple, randomized, placebo-controlled, clinical trials have been conducted, and they indicate that rEpo treatment can decrease the number of transfusion needed (1-3, 5, 34). In fact, this use of rEpo has been viewed as physiologic, because preterm infants appear to have a very limited capacity to increase their serum concentrations of Epo during anemia or as a compensation for blood loss (3, 34).

The action of Epo occurs by way of its binding to specific cell-surface receptors. The Epo-R is a member of the superfamily of hematopoietic cytokine receptors, which includes receptors for: IL-2, IL-3, IL-4, IL-5, IL-6, IL-7, granulocyte/macrophage and granulocyte colony-stimulating factors, prolactin, and growth hormone. The extracellular domains of these molecules share homology in the region required for receptor binding and activation. The binding of Epo to its receptor is followed by receptor-mediated endocytosis of Epo, and involves tyrosine phosphorylation (35).

The conventional understanding has been that the action of Epo was restricted to the proliferation and differentiation of erythroid progenitor cells, because these were the cells known

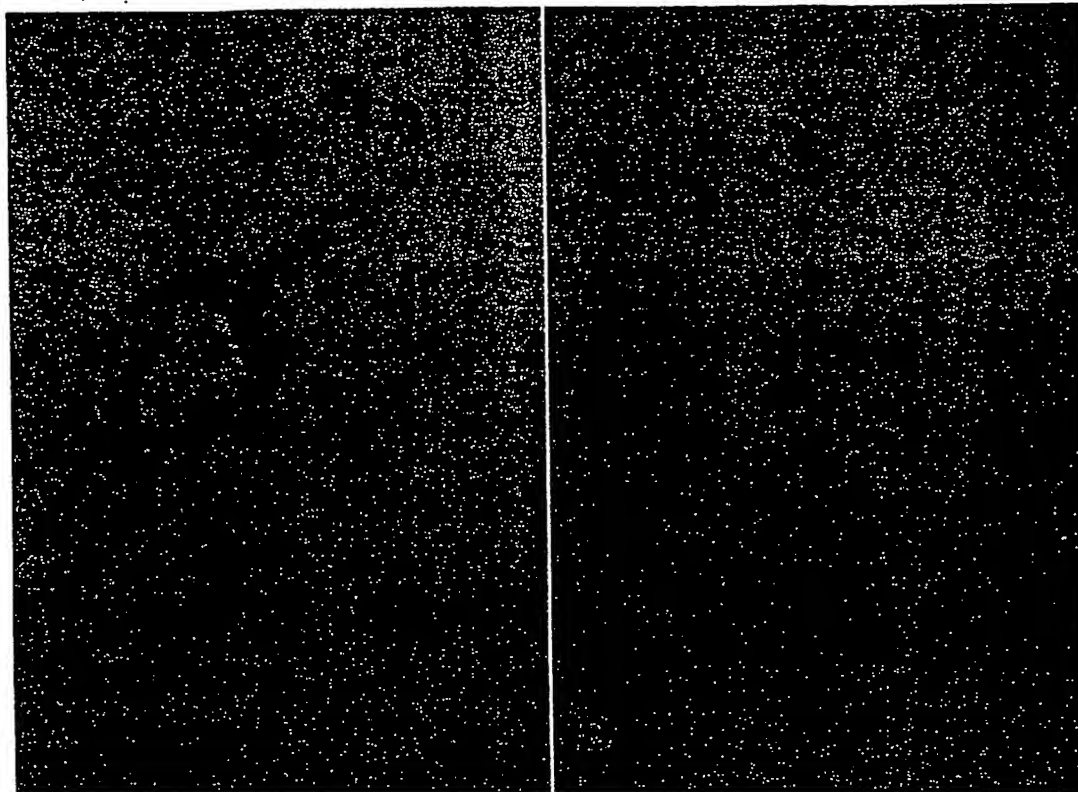


Figure 3. Immunofluorescent cytochemical stains of a spinal cord from a 17-wk gestation fetus showing (panel A) the cells to which anti-Epo-R antibody is bound. Panel B is a negative control.

to express Epo-R (12–17). Contrary to this belief, functional Epo-R have now been demonstrated on several nonerythroid tissues. Such receptors in endothelial cells obtained from multiple sources (human umbilical vein, bovine pulmonary artery, and bovine adrenal capillary) not only show mitogenic activity when stimulated by rEpo, but also stimulate the release of angiotensin-1 (36). Of particular concern are the reports of developmentally regulated, functional Epo-R on cells of neural origin (21). Indeed, previous and present studies suggest that the effects of Epo in the fetus might not be limited to erythropoiesis, as both the receptor and its ligand are present within the developing CNS during fetal development. The existence of alternatively spliced isoforms of the Epo-R is controversial, and further study will be required to know whether the receptors we identified represent alternatively spliced isoforms, or whether they are the same as the receptors found on erythroid cell lines. Although the physiologic significance of this ligand-receptor pair in the human fetal CNS is unclear, we maintain that further studies are indicated to delineate potential neurodevelopmental effects of rEpo administration for anemia of prematurity. For example, it would be important to know whether rEpo, used at doses appropriate to treat anemia of prematurity, crosses the blood brain barrier in premature human infants. Localization of Epo-R within the human brain, brainstem, and spinal cord would be interesting, and might help to direct further neurodevelopmental studies. For example, if there was a preponderance of such receptors in the reticular

activating system, one might pay particular attention to the effects of rEpo on symptoms of apnea. Such a finding might also shed light on the association (real or coincidental) of rEpo treatment with sudden infant death syndrome. It is also possible that rEpo might have beneficial neurodevelopmental effects, however, all these potential effects, good or bad, are at this point speculation, and a combination of further laboratory elucidation of the possible function of Epo within the CNS and long-term clinical studies following treated infants would answer these questions.

**Acknowledgments.** We thank Jenny Harcum, R.N., for help in obtaining specimens, and Yan Du for technical assistance.

## REFERENCES

1. Maier RF, Oblander M, Scigalla P, Linderkamp O, Duc G, Hieronimi G, Halliday HL, Versmold HT, Moriette G, Jorch G 1994 The effect of epoietin- $\beta$  (recombinant human erythropoietin) on the need for transfusion in very-low-birth-weight infants. *N Engl J Med* 330:1173–1178
2. Meyer MP, Meyer JH, Commerford A, Hann FM, Sive AA, Moller G, Jacobs P, Malan AF 1994 Recombinant human erythropoietin in the treatment of the anemia of prematurity: results of a double-blind, placebo-controlled study. *Pediatrics* 93:918–923
3. Ohls RK, Hunter DD, Christensen RD 1993 A randomized, placebo-controlled trial of recombinant erythropoietin as treatment for the anemia of bronchopulmonary dysplasia. *J Pediatr* 123:996–1000
4. Ohls RK 1995 Recombinant human erythropoietin to prevent and treat the anemia of prematurity. *Erythropoiesis* 6:35–45
5. Shannon KM, Keith III JF, Mentzer WC, Ehrenkranz RA, Brown MS, Widness JA, Gleason CA, Bifano EM, Millard DD, Davis CB, Stevenson DK, Alverson DC, Simmons CF, Brim M, Abels RI, Phibbs RH 1995 Recombinant human erythropoi-

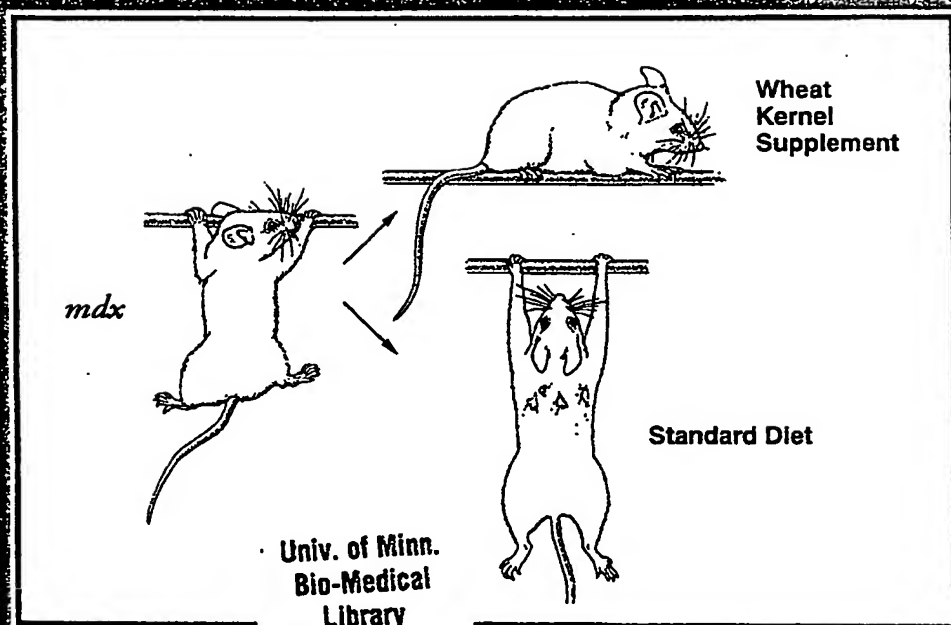
- erin stimulates erythropoiesis and reduces erythrocyte transfusions in very low birth weight preterm infants. *Pediatrics* 95:1-8
6. Christensen RD 1989 Recombinant erythropoietic growth factors as an alternative to erythrocyte transfusion for patients with "anemia of prematurity." *Pediatrics* 83:793-796
7. Shireman TI, Hilsenrath PE, Strauss RG, Widness JA, Mutnick AH 1994 Recombinant human erythropoietin vs transfusions in the treatment of anemia of prematurity. A cost-benefit analysis. *Arch Pediatr Adolesc Med* 148:582-588
8. Fein J, Hilsenrath JA, Widness RG, Strauss RG, Mutnick AH 1995 A cost analysis comparing erythropoietin and red cell transfusions in the treatment of anemia of prematurity. *Transfusion* 35:936-943
9. Hoffman HJ, Damm K, Hillman L, Krongrad E 1988 Risk factors for SIDS: results of the National Institute of Child Health and Human Development SIDS cooperative epidemiological study. *Ann NY Acad Sci* 533:13-30
10. Hoffman HJ, Hillman LS 1992 Epidemiology of the sudden infant death syndrome: maternal, neonatal, and postneonatal risk factors. *Clin Perinatol* 19:717-737
11. Emmerson AJB, Coles BJ, Stern CMM, Pearson TC 1993 Double blind trial of recombinant erythropoietin in preterm infants. *Arch Dis Child* 68:291-296
12. Mufson RA, Geisler TG 1987 Binding and internalization of recombinant human erythropoietin in murine erythroid precursor cells. *Blood* 69:1485-1490
13. Miglaccio AR, Miglaccio G, D'Andrea A, Baiocchi M, Crota S, Nicolis S, Otrolenghi S, Adamson JW 1991 Response to erythropoietin in erythroid subclones of the factor-dependent cell line 32D is determined by translocation of the erythropoietin receptor to the cell surface. *Proc Natl Acad Sci USA* 88:11086-11090
14. Sawyer ST, Krantz SB, Luna J 1987 Identification of the receptor for erythropoietin by cross-linking to Friend virus-infected erythroid cells. *Proc Natl Acad Sci USA* 84:3690-3694
15. Sawyer ST, Krantz SB, Sawada K 1989 Receptors for erythropoietin in mouse and human erythroid cells and placenta. *Blood* 74:103-109
16. Fraser JK, Lin FK, Berridge MV 1988 Expression and modulation of specific, high affinity binding sites for erythropoietin on the human erythroleukemic cell line K562. *Blood* 71:104-109
17. Hoshino S, Teramura M, Takahashi M, Motoji T, Oshimi K, Ueda M, Mizoguchi H 1989 Expression and characterization of erythropoietin receptors on normal human bone marrow cells. *Int J Cell Cloning* 7:156-167
18. Anagnostou A, Lee ES, Kessimian N, Levinson R, Steiner M 1990 Erythropoietin has a mitogenic and positive chemotactic effect on endothelial cells. *Proc Natl Acad Sci USA* 87:5978-5982
19. Anagnostou A, Liu Z, Steiner M, Chin K, Lee ES, Kessimian N, Noguchi CT 1994 Erythropoietin receptor mRNA expression in human endothelial cells. *Proc Natl Acad Sci USA* 91:3974-3978
20. Masuda S, Nagao M, Takahata K, Konishi Y, Gallyas FJ, Tabira T, Sasaki R 1993 Functional erythropoietin receptor of the cells with neural characteristics. *J Biol Chem* 268:11208-11216
21. Liu Z-Y, Chin K, Noguchi C 1994 Tissue specific expression of human erythropoietin receptor in transgenic mice. *Dev Biol* 166:159-169
22. Yasuda Y, Nagao M, Okano M, Masuda S, Sasaki R, Konishi H, Tanimura T 1993 Localization of erythropoietin and erythropoietin-receptor in postimplantation mouse embryos. *Dev Growth Differ* 35:711-722
23. Juul SE, Hargum J, Li Y, Christensen RD 1996 Erythropoietin is present in the cerebrospinal fluid of neonates. *Pediatr Res* 39:288A(abstr)
24. Masuda S, Okano M, Yamagishi K, Nagao M, Ueda M, Sasaki R 1994 A novel site of erythropoietin production. *J Biol Chem* 269:19488-19493
25. Tan CC, Eckardt K-U, Firth JD, Ratcliffe PJ 1992 Feedback modulation of renal and hepatic erythropoietin mRNA in response to graded anemia and hypoxia. *Am J Physiol* 263:F474-F481
26. Birkfalvi A, Han ZC 1994 Angiogenic factors are hematopoietic growth factors and vice versa. *Leukemia* 8:523-529
27. Konishi Y, Chui D-H, Hirose H, Kunishita T, Tabira T 1993 Trophic effect of erythropoietin and other hematopoietic factors on central cholinergic neurons *in vitro* and *in vivo*. *Brain Res* 609:29-35
28. Chomczynski P, Sacchi N 1987 Single-step method of RNA isolation by acid guanidinium thiocyanate-phenol-chloroform extraction. *Anal Biochem* 162:156-159
29. Winkelman JC, Penny LA, Deaven LL, Forget BG, Jenkins RB 1990 The gene for the human erythropoietin receptor: analysis of the coding sequence and assignment to chromosome 19p. *Blood* 76:24-30
30. Wilson JT, Wilson LB, Reddy VB 1988 Nucleotide sequence of the coding portion of human alpha globin messenger RNA. *J Biol Chem* 263:2807-2815
31. Nakajima-Iijima S, Hamada H, Reddy P, Kakunaga T 1985 Molecular structure of the human cytoplasmic  $\beta$ -actin gene: interspecies homology of sequences in the introns. *Proc Natl Acad Sci USA* 82:6133-6137
32. Behrman RE, Shiono PH 1992 Neonatal risk factors. In: Fanaroff AA, Martin RJ (eds) *Neonatal-Perinatal Medicine—Diseases of the Fetus and Infant*. Mosby, St. Louis
33. Strauss RG 1995 Red blood cell transfusion practices in the neonate. *Clin Perinatol* 22:641-655
34. Ohls RK, Osborne KA, Christensen RD 1995 Efficacy and cost analysis of treating very low birth weight infants with erythropoietin during their first two weeks of life: a randomized, placebo controlled trial. *J Pediatr* 126:421
35. Dallman PR (ed) 1993 *Anemia of prematurity: the prospects for avoiding blood transfusion by treatment with recombinant human erythropoietin*. In: *Advances in Pediatrics*. Mosby, St. Louis
36. Carlini RG, Dusso AS, Obialo CI, Alvarez UM, Rothstein M 1993 Recombinant human erythropoietin (rHuEPO) increases endothelin-1 release by endothelial cells. *Kidney Int* 43:1010-1014



# PEDIATRIC RESEARCH



OFFICIAL PUBLICATION OF AMERICAN PEDIATRIC SOCIETY  
EUROPEAN SOCIETY FOR PEDIATRIC RESEARCH / SOCIETY FOR PEDIATRIC RESEARCH



9 4.96

SEPTEMBER 1996 VOLUME 40 NUMBER 3

## Tissue Specific Expression of Human Erythropoietin Receptor in Transgenic Mice

ZI-YAO LIU, KYUNG CHIN, AND CONSTANCE TOM NOGUCHI

Laboratory of Chemical Biology, NIDDK, National Institutes of Health, Bethesda, Maryland 20892

Accepted July 29, 1994

We have made transgenic mice using the human erythropoietin receptor (hEpoR) encoding gene contained within a 15-kb DNA fragment. The transgenic mice that incorporated the hEpoR transgene into the genome were analyzed for tissue specific expression of hEpoR mRNA using reverse transcriptase and DNA amplification. In the control animals, endogenous EpoR transcripts were identified in bone marrow and spleen; no transcripts were detected in heart, kidney, liver, or brain. In the transgenic mice, hEpoR transcripts were detected in bone marrow and spleen but not in heart, kidney, or liver, suggesting that the transgene contains sufficient genetic information to direct appropriate expression in hematopoietically active tissues. The hematological parameters of the transgenic mice were within normal limits, consistent with the relatively low level of hEpoR transcripts detected. Surprisingly, hEpoR transcripts but not mouse EpoR transcripts were detected in the brains of the transgenic mice. Brain hEpoR transcripts were observed in all transgenic mice assayed, indicating that transgene expression in the brain did not result from the effects of aberrant integration sites. Comparable expression of the transgene was also observed in the embryonic brain. Interestingly, we observed significant expression of the endogenous EpoR gene in the early embryonic brain (Day 10) of normal mice at levels comparable to that observed in the adult spleen and bone marrow. The level of endogenous EpoR expression in the brain decreased during embryonic development to nondetectable levels prior to birth preceding the decrease of endogenous EpoR expression in the fetal liver, while hEpoR expression in the brains of transgenic mice persisted throughout embryonic development into adulthood. These data suggest that the hEpoR transgene contains appropriate regulatory sequences to direct tissue specific expression in tissues associated with hematopoietic activity and in the embryonic brain, but lacks the control elements to provide levels of expression comparable to that of the endogenous gene or to selectively silence brain expression in the adult mouse. © 1994 Academic Press, Inc.

### INTRODUCTION

Erythropoietin (Epo), the primary regulator of erythropoiesis, stimulates the proliferation and differentia-

tion of erythroid cells by binding to a specific receptor, the erythropoietin receptor (EpoR), on the surface of erythroid precursors (Yousoufian *et al.*, 1993). The number of surface receptors on the cell surface increases from less than 200 and peaks at about 1100 as erythroid precursors mature from the BFU-E to the CFU-E stage and then decreases with terminal differentiation (Broudy *et al.*, 1991). EpoR are not found on mature erythrocytes. Binding of Epo to its receptor is followed by receptor-mediated endocytosis of erythropoietin and other molecular events including activation of the erythroid transcription factor, GATA-1, and expression of globin genes (Chiba *et al.*, 1991).

The murine and human EpoR cDNAs encode a polypeptide of 507 and 508 amino acids, respectively, with a single transmembrane domain (D'Andrea *et al.*, 1989; Winkelmann *et al.*, 1990; Jones *et al.*, 1990). Although erythropoietin binding to the EpoR stimulates tyrosine kinase activity, the cytoplasmic region of the EpoR contains no tyrosine kinase domain. The cytoplasmic domain does contain a negative-control domain in the C-terminal region (Yoshimura *et al.*, 1990; D'Andrea *et al.*, 1991), which functions *in vitro* as well as *in vivo* (de la Chapelle *et al.*, 1993). The extracellular domain contains regions homologous to several other cytokine receptors such as receptors for IL2, IL3, IL4, IL6, IL8, and IL7, GM-CSF, G-CSF, prolactin, neural ciliary factor, and growth hormone (Yousoufian *et al.*, 1993). The homology region includes a domain with four cysteines and another region containing a Trp-Ser-X-Trp-Ser amino acid motif close to the transmembrane domain which is required for receptor binding and activation (Yoshimura *et al.*, 1992; Quelle *et al.*, 1992; Miura *et al.*, 1993). Together, these receptors make up a superfamily of hematopoietic cytokine receptors.

The human EpoR gene includes a coding region separated into eight exons (Noguchi *et al.*, 1991; Maoouche *et al.*, 1991; Penny and Forget, 1991). The coding region shares about 80% homology with the murine EpoR, but little homology exists outside of this region (Yousoufian *et al.*, 1990; Kuramochi *et al.*, 1990). Both the human



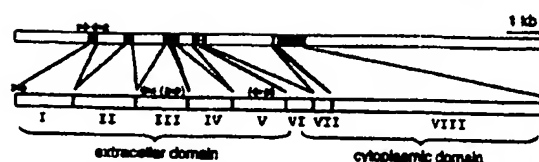


FIG. 1. Human erythropoietin receptor (hEpoR) gene. The 15-kb genomic fragment encoding hEpoR contains 2 kb 5' and 7 kb 3' of flanking DNA. The coding region is separated into eight exons with the single transmembrane domain encoded in exon 6 and the cytoplasmic domain encoded primarily in exons 7 and 8. The arrows 1 and 2 indicate the location of the primers used to detect the presence of the hEpoR transgene. Arrows 3 and 4 indicate the location of primers used to detect hEpoR mRNA. For the detection of the endogenous murine EpoR mRNA, specific primers located at positions 5 and 6 (in parentheses) and at positions 3 and 4 were selected.

and murine EpoR genes contain binding sites for the erythroid GATA-1 transcription factor (AGATAA) and the ubiquitous Sp1 transcription factor (CCGCC), immediately 5' of the transcription start site, but do not contain typical TATA or CAAT sequences in the vicinity of the cap site. The homology between the murine and human EpoR genes does not appear to extend to the IVS sequences or to the 5' region beyond the GATA-1 consensus binding region. We have previously shown that a fragment containing about 600 bp 5' of the transcription start site of the human EpoR gene could direct correctly initiated transcription *in vitro* (Noguchi *et al.*, 1991). Transfection assays with promoter/reporter gene constructs have also been used to characterize transcription activation of the EpoR gene (Noguchi *et al.*, 1992; Maouche *et al.*, 1994; Youssoufian, 1994).

Construction of transgenic mice containing the hEpoR gene provides a means for determining *cis*-acting control regions which confer tissue and developmental stage specificity of hEpoR gene expression. In the present study transgenic mice were produced using the entire hEpoR coding region with 5' and 3' flanking regions (Noguchi *et al.*, 1991). Tissues were analyzed to assess tissue specific transgene expression and compared with expression of the endogenous EpoR gene. Multiple transgenic founders or breeding lines were examined to avoid ambiguities due to possible integration site dependency. The data indicate that the 15-kb cloned hEpoR gene contains sufficient information to direct tissue specific expression in hematopoietically active tissues, but lacks regulatory elements which provide high levels of expression compared with the endogenous gene as well as elements which control brain specific developmental expression.

#### MATERIALS AND METHODS

**DNA construct.** The 15-kb human DNA fragment containing the EpoR-encoding gene (Fig. 1) included 2-kb 5' and 7-kb 3' DNA flanking the EpoR coding region (Noguchi *et al.*, 1991). This 15-kb DNA fragment was isolated from bacteriophage vector EMBL-3 SP6/T7 by digestion with restriction enzyme S81, purified by gel electrophoresis followed by electroelution and on an elutip-D column (Schleicher and Schuell, Inc.), and dialyzed into injection buffer (10 mM Tris-HCl, pH 7.5, 0.1 mM EDTA).

**Generation of transgenic mice.** DNA was introduced into the male pronucleus of fertilized mouse oocytes by

TABLE 1  
PRIMERS FOR PCR ANALYSES

Primer set	Sense (5'-3')	Antisense (5'-3')	Fragment size
hEpoR-gene	GAT CTG CCA CTT AGA GGC CGG TGG TCG GGA AGG GCC TGG TCA GCT GCG	CCT GCA GGC TCC AGC GTA GCG GTC CAC ACG CAG CTC ATC CTT ACC TTT CC	808
hEpoR-cDNA	ACC ACC TCG GGG CGT CCC TCT	AGC TTC CAT GGC TCA TCC	285
mEpoR-gene	GCG TGA GCA CTT GCC CAG GGT AAC AAG CAG CAG GTC AGT GC	ATG GGT TGG ATC CCC AGA ACC ACC AAA ATT GCA TGC ATG T	372
mEpoR-cDNA1	GGT TCT CCT CGC TAT CAC CGC ATC	TGG AAC AGC GAA GGT GTA GCG CGT	278
mEpo-cDNA2	AAA CTC AGG GTC CCC CTC TGG CCT	GAT GCG GTG ATA GCG AGG AGA ACC	376
hEpoR-gene-std	CCT GTT CAG CTG CGT TAG CCA GGT GCA GTG	GCT CAT CCT TAC OCT TTG CTT GTG GCC CTG GAC AGG T	412
hEpoR-cDNA-std	GCG TCC CTC TAG AGT TGC GCG T	TGG CTC ATC CGC TAG GCG TCA G	390
mEpoR-gene-std	CAG CAG GTC AGT GCC ACT TGC CAC TGT G	AAT TGC ATG CAT GTA CCA ACA CAC CCA G	446
mEpoR-cDNA-1-std	TAT CAC CGC ATC AAA CTC AGG GTG	GGT GTA GCG CGT CCT CCG TCA CCT	394
mβ-actin1	CCC CTG AAC OCT AAG GCC AAC CGT G	GCC AGT GGC CAT CTC CTG CTC GAA G	366
mβ-actin2	CCC CTG AAC OCT AAG GCC AAC CGT G	ACC ACC AGA CAA CAC TGT GTT GGC	581

Note. Fragment sizes when used in quantitative PCR reaction are 478, 411, 498, and 418 when using the hEpoR-gene, hEpoR-cDNA, mEpoR-gene, and mEpoR-cDNA1 primer sets, respectively.

microinjection. Approximately 2 to 5  $\mu$ l of DNA solution (1 to 5  $\mu$ g/ml) was injected to each fertilized embryo at the one cell stage. Incorporation of the transgene was identified by PCR screening of genomic DNA isolated from pieces of tail from each mouse tested. PCR primers were chosen from the region 5' of the start of transcription and within IVS 1 with little or no homology between the human and murine sequences (Table 1). Primers specific for the murine EpoR gene were used for a positive control for PCR (Table 1).

**cDNA preparation and PCR analysis.** After anesthesia with avertin, mice were sacrificed and tissues were harvested. Perfusion through the left ventricle with PBS was used to remove as much blood as possible from tissues. Messenger RNA was extracted and purified from bone marrow, spleen, brain, heart, kidney, and liver obtained from both normal and transgenic mice. Tissues were homogenized to a uniform suspension, diluted with 2 vol of 10 mM Tris-HCl, pH 7.4, 1 mM EDTA (TE), centrifuged, and mRNA separated from the supernatant on an oligo(dT)-cellulose Spun Column (Pharmacia LKB Biotechnology). The total amount and concentration of mRNA were determined by spectrophotometry (O.D. at 260 nm) and confirmed by gel electrophoresis. An aliquot of 0.5 to 1.0  $\mu$ g of mRNA in water treated with diethyl pyrocarbonate was used for cDNA preparation by reverse transcription (Gubler and Hoffman, 1988). Transcription of mRNA to cDNA was carried out using oligo(dT)<sub>18</sub> primers and avian myeloblastoma virus (AMV) reverse transcriptase (Boehringer Mannheim) in a total reaction volume of 20  $\mu$ l in buffer containing 50 mM Tris-HCl, pH 8.5, 8 mM MgCl<sub>2</sub>, 30 mM KCl, 0.01 mM DTT, 8U RNase inhibitor (Boehringer Mannheim), 1  $\mu$ M each dNTP, and 40 U AMV reverse transcriptase. The reaction was incubated at 42°C for 60 min. Products from the reverse transcription reaction were aliquoted and used directly for PCR analysis or frozen at -70°C.

Primers for PCR were chosen to give specific products for the hEpoR gene, hEpoR cDNA, murine EpoR gene, murine EpoR cDNA, and murine  $\beta$ -actin (Table 1). Primers to detect hEpoR cDNA from tissues of transgenic mice were selected from exon 1 (sense) and exon 3 (antisense); for murine EpoR, one pair of primers was selected from exon 2 (sense) and exon 5 (antisense) and a second pair of primers was chosen from similar regions for detection of hEpoR cDNA; for  $\beta$ -actin, primers were selected to give two different sizes of PCR products. PCR reactions were carried out using Ampli Taq DNA polymerase and Stoffel fragment (Perkin-Elmer Cetus) at a MgCl<sub>2</sub> concentration of 3.0 mM in a reaction volume of 50  $\mu$ l. The DNA thermal cycler was programmed for 30 to 35 cycles (94°C for 1 min, 55°C for 2 min and 72°C for 3 min).

**PCR quantitation.** Competitive PCR was used for quantitation of EpoR mRNA and to estimate transgene copy number. Internal standards were generated for each primer set by inserting a DNA fragment from elsewhere in the gene between the two specific primers. The standard for hEpoR cDNA was designed to give a PCR product distinguishable in size (418 bp) from the hEpoR cDNA (265 bp). This standard was generated by insertion of a cDNA fragment extending from exon 3 to exon 5 using the primer set, hEpoR-cDNA-std (Table 1). Standards for human and murine genomic EpoR and murine EpoR cDNA were similarly constructed using primer sets hEpoR-gene-std, mEpoR-gene-std, and mEpoR-cDNA1-std (Table 1). The PCR conditions were similar to that described above with reactions containing [ $\alpha$ -<sup>32</sup>P]dCTP and 1  $\mu$ l of serial dilutions of standard. Resultant PCR fragments (specific and standard) were analyzed by gel electrophoresis and radioactive counting of bands corresponding to sample (specific fragment) and competitor (standard). The concentration of the standard at which the intensity of the sample band and standard band are expected to be equal is used to determine the amount of sample present relative to the amount of standard.

**Hematological parameters.** Blood was analyzed using a Coulter Counter (Coulter Counter, Inc.) and a Sysmex R-1000 (TOA Medical Electronics (U.S.A.), Inc.) for red blood cell (RBC), white blood cell (WBC), platelet, and reticulocyte counts. Hemoglobin was determined using Drabkin's solution (Sigma) and spectrophotometry (540 nm). Hematocrit was determined by microcentrifugation.

**Embryo preparation.** Embryos were taken from pregnant mice after gestation of 10, 12, 14, 16, and 18 days and dissected using stereo microscopy. Tissues (brain and liver) were immediately frozen in liquid nitrogen and prepared for mRNA extraction as described above. Breeding of a male mouse homozygous for the transgene was used to obtain embryos containing the transgene.

## RESULTS

### Transgenic Mice

We had previously cloned and sequenced the erythropoietin receptor gene from a human placental genomic library (Noguchi *et al.*, 1991). The 15-kb genomic DNA fragment containing the human EpoR with 2 kb of 5' flanking sequence and 7 kb of 3' flanking sequence (Fig. 1) was used to produce transgenic mice. To determine successful incorporation of the hEpoR transgene into the mouse genome, DNA was prepared from pieces of tail taken from each mouse to be tested. Presence of hEpoR in the mouse genome was determined by PCR analysis (Fig. 2). Primers for PCR screening of the

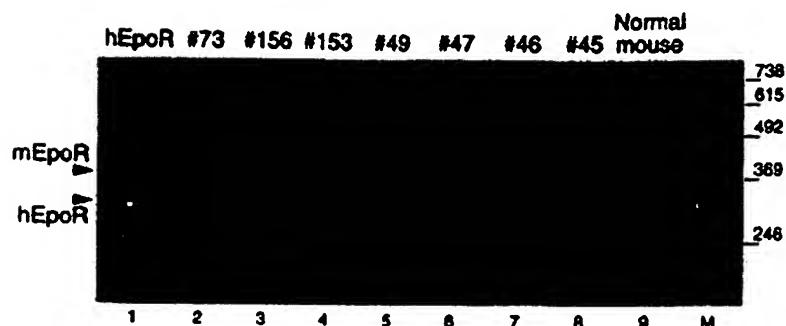


FIG. 2. Detection of hEpoR transgene in genomic DNA isolated from mouse tails. The control lanes (hEpoR and normal mouse) indicate the size of the expected PCR product from the hEpoR transgene or endogenous murine EpoR gene using specific primers for hEpoR or murine EpoR, respectively. PCR analysis demonstrates the presence of the transgene in mice 73, 156, 49, 47, and 45. Lane M is the marker lane.

transgene were selected from a region within the hEpoR with low homology to the murine EpoR in the 5' promoter region and IVS1 region and produced a specific PCR product of 303 bp (Table 1) from genomic DNA prepared from mice with successful incorporation of the transgene. Primers specific for the mouse EpoR gene were also used in PCR analysis as a control and produced a specific PCR product of 372 bp in all the mice tested (Fig. 2). The transgene was detected in 12 live births resulting from initial transplantation of oocytes injected with the transgene. Mice 47, 45, and 49 were chosen for further breeding to obtain progeny for further analysis.

#### Hematological Parameters

Hematological parameters were measured in both normal and transgenic mice. The six founders examined exhibited similar hematologic profiles as normal mice (Table 2). We found that the RBC count, WBC count, hematocrit, and hemoglobin of hEpoR transgenic mice were within normal limits (Table 1).

#### Tissue Specific Expression for EpoR

Expression of the endogenous murine EpoR gene was determined in normal and transgenic mice by mRNA extraction, reverse transcription, and PCR analysis. Tissues from spleen, liver, kidney, heart, brain, and bone

marrow were harvested and mRNA extracted. cDNA was produced from mRNA using an oligo(dT)<sub>18</sub> primer and reverse transcriptase. Specific primers for murine EpoR cDNA taken from exon 3 (sense) and exon 5 (antisense) (Table 1) were used to determine the presence of murine EpoR cDNA generated from mRNA obtained from the various tissues (Fig. 3). A mouse EpoR-specific PCR product of 372 bp was detected in spleen and bone marrow, both tissues with hematopoietic activity. No mouse EpoR-specific PCR product was detected in tissues lacking hematopoietic activity including liver, kidney, heart, and brain. Primers specific for  $\beta$ -actin (specific PCR product of 581 bp) was used in coamplification with the mouse EpoR to provide an indication of the relative amounts of mRNA used in the assay. This pattern of expression for the endogenous murine EpoR gene was observed in all normal (six mice) and all transgenic animals tested. Transgene expression was not observed in the thymus even after phenylhydrazine treatment of the transgenic mouse (data not shown).

Tissue-specific expression of the transgene was determined for hEpoR transgenic mice using similar PCR assays and the primers indicated in Table 1. Figure 4 (left) illustrates the results from transgenic mouse 156. As with the expression of the endogenous EpoR, expression of the transgene was detected in spleen and bone marrow, but not in heart, kidney, and liver. Surprisingly,

TABLE 2  
HEMATOLOGICAL PARAMETERS OF hEpoR TRANSGENIC MICE

	RBC (10 <sup>6</sup> / $\mu$ l)	WBC (10 <sup>3</sup> / $\mu$ l)	RET (%)	HCT (%)	Hb (g/dl)
Normal (6)	7.7 $\pm$ 1.1	1.8 $\pm$ 0.8	2.9 $\pm$ 1.3	40.0 $\pm$ 3.6	12.5 $\pm$ 0.8
Transgenic (4)	7.7 $\pm$ 1.0	2.5 $\pm$ 1.0	4.2 $\pm$ 1.3	39.0 $\pm$ 6.0	13.2 $\pm$ 0.9

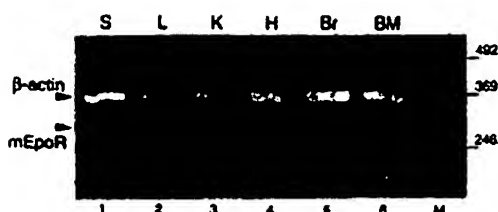


FIG. 3. Tissue-specific expression of murine EpoR transcripts. PCR analysis of mRNA from spleen, liver, kidney, heart, brain, and bone marrow (lanes 1, 2, 3, 4, 5, and 6, respectively) harvested from a normal mouse was carried out using primers corresponding to mEpoR-cDNA1 (Table 1) to detect tissue specific expression of the endogenous murine EpoR gene (mEpoR). The mEpoR PCR product was detected in spleen and bone marrow. As a control, primers corresponding to mβ-actin1 (Table 1) were selected for coamplification of murine β-actin. Lane M is the marker lane.

hEpoR transcripts were also detected in the adult brain. Restriction enzyme digestion was used to confirm that the expected PCR product provided the appropriate digestion pattern predicted from the hEpoR sequence. The PCR products were further analyzed by blot hybridization and only the fragment of the expected size hybridized to a  $^{32}$ P-labeled probe specific for hEpoR cDNA. To eliminate the possibility that expression of the transgene in the adult brain was a consequence of the site of transgene integration, four additional transgenic mice (Nos. 8, 30, 33, and 73) derived from different microinjections of the transgene into oocytes were examined (Fig. 5). For these mice, analysis of mRNA prepared from various tissues indicated that the hEpoR transcripts could be detected in hematopoietically active tissues, spleen, and bone marrow, but not in liver, kidney, or heart. Again, hEpoR transcripts were also detected in the adult brain (Fig. 5). The tissue specificity

of transgene expression for these mice (Fig. 5) and the remaining six independent founders or lines of hEpoR transgenic mice generated (data not shown) are similar to the results observed for transgenic mouse 156 (Fig. 4).

The level of transgene expression was determined using quantitative PCR, in which the PCR amplification for human EpoR was carried out in presence of specific standard DNA (Fig. 6). The standards were designed to be coamplified to give a PCR product distinguishable in size from the human EpoR cDNA product (Table 1). When the standard is added in greater or lesser amounts than the level of hEpoR cDNA present, DNA amplification results in PCR products corresponding predominantly to the standard or hEpoR cDNA PCR product, respectively. The PCR products corresponding to the standard and hEpoR cDNA are equal when the amount of standard added is the same as the amount of EpoR cDNA present. Quantitation of EpoR cDNA was carried out by adding ( $\alpha$ - $^{32}$ P)dCTP and varying amounts of the standard. Determination of the radioactivity incorporated into the specific PCR product corresponding to EpoR cDNA and to the standard was used to determine the amount of EpoR cDNA present in the reaction mix (Fig. 6). The level of transgene expression in the adult brain was found to vary from  $4.7 \times 10^{-4}$  to  $17.6 \times 10^{-4}$  ng/ $\mu$ g mRNA (Table 3). The hEpoR transgene expression in bone marrow ( $3.8 \times 10^{-3}$  ng/ $\mu$ g mRNA) and spleen ( $3.0 \times 10^{-3}$  ng/ $\mu$ g mRNA) was about 3 to 10 times higher than that observed in the adult brain but was as low as one log unit less than the levels of endogenous murine EpoR expression in bone marrow ( $1.6 \times 10^{-2}$  ng/ $\mu$ g mRNA) and spleen ( $8.0 \times 10^{-2}$  ng/ $\mu$ g mRNA) (Table 4). Quantitative PCR of genomic DNA from the transgenic mice indicated that the estimated copy number was low (about 5 or less).

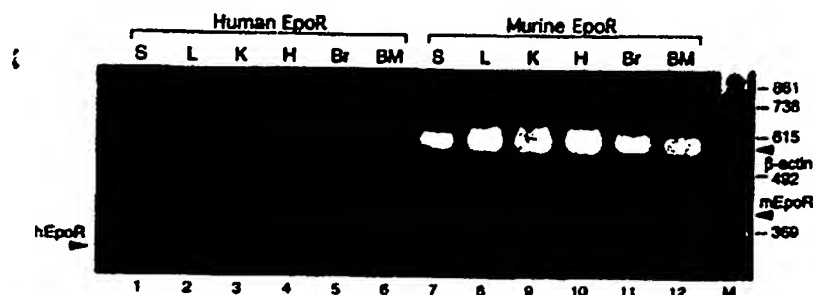


FIG. 4. Analysis of tissue specific expression of hEpoR and murine EpoR transcripts in transgenic mouse 156. PCR analysis of mRNA from spleen, liver, kidney, heart, brain, and bone marrow were analyzed for expression of the hEpoR transgene (lanes 1, 2, 3, 4, 5, and 6, respectively) and for expression of the endogenous murine EpoR gene (lanes 7, 8, 9, 10, 11, and 12, respectively). Primer sets mEpoR-cDNA2 and mβ-actin2 (Table 1) were used to give PCR products (mEpoR and β-actin, respectively) differing in size from the product hEpoR obtained with primer set hEpoR-cDNA (Table 1). The hEpoR PCR fragment is detected in spleen, brain, and bone marrow, and the mEpoR PCR fragment is detected in spleen and bone marrow. Lane M is the marker lane.

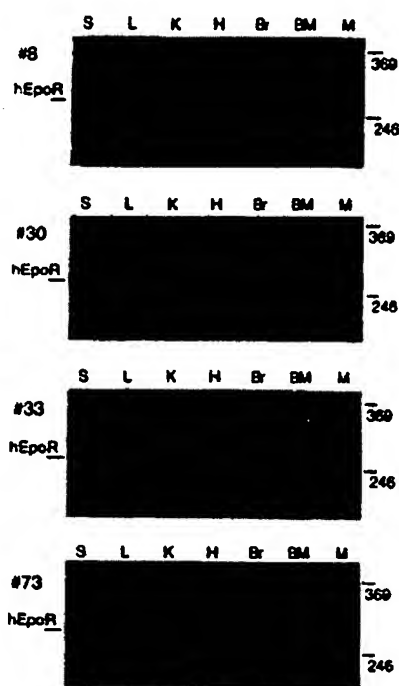


FIG. 5. Tissue-specific expression of hEpoR in transgenic mice. PCR analysis of mRNA from spleen, liver, kidney, heart, brain, and bone marrow (S, L, K, H, Br, and BM, respectively) harvested from transgenic mice 8, 30, 33, and 73 representing different lines was used to determine the presence of hEpoR transcripts. PCR fragments corresponding to hEpoR transcripts were detected in spleen, brain, and bone marrow in all transgenic animals analyzed. Lane M is the marker lane.

#### Developmental Expression of Endogenous EpoR

The developmental expression of the endogenous murine EpoR gene was examined in embryos at Days 10, 12, 14, 16, and 18 of development (relative to day zero when the vaginal plug appears in the pregnant female). In the fetal liver, which is known to be the hematopoietic organ during development, endogenous EpoR transcripts were detectable at Day 12 (when the liver could be identified by microscopic dissection) and later. The level of expression decreased with development and was no longer detectable at birth or in the adult mouse (Fig. 7). Quantitative PCR analysis of murine EpoR transcripts was used to determine the amount of endogenous transcript present in the fetal liver during development (Table 4). The highest level of expression of the endogenous EpoR gene at  $7.0 \times 10^{-1}$  ng/ $\mu$ g mRNA was detected in the fetal liver at Day 12 which was one log unit or greater than the levels detected in the adult tissues with hematopoietic activity (Table 4). The murine EpoR expression in the fetal liver decreased with increasing embryonic age

to  $5.0 \times 10^{-5}$  ng/ $\mu$ g mRNA at Day 18 and the endogenous EpoR gene appeared to be inactive after birth.

Surprisingly, endogenous murine EpoR gene expression was detected in the fetal brain. At Day 10, the level of murine EpoR expression in the brain was  $4.7 \times 10^{-2}$  ng/ $\mu$ g mRNA, greater than the level of endogenous EpoR transcripts detected in adult bone marrow or adult spleen (Table 4). EpoR expression in the brain continued to decrease with development and was no longer detected at Day 16 or later. The peak level of EpoR expression detected in the fetal brain (Day 10) was at least one log unit lower than the peak level of expression detected in the fetal liver (Day 12) and was generally at least two log units lower than the level of expression in the fetal liver at a comparable age.

#### Expression of hEpoR Transgene in Fetal Brain

Examination of embryonic brain tissue of transgenic mice revealed the presence of hEpoR mRNA throughout development. Quantitation of the level of transgene expression indicated that the activity of the transgene in brain remained steady from the early embryonic stage (Day 10) through birth and during adulthood at about  $1 \times 10^{-3}$  ng/ $\mu$ g mRNA (Table 4). This level is more than one and two orders of magnitude lower than the peak level detected for the endogenous EpoR in the embryonic mouse brain at 10 days and in the embryonic mouse liver at Days 12 and 14 (Figs. 7 and 8), respectively. The persistent expression of the hEpoR transgene in the embryonic and adult brain suggests that the transgene lacks the appropriate control elements necessary to regulate hEpoR expression in the developing brain.

#### DISCUSSION

We have made transgenic mice using the hEpoR gene contained within a 15-kb DNA fragment with 2 kb of 5' and 7 kb of 3' flanking sequence (Noguchi *et al.*, 1991). Examination of tissue-specific RNA demonstrated that murine EpoR mRNA corresponding to expression of the endogenous EpoR gene could be detected in spleen and bone marrow, the expected hematopoietically active tissues, but not in liver, kidney, heart, and brain (Fig. 3) or thymus. RNA isolated from various tissues taken from hEpoR transgenic mice were also examined to determine the transcription activity of the hEpoR transgene. Much of the hEpoR activity was restricted to low-level-specific expression in hematopoietically active tissues. Specifically, hEpoR transcripts were observed in spleen and bone marrow, indicating that the transgene contained sufficient information to provide tissue-specific expression (Figs. 4 and 5). The expression of the EpoR gene in tissues with hematopoietic activity is likely to be related in part to the erythroid expression of GATA-1.

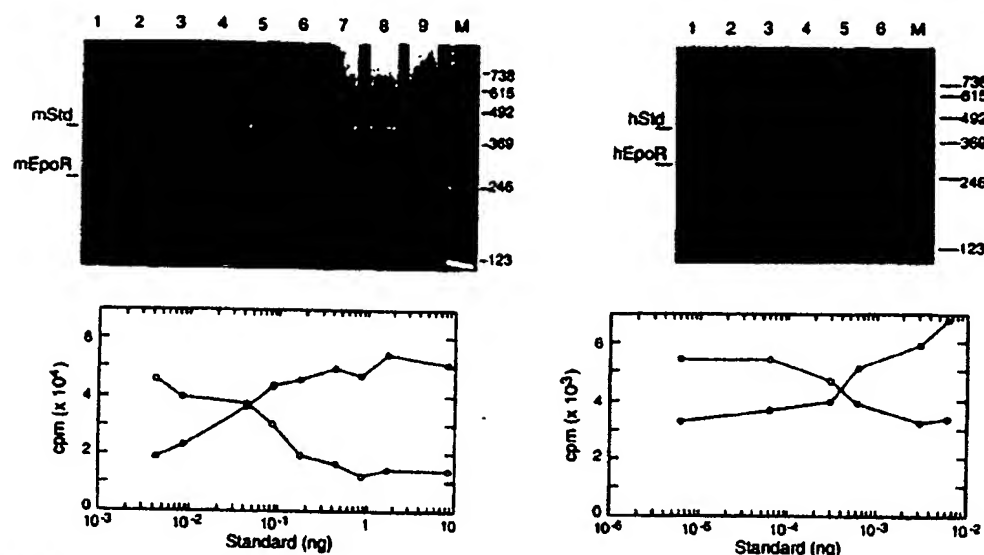


FIG. 6. Quantitation of EpoR transcripts using competitive PCR. Standards for the murine EpoR cDNA and hEpoR cDNA were constructed using primers mEpoR-cDNA-std and hEpoR-cDNA-std (Table 1), respectively. Reaction mixtures containing increasing amounts of standard and a fixed amount of cDNA made from tissue specific mRNA and  $(\alpha\text{-}^{32}\text{P})\text{dCTP}$  were analyzed using PCR amplification and primers corresponding to mEpoR-cDNA1 (left) and hEpoR-cDNA (right). Relative intensities of the appropriate PCR product were determined by the amount of  $(\alpha\text{-}^{32}\text{P})\text{dCTP}$  incorporated. The cpm (counts per minute) corresponding to the mEpoR or hEpoR PCR fragment (open circles) and to the standard (solid circles) were plotted against the amount of standard in each reaction. The point at which the two lines intersect is used to quantitate the corresponding amount of EpoR transcripts. Lane M is the marker lane.

In transfection assays, increasing GATA-1 levels transactivates transcription activity of the murine EpoR gene (Zon *et al.*, 1991; Chiba *et al.*, 1991) and the human EpoR gene (Noguchi *et al.*, 1992; Maouche *et al.*, 1994) mediated via GATA-1 binding sites in the promoter and elsewhere (Heberlein *et al.*, 1992). Although the fetal liver is the site of erythropoiesis during embryonic development, the lack of EpoR expression in the adult liver is consistent with the loss of erythropoiesis in the liver at birth. Also of interest is the fact that while Epo is produced in the adult kidney, no EpoR mRNA was detected in the kidney. The lack of endogenous and transgene expression in the adult liver, kidney, heart, and thymus suggests that the transgene contains the appropriate regu-

latory elements to silence the hEpoR gene in a tissue-specific manner.

The levels of transgene expression were about one order of magnitude less than that of the endogenous gene (Tables 3 and 4). This could be due to omission of an enhancer located more distal from the gene beyond the 2 kb 5' or 7 kb 3' of the flanking region included in the transgene construct. For example, for the  $\beta$ -globin cluster contains a locus control region (LCR) consisting of 4 DNase I hypersensitive sites located in the upstream 5' flanking region which provides high-level and site-independent expression of globin genes in transgenic mice (Fraser *et al.*, 1993). Although  $\beta$ -globin gene expression can be detected in erythroid tissues in transgenic mice without the incorporation of the LCR into the  $\beta$ -globin transgene construct, only very low levels of globin expression are observed. Inclusion of the LCR results in high level expression which can be comparable to levels of the endogenous gene in erythroid tissues depending on the construct used and developmental phase examined.

A repetitive element localized to the 1-kb 5' region of the murine EpoR which is capable of transcriptional inhibition of the murine EpoR has recently been identified (Yousoufian and Lodish, 1993). While no analogous sequence has yet been observed in the human EpoR, it is

TABLE 3  
TRANSGENE EXPRESSION IN BRAIN

Mouse ID No.	hEpoR cDNA (ng)/ $\mu\text{g}$ mRNA
120	$17.6 \times 10^{-4}$ $18.6 \times 10^{-4}$ $15.0 \times 10^{-4}$
168	$14.4 \times 10^{-4}$
94	$8.0 \times 10^{-4}$
190	$4.7 \times 10^{-4}$



TABLE 4  
QUANTITATION OF MOUSE AND HUMAN EpoR mRNA

Age*	Brain (ng)	Liver (ng)	Bone marrow (ng)	Spleen (ng)
Normal				
10 d	$4.1 \times 10^{-3}$			
12 d	$2.7 \times 10^{-3}$	$6.0 \times 10^{-1}$		
14 d	$1.0 \times 10^{-4}$	$3.0 \times 10^{-1}$		
16 d	0	$1.0 \times 10^{-2}$		
18 d	0	$2.4 \times 10^{-4}$		
Adult	0	0	$18 \times 10^{-2}$	$8.0 \times 10^{-1}$
Transgenic				
10 d	$1.2 \times 10^{-3}$			
12 d	$1.0 \times 10^{-3}$			
14 d	$1.2 \times 10^{-3}$			
16 d	$1.2 \times 10^{-3}$			
18 d	$1.3 \times 10^{-3}$			
Adult	$1.1 \times 10^{-3}$		$3.8 \times 10^{-3}$	$3.0 \times 10^{-3}$

\* Indicates age of embryos in days.

possible that the presence of such a sequence in the transgene without appropriate flanking regions could result in a low level of activity when the gene is expressed.

The hematological parameters of the transgenic mice were within normal limits (Table 2). The low level of transgene expression compared to the endogenous levels indicates that if translated into protein, the increase in the number of EpoR produced would be minimal. Furthermore, it is unclear that increasing the level of EpoR in cells already expressing EpoR would render those cells more sensitive to erythropoietin or have an adverse effect. During erythropoiesis, the early erythroid precursors, BFU-E, have a significantly lower number of

EpoR on the cell surface and do not appear to require erythropoietin for cell proliferation (Yousoufian *et al.* 1993). As these cells mature into later erythroid precursors, CFU-E, they become dependent on erythropoietin for cell proliferation and cell survival as erythropoietin appears to forestall apoptosis in these cells. In CFU-E the number of EpoR dramatically increases in excess of 1000 per cell (Broudy *et al.*, 1991). However, there is no evidence to suggest that the increase in EpoR alone renders these cells erythropoietin sensitive. In tissue culture, OCIM1 erythroleukemia cells have about 300 EpoR per cell and yet these cells are not dependent on erythropoietin for growth nor are they erythropoietin responsive (Papayannopoulou *et al.*, 1988).

The detection of hEpoR transcripts in the brain was observed in all the transgenic mice assayed (Figs. 4 and 5). Brain hEpoR transcripts were found in mice representing all 12 different integrations (founders) of the hEpoR transgene generated, indicating that this observation is not likely due to aberrant transcription resulting from site-specific integration of the transgene. Examination of expression in the embryonic brain of transgenic mice indicated that hEpoR transcripts were also detected in the brain during early embryonic development (Fig. 7). The level of hEpoR detected in the brain during embryonic development was comparable to the level detected in the adult transgenic mouse brain (Fig. 8).

The hEpoR expression in nonhematopoietic tissue is perhaps linked to transactivation of EpoR by GATA-1 (Zon *et al.*, 1991; Chiba *et al.*, 1991; Noguchi *et al.*, 1992; Maouche *et al.*, 1994) and the detection of other GATA-like proteins, GATA-2 and GATA-3, in the embryonic brain (Yamamoto *et al.*, 1990). Although GATA-1 appears to be restricted largely to hematopoietic cells (Evans and Felsenfeld, 1989; Tsai *et al.*, 1989; Martin *et al.*, 1990; Romeo *et al.*, 1990), recent data suggest that the

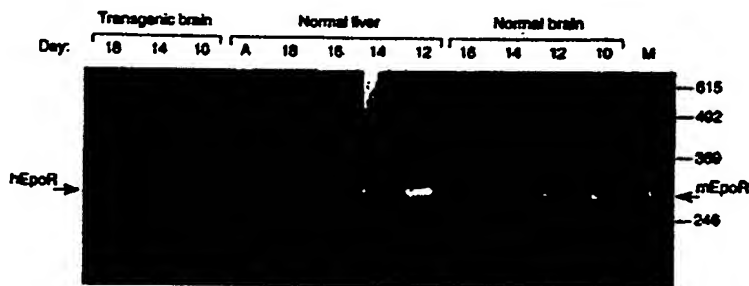


FIG. 7. Developmental expression of EpoR. Brain mRNA from normal embryos and embryos containing the hEpoR transgene varying in age from 10 days to 18 days and liver mRNA from normal embryos from 12 days to 18 days were analyzed by PCR for EpoR expression using primers hEpoR-cDNA for the hEpoR transgene and mEpoR-cDNA1 for the endogenous murine EpoR. PCR analysis of normal mouse adult liver mRNA is shown in lane A. Lane M is the marker lane.

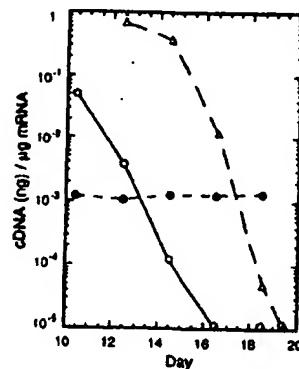


FIG. 8. Quantitation of EpoR transcripts in mouse embryos. Levels of the endogenous murine EpoR mRNA in brain (open circles) and liver (open triangles) of normal embryos beginning at Day 10 and extending to birth were quantitated by PCR. The level of transgene hEpoR expression was also determined in brain (closed circles) during embryonic development.

GATA consensus sequence, AGATAA, contained in the antisense direction in the proximal promoter for the hEpoR can bind GATA-1, GATA-2, and GATA-3 with similar specificity (Merika and Orkin, 1993; Ko and Engel, 1993).

During the early stages of gestation, erythropoiesis occurs in the yolk sac. The site of erythropoiesis shifts to the fetal liver during fetal life. In the adult, the major site of erythropoiesis is the bone marrow and spleen. Expression of the endogenous murine EpoR gene was detected in the fetal liver and at Day 12 was up to two log units greater than the level of endogenous EpoR transcripts detected in the adult hematopoietically active tissues (spleen or bone marrow) (Table 4). After Day 14, the level of endogenous murine EpoR transcripts in the fetal liver rapidly decreased with maturation and murine EpoR transcripts in the liver were no longer detected at birth (Fig. 8). During this time the proportion of CFU-E has been reported to decline from 5.9 to 0.3% with a comparable proportional decrease in the number of Epo binding sites per liver cell (Masuda *et al.*, 1992). The decreased production of EpoR mRNA in the fetal liver appears to follow the decreased production of erythroid precursors.

Examination of the fetal brain also indicated that the endogenous murine EpoR gene was active (Fig. 7). Murine EpoR RNA transcripts were detected during early (Day 10) embryonic development of the brain at a level comparable to the level observed in the adult spleen and bone marrow (Table 4), and one order of magnitude less than the maximal levels observed in the fetal liver (on Day 12). Expression of the endogenous murine EpoR gene in the embryonic brain decreased with maturation.

By Day 16, endogenous murine EpoR transcripts in the embryonic brain could no longer be detected. The presence of murine EpoR RNA transcripts in the embryonic brain suggests a possible additional role for the erythropoietin receptor beyond that usually associated with erythropoiesis. It is possible that the hEpoR transcripts detected in the adult brains of hEpoR transgenic mice mimic the normal tissue expression, which is ordinarily below detection limits. Alternatively, the persistent expression, of the hEpoR transgene in the adult brain might be due to the lack of appropriate control elements to silence hEpoR expression in the adult brain or that the regulatory elements for murine EpoR expression are different from that for hEpoR. For example, regulatory elements within IVS 1 (Heberlein *et al.*, 1992) and within a repetitive sequence in the 5' region of the EpoR encoding gene (Yousoufian and Lodish, 1993) have been suggested for the murine EpoR, but no comparable sequences have yet been identified for the human EpoR.

These data suggest that erythropoietin may have a yet unidentified function when binding to nonerythroid cells. Recently, EpoR mRNA transcripts have been found on PC12 cells with neural characteristics derived from rat adrenal medulla (Masuda *et al.*, 1993). These cells exhibit functional erythropoietin receptors on their surface. We have observed expression of hEpoR in human neuroblastoma and glial cell lines (unpublished results). Significant levels of functional erythropoietin receptors have also been detected on human umbilical vein endothelial cells and bovine pulmonary artery endothelial cells (Anagnostou *et al.*, 1990, 1994; Carlini *et al.*, 1993) and in embryonal stem cells (which lack significant amounts of GATA-1) (Heberlein *et al.*, 1992). Detection of EpoR transcripts in the embryonic or adult brain does not demonstrate that these tissues contain a functional surface receptor capable of binding erythropoietin. For example, although GATA-1 and EpoR gene expression are linked in nonerythroid 32D cells, the limitation of Epo binding to cells with erythroid characteristics suggests that other factors are also necessary for EpoR protein translocation to the cell surface in erythroid-specific lineages (Migliaccio *et al.*, 1991). Nevertheless, the fact that erythropoietin is able to stimulate the response of PC12 neuronal cells or umbilical vein endothelial cells in culture raises the possibility that the endogenous murine EpoR transcripts detected in the early embryonic brain could have a function alternative to the stimulation of erythropoiesis. That neuropoiesis and hematopoiesis may be linked is suggested by the *in vitro* stimulatory effect that neuropeptide substance P has on hematopoiesis for erythroid and granulocytic progenitors (Rameshwar *et al.*, 1993). EpoR expression may be involved in



the development of the brain, a possibility consistent with recognized the similarities of neuropoietic and hematopoietic cytokines (Bazan, 1991).

We thank H. Hiruma, E. P. Peten, and L. Striker for technical advice, Kun Shen for technical assistance, and J. G. Yuan and A. N. Schechter for helpful discussion.

#### REFERENCES

- Anagnostou, A., Lee, E. S., Kessiman, N., Levinson, R., and Steiner, M. (1990). Erythropoietin as a mitogenic and positive chemotactic effect on endothelial cells. *Proc Natl Acad Sci USA* 87, 5978-5982.
- Anagnostou, A., Liu, Z., Steiner, M., Chin, K., Lee, E. S., Kessiman, N., and Noguchi, C. T. (1994). Erythropoietin receptor mRNA expression in human endothelial cells. *Proc Natl Acad Sci USA* 91, 3974-3978.
- Arcaci, R. J., King, A. A. J., Simon, M. C., Orkin, S. H., and Wilson, D. B. (1993). Mouse GATA-4: A retinoic acid-inducible GATA-binding transcription factor expressed in endodermally derived tissues and heart. *Mol Cell Biol* 13, 2235-2246.
- Bazan, J. F. (1991). Neuropoietic cytokines in the hematopoietic fold. *Neuron* 7, 197-208.
- Broudy, V. C., Lin, N., Brice, M., Nakamoto, B., and Papayannopoulou, T. (1991). Erythropoietin receptor characteristics on primary human erythroid cells. *Blood* 77, 2583-2590.
- Carlini, R. G. (1993). Recombinant human erythropoietin (rHuEPO) increases endothelin-1 release by endothelial cells. *Kidney Int* 43, 1010-1014.
- Chiba, T., Ikawa, Y., and Todokoro, K. (1991). GATA-1 transactivates erythropoietin receptor gene, and erythropoietin receptor-mediated signals enhance GATA-1 gene expression. *Nucleic Acids Res* 19, 3843-3848.
- D'Andrea, A. D., Lodish, H. F., and Wong, G. G. (1989). Expression cloning of the murine erythropoietin receptor. *Cell* 57, 277-285.
- D'Andrea, A., Yoshimura, A., Youssoufian, H., Zon, L. I., Koo, J.-W., and Lodish, H. F. (1991). The cytoplasmic region of the erythropoietin receptor contains nonoverlapping positive and negative growth-regulatory domains. *Mol Cell Biol* 11, 1980-1987.
- de la Chapelle, A., Traskelin, A.-L., and Juvonen, E. (1993). Truncated erythropoietin receptor causes dominantly inherited benign human erythrocytosis. *Proc Natl Acad Sci USA* 90, 4495-4499.
- Evans, T. M., and Felsenfeld, G. (1989). The erythroid-specific transcription factor Eryf1: A new finger protein. *Cell* 58, 877-885.
- Fraser, P., Pruzina, S., Antoniou, M., and Grosfeld, F. (1993). Each hypersensitive site of the human beta-globin locus control region confers a different developmental pattern of expression on the globin genes. *Genes Dev* 7, 105-113.
- Gubler, U., and Hoffman, B. J. (1983). A simple and very efficient method for generating cDNA libraries. *Gene* 25, 263-289.
- Heberlein, C., Flacher, K. D., Stoffel, M., Nowock, J., Ford, A., Tessmer, U., and Stocking, C. (1992). The gene for erythropoietin receptor is expressed in multipotential hematopoietic and embryonal stem cells: Evidence for differentiation stage-specific regulation. *Mol Cell Biol* 12, 1815-1826.
- Jones, S. S., D'Andrea, A. D., Haines, L. L., and Wong, G. G. (1990). Human erythropoietin receptor: Cloning, expression, and biologic characterization. *Blood* 76, 31-35.
- Ko, L. J., and Engel, J. D. (1993). DNA-binding specificities of the GATA transcription factor family. *Mol Cell Biol* 13, 4011-4022.
- Kuramochi, S., Ikawa, Y., and Todokoro, K. (1990). Characterization of murine erythropoietin receptor genes. *J Mol Biol* 218, 567-575.
- Maouche, L., Cartron, J. P., and Chretien, S. (1994). Different domains regulate the human erythropoietin receptor gene transcription. *Nucleic Acids Res* 22, 338-346.
- Maouche, L., Tournamille, C., Hattab, C., Boffa, G., Cartron, J. P., and Chretien, S. (1991). Cloning of the gene encoding the human erythropoietin receptor. *Blood* 78, 2557-2563.
- Martin, D. I. K., Zon, L. I., Mutter, G., and Orkin, S. H. (1990). Expression of an erythroid transcription factor in megakaryocytic and mast cell lineages. *Nature* 344, 444-447.
- Masuda, S., Nagao, M., Takahata, K., Konishi, Y., Gallyas, F., Jr., Tabira, T., and Sasaki, R. (1993). Functional erythropoietin receptor of the cells with neural characteristics. *J Biol Chem* 268, 11208-11216.
- Merika, M., and Orkin, S. H. (1993). DNA-binding specificity of GATA family transcription factors. *Mol Cell Biol* 13, 3999-4010.
- Migliaccio, A. R., Migliaccio, G., D'Andrea, A., Baiocchi, M., Crotta, S., Nicolai, S., Ottolenghi, S., and Adamson, J. W. (1991). Response to erythropoietin in erythroid subclones of the factor-dependent cell line 32D is determined by translocation of the erythropoietin receptor to the cell surface. *Proc Natl Acad Sci USA* 88, 11068-11090.
- Miura, O., Cleveland, J. L., and Ihle, J. N. (1993). Inactivation of erythropoietin receptor function by point mutations in a region having homology with other cytokine receptors. *Mol Cell Biol* 13, 1788-1796.
- Noguchi, C. T., Bae, K. S., Chin, K., Wada, Y., Schechter, A. N., and Hankins, W. D. (1991). Cloning of the human erythropoietin receptor gene. *Blood* 78, 2548-2556.
- Noguchi, C. T., Chin, K., Oda, N., and Kim, I.-H. (1992). Transcription regulation of the human erythropoietin receptor gene. *Blood* 80(Suppl. 1), 152a.
- Papayannopoulou, T., Nakamoto, B., Kurachi, S., Tweeddale, M., and Mesner, H. (1988). Surface antigenic profile and globin phenotype of two new human erythroleukemia lines: Characterization and interpretations. *Blood* 72, 1029-1038.
- Penny, L. A., and Forget, B. G. (1991). Genomic organization of the human erythropoietin receptor gene. *Genomics* 11, 974-980.
- Quelle, D. E., Quelle, F. W., and Wojchowski, D. M. (1992). Mutations in the WSAWSE and cytosolic domains of the erythropoietin receptor affect signal transduction and ligand binding and internalization. *Mol Cell Biol* 12, 4553-4561.
- Rameshwar, P., Ganea, D., and Gascon, P. (1993). In vitro stimulatory effect of substance P on hematopoiesis. *Blood* 81, 391-398.
- Romeo, P.-H., Frandini, M.-H., Joulin, V., Mignotta, V., Prenant, M., Valinchenker, W., Marguerie, G., and Usan, (1990). Megakaryocytic and erythrocytic lineages share specific transcription factors. *Nature* 344, 447-449.
- Tsai, S. F., Martin, D. I. K., Zon, L. I., D'Andrea, A. D., Wong, G. G., and Orkin, S. H. (1989). Cloning of cDNA for the major DNA-binding protein of the erythroid lineage through expression in mammalian cells. *Nature* 339, 446-451.
- Winkelman, J. C., Penny, L. A., Deaven, L. L., Forget, B. G., and Jenkins, R. B. (1990). The gene for the human erythropoietin receptor: Analysis of the coding sequence and assignment to chromosome 19p. *Blood* 76, 24-30.
- Yamamoto, M., Ko, L. J., Leonard, M. W., Beng, H., Orkin, S. H., and Engel, J. D. (1990). Activity and tissue-specific expression of the transcription factor NF-E1 multigene family. *Genes Dev* 4, 1650-1662.
- Yoshimura, A., Longmore, G., and Lodish, H. F. (1990). Point mutation in the exoplasmic domain of the erythropoietin receptor resulting in hormone-independent activation and tumorigenicity. *Nature* 348, 647-649.
- Yoshimura, A., Zimmer, T., Neumann, D., Longmore, G., Yoshimura, Y., and Lodish, H. F. (1992). Mutations in the WSXWS motif of the

- erythropoietin receptor abolish processing, ligand binding, and activation of the receptor. *J. Biol. Chem.* 267, 11619-11625.
- Yousseoufian, H. (1994). Structure, function, and activation of the erythropoietin receptor. *Blood* 83, 1428-1435.
- Yousseoufian, H., and Lodish, H. F. (1993). Transcriptional inhibition of the murine erythropoietin receptor gene by an upstream repetitive element. *Mol. Cell. Biol.* 13, 98-104.
- Yousseoufian, H., Longmore, G., Neumann, D., Yoshimura, A., and Lodish, H. F. (1993). Structure, function and activation of the erythropoietin receptor. *Blood* 81, 2228-2235.
- Yousseoufian, H., Zon, L. I., Orkin, S. H., D'Andrea, A. D., and Lodish, H. F. (1990). Structure and transcription of the mouse erythropoietin receptor gene. *Mol. Cell. Biol.* 10, 3675-3682.
- Zon, L. I., Yousseoufian, H., Mather, C., Lodish, H. F., and Orkin, S. H. (1991). Activation of the erythropoietin receptor promoter by transcription factor GATA-1. *Proc. Natl. Acad. Sci. USA* 88, 10638-10641.

# Transgenic Mice Containing the Human Erythropoietin Receptor Gene Exhibit Correct Hematopoietic and Neural Expression

Chun Liu, Kim Yu, Kun Shen, Ziyao Liu, and Constance T. Noguchi

Laboratory of Chemical Biology, National Institute of Diabetes, Digestive and Kidney Diseases, National Institutes of Health, Bethesda, MD

8) NOTICE: THIS MATERIAL MAY BE PROTECTED  
BY COPYRIGHT LAW (TITLE 17 U.S. CODE)

The erythropoietin receptor (EpoR), known for its role in the proliferation and differentiation of erythroid cells, has been detected in nonhematopoietic tissues. We have reported previously that in addition to hematopoietic expression, EpoR is expressed at high levels in embryonic mouse brain and decreased to nondetectable levels by birth. While using transgenic mice to characterize human EpoR expression, we observed that a 15-kb human EpoR transgene (expressed in hematopoietic tissues but at a reduced level) also exhibited in the embryonic brain low levels of expression that persisted through adulthood. To examine further the basis of tissue and developmental specificity of the human EpoR gene, we produced additional transgenic mice using an 80-kb human EpoR genomic fragment isolated from a P1 phagemid human library. We found that this transgene is expressed appropriately in hematopoietic tissues (including yolk sac, fetal liver, adult spleen, and bone marrow) at levels comparable to the endogenous murine EpoR. The 80-kb transgene also provided high-level expression in the embryonic brain that paralleled the levels of the endogenous murine EpoR and was no longer detectable after birth. These data suggest that the high level of embryonic brain expression may be relevant to the human EpoR gene and that the transgenic mouse with an 80-kb fragment is a suitable model for studying the regulation and possible functional importance of human EpoR expression in the developing embryo.

## INTRODUCTION

The human EpoR gene encodes a single polypeptide of 508 amino acids in eight exons with a single transmembrane spanning region (1). Erythropoietin binding to its receptor stimulates phosphorylation and other signal transducing events, mediated via activation of JAK2 (2). The EpoR shares homology with other receptors such as receptors for interleukins 2-7 (IL2-IL7), granulocyte colony-stimulating factor (G-CSF), granulocyte-macrophage colony-stimulating factor (GM-CSF), leukemia inhibiting factor (LIF), and ciliary neurotropic factor (CNTF) that

compose a superfamily of hematopoietic cytokine receptors (3). The coding regions for the human and murine EpoR genes share a high degree of homology (82%), and their proximal promoters contain binding sites for the transcription factors GATA-1 (at -49 bp 5'), a largely erythroid specific factor, and SP1 (at -19 bp 5') but no TATA sequences (1,4). However, the homology does not appear to extend 5' beyond the GATA-1 binding motif. The murine EpoR contains within 481 bp 5' of the coding region three potential protein-binding CACCC motifs, which have been shown to be important in regulation of globin gene expression in erythroid cells (4). In contrast, the human EpoR contains several CACCC sequences beyond 500 bp upstream from the coding region, but deletion of these motifs does not have a major effect on transcription activity of the proximal promoter (5). The 5' flanking region of the human EpoR gene contains several stretches of species-specific Alu-repetitive elements that may be important for downregulating the promoter activity in nonerythroid cells (1,6). The murine EpoR gene contains a species-specific sequence located between -1703 and -1063 bp 5' and associated with negative regulation that does not appear to be tissue-specific or specific for the EpoR pro-

**Keywords:** brain; development; erythropoiesis.

**Abbreviations:** Epo, erythropoietin; EpoR, erythropoietin receptor; hEpoR, human erythropoietin receptor; mEpoR, mouse erythropoietin receptor.

Address correspondence and reprint requests to: Constance T. Noguchi, Ph.D., Laboratory of Chemical Biology, National Institute of Diabetes, Digestive and Kidney Diseases, National Institutes of Health, Bethesda, MD 20892-1822.

The author was invited to present this work at the May 1996 clinical meetings of the Tri-Societies (AAP, ASCZ, and AFCD). Consequently, this paper may contain previously published data.

Received 11 June 1996; Accepted 10 July 1996.

moter (7). These differences raise the possibility that the human and murine EpoR expression may exhibit species-specific expression patterns.

Binding of erythropoietin to its receptor results in the proliferation of erythroid progenitors and differentiation along the erythroid pathway, with subsequent activation of the production of the erythroid transcription factor GATA-1, the heme biosynthetic enzymes, and hemoglobin (3). It is likely that the appearance of EpoR on nonhematopoietic cells (e.g., endothelial cells) is related to the mitogenic effect of erythropoietin or is a viability factor in preventing apoptosis (8). Functional EpoR also has been observed on neuronal cells, and erythropoietin has been reported to support survival of damaged neurons *in vivo* (9,10).

We have observed significant levels of transcripts from the endogenous mouse EpoR gene in the early embryonic brain, which was downregulated with development (11). We also found that transgenic mice produced with a 15-kb human EpoR genomic DNA fragment provided reduced expression in hematopoietically active tissues but also provided in the mouse brain a low level of expression that persisted through adulthood. To address the reasons for reduced expression in hematopoietic tissue and the basis for the neural expression of the EpoR gene and to determine whether the difference in human and mouse EpoR brain expression was due to species-specific regulatory mechanisms, a P1 phagemid library was screened to obtain larger human genomic DNA fragments containing additional flanking regions of the EpoR gene. Transgenic mice produced with this longer (80-kb) human genomic DNA fragment were found to mimic the pattern of EpoR expression observed for the endogenous murine EpoR gene in both hematopoietic tissues and brain. These data suggest that the high level of EpoR embryonic brain expression observed in the mouse is relevant to the human EpoR gene and that these EpoR transgenic mice are a suitable model for investigating the regulatory basis for that expression and its possible functional significance.

## MATERIALS AND METHODS

### Preparation of DNA for Microinjection

DNA containing the human EpoR gene in bacterial phage lambda or P1 phagemid (Genome Systems Inc, St. Louis, MO) was harvested from bacterial cultures by alkaline lysis. From CsCl<sub>2</sub> purified phage DNA, the DNA fragment containing 15-kb human EpoR was recovered after restriction enzyme digestion and gel purification. The phagemid containing the 80-kb human EpoR was purified using GeneClean (Bio 101, La Jolla, CA).

### Production of Transgenic Mice

Purified DNA containing the human EpoR gene was injected into fertilized eggs and reimplanted into pseudopregnant foster mothers. Polymerase chain reaction (PCR) with tail DNA was used for rapid screening of 2-week-old offsprings. Mice containing human EpoR transgene were bred for further analysis. Primers used to detect the human EpoR transgene were 5'-GTTCGAGAGCAAAGGTAAGG-3' (sense) and 5'-CGATCAGGAGTCTTGGATCC-3' (antisense).

### Screening for EpoR Expression Using RT-PCR

Total RNA was prepared from adult and staged embryos. Reverse transcriptase-PCR (RT-PCR) analysis was carried out using the GeneAmp RT-PCR kit (Perkin Elmer, Foster City, CA). Primers used to detect the human EpoR transcript were from exons 1 and 3: 5'-ACC-ACCTCGGGGCGTCCCTCT-3' (sense) and 5'-AGC-TTCCATGGCTCATCC-3' (antisense). Primers used to detect the mouse EpoR transcript were from exons 1 and 3: 5'-AAACTCAGGGTGCCCTCTGGCCT-3' (sense) and 5'-GATGCGGTGATAGCGAGGAGA-ACC-3' (antisense). Control primers for the mouse ribosomal protein s16 were: 5'-CTGGAGCCTGTTTT-GCTTCTG-3' (sense) and 5'-TGAGATGGACTGTC-GGATGG-3' (antisense), which give a 110-bp band for cDNA and a 198-bp band for genomic DNA.

### Quantitation of EpoR mRNA

PCR standards for quantitation of human and murine EpoR were generated to provide a PCR product of different size when coamplified with sample, as previously described (11). Quantitation was carried out using coamplification with serial dilutions of standard at known concentrations. Initially, PCR reactions were used, with increasing amounts of sample and concomitant decreasing amount of standard, using two-fold increases or decreases to estimate the dilution where sample and standard PCR products had similar intensities when analyzed by gel electrophoresis. A second set of PCR reactions was used, with a fixed amount of sample and increasing amount of standard bracketing the crossing point determined by the first set of PCR reactions and analyzed by gel electrophoresis. Alternatively, to conserve the total amount of sample needed, the amount of standard was fixed and the amount of sample was varied. Band intensities (corrected for fragment size) were plotted, and the crossing point at which the intensity of the standard equals the intensity of the sample provided an estimate for the amount of EpoR cDNA present in the sample.

## RESULTS

Previously, we have reported on the expression of the endogenous murine EpoR gene and a 15-kb human EpoR gene in transgenic mice (11). During development, the endogenous EpoR is expressed at high level in the fetal liver between days 12 and 14 (Fig. 1), when the site of erythropoiesis switches from the yolk sac to the fetal liver (11). The level of EpoR expression in the liver decreases with age and no longer is detectable at birth or in the adult. Examination of endogenous EpoR transcripts in the embryonic brain revealed significant levels at embryonic day 10 comparable to levels observed for adult spleen and bone marrow. The level of endogenous embryonic brain transcripts decreased with development, parallel to the decrease observed in fetal liver. The 15-kb human EpoR transgene was expressed appropriately in adult spleen and bone marrow, indicating that it contained sufficient information to direct appropriate expression in hematopoietic tissues, although expression of the transgene was three- to four-fold lower than that of the endogenous EpoR gene. Transgene expression was not detected in mRNA harvested from heart, kidney, or liver, as expected for an appropriately regulated EpoR gene. In contrast, low level of human EpoR expression (but not endogenous EpoR expression) was detected in adult brain. Analysis of embryonic brain expression of the 15-kb transgene indicated that the transgenic EpoR transcripts were expressed in day 10 brain but at two orders of magnitude lower than that of the endogenous gene (see Fig. 1), and persisted at this low level throughout development to adulthood.

We screened a human P1 phagemid library using PCR primers specific for the 3' and 5' region of human EpoR gene. We isolated two different clones containing the original 15-kb human EpoR DNA fragment with extended 3' and 5' regions. One of these was chosen for the further production of transgenic mice. RT-PCR analysis was used to determine transgene expression in bone marrow, liver, spleen, brain, and heart and was analyzed by agarose gel electrophoresis (Fig. 2). To distinguish PCR products specific for EpoR cDNA from nonspecific bands, we used Southern blot hybridization with a probe specific for human or mouse EpoR that would not cross-hybridize to the PCR primers used (see Fig. 2 a and b). High-level expression of the transgene was observed in spleen and bone marrow (see Fig. 2b, right) comparable to that observed for the endogenous EpoR gene (see Fig. 2, a and b right). No human or mouse EpoR-specific PCR products were detected for adult liver, brain, or heart. RT-PCR of the chromosomal protein s16 was used as a control (see Fig. 2c).

We used a modified quantitative RT-PCR analysis of EpoR expression that also allowed for determi-

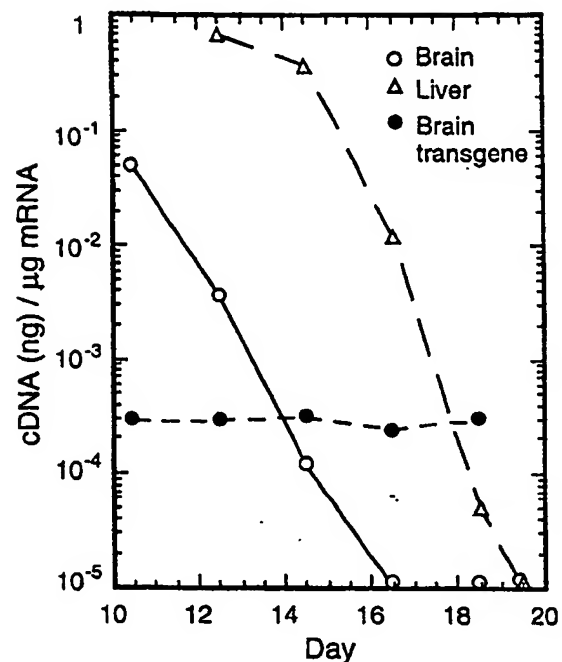
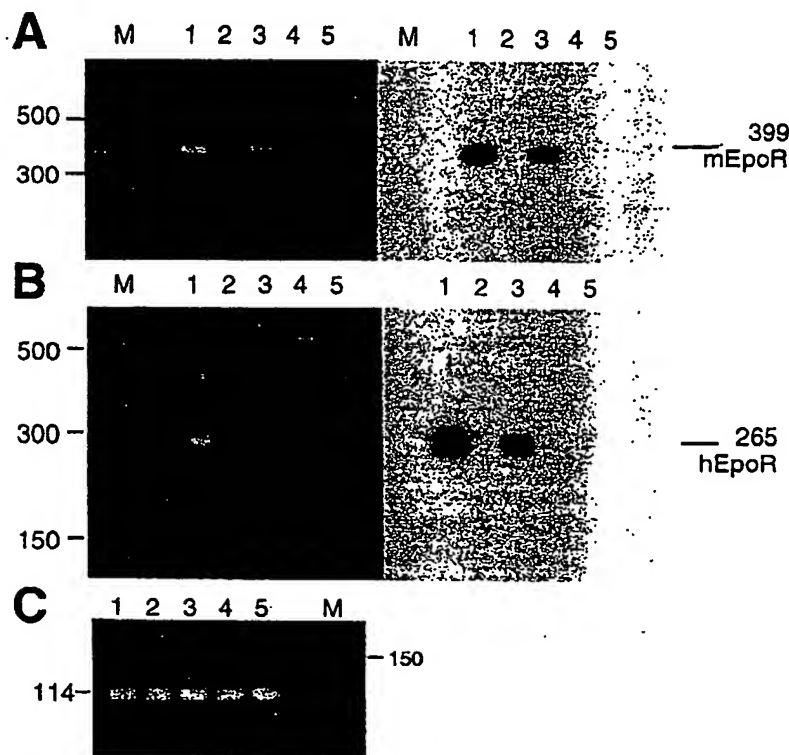


Figure 1. Quantitation of (EpoR) transcripts in mouse embryos.

Levels of the endogenous murine erythropoietin receptor (EpoR) mRNA in brain (open circles) and liver (open triangles) beginning at day 10 and extending to birth were determined by quantitative reverse transcriptase-polymerase chain reaction. The level of 15-kb transgene hEpoR expression also was determined in brain (closed circles) during embryonic development. (Reprinted with permission from Reference 11.)

nation of EpoR RNA transcripts in the small amounts of yolk sac and early embryonic brain (Fig. 3). Analysis of hematopoietic tissues indicated that this 80-kb human EpoR transgene was expressed correctly in yolk sac, fetal liver, adult spleen, and adult bone marrow (Table 1). These levels were comparable to expression of the endogenous murine EpoR gene (Fig. 4). In the embryonic brain at day 12, the 80-kb transgene expression was 80% of that observed for the endogenous murine EpoR expression and approximately an order of magnitude greater than expression obtained with the 15-kb transgene. As with the endogenous gene, the 80-kb transgene expression in the brain was downregulated with development to nondetectable levels by 2 months after birth. These data suggest that although the 15-kb transgene containing the human EpoR gene is able to direct moderate expression in hematopoietic tissues, it is not able to maintain appropriate control in nonhematopoietic tissue (i.e., brain) because additional flanking sequences are required. Also, the significant levels of EpoR transcripts detected in the embryonic brain suggest a possible role for the EpoR in brain development, including the human, and an alternate function for EpoR in addition



**Figure 2.** Expression of the 80-kb human erythropoietin receptor (EpoR) transgene.

Polymerase chain reaction (PCR) analysis was used to determine the presence of human EpoR transcripts in bone marrow (lane 1), liver (lane 2), spleen (lane 3), brain (lane 4), and heart (lane 5). Specific primers for the mouse and human EpoR were used to detect the endogenous mEpoR (a) and the hEpoR transgene (b), respectively. Both the endogenous gene and the transgene were detected in the bone marrow and the spleen. The left panels are ethidium bromide-stained gels, and the right panels are Southern blot analysis of the corresponding gels, using EpoR-specific probes. As control, the same cDNA samples were used also for amplification, using PCR primers for ribosomal protein  $\beta$ 16 (c).

to its role in the proliferation and differentiation of erythroid cells.

## DISCUSSION

A 15-kb human EpoR transgene contained sufficient regulatory sequences to direct a relatively low level of

hematopoietic expression in spleen and bone marrow (11). By using an extended transgene of 80-kb that included more 3' and 5' flanking sequence, the human EpoR transgene provided hematopoietic expression in adult tissues (spleen and bone marrow) as well as embryonic yolk sac and fetal liver, close to levels observed for the endogenous EpoR gene. The homology beyond the coding region and proximal promoter for

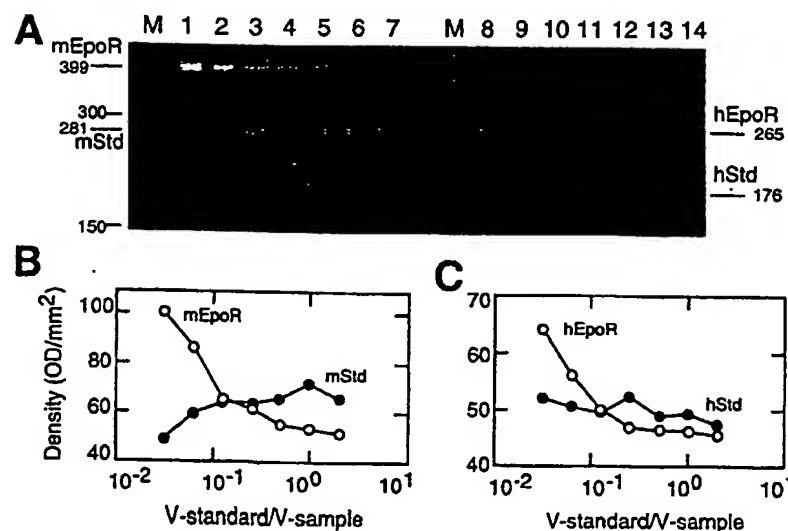


**Figure 3.** Analysis of erythropoietin receptor (EpoR) transcripts in 12-day embryonic brain.

cDNA from 12-day embryonic brain were used for competitive polymerase chain reaction (PCR). Lanes 1–7 correspond to PCR reaction mixtures with 16, 8, 4, 2, 1, 0.5, and 0.25 volumes of sample cDNA and one volume of standard DNA for mouse EpoR at  $1.3 \times 10^{-9}$   $\mu$ g/ $\mu$ l. Lanes 8–14 contain similar volume ratios with standard DNA for human EpoR at  $1.0 \times 10^{-9}$   $\mu$ g/ $\mu$ l. The intensities of the bands corresponding to each PCR product were determined, adjusted for fragment size and plotted against the volume ratio of standard to sample (V-standard:V-sample) used in the reaction. The volume ratio at which the two lines cross is used to calculate the sample cDNA concentration. Open circles indicate intensities for the sample bands; filled circles indicate intensities for the standard bands.

**Table 1. Expression of human erythropoietin receptor transgene in hematopoietic tissues**

Tissue	cDNA(fg)/RNA( $\mu$ g)
Yolk sac	110 $\pm$ 10
Fetal liver	284 $\pm$ 22
Adult spleen	3.1 $\pm$ 1.4
Adult bone marrow	6.1 $\pm$ 1.1

the human and murine EpoR genes is limited, and the 15-kb human EpoR transgene provided a low but persistent level of expression in the embryonic and adult brain. In contrast, the endogenous murine EpoR and the 80-kb human EpoR transgene provided significant levels of expression in the embryonic brain, comparable to levels detected for adult bone marrow. Brain expression decreased with development to nondetectable levels by 2 months after birth. These data suggest that EpoR may play a role in brain development and that the human EpoR transgenic mouse produced with the 80-kb transgene can be a useful model for studying the expression of the human EpoR in the brain.

The biological significance of EpoR expression in the embryonic brain may be related to the neuronal expression of other members of the hematopoietic cytokine receptor superfamily, such as receptors for LIF, CNTF, and gp130 (12). These receptors function by formation of homomultimers or heteromultimers and exhibit neurotrophic properties. LIF and CNTF can support the survival of primary embryonic sen-

sory neurons in culture. In view of the structural relationship between EpoR and receptors for LIF, CNTF and gp130, it is possible that EpoR may be involved in other signaling processes in addition to the stimulation of erythroid cell proliferation and differentiation. As with receptors for LIF, CNTF, and gp130, other proteins on neural cells may be involved in the interaction with cytokine stimulus, and EpoR may act as a partner in a heteromultimeric receptor complex.

Although EpoR has long been recognized for its role in erythropoiesis, recent data show that expression (and possibly function) is not restricted to hematopoietic tissues. Human umbilical vein endothelial cells contain EpoR mRNA, express EpoR on their surface, and respond to erythropoietin stimulation (8). EpoR brain expression may be related to EpoR expression on vascular endothelium and the development of brain vasculature. PC12 cells that exhibit neuronal characteristics express EpoR and exhibit an erythropoietin response (9). Septal cholinergic cell line SN6 and primary septal neurons express EpoR and respond with elevated choline acetyltransferase activity on erythropoietin stimulation, and Epo improves the survival rate of injured neurons *in vivo* (10). Digicaylioglu et al. (13) recently have shown that I<sup>125</sup> erythropoietin is capable of binding to specific areas of adult brain, suggesting that despite the downregulation of the EpoR message by birth, functional EpoR protein still is expressed in the adult brain. We also have detected EpoR expression in human neuronal cell lines (NT2 and SHY5Y) and on preliminary screening of mRNA derived from human fetal brain, at approximately 20 weeks (CloneTech, Palo Alto, CA). The expression of erythropoietin in brain would increase the significance of these findings of brain EpoR expression. Such a possibility is suggested by the report on the oxygen-dependent production of erythropoietin in astrocytes cultured from rat fetus (14). Erythropoietin production with appropriate oxygen response further suggests the possibility that Epo/EpoR expression in the brain may act as an oxygen sensor. These studies together with the data in this article suggest that EpoR may play a role in the embryonic development of the brain or, possibly, brain vasculature development.

Recent reports on the EpoR knockout mouse indicate that EpoR expression is required absolutely for development (15,16). Homozygous EpoR knockout mice do not survive beyond day 13.5 and die in utero due to insufficient hematopoiesis. Selective rescue of these mice with hematopoietic-specific expression of EpoR—by mating with transgenic mice with transgene expression restricted to hematopoietic tissues—should be useful in determining the functional significance of EpoR brain expression in the developing and adult brain.

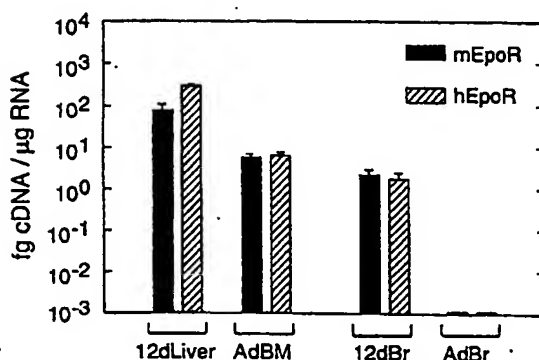


**Figure 4. Quantitation of erythropoietin receptor (EpoR) expression in different tissues.** Expression level of the 80-kb transgene was comparable to that of the endogenous EpoR in hematopoietic tissues, 12-day liver (12dLiver) and adult bone marrow (AdBM). In 12-day embryonic brain (12dBr), the 80-kb transgene was expressed at a level similar to the endogenous EpoR gene and, in adult brain (AdBr), both the transgene and the endogenous gene were undetectable at a resolution of 10<sup>-3</sup> fg cDNA/per  $\mu$ g of RNA.

## ACKNOWLEDGMENT

We thank Dr. Alan N. Schechter for suggestions in preparation of the manuscript.

## REFERENCES

1. Noguchi C.T., Bae K.J., Chin K., et al. Cloning of the human erythropoietin receptor gene. *Blood* 78: 2548-2556, 1991.
2. Withuhn B.A., Quelle F.W., Silvennoinen O., et al. JAK2 associates with the erythropoietin receptor and is tyrosine phosphorylated and activated following stimulation with erythropoietin. *Cell* 74: 227-236, 1993.
3. Youssoufian H., Longmore G., Neumann D., et al. Structure, function, and activation of the erythropoietin receptor. *Blood* 81: 2223-2236, 1993.
4. Youssoufian H., Zon L.I., Orkin S.H., et al. Structure and transcription of the mouse erythropoietin receptor gene. *Mol. Cell. Biol.* 10: 3675-3682, 1990.
5. Chin K., Oda N., Shen K., and Noguchi C.T. Regulation of transcription of the human erythropoietin receptor gene by proteins binding to GATA-1 and Sp1 motifs. *Nucleic Acids Res.* 23: 3041-3049, 1995.
6. Maouche L., Cartron P.C. and Chretien S. Different domains regulate the human erythropoietin receptor gene transcription. *Nucleic Acids Res.* 22: 338-346, 1994.
7. Youssoufian H. and Lodish H.F. Transcriptional inhibition of the murine erythropoietin receptor gene by an upstream repetitive element. *Mol. Cell. Biol.* 13: 98-104, 1993.
8. Anagnostou A., Liu Z., Steiner M., et al. Erythropoietin receptor mRNA expression in human endothelial cells. *Proc. Natl. Acad. Sci. U.S.A.* 91: 3974-3978, 1994.
9. Masuda S., Nagao M., Takahata K., et al. Functional erythropoietin receptor of the cells with neural characteristics. Comparison with receptor properties of erythroid cells. *J. Biol. Chem.* 268: 11208-11216, 1993.
10. Tabira T., Konishi Y. and Gallyas F. Jr. Neurotrophic effect of hematopoietic cytokines on cholinergic and other neurons in vitro. *Int J Dev Neurosci* 13: 241-252, 1995.
11. Liu Z.Y., Chin K. and Noguchi C.T. Tissue specific expression of human erythropoietin receptor in transgenic mice. *Develop. Biol.* 166: 159-169, 1994.
12. Kishimoto T. Signal transduction through homo- or heterodimers of gp130. *Stem Cells* 12: 37-45, 1994.
13. Digicaylioglu M., Bichet S., Marti H.H., et al. Localization of specific erythropoietin binding sites in defined areas of the mouse brain. *Proc. Natl. Acad. Sci. U.S.A.* 92:3717-3720, 1995.
14. Masuda S., Okano M., Yamagishi K., et al. A novel site of erythropoietin production: Oxygen-dependent production in cultured rat astrocytes. *J. Biol. Chem.* 269: 19488-19493, 1994.
15. Wu H., Liu X., Jaenisch R., and Lodish H.F. Generation of committed BFU-E and CFU-E progenitors does not require erythropoietin receptor. *Cell* 83: 59-67, 1995.
16. Lin C.S., Lim S.K., D'Agati V., and Constantini F. Differential effects of an erythropoietin receptor gene disruption on primitive and definitive erythropoiesis. *Genes Dev.* 10: 154-164, 1996.



# PROCEEDINGS OF THE ASSOCIATION OF AMERICAN PHYSICIANS

Univ. of Minn.  
Bio-Medical  
Library

VOLUME 108 • NUMBER 6 • 1996

## CONTENTS

### REVIEWS

Crystal Structure of Macrophage  
Migration Inhibitory Factor (MIF), a  
Glucocorticoid-Induced Regulator of  
Cytokine Production, Reveals a  
Unique Architecture *Lolis, Bucala*

Rational Design, Analysis, and Potential  
Utility of GM-CSF Antagonists  
*Monfardini, Kieker-Emmons, VonFeldt,  
Godillor, Voet, Weiner, Williams*

Molecular Medical Approaches for  
Alleviating Infertility and Understanding  
Assisted Reproductive Technologies  
*Sutorzky, Hewitson, Simerly, Schatten*

Determination of the True Prevalence of  
Infection with the Human T-Cell  
Lymphotropic Viruses (HTLV-III)  
May Require a Combination of  
Biomolecular and Serologic Analyses  
*Pancake, Zucker-Franklin, Marmor, Egler*

### MOLECULAR GENETICS

Transgenic Mice Containing the Human  
Erythropoietin Receptor Gene Exhibit  
Correct Hematopoietic and Neural  
Expression *Liu, Yu, Shen, Liu, Noguchi*

### IMMUNITY/INFECTION

Interaction of Tumor Necrosis Factor- $\alpha$   
and Granulocyte Colony-Stimulating  
Factor on Neutrophil Apoptosis, Receptor  
Expression, and Bactericidal Function  
*Sullivan, Gelrud, Carper, Mandell*

Antibodies to  $\beta_2$  Glycoprotein I:  
Standardized Immunoassay and a  
Reference Interval for Healthy  
Controls *Najney, Erickson, Keil, DeBart*

### VASCULAR BIOLOGY

Menstrual Cyclic Variation of  
Endothelium-Dependent Vasodilation of  
the Brachial Artery: Possible Role of  
Estrogen and Nitric Oxide  
*Kawano, Motoyama, Kugiyama, Hirashima,  
Ohgushi, Yoshimura, Ogawa, Okumura, Yasue*

### DEMOGRAPHY OF HELICOBACTER

Racial Differences in Gastric Function  
among African Americans and Caucasian  
Americans: Secretion, Serum Gastrin, and  
Histology *Cryer, Feldman*

• AUTHOR INDEX

• SUBJECT INDEX

## Regulated Human Erythropoietin Receptor Expression in Mouse Brain\*

(Received for publication, July 14, 1997, and in revised form, October 7, 1997)

Chun Liu, Kun Shen, Ziyao Liu, and Constance Tom Noguchi†

From the Laboratory of Chemical Biology, NIDDK, National Institutes of Health, Bethesda, Maryland 20892-1R22

Erythropoietin (Epo) is known for its role in erythropoiesis and acts by binding to its receptor (EpoR) on the surface of erythroid progenitors. EpoR activity follows the site of hematopoiesis from the embryonic yolk sac to the fetal liver and then the adult spleen and bone marrow. Expression of EpoR has also been observed in selected cells of non-hematopoietic origin, such as the embryonic mouse brain during mid-gestation, at levels comparable to adult bone marrow. EpoR transcripts in brain decrease during development falling by birth to less than 1–3% of the level in hematopoietic tissue. We have now recapitulated this pattern of expression using a human EpoR transgene consisting of an 80-kb human EpoR genomic fragment. The highest level of expression was observed in the embryonic yolk sac and fetal liver, analogous to the endogenous gene, in addition to expression in adult spleen and bone marrow. Although activity of this transgene in brain is initially lower than the endogenous gene, it does exhibit the down-regulation observed for the endogenous gene in adult brain. The expression pattern of hybrid transgenes of an hEpoR promoter fused to  $\beta$ -galactosidase in 9.5-day embryos suggested that the hEpoR promoter region between -1778 and -150 bp 5' of the transcription start site is necessary to direct EpoR expression in the neural tube. EpoR expression in the neural tube may be the origin of the EpoR transcripts detected in brain during development. These data demonstrate that both the mouse and human EpoR genes contain regulatory elements to direct significant levels of expression in a developmentally controlled manner in brain and suggest that in addition to its function during erythropoiesis, EpoR may play a role in the development of selected non-hematopoietic tissue.

The erythropoietin receptor (EpoR)<sup>1</sup> on erythroid progenitor cells is the primary target for erythropoietin (Epo) binding resulting in proliferation and differentiation along the erythroid lineage and is critical for normal erythroid development (1, 2). In hematopoietic cells, the EpoR gene is active early and EpoR mRNA is expressed at moderate levels in the pluripotent hematopoietic stem cell (3). Primary erythroblasts contain a low level of surface erythropoietin receptors, and the number of receptor increase to more than 1000/cell as erythropoiesis con-

tinues upon Epo stimulation (4). Late in erythropoiesis, there is a rapid reduction in EpoR expression, and dependence upon Epo declines as cells progress toward terminal differentiation (5). The EpoR gene contains eight exons with a single transmembrane region (6–8) but no intrinsic tyrosine kinase domain (9). Protein phosphorylation and signal transduction via Epo-EpoR stimulation depends in part on activation of JAK2/STAT5 (10, 11) as well as other kinase pathways (12, 13). *In vitro*, cells of other lineages respond to Epo stimulation including hematopoietic cells such as megakaryocytes, which differentiate in the presence of Epo (14), and B lymphocytes, which exhibit a proliferative response (15).

We have reported that in addition to expression in hematopoietic tissues, EpoR expression can be detected in day 10.5 embryonic mouse brain at high levels comparable to that in adult hematopoietic tissue. EpoR expression in brain decreases with development and is not readily detectable at or after birth (16). Embryonic EpoR expression in the brain may be related to EpoR expression on other non-hematopoietic cells such as those of endothelial or neuronal origin. For example, human umbilical vein endothelial cells express EpoR and are responsive to Epo (17, 18). EpoR mRNA has also been observed in rat brain capillary endothelial cells (19), and functional EpoR has been detected in cultured rodent cells with neuronal characteristics (20, 21) and primary rat hippocampal neurons (22).

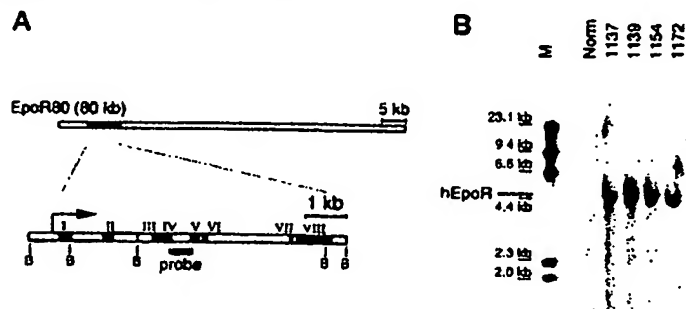
In an attempt to create an hEpoR transgenic mouse exhibiting developmental control in both hematopoietic cells and brain, we isolated a larger (80 kb) human genomic fragment containing the EpoR gene for production of transgenic mice. In a preliminary report, we showed that this transgene was able to direct readily detectable levels of hEpoR transgene expression in fetal liver and adult bone marrow with little or no expression in the adult brain (23). We now show that the 80-kb hEpoR transgene is developmentally regulated to mimic both the pattern of the endogenous mEpoR gene expression in hematopoietic tissue and brain. The highest levels of hEpoR transgene and endogenous mEpoR gene expression are observed in hematopoietically active embryonic tissue (yolk sac and fetal liver). In the brain, hEpoR expression in the developing embryo is followed by down-regulation of expression so that the levels of endogenous mEpoR gene and hEpoR transgene expression are reduced about 2 orders of magnitude or more in adult brain. Reporter gene constructs using hEpoR promoter fragments to drive  $\beta$ -galactosidase gene expression in early transgenic mouse embryos suggest that the region flanking the hEpoR proximal promoter is necessary to drive EpoR expression in the early embryonic neural tube. These data demonstrate that both human and mouse EpoR genes are actively transcribed in hematopoietic tissue and the developing embryonic brain and suggest that, in addition to its role in erythropoiesis, EpoR may be functionally important in the development of select non-hematopoietic tissue.

\* The costs of publication of this article were defrayed in part by the payment of page charges. This article must therefore be hereby marked "advertisement" in accordance with 18 U.S.C. Section 1734 solely to indicate this fact.

† To whom correspondence should be addressed. Tel.: 301-496-1164; Fax: 301-402-0101; E-mail: cnoguchi@helix.nih.gov.

The abbreviations used are: Epo, erythropoietin; EpoR, erythropoietin receptor; hEpoR, human erythropoietin receptor; mEpoR, mouse erythropoietin receptor; kb, kilobase(s); bp, base pair(s); PCR, polymerase chain reaction; RT, reverse transcriptase.

**Fig. 1.** A, human EpoR gene fragment used to make transgenic mice. The 15-kb hEpoR DNA fragment contains 2 kb 5' and 7 kb 3' of the coding region. The 80-kb hEpoR DNA fragment contains 6 kb 5' and 60 kb 3' of the coding region. A hEpoR cDNA probe from exon IV to exon V was constructed to detect the presence of the transgene. B, Southern blot analysis of DNA from normal (Norm) and different transgenic mice (1137, 1139, 1154, and 1172). Genomic DNA was digested with *Bam*HI and used to confirm the presence of hEpoR after preliminary screening by PCR. M, marker DNA.



#### MATERIALS AND METHODS

**Human EpoR Gene.**—An 80-kb EpoR genomic clone was isolated from a human P1 phagemid library (Genome Systems, St. Louis, MO). P1 phagemid DNA was prepared for direct injection as described previously (24). DNA was further purified by isopropanol precipitation, ethanol precipitation, and treatment with RNase and phenol/chloroform. Final treatment included Gene-clean (Bio 101, Vista, CA) and filtration through a 0.22- $\mu$  sterile filter. The DNA was centrifuged again to remove any remaining glass beads and was dialyzed against injection buffer (10 mM Tris-HCl, pH 7.5, with 0.1 mM EDTA) (16).

**Production of Transgenic Mice.**—Transgenic mice were generated using B6C3F1 (female)  $\times$  B6D2F1 (male) as described previously (16). The B6C3F1 results from C57BL/6N  $\times$  C3H/HeN and the B6D2F1 results from C57BL/6N  $\times$  DBA/2N. DNA was injected into the male pronucleus of embryonic day 2 (E2) fertilized mouse eggs. The injected eggs were reimplanted into surrogate dams. Screening for positive newborns was done by isolation of genomic DNA from a 0.5-cm piece of the tail at 2 weeks of age. The DNA was subjected to polymerase chain reaction (PCR) using a pair of primers selected from the human EpoR gene as described previously. Mice positive for the hEpoR were further analyzed and confirmed by Southern blot analysis. For each mouse, 10  $\mu$ g of genomic DNA was digested with *Bam*HI, loaded on a 0.7% agarose gel for electrophoresis, and transferred to a nylon membrane using a TurboBlotter (Schleicher & Schuell). The membrane was subsequently probed using a nonradioactive labeled probe (Boehringer Mannheim) spanning exons 4 and 5 of the hEpoR cDNA. Positive progeny were then bred for further analysis.

**Screening for EpoR Expression.**—Total RNA was prepared from various tissues using STAT-60 (Tel-Test B, Friendswood, TX) and treated with RNase-free DNase (Promega, Madison, WI) at 5 units/100  $\mu$ g of RNA at 37  $^{\circ}$ C for 30 min followed by phenol/chloroform extraction and ethanol precipitation. One microgram of isolated total RNA was reverse-transcribed for 15 min in a 20- $\mu$ l reaction mixture using reverse transcriptase (Perkin-Elmer). One microliter of RT product was then amplified by polymerase chain reaction (PCR) using a primer pair designed to detect the human EpoR transcript from exons 1 and 3: 5'-ACGACCTCGGGCGTCCCTCT-3' (sense) and 5'-AGCTCCATGCGTCATCC-3' (antisense). Primers used to detect the mouse EpoR transcript were (from exons 1 and 3): 5'-AACTCAGGCTGCCCCCTCTGGCT-3' (sense) and 5'-GATGCGGTGATAGCCAGGAGAACC-3' (antisense). Positive control primers for the mouse ribosomal protein S16: (5'-CTGGAGCTGTTTCTCTCTG-3' (sense) and 5'-TGAGATGGA-CTGTCGGATGG-3' (antisense)) gave a 110-bp band PCR product for cDNA and a 198-bp band for genomic DNA.

**Generation of DNA Standards for Quantitative PCR.**—Specific DNA standards were produced such that when they were co-amplified using primers for a specific cDNA, the product obtained from the DNA standard would be slightly shorter than the product obtained from the cDNA of interest. Primer pairs of 50 bp long were designed to contain 20 bp at the 5' end matching the respective sequences of the cDNA specific primers. The remaining 30 bp at the 3' end were then selected to match a sequence within the amplified cDNA fragment that would produce a PCR product distinguishable in size from the original PCR-amplified cDNA product. Fifty nanograms of specific cDNA was used in a 100- $\mu$ l PCR reaction mixture. The resulting PCR products were separated on 1% agarose gels and electrophoresed (Schleicher & Schuell). Concentration of DNA standard was determined by UV absorbance at 260 nm.

**Quantitation of EpoR mRNA.**—mRNA was reverse-transcribed and the product subjected to quantitative PCR involving two sets of co-amplification with standard cDNA. We used a modified quantitative RT-PCR procedure incorporating serial dilutions of sample and specific

standard DNA to determine the level of EpoR expression. For the first set, seven reactions were set up with increasing amount of sample and decreasing amount of standard. The dilutions in which intensities of the cDNA PCR product and the PCR product for the DNA standard were similar were used to estimate the initial amount of message present in the RT-PCR reaction (23). After this initial estimation of the expression level, a second set of PCR was carried out using a fixed amount of sample and an increasing amount of standard bracketing the estimated crossing point. When the amount of sample was limited, the amount of standard was fixed and that of the sample varied to minimize the total amount of sample required. This method of PCR quantitation was sensitive to differences of 2-fold or more.

**Phenylhydrazine Treatment.**—Normal and transgenic mice were injected with phenylhydrazine at a dose of 0.03 g/g of body weight for two days and at 0.015 g/g of body weight for 3 days. Mice were sacrificed on the 7th day from the initial treatment. The reticulocyte count was determined for each mouse and RNA prepared from different tissues.

**EpoR/ $\beta$ -Galactosidase Reporter Gene.**—A reporter gene construct was made containing a hEpoR promoter fragment extending 1778 bp 5' of the transcription start site and 3' to include the untranslated transcribed region and linked to a  $\beta$ -galactosidase reporter gene. Transgenic mice were constructed as described above and embryos harvested and stained for  $\beta$ -galactosidase activity (25). The number of days after vaginal plug formation was used to identify the age of embryos. Embryos were embedded in paraffin and 10- $\mu$ m sagittal sections were made and counterstained with hematoxylin-eosin.

#### RESULTS

Transgenic mice were generated from an 80-kb human EpoR clone isolated from a genomic P1 phagemid library. This construct contained flanking genomic DNA extending 6 kb 5' and 60 kb 3' of the hEpoR coding region (Fig. 1A). Integration of the transgene was determined by PCR and confirmed by Southern blot analysis as described under "Materials and Methods" (Fig. 1B). Two independent lines of transgenic mice were used for further analysis. At least three mice were analyzed, each independently, from the two lines. Transgene copy number for these lines was low (less than five).

**Tissue Distribution of hEpoR Transgene Expression.**—To examine transgene activity in the adult mouse, RNA was isolated from various tissues and analyzed for endogenous mEpoR gene and hEpoR transgene expression. In hematopoietic tissues, bone marrow, and spleen, both mEpoR and hEpoR transcripts were readily detected (Fig. 2). Expression of the hEpoR transgene in hematopoietic tissue in addition to endogenous mEpoR expression did not result in increased stimulation of erythropoiesis, as no difference was observed in blood hematocrit compared with normal control mice. Mice carrying the 80-kb transgene showed no gross morphological abnormalities. Analysis of expression in non-hematopoietic tissue indicated that no RNA transcripts could be detected in adult liver, heart, leg muscle, or kidney corresponding to either endogenous mEpoR or transgenic hEpoR expression (Fig. 2).

**Developmental Expression of the EpoR Transgene in Hematopoietic Tissues.**—We have previously reported that a 15-kb hEpoR transgene provided hematopoietic specific expression in

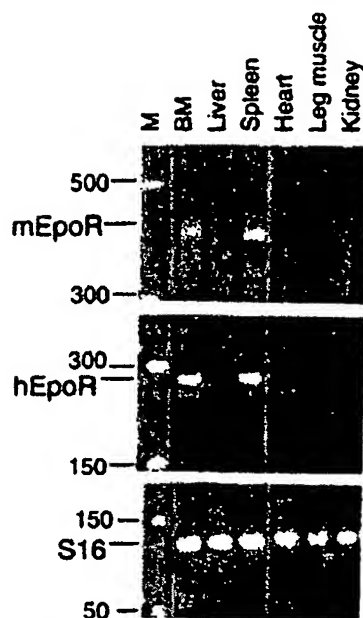


FIG. 2. Expression of EpoR. RNA was isolated and subjected to RT-PCR to determine EpoR expression from bone marrow (BM), liver, spleen, heart, leg muscle, and kidney. PCR reaction products using primers specific for the endogenous mouse EpoR (*mEpoR*), human EpoR (*hEpoR*) transgene, and mouse ribosomal protein S16 (*S16*) as control are indicated. M, marker DNA.

spleen and bone marrow of adult mice but at levels lower than the endogenous gene (16). We now examine the expression of the 80-kb hEpoR transgene in developing hematopoietic tissue and find expression levels more comparable to those observed for the endogenous gene. As observed for the mouse EpoR, the hEpoR transgene was expressed in yolk sac, fetal liver, and adult spleen and bone marrow. The level of hEpoR expression was determined using quantitative RT-PCR as described above and compared with the level detected for endogenous mEpoR. The highest level of hEpoR mRNA was observed in embryonic hematopoietic tissues (Fig. 3). Human EpoR transgene expression levels in yolk sac (110 fg/ $\mu$ g of RNA) and fetal liver (262 fg/ $\mu$ g of RNA) were similar to mEpoR expression in yolk sac (80 fg/ $\mu$ g of RNA) and in fetal liver (104 fg/ $\mu$ g of RNA). As with endogenous mEpoR expression, hEpoR expression in the fetal liver decreased during development to undetectable levels at birth as the site of hematopoiesis switches to the spleen and bone marrow. In the adult, the level of EpoR expression in the bone marrow was 7.1 fg/ $\mu$ g of RNA for hEpoR and 3.1 fg per  $\mu$ g of RNA for mEpoR. EpoR transcripts in the spleen was determined to be 4.4 fg/ $\mu$ g of RNA for hEpoR and 11.7 fg/ $\mu$ g of RNA for mEpoR. Treatment with phenylhydrazine to induce hemolytic anemia and increase erythropoietic activity resulted in an increase in the percentage of reticulocytes from less than 2% to more than 20% in both normal and transgenic mice. Accompanying the increase in spleen size by 3–4-fold was an increase in endogenous mEpoR gene and hEpoR transgene expression in response to the induced anemic stress (Fig. 4). In contrast, no EpoR expression was observed before or after phenylhydrazine treatment in thymus, a tissue related to lymphoid activity.

**Transgene Expression during Brain Development**—We have previously reported that in spite of regulated hematopoietic tissue expression, a 15-kb hEpoR transgene was not develop-

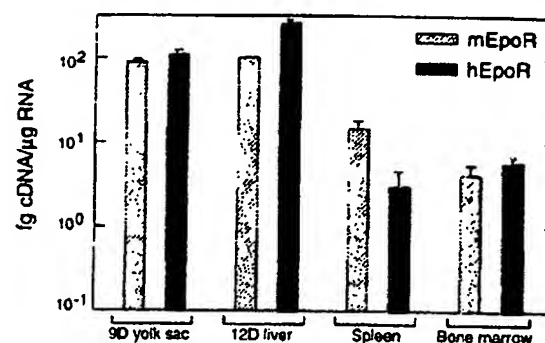
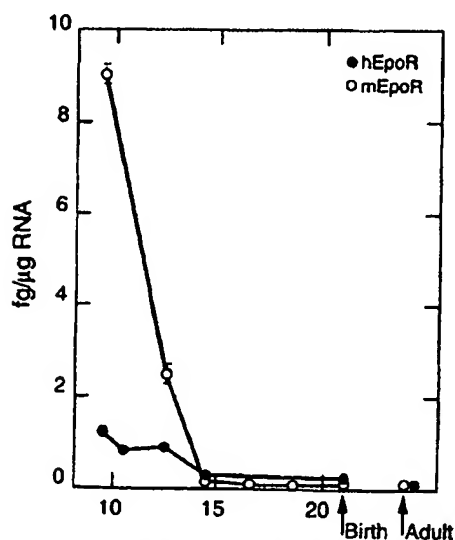
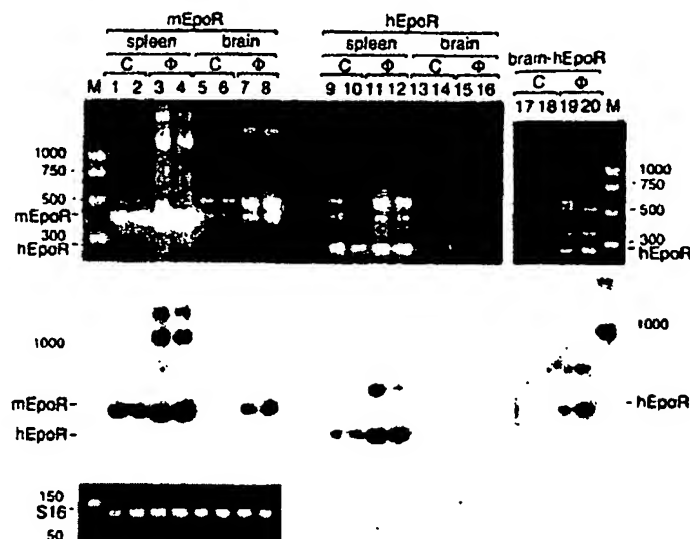


FIG. 3. Developmental expression of hEpoR transgene in hematopoietic tissues. The level of hEpoR expression was determined by quantitative RT-PCR and compared with endogenous mEpoR expression in yolk sac (9.5 day), fetal liver (12.5 day), spleen (adult), and bone marrow (adult). Standard deviations from analysis of three to six individual mice are shown.

mentally regulated in the brain (16). In contrast, the endogenous mEpoR was expressed in embryonic brain tissues at day 10.5 at a level close to that in adult spleen and bone marrow and then decreased with development, dropping by more than 3 orders of magnitude at birth. These data suggested that the hEpoR transgene did not contain regulatory elements to provide control of brain expression and/or that developmental control of EpoR in brain may be different between human and mouse. In the present study, we found that the more distal flanking regions of the hEpoR gene were able to provide regulation in both hematopoietic tissue and brain. An 80-kb human EpoR gene fragment was used to produce transgenic mice; transgenic mice were mated and embryos harvested at different days of development. RNA isolated from brains of 10.5-day embryos exhibited transgene expression of 1.5 fg/ $\mu$ g of RNA (Fig. 5). This level of expression persisted through day 12.5 and then started to decrease with the decrease in endogenous mEpoR expression. Although the 80-kb hEpoR transgene was not able to provide the high level of EpoR expression observed for the endogenous mEpoR gene in the early embryonic (day 10.5) brain, these data suggest that the additional distal flanking genomic sequences provided much of the regulation required for developmental control of brain expression not observed previously.

**Human EpoR Promoter Activity in Neural Tube**—To determine whether the 5' DNA region flanking the first exon of hEpoR could direct reporter gene activity in non-hematopoietic tissues *in vivo* and to identify the possible site of hEpoR expression in the early embryonic brain, the hEpoR promoter linked to a  $\beta$ -galactosidase reporter gene was used to generate transgenic mice. The reporter gene construct contained an hEpoR promoter fragment extending 5' from the ATG start site for transcription to -1778 bp 5' of the transcription start site. Mice testing positive for the transgene were mated with normal mice. Embryos were harvested at day 9.5 postcoitus, and whole embryos were stained for  $\beta$ -galactosidase activity. Staining was observed in the ventral neural tube in two independently generated transgenic mouse lines in the region extending from the anterior to posterior segmental neuroepithelium, the ventral isthmal neuroepithelium, and the pontine neuroepithelium (Fig. 6). However, not all of the transgenic lines exhibited staining at embryonic day 9.5. No staining of the neural tube was observed in normal mice or in transgenic mice containing a shorter promoter that extend to only 150 bp 5' from the transcription start site (Fig. 6). These data suggest that the promoter region between -1778 and -150 bp is necessary to

**FIG. 4. Induction of erythropoietin receptor expression by anemic stress.** EpoR expression was determined using RT-PCR analysis of RNA harvested from spleen and brain tissues of untreated or control (C) and phenylhydrazine treated (Φ) hEpoR transgenic mice. The reaction products (top panel) were analyzed by blot hybridization (center panel) as described in the text to confirm the identities of the mEpoR and hEpoR specific bands. Results for endogenous mEpoR and the hEpoR transgene are shown in lanes 1–8 and lanes 9–20, respectively. Analyses of two untreated mice are included in lanes 1, 5, 9, 13, and 17 and lanes 2, 6, 10, 14, and 18, respectively. Analyses of two treated mice are included in lanes 3, 7, 11, 15, and 19 and lanes 4, 8, 12, 16, and 20, respectively. For hEpoR expression in brain tissue, results obtained by increasing the cycle number from 35 (for lanes 1–16) to 40 (for lanes 17–20) are also shown. Determination of S16 was used as a control (bottom panel). Marker lanes are indicated (M).



**FIG. 5. Quantitation of hEpoR transgene expression in embryonic brain.** Quantitative RT-PCR analysis was used to determine the level of mEpoR and hEpoR in RNA prepared from embryonic brain tissue at different days of development and from adult brain tissue. Standard deviations from analysis of three to six individual mice are shown.

drive transgene expression in the neural tube. To confirm that the staining pattern was relevant to EpoR gene expression, tissue corresponding to the  $\beta$ -galactosidase stained region was dissected from normal mice and mice containing the 80-kb hEpoR transgene. Both mEpoR and hEpoR transcripts were detected and quantified by RT-PCR. The levels of hEpoR transgene and mEpoR gene expression in the neural tube were comparable to that in adult hematopoietic tissue and were 5.1 fg/μg of RNA compared with 3.0 fg/μg of RNA for the endogenous mEpoR gene. The expression of EpoR in neural tube at day 9.5 may be the origin of the embryonic brain expression detected later in development.

**EpoR Transcripts in Adult Brain.** Our initial screening for EpoR expression in the adult brain showed no detectable tran-

scripts, which suggests that if EpoR is expressed, it is at levels less than 0.1 fg/mg of RNA as determined by the quantitative PCR procedure described above. We increased the sensitivity of our analysis and reexamined RNA isolated from normal and transgenic mouse brain tissue. By increasing the PCR cycle number from 30 to 35, we were able to detect mEpoR expression. The PCR product was digested by restriction enzymes *XhoI* and *XbaI* and hybridized to mEpoR specific probe to confirm its identity (Fig. 7). This level of expression corresponded to more than 2 orders of magnitude lower than that seen in adult spleen. Comparable results were also obtained for expression in adult brain of the 80-kb hEpoR transgene. As a negative control, increasing the PCR cycle number showed no mEpoR or hEpoR expression in adult liver. No PCR products were observed when reverse transcriptase was omitted from the reaction mixture.

#### DISCUSSION

The murine system has provided unique insights into the regulation of erythropoiesis by EpoR. Null mutations of both Epo and EpoR gene in mice demonstrated that Epo and EpoR were crucial for definitive erythropoiesis and that interrupted erythroid development in fetal liver was lethal around embryonic day 13.5 [1, 2]. We used the transgenic mouse to examine the developmental regulation of the human EpoR gene. We demonstrated that in transgenic mice produced from the 80-kb hEpoR transgene, appropriate expression of hEpoR was recovered in hematopoietic tissues. The highest level of EpoR expression for the endogenous mEpoR gene and the 80-kb hEpoR transgene occurred in hematopoietic embryonic tissue. The levels of mEpoR and hEpoR RNA transcripts in yolk sac and fetal liver were 1.5–2 orders of magnitude higher than the levels observed in adult spleen and bone marrow. We have previously shown that a 15-kb human EpoR gene fragment provided expression but at low levels in adult hematopoietic tissues of transgenic mice [16]. The similarity between endogenous mEpoR gene and hEpoR transgene expression in these tissues suggests that the 80-kb hEpoR transgenic mouse can be used to examine the developmental expression of hEpoR in hematopoietic tissue.

In addition to detection of EpoR in known hematopoietic tissues, we detected endogenous mEpoR expression in the embryonic mouse brain at high levels, which was down-regulated



FIG. 6. hEpoR/ $\beta$ -galactosidase reporter gene expression at embryonic day 9.5. EpoR promoter extending to 150 bp 5' (A) and to 1778 bp 5' (B and C) of the start site for transcription were used to drive  $\beta$ -galactosidase expression in transgenic mice. Embryos were harvested at day 9.5 and stained for  $\beta$ -galactosidase activity. Photographs of embryos (A and B) are at 1:15 enlargements. An embryo was sectioned and counterstained with hematoxylin-eosin and photographed at 1:38 enlargement (C).

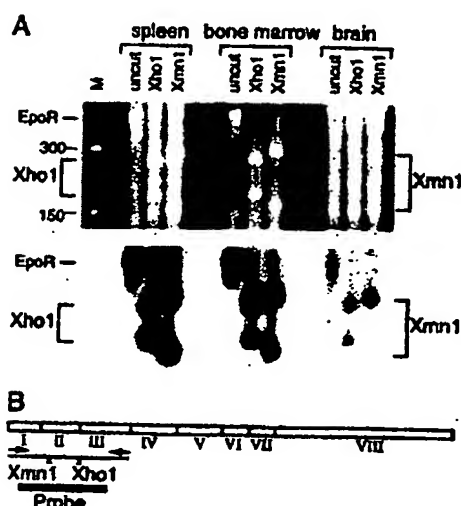
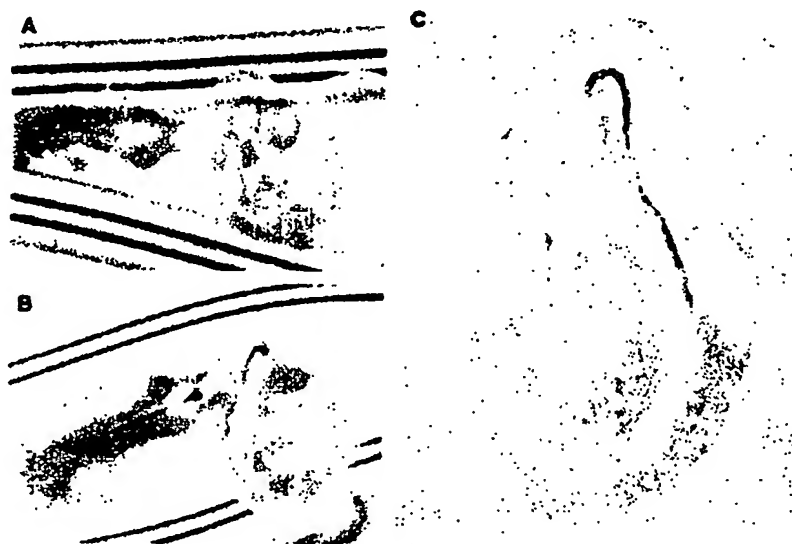


FIG. 7. EpoR transcripts detected in adult mouse brain. A, increasing PCR cycle number and analyzing RT-PCR products with a mEpoR specific probe confirmed the presence of low level EpoR RNA transcripts in the adult brain compared with spleen and bone marrow. XhoI and XmnI restriction enzyme digestion was used to demonstrate specificity of the procedure. B, location of XhoI and XmnI restriction enzyme sites in the expected EpoR RT-PCR product.

with development (16). We have now shown that endogenous mEpoR was expressed in the adult brain, but at a level of about 2 orders of magnitude lower than that observed in the embryonic brain at day 10.5. The mEpoR and hEpoR transgene expression we observed in day 9.5 neural tube may be the origin of the EpoR expression detected in the brain at day 10.5 and later and may be related to detection of EpoR localized to the neural plate earlier in development (26). Specific localized binding of radiolabeled Epo to adult mouse brain sections has also been detected (27). These observations suggest that the EpoR message detected in the rodent brain is developmentally regulated and processed into Epo binding protein. The 15-kb hEpoR genomic DNA fragment contained much of the homology between the murine and human EpoR genes within the

coding region and extending 5' to the GATA-1 binding site in the EpoR proximal promoter (28, 29). Further 5' are species-specific repetitive elements that have been associated with negative regulation (30–32). However, this human EpoR transgene was expressed at a low level in an unregulated manner in embryonic and adult brain. To include additional regulatory elements, an expanded 80-kb hEpoR genomic fragment was isolated and used to produce transgenic mice.

Analysis of the 80-kb hEpoR transgene demonstrated that embryonic brain expression for both hEpoR and mEpoR decreased in a parallel fashion with further development dropping by about 2 orders of magnitude or more in the adult. The behavior of the hEpoR promoter/ $\beta$ -galactosidase reporter gene constructs suggested that the region from –1778 to –150 bp of the transcription start site was necessary to provide staining of  $\beta$ -galactosidase in the embryonic day 9.5 neural tube. RNA prepared from neural tube of normal and hEpoR transgenic mice at embryonic day 9.5 also showed high level expression of mEpoR and hEpoR and may be the origin of EpoR brain expression observed during development. EpoR expression has been observed in the central nervous system of mid-trimester human fetuses (33) and in brain of adult monkeys (34). GATA-1 is an important transactivator of EpoR expression in hematopoietic cells (28, 29, 35). Although GATA-1 is not expressed in the brain, the brain expresses significant levels of GATA-3, which is capable of binding similar DNA motifs. Targeted disruption of the GATA-3 gene causes severe abnormalities in the embryonic nervous system and in fetal liver hematopoiesis (36). The developmental expression of EpoR expression observed for the endogenous mEpoR gene and the hEpoR transgenes suggests that EpoR expression in non-hematopoietic cells may share some common regulatory controls with hematopoietic expression, but requires additional *cis*-acting DNA elements.

Although the physiological function *in vivo* of EpoR expression in non-hematopoietic cells is not yet known, it may be directly related to EpoR activity reported for endothelial cells. Epo stimulation of cultured endothelial cells increases protein phosphorylation and induces nuclear translocation of STAT-5 (37). Epo can also increase intracellular calcium and increase endothelin-1 secretion (38) in a dose-dependent manner (39). The involvement of EpoR in endothelial cells may originate

from the close relationship between hematopoiesis and vasculogenesis (40) and between hematopoiesis and angiogenesis later in development (41). Stimulation of EpoR in the brain may not require Epo to cross the blood-brain barrier, as oxygen-dependent Epo production has been observed in cultured rat astrocytes (42) and that Epo expression in the adult brain can be up-regulated by hypoxia in mice (27) and monkeys (34). Expression of EpoR in non-hematopoietic cells may allow for Epo activation in the early embryo to stimulate proliferation or to control apoptosis as those cells differentiate and mature.

## REFERENCES

- Wu, H., Liu, X., Jaenisch, R., and Lodish, H. F. (1995) *Cell* 83, 59-67.
- Lin, C. S., Lum, S. K., V. D. A., and Cortantini, P. (1996) *Genes Dev.* 10, 151-164.
- Orlic, D., Andersson, S., Diezicker, L. G., Sorrentino, D. P., and Dodine, D. M. (1995) *Proc. Natl. Acad. Sci. U. S. A.* 92, 4601-4605.
- Droudy, V. C., Lin, N., Brier, M., Nakamoto, B., and Papayannopoulos, T. (1991) *Blood* 77, 2583-2590.
- Wickrema, A., Krantz, S. B., Winkelmans, J. C., and Bonchaurant, M. C. (1992) *Blood* 80, 1940-1949.
- Noguchi, C. T., Bao, K. S., Chiu, K., Wada, Y., Schechter, A. N., and Hankins, W. D. (1991) *Blood* 78, 2548-2556.
- Penny, L. A., and Forget, B. G. (1991) *Genomics* 11, 974-980.
- Maoache, L., Turramille, C., Huttah, C., Boffa, G., Cartron, J. P., and Chretien, S. (1991) *Blood* 78, 2557-2563.
- Yousoufian, H., Longmore, G., Neumann, D., Yoshimura, A., and Lodish, H. F. (1993) *Blood* 81, 2223-2238.
- Quelle, P. W., Wang, D., Nonaka, T., Thierfelder, W. B., Stravopodis, D., Weinstein, Y., and Ihle, J. N. (1996) *Mol. Cell. Biol.* 16, 1622-1631.
- Sawyer, S. T., and Penta, K. (1996) *J. Biol. Chem.* 271, 32430-32437.
- Barber, D. L., Corless, C. N., Xia, K., Roberts, T. M., and D'Andrea, A. D. (1997) *Blood* 89, 55-64.
- Klingmüller, U., W. H., Haio, J. G., Toker, A., Duckworth, B. C., Cantley, L. C., and Lodish, H. F. (1997) *Proc. Natl. Acad. Sci. U. S. A.* 94, 3016-3021.
- Ishibashi, T., Kozlowski, J. A., and Bernstein, S. A. (1987) *J. Clin. Invest.* 79, 288-289.
- Kimata, H., Yoshida, A., Ishioka, C., Masuda, S., Sasaki, R., and Mikawa, H. (1991) *Clin. Exp. Immunol.* 85, 151-156.
- Liu, Z. Y., Chiu, K., and Noguchi, C. T. (1994) *Dev. Biol.* 166, 159-169.
- Anagnostou, A., Lee, E. S., Krasnianski, N., Levinson, R., and Steiner, M. (1990) *Proc. Natl. Acad. Sci. U. S. A.* 87, 5978-5982.
- Anagnostou, A., Liu, Z., Steiner, M., Chiu, K., Lee, E. S., Krasnianski, N., and Noguchi, C. T. (1994) *Proc. Natl. Acad. Sci. U. S. A.* 91, 3974-3978.
- Yamaji, R., Okada, T., Moriya, M., Naito, M., Tsuruo, T., Miyatake, K., and Nakano, Y. (1996) *Eur. J. Biochem.* 239, 494-500.
- Masuda, S., Nagao, M., Takahashi, K., Konishi, Y., Gallyas, F., Jr., Tabira, T., and Sasaki, R. (1993) *J. Biol. Chem.* 268, 11208-11216.
- Tabira, T., Konishi, Y., and Gallyas, F., Jr. (1995) *Int. J. Dev. Neurosci.* 13, 241-252.
- Monshita, E., Narita, H., Nishida, M., Kawashima, N., Yamagishi, K., Masuda, S., Nagao, M., Hara, H., and Sasaki, R. (1996) *Blood* 88, 165-171.
- Liu, C., Yu, K., Shen, K., Liu, Z., and Noguchi, C. T. (1996) *Proc. Assoc. Am. Physicians* 108, 449-454.
- Callow, M. J., Stoltzfus, L. J., Law, R. M., and Rubin, E. M. (1994) *Proc. Natl. Acad. Sci. U. S. A.* 91, 2130-2134.
- Whiting, J., Marshall, H., Cook, M., Krumlauf, R., Rigby, P. W., Stuetz, D., and Alleman, R. K. (1991) *Genes Dev.* 5, 2045-2059.
- Yasuda, Y., Nagao, M., Okano, M., Masuda, S., Sasaki, R., Konishi, H., and Taniguchi, T. (1993) *Dev. Growth Differ.* 4, 711-722.
- Digicaylioglu, M., Bichet, S., Maru, H. H., Wenger, R. H., Rivas, L. A., Bauer, C., and Gassmann, M. (1995) *Proc. Natl. Acad. Sci. U. S. A.* 92, 3717-3720.
- Yousoufian, H., Zou, L., Orkin, S. H., AD, D. A., and Lodish, H. F. (1990) *Mol. Cell. Biol.* 10, 3675-3682.
- Chiu, K., Oda, N., Shen, K., and Noguchi, C. T. (1995) *Nucleic Acids Res.* 23, 3041-3049.
- Maoache, L., Cartron, J. P., and Chretien, S. (1994) *Nucleic Acids Res.* 22, 338-346.
- Yousoufian, H., and Lodish, H. F. (1993) *Mol. Cell. Biol.* 13, 98-104.
- Yousoufian, H. (1994) *Blood* 83, 1428-1435.
- Li, Y., Junil, S. E., Morris-Wiman, J. A., Colhoun, D. A., and Christensen, R. D. (1996) *Pediatr. Res.* 40, 376-380.
- Marti, H. H., Wenger, R. H., Rivas, L. A., Straumann, U., Digicaylioglu, M., Henna, V., Yockawa, Y., Bauer, C., and Gassmann, M. (1996) *Eur. J. Neurosci.* 8, 666-678.
- Chiba, T., Ikawa, Y., and Todokoro, K. (1991) *Nucleic Acids Res.* 19, 3843-3848.
- Pandolfi, P. P., Rath, M. F., Kuris, A., Leonard, M. W., Drivetzak, E., Gravel, P. G., Engel, J. D., and Lindenbaum, M. H. (1995) *Nat. Genet.* 11, 40-44.
- Haller, H., Christel, C., Dannenberg, L., Thiele, P., Lindschau, C., and Luft, F. C. (1998) *Kidney Int.* 50, 481-488.
- Carlini, R. G., Gupta, A., Lapis, H., and Rothstein, M. (1995) *J. Cardiovasc. Pharmacol.* 28, 849-852.
- Nitta, K., Uchida, K., Kimata, N., Kawashima, A., Yumura, W., and Nishi, H. (1995) *Eur. J. Pharmacol.* 293, 491-494.
- Flamme, I., and Risau, W. (1992) *Development* 116, 435-439.
- Asahara, T., Murohara, T., Sullivan, A., Silver, M., van der Zee, R., Li, T., Witzenbichler, B., Schatteman, G., and Isner, J. M. (1997) *Science* 275, 964-967.
- Masuda, S., Okano, M., Yamagishi, K., Nagao, M., Ueda, M., and Sasaki, R. (1994) *J. Biol. Chem.* 269, 19488-19493.

# Erythropoietin Gene Expression in Human, Monkey and Murine Brain

Hugo H. Marti, Roland H. Wenger, Luis A. Rivas, Urs Straumann, Murat Digicaylioglu, Volker Henn<sup>1</sup>, Yasuhiro Yonekawa<sup>2</sup>, Christian Bauer and Max Gassmann

Institute of Physiology, <sup>1</sup>Department of Neurology and <sup>2</sup>Department of Neurosurgery, Zürich University Medical School, Zürich, Switzerland

**Keywords:** astrocyte, hypoxia, VEGF, erythropoietin receptor, quantitative RT-PCR

## Abstract

The haematopoietic growth factor erythropoietin is the primary regulator of mammalian erythropoiesis and is produced by the kidney and the liver in an oxygen-dependent manner. We and others have recently demonstrated erythropoietin gene expression in the rodent brain. In this work, we show that cerebral erythropoietin gene expression is not restricted to rodents but occurs also in the primate brain. Erythropoietin mRNA was detected in biopsies from the human hippocampus, amygdala and temporal cortex and in various brain areas of the monkey *Macaca mulatta*. Exposure to a low level of oxygen led to elevated erythropoietin mRNA levels in the monkey brain, as did anaemia in the mouse brain. In addition, erythropoietin receptor mRNA was detected in all brain biopsies tested from man, monkey and mouse. Analysis of primary cerebral cells isolated from newborn mice revealed that astrocytes, but not microglia cells, expressed erythropoietin. When incubated at 1% oxygen, astrocytes showed >100-fold time-dependent erythropoietin mRNA accumulation, as measured with the quantitative reverse transcription-polymerase chain reaction. The specificity of hypoxic gene induction in these cells was confirmed by quantitative Northern blot analysis showing hypoxic up-regulation of mRNA encoding the vascular endothelial growth factor, but not of other genes. These findings demonstrate that erythropoietin and its receptor are expressed in the brain of primates as they are in rodents, and that, at least in mice, primary astrocytes are a source of cerebral erythropoietin expression which can be up-regulated by reduced oxygenation.

## Introduction

The haematopoietic growth factor erythropoietin regulates erythroid differentiation in the haematopoietic organs, including the bone marrow, spleen and fetal liver, by preventing apoptosis of erythroid progenitor cells (for reviews see Krantz, 1991; Jelkmann, 1992; Koury and Bondurant, 1992). When individuals are subjected to hypoxic conditions, formation of erythropoietin is governed by an operationally defined oxygen sensor that leads to the accumulation of mRNA, resulting in elevated erythropoietin serum levels (Krantz, 1991; Jelkmann, 1992). However, the mechanisms by which cells perceive changes in oxygen concentration remain to be elucidated. The localization of erythropoietin synthesis was originally deduced from organ extirpation experiments and more recently from the analysis of erythropoietin mRNA distribution, to reveal that the kidney and liver are the dominant organs of erythropoietin production (for review see Jelkmann, 1992). In the kidney, peritubular interstitial fibroblasts have been identified as erythropoietin-producing cells (Koury *et al.*, 1988), whereas in the liver both hepatocytes and the non-parenchymal Ito cells have been found to express erythropoietin (Koury *et al.*, 1991; Maxwell *et al.*, 1994).

Induced erythropoietin gene expression in cell culture has been

observed after exposing the human hepatoma cell lines HepG2 and Hep3B to either 1% oxygen or cobalt chloride (Goldberg *et al.*, 1987). Molecular analysis using these cell lines as well as transgenic mice carrying the human erythropoietin transgene (Semenza *et al.*, 1991) has revealed the presence of an oxygen-dependent transcriptional enhancer lying 3' to the poly(A) addition site of the erythropoietin gene (Pugh *et al.*, 1991). The nuclear hypoxia-inducible factor 1 (HIF-1), a basic helix-loop-helix heterodimeric transcription factor (Wang *et al.*, 1995), was found to bind to this enhancer sequence in response to reduced oxygen concentrations (Semenza and Wang, 1992). Significantly, oxygen-dependent HIF-1 expression was observed not only in erythropoietin-producing HepG2 and Hep3B cells but also in various other cell lines that do not produce erythropoietin (Wang and Semenza, 1993). In addition, an oxygen-sensing mechanism similar to that regulating gene expression of erythropoietin has also been suggested for the gene encoding the vascular endothelial growth factor (VEGF) in Hep3B cells (Goldberg and Schneider, 1994; Levy *et al.*, 1995), as well as for glycolytic enzymes such as phosphoglycerate kinase 1, aldolase A, pyruvate kinase M and lactate dehydrogenase A (Firth *et al.*, 1994). These

findings demonstrate that erythropoietin is widespread in the brain. So far, erythropoietin is considered to be a target for its role in the nervous system, e.g. in the survival of tumours of haemangioblasts (Semenza *et al.*, 1993). Detection of erythropoietin receptor mRNA in the brain (Semenza *et al.*, 1992) and our findings support the hypothesis that erythropoietin is so far unknown in the brain, growth factor erythropoietin brain barrier situation in the brain is well established. We expect that in mice and in mice and in mice, we have demonstrated that erythropoietin receptor transpolymerase chain reaction cultures from the productively investigated to a reduced

## Materials and Methods

### Human brain

Human brain men, aged 1–4 years, amygdala/hippocampus treatment of protocol was from the test in liquid nitrogen

### Animals

Animals were the Kantonale used for neuro prior to perfusion kg body wt containing ci analysed du instrumentat kidney and h frontal and o and nucleus. Stimulation mice was a functional at 4 h in an air

Correspondence to: Hugo H. Marti, Institute of Physiology, University of Zürich-Irchel, Winterthurerstrasse 190, CH-8057 Zürich, Switzerland

Received 14 July 1995, revised 24 October 1995, accepted 27 October 1995



findings demonstrate that the ability to sense low oxygen concentrations, which leads to up-regulated expression of certain genes, is widespread in mammalian cells (Maxwell *et al.*, 1993).

So far, erythroid precursor cells have been considered to be the main target for erythropoietin. However, recent reports suggest that, beside its role in erythropoiesis, erythropoietin might exert a function in the nervous system; erythropoietin production has been observed in tumours of the human central nervous system, such as cerebellar haemangioblastoma (Trimble *et al.*, 1991) and meningioma (Bruneval *et al.*, 1993). In addition, erythropoietin has been shown to support the survival of lesioned neurons in rats *in vivo* and to augment choline acetyltransferase activity in primary cultured neurons (Konishi *et al.*, 1993). Detection of erythropoietin mRNA in the rat brain (Tan *et al.*, 1992) and our localization of specific erythropoietin binding sites in defined areas of the mouse brain (Digicaylioglu *et al.*, 1995) also support the notion that erythropoietin and its receptor are involved in so far unknown neuronal processes. Erythropoietin gene expression in the brain, in contrast to the kidney and liver, implies that this growth factor acts locally, since transport of cerebrally produced erythropoietin to the blood is most probably impeded by the blood-brain barrier (for review see Bradbury, 1993). By analogy to the situation in the kidney and liver, where erythropoietin gene expression is well established in all mammals, including primates, one would expect that cerebral erythropoietin gene expression is not restricted to mice and rats but also occurs in other species. To test this hypothesis, we analysed human, monkey (*Macaca mulatta*) and mouse brain biopsies for the presence of erythropoietin and erythropoietin receptor transcripts by means of quantitative reverse transcription-polymerase chain reaction (RT-PCR), and established primary cell cultures from the mouse brain to identify possible candidate cells for the production of erythropoietin in this organ. Furthermore, we investigated the ability of the brain to sense and respond specifically to a reduced oxygen supply.

## Materials and methods

### Human brain biopsies

Human brain material was obtained from two women and four men, aged 19–31 years, who had undergone trans-sylvian selective amygdalohippocampopectomy (Yasargil *et al.*, 1993) for the treatment of intractable temporal lobe epilepsy. The experimental protocol was approved by the University ethical committee. Biopsies from the temporal cortex, amygdala and hippocampus were frozen in liquid nitrogen.

### Animals

Animals were handled in accordance with a protocol approved by the Kantonales Veterinäramt Zürich. Adult male monkeys (*M. mulatta*) used for neuroanatomical studies were subjected to hypoxic conditions prior to perfusion with fixatives. Anaesthetized (40 mg pentobarbital/kg body wt *i.p.*) and intubated animals breathed a gas mixture containing either 8 or 20% oxygen for 2 h. Arterial blood gases were analysed during ventilation using a blood gas analyser (IL 1304, Instrumentation Laboratory, Milan, Italy). Tissue samples from the kidney and liver as well as from various areas of the brain (temporal, frontal and occipital cortex, cerebellum, hypothalamus, hippocampus and nucleus caudatus) were taken and transferred to liquid nitrogen.

Stimulation of erythropoietin production in adult male C57BL/6 mice was achieved by carbon monoxide inhalation resulting in functional anaemia (Eckardt *et al.*, 1992). Animals were exposed for 4 h in an airtight chamber that was supplied with a mixture of normal

air supplemented with 0.1% carbon monoxide. Immediately after exposure, mice were killed by decapitation, and after collecting blood, the kidneys, liver, brain, testis, spleen and samples of skeletal muscle were removed and frozen in liquid nitrogen. Hypoxic stimulation was monitored by determination of serum erythropoietin concentration using a radioimmunoassay as described (Eckardt *et al.*, 1988).

### Primary brain cell culture

Primary glial cell cultures were prepared from brains of newborn C57BL/6 mice as described (Frei *et al.*, 1986, 1987). Following removal of the meninges, the brains were mechanically dissociated by pressing through nylon sieves. The cells were seeded in DME medium (Gibco-BRL) containing 20% fetal calf serum (FCS; Boehringer Mannheim), 100 U/ml penicillin, 100 µg/ml streptomycin, 1 × Minimal Essential Medium non-essential amino acids, 2 mM L-glutamine and 1 mM sodium pyruvate (all from Gibco-BRL) in 175 cm<sup>2</sup> tissue culture flasks (two brains per flask), and were cultured in a humidified atmosphere containing 5% CO<sub>2</sub> at 37°C. Fresh medium with reduced FCS concentrations was added to the cells at days 6 (10% FCS) and 9 (5% FCS) of culture. Confluent cultures at day 13 were used to harvest both microglia cells and astrocytes. After agitating the confluent culture (500 r.p.m.) for 1 h, the adherent cells were saved for astrocyte preparation (see below), and the floating cells were transferred to a fresh tube to isolate microglia cells. After 10 min of gravity sedimentation at room temperature, the sediment was discarded and the supernatant containing floating cells was incubated at 37°C for 2 h in a flask and then gently agitated (70 r.p.m.) for an additional 10 min. Subsequently, the non-adherent cells present in the medium were removed while the remaining adherent cells were identified as microglia cells by immunofluorescence. The isolation of astrocytes followed the same protocol until day 13, when the floating microglia cells were removed (see above). The adherent cells were trypsinized and subcultured in medium containing 5% FCS. After 3 additional days, >95% of these first-passage cells were identified as astrocytes by immunofluorescence. Exposure to a low oxygen concentration was performed with confluent astrocytes: after replacing the medium (5% FCS), the cells were incubated for 6–94 h at either 20% O<sub>2</sub> (140 mm Hg, normoxia) or 1% O<sub>2</sub> (7 mm Hg, hypoxia) with or without addition of 100 µM CoCl<sub>2</sub> or 15 ng/ml human recombinant interleukin-6 (IL-6; R&D Systems, Basel, Switzerland) in a Forma Scientific incubator (Model 3319, Brouwer, Luzern, Switzerland).

### Immunofluorescent staining for glial fibrillary acidic protein and Fc receptor

For immunofluorescent staining, antibodies were diluted in phosphate-buffered saline containing 0.1% bovine serum albumin. Whereas astrocytes were directly cultured on glass slides, the microglia cells were cytopsed at a density of 1000 cells per slide. For staining of the astrocyte-specific intermediate filaments, slides were incubated with a 1:400 dilution of a rat anti-glial fibrillary acidic protein (GFAP) antiserum (Sigma) for 30 min at 25°C. To examine the Fc (IgG<sub>1/2b</sub>) receptor, a marker for microglia cells (Frei *et al.*, 1987), cells were incubated with monoclonal rat anti-mouse Fc receptor antibody (New England Nuclear) using a 1:1000 dilution for 30 min at 25°C. Subsequently, the cells were washed three times in PBS and incubated for 30 min with a 1:100 dilution of a biotinylated anti-rat IgG antibody (Sigma). As negative controls, cells were incubated with the second antibody alone. After washing, fluorescein isothiocyanate-conjugated streptavidin (Sigma) at 1:100 dilution was incubated for 30 min and the slides were examined in a Zeiss laser scanning fluorescence microscope.

### RNA preparation and Northern blot analysis

Frozen tissue was weighed and total RNA was isolated according to Chomczynski and Sacchi (1987). Resuspended RNA was quantified by spectrophotometric absorbance at 260 nm and tested for integrity by 1% agarose gel electrophoresis containing 0.05% sodium dodecyl sulphate in the running buffer. Total RNA (10 µg) was denatured in formaldehyde/formaldehyde and electrophoresed through a 1% agarose gel containing 6% formaldehyde as described (Sambrook *et al.*, 1989). After pressure blotting (Stratagene) to nylon membranes (Biodyne A, Pall, Winiger, Wohlen, Switzerland), the RNA was hybridized to <sup>32</sup>P-labelled probes following the manufacturer's (Pall) instructions. The radioactive signal was recorded and quantified using a phosphorimager (Molecular Dynamics, Paul Bucher, Basel, Switzerland). The mouse VEGF probe was derived from a 644 bp PCR fragment generated by using primers 5'-GCGGGCTGCCTC-GCAGTC-3' and 5'-TCACCGCCTTGGCTTGTAC-3' respectively (corresponding to bp 16-33 and 659-640 of the mouse VEGF cDNA sequence; numbering according to Claffey *et al.*, 1992). The contrapins probe was a kind gift from Dr Y. Suzuki (Osaka, Japan). Complement C3 cDNA was purchased from ATCC (phACT235, ATCC No. 61600, Rockville, MD) and the human actin probe was obtained from Clontech.

### Construction of competitor erythropoietin cRNA templates

The human competitor erythropoietin template was constructed by deleting a 102 bp *PvuII*-*PvuII* erythropoietin cDNA fragment (corresponding to bp 2405-2642 of the genomic erythropoietin sequence; numbering according to Jacobs *et al.*, 1985) from the human erythropoietin cDNA-containing plasmid pc49f. The *KpnI*-*SacI* erythropoietin cDNA fragment (1307-3052), harbouring the 102 bp deletion, was subcloned into vector pSP64polyA (Promega, Catalys, Wallisellen, Switzerland), giving rise to plasmid pEPO64. After cleavage with *EcoRI* and gel purification, the linearized plasmid was transcribed *in vitro* using SP6 RNA polymerase (Fermentas, Mächler, Basel, Switzerland) according to the manufacturer's directions, and the synthesized cRNA was quantified by absorbance at 260 nm. The resulting competitor product, following RT-PCR, was 178 bp long compared to 280 bp of the amplified target erythropoietin mRNA using the same primer set, allowing easy separation of both fragments by agarose gel electrophoresis. The mouse competitor erythropoietin template was obtained by deleting the *ScaI*-*SmaI* fragment (corresponding to bp 1568-2980; numbering according to Shoemaker and Mitsock, 1986) located in exon 2 and 5 of the mouse genomic erythropoietin fragment *BamHI*-*XbaI* (856-3463 bp) subcloned into pSP64polyA (*BamHI*-*SmaI*), giving rise to pLR1-EPO. The mouse competitor erythropoietin cRNA was obtained as described above and the RT-PCR product was 492 bp long, compared to 395 bp of the amplified target erythropoietin mRNA.

### Quantitation of erythropoietin mRNA by competitive RT-PCR

Both competitor and sample RNA species were reverse-transcribed into cDNA using Promega's Reverse Transcription System. To melt secondary structures, the RNA was denatured at 60°C for 10 min and chilled on ice. Subsequently, a series of 20 µl reaction mixtures containing 1 µg total RNA, each spiked with 0.2 fg to 20 pg of synthetic erythropoietin cRNA, 1 × reverse transcription buffer (10 mM Tris-HCl (pH 8.8 at 25°C), 50 mM KCl and 0.1% Triton X-100), 1 mM each dNTP's, 5 mM MgCl<sub>2</sub>, 20 U rRNasin, 15 U avian myeloblastosis virus reverse transcriptase and 0.5 µg oligo(dT)<sub>15</sub> primer were incubated for 1 h at 42°C. The reaction was terminated by heating the samples for 5 min at 75°C. Two negative controls

were carried out for each RT-PCR set by omitting either avian myeloblastosis virus reverse transcriptase or RNA from the reaction mixture.

PCR for human and monkey erythropoietin was performed with a sense primer located in exon 3 (5'-CGTCCCAGACACCAAAGTT-3') and the antisense primer located in exon 5 (5'-AGTGATGGTTCGGAGTGGGA-3') corresponding to bp 1639-1657 and 2666-2682 respectively (numbering according to Jacobs *et al.*, 1985) in a reaction mixture containing 1 × polymerization-buffer (10 mM Tris-HCl (pH 9.0 at 25°C), 50 mM KCl, 0.01% (wt/vol) gelatin, 0.1% Triton X-100, 1.5 mM MgCl<sub>2</sub>), 0.2 mM each dNTP's, 25 pmol of each primer, 0.2 U Super Taq Polymerase (Staehelin, Basel, Switzerland) and 5 µl from each reverse transcription reaction in a final volume of 50 µl. After initial denaturation for 1 min at 94°C, Taq polymerase was added and PCR was performed for 30-35 cycles (GeneAmp PCR System 9600 thermocycler, Perkin Elmer Cetus) with denaturation at 94°C for 1 min, primer annealing at 55°C for 1 min, elongation at 72°C for 1.5 min, and final elongation at 72°C for 5 min. PCR for mouse erythropoietin was performed as described (Digicaytliglu *et al.*, 1995).

Following agarose gel electrophoresis, the relative amount of target cDNA versus competitor DNA was quantitated by pixel analysis of video camera recordings. Coaccumulation of the two cDNA species was verified by erythropoietin RT-PCR analysis using either the competitor cRNA template (250 fg/assay) or 0.125 µg total RNA from kidney of stimulated mice containing ~250 fg erythropoietin mRNA/µg total RNA. The reactions were stopped after 25, 27, 29, 31 and 33 cycles and the amplified products were separated by gel electrophoresis. Analysis of the ethidium bromide-stained gel revealed a similar increase in both products after the same number of amplification cycles. Reproducibility of erythropoietin mRNA quantitation by competitive RT-PCR was verified by quadruplicate measurements of dilution series from the same sample, resulting in essentially identical values.

### Detection of erythropoietin receptor mRNA by RT-PCR

Reverse transcription of total RNA samples was performed as described above. An aliquot (3 µl) from this reaction was used as a template for amplification (30-35 cycles). For primate erythropoietin receptor, RT-PCR was performed using the sense primer located in exon 3 (5'-ACCGTGTCCATCCATCAAT-3') and the antisense primer in exon 7 (5'-GCCTTCAAACCTCGCTCTCTG-3') (corresponding to bp 401-420 and 885-866 respectively of the human erythropoietin receptor cDNA sequence; numbering according to Jones *et al.*, 1990). The amplification profile was 94°C for 1 min, 60°C for 1 min and 72°C for 1.5 min. The resulting erythropoietin receptor product was 485 bp long. One hundred femtograms of human erythropoietin receptor cDNA was used as a positive control. Murine erythropoietin receptor mRNA was detected as described (Digicaytliglu *et al.*, 1995) using total RNA from murine erythroleukaemia (MEL) cells as positive control (D'Andrea *et al.*, 1989).

### Presentation of data and statistics

Where appropriate, data are given as mean ± SD of *n* experiments. Student's *t*-test was used to evaluate the significance of differences.

### Results

#### Hypoxic induction of erythropoietin mRNA in the primate brain

Human brain biopsies were used to test whether erythropoietin is transcribed in this organ as it is in the rodent brain. To this end, we

Fig. 1. Detecti  
temporal cortex  
(B) was reverse  
(A) or quantita  
178 bp. No RT

look advanta  
who had un  
RNA sample  
PCR, reveal  
brain areas, a  
280 bp eryth  
fragment len  
mRNA levels  
PCR assay. T  
samples spiked  
cRNA added  
by PCR using  
variability in  
A representat  
is shown in f  
± 0.5 fg eryd  
in human hip  
and amygdala  
Because it  
regulation in  
monkeys to  
of the brain of  
spontaneousl  
(normoxia) or  
concentration

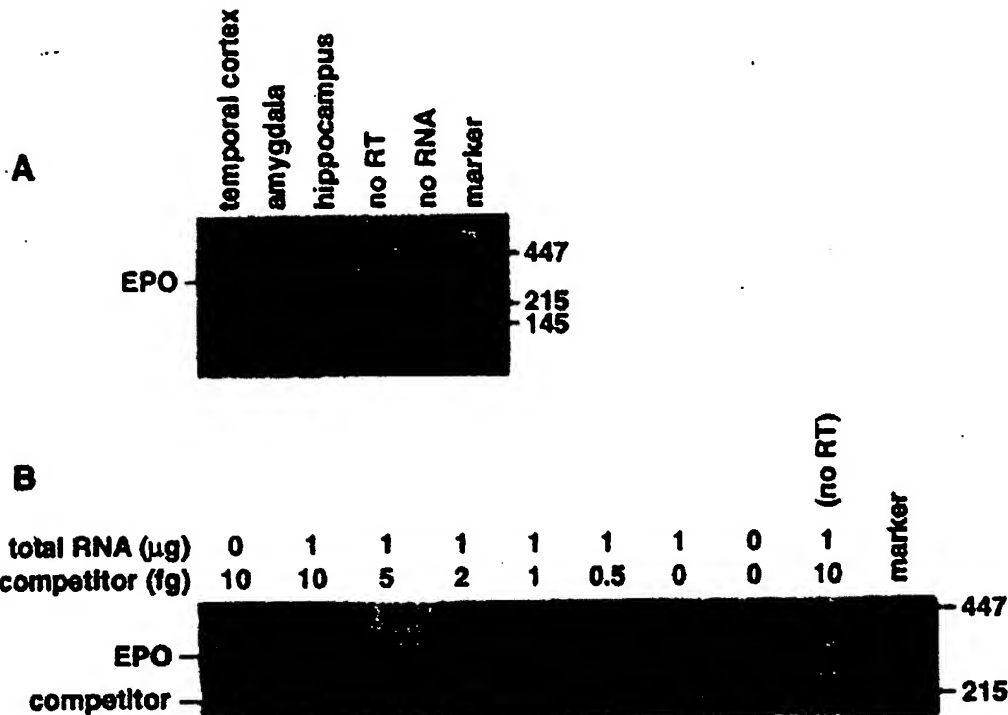


Fig. 1. Detection and quantitation of erythropoietin (EPO) transcripts in human brain tissues by RT-PCR. One microgram each of total RNA from human quadruplex temporal cortex, amygdala and hippocampus (A) or 1 μg of total RNA from hippocampus spiked with the indicated amount of competitor erythropoietin cRNA (B) was reverse-transcribed and amplified. After gel electrophoresis in 1.4% agarose, the reaction products were stained with ethidium bromide and photographed (A) or quantitated by pixel analysis of a video camera recording (B). The RT-PCR product length for primate erythropoietin is 280 bp and for the competitor 178 bp. No RT, no reverse transcriptase added.

## PCR

performed to take advantage of the therapeutic treatment of six epileptic patients who had undergone unilateral amygdala-hippocampectomy. Total RNA samples isolated from these biopsies were analysed by RT-PCR, revealing that erythropoietin mRNA was present in all three brain areas, as exemplified in Figure 1A. The identity of the amplified 280 bp erythropoietin product was further confirmed by restriction fragment length analysis (not shown). To quantify erythropoietin mRNA levels in the primate brain, we established a competitive RT-PCR assay. This technique involves reverse transcription of the test samples spiked with varying amounts of a synthetic erythropoietin cRNA added as standard, and coamplification of the cDNA products by PCR using primers common to both templates, thus correcting for variability in the efficiency of reverse transcription and amplification. A representative quantitation experiment from a hippocampus biopsy is shown in Figure 1B. Independent measurements revealed that  $1.5 \pm 0.5$  fg erythropoietin mRNA per μg total RNA ( $n = 3$ ) was present in a human hippocampus as well as in the biopsies of temporal cortex and amygdala.

Because it was not possible to investigate erythropoietin mRNA regulation in the brain of humans after oxygen deprivation, we used monkeys to test whether erythropoietin mRNA is up-regulated in the brain of hypoxic primates. Each two anaesthetized monkeys spontaneously breathed a gas mixture containing either 20% (normoxia) or 8% oxygen (hypoxia), the latter mimicking the oxygen concentration found at an altitude of 7500 m above sea level. Blood

gas analysis revealed that after 2 h exposure to 8% oxygen, the arterial  $pO_2$  was 44 mm Hg (5.9 kPa) and the oxygen saturation was diminished to 58.5%, compared to 75 mm Hg (10.0 kPa) and 92.0% respectively in the normoxic control animals. Furthermore, erythropoietin serum levels were found to be elevated by a factor of 2.5 as measured by radioimmunoassay. These findings confirmed that the exposed animals were indeed hypoxic. Competitive RT-PCR analysis revealed that erythropoietin mRNA levels increased more than 200 times ( $P < 0.01$ ) in the hypoxic kidney, reaching a concentration of  $1667 \pm 416$  fg erythropoietin mRNA/μg total RNA (Fig. 2). Similar to human biopsies (see above), normoxic monkey brain biopsies contained  $1.16 \pm 0.4$  fg erythropoietin mRNA/μg total RNA, independently of the sample's origin (e.g. temporal, frontal or occipital cortex, cerebellum, hypothalamus, hippocampus or nucleus caudatus). Hypoxic exposure led to an increase of ~3-fold ( $P < 0.001$ ) in the erythropoietin mRNA concentration in brain tissue (Fig. 2).

## Quantitation of erythropoietin mRNA in hypoxic mouse organs

Exposure of animals to 0.1% carbon monoxide results in functional anaemia and represents a strong stimulus for erythropoietin expression (Eckardt *et al.*, 1992). Since inhalation of carbon monoxide by the monkeys was not practicable, we exposed mice to 0.1% carbon monoxide for 4 h (see Materials and methods). Blood sample analysis revealed that ~50% of the haemoglobin was bound to carbon monoxide

TABLE 1. Serum immunoreactive erythropoietin protein and mRNA levels in different organs from unstimulated and carbon monoxide-treated mice

Mouse no.	RIA (mU/ml)	Competitive RT-PCR (fg erythropoietin mRNA/ $\mu$ g total RNA)					
		Serum EPO	Kidney	Liver	Brain	Testis	Spleen
Unstimulated (20% O <sub>2</sub> )							
1	27.3 $\pm$ 0.1	10	<0.2	2	1	<0.2	<0.2
2	28.2 $\pm$ 2.5	10	<0.2	1.5	1.5	0.2	n.d.
3	24.0 $\pm$ 1.3	10	<0.2	2	1	<0.2	<0.2
Stimulated (0.1% CO, 4 h)							
4	953 $\pm$ 7	1500	100	30	4	0.2	<0.2
5	1024 $\pm$ 30	2000	50	30	2	0.35	<0.2
6	1195 $\pm$ 34	2000	100	30	4	n.d.	<0.2

Quantitation of erythropoietin (EPO) mRNA in stimulated and control mice was performed as described in the legend to Figure 3. Serum erythropoietin levels are expressed as mean  $\pm$  SD. n.d., not determined.

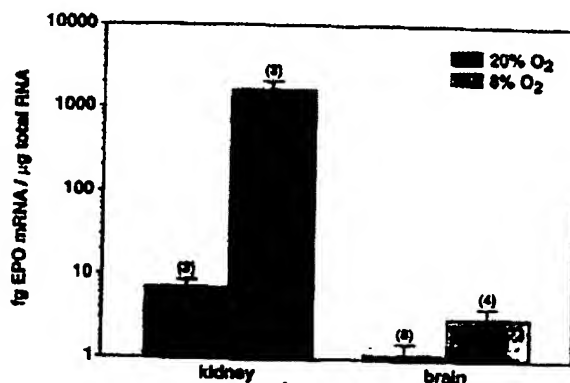


Fig. 2. Quantitation of erythropoietin (EPO) mRNA in normoxic and hypoxic monkeys. Total RNA was isolated from normoxic and hypoxic monkeys previously breathing 20 and 8% O<sub>2</sub> respectively for 2 h, and the erythropoietin mRNA level was quantitated by competitive RT-PCR. Biopsies were taken from the kidney (positive control) and different areas of the brain. The difference between normoxic and hypoxic organs was significant according to Student's *t*-test (kidney,  $P < 0.01$ ; brain,  $P < 0.001$ ,  $n = 3-8$  as indicated).

(as measured by the IL-CO-Oximeter 282, Milan, Italy). Hypoxic stimulation of erythropoietin production was confirmed by a 40-fold increase in serum erythropoietin protein level (as shown in Table 1). Quantitation of mouse erythropoietin mRNA in several organs was performed by competitive RT-PCR, as exemplified by mouse no. 1 (normoxia) and no. 6 (carbon monoxide-exposed) in Figure 3. Table 1 summarizes the values measured in six animals. In the kidney, the main erythropoietin-producing organ, induction was nearly 200-fold; erythropoietin mRNA levels increased from 10 fg/ $\mu$ g total RNA in control mice ( $n = 3$ ) to  $1833 \pm 289$  fg/ $\mu$ g total RNA in carbon monoxide-treated animals ( $n = 3$ ). Hepatic erythropoietin mRNA rose from barely detectable levels to 100 fg/ $\mu$ g total RNA. In the brain, we observed an increase in erythropoietin mRNA levels from  $1.83 \pm 0.29$  fg erythropoietin mRNA/ $\mu$ g total RNA in control mice to 30 fg/ $\mu$ g total RNA in carbon monoxide-treated animals, representing an induction factor of  $\sim 20$  (see also Fig. 3). Low level erythropoietin mRNA was also found in testis ( $1.17 \pm 0.29$  fg/ $\mu$ g total RNA) as well as in the spleen of control mice. Interestingly, while no erythropoietin transcripts were detected in skeletal muscle, independently of whether or not the mice were exposed to carbon

monoxide, exposure to carbon monoxide led to a 3-fold induction of testicular erythropoietin mRNA.

#### Oxygen-dependent expression of erythropoietin and VEGF in cultured mouse astrocytes

In an attempt to identify erythropoietin-producing cells in the mouse brain and to examine at a cellular level whether other genes besides erythropoietin are up-regulated by hypoxia in this organ, we cultured primary cells derived from the neonatal mouse brain. By analogy to the situation in the kidney and liver, where non-parenchymal cells are the main source of erythropoietin, we surmised that the glial cells in the brain, mainly astrocytes and microglia cells, might be a source of erythropoietin production. Thus, we established cultures enriched in microglia cells and astrocytes. The identity of the two cell types was verified using antibodies raised against the Fe receptor (IgG<sub>1</sub>) (microglia cells) and GFAP (astrocytes). Immunofluorescence analysis revealed that  $>90\%$  of the cells in the microglia fraction were positive for the Fe receptor whereas GFAP-positive cells represented  $<5\%$  of all cells (Fig. 4). On the other hand,  $>95\%$  of the cells present in the astroglia fraction were GFAP-positive (Fig. 4), thus showing efficient separation of the two cell types.

Analysis of total RNA from normoxic cells revealed the presence of erythropoietin mRNA in primary astrocytes only. Quantitative RT-PCR revealed that the erythropoietin mRNA level in these cells was up-regulated more than 100-fold by hypoxia (1% oxygen) in a time-dependent manner (Fig. 5). A very faint erythropoietin RT-PCR signal was found in cultured primary microglia and oligodendrocytes only after hypoxic induction (data not shown), most probably resulting from contaminating astrocytes. These results identified astrocytes as erythropoietin-producing cells and demonstrated that these cells are capable of increasing the erythropoietin mRNA level in an oxygen-dependent manner. Interestingly, addition of cobalt chloride, which is known to induce erythropoietin expression in human hepatoma cell lines (Goldberg *et al.*, 1987), showed no significant stimulatory effect in astrocytes (Fig. 5).

To verify that hypoxic up-regulation in these cells was specific we analysed the mRNA levels of other genes after reduced oxygenation. We chose conalbumin and complement C3 because these genes are known to be expressed in astrocytes. We also investigated the regulation of VEGF mRNA, a potent inducer of angiogenesis (reviewed in Plate *et al.*, 1994), since this gene is expressed in the mammalian brain (Breier *et al.*, 1992) and since hypoxic VEGF regulation has been observed in human glioblastomas (Shweiki *et al.*, 1992). In addition, it has been suggested that there exist similarities

Fig. 3. Quantitation of erythropoietin (EPO) mRNA in stimulated and control mice was performed as described in the legend to Figure 3. Serum erythropoietin levels are expressed as mean  $\pm$  SD. n.d., not determined.

between the expression of VEGF and erythropoietin (Potter, 1992). For synergistic cell line (F. fold synergism with 1 astrocytes, expression moderately this gene is (Potter, 1992). VEGF in IL-6 affect Detection man, mon Assuming and consid





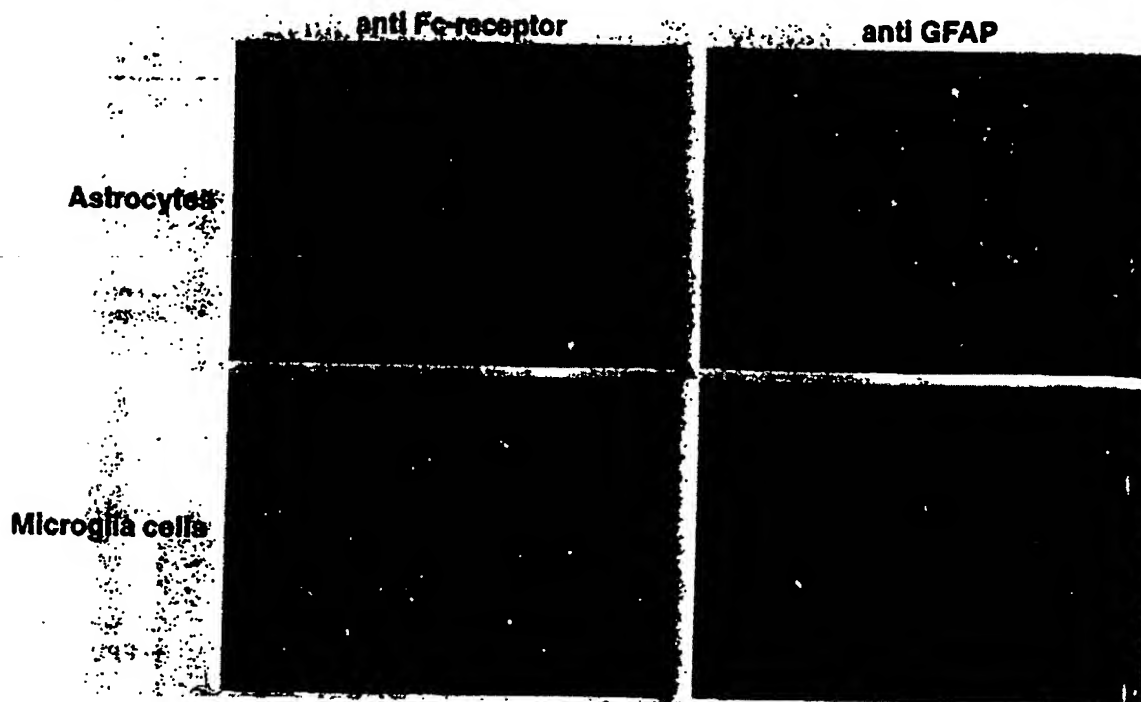


FIG. 4. Identification of astrocytes and microglia cells by immunofluorescence. Primary astrocytes and microglia cells were prepared from 1-day-old mice. Astrocytes and microglia cells were incubated with antibodies raised against the Fc receptor, specific for microglia cells, or GFAP, specific for astrocytes.

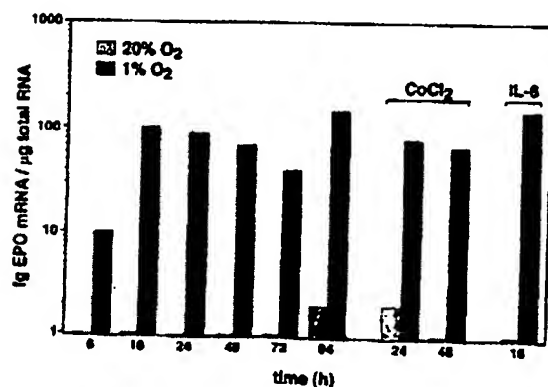


FIG. 5. Quantitation of erythropoietin (EPO) mRNA levels in primary murine astrocytes. Cells were incubated for 6–96 h at 20 or 1% O<sub>2</sub> with or without 100 μM CoCl<sub>2</sub> chloride or 15 ng/ml IL-6. Total RNA was isolated after stimulation of the cells and the erythropoietin mRNA level was determined by competitive RT-PCR.

caudatus) and the mouse. Histological examination of the human brain samples used in this study showed a reactive gliosis in the hippocampus and amygdala (data not shown). This might lead to the speculation that erythropoietin expression is enhanced under these pathological conditions. However, comparable concentrations of erythropoietin mRNA were also found in the normal brain of both monkey and mouse. Together with similar observations in the rodent

brain (Tan *et al.*, 1992; Masuda *et al.*, 1994; Digicaylioglu *et al.*, 1995) our findings support the hypothesis that erythropoietin plays a physiological role in the mammalian brain, including the human brain. This notion is strengthened by the relatively high constitutive erythropoietin mRNA level found in the normoxic mouse brain: when taking organ weight into account and assuming identical transcription efficiencies, accumulation of cerebral erythropoietin mRNA was considerably higher than in the liver and represented ~10% of the constitutive renal erythropoietin production. Furthermore, we showed that erythropoietin gene expression in the brain responds to the physiological stimuli of hypoxia and anaemia (resulting from exposure to carbon monoxide) with an increase in the erythropoietin mRNA level. In comparison to the normoxic control mice, hypoxic up-regulation of erythropoietin mRNA was 10 times higher in the kidney and 2–5 times higher in the liver, compared to the brain. This observation can be explained by assuming that cerebrally produced erythropoietin would remain in the brain as the blood–brain barrier insulates this organ from the bloodstream and most probably hinders renal erythropoietin from entering this tissue. Thus, erythropoietin might act locally as a paracrine rather than as an endocrine factor. As such, much lower amounts of erythropoietin could be sufficient to achieve local concentrations similar to those in the bone marrow to which erythropoietin has to be transported upon release by the kidney into the bloodstream and subsequent dilution. Alternatively, it is possible that the threshold level of the oxygen sensor is different in the brain compared to the kidney and liver, suggesting that the response to hypoxia is specifically modulated in every organ.

So far, erythropoietin is thought to exert its function exclusively by binding to the erythropoietin receptor. Thus, paracrine action

FIG. 6. Quantitation of erythropoietin (EPO) mRNA levels in primary murine astrocytes. Cells were incubated for 6–96 h at 20 or 1% O<sub>2</sub> with or without 100 μM CoCl<sub>2</sub> chloride or 15 ng/ml IL-6. Total RNA was isolated after stimulation of the cells and the erythropoietin mRNA level was determined by competitive RT-PCR.

erythropoietin receptor in erythropoietin mouse brain receptor mRNA (Yasu PC12 and S 1993). In it gene is exp

Hypoxia in primary

While we murine astrocytes, the erythropoietin mRNA level in the erythropoietin mouse brain is higher than the much in our finding transformed produced

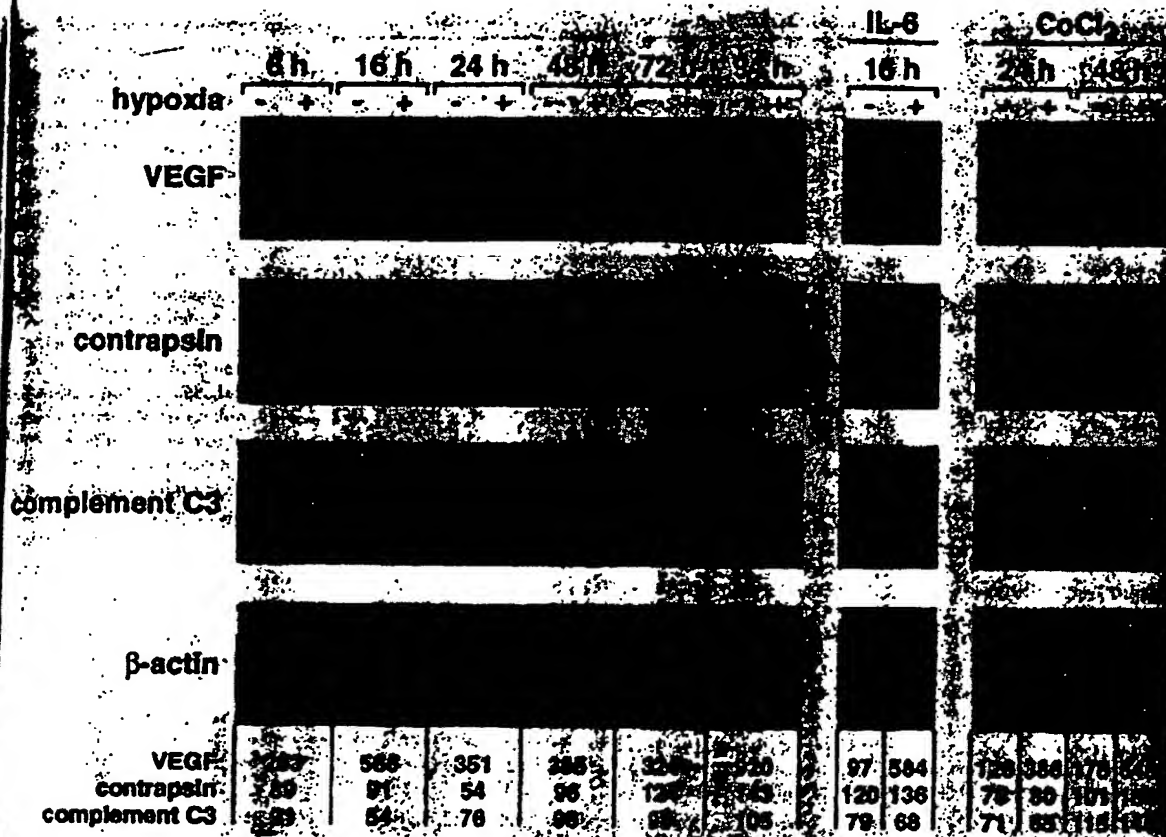


Fig. 6 Quantitative Northern blot analysis of primary astrocytes. Cells were incubated at 20% (-) or 1% O<sub>2</sub> (+) as described in Figure 5. Equal amounts (10 µg) of total RNA were loaded on each lane. After blotting, the membrane was hybridized to probes encoding VEGF, contrapsin, complement C3 and β-actin, the latter serving as a loading, blotting and internal normalization control. The signals were evaluated by phosphorimager analysis, and the values, normalized to β-actin, are shown as percentages of the corresponding normoxic and untreated control value at the bottom of the figure.

erythropoietin in the brain implies the presence of erythropoietin receptor in this organ. We recently reported the presence of specific erythropoietin binding sites and erythropoietin receptor mRNA in the mouse brain (Digicaylioglu *et al.*, 1995). In addition, erythropoietin receptor mRNA has also been observed in the developing mouse brain (Yasuda *et al.*, 1993) and in the non-erythroid clonal cell lines PC12 and SN6, which display neuronal characteristics (Masuda *et al.*, 1993). In this study, we have shown that the erythropoietin receptor gene is expressed in all tested areas of human and monkey brain.

#### Hypoxia-inducible erythropoietin and VEGF gene expression in primary astrocytes

While we detected erythropoietin mRNA in primary cultures of murine astrocytes, only very small amounts were observed in microglia. Hypoxic induction of astrocytes led to a 100-fold increase in the erythropoietin mRNA level. This increase is considerably higher than that found *in vivo* (see above), but can be explained by the much more severe reduction in oxygen concentration used *in vitro*. Our findings are in agreement with a recent report demonstrating that transformed rat astrocytes harbouring the SV40 large T-antigen produced erythropoietin in an oxygen-dependent manner (Masuda

*et al.*, 1994). Interestingly, cobalt chloride, an inducer of erythropoietin production in the hepatoma cell lines HepG2 and Hep3B (Goldberg *et al.*, 1987), had no effect on erythropoietin mRNA levels in primary astrocytes, a phenomenon which has also been reported for primary cultures of rat hepatocytes, which represent the only other primary cells capable of erythropoietin production (Eckardt *et al.*, 1993). Addition of IL-6 to the primary astrocytes synergistically increased hypoxic erythropoietin mRNA levels by 50%, whereas IL-6 alone had no effect under normoxic condition. These findings very closely resemble previous results obtained with the hepatoma cell line Hep3B (Faquin *et al.*, 1992). However, it is unknown how erythropoietin-producing primary hepatocytes respond to IL-6. Unfortunately, the lack of a regulated erythropoietin-producing cell line of renal origin impedes a comparison with astrocytes.

To test whether oxygen-dependent gene expression in primary astrocytes is restricted to erythropoietin, we analysed the mRNA level of VEGF, another hypoxia-inducible gene. We showed that astrocytes are a source of VEGF production in the brain and that stimulation by hypoxia or cobalt chloride led to a significant increase in VEGF mRNA levels, whereas addition of IL-6 had no effect. These results were confirmed by a recent study, published while this

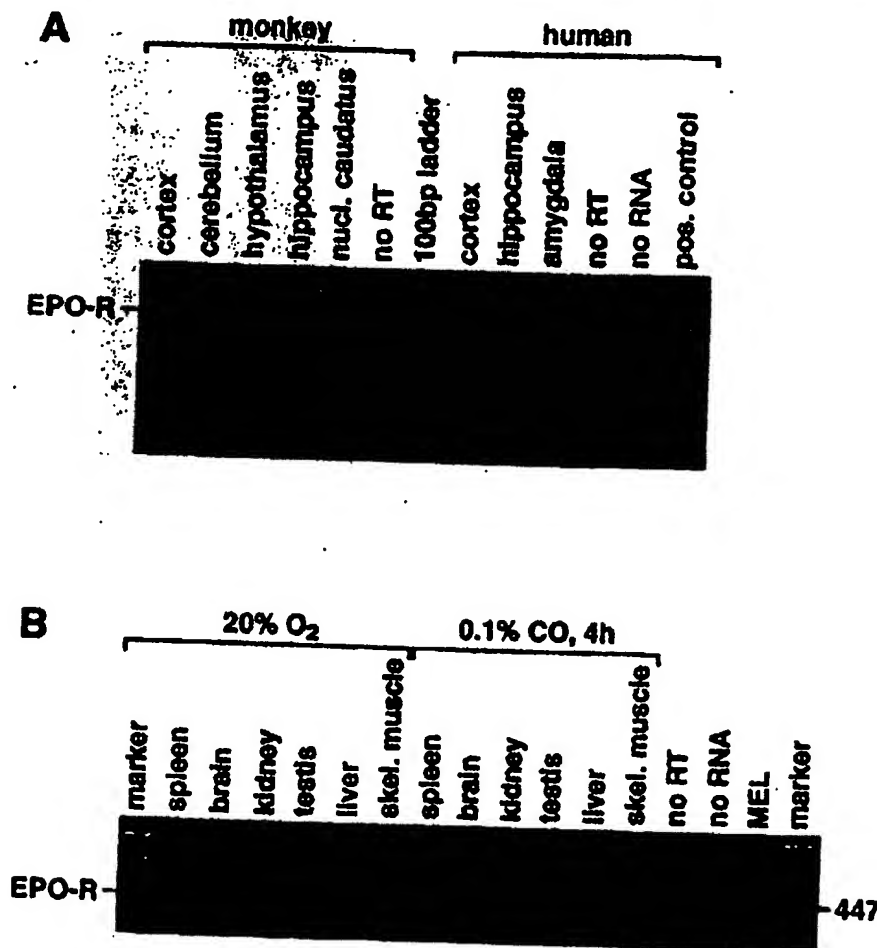


FIG. 7. Detection of erythropoietin receptor (EPO-R) mRNA in different regions of the primate (monkey and human) brain (A) and in mouse organs (B). One microgram of total RNA was analysed by RT-PCR specific for primate (A) or mouse (B) erythropoietin receptor. The RT-PCR product for primate erythropoietin receptor is 485 bp, and that for the mouse EPO receptor is 452 bp. No RT, no reverse transcriptase added; positive control, human erythropoietin receptor cDNA; MEL, murine erythroleukaemia cells (positive control for murine erythropoietin receptor).

manuscript was under revision, showing hypoxia-inducible VEGF expression in rat astrocytes (Ijichi *et al.*, 1995). By contrast, complement C3 and contraspin showed no significant effect upon stimulation by either stimulus. In conclusion, we showed that astrocytes expressed erythropoietin and VEGF in an oxygen-dependent manner and that cobalt chloride mimicked this up-regulation of VEGF but not of erythropoietin transcription.

#### Putative physiological role of erythropoietin in the brain

At present, the physiological function of erythropoietin in the nervous system remains to be clarified. By analogy to other ligands that bind to members of the cytokine receptor superfamily (including the erythropoietin receptor), erythropoietin might represent a polyfunctional growth factor. We recently proposed that the significant increase in erythropoietin mRNA in the brain upon hypoxic stimulation might represent a rapid adaptive mechanism of this organ to hypoxia (Digicaylioglu *et al.*, 1995). In this context, it is noteworthy that

erythropoietin and erythropoietin receptor mRNA expression was found in areas containing populations of neurons which are particularly susceptible to hypoxia, such as the hippocampus (CA1), neocortex and cerebellum (Haddad and Jiang, 1993). Furthermore, assuming that the erythropoietin receptor is present on neurons, as observed with neuron-like PC12 cells (Masuda *et al.*, 1993) and neuroblastoma cell lines (H. H. Marti, R. H. Wenger and M. Gassmann, unpublished observations), one could postulate that erythropoietin exerts a neurotrophic activity in the brain. In view of its role during erythropoiesis, erythropoietin might act as a survival factor preventing apoptosis as well as a differentiating factor during development. Interestingly, *in vivo* experiments have demonstrated that erythropoietin promotes the survival of lesioned neurons after fimbria-fornix transections in rats (Konishi *et al.*, 1993). Furthermore, erythropoietin augmented choline acetyltransferase activity in mouse embryonic primary cortical neurons (Konishi *et al.*, 1993) and increased monoamine and calcium levels in the pheochromocytoma-derived cell line PC12 (Masuda

*et al.*, 1993). In the brain development has been detected (Masuda *et al.*, 1993). Finally, erythropoietin and erythropoietin VEGF; erythropoietin (Amagnotou, 1990) and erythropoietin (Cartini *et al.*, 1990).

The view of erythropoietin as a hormone, selecting exclusively erythropoietin body. A more as well as du containing the promoters.

#### Acknowled

The authors thank the erythropoietin (Ciba-Geigy) and MEL (plasmid pc49 erythropoietin) for help during the patients, W. Massey, I. Forstner, and this Foundation (Stiftung, and Zürich M. D. Foundation).

#### Abbreviati

GFAP  
IL-6  
MEL  
PBS  
PCR  
RT  
VEGF

#### Reference

Amagnotou, (1990) Erythropoietin and endothelial  
Noguchi, C  
Brady, M.  
Breier, G., A  
vascular en  
Bruneval, P.  
X., Varet,  
cells in a  
1593-1597  
Cartini, R. G  
erythropoie



et al., 1993). During embryogenesis, erythropoietin might be involved in brain development: expression of erythropoietin and its receptor has been detected in the developing brain of 8- to 10-day old embryos (Yasuda et al., 1993) as well as in blastocyst-derived embryonic stem cells and embryoid bodies, which resemble the 6-8 day egg cylinder stage (Schmitt et al., 1991; Keller et al., 1993; Gassmann et al., 1995). Finally, oxygen-dependent expression of the cytokines erythropoietin and VEGF in astrocytes leads to the speculation that erythropoietin might play a role in angiogenesis in concert with VEGF: erythropoietin receptor is expressed on endothelial cells (Anagnostou et al., 1994) and erythropoietin has been shown to exert mitogenic and chemotactic effects on endothelial cells (Anagnostou et al., 1990) and to induce angiogenesis from rat aortic rings *in vitro* (Carlini et al., 1995).

The view of erythropoietin as a monofunctional haematopoietic hormone, solely produced by the fetal liver and adult kidney and acting exclusively on erythroid precursor cells, needs to be revised: erythropoietin and its receptor are widely expressed throughout the body. A more defined role for erythropoietin in brain and other organs as well as during embryogenesis requires studies in transgenic mice containing the erythropoietin gene under the control of tissue-specific promoters.

#### Acknowledgements

The authors thank N. Arnold and S. Aschkenasy for their help in constructing the erythropoietin competitors. The monkeys were kindly provided by R. Pfister (Ciba-Geigy, Basel, Switzerland), human erythropoietin cDNA (plasmid pc49f) by E. Goldwasser, mouse erythropoietin cDNA by Y. Suzuki, erythropoietin receptor cDNA by A. D'Andrea, Fc receptor antibodies by K. Frei, and MEL cells by P. Ratcliffe. We thank V. Furrer for excellent technical help during the monkey experiments, H.-G. Wieser and D. Köntz for evaluating the patients, W. Baier-Kustermann for doing the erythropoietin radioimmunoassay, I. Forster for critical reading of the manuscript and C. Gasser for the artwork. This study was supported by grants from the Swiss National Science Foundation (31-36369.92), the EMDO-, Hartmann Müller- and Sandoz-Stiftung, and the Stiftung für Wissenschaftliche Forschung an der Universität Zürich. M. D. was the recipient of a fellowship from the Theodore Ott Foundation.

#### Abbreviations

GFAP	glial fibrillary acidic protein
IL-6	interleukin-6
MEL	murine erythroleukaemia
PBS	phosphate-buffered saline
PCR	polymerase chain reaction
RT	reverse transcription
VEGF	vascular endothelial growth factor

#### References

- Anagnostou, A., Lee, E. S., Kessimian, N., Levinson, R. and Steiner, M. (1990) Erythropoietin has a mitogenic and positive chemotactic effect on endothelial cells. *Proc. Natl Acad. Sci. USA*, **87**, 5978-5982.
- Anagnostou, A., Liu, Z., Steiner, M., Chin, K., Lee, E. S., Kessimian, N. and Noguchi, C. T. (1994) Erythropoietin receptor mRNA expression in human endothelial cells. *Proc. Natl Acad. Sci. USA*, **91**, 3974-3978.
- Bradbury, M. W. (1993) The blood-brain barrier. *Exp. Physiol.*, **78**, 453-472.
- Breier, G., Albrecht, U., Sterrer, S. and Risau, W. (1992) Expression of vascular endothelial growth factor during embryonic angiogenesis and endothelial cell differentiation. *Development*, **114**, 521-532.
- Bruneval, P., Sassy, C., Mayeux, P., Belair, M.-F., Casadevall, N., Roux, F.-X., Varet, B. and Lacombe, C. (1993) Erythropoietin synthesis by tumor cells in a case of meningioma associated with erythrocytosis. *Blood*, **81**, 1593-1597.
- Carlini, R. G., Reyes, A. A. and Rothstein, M. (1995) Recombinant human erythropoietin stimulates angiogenesis *in vitro*. *Kidney Int.*, **47**, 740-745.
- Chomczynski, P. and Sacchi, N. (1987) Single-step method of RNA isolation by acid guanidinium thiocyanate-phenol-chloroform extraction. *Anal. Biochem.*, **162**, 156-159.
- Claffey, K. P., Wilkison, W. O. and Spiegelman, B. M. (1992) Vascular endothelial growth factor. Regulation by cell differentiation and activated second messenger pathways. *J. Biol. Chem.*, **267**, 16317-16322.
- D'Andrea, A. D., Lodish, H. F. and Wang, O. G. (1989) Expression cloning of the murine erythropoietin receptor. *Cell*, **57**, 277-285.
- Digicaylioglu, M., Bichet, S., Marti, H. H., Wenger, R. H., Rivas, L. A., Bauer, C. and Gassmann, M. (1995) Localization of specific erythropoietin binding sites in defined areas of the mouse brain. *Proc. Natl Acad. Sci. USA*, **92**, 3717-3720.
- Eckardt, K.-U., Kurtz, A., Hirth, P., Scigalla, P., Wiecek, L. and Bauer, C. (1988) Evaluation of the stability of human erythropoietin in samples for radioimmunoassay. *Klin. Wochenschr.*, **66**, 241-245.
- Eckardt, K.-U., Ratcliffe, P. J., Tan, C. C., Bauer, C. and Kurtz, A. (1992) Age-dependent expression of the erythropoietin gene in rat liver and kidneys. *J. Clin. Invest.*, **89**, 753-760.
- Eckardt, K.-U., Pugh, C. W., Ratcliffe, P. J. and Kurtz, A. (1993) Oxygen-dependent expression of the erythropoietin gene in rat hepatocytes *in vitro*. *Pflügers Arch.-Eur. J. Physiol.*, **423**, 356-364.
- Faquin, W. C., Schneider, T. J. and Goldberg, M. A. (1992) Effect of inflammatory cytokines on hypoxia-induced erythropoietin production. *Blood*, **79**, 1987-1994.
- Firth, J. D., Ebert, B. L., Pugh, C. W. and Ratcliffe, P. J. (1994) Oxygen-regulated control elements in the phosphoglycerate kinase 1 and lactate dehydrogenase A genes: similarities with the erythropoietin 3' enhancer. *Proc. Natl Acad. Sci. USA*, **91**, 6496-6500.
- Frei, K., Bodmer, S., Schwerdel, C. and Fontana, A. (1986) Astrocyte-derived interleukin 3 as a growth factor for microglia cells and peritoneal macrophages. *J. Immunol.*, **137**, 3521-3527.
- Frei, K., Siepl, C., Groscurth, P., Bodmer, S., Schwerdel, C. and Fontana, A. (1987) Antigen presentation and tumor cytotoxicity by interferon- $\gamma$ -treated microglia cells. *Eur. J. Immunol.*, **17**, 1721-1728.
- Gassmann, M., Wartenberg, M., McClanahan, T., Fandrey, J., Bichet, S., Kreuter, R., Acker, H. and Bauer, C. (1995) Differentiating embryonic stem cells as an *in vitro* model of early erythropoiesis. *Toxicol. In Vitro*, **9**, 429-438.
- Goldberg, M. A. and Schneider, T. J. (1994) Similarities between the oxygen-sensing mechanisms regulating the expression of vascular endothelial growth factor and erythropoietin. *J. Biol. Chem.*, **269**, 4355-4359.
- Goldberg, M. A., Glass, G. A., Cunningham, J. M. and Bunn, H. F. (1987) The regulated expression of erythropoietin by two human hepatoma cell lines. *Proc. Natl Acad. Sci. USA*, **84**, 7972-7976.
- Haddad, G. G. and Jiang, C. (1993) O<sub>2</sub> deprivation in the central nervous system: on mechanisms of neuronal response, differential sensitivity and injury. *Prog. Neurobiol.*, **40**, 277-318.
- Ijichi, A., Sakuma, S. and Toftlon, P. J. (1995) Hypoxia-induced vascular endothelial growth factor expression in normal rat astrocyte cultures. *Glia*, **14**, 87-93.
- Jacobs, K., Shoemaker, C., Rudersdorf, R., Neill, S. D., Kaufman, R. J., Mufson, A., Sechra, J., Jones, S. S., Hewick, R., Fritsch, E. F., Kawakita, M., Shimizu, T. and Miyake, T. (1985) Isolation and characterization of genomic and cDNA clones of human erythropoietin. *Nature*, **313**, 806-810.
- Jellmann, W. (1992) Erythropoietin: structure, control of production, and function. *Physiol. Rev.*, **72**, 449-489.
- Jones, S. S., D'Andrea, A. D., Haines, L. L. and Wong, G. G. (1990) Human erythropoietin receptor: cloning, expression, and biologic characterization. *Blood*, **76**, 31-35.
- Keller, G., Kennedy, M., Papayannopoulou, T. and Wiles, M. V. (1993) Hematopoietic commitment during embryonic stem cell differentiation in culture. *Mol. Cell. Biol.*, **13**, 473-486.
- Konishi, Y., Chui, D.-H., Hirose, H., Kumishima, T. and Tabira, T. (1993) Trophic effect of erythropoietin and other haematopoietic factors on central cholinergic neurons *in vitro* and *in vivo*. *Brain Res.*, **609**, 29-35.
- Koury, S. T., Bondurant, M. C. and Koury, M. J. (1988) Localization of erythropoietin synthesizing cells in murine kidneys by *in situ* hybridization. *Blood*, **71**, 524-527.
- Koury, S. T., Bondurant, M. C., Koury, M. J. and Semenza, G. L. (1991) Localization of cells producing erythropoietin in murine liver by *in situ* hybridization. *Blood*, **77**, 2497-2503.
- Koury, M. J. and Bondurant, M. C. (1992) The molecular mechanism of erythropoietin action. *Eur. J. Biochem.*, **210**, 649-663.
- Krantz, S. B. (1991) Erythropoietin. *Blood*, **77**, 419-434.
- Levy, A. P., Levy, N. S., Wegner, S. and Goldberg, M. A. (1995) Transcriptional

- regulation of the rat vascular endothelial growth factor gene by hypoxia. *J. Biol. Chem.*, 270, 13333-13340.
- Masuda, S., Nagao, M., Takahata, K., Konishi, Y., Gallyas, F., Tabira, T. and Sasaki, R. (1993) Functional erythropoietin receptor of the cells with neural characteristics. *J. Biol. Chem.*, 268, 11208-11216.
- Masuda, S., Okano, M., Yamagishi, K., Nagao, M., Ueda, M. and Sasaki, R. (1994) A novel site of erythropoietin production: oxygen-dependent production in cultured rat astrocytes. *J. Biol. Chem.*, 269, 19488-19493.
- Maxwell, P. H., Pugh, C. W. and Ratcliffe, P. J. (1993) Inducible operation of the erythropoietin 3' enhancer in multiple cell lines: evidence for a widespread oxygen-sensing mechanism. *Proc. Natl Acad. Sci. USA*, 90, 2423-2427.
- Maxwell, P. H., Ferguson, D. J. P., Osmond, M. K., Pugh, C. W., Heryet, A., Doe, B. G., Johnson, M. H. and Ratcliffe, P. J. (1994) Expression of a homologously recombined erythropoietin-SV40 T antigen fusion gene in mouse liver: evidence for erythropoietin production by its cells. *Blood*, 84, 1823-1830.
- Plate, K. H., Breier, G. and Risau, W. (1994) Molecular mechanisms of developmental and tumor angiogenesis. *Brain Pathol.*, 4, 207-218.
- Potter, H. (1992) The involvement of astrocytes and an acute phase response in the amyloid deposition of Alzheimer's disease. *Prog. Brain Res.*, 94, 347-358.
- Pugh, C. W., Tan, C. C., Jones, R. W. and Ratcliffe, P. J. (1991) Functional analysis of an oxygen-regulated transcriptional enhancer lying 3' to the mouse erythropoietin gene. *Proc. Natl Acad. Sci. USA*, 88, 10553-10557.
- Sambrook, J., Fritsch, E. F. and Maniatis, T. (1989) *Molecular Cloning: A Laboratory Manual*. Cold Spring Harbor Laboratory Press, Cold Spring Harbor, NY.
- Schmitt, R. M., Bruyns, E. and Snodgrass, H. R. (1991) Hematopoietic development of embryonic stem cells *in vitro*: cytokine and receptor gene expression. *Genes Dev.*, 5, 728-740.
- Semenza, G. L. and Wang, G. L. (1992) A nuclear factor induced by hypoxia via *de novo* protein synthesis binds to the human erythropoietin enhancer at a site required for transcriptional activation. *Mol. Cell. Biol.*, 12, 5447-5454.
- Semenza, G. L., Koury, S. T., Neiffelt, M. K., Gearhart, J. D. and Antonarakis, S. E. (1991) Cell-type-specific and hypoxia-inducible expression of the human erythropoietin gene in transgenic mice. *Proc. Natl Acad. Sci. USA*, 88, 8725-8729.
- Shoemaker, C. B. and Mitsch, L. D. (1986) Murine erythropoietin gene cloning, expression, and human gene homology. *Mol. Cell. Biol.*, 6, 809-811.
- Shweiki, D., Iin, A., Soffer, D. and Keshet, E. (1992) Vascular endothelial growth factor induced by hypoxia may mediate hypoxia-initiated angiogenesis. *Nature*, 359, 843-845.
- Tan, C. C., Eckardt, K. U., Firth, J. D. and Ratcliffe, P. J. (1992) Fecund modulation of renal and hepatic erythropoietin mRNA in response to graded anemia and hypoxia. *Am. J. Physiol.*, 263, F474-F481.
- Trimble, M., Caro, J., Talalla, A. and Braun, M. (1991) Secondary erythrocytosis due to a cerebellar hemangioblastoma: demonstration of erythropoietin mRNA in the tumor. *Blood*, 78, 599-601.
- Wang, G. L. and Semenza, G. L. (1993) General involvement of hypoxia-inducible factor 1 in transcriptional response to hypoxia. *Proc. Natl Acad. Sci. USA*, 90, 4304-4308.
- Wang, G. L., Jiang, B. H., Rue, E. A. and Semenza, G. L. (1995) Hypoxia-inducible factor 1 is a basic helix-loop-helix PAS heterodimer regulated by cellular O<sub>2</sub> tension. *Proc. Natl Acad. Sci. USA*, 92, 5510-5514.
- Yasargil, M. G., Wieser, H. G., Valavanis, A., von Ammon, K. and Roth, P. (1993) Surgery and results of selective amygdala-hippocampectomy in one hundred patients with nonlesional limbic epilepsy. *Neurosurg. Clin. N. Am.*, 4, 243-261.
- Yasuda, Y., Nagao, M., Okano, M., Masuda, S., Sasaki, R., Konishi, H. and Tanumura, T. (1993) Localization of erythropoietin and erythropoietin receptor in postimplantation mouse embryos. *Dev. Growth Differ.*, 4, 711-722.

Embryonic  
clamping of  
filamentous  
acetylcholine  
0.5 ms and  
or procaine  
appeared v  
was follows  
end of puls  
peak with -  
5 ms pulse  
quantitative  
procaine bi  
desensitiza  
procaine, a

At the neur  
variety of  
substances  
1977; Neha  
Albuquerque  
physostigmi  
binding of  
that unbindi  
The effec  
the steady  
continuous  
at very high  
receptors of  
et al., 1987  
1992). As a  
ize in the ma  
half of th  
acetylcholin  
of 10<sup>-6</sup> M  
think, there  
desensitizat

Research report

# Insulin-like growth factors and insulin stimulate erythropoietin production in primary cultured astrocytes

Seiji Masuda<sup>\*</sup>, Mariko Chikuma, Ryuzo Sasaki

Department of Food Science and Technology, Faculty of Agriculture, Kyoto University, Kitashirakawa-oiwakecho, Sakyo-ku, Kyoto 606-01, Japan

Accepted 1 October 1996

## Abstract

Erythropoietin (EPO) is established as a major regulator of erythropoiesis. However, we and others have shown that neurons express erythropoietin receptor (EPO-R), that astrocytes produce EPO and that EPO may act as a neurotrophic factor in the CNS. We also found that EPO production is activated by insulin and insulin-like growth factors (IGFs) in astrocytes in a dose-dependent manner and that IGF-I was the most potent activator. The concentrations required for half-maximal activation were 3 nM IGF-I, 10 nM IGF-II and 100 nM insulin. The oxygen concentration regulates EPO production; hypoxia stimulates EPO production in astrocytes. The stimulatory effect of IGFs and insulin on EPO production in astrocytes was not affected by the oxygen concentration of astrocyte culture. Insulin and IGFs did not increase the total protein synthesis of astrocytes but increased EPO mRNA levels, indicating that EPO production is stimulated at the mRNA level. It appeared that the growth factor-induced accumulation of EPO mRNA in astrocytes was caused by activation of the tyrosine kinase-signal transduction pathway, because tyrosine phosphorylation of receptors for IGF-I and insulin was activated when astrocytes were stimulated by these growth factors.

**Keywords:** Erythropoietin; Insulin; Insulin-like growth factor-I; Insulin-like growth factor-II astrocyte; Oxygen; mRNA

## 1. Introduction

Erythropoiesis is regulated by EPO, a glycoprotein, that stimulates the proliferation and differentiation of erythroid precursor cells [23]. In adults, the kidney is a major site of EPO production [17] and kidney EPO travels through the circulation to reach erythropoietic sites such as the bone marrow and spleen (in mice). In the fetus, EPO is produced by the liver where the erythropoiesis takes place [46]. Oxygen is a primary regulator of EPO production [6,16,22]; hypoxia increases EPO production by activating transcription of the EPO gene and also stabilizing EPO mRNA.

**Abbreviations:** EPO, erythropoietin; IGF, insulin-like growth factor; PBS, 10 mM phosphate-buffered saline; EGTA, ethylene glycol bis(β-aminoethyl ether)-N,N,N',N'-tetraacetic acid; APMSP, (p-aminidophenyl)methanesulfonyl fluoride; PCR, polymerase-chain reaction; RT-PCR, reverse transcription-PCR; CNS, central nervous system; EIA, enzyme-linked immunosorbent assay.

<sup>\*</sup> Corresponding author. Kyoto University, Faculty of Agriculture, Department of Food Science and Technology, Kitashirakawa-oiwakecho Sakyo-ku, Kyoto 606-01, Japan. Fax: +81 (75) 753-6274.

It has been thought that EPO exclusively acts on erythroid precursor cells in vivo. However, a number of evidence indicate that an EPO-EPOR system in the CNS is independent of that for erythropoiesis. We showed that neuronal cell lines, brain tissues and primary cultured neurons from rat embryos express EPOR protein as well as its mRNA [26,31,32]. Using radiolabeled EPO, EPO binding sites have been detected in some parts of the adult mouse brain, including the hippocampus and cerebral cortex, where there are neurons vulnerable to ischemia [14]. EPO mRNA is expressed in the adult rat brain and its expression is hypoxia-inducible [44]. A search for EPO-producing cells in the rat brain revealed that astrocytes produced EPO in an oxygen-dependent manner. The increased EPO production at low oxygen was due to an increase in EPO mRNA [27], which was confirmed in mouse astrocytes [28]. mRNAs for EPO and EPOR are also expressed in the brains of adult primates [28].

EPO augments choline acetyltransferase in mouse embryonic primary septal neurons and supports the survival of septal cholinergic neurons in adult rats that have undergone fimbria fornix transection [20]. The binding of EPO

to neuronal cell line, PC12, induces a rapid and transient influx of  $\text{Ca}^{2+}$  from the outside of the cells [26]. EPO protects cultured hippocampal and cortical neurons from glutamate-induced cell death [31]. These findings support the notion that EPO in the CNS acts on neurons in a paracrine fashion and therefore it is important to understand how EPO production in astrocytes is regulated.

We found that EPO production in astrocytes is stimulated by insulin, IGF-I and IGF-II. Here, we showed that stimulation operates at the level of EPO mRNA through a pathway independent of the low oxygen-induced activation of EPO production.

## 2. Materials and methods

### 2.1. Materials

Materials were obtained from the indicated sources: Dulbecco's modified Eagle's medium (Gibco, Grand Island, NY, USA); fetal calf serum (Bio Whittaker, Walkersville, MD, USA); bovine insulin (Sigma, St. Louis, MO, USA); recombinant human IGF-I and IGF-II (R&D Systems, Minneapolis, MN, USA); protein A and ECL detection system (Pharmacia, Uppsala, Sweden); anti-phosphotyrosine monoclonal antibody, RC20, (Transduction Laboratories, Lexington, KY, USA); anti-IGF-I receptor  $\beta$ -chain polyclonal antibody and IGF-II receptor  $\beta$ -chain polyclonal antibody (Santa Cruz Biotechnology, Santa Cruz, CA, USA); protein assay kit (Bio-Rad Laboratories, Hercules, CA, USA); total RNA isolation kit (Ambion, Austin, TX, USA); avidin-biotin-peroxidase complex (Vector Laboratories, Burlingame, CA, USA); [ $^{35}\text{S}$ ]methionine (Dupont, Wilmington, DE, USA); genistein (Extrasynthese, Geney, France).

### 2.2. Cell culture

Astrocytes were cultured with Dulbecco's modified Eagle's medium supplemented with 10% fetal calf serum in a T-flask as described previously [27]. The cells were cultured under a 5%  $\text{O}_2$ , 5%  $\text{CO}_2$ , 90%  $\text{N}_2$  atmosphere unless otherwise indicated. After 2 weeks, EPO production from astrocytes was confirmed by EIA [34]. The medium was changed every 3 days. Astrocytes producing EPO were seeded in 12-well plates at a density of  $10^5/\text{cm}^2$  and cultured for 1 week. Experiments were started by adding various amounts of IGFs or insulin. At intervals, EPO in the spent medium was measured by EIA. To measure the amounts of cellular proteins, the cells were washed three times with PBS, denatured in 1 ml of 0.1 N HCl for 20 min, then dissolved in 1 ml of 1 N NaOH. Proteins in the lysates were determined with protein assay kit using bovine immunoglobulins as a standard.

Hep3B cells were maintained in Dulbecco's modified Eagle's medium supplemented with 10% fetal calf serum

under 21% oxygen. For experiments, Hep3B cells were plated in a 6-well plate at a density of  $10^4/\text{cm}^2$  and cultured for 24 h under 21% oxygen. The cells in fresh media containing various amounts of insulin were placed under 21 or 5% oxygen for 48 h. EPO in the spent medium and cellular proteins were determined.

### 2.3. Measurement of de novo protein synthesis

The cells were cultured with or without IGFs or insulin for 24 h. [ $^{35}\text{S}$ ]methionine (50  $\mu\text{Ci}$ ) was added at zero time. Incorporation of the radioactive amino acids into nascent protein was measured by measuring the radioactivity in the acid-insoluble fraction. The background incorporation was assessed by adding 10  $\mu\text{g}/\text{ml}$  cycloheximide as an inhibitor of protein synthesis.

### 2.4. Competitive RT-PCR for EPO mRNA

We estimated EPO mRNA levels by competitive RT-PCR. The full-length rat EPO cDNA, REPO1.5 [33], was inserted into the *EcoRI* site of pUC19. *HincII* and *SnaBI* digestion of the plasmid containing EPO cDNA and subsequent ligation between these sites yielded a competitor DNA that lacks a portion of the inner part of EPO cDNA. Total RNA was prepared from astrocytes cultured with or without 100 nM IGFs or 1  $\mu\text{M}$  insulin for 16 h using a total RNA isolation kit (Ambion, Austin, TX, USA). The RT reaction proceeded using a random nanomere primer and 1  $\mu\text{g}$  of heat denatured RNA. To estimate EPO mRNA, the transcribed cDNA was co-amplified by PCR in the presence of various amounts of competitor DNA, sense (REP62F, 5'-TCCTTGCTACTGATTCTCTGG-3') and antisense primers (REP512R, 5'-AAGTATCCGCTGAGAGGTTTCG-3'). Amplification of the competitor DNA and the transcribed EPO cDNA by PCR gave products of 282 and 451 bp, respectively. Each of 40 PCR cycles consisted of an incubation for 1 min at 94°C for denaturation, 2 min at 65°C for annealing and 3 min at 72°C for elongation. The amplified DNA was fractionated by electrophoresis, stained with ethidium bromide and densitometrically analyzed.

### 2.5. Detection of phosphorylated IGF-I receptor and insulin receptor by Western blotting

The cells were incubated with 100  $\mu\text{M}$  orthovanadate for 30 min to inhibit phosphatase activity, then 30 nM IGF-I or 1  $\mu\text{M}$  insulin was added. The cells were incubated at 37°C for 10 min, then washed with ice-cold PBS containing 1 mM EGTA, 10  $\mu\text{M}$  APMSF, 10  $\mu\text{M}$  leupeptin and 100  $\mu\text{M}$  orthovanadate. The cells were lysed by an incubation for 1 h in ice-cold PBS containing 1% NP40, 1 mM EGTA, 10  $\mu\text{M}$  APMSF, 10  $\mu\text{M}$  leupeptin and 100  $\mu\text{M}$  orthovanadate. After centrifugation at 10000  $\times g$  for 20 min, the solubilized proteins in the supernatant

Fig.  
CO.  
B, c  
EacI

Ins

K

Fig.  
5%  
with

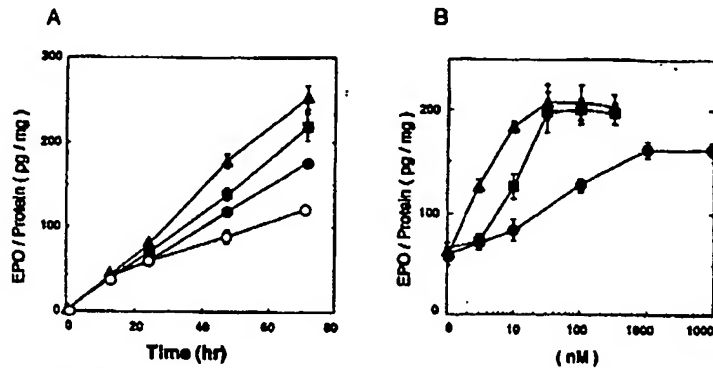


Fig. 1. Stimulation of EPO production of astrocytes by IGFs or insulin. In A, cells were cultured with IGFs or insulin for 12, 24 and 48 h in 5% O<sub>2</sub>, 5% CO<sub>2</sub> and 90% N<sub>2</sub>, then EPO in the spent medium was assayed with EIA. No addition, (○); 1 μM insulin, (●); 30 nM IGF-I, (▲); 30 nM IGF-II, (■). In B, cells were cultured with different concentrations of IGFs or insulin for 48 h in 5% O<sub>2</sub>, 5% CO<sub>2</sub> and 90% N<sub>2</sub>. Insulin, (●); IGF-I, (▲); IGF-II, (■). Each point is the mean ± S.D. (n = 3).

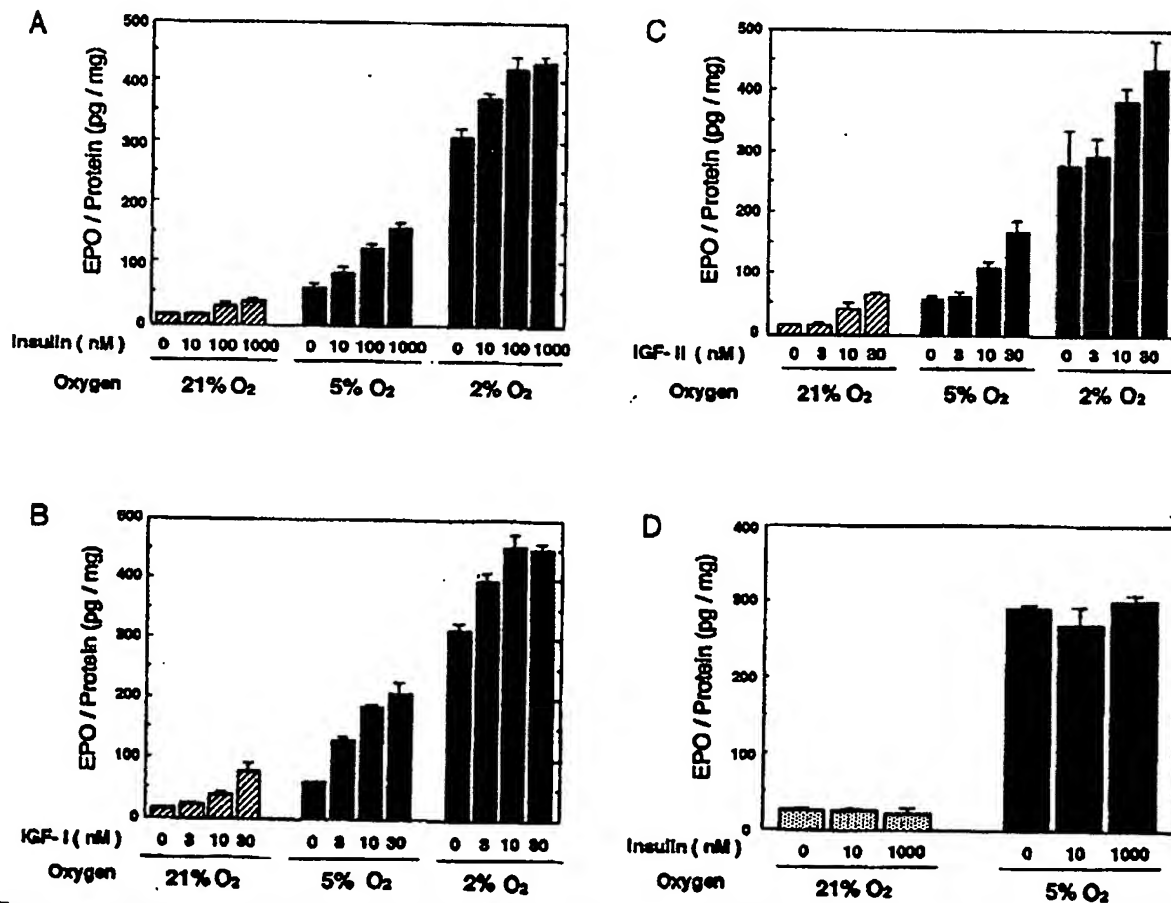


Fig. 2. Oxygen dependence of EPO production in the presence of IGFs or insulin. Astrocytes were cultured under various levels of oxygen tensions (21%, 5% and 2%) for 48 h in the presence of growth factors at the concentrations indicated. A: insulin. B: IGF-I. C: IGF-II. In D, Hep3B cells were cultured with insulin at the concentrations indicated under 21% and 5% oxygen for 48 h. Each point is the mean ± S.D. (n = 3).

were recovered. To immunoprecipitate the IGF-I receptor or insulin receptor, 3  $\mu$ g of anti-IGF-I receptor antibody or anti-insulin receptor antibody was added to each sample and the mixtures were incubated for 1 h at 4°C. The supernatant was mixed with 10  $\mu$ l protein A gel and rotated end over end at 4°C overnight. The gel was pelleted by centrifugation at 1000  $\times$  g for 5 min at 4°C and washed three times with ice-cold PBS containing 1% NP40, 1 mM EGTA, 10  $\mu$ M APMSF, 10  $\mu$ M leupeptin and 100  $\mu$ M orthovanadate. The immunoprecipitated proteins were recovered in the SDS buffer consisting of 60 mM Tris-HCl, pH 6.8, 2% SDS, 10% glycerol, 1.4 M 2-mercaptoethanol and 0.001% bromophenol blue and boiled for 3 min. The proteins were separated by electrophoresis on a 7.5% SDS-polyacrylamide gel. Western blotting proceeded as described previously [27]. Briefly, separated proteins were transferred to a nitrocellulose membrane and detected using RC20, avidin-biotin-peroxidase complex and the ECL detection system.

### 3. Results

#### 3.1. Dose-dependent and oxygen-independent stimulation of EPO production by IGFs and insulin

To examine whether neurons are involved in regulating EPO production by astrocytes, the conditioned medium of cultured hippocampal neurons from a day-19 rat embryo was added to cultured astrocytes. EPO production doubled but further examination revealed that this increase was due to the insulin included in the neuron culture medium. This finding prompted us to investigate stimulatory effect of insulin and IGFs on the EPO production by astrocytes in detail, because these growth factors are ubiquitous in the CNS [4]. Astrocytes were cultured under 5% oxygen in the presence or absence of insulin and IGFs, then EPO levels in the culture media were assayed by EIA at intervals. EPO production was stimulated by IGFs or insulin within 24 h and was sustained for at least 72 h (Fig. 1A). They stimulated EPO production in a dose-dependent manner (Fig. 1B). Insulin induced stimulation at a concentration of 10 nM, but 1  $\mu$ M insulin was required for the maximal 2-fold increase. IGF-II was more active at lower concentrations. IGF-I was the most potent stimulator, causing a 2-fold increase at 3 nM and a maximal 3.5-fold increase at 30 nM. Half-maximal stimulation of EPO production was achieved by 3 nM IGF-I, 10 nM IGF-II and 100 nM insulin. To determine whether or not the stimulation by these factors was oxygen-dependent, astrocytes were cultured with IGFs or insulin under various oxygen concentrations and the amount of EPO produced over 48 h was assayed (Fig. 2A–C). In agreement with published results [27], EPO production was significantly activated by low oxygen tension. However, insulin and IGFs increased EPO production under all oxygen concentrations tested. Further-

more, the effects of growth factors and hypoxia were additive and the dose-response curves of individual growth factor under different oxygen concentrations were essentially similar. These results suggest that there are different mechanisms of EPO induction by these two stimuli.

Hep3B, a human hepatoma-derived cell line, produces EPO in an oxygen-dependent manner. Therefore, it has been widely used for studying the regulatory mechanism of EPO biosynthesis. In consistent with the results described previously [16], EPO production by Hep3B cells was stimulated by low oxygen tension but culturing the cells with insulin did not stimulate EPO production under 21 and 5% oxygen (Fig. 2D). The insulin receptor is expressed in Hep3B cells [11].

#### 3.2. Protein synthesis induced by IGFs and insulin

Insulin and IGFs stimulate protein synthesis in a variety of cell types and their effect upon EPO production might be derived from an increase in overall protein synthesis. Astrocytes were cultured with or without IGFs and insulin in the presence of [<sup>35</sup>S]methionine. We assayed EPO levels in the culture supernatants and the amount of [<sup>35</sup>S]methionine incorporated into proteins in the cells. The specific incorporation was calculated by subtracting the background incorporation, which was assessed in the presence of cycloheximide, from the total. Fig. 3 shows a slight stimulation of protein synthesis but to a far lesser degree than that of EPO production. The low response of protein synthesis to insulin and IGFs may be ascribed to the astrocytes being confluent.

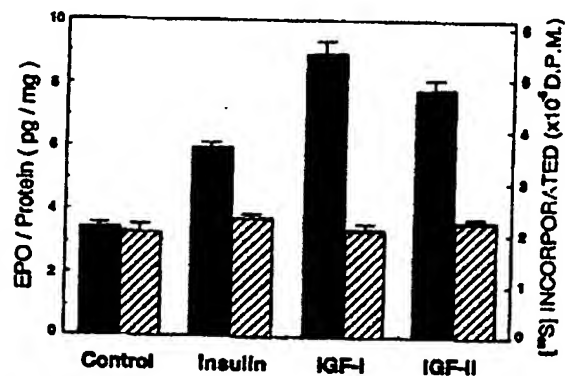


Fig. 3. Effect of IGFs or insulin on EPO production and de novo protein synthesis of astrocytes. Astrocytes were cultured for 20 h in the absence or presence of 1  $\mu$ M insulin, 30 nM IGF-I or 30 nM IGF-II. EPO produced for 20 h was determined with EIA and protein synthesis was measured by the incorporation of [<sup>35</sup>S]methionine into the acid-insoluble fraction of cell lysates as described in Section 2. The background incorporation (4325  $\pm$  256 dpm) obtained from the culture in the presence of cycloheximide was subtracted from the total. EPO production is shown by filled columns and protein incorporation by hatched columns. Each column is the mean  $\pm$  S.D. ( $n = 3$ ).

Fig.  
com:  
12-  
lane:  
EPO  
prod

3.3.

the  
the  
rev  
was  
am  
cD  
sho  
agr  
am  
zyn  
of  
ban  
der  
ast  
0.1

Fig  
5 n  
the  
Lar  
μM



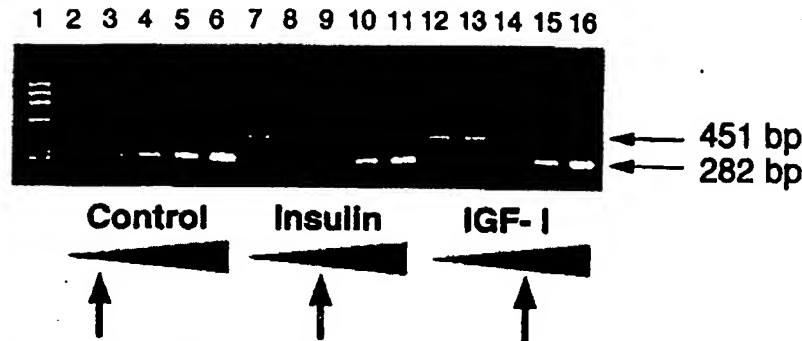


Fig. 4. Competitive RT-PCR for calculating the EPO mRNA. Astrocytes were stimulated with insulin or IGFs for 16 h. Total RNA was recovered and competitive RT-PCR was performed. Lane 1,  $\phi$  × 174 *Hae*III digested marker; lanes 2–6, no growth factor; lanes 7–11, stimulated by insulin; lanes 12–16, stimulated by IGF-I. Competitor DNA was included in the PCR reaction mixtures as follows: lanes 2, 7 and 12, 0.5 fg; lanes 3, 8 and 13, 5 fg; lanes 4, 9 and 14, 15 fg; lanes 5, 10 and 15, 50 fg; lanes 6, 11 and 16, 500 fg. The amplified products of 451 and 282 bp were derived from transcribed EPO cDNA and the competitor DNA, respectively. The band intensity was measured by densitometry and the ratio of EPO cDNA-derived product/competitor-derived product was calculated. Arrows indicate reversal points of the band intensity of the amplified products.

### 3.3. Accumulation of EPO mRNA by IGFs and insulin

To determine whether or not IGFs and insulin elevated the level of EPO mRNA, total RNA was recovered from the astrocytes cultured with or without growth factors and reverse-transcribed. EPO-specific mRNA in the total RNA was quantified by competitive PCR. The primers predict amplified fragments of 451 bp for the transcribed EPO cDNA and of 282 bp for the competitor DNA. Fig. 4 shows that the amplified DNAs migrated with sizes that agreed well with those predicted. The validity of the amplified products was also confirmed by restriction enzyme mapping (data not shown). The approximate content of EPO mRNA was calculated from the point where the band intensity of the EPO cDNA- and competitor DNA-derived products reversed. The content of EPO mRNA in astrocytes cultured in the absence of growth factors was 0.18 fg/ $\mu$ g total RNA. Culture with insulin and IGF-I

increased EPO mRNA levels to 0.44 and 0.80 fg, respectively (Fig. 4). IGF-II (30 nM) increased EPO mRNA to 0.60 fg/ $\mu$ g total RNA (data not shown). These growth factor-dependent increases in EPO mRNA were comparable to those of EPO production when astrocytes were cultured with these growth factors (see Fig. 1).

### 3.4. Phosphorylation of IGF-I and insulin receptor

Receptors for IGF-I and insulin consists of an extracellular  $\alpha$ -subunit and a transmembrane  $\beta$ -subunit peptide, which are linked by a disulfide bond in the extracellular site [36]. Following the binding of these ligands to the  $\alpha$ -subunit of insulin or IGF-I receptor, the tyrosine kinase in the  $\beta$ -subunit undergoes autophosphorylation and activation [18,39]. The latter results in the tyrosine residues of several intracellular signal transducers being phosphorylated. To demonstrate the involvement of the receptor for

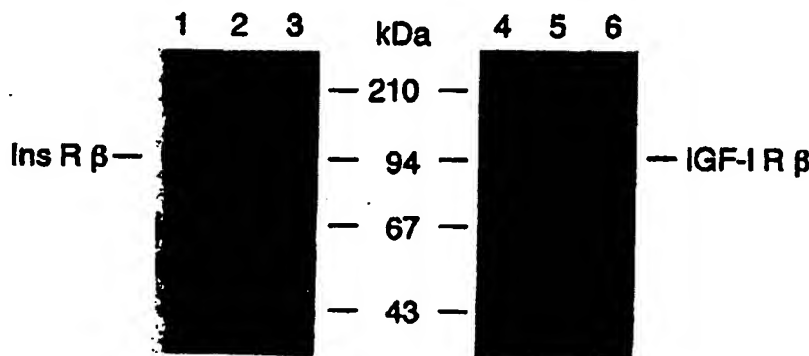


Fig. 5. Phosphorylation of the  $\beta$ -subunit of the insulin and IGF-I receptors in astrocytes. Astrocytes were stimulated with 1  $\mu$ M insulin or 30 nM IGF-I for 5 min and the receptor of each growth factor was immunoprecipitated by the receptor-specific antibody. InsR  $\beta$  and IGF-IR  $\beta$  represent phosphorylation of the insulin and IGF-I receptor-specific  $\beta$ -subunits, respectively. Phosphorylation of the receptor was detected by the anti-phosphotyrosine antibody, RC20. Lanes 1–3, immunoprecipitated by anti-insulin receptor antibody; lanes 4–6, immunoprecipitated by anti-IGF-I antibody; lanes 1 and 4, stimulated by 1  $\mu$ M insulin; lanes 2 and 5, stimulated by 30 nM IGF-I; lanes 3 and 6, no stimulation.



IGF-I or insulin in the stimulation of EPO production, we tested receptor phosphorylation. Astrocytes were stimulated with IGF-I or insulin for 5 min and the cells were solubilized. IGF-I receptor or insulin receptor was immunoprecipitated by anti-IGF-I or anti-insulin receptor  $\beta$ -subunit antibody and detected by an anti-phosphotyrosine antibody (Fig. 5). In these experiments, the IGF-I (30 nM) and insulin (1  $\mu$ M) concentrations were those that maximally activated EPO production (see Fig. 1B). Both  $\beta$ -subunits of IGF-1 and insulin receptors were phosphorylated by adding either IGF-I or insulin. The size of the IGF-I receptor  $\beta$ -subunit (95 kDa) was in good agreement with that of the glial type; the neuronal IGF-1 receptor  $\beta$ -subunit has a molecular mass of 91 kDa [43].

We examined effect of genistein, an inhibitor of tyrosine kinase, on the stimulation of EPO production by IGF-I. Astrocytes were cultured under 5% oxygen for 48 h in the presence or absence of IGF-I. IGF-I (30 nM) caused a 3-fold enhancement in EPO production. When the inhibitor was added at 30  $\mu$ M in the cultures, the enhancement was reduced to 1.2-fold, which supports that the stimulation of EPO production by IGF-I is mediated through tyrosine phosphorylation of the receptor.

#### 4. Discussion

Several lines of evidence indicate that the EPO/EPOR system independent of that in erythropoiesis is present in the CNS where astrocytes produce EPO and neurons express EPOR [26,27,31,32] and that EPO supports survival of neurons [20,31]. Therefore, regulation of EPO production by astrocytes may differ from that by the cells (liver and renal) involved in erythropoietic system, although the oxygen concentration is a common regulatory signal of EPO production in the liver, kidney and brain [6,16,22,27]. We found that EPO production in primary cultured astrocytes was activated by insulin and IGFs. The widespread distribution of insulin and IGFs and their receptors in the CNS [3,4,7,10,12,25,35,41,43] suggests that these growth factors are involved in the regulation of EPO production in the brain. IGFs and insulin have been shown to directly act on neurons as neurotrophic factors [1,5,9,13,15,19,21,24,29,37] and they also appear to indirectly act on neurons by activating production of brain EPO, which supports neuronal survival. Interestingly, neurite promoting activity of IGF-I and insulin in mouse motoneurons is astrocyte-dependent [2] and a 17-mer peptide sequence in EPO stimulates neurite outgrowth of neuroblastoma cell lines [8].

Studies using Hep3B cells have demonstrated that the cis-acting element responsible for hypoxic activation of EPO gene transcription is located at its 3'-flanking region to which binding of HIF (hypoxia-inducible factor, a heterodimer of *trans*-acting proteins) potentiates gene transcription [42]. Phosphorylation of one of the heterodimer

converts HIF to an active form [45]. EPO production in astrocytes, however, was activated by insulin and IGFs in an oxygen concentration-independent manner, suggesting that these growth factors exert their effects through a pathway different from that of hypoxia-induced activation. Hypoxic stimulation of EPO production in Hep3B cells is partly attributable to stabilizing EPO mRNA by binding of an yet unidentified protein whose production also appears to be hypoxia-inducible [38]. Although it was clear that the growth factor-induced stimulation of EPO production by astrocytes is due to an increase of EPO mRNA, it remains to be investigated whether the increase is caused by the transcriptional activation or an elongated mRNA life-span.

EPO production in astrocytes was stimulated by insulin, IGF-I and IGF-II. These growth factors cross-bind to their receptors with different affinities. The receptor with the highest affinity to IGF-II among these ligands is identical to the mannose-6-phosphate receptor [30], which has a very short intracellular domain and plays a key role in sorting cellular proteins into lysosomes. The stimulation of EPO production by IGF-II, therefore, is likely mediated via the receptor for insulin or IGF-I. In general, the affinities of these ligands to the insulin and IGF-I receptors are insulin > IGF-II > IGF-I and IGF-I > IGF-II > insulin, respectively [40]. IGF-I and IGF-II at low doses stimulated EPO production in astrocytes, whereas a high concentration was required for insulin. These findings indicated that the stimulation of these growth factors was largely mediated via the IGF-I receptor, although some contribution of an insulin receptor-mediated signal could not be excluded. In fact, the insulin receptor was tyrosine phosphorylated when IGF-I or insulin was added.

#### Acknowledgements

This work was supported by a Grant-in-Aid for Scientific Research from the Ministry of Education, Science and Culture of Japan.

#### References

- [1] Alizeman, Y. and DeVeellis, J., Brain neurons develop in a serum and glial free environment: effects of transferrin, insulin, insulin-like growth factor I and thyroid hormone on neuronal survival, growth and differentiation, *Brain Res.*, 406 (1987) 32–42.
- [2] Ang, L.C., Bhaumick, B. and Jurlink, B.H.J., Neurite promoting activity of insulin, insulin-like growth factor I and nerve growth factor on spinal motoneurons is astrocyte dependent, *Dev. Brain Res.*, 74 (1993) 83–88.
- [3] Araujo, D.M., Lapchak, P.A., Collier, B., Chabot, J.G. and Quirion, R., Insulin-like growth factor-I (somatomedin-C) receptors in the rat brain: distribution and interaction with the hippocampal cholinergic system, *Brain Res.*, 484 (1989) 130–138.
- [4] Baskin, D.G., Wilcox, B.J., Figlewicz, D.P. and Dorsa, D.M., Insulin and insulin-like growth factors in the CNS, *Trends Neurosci.*, 11 (1988) 107–111.

- [5] Beilharz, E.J., Bassett, N.S., Sirmann, E.S., Williams, C.E. and Gluckman, P.D.: Insulin-like growth factor II is induced during wound repair following hypoxic-ischemic injury in the developing rat brain, *Mol. Brain Res.*, 29 (1995) 81–91.
- [6] Beru, N., McDonald, J., Lacombe, C. and Goldwasser, E., Expression of the erythropoietin gene, *Mol. Cell Biol.*, 6 (1986) 2571–2575.
- [7] Barde, Y.-A., Trophic factors and neuronal survival, *Neuron*, 2 (1989) 1525–1534.
- [8] Campana, W.M., Carson, G.S., Misasi, R. and O'Brien, J.S., Identification of a neurotrophic factor sequence in erythropoietin, *J. Neurochem.*, 64 (Suppl.) (1995) S24D.
- [9] Cheng, B. and Mattson, M.P., IGF-I and IGF-II protect cultured hippocampal and septal neurons against calcium-mediated hypoglycemic damage, *J. Neurosci.*, 12 (1992) 1558–1566.
- [10] Chermak, S.D., Insulin-like growth factor-I (IGF-I) production by astroglial cells: regulation and importance for epidermal growth factor-induced cell replication, *J. Neurosci. Res.*, 34 (1993) 189–197.
- [11] Chou, C.K., Su, T.S., Chang, C.M., Hu, C.P., Huang, M.Y., Suen, C.S., Chou, N.W. and Ting, L.P., Insulin suppresses hepatitis B surface antigen expression in human hepatoma cells, *J. Biol. Chem.*, 264 (1989) 15304–15308.
- [12] Devaskar, S.U., Giddings, S.J., Rajakumar, P.A., Carnaghi, L.R., Melon, R.K. and Zahm, D.S., Insulin gene expression and insulin synthesis in mammalian neuronal cells, *J. Biol. Chem.*, 269 (1994) 8446–8454.
- [13] DiCicco-Bloom, E. and Black, I., Insulin growth factors regulate the mitotic cycle in cultured rat sympathetic neuroblasts, *Proc. Natl. Acad. Sci. USA*, 85 (1988) 4066–4070.
- [14] Digicaylioglu, M., Bichet, S., Marti, H.H., Wegner, R.H., Rivas, L.A., Bauer, C. and Gassmann, M., Localization of specific erythropoietin binding sites in defined areas of the mouse brain, *Proc. Natl. Acad. Sci. USA*, 92 (1995) 3717–3720.
- [15] Enberg, G., Tham, A. and Sara, V.R., The influence of purified somatomedins and insulin on foetal rat brain DNA synthesis in vitro, *Acta Physiol. Scand.*, 125 (1985) 305–308.
- [16] Goldberg, M.A., Dunning, S.P. and Bunn, H.F., Regulation of the erythropoietin gene: evidence that the oxygen sensor is a heme protein, *Science*, 242 (1988) 1412–1415.
- [17] Jacobson, L.O., Goldwasser, E., Fried, W. and Plzak, L., Role of the kidney in erythropoiesis, *Nature*, 179 (1957) 633–634.
- [18] Kasuga, M., Karlsson, F.A. and Kahn, C.R., Insulin stimulates the phosphorylation of the 95 k subunits of its own receptor, *Science*, 215 (1982) 185–187.
- [19] Kausel, B., Michel, P.P., Schwaber, J.S. and Hefti, F., Selective and nonselective stimulation of central cholinergic and dopaminergic development in vitro by nerve growth factor, basic fibroblast growth factor, epidermal growth factor, insulin and the insulin-like growth factors I and II, *J. Neurosci.*, 10 (1990) 558–570.
- [20] Konishi, Y., Chui, D.-H., Hirose, H., Kunishita, T. and Tabira, T., Trophic effect of erythropoietin and other hematopoietic factors on central cholinergic neurons in vitro and in vivo, *Brain Res.*, 609 (1993) 29–35.
- [21] Konishi, Y., Takahashi, K., Chui, D.-H., Rosenfeld, R.G., Hideno, M. and Tabira, T., Insulin-like factor II promotes in vitro cholinergic development of mouse septal neurons: comparison with the effects of insulin-like growth factor I, *Brain Res.*, 649 (1994) 53–61.
- [22] Koury, S.T., Koury, M.J., Bondurant, M.C., Caro, J. and Graber, S.E., Quantitation of erythropoietin-producing cells in kidney of mice by in situ hybridization: correlation with hematocrit, renal erythropoietin mRNA, and serum erythropoietin concentration, *Blood*, 74 (1989) 645–651.
- [23] Krantz, S.B., Erythropoietin, *Blood*, 77 (1991) 419–434.
- [24] Lenoir, D. and Plonegger, P., Insulin-like growth factor I (IGF-I) stimulates DNA synthesis in fetal rat brain cell cultures, *Dev. Brain Res.*, 7 (1983) 205–213.
- [25] Marks, J.L., Porto, D., Jr., Stahl, W.L. and Beakins, D.G., Localization of insulin receptor mRNA in rat brain by in situ hybridization, *Endocrinology*, 127 (1990) 3234–3236.
- [26] Masuda, S., Nagao, M., Takahata, K., Konishi, Y., Gallyas, F., Jr., Tabira, T. and Sasaki, R., Functional erythropoietin receptor of the cells with neural characteristics: comparison with receptor properties of erythroid cells, *J. Biol. Chem.*, 268 (1993) 11208–11216.
- [27] Masuda, S., Okano, M., Yamagishi, K., Nagao, M., Ueda, M. and Sasaki, R., A novel site of EPO production: oxygen-dependent production in cultured rat astrocytes, *J. Biol. Chem.*, 269 (1994) 19488–19493.
- [28] Marti, H.H., Wenger, R.H., Rivas, L.A., Straumann, U., Digicaylioglu, M., Henn, V., Yonchara, Y., Bauer, C. and Gassmann, M., Erythropoietin gene expression in human, monkey and murine brain, *Eur. J. Neurosci.*, 8 (1996) 666–676.
- [29] Mill, J.F., Chao, M.V. and Ichi, D.N., Insulin, insulin-like growth factor II, and nerve growth factor effects on tubulin mRNA levels and neurite formation, *Proc. Natl. Acad. Sci. USA*, 82 (1985) 7126–7130.
- [30] Morgan, D.O., Edman, J.C., Standring, D.N., Fried, V.A., Smith, M.C., Roth, R.A. and Rutter, W.J., Insulin-like growth factor II receptor as a multifunctional binding protein, *Nature*, 329 (1987) 301–307.
- [31] Morishita, E., Masuda, S., Nagao, M., Yasuda, Y. and Sasaki, R., Erythropoietin receptor is expressed in rat hippocampal and cerebral cortical neurons, and erythropoietin prevents in vitro glutamate-induced neuronal death, *Neuroscience*, 76 (1997) 105–116.
- [32] Morishita, E., Narita, H., Nishida, M., Kawashima, N., Yamagishi, K., Masuda, S., Nagao, M. and Sasaki, R., Anti-erythropoietin receptor monoclonal antibody: epitope mapping, quantification of the soluble receptor, and detection of the solubilized transmembrane receptor and the receptor-expressing cells, *Blood*, 88 (1996) 465–471.
- [33] Nagao, M., Suga, H., Okano, M., Masuda, S., Narita, H., Ikura, K. and Sasaki, R., Nucleotide sequence of rat erythropoietin, *Biochim. Biophys. Acta*, 1171 (1992) 99–102.
- [34] Okano, M., Masuda, S., Narita, H., Masushige, S., Kato, S., Imagawa, S. and Sasaki, R., Retinoic acid up-regulates erythropoietin production in hepatoma cells and in vitamin A-depleted rats, *FEBS Lett.*, 349 (1994) 229–233.
- [35] Pabro, F. and Rosa, E.J., The developing CNS: a scenario for the action of proinsulin and insulin-like growth factors, *Trends Neurosci.*, 18 (1995) 143–150.
- [36] Plich, P.F. and Czech, M.P., The subunit of the high affinity insulin receptor, *J. Biol. Chem.*, 255 (1980) 1722–1731.
- [37] Reao-Plata, E., Rechler, M.M. and Ichi, D.N., Effects of insulin, insulin-like growth factor-II and nerve growth factor on neurite formation and survival in cultured sympathetic and sensory neurons, *J. Neurosci.*, 6 (1986) 1211–1219.
- [38] Rooden, J.J., MacMillan, L.A., Beckman, B.S., Goldberg, M.A., Schneider, T., Bunn, H.F. and Malter, J.S., Hypoxia up-regulates the activity of a novel erythropoietin mRNA binding protein, *J. Biol. Chem.*, 266 (1991) 16594–16598.
- [39] Roth, R.A. and Cassell, D.J., Insulin receptor: evidence that it is a protein kinase, *Science*, 219 (1983) 299–301.
- [40] Roth, R.A., Steel-Pinkins, G., Hari, J., Stover, C., Pierce, S., Turner, J., Edman, J.C. and Rutter, W.J., Insulin and insulin-like growth factor receptors and responses, *Cold Spring Harbor Symp.*, LIII (1988) 537–543.
- [41] Rotwein, P., Burgess, S.K., Milbrndt, J.D. and Kreuse, J.E., Differential expression of insulin-like growth factor genes in rat central nervous system, *Proc. Natl. Acad. Sci. USA*, 85 (1988) 265–269.
- [42] Semenza, G.L. and Wang, G.L., A nuclear factor induced by hypoxia via de novo protein synthesis binds to the human erythropoietin gene enhancer at a site required for transcriptional activation, *Mol. Cell Biol.*, 12 (1992) 5447–5454.
- [43] Shemer, J., Raizada, M.K., Masters, B.A., Ota, A. and LeRoith, D.,

- Insulin-like growth factor I receptors in neuronal and glial cells, *J. Biol. Chem.*, 262 (1987) 7693-7699.
- [44] Tan, C.C., Eckardt, K.U., Firth, J.D. and Ratcliffe, P.J., Feedback modulation of renal and hepatic erythropoietin mRNA in response to graded anemia and hypoxia, *Am. J. Physiol.*, 263 (1992) F474-F481.
- [45] Wang, G.L. and Semenza, G.L., Characterization of hypoxia-inducible factor 1 and regulation of DNA binding activity by hypoxia, *J. Biol. Chem.*, 268 (1993) 21513-21518.
- [46] Zanjani, E.D., Foster, J., Burlington, H., Mann, L.I. and Wasserman, L.R., Liver as the primary site of erythropoietin formation in the fetus, *J. Lab. Clin. Med.*, 89 (1977) 640-644.



Dis

## Abstract

In five  
lobster),  
sensory  
numerous  
net- or b  
separate,  
immunor  
condense  
chemosen  
classes o

## Keywords

## 1. Intro

In ar.  
have be.  
but not  
insects  
as sens  
[4,17,43  
another  
implicat  
mechan  
insects  
data ind  
transmit  
Amo  
evidenc  
olfactor  
[37]. Di  
tion, ho  
few, pre

\* Corre  
sult Ham  
Fax: +49

0006-8997  
PU S006

G00043121.0358

## Functional Erythropoietin Receptor of the Cells with Neural Characteristics

### COMPARISON WITH RECEPTOR PROPERTIES OF ERYTHROID CELLS\*

(Received for publication, November 16, 1992, and in revised form, February 1, 1993)

Seiji Masuda, Masaya Nagao, Kyoya Takahata†, Yoshihiro Konishi§, Ferenc Gallyas, Jr.§, Takeshi Tabira§, and Ryuzo Sasaki¶

From the Department of Food Science and Technology, Faculty of Agriculture, Kyoto University, Kyoto 606, the †Department of Bioresources Chemistry, Faculty of Agriculture, Okayama University, Okayama 700, and the §Division of Demyelinating Disease and Aging, National Institute of Neuroscience, National Center of Neurology and Psychiatry, Tokyo 187, Japan

Radiolabeled erythropoietin (Epo) was bound specifically to the cells of two non-erythroid clonal lines, PC12 and SN6, which expressed neuronal characteristics. The binding was time-, cell number-, and dose-dependent and was reversible. Although the cloned Epo receptor from PC12 cells (derived from rat adrenal medulla) was identical to that from rat erythroid cells, significant differences in the ligand binding properties between two cell lineages were found; 1) PC12 cells had a single class of binding sites with very low affinity ( $K_d = 16$  nM), whereas erythroid cells had two classes of binding sites with different affinities ( $K_d = 95$  pM for high affinity sites and 1.9 nM for low affinity sites), and 2) cross-linking experiments revealed one cross-linked product of 105 kDa for PC12 cells and two products of 140 and 120 kDa for erythroid cells. Taken together with additional results, the presence of a putative accessory protein(s) that may alter the ligand binding affinity through interaction with Epo receptor is discussed. The binding of Epo to PC12 cells caused a rapid increase in the cytosolic concentration of free calcium. The presence of EGTA had no effect on the Epo binding but completely inhibited the calcium increase, indicating that Epo stimulated the calcium influx from outside of the cells. The addition of Epo to the culture media of PC12 cells elevated the intracellular concentrations of monoamines.

The action of Epo on erythroid precursor cells has been only a generally accepted function; Epo supports survival of the cells and stimulates their proliferation and differentiation (see Ref. 1 for review). Epo, however, acts *in vitro* on other cells besides erythroid cells; Epo promotes differentiation of megakaryocytes (2), has a mitogenic and positive chemotactic effect on endothelial cells (3), and enhances the immunoglobulin production by B lymphocytes and their proliferation (4). Epo-R is present in the cells from rodent placentas (5). A physiological significance of these findings remains to be proven but such findings of non-erythroid cells bearing Epo receptors may provide us with an opportunity to find a new physiological function of Epo.

Cells derived from the neural crest lineage appear to display in culture either neuronal or chromaffin phenotypes. NGF induces neuronal characteristics and corticosteroids potentiate chromaffin properties (6). The rat cell line PC12, which has been established from an adrenal medullary pheochromocytoma, has similar bipotent properties; the cells express more neuronal properties with exposure to NGF and keep chromaffin properties with corticosteroids (7-9). The cell line SN6, a clonal hybrid cell line developed from the septal region of the mouse basal forebrain, expresses characteristics typical of cholinergic neurons (10). Here we report the presence of Epo-R in these two cell lines, molecular properties of Epo-R on PC12 cells compared with that on erythroid cells, and the Epo-induced increase in intracellular concentrations of calcium and monoamines of PC12 cells. The presence of Epo-R on these neural cell lines can be rationalized on the basis of recent findings that Epo augments choline acetyltransferase activity in primary cultured neurons and supports the *in vivo* survival of lesioned neurons (11), although the physiological significance of these findings has not been verified. Comparison of Epo-R on the neural cells with that on erythroid cells, therefore, is important for studying a new physiological function of Epo and also for understanding the Epo-induced signal transduction pathway, including identification of protein(s) on neural cells involved in the interaction with Epo.

#### EXPERIMENTAL PROCEDURES

**Materials**—Materials were purchased from the indicated sources: FCS and horse serum, Whitaker M. A. Bioproduct; DMEM and MEM, GIBCO; keyhole limpet hemocyanin and ethylene glycol-bis(succinimidylsuccinate), Pierce Chemical Co.; CH-Sepharose 4B gel, Pharmacia; CHAPS, EGTA, and fura-2AM, Dojin Chemicals; APMSF, mouse epidermal growth factor, and bradykinin, Wako Pure Chemical Industries; leupeptin, pepstatin, and antipain, Peptide Institute; block ace, Snow Brand Milk Products; enhanced chemiluminescence Western blotting detection system and Hybond N filter, Amersham; human IL-1 $\beta$  and G-CSF, R & D System, Inc.; mouse IL-

Epo<sup>1</sup> is a major physiological regulator of erythropoiesis.

\* This work was supported by grants-in-aid from the Ministry of Education, Science and Culture of Japan (to R. S.), the Science and Technology Agency (to T. T.), Health Science Foundation (to T. T.), and the Ryoichi Naito Foundation for Medical Research (to R. S.). The costs of publication of this article were defrayed in part by the payment of page charges. This article must therefore be hereby marked "advertisement" in accordance with 18 U.S.C. Section 1734 solely to indicate this fact.

† To whom correspondence should be addressed: Dept. of Food Science and Technology, Faculty of Agriculture, Kyoto University, Kyoto 606, Japan. Tel.: 81-75-753-6271; Fax: 81-75-753-6274.

¶ The abbreviations used are: Epo, erythropoietin; Epo-R, erythropoietin receptor; NGF, nerve growth factor; HuEpo, human erythropoietin; rHuEpo, recombinant human erythropoietin; DMEM, Dulbecco's modified Eagle's medium; MEM, minimum essential medium; PBS, phosphate-buffered saline; FCS, fetal calf serum; CHAPS, 3[(3-cholamidopropyl)dimethylammonio]-1-propanesulfonate; APMSF, (p-amidinophenyl)methanesulfonyl fluoride; IL, interleukin; GM-CSF, granulocyte/macrophage-colony-stimulating factor; RT-PCR, reverse transcriptase-polymerase chain reaction; DOPAC, 3,4-dihydroxyphenylacetic acid; HVA, homovanillic acid; MDOPA, 3-methoxy-DOPA.

3, Collaborative Research, Inc.; human IL-6; tumor necrosis factor and GM-CSF, Genzyme; human EDF (activin A), a kind gift from Dr. Eto of Ajinomoto; human HGF, a kind gift from Dr. Higashio of Snow Brand Milk Products; mouse NGF, Biochemical Technologies Inc.; bovine insulin, Sigma; Oligo(dT)-Latex, Takara.

**Cells and Cell Culture**—PC12 pheochromocytoma cells were cultured in DMEM supplemented with 10% horse serum and 5% FCS under a humidified atmosphere containing 10% CO<sub>2</sub>, and SN6.10.2.2 cells (a kind gift from Dr. B. H. Wainer) were cultured in DMEM supplemented with 10% FCS in the presence of 5% CO<sub>2</sub>. The latter is a subclone of the SN6 cell line (10). PC12 and SN6 cells were removed from the flasks and dissociated by pipetting to yield single cell suspensions. The spleen single cell suspension enriched with Epo-responsive cells was prepared from Wistar rats made anemic by injections of phenylhydrazine (12). Chromaffin cells were prepared from rat adrenal medullas (13). Adrenal glands were removed from 6-week-old Wistar rats. Medullas were carefully freed from capsular and cortical tissue. The medullary tissue was cut into small pieces and kept in Ca<sup>2+</sup>-free Hanks' balanced salt solution at 37 °C for 20 min. The dissected medullas were transferred to MEM containing 10% FCS, 0.15% collagenase, 30 µg/ml DNase I, 10 mM HEPES and digested at 37 °C for 100 min with constant shaking. Every 20 min during digestion, the digestion medium was renewed. The cells were washed three times with MEM containing 10% FCS by centrifugation at 50 × g for 3 min. More than 90% of the cells were viable judging from staining with trypan blue.

**Epo and Its Binding to the Cells**—Recombinant HuEpo was produced (14) and isolated (15) as described previously. The fully deglycosylated rHuEpo was prepared by the procedures also described previously (16). Rat Epo was isolated from the sera of anemic animals.<sup>2</sup> Quantities of rHuEpo and rat Epo were measured by sandwich-type enzyme-linked immunosorbent assay (15, 17). Recombinant HuEpo was radioiodinated at a specific activity of 1.11 MBq/µg protein (18). Experiments for the binding of [<sup>125</sup>I]-rHuEpo to cells were done as described previously (19). Binding assay mixtures contained cells, 20 mM HEPES, pH 7.4, 0.1% bovine serum albumin, 0.1% NaN<sub>3</sub> (an inhibitor of the ligand internalization), and rHuEpo in a total volume of 150 µl PBS. Incubations for binding were done at 15 °C for 3 h unless otherwise indicated. The cells were pelleted, washed once with PBS, and suspended in 200 µl of PBS. The suspension was layered on an 800-µl cushion buffer (PBS containing 10% bovine serum albumin), and the cells were separated from the unbound ligand by centrifugation. The tube contents were frozen in solid CO<sub>2</sub>/ethanol. The tip was cut off just above the cell pellet, and the radioactivity was counted. Specific binding was defined as the difference in bound radioactivity between samples incubated in the absence and the presence of 200-fold unlabeled Epo. Scatchard plot analyses of the binding data were performed by the LIGAND program (20).

**Internalization of Epo Bound to PC 12 Cells**—Internalization of [<sup>125</sup>I]-rHuEpo bound to PC 12 cells was measured by the low-pH method (21). Binding assay mixtures containing 5.6 × 10<sup>6</sup> cells, 7.5 nM [<sup>125</sup>I]-rHuEpo, and no NaN<sub>3</sub> were incubated at 15 °C for 3 h or at 37 °C for 1 h. The cell-associated ligand at 15 °C is equivalent to the cell surface receptor-bound ligand, whereas that at 37 °C contains both the receptor-bound ligand and the internalized ligand. Cells were washed three times with PBS and then suspended in ice-cold 0.25 M acetic acid, pH 2.5, containing 0.5 M NaCl or in PBS. The receptor-bound Epo should be released upon incubation at the acidic pH, but the internalized Epo should remain cell-associated. The cell suspensions were incubated at 0 °C for 3 min and layered on the cushion buffer. After centrifugation, the tube contents were frozen, and the tips were cut off as described previously. Radioactivity of the tips represents the internalized Epo and that of the supernatant represents Epo released from Epo-receptor complexes on the cell surface. Control runs were done in the presence of 200-fold unlabeled Epo.

**Cross-linked Products**—Cross-linked products between [<sup>125</sup>I]-rHuEpo and EPO-R were prepared as described previously (18). Briefly, cells (1.5 × 10<sup>7</sup>) were incubated with 6 nM [<sup>125</sup>I]-rHuEpo at 4 °C overnight. The cells were washed and then incubated for cross-linking with 0.4 mM ethylene glycolbis(succinimidylsuccinate) at 0 °C for 1 h. Cross-linked products were extracted by the extraction buffer containing 2% Triton X-100, 10 µM APMSE, 10 µM pepstatin, 10 µM leupeptin, and 1 mM EGTA and then analyzed by SDS-polyacrylamide gel electrophoresis.

**Anti-mouse Epo-R Antiserum**—Recombinant mouse soluble Epo-

R lacking cytoplasmic and transmembrane domains was produced and isolated (22). Rabbit anti-mouse soluble Epo-R antiserum was prepared by injection of the isolated soluble Epo-R. Rabbit anti-NH<sub>2</sub>-terminal mouse Epo-R antiserum was prepared using the 15 NH<sub>2</sub>-terminal amino acid peptide conjugated to keyhole limpet hemocyanin as an antigen (22).

**Preparation of rHuEpo-fixed Gel**—For preparation of the Epo-fixed gel, 150 mg of rHuEpo in 100 mM NaHCO<sub>3</sub> was gently mixed with 9 ml of CH-Sepharose 4B gel at 20 °C for 1 h and at 4 °C overnight. The gel was pelleted by centrifugation and then suspended in 100 mM Tris-HCl, pH 8.0, to block the remaining sites on the gel. Washings of the gel were done four times each with the acidic solution (50 mM acetic acid containing 500 mM NaCl) and then with the basic solution (50 mM Tris containing 500 mM NaCl). The Epo-fixed gel was kept in PBS containing 0.1% NaN<sub>3</sub> at 4 °C before use.

**Immunological Detection of Epo-R Solubilized from PC12 Cells and Rat Erythroid Cells by Western Blotting**—Epo-R solubilized from PC12 cells and rat spleen erythroid cells was concentrated using the Epo-fixed gel and then identified with the Western blotting technique. About 10<sup>6</sup> cells were lysed by incubation at 4 °C for 1 h in 2 ml buffer A, PBS containing 0.5% (w/v) CHAPS, 10 µM APMSE, 10 µM leupeptin, and 1 mM EGTA. The lysate was centrifuged 12,000 × g for 30 min at 4 °C. The supernatant was mixed with 15 µl of rHuEpo-fixed gel (15 mg of rHuEpo/ml of gel) overnight at 4 °C. The gel was pelleted by centrifugation and washed three times with 500 µl of buffer A. Proteins bound to the Epo-fixed gel were solubilized in 50 µl of SDS-buffer consisting of 60 mM Tris-HCl, pH 6.8, 2% SDS, 10% glycerol, 1.4 M 2-mercaptoethanol, and 0.001% bromophenol blue. Solubilized proteins were separated by electrophoresis with SDS, 9% polyacrylamide gel. Western blotting was carried out according to the method of Burnette (23) with some modifications. Briefly, polyacrylamide gel was immersed in 50 ml of transfer buffer consisting of 48 mM Tris, 39 mM glycine, 1.3 mM SDS, and 20% methanol for 15 min, with two changes in buffer solution. The proteins in gel were transferred to a 0.45-µm nitrocellulose filter at 1.2 mA/cm<sup>2</sup> for 40 min. The nitrocellulose filter was immersed in 15 ml of block ace at 4 °C overnight for blocking. The filter was then dipped into 15 ml of buffer B consisting of 0.05% Tween 20, 5% block ace in PBS, and the anti-soluble Epo-R antiserum. After the incubation for 1 h at room temperature, the filter was washed three times with buffer B and then immersed in 15 ml of buffer B containing peroxidase-fixed goat anti-rabbit IgG (1 µg/ml) for 1 h at room temperature and then washed five times with buffer B. The antigen, Epo-R, was visualized using the enhanced chemiluminescence Western blotting detection system.

**Northern Analysis of Epo-R mRNA from PC 12 Cells and Erythroid Cells**—Total RNA from PC12 cells was prepared using the method for preparation of cytoplasmic RNA (24). Total RNA from anemic rat spleen and fetal mouse liver cells was prepared according to the manufacturer's instruction (Pharmacia) using guanidinium isothiocyanate, CsCl, and trifluoroacetic acid. Poly(A)<sup>+</sup> RNA was isolated using oligo(dT)-Latex. Poly(A)<sup>+</sup> RNA (8 µg) treated with glyoxal/dimethyl sulfoxide (24) was loaded in each lane of a 1% agarose gel. After electrophoresis, the RNA was blotted onto Hybond N filter, and the filter was hybridized with the <sup>32</sup>P-labeled coding region of rat Epo-R cDNA between the F and R primers (see below) as a probe.

**Nucleotide Sequence of Epo-R cDNA from PC12 Cells and Rat Erythroid Cells**—The coding regions of Epo-R cDNAs from anemic rat spleen cells and PC12 cells were obtained using the RT-PCR method (25). Primers N (5'-GGCAAGCTTGGGCTGCATCATG-3'), C (5'-GCTCTAGAGTAGGCTGGAGTCTCTA-3'), F (5'-GTTCG-AGCAACCTGCG-3'), and R (5'-GTCCAGGATGGTGTACTCA-3') were synthesized to amplify the coding region of Epo-R from PC12 cells and rat erythroid cells. The underlined sequences in the primers N, C, F, and R correspond to the mouse Epo-R cDNA sequences, 18-30, 1564-1549, 640-656, and 1314-1296, respectively (numbered according to Ref. 26); RT-PCR using primers N and C amplifies the whole coding region of Epo-R. The 5' eight nucleotides in primers N and C were added for creation of restriction sites. Single-stranded cDNAs were synthesized by Molony murine leukemia virus reverse transcriptase (Bethesda Research Laboratories) using poly(A)<sup>+</sup> RNA from anemic rat spleen cells and PC12 cells as templates. PCR was performed between primers N and C, N and R, or F and C using single-stranded cDNAs as templates. Nucleotide sequences of RT-PCR products were determined by the direct sequencing method (27) and those of cloned RT-PCR products by the dideoxy sequencing method using Sequenase (28).

**Calcium Concentration**—Intracellular calcium concentrations were

<sup>2</sup> M. Okano, H. Suga, S. Masuda, M. Nagao, H. Narita, K. Ikura, and R. Sasaki, manuscript in preparation.

determined using the fluorescent calcium indicator fura-2 (29, 30). PC12 cells were loaded with 10  $\mu$ M fura-2AM, the ester form of fura-2, by incubating the cell suspensions in PBS at  $2 \times 10^6$  cells/ml for 45 min at 37 °C. The cells were washed three times by an isotonic buffer consisting of 125 mM NaCl, 5 mM KCl, 1.2 mM MgCl<sub>2</sub>, 1.2 mM KH<sub>2</sub>PO<sub>4</sub>, 5 mM NaHCO<sub>3</sub>, 1 mM CaCl<sub>2</sub>, 6 mM glucose, 25 mM HEPES, and 1 mM CaCl<sub>2</sub> and resuspended in the same buffer. One-milliliter aliquots of the cell suspension were pipetted into tubes and the tubes were kept on ice for 1 h. Cells were resuspended in the same buffer warmed at 37 °C. Fluorescence measurements were made in 1-ml samples continuously stirred in quartz-glass cuvettes and thermostatically maintained at 37 °C. Fluorescence was monitored with a Shimadzu RF-5000 spectrofluorimeter, with excitation at dual wavelengths (340 and 380 nm) and emission at 490 nm; ratios of fluorescence intensities emitted when excited at 340 and 380 nm were recorded.

**Intracellular Monoamine Concentrations of PC12 Cells**—PC12 cells ( $1.2 \times 10^6$  cells/3 ml of medium) were cultured in a 35-mm plastic dish for 2 days in the presence of Epo at 3 nM or in its absence. Cells were thoroughly washed with PBS and suspended in 100  $\mu$ l PBS. An aliquot (20  $\mu$ l) of the suspension was used for measurement of protein according to Lowry's method after the lysis of cells in 1% SDS. The remainder (80  $\mu$ l) of the cell suspension was homogenized with 200  $\mu$ l of 0.1 M perchloric acid. After centrifugation, the supernatant was passed through a 0.22- $\mu$ m filter. Monoamine contents in the filtrate were measured with ESA's Coulometric-detector Array Gradient System (Neurochem Nikko Bioscience).

## RESULTS

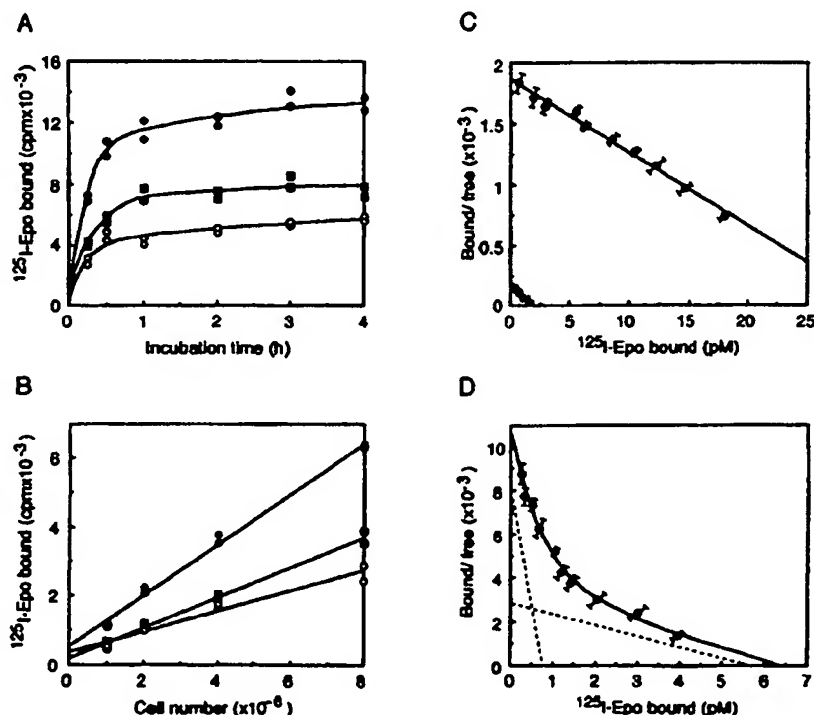
**Binding of Epo to Rat Neuronal and Erythroid Cells**—Fig. 1A shows the time-dependent binding of <sup>125</sup>I-rHuEpo to PC12 cells. The maximum specific binding occurred within 3 h of incubation at 15 °C. There were proportional increases in the specific binding as the number of PC12 cells increased (Fig. 1B). Similar results for the time- and cell number-dependent binding were obtained with SN6 cells and rat spleen cells enriched with Epo-responsive cells (data not shown). Scatchard transformation of ligand-saturation curves of PC12 and

SN6 cells yielded straight lines (Fig. 1C), indicating that these cells had a single class of binding sites. There were 1390 sites/cell with a  $K_d$  (dissociation constant) of 16 nM on PC12 cells and 84 sites/cell with a  $K_d$  of 10 nM on SN6 cells. A Scatchard plot of rat spleen erythroid cells was biphasic (Fig. 1D); erythroid cells had high-affinity binding sites (33 sites/cell,  $K_d$  = 95 pM) and low-affinity binding sites (252 sites/cell,  $K_d$  = 1.9 nM).

We examined whether the binding of Epo to PC12 cells was reversible. Radioiodinated rHuEpo was bound to cells by incubating the binding mixture at 15 °C for 3 h. The cells were washed thoroughly to remove the free ligand. The washed cells were again incubated at 15 °C, and the decrease in the bound ligand during incubation was measured. Fig. 2 shows the time-dependent release of radioactivity from PC12 cells and rat erythroid cells. The dissociated radioactivity was precipitated almost completely by 5% trichloroacetic acid and migrated in SDS-polyacrylamide gel with a molecular size similar to that of <sup>125</sup>I-rHuEpo; binding of Epo to PC12 cells as well as to erythroid cells is reversible. Epo appears to dissociate more rapidly from PC12 cells than erythroid cells. Since the unlabeled Epo is not added in the ligand-dissociation mixture, however, the time-dependent release of Epo in Fig. 2 reflects both dissociation of Epo from the cells and reassociation of the dissociated ligand.

Table I shows that Epo bound to PC12 cells was internalized at 37 °C but not at 15 °C. After the cells were incubated with <sup>125</sup>I-rHuEpo at 15 or 37 °C, the cell-associated Epo was exposed to a neutral pH or an acidic pH and then centrifuged. At the acidic pH the ligand bound to the cell surface receptor would be released from the cells, and therefore the radioactivity should appear in the supernatant after centrifugation. But the internalized ligand would not be released from the cells upon low-pH treatment, and therefore, the radioactivity

**FIG. 1.** Binding of <sup>125</sup>I-rHuEpo to PC12, SN6, and rat spleen erythroid cells. **A**, time dependence of binding to PC12 cells. Binding mixtures contained 7.5 nM <sup>125</sup>I-rHuEpo and  $4.5 \times 10^6$  cells. ●, total binding; ○, nonspecific binding; ■, specific binding. **B**, cell number-dependency of binding to PC12 cells. ●, total binding; ○, nonspecific binding; ■, specific binding. Binding mixtures contained 5 nM <sup>125</sup>I-rHuEpo. **C**, Scatchard plots of ligand-saturation curves of PC12 cells (●) and SN6 cells (○). Binding mixtures contained  $2 \times 10^6$  PC12 cells or SN6 cells. **D**, Scatchard plot of rat erythroid cells. Binding mixtures contained  $2 \times 10^6$  cells. Each point in Scatchard plots is the mean  $\pm$  S.D. of quadruplicate assays (C and D).





should be associated with the pelleted cells. When Epo was bound to the cells at 15 °C and then the cell-associated Epo was exposed to the neutral pH, most of the radioactivity was associated with the pelleted cells. The radioactivity, however,

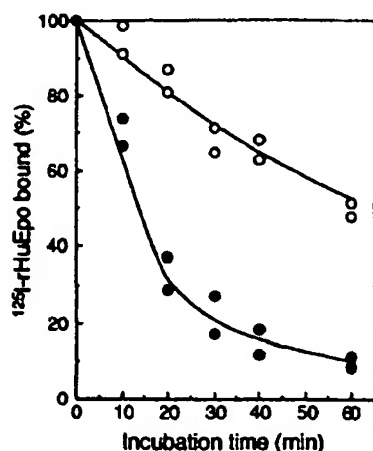


FIG. 2. Reversible binding of Epo to PC12 cells and rat erythroid cells. Binding mixtures were as described under "Experimental Procedures" except that the mixtures of rat spleen erythroid cells contained 0.5 nM  $^{125}\text{I}$ -rHuEpo and  $4 \times 10^6$  cells, and the mixtures of PC12 cells contained 5 nM  $^{125}\text{I}$ -rHuEpo and  $2.5 \times 10^6$  cells. The mixtures were incubated at 15 °C for 3 h for binding of Epo and then the cells were washed three times by PBS. The washed cells were suspended in 150  $\mu\text{l}$  of PBS. The suspensions were incubated at 15 °C for indicated periods and centrifuged on the cushion buffer. Radioactivity of the cell-associated Epo was counted. The total cell-associated radioactivity of rat spleen cells at zero time was  $4454 \pm 183$  cpm (mean of duplicate assays  $\pm$  deviation of duplicate values), and the nonspecific binding was  $1194 \pm 37$  cpm; therefore, specific binding was 3260 cpm. The total and nonspecific binding of PC12 cells was  $6536 \pm 289$  and  $3763 \pm 176$  cpm, respectively; specific binding was 2773 cpm. Specific binding was defined as 100%. Nonspecific binding at each point was measured using the cells bound to  $^{125}\text{I}$ -Epo in the presence of 200-fold unlabeled Epo in the binding mixtures. O, rat erythroid cells; ●, PC12 cells. The supernatants that contained the radioactivity released from the cells were used for identification of the released radioactive material (see text).

was almost completely removed from the cells when the cell-associated Epo was exposed at the acidic pH. When the binding was done at 37 °C, approximately 40% of the total specific binding was still cell-associated after exposure to the acidic pH, in agreement with erythroid cells (21). The specific binding of Epo to PC12 cells at 15 °C is indeed equivalent to the receptor-bound ligands on the cell surface, but a significant portion of the ligands bound to the cells at 37 °C is internalized.

The culture of PC12 cells in the presence of NGF caused neurite growth. When Epo binding was tested for PC12 cells cultured for 3 days in the presence of 2 nM NGF, there were no significant changes in the characteristics of Epo binding, including the number of binding sites.

PC12 cells were derived from rat adrenal chromaffin cells (6). The natural chromaffin cells were prepared from rat adrenal medullas, and the specific binding of  $^{125}\text{I}$ -rHuEpo at 10 nM was tested using  $4 \times 10^5$  cells. There was specific and reproducible binding ( $410 \pm 20$  cpm in triplicate assays), but low numbers of the available cells did not allow us to carry out further characterization of the binding.

**Specificity of Binding of Epo to PC12 Cells—Affinities of Epo binding sites on PC12 and SN6 cells are much lower than those on erythroid cells, and Epo is a heavily glycosylated protein (1, 16). It is possible that the Epo binding to these neuronal cells occurs through recognition of sugar chains attached to Epo, like a lectin-glycoprotein interaction. This possibility, however, was excluded by the results that the deglycosylated form of rHuEpo inhibited the specific binding of  $^{125}\text{I}$ -rHuEpo with a potency similar to that of the fully glycosylated rHuEpo and that metal chelators (EGTA and EDTA) and monosaccharides (GalNAc and Gal), which are inhibitors of the interaction among some lectins and glycoproteins, showed no effect on the specific binding (Table II). Rat Epo also inhibited the specific binding of  $^{125}\text{I}$ -rHuEpo with an efficiency similar to that of the unlabeled rHuEpo, indicating that the low affinity of PC12 cells was not due to a combination heterogeneous in origin of the ligand and target cells. The monoclonal antibodies (R2 and R6) against rHuEpo decreased the binding, probably by deprivation of free ligand, but the control antibody directed against transglutaminase**

TABLE I  
Internalization of Epo bound to PC12 cells

Radioiodinated rHuEpo was bound to PC12 cells under the different conditions, and the cells were then separated from the free ligand as described under "Experimental Procedures." The cells were subjected to the postbinding treatment for 3 min on ice and centrifuged. Radioactivity of the supernatant and pelleted fractions was counted. Radioactivity due to nonspecific binding was measured with the experiments in which 200-fold unlabeled Epo was added to the binding mixtures. Each value is the mean of duplicate assays  $\pm$  deviation of duplicate values. The values in parentheses indicate specific binding. Total radioactivity represents the sum of supernatant and pellet radioactivity.

Binding conditions		Postbinding treatment	Radioactivity		
Temperature and time	Unlabeled Epo		Supernatant	Pellet	Total
cpm/10 <sup>6</sup> cells					
15 °C, 3 h	-	pH 7.4	194 ± 14	3064 ± 87	3258 ± 73
	+		134 ± 7	1528 ± 56	1662 ± 49
	-		(60)	1536	(596)
	-	pH 2.5	2850 ± 44	472 ± 30	3322 ± 15
	+		1356 ± 63	363 ± 45	1719 ± 108
	-		(1494)	109	(1603)
37 °C, 1 h	-	pH 7.4	235 ± 49	3738 ± 6	3973 ± 43
	+		121 ± 14	1339 ± 81	1460 ± 95
	-		(114)	2399	(2513)
	-	pH 2.5	2563 ± 102	1369 ± 28	3932 ± 130
	+		1081 ± 44	361 ± 32	1442 ± 12
	-		(1482)	1008	(2490)



TABLE II

## Specific binding of Epo to PC12 cells

Binding mixtures contained 5 nM [<sup>125</sup>I]-rHuEpo and 2.5 × 10<sup>6</sup> PC12 cells. The substance was added to the binding mixture just before the labeled Epo was added. Nonspecific binding measured in the presence of 200-fold unlabeled Epo was 3420 cpm (mean of duplicate, 3314 and 3525 cpm). Each value is the mean of duplicate assays ± deviation of duplicate values. Specific binding (%) was calculated from the mean value.

Substances	Concentration	Specific binding of [ <sup>125</sup> I]-rHuEpo	
		cpm	%
rHuEpo	5 nM	2592 ± 46	100
Deglycosylated rHuEpo	5 nM	1451 ± 34	56
Rat Epo	5 nM	1470 ± 18	57
GalNAc	10 mM	1486 ± 19	57
Gal	5 mM	2348 ± 49	91
EGTA	10 mM	2768 ± 103	107
EDTA	15 mM	2627 ± 33	101
R2*	40 μg/ml	1083 ± 30	42
R6*	80 μg/ml	206 ± 24	8
Anti-TG*	40 μg/ml	2454 ± 67	95

\* rHuEpo-directed monoclonal antibodies (15).

\* Transglutaminase-directed monoclonal antibodies (41).

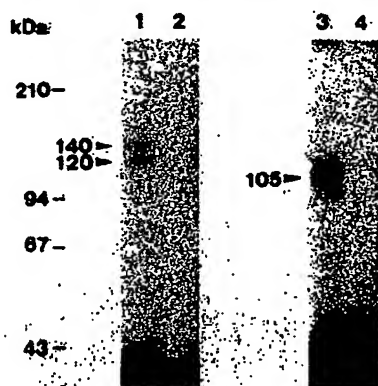


FIG. 3. Affinity cross-linkage of [<sup>125</sup>I]-rHuEpo to PC12 cells and rat erythroid cells. Binding mixtures of rat erythroid cells contained 2 nM [<sup>125</sup>I]-rHuEpo and 2 × 10<sup>6</sup> cells, and those of PC12 cells contained 6 nM ligand and 1.5 × 10<sup>6</sup> cells. Lanes 1 and 2, rat erythroid cells; lanes 3 and 4, PC12 cells. Incubations for binding were done in the presence of 200-fold unlabeled ligand (lanes 2 and 4) or in its absence (lanes 1 and 3).

showed little effect. No inhibition of the binding was found in the presence of the following individual growth factor at 20 nM IL-1β, 20 nM IL-3, 200 nM IL-6; 200 nM G-CSF, 200 nM GM-CSF, 200 nM EDF (activin A), 200 nM tumor necrosis factor, 80 nM hepatocyte growth factor, 1 μM epidermal growth factor, 200 nM NGF, and 20 μM insulin. These properties of the Epo binding sites on PC12 cells demonstrate that the cells express Epo-specific receptors which interact with the polypeptide part of the ligand.

**Cross-linked Products**—Epo receptors on PC12 cells and rat erythroid cells were affinity-labeled by a chemical cross-linker, solubilized with Triton X-100, and then analyzed by SDS-polyacrylamide gel electrophoresis under reducing conditions (Fig. 3). There were two cross-linked products of rat erythroid cells with the molecular masses of 120 and 140 kDa, and a single product of PC12 cells with a 105-kDa molecular mass. These products were not detected when an excess of unlabeled Epo was added to the binding mixture. Subtracting the molecular mass of Epo, 35 kDa, from those of the cross-

linked products gave the apparent size of the component cross-linked to Epo in each product; 85 and 105 kDa of erythroid cells and 70 kDa of PC12 cells.

**Immunohistochemical Detection of Epo-R of PC12 Cells and Erythroid Cells**—Rabbit anti-mouse Epo-R antiserum was prepared by using the soluble form of mouse Epo-R as an antigen. This antiserum was used to identify Epo-R of erythroid cells and PC12 cells. Epo-R was solubilized from cells and concentrated by the Epo-fixed gel. The concentrated Epo-R was detected by the Western blotting technique (Fig. 4). Epo-R of mouse erythroid cell line, TSA8, was detected as a single band with a molecular size of 68 kDa (lane 1). A band with a similar size was found for rat spleen cells (lane 2). These bands were undetectable when the antiserum was preadsorbed with the antigen, soluble form of mouse Epo-R (lanes 4 and 5). PC12 cells yielded one major band at 62 kDa; and two additional minor bands at 58 and 54 kDa (lane 3). The major 62-kDa band appears to be Epo-R on PC12 cells, because the minor bands were still detected by the preadsorbed antiserum (lane 6). Experiments using the anti-NH<sub>2</sub>-terminal antiserum also showed Epo-R of 68 kDa in TSA8 and 62 kDa in PC12 cells.

**Northern Blotting of Epo-R mRNA**—Poly(A)<sup>+</sup> RNA was isolated from fetal mouse liver cells, rat spleen cells, and PC12 cells and subjected to Northern hybridization using rat Epo-R cDNA as a probe (Fig. 5). The rat probe hybridizes with mRNA from fetal mouse liver cells (lane 1), rat spleen cells (lane 2), and PC12 cells (lane 3). The size (2.1 kilobases) of rat mRNA agrees with that from mouse cells (26, 31).

**Nucleotide Sequence of Epo-R of PC12 Cells and Rat Erythroid Cells**—The affinity of Epo to PC12 Epo-R is very low as compared with that of erythroid cells (Fig. 1); and the size of PC12 Epo-R is smaller than that of erythroid cells (Fig. 4). In order to know whether this low affinity is due to expression of a deletion-mutant Epo-R on PC12 cells, we determined the nucleotide sequence of the entire coding region of Epo-R cDNA from rat erythroid cells and PC12 cells. The nucleotide sequence of PC12 cells was identical to that of rat erythroid cells. Fig. 6 shows the nucleotide sequence of rat Epo-R and its deduced amino acid sequence: the matured rat Epo-R consists of 483 amino acids, and its calculated molecular weight is 52,794. For comparison, the amino acid sequences of mouse (26) and human (32, 33) Epo-R are shown. The amino acid sequences of the matured proteins were 82% conserved between the rat and human Epo-Rs. Homology between rat and mouse increased to 94%. Insertion of one amino acid occurs at position 49 in human Epo-R. The

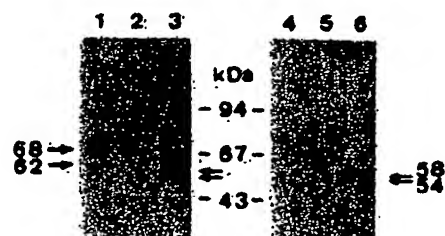


FIG. 4. Immunohistochemical identification of Epo-R of PC12 cells and erythroid cells. Rat spleen, erythroid cells, PC12 cells, and mouse erythroleukemia cells (TSA8) were solubilized by CHAPS. Epo-R in the lysates was concentrated using the Epo-fixed gel. The concentrated Epo was detected by the Western blotting technique using anti-soluble Epo-R antiserum. In A, the anti-soluble Epo-R antiserum was used without the antigen preadsorption, whereas, in B, the antiserum was preincubated with excess antigen, soluble Epo-R. Lanes 1 and 4, TSA8 cells; lanes 2 and 5, rat spleen cells; lanes 3 and 6, PC12 cells.

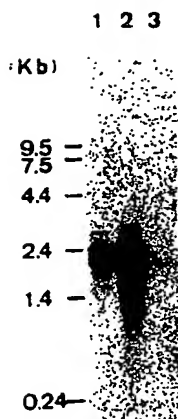


FIG. 5. Northern blot analyses of Epo-R mRNA. Poly(A)<sup>+</sup> RNA from fetal mouse liver cells (lane 1), rat spleen cells (lane 2), and PC12 cells (lane 3) was loaded in each lane of 1% agarose gel. RNA blotted to the filter was hybridized with <sup>32</sup>P-labeled rat Epo-R cDNA probe.

presence of 4 spaced cysteines near the amino terminus (positions 28, 38, 66, and 82) and a WS-motif (WSXWS at positions 208–212) in the extracellular region is the characteristic conserved features of a new cytokine receptor family to which receptors of Epo, IL-2, IL-3, IL-4, IL-5, IL-6, IL-7, GM-CSF, G-CSF, and prolactin belong (34, 35). The WS motif of Epo-R appears to be critical for protein folding, ligand binding, and signal transduction (36, 37). One N-glycosylation site (NYS at positions 51–53) is conserved in rodent and human Epo-Rs. In the cytoplasmic domain, there is a well conserved region (positions 248–295) proximal to the transmembrane domain. This region is homologous to the IL-2 receptor chain (34) and contains the sequence that appears to play a key role in expression of the growth signal including tyrosine-kinase activity (38–40). Forty amino acid residues in the carboxyl terminus have been proposed as a negative regulatory region (40). This regulatory region is preceded with a highly conserved region (positions 418–446) whose significance is not known.

**Effects of Epo on Cultured PC12 Cells**—There were no effects on [<sup>3</sup>H]thymidine incorporation into DNA of PC12 cells. Incubation of PC12 cells with Epo caused a rapid and transient increase in the cytosolic free calcium concentration (Fig. 7A). This increase was completely abolished by the Epo-directed monoclonal antibodies R2 and R6 (not shown). An increase in the calcium concentration also occurred with the addition of bradykinin, a control compound that has been known (30) to mobilize calcium from intracellular stores to the cytoplasmic fraction (Fig. 7A). EGTA abolished the increase in calcium by Epo but had no effect on the bradykinin-induced increase (Fig. 7B). Epo-induced increase in the cytosolic concentration was dose-dependent; when Epo was added at 30 pM, 900 pM, 3 nM, and 6 nM, increases of the calcium concentration in percent were  $10 \pm 6.3$  ( $n = 10$ ),  $49 \pm 13.9$  ( $n = 12$ ,  $p < 0.025$ ),  $60 \pm 13.9$  ( $n = 12$ ,  $p < 0.025$ ), and  $70 \pm 17.0$  ( $n = 7$ ,  $p < 0.025$ ), respectively, where the calcium concentration without addition of Epo was defined as 100 and the increased values were means  $\pm$  S.E. Addition of Epo at 9 nM resulted in a rather low increase of  $36 \pm 11.6$  ( $n = 12$ ,  $p < 0.025$ ) by an unknown reason.

A culture of PC12 cells in the presence of Epo elevated intracellular concentrations of monoamines such as DOPA, dopamine, DOPAC, and HVA; MDOPA remained unchanged (Fig. 8). This may suggest that tyrosine hydroxylase, a key

enzyme in the biosynthetic pathway of the four monoamines that increased, is activated or accumulated.

#### DISCUSSION

Stimulation of erythropoiesis has been thought to be an exclusive physiological function of Epo. Findings that Epo-R exists on megakaryocytes (2), endothelial cells from human umbilical vein and bovine adrenal capillary (3), B-lymphocytes (4), rodent placenta cells (5), multipotential hematopoietic stem cells (42), and embryonic stem cells (42, 43), however, may suggest yet unidentified functions of Epo, although some of these findings may not be physiologically meaningful. The PC12 pheochromocytoma cell line has been a widely used model system for studying the action mechanism of NGF on neurons, because this cell line undergoes neurite outgrowth responding to NGF (7). SN6 cells display some properties of cholinergic neurons such as high choline acetyltransferase activity and neurite extension (8). In this paper we described that these cell lines had Epo-binding proteins. Detailed analyses of PC12 cells and rat erythroid cells, including nucleotide sequence analyses of Epo-R, revealed that the Epo-binding protein on PC12 cells is the counterpart of erythroid cells. Expression of Epo-R on these neural cell lines seems not to be accidental, because Epo augments choline acetyltransferase activity in mouse embryonic primary septal neurons and supports survival of septal cholinergic neurons in adult rats (11). Epo exerts its activity on these neurons at a nanomolar range (11), which is comparable with  $K_d$  of Epo-R on PC12 and SN6 cells. A prerequisite for inference of a physiological significance of Epo-R in nerve cells is to demonstrate production of Epo in brain. Currently we are attempting to find Epo production in brain tissue.

Immunochemical detection of solubilized Epo-R showed that the size (62 kDa) of Epo-R from PC12 cells was smaller than that (68 kDa) from rat erythroid cells. Analyses of PC12 mRNA by Northern blotting and its nucleotide sequence, however, were indicative of expressing neither a mutated Epo-R nor an alternative splicing-derived Epo-R. Neural cells may differ from erythroid cells in post-translational processing of Epo-R, resulting in expression of Epo-R with different sizes. One putative N-glycosylation site existing in the extracellular domain of Epo-R could be a cause for the size difference, but the difference could also result from other processings such as proteolysis and phosphorylation. Proteolytic removal of the NH<sub>2</sub>-terminal region from PC12 Epo-R is unlikely, because the antiserum against the NH<sub>2</sub>-terminal peptide reacts with the solubilized Epo-R.

The ligand affinity of Epo-R on neural cells ( $K_d = 10 \sim 16$  nM) is significantly lower than those on erythroid cells ( $K_d = 95$  pM for high affinity site and 1.9 nM for low affinity site). The low affinity of Epo-R on PC12 cells might be related to a post-translational processing that yields Epo-R with a smaller size. But the N-linked sugar, if it causes the difference in Epo-R size, is not responsible for the affinity difference, because the N-glycosylation site-defective mutant of mouse Epo-R (44) and its extracellular soluble domain (22) are similar to the respective wild-type counterpart in binding with Epo.

A more intriguing hypothesis to account for the affinity difference is that there are accessory proteins that interact with Epo-R, altering interaction of Epo-R with the ligand. Cross-linking experiments revealed the presence of two proteins with 105 and 85 kDa in erythroid cells and a 70-kDa protein in PC12 cells (the size of Epo, 35 kDa, has been subtracted from the cross-linked products) (see Fig. 3). The two proteins found in rat erythroid cells are consistent with

	ATGGACCAACTCAGGTTGGCCGGCTGGCTCTGGGTTAGCCCGCTGTGTCTCTACTTGGT	80	CTCATCTCACTGTTGCTGACTGTGCTGGCCCTGCTGTCACCGCGGGGCTCTGGCGAC	837
RT	H D Q L R V A R V P R V S P L C L L L A		L I S L L L T V L A L L S H R R A L R Q	
MS	. . . . . P L . . . . . G . . . . .		. . . . . . . . . . . . . . . . . . . .	
HU	. . . . . Q A S L . . . . . Q . . . . .		V . . L V . . . . . . . . . . . Q . .	
	GGGGCAACCTCGGGCATCTCAACGAGCTCCGGGACCCCAAGTTTGAGAGCAAAAGCCGCG	120	AGATCTGGCCTGGCATCCAGCGCCAGAGAAATGAGTTTGAGGGTCTCTTCAACACCCAC	867
RT	G A A V A . . . . . S P L P D P E F E S K A A		K I I M P G I P S P E B E F E G L F T Y H	
MS	. . . . . P . . . . . . . . . . . . . . . .		. . . . . . . . . . . S . . . . . . . .	
HU	. . . . . P P . . . . . N . . . . . . . . . .		. . . . . . . . . . . . . . . . . . . .	
	CTCTTGCAATCCCGGGGCTCGCAAGAATCTCTATGCTTCAACGAGCTCTGGAGACTTG	180	AAAGCTAACTTCAGCTATGGCTGTTGCAAGCCGATGGCTGTCTGTGTGTGGAGCCCAAGT	937
RT	L L A S R G S E E L L C P T T Q R L E D L		K G H F Q L M L L Q R D Q C L M V S P S	
MS	. . . . . . . . . . . . . . . . . . . .		. . . . . . . . . . . . . . . . . . . .	
HU	. . . . . . . . . . . . . . . . . . . .		. . . . . . . . . . . . . . . . . . . .	
	GTCTTTTCTGGAGGAGCGGGCAACTCGGGATGGCG---TTCAACTACAGCTTCTCT	237	AGCCCCCTCCCTGAGGATACACTGGGCACTAGAGTCTCTCTAGACGAGAGCTGGGGA	1017
RT	V C P M E E A A H S G R G - F H Y S P S		S P F P S D P P A H L L V L S S R R M G	
MS	. . . . . . . . . . . S A . V . . . . .		. . . . . S . . . . . . . . . . . P . . A	
HU	. . . . . . . . . . . S A . V . . . . .		. . . . . . . . . . . . . . . . . . . .	
	TACCACTCGAAGGTGAATCAAGAAAGTCAITGGCTGTCAGCAGCGCCGCCACCGCTCGGC	287	GTGATCAGCGCTGGGATCAGCGGCGAGAGACAGGCGCCCTTACTCGAGCCATGGGCG	1077
RT	. . . . . Q L E G E S R K S C R L E Q A P T V R		V T Q A G D A G A E D K C P L L S P V G	
MS	. . . . . . . . . . . . . . . . . . . .		. . . . . . . . . . . . . . . . . . . .	
HU	. . . . . . . . . . . . . . . . . . . .		. . . . . T M . . V E P . . T D E . . . . .	
	CGCTCCATCGCTTCTGGTCTTCACTGGCGACCGCGGAGACGTGGAGTTTGTGGCACTG	357	AGTCACGGCGCCAGGACACCTACCTGATTTGATGAATGTTGCTACCCCGGTGGCCA	1137
RT	G S N R F M C S L P T A D T S S F V P L		S E R A Q D T Y L V L D D M L L P R C F	
MS	. . . . . V . . . . . . . . . . . . . . . .		. . . . . . . . . . . . . . . . . . . .	
HU	. . . . . A V . . . . . . . . . . . . . . . .		. . . . . . . . . . . . . . . . . . . .	
	GAGCTGCAGGTGACGAGGGCTCCGGA TCTGCTGCTAGCACCGCATCATCCATCAAT	417	TGCAGTGAGAACCTCTCTGGGCTGGGACAGTGTAGACCCCTCCGACTATGATGAAGGT	1197
RT	E L Q V T E A S G S P R Y H R I I N I H		C S E N L S G P G D S V D P A T H D E G	
MS	. . . . . . . . . . . . . . . . . . . .		. . . . . . . . . . . . . . . . . . . .	
HU	. . . . . . . . . . . . . . . . . . . .		. . . . . P . . . D . P . . . . . G . . . . .	
	GAGTAGTGTCTCTGAGGACCGCCCGCGGGCTGCTGGCGCGGACGACGAAGAGGCGAGC	477	TCAGAAATCTCTCTGGCCCTCTGAGTGGCTTCAAGGCCGACGCCAGAGGCCGACCTCG	1257
RT	E V V L L D A P A G L L A R R A E R G S		S E T A E S C P S D L A S K P R P E G T S	
MS	. . . . . . . . . . . . . . . . . . . .		. . . . . . . . . . . . . . . . . . . .	
HU	. . . . . . . . . . . . . . . . . . . .		. . . . . . . . . . . . . . . . . . . .	
	CACGTGTGCTGGGTGCTGGCACTCGCGGGCTGCTATGACCAACCCGATCCGCTAC	537	CTTCCAGCTTTGAGTACCACTCTGGAGCCAGCTCTAAGCTCTGTGGCTCGGGCA	1317
RT	H V V L E M L P P P G A P H T T H I Y		P S S F E Y T I L D P S S K L L C P R A	
MS	. . . . . . . . . . . . . . . . . . . .		. . . . . . . . . . . . . . . . . . . .	
HU	. . . . . . . . . . . . . . . . . . . .		. . . . . A A . . . . . . . . . . . Q . . . .	
	GAGGTGAGCTGTGAGCAGCGCAACCGGCTGGGCGACACAAAGCGTGAGAGCTCTGGAA	597	CTGGCTCTCAGCTACCGCCCACTCACCTTCACTGAAGTACTGTACTTGTGTGTCTC	1377
RT	E V D V S A G H R A G G T G R V E V L E		L P P E L P P T P P E L K Y L Y L V V S	
MS	. . . . . . . . . . . . . . . . . . . .		. . . . . . . . . . . . . . . . . . . .	
HU	. . . . . . . . . . . . . . . . . . . .		. . . . . C . . . . . . . . . . . . . . . .	
	GGCGCACTGAGTGTGTCTGAGCAACTGCGGGCGGGGACCGCTACACCTTCCGCTGT	657	GATTCGGCATCTCAACAGATTACAGCTCAGGGGCTCCAGGAGCTCAGCGGAGCTCA	1437
RT	G R T E C V L S H L R G G T R Y T P A V		D S G I S T D Y S S G S G S Q Q V H G D S	
MS	. . . . . . . . . . . . . . . . . . . .		. . . . . . . . . . . . . . . . . . . .	
HU	. . . . . . . . . . . . . . . . . . . .		. . . . . . . . . . . . . . . . . . . .	
	CGAGACCGCATGGCGAGCGGAGCTTCAGCGGATCTGAGAGCGCTGTGTCTGAGCGCGG	717	TCTGACGGGCGGCTACTCCACCCGCTATGAGAATAGCCTGTTTTCAGACAGAGCCCTCTG	1497
RT	R A R H A E F S F S G F V S A V S E P A		S D G P Y S H P V E H L V P D T E P L	
MS	. . . . . . . . . . . . . . . . . . . .		. . . . . . . . . . . . . . . . . . . .	
HU	. . . . . . . . . . . . . . . . . . . .		. . . . . . . . . . . . . . . . . . . .	
	TGCTACTCACTGCTAGCACTTGCACTCTTCACTCTGAGCGCTGTCTCTCAATCTGTCTC	777	CGGGCCAGCTACGTTGGCTGCTCTAG	1527
RT	S L L T A S D L D P L I L T L S L I L V		R P S Y V A C S .	
MS	. . . . . . . . . . . . . . . . . . . .		. . . . . . . . . . . . . . . . . . . .	
HU	. . . . . . . . . . . . . . . . . . . .		. . . . . H . . . . . . . . . . . . . . .	

FIG. 6. Nucleotide sequence of rat Epo-R and amino acid sequences of rat, mouse, and human Epo-R. The nucleotide sequence of rat Epo-R is presented in the first line. Amino acid sequences of rat (RT), mouse (MS), and human (HU) Epo-R are presented in the second, third, and fourth lines, respectively. Position 1 was given to the putative NH<sub>2</sub>-terminal amino acid of the matured protein (26). The transmembrane domain is underlined. Amino acid sequences of mouse (26) and human (32, 33) were cited from the indicated sources. The nucleotide sequence data reported in this paper will appear in the DDBJ, EMBL, and GenBank Nucleotide Sequence Databases with accession number D13566.

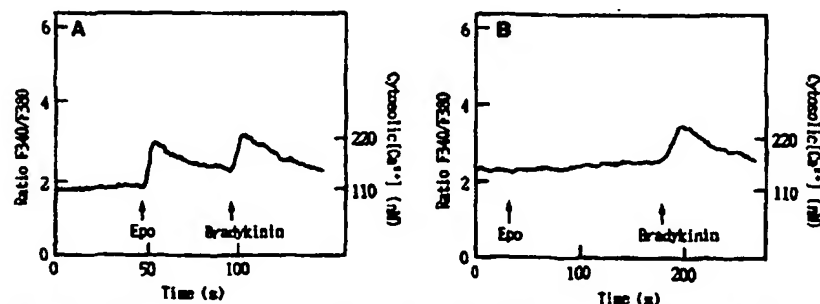


FIG. 7. **A** Epo-induced increase in cytosolic calcium concentration of PC12 cells. **A**, Epo at 3 nM and bradykinin at 0.1 mM were added to the fura-2 AM-loaded PC12 cells at the indicated time. The ratio  $F_{340}/F_{380}$  represents the ratio of fluorescence at 490 nm when excited at 340 nm to that when excited at 380 nm. **B**, experimental conditions were as in **A**, except that 1 mM EGTA was present in the assay mixture. EGTA inhibits an Epo-induced increase in the cytosolic calcium concentration but does not inhibit a bradykinin-induced increase.

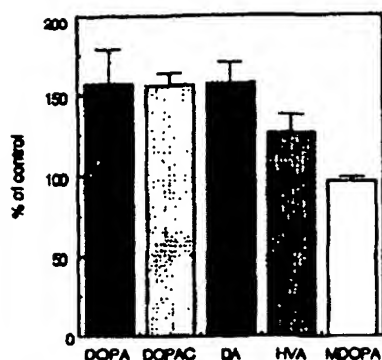


FIG. 8. Effects of Epo on intracellular monoamine concentrations of PC12 cells. The control cells cultured without Epo contained DOPA, DOPAC, dopamine, HVA, and MDOPA with averages of 5.4, 2.2, 5.3, 0.5, and 0.7 ng/mg protein, respectively. These values were defined as 100%. Triplicate cultures were done with and without Epo. The values are means  $\pm$  S.D.

those reported previously in rat source (45) and the presence of two components with similar sizes has been shown in erythroid cells from human and mouse (for review see Refs. 1 and 46). No conclusive evidence for these proteins being derived from cloned Epo-R cDNA has been reported. The molecular weight of Epo-R predicted from cloned mouse (26) and rat cDNA (this paper) is about 53,000, and the size of Epo-R detected by immunoblotting (Ref. 47 and this paper) or by ligand blotting technique (48, 49) is around 65 kDa; this size of Epo-R is much smaller than two proteins included in cross-linked products of erythroid cells. From these, it has been suspected that erythroid cross-linked products may consist of Epo, Epo-R, and an unidentified accessory protein. It has been reported recently, however, that erythroid cross-linked products before denaturation are precipitated by the antiserum against the cytoplasmic domain of mouse Epo-R, but, surprisingly, they are not precipitated upon denaturation (boiling of the cross-linked products for 5 min in Laemmli SDS-electrophoresis buffer) (50). The cross-linked products either before or after denaturation could be precipitated by the antiserum against Epo. These results have been interpreted as a strong indication of the following. 1) Epo interacts with Epo-R, but the reagent used does not efficiently cross-link between Epo and Epo-R; 2) Epo is cross-linked with accessory protein(s) which is immunochemically unrelated to Epo-R, and 3) before denaturation of cross-linked products, Epo-R is retained in complexes through noncovalent interaction with Epo or both Epo and an accessory protein, but Epo-R is dissociated from the complexes upon denaturation. By using the antiserum against the extracellular domain of mouse Epo-R, we performed similar experiments of erythroid cross-linked products, and the data obtained were consistent with those already reported (50). The 105-kDa cross-linked product of PC12 cells could not be precipitated either before or after denaturation,<sup>3</sup> although our antiserum reacted with the solubilized Epo-R of PC12 cells on the Western blotting filter (see Fig. 4). The PC12-derived cross-linked product was precipitated by the antiserum against Epo, regardless of denaturation of the product. From these results of the PC12 cells, we infer that most of the Epo-R associated with the PC12 cross-linked product may have dissociated during solubilization of the cross-linked product so that the cross-linked product even before being subjected to the denaturation treat-

ment can not be precipitated by the Epo-R antiserum. This inference is supported by rapid dissociation of Epo-Epo-R complexes on PC12 cells (see Fig. 2). Based on such information, our hypothesis is that the cloned Epo-R is a common molecule required for Epo binding, but the ligand affinity is modulated by multiple accessory proteins of which expression may be cell type-specific. Affinity of the Epo-R on endothelial cells is also very low ( $K_d = 2-8$  nM), and the size of a major cross-linked product is around 79 kDa (4). Homodimerization of the cloned Epo-R has been implicated in the signal transduction pathway of Epo (51), but this does not exclude the possible involvement of a heterosubunit in the pathway. For high affinity receptor sites of IL-2 (52), IL-3 (53), IL-5 (54), IL-6 (55), and GM-CSF (53), oligomerization of heterosubunits is required.

Epo caused a rapid increase in calcium in PC12 cells. EDTA did not interfere with binding of Epo to the cells (Table II) but inhibited the Epo-induced increase of calcium, indicating that Epo stimulates mostly the calcium influx from outside of PC12 cells. The role of calcium in Epo-signal transduction of erythroid cells has been controversial (56-60). Several studies have indicated significant alterations in intracellular free calcium concentration or calcium influx in response to Epo (56-59). Experiments with purified Epo-responsive mouse erythroid cells that probably express Epo-R at the highest number, however, showed that the Epo action was not accompanied by an acute alteration in intracellular calcium concentration (60). It has been pointed out that the conflicting data may result from different maturation stages of the cells used (60). The data may also be dependent on whether or not the cells have been exposed *in vivo* to a high Epo concentration before the cells were prepared from animals. Further studies are necessary to find a definitive role of calcium in Epo-signal transduction.

**Acknowledgment**—We thank Yoko Tanaka for help in the preparation of the manuscript.

#### REFERENCES

- Krantz, S. B. (1991) *Blood* 77, 419-434
- Ishibashi, T., Kozio, J. A., and Burstein, S. A. (1987) *J. Clin. Invest.* 79, 286-289
- Angelos, A., Lee, E.-S., Kessimian, N., Levinson, R., and Steiner, M. (1990) *Proc. Natl. Acad. Sci. U. S. A.* 87, 5978-5982
- Kimoto, H., Yoshida, A., Ishioka, C., Masuda, S., Sasaki, R., and Mikawa, H. (1991) *Clin. Exp. Immunol.* 85, 151-156
- Sawyer, S. T., Krantz, S. B., and Sawada, K. (1989) *Blood* 74, 103-109
- Doupe, A. J., Landis, S. C., and Patterson, S. C. (1985) *J. Neurosci.* 5, 2119-2142
- Greene, L. A., and Tischler, A. S. (1976) *Proc. Natl. Acad. Sci. U. S. A.* 73, 2424-2428
- Greene, L. A., and Tischler, A. S. (1982) *Adv. Cell Neurobiol.* 3, 373-414
- Federoff, H. J., Grabczyk, E., and Fishman, M. C. (1988) *J. Biol. Chem.* 263, 19290-19295
- Hammond, D. N., Weiner, B. H., Tonagrad, J. H., and Heller, A. (1986) *Science* 234, 1237-1240
- Konishi, Y., Chui, D.-H., Hirose, H., Kunishita, T., and Tabira, T. (1993) *Brain Res.*, in press
- Krytal, G. (1983) *Exp. Hematol.* 11, 649-660
- Osawa, M., Ishikawa, T., and Irimajiri, A. (1984) *Nature* 307, 66-68
- Goto, M., Akai, K., Murakami, A., Hashimoto, C., Tsuda, E., Ueda, M., Kawanishi, G., Takahashi, N., Ishimoto, A., Chiba, H., and Sasaki, R. (1988) *Bio/Technology* 6, 67-71
- Goto, M., Murakami, A., Akai, K., Kawanishi, G., Ueda, M., Chiba, H., and Sasaki, R. (1989) *Blood* 74, 1415-1423
- Tsuda, E., Kawanishi, G., Ueda, M., Masuda, S., and Sasaki, R. (1990) *Eur. J. Biochem.* 188, 405-411
- Okano, M., Ohnata, H., and Sasaki, R. (1992) *J. Nutr.* 122, 1376-1383
- Sasaki, R., Yanagawa, S., Hitomi, K., and Chiba, H. (1987) *Eur. J. Biochem.* 168, 43-48
- Yamaguchi, K., Akai, K., Kawanishi, G., Ueda, M., Masuda, S., and Sasaki, R. (1991) *J. Biol. Chem.* 266, 20434-20439
- Munson, P. J., and Rodbard, D. (1980) *Anal. Biochem.* 107, 220-239
- Sawyer, S. T., Krantz, S. B., and Goldwasser, E. (1987) *J. Biol. Chem.* 262, 5564-5568
- Nagao, M., Masuda, S., Abe, S., Ueda, M., and Sasaki, R. (1992) *Biochem. Biophys. Res. Commun.* 188, 888-897
- Burnette, W. N. (1981) *Anal. Biochem.* 112, 195-203
- Sambrook, J., Fritsch, E. F., and Maniatis, T. (1989) *Molecular Cloning: A Laboratory Manual*, 2nd Ed., Cold Spring Harbor Laboratory, Cold Spring Harbor, NY

<sup>3</sup>S. Masuda, M. Nagao, and R. Sasaki, unpublished data.

25. Vera, G., Gibbs, R. A., Scherer, S. E., and Caskey, C. T. (1987) *Science* **237**, 415-417.
26. D'Andrea, A. D., Lodish, H. F., and Wong, G. G. (1989) *Cell* **57**, 277-285.
27. Carothers, A. M., Urlaub, G., Mucha, J., Grunberger, D., and Chasin, L. A. (1989) *BioTechniques* **7**, 497-499.
28. Tabor, S., and Richardson, C. C. (1989) *J. Biol. Chem.* **264**, 6447-6458.
29. Gryniewicz, G., Poenie, M., and Tsien, R. Y. (1985) *J. Biol. Chem.* **260**, 3440-3450.
30. Calker, D., Takahata, K., and Heumann, R. (1989) *J. Neurochem.* **52**, 38-45.
31. Masuda, S., Hisada, Y., and Sasaki, R. (1992) *FEBS Lett.* **298**, 169-172.
32. Winkelmann, J. C., Penny, L. A., Deaven, L. L., Forget, B. G., and Jenkins, R. B. (1990) *Blood* **76**, 24-30.
33. Jones, S. S., D'Andrea, A. D., Haines, L. L., and Wong, G. G. (1990) *Blood* **76**, 31-35.
34. D'Andrea, A. D., Fasman, G. D., and Lodish, H. F. (1989) *Cell* **58**, 1023-1024.
35. Bazan, J. F. (1989) *Biochem. Biophys. Res. Commun.* **164**, 788-793.
36. Yoshimura, A., Zimmers, T., Neumann, D., Longmore, G., Yoshimura, Y., and Lodish, H. F. (1992) *J. Biol. Chem.* **267**, 11619-11625.
37. Chiba, T., Amanuma, H., and Todokoro, K. (1992) *Biochem. Biophys. Res. Commun.* **184**, 485-490.
38. Miura, O., D'Andrea, A., Kabat, D., and Ihle, J. N. (1991) *Mol. Cell. Biol.* **11**, 4895-4902.
39. Chiba, T., Kishi, A., Sugiyama, M., Amanuma, H., Machida, M., Nagata, Y., and Todokoro, K. (1992) *Biochem. Biophys. Res. Commun.* **188**, 1236-1241.
40. D'Andrea, A. D., Yoshimura, A., Youssoufian, H., Zon, L. I., Koo, J.-W., and Lodish, H. F. (1991) *Mol. Cell. Biol.* **11**, 1980-1987.
41. Ikura, K., Yanagawa, S., Okumura, K., Sasaki, R., and Chiba, H. (1984) *Agric. Biol. Chem.* **48**, 1835-1840.
42. Heberlein, C., Fischer, K.-D., Stoffel, M., Nowack, J., Ford, A., Tessmer, U., and Stocking, C. (1992) *Mol. Cell. Biol.* **12**, 1815-1826.
43. Schmitt, R. M., Bruyns, E., and Snodgrass, H. R. (1991) *Genes & Dev.* **5**, 728-740.
44. Nagao, M., Matsumoto, S., Masuda, S., and Sasaki, R. (1993) *Blood*, in press.
45. Mayeux, P., Billat, C., and Jacquot, R. (1987) *J. Biol. Chem.* **262**, 13985-13990.
46. D'Andrea, A. D., and Zon, L. I. (1990) *J. Clin. Invest.* **86**, 681-687.
47. Yoshimura, A., D'Andrea, A. D., and Lodish, H. F. (1990) *Proc. Natl. Acad. Sci. U. S. A.* **87**, 4139-4143.
48. Atkins, H. L., Broudy, V. C., and Papayannopoulou, T. (1991) *Blood* **77**, 2577-2582.
49. Wognum, A. W., Lanadrop, P. M., Humphries, R. K., and Krystal, G. (1990) *Blood* **76**, 697-705.
50. Mayeux, P., Lacombe, C., Casadevall, N., Chretien, S., Dusenter, I., and Gisselbrecht, S. (1991) *J. Biol. Chem.* **266**, 23380-23385.
51. Watowich, S. S., Yoshimura, A., Longmore, G. D., Hilton, D. J., Yoshimura, Y., and Lodish, H. F. (1992) *Proc. Natl. Acad. Sci. U. S. A.* **89**, 2140-2144.
52. Hatakeyama, M., Tsuda, M., Minamoto, S., Kono, T., Doi, T., Miyata, T., Miyasaka, M., and Taniguchi, T. (1989) *Science* **244**, 551-556.
53. Kitamura, T., Sato, N., Arai, K.-I., and Miyajima, A. (1991) *Cell* **66**, 1165-1174.
54. Tavernier, J., Devos, R., Cornelis, S., Tuypens, T., Van der Heyden, J., Fiers, W., and Plautinck, G. (1991) *Cell* **66**, 1175-1184.
55. Taga, T., Hibi, M., Hirata, Y., Yamasaki, K., Yasukawa, K., Matsuda, T., Hirano, T., and Kishimoto, T. (1989) *Cell* **58**, 573-581.
56. Masiati, J., and Spivak, J. L. (1979) *J. Clin. Invest.* **64**, 1573-1579.
57. Sayer, S. T., and Krantz, S. B. (1984) *J. Biol. Chem.* **259**, 2769-2774.
58. Mladenovic, J., and Kay, N. E. (1983) *J. Lab. Clin. Med.* **112**, 23-27.
59. Miller, B. A., Scaduto, R. C., Jr., Tillotson, D. L., Botti, J. J., and Cheung, J. Y. (1988) *J. Clin. Invest.* **82**, 309-315.
60. Imagawa, S., Smith, B. R., Palmer-Crocker, R., and Bunn, H. F. (1989) *Blood* **73**, 1452-1457.

## Evidence for specific binding and stimulatory effects of recombinant human erythropoietin on isolated adult rat Leydig cells

Roberto Mioni, Francesco Gottardello, Paola Bordon, Gianni Montini<sup>1</sup> and Carlo Foresta

*Institute of Medical Semiotics, Third Chair of Medical Pathology and Pediatric Department<sup>1</sup>, University of Padua, Padua, Italy*

Mioni R, Gottardello F, Bordon P, Montini G, Foresta C. Evidence for specific binding and stimulatory effects of recombinant human erythropoietin on isolated adult rat Leydig cells. *Acta Endocrinol* 1992;127:459-65. ISSN 0001-5598

The presence of specific binding of recombinant human erythropoietin and its effect on testosterone production were evaluated in isolated intact adult rat Leydig cells. Maximal specific binding was observed after 135 min incubation at 34°C. Scatchard analysis of the binding data revealed two distinct classes of binding sites for [<sup>125</sup>I]-recombinant human erythropoietin with dissociation constant of (Kd1)  $1.9 \times 10^{-10}$  mol/l and (Kd2)  $1.37 \times 10^{-8}$  mol/l respectively and binding capacity of (Bmax1) 12.3 fmol/10<sup>6</sup> cells and (Bmax2) 42.8 fmol/10<sup>6</sup> cells, respectively. GnRH, hCG, IGF-I and EGF did not induce any modification of recombinant human erythropoietin-specific binding. Recombinant human erythropoietin added to isolated adult rat Leydig cells exerted a stimulatory effect on testosterone production reaching its maximal effect at the dose of  $10^{-10}$  mol/l (testosterone production from  $14.9 \pm 1.7$  to  $45.1 \pm 6.2$  pmol/10<sup>6</sup> cells/3 h). Addition of anti-recombinant human erythropoietin serum completely blocked the recombinant human erythropoietin-stimulated testosterone production. These results show that purified adult rat Leydig cells possess recombinant human erythropoietin specific binding, and suggest that this glycoprotein directly influences rat Leydig steroidogenesis.

Carlo Foresta, Institute of Medical Semiotics, Third Chair of Medical Pathology, University of Padua, Via Ospedale Civile 105, 35128 Padova, Italy

Growth factors, a family of polypeptides with molecular weights of about 40 kD or less, are intimately involved in the regulation of growth, differentiation and development of mammalian cells. Most of these peptides exert their effects, by paracrine or endocrine mechanisms, activating specific cell surface receptors (1-5). Recent evidence suggests that several growth factors are involved in the regulation of testicular functions. In particular, it has been observed that, e.g., epidermal growth factors (EGF), insulin-like growth factor-I (IGF-I), transforming growth factor- $\beta$  (TGF- $\beta$ ), fibroblast growth factor (FGF) and insulin were able to influence Leydig steroidogenesis through the binding to specific plasma membrane receptors (6-10). Erythropoietin (EPO), a 34 kD glycoprotein hormone, principally secreted by the kidney, is an essential growth factor for normal erythropoiesis (11-15). It regulates the proliferation and terminal differentiation of pro-erythroblasts and their immediate precursors, the colony-forming unit erythroid cells (CFU-e), acting on specific receptors (15-17). Recently, it has been observed that the receptors of erythropoietin, EGF, IGF-I and interleukins 2, 3, 4 and 6 are homologous in their structural features, in accordance with the existence of a superfamily of growth factors (18, 19). To date, there are no clear physiological explanations for this receptor-structure homology, unless these factors may influence cellular functions activating a common signal transduction pathway. The aim of this study was

to investigate whether erythropoietin, as well as other growth factors (6-10), influences steroidogenesis in isolated adult rat Leydig cells and if this effect is mediated by specific receptors.

### Materials and methods

#### Materials

Medium-199 with Hanks' salts with L-glutamine, penicillin and streptomycin were obtained from the Grand Island Biological Co (Grand Island, NY); collagenase (type II), BSA (fraction V), HRPES, soybean trypsin inhibitor (type 1s), TRIS (hydroxymethyl)-amino-methan, and GnRH (Gly-6) were from Sigma (St Louis, MO); Percoll was from Pharmacia Fine Chemicals AB (Uppsala, Sweden); highly purified hCG (48600 UI/g) was from Serono (Rome, Italy); EGF (0.1 g/l) was from BioMacor (Rehovot, Israel); human recombinant IGF-I (0.1 g/l) was from Calbiochem (San Diego, CA). rHuEPO (10<sup>6</sup> U/l) was from Cilag GmbH (Aksbach-Hahnlein, Germany); human erythropoietin was produced by recombinant DNA technology and obtained by inoculation of isolated gene in mammalian cell cultures. The specific erythropoietin activity was approximately 110,000 U per mg of glycoprotein and determined by both in vitro and in vivo <sup>59</sup>Fe-uptake methods (20). High specific activity [<sup>125</sup>I]-labeled erythropoietin was



obtained from Amersham, UK (specific activity 3000–4000 Ci/mmol; 111–148 TBq/mmol). Rabbit anti-rHuEPO serum, which neutralized about 1.5 U of rHuEPO at a dilution of 1:200, was generously provided by Dr V. Ferrari (Department of Pediatrics, University of Padua, Padua, Italy).

#### Isolation and purification of Leydig cells

Adult male rats of the Sprague-Dawley strain (280–320 g) were used. Testicular interstitial cells were prepared through decapsulation and collagenase digestion. Briefly, 12–14 decapsulated testes were placed in sterile polyethylene vials (50 cm<sup>3</sup>) containing medium-199 (3 ml/testis) with Hanks' salts and L-glutamine, 0.2% BSA (fraction V), 1 g/l collagenase (type II), and shaken (90 cycles/min), in controlled atmosphere (pO<sub>2</sub> 95%–pCO<sub>2</sub> 5%) at 34°C. After 15–20 min, 15 ml of medium-199 was added to each vial and the suspension was filtered through sterile nylon gauze (mesh 0.5–0.8 mm) into a sterile 50 cm<sup>3</sup> centrifuge tube. Erythrocytes (about 75–85%) were removed by the addition of a Percoll cushion (5 ml of 60% v/v, in the bottom of each vial), followed by centrifugation for 10 min at 800 × g at 22°C. Cells, at the medium-199/Percoll 60% interface, were then carefully aspirated, rinsed twice in 5 ml of medium-199. After centrifugation at 100 × g for 10 min at 22°C, cells were resuspended in medium-199 to give approximately 40 × 10<sup>6</sup> cells/l. Purification of Leydig cells was obtained by layering 5 ml of crude interstitial cell suspension (20–25 × 10<sup>6</sup> cells/l) on top of each vial, containing a previously prepared discontinuous Percoll density gradient (20–60%), and then centrifuged at 800 × g for 20 min at room temperature. The fractions were collected from the bottom of the tubes with a peristaltic pump (minipuls-3 Gilson, Villiers, France), and then rinsed twice in isotonic medium-199 to remove any residual Percoll. Purified Leydig cells (85–92% staining positively for 3-β-OH-steroid-dehydrogenase activity (21)) were resuspended in medium-199. Cell concentration (about 1.0–1.2 × 10<sup>6</sup> Leydig cells/testis) and viability (over 90%) were determined using a hemocytometer and trypan blue method, respectively.

#### Measurement of radiolabeled erythropoietin binding to intact rat Leydig cell

Binding assays were performed with [<sup>125</sup>I]-rHuEPO in purified adult rat Leydig cell suspensions. Aliquots (0.25 ml) of Leydig cell suspension (1.0 × 10<sup>6</sup> cells/l) were incubated with 2.0 nmol/l [<sup>125</sup>I]-rHuEPO, with or without unlabeled rHuEPO, for various periods of time from 0 to 180 min and at different temperatures (4°C, 34°C). Both cells and rHuEPO were in binding buffer consisting of medium-199 with 25 mmol/l HEPES (pH 7.4) and 1% BSA (fraction V). For equilibrium studies, aliquots of purified intact adult Leydig cells (final concentration

1.0 × 10<sup>6</sup> cells/l) were incubated, at 34°C for 3 h, in sterile multi-well tissue culture dishes, with medium-199 added to a final volume of 0.25 ml. Each well containing an increasing concentration of [<sup>125</sup>I]-rHuEPO (2.7 pmol/l to 3.8 nmol/l, giving 28,000–1,800,000 cpm). Non-specific binding was measured in the presence of a 1000-fold molar excess of unlabeled rHuEPO. After incubation, cell suspensions were transferred to microcentrifuge tubes and washed twice with 2 ml of ice-cold Dulbecco's phosphate buffered saline with 1% BSA (PBS-1% BSA pH 8.0). After centrifugation at 800 × g for 5 min at 4°C, radioactivity was measured, both in the supernatant and in the pellet in a gamma-spectrometer for 120 sec. With the same experimental conditions, we determined the intracellular radioactivity in the cells both in binding and equilibrium studies: after incubation with [<sup>125</sup>I]-rHuEPO in the presence and absence of 1000-fold molar excess of unlabeled rHuEPO, each aliquot was rinsed twice in PBS-1% BSA (pH 7.4). Then, 2 ml of 50 mmol/l glycine-buffered saline (pH 3) were added for 2 min into all the tubes on ice to remove surface-bound rHuEPO. After washing twice in PBS-1% BSA, the cells were resuspended with 0.5 ml of medium-199 and centrifuged at 100 × g for 15 min at 4°C. Radioactivity was measured both in the supernatant and in the pellet, previously dissolved in 0.5 mmol/l NaOH. The bound radioactivity in microcentrifuge tube without cells was less than 0.3% of the total counts, added. Displacement studies were performed with rHuEPO and unrelated peptides (hCG, GnRH, RGF, IGF-I) at doses ranging from 10<sup>-10</sup> mol/l to 10<sup>-7</sup> mol/l.

#### Effects of rHuEPO on testosterone production

Aliquots (0.5 ml) of purified Leydig cell suspensions, prepared as described above (1.0 × 10<sup>6</sup> cells/l), were incubated in medium-199 with Hanks' salts, L-glutamine, TRIS, 0.1% BSA (fraction V), penicillin (10<sup>4</sup> U/l), streptomycin (1 g/l), at pH 7.4, in polyethylene sterile tubes containing rHuEPO, dissolved in medium-199, at doses ranging from 10<sup>-13</sup> to 10<sup>-9</sup> mol/l, in a shaking-rack (90 cycles/min) at 34°C for 3 h, in a controlled atmosphere (pO<sub>2</sub> 95%–pCO<sub>2</sub> 5%). To a different set of tubes, under the same experimental conditions, anti-rHuEPO serum was added. Furthermore, the effects of hCG on rHuEPO-stimulated testosterone production were evaluated, incubating two doses of hCG, 10<sup>3</sup> ng/l and 10<sup>4</sup> ng/l respectively, in different aliquots of Leydig cell suspension containing rHuEPO at the doses ranging from 2 · 10<sup>-12</sup> to 10<sup>-10</sup> mol/l, at the time and conditions reported above. After incubation, all the tubes were immersed in an ice-water bath (0°C) and then centrifuged at 1500 × g for 15 min at 4°C. Each supernatant was immediately stored at -20°C until hormone assay. Cell viability (over 90%) in the resuspended pellets from each tube was determined by the trypan blue method.



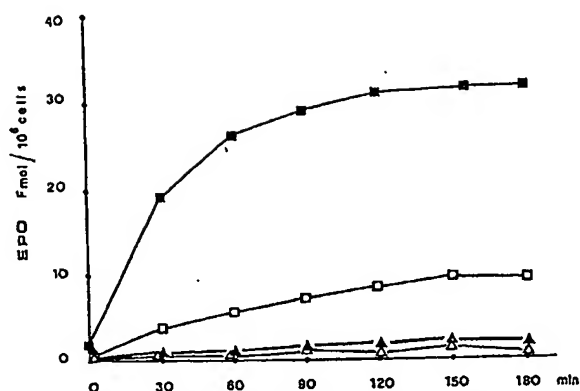


Fig. 1. The binding of [<sup>125</sup>I]-rHuEPO to intact adult rat Leydig cells was performed as a function of different times and temperatures (■ 34°C, □ 4°C). The intracellular radioactivity was measured (▲ 34°C, △ 4°C) after rinsing the cells in 50 mmol/l glycine-saline buffered (pH 3) and dissolving in 0.5 mmol/l of NaOH. The results represent the specific binding for each time interval, and correspond to the mean of three different experiments done in duplicate.

#### Hormone measurements

Testosterone production of Leydig cell incubations was measured by the RIA method as previously described (22). The sensitivity was estimated as 3.6 fmol/l and intra- and interassay coefficients of variation were 7.8% and 7.0% respectively.

#### Statistical analysis

For the analysis of binding and equilibrium data, each point was considered as the mean of three independent experiments, each done in duplicate. Scatchard analysis and displacement studies were performed using the EBDA and Ligand computer programs (23–24). For hormone production, results of three independent experiments were considered and expressed as mean ± SEM and analysed by Student's *t*-test for unpaired data.

#### Results

##### Binding study

The specific binding of [<sup>125</sup>I]-rHuEPO was considered as the difference between total counts in the pellet and the amount trapped in the pellet in the presence of a 1000-fold excess of unlabeled rHuEPO. Fig. 1 shows that [<sup>125</sup>I]-rHuEPO specifically binds, in a time- and temperature-dependent manner, to intact adult rat Leydig cells. Maximal specific binding was reached after 135 min of incubation at 34°C, maintaining a steady state up to 180 min. At 4°C maximal specific binding was observed after 165 min and reached only 20% of that obtained at 34°C.

Furthermore, the intracellular radioactivity, in the Leydig cells, was calculated at both 34° and 4°C. After glycine treatment the extracellular radioactivity was completely removed and no activity was found in the supernatant of resuspended cells (data not shown).

The saturation curves of [<sup>125</sup>I]-rHuEPO binding to rat Leydig cells and of its intracellular measurement are shown in Fig. 2. The incubation of Leydig cell suspensions with increasing concentration of [<sup>125</sup>I]-rHuEPO demonstrated the existence of a saturable binding. Furthermore, Scatchard analysis of these binding data revealed the existence of two classes of binding sites: (a) one with high affinity ( $K_{d1} = 1.9 \times 10^{-10}$  mol/l) and binding capacity ( $B_{max1}$ ) of 12.3 fmol/10<sup>6</sup> cells; (b) the other with low affinity ( $K_{d2} = 1.37 \times 10^{-8}$  mol/l) and binding capacity ( $B_{max2}$ ) of 42.8 fmol/10<sup>6</sup> cells respectively (Fig. 3). Displacement study of [<sup>125</sup>I]-rHuEPO, obtained with incubation of unrelated peptides (hCG, GnRH, EGF and IGF-I), did not evidence any effect on the specific rHuEPO binding to intact rat Leydig cells (Fig. 4).

##### Hormonal production

rHuEPO influenced testicular steroidogenesis, inducing a stimulatory effect on testosterone production in isolated adult rat Leydig cells. Fig. 5 shows the effect of increasing doses of rHuEPO on Leydig cell steroidogenesis. This glycoprotein begins to stimulate testosterone production at the dose of  $10^{-11}$  mol/l and produces its maximal effect at  $10^{-10}$  mol/l, maintaining a steady state up to  $10^{-9}$  mol/l. When rHuEPO was incubated

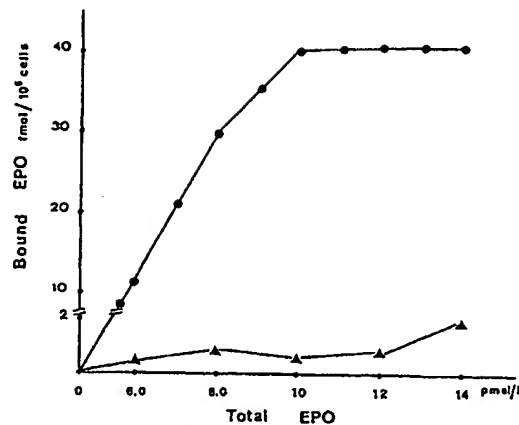


Fig. 2. Intact rat Leydig cells were incubated with increasing concentrations of [ $^{125}$ I]-rHuEPO (●). The intracellular radioactivity was also determined (▲). These curves are obtained with the mean of three different experiments done in duplicate. Non-specific binding for each concentration was determined by the addition of 1000-fold excess of unlabeled hormone.

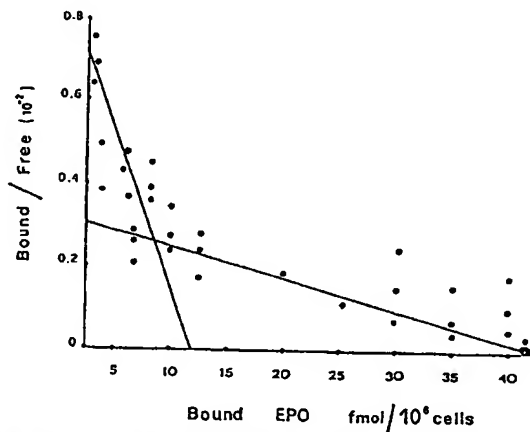


Fig. 3. Scatchard analysis of the specific binding of [ $^{125}$ I]-rHuEPO to purified adult rat Leydig cells is shown. Two specific binding sites are observed:  $Kd1 = 1.9 \times 10^{-10}$  mol/l, with about 1800 sites/cell, and  $Kd2 = 1.37 \times 10^{-8}$  mol/l, with about 6400 sites/cell. The points summarized three independent experiments, each done in duplicate. Increased amounts of radiolabeled rHuEPO were added to the cells with or without an excess of unlabeled rHuEPO for each point.

with its neutralizing antiserum, rHuEPO-stimulated testosterone production was completely blocked. The stimulatory effect of the different doses of rHuEPO on Leydig cell steroidogenesis was significantly enhanced when hCG was added in the medium at low ( $10^3$  ng/l) and higher ( $10^4$  ng/l) concentrations (Fig. 6).

#### Discussion

Our data show that rHuEPO specifically binds to intact rat Leydig cells and exerts a stimulatory effect on testosterone production. The amount of this binding is influenced by the temperature, reaching the highest values at  $34^\circ\text{C}$ , as well as for hCG and other hormones

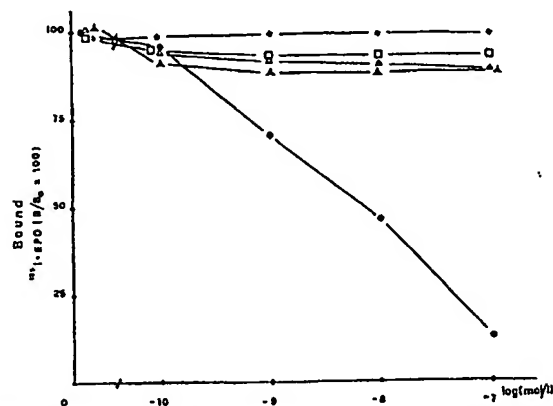


Fig. 4. Displacement study was performed in Leydig cells, incubating at 34°C for 3 h [ $^{125}$ I]-rHuEPO, at the dose of 1.0 nmol/l, with increasing concentrations of unlabeled rHuEPO ( $\bullet$ ), GnRH ( $\blacktriangle$ ), hCG ( $\triangle$ ), IGF-I ( $\square$ ) and BGF ( $\nabla$ ) respectively. Each point represents the mean of three experiments.

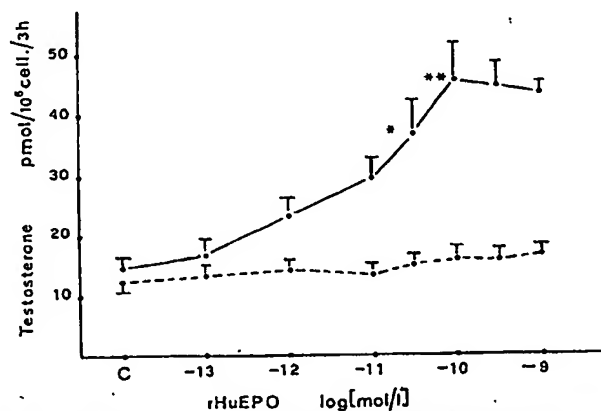


Fig. 5. The effects of rHuEPO on testosterone production in purified adult rat Leydig cells is summarized. Increasing concentrations of rHuEPO were incubated at 34°C for 3 h. In the same experimental conditions, through the addition of anti-rHuEPO serum (Ab-rHuEPO dashed line; for dilution see Materials and Methods), the stimulatory effect of rHuEPO on testosterone production was completely blocked. Statistical differences were: \* $p < 0.05$  versus control; \*\* $p < 0.01$  versus control.

(25, 27). At high temperature, rHuEPO may be internalized, resulting in an overestimation of cell surface binding; however, the low measurement of the internalized [ $^{125}$ I]-rHuEPO (rate of internalization  $< 0.05$  fmol/ $10^6$  cells/min at 34°C) excludes this possibility.

The Scatchard analysis of [ $^{125}$ I]-rHuEPO binding to intact rat Leydig cells revealed two classes of binding

sites, with respectively: (a) high affinity ( $Kd1 = 190$  pmol/l) and binding capacity of 12.3 fmol/ $10^6$  cells and (b) low affinity ( $Kd2 = 13.7$  nmol/l) and binding capacity of 42.8 fmol/ $10^6$  cells. These binding data can be compared with those obtained by several authors in other cellular systems (28–31). In particular, it has been observed that erythropoietin exerts its effects on spleen

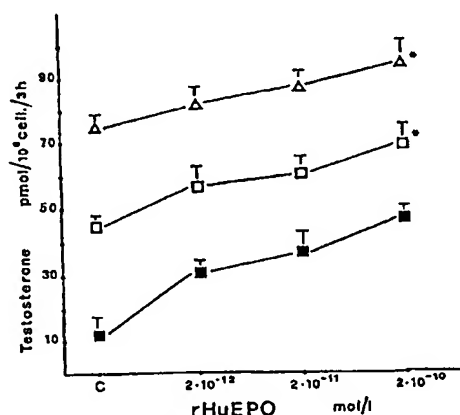


Fig. 6. The effects of M-199 (■) and hCG, at doses of  $10^{-6}$  ng/l (□) and  $10^{-8}$  ng/l (Δ) respectively, on testosterone production stimulated by increasing doses of rHuEPO in isolated Leydig cells. M-199 and hCG were added to each tube at zero time. Statistical differences were considered between each dose of hCG with rHuEPO and control. \* $p < 0.05$ .

and liver erythroid progenitor cells, through the activation of specific binding of comparable affinities ( $K_d < \text{nmol}$  range) to those observed in our study, suggesting an involvement of similar receptors (32–34). Recent observations have shown that some growth factors, rHuEPO included, possess a common binding domain (18, 19, 35); therefore, a cross-linking reaction of rHuEPO with these receptors may exist (36–39). However, our displacement study with several unrelated peptides, such as hCG, GnRH, EGF and IGF-I, suggests the specificity of rHuEPO binding to rat Leydig cells. In accordance with this observation, rHuEPO did not induce any stimulatory effect on rat Leydig cells, in the presence of rHuEPO-antisera. Our present data show that rHuEPO was able to stimulate rat Leydig cell testosterone production. The stimulatory activity of this glycoprotein is dose-related up to  $10^{-11}$  mol/l, reaching a steady state at higher doses. The most effective rHuEPO concentrations were comparable to those observed in rat plasma levels during pharmacokinetic studies of a single iv bolus of 30–60 U/kg of rHuEPO (40, 41). The maximal stimulatory effect, observed at low doses (under  $10^{-11}$  mol/l), may be due to the activation of a partial fraction of the total specific receptor sites. In fact, in adult rat Leydig cells, this phenomenon is well known with other physiologic agonists, as well as LH or hCG, that are able to reach the maximal stimulatory effect binding only 1% of their specific receptors (21, 42).

In the presence of hCG, rHuEPO still exerts a stimula-

tory effect on testosterone production, suggesting that this hormone influences rat Leydig cell steroidogenesis without interfering with hCG-activated receptor systems and involving different post-receptor mechanisms. A direct stimulatory effect of testosterone on colony forming units-erythroid cells has been demonstrated and several clinical studies have shown that androgens have been commonly used in the treatment of various hemopoietic disorders (43, 44). Our results suggest that erythropoietin may influence hemopoiesis, also involving the most important endogenous source of androgen production in the male, the testis. This hypothesis is further supported by recent data showing that in male patients undergoing chronic hemodialysis the treatment with recombinant human erythropoietin improved sexual function and increased basal plasma testosterone levels (45, 46). These observations have justified emphasizing the normalization of the high plasma PRL levels or with the improvement of anemia (47, 48). However, in view of our data, a direct rHuEPO effect on testicular functions cannot be ruled out.

In conclusion, our study shows that rHuEPO influences rat Leydig steroidogenesis by stimulating testosterone production through a direct specific receptor mechanism and suggests a possible linkage between the erythropoietic system and testicular function.

## References

- Burges AW. Epidermal growth factors and transforming growth factors- $\alpha$ . *Br Med Bull* 1989;45:401–24.
- Dudgeon TJ, Baron M, Cooke RM, Campbell ID, Edwards RM, Fallow A. Structure and function of hEGF: receptor binding and NMR. *FEBS Lett* 1990;261:392–6.
- Campbell ID, Cooke RM. Structure function relationships in EGF, TGF- $\alpha$  and IGF-I. *J Cell Sci* 1990;(Suppl 13):5–10.
- Wakefield L. Growth factors: an overview. In: Iddori A, Fabbri A, Dufau ML, eds. *Hormonal communicating events in the testis*. New York: Raven Press, 1990;70:181–90.
- Walsh JH, Karnes WF, Cuttitta F, Walker A. Autocrine growth factors and solid tumor malignancy. *West J Med* 1991;155:152–60.
- Bartlett JMS, Spiteri-Grech J, Nieschlag E. Regulation of insulin-like growth factor-I and stage specific levels of epidermal growth factor in stage synchronized rat testes. *Endocrinology* 1990;127:747–58.
- Bellè A, Zheng W. Growth factors as autocrine and paracrine modulators of male gonadal function. *J Reprod Fertil* 85/2:1989:771–93.
- Foresta C, Caretto A, Varotto A, Rossato M, Scandellari C. Epidermal growth factor receptors (EGFR) localisation in human testis. *Arch Androl* 1991;27:17–21.
- Morera AM, Chauvin MA, Felge JJ, Guillaumont P, Keramidas M, Mauduit C, et al. Interaction between systemic hormones and local growth factors in the control of the testis function: the example of gonadotropins and transforming growth factor- $\beta$ . In: Iddori A, Fabbri A, Dufau ML, eds. *Hormonal communicating events in the testis*. New York: Raven Press, 1990;70:191–202.
- Sordollet C, Chauvin MA, Revol A, Morera AM, Benahmed M. Fibroblast growth factor is a regulator of testosterone secretion in cultured immature Leydig cells. *Mol Cell Endocrinol* 1989;58:283–6.
- Ishibashi T, Koziol JA, Burstein SA. Human recombinant erythro-

- poietin promotes differentiation of murine megakaryocytes in vitro. *J Clin Invest* 1987;79:286-93
12. Berridge MV, Fraser JK, Carter JM, Lin FK. Effect of recombinant human erythropoietin on megakaryocytes and on platelet production in the rat. *Blood* 1988;73:970-7
  13. Krantz SB. Erythropoietin. *Blood* 1990;77:419-34
  14. Fukamachi H, Saito T, Tojo A, Kitamura T, Urabe A, Takaku F. Binding of erythropoietin to CFU-e derived from fetal liver cells. *Exp Hematology* 1987;15:833-7
  15. D'Andrea AD, Zon LI. Erythropoietin receptor. *J Clin Invest* 1990;86:681-7
  16. Graber SE, Krantz SB. Erythropoietin and the control of red blood cell production. *Annu Rev Med* 1978;29:51-66
  17. Goldwasser E, Krantz SB, Wang FF. Erythropoietin and erythroid differentiation. In: Ford RJ, Maizel AL, eds. *Mediators in cell growth and differentiation*. New York: Raven Press, 1985:103-18
  18. D'Andrea AD, Fasman G, Lodish HF. Erythropoietin receptor and interleukin-2 receptor  $\beta$ -chain: a new receptor family. *Cell* 1989;58:1023-4
  19. Bazan JP. A novel family of growth factor receptors. *Biochem Biophys Res Commun* 1989;164:788-95
  20. Egrie JC, Strickland TW, Lane J, Aoki K, Cohen AM, Smalling R. Characterization and biological effects of recombinant human erythropoietin. *Immunobiol* 1986;172:213-24
  21. Mendelson C, Dufau ML, Catt KJ. Gonadotropin binding and stimulation of cyclic adenosine 3',5'-monophosphate and testosterone production in isolated Leydig cells. *J Biol Chem* 1975;250:8818-23
  22. Foresta C, Russa G, Rizzotti A, Lembo A, Valente ML. Mastroglioma I. Varicocele and infertility. *J Androl* 1984;5:135-7
  23. Munson FJ, Rodbard D. Ligand: a versatile computerized approach for characterization of ligand-binding systems. *Anal Biochem* 1980;107:220-39
  24. McPherson GA. A practical computer-based approach to the analysis of radioligand binding experiments. *Comput Programs Biomed* 1983;17:107-13
  25. Schwars S, Krude H, Nelboeck E, Berger P, Mers WB, Wick G. Relationship of orientation with affinity and activity of receptor-bound glycosylation of human chorionic gonadotropin (hCG) as visualized by monoclonal antibodies (MCA). *J Receptor Res* 1991;11:437-58
  26. Habib FK, Maddy QS, Gelly KJ. Characterisation of receptors for 1,25-dihydroxyvitamin D<sub>3</sub> in the human testis. *J Steroid Biochem* 1990;35:195-9
  27. Ullisse S, Fabbri A, Dufau ML. Corticotropin-releasing factor receptors and actions in rat Leydig cells. *J Biol Chem* 1989;264:2156-63
  28. Sawyer ST, Krantz SB, Luna J. Identification of the receptor for erythropoietin by cross-linking to Friend virus-infected erythroid cells. *Biochemistry* 1987;84:3690-4
  29. Todokoro K, Kanazawa S, Amanuma H, Ikawa Y. Specific binding of erythropoietin to its receptor on responsive mouse erythroleukemia cells. *Proc Natl Acad Sci USA* 1987;84:4126-30
  30. Weiss TL, Barker ME, Sellock SE, Wintoub BV. Erythropoietin binding and induced differentiation of Rauscher erythroleukemia cell line red. *J Biol Chem* 1989;264:1804-10
  31. Fraser JK, Tam AS, Lin FR, Berridge MV. Expression and specific high-affinity binding sites for erythropoietin on rat and mouse megakaryocytes. *Exp Hematol* 1989;17:10-16
  32. Kolke K, Shimizu T, Miyake T, Ihle JN, Ogawa M. Hemopoietic colony formation by mouse spleen cells in serum free culture supported by purified erythropoietin and for interleukine-3. In: Levine RP, William N, Levine J, Svatt BL, eds. *Megakaryocyte development and function*. New York: Liss, 1986:33-49
  33. Sawada K, Krantz SB, Kans JS, Desypris EN, Sawyer S, Glick AD, et al. Purification of human erythroid colony-forming units and demonstration of specific binding of erythropoietin. *J Clin Invest* 1987;80:357-66
  34. Tojo A, Fukamachi H, Kasuga M, Urabe A, Takaku F. Identification of erythropoietin receptors on fetal liver erythroid cell. *Biochem Biophys Res Commun* 1987;148:443-8
  35. Rothwell N. The endocrine significance of cytokines. *J Endocrinol* 1991;128:171-3
  36. Verhoeven G, Cailleau J. Stimulatory effects of epidermal growth factor on steroidogenesis in Leydig cells. *Mol Cell Endocrinol* 1986;47:99-106
  37. Lin T, Haskell J, Vinson N, Terracio L. Direct stimulatory effects of insulin-like growth factor-I on Leydig cell steroidogenesis in primary culture. *Biochem Biophys Res Commun* 1986;137:950-6
  38. Guo H, Calkins JH, Sigel MH, Lin T. Interleukin-2 is a potent inhibitor of Leydig cell steroidogenesis. *Endocrinology* 1990;127:1234-9
  39. Moore C, Moger WH. Interleukin-1 $\alpha$  induces changes in androgen and cyclic adenosine 3',5'-monophosphate release in adult rat Leydig cells in culture. *J Endocrinol* 1991;129:381-90
  40. Emmanouel DS, Goldwasser E, Katz AL. Metabolism of pure human erythropoietin in the rats. *Am J Physiol* 1984;247:168-76
  41. Ohishi N. Pharmacokinetics of recombinant human erythropoietin in rats. II. Intern ISSX Meet, Kyoto, Japan 1988. Abstract b58
  42. Huhtaniemi IT, Clayton RN, Catt KJ. Gonadotropin binding and Leydig cell activation in the rat testis in vivo. *Endocrinology* 1982;111:982-7
  43. Thomsen K, Riis B, Krabbe S, Christiansen C. Testosterone regulates the hemoglobin concentration in male puberty. *Acta Paediatr Scand* 1986;75:793-6
  44. Claustres M, Sultan C. Stimulatory effects of androgens on normal children's bone marrow in culture: effects on BFU-e, CFU-e and uroporphyrinogen-I synthase activity. *Hormon Res* 1986;23:91-8
  45. Haley NR, Matsumoto AM, Eschbach JW, Adamson JW. Low testosterone (T) levels increase in male hemodialysis patients (HDP) treated with recombinant human erythropoietin (rHuEPO). *Kidney Intern* 1989;35:Abstract 194
  46. Kokot F, Wiecek A, Grzeszczak W, Klepacka J, Klin M, Lao M. Influence of erythropoietin treatment on endocrine abnormalities in haemodialyzed patients. In: Beldamius CA, Scigalla P, Wiecek L, Koch KM, eds. *Erythropoietin: from molecular structure to clinical application*. 1989;76:257-72
  47. Schaeffer RM, Kokot F, Wernze H, Geiger H, Heidland A. Improved sexual function in hemodialysis patients on recombinant erythropoietin: a possible role for prolactin. *Clin Nephrol* 1989;31:1-5
  48. Bommer J, Kugel M, Schwobel B, Riis B, Barth HP, Seeling R. Improved sexual function during recombinant human erythropoietin therapy. *Nephrol Dial Transplant* 1990;5:204-7

Received January 16th, 1992  
Accepted July 17th, 1992

Akihiko Okada  
Yoshikazu Kinoshita  
Toru Maekawa  
Md. Sazzad Hassan  
Chiharu Kawanami  
Masakyo Asahara  
Yumi Matsushima  
Kiyohiko Kishi  
Hirohisa Nakata  
Yoko Naribayashi  
Tsutomu Chiba

Division of Gerontology, Department of  
Medicine, Kobe University School of  
Medicine, Kobe, Japan

#### Key Words

Erythropoietin  
Gastric mucosal lesion  
RGM-1 cells  
Gastric mucosal cell growth

## Erythropoietin Stimulates Proliferation of Rat-Cultured Gastric Mucosal Cells

#### Abstract

Most anemic patients with chronic renal failure have gastric mucosal lesions. However, these gastric lesions are often improved after the administration of recombinant human erythropoietin (rHuEPO). We have used the rat gastric mucosal cell line RGM-1, to examine the possibility that rHuEPO might directly stimulate the growth of gastric mucosal cells in vitro. Our results show that rHuEPO dose-dependently increased [ $^3\text{H}$ ]thymidine incorporation into RGM-1 cells and their expression of c-myc gene. In addition,  $^{125}\text{I}$ -rHuEPO, specifically bound to RGM-1 cells, and moreover, erythropoietin receptor gene expression was detected by RT-PCR. We conclude that rHuEPO has a direct growth-promoting effect on RGM-1 cells, suggesting possible usefulness of rHuEPO administration for the treatment of gastric mucosal damage in patients with chronic renal failure.

#### Introduction

Erythropoietin is the major regulatory factor of erythropoiesis, and it is well known that erythropoietin production in the cortical peritubular cells of the kidney is impaired in patients with chronic renal failure with resulting anemia [1]. Recently, recombinant human erythropoietin (rHuEPO) has been widely used for the treatment of anemia in these patients. On the other hand, many patients with chronic renal failure have also been reported to have erosive lesions of the gastric mucosa which may cause gastrointestinal bleeding [2]. Interestingly, a remarkable improvement in these lesions by the administration of rHuEPO has recently been reported [3, 4]. Recovery from anemia may restore the oxygen supply to the gastric mucosa, and help to heal the gastric mucosal lesions. However, it is not known whether erythropoietin has a direct stimulatory effect on the healing of gastric mucosal lesions. Therefore, the present study is designed

to test the hypothesis that erythropoietin has a direct growth-promoting effect on the gastric mucosal epithelial cells. For this purpose, we have used the recently established normal rat gastric mucosal cell line RGM-1 [5] as a model of gastric epithelial cells.

#### Materials and Methods

##### Cells and Cell Culture

The rat gastric mucosal cell line RGM-1 [5] was grown in DMEM/Ham F-12 containing 100 U/ml penicillin, 100  $\mu\text{g}/\text{ml}$  streptomycin and 20% fetal calf serum (FCS) and subcultured every 3 days. The erythroid cell line TSA8 (a gift from Prof. Sasaki, Department of Food Science and Technology, Kyoto University, Kyoto, Japan) [6], was cultured in RPMI 1640 containing 100 U/ml penicillin, 100  $\mu\text{g}/\text{ml}$  streptomycin and 10% FCS.

##### Binding Studies

$^{125}\text{I}$ -rHuEPO cell-binding experiments were done according to the method of Masuda et al. [6], with minor modifications. The rHuEPO was a gift from Chugai Pharmaceutical Co. Ltd. (Tokyo,

#### KARGER

E-Mail: karger@karger.ch  
Fax: +41 61 306 12 34  
http://www.karger.ch

© 1996 S. Karger AG, Basel  
0012-2823/96/0575-0328\$10.00/0

This article is also accessible online at  
http://BioMedNet.com/

Tsutomu Chiba, MD, PhD  
Division of Gerontology, Department of Medicine  
Kobe University School of Medicine  
7-5-2 Kusunoki-cho, Chuo-ku  
Kobe 650 (Japan)

Received:  
November 8, 1995  
Accepted:  
January 16, 1996

Japan). In brief, dispersed RGM-1 or TSA8 cells ( $5 \times 10^4$ /tube) were incubated in 200  $\mu$ l phosphate-buffered saline (PBS) containing 20 mM HEPES (pH 7.4), 0.1% FCS, and 0.1% NaN<sub>3</sub> with <sup>125</sup>I-rHuEPO (111–148 TBq/mmol; Amersham, UK) in the presence or absence of unlabeled rHuEPO (50 U/tube) at 15°C. After 3 h, the cells were washed once with ice-cold PBS and resuspended in 200  $\mu$ l of PBS. The suspension was immediately layered onto 800  $\mu$ l of cushion buffer (PBS containing 10% FCS), and the cells were separated from the unbound ligand by centrifugation. The tube contents were snap-frozen in solid CO<sub>2</sub> ethanol, and the tip of the tube was cut off just above the cell pellet, and the radioactivity bound to the cells was counted. Nonspecific binding was assessed as the fraction of label that remained bound in the presence of an excess amount of unlabeled rHuEPO (50 U/tube). All calculations were performed using a SAS statistical analyzing system (SAS Institute Inc., Tokyo, Japan).

#### Measurement of DNA Synthesis

The mitogenic effect of rHuEPO was determined by measuring the incorporation of [<sup>3</sup>H]thymidine (Amersham) into the DNA of RGM-1 cells as previously described [7]. Subconfluent RGM-1 cells were rendered quiescent by serum deprivation for 6 h. The quiescent cells were exposed to various concentrations (0–8 U/ml) of rHuEPO in DMEM for 24 h. [<sup>3</sup>H]thymidine (8  $\mu$ Ci/tube) was then added and the cells were incubated for a further 4 h. The incubation was terminated by removing the medium and, after washing the cells 3 times in ice-cold PBS, 6% trichloroacetic acid (TCA) was added. TCA-precipitable [<sup>3</sup>H]thymidine, which had been incorporated into the DNA, was measured using a liquid scintillation counter.

#### Northern Blot Analysis

Northern blot analysis was used to investigate the expression of c-myc or erythropoietin-receptor (EPO-R) mRNA in RGM-1 cells. The total RNAs were obtained from RGM-1 cells by extraction with guanidine thiocyanate (GTC), followed by cesium chloride centrifugation as described previously [8]. The total RNAs were separated by electrophoresis on 0.66 M formaldehyde-1% agarose gel containing 0.4 M 3-(n-monomorpho)propane sulfate, 0.1 M sodium acetate and 0.02 M ethylenediaminetetraacetic acid (EDTA). The nucleic acid was transferred to nitrocellulose membranes (Schleicher & Schüll, Dassel, Germany) and fixed using ultraviolet (UV) cross-linking. The mouse EPO-R cDNA probe, used for the Northern blot analysis, was obtained by RT-PCR using the synthetic oligonucleotide primers; 5'-CAGTGAGCATGCCAGG-3' and 5'-GGGTCCAGGATGGTGTGTA-3' to amplify the total mRNA extracted from fetal mouse liver. The primers were designed to amplify a section of the EPO-R cDNA within its open reading frame (nucleotides 1122–1334) [9]. The 213-bp PCR product was cloned into a pCR-II plasmid vector using a TA cloning kit (Invitrogen, San Diego, Calif., USA). The plasmid was digested with EcoRI, and the <sup>32</sup>P-radiolabeled DNA probe was synthesized using a random prime labeling kit (Boehringer-Mannheim, Germany). The nucleotide sequence of the probe was found to be identical to that reported for the EPO-R cDNA [10] using a Sequence Version 2.0, DNA sequencing kit (United States Biochemical, Cleveland, Ohio, USA). The human c-myc DNA probe (467 bp) was purchased from Takara Shuzo, Japan. Hybridization was carried out at 42°C for 16 h and filters were washed twice for 20 min each at 53°C in 0.1 × SSC/0.1% sodium dodecyl sulfate (SDS) as described previously [11]. The signal intensity was quantified with a bioimaging analyzer model BAS2000 (Fujix, Tokyo, Japan) [12].

#### RT-PCR

Five micrograms of total RNA extracted from the rat fetal liver and the RGM-1 cells were used to synthesize a first-strand cDNA by a superscript amplification system (Bethesda Research Laboratories Inc., Md., USA). The first-strand cDNA was then amplified by the PCR method with a set of primers synthesized according to the sequence of rat EPO-R. The primers used were 5'-CAGTGAGCGGGCCAGG-3' and 5'-GGGTCCAGGATGGTGTGTA-3' with resulting amplification of 213 bp DNA fragment.

#### Statistical Analysis

Statistical analysis was carried out using the analysis of variance followed by Dunnett's t test. All the values are expressed as the mean  $\pm$  SEM. Differences between groups were considered statistically significant for p values of <0.05.

## Results

#### Binding Studies

Although total binding of <sup>125</sup>I-rHuEPO to the RGM-1 cells was small and its nonspecific binding was relatively high, it was clear that a small amount of <sup>125</sup>I-rHuEPO specifically bound to the RGM-1 cells (fig. 1). This binding datum was in a sharp contrast to the large specific binding of <sup>125</sup>I-rHuEPO to the TSA8 erythroid cells, which possess a large amount of EPO-R [6]. Thus, RGM-1 cells appear to possess a small number of specific binding sites for erythropoietin.

#### Effect of rHuEPO on DNA Synthesis

In quiescent RGM-1 cells, the basal level of [<sup>3</sup>H]thymidine incorporation into DNA was  $11,587 \pm 562$  cpm/ $10^5$  cells. The addition of rHuEPO (1–8 U/ml) caused a dose-dependent and significant increase of [<sup>3</sup>H]thymidine incorporation into RGM-1 cells, the effect was maximal at 8 U/ml erythropoietin ( $p < 0.05$ ) (fig. 2). Further increase of [<sup>3</sup>H]thymidine incorporation was not observed even at higher concentrations. Similar to rHuEPO, the addition of FCS (final concentration 20%), a positive control, also increased [<sup>3</sup>H]thymidine incorporation into RGM-1 cells ( $21,242 \pm 532$  cpm/ $10^5$  cells).

#### Effect of rHuEPO on c-myc Gene Expression

In immediate early response genes, c-myc gene expression is reported not to be restricted to a brief period at the G<sub>0</sub>-G<sub>1</sub> transition but to be continuously expressed in proliferating cells in a cell-cycle-independent manner [13]. Therefore, as a marker of cell proliferation, c-myc gene expression was checked. Northern blot analysis demonstrated that c-myc gene expression in RGM-1 cells was greatly increased by rHuEPO administration in a dose-



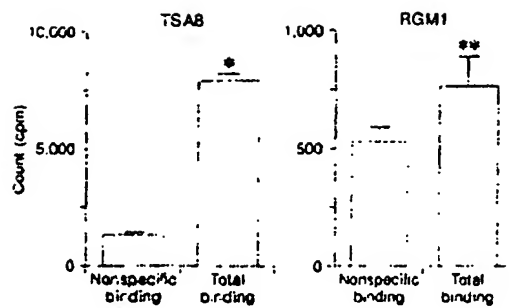


**Fig. 1.** The binding of <sup>125</sup>I-rHuEPO to TSA8 and RGM-1 cells. The radioactivity bound to the cells was counted after 3 h incubation at 15°C as described in the Materials and Methods section. Values are expressed as the mean  $\pm$  SEM of quadruplicate assays. Nonspecific binding was assessed as the fraction of label that remained bound in the presence of an excess amount of unlabeled rHuEPO (50 U/tube). \*  $p < 0.01$  for nonspecific binding vs. total binding in TSA8 cells. \*\*  $p < 0.05$  for nonspecific binding vs. total binding in RGM-1 cells.

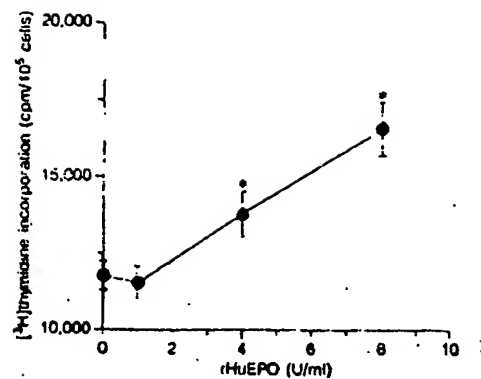


**Fig. 2.** The effect of rHuEPO on [<sup>3</sup>H]thymidine incorporation into RGM-1 cells. [<sup>3</sup>H]thymidine incorporation was measured as described in the Materials and Methods section. Values are expressed as the mean  $\pm$  SEM of 6 separate experiments. \*  $p < 0.05$  for rHuEPO-mediated incorporation vs. the basal level.

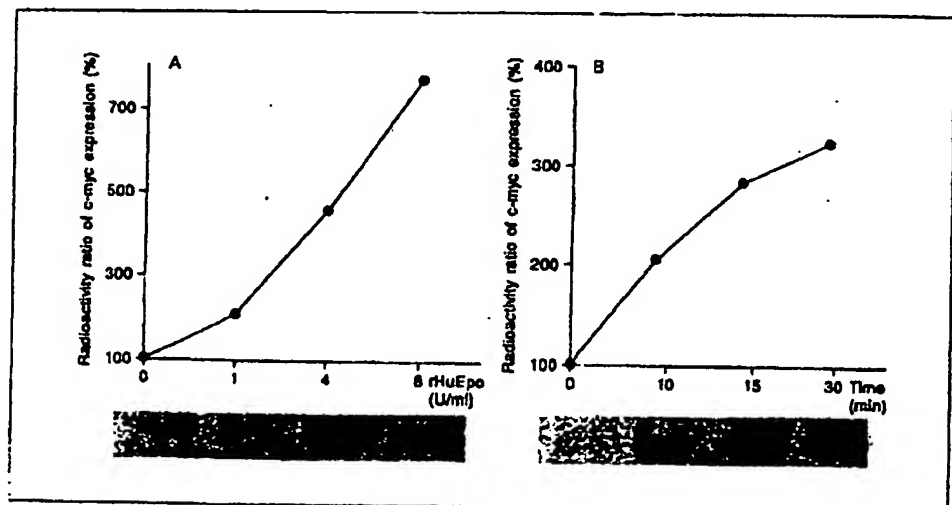


**Fig. 3.** The effect of rHuEPO on c-myc gene expression in RGM-1 cells. **A** Quiescent RGM-1 cells were treated with various concentrations (0–8 U/ml) of rHuEPO or FCS (final concentrations 20%) for 1 h. **B** Quiescent RGM-1 cells were treated with 8 U/ml rHuEPO for the periods indicated. Total cellular RNA (20  $\mu$ g/lane) was isolated and hybridized with the <sup>32</sup>P-labeled c-myc cDNA probe. The signal intensity of the c-myc gene expression was quantified using a bioimaging analyzer model BAS2000 (Fujix, Tokyo, Japan). Values are expressed as the percentage of radioactivity in unstimulated condition. In FCS-stimulated RGM-1 cells, tenfold increase of c-myc gene expression was observed (data not shown).

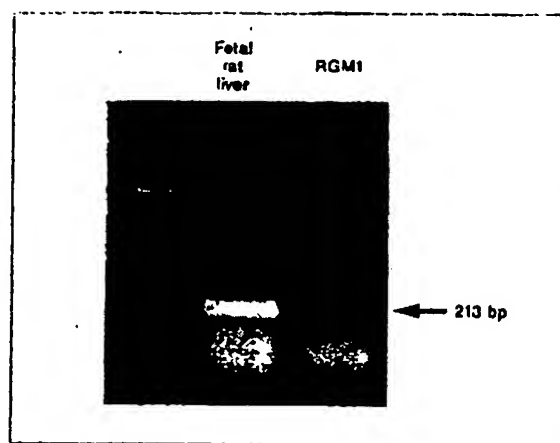
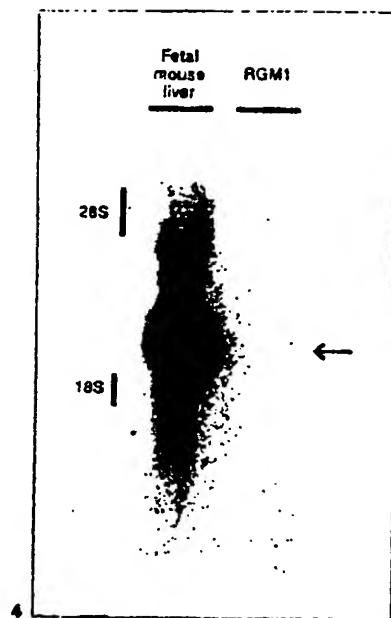


Fig. 4. Northern blot analyses of EPO-R mRNA. Total RNA (20 µg/lane) from RGM-1 and mouse liver cells was isolated, and hybridized with the <sup>32</sup>P-labeled mouse EPO-R cDNA probe. The arrow indicates the signal for EPO-R mRNA.

Fig. 5. RT-PCR detection of EPO-R mRNA. 213 bp EPO-R cDNA was amplified not only in fetal rat liver but also in RGM-1 cells.

dependent fashion (1–8 U/ml) (fig. 3A). As early as 15 min after the addition of 8 U/ml rHuEPO, there was a rapid increase in c-myc gene expression, and this increase was maximal after 30 min (fig. 3B). In contrast, erythropoietin did not stimulate c-myc gene expression of rat fibroblastic cells which lack EPO-R (data not shown).

#### EPO-R mRNA Expression in RGM-1 Cells

Although mouse fetal liver expressed considerable amounts of EPO-R mRNA, we failed to detect any transcripts of this gene in RGM-1 cells by the Northern blot analysis (fig. 4). The more sensitive RT-PCR method, however, clearly demonstrated the presence of EPO-R mRNA in RGM-1 rat gastric epithelial cells (fig. 5). These results indicated that the RGM-1 cells have weak but detectable gene expression of EPO-R.

#### Discussion

Erythropoietin has been believed to act only on the progenitor cells of erythrocytes, and to regulate their proliferation and differentiation through the interaction with its receptor [1]. Recently, it has also been shown to stimulate the proliferation of nonerythroid cells [7, 14]. Eryth-

ropoietin has a chemotactic and mitogenic effect on endothelial cells [15], and it increases both the immunoglobulin production by B lymphocytes and their proliferation [16]. Although the physiological significance of these findings is not known, evidence for the action of erythropoietin on nonerythroid cells may provide us with an opportunity to find a novel physiological role for this protein.

Our results demonstrate for the first time that rHuEPO has direct growth-promoting activity on rat gastric mucosal cell line RGM-1. rHuEPO dose-dependently increased DNA synthesis and c-myc gene expression in RGM-1 cells. We also found that, in addition to mouse TSA8 erythroid cells, <sup>125</sup>I-rHuEPO specifically bound to RGM-1 cells. These data suggest that rHuEPO exerts its effect on RGM-1 cells through its specific binding sites.

It is well known that patients with chronic renal failure often develop gastric mucosal lesions [2]. There are several reasons why gastric mucosal lesions may develop in patients with chronic renal failure. It has been shown that the permeability of the gastric mucosa to H<sup>+</sup> ions is increased in uremic rats [17]. Moreover, gastric mucosal blood flow as well as mucosal hexosamine content appear to be decreased in rats with renal failure [18]. rHuEPO has recently become available for the treatment of anemia in patients with chronic renal failure. Interestingly, it has

been shown that gastric mucosal lesions in those patients were greatly improved after administration of rHuEPO [3, 4]. It might be considered that rHuEPO acts indirectly to promote gastric mucosal healing by restoring the oxygen supply to this tissue in patients with chronic renal failure. However, our data clearly show that rHuEPO has a growth-promoting effect on RGM-1 cells. This lends support to the idea that rHuEPO may act directly to enhance the growth of gastric mucosal cells in patients with chronic renal failure, resulting in repair of the gastric mucosal damage.

In addition to the presence of specific binding sites for <sup>125</sup>I-rHuEPO and growth-promoting activity of rHuEPO, we detected weak but distinct gene expression of EPO-R mRNA in RGM-1 cells. Therefore, rHuEPO may have exerted its growth-promoting effect on RGM-1 cells through its receptor whose cDNA has recently been cloned [10]. An alternative explanation might be that rHuEPO cross-reacted with other cytokine receptors on

the RGM-1 cells. It is known that erythropoietin induces tyrosine phosphorylation in the  $\beta$  chain of the granulocyte-macrophage colony-stimulating factor [19].

Although the growth-promoting activity of erythropoietin on gastric mucosal cells in vitro may not be physiologically relevant because its plasma concentration in vivo is very low [20], the present study emphasizes the possible usefulness of erythropoietin administration for the treatment of gastric mucosal damage in patients with chronic renal failure.

#### Acknowledgements

This study was supported in part by Grants-in-Aid for Scientific Research from the Ministry of Education, Science and Culture, and the Ministry of Health and Welfare, Japan. We wish to thank Prof. Sasaki, Department of Food Science and Technology, Kyoto University, for supplying the TSA8 cells, and Chugai Pharmaceutical Co. Ltd, Japan, for providing the rHuEPO.

#### References

- Krantz SB: Erythropoietin. *Blood* 1991;77:419-434.
- Chachati A, Godon JP: Effect of haemodialysis on upper gastrointestinal tract pathology in patients with chronic renal failure. *Nephrol Dial Transplant* 1987;1:233-237.
- Ito K, Ito E, Matsuo H, Sudo H, Nakamura O, Sudo Y: Relationship between renal disease and stomach. *Res Gastrointest Blood Flow* 1991;7:57-70.
- Ito K: Upper gastrointestinal disease and chronic renal failure. In: Matuo H, Tamakuma M (eds): *Gastrointestinal Disease*. Tokyo, Ishiyaku, 1993, pp 102-104.
- Hessan S, Kinoshita Y, Min D, Nakata H, Kishi K, Matsushima Y, Asahara M, He-Yao W, Okada A, Mackawa T, Matsui H, Chiba T: Presence of prostaglandin EP<sub>4</sub> receptor gene expression in rat gastric mucosal cell line. *Digestion*, in press.
- Masuda S, Nagao M, Takahata K, Konishi Y, Gallyas F Jr, Tabira Y, Sasaki R: Functional erythropoietin receptor of the cells with neural characteristics. *J Biol Chem* 1993;268:11208-11216.
- Kinoshita Y, Fukae M, Yamatani T, Chiba T, Nakai M, Tsutsumi M, Fujita T: Possible involvement of inositol phosphates and calmodulin in calcitonin-induced stimulation of phosphate transport in LLC-PK1 cells. *Biochem Biophys Res Commun* 1987;144:741-748.
- Nakata H, Matsui T, Ito M, Taniguchi T, Narabayashi Y, Arima N, Nakamura A, Kinoshita Y, Chihara K, Hosoda S, Chiba T: Cloning and characterization of gastrin receptor from ECL carcinoid tumor of *Mastomys natalensis*. *Biochem Biophys Res Commun* 1992;187:1151-1157.
- Tojo A, Fukamachi H, Kasuga M, Urabe A, Takaku F: Identification of erythropoietin receptors on fetal liver erythroid cells. *Biochem Biophys Res Commun* 1987;148:443-448.
- D'Andrea AD, Lodish HF, Wong GG: Expression cloning of the murine erythropoietin receptor. *Cell* 1989;57:277-285.
- Takeuchi K, Okabe S: Importance of pepsin and stomach distension in morphological alteration of stress-induced gastric lesions in pylorus-ligated rats. *Dig Dis Sci* 1988;33:52-59.
- Asahara M, Kinoshita Y, Nakata H, Matsushima Y, Narabayashi Y, Nakamura A, Matsui T, Chihara K, Yamamoto J, Ichikawa A, Chiba T: Gastrin receptor genes are expressed in gastric parietal cells and enterochromaffin-like cells of *Mastomys natalensis*. *Dig Dis Sci* 1994;39:2149-2156.
- Even GI, Littlewood TD: The role of c-myc in cell growth. *Curr Opin Genet Dev* 1993;3:44-49.
- Gogusev J, Zhu DL, Herembert T, Ammar-guella F, Marche P, Druke T: Effect of erythropoietin on DNA synthesis, proto-oncogene expression and phospholipase C activity in rat vascular smooth muscle cells. *Biochem Biophys Res Commun* 1994;199:977-983.
- Anagnostou A, Lee ES, Kessimian N, Levinson R, Steiner M: Erythropoietin has a mitogenic and positive chemotactic effect on endothelial cells. *Proc Natl Acad Sci USA* 1990;87:5978-5982.
- Kimata H, Yoshida A, Ishioka C, Masuda S, Sasaki R, Mikawa H: Human recombinant erythropoietin directly stimulates B cell immunoglobulin production and proliferation in serum-free medium. *Clin Exp Immunol* 1991;85:151-156.
- Nisizaki Y, Guth PH, Quintero E, Bover J, Del Rivero M, Kaunitz JD: Prostaglandin E<sub>2</sub> enhances gastric defense mechanisms against acid injury in uremic rats. *Gastroenterology* 1994;107:1382-1389.
- Suzuki Y, Kameyama J, Nishina M, Tsukamoto M, Nishiyama N, Ishihara K, Hotta K: Pathogenesis of water-immersion stress-induced gastric ulcers in rats with renal failure. *Scand J Gastroenterol Suppl* 1989;162:127-130.
- Hanazono Y, Sasaki K, Nitta H, Yazaki Y, Hirai H: Erythropoietin induces tyrosine phosphorylation of the  $\beta$  chain of the GM-CSF receptor. *Biochem Biophys Res Commun* 1995;208:1060-1066.
- Horina JH, Petritsch W, Schmid CR, Reich G, Wenzel H, Silly H, Krejs GJ: Treatment of anemia in inflammatory bowel disease with recombinant human erythropoietin. *Gastroenterology* 1993;104:1828-1831.

# Receptors for Erythropoietin in Mouse and Human Erythroid Cells and Placenta

By Stephen T. Sawyer, Sanford B. Krantz, and Ken-ichi Sawada

High and lower affinity receptors for erythropoietin (EP) were initially identified on a very pure population of EP-responsive erythroblasts obtained from the spleens of mice infected with anemia strain of Friend virus (FVA). The structure of the receptor for EP in these cells was determined to be proteins of 100 and 85 Kd by cross-linking  $^{125}\text{I}$ -EP. In this investigation, studies on the receptors for EP were extended to other mouse erythroid cells and human erythroid cells as well as to the placentas of mice and rats. Only lower affinity receptors for EP were detected on erythroblasts purified from the spleens of mice infected with the polycythemia strain of Friend virus and a murine erythroleukemia cell line, both of which are not responsive to EP in culture. Internalization of  $^{125}\text{I}$ -EP was observed in both groups of cells. The structure of the receptor determined by cross-linking  $^{125}\text{I}$ -EP was two equally labeled proteins of 100 Kd and 85 Kd molecular mass in all these

mouse erythroid cells. The structure of the receptor was found to be very similar in human erythroid colony forming cells cultured from normal blood. These cells respond to EP with erythroid maturation and were previously shown to have high and lower affinity receptors. Placentas from mice and rats were found to have only lower affinity receptors for EP, and when placental membranes were cross-linked to  $^{125}\text{I}$ -EP, the same 100 Kd and 85 Kd bands were found as seen in mouse and human erythroid cells. The structure of the receptor was similar in cells that have high affinity receptors (FVA-infected and human erythroid colony-forming cells) and nonresponsive erythroid cells and placenta that have lower affinity receptors, but only the cells with the high affinity receptors respond to the addition of EP with erythroid maturation.

©1989 by Grune Stratton, Inc.

**S**PECIFIC BINDING of erythropoietin (EP) was first observed in erythroblasts purified from spleens of mice infected with the anemia strain of Friend virus (FVA).<sup>1,2</sup> These immature FVA-infected erythroid cells (FVA cells) respond to physiological levels of EP in culture by progressing to near erythroid maturation.<sup>4,5</sup>  $^{125}\text{I}$ -EP binds to higher and lower affinity receptors on the surface of these FVA cells and is subsequently internalized and degraded in the lysosomal compartment.<sup>1</sup> In our initial investigation,  $^{125}\text{I}$ -EP binding was also observed in murine erythroleukemia (MEL) cells, clone 745, but only to lower affinity receptors.<sup>1</sup> In this study, we characterize the internalization of  $^{125}\text{I}$ -EP in these MEL cells, which are not responsive to EP in culture, and the binding and internalization of  $^{125}\text{I}$ -EP in erythroid cells purified from the spleens of mice infected with the polycythemia strain of Friend virus (FVP cells), which spontaneously differentiate *in vitro* in the absence of exogenously added EP. The existence of receptors for EP in membranes prepared from placentas from mice and rats is also identified.

When  $^{125}\text{I}$ -EP bound to FVA cell membranes was cross-linked by disuccinimyl suberate (DSS) to the receptor, two labeled bands corresponding to proteins of molecular weights of 100 and 85 Kd were observed on sodium dodecyl sulfate polyacrylamide gel electrophoresis (SDS-PAGE).<sup>3</sup> No evidence of disulfide bridges between these two proteins was found. More recently other investigators have presented evidence that suggests the existence of additional lower molecular weight proteins in the receptor,<sup>7-10</sup> and have suggested that the multiply labeled proteins may be subunits of a very large complex that is bridged by disulfide bonds.<sup>8,10</sup> We have examined this possibility by cross-linking  $^{125}\text{I}$ -EP to the receptor in MEL cells, FVP cells, human erythroid colony-forming cells (CFU-E), and placentas from mice and rats. The data presented here show a remarkable similarity of the receptors for EP in human, mouse, and rat tissues and in EP responsive and nonresponsive erythroid cells. No evidence of additional subunits of the receptor or a larger complex of subunits was detected in any of these sources of receptor.

## MATERIALS AND METHODS

Human recombinant EP was purchased from AmGen Biologicals (Thousand Oaks, CA). Na  $^{125}\text{I}$  was obtained from Amersham. DSS and IODO-GEN (1,3,4,6-tetra-chloro-3 $\alpha$ , 6 $\alpha$ -diphenylglycouril) were obtained from Pierce (Rockford, IL). Friend virus, pseudotype SPFFV<sub>1</sub>/FRE c1-3/MuLV (201) originally obtained from W.D. Hankins (National Institutes of Health [NIH]) and FVP obtained from R. Holdenreid (NIH) were maintained by the passage of infectious plasma in BALB/c mice. MEL cells, clone 745, were obtained from W. LeSturgeon, Vanderbilt University.

**Cells and plasma membrane preparation.** Immature erythroid cells were purified from the spleens of CD<sub>2</sub>F<sub>1</sub> mice infected with FVA or FVP by velocity sedimentation at unit gravity through a continuous gradient of bovine serum albumin as described previously.<sup>4,5</sup> To prepare plasma membranes from FVA- or FVP-infected erythroid cells, the total spleen was disrupted to a single cell suspension and the erythrocytes were lysed by exposure to 150 mmol/L NH<sub>4</sub>Cl/15 mmol/L Tris HCl, pH 7.65, at 37°C for 30 seconds. The NH<sub>4</sub>Cl/Tris solution was diluted fourfold with Iscove's modified Dulbecco's medium and the cells were pelleted by centrifugation at 500 g for 15 minutes. The pellet was resuspended in NH<sub>4</sub>Cl/Tris and the procedure was repeated. The cells were then washed in 105 mmol/L NaCl and 10 mmol/L Tricine, pH 7.4, three times and resuspended in 10 mmol/L KCl and 10 mmol/L Tricine.

From the Division of Hematology, Department of Medicine Vanderbilt University School of Medicine and Veterans Administration Medical Center, Nashville.

Submitted August 9, 1988; accepted March 3, 1989.

Supported by grants from the National Institutes of Health, DK-39781, AM-15555, T32 DK-07186 and VA Medical Research Funds.

Address reprint requests to Stephen T. Sawyer, PhD, Division of Hematology, Room C-3101, Medical Center North, Vanderbilt University School of Medicine, Nashville, TN 37232.

The publication costs of this article were defrayed in part by page charge payment. This article must therefore be hereby marked "advertisement" in accordance with 18 U.S.C. section 1734 solely to indicate this fact.

©1989 by Grune & Stratton, Inc.  
0006-4971/89/7401-0034\$3.00/0

pH 7.4, containing a mixture of proteinase inhibitors (2 mmol/L EGTA, 5 mmol/L EDTA, 1  $\mu$ g leupeptin/mL, 5 mmol/L benzamide, 1 mmol/L iodoacetamide, 10  $\mu$ g/mL tosylamide-2-phenylethyl-chloromethyl ketone, 10  $\mu$ g/mL p-tosyl-L-arginine methylester, 1  $\mu$ g/mL n-d-tosyl-L-Tyrosine chloromethylketone, 2  $\mu$ g/mL aprotinin, 1  $\mu$ g/mL pepstatin, and 0.1 mmol/L penicillimethyl-sulfonylfluorine).

Plasma membrane fractions of MEL cells, FVP cells, and FVA cells were prepared in identical fashion as described previously<sup>3</sup> except that the above described mixture of proteinase inhibitors was included at every step. Briefly, the cells were swollen in hypotonic medium, and disrupted with ten strokes of a teflon, motor-driven homogenizer. The cell debris was discarded after low speed centrifugation, and a crude membrane pellet was obtained after one hour centrifugation at 150,000 g. This pellet was resuspended in a solution containing a final concentration of 40% sucrose, which became the bottom of a discontinuous sucrose gradient composed of solutions of 35%, 31%, 25%, and 8.5% sucrose. The light membrane fractions at the 35%/31% interface and 31%/25% interface were collected as the plasma membrane fraction.

Placenta membranes were prepared in a similar fashion. Placentas from CD<sub>2</sub>F<sub>1</sub> mice were taken at days 14 and 18 of gestation, and placentas from Sprague Dawley rats were taken at 18 to 20 days of gestation. Placentas were washed in phosphate buffered saline containing the above mentioned cocktail of protease inhibitors and finely minced. The minced placenta was then homogenized, centrifuged, and crude membranes were fractionated on discontinuous sucrose gradient exactly as described above for the erythroid cells.

Human CFU-E were obtained as described previously.<sup>11</sup> Briefly, erythroid burst forming units were partially purified from normal human blood. These cells were then cultured in the presence of EP to the stage where the cells were not producing a significant level of hemoglobin and were capable of forming colonies of eight to 49 cells when further cultured in the presence of EP. At this stage the cells were removed from culture and purified additionally by removing adherent cells and by Ficoll-Hypaque density centrifugation. Purity of the cells was >50% and receptors for EP have been found on the cell surface at about 1,000 receptors per cell.<sup>12</sup>

**Iodination of EP.** EP was iodinated using IODO-GEN.<sup>1</sup> Two micrograms of IODO-GEN were coated on the walls of a conical reaction vial. EP (50 units, ~4  $\mu$ g protein) and 20  $\mu$ Ci <sup>125</sup>I were incubated in the reaction vial for five minutes at room temperature in a final volume of 50  $\mu$ L of 0.5 mol/L phosphate buffer, pH 7.0, containing 0.02% Tween 20. After the incubation, the contents of the reaction vial were transferred to a tube containing 10 mg KI in phosphate buffered saline, 0.1% bovine serum albumin, and 0.02% Tween 20; <sup>125</sup>I-EP was separated from the free <sup>125</sup>I by chromatography over a Biogel P6 column. This procedure provided EP with 0.3 to 1.0 molecule of <sup>125</sup>I per molecule (25 to 75  $\mu$ Ci/ $\mu$ g) and with full biological activity when assayed in these FVA-infected erythroid cells.<sup>4</sup>

**Binding <sup>125</sup>I-EP.** <sup>125</sup>I-EP was incubated with from 10 to 40  $\mu$ g protein of the plasma membrane fraction from FVA cells, FVP cells, MEL cells, and placentas from mice and rats at 37°C for the time indicated in 100 mmol/L phosphate buffer, pH 7.4, containing 1 mmol/L EGTA and 0.1% bovine serum albumin. The binding mixture was then applied to 0.2  $\mu$ m Millipore filters (EHWP) and washed with 10 mL of phosphate buffered saline containing 0.1% bovine serum albumin. The filters were then counted in a gamma counter. Nonspecific binding was determined in the presence of 100 to 200 units of EP/mL and was subtracted.

FVA cells, FVP cells, and MEL cells were washed and resuspended in binding medium (Iscoe's modified Dulbecco's medium) supplemented to contain 20 mmol/L HEPES, pH 7.4, and 2% bovine serum albumin. The cells were allowed to stand for one hour at 37°C in a 5% CO<sub>2</sub> atmosphere before the initiation of binding

studies. For binding at 37°C labeled EP was added to the cells in the binding medium at varying concentrations for different times in the incubator. The concentration of cells was 10<sup>7</sup> cells/mL or less. Binding was terminated by sedimenting the cells through dibutyl phthalate oil (0.5 mL) for one minute in a minifuge (8,000 g). The tube was frozen at -80°C, and the tip containing the cell pellet was cut off. Radioactivity in the tip was determined by counting the tip in a gamma counter. Nonspecific binding of the labeled EP was determined by adding a 20 to 100-fold excess of unlabeled EP in the binding assay (100 to 200 units EP/mL).

For binding at 0°C, the protocol was essentially the same as at 37°C except that the cells were cooled for one hour in an ice bath at 4°C, and the incubation was carried out in sealed 1.5 mL minifuge tubes in the ice bath.

For determination of the binding affinities by the method of Scatchard,<sup>13</sup> the cells were incubated for 20 hours at 4°C. This time is sufficient for the binding to plateau, the cell viability as measured by trypan blue exclusion to remain >90% viable, and bound EP to be substantially released. However the binding of <sup>125</sup>I-EP is not totally reversible at 20 hours (60% of <sup>125</sup>I-EP bound was released). <sup>125</sup>I-EP bound to FVA cells was not totally reversible during a reasonable period at 4°C. Extrapolation of the second order release curve showed 90% of bound <sup>125</sup>I-EP was released at 72 hours. However, binding at 4°C for this length of time or greater is not feasible since the cells are not stable and they disintegrate. Nevertheless, binding at 48 hours at 4°C did not affect the binding constant for FVA cells. Therefore these studies were carried out at 20 hours for convenience.

**Determination of surface-bound and internalized EP.** An acid wash, which has been used previously to remove surface-bound ligands,<sup>1,14</sup> was used to remove surface-bound labeled EP from the cell surface. At the indicated times after labeled EP was added to the cells, the cells were cooled to 0°C by the addition of a ninefold excess of cold binding medium and transferred to an ice bath. After three washes to remove unbound ligand, the cells were pelleted by centrifugation in a minifuge for 30 seconds and resuspended in cold 0.5 mmol/L NaCl and to 0.25 mmol/L acetic acid, pH 2.5. After three minutes, the cells were centrifuged through dibutyl phthalate oil. The tube was frozen, and the tip containing the pellet was cut off and counted. The aqueous phase also was counted. Parallel experiments were performed with a large excess of unlabeled EP in the binding assay, and the cells were treated with the high salt, pH 2.5, wash to determine the distribution of the nonspecifically bound EP between the acid labile and stable radioactivity. After nonspecific radioactivity was subtracted, the labeled EP in the acid wash was considered surface bound, while the labeled EP resistant to the acid wash was considered internalized.

**Cross-linking of <sup>125</sup>I-EP.** <sup>125</sup>I-EP was cross-linked to the surface of human erythroid colony-forming cells with DSS in a similar fashion as described previously for FVA cells.<sup>3</sup> <sup>125</sup>I-EP was added to 10<sup>7</sup> cells for 30 minutes at 37°C. DSS was added at 500  $\mu$ M for 15 minutes at 0°C. The cells were washed three times with 150 mmol/L Tris-HCl, pH 7.4, to quench the cross-linking reaction and remove unbound EP. The cells were then extracted for one minute at 0°C with a solution containing 1.0% Triton X-100, 20 mmol/L HEPES, pH 7.4, containing the mixture of 11 protease inhibitors described above. The disrupted cell preparation was then centrifuged at 1,000 g for one minute to remove nuclei and cell debris; the supernatant and pellet were both analyzed by SDS-PAGE.

<sup>125</sup>I-EP was bound to receptors on the plasma membrane fraction and was cross-linked in a similar fashion as described previously.<sup>3</sup> Membranes were incubated with 7.5 units of <sup>125</sup>I-EP per milliliter in 100 mmol/L phosphate buffer, pH 7.4, containing 1 mmol/L EGTA and 0.1% bovine serum albumin for 15 minutes at 37°C. The mixture was transferred to an ice bath, and DSS was added to a final

concentration of 200  $\mu\text{mol/L}$  for 15 minutes. Tris-HCl, pH 8.0, was added to a final concentration of 150 mmol/L, and the membranes were pelleted by centrifugation at 13,000 g for 30 minutes. The pellet was resuspended in 10 mmol/L Tris-HCl, pH 7.4, and 100 mmol/L NaCl and washed twice. The pellet was suspended in sample buffer, boiled for three minutes and sonicated briefly. The material was analyzed by SDS-PAGE as described by Laemmli.<sup>15</sup>

## RESULTS

**Binding and internalization of  $^{125}\text{I}$ -EP.** FVP cells were purified from the spleens of mice infected with the polycythemia strain of the virus. Surface receptors were quantitated by measuring the binding of  $^{125}\text{I}$ -EP at 0°C for 20 hours. Figure 1 shows the amount of bound  $^{125}\text{I}$ -EP when increasing concentrations of  $^{125}\text{I}$ -EP were added. In Fig 1 the data were plotted by the method of Scatchard.<sup>15</sup> The intercept reveals a total of 650 surface receptors. The slope reveals a single class of receptors having a dissociation constant of 700 pmol/L. Binding to FVA cells is also shown in Fig 1 to illustrate the two classes of  $^{125}\text{I}$ -EP binding sites in these cells compared with the single class of receptors found in FVP cells.  $^{125}\text{I}$ -EP was also bound to FVP cells at 37°C (Fig 2B) and the internalization of  $^{125}\text{I}$ -EP by FVP, FVA,

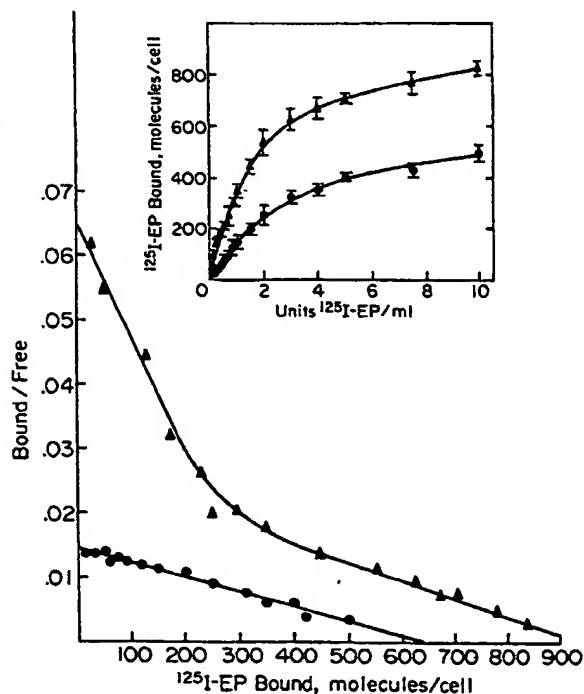


Fig 1. Binding of  $^{125}\text{I}$ -EP to FVP cells and FVA cells. Immature erythroid cells were purified from mice infected with the polycythemia and FVA. These cells were then incubated with the indicated concentration of  $^{125}\text{I}$ -EP for 20 hours at 0°C. Nonspecific binding was determined in the presence of a 20-fold excess of unlabeled EP. Nonspecific binding was <20% and was subtracted. Data are the mean of triplicates  $\pm$  SD. At the maximum binding for FVA cells approximately 5,000 cpm of  $^{125}\text{I}$ -EP were specifically bound per  $10^6$  cells. The binding data were plotted by the method of Scatchard.<sup>15</sup>  $\Delta$ , FVA cells;  $\bullet$ , FVP cells.

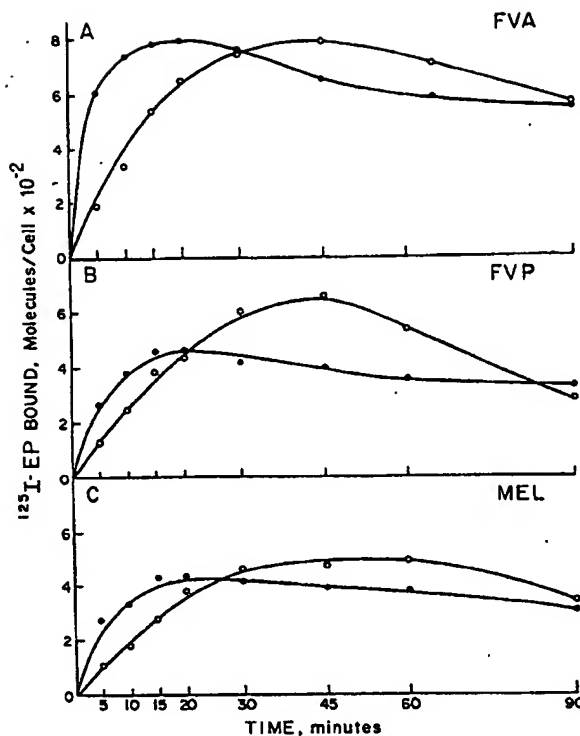


Fig 2. Binding and internalization of  $^{125}\text{I}$ -EP by FVA cells, FVP cells, and MEL cells.  $^{125}\text{I}$ -EP was added to the cells at  $t = 0$  and incubated for the indicated time at 37°C. The surface bound hormone ( $\bullet$ ) and internalized hormone ( $\circ$ ) were determined by extracting surface  $^{125}\text{I}$ -EP from the cell with a pH 2.5, high salt wash as described in the Materials and Methods section.

and MEL cells were compared (Fig 2). FVP cells bind 900 molecules of  $^{125}\text{I}$ -EP after 30 minutes at 37°C and the binding slowly falls to a plateau level of 600 total molecules by 90 minutes (sum of surface and internal radioactivity). As previously reported,<sup>1</sup> FVA cells bind 1,500 molecules at 30 minutes after which the level falls to 1,000 molecules of EP. MEL cells bind 850 molecules of EP at 37°C, which is compatible with our earlier report of 760 receptors on the cell surface. A pH 2.5, 0.5 mol/L NaCl wash was used to strip away surface bound  $^{125}\text{I}$ -EP to discriminate surface bound hormone from internalized hormone and degradation products. FVP cells and MEL cells internalized  $^{125}\text{I}$ -EP in a similar fashion as FVA cells. As previously reported for FVA cells, intracellular radioactivity predominated after 30 minutes of incubation with  $^{125}\text{I}$ -EP at 37°C. Additional experiments were carried out to show that the internalized  $^{125}\text{I}$ -EP was degraded to  $^{125}\text{I}$ -iodotyrosine (data not shown).

Plasma membrane fractions from FVA cells, FVP cells, and MEL cells were tested for  $^{125}\text{I}$ -EP binding. Smooth membrane from mouse and rat placenta were also prepared, and  $^{125}\text{I}$ -EP binding was quantitated (Fig 3 and Table 1). Binding was determined for a range of increasing concentrations of  $^{125}\text{I}$ -EP and plotted by the method of Scatchard, the number of receptors was determined from the intercept while the dissociation constant was determined from the slope. In

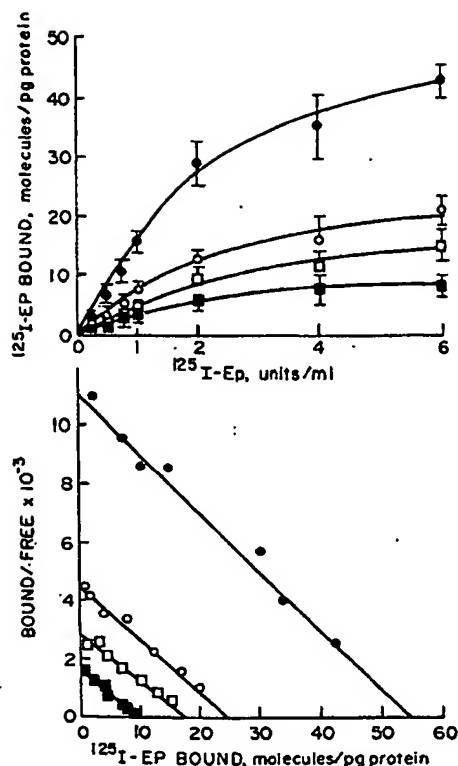


Fig 3. Binding of  $^{125}\text{I}$ -EP to membranes from FVP cells, MEL cells, and placentas from mice and rats. Membranes were prepared and binding of  $^{125}\text{I}$ -EP were carried out as described in the Materials and Methods section. Binding was performed in triplicate and the mean  $\pm$  SD is shown. Nonspecific binding was carried out in an excess of unlabeled EP and subtracted. In these membranes, nonspecific binding was similar; at the highest concentration of  $^{125}\text{I}$ -EP, this nonspecific binding was 15% of total in FVP membranes and increased up to 65% in rat placentas. In the lower panel, the data were plotted by the method of Scatchard. FVP, (●); MEL, (○); mouse placenta, (□); rat placenta (■).

contrast to FVA cell membranes, which have higher and lower affinity receptors, the other membranes showed a single class of receptors with a (Kd) dissociation constant from 600 pmol/L to 1.0 nmol/L (Table 1). FVA and FVP cell membranes contained more receptors (72 and 54 receptors/pg protein) than membranes from MEL cells (27 receptors/pg protein), and all the erythroid cell membranes

Table 1.  $^{125}\text{I}$ -EP Binding to Membranes From Erythroid Cells and Placentas

Membrane Source	Receptors/pg Protein	Binding Affinity (Kd)
FVA cells	72	80 pmol/L, 600 pmol/L <sup>3</sup>
FVP cells	54	800 $\pm$ 200 pmol/L*
MEL cells	27	900 $\pm$ 100 pmol/L
Mouse placenta	19	1,000 $\pm$ 400 pmol/L
Rat placenta	9	900 $\pm$ 200 pmol/L

\*Binding affinities shown are the mean of two to four determinations  $\pm$  the variance in these determinations.

contain more receptors than placenta membranes (mouse 19 and rat 9 receptors/pg protein) when normalized for protein content. These data are from Fig 3. Other preparations of membranes had similar numbers of receptors. Inclusion of additional inhibitors of proteinase activity increased the receptors/protein ratio by 70% in FVA cells over the previously reported value.<sup>3</sup>

**Cross-linking of  $^{125}\text{I}$ -EP to receptors.**  $^{125}\text{I}$ -EP bound to membranes prepared from FVA cells, FVP cells, MEL cells, and placentas from mice and rats was cross-linked to the receptor for EP using DSS. As shown by the autoradiograph in Figs 4 and 5, the  $^{125}\text{I}$ -EP became covalently attached to two discretely migrating proteins such that the complex migrated at 140 Kd and 125 Kd. Subtraction of the molecular mass of EP lead to the apparent molecular mass of 100 Kd and 85 Kd. These bands were identical in each sample (FVA cells, FVP cells, MEL cells, and placenta from mouse and rat). In Fig 4 the SDS-PAGE is run in the absence of reducing agent. The results are identical to the SDS-PAGE of the same samples  $^{125}\text{I}$ -EP cross-linked membranes run in the presence of reducing agent (shown in Fig 5). This indicates the absence of disulfide bridges between the two labeled proteins of 100 Kd and 85 Kd in all these erythroid cells and placentas.

Intact cells were used to identify the receptor for EP in human erythroid cells. After binding  $^{125}\text{I}$ -EP to these cells at 37°C, DSS was added to the binding mixture. The cells were disrupted and both the extract (Fig 6C) and cell debris fraction (6B) were analyzed by SDS-PAGE.  $^{125}\text{I}$ -EPO cross-

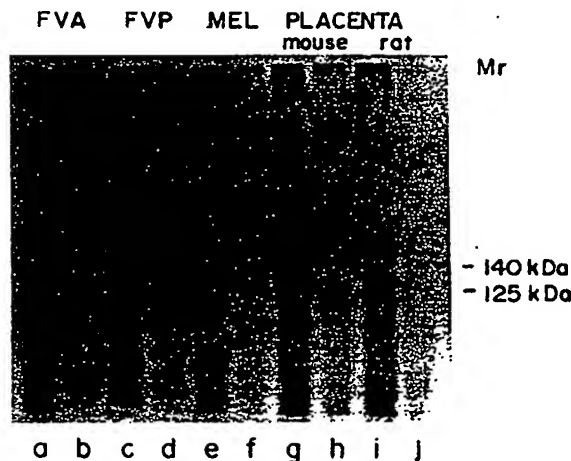


Fig 4. Cross-linking of  $^{125}\text{I}$ -EP to membranes from FVA cells, FVP cells, MEL cells, and placentas from mice and rats. Binding and cross-linking was performed as described in Materials and Methods. Nonspecific binding was done in the presence of 200 U/mL unlabeled EP. The cross-linked membranes were dissolved in sample buffer without reducing agents and radioactivity was counted in a gamma counter. Equal amounts of radioactivity were loaded (an equal volume of extract of the corresponding nonspecific sample was loaded) on a 5% acrylamide gel. The dried gel was subject to autoradiography. FVA cells, lanes a, b; FVP cells, c, d; MEL cells, e, f; mouse placenta, g, h; rat placenta, i, j. Nonspecific cross-linking is shown in lanes b, d, f, h, and j.



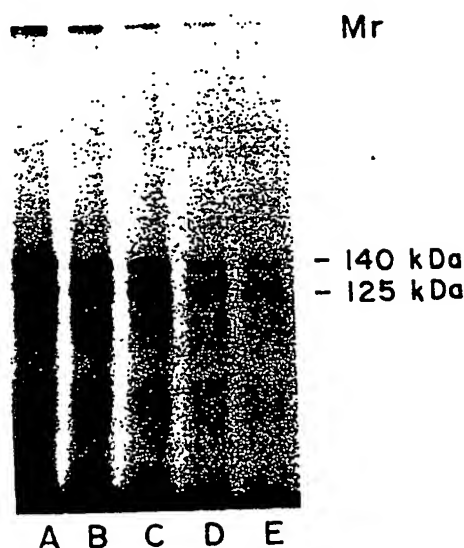


Fig 5. Cross-linking of  $^{125}\text{I}$ -EP to membranes from FVA cells, FVP cells, MEL cells, and placentas from mice and rats. One milligram of membrane protein was incubated with 5 units of  $^{125}\text{I}$ -EP for 15 minutes and cross-linked with 0.2 mmol/L DSS. The samples were analyzed by SDS-PAGE in the presence of  $\beta$ -mercaptoethanol and autoradiography. Lane A, FVA cells; B, FVP cells; C, MEL cells; D, mouse placenta; E, rat placenta.

linked proteins were found to migrate in the gel at a position corresponding to a molecular mass of 140 Kd and approximately 130 Kd. While the 140 Kd band is identical to that found in mouse tissues, the lesser molecular weight band appears just slightly larger than the corresponding band in mouse FVA cells (Fig 6D). A minor band that migrates at 110 Kd was also seen in the cell extract but not in the cell debris fraction. The presence of this band was variable from one experiment to another and may be a proteolytic fragment of the larger cross-linked bands. The gel pattern was identical in the presence and absence of reducing agents.

#### DISCUSSION

Following the appearance of our report of the structure of the receptor in FVA cells as two proteins of 100 Kd and 85 Kd molecular mass,<sup>3</sup> Todakaro et al<sup>7</sup> reported that the receptor in an EP responsive cell line was composed of three subunits of 119, 94, and 63 Kd, which were not connected through disulfide bridges. In addition, three erythroid cell lines unresponsive to EP (including clone 745 MEL cells) were found to have only the 63 Kd band cross-linked to  $^{125}\text{I}$ -EP. However, Sasaki et al<sup>10</sup> reported identical 100 Kd and 85 Kd subunits of the receptor for EP in EP-responsive TSA8 erythroid cells, FVA cells, mouse fetal liver cells, and spleens from anemic mice. Tojo et al reported the EP receptor as bands of 110 and 95 Kd in fetal mouse liver,<sup>16</sup> while Mayeux et al reported two proteins of molecular mass of 94 and 78 Kd in fetal rat liver<sup>8</sup>; and Pekonen et al described two proteins of 85 Kd and 41 Kd in human fetal liver.<sup>9</sup>

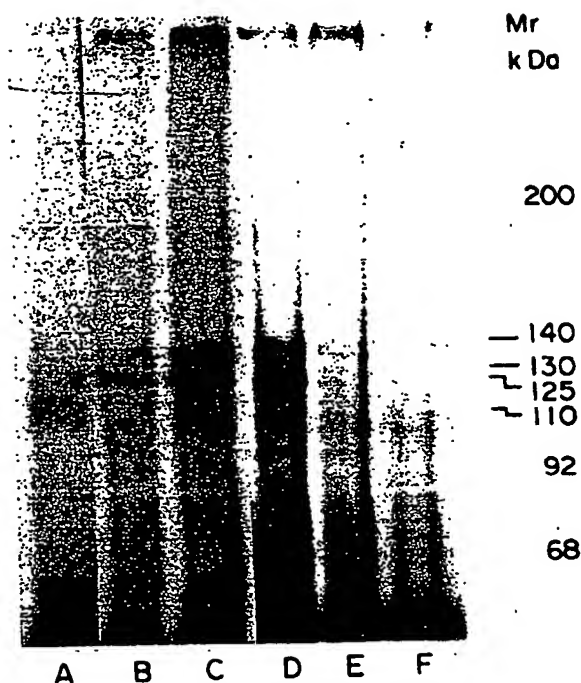


Fig 6. Cross-linking of  $^{125}\text{I}$ -EP to human erythroid colony-forming cells and FVA cells.  $^{125}\text{I}$ -EP was bound to the cells and cross-linked as described in Materials and Methods. Nonspecific binding was determined in the presence of 100 units of unlabeled EP, lanes A and F. The cells were extracted with detergent and centrifuged at 1,000 g. Cell extract, lanes A, C, D, and F; cell debris, B lanes and E. Human erythroid colony-forming cells, lanes A, B, and C; FVA cells, lanes D, E, and F.

In view of the possibility that different subunits of the receptor might exist in different animal species or different cell lines, we compared the structure of receptors for EP in different erythroid cells. In contrast to the finding of others,<sup>7,10</sup> we found that the structure of the receptor for EP in the MEL cells consisted of the same 100 Kd and 85 Kd proteins found in FVA cells and all other tissues tested in this study. In addition, the rat and human receptor were similar to the mouse receptor, in contrast to reports of lower molecular weight receptors.<sup>8,9</sup> We suspect that the lower molecular weight proteins cross-linked to  $^{125}\text{I}$ -EP in these earlier reports are proteolytic fragments of the larger molecular weight proteins. In early experiments we observed a band of 70 Kd when  $^{125}\text{I}$ -EP was cross-linked to intact MEL cells and the cross-linked complex was extracted with Triton X-100. In other studies to be published elsewhere, the receptor for EP in FVA cells was observed to be degraded to a series of lower molecular weight protein after cross-linking to  $^{125}\text{I}$ -EP to intact cells. This could be prevented by the addition of proteinase inhibitors. While the cross-linked receptor is very insoluble in nonionic detergents, the degradation fragments are more easily extracted. Earlier reports on the EP receptor in MEL and fetal rat liver cells used Triton X-100 extraction of cross-linked receptor from intact cells. Likewise, an additional minor band was seen in the soluble extract of cross-

linked receptor from human CFU-E but not in the insoluble fraction (Fig 6). Preparation of plasma membranes from cells eliminates the need to extract the receptor from the intact cell and lowers the ratio of receptor to proteinase activity during the cross-linking reaction.

In contrast to our work and the work of Todokoro et al., Sasaki et al showed that the cross-linked bands mostly did not enter the gel or a minor band was observed at 210 Kd in the absence of reducing agent during SDS-PAGE.<sup>10</sup> Mayeux et al reported the existence of 94 and 78 Kd proteins cross-linked to <sup>125</sup>I-EP in fetal rat liver cells and also suggested that these proteins were subunits of a large molecular weight complex bridged by disulfide bonds.<sup>8</sup> In this study no evidence of disulfide bridging between the 100 and 85 Kd proteins of the EP receptor was detected in any cell or tissue examined. The observations of large molecular weight proteins cross-linked to <sup>125</sup>I-EP on SDS-PAGE in the absence of reducing agents may be due to the incomplete solubilization of the cross-linked membranes. Mild treatment of <sup>125</sup>I-EP cross-linked to FVA cell membranes and SDS-PAGE in the absence of reducing agents leads to a weakly labeled band at 230 Kd and most of the radioactivity at the top of the running gel and stacking gel. This radioactive material was cut out of an unfixed gel and rerun on SDS-PAGE in the presence of  $\beta$ -mercaptoethanol. Only 1% of this radioactivity was found in the 100 and 85 Kd cross-linked bands while 99% was noncross-linked <sup>125</sup>I-EP (data not shown). Mild sonication of the cross-linked membrane in sample buffer for SDS-PAGE containing no reducing agent converted the higher molecular weight cross-linked material into the clear 100 and 85 Kd proteins. This strongly suggested the absence of disulfide bridges between the 100 and 85 Kd proteins.

This study reports the structure of the normal human erythroid receptor for EP. The human receptor is virtually identical to the mouse and rat receptor, however a slight increase in the molecular mass of the lesser protein of the human receptor compared with mouse and rat may occur. Other experiments show the very slight difference in migration of the two proteins of the human receptor compared with that in FVA cells. We suspect that the lower band of the receptor for EP may be due to the cleavage of the 100 Kd band by proteinase. If this is the case, a subtle difference in the amino acid sequence of the human 100 Kd receptor protein could lead to a different site of cleavage and therefore a fragment of slightly larger molecular mass.

It is of interest that the receptor for EP is remarkably similar in mouse, rat, and human tissue. Furthermore, the

similarity of receptor in erythroid cells and placenta is also of interest in that the function of the receptor in the placenta is not proven. This is the first report of the existence of receptors for EP in placenta. The finding in this laboratory that <sup>125</sup>I-EP crossed from maternal circulation to the fetus in pregnant mice<sup>17</sup> led us to investigate the existence of receptors for EP in the placenta. We think that the placental receptors for EP may be involved in the transplacental transfer of <sup>125</sup>I-EP but additional experiments are necessary to prove the physiological relevance of the transfer of EP to the fetus and the receptor mediated nature of the transfer.

The nearly identical structure of the receptors in the normal human erythroid cells and normal placentas compared with the receptors in mouse erythroid cells that proliferate in response to infection with the Friend virus indicates that the Friend virus does not stimulate erythroid development through a gross modification of the structure of the receptor for EP. The two strains of Friend virus, FVA, and FVP, lead to different responses when either mice or bone marrow cells are infected. FVA infection generates erythroid cells comparable with CFU-E in that the cells are responsive to EP and respond by undergoing erythroid maturation and growth. In contrast, FVP infection results in a proliferation of erythroid cells that are apparently undergoing erythroid maturation independently of EP. In culture these cells do not respond to EP.<sup>4,18</sup> It is possible that autocrine production of EP by FVP cells might be responsible for this apparent independence of regulation by EP, but preliminary experiments in our laboratory have failed to detect production of mRNA coding for EP in FVP cells.

The presence of receptors for EP on MEL and FVP cells on which EP has no apparent effect suggests that the normal mechanism by which EP triggers these cells has been altered. In this regard, we studied internalization of <sup>125</sup>I-EP by MEL and FVP cells. <sup>125</sup>I-EP was internalized in these cells in exactly the same manner as the EP-responsive FVA cells. In earlier work, the higher affinity receptors on the FVA cells appeared to be preferentially endocytosed<sup>1</sup>; however, this study shows equal endocytosis of higher and lower affinity receptor since FVP and MEL have only lower affinity receptor for EP. The presence of higher affinity receptors on FVA cells and human CFU-E<sup>12</sup> may be responsible for their capacity to respond to EP with erythroid maturation. However, the molecular mechanism for this effect is still unknown since the present study shows that the structure of the receptor for EP in cells containing either higher and lower affinity receptor or only affinity receptors is identical in gross structure.

#### REFERENCES

1. Sawyer ST, Krantz SB, Goldwasser E: Binding and receptor mediated endocytosis of erythropoietin in Friend virus-infected erythroid cells. *J Biol Chem* 262:5554, 1987
2. Krantz SB, Goldwasser E: Specific binding of erythropoietin in spleen cells infected with the anemia strain of Friend virus. *Proc Natl Acad Sci USA* 81:7574, 1984
3. Sawyer ST, Krantz SB, Luna J: Identification of the receptor for erythropoietin by cross-linking to Friend virus-infected erythroid cells. *Proc Natl Acad Sci USA* 84:3690, 1987
4. Koury MJ, Sawyer ST, Bondurant MC: Splenic erythroblasts in anemia-inducing Friend disease: A source of cells for studies of erythropoietin-mediated differentiation. *J Cell Physiol* 121:526, 1984
5. Sawyer ST, Koury MJ, Bondurant MC: Large-scale procurement of erythropoietin-responsive erythroid cells. *Methods Enzymol* 147:340, 1987
6. Koury MJ, Bondurant MC, Atkinson JB: Erythropoietin control of terminal erythroid differentiation: Maintenance of cell viability

ity, production of hemoglobin, and development of the erythrocyte membrane. *Blood Cells* 13:217, 1987

7. Todokoro K, Kanazawa S, Amanuma H, Ikawa Y: Specific binding of erythropoietin to its receptor on responsive mouse erythroleukemia cells. *Proc Natl Acad Sci USA* 84:4126, 1987

8. Mayeux D, Billat C, Jacquot R: The erythropoietin receptor of rat erythroid progenitor cells. *J Biol Chem* 262:13985, 1987

9. Pekonen F, Rosenlof K, Rutanen E-M, Fyhrquist F: Erythropoietin binding sites in human foetal tissues. *Acta Endocrinol (Copenh)* 116:561, 1987

10. Sasaki R, Yanagawa S, Hitomi K, Chiba H: Characterization of erythropoietin receptor of murine erythroid cells. *Eur J Biochem* 168:43, 1987

11. Sawada K, Krantz SB, Kans J, Dessypris EN, Sawyer ST, Glick AD, Civin CI: Purification of human erythroid colony-forming units and demonstration of specific binding of erythropoietin. *J Clin Invest* 80:347, 1987

12. Sawada K, Krantz SB, Sawyer ST, Civin CI: Quantitation of

specific binding of erythropoietin to human erythroid colony-forming cells. *J Cell Physiol* 137:337, 1988

13. Scatchard G: The attraction of proteins for small molecules and ions. *Ann NY Acad Sci* 51:660, 1949

14. Sawyer ST, Krantz SB: Transferrin receptor number, synthesis, and endocytosis during erythropoietin-induced maturation of Friend virus-infected erythroid cells. *J Biol Chem* 261:9187, 1986

15. Laemmli UK: Cleavage of structural proteins during the assembly of the head of bacteriophage T4. *Nature* 227:680, 1970

16. Tojo A, Fukamachi H, Kasuga M, Urabe A, Takaku F: Identification of erythropoietin receptors on fetal liver erythroid cells. *Biochem Biophys Res Commun* 148:443, 1987

17. Koury MJ, Bondurant MC, Graber SE, Sawyer ST: Erythropoietin messenger RNA levels in developing mice and transfer of <sup>125</sup>I-erythropoietin by the placenta. *J Clin Invest* 82:154, 1988

18. Ruscetti S, Wolff L: Spleen focus-forming virus: Relationship of an altered envelope gene to the development of a rapid erythroleukemia. *Curr Top Microbiol Immunol* 112:21, 1984

VOL 74, NO 1

JULY 1989

# BLOOD

*The Journal of  
The American Society of  
Hematology*

*American Society of Hematology  
Thirty-First Annual Meeting  
December 2-5, 1989  
Atlanta, Georgia  
(see page 527 for registration information)  
ABSTRACT DEADLINE: AUGUST 24, 1989*

Table of Contents v

GRUNE & STRATTON  
Harcourt Brace Jovanovich, Inc.

E000080

C00024646

## Human, rat, and mouse kidney cells express functional erythropoietin receptors

CHRISTOF WESTENFELDER, DIANA L. BIDDLE, and ROBERT L. BARANOWSKI

Division of Nephrology, VA and University of Utah Medical Centers, Salt Lake City, Utah, USA

Cells of human, rat, and mouse kidney express functional erythropoietin receptors.

**Background.** Erythropoietin (EPO), secreted by fibroblast-like cells in the renal interstitium, controls erythropoiesis by regulating the survival, proliferation, and differentiation of erythroid progenitor cells. We examined whether renal cells that are exposed to EPO express EPO receptors (EPO-R) through which analogous cytokine responses might be elicited.

**Methods.** Normal human and rat kidney tissue and defined cell lines of human, rat, and mouse kidney were screened, using reverse transcription-polymerase chain reaction, nucleotide sequencing, ligand binding, and Western blotting, for the expression of EPO-R. EPO's effects on DNA synthesis and cell proliferation were also examined.

**Results.** EPO-R transcripts were readily detected in cortex, medulla, and papilla of human and rat kidney, in mesangial (human, rat), proximal tubular (human, mouse), and medullary collecting duct cells (human). Nucleotide sequences of EPO-R cDNAs from renal cells were identical to those of erythroid precursor cells. Specific <sup>125</sup>I-EPO binding revealed a single class of high- to intermediate-affinity EPO-Rs in each tested cell line (K<sub>D</sub> 96 pM to 1.4 nM; B<sub>max</sub> 0.3 to 7.0 fmol/mg protein). Western blots of murine proximal tubular cell membranes revealed an EPO-R protein of approximately 68 kDa. EPO stimulated DNA synthesis and cell proliferation dose dependently.

**Conclusion.** This is the first direct demonstration, to our knowledge, that renal cells possess EPO-Rs through which EPO stimulates mitogenesis. This suggests currently unrecognized cytokine functions for EPO in the kidney, which may prove beneficial in the repair of an injured kidney while being potentially detrimental in renal malignancies.

Erythropoietin (EPO) is a 34 kDa glycoprotein hormone that controls erythropoiesis by receptor-mediated regulation of survival, proliferation, and differentiation of erythroid progenitor cells [1]. In the adult, EPO is secreted primarily by fibroblast-like interstitial cells of the renal cortical labyrinth and, to a smaller degree, by

the liver [1-5]. Renal EPO is first secreted into peritubular capillary blood that also contains residual EPO [1, 6]. From here, renal veins deliver the hormone into the systemic circulation [1, 6].

Intriguingly, EPO-producing cells are also in direct contact with the basal aspects of proximal and distal tubular cells [1-5, 7]. We reasoned that this anatomical relationship between EPO-secreting cells, the intrarenal capillary network, and tubular and other renal cells could facilitate endocrine and paracrine actions of EPO within the kidney itself. This would require that potential targets, such as renal tubular cells, possess functional EPO receptors (EPO-Rs) on their surface [8]. This has, however, not been systematically investigated to date, and as a consequence, endocrine or paracrine actions of EPO within the kidney have not been considered. This is primarily due to the assumption, until recently, that EPO-Rs existed only on erythroid progenitor cells and that, therefore, EPO's effects were restricted to these cells [8].

Recently, however, Anagnostou et al showed that vascular endothelial cells possess EPO-Rs and proliferate and migrate in response to EPO [9, 10]. Others have demonstrated that EPO-Rs are present in rodent placenta [11], rat brain and neuronal PC12 and SN6 cells [12, 13], testicular Leydig cells [14], and gastric epithelial cells [15]. In Leydig cells, EPO stimulates testosterone synthesis, and in gastric mucosal cells, it stimulates mitogenesis. In the brain of gerbils, EPO was shown to ameliorate the injury caused by ischemia [16], whereas in glomerular mesangial cells, it was found to activate calcium channels, potentially resulting in cellular contraction [17]. Taken together, these observations provide growing evidence in support of the notion that EPO may possess important physiological functions in various nonhemopoietic cells.

To explore EPO's nonhemopoietic functions further, we conducted a systematic search for EPO-R in human and rat kidney tissue and in various lines of cultured renal cells. We detected authentic EPO-R transcript and protein expression and specific binding of EPO to cell

**Key words:** EPO, mitogenesis, erythropoiesis, injury repair, renal malignancies.

Received for publication June 23, 1998  
and in revised form September 15, 1998  
Accepted for publication September 22, 1998

© 1999 by the International Society of Nephrology

surface receptors. Receptor activation stimulated mitogenesis *in vitro*, demonstrating that EPO may act through its receptors in the kidney as a currently unrecognized cytokine.

## METHODS

### Human kidney

Normal tissue from two different nephrectomy specimens was obtained with our Institutional Review Board (IRB) approval. Tissues were immediately placed into chilled phosphate-buffered saline (PBS), rinsed free of blood, frozen in liquid nitrogen, and dissected into cortex, outer medulla, and papilla. The samples were stored at  $-70^{\circ}\text{C}$  until RNA was extracted. mRNA from normal human fetal liver (week 19) served as a positive control.

### Rat kidney

For all studies (approved by the Institutional Animal Care and Use Committee), normal, adult, male Sprague-Dawley rats weighing 300 to 350 g were used. Animals had free access to food and water. Before sacrifice, rats were anesthetized (ketamine, 1 mg, and acepromazine, 0.1 mg/100 g body wt i.p.), and hearts and kidneys were rapidly removed, placed in chilled PBS, rinsed free of blood, frozen in liquid nitrogen, and stored at  $-70^{\circ}\text{C}$  until RNA was extracted. Kidneys were dissected into cortex, outer medulla, and papilla.

Because anemia causes the accumulation of EPO-R-expressing erythroid progenitor cells, it was necessary to obtain negative and positive controls [8]. Accordingly, using a modification of a previously reported method [18], adult male Balb C mice ( $N = 3$ ), weighing 40 to 50 g, were made anemic with a 5 mg/ml solution of phenylhydrazine in PBS administered once a day for three days (50 mg/kg body wt i.p.). Sham animals ( $N = 3$ ) were treated with an equal volume of PBS. After two additional days, hematocrits in phenylhydrazine-treated animals had decreased from  $46 \pm 2\%$  to  $31 \pm 3\%$  ( $P < 0.05$ ), whereas they remained stable in sham animals ( $46 \pm 2\%$  and  $46 \pm 2\%$ ). Animals were then sacrificed under nembutal anesthesia (40 mg/kg body wt i.p.), and spleens were harvested, immediately frozen in liquid nitrogen, and stored at  $-70^{\circ}\text{C}$ . Subsequently, RNA was extracted, and cell membranes were prepared for Western blotting, as described later here.

### Cell lines

Defined, normal human proximal tubular cells (HCTs; Genetics Corp., San Diego, CA, USA) at passage 2 and normal human medullary collecting duct cells (HMCs) at passages 2 and 3 were grown to high subconfluence in a 1:1 mixture of Dulbecco's modified Eagle's medium (DMEM) and F12 containing  $1 \times$  insulin, transferrin, selenium (Sigma, St. Louis, MO, USA), epithelial growth

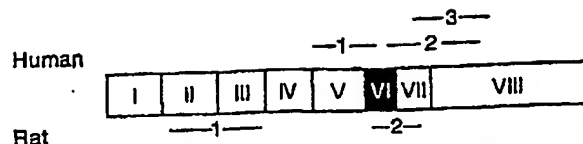


Fig. 1. Schema of the mRNA that encodes the erythropoietin receptor [24, 25]. It is composed of eight exons; exons I through V represent the extracellular domain (N-terminus), exon VI, the single transmembrane domain, and exons VII and VIII, the cytoplasmic domain (C-terminus). Regions of the human EPO-R transcript that are bound by the three PCR primers (1 through 3) are shown above, and PCR primers (1 and 2) utilized for rat and mouse EPO-R transcripts, below the diagram (not to scale).

factor (10 ng/ml), T3 (4 pg/ml), and 10% newborn calf serum (NCS; Hyclone, Logan, UT, USA) at  $37^{\circ}\text{C}$  in 5%  $\text{CO}_2/\text{air}$  [19]. Defined, normal mesangial cells obtained from adult human (HMCs) and rat (RMCs) kidney at passages 2 to 3 were grown to high subconfluence in DMEM with 10% NCS at  $37^{\circ}\text{C}$  in 5%  $\text{CO}_2/\text{air}$ . Transformed murine proximal tubular cells (MCTs) are a well-defined cell line that retains many characteristics of native proximal tubular cells [20]. They were grown in DMEM with 10% NCS at  $37^{\circ}\text{C}$  in 5%  $\text{CO}_2/\text{air}$ . A human erythroleukemia cell line that expresses high numbers of EPO-Rs, OCIM 1 cells [21], served as positive controls. They were grown at  $37^{\circ}\text{C}$  in 5%  $\text{CO}_2/\text{air}$  in suspension culture, using Iscove's modified Dulbecco's media, containing 10% heat-inactivated fetal calf serum (FCS) and  $5 \times 10^{-4} \text{ M}$   $\beta$ -mercaptoethanol. HeLa cells (ATTC, Rockville, MD, USA) served as negative human controls. They were grown in MEM and 10% NCS. HCD 57, an EPO-dependent murine erythroleukemia cell line with high level expression of EPO-Rs [22], served as the positive control. They were grown in suspension culture media as described for OCIM 1 cells. In addition, 1 U/ml of human EPO was added to the culture media. Mouse NIH 3T3 cells, embryonic mouse fibroblasts, served as negative controls (ATTC). They were grown in DMEM with 10% NCS at  $37^{\circ}\text{C}$  in 5%  $\text{CO}_2/\text{air}$ .

### mRNA isolation, RT-PCR, and gel electrophoresis

Total RNA was isolated from tissues and cultured cells by an acid guanidinium-thiocyanate-phenol-chloroform method [23], using TRI Reagent (Molecular Research Center, Inc., Cincinnati, OH, USA). For the reverse transcription-polymerase chain reactions (RT-PCR) 1  $\mu\text{g}$  of total mRNA was reverse transcribed (M-MLV reverse transcriptase; GIBCO, Grand Island, NY, USA), and the resulting cDNAs were subjected to 35 cycles of the PCR. The amplification of the examined cDNAs was linear up to 40 PCR cycles for all primer sets used in this study. For human samples, three sets of PCR primers were chosen, each specific to a different domain of human EPO-R cDNA (Fig. 1). Their individual sequences



and respective positions within the coding sequence are as follows [24]: (1) sense, 5'-CCTGGTGGAGCCTGTGT-3', antisense, 5'-CACGACGACTGGCAGAG-3', yielding a 104 bp PCR product of nucleotides 704-807 located on exons V and VI, spanning extracellular and transmembrane domains; (2) sense, 5'-TCGTGGTCATCCTGGTGCTGCTGA-3', antisense, 5'-ACCTTCAGGAGAGTCTCGCGACGA-3', yielding a 240 bp PCR product of nucleotides 776-1015, located on exons VI and VIII, representing transmembrane and cytoplasmic domains; and (3) sense, 5'-CCCAGCCCAGAGAGCAGATT-3', antisense, 5'-TAGGAGGACGAGTAGACGAAA-3', yielding a 372 bp PCR product of nucleotides 885-1229 on exons VII and VIII, representing cytoplasmic domains of the human EPO-R.

For rat and mouse EPO-R cDNAs, two sets of primers were used for PCR amplification of homologous sequences (Fig. 1) [12, 25]: (1) sense, 5'-TCTGGGAGGC GGCGAACT-3', antisense, 5'-GAGGAGCGATGGTG GCGTAGT-3', yielding a 219 bp PCR product of nucleotides 188-406 on exons II and III, representing an extracellular domain; and (2) sense, 5'-CGCTGTCTCTCAT TCTCGTC-3', antisense, 5'-GGTTCGGGTCTCTTAC TCAA-3', yielding a 118 bp PCR product of nucleotides 758-875 on exons VI and VII, representing transmembrane to cytoplasmic domains of the rat/mouse EPO-R.

All primer pairs were chosen to span introns (Fig. 1), thus facilitating control for contamination by genomic DNA. All cell and tissue extracts were subjected to the PCR reaction once with and once without an initial reverse transcription.

As internal controls, human and mouse/rat  $\beta$ -actin mRNAs were simultaneously reverse transcribed and PCR amplified. The primers used for human  $\beta$ -actin cDNA had the following sequence: sense, 5'-TGTCACCTTCCAGCAGATGT-3', antisense, 5'-CACCTT CACCGTTCCAGTTT-3', yielding a 249 bp product. The primers used for rat/mouse  $\beta$ -actin cDNA had the following sequence: sense, 5'-AGAGGGAAATCGTG CGTGACA-3', antisense, 5'-CACTGTGTTGGCATA GAGGTC-3', yielding a 279 bp product.

All PCR products were size fractionated on 2.5% NuSieve agarose and 1% agarose gel (FMC Bioproducts, Rockland, ME, USA), stained with ethidium bromide, and band locations were recorded by photographing them under ultraviolet light. Size standards of DNA were run in parallel (pBR322 DNA MSP I digest; New England Biolabs, Beverly, MA, USA).

#### Nucleotide sequencing

Besides the use of appropriate negative and positive controls, unequivocal proof for the authenticity of renal EPO-R transcripts was obtained by subcloning and sequencing of the respective PCR products. Accordingly, PCR products generated with the species-specific first

and second EPO-R primer sets (Fig. 1) from HCT and MCT mRNAs were subcloned (pCR 3.1 vector; Original TA Cloning Kit; Invitrogen, San Diego, CA, USA). The obtained subclones then underwent automated fluorescent DNA sequencing at the University of Utah Core Sequencing Facility.

#### Erythropoietin binding to cells

Cells were grown to subconfluence, as described earlier here, and were mechanically harvested. They were then washed at 4°C for three minutes with 0.5 M NaCl and 0.25 M acetic acid (pH 2.5) in order to remove EPO bound to the cell surface [12] and were washed twice more with PBS (pH 7.3). Binding assays were carried out by placing approximately  $1 \times 10^6$  cells in an incubation mixture, containing PBS with 0.1% bovine serum albumin, 0.1% NaN<sub>3</sub>, to inhibit internalization, and a 200-fold excess of recombinant human erythropoietin (rHuEPO) in a total volume of 170  $\mu$ L. <sup>125</sup>I-rHuEPO (specific activity 948 Ci/mmol; Amersham, Arlington Heights, IL, USA) was added to cell aliquots in increasing concentrations (40 to 620 pM) and was incubated for three hours at 15°C. The cells were then pelleted and washed three times with 200  $\mu$ L of ice-cold PBS, and cell-associated radioactivity was measured with a gamma counter. By measuring the difference in radioactivity when cells were incubated either in the presence or in the absence of 200-fold excess unlabeled EPO (recombinant human EPO; Amgen, Royal Oaks, CA, USA), the amount of specific EPO binding was determined. Assay conditions were designed to keep total EPO binding (specific plus nonspecific) below 10% of the total amount of radioligand added. To obtain  $K_d$  and  $B_{max}$ , both linear Scatchard [26] and nonlinear (GraphPad Software, Inc., San Diego, CA, USA) regression analyses of the equilibrium-binding data were performed. The time course of ligand binding was determined by incubating <sup>125</sup>I-rHuEPO at a concentration of 620 pM with approximately  $1 \times 10^6$  cells at 15°C for four hours. To test whether specific EPO binding has a linear correlation with the number of cells used, increasing numbers of cells, from 0 to  $9 \times 10^6$ , were incubated with <sup>125</sup>I-rHuEPO (620 pM) for three hours at 15°C both in the absence and the presence of 200-fold excess unlabeled EPO.

#### Immunological detection of erythropoietin receptor protein

Murine proximal tubular cells (approximately  $5 \times 10^6$ ), grown in 75 cm<sup>2</sup> flasks, were washed twice with ice-cold PBS and were collected by scraping and centrifuging. The pellet was frozen at -70°C. Spleens from anemic and sham mice were obtained, rinsed free of blood, and frozen at -70°C. Cell membranes from MCTs and spleens were prepared as previously reported [17]. In brief, approximately 50 mg of spleen tissue or  $5 \times 10^6$  MCTs were homogenized in a polytron in 1 mL hypotonic



buffer (50 mM Tris-HCl, pH 7.4, 2 mM  $\text{Na}_2\text{VO}_4$ , 50 mM  $\text{Na}^+$ , 10 mM  $\text{Na}_2\text{P}_2\text{O}_7$ , 1 mM phenylmethylsulfonyl fluoride), and incubated for 30 minutes at 4°C. The sample was centrifuged at 4°C for 20 minutes at  $6000 \times g$ . Membrane proteins in the pellet were extracted over 60 minutes at 4°C with lysis buffer (PBS containing 5 mM ethylenediaminetetraacetic acid, pH 7.4, 1% Triton X-100, 0.5 mM phenylmethylsulfonyl fluoride). Following centrifugation for 20 minutes at  $6000 \times g$  at 4°C, the supernatant, containing cell membrane protein, was collected.

These cell membrane protein preparations from spleen and MCTs were then immunoprecipitated by adding 10  $\mu\text{l}$  of an affinity-purified antibody directed against the C-terminus of the murine EPO-R (Santa Cruz Biotechnology, Santa Cruz, CA, USA). This mixture was incubated overnight at 4°C. Protein A/G Plus-Agarose (Santa Cruz Biotechnology) was then added, and the mixture was incubated for another three hours at 4°C. After four washes in lysis buffer, the pelleted agarose antibody complex was suspended in 40  $\mu\text{l}$  2  $\times$  Laemmli's sample buffer and heated at 100°C for four minutes prior to electrophoresis on 9% sodium dodecyl sulfate-polyacrylamide gel, as previously reported [27, 28]. The separated protein bands were then electrophoretically transferred to Hybond-P membrane (Amersham). These were incubated for two hours at room temperature in a mixture of blocking buffer (TBS-T: 10 mM Tris-buffered saline, pH 8.0, 0.1% Tween 20) and 5% nonfat powdered milk in order to prevent binding to nonspecific sites. A 1:1000 dilution of the primary antibody in blocking buffer was then added to the membranes, and they were incubated at room temperature for 45 minutes. After three washes in TBS-T, the second antibody was added (1:1000 dilution of a horseradish peroxidase-conjugated anti-rabbit IgG), followed by a one-hour incubation at room temperature. After four washes in TBS-T, the protein bands were made visible, using a chemiluminescence detection system (ECL, Amersham) and recorded on radiographic film as previously reported [27].

The specificity of anti-EPO-R antibody binding by MCT protein extracts was further assessed by reacting the primary blots, prepared as described earlier here, with a 1:1000 dilution of primary antibody that had been neutralized (17 hours at 4°C) with a 10-fold (by mass) excess of EPO-R antigen (C-terminal peptide; Santa Cruz Biotechnology). The remaining steps of the immunodetection protocol were then performed as described earlier here.

#### DNA synthesis

Cells were grown in 24-well plates. Once attached and subconfluent, the cells were serum deprived for 24 hours. The effect of EPO on DNA synthesis, determined by [ $^3\text{H}$ ]-thymidine incorporation, was assessed by incubat-

ing the cells for 20 additional hours with varying concentrations of EPO or 10% NCS. The cells were then pulsed with 0.5  $\mu\text{Ci}$  [ $^3\text{H}$ ]-thymidine (specific activity 70 to 90 Ci/mmol; New England Nuclear, Boston, MA, USA) and incubated for four more hours before being washed with 750  $\mu\text{l}$  cold PBS and again with cold 5% trichloroacetic acid. Next, 750  $\mu\text{l}$  of 0.25 M NaOH in 0.1% sodium dodecyl sulfate were added for 30 minutes in order to solubilize proteins. Radioactivity was determined by scintillation counting, with counts expressed as cpm per microgram of protein. Protein was measured by the BCA Protein Assay (Pierce, Rockford, IL, USA).

#### Cell proliferation

All tested cells were seeded at  $1 \times 10^4$  per well in 96-well plates and allowed to attach overnight in appropriate serum-containing media. Cells were made quiescent by incubation in serum-free media for 24 hours. Newborn calf serum (10%) or EPO, at incremental concentrations, was then added, and the incubation was continued for 48 hours. At this time, media were removed and replaced with fresh media (without phenol red and serum) containing 5 mg/ml MTT [3-(4,5-dimethylthiazol-2-yl)-2,5-diphenyltetrazolium bromide; Thiazolyl blue; Sigma] and cells were incubated at 37°C for an additional three hours. After this, the media were removed, and 100  $\mu\text{l}$  of 0.04 N HCl in isopropanol were added to each well in order to solubilize the blue MTT reduction product formed in viable cells. The absorbance was read on a microplate reader at 570 nm with background subtraction at 650 nm. Media D-glucose concentration at the time of the MTT assay was well maintained, thus preventing an underestimation of cell numbers [29]. In addition, cell proliferation was assessed by hemocytometer counting of trypsinized cells. There was an excellent linear correlation ( $r = 0.99$ ) between cell counts and results obtained by the MTT assay.

#### Data reporting and statistical analysis

All data on rat and human tissues and individual cell lines are representative of at least three to six replications or independent experiments, respectively. Data are reported as means  $\pm$  SE. Differences between data means were analyzed for statistical significance ( $P < 0.05$ ) using Student's *t*-test for paired and independent populations, as well as analysis of variance [30]. Apparent  $K_d$  and  $B_{\text{max}}$  values for  $^{125}\text{I}$ -EPO binding were derived by both linear Scatchard [26] and nonlinear (GraphPad Software) regression analyses of the equilibrium-binding data.

## RESULTS

### Erythropoietin receptor transcripts in human and rat kidney

Figure 2 shows ethidium bromide-stained agarose gels of EPO-R PCR products obtained from normal human

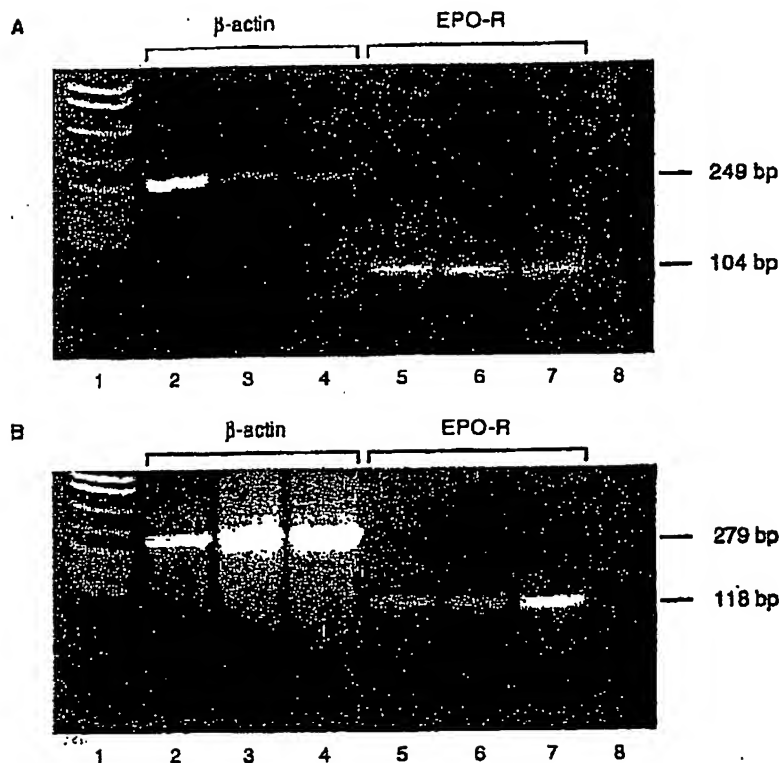


**Fig. 2.** Erythropoietin receptor (EPO-R) transcripts in human and rat kidney. (A) Ethidium bromide-stained gel shows the expected 104 bp EPO-R PCR products (first primer set in Fig. 1) from human renal cortex (lane 5), medulla (lane 6), and papilla (lane 7). The first lane shows a DNA ladder. Lanes 2 through 4 show the corresponding 249 bp β-actin PCR products, and lane 8 demonstrates that deletion of the RT reaction prevents subsequent formation of PCR products (tested on papilla, lane 7). (B) Ethidium bromide-stained gel shows the expected 118 bp EPO-R PCR products (first primer set in Fig. 1) from rat renal cortex (lane 5), medulla (lane 6), and papilla (lane 7). Other lane explanations as in (A).

(Fig. 2A) and rat (Fig. 2B) kidney. The bands in lanes 5 (cortex), 6 (medulla), and 7 (papilla) of Figure 2A represent the expected 104 bp PCR products of the human EPO-R cDNA. The first lane shows DNA size standards, and lane 8 demonstrates that deletion of the reverse transcription step yields no detectable PCR product in papillary tissue (lane 7). The bands in lanes 2 through 4 represent the 249 bp β-actin PCR products from cortex, medulla, and papilla, respectively. Bands of comparable intensity were obtained with the other two primer sets, yielding expected PCR products of 240 bp and 372 bp. Human fetal liver served as the positive control; it yielded identical PCR products (104, 240, and 372 bp) as shown in Figure 3A.

Figure 2B depicts, in lanes 5 (cortex), 6 (medulla), and 7 (papilla), the expected 118 bp PCR products of the rat EPO-R cDNA, and lanes 2 through 4 show the corresponding 279 bp β-actin PCR product from renal cortex, medulla, and papilla, respectively. The first lane shows DNA size standards, and lane 8 demonstrates that deletion of the reverse transcription step yields no detectable PCR product in papillary tissue (lane 7). Bands of similar intensity were obtained with the other primer set, yielding the expected PCR product of 219 bp. Spleen from anemic mice served as positive control (Fig. 3B); it

yielded PCR products of predicted sizes (118 and 219 bp for EPO-R; 279 bp for β-actin), whereas rat myocardium showed no EPO-R message (Fig. 3C).

#### Erythropoietin receptor transcripts in renal cells

Because the renal circulation may contain erythroid progenitor cells that express EPO-Rs and because the kidney is composed of vascular, interstitial, glomerular, and distinct tubular cells, we next screened for the presence of EPO-R message in defined renal cell lines grown in culture. Figure 4A shows the data from HCTs and HMCs. Bands in lanes 4, 6, and 8 depict the expected 104, 240, and 372 bp products of the human EPO-R in HCT cells. Bands in lanes 5, 7, and 9 show the corresponding signals from HMCs. In lane 1 DNA size standards and in lanes 2 and 3, the respective 249 bp β-actin signals are depicted. Figure 4B shows the data from HMCs. Lane 2 shows the β-actin signal, and lanes 3 through 6 show the EPO-R PCR products of expected sizes (372 bp, 240 bp, and 104 bp). Figure 5A confirms that EPO-R transcripts from human erythroleukemia cells (OCIM 1) are comparable to those obtained in renal cells (positive control: bands in lanes 3, 4, and 5 represent EPO-R PCR products, lane 1 DNA size standards, and lane 2 β-actin signal, respectively), whereas no such mes-

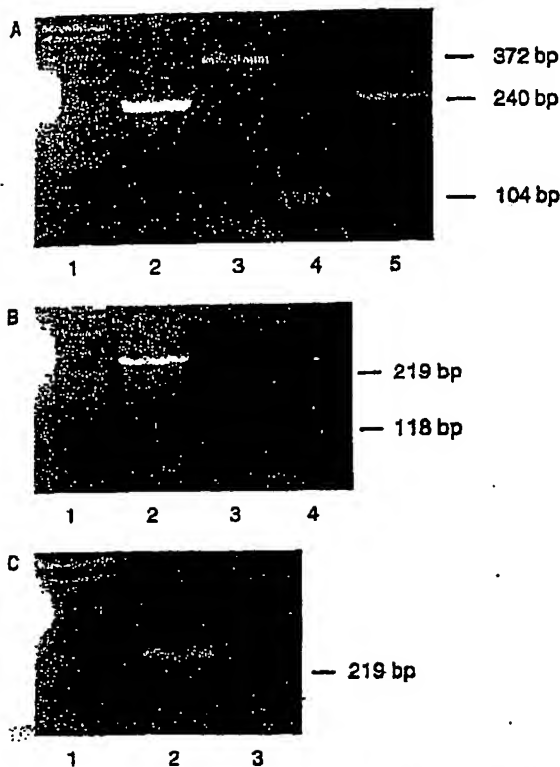


Fig. 3. EPO-R transcripts in human, mouse, and rat control tissues. (A) Fetal human liver verified as a positive control. Gel shows the EPO-R PCR products obtained with the three primer sets (Fig. 1): 372 bp (lane 1), 240 bp (lane 4), and 240 bp (lane 5). Lane 1 depicts a DNA ladder, lane 2 the 240 bp  $\beta$ -actin signal. (B) Anemic mouse spleen (positive control). Gel shows the EPO-R PCR products obtained with the two mouse/rat primer sets (Fig. 1): 219 bp (lane 3) and 118 bp (lane 4). Lane 1 depicts a DNA ladder, and lane 2 shows the 279 bp  $\beta$ -actin signal. (C) Rat myocardium (negative control). EPO-R expression (219 bp PCR product) was not detected (lane 3). Lane 1 depicts a DNA ladder and lane 2 the 279 bp  $\beta$ -actin signal.

message is detected in HeLa cells (negative control: lane 7 shows no 372 bp EPO-R PCR product; lane 6 is the  $\beta$ -actin signal). Together, these data demonstrate that HCTs, collecting duct, as well as glomerular mesangial cells express EPO-R mRNA.

Figure 4C depicts corresponding data from MCTs and RMCs. Bands in lanes 4 and 6 represent the expected 118 bp and 219 bp PCR products of the mouse EPO-R in MCTs. Bands in lanes 5 and 7 represent those from RMCs. Bands in lanes 2 and 3 represent the respective  $\beta$ -actin signals, and lane 1 shows DNA size standards. Figure 5B confirms that EPO-R transcripts from murine erythroleukemia cells (HCD 57, positive control) are comparable to those obtained in renal cells. Lanes 3 and 4 show 118 bp and 219 bp EPO-R PCR products, lane 1 DNA size standards, lane 2  $\beta$ -actin signal), whereas no

EPO-R message is detected in NIH 3T3 cells (negative control: lanes 6 and 7 correspond to lanes 3 and 4, and lane 5 represents  $\beta$ -actin). Collectively, these data demonstrate that murine proximal tubular and rat glomerular mesangial cells express EPO-R mRNA.

#### Sequencing of EPO-R cDNA

To directly show that the PCR products derived from renal cells represent authentic EPO-R message, generated cDNAs were subcloned, and their sequences were analyzed. Thus, sequencing of EPO-R cDNAs generated from HCT mRNA, using both set 1 (104 bp, exons V and VI) and set 2 (240 bp, exons VII and VIII) of PCR primers (Fig. 1; Methods section), yielded results identical to published EPO-R DNA sequences [19]. The sequences of cDNAs generated from MCTs and rat kidney cortex by set 1 (219 bp, exons II and III; Fig. 1; Methods section) and set 2 (118 bp) of primer pairs specific to rat/mouse EPO-R were also identical to published EPO-R DNA sequences [20]. These data prove unequivocally that HCTs and MCTs as well as rat kidney cortex express authentic EPO-R transcripts.

#### Specific erythropoietin binding to cell surface and immunologic detection of erythropoietin receptor protein

In MCTs and HCTs, and in HMCDs, specific binding of  $^{125}$ I-EPO to cell surface EPO-R was examined. Figure 6A shows equilibrium binding data in MCTs. Specific binding of  $^{125}$ I-EPO in these cells occurred to a single class of high-affinity receptors ( $K_d$   $96.1 \pm 6.1$  pM;  $B_{max}$   $0.3 \pm 0.07$  fmol/mg protein;  $N = 3$ ), and binding became saturated over time (Fig. 6B). Nonlinear and Scatchard analyses yielded comparable results. There was excellent linear correlation ( $r = 0.99$ ) between specific ligand binding in tested cell lines and cell numbers. The apparent  $K_d$  in HCT cells was  $1.1 \pm 0.1$  nM and  $B_{max}$   $1.6 \pm 0.2$  fmol/mg ( $N = 3$ ), and in HMCDs ( $N = 3$ ) the apparent  $K_d$  was  $1.3 \pm 0.2$  nM and  $B_{max}$   $7.0 \pm 0.8$  fmol/mg protein.

Western blots for EPO-R protein (Fig. 7) were generated after initial immunoprecipitation of MCT and mouse spleen cell membrane protein with anti-EPO-R antibody. Lane 1 on Figure 7A shows a representative Western blot from MCTs. Two immunoreactive protein bands of approximate molecular mass of 68 and 90 kDa, respectively, are identified. When anti-EPO-R antibodies were first neutralized with an excess of specific antigen (C-terminal EPO-R peptide; Methods section), no EPO-R-specific immunoreactivity was detected (lane 2). Lane 3 shows molecular weight standards. These data imply that the detected bands possess EPO-R-specific antigenicity. As positive control, spleen cell membrane proteins from anemic mice were utilized. In these, immunoreactive protein bands of comparable molecular mass

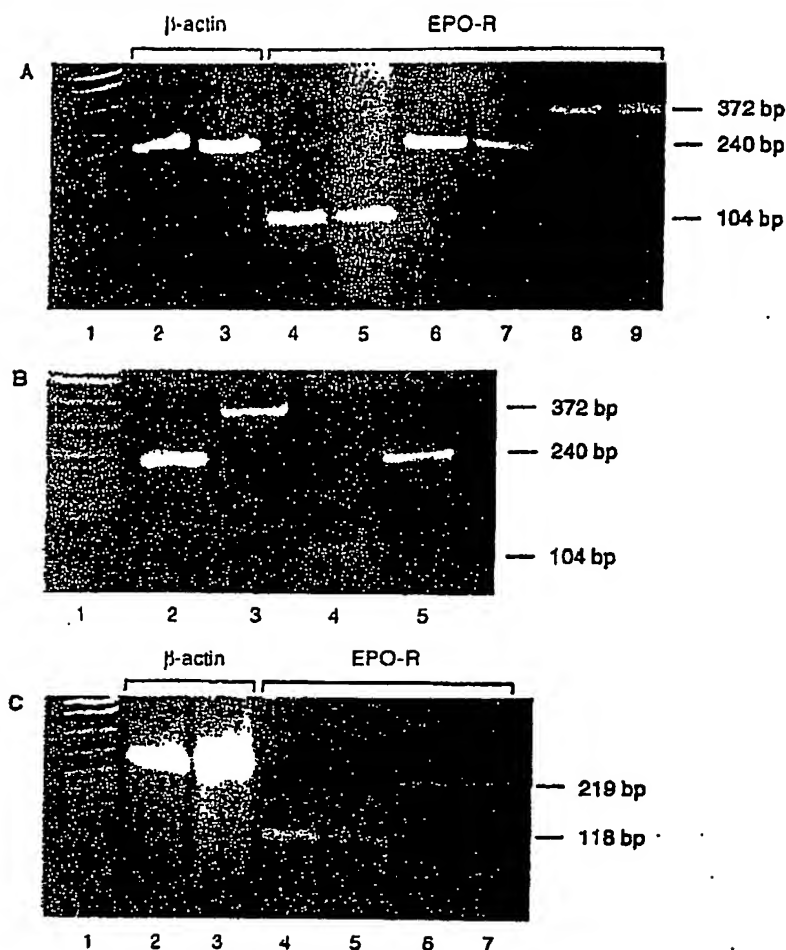


Fig. 4. EPO-R transcripts in renal cells. (A) Human proximal tubular and mesangial cells. Gel shows in lanes 4, 6, and 8 the expected 104, 240, and 372 bp PCR products of the human EPO-R in proximal tubular cells (HCT), and in lanes 5 and 9 those in mesangial cells (HMC). The first lane shows a DNA ladder, lanes 2 and 3, the 249 bp  $\beta$ -actin signals from HCT and HMC, respectively. (B) Human medullary collecting duct cells. Gel shows all three EPO-R PCR products (lanes 3 through 5, 372, 104, 240 bp), a DNA ladder (lane 1) and  $\beta$ -actin signal (lane 2). (C) Mouse proximal tubular and rat mesangial cells. Lanes 4 and 6 depict the expected 118 and 219 bp PCR products of the EPO-R in mouse proximal tubular (MCTs), and lanes 5 and 7 those in rat mesangial cells (RMCs), respectively. Lane 1 shows a DNA ladder and lanes 2 and 3 the corresponding 279 bp  $\beta$ -actin signals for each cell line.

(68 and 90 kDa) were identified (lane 2 on Fig. 7B); however, the 68 kDa protein was not detected in normal spleen (lane 1), whereas the 90 kDa band was detectable both in normal and anemic spleens (lanes 1 and 2). This pattern suggests that the 68 kDa protein likely represents the EPO-R, because anemia stimulates the accumulation of erythroid progenitor cells in the spleen, that is, cells that express the EPO-R [8]. Lane 3 shows molecular weight standards.

#### Mitogenic action of erythropoietin in MCTs

Figure 8A shows that EPO dose dependently stimulates DNA synthesis in MCTs. Figure 8B shows that 48 hours after EPO was added, MCT proliferation was stimulated significantly and dose dependently. This proliferative response was smaller but also evident 24 hours after EPO addition. The addition of 10% NCS to quiescent MCTs served as the positive control.

#### DISCUSSION

The unique anatomical relationship between EPO-producing interstitial fibroblasts and adjacent tubular cells [1, 6] prompted us to ask whether renal cells possess biologically active EPO-Rs that would enable them to respond to EPO. In our examination of human and rat kidney as well as various renal cell lines, we detected authentic, species-specific EPO-R expression at both the transcriptional and the translational level, a single class of moderate- to high-affinity EPO-Rs, and specific, dose-dependent, mitogenic activity of EPO *in vitro*. These findings, when considered as a whole, make this the first study, to our knowledge, to demonstrate conclusively that renal cells in culture possess functional EPO-Rs through which EPO can elicit mitogenic and possibly other cytokine actions. We are currently investigating how these initial *in vitro* observations may apply to the biology of the normal and diseased kidney.

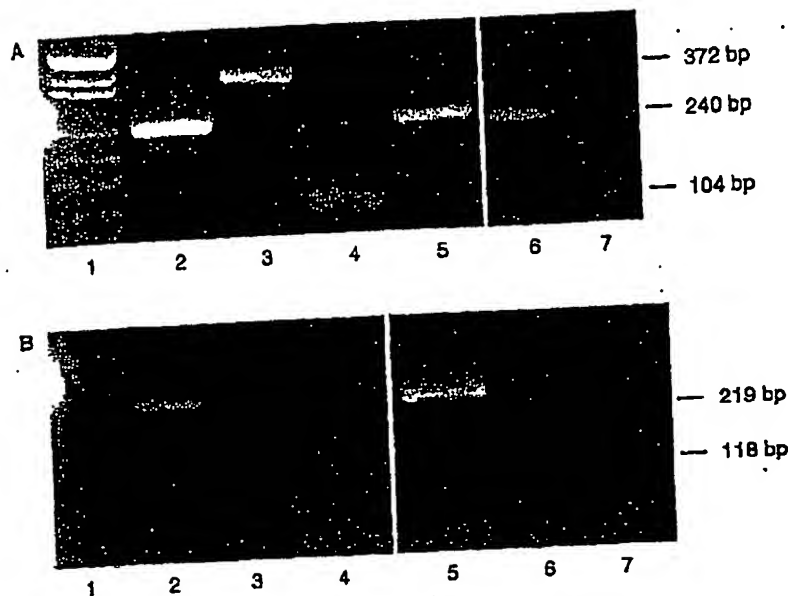


Fig. 5. EPO-R transcripts in control cells. (A) Human cells. In OCIM 1 cells (positive control), all three EPO-R PCR products are detected (lanes 3 through 5, 372, 240, 104 bp). Lane 1 shows a DNA ladder and lane 2 the  $\beta$ -actin signal. In HeLa cells (negative control), no EPO-R message (lane 7, 240 bp) is detected. Lane 6 represents  $\beta$ -actin message. (B) Mouse cells. In HCD 57 cells (positive control), two EPO-R PCR products are shown (lanes 3 and 4, 219 bp, 118 bp). In NIH 3T3 cells (negative control), corresponding EPO-R message is not detected (lanes 6 and 7). Lane 1 shows DNA ladder, and lanes 2 and 5 show  $\beta$ -actin from respective cell lines.

Given our findings, one would expect that clinically occurring or experimentally induced alterations in renal EPO production *per se* would result in detectable changes in renal structure and function. Chronic anemias that are not caused by sickle cell disease or other hemolytic disorders have not been reported to cause significant tomical or functional changes in the kidney [31]. This indicate that elevated EPO levels cause down-regulation of EPO-R expression in the kidney or that the trophic effects of EPO are suppressed by counteracting factors or that renal histology and function in such conditions have not been specifically examined. Severe, more acute anemia induced in rats was shown to lead to significant injury in S1 segments of proximal tubular cells and additional morphological changes in the interstitium of the cortical labyrinth [32]. Whether the associated increase in EPO production influenced the observed histologic picture or renal function in this study is not known.

Acquired renal cysts may be another condition in which EPO's renotrophic effects could be significant. Although cyst fluid is often found to contain increased levels of EPO [33], it is unknown whether cyst growth is, at least in part, the result of EPO's growth-promoting capability or whether the latter contributes to the increased incidence of renal cell carcinomas noted in these patients. Similarly, a significant percentage of patients with autosomal dominant polycystic kidney disease and end-stage renal failure has relatively normal EPO and hematocrit levels [34], and renal cyst fluid has also been found to be rich in EPO [35]. Again, it is unexplored

whether EPO's proliferative actions do, in fact, stimulate cystogenesis in this condition. Finally, a small percentage of patients with renal cell carcinoma produces increased amounts of EPO [36]. Preliminary data from our laboratory demonstrate that EPO stimulates mitogenesis in human and rat renal carcinoma cell lines, raising the concern that the administration of EPO for the treatment of anemia could conceivably hasten the growth of some renal malignancies.

Only one study published to date has shown that EPO treatment of rats with *cis*-platinum-induced acute renal failure enhances functional recovery [37]. Because most forms of acute renal failure caused by acute tubular necrosis are associated with a transient depression of renal EPO synthesis [38-40], EPO replacement may thus serve to hasten the repair of the injured kidney.

Recent work on the biological functions of EPO in nonerythroid cells has demonstrated that vascular endothelial cells express EPO-Rs and that EPO acts in these as a mitogen and a motogen [9, 10], as vasoconstrictor and activator of angiogenesis, in part via induction of endothelin-1 [41, 42]. We reported that incubation of vascular endothelial cells with EPO causes significant changes in the expression of immediate early response genes (*c-jun*, *c-myc*) and the genes of several vasoactive peptides (atrial, brain, and C-type natriuretic peptide, and endothelin-1) [43]. These findings reconfirm the ability of vascular endothelial EPO-Rs to transmit mitogenic and other transactivating signals. It was recently reported that EPO increases  $Ca^{2+}$  influx in glomerular mesangial cells [17], a response previously observed in vascular

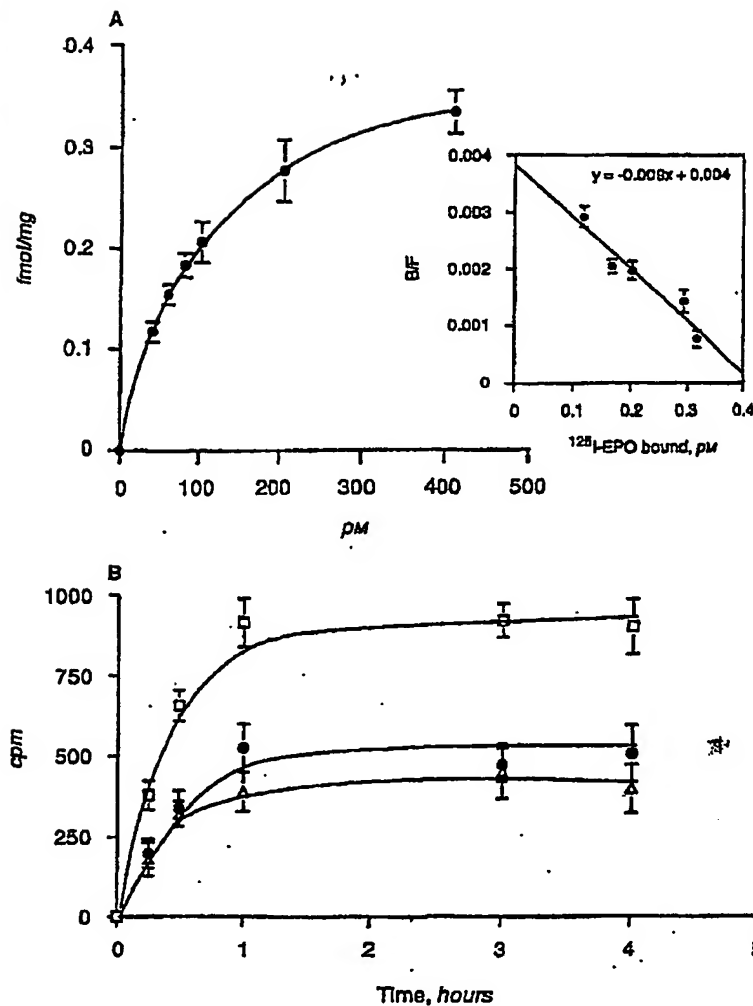


Fig. 6. Specific  $^{125}\text{I}$ -EPO binding in murine proximal tubular cells (MCTs). (A) Equilibrium binding curve and Scatchard plot (insert) of  $^{125}\text{I}$ -rhEPO binding in MCTs (means  $\pm$  se). Apparent  $K_d$  derived by Scatchard or nonlinear analysis, was  $96.1 \pm 6.1$  pM ( $N = 3$ ).  $B_{\text{max}}$  was  $0.3 \pm 0.07$  fmol/mg protein; there was only a single class of high-affinity receptors. (B) Time dependence of total ( $\square$ ), nonspecific ( $\Delta$ ), and specific  $^{125}\text{I}$ -EPO binding ( $\bullet$ ) to MCTs (means  $\pm$  se). Binding, assessed at 0.25, 0.5, 1, 2, 3, and 4 hours, reached a plateau at approximately 2 hours.

smooth muscle cells [44]. This response occurs via an EPO-R-operated  $\text{Ca}^{2+}$  channel, which, in turn, is activated by tyrosine phosphorylation of phospholipase C- $\gamma$ 1. This mechanism may be an additional explanation for the ability of EPO to generate clinical hypertension.

In neuronal cells, EPO-Rs have been located and were found to increase intracellular calcium and protect against glutamate neurotoxicity [12, 13, 16, 45]. It appears that some of the *in vitro* functions of EPO in Leydig cells, placental endothelial cells, and gastric epithelial cells are also found *in vivo* [11, 14, 15].

Specific binding of EPO to cultured renal cells occurred to a single class of receptors and with relatively low  $B_{\text{max}}$  values, a pattern also found in erythroid progenitor and other nonerythroid cells [8]. Binding affinity was

highest in MCTs ( $K_d$  approximately 96 pM), intermediate in HCTs ( $K_d$  approximately 1.1 nM), and low in HMCs ( $K_d$  approximately 1.3 nM). Serum levels of EPO under nonanemic and nonhypoxic conditions are between 5 and 35 mU/ml, that is, in the low picomolar range [1]. These concentrations are well below the  $K_d$  values we identified in cultured renal cells. Although not known, it appears conceivable that EPO concentrations in the interstitium of the renal cortical labyrinth, that is, in the immediate vicinity of EPO secreting and adjacent tubular cells exceed those seen in the periphery. These higher local concentrations of EPO may, in turn, be sufficient to activate EPO-Rs *in vivo*. Furthermore, ambient EPO concentrations in the kidney can be dramatically increased by tissue hypoxia or the administration



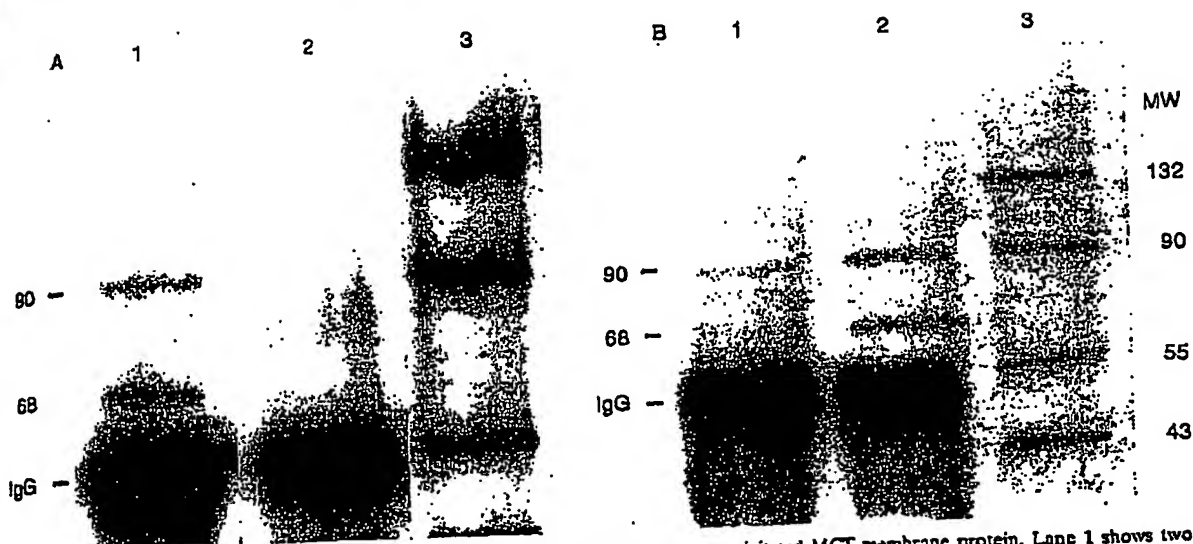


Fig. 7. Immunodetection of EPO-R protein in MCT. (A) Western blots of immunoprecipitated MCT membrane protein. Lane 1 shows two EPO-R immunoreactive bands of approximate molecular mass of 68 and 90 kDa, respectively. Lane 2 demonstrates that preincubation of anti-EPO-R antibody with excess EPO-R antigen prevents the detection of EPO-R proteins, confirming immunospecificity of the anti-EPO-R antibody. Lane 3 shows molecular weight markers. (B) Western blots of immunoprecipitated mouse spleen cell membrane protein. Lane 1 shows immunoreactive bands of approximate molecular mass of 68 and 90 kDa, respectively. These were obtained from anemic animals. Lane 2 shows no immunoreactive bands from nonanemic mouse spleen. In these, no 68 kDa protein was detected, whereas the 90 kDa band remained detectable, thus suggesting that the smaller protein represents the EPO-R. Lane 3 shows molecular weight markers.

of recombinant EPO [1]. Under these circumstances, even if EPO-R-binding affinities and surface expression were as low as those found in this *in vitro* study, EPO-R activation could occur. An additional factor in this regard may be the surface distribution of EPO-Rs. Renal tubular cells, distinct from erythroid progenitor cells, grow in polarized monolayers. A large number of hormone and cytokine receptors in tubular cells are concentrated on their basolateral side [46]. If EPO-Rs in tubular cells were likewise preferentially expressed in a basolateral distribution, their endocrine or paracrine stimulation *in vivo* would be facilitated, whereas *in vitro* activation may be difficult. Under the latter culture conditions, apically added EPO may not reach basolaterally located EPO-Rs in concentrations sufficient to initiate a physiologic response. These possibilities await investigation. Finally, the as yet undefined expression pattern and ligand-binding kinetics of the EPO-R in the kidney, whether regulated, constitutive, or altered by pathologic conditions, are expected to modify biological responses to EPO further.

We detected in murine proximal tubular cells two EPO-R immunoreactive proteins of approximately 68 and 90 kDa, respectively (Fig. 7). The cloned murine EPO-R cDNA encodes a 55 kDa polypeptide, and the EPO-R is post-translationally modified by N-linked glycosylation and phosphorylation, increasing its mass to 78 kDa and above [47, 48]. The 68 kDa protein that we consistently detected in MCTs and in anemic mouse

spleen was also found in HCD 57 cells (not shown). This moiety of EPO-R has been previously described in the latter cells [22], strongly suggesting that MCTs express this receptor protein as well. The fact that experimental anemia induced the expression of the 68 kDa protein, whereas it only modestly affected that of the 90 kDa protein, supports the notion that the former is likely the EPO-R. The exact nature of the 90 kDa protein requires additional investigation.

The mitogenic response elicited by EPO was dose dependent and specific. It was, not unexpectedly, less in magnitude than that elicited by 10% NCS (Fig. 8) and became most prominent after 48 hours of incubation, a pattern also observed when MCTs are stimulated with other growth factors [20]. Although it remains to be proven, it is conceivable that EPO stimulates mitogenesis in renal cells not only through its own receptor but also via as yet unidentified mediators or pathways. Such indirect action has recently been reported in vascular endothelial cells, in which EPO stimulates angiogenesis, at least in part, via induction of endothelin-1 synthesis [41, 42].

It is of note that cells of the neuronal type express EPO-Rs on their surface but fail to undergo mitosis when exposed to EPO [12]. Vascular endothelial and gastric mucosal cells, by contrast, proliferate when exposed to EPO through mitogenic signals transmitted by its receptor, as well as through induction of endothelin-1 synthesis



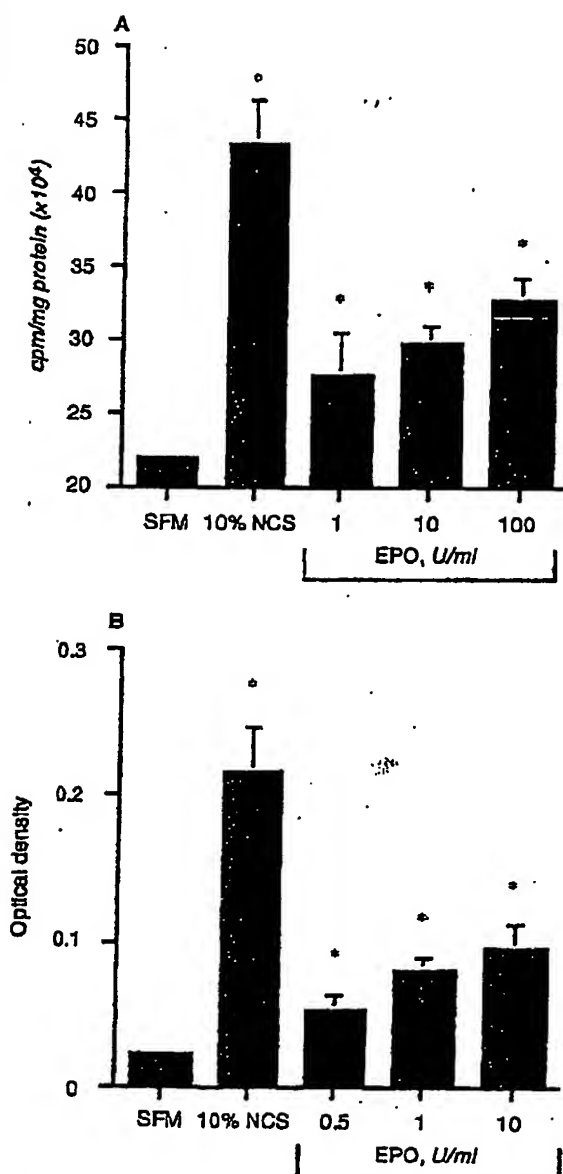


Fig. 8. DNA synthesis and cell proliferation in response to EPO in MCTs. (A) DNA synthesis in quiescent MCTs, assessed by [ $^3$ H]thymidine incorporation, was stimulated by EPO dose dependently and significantly. Ten percent NCS served as positive control. \* $P < 0.05$  compared with quiescent control cells (first column). (B) Cell proliferation in response to EPO in quiescent MCTs. EPO increased cell numbers dose dependently and significantly (after 48 hours of incubation). Ten percent NCS served as positive control. Abbreviations are: MCTs, murine proximal tubule cells; EPO, erythropoietin; NCS, newborn calf serum; SFM, serum free media; \* $P < 0.05$  compared with quiescent control cells (first column).

in the former [9, 10, 15, 40, 41]. Although we show that EPO acts as a mitogen in renal cells, it is very unlikely that renal cells depend exclusively on EPO for their *in vitro* or *in vivo* growth or survival. Erythroid progenitor cells, at certain stages, depend for growth and survival on EPO and in addition on interleukin-3, insulin-like growth factor-I, stem cell factor, and other cytokines [1, 8, 49]. Some of the same growth factors, for example, insulin-like growth factor-I, but also epidermal growth factor and hepatocyte growth factor, act as mitogens and survival factors when the kidney is injured as in acute tubular necrosis [50]. Following toxic or ischemic tubular injury, adaptive increases in cytokine or cytokine receptor expression or the administration of renotropic growth factors appear to aid the tubular repair process by stimulating cell proliferation and inhibiting apoptosis [50]. It is conceivable that EPO elicits analogous effects in acute tubular necrosis, as was suggested by Vaziri, Zhou and Liao [37].

In summary, we have shown that cortex, medulla, and papilla of both human and rat kidney express species-specific EPO-R mRNAs. More specifically, authentic EPO-R transcripts are expressed in HCTs and MCTs, HMCs, RMCs, and HMCDs. EPO binding occurs to a single class of receptors. EPO-R protein has been identified in mouse proximal tubular cells, and in these, EPO stimulates DNA synthesis and cell proliferation. In conclusion, our data show that EPO acts *in vitro* as a renotropic mitogen and that the expression of authentic EPO-R, a member of the cytokine receptor superfamily [51], in renal tubular and mesangial cells and in kidney cortex, medulla, and papilla has allowed us to identify the critical system through which endocrine and paracrine actions of EPO may be elicited. Although its functions *in vivo* remain to be identified, EPO may play a role in renal development, cell survival, cell proliferation, cell migration, and differentiation.

#### ACKNOWLEDGMENTS

This work was funded by grants from the Department of Veterans Affairs Merit Review Program and from the Dialysis Research Foundation, Ogden, Utah, USA. Portions of this work have been presented at the XIVth Congress of the International Society of Nephrology, Sydney, Australia, May 1997; the 10th Symposium on Molecular Biology of Hemopoiesis, Hamburg, Germany, June 1997; and the Annual Meeting of the American Society of Nephrology, Austin, TX, November 1997. The technical assistance of Ms. Monica Stevens is gratefully acknowledged. We thank Drs. E. Nielson for the MCTs, K. Ward and T. Morgan for technical advice and human fetal liver mRNA, D. Terreros for human kidney tissue, G. Boulger for genomic DNA from human prostate, D.E. Kohan for human proximal tubular, collecting duct, and glomerular mesangial cells, and S.T. Sawyer for HCD 57 cells.

Reprint requests to Christof Westenfelder, M.D., Section of Nephrology (111 N), VA Medical Center, 500 Foothill Boulevard, Salt Lake City, Utah 84143, USA.  
E-mail: Westenfelder@polnet

## APPENDIX

Abbreviations used in this article are: EGF, epithelial growth factor; EPO, erythropoietin; EPO-R, erythropoietin receptor; HCT, human proximal tubule cells; HMC, human mesangial cells; HMCD, human medullary collecting duct cells; IGF, insulin-like growth factor; MCT, murine tubular cells; MTT, 3-(4,5-dimethylthiazol-2-yl)-2,5-diphenyltetrazolium bromide; NCS, newborn calf serum; OCIM, human erythroleukemia cell line; PBS, phosphate buffered saline; rHuEPO, recombinant human erythropoietin; RMC, rat mesangial cells; RT-PCR, reverse transcription-polymerase chain reaction.

## REFERENCES

1. JANTZ S: Erythropoietin. *Blood* 77:419-434, 1991
2. LACOMBE C, DA SILVA J, BRUNEVAL P, FOURNIER J, WENDLING F, CASADEVALL N, CAMILLERI J-P, BARIETY J, VARET B, TAMBOURIN P: Peritubular cells are the site of erythropoietin synthesis in the murine hypoxic kidney. *J Clin Invest* 81:620-623, 1988
3. KOURY S, BONDURANT M, KOURY M: Localization of erythropoietin synthesizing cells in murine kidneys by in situ hybridization. *Blood* 71:524-527, 1988
4. BACHMANN S, LE HIR M, ECKARDT K: Colocalization of erythropoietin messenger RNA and ecto-5'-nucleotidase immunoreactivity in peritubular cells of rat renal cortex indicates that fibroblasts produce erythropoietin. *J Histochem Cytochem* 41:335-341, 1993
5. MAXWELL P, OSNOND M, PUGH C, HERYET A, NICHOLLS L, TAN JOE B, FERGUSON D, JOHNSON M, RATCLIFFE PJ: Identification of the renal erythropoietin-producing cells using transgenic mice. *Kidney Int* 44:1149-1162, 1993
6. KRAIZ W, KAISLING B: Structural organization of the mammalian kidney. In *The Kidney: Physiology and Pathophysiology*, edited by SELDIN DW, GIEBISCH G. New York, Raven Press, 1992, pp 707-777
7. ECKARDT KU, KOURY ST, TAN CC, SCHUSTER SJ, KAISLING B, RATCLIFFE PJ, KURTZ A: Distribution of erythropoietin producing cells in rat kidneys during hypoxic hypoxia. *Kidney Int* 43:815-823, 1993
8. YOUSSEFIAN H, LONGMORE G, NEUMANN D, YOSHIMURA A, LODISH HF: Structure, function, and activation of the erythropoietin receptor. *Blood* 81:2223-2236, 1993
9. ANAGNOSTOU A, LEE ES, KESSIMIAN N, LEVINSON R, STEINER M: Erythropoietin has a mitogenic and positive chemotactic effect on endothelial cells. *Proc Natl Acad Sci USA* 87:5978-5982, 1990
10. ANAGNOSTOU A, LIU Z, STEINER M, CHIN K, LEE ES, KESSIMIAN N, NAGUCHI CT: Erythropoietin receptor mRNA expression in human endothelial cells. *Proc Natl Acad Sci USA* 91:3974-3978, 1994
11. SAWYER S, KRANTZ S, SAWADA K: Receptors for erythropoietin in mouse and human erythroid cells and placenta. *Blood* 74:103-107, 1989
12. MASUDA S, NAGAO M, TAKAHATA K, KONISHI Y, GALLIAS FJ, TABARA T, SASAKI R: Functional erythropoietin receptor of the cells with neural characteristics: Comparison with receptor properties of erythroid cells. *J Biol Chem* 268:11208-11216, 1993
13. MORISHITA E, NARITA H, NISHIDA M, KAWASHIMA N, YAMAGISHI K, MASUDA S, NAGAO M, HATTA H, SASAKI R: Anti-erythropoietin receptor monoclonal antibody: Epitope mapping, quantification of the soluble receptor, and detection of the solubilized transmembrane receptor and the receptor-expressing cells. *Blood* 88:465-471, 1996
14. MIDDI R, GOTTARDELLO P, BORDON P, MONTINI G, FORESTA C: Evidence for specific binding and stimulatory effects of recombinant human erythropoietin on isolated adult rat Leydig cells. *Acta Endocrinol (Copenh)* 127:459-465, 1992
15. OKADA A, KINOSHITA Y, MAEKAWA T, HASSAN MS, KAWANAMI C, ASAHARA M, MATSUSHIMA Y, KISHI K, NAKATA H, NARIBAYASHI Y, CHIBA T: Erythropoietin stimulates proliferation of rat cultured gastric mucosal cells. *Digestion* 57:328-332, 1996
16. SAKANAKA M, WEN TC, MATSUDA S, MASUDA S, MORISHITA E, NAGAO M, SASAKI R: In vivo evidence that erythropoietin protects neurons from ischemic damage. *Proc Natl Acad Sci USA* 95:4635-4640, 1998
17. MARRERO MB, VENEMA RC, MA H, LING BN, EATON DC: Erythropoietin receptor-operated  $Ca^{2+}$  channels: Activation by phospholipase C- $\gamma$  1. *Kidney Int* 53:1259-1268, 1998
18. MASUDA S, HISADA Y, SASAKI R: Developmental changes in erythropoietin expression of fetal mouse liver. *FEBS Lett* 298:169-172, 1992
19. KOHAN DE: Endothelin production by human inner medullary collecting duct cells. *J Am Soc Nephrol* 3:1719-1721, 1993
20. HAVERTY TP, KELLY CJ, HINES WH, AMENTA PS, WATANABE M, HARPER RA, KEPALIDES NA, NEILSON EG: Characterization of a renal tubular epithelial cell line which secretes the autologous target antigen of autoimmune experimental interstitial nephritis. *J Cell Biol* 107:1359-1368, 1988
21. EHRENMANN K, ST JOHN T: The erythropoietin receptor gene: Cloning and identification of multiple transcripts in an erythroid cell line OCIM1. *Exp Hematol* 19:973-977, 1991
22. SAWYER ST, PENTA K: Association of JAK2 and STAT3 with erythropoietin receptors: Role of receptor phosphorylation in erythropoietin signal transduction. *J Biol Chem* 271:32430-32437, 1996
23. CHOMCZYNSKI P, SACCHI N: Single-step method of RNA isolation by acid guanidinium thiocyanate-phenol-chloroform extraction. *Anal Biochem* 162:156-159, 1987
24. JONES SS, D'ANDREA AD, HAINES LL, WONG GG: Human erythropoietin receptor: Cloning, expression, and biologic characterization. *Blood* 76:31-35, 1990
25. D'ANDREA AD, LODISH HF, WONG GG: Expression cloning of the murine erythropoietin receptor. *Cell* 57:277-285, 1989
26. SCATCHARD G: The attractions of proteins for small molecules and ions. *Ann NY Acad Sci* 51:660-672, 1949
27. MADDOCK AL, WESTENFELDER C: Urea induces the heat shock response in human neuroblastoma cells. *J Am Soc Nephrol* 7:275-282, 1996
28. LAEMMLI UK: Cleavage of structural proteins during the assembly of the head of bacteriophage T4. *Nature* 227:680-685, 1970
29. VISTICA DT, SKEHAN P, SCUDIERO D, MONKS A, PRITMAN A, BOYD MR: Tetrazolium-based assays for cellular viability: A critical examination of selected parameters affecting formazan production. *Cancer Res* 51:2515-2520, 1991
30. SNEDECOR GW, COCHRAN WG: *Statistical Methods* (6th ed). Ames, Iowa State University Press, 1978
31. ALLON M: Renal abnormalities in sickle cell disease. *Arch Intern Med* 150:501-504, 1990
32. KAISLING B, SMESS S, RUNNE B, LE HIR M: Effects of anemia on morphology of rat renal cortex. *Am J Physiol* 264:F608-F617, 1993
33. FRANEK E, KOKOT P, WIECER A, PAWLOWSKI W, MYRTA J, SZEWCEK W, BAR A: Erythropoietin concentration in cyst fluid in patients with simple renal cysts. *Nephron* 67:431-435, 1994
34. FICK GM, GABOW PA: Hereditary and acquired cystic disease of the kidney. *Kidney Int* 46:951-964, 1994
35. ECKARDT KU, MÜLLMANN M, NEUMANN R, BRUNKHORST R, BURGER HU, LONNEMANN G, SCHOLZ H, KEUSCH G, BUCHHOLZ B, FREI U, BAUER C, KURTZ A: Erythropoietin in polycystic kidneys. *J Clin Invest* 84:1160-1166, 1989
36. DA SILVA J, LACOMBE C, BRUNEVAL P, CASADEVALL N, LEFORNIER M, CAMILLERI JP, BARIETY J, TAMBOURIN P, VARET B: Tumor cells are the site of erythropoietin synthesis in human renal cancers associated with polycythemia. *Blood* 75:577-582, 1990
37. VAZIRI ND, ZHOU XJ, LAO SY: Erythropoietin enhances recovery from cisplatin-induced acute renal failure. *Am J Physiol* 266:F360-F366, 1994
38. WOOD PA, HRUSHESKY WJ: Cisplatin-associated anemia: An erythropoietin deficiency syndrome. *J Clin Invest* 95:1650-1659, 1995
39. NIELSEN OJ, THAYSEN JH: Erythropoietin deficiency in acute tubular necrosis. *J Intern Med* 227:373-380, 1990
40. TAN CC, TAN LH, ECKARDT KU: Erythropoietin production in rats with post-ischemic acute renal failure. *Kidney Int* 50:1958-1964, 1996
41. CARLINI R, DUSSO A, OBIALO C, ALVEREZ U, ROTHSTEIN M: Recombinant human erythropoietin (rHuEPO) increases endothelin-1 release by endothelial cells. *Kidney Int* 43:1010-1014, 1993
42. CARLINI R, REYES A, ROTHSTEIN M: Recombinant human erythropoietin stimulates angiogenesis in vitro. *Kidney Int* 47:740-745, 1995

43. WESTENFELDER C, BRUCE H, BARANOWSKI RL: New biologic actions of erythropoietin in rat vascular endothelial cells. (abstract) *J Am Soc Nephrol* 4:573, 1993
44. NEUSSER M, TAPEL M, SIOZEK W: Erythropoietin increases cytosolic free calcium concentration in vascular smooth muscle cells. *Cardiovasc Res* 27:1233-1236, 1993
45. MORISHITA E, MASUDA S, NAGAO M, YASUDA Y, SASAKI R: Erythropoietin receptor is expressed in rat hippocampal and cerebral cortical neurons, and erythropoietin prevents in vitro glutamate-induced neuronal death. *Neuroscience* 76:105-116, 1997
46. GUNDER WG, MOREL F: Biochemical characterization of individual nephron segments, in *Handbook of Physiology, Section 8: Renal Physiology*, edited by WINDHAGER EE, New York, Oxford University Press, 1992, pp 2119-2164
47. SAWYER ST, HANKINS WD: The functional form of the erythropoietin receptor is a 78-kDa protein: Correlation with cell surface expression, endocytosis, and phosphorylation. *Proc Natl Acad Sci USA* 90:6849-6853, 1993
48. TARR K, WATOWICH SS, LONGMORE GD: Cell surface organization of the erythropoietin receptor complex differs depending on its mode of activation. *J Biol Chem* 272:9099-9107, 1997
49. WATOWICH SS, WU H, SOCOLOVSKY M, KLINGMÜLLER U, C-INCANTANESCU SN, LODISH HF: Cytokine receptor signal transduction and the control of hematopoietic cell development. *Annu Rev Cell Dev Biol* 12:51-123, 1996
50. HAMMERMAN M, MÜLLER S: Therapeutic use of growth factors in renal failure. *J Am Soc Nephrol* 5:1-11, 1994
51. BAZAN JF: A novel family of growth factor receptors: A common binding domain in the growth hormone, prolactin, erythropoietin and IL-6 receptors, and the p75 IL-2 receptor beta-chain. *Biochem Biophys Res Commun* 164:788-795, 1989

# The Expression and Role of Human Erythropoietin Receptor in Erythroid and Nonerythroid Cells

DONNA M. WILLIAMS,<sup>a,b</sup> TERESA A. ZIMMERS,<sup>b</sup>  
JACALYN H. PIERCE,<sup>c</sup> PAMELA N. PHARR,<sup>d</sup>  
ALAN N. SCHECHTER,<sup>b</sup> STEPHEN T. SAWYER,<sup>e</sup>  
SANDRA K. RUSCETTI,<sup>f</sup> JERRY L. SPIVAK,<sup>a</sup>  
AND W. DAVID HANKINS<sup>a,g</sup>

<sup>a</sup>*Department of Medicine  
Division of Hematology  
Johns Hopkins School of Medicine  
Baltimore, Maryland 21205*

<sup>b</sup>*Laboratory of Chemical Biology  
National Institute of Diabetes, Digestive and Kidney Diseases  
National Institutes of Health  
Bethesda, Maryland 20892*

<sup>c</sup>*Laboratory of Chemical and Molecular Biology  
National Cancer Institute  
National Institutes of Health  
Bethesda, Maryland 20892*

<sup>d</sup>*Medical University of South Carolina and  
Veterans Affairs Medical Center  
Charleston, South Carolina 29403*

<sup>e</sup>*Department of Medicine  
Division of Hematology  
Vanderbilt University School of Medicine  
Nashville, Tennessee 37232-2287*

<sup>f</sup>*Laboratory of Molecular Oncology  
National Cancer Institute  
Frederick, Maryland 20702-1201*

## INTRODUCTION

During the past few years, our laboratory has investigated the erythropoietin receptor (EPOR) with regard to its structure-function relationships, role in development, transcriptional regulation, and the mechanism by which it conveys a signal upon interaction with its ligand. We began to focus on the EPOR as the result of three related developments. First, our recent studies indicated that erythropoietin (EPO) functioned as a viability factor rather than as an inducer of erythropoiesis.<sup>1</sup>

<sup>g</sup> To whom correspondence should be addressed.

Second, we isolated and characterized erythroid cell lines exclusively dependent on EPO.<sup>2</sup> Third, the EPOR cDNA was cloned and sequenced.<sup>3</sup>

Our suspicion that EPO may be primarily a permissive, viability factor emanated from our studies in a murine leukemia model. In the mid 1970s, Dr. Charlotte Friend<sup>4</sup> and others reported that the cells transformed by the spleen focus-forming virus (SFFV) had become blocked in erythroid maturation and independent of EPO. Toward understanding the abrogation of EPO requirements by these leukemic cells, we developed a direct hemopoietic precursor transformation system that would permit us to study, *in vitro*, virus-induced changes in the growth and differentiation of hemopoietic progenitors.<sup>5</sup>

Using this system we were surprised to find that erythroid cells transformed *in vitro* by SFFV were neither blocked in maturation nor EPO-independent.<sup>6</sup> These unexpected findings led us to test the generality of this new information in a variety of other primary transformants. We found that many oncogenes, including *ras*, *abl*, *mos*, *src* and others, all conveyed a growth advantage to hemopoietic progenitors in the myeloid, erythroid, or lymphoid lineages.<sup>7-9</sup> Because we could isolate and examine the virally transformed hemopoietic cells *in vitro*, we learned that all the transformants, like the SFFV transformants, retained two properties of their uninfected counterparts. The transformed blood progenitor was capable of terminal differentiation, and they were still dependent on lineage-specific growth factors for their survival. Collectively, these *in vitro* results suggested that our preconceived notions that leukemia cells were hormone-independent (and therefore autonomous) and blocked in maturation (and therefore immortal) may have been wrong.

Based on these observations, in 1983 we published an alternative model of transformation<sup>10</sup> in which we suggested that neoplastic transformation, either by viruses, chemicals, mutations, or unknown mechanisms, may produce cells that grow abnormally but nonetheless retain many properties of their normal counterparts such as hormone dependence and the ability to differentiate. It was suggested that if this model were correct, then the retention of specific hormone dependence by cancer cells could be exploited for the development of new therapeutic approaches to eradicate the tumor. Furthermore, the hormone sensitivity might also be useful in the detection, diagnosis, and staging of cancer.

We therefore sought to test the *in vivo* validity of this model by examining the hormone sensitivity of an aggressive transplantable erythroleukemia in mice. Injection of newborn mice with the helper virus isolated from the Friend leukemia virus complex produces such a leukemia.<sup>11</sup> When we placed these erythroleukemic spleens into culture in the presence of a variety of hemopoietic hormones and growth factors, we observed that EPO was the only hormone that would support growth of these colonies. We had anticipated that EPO would merely stimulate proliferation and differentiation. However, we observed a dramatic "all or none" effect.<sup>12</sup> In the absence of EPO, the cells died. In the presence of EPO, the cells thrived and proliferated but would not differentiate until another agent, hemin, was included in the medium.<sup>13</sup> These observations suggested that EPO may act primarily as a viability agent rather than as an inducer of differentiation. Consequently, our research focus turned from an investigation of the induction of erythroid-specific genes by EPO to investigations of how and when the EPOR is expressed and of the new properties its expression conveyed to red cell precursors.

The following progress report on our EPOR studies is presented in three categories: (a) descriptive studies in which we have quantified EPOR mRNA expression, EPO binding, and internalization; (b) experimental studies in which we have mutated the EPOR and used gene transfer technology to study receptor function in erythroid and nonerythroid cells; and (c) applied studies in which we

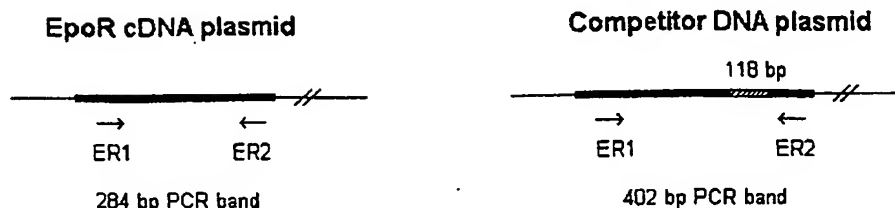


**FIGURE 1.** Construction of competitor DNA used for PCR quantitation of EPOR transcripts. First, the 5' portion of the EPOR cDNA (–10 to +423 bp relative to the translational start site) was cloned into the plasmid pBluescript II SK<sup>+</sup> (Stratagene) (left panel). Second, a 118 bp *Hae*III digested fragment of phi X-174 DNA was cloned into an *Eco*RV site within the EPOR cDNA gene (right panel). The relative positions of the PCR primers ER1 and ER2 and the size of their respective PCR products are as indicated.

have attempted to develop antihormone therapies for leukemias by interfering with ligand-receptor interactions.

## DESCRIPTIVE STUDIES

### *Detection and Quantitation of EPOR Transcripts by PCR*

In our initial studies, we sought to define the time course of EPOR expression at the transcriptional level during erythroid cell development. For this purpose, we used a polymerase chain reaction (PCR) quantitative assay<sup>14</sup> that we tailored for detection and quantitation of EPOR transcripts. To define primer sequences that would specifically amplify the EPOR transcripts, we cloned and sequenced the gene for the human EPOR.<sup>15</sup> From these sequences, we designed primers, ER1 and ER2 (FIG. 1), that when tested, allowed detection of EPOR transcripts in erythroid cells such as OCIM-1,<sup>16</sup> TF-1,<sup>17</sup> K562,<sup>18</sup> and peripheral blood mononuclear cells but not in nonerythroid cells such as HeLa<sup>19</sup> and kidney. Next, we devised a competitive PCR assay for quantitation of EPOR transcripts<sup>20</sup> (manuscript in preparation). In brief, we constructed a sequence of DNA that would compete for the EPOR primers, ER1 and ER2, with the mRNA-derived cDNA. This was done by inserting unrelated sequences derived from phi X-174 bacteriophage into a fragment of the cloned human EPOR cDNA (FIG. 1). When this competitive fragment was included in the reaction mixture along with the mRNA-derived cDNA, we could observe two bands of different sizes representing DNA fragments amplified from mRNA transcripts and competitor DNA. By quantitating the radioactivity incorporated into each of these bands, we could precisely define the number of copies of competitor that was necessary to compete out the mRNA-derived cDNA. This allowed us to calculate the absolute number of copies of EPOR transcripts per microgram of cellular RNA.

FIGURE 2 demonstrates that this technique was sensitive enough to reproducibly quantitate the number of EPOR transcripts, even in peripheral blood mononuclear cells in which the number of erythroid progenitors is very low. The absolute number of copies of EPOR mRNA in normal blood was determined to be

approximately  $6 \times 10^3$  per microgram of RNA. When measured in an erythroid cell line, OCIM-1, the number of transcripts was approximately 1000-fold higher. By comparison, no transcripts were detected in HeLa cells that were nonerythroid. Therefore, this assay is both sensitive and specific and should allow us to study EPOR expression during erythropoiesis in cell culture, developing tissues, and clinical samples. Furthermore, we suggest that various hemopoietic progenitors may be detected and defined on the basis of specific cytokine receptor transcripts. We call this the receptor transcript phenotyping (RTP). In addition to distinguishing various populations of normal hemopoietic cells, this RTP assay may be particularly valuable in defining leukemia types and subtypes that are now classified primarily by immunophenotyping. It follows that the receptor proteins, encoded

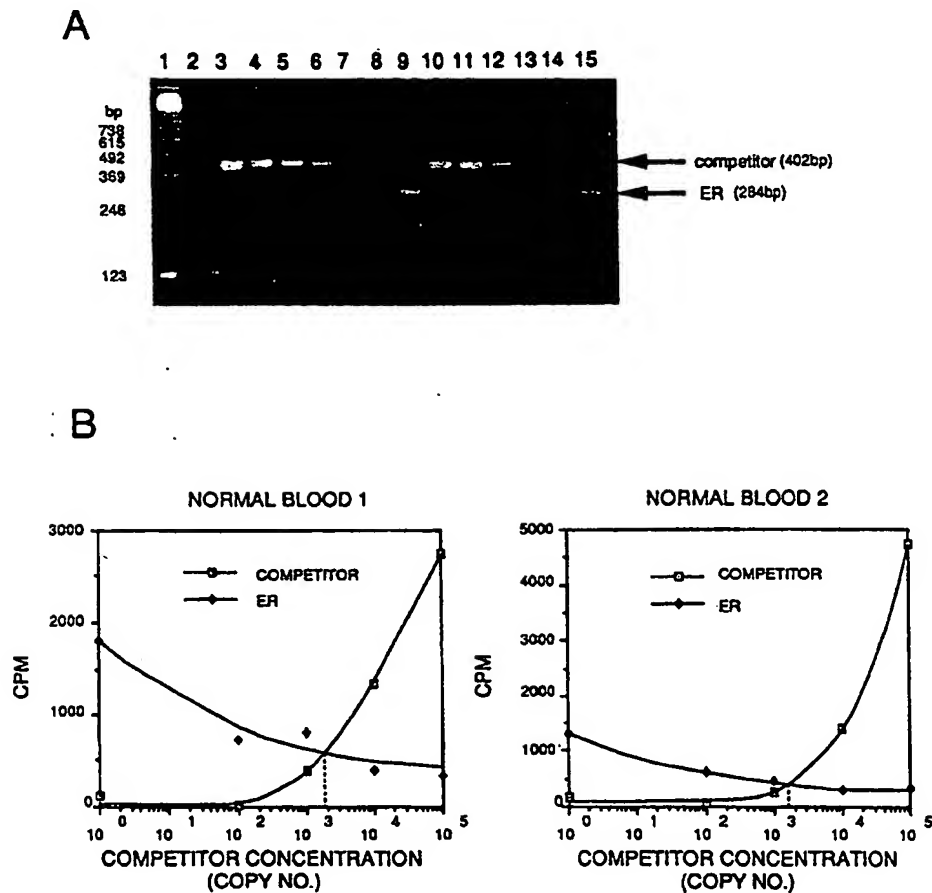


**FIGURE 2.** Absolute quantitation of EPOR RNA in normal peripheral blood. **A:** PCR reactions using primers ER1 and ER2 (lanes 2–15). Template DNA used was either no DNA (lane 2),  $10^6$  copies of competitor plasmid alone (lane 3), or cDNA reverse transcribed from peripheral blood from one of two normal individuals either alone (lanes 9 and 15) or in the presence of decreasing amounts of competitor plasmid (from  $10^6$  to  $10^2$  copies by log increments, lanes 4–8 for individual 1 and lanes 10–14 for individual 2). **B:** Diagram of counts per minute ( $^{32}$ P) present in PCR products generated in **A**.



by such transcripts, provide reasonable targets for lineage-specific approaches to antileukemia therapies.

**Characterization of EPO Binding, Internalization, and Response in an EPO-Dependent Erythroid Cell Line (HCD Cells)**

As discussed above, the erythroleukemia cells derived from virally infected animals remained hormone dependent *in vitro*. From these cells, we were able to develop permanent cell lines (HC cells and their clonal derivative HCD cells),

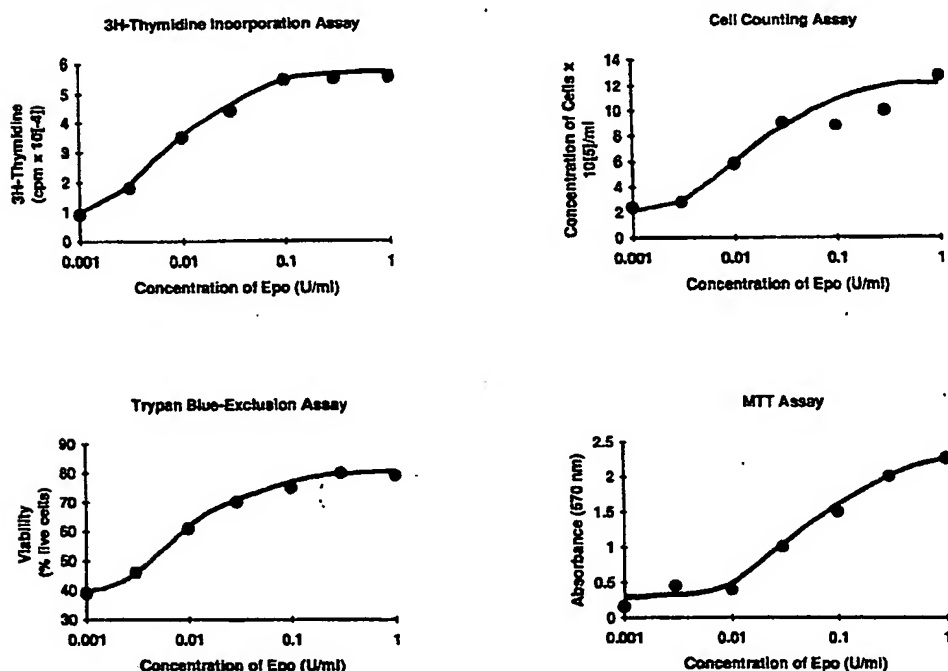


**FIGURE 3.** Effect of EPO on proliferation of HC cells as measured using four assays: [<sup>3</sup>H]thymidine uptake, cell count, Trypan blue exclusion, and MTT (3-(4,5-dimethylthianon-2- $\mu$ L)-2,5-diphenyl tetrazolium bromide) reduction. HC cells were suspended in medium containing IMDM, 30% FBS, and  $5 \times 10^{-5}$ M B-mercaptoethanol at a density of 250,000 cells/mL and dispensed into 96-well plates (0.1 mL/well). EPO concentrations varied from .001 to 1 U/mL in 1/2 log increments as indicated. EPO was added to triplicate wells for each concentration, and then cells were incubated for 72 hours at 37°C prior to assay.

which have been maintained for over three years in our laboratory.<sup>2</sup> These cells retain an absolute dependence on EPO and exhibit an exclusive and extraordinary sensitivity to the hormone. The response to the hormone can be assayed in a number of ways. For example, as shown in FIGURE 3, one can assess the effect of EPO on HC cells by tritiated-thymidine uptake,<sup>21</sup> MTT<sup>22</sup> proliferation assays, total cell counts, and, importantly, by assessing the number of viable cells using Trypan blue exclusion. Thus, as shown in FIGURE 3, if no EPO is added there are few, if any, viable cells after three days in culture. If, on the other hand,

increasing amounts of EPO are added, one sees increasing numbers of viable cells. It was this data that first suggested that a primary role of EPO may be as a survival factor rather than an inducer of erythroid differentiation.

The HC cells have been very useful in studying details of the EPO response. For example, Spivak and his colleagues<sup>23</sup> have synchronized these cells and studied EPO-induced phosphorylation and proliferation in relation to cell cycle. In another study, Ruscetti *et al.*,<sup>24</sup> demonstrated that the need for EPO could be abrogated in HC cells by superinfection with the spleen focus-forming virus. Interestingly, the phosphorylation pattern was quite different from that induced by EPO. Finally, Sawyer<sup>25</sup> and his colleagues have extensively characterized the binding of radioactive EPO to HCD cells. We believe that these studies have identified the biologically active form of the EPOR. Briefly, we deprived the HCD cells of EPO, which caused a tenfold accumulation in the number of binding sites. Surprisingly, the previously characterized 62–66 kDa form of the EPOR<sup>26</sup> did not change upon starvation and refeeding. However, a 78 kDa highly glycosylated form, not previously recognized, correlated precisely with the biologic activity, the accumulation upon starving, and the disappearance of binding sites upon refeeding. The 78 kDa form of EPOR was exclusively phosphorylated on tyrosine. Perhaps the most significant observation was that the phosphorylation, internalization, and down-regulation of the receptor all occurred over only a 20–30 minute period after EPO addition. Therefore, it may be appropriate to view the EPO stimulus response as a circumscribed phenomenon that occurs in minutes rather than in hours. The long-term EPO effects<sup>27</sup> (*e.g.*, hemoglobin synthesis or other differentiation event) that require prolonged exposure to EPO could be considered as sequelae to the initial ligand-receptor interaction. Alternatively, these long-term (2–3 day) responses may emanate from the cumulative effect of many successive individual responses.

## EXPERIMENTAL STUDIES

### *Gene-Transfer Studies of Wild-Type and Mutated Human EPOR in Nonerythroid Cell Lines*

In an effort to learn more about the function of the EPOR, we have initiated gene-transfer studies of both the wild-type and a series of mutated human EPOR genes. The first mutation we analyzed was a change in amino acid 129 from Arg to Cys<sup>28</sup> (manuscript in preparation). We transfected both the human wild-type and mutated EPOR into an IL-3-dependent myeloid cell line, 32D, and isolated stable transformants (32D-HER and 32D-MHER, respectively). We subsequently characterized these cell lines in terms of their response to EPO for proliferation, tyrosine phosphorylation, and differentiation. As shown in the top panel of FIGURE 4, 32D cells that expressed the wild-type EPOR were no longer dependent upon IL-3 and exhibited a dependent proliferation response to EPO. As seen in the bottom panel of FIGURE 4, 32D cells that expressed the mutated EPOR were rendered factor independent. In addition to this proliferative response, both wild-type and mutated EPOR conveyed to the 32D the ability to carry out a specific pattern of tyrosine phosphorylation in response to EPO (data not shown). Mock transfected cells do not respond to EPO. When we compared the phosphorylation banding pattern induced by IL-3 and EPO in these cells, ligand-specific substrates were observed, although certain proteins were phosphorylated in response to either cytokine. One of the EPO-specific phosphorylation substrates was identified as the EPO receptor itself. Further downstream components of the EPO signal

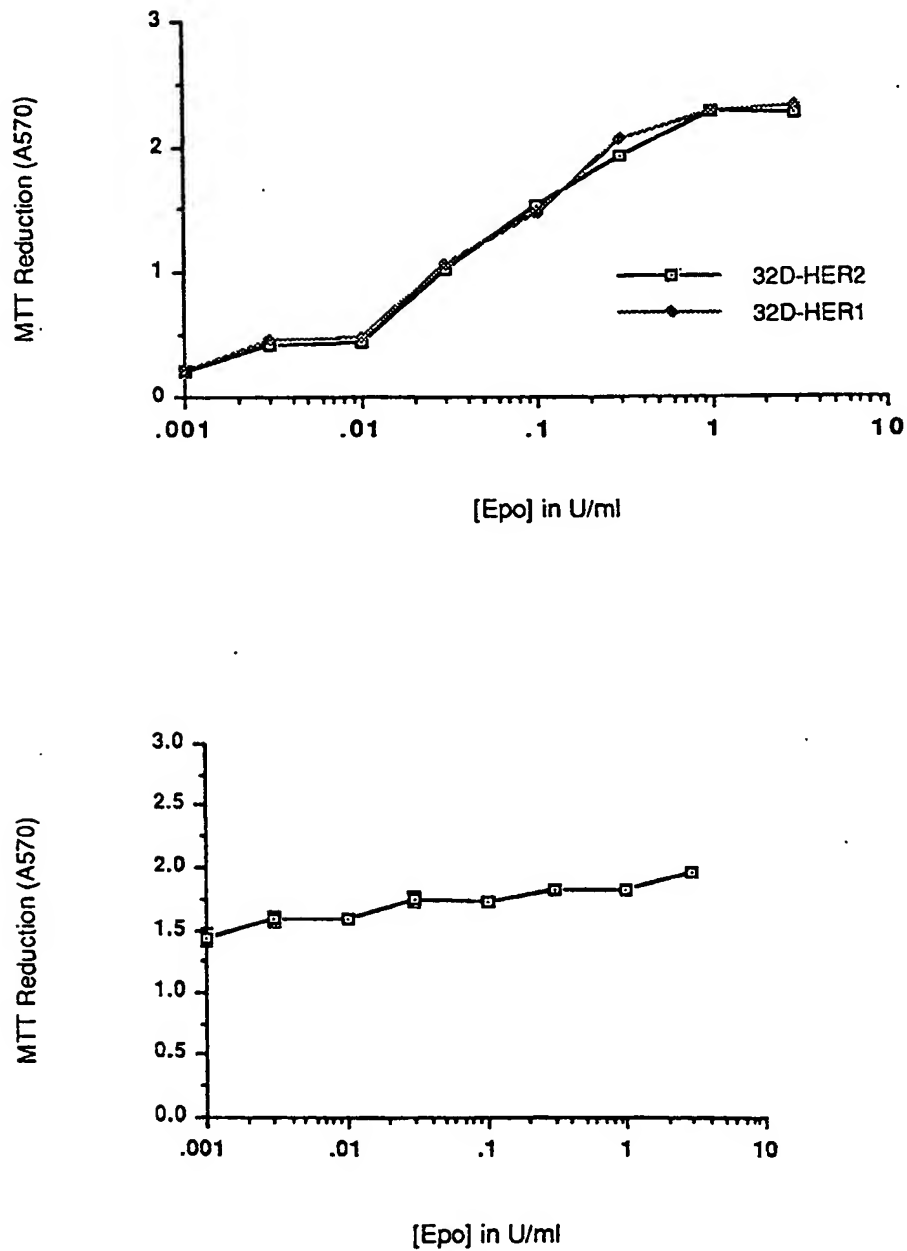


**FIGURE 4.** MTT proliferation assay of 32D cells stably transfected with wild-type (32D-HER) (top) or mutated EPOR (32D-MHER) (bottom). Assays were performed as described in the legend for FIGURE 3.

transduction pathway are currently being investigated in our laboratory. It should be noted in passing that we have not observed any evidence that the EPOR can support erythroid differentiation in the transfected 32D cells.

We also tested the effect of EPOR in 32D cells on granulocyte-colony stimulating factor (G-CSF)-induced differentiation. Perhaps the most interesting result observed in these gene transfer studies was that G-CSF-induced differentiation of 32D cells was inhibited by the EPOR if EPO was present. As shown in TABLE 1, differentiation, as indicated by myeloperoxidase staining and Wright-Giemsa staining of segmented nuclei, was induced by G-CSF in the 32D cells. Upon transfer of the wild-type EPOR into these cells, the G-CSF inductions remained intact. However, when EPO was added to the 32D cells expressing the EPOR, G-CSF did not induce these two markers of myeloid differentiation. As expected, EPO did not block G-CSF induction in control, mock transfected, 32D cells. This result may suggest competition by these two growth factors, EPO and G-CSF, at the cell membrane level, at the intracellular signal transduction pathway level, or at the gene activation level. Alternatively, EPO might trigger the down-regulation of the G-CSF receptor. Studies are now in progress to further explore the interaction of these two regulatory pathways in 32D cells.

TABLE 1. Assay for Neutrophilic Differentiation Induced by G-CSF

Cells	Growth Factors	Myeloperoxidase Staining	Segmented Nuclei Staining
32D	G-CSF	Yes	Yes
	EPO + G-CSF	Yes	Yes
32D-HER	G-CSF	Yes	Yes
	EPO + GCSF	No	No

#### *Gene-Transfer Studies of Mutated EPOR in Primary Hemopoietic Cells*

As discussed above, expression of the mutated EPOR in myeloid cells in culture abrogated their IL-3 dependence. This led us to speculate that upon infection of primary hemopoietic cells (*i.e.*, from bone marrow, spleen, or fetal liver), one might observe the abrogation of growth factor requirements in a number of lineages. That is, the mutated EPOR might lead to the production of growth factor-independent myeloid, lymphoid, and erythroid colonies. To address this subject, we tested the ability of a constitutively activated murine EPOR<sup>29</sup> to alter the growth requirements of primary hematopoietic precursors that terminally differentiate in culture.<sup>30</sup> Two recombinant retroviruses expressing the mutated EPOR were used to infect fetal liver cells that served as a source of hematopoietic progenitors. Methylcellulose cultures were incubated in the absence of any growth factor or in combination with selected growth factors. In contrast to the cell line studies, in which erythroid, lymphoid, and myeloid cells were rendered factor independent by the mutated EPOR,<sup>31</sup> only factor-independent erythroid cells were observed in the primary cultures. Specifically, the mutated EPOR completely abrogated the EPO requirement of erythroid colony-forming units to form erythrocytes after 2-5 days in culture and did not interfere with the differentiation program of these cells. However, in the absence of growth factors, the mutated EPOR did not enhance the growth of erythroid burst-forming unit development. (Erythroid burst-forming

units are descendants of progenitors from an earlier stage of the erythroid cell lineage than erythroid colony-forming units.)

At least two conclusions can be drawn from these results. First, in primary cells, the EPOR was functional only in the erythroid progenitors. Perhaps only erythroid progenitors express specific proteins that interact with the EPOR to render it functional (*i.e.*, partner or chaperon proteins). Second, the apparent action of the constitutively activated EPOR was not only restricted to the erythroid lineage but it was also restricted to a relatively narrow window in the erythroid lineage. Thus, this assay system may not only allow one to rapidly assess the function of cloned receptors, but it may also help to define the temporal importance of these receptors during development.

### APPLIED EPOR STUDIES

As a result of our observation that certain leukemia cells retained hormone sensitivity, we have begun to examine whether such leukemias might be controlled, suppressed, or eradicated by interfering with hormone-receptor interactions. TABLE 2 lists five such approaches that we are currently investigating using the EPO-dependent erythroleukemias as a model. To give one example of our current studies, we have recently explored the possibility of using the ligand-binding portion of the EPOR to inhibit EPO action. Accordingly, we have synthesized, in collaboration with Linda Mulcahy and Linda Jolliffe at the Robert Wood Johnson Pharmaceutical Research Institute, the exoplasmic domains of the several variants of murine and human erythropoietin receptors. This "soluble" receptor binds EPO and is clearly capable of inhibiting EPO-dependent viability and proliferation in the HC cells (FIG. 5). We are currently testing the activity of the soluble receptor in animals to determine its effect on normal and malignant erythropoiesis *in vivo*.

### SUMMARY

In this paper we have discussed our recent progress on understanding the role of the EPOR in erythroid development. The major suggestions stemming from our studies are that (1) the EPOR conveys viability and/or proliferation but does not induce erythroid differentiation; (2) EPO-dependent cell lines (HC cells) provide a useful model for studies of the interaction of EPO with its receptor; (3) a highly glycosylated 78 kDa protein on the cell surface appears to be the mature, biologically active form of the EPO receptor; (4) the EPOR, when activated by ligand binding, may inhibit the induction of myeloid differentiation by G-CSF; and (5) the hormone sensitivity of leukemia cells may be exploited for the development of new approaches to target and deliver drugs that specifically control the

TABLE 2. Antihormone Approaches to Cancer Therapy

- 
- Radiolabeled hormone
  - Soluble receptor
  - Hormone analogues
  - Hormone/receptor antibodies
  - Hormone-toxin conjugate
-

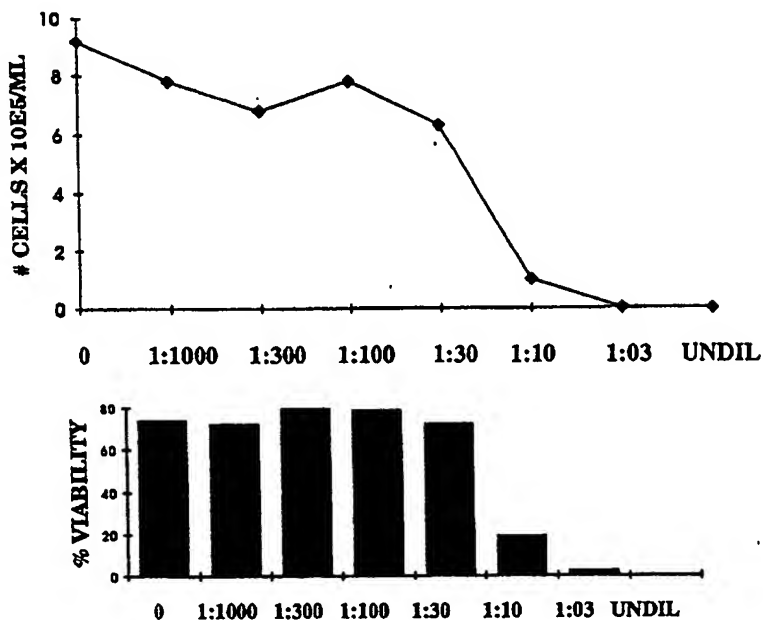


FIGURE 5. Inhibition of EPO-dependent proliferation of HC cells by soluble EPOR. The effect of increasing concentrations of soluble EPOR on HC cell counts (upper panel) and viability as measured by Trypan blue exclusion (lower panel) after incubation for 72 hours at 37°C.

growth of leukemia cells. In particular, a soluble form of EPOR bound EPO and inhibited EPO-dependent growth *in vitro*. Therefore this approach may also be useful as an antihormone therapy for erythroid leukemia *in vivo*.

#### REFERENCES

1. HOSSAIN, A., J. K. KIM & W. D. HANKINS. 1986. Treatment of a fatal transplantable erythroleukemia by procedures that lower endogenous erythropoietin. *J. Cell Biochem.* 30: 311-318.
2. HANKINS, W. D., K. L. CHIN, R. DONS & G. SIGOUNAS. 1989. Erythropoietin-dependent and erythropoietin-producing cell lines. Implications for research and for leukemia therapy. *Ann. N.Y. Acad. Sci.* 554: 21-28.
3. D'ANDREA, A. D., H. F. LODISH & G. G. WONG. 1989. Expression cloning of the murine erythropoietin receptor. *Cell* 57: 277-285.
4. FRIEND, C., W. SCHER, J. G. HOLLAND & T. SATO. 1971. Hemoglobin synthesis in murine virus-induced leukemic cell *in vitro*: stimulation of erythroid differentiation by dimethyl sulfoxide. *Proc. Natl. Acad. Sci. USA* 68: 378-382.
5. HANKINS, W. D., T. A. KOST, M. J. KOURY & S. B. KRANTZ. 1978. Erythroid bursts produced by Friend leukemia virus *in vitro*. *Nature* 276: 506-508.
6. KOURY, M. J., M. BONDURANT, D. T. DUNCAN, S. B. KRANTZ & W. D. HANKINS. 1982. Specific differentiation events induced by erythropoietin in cells infected *in vitro* with the anemic strain of Friend virus. *Proc. Natl. Acad. Sci. USA* 79: 635-639.
7. ANDERSON, S. M., S. P. KLINKEN & W. D. HANKINS. 1985. A murine recombinant retrovirus containing the *src* oncogene transforms erythroid precursor cells *in vitro*. *Mol. Cell. Biol.* 5: 3369-3375.

8. PHARR, P. N., M. OGAWA & W. D. HANKINS. 1987. *In vitro* retroviral transfer of *ras* genes to single hemopoietic progenitors. *Exp. Hematol.* 15: 323-330.
9. HANKINS, W. D., I. B. PRAGNELL & T. KOST. 1982. Myeloproliferative virus causes erythroid transformation *in vitro*. *Mol. Cell. Biol.* 2: 138-146.
10. HANKINS, W. D. 1983. Increased erythropoietin sensitivity after *in vitro* transformation of hematopoietic precursors by RNA tumor viruses. *J. Natl. Cancer Inst.* 70: 725-734.
11. OLIFF, A., S. RUSCETTI, E. C. DOUGLAS & E. M. SCOLNICK. 1981. Isolation of transplantable erythroleukemia cells from mice infected with helper-independent Friend murine leukemia virus. *Blood* 58: 244-254.
12. HANKINS, W. D., K. CHIN & G. SIGOUNAS. 1988. Hormone associated therapy of leukemia: reflections. *In Progress in Clinical Biological Research*. W. D. Hankins & D. Puett, Eds.: Vol. 262: 257-267. Alan R. Liss, Inc. New York.
13. SIGOUNAS, G., H. CAO, H. FOX, A. N. SCHECHTER & W. D. HANKINS. 1987. Hemin inducibility of erythropoietin-dependent cell lines. *Blood* 70(Suppl. 1): 161a.
14. GILLILAND, G., S. PERRIN, K. BLANCHARD & H. F. BUNN. 1990. Analysis of cytokine mRNA and DNA: Detection and quantitation by competitive polymerase chain reaction. *Proc. Natl. Acad. Sci. USA* 87: 2725-2729.
15. NOGUCHI, C. T., K. S. BAE, K. CHIN, Y. WADA, A. N. SCHECHTER & W. D. HANKINS. 1991. Cloning of the human erythropoietin receptor gene. *Blood* 78: 2548-2556.
16. PAPAYANNOPOULOU, T., B. NAKAMOTO, S. KURACHI, M. TWEEDDALE & H. MESSNER. 1988. Surface antigenic profile and globin phenotype of two new human erythroleukemia lines: characterization and interpretations. *Blood* 72: 1029-1038.
17. KITAMURA, T., A. TOJO, T. KUWAKI, S. CHIBA, K. MIYAZONO, A. URABE & F. TAKAKU. 1989. Identification and analysis of human erythropoietin receptors on a factor-dependent cell line, TF-1. *Blood* 73: 375-380.
18. LOZZIO, C. B. & B. B. LOZZIO. 1975. Human chronic myelogenous leukemia cell-line with positive Philadelphia chromosome. *Blood* 45: 321-334.
19. GEY, G. O., W. D. COFFMAN & M. T. KUBICEK. 1952. Tissue culture studies of the proliferative capacity of cervical carcinoma and normal epithelium. *Cancer Res.* 12: 364-365.
20. HANKINS, W. D., F.-S. XU, D. M. WILLIAMS, T. A. ZIMMERS, A. N. SCHECHTER & C. T. NOGUCHI. 1990. Cloning of the human erythropoietin receptor and PCR quantitation of mRNA transcripts in peripheral blood clinical samples. *Blood* 76 (Suppl. 1): 96a.
21. RUSCETTI, S. K. 1986. Employment of a <sup>3</sup>H-thymidine-incorporation assay to distinguish the effects of different Friend erythroleukemia-inducing retroviruses on erythroid cell proliferation. *J. Natl. Cancer Inst.* 77: 241-245.
22. MOSMANN, T. 1983. Rapid colorimetric assay for cellular growth and survival: application to proliferation and cytotoxicity assays. *J. Immunol. Methods* 65: 55-63.
23. SPIVAK, J. L., T. PHAM, M. ISAACS & W. D. HANKINS. 1991. Erythropoietin is both a mitogen and a survival factor. *Blood* 77: 1228-1233.
24. RUSCETTI, S. K., N. J. JANESCH, A. CHAKRABORTI, S. T. SAWYER & W. D. HANKINS. 1990. Friend spleen focus-forming virus induces factor independence in an erythropoietin-dependent erythroleukemia cell line. *J. Virol.* 63: 1057-1062.
25. SAWYER, S. T. & W. D. HANKINS. 1993. The functional form of the erythropoietin receptor is a 78 kDa protein: correlation with cell surface expression, endocytosis and phosphorylation. *Proc. Natl. Acad. Sci. USA* 90: 6849-6853.
26. YOSHIMURA, A., A. D. D'ANDREA & H. F. LODISH. 1990. Friend spleen focus-forming virus gp55 interacts with the erythropoietin receptor in the endoplasmic reticulum and affects receptor metabolism. *Proc. Natl. Acad. Sci. USA* 87: 4193-4197.
27. KOURY, M. J. & M. C. BONDURANT. 1990. Erythropoietin retards DNA breakdown and prevents programmed death in erythroid progenitor cells. *Science* 248: 378-381.
28. ZIMMERS, T. A., W. D. HANKINS, D. M. WILLIAMS, L.-M. WANG, A. N. SCHECHTER & J. H. PIERCE. 1993. Analysis of human erythropoietin receptor function by mutagenesis and gene transfer. *J. Cell Biochem. (Suppl. 17B)*: 84.
29. YOSHIMURA, A., G. LONGMORE & H. F. LODISH. 1990. Point mutation in the exoplasmic domain of the erythropoietin receptor resulting in hormone-independent activation and tumorigenicity. *Nature* 348: 647-649.



30. PHARR, P. N., D. HANKINS, A. HOFBAUER, H. LODISH & G. D. LONGMORE. 1993. Expression of a constitutively active erythropoietin receptor in primary hematopoietic progenitors abrogates erythropoietin dependence and enhances erythroid colony-forming unit, erythroid burst-forming unit and granulocyte/macrophage progenitor growth. *Proc. Natl. Acad. Sci. USA* 90: 938-942.
31. YOSHIMURA, A., G. LONGMORE & H. F. LODISH. 1990. Pointmutation in the extracellular domain of the erythropoietin receptor resulting in hormone-independent activation and tumorigenicity. *Nature* 348: 647-649.

### DISCUSSION OF THE PAPER

ALAN D. D'ANDREA (*Dana-Farber Cancer Institute, Boston, MA*): One of the things that came out of this session for me is that early in development certain growth factors like activin A seem to have a very broad impact or very broad effect on mesoderm induction. But as we will be seeing tomorrow for instance, from John Yu's talk, activin A has a pretty confined effect on erythropoiesis and erythroid differentiation, which is obviously in a more differentiated organism.

EUGENE GOLDWASSER (*The University of Chicago, Chicago, IL*): Perhaps I could tell you the results of one experiment that obviously needs confirmation. We made an M-CSF ricin A chain conjugate. We incubated that with marrow cells and then scored for erythroid bursts after adding EPO, and we pretty much wiped out burst formation, which would suggest that the early cells, the burst former or its precursor, had CSF receptors. The reciprocal experiment, which would be more interesting from my point of view, is a little hard to do because the conjugate formation isn't nearly as simple as it is with the CSFs, but we're clearly working in that direction.

MARK J. KOURY (*Vanderbilt University, Nashville, TN*): I have a couple of questions. With regard to the receptor transcripts in the peripheral blood, those preparations, it seems to me, are not from the front end. You could be looking at the back end. That is perhaps a cell that was nucleated or even more likely a reticulocyte that was in your preparation. Isn't that possible, so that it's actually a very late-stage cell after it has been through, rather than on a precursor. Is that possible? It seems to me that's a likely cell to be out there; there's a lot more reticulocytes than there are erythroid precursors floating around.

W. DAVID HANKINS (*The Johns Hopkins University School of Medicine, Baltimore, MD*): By putting peripheral blood cells in culture and doing the right kind of things, you can get erythroid precursors to develop, so we know that there are some CFU-E and BFU-E cells there, but their numbers are very low. I think it would be wonderful if we were able to pick up the message, whatever it means, and then you could begin to answer your question. Has anyone actually shown whether reticulocytes have the EPO receptor?

KOURY: I wasn't sure myself.

GOLDWASSER: They don't have receptors, but they might be decaying off, and the cells may have some message left in them.

KOURY: Yes, that's what I was thinking. I'm talking about the message, not the receptor itself.

HANKINS: The message would have a very short half-life, but again it doesn't really matter if they are reticulocytes or CFU-E. I think that this assay may provide one with a way to begin to look at those kinds of things.

KOURY: The other question was about the 32D competition. I couldn't follow how you selected for those cells after the EPO-R transfection.

HANKINS: We selected for them first of all by G418, so we put on a selectable marker and selected cells. Then we checked them to see whether they had the EPO receptor, the way I talked about, and made sure they had the human receptor. It was at that point that we started growing them in IL-3 and then adding EPO the same way Alan D'Andrea did. We added G-CSF either in the presence or absence of EPO. And what we're interested in doing, of course, is adding G-CSF and then asking if you can block it at various points down the pathway by adding EPO.

ANNA RITA MIGLIACCIO (*Lindsley F. Kimball Research Institute, New York, NY*): When an EPO receptor was transfected in a GM-CSF-responsive cell line (FDCP-1), it suppressed the number of GM-CSF receptors expressed on the surface (Quelle and Wojchowski, *Proc. Natl. Acad. Sci. USA* **88**: 4801-4805, 1991). In that case, it was shown that the EPO receptor on the cell surface down-modulated the number of GM-CSF receptors on the surface. Have you any evidence that GM-CSF binds to these cell lines?

HANKINS: No, I don't, but there's an excellent possibility. It may do something to the receptors, it may compete at the phosphorylation pathway, or it may favor proliferation over differentiation. We have a lot of things to work on.

D'ANDREA: Along those lines, Quelle and Wojchowski (*Proc. Natl. Acad. Sci. USA* **88**: 4801-4805, 1991) have shown that when you stimulate the EPO receptor you down-regulate the cell-surface expression of the GM-CSF receptor. I think that cell-surface expression is very important, because what you are saying is that when you add EPO to these cells you are getting down-regulation of the cell-surface G-CSF receptor.

I've been very struck by these early bursts that you see with FVP. Are the 5-day bursts from the FVP the same size as the 10-day bursts that you see with EPO? Doesn't this suggest that FVP is infecting a later cell? In fact, are you getting your bursts quicker?

HANKINS: I'll try to give you a short answer to that. We spent a long time in Nashville trying to identify the target cell for SFFV. The target cell turned out to be a 5-day or intermediate BFU-E, and not one of those early ones that you are talking about, the 10-day or 8-day BFU-E.

ANNALS OF THE NEW YORK ACADEMY OF SCIENCES  
Volume 718

**MOLECULAR, CELLULAR,  
AND DEVELOPMENTAL BIOLOGY  
OF ERYTHROPOIETIN  
AND ERYTHROPOIESIS**

*Edited by Ivan N. Rich and Terence R. J. Lappin*



*The New York Academy of Sciences  
New York, New York  
1994*

# The Expression and Role of Human Erythropoietin Receptor in Erythroid and Nonerythroid Cells

DONNA M. WILLIAMS,<sup>a,b</sup> TERESA A. ZIMMERS,<sup>b</sup>  
JACALYN H. PIERCE,<sup>c</sup> PAMELA N. PHARR,<sup>d</sup>  
ALAN N. SCHECHTER,<sup>b</sup> STEPHEN T. SAWYER,<sup>e</sup>  
SANDRA K. RUSCETTI,<sup>f</sup> JERRY L. SPIVAK,<sup>a</sup>  
AND W. DAVID HANKINS<sup>a,g</sup>

<sup>a</sup>*Department of Medicine  
Division of Hematology  
Johns Hopkins School of Medicine  
Baltimore, Maryland 21205*

<sup>b</sup>*Laboratory of Chemical Biology  
National Institute of Diabetes, Digestive and Kidney Diseases  
National Institutes of Health  
Bethesda, Maryland 20892*

<sup>c</sup>*Laboratory of Chemical and Molecular Biology  
National Cancer Institute  
National Institutes of Health  
Bethesda, Maryland 20892*

<sup>d</sup>*Medical University of South Carolina and  
Veterans Affairs Medical Center  
Charleston, South Carolina 29403*

<sup>e</sup>*Department of Medicine  
Division of Hematology  
Vanderbilt University School of Medicine  
Nashville, Tennessee 37232-2287*

<sup>f</sup>*Laboratory of Molecular Oncology  
National Cancer Institute  
Frederick, Maryland 20702-1201*

## INTRODUCTION

During the past few years, our laboratory has investigated the erythropoietin receptor (EPOR) with regard to its structure-function relationships, role in development, transcriptional regulation, and the mechanism by which it conveys a signal upon interaction with its ligand. We began to focus on the EPOR as the result of three related developments. First, our recent studies indicated that erythropoietin (EPO) functioned as a viability factor rather than as an inducer of erythropoiesis.<sup>1</sup>

<sup>g</sup> To whom correspondence should be addressed.

## Brain capillary endothelial cells express two forms of erythropoietin receptor mRNA

Ryoichi YAMAJI<sup>1</sup>, Tadayuki OKADA<sup>1</sup>, Maki MORIYA<sup>1</sup>, Mikihiko NAITO<sup>2</sup>, Takashi TSURUO<sup>2</sup>, Kazutaka MIYATAKE<sup>1</sup> and Yushihisa NAKANO<sup>1</sup>

<sup>1</sup> Department of Applied Biological Chemistry, Osaka Prefecture University, Japan

<sup>2</sup> Institute of Molecular and Cellular Biosciences, University of Tokyo, Japan

(Received 31 January/13 May 1996) – EJB 96 0135/1

To study the existence of the erythropoietin receptor (Epo-R) mRNA in brain capillary endothelial cells, the reverse transcription (RT) PCR was performed using total RNAs from rat brain capillary endothelial cells (RBECs) and MBEC4, which is one of the established mouse brain capillary endothelial cell lines. Southern analysis of the RT-PCR products indicated that both RBECs and MBEC4 expressed an authentic form of Epo-R mRNA as a minor form and an intron-5-inserted form of Epo-R mRNA, thus a soluble form of Epo-R mRNA, as a major form. Furthermore, the effect of recombinant human erythropoietin (rHuEpo) on the DNA synthesis in RBECs was analyzed. rHuEpo showed a dose-dependent mitogenic action on RBECs as a competence factor. Radioiodinated rHuEpo was bound specifically to RBECs with time, cell number and dose dependencies. Binding studies with <sup>125</sup>I-rHuEpo showed that RBECs had a single class of receptors with low-affinity ( $K_d = 860$  pM) and that the number of sites/cell (10300) was abundant. These results suggest that brain capillary endothelial cells express not only an authentic form of Epo-R but also a soluble form of Epo-R and that erythropoietin acts directly on brain capillary endothelial cells as a competence factor.

**Keywords:** erythropoietin; recombinant human erythropoietin; erythropoietin receptor; brain capillary endothelial cells.

Hypoxemia resulting from lung and heart diseases, anemia and high-altitude residence induces a series of modifications in the mammals. As an adaptation mechanism to hypoxia, mammals increase the number of the capillaries/tissue mass [1] and the erythrocytes in the blood [2] to maintain an adequate O<sub>2</sub> delivery.

Erythropoietin (Epo) is a serum glycoprotein hormone required for survival, proliferation, and differentiation of committed erythroid progenitor cells and its production is accelerated in the kidney by hypoxia [3–5]. Recently, it has been reported that Epo may act on such non-erythroid cells as endothelial cells [6–9], smooth muscle cells [10], B lymphocytes [11], rodent placenta cells [12], embryonic stem cells [13, 14], megakaryocytes [15], and cells with neural characteristics (PC12 cells and SN6 cells) [16] in addition to erythroid progenitor cells and that Epo mRNA and Epo receptor (Epo-R) mRNA express in mouse brain [17]. *In vitro* experiments have shown that recombinant human Epo (rHuEpo) has a proliferative and a positive chemotactic effect on human umbilical vein endothelial cells (HUVECs) and bovine adrenal capillary endothelial cells [6], increases endothelin-1 release in bovine pulmonary artery endothelial cells [8] and stimulates angiogenesis in rat thoracic aortas

[9]. Although these results suggest that Epo may function as an angiogenic factor for adapting to hypoxia, after embryogenesis, angiogenesis proceeds by the growth of new capillary vessels from an established microvasculature following stimulation by various physiological or pathological processes [18, 19]. Furthermore, the mean microvessel density increases in brain [20] and no new capillaries develop in muscle [21] under hypoxic conditions such as exposure to high altitudes, implying that capillary endothelial cells from various tissues each has specific characteristics.

HUVECs express Epo-R mRNA [17]. In the present study, we use rat brain capillary endothelial cells (RBECs) and MBEC4, which is one of the established mouse brain capillary endothelial cell lines [22], to analyze the existence of Epo-R mRNA in brain capillary endothelial cells, which have been thought to be associated with angiogenesis under hypoxic conditions, and provide evidence that both RBECs and MBEC4 express two forms of Epo-R mRNA, an authentic form (aEpo-R) and a soluble form (sEpo-R). Furthermore, we report that rHuEpo acts directly on RBECs as a mitogenic factor with competence activity and that RBECs have a single class of Epo-R which are abundant compared to those in erythroid progenitor cells.

## MATERIALS AND METHODS

**Materials.** Epo used throughout the present experiments was rHuEpo (200000 IU/mg) kindly provided by Kirin Brewery (Gunma, Japan). The following materials were purchased from the indicated sources: Dulbecco's modified Eagle's medium (DMEM), minimum essential medium (MEM) and Hanks' solu-

Correspondence to Y. Nakano, Department of Applied Biological Chemistry, Osaka Prefecture University, Sakai, Osaka, Japan 593.  
Fax: +81 722 50 7318.

**Abbreviations.** Epo, erythropoietin; rHuEpo, recombinant human Epo; Epi-R, Epo receptor; sEpo-R, soluble form of Epo-R; aEpo-R, authentic form of Epo-R; RBECs, rat brain capillary endothelial cells; HUVECs, human umbilical vein endothelial cells; bFGF, basic fibroblast growth factor; RT-PCR, reverse-transcription polymerase chain reaction; DMEM, Dulbecco's modified Eagle's medium; MEM, minimum essential medium; NaCl/P, phosphate-buffered saline.

tion, Nissui Pharmaceutical Co.; fetal calf serum, reverse transcriptase (Superscript II RNase H<sup>-</sup>) and human transferrin, Gibco; pGEM-T vector, Promega; collagenase, Wako Pure Chemical Industries; dextran T70, Percoll and Sephadex G-25 (NAP 10 column), Pharmacia Biotech; Taq DNA polymerase, Toyobo; bovine insulin, Sigma; basic fibroblast growth factor (bFGF), Intergen Inc.; Iodo-gen (1,3,4,6-tetrachloro-3 $\alpha$ ,6 $\alpha$ -diphenylglycyl), Pierce; [<sup>3</sup>H]thymidine and Na<sup>125</sup>I, New England Nuclear.

**Isolation and culture of RBECs.** RBECs were isolated from 7-week-old male Wistar rat brains with 0.5% collagenase in Hanks' solution with minor modification of the method described by Bowman et al. [23]. Briefly, the aseptically removed five brains were rinsed several times with sterile ice-cold phosphate-buffered saline (NaCl/P; 137 mM NaCl, 2.68 mM KCl, 8.1 mM Na<sub>2</sub>HPO<sub>4</sub>, 1.47 mM KH<sub>2</sub>PO<sub>4</sub>, pH 7.4), cleaned of meninges, and minced into 1–2-mm pieces in 2–3 ml DMEM supplemented with 5% fetal calf serum. These were incubated in 15 ml Hanks' solution containing 0.5% collagenase at 37°C for 1.5 h with shaking, followed by the addition of 15 ml DMEM containing 10% fetal calf serum to stop the enzymatic reaction, and centrifuged at 400×g for 3 min. The pellet was suspended with 15 ml MEM containing 13% dextran T70 and centrifuged at 6000×g for 10 min. The pellet was suspended in Hanks' solution containing 0.5% collagenase, incubated at 37°C for 20 min with shaking to remove the pericytes and the basement membrane and then passed through a 100- $\mu$ m nylon mesh. The filtrate was passed through a 50- $\mu$ m nylon mesh and rinsed with DMEM containing 5% fetal calf serum. The 50- $\mu$ m nylon mesh which was used to trap the capillary segments was placed upside down in the petri dish and rinsed out with the same medium to place the segments into the dish. After centrifugation at 400×g for 3 min, the pellet was suspended in 2 ml DMEM supplemented with 10% fetal calf serum. Percoll gradient was prepared as follows: nine parts Percoll and ten parts MEM. Percoll gradients were established by centrifuging at 27000×g for 1 h and the suspended pellet was layered over 7-ml Percoll gradients and centrifuged at 500×g for 10 min. The band containing capillary fragments and clumps of cells were transferred to another fresh tube and rinsed with DMEM containing 10% fetal calf serum by centrifuging at 400×g for 2 min to remove Percoll. The pellet was suspended in DMEM supplemented with 20% fetal calf serum, seeded into dishes coated with collagen (type I) and cultured at 37°C in a 5% CO<sub>2</sub>/95% air atmosphere at 100% humidity. The cells were subcultured by trypsinization using NaCl/P, containing 0.25% trypsin and 0.02% EDTA. Endothelial cell identity was confirmed using rabbit antiserum to human-factor-VIII-related antigen (Dako Japan Co.) and by incorporation of fluorescent 1,1'-dioctadecyl-3,3,3',3'-tetraethylindocarbocyanine perchlorate acetylated low-density lipoprotein (Biomedical Technologies). The cells from passage 4 were used in the present study. The buffers and media used for isolation and culture of capillary endothelial cells contained amphotericin B (250  $\mu$ g/ml), sodium deoxycholate (205  $\mu$ g/ml) and gentamicin sulfate (50  $\mu$ g/ml).

**Cell culture.** MBEC4 was maintained in DMEM supplemented with 10% fetal calf serum and antibiotics under a humidified atmosphere containing 5% CO<sub>2</sub>. MBEC4 was seeded into the collagen-coated dishes.

**Primers.** The nucleotide sequences of the primers are based on the published sequence of the rat Epo-R [16]. The primers used are summarized in Table 1 and their locations are shown in Fig. 1.

**Probes.** Total RNA was prepared from phenylhydrazine-treated rat spleen by the acid guanidium thiocyanate/phenol/chloroform extraction method [24]. The rats were injected intra-

peritoneally with 15 mg/ml phenylhydrazine (40 mg/kg) twice at one-day intervals. Next day after the last injection, the spleen was removed. The Epo-R cDNA fragments were obtained with the reverse transcription (RT) PCR method using the following primer combinations: (a) primers RE1 and RE7 and (b) RE6 and RE8. The regions amplified with these primers cover the whole coding region of the Epo-R cDNA. The first-strand Epo-R cDNA was synthesized using 20  $\mu$ g heat-denatured RNA, 0.5  $\mu$ g oligo(dT) primer, 10 mM dithiothreitol, 50 U RNase inhibitor from human placenta, 1 mM dNTP and 200 U reverse transcriptase in a volume of 25  $\mu$ l. The reaction was performed at 48°C for 60 min. The PCR of 0.5  $\mu$ l of the synthesized first-strand cDNA was performed using 200  $\mu$ M dNTP, 500 nM each of primers RE1 and RE7 or RE6 and RE8 and 2.5 U Taq DNA polymerase in a volume of 100  $\mu$ l and using a programmed thermo-controller (PC-700, Astec Co. Ltd, Japan) programmed with the following conditions: 5 min at 94°C followed by 30 cycles of 1 min at 94°C, 2 min at 55°C, 1 min at 72°C, followed by a single extension of 10 min at 72°C. Each RT-PCR product cloned into pGEM-T vector was sequenced and identified to be the Epo-R cDNA fragment targeted (903 bp for primers RE1 and RE7 and 740 bp for primers RE6 and RE8). The EcoRI-digested fragments of the cloned RT-PCR products were labeled with digoxigenin-11-dUTP using the DIG DNA labeling kit (Boehringer Mannheim) according to the manufacturer's instructions. The labeled Epo-R cDNA fragments (903-bp fragment and 740-bp fragment) were used as probes A and B, respectively, in the present study.

**Detection of Epo-R mRNA.** Total RNAs from RBECs and MBEC4 were prepared and the first strand cDNAs were synthesized as described above. The PCR was performed according to the above program using the following primer combination: (a) primers E1 and E7A, (b) primers E5 and E7B, (c) primers E5 and E6A and (d) primers E6B and E8. The amplified products were detected by Southern blotting using the digoxigenin-labeled rat Epo-R cDNA fragment, probe A or probe B.

**DNA synthesis.** The mitogenic effect of rHuEpo was determined by measuring [<sup>3</sup>H]thymidine incorporation into the DNA of RBECs cultured in the collagen-coated 12-well plates. The cells were plated at a concentration of 3.0×10<sup>4</sup> cells/well in 900  $\mu$ l DMEM supplemented with 20% fetal calf serum and cultured for 24 h. The medium was removed and the cells were rinsed twice with MEM. The cells were incubated in the serum-free medium composed of MEM supplemented with either insulin (5 mg/l), transferrin (5 mg/l) and selenious acid (5  $\mu$ g/l) or transferrin (5 mg/l) and selenious acid (5  $\mu$ g/l) for 24 h to make them quiescent. The medium was replaced with serum-free medium containing various concentrations of rHuEpo or bFGF, which were dissolved in NaCl/P, containing 0.1% BSA, and the cells were incubated for 20 h. NaCl/P, containing 0.1% BSA was added to the medium for control cells. Subsequently the cells were pulsed with 0.1  $\mu$ Ci/ml [<sup>3</sup>H]thymidine. After a 4-h incubation period, the cells were rinsed twice with 2 ml ice-cold NaCl/P, incubated with 1 ml ice-cold 10% trichloroacetic acid at 4°C for 20 min and subsequently rinsed twice with 1 ml ice-cold 8% trichloroacetic acid. The trichloroacetic-acid-insoluble material was solubilized with 700  $\mu$ l 2 M NaOH and the radioactivity was determined by standard liquid scintillation spectrometric techniques.

**Iodination of rHuEpo.** rHuEpo was labeled with <sup>125</sup>I using Iodo-gen: 10  $\mu$ g Iodo-gen in chloroform was coated onto the wall of a conical vial by incubation at 40°C. After the vial was rinsed with 0.2 M sodium phosphate pH 7.0, 0.5 mCi Na<sup>125</sup>I and 0.2 M sodium phosphate were added to the vial in a volume of 20  $\mu$ l and incubated for 2.5 min at room temperature. The mixture was removed from the reaction vial and transferred to a

**Table 1.** Oligonucleotide primers used for amplification of Epo-R cDNA. The primer sequences correspond to the rat Epo-R cDNA sequence [16]. The underlined sequences in the primers RE1, RE7A, RE7B and RE8 were designed for *Eco*RI restriction sites.

Primer	Primer sequences: 5' to 3'	Position (bp)
RE1	<u>AAGAATTC</u> ATGGACCAACTCAGGGTGGCCC	1-22
RE6	<u>CCGAATTC</u> CACTGTGTGCTGACTGTGCTGGC	785-806
RE7	<u>TGGAATTC</u> ACCCTTGTGGGTGGTGAAGAGA	903-882
RE8	<u>CTGAATTC</u> CTAGGAGCAGGCCACGTAGCTG	1524-1503
E1	ATGGACCAACTCAGGGTGGCCC	1-22
E5	TGAGTGTGTCTTGAGCAACCT	606-626
E6A	GACGAGAATGAGAGACAGCGT	777-757
E6B	CACTGTGTGCTGACTGTGCTGGC	785-806
E7A	ACCCTTGTGGGTGGTGAAGAGA	903-882
E7B	TCATTCTCTGGGCTTGGGATG	872-852
E8	CTAGGAGCAGGCCACGTAGCTG	1524-1503

tube containing 3.6  $\mu$ l rHuEpo (1.4 mg/ml). After incubation for 10 min at room temperature, 81.4  $\mu$ l NaCl/P, containing 20 mg/ml of KI and 6% BSA was added.  $^{125}$ I-rHuEpo was separated from free  $^{125}$ I by chromatography on a Sephadex G-25 (NAP 10) column (1.3 $\times$ 2.6 cm) equilibrated with NaCl/P, containing 0.1% BSA. The biological activity of  $^{125}$ I-rHuEpo was assayed by utilizing its stimulatory effect of the incorporation of [ $^3$ H]thymidine into DNA of spleen cells from phenylhydrazine-treated mice according to Sasaki et al. [25]. The specific radioactivity of  $^{125}$ I-rHuEpo was estimated to be 1600 Ci/mmol and  $^{125}$ I-rHuEpo retained full biological activity.

**Binding of radioactive rHuEpo to RBECs.** RBECs were cultured in the collagen-coated 35-mm dishes in DMEM supplemented with 20% fetal calf serum for 24 h. The cells were washed with ice-cold binding buffer (MEM containing 10 mM Hepes pH 7.2 and 0.3% BSA) and incubated in 1 ml binding buffer for 5 min at 4°C. After the binding buffer was changed to 1 ml ice-cold binding buffer containing various concentrations of  $^{125}$ I-rHuEpo, the cells were incubated for different times at 4°C. The cells were separated from the unbound radioactive ligand by washing three times with ice-cold NaCl/P, containing 0.1% BSA and lysed with 1 ml 0.4 M NaOH. The radioactivity in the lysate was determined by a  $\gamma$ -counter. Nonspecific binding of the labeled rHuEpo was determined by adding a 500-fold excess of unlabeled rHuEpo in the binding assay.

## RESULTS

**Southern blot analysis of RT-PCR products.** To study the existence of Epo-R mRNA in brain capillary endothelial cells, total RNAs from RBECs and MBEC4 were prepared. When the RT-PCR using primers E1 and E7A was performed, Southern

blot analysis detected two bands (Fig. 2A). One was a minor band of 903 bp, which is the exact size expected from Epo-R mRNA in rat erythroid cells and PC12 cells [16] and in mouse erythroleukemia SKT6 cells and 32D Epo and 32D GM cells, which are subclones of the murine 32D cell line [26, 32]. The other was a major band of 981 bp, which is the fragment size expected from the results in the present study and the sEpo-R mRNA in SKT6 cells, 32D Epo cells and 32D GM cells [26, 32]. In addition, amplification using primers E5 and E7B resulted in two bands (Fig. 2B). The minor band was 267 bp, which is consistent with the exact size expected from rat and murine Epo-R mRNAs [16, 26, 32]; the major band was 345 bp, which is the fragment size expected from the results in the present study and murine sEpo-R mRNA [26, 32]. As shown in Fig. 2C, when the RT-PCR was performed using primers E5 and E6A in the presence of reverse transcriptase, Southern blot analysis detected two bands; one of these was a minor band of 172 bp, which is the fragment size expected from rat and murine Epo-R mRNAs [16, 26, 32], while the other was a major band of 250 bp, which is the fragment size expected from the results in the present study and murine sEpo-R mRNA [26, 32]. However, Southern blot analysis detected no bands when the RT-PCR was performed in the absence of reverse transcriptase. In contrast, the amplification using primers E6B and E8 yielded a single band of 740 bp, which is the fragment size expected from rat and murine Epo-R mRNAs [16, 26, 32] (Fig. 2D). As shown in Fig. 2, when the RT-PCR of the phenylhydrazine-treated rat spleen was performed using each primer combination described above, Southern blot analysis showed that erythroid progenitor cells expressed the aEpo-R mRNA as a major form and the intron-5-inserted form of Epo-R mRNA as a minor form. Furthermore, Southern blot analysis detected three bands containing the band corresponding to the intron-5-inserted form of Epo-R mRNA (Fig. 2A) and one band (Fig. 2D) in addition to the band corresponding to the aEpo-R mRNA in erythroid progenitor cells. These results suggest the occurrence of some alternatively spliced Epo-R mRNAs due to insertions and deletions in erythroid progenitor cells.

**Stimulatory effect of rHuEpo on DNA synthesis.** The effect of rHuEpo on the incorporation of [ $^3$ H]thymidine into DNA was analyzed in quiescent RBECs which were cultured in the serum-free medium composed of MEM supplemented with insulin, transferrin and selenious acid. As shown in Fig. 3, addition of increasing concentrations of rHuEpo to RBECs resulted in a dose-dependent increase in [ $^3$ H]thymidine incorporation. When rHuEpo was added to RBECs at 1 U/ml, the stimulation of DNA synthesis was maximum within a concentration of up to 10 U/ml tested.

**Competence activity of rHuEpo to RBECs.** To determine whether rHuEpo functions as a competence factor or a pro-

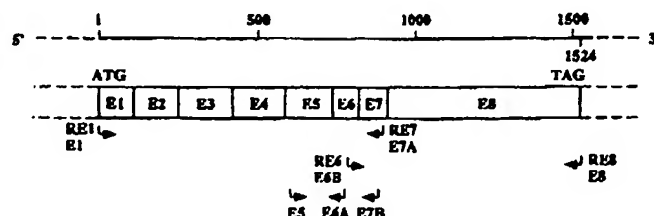


**Fig. 1.** Schematic presentation of rat Epo-R cDNA. Exons (E) are indicated by boxes. The top row represents the number of base pairs of the Epo-R cDNA. The positions of exons of the rat Epo-R cDNA are deduced from the mouse genomic sequence [16]. The arrows indicate the location of the primers used for PCR.

**Fig. 2.** Southern blot analysis of RT-PCR products. Lanes 1: amplification of RBECs phenylhydrazine-treated spleen (lanes 1) present amplification of MBEC4 mRNA (lanes 2).

**Fig. 3.** Effect of rHuEpo on DNA synthesis of RBECs. Cells were cultured in the serum-free medium composed of MEM supplemented with insulin, transferrin and selenious acid. After 20 h, [ $^3$ H]thymidine incorporation was measured.

gression component and selected in Fig. 3. Transferrin incorporation to the bFGF absence



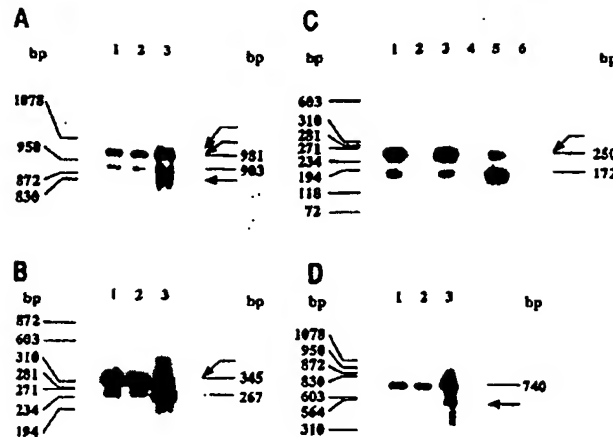


**Fig. 2.** Detection of Epo-R mRNAs. Total RNAs were prepared from RBECs, MBEC4 and phenylhydrazine-treated spleen and the first-strand cDNA was synthesized. (A) The RT-PCR products amplified using primers E1 and E7A were detected by Southern blot analysis using probe A. Lanes 1, 2 and 3 show the RT-PCR products from RBECs, MBEC4 and phenylhydrazine-treated spleen, respectively. (B) The RT-PCR products amplified using primers E5 and E7B were analyzed by Southern blot analysis using probe A. Lanes 1, 2 and 3 show the RT-PCR products from RBECs, MBEC4 and phenylhydrazine-treated spleen, respectively. (C) The RT reaction using total RNAs prepared from RBECs, MBEC4 and phenylhydrazine-treated spleen was performed in the presence or absence of reverse transcriptase. The RT reaction products were amplified using primers E5 and E6A. The RT-PCR products were analyzed by Southern blotting using probe A. Lanes 1–6 show the following RT-PCR products: lanes 1 and 2, RBECs; lanes 3 and 4, MBEC4; lanes 5 and 6, phenylhydrazine-treated spleen. Lanes 1, 3 and 5 show the RT-PCR products in the presence of reverse transcriptase and lanes 2, 4 and 6 show the RT-PCR products in the absence of reverse transcriptase. (D) The RT-PCR products amplified using primers E6B and E8 were detected by Southern blotting using probe B. Lanes 1, 2 and 3 show the RT-PCR products from RBECs, MBEC4 and phenylhydrazine-treated spleen, respectively. Each arrow in A–D indicates the RT-PCR product of the alternatively spliced Epo-R mRNA except for aEpo-R mRNA in rat erythroid progenitor cells. For estimation of molecular mass,  $\lambda$  DNA fragments digested with *Hind*III and *3'αEco*RI and  $\phi$ X174 fragments digested with *Hae*III were used in A and C and  $\phi$ X174 fragments digested with *Hae*III were used in B and D.

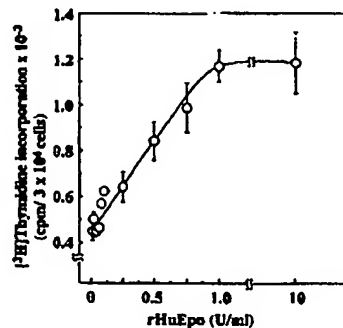


**Fig. 3.** Effect of rHuEpo on  $[^3\text{H}]$ thymidine incorporation into DNA of RBECs. RBECs were rendered quiescent by culturing in the serum-free medium (insulin, transferrin and selenious acid medium) for 24 h. After RBECs were treated with various concentrations of rHuEpo for 20 h,  $[^3\text{H}]$ thymidine incorporation was measured. Values are indicated as means  $\pm$  SEM of three experiments performed in triplicate.

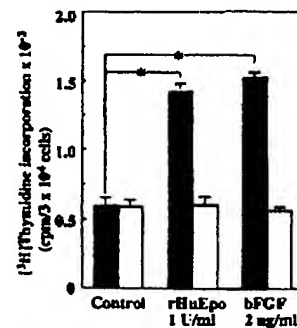


**Fig. 4.** Effect of insulin on DNA synthesis by rHuEpo in RBECs. RBECs were cultured with rHuEpo (1 U/ml) or bFGF (2 ng/ml) in insulin, transferrin and selenious acid medium or transferrin and selenious acid medium, thus in the presence (closed box) or absence (open box) of insulin, at 37°C for 20 h and then  $[^3\text{H}]$ thymidine incorporation was measured. Results are means  $\pm$  SEM of three experiments performed in triplicate. Statistically significant differences between control and rHuEpo or bFGF in the presence of insulin are indicated by: \* $P < 0.01$ .

gression factor, RBECs were cultured in the serum-free medium composed of MEM supplemented with either insulin, transferrin and selenious acid or transferrin and selenious acid. As shown in Fig. 4, when RBECs were cultured in MEM with insulin, transferrin and selenious acid, rHuEpo at 1 U/ml accelerated an incorporation of  $[^3\text{H}]$ thymidine into DNA; bFGF, which functions as a competence factor, also stimulated the DNA synthesis to the same level as rHuEpo. In contrast, neither rHuEpo nor bFGF had any influence on DNA synthesis in RBECs in the absence of insulin, a progression factor.

**Binding of rHuEpo to RBECs.** Fig. 5A shows the time dependency of the binding of  $^{125}\text{I}$ -rHuEpo to RBECs. When RBECs ( $10^5$  cells) were incubated in the presence of 450 pM  $^{125}\text{I}$ -rHuEpo at 4°C, the maximum specific binding reached equilibrium within 4 h and remained constant for at least 6 h. As shown in Fig. 5B, the specific binding was proportional to cell density throughout the range tested ( $2\text{--}12 \times 10^4$  cells/ml) after incubating for 4 h at 4°C in the presence of 450 pM labeled rHuEpo.

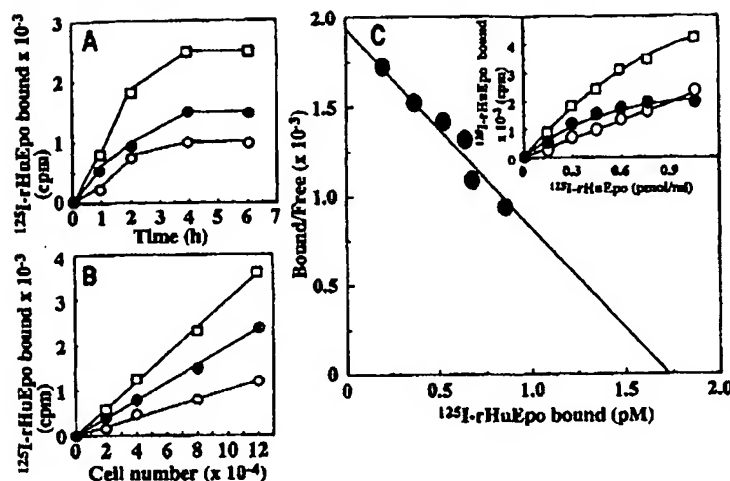


Fig. 5. Binding of radiolabeled rHuEpo to RBECs. (A) Time dependence of  $^{125}\text{I}$ -rHuEpo binding to RBECs. RBECs ( $10^5$  cells) were incubated with 450 pM  $^{125}\text{I}$ -rHuEpo for the indicated times at  $4^\circ\text{C}$ . (B) The effect of cell number on  $^{125}\text{I}$ -rHuEpo binding to RBECs. RBECs were incubated with 450 pM rHuEpo for 4 h at  $4^\circ\text{C}$ . (C) Scatchard analysis of the binding of  $^{125}\text{I}$ -rHuEpo to RBECs. RBECs ( $10^5$  cells) were incubated for 4 h at  $4^\circ\text{C}$  with the indicated concentrations of  $^{125}\text{I}$ -rHuEpo. Inset: direct representation of total, nonspecific and specific radioactivity bound to the cells as a function of the concentration of  $^{125}\text{I}$ -rHuEpo added. Nonspecific binding (O) was determined in the presence of 500-fold unlabeled rHuEpo. Specific binding ( $\bullet$ ) was calculated by subtraction of nonspecific binding from total binding ( $\square$ ). Results are the mean of three experiments in triplicate.

The  $K_d$  and the number of binding sites were evaluated by Scatchard plots (Fig. 5C; the inset represents the ligand-saturation curves). Data analyzed by the method of Scatchard indicate that RBECs have a single class of binding sites for Epo and express 10300 receptors/cell with a  $K_d$  of 860 pM.

## DISCUSSION

Mammals have adaptation mechanisms to hypoxia such as induction of the growth of new capillary blood vessels [1] and promotion of erythropoiesis [2]. Adenosine [27] and vascular endothelial growth factor [28–30] are the major candidates for angiogenic factors under hypoxic conditions and Epo has been thought to play a physiological role in erythropoiesis [3–5]. Endothelial cells and hematopoietic cells have a common origin in embryogenesis and it has been reported that angiogenic factors are hematopoietic growth factors and vice versa [31]. Recently, it has been reported that rHuEpo has a proliferative and a positive chemotactic effect on HUVECs and bovine adrenal capillary endothelial cells [6] and stimulates angiogenesis in rat thoracic aortas [9], suggesting that Epo acts on endothelial cells as an angiogenic factor. Furthermore, when the RT-PCR was performed using primers based on nucleotide sequences from exon 5 (sense) and exon 6 (antisense) of human Epo-R gene to assess expression of Epo-R mRNA in HUVECs, the aEpo-R mRNA was detected but not the intron-5-inserted form of Epo-R [7]. However, in the present study, the RT-PCR using primers E5 and E6, which are located in exon 5 and exon 6, respectively, provided evidence that two forms of Epo-R mRNA were expressed in rat and mouse brain capillary endothelial cells. In addition, each RT-PCR using primers E1 plus E7A and primers E5 plus E7B resulted in the amplification of two cDNA fragments containing a cDNA fragment targeted. It has been reported that SKT cells express an alternatively spliced Epo-R mRNA which is inserted intron 5 and part of intron 6 [26] and that 32D Epo and 32D GM cells, subclones of the murine 32D cell line, express several alternatively spliced Epo-R mRNAs

which result from retention of intron 5, part of intron 6, or intron 5 and part of intron 6, or loss of exon 5 [32] in addition to the aEpo-R mRNA. Taken into consideration with these results, the present results indicate that brain capillary endothelial cells express an intron-5-inserted form of Epo-R mRNA, thus the sEpo-R mRNA, as a major form and the aEpo-R mRNA as a minor form. Possible explanations for the difference between the results in HUVECs and the present results are the following: (a) The sEpo-R mRNA in human erythroid progenitor cells results from retention of part of intron 4 (104-bp insert) [33, 34]; in contrast, alternatively spliced mRNAs encoding sEpo-R in SKT6 cells, 32D Epo cells and 32D GM cells result from retention of intron 5 or intron 5 and part of intron 6 or loss of exon 5, but not retention of part of intron 4. (b) Expression of sEpo-R mRNA is characteristic of brain capillary endothelial cells, but not large vessel endothelial cells. We are now attempting to study whether HUVECs express sEpo-R mRNA resulting from retention of part of intron 4.

In the present study, we have cloned the full-length intron-5-inserted form of Epo-R cDNA from RBECs and the phenylhydrazine-treated rat spleen by RT-PCR using primers E1 and E7A and the RT-PCR products using primers E5 and E7B from RBECs and MBEC4. Sequence analysis showed that these cDNAs contained intron 5 but not intron 6. The nucleotide sequence of intron 5 for Balb/c murine sEpo-R reported previously is 78 bp long [26], whereas the nucleotide sequences of intron 5 for these cDNAs were 79 bp (data not shown). This difference is not due to differences between mouse species because MBEC4 are endothelial cells from Balb/c mouse. We are now studying whether our results are due to a PCR artifact. Therefore, in this report, the sizes of aEpo-R and sEpo-R mRNAs are indicated as the sizes expected from the known nucleotide sequence.

Cell proliferation requires at least two kinds of factors, a competence factor which leads cell from  $G_0$  to  $G_1$  phase, and a progression factor for the transfer of cells from  $G_1$  to S phase. bFGF and insulin are the competence factor and the progression

factor  
DN,  
stim  
indi  
as b  
the  
in r  
phy  
mia  
and  
tivel  
cells  
to bl  
caps  
the l  
cells  
ical  
oxia  
Epo  
phys  
theli  
dium  
Sept  
Pro  
anal  
or a  
DPK  
whi  
lumi  
tem  
both  
into  
dium  
cont  
of p  
to th  
not  
secre  
rHuE  
wher  
I  
and  
cell  
On t  
cell  
pM)  
and  
of 7  
the  
stud  
affin  
relat  
and  
othe  
cyte  
ende  
conc  
on t  
with  
astr  
unde  
cells

factor, respectively [35]. Both rHuEpo and bFGF stimulated the DNA synthesis in RBECs in the presence of insulin, whereas no stimulation was observed in the absence of insulin. These results indicate that rHuEpo functions as a competence factor as well as bFGF for RBECs.

rHuEpo maximally stimulated DNA synthesis of RBECs at the concentration of 1 U/ml. The serum concentrations of Epo in most animals are in the range of 10–30 mU/ml under normal physiological conditions and increase more than 100-fold in anemia [36, 37]. Furthermore, Epo concentration increases to 1.4 and 2.1 U/ml in rats exposed to 9% and 7.5% hypoxia, respectively, for 8 h [38]. The present study suggested that endothelial cells expressed sEpo-R, which is released from endothelial cells to blood, as a major form in addition to aEpo-R. sEpo-R has the capability to bind to Epo [39]. Therefore, sEpo-R may inhibit the binding of Epo circulating in blood to Epo-R on endothelial cells and thus function as an antagonist under normal physiological conditions. However, when excess Epo is induced by hypoxia, sEpo-R may be unable to prevent the binding of Epo to Epo-R on endothelial cells which are in G<sub>0</sub> phase under normal physiological conditions. In such cases, Epo may act on endothelial cells as a competent factor.

To assess whether sEpo-R accumulates in the culture medium, the conditioned medium was incubated with ConA-Sepharose resin or Epo-bound activated CH-Sepharose resin. Proteins bound to the resin were subjected to SDS/PAGE and analyzed by Western blot using anti-Epo-R polyclonal antibody or an antibody to amino-terminal peptides of Epo-R (ASSPSLP-DPKFESKAC). However, a positive band was not detected when the detection assay was performed by the enhanced chemiluminescence assay using Super Signal CL-HRP substrate system from Pierce (data not shown). On the other hand, although both rHuEpo and bFGF raised an incorporation of [<sup>3</sup>H]thymidine into DNA when RBECs were incubated in the serum-free medium and then the medium was replaced by serum-free medium containing rHuEpo or bFGF, only bFGF raised an incorporation of [<sup>3</sup>H]thymidine into DNA when rHuEpo or bFGF was added to the serum-free medium without replacing the medium (data not shown). These results imply a possibility that sEpo-R secreted from RBECs to the medium inhibits the binding of rHuEpo to Epo-R on RBECs. We are attempting to demonstrate whether sEpo-R accumulates in the medium.

RBECs had a single class of Epo-R with a  $K_d$  of 860 pM and expressed 10300 sites/cell. Epo-R expressed 27000 sites/cell with an affinity in the nanomolar range on HUVECs [6]. On the other hand, some erythroid progenitor cells and erythroid cell lines express Epo-R with both high-affinity ( $K_d$  = 90–410 pM) and low-affinity ( $K_d$  = 400–6100 pM) Epo binding sites and others express only a single class of binding sites with a  $K_d$  of 70–1390 pM [40]. A common characteristic of both is that the number of receptor sites/cell is less than 4000. The present study indicates that Epo-R on RBECs is classified into a low-affinity type and that endothelial cells express abundant Epo-R relative to the erythroid cells.

Since hypoxia is observed to induce Epo mRNA in testis and brain [38], Epo production is expected to be stimulated in other organs outside kidney under hypoxic conditions. Astrocytes, which are in close apposition to and interact directly with endothelial cells of brain capillary, produce Epo under hypoxic conditions [41]. The present study suggests that Epo acts directly on brain capillary endothelial cells as a novel mitogenic factor with a competence activity through a paracrine mechanism from astrocytes and an endocrine mechanism from kidney and testis under hypoxic conditions.

The present study indicated that brain capillary endothelial cells expressed sEpo-R mRNA as a major form. Since cells and

tissues expressing sEpo-R as a major form have not been found yet, brain capillary endothelial cells would be very useful to gain information concerning the physiological function of sEpo-R.

This work was supported by Grant-in-Aid (05660146) for scientific research (to Yoshihisa NAKANO) from the Japanese Ministry of Education, Science, and Culture. We thank Kirin Brewery (Gunma, Japan) for their kind gift of rHuEpo.

## REFERENCES

- Bouverot, P. (1985) Diffusive processes, in *Adaptation to altitude-hypoxia in vertebrates* (Bouverot, P., ed.) pp. 94–119. Springer-Verlag, New York.
- Bouverot, P. (1985) Circulatory adaptations, in *Adaptation to altitude-hypoxia in vertebrates* (Bouverot, P., ed.) pp. 61–93. Springer-Verlag, New York.
- Jacobson, L. O., Goldwasser, E., Fried, W. & Plzak, L. (1957) Role of the kidney in erythropoiesis, *Nature* **179**, 633–634.
- Jeikmann, W. (1992) Erythropoietin: Structure, control of production, and function, *Physiol. Rev.* **72**, 449–489.
- Krantz, S. B. (1991) Erythropoietin, *Blood* **77**, 419–434.
- Anagnostou, A., Lee, E. S., Kessimian, N., Levinson, R. & Steiner, M. (1990) Erythropoietin has a mitogenic and positive chemotactic effect on endothelial cells, *Proc. Natl Acad. Sci. USA* **87**, 5978–5982.
- Anagnostou, A., Liu, Z., Steiner, M., Chin, K., Lee, E. S., Kessimian, N. & Noguchi, C. T. (1994) Erythropoietin receptor mRNA expression in human endothelial cells, *Proc. Natl Acad. Sci. USA* **91**, 3974–3978.
- Carlini, R. G., Dusso, A. S., Obialo, C. I., Alvarez, U. M. & Rothstein, M. (1993) Recombinant human erythropoietin (rHuEPO) increases endothelin-1 release by endothelial cells, *Kidney Int.* **43**, 1010–1014.
- Carlini, R. G., Reyes, A. A. & Rothstein, M. (1995) Recombinant human erythropoietin stimulates angiogenesis *in vitro*, *Kidney Int.* **47**, 740–745.
- Gogusev, J., Zhu, D.-L., Hérembert, T., Ammarguelli, F., Marche, P. & Druke, T. (1994) Effect of erythropoietin on DNA synthesis, proto-oncogene expression and phospholipase activity in rat vascular smooth muscle cells, *Biochem. Biophys. Res. Commun.* **199**, 977–983.
- Kimata, H., Yoshida, A., Ishioka, C., Masuda, S., Sasaki, R. & Mikuwa, H. (1991) Human recombinant erythropoietin directly stimulates B cell immunoglobulin production and proliferation in serum-free medium, *Clin. Exp. Immunol.* **85**, 151–156.
- Sawyer, S. T., Krantz, S. B. & Sawada, K.-I. (1989) Receptors for erythropoietin in mouse and human erythroid cells and placenta, *Blood* **74**, 103–109.
- Heberlein, C., Fischer, K.-D., Stoffel, M., Nowock, J., Furd, A., Tessmer, U. & Stocking, C. (1992) The gene for erythropoietin receptor is expressed in multipotential hematopoietic and embryonal stem cells: evidence for differentiation stage-specific regulation, *Mol. Cell. Biol.* **12**, 1815–1826.
- Schmitt, R. M., Bruyas, E. & Snodgrass, H. R. (1991) Hematopoietic development of embryonic stem cells *in vitro*: cytokine and receptor gene expression, *Genes & Dev.* **5**, 728–740.
- Ishibashi, T., Koziol, J. A. & Burstein, S. A. (1987) Human recombinant erythropoietin promotes differentiation of murine megakaryocytes *in vitro*, *J. Clin. Invest.* **79**, 286–289.
- Masuda, S., Nagao, M., Takahata, K., Konishi, Y., Gallyas, F. J., Tabira, T. & Sasaki, R. (1993) Functional erythropoietin receptor of the cells with neural characteristics, *J. Biol. Chem.* **268**, 11208–11216.
- Digacaylinglu, M., Bichel, S., Marti, H. H., Wenger, R. H., Rivas, L. A., Bauer, C. & Gassmann, M. (1995) Localization of specific erythropoietin binding sites in defined areas of the mouse brain, *Proc. Natl Acad. Sci. USA* **92**, 3717–3720.
- Ausprunk, D. H. & Folkman, J. (1977) Migration and proliferation of endothelial cells in preformed and newly formed blood vessels during tumor angiogenesis, *Microvascul. Res.* **14**, 53–65.
- Montesano, R. (1992) Regulation of angiogenesis *in vitro*, *Eur. J. Clin. Invest.* **22**, 504–515.

20. Lamanna, J. C., Vendel, L. M. & Farrell, R. M. (1992) Brain adaptation to chronic hypobaric hypoxia in rats, *J. Appl. Physiol.* **72**, 2238–2243.
21. Hoppeler, H., Howald, H. & Cerretelli, P. (1990) Human muscle structure after exposure to extreme altitude, *Experientia* **46**, 1185–1187.
22. Tatsuta, T., Naito, M., Oh-hara, T., Sugawara, I. & Tsuruo, T. (1992) Functional involvement of P-glycoprotein in blood-brain barrier, *J. Biol. Chem.* **267**, 20383–20391.
23. Bowman, P., Betz, A. L., AR, D., Wolinsky, J. S., Penney, J. B., Shivers, R. R. & Goldstein, G. W. (1981) Primary culture of capillary endothelium from rat brain, *In vitro* **17**, 353–362.
24. Chomczynski, P. & Sacchi, N. (1987) Single-step method of RNA isolation by acid guanidinium thiocyanate-phenol-chloroform extraction, *Anal. Biochem.* **162**, 156–159.
25. Sasaki, R., Ohnata, H., Yanagawa, S.-I. & Chiba, H. (1985) Dietary protein-induced changes of the erythropoietin level in rat serum, *Agric. Biol. Chem.* **49**, 2671–2683.
26. Kuramochi, S., Ikawa, Y. & Todokoro, K. (1990) Characterization of murine erythropoietin receptor genes, *J. Mol. Biol.* **216**, 567–575.
27. Meininger, C. J., Schelling, M. E. & Granger, H. J. (1988) Adenosine and hypoxia stimulate proliferation and migration of endothelial cells, *Am. J. Physiol.* **255**, H554–H562.
28. Goldberg, M. A. & Schneider, T. J. (1994) Similarities between the oxygen-sensing mechanisms regulating the expression of vascular endothelial growth factor and erythropoietin, *J. Biol. Chem.* **269**, 4355–4359.
29. Ladoux, A. & Frelin, C. (1993) Hypoxia is a strong inducer of vascular endothelial growth factor mRNA expression in the heart, *Biochem. Biophys. Res. Commun.* **195**, 1005–1010.
30. Shweiki, D., Ikin, A., Soffer, D. & Keshet, E. (1992) Vascular endothelial growth factor induced by hypoxia may mediate hypoxia-initiated angiogenesis, *Nature* **359**, 843–848.
31. Bikfalvi, A. & Han, Z. C. (1994) Angiogenic factors are hematopoietic growth factors and vice versa, *Leukemia* **8**, 523–529.
32. Barron, C., Migliaccio, A. R., Migliaccio, G., Jiang, Y., Adamson, J. W. & Ottolenghi, S. (1994) Alternatively spliced mRNAs encoding soluble isoforms of the erythropoietin receptor in murine cell lines and bone marrow, *Gene* **147**, 263–268.
33. Nakamura, Y., Komatsu, N. & Nakauchi, H. (1992) A truncated erythropoietin receptor that fails to prevent programmed cell death of erythroid cells, *Science* **257**, 1138–1141.
34. Todokoro, K., Kuramochi, S., Nagasawa, T., Abe, T. & Ikawa, Y. (1991) Isolation of cDNA encoding a potential soluble receptor for human erythropoietin, *Gene* **106**, 283–284.
35. Scher, C. D., Shepard, R. C., Antoniades, H. N. & Stiles, C. D. (1979) Platelet-derived growth factor and the regulation of the mammalian fibroblast cell cycle, *Biochim. Biophys. Acta* **560**, 217–241.
36. Garcia, J. F., Ehbe, S. N., Hollander, L., Cutting, H. O., Miller, M. E. & Cronkite, E. D. (1982) Radioimmunoassay of erythropoietin: circulating levels in normal and polycythemic human beings, *J. Lab. Clin. Med.* **99**, 624–635.
37. Koeffler, H. P. & Goldwasser, E. (1981) Erythropoietin radioimmunoassay in evaluating patients with polycythemia, *Ann. Int. Medicine* **94**, 44–47.
38. Tan, C. C., Eckardt, K.-U., Firth, J. D. & Ratcliffe, P. J. (1992) Feedback modulation of renal and hepatic erythropoietin mRNA in response to graded anemia and hypoxia, *Am. J. Physiol.* **263**, F474–F481.
39. Nagao, M., Masuda, S., Abe, S., Ueda, M. & Sasaki, R. (1992) Production and ligand-binding characteristics of the soluble form of murine erythropoietin receptor, *Biochem. Biophys. Res. Commun.* **188**, 888–897.
40. Sawyer, S. T. (1990) Receptors for erythropoietin distribution, structure, and role in receptor-mediated endocytosis in erythroid cells, in *Blood cell biochemistry* (Harris, J. R., ed.) vol. 1, pp. 365–402. Plenum, New York.
41. Masuda, S., Okano, M., Yamagishi, K., Nagao, M., Ueda, M. & Sasaki, R. (1994) A novel site of erythropoietin production, *J. Biol. Chem.* **269**, 19488–19493.



the project

protein atlas

dictionary

disclaimer

submission of antibodies

## CSF2RB expression profiles. Validation score: N/A

**Gene data**

Description: **Cytokine receptor common beta chain precursor (GM-CSF/IL-3/IL-5 receptor common beta-chain) (CD131 antigen) (CDw131).**  
 Source: **P32927** (Uniprot)  
 Chromosome: **22:q12.3**  
 Ensembl ID: **ENSG00000100368**

Splice variant 1: **Protein Ensembl ID: ENSP00000262825** **Transcript Ensembl ID: ENST00000262825** **No of aa: 897** **Mw: 97 kDa** **Signal Peptide: Yes** **TM Region(s): Yes**

**Normal Tissues - IHC**

**Adrenal gland** cortical cells **Lymph node** lymphoid cells outside reaction centra  
**Appendix** glandular cells **Nasopharynx** reaction center cells  
 lymphoid cells **Oral mucosa** respiratory epithelial cells  
**Bone marrow** bone marrow poietic cells **Ovary** squamous epithelial cells  
 glandular cells **Pancreas** follicle cells  
**Breast** respiratory epithelial cells **Parathyroid gland** ovarian stromal cells  
**Bronchus** cells in granular layer **Placenta** exocrine glandular cells  
**Cerebellum** cells in molecular layer **Prostate** islet cells  
 purkinje cells **Rectum** glandular cells  
 glial cells **Salivary gland** decidual cells  
**Cerebral cortex** neuronal cells **Seminal vesicle** trophoblastic cells  
 glandular cells **Skeletal muscle** glandular cells  
 squamous epithelial cells **Skin** glandular cells  
 cells in endometrial stroma **Small intestine** glandular cells  
 glandular cells **Smooth muscle** glandular cells  
 cells in endometrial stroma **Soft tissue 1** smooth muscle cells  
 glandular cells **Soft tissue 2** mesenchymal cells  
 glandular cells **Spleen** mesenchymal cells  
 glandular cells **Stomach 1** cells in red pulp  
 glandular cells **Stomach 2** cells in white pulp  
 myocytes **Testis** glandular cells  
 glial cells **Thyroid gland** glandular cells  
 neuronal cells **Tonsil** lymphoid cells outside reaction centra  
 cells in glomeruli **Urinary bladder** reaction center cells  
 cells in tubules **Vagina** squamous epithelial cells  
 glial cells **Vulva/anal skin** urothelial cells  
 neuronal cells **Vulva/anal skin** squamous epithelial cells  
 bile duct cells **Vulva/anal skin** squamous epithelial cells  
 hepatocytes **Vulva/anal skin** squamous epithelial cells  
 alveolar cells **Vulva/anal skin** squamous epithelial cells  
 macrophages **Vulva/anal skin** squamous epithelial cells

**Annotation Summary - IHC**

Normal tissues exhibited moderate cytoplasmic staining. Strong cytoplasmic immunoreactivity, occasionally combined with nuclear positivity, was observed for example in neuronal cells and trophoblastic cells. Malignancies displayed similar staining pattern as normal cells, mainly weak to moderate cytoplasmic and rare nuclear staining. A few malignant gliomas and liver cancers showed strong cytoplasmic positivity.

## Navigation

Home

Search result

CAB010251

## Expression profile

Normal tissues

Cancer tissues

Cells IHC

Antibody info

## Search

## Protein expression

- Strong
- Moderate
- Weak
- Negative
- Not represented



alph. sort order		Cancer Tissues - IHC	
<u>Breast cancer</u> <u>Cervical cancer</u> <u>Colorectal cancer</u> <u>Endometrial cancer</u> <u>Head &amp; neck cancer</u> <u>Liver cancer</u> <u>Lung cancer</u> <u>Malignant carcinoid</u> <u>Malignant glioma</u> <u>Malignant lymphoma</u> <u>Malignant melanoma</u> <u>Ovarian cancer</u> <u>Pancreatic cancer</u> <u>Prostate cancer</u> <u>Renal cancer</u> <u>Skin cancer</u> <u>Stomach cancer</u> <u>Testis cancer</u> <u>Thyroid cancer</u> <u>Urothelial cancer</u>			
		Cell lines - IHC	
<u>HEL</u> <u>HL-60</u> <u>HMC-1</u> <u>K-562</u> <u>NB-4</u> <u>THP-1</u> <u>U-937</u>	Myeloid	<u>CACO-2</u> <u>CAPAN-2</u> <u>Hep-G2</u> Breast, female reproductive system <u>AN3-CA</u> <u>EFO-21</u> <u>HeLa</u> <u>MCF-7</u> <u>SiHa</u> <u>SK-BR-3</u> Urinary, male reproductive system <u>NTERA-2</u> <u>PC-3</u> <u>RT-4</u>	
	Lymphoid	Skin <u>A-431</u> <u>HaCaT</u> <u>SK-MEL-30</u> <u>WM-115</u> Sarcoma <u>RH-30</u> <u>U-2 OS</u> <u>U-2197</u> Miscellaneous <u>BEWO</u> <u>HEK 293</u> <u>HTH 83</u> <u>TIME</u>	
	Brain		
<u>Daudi</u> <u>HDLM-2</u> <u>Karpas-707</u> <u>KM3</u> <u>LP-1</u> <u>MOLT-4</u> <u>RPMI-8226</u> <u>U-266/70</u> <u>U-266/84</u> <u>U-698</u>			
<u>D341 Med</u> <u>SH-SY5Y</u> <u>U-138MG</u> <u>U-251MG</u> <u>U-87MG</u>			
<u>A-549</u> <u>SCLC-21H</u>	Lung		
		Cells - IHC	
<u>Leukemia, AML</u> <u>Leukemia, AML</u> <u>Leukemia, B-ALL</u> <u>Leukemia, B-CLL subtype 1</u> <u>Leukemia, B-CLL subtype 2</u> <u>Leukemia, B-CLL subtype 3</u>		<u>Leukemia, B-CLL subtype 4</u> <u>Leukemia, CML</u> <u>Leukemia, CML</u> <u>Leukemia, T-ALL</u> <u>PBMC</u> <u>PBMC</u>	



Send questions, comments or suggestions to [contact@hpa.se](mailto:contact@hpa.se) | FAO





## Appendix C

1. Bianchi et al., entitled "Protective effect of erythropoietin and its carbamylated derivative in experimental cisplatin peripheral neurotoxicity", Clin. Canc. Res. 2006, 12: 2607-2612.
2. Bodo et al., entitled "Human hair follicles are an extrarenal source and a nonhematopoietic target of erythropoietin", FASEB J. 2007, 21: 3346-3354.
3. Brines et al., entitled "Erythropoietin mediates tissue protection through an erythropoietin and common  $\beta$ -subunit heteroreceptor", PNAS 2004, 101: 14907-14912.
4. Brines et al., entitled "Tissue protective cytokines for the treatment and prevention of sepsis and the formation of adhesions", WO/2005/032467.
5. Chong et al., entitled "Vascular injury during elevated glucose can be mitigated by erythropoietin and Wnt signaling", Curr. Neurovasc. Res. 2007, 4: 194-204.
6. Contaldo et al., entitled "Human recombinant erythropoietin protects the striated muscle microcirculation of the dorsal skinfold from postischemic injury in mice", Am. J. Physiol. Heart Circ. Physiol. 2007, 293: H274-H283.
7. Guneli et al., entitled "Erythropoietin protects the intestine against ischemia/reperfusion injury in rats" Mol. Med. 2007, 13: 509-517.
8. Holstein et al., entitled "Erythropoietin (EPO) - EPO-receptor signaling improves early endochondral ossification and mechanical strength in fracture healing", Life Sci. 2007: 893-900.
9. Kitamura et al., entitled "Nonerythropoietic derivative of erythropoietin protects against tubulointerstitial injury in a unilateral ureteral obstruction model", Nephrol. Dial. Transplant. 2008, 0: 1-8.
10. Monge et al., entitled "The effect of erythropoietin on gentamicin-induced auditory hair cell loss", Laryngoscope 2006, 116: 312-316.
11. Moon et al., entitled "Erythropoietin, modified to not stimulate red blood cell production, retains its cardioprotective properties", J. Pharmacol. Exp. Ther. 2006, 316: 999-1005.
12. Savino et al., entitled "Delayed administration of erythropoietin and its non-erythropoietic derivatives ameliorates chronic murine autoimmune encephalomyelitis", J. Neuroimmunol. 2006, 172: 27-37.
13. Tascilar et al., entitled "Protective effects of erythropoietin against acute lung injury in a rat model of acute necrotizing pancreatitis", World J. Gastroenterol. 2007, 13: 6172-6182.
14. Wang et al., entitled "Post-ischemic treatment with erythropoietin or carbamylated erythropoietin reduces infarction and improves neurological outcome in a rat model of focal cerebral ischemia", Brit. J. Pharmacol. 2007, 151: 1337-1384.

15. Yazihan et al., Turk. J. entitled "Erythropoietin attenuates hydrogen peroxide-induced damage of hepatocytes", Gastroenterol. 2007, 18: 239-244.

## Protective Effect of Erythropoietin and Its Carbamylated Derivative in Experimental Cisplatin Peripheral Neurotoxicity

Roberto Bianchi,<sup>1</sup> Michael Brines,<sup>3</sup> Giuseppe Lauria,<sup>2</sup> Costanza Savino,<sup>1</sup> Alessandra Gilardini,<sup>4</sup> Gabriella Nicolini,<sup>4</sup> Virginia Rodriguez-Menendez,<sup>4</sup> Norberto Oggioni,<sup>4</sup> Annalisa Canta,<sup>4</sup> Paola Penza,<sup>2</sup> Raffaella Lombardi,<sup>2</sup> Claudio Minoia,<sup>5</sup> Anna Ronchi,<sup>5</sup> Anthony Cerami,<sup>3</sup> Pietro Ghezzi,<sup>1,3</sup> and Guido Cavaletti<sup>4</sup>

**Abstract** **Purpose:** Antineoplastic drugs, such as cisplatin (CDDP), are severely neurotoxic, causing disabling peripheral neuropathies with clinical signs known as chemotherapy-induced peripheral neurotoxicity. Cotreatment with neuroprotective agents and CDDP has been proposed for preventing or reversing the neuropathy. Erythropoietin given systemically has a wide range of neuroprotective actions in animal models of central and peripheral nervous system damage. However, the erythropoietic action is a potential cause of side effects if erythropoietin is used for neuroprotection. We have successfully identified derivatives of erythropoietin, including carbamylated erythropoietin, which do not raise the hematocrit but retain the neuroprotective action exerted by erythropoietin. **Experimental Design:** We have developed previously an experimental chemotherapy-induced peripheral neurotoxicity that closely resembles CDDP neurotoxicity in humans. The present study compared the effects of erythropoietin and carbamylated erythropoietin (50 µg/kg/d thrice weekly) on CDDP (2 mg/kg/d i.p. twice weekly for 4 weeks) neurotoxicity *in vivo*. **Results:** CDDP given to Wistar rats significantly lowered their growth rate ( $P < 0.05$ ), with slower sensory nerve conduction velocity ( $P < 0.001$ ) and reduced intraepidermal nerve fiber density ( $P < 0.001$  versus controls). Coadministration of CDDP and erythropoietin or carbamylated erythropoietin partially but significantly prevented the sensory nerve conduction velocity reduction. Both molecules preserved intraepidermal nerve fiber density, thus confirming their neuroprotective effect at the pathologic level. The protective effects were not associated with any difference in platinum concentration in dorsal root ganglia, sciatic nerve, or kidney specimens. **Conclusions:** These results widen the spectrum of possible use of erythropoietin and carbamylated erythropoietin as neuroprotectant drugs, strongly supporting their effectiveness.

Chemotherapy-induced peripheral neurotoxicity (CIPN) is a major clinical problem because it is a dose-limiting side effect of important and effective antineoplastic drugs (1). The incidence, severity, and clinical symptoms and signs of CIPN depend on the drug given and its schedules. Severe neuropathy can occur in 3% to 7% of treated cases with single agents but can increase to 38% with combined regimens (2, 3). Moreover, even when CIPN is not dose-limiting, it may severely affect the

quality of life of cancer patients and cause chronic discomfort. Therefore, effective prevention and/or treatment of CIPN would be a major advance for cancer patients.

Cisplatin (CDDP) and the other platinum-derived drugs are among the most effective antineoplastic agents, but they are severely neurotoxic. The clinical features of CDDP neurotoxicity in humans are mainly ataxia, pain, and sensory impairment secondary to accumulation of CDDP in the dorsal root ganglia (DRG) and subsequent damage, resulting in secondary nerve fiber axonopathy.

We have developed an experimental model of peripheral neurotoxicity induced by CDDP (4–9) that closely resembles CDDP neurotoxicity in humans. It involves the reversible primary involvement of DRG neurons, with secondary sensory axonal neuropathy and sparing of the motoneurons. This model has already been used to investigate the mechanisms of neurotoxic action of CDDP (4, 5, 7, 9) and to test the effect of putative neuroprotective agents (6, 8–13). Among these agents, cotreatment with neurotrophic agents has been proposed as a means of preventing or reversing CIPN (14).

Among the several substances with trophic action on central neurons and peripheral nerves, erythropoietin has a

**Authors' Affiliations:** <sup>1</sup>"Mario Negri" Institute for Pharmacological Research; <sup>2</sup>"Basta" National Neurological Institute, Milan, Italy; <sup>3</sup>Kenneth S. Warren Institute, Kitchawan, New York; <sup>4</sup>University of Milan "Bicocca," Monza, Italy; and <sup>5</sup>"Maugeri" Foundation, Pavia, Italy

Received 10/8/06; revised 1/16/07; accepted 1/26/07.

Grant support: Fondazione Banca Del Monte di Lombardia (G. Cavaletti).

The costs of publication of this article were defrayed in part by the payment of page charges. This article must therefore be hereby marked advertisement in accordance with 18 U.S.C. Section 1734 solely to indicate this fact.

Requests for reprints: Roberto Bianchi, Molecular Biochemistry and Pharmacology, "Mario Negri" Institute for Pharmacological Research, Via Eritrea, 62, Milan 20157, Italy. Phone: 39-239014484; Fax: 39-02-3546277; E-mail: robbia@marionegri.it

© 2006 American Association for Cancer Research.  
doi:10.1158/1078-0432.CCR-05-2177

wide range of neuroprotective effects *in vivo*. Erythropoietin receptors are expressed both in nerve axons and Schwann cells and in DRG neurons and are overexpressed after nerve injury (15-17), presenting a target for pharmacotherapy. In primary neuronal cultures or neuronal cell lines, recombinant human erythropoietin protects from apoptosis (18, 19). *In vivo*, erythropoietin protects neurons from cerebral ischemia and traumatic injury (20) and reduces the severity of experimental autoimmune encephalomyelitis, spinal cord injury, and sciatic nerve compression (21). We recently found that erythropoietin both protects against and lowers the severity of experimental diabetic neuropathy (22). Erythropoietin is also protective against peripheral neuropathy induced by CDDP in rats, evaluated by electrophysiology (compound muscle action potential) and histologic examination of the number of nerve fibers (23).

One major issue in the use of erythropoietin is its erythrodifferentiating action that could be cause of several side effects, including vascular perfusion defects (24). In mice, the increase in hematocrit induced by erythropoietin causes vasoconstriction and cardiac dysfunction due to nitric oxide depletion and endothelin activation (25, 26). In animals and humans, erythropoietin can lead to hypertension (27, 28) or thrombosis (29).

Recently, we have identified derivatives of erythropoietin, including carbamylated erythropoietin (30) and asialo-erythropoietin (21), which are nonerythropoietic but retain neuroprotective action in different animal models, including cerebral ischemia, spinal cord injury, and diabetic neuropathy.

In this study, we investigated the potential role of erythropoietin and carbamylated erythropoietin for neuroprotection against CIPN induced by CDDP.

Because carbamylated erythropoietin does not increase the hematocrit and does not bind the hemopoietic, homodimeric erythropoietin receptor, the present model should enable us to dissociate a peripheral neuroprotective action of erythropoietin from a hemopoietic effect and determine whether neuroprotection can be achieved without the risk associated with the use of erythropoietin in nonanemic patients.

## Materials and Methods

**Animal husbandry.** All the procedures involving animals and their care were conducted in conformity with the institutional guidelines in compliance with national (Law by Decree No. 116, February 18, 1992, *Gazzetta Ufficiale della Repubblica Italiana*, Suppl. 40) and international (European Economic Community Council Directive 86-609, December 12, 1987, in *Official Journal of Law*, p. 358; Guide for the Care and Use of Laboratory Animals, U.S. National Research Council, 1996) laws and policies. The protocols for the investigation were reviewed and approved by the Animal Care and Use Committees of the Istituto di Ricerche Farmacologiche "Mario Negri" (Milan) and the Faculty of Medicine, University of Milano "Bicocca".

A total of 72 female Wistar rats (200-220 g at the beginning of the experiment; Harlan Italia, Correzzana, Italy) were used for the study. They were housed in a limited access animal facility with room temperature and relative humidity  $22 \pm 2^\circ\text{C}$  and  $55 \pm 10\%$  and unrestricted access to food and water. Artificial lighting provided a 24-hour cycle of 12-hour light/12-hour dark (light 7 a.m.-7 p.m.).

**Drugs.** CDDP (Platamine) was purchased from Pharmacia Italia (Milan, Italy). Erythropoietin was obtained from Dragon Pharmaceuticals (Vancouver, British Columbia, Canada). Carbamylated erythro-

poietin was prepared as described (30) and was kindly provided by H. Lundbeck (A/S, Valby, Copenhagen, Denmark).

**In vivo studies.** Two separate experiments were done. In a first experiment, we studied the effects of erythropoietin on CDDP-induced neuropathy. Thirty-two rats were randomly divided into four groups (8 per group): CDDP, CDDP plus erythropoietin, erythropoietin, and untreated controls. CDDP was dissolved in sterile saline and rats were injected with CDDP 2 mg/kg i.p. twice weekly for 8 times using a volume of 4 mL/kg (31, 32). The CDDP plus erythropoietin group was treated with the same dose of CDDP plus erythropoietin (50 µg/kg i.p. thrice weekly). The erythropoietin group received only the drug as above. In a second experiment, we studied the effect of carbamylated erythropoietin (50 µg/kg i.p. thrice weekly) on CDDP-induced neuropathy. Forty rats were randomly divided into five groups (8 per group): CDDP, CDDP plus erythropoietin, CDDP plus carbamylated erythropoietin, carbamylated erythropoietin, and control.

In both experiments, control rats received sham i.p. injections with the CDDP solvent.

**Methods of evaluation.** General conditions of the animals were recorded daily, and weight was measured at the time of drug administration.

At the end of the treatment, each rat's sensory nerve conduction velocity (SNCV) was determined in the tail using a previously described method (6, 9). Briefly, antidromic SNCV was assessed by stimulating the tail nerve with ring electrodes placed 5 and 10 cm proximally to the recording ring electrodes placed distally in the tail. The latencies of the potentials recorded at the two sites after nerve stimulation were determined (peak-to-peak) and the nerve conduction velocity was calculated accordingly. All the neurophysiologic measurements were done under standard conditions in a temperature-controlled room.

At the end of the experiment, the animals were euthanized under general xylazine/ketamine anesthesia and tissue specimens were obtained.

Peripheral nerve damage was assessed on pathologic grounds by skin biopsy and an estimate of intraepidermal nerve fiber (IENF) density in the hindpaw footpad (33). Briefly, skin specimens were fixed in 2% paraformaldehyde-lysine periodate for 24 hours at  $4^\circ\text{C}$ , cryoprotected overnight, and serially cut with a cryostat to obtain 20 µm sections. Three sections were randomly selected and immunostained with polyclonal anti-PGP 9.5 (Biogenesis, Poole, United Kingdom) using a free-floating protocol (33). Three blinded observers counted the total number of IENF in each section under a light microscope at high magnification using a microscope-mounted video camera. Individual fibers were counted as they crossed the dermal-epidermal junction, and secondary branching within the epidermis was excluded. The length of the epidermis was measured using a computerized system (Microscience, Seattle, WA) to obtain the linear density of IENF.

Whole blood was obtained through abdominal aorta puncture, collected into a heparinated tube for hematocrit determination, and centrifuged at 2,500 rpm for 20 minutes at  $4^\circ\text{C}$ . Total and erythrocyte capillary tube length was measured and the hematocrit was calculated as a percentage by dividing the particulate by total length and multiplying it by 100.

Sciatic nerves, DRG, and kidneys of rats from all CDDP-treated groups were obtained, snap-frozen in liquid nitrogen, and kept at  $-80^\circ\text{C}$  until used to determine the platinum concentration by inductively coupled plasma-tandem mass spectrometry according to the previously reported protocol (6).

**Statistics.** The differences between all experimental groups in body weight, SNCV, IENF density, and tissue platinum concentrations were examined by ANOVA and the Tukey-Kramer post-test.

## Results

**General toxicity.** All the rats completed the studies, with no evidence of severe general toxicity. In each experiment, at

**Table 1.** Physiologic variables of rats treated with CDDP and/or cotreated with erythropoietin and carbamylated erythropoietin

Group	Experiment 1			Experiment 2		
	Baseline body weight (g)	Final body weight (g)	Hematocrit (%)	Baseline body weight (g)	Final body weight (g)	Hematocrit (%)
Control + vehicle	186 ± 2	221 ± 3	51.9 ± 1.0	184 ± 6	256 ± 9	50.0 ± 1.8
CDDP + vehicle	197 ± 3	199 ± 3*	47.6 ± 1.2	181 ± 3	212 ± 6*	52.3 ± 1.1
Control + erythropoietin	196 ± 2	222 ± 3	82.4 ± 1.5 <sup>†</sup>			
Control + carbamylated erythropoietin				184 ± 3	248 ± 6	56.4 ± 2.3
CDDP + erythropoietin	195 ± 3	209 ± 6	84.3 ± 1.2 <sup>†</sup>	182 ± 5	229 ± 7	76.2 ± 6.3 <sup>†</sup>
CDDP + carbamylated erythropoietin				180 ± 5	230 ± 5	61.0 ± 1.3

NOTE: Data are mean ± SE (8 per group). Statistics by ANOVA with Tukey-Kramer HSD test for multiple comparisons.

\*P < 0.01 versus control and control + erythropoietin (experiment 1).

†P < 0.01 versus all the other groups (experiment 2).

‡P < 0.01 versus control and CDDP (experiment 1).

§P < 0.01 versus all the other groups (experiment 2).

baseline, there was no difference in body weight between groups. CDDP alone significantly reduced weight gain (Table 1); CDDP-treated rats weighed 10% and 17% less than the control groups in experiments 1 and 2, respectively ( $P < 0.01$  in both cases), and the coadministration of erythropoietin or carbamylated erythropoietin reduced the difference by ~50%.

Hematocrit was significantly higher in both erythropoietin-treated groups ( $P < 0.01$ ), whereas carbamylated erythropoietin did not produce any significant change from control rats (Table 1).

**Tail nerve neurophysiologic evaluation.** In each experiment, baseline SNCV did not differ in the two groups. In the first experiment, tail SNCV studies at the end of the treatment showed that the erythropoietin and control groups were very similar (Fig. 1A). This was confirmed in the second experiment, which, in addition, showed similar results for carbamylated erythropoietin (Fig. 1B). CDDP, however, reduced mean SNVC by 26% and 30% compared with control in experiments 1 and 2, respectively ( $P < 0.001$ ). In both experiments, erythropoietin had a partial, but highly significant, protective effect (Fig. 1A and B) and SNCV compared with the CDDP group, although it remained different from control (mean of experiments 1 and 2, -15.7% and -17.8%, respectively;  $P < 0.001$ ). Similarly, carbamylated erythropoietin partially prevented the decrease in SNVC induced by CDDP ( $P < 0.05$ ; Fig. 1B).

**IEFN density.** In footpad skin, both the neurotoxic effect of CDDP and the neuroprotective action of erythropoietin and carbamylated erythropoietin were confirmed at the pathologic level. Figure 2 summarizes the results of the two experiments. Erythropoietin and carbamylated erythropoietin coadministered did not affect IEFN density in control rats (data not shown). CDDP significantly reduced the epidermal innervation density (mean 13.1% lower than control) and caused diffuse morphologic changes of nerve fibers, indicating axonal degeneration (Fig. 3). Erythropoietin and carbamylated erythropoietin coadministered significantly ( $P < 0.001$ ) protected against from the loss of IEFN induced by CDDP (Figs. 2 and 3).

**Tissue platinum concentration.** Platinum in control specimens was below the limit of detection of the inductively coupled plasma-mass spectrometry method (i.e.,  $<0.001 \mu\text{g/g}$  tissue), but it was detectable in specimens from CDDP-treated rats. No significant differences were observed between CDDP and CDDP plus erythropoietin groups ( $7.64 \pm 0.82$  versus  $9.11 \pm 1.84$ ,  $1.86 \pm 0.41$  versus  $1.67 \pm 0.23$ , and

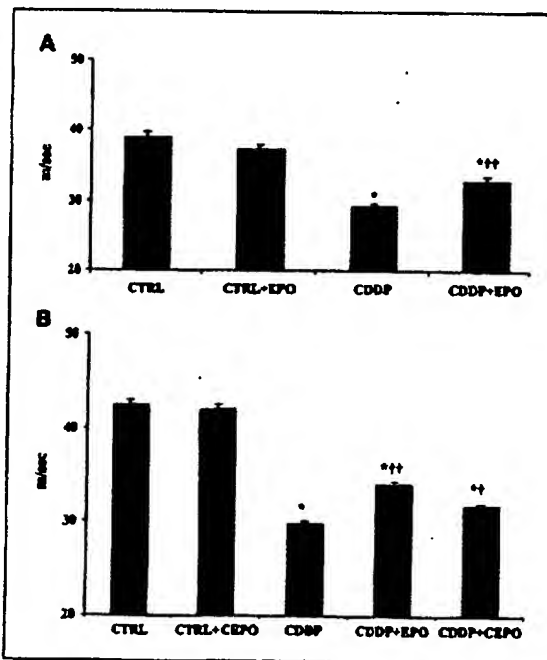


**Fig. 1.** SNCV at the end of the treatment. Columns, mean (in m/s) of seven to eight per group; bars, SE. A, experiment 1. \*,  $P < 0.001$  versus control (CTRL) and control + erythropoietin (EPO); †,  $P < 0.01$  versus CDDP. B, experiment 2. \*,  $P < 0.001$  versus control and control + carbamylated erythropoietin (CEPO); ‡,  $P < 0.01$  versus CDDP; §,  $P < 0.05$  versus CDDP; ††,  $P < 0.01$  versus CDDP.

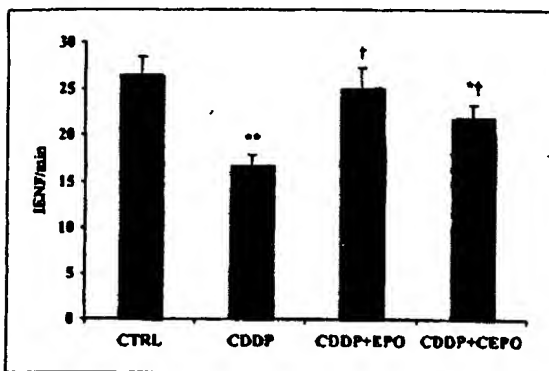


Fig. 2. Erythropoietin restores the loss of intraepidermal fibers in CDDP-treated rats. Skin biopsies were obtained at the end of the treatment. Columns: mean (number of IENF/mmo) of seven to eight per group; bars: SE. \*,  $P < 0.05$  versus control (CTRL); \*\*,  $P < 0.001$  versus control; †,  $P < 0.001$  versus CDDP.

2.38 versus 3.16  $\mu\text{g/g}$  tissue for kidney, sciatic nerves, and pooled DRG samples, respectively). Hence, the protective effect of erythropoietin was not associated with any difference in platinum concentration in DRG, sciatic nerve, or kidney specimens.

### Discussion

CIPN is a major limitation in the current treatment of cancer with platinum drugs, because it frequently requires a dose reduction or even treatment withdrawal, on account of adverse effects. Therefore, effective strategies to prevent or reduce the severity of CIPN are a major goal of preclinical research, with a view to clinical application. *In vitro* studies have been frequently used for screening putative neuroprotective agents, because they are faster and cheaper than *in vivo* testing. However, the latter reproduce the clinical picture in humans more reliably, including the effects of drug metabolism and bioavailability and tissue distribution, with respect to the target organs in particular.

The peripheral neuropathy induced in rats by repeated administration of CDDP is qualitatively similar to that in humans, involving the degeneration of sensory nerve fibers caused by DRG neuronopathy. The model of CIPN used in this study has already been extensively characterized in our laboratory (4–9) and has been used to assess the effectiveness of several putative neuroprotective agents. Some were not effective (9, 31), whereas others had at least a partial effect (6, 8, 10, 12, 13). The usefulness and reliability of the preclinical results were further strengthened when one of these neuroprotectants (reduced glutathione) was evaluated in a randomized, double-blind, placebo-controlled clinical trial in ovarian cancer patients (32), which confirmed its partial protective effect against CDDP neurotoxicity, previously evidenced in the animal model.

The use of neurophysiologic tests to assess the effect of neurotoxic or neuroprotective agents is well established (6–8, 34–36). They are also largely used in clinical practice in human neuropathies. However, pathologic confirmation of the neurophysiologic results is always advisable. In our

CDDP model, we have extensively reported the pathologic features in DRG, sciatic nerves, and tibial nerves (5). In the present study, for the first time, we investigated the effect of CDDP at the pathologic level by quantifying IENF density in the footpad skin using a standardized method (33). This procedure is currently used to assess the degeneration of skin nerve fibers in human peripheral neuropathies (37). Skin biopsy for IENF density quantification is a reliable and minimally invasive technique in patients. It showed both degeneration and regeneration of nerve fibers in experimental and human diabetic neuropathies (22, 38, 39) and it might be proposed as an outcome measure in clinical trials with neurotoxic drugs. SNCV and IENF density studies explore different nerve fiber populations: SNCV evaluation mostly

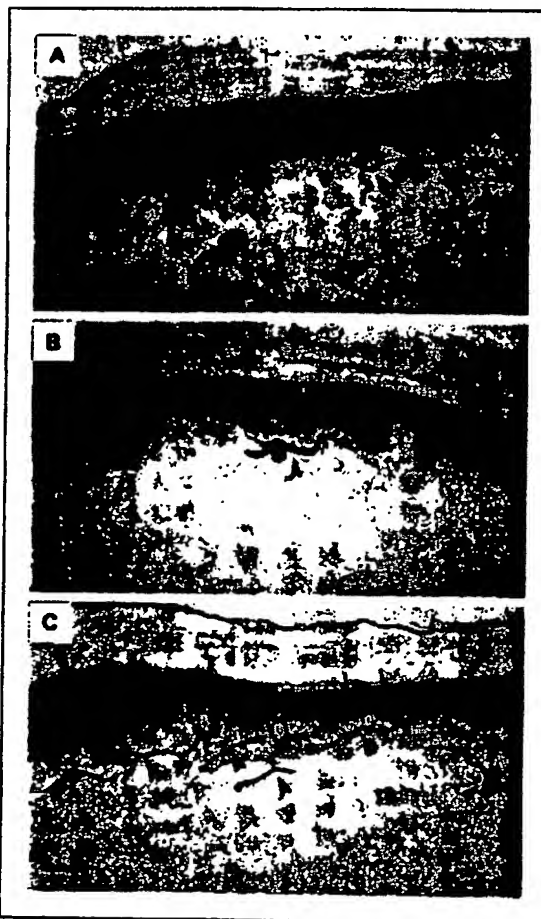


Fig. 3. Microphotographs are skin biopsies from the hindpaw footpad of Wistar rats. Sections were immunostained with the panaxonal marker PGP 9.5. Arrows, IENF; arrowheads, dermal nerve bundles. Bar, 30  $\mu\text{m}$ . A, normal epidermal and dermal innervation density. B, reduced density of IENF and dermal nerve bundles in CDDP-induced neuropathy. IENF show weaker and fragmented PGP 9.5 immunoreactivity indicative of axonal degeneration. C, normal density and morphology of IENF and dermal nerve bundles in a rat cotreated with CDDP and carbamylated erythropoietin.

reflects changes in large myelinated fibers, whereas IENF density is an estimate of small-diameter fibers that are affected early in most peripheral neuropathies.

Erythropoietin, a 165-amino acid sialoglycoprotein, is essential in the regulation of erythropoiesis. Among its several clinical applications, erythropoietin is a very effective, well tolerated, and widely used treatment for anemia in cancer patients undergoing chemotherapy. However, the bone marrow is not the only target tissue of erythropoietin, and the wide expression of functional receptors for erythropoietin explains its nonerythropoietic functions, including its neuroprotective action on the injured nervous system (40). Rat models have been used to test the protective effect of erythropoietin (15, 16, 22), which was recently confirmed in an experimental model of CDDP (23). However, this rat model involved a motor, demyelinating neuropathy that did not reproduce the typical effects of CDDP in humans (i.e., sensory impairment with axonal damage in the peripheral nerves), thus raising some concern about the relevance of the positive results for potential clinical application.

Because, in rats, both DRG and peripheral nerves express the erythropoietin receptor (15, 16), our model of CDDP-induced DRG sensory neuronopathy with secondary axonal neuropathy seems adequate to assess the use of erythropoietin as a neuroprotective agent. The effect of a nonerythropoietic erythropoietin derivative, such as carbamylated erythropoietin, which showed tissue-protecting properties in several animal models of peripheral nerve damage (30), was also evaluated.

Our study shows that erythropoietin or carbamylated erythropoietin alone have no effect on the normal function of the peripheral nerves but had significant and reproducible neuroprotective effects in CDDP-induced neurotoxicity. These results were supported both by the neurophysiologic findings showing the improvement of tail SNCV and at the pathologic level by the higher density of IENF in the footpad skin.

A major concern in the use of neuroprotectant drugs to prevent CIPN is interference with the antineoplastic activity of chemotherapy. Although the effects of erythropoietin on tumor growth is still controversial, Sigounas et al. (41) suggested a synergy between erythropoietin and chemotherapeutic agents in a murine cancer model. We investigated whether erythropoietin or carbamylated erythropoietin affected the tissue distribution of CDDP by measuring the concentration of platinum in the kidney (where it accumulates after CDDP administration and CDDP-DNA adducts are present; 11) and in the peripheral nervous system. We found no difference in platinum tissue concentrations, supporting the opinion that erythropoietin and carbamylated erythropoietin do not interfere with CDDP.

The mechanism of neuroprotection of erythropoietin and carbamylated erythropoietin in our experimental paradigm is still an open issue. Based on current knowledge, a direct protective effect of erythropoietin and carbamylated erythropoietin can be suggested on sensory neurons and/or peripheral nerves through the direct binding to the erythropoietin receptor, which is widely expressed in the peripheral nervous system and overexpressed after nerve injury (16, 17). Carbamylated erythropoietin does not bind to the classic erythropoietin receptors expressed by bone marrow (30). This

affinity for the neural-type erythropoietin receptor shared by erythropoietin and carbamylated erythropoietin suggests that high circulating levels of erythropoietin or carbamylated erythropoietin might have an effect on damage prevention and/or repair. We already reported that erythropoietin reduced the severity of experimental diabetic neuropathy in two different experimental paradigms (22), thus raising the possibility that it has a "nonspecific" neuroprotective effect against different types of injury of the peripheral nervous system as shown recently *in vitro* (17).

The major point of concern in proposing of erythropoietin for neuroprotection in clinical practice is the risk of a marked increase in hematocrit with long-term treatment as observed in our experiment. However, short-term administration of erythropoietin as a neuroprotectant in clinical trials of stroke has not resulted in elevated hematocrit (42) and the optimal schedule (dose and timing) of erythropoietin treatment for the prevention of CIPN still needs to be defined. Recent data suggest that erythropoietin in combination with other growth factors (and possibly with other neuroprotectants) may synergistically activate neuroprotective pathways that allow a lower dose of erythropoietin to be used (43).

A different approach to minimize the erythropoietic effect of erythropoietin is modification of the molecule as has been done with carbamylated erythropoietin. Extensive studies of the relationship between the structure and the activity of the erythropoietin molecule identified regions and amino acids essential for its binding receptor (44) and found that several chemical modifications abolish the hematopoietic bioactivity (45, 46). Previous studies and our results are encouraging because carbamylated erythropoietin maintained its neuroprotective effect without changing the hematocrit (30). These findings open up the possibility of distinguishing between the tissue-protective action of erythropoietin and its potentially detrimental effects (e.g., endothelial activation and platelet reactivity, prothrombotic effects, and excessive erythropoiesis with chronic dosing; refs. 47, 48).

When considering the differences between erythropoietin and carbamylated erythropoietin, it is important to note that these two molecules have very similar pharmacokinetic variables and plasma half-life in particular (30), in contrast to asialo-erythropoietin that has a very short half-life (21). We have shown that, whereas erythropoietin bind the classic homodimeric erythropoietin receptor, carbamylated erythropoietin does not (30), but both molecules require the presence of the  $\beta$  common subunit shared by the granulocyte-macrophage colony-stimulating factor and the interleukin-3 and interleukin-5 receptors, as knockout mice deficient in this transducer do not show protective effects of either carbamylated erythropoietin or erythropoietin (49).

In conclusion, these results we obtained in a model of CIPN that reproduces the clinical features of the effects of CDDP in humans widen the spectrum of possible use of erythropoietin and carbamylated erythropoietin as neuroprotectant drugs, strongly supporting their effectiveness. However, they also indicate the need for further preclinical studies to optimize their effectiveness, to determine the exact mechanism and site of action, and to clarify the issues of long-term tolerability and safety *in vivo*, with the final aim of identifying the best strategy for clinical application.



## References

- Quasthoff S, Hartung HP. Chemotherapy-induced peripheral neuropathy. *J Neurol* 2002;249:9-17.
- Connelly E, Markman M, Kennedy A, et al. Paclitaxel delivered as a 3-hr infusion with cisplatin in patients with gynecologic cancers: unexpected incidence of neurotoxicity. *Gynecol Oncol* 1996;62:168-8.
- Ross PG, Blessing JA, Gershenson DM, McGhee R. Paclitaxel and cisplatin as first-line therapy in recurrent or advanced squamous cell carcinoma of the cervix: a Gynecologic Oncology Group study. *J Clin Oncol* 1999;17:2676-80.
- Barajon I, Bersani M, Quarto M, et al. Neuropeptides and morphological changes in cisplatin-induced dorsal root ganglion neuropathy. *Exp Neurol* 1998;138:93-104.
- Cavaletti G, Tredici G, Marmiroli P, et al. Morphometric study of the sensory neuron and peripheral nerve changes induced by chronic cisplatin (DDP) administration in rats. *Acta Neuropathol (Berl)* 1992;84:364-71.
- Cavaletti G, Minola C, Schiappati M, Tredici G. Protective effects of glutathione on cisplatin neurotoxicity in rats. *Int J Radiat Oncol Biol Phys* 1994;29:771-8.
- Cavaletti G, Tredici G, Marmiroli P, et al. Off-treatment course of cisplatin-induced dorsal root ganglion neuropathy in rats. *In vivo* 1994;8:313-6.
- Tredici G, Cavaletti G, Petruccioli MG, et al. Low-dose glutathione administration in the prevention of cisplatin-induced peripheral neuropathy in rats. *Neurotoxicology* 1994;15:701-4.
- Tredici G, Tredici S, Fabbri D, et al. Experimental cisplatin neuropathy in rats and the effect of retinoic acid administration. *J Neurooncol* 1998;36:31-40.
- Tredici G, Braga M, Nicolini G, et al. Effect of recombinant human nerve growth factor on cisplatin neurotoxicity in rats. *Exp Neurol* 1999;159:581-8.
- Meijer C, DeVries EG, Marmiroli P, et al. Cisplatin-induced DNA-platination in experimental dorsal root ganglia neuropathy. *Neurotoxicology* 1999;20:883-7.
- Pisano C, Pratesi G, Laccabue D, et al. Paclitaxel and Cisplatin-induced neurotoxicity: a protective role of acetyl-L-carnitine. *Clin Cancer Res* 2003;9:5766-67.
- Hausheer F, Cavaletti G, Tredici G, et al. Oral and intravenous BNP77797 protects against platinum neurotoxicity without *in vitro* and *in vivo* tumor protection. *Proceedings of the 90th AACR Meeting; Philadelphia, PA; 1999*. pp. 398.
- Cavaletti G, Marmiroli P. Chemotherapy-induced peripheral neurotoxicity. *Expert Opin Drug Saf* 2004;3:535-46.
- Campana WM, Myers RR. Erythropoietin and erythropoietin receptors in the peripheral nervous system: changes after nerve injury. *FASEB J* 2001;15:1804-8.
- Campana WM, Myers RR. Exogenous erythropoietin protects against dorsal root ganglion apoptosis and pain following peripheral nerve injury. *Eur J Neurosci* 2003;15:1497-508.
- Kerwer SC, Buddenfioght U, Fischer A, et al. A novel endogenous erythropoietin mediated pathway prevents axonal degeneration. *Ann Neurol* 2004;55:815-26.
- Digicaylioglu M, Lipton SA. Erythropoietin-mediated neuroprotection involves cross-talk between Jak2 and NF- $\kappa$ B signaling cascades. *Nature* 2001;412:641-7.
- Siren AL, Fratelli M, Brines M, et al. Erythropoietin prevents neuronal apoptosis after cerebral ischemia and metabolic stress. *Proc Natl Acad Sci U S A* 2001;98:4044-9.
- Brines ML, Ghezzi P, Keenan S, et al. Erythropoietin crosses the blood-brain barrier to protect against experimental brain injury. *Proc Natl Acad Sci U S A* 2000;97:10528-31.
- Erbayraktar S, Grasso G, Shacter A, et al. Asialoerythropoietin is a nonerythropoietic cytokine with broad neuroprotective activity *in vivo*. *Proc Natl Acad Sci U S A* 2003;100:6741-6.
- Bianchi R, Buyukakilli B, Brines M. Erythropoietin both protects from and reverses experimental diabetic neuropathy. *Proc Natl Acad Sci U S A* 2004;101:623-8.
- Orhan B, Yalcin S, Nuru G, et al. Erythropoietin against cisplatin-induced peripheral neurotoxicity in rats. *Med Oncol* 2004;21:197-203.
- Natali A, Toschi E, Baldeweg S. Haemostatic type 2 diabetes, and endothelium-dependent vasodilation of resistance vessels. *Eur Heart J* 2005;26:484-71.
- Quaschnig T, Ruschitzka F, Stallmach T, et al. Erythropoietin-induced excessive erythrocytosis activates the tissue endothelin system in mice. *FASEB J* 2003;17:259-61.
- Ruschitzka FT, Wenger RH, Stallmach T, et al. Nitric oxide prevents cardiovascular disease and determines survival in polyglobular mice overexpressing erythropoietin. *Proc Natl Acad Sci U S A* 2000;97:11609-13.
- Lim VS. Recombinant human erythropoietin in predialysis patients. *Am J Kidney Dis* 1991;18:34-7.
- Veret B, Casadevall M, Lacombe C, Navesux P. Erythropoietin: physiology and clinical experience. *Semin Hematol* 1990;27:25-31.
- Bokemeyer C, Aspro MS, Coudi A, et al. EORTC guidelines for the use of erythropoietic proteins in anemic patients with cancer. *Eur J Cancer* 2004;40:2201-16.
- Leist M, Ghezzi P, Grasso G, et al. Derivatives of erythropoietin that are tissue protective but not erythropoietic. *Science* 2004;308:239-42.
- Cavaletti G, Braga M, Dondi E, et al. Effect of recombinant human NGF or GDNF on cisplatin neurotoxicity in rats. *Ital J Anat Embryol* 1999;104:85.
- Cascinu S, Cordella L, Del Ferro E, et al. Neuroprotective effect of reduced glutathione on cisplatin-based chemotherapy in advanced gastric cancer: a randomized double-blind placebo-controlled trial. *J Clin Oncol* 1995;13:26-32.
- Lauria G, Lombardi R, Borgna M, et al. Intraepidermal nerve fiber density in rat foodpad: neuropathologic-neurophysiologic correlation. *J Peripher Nerv Syst* 2005;10:199-205.
- Apfel SC, Arezzo JC, Lipson L, Kessler JA. Nerve growth factor prevents experimental cisplatin neuropathy. *Ann Neurol* 1992;31:76-80.
- Apfel SC, Lipton RB, Arezzo JC, Kessler JA. Nerve growth factor prevents toxic neuropathy in mice. *Ann Neurol* 1991;29:87-90.
- Wang MS, Davis AA, Culver DG, et al. Calcitonin inhibition protects against Taxol-induced sensory neuropathy. *Brain* 2004;127:671-9.
- McArthur JC, Stocks EA, Hauer P, et al. Epidermal nerve fiber density: normative reference range and diagnostic efficiency. *Arch Neurol* 1998;55:1513-20.
- Lauria G, McArthur JC, Hauer PE, et al. Neuropathological alterations in diabetic truncal neuropathy: evaluation by skin biopsy. *J Neurol Neurosurg Psychiatry* 1998;65:782-6.
- Polydefkis M, Hauer P, Sheth S, et al. The time course of epidermal nerve fiber regeneration: studies in normal controls and in people with diabetes, with and without neuropathy. *Brain* 2004;127:1606-15.
- Buoni M, Cavallaro E, Floccari F, et al. The pleiotropic effects of erythropoietin in the central nervous system. *J Neuropathol Exp Neurol* 2003;62:226-36.
- Sigounas G, Seltz S, Sigounas VY. Erythropoietin modulates the anticancer activity of chemotherapeutic drugs in a murine lung cancer model. *Cancer Lett* 2004;214:171-9.
- Ehrenreich H, Hasselblatt M, Dombrowski C, et al. Erythropoietin therapy for acute stroke is both safe and beneficial. *Mol Med* 2002;8:495-505.
- Digicaylioglu M, Garden G, Timberlake S, et al. Acute neuroprotective synergy of erythropoietin and insulin-like growth factor I. *Proc Natl Acad Sci U S A* 2004;101:9856-60.
- Grodberg J, Davis KL, Sytkowski AJ. Alanine scanning mutagenesis of human erythropoietin identifies four amino acids which are critical for biological activity. *Eur J Biochem* 1993;218:597-601.
- Mun KC, Golper TA. Impaired biological activity of erythropoietin by cyanate carbamylation. *Blood Purif* 2000;18:13-7.
- Setake R, Kozutsumi H, Takeuchi M, Asano K. Chemical modification of erythropoietin: an increase in *in vitro* activity by guanidination. *Biochim Biophys Acta* 1990;1038:125-9.
- Raine AE. Hypertension, blood viscosity, and cardiovascular morbidity in renal failure: implications of erythropoietin therapy. *Lancet* 1988;1:97-100.
- Stohlawetz PJ, Dzido L, Margovich N, et al. Effects of erythropoietin on platelet reactivity and thrombopoiesis in humans. *Blood* 2000;95:2963-9.
- Brines M, Grasso G, Fiordaliso F, et al. Erythropoietin mediates tissue protection through an erythropoietin and common  $\beta$ -subunit heteroreceptor. *Proc Natl Acad Sci U S A* 2004;101:14907-12.

## Human hair follicles are an extrarenal source and a nonhematopoietic target of erythropoietin

Enikő Bodó,<sup>\*,1</sup> Arno Kromminga,<sup>†,1</sup> Wolfgang Funk,<sup>‡</sup> Magdalena Laugsch,<sup>§</sup> Ute Duske,<sup>†</sup> Wolfgang Jelkmann,<sup>§</sup> and Ralf Paus<sup>\*,2</sup>

<sup>\*</sup>Department of Dermatology, University of Lübeck, Lübeck, Germany; <sup>†</sup>Institute for Immunology, Clinical Pathology, Molecular Medicine, Hamburg, Germany; <sup>‡</sup>Klinik Dr. Kozłowski, Munich, Germany; and <sup>§</sup>Department of Physiology, University of Lübeck, Lübeck, Germany

**ABSTRACT** Erythropoietin primarily serves as an essential growth factor for erythrocyte precursor cells. However, there is increasing evidence that erythropoietin (EPO)/EPO receptor (EPO-R) signaling operates as a potential tissue-protective system outside the bone marrow. Arguing that growing hair follicles (HF) are among the most rapidly proliferating tissues, we have here explored whether human HFs are sources of EPO and targets of EPO-R-mediated signaling. Human scalp skin and microdissected HFs were assessed for EPO and EPO-R expression, and the effects of EPO on organ-cultured HFs were assessed in the presence/absence of a classical apoptosis-inducing chemotherapeutic agent. Here, we show that human scalp HFs express EPO on the mRNA and protein level *in situ*, up-regulate EPO transcription under hypoxic conditions, and express transcripts for EPO-R and the EPO-stimulatory transcriptional cofactor hypoxia-inducible factor-1 $\alpha$ . Although EPO does not significantly alter human hair growth *in vitro*, it significantly down-regulates chemotherapy-induced intrafollicular apoptosis and changes the gene expression program of the HFs. The current study points to intriguing targets of EPO beyond the erythropoietic system: human HFs are an extrarenal site of EPO production and an extrahematopoietic site of EPO-R expression. They may recruit EPO/EPO-R signaling *e.g.*, for modulating HF apoptosis under conditions of hypoxia and chemotherapy-induced stress.—Bodó, E., Kromminga, A., Funk, W., Laugsch, M., Duske, U., Jelkmann, W., Paus, R. Human hair follicles are an extrarenal source and a non-hematopoietic target of erythropoietin. *FASEB J.* 21, 3346–3354 (2007)

**Key Words:** anagen hair follicles • tissue protection • hemoglobin alpha-1 • kinesin light chain 3 • aminase oxidase • calmagin • RAS-like family 10

THE GLYCOPROTEIN HORMONE ERYTHROPOIETIN (EPO) serves as an essential viability and growth factor for erythrocyte precursor cells (1–5). EPO is the main regulator of maintenance of the blood cell mass by stimulating the proliferation and differentiation of precursor cells and by inhibiting apoptosis of erythroid cells in the bone marrow (1–5).

The classical site of EPO synthesis is peritubular interstitial cells of the kidney when stimulated by hypoxia (1, 2, 6, 7). A primary mediator of hypoxia-induced EPO gene expression is the hypoxia-inducible dimeric transcription factor 1 (HIF-1  $\alpha/\beta$ ; refs. 1, 8, 9). However, HIF-1 $\alpha$  and HIF-1 $\beta$  mRNAs are continuously produced and remain essentially unaltered by the induction of hypoxia (1, 10, 11). Instead, oxygen sensing and activation of the EPO gene are initiated by post-translational modifications of the HIF-1 $\alpha$  protein (1). EPO activates a specific receptor [erythropoietin receptor (EPO-R)] of the cytokine receptor gene family, the (mainly Jak2 and STAT5-mediated) signaling of which is thought to chiefly induce changes in gene expression that result in inhibition of the proapoptotic machinery of EPO-R expressing target cells, thereby suppressing apoptosis (1, 2, 5–7).

Recently, however, it has surfaced that the apoptosis-inhibiting property of EPO is not restricted to erythropoietic cells and that apoptosis in several other tissues can be suppressed by EPO. Apparently, EPO serves as a potent paracrine-autocrine cell-protective factor protecting from, for example, ischemia-induced apoptosis (1, 3, 4). One of the best studied fields is the nervous system (1, 3, 4): functional EPO-R have been demonstrated on neuronal cells (1, 12, 13), and application of EPO has neuroprotective effects in *in vivo* animal studies (14–17) via regulation of, for example, bcl-x<sub>l</sub> (18), an antiapoptotic factor. EPO even may reduce infarct size and may improve recovery of stroke patients (16, 19). Also, human recombinant EPO was reported to prevent lipopolysaccharide-induced apoptosis in bovine pulmonary artery endothelial cells (20) and to reduce necrosis and apoptosis during experimental injury in the kidney *in vivo* (21). Furthermore, human fetal liver, placenta, retina, and adrenal cortex all have been reported to express EPO, respectively, EPO-R (22).

<sup>1</sup> These authors contributed equally to this work.

<sup>2</sup> Correspondence: Department of Dermatology, University Hospital Schleswig-Holstein, University of Lübeck, Ratzeburger Allee 160, D-23538 Lübeck, Germany. E-mail: ralf.paus@uk-sh.de

doi: 10.1096/fj.07-8628com

Whether or not EPO/EPO-R signaling plays a role in human skin biology and pathology is as yet unknown. Recombinant, subcutaneously administered human EPO has been applied successfully to enhance wound healing in the skin of C57BL/6 mice, where EPO increased significantly the area of reepithelialization and accelerated the wound closure in deep-dermal second burn (23). Selzer *et al.* (24) reported EPO-R expression in transformed human melanocytes *in vitro* but not in normal neonatal and adult primary human melanocytes. In contrast, Kumar *et al.* (25) have described highly expressed EPO-R and very weak, if any, EPO signals by Western blotting and immunocytochemistry in cultured human primary melanocytes. Note, however, that the non-specific C-20 antibody against EPO-R (26) was used for the latter study. Recently, an antibody that reportedly recognizes the soluble form EPO-R was claimed to demarcate immunoreactivity in cutaneous mast cells (27). Very recently, LeBaron *et al.* (28) demonstrated that hair follicle (HF) dermal papilla fibroblasts are EPO target cells and respond to EPO treatment by an activation of EPO-R signaling. Thus, the cutaneous targets of EPO-induced signaling and whether mammalian skin expresses specific EPO-R and/or its ligand *in situ* remain unclear.

Arguing that growing (anagen) HFs are among the most rapidly proliferating and most damage-sensitive tissues in the human body (29, 30), we have here explored whether human HFs are sources of EPO expression and targets of EPO-R-mediated signaling. Matrix keratinocytes of human anagen VI HFs are characterized by a very high proliferative potential (29) and must be perfused entirely via the HF mesenchyme. Therefore, they may continuously experience conditions of relative hypoxia and have even been claimed to primarily resort to anaerobic glycolysis to meet their energy requirements (31).

To investigate the EPO/EPO-R system in the skin and HFs has become particularly important since human skin and human pilosebaceous units operate as endocrine organs that synthesize classical (neuro)endocrine messengers (TSH, CRH, ACTH,  $\alpha$ -MSH, prolactin, and melatonin; refs. 32–39) and display a fully functional peripheral equivalent of the central hypothalamic-pituitary-adrenal stress response axis (36, 40).

Here, we show that normal human skin joins the growing list of tissues that recruit the EPO/EPO-R system for cell protection and that healthy human HFs are an extrarenal site of EPO and an extrahematopoietic site of EPO-R expression.

## MATERIALS AND METHODS

### HF organ culture and hypoxia treatment

Anagen VI HFs were isolated from normal human scalp skin obtained after written patient consent from healthy females undergoing routine face-lift surgery for cosmetic purposes as described previously (41), adhering to Helsinki guidelines. HFs were microdissected and organ-cultured as described

previously (39, 41, 42). Isolated HFs were maintained in supplemented, serum-free Williams' E medium (Biochrom, Cambridge, UK) supplemented with 2 mmol/l L-glutamine (Invitrogen, Paisley, UK), 10 ng/ml hydrocortisone (Sigma-Aldrich, Taufkirchen, Germany), 10  $\mu$ g/ml insulin (Sigma-Aldrich), and 1% antibiotic/antimycotic mixture (100 $\times$ , Life Technologies, Germany, Karlsruhe). HFs were first incubated overnight, and the next day medium was exchanged and vehicle (culture medium)/EPO (100 U/ml, Epoetin beta; Roche/Boehringer Mannheim, Mannheim, Germany) was added to each well. HFs were treated over 9 days, and hair shaft length measurements were performed every second day on each individual HF, using a Zeiss inverted binocular microscope with an eyepiece measuring graticule.

In selected experiments, microdissected HFs were first cultured under normoxic conditions (humidified atmosphere at 37°C, 5% CO<sub>2</sub>, and 95% air; ref. 43) for 12 h. Then, HFs were placed in an InvivoO<sub>2</sub> 400 hypoxia workstation (Ruskin Technology, Leeds, United Kingdom) with a gas mixture of 3% O<sub>2</sub>, 5% CO<sub>2</sub>, and balance N<sub>2</sub> for additional 24 h to induce conditions of relative hypoxia (43).

### Apoptosis induction in human HFs by chemotherapy

To explore potential cytoprotective effects of EPO, HFs were first incubated overnight without any treatment, and the next day (day 1) medium was exchanged and vehicle (culture medium)/EPO (100 U/ml) was added to each well. After 24 h preincubation, HFs were cotreated with the key toxic metabolite of the potent alopecia-inducing cytostatic agent cyclophosphamide [4-hydroperoxycyclophosphamide (4-HC), Niomec, Bielefeld; refs. 44, 45] for 4 days. In this assay system, we had previously shown that keratinocyte growth factor (FGF7) operates as a potent cytoprotective agent (45).

### Immunohistochemistry and quantitative immunohistology

For the detection of EPO in human scalp skin, the highly sensitive EnVision (Dako, Glostrup, Denmark) technique (46) was performed. The staining specificity was verified using human kidney cryosections as positive control. Acetone-fixed, 8  $\mu$ m thick cryoslides of human scalp skin were preincubated with 10% normal goat serum (in TBS, Dako) for 20 min and then incubated with a rabbit anti-human EPO antiserum (1:50 in TBS, generated by hyperimmunization of rabbits with recombinant human EPO) overnight at 4°C. Slides were then treated with the EnVision secondary antibody solution (Dako, 45 min) against rabbit/mouse immunoglobulin followed by a counterstaining with hematoxylin (Sigma-Aldrich). Negative control experiments were performed by omitting primary antibody and by the absence of EPO immunoreactivity in sections showing human kidney epithelium. Instead, specific immunoreactivity in peritubular/interstitial kidney fibroblasts was used as a positive control (see Fig. 1A).

For detection of experimentally induced apoptosis, the terminal dUTP nick end-labeling (TUNEL) staining was performed, using murine spleen sections as positive control (47). Cryostat sections were fixed in paraformaldehyde and ethanol-acetic acid (2:1) and were labeled with digoxigenin-deoxyUTP (ApoTag Fluorescein In Situ Apoptosis detection kit; Intergen, Purchase, NY, USA, 60 min, 37°C). The enzyme reaction was stopped (stop buffer, ApoTag Fluorescein In Situ Apoptosis Detection Kit), and slides were labeled with a FITC-conjugated antidigoxigenin antibody (Apoptosis Kit). Negative controls were performed by omitting TdT enzyme.

For a simultaneous labeling of proliferating and apoptotic cells, the Ki-67/TUNEL double-staining was applied as de-



**Figure 1.** Normal human skin and hair follicles express EPO protein in situ. EPO immunoreactivity (EnVision technique) is localized to central outer root sheath (B) keratinocytes (ORS) of growing hair follicles and blood vessels (BV) of skin (D). All cell types of hair bulb (C) and epidermis were negative (A). Frozen sections of human kidney (E) served as positive (peritubular interstitial cells, open arrows) and negative (epithelial cells, arrow) control. NC = negative control (by omitting primary antibody); DP = dermal papilla; MK = matrix keratinocytes; HS = hair shaft; scale bars = 50  $\mu$ M.

scribed earlier (42). Quantitative immunohistomorphometry was performed as described previously (39): Ki-67, TUNEL, or DAPI+ cells were counted in a previously defined reference region of the HF matrix, and the percentage of Ki-67+/TUNEL+ cells was determined.

#### Quantitative real-time polymerase chain reaction

Total RNA was extracted from HF cultured under normoxic and hypoxic conditions, respectively, using the RNA easy kit (Qiagen, Hilden, Germany) and was reverse-transcribed using random hexamers as primers and Transcriptor Reverse Transcriptase (Roche, Mannheim, Germany). A specific EPO cDNA fragment of 158 bp covering the region 537–694 according to the most recent accession number of the GenBank DNA databank was amplified by real-time polymerase chain reaction (PCR; 95°C for 10 min; 35 cycles of 95°C for 10 s, 68°C for 10 s, 72°C for 16 s) using undisclosed primer pairs from LC Search (Heidelberg, Germany). SybrGreen was used for staining of the PCR products. The amount of cDNA in all samples was standardized by the amplification of the housekeeping gene GAPDH (Roche, Mannheim, Germany). The specificity of the amplification reactions was assessed by a melting curve analysis. The second derivative maximum analysis of the relative quantification software package, version 1.0 (Roche), was used for a relative quantification of specific EPO PCR products. The PCR products were also visualized using a 0.7% agarose gel with ethidium bromide.

#### ELISA analysis of secreted EPO in culture medium

EPO in the supernatant of the cultured HFs was analyzed using a commercial sandwich ELISA from R&D Systems (Minneapolis, MN, USA). This ELISA makes use of an immobilized monoclonal murine catching antibody that binds EPO. The second polyclonal (rabbit) detecting antibody is conjugated with horse-radish peroxidase and binds immobilized EPO. Before the analysis, HF culture supernatant was up-concentrated 10-fold using centrifugal Microcon filter unit YM-10 (cut-off 10 kDa; Millipore, Billerica, MA, USA). YM-10 filters were centrifuged at 14,000 g for 10 min at room temperature.

#### Microarray analysis of selected candidate genes

Gene expression analysis of HFs from two different individuals (both female) using Human Whole Genome Oligo Microarray (44 K) was performed as a commercial service by Miltenyi Biotec GmbH (Cologne, Germany). Twenty HFs per group were treated with vehicle/EPO (100 U/ml) for 6 h, and total RNA was isolated according to standard protocols (Trizol, Sigma-Aldrich). Quality of total RNA was controlled

via the Agilent 2100 Bioanalyzer System. Linear amplification of RNA and hybridization of whole genome oligo microarray were performed according to Agilent's standard protocols. All compared test and control HFs were derived from one defined scalp skin region of the same donor, and the gene expression profiles of two donors were compared independently.

"Differentially regulated" candidate genes were selected according the following rigid selection criteria: only those genes were further evaluated whose transcription had changed >1.5-fold and with a *P* value of < 0.01, and this in an equidirectional manner (*i.e.*, the transcription was significantly up- and down-regulated, respectively, in both individuals). In a separate analysis, those genes were selected whose transcription was substantially modulated (*i.e.*, >5-fold, *P* < 0.01) in HF RNA extracts of only one of the two examined patients (Table 1).

## RESULTS

First, we asked, whether human scalp skin transcribes and translates EPO. As shown in Fig. 1, with the use of a specific antibody and human kidney sections as positive and negative control (Fig. 1A), EPO-like specific immunoreactivity was mainly found in the HF epithelium and in large blood vessels (Fig. 1A–D); epidermal/follicular melanocytes did not seem to express EPO. The most intensive staining was seen in central outer root sheath keratinocytes (Fig. 1B).

Moreover, EPO was secreted into the culture medium as demonstrated by ELISA (data not shown). These microdissected human scalp HFs (< ~50 cell layers the central ORS/ follicle,  $2.5 \times 10^5$  cells/experiment) secreted 2.4 mU/ml EPO protein into the medium after 48 h of organ culture under serum-free conditions (in comparison, the normal EPO concentration in human serum is between 3–17 mU/ml; ref. 48).

By quantitative, real-time reverse transcriptase (RT)-PCR, both EPO and EPO-R transcripts were detected in freshly microdissected hair bulbs of human scalp HFs in the growth phase of the hair cycle (anagen VI; ref. 29; Fig. 2A, B). We could also detect transcripts for HIF-1 $\alpha$ , a main mediator of EPO production, in microdissected, organ-cultured human scalp HFs (Fig. 2; see Supplemental Fig. S1). Since commercially available anti-EPO-R antibodies cannot reliably detect EPO-R antigen because of their low specificity and affinity (26), we

TABLE 1. EPO administration causes differential gene expression changes

Abbreviation	Sequence Description	Accession number	Fold Change
LOC126536	Homo sapiens hypothetical protein LOC126536	NM_001034966	-27.1
CTSZ	Homo sapiens cathepsin Z	NM_001336	-25.0
FABP1	Homo sapiens fatty acid binding protein 1	NM_001443	-23.5
PRDM14	Homo sapiens PR domain containing 14	NM_024504	-20.6
APOB48R	Homo sapiens apolipoprotein B48 receptor	NM_018690	-19.8
TPH2	Homo sapiens tryptophan hydroxylase 2	NM_173353	-18.6
CHIT1	Homo sapiens chitinase 1	NM_003465	-13.3
PLCB2	Homo sapiens phospholipase C, beta 2	NM_004573	-11.4
RPS4Y1	Homo sapiens ribosomal protein S4, Y-linked	NM_001008	-9.9
MIA2	Homo sapiens melanoma inhibitory activity 2	NM_054024	-9.9
UCP2	Homo sapiens uncoupling protein 2	NM_003355	-9.4
RBMV1E	Homo sapiens RNA binding motif protein, Y-linked, family 1, member E	NM_001006118	-9.4
CDW52	Homo sapiens CDW52 antigen	NM_001803	-9.2
KCNV2	Homo sapiens potassium channel, subfamily V, member 2	NM_133497	-8.7
ZNF409	Homo sapiens mRNA for KIAA1056 protein	AB028979	-8.4
FBXL18	Homo sapiens hypothetical protein FLJ11467	NM_024963	-8.3
RPS4Y2	Homo sapiens ribosomal protein S4, Y-linked 2	NM_001039567	-8.0
L3MBTL	Homo sapiens mRNA for KIAA0681 protein	AB014581	-7.9
LRRC21	Homo sapiens leucine rich repeat containing 21	NM_015613	-7.4
SLC24A1	Homo sapiens mRNA for KIAA0702	AB014602	-7.3
GAGED3	Homo sapiens G antigen, family D, 3	NM_130777	-7.2
CCL19	Homo sapiens chemokine (C-C motif) ligand 19	NM_006274	-7.1
DNAI2	Homo sapiens mRNA for intermediate dynein chain	AJ295276	-7.0
DDI1	Homo sapiens DNA-damage inducible protein 1	NM_001001711	-6.9
ADAMTS10	Homo sapiens a disintegrin-like and metalloprotease (reprolysin type) with thrombospondin type 1 motif, 10	NM_030957	-6.8
TM7SF4	Homo sapiens DC-specific transmembrane protein	NM_030788	-6.8
HK3	Homo sapiens hexokinase 3 (white cell), nuclear gene encoding mitochondrial protein	NM_002115	-6.6
CART1	Homo sapiens cartilage paired-class homeoprotein 1	NM_006982	-6.6
PDE6C	Homo sapiens phosphodiesterase 6C, cGMP-specific, cone, alpha prime	NM_006204	-6.4
AOC2	Homo sapiens amine oxidase, copper containing 2, transcript variant 1	NM_001158	-6.3
IL20	Homo sapiens interleukin 20	NM_018724	-6.1
NM_001012763	Homo sapiens gonadotropin-releasing hormone receptor, transcript variant 2	NM_001012763	-6.0
TDGF1	Homo sapiens teratocarcinoma-derived growth factor 1	NM_003212	-6.0
LCP1	Homo sapiens lymphocyte cytosolic protein 1	NM_002298	-5.6
KCNH6	Homo sapiens cDNA FLJ33650 fis, highly similar to Rattus norvegicus potassium channel	NM_030779	-5.4
PRDM7	Homo sapiens PR domain containing 7	NM_052996	-5.4
FFR1	Homo sapiens formyl peptide receptor	NM_002029	-5.3
M27126	Human lymphocyte antigen	M27126	-5.2
PDLIM2	Homo sapiens PDZ and LIM domain 2	NM_176871	-5.2
CLGN	Homo sapiens calmagin	NM_004362	-5.2
EDN3	Homo sapiens endothelin 3, transcript variant 2	NM_207032	+5.4
LOC440040	PREDICTED: Homo sapiens similar to Metabotropic glutamate receptor 5 precursor	XM_495873	+6.2
PTPRB	Homo sapiens protein tyrosine phosphatase, receptor type	NM_002837	+6.6
ABCA13	Homo sapiens ATP binding cassette gene, sub-family A, member 13	NM_152701	+7.6

Table lists genes whose transcription was substantially modulated by EPO treatment (>5-fold,  $P < 0.01$ ) in HF RNA extracts of only one of the two examined patients. HFs were treated with vehicle or EPO (100 U/ml), and microarray analysis (Human Whole Genome Microarray; expression differences visualized by Agilent technique) was performed. Down-regulation = green, up-regulation = red.

could not investigate the precise localization of EPO-R protein expression in the HFs.

Since renal EPO production is primarily stimulated by hypoxia (1), we cultured HFs under hypoxic conditions and compared the EPO, EPO-R, and HIF-1 $\alpha$  steady-state transcript levels to the normoxic ones by quantitative real time PCR. Both HIF-1 and EPO-R steady-state transcript levels were unchanged under hypoxic conditions (Fig. 2; see Supplemental Fig. S1).

However, there was a significant up-regulation of EPO mRNA in hypoxia-treated HFs (Fig. 2; Supplemental Fig. S1), suggesting that, just as in the kidney, EPO production in human HFs is inducible by hypoxia.

Next, we investigated how EPO-R activation influences key HF parameters, such as hair shaft elongation or proliferation/apoptosis of human hair matrix keratinocytes *in situ* under normoxic standard organ-culture conditions. However, HFs treated with EPO for 9

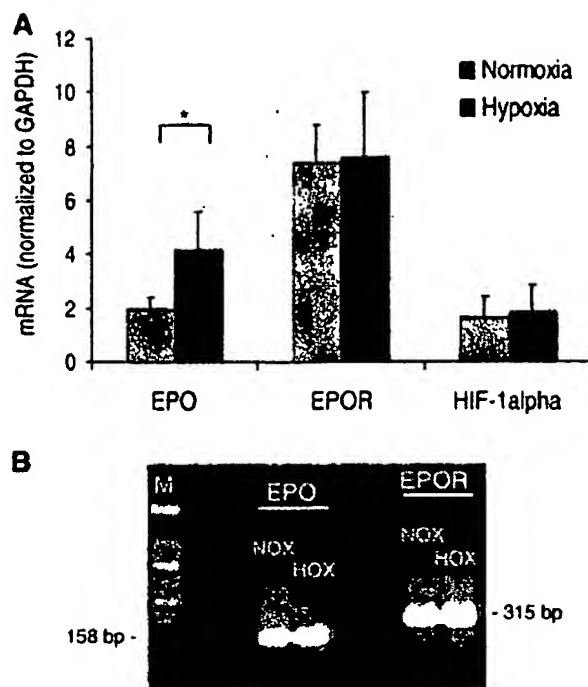


**Figure 2.** Detection of EPO, EPO-R, and HIF-1 $\alpha$  mRNA by real-time PCR in extract isolated from microdissected hair follicles. **A)** Freshly microdissected and cultured HF (n=30/group) were analyzed by quantitative real-time RT-PCR for EPO, EPO-R, and HIF-1 $\alpha$ . Organ cultured hair follicles up-regulate EPO but not EPO-R and HIF-1 $\alpha$  mRNA under hypoxic conditions (3% O<sub>2</sub>). \*P < 0.05; mean  $\pm$  SE. **B)** PCR products for EPO and EPO-R were visualized on a 0.7% agarose gel with ethidium bromide (note that these PCR products are obtained at the very end of the PCR reactions (after 35 cycles). At that time point, concentration differences can not be observed.) M = marker; NOX = normoxia; HOX = hypoxia.

days failed to show significant changes in hair shaft elongation (Fig. 3). Also, proliferation/apoptosis of hair matrix keratinocytes under standard culture conditions remained essentially unaltered after EPO administration (Fig. 3).

In contrast, chemotherapy-induced intrafollicular apoptosis *in situ* was inhibited by prior and concomitant EPO administration (Fig. 4): When organ-cultured human anagen HF were exposed to a key toxic metabolite of the potent alopecia-inducing cytostatic agent cyclophosphamide [4-hydroperoxy-cyclophosphamide (4-HC); 44, 45], the massive apoptosis induced in the HF epithelium by 4-HC was significantly reduced (from  $6.6 \pm 2.4$  to  $3.0 \pm 1.3$ ) by EPO (as measured by quantitative immunohistomorphometry of TUNEL+ cells in the hair matrix; ref 39; Fig. 4). In view of the unavailability of sufficiently specific antibodies for the immunohistological detection of EPO-R protein, this finding also serves as indirect evidence that the detected EPO-R transcripts are translated into functionally active EPO-R.

To obtain further evidence of EPO-R functionality

and to search for previously unknown target genes for extraerythropoietic EPO-R-mediated signaling, we, finally, subjected two independent sets of organ-cultured human scalp HF (derived from 2 different, healthy female face lift patients) to DNA microarray after stimulation with EPO (100 U/ml; Fig. 5). This was performed as a commercial service (Human Whole Genome Oligo Microarray, Miltenyi), and rigid selection criteria were employed to single-out "differentially expressed" genes.

When only equidirectional expression changes in HF RNA extracts from both individuals with a P value of <0.01, and fold changes of >1.5 were accepted as strong indications for "differential gene expression," only two up-regulated and three down-regulated genes were identified: hemoglobin alpha-1 (HBA1), kinesin light chain 3 (KLC3), aminase oxidase (copper containing 2, AOC2), calmeglin (CLGN), and RAS-like family 10, member B (RASL10B), respectively (Fig. 5). The complete list of genes whose expression changed markedly (5–27-fold) in at least one of two examined patients is shown in Table 1.

## DISCUSSION

Here, we provide the first evidence that normal human skin expresses EPO and functional EPO-Rs *in situ* and that human scalp HF are important extrarenal sources and extrahematopoietic targets of EPO-induced signaling. We show that EPO protein is exclusively produced by outer root sheath keratinocytes of human anagen VI HF and is secreted into the organ culture medium. In contrast to what has been reported for cultured melanocytes and melanoma cells (24, 25), neither epidermal nor follicular melanocytes in normal human skin *in situ* showed convincing, specific immunoreactivity for EPO protein with the antibody employed here.

As a prototypic neuroectodermal-mesodermal interaction system (29), human HF organ culture offers itself as an instructive and physiologically relevant, novel research tool for dissecting the intriguing but still unclear extraerythropoietic functions of EPO in peripheral tissues in the human system. Similar to its effect on kidney, liver, and brain (1, 49), hypoxia stimulated EPO production in human HF *in situ*, suggesting that the latter utilize a classical hypoxia-sensing system employed elsewhere in the human body (7). Since we also show that HF transcribe the main "oxygen sensor" HIF-1 $\alpha$ , these cutaneous miniorgans may be able to detect insufficient O<sub>2</sub> levels via the oxygen-dependent level of HIF-1 $\alpha$ . This may represent an important mechanism for regulating the metabolic balance of the extremely fast-renewing and proliferating cell population of hair matrix keratinocytes. The regulation of HIF-1 $\alpha$  generally occurs by post-translational modifications; hypoxic cells show an increase in HIF-1 $\alpha$  protein levels, while the HIF-1 $\alpha$  mRNA levels remain unchanged at low pO<sub>2</sub> (1, 50). We have here shown that, as described elsewhere (1, 50), HIF-1 $\alpha$

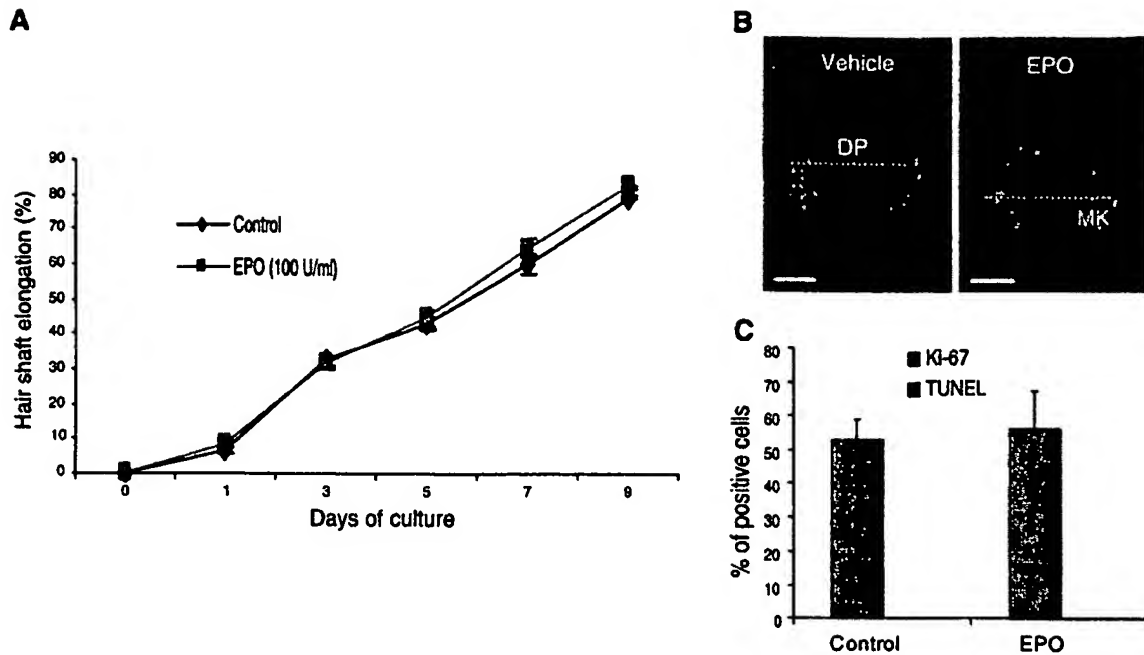


**Figure 3.** EPO does not significantly influence hair shaft elongation and proliferation/apoptosis of matrix keratinocytes *in vitro*. **A**) Hair follicles were treated with vehicle/EPO (100 U/ml) and hair shaft length was measured every second day.  $P > 0.05$ ; mean  $\pm$  SE. **B, C**) Cryosections of cultured, vehicle/EPO treated hair follicles were double labeled with Ki-67(red)/TUNEL(green) staining. Ki-67/TUNEL positive cells were counted below Auber's line (indicated in white) and percentage of positive cells was compared between vehicle and EPO-treated follicles.  $P > 0.05$ , mean  $\pm$  SE; scale bars = 50  $\mu$ m.

transcription was not changed by hypoxia in organ cultured HF at mRNA levels. This suggests that intrafollicular HIF-1 $\alpha$  production is regulated at the post-transcriptional level, as well.

Although the precise role of intrafollicular EPO production for human HF biology remains to be fully explored, due to its potent antiapoptotic properties (3, 4, 6), EPO may serve as an endogenous HF cytoprotectant, similar to what has been reported for keratinocyte growth factor (45) or melatonin (38). It now deserves to be assessed whether EPO can be exploited clinically as an anti-hair loss agent, for example, in chemotherapy-induced alopecia. Our data provide further evidence for the emerging concept that EPO may play a role as a general protective factor (wound

healing, chemotherapy-induced apoptosis) for the skin (2, 3, 23, 45).

Furthermore, in the light of the previously reported wound healing-promoting effect of EPO (23), it is intriguing to ask whether HF-derived EPO may also serve to facilitate wound healing. Not the least in view of the fact that HF-derived keratinocytes are a major cell source for reepithelization during wound healing (51) and that the HF connective tissue sheath is a likely source for granulation tissue formation (52), this possibility deserves systematic further analysis.

As shown by microarray analysis, EPO administration changed the gene expression (hemoglobin alpha-1, kinesin light chain 3, aminase oxidase, calmeglin, and RAS-like family 10) program of human HF. Although

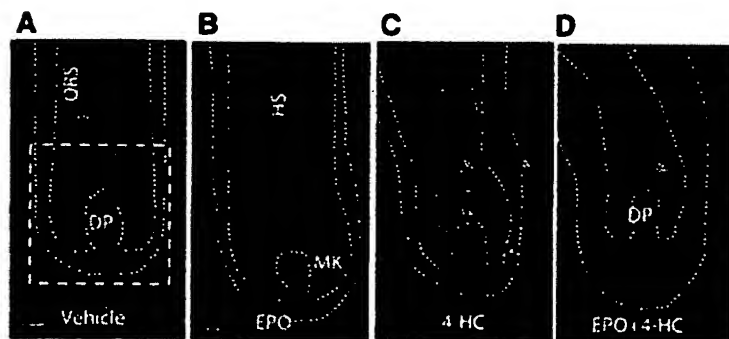


**Figure 4.** EPO (100 U/ml) reduces the massive apoptosis induced by the cyclophosphamide metabolite 4-hydroperoxycyclophosphamide (4-HC). HF were incubated overnight without any treatment, the next day (day 1) medium was exchanged and vehicle (culture medium)/EPO (100 U/ml) was added to each well. After 24 h preincubation, HF were cotreated with key toxic metabolite of the potent alopecia-inducing cytostatic agent 4-HC for 4 days. Apoptotic cells were detected by TUNEL immunostaining (green). EPO reduced number of apoptotic cells after 4-HC treatment. Scale bars = 50  $\mu$ m;  $n = 10$  HF/group.



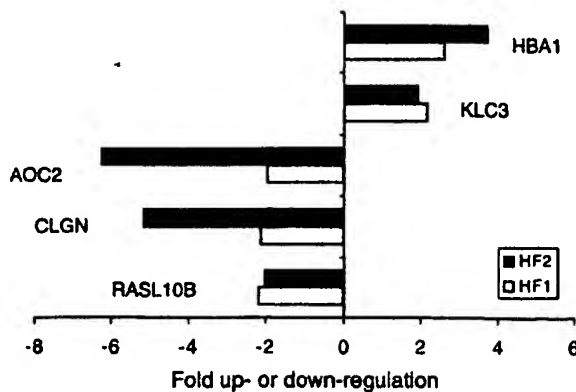


**Figure 5.** EPO administration causes differential gene expression changes. HFs of 2 different female donors (HF1 and HF2) were treated with vehicle or EPO (100 U/ml) and microarray analysis (Human Whole Genome Microarray, Miltenyi; expression differences visualized by Agilent technique) was performed. When only genes with equidirectional changes in both individuals were included, where, in addition,  $P$  value was  $<0.01$  and fold-changes were  $>1.5$ , five differentially regulated genes were identified: hemoglobin alpha-1 (HBA1), kinesin light chain 3 (KLC3), aminase oxidase (copper containing 2, AOC2), calmodulin (CLGN), and RAS-like family 10, member B (RASL10B). The genes whose transcription changed substantially (5–27-fold,  $P<0.01$ ) in only one patient are listed separately in Table 1.

the newly identified candidates as EPO-target genes and their functional significance need to be confirmed and clarified in further experiments, our results invite one to speculate on the potential involvement of some of these novel EPO-target genes in skin or hair biology. For example, kinesin molecules are involved in melanosomal movement along melanocyte dendrites (obligate event of the maintenance of the skin color) (53). In addition, the down-regulation of RAS10B, a new member of the Ras superfamily with tumor suppressor potential (54), may be related to the antiapoptotic features of EPO. Furthermore, here we provide the first evidence that, beyond expressing the beta globin gene (55), HFs, unexpectedly, transcribe the alpha chain of hemoglobin and that this transcription is upregulated by EPO.

When the genes whose transcription was markedly modulated in only one of the two examined patients (Table 1) are included as candidate EPO-target genes in human HFs, our results point to several genes coding for enzymes or receptors with relevance to skin neuroendocrinology. One of the most interesting is tryptophan hydroxylase 2 (TPH2). TPH (TPH1) plays a pivotal role in the synthesis of serotonin as catalyzer of the rate-limiting step of the serotonin synthesis in the skin [as reviewed by Slominski *et al.* (56)]. TPH and also serotonin and serotonin receptor were described to be expressed in whole human, C57BL/6 mice and hamster skin and several cultured skin cells (HaCaT cells, melanocytes, and melanoma cell lines; refs. 56–58). Furthermore, serotonin is involved in human skin physiology as regulator of cell proliferation, vasoactive

agent and immune modulator (56). TPH 2 has been described to localize to the central nervous system and not to the skin (56). Here we provide the first evidence that TRH 2 is translated by human HFs and its expression is inhibited by EPO. This raises the intriguing question of whether, for example, EPO influences the serotonergic system *via* modulation of TPH 2 transcription.

Naturally, these analyses do not allow one to conclude whether EPO modulated the intrafollicular expression of these genes directly or indirectly, for example, by changing the secretion or surface expression of molecules, which then implemented the observed differential gene expression. Nevertheless, these data clearly demonstrate that the stimulation of normal, EPO-R-expressing human scalp HFs with EPO elicits defined and reproducible gene expression changes, thus providing further evidence for the functional activity of HF EPO-R. Last but not least, these initial microarray data indicate that human HF organ culture offers an excellent discovery tool for identifying novel EPO target genes in peripheral tissue biology, as a key element in the ongoing endeavor to explore nonclassical EPO functions in the human system. J

The authors are grateful to A. Becker for excellent technical assistance. This work was supported in part by a grant from Deutsche Forschungsgemeinschaft (DFG) to R. Paus (Pa 345/11–2).

## REFERENCES

- Jelkmann, W. (2004) Molecular biology of erythropoietin. *Intern. Med.* **43**, 649–659
- Ghezzi, P., and Brines, M. (2004) Erythropoietin as an antiapoptotic, tissue-protective cytokine. *Cell Death Differ.* **11**, S37–44
- Savino, R., and Ciliberto, G. (2004) A paradigm shift for erythropoietin: no longer a specialized growth factor, but rather an all-purpose tissue-protective agent. *Cell Death Differ.* **11**, S2–4
- Brines, M., and Cerami, A. (2006) Discovering erythropoietin's extra-hematopoietic functions: biology and clinical promise. *Kidney Int.* **70**, 246–250
- Rosser, J., and Eckardt, K. U. (2005) Erythropoietin receptors: their role beyond erythropoiesis. *Nephrol. Dial. Transplant.* **20**, 1025–1028
- Kaushansky, K. (2006) Lineage-specific hematopoietic growth factors. *N. Engl. J. Med.* **354**, 2034–2045
- Dame, C. (2003) Molecular biology of the erythropoietin receptor in hematopoietic and non-hematopoietic tissues. In *Erythropoietins and Erythropoiesis* (Molineux, G., Foote, M., and Elliott, S., eds) pp. 35–63. Birkhauser Verlag, Switzerland
- Wang, G. L., and Semenza, G. L. (1993) General involvement of hypoxia-inducible factor 1 in transcriptional response to hypoxia. *Proc. Natl. Acad. Sci. U. S. A.* **90**, 4304–4308
- Wang, G. L., Jiang, B. H., Rue, E. A., and Semenza, G. L. (1995) Hypoxia-inducible factor 1 is a basic-helix-loop-helix-PAS heterodimer regulated by cellular O<sub>2</sub> tension. *Proc. Natl. Acad. Sci. U. S. A.* **92**, 5510–5514
- Gradin, K., McGuire, J., Wenger, R. H., Kvietkova, I., Whitelaw, M. L., Toftgard, R., Tora, L., Gassmann, M., and Poellinger, L. (1996) Functional interference between hypoxia and dioxin signal transduction pathways: competition for recruitment of the Arnt transcription factor. *Mol. Cell Biol.* **16**, 5221–5231
- Wood, S. M., Gladle, J. M., Pugh, C. W., Hankinson, O., and Ratcliffe, P. J. (1996) The role of the aryl hydrocarbon receptor nuclear translocator (ARNT) in hypoxic induction of gene

- expression. Studies in ARNT-deficient cells. *J. Biol. Chem.* 271, 15117-15123
12. Masuda, S., Nagao, M., Takahata, K., Konishi, Y., Gallyas, F., Jr., Tabira, T., and Sasaki, R. (1993) Functional erythropoietin receptor of the cells with neural characteristics. Comparison with receptor properties of erythroid cells. *J. Biol. Chem.* 268, 11208-11216
13. Konishi, Y., Chui, D. H., Hirose, H., Kunishita, T., and Tabira, T. (1993) Trophic effect of erythropoietin and other hematopoietic factors on central cholinergic neurons in vitro and in vivo. *Brain Res.* 609, 29-35
14. Sakanaka, M., Wen, T. C., Matsuda, S., Masuda, S., Morishita, E., Nagao, M., and Sasaki, R. (1998) In vivo evidence that erythropoietin protects neurons from ischemic damage. *Proc. Natl. Acad. Sci. U. S. A.* 95, 1635-1640
15. Sadamoto, Y., Igase, K., Sakanaka, M., Sato, K., Otsuka, H., Sakaki, S., Masuda, S., and Sasaki, R. (1998) Erythropoietin prevents place navigation disability and cortical infarction in rats with permanent occlusion of the middle cerebral artery. *Biochem. Biophys. Res. Commun.* 253, 26-32
16. Hasselblatt, M., Ehrenreich, H., and Siren, A. L. (2006) The brain erythropoietin system and its potential for therapeutic exploitation in brain disease. *J. Neurosurg. Anesthesiol.* 18, 132-138
17. Siren, A. L., Fratelli, M., Brines, M., Goemans, C., Casagrande, S., Lewczuk, P., Keenan, S., Gleiter, C., Pasquali, C., Capobianco, A., et al. (2001) Erythropoietin prevents neuronal apoptosis after cerebral ischemia and metabolic stress. *Proc. Natl. Acad. Sci. U. S. A.* 98, 4044-4049
18. Wen, T. C., Sadamoto, Y., Tanaka, J., Zhu, P. X., Nakata, K., Ma, Y. J., Hata, R., and Sakanaka, M. (2002) Erythropoietin protects neurons against chemical hypoxia and cerebral ischemic injury by up-regulating Bcl-xL expression. *J. Neurosci. Res.* 67, 795-803
19. Ehrenreich, H., Hasselblatt, M., Dembowski, C., Cepek, L., Lewczuk, P., Stiefel, M., Rustenbeck, H. H., Breiter, N., Jacob, S., Knerlich, F., et al. (2002) Erythropoietin therapy for acute stroke is both safe and beneficial. *Mol. Med.* 8, 495-505
20. Carlini, R. G., Alonzo, E. J., Dominguez, J., Blanca, I., Weisinger, J. R., Rothstein, M., and Bellorin-Font, E. (1999) Effect of recombinant human erythropoietin on endothelial cell apoptosis. *Kidney Int.* 55, 546-553
21. Sharples, E. J., and Yaqoob, M. M. (2006) Erythropoietin and acute renal failure. *Semin. Nephrol.* 26, 325-331
22. Juul, S. E., Yachnis, A. T., and Christensen, R. D. (1998) Tissue distribution of erythropoietin and erythropoietin receptor in the developing human fetus. *Early Hum. Dev.* 52, 235-249
23. Galeano, M., Altavilla, D., Bitto, A., Minutoli, L., Calo, M., Lo Cascio, P., Polito, F., Giugliano, G., Squadrito, G., et al. (2006) Recombinant human erythropoietin improves angiogenesis and wound healing in experimental burn wounds. *Crit. Care Med.* 34, 1139-1146
24. Selzer, E., Wacheck, V., Kodym, R., Schlagbauer-Wadl, H., Schlegel, W., Pehamberger, H., and Jansen, B. (2000) Erythropoietin receptor expression in human melanoma cells. *Melanoma Res.* 10, 421-426
25. Kumar, S. M., Acs, G., Fang, D., Herlyn, M., Elder, D. E., and Xu, X. (2005) Functional erythropoietin autocrine loop in melanoma. *Am. J. Pathol.* 166, 823-830
26. Elliott, S., Busse, L., Bass, M. B., Lu, H., Sarosi, I., Sinclair, A. M., Spahr, C., Um, M., Van, G., and Begley, C. G. (2006) Anti-Epo receptor antibodies do not predict Epo receptor expression. *Blood* 107, 1892-1895
27. Isogai, R., Takahashi, M., Aisu, K., Horiuti, Y., Aragane, Y., Kawada, A., and Tezuka, T. (2006) The receptor for erythropoietin is present on cutaneous mast cells. *Arch. Dermatol. Res.* 297, 389-394
28. Lebaron, M. J., Ahonen, T. J., Nevalainen, M. T., and Rui, H. (2006) In vivo response-based identification of direct hormone target cell populations using high-density tissue arrays. *Endocrinology* 148, 989-1008
29. Paus, R., and Cotsarelis, G. (1999) The biology of hair follicles. *N. Engl. J. Med.* 341, 491-497
30. Stenn, K. S., and Paus, R. (2001) Controls of hair follicle cycling. *Physiol. Rev.* 81, 449-494
31. Philpott, M. P., and Kealey, T. (1991) Metabolic studies on isolated hair follicles: hair follicles engage in aerobic glycolysis and do not demonstrate the glucose fatty acid cycle. *J. Invest. Dermatol.* 96, 875-879
32. Slominski, A., and Wortsman, J. (2000) Neuroendocrinology of the skin. *Endocr. Rev.* 21, 457-487
33. Slominski, A., Wortsman, J., Kohn, L., Ain, K. B., Venkataraman, G. M., Pisarchik, A., Chung, J. H., Giuliani, C., Thornton, M., Slugocki, G., and Tobin, D. J. (2002) Expression of hypothalamic-pituitary-thyroid axis related genes in the human skin. *J. Invest. Dermatol.* 119, 1449-1455
34. Slominski, A., Wortsman, J., Pisarchik, A., Zbytek, B., Linton, E. A., Mazurkiewicz, J. E., and Wei, E. T. (2001) Cutaneous expression of corticotropin-releasing hormone (CRH), urocortin, and CRH receptors. *FASEB J.* 15, 1678-1693
35. Zouboulis, C. C., Seltmann, H., Hiroi, N., Chen, W., Young, M., Oeff, M., Scherbaum, W. A., Orfanos, C. E., McCann, S. M., and Bornstein, S. R. (2002) Corticotropin-releasing hormone: an autocrine hormone that promotes lipogenesis in human sebocytes. *Proc. Natl. Acad. Sci. U. S. A.* 99, 7148-7153
36. Ito, N., Ito, T., Kromminga, A., Bettermann, A., Takigawa, M., Kees, F., Straub, R. H., and Paus, R. (2005) Human hair follicles display a functional equivalent of the hypothalamic-pituitary-adrenal axis and synthesize cortisol. *FASEB J.* 19, 1332-1334
37. Paus, R., Theoharides, T. C., and Arck, P. C. (2006) Neuroimmunendocrine circuitry of the "brain-skin connection." *Trends Immunol.* 27, 32-39
38. Kobayashi, H., Kromminga, A., Dunlop, T. W., Tychsen, B., Conrad, F., Suzuki, N., Memezawa, A., Bettermann, A., Aiba, S., Carlberg, C., and Paus, R. (2005) A role of melatonin in neuroectodermal-mesodermal interactions: the hair follicle synthesizes melatonin and expresses functional melatonin receptors. *FASEB J.* 19, 1710-1712
39. Foitzik, K., Krause, K., Conrad, F., Nakamura, M., Funk, W., and Paus, R. (2006) Human scalp hair follicles are both a target and a source of prolactin, which serves as an autocrine and/or paracrine promoter of apoptosis-driven hair follicle regression. *Am. J. Pathol.* 168, 748-756
40. Slominski, A., Wortsman, J., Luger, T., Paus, R., and Solomon, S. (2000) Corticotropin releasing hormone and proopiomelanocortin involvement in the cutaneous response to stress. *Physiol. Rev.* 80, 979-1020
41. Philpott, M. P., Green, M. R., and Kealey, T. (1990) Human hair growth in vitro. *J. Cell Sci.* 97, 463-471
42. Bodó, E., Biró, T., Telek, A., Czifra, G., Griger, Z., Tóth, B. I., Mescalchin, A., Ito, T., Bettermann, A., Kovács, L., and Paus, R. (2005) A hot new twist to hair biology: involvement of vanilloid receptor-1 (VR1/TRPV1) signaling in human hair growth control. *Am. J. Pathol.* 166, 985-998
43. Marxsen, J. H., Stengel, P., Doege, K., Heikkinen, P., Jokilehto, T., Wagner, T., Jelkmann, W., Jaakkola, P., and Metzzen, E. (2004) Hypoxia-inducible factor-1 (HIF-1) promotes its degradation by induction of HIF- $\alpha$ -prolyl-4-hydroxylases. *Biochem. J.* 381, 761-767
44. Bodó, E., Tobin, D., Funk, W., and Paus, R. (2006) Development and characterization of an in vitro-assay for the study of human chemotherapy-induced dystrophy. *J. Invest. Dermatol. Suppl.* 126, P126
45. Braun, S., Krampert, M., Bodo, E., Kümin, A., Born-Berclaz, C., Paus, R., and Werner, S. (2006) Keratinocyte growth factor protects epidermis and hair follicles from cell death induced by UV irradiation, chemotherapeutic, and cytotoxic agents. *J. Cell Sci.* 119, 4841-4849
46. Ito, T., Ito, N., Bettermann, A., Tokura, Y., Takigawa, M., and Paus, R. (2004) Collapse and restoration of MHC class-I-dependent immune privilege: exploiting the human hair follicle as a model. *Am. J. Pathol.* 164, 623-634
47. Lindner, G., Botchkarev, V. A., Botchkareva, N. V., Ling, G., van der Veen, C., and Paus, R. (1997) Analysis of apoptosis during hair follicle regression (catagen). *Am. J. Pathol.* 151, 1601-1617
48. National Committee for Clinical Laboratory Standards (1992) How to define, determine, and utilize reference intervals in the clinical laboratory. NCCLS Document C28-P, Vol. 12, pp. 1-47
49. Liu, R., Suzuki, A., Guo, Z., Mizuno, Y., and Urabe, T. (2006) Intrinsic and extrinsic erythropoietin enhances neuroprotection against ischemia and reperfusion injury in vitro. *J. Neurochem.* 96, 1101-1110
50. Bruegge, K., Jelkmann, W., and Metzzen, E. (2007) Hydroxylation of hypoxia-inducible transcription factors and chemical

- compounds targeting the HIF- $\alpha$  hydroxylases. *Current Med. Chem.* **14**, 103–112
51. Ito, M., Liu, Y., Yang, Z., Nguyen, J., Liang, F., Morris, R. J., and Cotsarelis, G. (2005) Stem cells in the hair follicle bulge contribute to wound repair but not to homeostasis of the epidermis. *Nat. Med.* **11**, 1351–1354
  52. Jahoda, C. A., and Reynolds, A. J. (2001) Hair follicle dermal sheath cells: unsung participants in wound healing. *Lancet* **358**, 1445–1448
  53. Hara, M., Yaar, M., Byers, H. R., Goukassian, D., Fine, R. E., Gonsalves, J., and Gilchrist, B. A. (2000) Kinesin participates in melanosomal movement along melanocyte dendrites. *J. Invest. Dermatol.* **114**, 438–443
  54. Zou, H., Hu, L., Li, J., Zhan, S., and Cao, K. (2006) Cloning and characterization of a novel small monomeric GTPase, RasL10B, with tumor suppressor potential. *Biotechnol. Lett.* **28**, 1901–1908
  55. Liu, T. C., Chang, J. G., Lin, C. P., Lee, L. S., Lin, S. F., Liu, H. W., and Chen, T. P. (1990) Detection of beta-globin gene from single hairs. *Gaoxiong Yi. Xue. Ke. Xue. Za. Zhi.* **6**, 181–185
  56. Slominski, A., Wortsman, J., and Tobin, D. J. (2005) The cutaneous serotonergic/melatonergic system: securing a place under the sun. *FASEB J.* **19**, 176–194
  57. Slominski, A., Pisarchik, A., Semak, I., Sweatman, T., and Wortsman, J. (2003) Characterization of the serotonergic system in the C57BL/6 mouse skin. *Eur. J. Biochem.* **270**, 3335–3344
  58. Slominski, A., Pisarchik, A., Semak, I., Sweatman, T., Wortsman, J., Szczesniowski, A., Slugocki, G., McNulty, J., Kauser, S., Tobin, D. J., *et al.* (2002) Serotonergic and melatonergic systems are fully expressed in human skin. *FASEB J.* **16**, 896–898

Received for publication March 22, 2007.

Accepted for publication April 26, 2007.

# Erythropoietin mediates tissue protection through an erythropoietin and common $\beta$ -subunit heteroreceptor

Michael Brines<sup>\*,†</sup>, Giovanni Grasso<sup>\*,§</sup>, Fabio Fiordaliso<sup>‡</sup>, Alessandra Sfacteria<sup>\*,§</sup>, Pietro Ghezzi<sup>\*,†</sup>, Maddalena Fratelli<sup>‡</sup>, Roberto Latini<sup>‡</sup>, Qiao-wen Xie<sup>\*,†</sup>, John Smart<sup>\*,†</sup>, Chiao-Ju Su-Rick<sup>\*,†</sup>, Eileen Pobre<sup>\*,†</sup>, Deborah Diaz<sup>\*,†</sup>, Daniel Gomez<sup>\*,†</sup>, Carla Hand<sup>\*,†</sup>, Thomas Coleman<sup>\*,†</sup>, and Anthony Cerami<sup>\*,†</sup>

<sup>\*</sup>Kenneth S. Warren Institute and <sup>†</sup>Warren Pharmaceuticals, Ossining, NY 10563; <sup>‡</sup>Mario Negri Pharmacological Research Institute, 20157 Milan, Italy; and <sup>§</sup>University of Messina, 98122 Messina, Italy

Contributed by Anthony Cerami, September 2, 2004

The cytokine erythropoietin (Epo) is tissue-protective in preclinical models of ischemic, traumatic, toxic, and inflammatory injuries. We have recently characterized Epo derivatives that do not bind to the Epo receptor (EpoR) yet are tissue-protective. For example, carbamylated Epo (CEpo) does not stimulate erythropoiesis, yet it prevents tissue injury in a wide variety of *in vivo* and *in vitro* models. These observations suggest that another receptor is responsible for the tissue-protective actions of Epo. Notably, prior investigation suggests that EpoR physically interacts with the common  $\beta$  receptor ( $\beta$ cR), the signal-transducing subunit shared by the granulocyte-macrophage colony stimulating factor, and the IL-3 and IL-5 receptors. However, because  $\beta$ cR knockout mice exhibit normal erythrocyte maturation,  $\beta$ cR is not required for erythropoiesis. We hypothesized that  $\beta$ cR in combination with the EpoR expressed by nonhematopoietic cells constitutes a tissue-protective receptor. In support of this hypothesis, membrane proteins prepared from rat brain, heart, liver, or kidney were greatly enriched in EpoR after passage over either Epo or CEpo columns but covalently bound in a complex with  $\beta$ cR. Further, antibodies against EpoR coimmunoprecipitated  $\beta$ cR from membranes prepared from neuronal-like P-19 cells that respond to Epo-induced tissue protection. Immunocytochemical studies of spinal cord neurons and cardiomyocytes protected by Epo demonstrated cellular colocalization of Epo  $\beta$ cR and EpoR. Finally, as predicted by the hypothesis, neither Epo nor CEpo was active in cardiomyocyte or spinal cord injury models performed in the  $\beta$ cR knockout mouse. These data support the concept that EpoR and  $\beta$ cR comprise a tissue-protective heteroreceptor.

**E**rythropoietin (Epo) is a cytokine characterized by remarkable tissue-protective activity in preclinical models of neuronal, retinal, cardiac, and renal ischemic injury (reviewed by Grasso *et al.* in ref. 1). A recent positive clinical study showing that administration of recombinant human Epo (rhEpo) benefits stroke patients (2) provides hope that additional translation from preclinical models of tissue protection into other human diseases will occur. The broad efficacy of Epo observed in model systems depends on Epo's key role in multiple protective pathways activated in many diseases, including an inhibition of apoptosis, restoration of vascular autoregulation, attenuation of inflammatory responses, and augmentation of restorative functions, including the direct recruitment of stem cells (1).

The signaling pathways in these responses have not been fully clarified but are known to involve multiple second messenger systems (reviewed by Ghezzi and Brines in ref. 3). Notably, the results of previous studies have shown that the affinity of Epo for the neuronal-type receptor is substantially lower than that of Epo for the red-cell precursor receptor homodimer (EpoR)<sub>2</sub> (4). Further, neuronal proteins associated with Epo in cross-linking studies are smaller than those isolated from bone marrow (5). Finally, our recent work identifying Epo derivatives that lack hematopoietic activity yet retain full tissue protection confirm the distinct nature of the tissue-protective Epo receptor (EpoR) (6).

Several laboratories have previously reported a physical association (7) and functional interaction (8) of EpoR with the common  $\beta$  receptor ( $\beta$ cR) subunit, also known as CD131, which provides increased ligand-binding affinity to the receptor complex and is also the signal-transducing component common to the granulocyte-macrophage colony stimulating factor (GM-CSF), IL-3, and IL-5 receptors (reviewed in ref. 9). However, the significance of these observations was questioned when it was shown that  $\beta$ cR knockout mice exhibit normal hematopoiesis (10).

In light of the successful separation of Epo hematological and tissue-protective activities, we reassessed the relationship between EpoR and  $\beta$ cR in tissues exhibiting Epo protection as a potential explanation of how a nonerythropoietic Epo initiates tissue protection. A number of studies involving cells within the CNS, including microglia, have reported expression of  $\beta$ cR and responsiveness to IL-3, IL-5, and GM-CSF *in vivo* and *in vitro* (11), indicating that  $\beta$ cR is functionally present in brain cells. Other tissues, however, have not been examined for coexpression of EpoR and  $\beta$ cR. In the present communication, we demonstrate that EpoR and  $\beta$ cR are coexpressed in Epo-sensitive cells within protected tissues. Moreover, EpoR and  $\beta$ cR copurify on a variety of affinity resins and in immunoprecipitation experiments. Finally, Epo is not tissue-protective in the  $\beta$ cR knockout mouse. Together, these results are consistent with a model wherein tissue protection is mediated through a heteroreceptor complex comprising both EpoR and  $\beta$ cR.

## Methods

**Animals.** All protocols were approved by the Animal Use and Care Committee of the Kenneth S. Warren Institute in accordance with the directives of the Guide for the Care and Use of Laboratory Animals. The  $\beta$ cR knockout mice used for these experiments are described in ref. 10, and we thank L. Robb (Royal Melbourne Hospital, Victoria, Australia), C. G. Begley (Amgen), J. A. Whitsett (Children's Hospital Center, Cincinnati), and W. Hull (Children's Hospital Center, Cincinnati) for providing this strain. Confirmation of  $\beta$ cR<sup>-/-</sup> was accomplished for each mouse by PCR genotyping with primers described in ref. 10. Control strain-matched, wild-type mice (C57/BL6) and Sprague-Dawley rats were obtained from Taconic Farms.

**Abbreviations:**  $\beta$ cR, common  $\beta$  receptor; Epo, erythropoietin; CEpo, carbamylated Epo; EpoR, Epo receptor; GM-CSF, granulocyte-macrophage colony stimulating factor; rhEpo, recombinant human Epo.

<sup>†</sup>M.B., P.G., Q.X., C.S.-R., E.P., D.D., D.G., C.H., T.C., and A.C. are minority stockholders of Warren Pharmaceuticals, which is engaged in commercializing tissue-protective cytokines.

<sup>‡</sup>To whom correspondence should be addressed at: Kenneth S. Warren Institute, 712 Kitchawan Road, Kitchawan, NY 10562. E-mail: mbrines@kswi.org.

<sup>§</sup>G.G. and F.F. contributed equally to this work.

© 2004 by The National Academy of Sciences of the USA

**Materials.** All reagents not specified were of the highest purity and obtained from local suppliers. Carbamylated Epo (CEpo) was prepared as described in ref. 6 and confirmed to be nonerythropoietic at concentrations up to 10  $\mu\text{g/ml}$  by using TF-1 and UT-7 cells. Epo was a generous gift from Dragon Pharmaceuticals (Vancouver).

**Immunocytochemistry.** Animals were perfused with 4% paraformaldehyde, and tissues were removed, embedded in paraffin, cut into 6- $\mu\text{m}$ -thick sections, and processed as described in ref. 12. Antibodies used ( $\beta\text{cR}$ : K-17, N-20; EpoR: M-20, H194) were obtained from Santa Cruz Biotechnology.

**Affinity Purification of Cell Membranes.** Epo and CEpo columns were prepared by adding 3.5 mg of recombinant protein to cyanogen bromide-activated Sepharose 4B in a conical tube and slowly rotating it at 4°C for 48 h. Efficiency of coupling ( $\approx 100\%$ ) was determined by UV spectrometry of the supernatant. Membranes obtained from freshly dissected organs from normal rats were minced and homogenized in phosphate buffer with a protease inhibitor mixture of phenylmethylsulfonylfluoride (1 mM) and aprotinin (10  $\mu\text{g/ml}$ ). After centrifugation (30 min at 15,000  $\times g$  in microfuge tubes), the supernatant was passed over a lentil lectin Sepharose 4B column (Amersham Biosciences). Retained glycoproteins were eluted by  $\alpha$ -methylmannose (10  $\mu\text{M}$ ) and subsequently analyzed by Western blotting or affinity purification over Epo or CEpo columns.

**EpoR Immunoprecipitation.** P19 cells were grown to 70% confluence as described in ref. 13, treated with 10 ng/ml Epo or saline for 15 min, and detached by gently swirling the flask. The cells were collected by centrifugation (7 min at 1,000  $\times g$ ) and resuspended in lysis buffer [Tris-buffered saline with protease inhibitors phenylmethylsulfonylfluoride (1 mM) and aprotinin (10  $\mu\text{g/ml}$ ), 2 mM  $\text{CaCl}_2$ , 1% Triton, and 1% Nonidet P-40]. Freezing and vortexing were avoided. After removal of cellular debris by centrifugation for 10 min (1,000  $\times g$ ), the lysate was diluted to a final concentration of  $\approx 1$  mg of protein per ml and was incubated with protein A Sepharose (10  $\mu\text{l}$  of drained gel per ml; Amersham Biosciences) for 1 h at room temperature to reduce nonspecific binding. The supernatant was then incubated with protein A Sepharose (10  $\mu\text{l}$  of gel per ml) that was previously coupled to the antibody for 1 h and then washed three times with lysis buffer. Either an antibody against the common  $\beta$  chain (K17, Santa Cruz Biotechnology) or a mixture of two antibodies against EpoR (M20 and H194, Santa Cruz Biotechnology) at a final dilution of 1:200 was used for an overnight incubation at 4°C. The protein A Sepharose beads, either alone (nonspecific) or antibody-coupled (specific), were then washed five times with low-detergent lysis buffer (the same as above but

containing 0.5% Triton without Nonidet P-40), and bound proteins were dissociated by the addition of 30  $\mu\text{l}$  of 2 $\times$  Laemmli sample buffer with 5% 2-mercaptoethanol and run on a 10% SDS/PAGE. Immunoblotting was performed with either the antibody against  $\beta\text{cR}$  (K17, Santa Cruz Biotechnology) or an antibody against EpoR (H194, Santa Cruz Biotechnology) at 1:200 and with 1:50,000 anti-rabbit horseradish peroxidase secondary antibody (Sigma) and was detected by the ECL Plus system (Amersham Biosciences).

**Spinal Cord Injury.** Spinal cord compression in mice was performed by using a slight modification of the protocol of Farooque (14) under isoflurane anesthesia and a controlled core temperature of 35–37°C. Briefly, C57/BL6 wild-type or  $\beta\text{cR}$  knockout mice (15) of 8–16 weeks of age (10 animals per group) were subjected to a T3 laminectomy, and a 2-mm stainless steel rod (15 g) was then applied to the dura with a micromanipulator for 4 min. A single dose of CEpo or Epo (10  $\mu\text{g/kg}$ ) was administered i.p. immediately after injury. During recovery, animals were assessed in a blinded fashion by using the scoring system of Basso *et al.* (16) and of Tarlov (17). The bladders were manually expressed twice daily for each animal until neurogenic function developed, usually by 10 days.

**Isolated Ventricular Cardiomyocytes in Primary Culture.** Left ventricular cardiomyocytes were isolated from adult wild-type C57/BL6 or  $\beta\text{cR}$  knockout mice (15) as described in ref. 18. Briefly, hearts were perfused via the aorta with collagenase buffer (type II, Worthington) gassed with 85%  $\text{O}_2$  and 15%  $\text{N}_2$  at 37°C. Left ventricular myocytes were then isolated by mechanical dissociation, separated by differential centrifugation, plated on laminin-coated dishes, and maintained in minimum essential medium with Hanks' salts and L-glutamine. One hour after plating, the medium was changed, and Epo (100 ng/ml) or control buffer was added to the myocytes in a blinded fashion 30 min before apoptosis was triggered by staurosporine (0.1  $\mu\text{M}$ ; Sigma). After 16 h of incubation, cardiomyocytes were fixed and processed for *in situ* terminal deoxynucleotidyltransferase (TdT) detection of apoptosis (Roche Diagnostics). The number of TdT-labeled cells was determined by counting at least 500 myocytes in each culture dish and expressed as a percentage of the total number of cells. Omission of biotin-16-dUTP or TdT was used to generate negative controls.

**Statistics.** Unless otherwise indicated, all results are displayed as means  $\pm$  SEM of replicates. One-way analysis of variance followed by Dunnett's test or the nonparametric Kruskal–Wallace analysis were used for statistical evaluation as appropriate.

## Results

**Evidence for a Heteromeric Complex Consisting of EpoR and  $\beta\text{cR}$ .** Working on the assumption that tissue protection is mediated via a typical glycosylated cytokine receptor, adult rat brain, kidney,

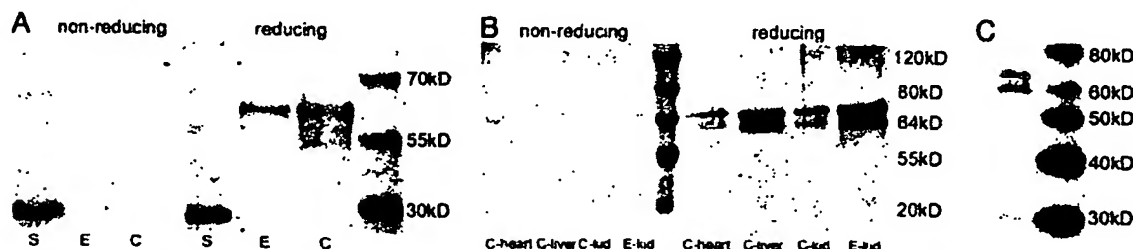


**Fig. 1.** Despite having no affinity for CEpo, EpoR is bound to a CEpo affinity column but within a complex. (A) Rat brain membrane proteins sequentially purified over a lentil lectin column and Epo or CEpo affinity columns were subjected to EpoR Western blotting in either a reduced or nonreduced state. Bands ( $\approx 64$  kDa) consistent with the EpoR were visualized only under reduced conditions. S, soluble EpoR-positive control (29 kDa); E, Epo affinity column; C, CEpo affinity column. (B) Membranes prepared from heart, kidney (kid), and liver show results similar to those for brain membranes but as a distinct doublet. (C) In contrast, cell membranes obtained from TF-1 cells and run under nonreducing conditions show the doublet EpoR.

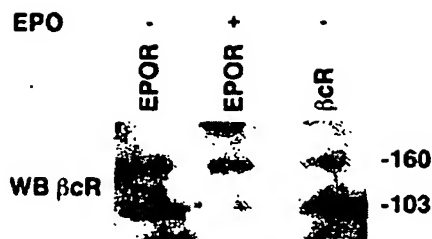


**Fig. 2.** EpoR and  $\beta$ cR are present as a complex in neuronal lysates. Immunoprecipitation of membranes prepared from P19 mouse neuroblastoma cells demonstrate that either anti-EpoR or anti- $\beta$ cR pulls down a protein consistent with  $\beta$ cR ( $\sim 130$  kDa), as well as a smaller molecular species. Equivalent results were obtained in the presence or absence of Epo.

and liver membrane preparations were first glycoprotein-enriched by passage over a lentil lectin column and then exposed to either an Epo or CEpo affinity column. Immunoblotting of reduced or nonreduced eluted proteins from either column with an anti-EpoR antibody visualized a principal band of  $\sim 64$  kDa

molecular mass, consistent with previous reports of EpoR (5), but only under reducing conditions (Fig. 1*A* and *B*). In contrast, membranes obtained from TF-1 cells, which signal via the homodimeric (EpoR) $_2$ , showed bands consistent with EpoR under both nonreducing (Fig. 1*C*) and reducing (data not shown) conditions. These data suggested that the tissue-protective receptor consisted of EpoR within a larger complex that displayed an affinity for the CEpo column.

EpoR and  $\beta$ cR have been previously described as a complex; by using immunoprecipitation, we determined this complex was present in neuron-like cells. Membranes were prepared from undifferentiated neuronal-like murine P19 cells with or without a brief Epo exposure and then immunoprecipitated by using a mixture of two antibodies against EpoR that were raised against different regions of the molecule. Western blotting of the precipitated proteins with anti- $\beta$ cR displayed a dominant band at the appropriate molecular mass for the  $\beta$ cR protein ( $\sim 130$  kDa), as well as another band at  $\sim 100$  kDa (Fig. 2). The presence of Epo during incubation and precipitation did not affect the results. Similar findings were obtained from membranes prepared from adult mouse heart (data not shown).

Because the tissue-protective receptor (with high affinity for

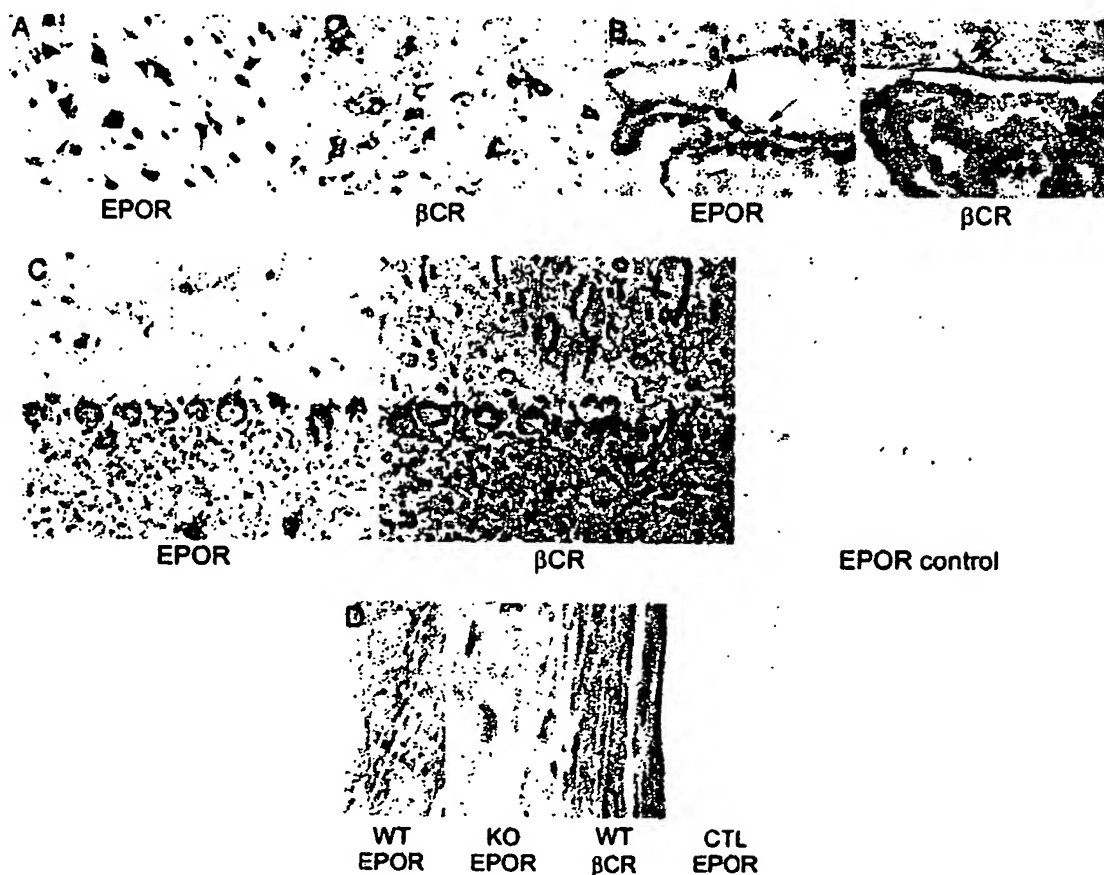


**Fig. 3.** Cells exhibiting tissue protection express both the EpoR and  $\beta$ cR subunit. (A) Spinal cord neurons within the central gray obtained from normal mice show prominent staining of the somata for both proteins. (B) Choroid plexus (arrow), as well as the ependymal cell layer (arrowhead), exhibit prominent staining for both EpoR and  $\beta$ cR. EpoR staining appears punctate. Radial glia (double arrow) are also doubly immunoreactive. (C) Purkinje cells of the cerebellum stain densely for EpoR in a punctate manner (Left), whereas anti- $\beta$ cR stains somata, as well as the proximal dendrites (arrow), more diffusely. Note that neuronal somata in the molecular layer, as well as granule cells, are also immunopositive for both proteins. Right illustrates negative control (primary antibody omitted). (D) Sections of myocardium obtained from normal mice show prominent EpoR and  $\beta$ cR immunostaining. Sections obtained from the  $\beta$ cR knockout mouse exhibit prominent EpoR immunoreactivity. CTL EpoR is a negative control in which the primary antibody was omitted.



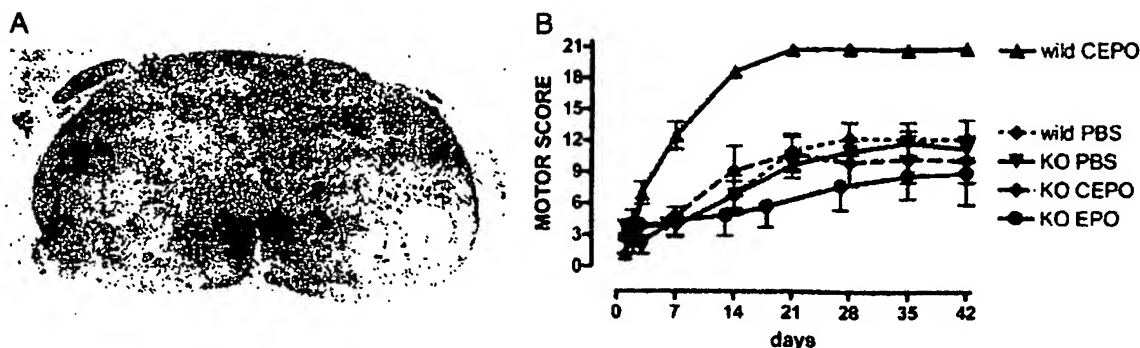


Fig. 4. CEpo restores motor function after spinal compression in wild-type mice but not in strain-matched  $\beta$ CR knockout mice. (A) Spinal cord morphology is normal in the  $\beta$ CR knockout mouse (hematoxylin/eosin-stained). (B)  $\beta$ CR knockout mice subjected to spinal cord compressive injury do not respond to either Epo or CEpo (10  $\mu$ g/kg of body weight) given i.p. as a single dose immediately after injury.

CEpo) contained both EpoR and  $\beta$ CR, individual cells responsive to nonerythropoietic tissue-protective cytokines should coexpress these proteins. In confirmation of this prediction, a heterogeneous distribution of distinctive cell types expressing immunoreactivity for both  $\beta$ CR and EpoR was observed in normal rat tissues. For example, spinal cord central gray neurons (Fig. 3A) were immunopositive for both receptors. However, the subcellular localization of the proteins differed in large and small neurons within the brain and spinal cord: EpoR staining was localized predominantly to the neuronal somata in a punctuate cytoplasmic pattern, extending rarely into the proximal dendrites (e.g., the Purkinje cells within the cerebellum) (Fig. 3C). In contrast, although  $\beta$ CR immunoreactivity colocalized within the same neuronal type, it appeared extensively distributed throughout both the cell body and dendritic processes. In a noncomprehensive nervous system survey, prominent colocalization of  $\beta$ CR and EpoR also was observed in the choroid plexus, ependymal cells (Fig. 3B), and radial glia. In contrast, EpoR and  $\beta$ CR expression in other tissues appeared diffusely colocalized, e.g., in cardiac myocytes (Fig. 3D). In many regions examined, small capillaries were also positive for the two receptor proteins (data not shown). Two other antibodies against  $\beta$ CR and EpoR (obtained from R & D Systems) produced similar staining patterns (data not shown).

**Studies in the  $\beta$ CR Knockout Mouse.** If the  $\beta$ CR is a critical component of the tissue-protective receptor, the  $\beta$ CR knockout mouse should be unresponsive to tissue-protective cytokines. This mouse model is grossly normal phenotypically and is fertile. It is immunologically abnormal, especially within the eosinophil lineage, and ultimately develops a progressive pulmonary fibrosis with advancing age. The original descriptions of the young  $\beta$ CR knockout mouse reported no abnormalities of tissues and organs. We confirmed these observations by extensive microscopic examination of hematoxylin/eosin- and Nissl-stained sections that revealed no abnormalities of the  $\beta$ CR knockout brain, spinal cord (Fig. 4A), liver, kidney, or heart.

**Spinal Cord Injury.** Normal or  $\beta$ CR knockout male mice of 8–16 weeks of age received a moderate compressive lesion of the spinal cord, followed immediately by a single i.p. dose of Epo or CEpo (10  $\mu$ g/kg of body weight) and were subsequently evaluated for motor function over 6 weeks. Mortality was similar between groups ( $\sim$ 10–20%). Wild-type mice responded to CEpo with a complete recovery within 4 weeks (Fig. 4). In contrast,  $\beta$ CR knockout animals exhibited no difference in motor function among the CEpo, Epo, or saline groups after 6 weeks. However, at earlier time points,  $\beta$ CR knockout animals receiving

Epo exhibited a poorer motor recovery. Calculation of the area under the curve showed a significant difference between the Epo and PBS animals ( $133 \pm 30$  vs.  $356 \pm 36$  motor-score days;  $P < 0.05$ ). The simplified scoring of Tarlov (17) gave a similar outcome to the Basso scale (16). Bladder function was regained in parallel to the motor function (data not shown).

**Primary Cardiomyocyte Survival.** Cardiomyocytes prepared from the hearts of young wild-type or  $\beta$ CR knockout mice (8–12 weeks) were incubated in the presence of rhEpo (100 ng/ml) or control buffer and then exposed to staurosporine (0.1  $\mu$ M). After a 16-h exposure, both the wild-type and  $\beta$ CR knockout cell cultures exhibited  $\sim$ 70% apoptosis (Fig. 5) ( $P < 0.001$ ). rhEpo added to the culture medium (100 ng/ml) improved survival, reducing apoptosis to  $\sim$ 40% in the wild-type cells ( $P < 0.001$ ). In contrast,  $\beta$ CR knockout cardiomyocytes did not respond to rhEpo.

## Discussion

We have recently shown that the hematopoietic and tissue-protective activities of Epo are distinct and separate (6), implicating the existence of different receptors. Epo is a member of the cytokine superfamily type I that is characterized by pleiotropic functionality. Receptors within this family often consist of heterogeneous combinations of proteins that can transduce different functions for the same ligand (e.g., gp130) (19). Despite our observations that CEpo does not bind to the EpoR dimer or monomer (6), there are several lines of evidence that firmly implicate the EpoR in tissue protection. First, under conditions of hypoxia or other metabolic stressors, brain cells greatly

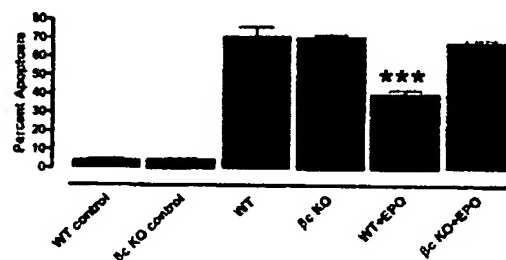


Fig. 5. rhEpo is tissue-protective of staurosporine-induced apoptosis for cardiomyocytes derived from wild-type cells but not identically prepared cells from  $\beta$ CR knockout mice. rhEpo was added (100 ng/ml) 30 min before the addition of staurosporine (0.1  $\mu$ g/ml). Each condition corresponds to between four and eight replications. \*\*\*,  $P < 0.001$  vs. staurosporine alone.



increase mRNA and immunoreactive EpoR (20, 21). Second, EpoR-neutralizing antibodies block neuroprotection (22). Third, EpoR knockout mice develop an abnormal brain and heart, characterized by massive cellular apoptosis. Fetal neurons can be cultured from the EpoR knockout embryos, and these display an increased sensitivity to stressors (e.g., ischemia) and do not respond to Epo (23).

As an initial approach to isolate the receptor with which CEpo interacts, we used a CEpo affinity column. Our preliminary work showed that an enrichment of glycosylated membrane proteins could be obtained if the membrane fraction was first passed over a lentil lectin column. Analysis of the proteins retained on the CEpo column showed that EpoR was indeed captured, despite exhibiting no affinity for CEpo. However, in this case, EpoR, unlike proteins prepared from TF-1 cells, was covalently bound to another protein (or proteins); it was only observable under reducing conditions (Fig. 1). The possibility that residual low levels of Epo contaminated the CEpo was eliminated by the demonstration that the CEpo used (tested up to 10  $\mu$ g/ml) possessed no erythropoietic activity in the TF-1 and UT-7 bioassays.

Further, proteins from membranes prepared from the neural-like P19 cells, immunoprecipitated by using anti-EpoR antibodies, and immunoblotted by using anti- $\beta$ cR, a receptor reported to be associated with EpoR (7), showed a band of a size consistent with  $\beta$ cR ( $\sim$ 130 kDa) but, again, only under reducing conditions (Fig. 2). An additional molecular species that could be a variant or breakdown product of  $\beta$ cR also was observed. Immunocytochemistry further supported the hypothesis of the tissue-protective receptor consisting of EpoR and  $\beta$ cR proteins, because these proteins appear colocalized in those cells (e.g., neurons) for which CEpo is tissue-protective *in vitro* and *in vivo* (Fig. 3).

Taken together, the colocalization and binding data suggest that tissue protection signals through the interaction of Epo or CEpo with an EpoR- $\beta$ cR heteromer. To test this hypothesis, we used a mouse model that lacked the  $\beta$ cR but was otherwise normal with respect to red cells and platelets, verifying a preserved hematopoietic action of Epo via the homodimer (EpoR)<sub>2</sub>. As expected in the strain-matched, wild-type animals, tissue-protective cytokines were fully active in a spinal cord injury model, confirming that mice are effectively protected from damage, as previously shown for the rat (6). In contrast, both CEpo and Epo did not protect  $\beta$ cR knockout mice from compressional spinal cord injury (Fig. 4), although the histology of the uninjured spinal cord was normal. Immunohistochemical examination of the brain and spinal cord for EpoR confirmed expression levels comparable to those of wild-type tissues, making it unlikely that the loss in efficacy for Epo or CEpo was explained by reduced or absent expression of EpoR.

The significantly reduced area under the curve for Epo compared with CEpo in the spinal cord injury model in  $\beta$ cR knockout mice is interesting and could depend on unopposed actions of Epo through the classical (EpoR)<sub>2</sub>. Particularly, platelet activation within the microvasculature (24) might delay or impair early recovery through development of microinfarctions. The  $\beta$ cR knockout model will be useful for distinguishing between the classical and tissue-protective effects of Epo.

$\beta$ cR knockout mice have been shown to exhibit defects in eosinophil and macrophage populations, which could well affect the rate of recovery from spinal cord injury. To eliminate this

possibility, as well as to examine the involvement of the  $\beta$ cR receptor in cytoprotective activities outside of the CNS, we used an *in vitro* model of primary cardiomyocytes obtained from the adult heart. In agreement with previous studies (25), Epo protects wild-type primary cardiomyocytes from staurosporine-mediated apoptosis (Fig. 5). In marked contrast, Epo had no cytoprotective effects on identically treated cardiomyocytes isolated from  $\beta$ cR knockout mice, despite the presence of abundant EpoR immunoreactive protein. In sum, these experiments are fully supportive of a role for  $\beta$ cR in the tissue-protective signaling of Epo and CEpo.

It is notable that the  $\beta$ cR knockout mice appeared histologically normal and did not appear to be more sensitive to injury (e.g., after exposure to staurosporine), as we would have predicted in the absence of a tissue-protective receptor. This lack of amplification of injury could depend on an additional IL-3-specific common  $\beta$  subunit highly homologous to  $\beta$ cR that is present only in the mouse. In the mouse, therefore, the  $\beta$ cR knockout will affect only GM-CSF and IL-5 signaling (26), not IL-3, which has itself been reported to possess tissue-protective properties. Notably, IL-3 and its receptors (both  $\alpha$  and  $\beta$ ) are locally made (27, 28) and act in a neurotrophic and neuroprotective manner (29, 30), including protection from spinal motor neuron transection (31). To answer this question, additional experiments using gene-silencing technology will need to be performed in another species, e.g., in the rat, for which abundant data relevant to tissue protection have been collected. If the IL-3-specific  $\beta$  subunit does confer protection, the role of tissue-protective cytokine receptors in the setting of injury may be even more dramatic than has been shown in these experiments.

Although the precise protein interactions of the EpoR and  $\beta$ cR have not been determined, they are likely homologous to the GM-CSF: $\beta$ cR stoichiometry, because receptor assembly in this cytokine family occurs through highly conserved structural and chemical mechanisms (32). In this system, the ligand GM-CSF displays negligible affinity for the GM-CSF receptor or  $\beta$ cR alone (33), similar to what we have observed for CEpo. In the presence of the ligand, however, a high-affinity receptor complex consisting of a 1:1:2 ratio of GM-CSF:GM-CSF receptor: $\beta$ cR is formed (33). Because at least four cytokines appear to use the  $\beta$ cR, multiple signaling possibilities exist in tissues expressing different  $\alpha$  receptors and clearly require further study. For example, previous investigators have described a hierarchy in signaling, presumably based on differences in affinity of  $\beta$ cR to the different  $\alpha$  receptor subunits (33).

Finally, although our experimental results identify  $\beta$ cR and EpoR as components of the receptor mediating tissue protection, further study will be required to understand many critical aspects of this association, e.g., whether other proteins also are members of the complex, the precise stoichiometry of the receptor subunits, and the signaling pathways. With this knowledge, rational development of tissue-protective cytokines can be initiated.

We thank Ulf Andersson Örom for technical assistance, Dr. Michael Yamin for critically reading the manuscript, and Drs. L. Robb, C. G. Begley, J. A. Whitsett, and W. Hull for providing the  $\beta$ cR knockout mice. This work was supported in part by the Kenneth S. Warren Institute and by Grants RBAU01AR5J and Fondo Integrativo Speciale per la Ricerca-Neurobiotecnologie from the Ministero della Istruzione, Università e Ricerca, Rome (to P.G.).

- Grasso, G., Sfacteria, A., Cerami, A., & Brines, M. (2004) *Neuroscientist* 10, 93–98.
- Ehrenreich, H., Hasselblatt, M., Dembowski, C., Cepck, L., Lewczuk, P., Stiefel, M., Rustenbeck, H. H., Breiter, N., Jacob, S., Knerlich, F., et al. (2002) *Mol. Med.* 8, 495–505.
- Ghezzi, P., & Brines, M. (2004) *Cell Death Differ.* 11, Suppl. 1, S37–S44.

- Livnah, O., Stura, E. A., Middleton, S. A., Johnson, D. L., Jolliffe, L. K., & Wilson, I. A. (1999) *Science* 283, 987–990.
- Masuda, S., Nagao, M., Takahata, K., Konishi, Y., Gallyas, F., Jr., Tabira, T., & Sasaki, R. (1993) *J. Biol. Chem.* 268, 11208–11216.
- Leist, M., Ghezzi, P., Grasso, G., Bianchi, R., Villa, P., Fratelli, M., Savino, C., Bianchi, M., Nielsen, J., Gerwien, J., et al. (2004) *Science* 305, 239–242.

7. Jubinsky, P. T., Krijanowski, O. I., Nathan, D. G., Tavernier, J. & Sieff, C. A. (1997) *Blood* 90, 1867–1873.
8. Blake, T. J., Jenkins, B. J., D'Andrea, R. J. & Gonda, T. J. (2002) *J. Leukocyte Biol.* 72, 1246–1255.
9. D'Andrea, R. J. & Gonda, T. J. (2000) *Exp. Hematol.* 28, 231–243.
10. Scott, C. L., Robb, L., Papaevangelou, B., Mansfield, R., Nicola, N. A. & Begley, C. G. (2000) *Blood* 96, 1588–1590.
11. Klampfer, L., Zhang, J. & Nimer, S. D. (1999) *Cytokine* 11, 849–855.
12. Celik, M., Gokmen, N., Erbayraktar, S., Akhisaroglu, M., Konak, S., Ulukus, C., Genc, S., Genc, K., Sagiroglu, E., Cerami, A. & Brines, M. (2002) *Proc. Natl. Acad. Sci. USA* 99, 2258–2263.
13. Brines, M. L., Ghezzi, P., Keenan, S., Agnello, D., de Lanerolle, N. C., Cerami, C., Itri, L. M. & Cerami, A. (2000) *Proc. Natl. Acad. Sci. USA* 97, 10526–10531.
14. Farooque, M. (2000) *Acta Neuropathol.* 100, 13–22.
15. Reed, J. A., Ikegami, M., Robb, L., Begley, C. G., Ross, G. & Whitsett, J. A. (2000) *Am. J. Physiol.* 278, L1164–L1171.
16. Basso, D. M., Beattie, M. S. & Bresnahan, J. C. (1995) *J. Neurotrauma* 12, 1–21.
17. Tarlov, I. M. (1972) *J. Neurosurg.* 36, 10–20.
18. Fiordaliso, F., Leri, A., Cesselli, D., Limana, F., Safai, B., Nadal-Ginard, B., Anversa, P. & Kajstura, J. (2001) *Diabetes* 50, 2363–2375.
19. Muller-Newen, G. (2003) *Sci. STKE* 2003, PE40.
20. Bernaudin, M., Marti, H. H., Roussel, S., Divoux, D., Nouvelot, A., MacKenzie, E. T. & Petit, E. (1999) *J. Cereb. Blood Flow Metab.* 19, 643–651.
21. Siren, A. L., Knerlich, F., Poser, W., Gleiter, C. H., Bruck, W. & Ehrenreich, H. (2001) *Acta Neuropathol.* 101, 271–276.
22. Campana, W. M., Misasi, R. & O'Brien, J. S. (1998) *Int. J. Mol. Med.* 1, 235–241.
23. Yu, X., Shacka, J. J., Fells, J. B., Suarez-Quian, C., Przygodzki, R. M., Beleslin-Cokic, B., Lin, C. S., Nikodem, V. M., Hempstead, B., Flanders, K. C., et al. (2002) *Development (Cambridge, U.K.)* 129, 505–516.
24. Stohlawetz, P. J., Dzirlo, L., Hergovich, N., Lackner, F., Mensik, C., Eichler, H. G., Kabma, E., Geisler, K. & Jilka, B. (2000) *Blood* 95, 2983–2999.
25. Calvillo, L., Latini, R., Kajstura, J., Leri, A., Anversa, P., Ghezzi, P., Salio, M., Cerami, A. & Brines, M. (2003) *Proc. Natl. Acad. Sci. USA* 100, 4802–4806.
26. Nishinakamura, R., Nakayama, N., Hirabayashi, Y., Inoue, T., Aud, D., McNeil, T., Azuma, S., Yoshida, S., Toyoda, Y., Arai, K., et al. (1995) *Immunity* 2, 211–222.
27. Konishi, Y., Kamegai, M., Takahashi, K., Kunishita, T. & Tabira, T. (1994) *Neurosci. Lett.* 182, 271–274.
28. Tabira, T., Chui, D. H., Fan, J. P., Shirabe, T. & Konishi, Y. (1998) *Ann. N.Y. Acad. Sci.* 840, 107–116.
29. Kamegai, M., Nijima, K., Kunishita, T., Nishizawa, M., Ogawa, M., Araki, M., Ueki, A., Konishi, Y. & Tabira, T. (1990) *Neuron* 4, 429–436.
30. Wen, T. C., Tanaka, J., Peng, H., Desaki, J., Matsuda, S., Maeda, N., Fujita, H., Sato, K. & Sakanaka, M. (1998) *J. Exp. Med.* 188, 635–649.
31. Iwasaki, Y., Ikeda, K., Ichikawa, Y., Igarashi, O., Iwamoto, K. & Kinoshita, M. (2002) *Neurol. Res.* 24, 643–646.
32. Rossjohn, J., McKinsty, W. J., Woodcock, J. M., McClure, B. J., Hercus, T. R., Parker, M. W., Lopez, A. F. & Bagley, C. J. (2000) *Blood* 95, 2491–2498.
33. McClure, B. J., Hercus, T. R., Cambareri, B. A., Woodcock, J. M., Bagley, C. J., Howlett, G. J. & Lopez, A. F. (2003) *Blood* 101, 1308–1315.

(12) INTERNATIONAL APPLICATION PUBLISHED UNDER THE PATENT COOPERATION TREATY (PCT)

(19) World Intellectual Property  
Organization  
International Bureau



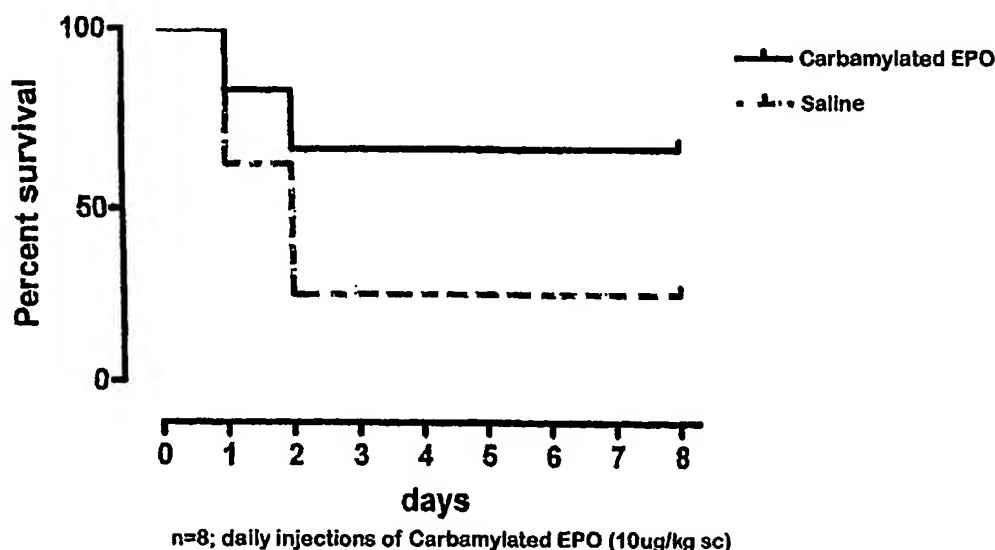
(43) International Publication Date  
14 April 2005 (14.04.2005)

PCT

(10) International Publication Number  
**WO 2005/032467 A2**

- (51) International Patent Classification<sup>7</sup>: **A61K**
- (21) International Application Number:  
PCT/US2004/031789
- (22) International Filing Date:  
29 September 2004 (29.09.2004)
- (25) Filing Language: English
- (26) Publication Language: English
- (30) Priority Data:  
60/506,149 29 September 2003 (29.09.2003) US
- (71) Applicant (for all designated States except US): **WARREN PHARMACEUTICALS, INC.** [US/US]; 712 Kitchawan Road, Ossining, NY 10562 (US).
- (72) Inventors; and
- (75) Inventors/Applicants (for US only): **BRINES, Michael** [US/US]; 1 Wopawaug Road, Woodbridge, CT 06525 (US). **CERAMI, Anthony** [US/US]; 49 Bramblebush Drive, Croton-on-Hudson, NY 10520 (US). **YILMAZ, Osman** [TR/TR]; 100 Sokad Kalaci, Apt. 24/17, Gottepe Izmir (TR). **COLEMAN, Thomas** [US/US]; 20 Emery Street, Mt. Kisco, NY 10549 (US).
- (74) Agents: **MULGREW, John, P. et al.**; Swidler Berlin Sheroff Friedman, LLP, 3000 K Street, N.W., Suite 300, Washington, DC 20007 (US).
- (81) Designated States (unless otherwise indicated, for every kind of national protection available): AE, AG, AL, AM, AT, AU, AZ, BA, BB, BG, BR, BW, BY, BZ, CA, CH, CN, CO, CR, CU, CZ, DE, DK, DM, DZ, EC, EE, EG, ES, FI, GB, GD, GE, GH, GM, HR, HU, ID, IL, IN, IS, JP, KE, KG, KP, KR, KZ, LC, LK, LR, LS, LT, LU, LV, MA, MD, MG, MK, MN, MW, MX, MZ, NA, NI, NO, NZ, OM, PG, PH, PL, PT, RO, RU, SC, SD, SE, SG, SK, SL, SY, TJ, TM, TN, TR, TT, TZ, UA, UG, US, UZ, VC, VN, YU, ZA, ZM, ZW.
- (84) Designated States (unless otherwise indicated, for every kind of regional protection available): ARIPO (BW, GH, GM, KE, LS, MW, MZ, NA, SD, SL, SZ, TZ, UG, ZM, ZW), Eurasian (AM, AZ, BY, KG, KZ, MD, RU, TJ, TM), European (AT, BE, BG, CH, CY, CZ, DE, DK, EE, ES, FI, FR, GB, GR, HU, IE, IT, LU, MC, NL, PL, PT, RO, SE, SI, SK, TR), OAPI (BF, BJ, CF, CG, CI, CM, GA, GN, GQ, GW, ML, MR, NE, SN, TD, TG).
- Published:  
— without international search report and to be republished upon receipt of that report
- For two-letter codes and other abbreviations, refer to the "Guidance Notes on Codes and Abbreviations" appearing at the beginning of each regular issue of the PCT Gazette.

(54) Title: **TISSUE PROTECTIVE CYTOKINES FOR THE TREATMENT AND PREVENTION OF SEPSIS AND THE FORMATION OF ADHESIONS**



(57) Abstract: A method of treating, preventing, delaying the onset, and/or reducing the effects of proinflammatory cytokines in conditions including, but not limited to, sepsis, adhesion formation, wounds, organ failure, chronic disease, general inflammatory conditions resulting from infection, scarring resulting from injury and incisions, and combinations thereof.

WO 2005/032467 A2

**TISSUE PROTECTIVE CYTOKINES FOR THE TREATMENT  
AND PREVENTION OF SEPSIS AND THE FORMATION OF ADHESIONS**

**FIELD OF THE INVENTION**

5           The present invention is directed to a method of treating, preventing, delaying the onset, and/or reducing the effects of sepsis and related complications. In particular, the present invention is directed to the use of tissue protective cytokines for the treatment, prevention, delay, and/or reduction of complications with regard to sepsis, adhesion formation, and organ failure. Furthermore, the tissue protective cytokines of the present  
10   invention are also contemplated for treatment, prevention, delay, and/or reduction of complications of general inflammatory conditions resulting from infection.

**BACKGROUND OF THE INVENTION**

          Several strategies exist for responding to infection, immune challenges, inflammation,  
15   and trauma in a host. One mechanism by which the host attempts to respond to these challenges is through the upregulation of cytokines, nonantibody proteins that act as intercellular regulators. Some cytokines, known as proinflammatory cytokines, counteract the challenges to the host by enhancing the disease in the hopes of ridding the host of the challenge and host cells damaged by the challenge. Proinflammatory cytokines include, but  
20   are not limited to, interleukins (IL), such as IL-1, IL-6, IL-8, and IL-18, and tumor necrosis factor (TNF).

          When released, the proinflammatory cytokines have the effect at the site of injury of increasing the release of antibodies and their compliments, T and B cell activation, the adhesion of platelets to blood vessel walls, and extravascularization of lymphocytes and  
25   macrophages. These changes lead to a localized environment at the site of injury including fever, tissue injury, tumor necrosis, induction of other cytokines and immunoregulation and apoptosis. This localized response is toxic not only to the source of the challenge to the host but also to the host cells within the penumbra of the proinflammatory cytokine response. Thus, it is not surprising that on a systemic level, such as may occur during overwhelming  
30   infection or serious trauma to the host, many of these proinflammatory cytokines are harmful  
\*   to the host producing fever, inflammation, tissue destruction, and, in some cases, shock and death.

Representative of the action of the various proinflammatory cytokines is TNF. TNF is a proinflammatory cytokine produced by many cell types, including macrophages, monocytes, lymphoid cells and fibroblasts in response to inflammation, infection, and other environmental challenges. TNF elicits a wide spectrum of cellular responses, including fever, shock, tissue injury, tumor necrosis, anorexia, induction of other cytokines and immunoregulatory molecules, cell proliferation, differentiation and apoptosis. When released TNF has an effect at the site of injury of increasing the release of antibodies and their compliments, T and B cell activation, the adhesion of platelets to blood vessel walls, and extravasuarization of lymphocytes and macrophages. Systemically, TNF acts upon the hypothalamus and liver. TNF stimulates the hypothalamus to release corticotropin releasing hormone, suppress appetite and induce fever. In response to TNF, the liver initiates an acute phase response resulting in the synthesis of several proteins including C-reactive protein, coagulation factors and compliment factors. Also, TNF induces insulin resistance. In the defined area of injury or infection, TNF is vital to removing the particular infectious agent and adapting the body's immune response to the particular injury.

On a systemic level, however, in which TNF as well as other proinflammatory cytokines may be present at higher concentrations or for prolonged times, TNF can have deleterious effects on the body. At high concentrations TNF activates an IL-1 & IL-6 cascade that results in cachexia (wasting). Additionally, TNF can lead to systemic edema, hypoproteinemia, and neutropenia which can result in disseminated extravascular coagulation and eventually multiple organ failure. In chronic diseases such as cancer, TNF can also interfere with vital endogenous functions within the host. For example, TNF may interfere with the ability of endogenous erythropoietin to maintain the hematocrit of the host, leading to a condition referred to as the anemia of chronic diseases (ACD). A typical course of treatment with recombinant erythropoietin may not counteract the effects of the proinflammatory cytokine, thereby requiring the administration of elevated doses of recombinant erythropoietin just to maintain the normal hematocrit of the host. Beyond the additional costs associated with the increased dosing, there is also the risk of adverse side effects from the increased doses of erythropoietin such as thrombosis. In addition to the conditions detailed below, proinflammatory cytokines, including, but not limited to, TNF are associated with diseases such as chronic inflammation, bacterial septic shock, bacterial toxic shock, graft vs. host disease, and HIV infection and AIDS.

### Sepsis

Sepsis is the body's response to any kind of infection, *e.g.*, bacterial, viral, parasitic, or fungal. Sites of infection are typically the lungs, the urinary tract, the abdomen, and the pelvis. In some cases, however, the actual site of infection cannot be detected. Although  
5 sepsis was once thought to be a systemic inflammatory response, it is now recognized that sepsis also includes prothrombotic diathesis and impaired fibrinolysis.

Once sepsis commences, widespread inflammation and clotting occurs throughout the body. Whereas in a healthy body, immune modulators would be released to fight the infection and heal the body, in sepsis, an overabundance of immune regulators is released.

10 The release of proinflammatory cytokines such as TNF, interleukin-1, and interleukin-18 lead to the inflammation of endothelial linings, elevation of the core temperature, loss of appetite, and anemia. In addition, inflammation of the lining of blood vessels activates the blood clotting process. Because sepsis decreases the body's natural production of protein C, which regulates blood clotting and controls inflammation, the body's ability to break down the  
15 formed blood clots is suppressed. This suppression leads to clotting in vital organs, limbs, fingers, and toes, which, in turn, leads to organ failure or gangrene.

Sepsis may present itself in varying degrees. For example, in cases of severe sepsis, which occurs when acute organ dysfunction or failure results, the body's normal defense reaction goes into overdrive, setting off a cascade of events that can lead to widespread  
20 inflammation and blood clotting in tiny vessels throughout the body. Septic shock occurs when a patient with severe sepsis experiences cardiovascular system failure. This failure causes the blood pressure to drop, which, in turn, deprives vital organs of an adequate oxygenated blood supply. Septicemia is a sepsis that has an infection in the bloodstream itself. In fact, septicemia may cause ischemia, *i.e.*, poor blood supply to at least one organ.  
25 For example, when blood flow to the kidneys is reduced to dangerously low levels for substantial time period, ischemic acute renal failure (ARF) may develop. The depressed blood flow also results in necrosis, or tissue death, in affected organs.

Providing the source of the sepsis can be identified, many cases of sepsis will respond to treatment. Once isolated, a treatment regime specific to the cause of infection is initiated.  
30 Known treatment includes the use of antibiotics, surgical excision of infected or necrotic tissues, drugs that increase activated protein, and steroids (in cases of septic shock). For example, a typical course of sepsis treatment includes administration of a broad spectrum antibiotic until the cause of infection is isolated. However, the mortality rate of sepsis

patients remains relatively high in cases of sepsis where the cause and/or area of infection is not ascertainable.

Depending on the severity of sepsis, anti-infection agents, draining techniques, fluids, drugs to raise the mean arterial blood pressure (MAP) such as norepinephrine and phenylephrine, drugs to improve renal function such as dopamine, drugs to increase oxygen delivery and oxygen consumption such as dobutamine and epinephrine, mechanical ventilators to support breathing, and dialysis for kidney failure may be used in the course of treatment. In addition, pharmacological agents that have been shown to have beneficial effects on immune responses following shock and sepsis include ATP-MgCl<sub>2</sub>, nonanticoagulant heparin, calcium channel blockers, chloroquine, cyclooxygenase inhibitors, PAF antagonists, anti-inflammatory cytokines, growth factors, dietary manipulation, anti-TNF antibodies, activated protein C (Xigris®, Eli Lilly, Indianapolis, Indiana), and sex hormones. Recovery from sepsis is greatest when the condition is quickly diagnosed and promptly treated.

Recombinant erythropoietin (rhu-EPO), commercially available under tradenames PROCrit® (from Ortho Biotech Inc., Raritan, NJ), EPOGEN® (from Amgen, Inc., Thousand Oaks, CA), and NEORECOMON (from Roche, Basel, Switzerland) has also recently been investigated with regard to treatment of various conditions related to sepsis. In addition, U.S. Patent Publication No. 2003/0083251 generally discloses the use of rhu-EPO to aid in the regeneration of renal tubular cells and prevention of apoptosis of the renal tubular cells in order to treat patients with ischemic ARF. Furthermore, US Patent Publication No. 2002/0061849 generally discloses the use of rhu-EPO to aid in the treatment of inflammation in a non-ischemic condition in one or more organs. However, because of erythropoietin's erythropoietic effects -- increased hematocrit, vasoconstriction, hyperactivation of platelets, pro-coagulant activity, and increased production of thrombocytes -- treatment with rhu-EPO poses additional risks given the widespread clotting in vital organs, limbs, fingers, and toes that is associated with sepsis.

#### Adhesions.

In addition to sepsis, proinflammatory cytokines, such as TNF, have been associated with the formation of adhesions, abnormal fibrous bands or connections between organs and other structures of the body, as well. Adhesions may be a complication of, or related to,



sepsis but also may occur independently. For example, adhesions may form as a result of surgery, trauma, infection, chemotherapy, and radiation. In fact, adhesions are almost an inevitable outcome of surgery, *i.e.*, about 93 percent of patients who have undergone abdominal surgery suffer from adhesions to some degree (compared with adhesion formation in about 10.4 percent of patients who had never undergone a previous abdominal operation).  
5 *See* D. Menzies and H. Ellis, *Intestinal Obstruction from Adhesions—How Big is the Problem?*, ANN. R. COLL. SURG. ENGL. 72: 60-3 (1990).

The formation of adhesions can cause severe pain and apply unnatural pressure or tension on organs or other structures of a patient. For example, adhesions in the abdominal  
10 region of the body may cause the intestines of a patient to become trapped or squeezed between organs or other structures of the body. In some cases, the intestines may become blocked or significantly obstructed due to nearby adhesions.

The formation of these abnormal connections between two parts of a body leads to a host of other conditions. For example, as cesarean sections are becoming a more common  
15 method of childbirth, women who undergo this major abdominal surgery are likely to form adhesions and, as a result, experience chronic pelvic pain. In addition, adhesions involving female reproductive organs may lead to infertility and dyspareunia.

A number of agents have been researched in connection with preventing and treating adhesions, *e.g.*, dextran, corticosteroids, phosphatidylcholine, phospholipase inhibitors, non-  
20 steroidal anti-inflammatory drugs, proteoglycans, heparin, and tissue plasminogen activator. *See, e.g.*, C.L. Kowalczyk and M.P. Diamond, *The Management of Adhesive Disease*, in PERITONEAL ADHESIONS 315-324 (K.H. Treutner and V. Schumpelick, eds., 1997). Some, but not all of these agents, are believed to be effective in the treatment of adhesions because of their ability to interfere with coagulation and fibrinolysis. Clinical experience with the  
25 majority of these agents, however, is limited due to bleeding complications. In addition, hyaluronic acid derivatives have been shown to prevent postsurgical adhesions, particularly in the intra-abdominal area. *See, e.g.*, J.M. Becker *et al.*, *Prevention of Postoperative Abdominal Adhesions by a Sodium Hyaluronate-based Bioresorbable Membrane: A Prospective, Randomized, Double-blind Multicenter Study*, in J. AM. COLL. SURG. 183 297-  
30 306 (1996). Furthermore, beta-glucan, which is a glucose polymer that binds with high affinity to the receptors on monocytes and neutrophils in a competitive manner, has been  
shown to have a reducing effect on the frequency of adhesion after experimentally developed intraabdominal sepsis in Wistar rats. A. Bedirli *et al.*, *Prevention of Intraperitoneal Adhesion*

*Formation Using Beta-Glucan After Ileocolic Anastomosis in a Rat Bacterial Peritonitis Model*, in AM. J. SURG. 185 339-343 (2003).

Surgery may also be used as a course of treatment for adhesions. Generally, a physician will perform surgery to sever the adhesions from the organ or other part of the body. Given that adhesions are often a complication of surgery, however, surgery to remove adhesions frequently results in the formation of new adhesions. While some surgical procedures involve placement of sleeves over organs adjacent to the areas affected by the surgery and thus, help to prevent adhesions involving these organs, such procedures have had mixed results. In addition, the organ sleeves also require additional surgery to remove the sleeves.

Thus, despite the increased awareness with regard to adhesions, research into treatment methods have met with limited success. Many physicians are unwilling or unable to address the treatment of adhesions and many insurance companies are unwilling to pay for treatments that are, at best, marginally successful.

#### Wound Healing.

Healing is an essential process of the body that reestablishes the integrity of damaged tissue. This process is often viewed in terms of wounds, ulcers or lesions of the skin resulting from various causes such as trauma, surgery, pressure (bed sores), burns, diabetes, etc. The severity of the wounds is characterized by the extent the wound penetrates the skin. Stage I wounds are characterized by redness or discoloration, warmth, and swelling or hardness. Stage II wounds, partial thickness wounds, penetrate the epidermis and superficial dermis of the skin. Stage III wounds, full thickness wounds, penetrate through the dermis of the skin but do not penetrate the membrane separating the skin from deeper organs. Stage IV wounds involve damage to the underlying muscle or bone.

Although all wounds heal through the same process: inflammation, epithelialization, angiogenesis, and the accumulation of matrix; the ease with which the wound heals is largely based on the severity of the wound and the health of the wounded individual. In general, Stage I and Stage II wounds heal through the regeneration of epithelial cells by the underlying dermis. Whereas, Stage III and IV wounds heal through the production of a scar. Proinflammatory cytokines, such as TNF, play a role in the healing of wounds, however, it is speculated that TNF may have an adverse effect on the accumulation of collagen in the

healing wound and ultimately on the time the wound takes to heal and the strength of the repaired tissue.

Several therapeutics as well as therapeutic methods have been developed to assist the body in healing wounds. Several compounds are considered to have a therapeutic effect on wound healing including, but not limited to, growth factors (epidermal growth factor, Insulin-like Growth Factor, human growth hormone, fibroblast growth factor, vascular endothelial growth factor, interleukin-6, and interleukin-10), nutritional supplements (arginine, glutamine, vitamin C, vitamin B5, Bromelain, Curcumin, zinc, copper), and herbal supplements (aloe vera, Centella). Furthermore, various therapeutic methods including, but not limited to, hyperbaric oxygen therapy, whirlpool therapy, ultrasound therapy, electrical stimulation, and magnetic therapy have been utilized to aid the body in healing wounds.

If a wound does not heal properly or fails to heal at all it can lead to several complications chief among them scarring and infection. Depending upon the severity of the wound, the body may generate scar tissue in healing the wound. Aside from the aesthetic concerns of a scar, the scar may impair movement of the individual depending upon its severity. Additionally, a wound presents an opportunity for bacteria and other infectious agents to enter the body. Depending upon the severity of infection it may spread and become systemic leading to sepsis or septicemia.

Rhu-EPO has also been investigated for its possible healing effects in rat models of random ischemic flaps. For example, rhu-EPO has been shown to reduce necrosis, decrease neutrophil infiltration, and prevent increased temperature with regard to ischemic skin flap injuries. See M. Buemi *et al.*, *Recombinant Human Erythropoietin Influences Revascularization and Healing in a Rat Model of Random Ischaemic Flaps*, ACTA DERM VENEREOL, 82: 411-417 (2002). This finding suggests that rhu-EPO administration can improve the wound healing process, both in early and late stages of injury, by reducing the inflammatory response, increasing the density of capillaries in ischemic flaps and allowing earlier repair of a damaged area. However, as mentioned above, because rhu-EPO has erythropoietic activity, the use of rhu-EPO for treatment of these conditions may cause a greater degree of clotting or complications than already initiated by the healing process.

In sum, no one agent or treatment strategy has demonstrated sufficient value for the management of sepsis cases, the incidence of sepsis, the formation of adhesions, wound healing or general inflammatory conditions. In fact, the mortality associated with sepsis and related conditions remains high. Every year, approximately 215,000 people die from severe sepsis and one out of every three patients who develop severe sepsis will die within a month.

And, cases of sepsis are expected to rise in the future due to the increased awareness of the condition and sensitivity for the diagnosis, the number of immunocompromised patients, the use of invasive procedures, the number of resistant microorganisms, and the growth of the elderly population. In addition, the chronic pain associated with adhesions and general inflammatory conditions is often untreated due to the lack of a successful treatment strategy.

Thus, there exists a need in the art for method and therapeutics for treating, preventing, delaying the onset of, and reducing the effects of proinflammatory cytokines for the purposes of limiting the penumbra of their action and further addressing their systemic effect. In particular, a need exists for treating, preventing, delaying the onset of, and reducing the effects of proinflammatory cytokines in conditions of sepsis, adhesions, wounds, chronic disease and general inflammatory conditions. In addition, it would be beneficial to provide methodologies that have the ability to repair or prevent damage to tissue in ischemic conditions.

## **SUMMARY OF THE INVENTION**

The present invention is directed to a method of treating, preventing, delaying the onset, and/or reducing the effects of sepsis, adhesions, general inflammatory conditions, and combinations thereof by administering at least one tissue protective cytokine in a therapeutically effective amount. In addition, the present invention relates to the prevention or reduction of scarring relating to injury and incisions using at least one tissue protective cytokine. The at least one tissue protective cytokine may be any tissue protective cytokine having tissue protective functionality. In one embodiment, however, the at least one tissue protective cytokine is a chemically modified EPO. In another embodiment, the chemically modified EPO is carbamylated EPO.

One embodiment of the present invention relates to a method of treating, preventing, delaying the onset of, or reducing the effects of proinflammatory cytokines in a mammal. Other embodiments relate to methods of treating, preventing, delaying the onset of a condition associated with an effect of proinflammatory cytokines. Some examples of conditions associated with the effects of proinflammatory cytokines include sepsis, adhesions, wounds, inflammation or chronic disease. These methods may involve the steps of administering a therapeutically effective amount of one or more tissue protective cytokines in a pharmaceutical carrier.

In addition, the present invention also is directed to pharmaceutical compositions that may be used in the methods described herein. For instance, one embodiment is directed

toward a pharmaceutical composition comprising an amount of at least one tissue protective cytokine effective in treating, preventing, delaying the onset of, or reducing the effects of proinflammatory cytokines in a mammal. Another embodiment is directed toward a pharmaceutical composition comprised of an amount of at least one tissue protective cytokine effective in treating, preventing, delaying the onset of a condition associated with proinflammatory cytokines in a mammal.

Some tissue protective cytokines used in the present invention may be chemically modified erythropoietin or mutated erythropoietin.

In some embodiments where a chemically modified erythropoietin is used, the chemically modified erythropoietin may include one or more of the following: i) an erythropoietin that lacks sialic acid moieties; ii) an erythropoietin having at least no sialic acid moieties; iii) an erythropoietin having at least no N-linked or no O-linked carbohydrates; iv) an erythropoietin having at least a reduced carbohydrate content by virtue of treatment of native erythropoietin with at least one glycosidase; v) an erythropoietin having at least one or more oxidized carbohydrates; vi) an erythropoietin having at least one or more oxidized carbohydrates and is chemically reduced; vii) an erythropoietin having at least one or more modified arginine residues; viii) an erythropoietin having at least one or more modified lysine residues or a modification of the N-terminal amino group of the erythropoietin molecule; ix) an erythropoietin having at least a modified tyrosine residue; x) an erythropoietin having at least a modified aspartic acid or a glutamic acid residue; xi) an erythropoietin having at least a modified tryptophan residue; xii) an erythropoietin having at least one amino group removed; xiii) an erythropoietin having at least an opening of at least one of the cystine linkages in the erythropoietin molecule; or xiv) a truncated erythropoietin. In another embodiment, the chemically modified erythropoietin lacks erythropoietin's erythropoietic effects. The chemically modified erythropoietin also may comprise carbamylated erythropoietin.

Similarly, in some embodiments involving a mutated erythropoietin, the mutated erythropoietin may be selected from one or more of the following mutations C7S, R10I, V11S, L12A, E13A, R14A, R14B, R14E, R14Q, Y15A, Y15F, Y15I, K20A, K20E, E21A, C29S, C29Y, C33S, C33Y, P42N, T44I, K45A, K45D, V46A, N47A, F48A, F48I, Y49A, Y49S, W51F, W51N, Q59N, E62T, L67S, L70A, D96R, K97D, S100R, S100E, S100A, S100T, G101A, G101I, L102A, R103A, S104A, S104I, L105A, T106A, T106I, T107A, T107L, L108K, L108A, S126A, F142I, R143A, S146A, N147K, N147A, F148Y, L149A, R150A, G151A, K152A, L153A, L155A, C160S, I6A, C7A, B13A, N24K, A30N, H32T,

N38K, N83K, P42A, D43A, K52A, K97A, K116A, T132A, I133A, T134A, K140A, P148A, R150B, G151A, K152W, K154A, G158A, C161A, or R162A. . In another embodiment, the mutated erythropoietin lacks erythropoietin's erythropoietic effects.

Two examples of proinflammatory cytokines are Interleukin and TNF. One or more effects of the proinflammatory cytokine may include fever, wasting, lethargy, anemia, edema, ischemia, organ failure and insulin resistance. Additional features and advantages of the present invention are described in greater detail below.

## 10 **BRIEF DESCRIPTION OF THE DRAWINGS**

Further features and advantages of the invention can be ascertained from the following detailed description that is provided in connection with the drawing(s) described below:

FIG. 1 is a graphical representation of the survival rate of Sprague Dawley rats after cecum ligation and puncture (CLP) and subsequent treatment with saline or a tissue protective cytokine of the invention;

FIG. 2 is a graphical representation of the adhesion score for Sprague Dawley rats following CLP and subsequent treatment with saline or a tissue protective cytokine of the invention;

FIG. 3 is a graphical representation of the illness score for Sprague Dawley rats subjected to CLP and subsequent treatment with saline or a tissue protective cytokine of the invention;

FIG. 4 is a graphical representation of the adhesion score for Sprague Dawley rats following CLP with and without sepsis introduction and subsequent treatment with saline and a tissue protective cytokine of the invention; and

FIG. 5 is a graphical representation of the serum TNF level for Sprague Dawley rats following CLP with and without sepsis introduction and subsequent treatment with saline and a tissue protective cytokine of the invention.

FIG. 6 is a chart demonstrating the core body temperature for Sprague Dawley rats treated with saline or a tissue protective cytokine after lippopolysaccharide (LPS) induced sepsis for a period of 24 hours.

FIGS 7 (a) and (b) are charts demonstrating the levels of IL-6 (Fig. 7a) or TNF (Fig 7b) in the serum of Sprague Dawley rats treated with saline or a tissue protective cytokine after LPS induced sepsis.

FIGS 8(a) and (b) are charts demonstrating the core body temperature of Sprague Dawley rats treated with a tissue protective cytokine peripherally (Fig. 8a) or centrally (Fig. 8b) after LPS induced sepsis.

FIG 9 is a graphic representation of the percentage of lesion healed in Sprague  
5 Dawley rats thirty-four (34) days after being subjected to an ischemic skin flap test and subsequently treated with saline or a tissue protective cytokine.

### **DETAILED DESCRIPTION OF THE INVENTION**

10 The present invention is directed to novel compositions for the treatment, prevention, delay, or reduction of the effects of proinflammatory cytokines, such as TNF, in conditions including, but not limited to, sepsis and sepsis-related conditions, adhesions, wound healing, and chronic disease. The effects of the proinflammatory cytokines addressed by the tissue protective cytokines include, but are not limited to, fever, wasting, lethargy, anemia, edema,  
15 ischemia, organ failure and insulin resistance. The compositions of the invention are also contemplated for the treatment, prevention, delay, or reduction of the effects of inflammatory conditions in one or more organ(s) or tissue(s) resulting from infection, such as in the case of meningitis. In particular, the present invention is directed to compositions including tissue protective cytokines that are successful in the treatment of the effects of proinflammatory  
20 cytokines in conditions including sepsis, adhesions, wound healing, chronic disease, and inflammatory conditions.

In addition, the compositions of the inventions are useful in treating, preventing, and/or reducing the appearance of scarring from injury. For example, when a tissue protective cytokine of the present invention is used in conjunction with abdominal surgery,  
25 scarring may be substantially reduced. In one embodiment, the tissue protective cytokines of the present invention are used to prevent scarring from surgical incisions.

### **Compositions of the Invention**

Any cytokine that exhibits tissue protective capability is contemplated for use with the  
30 present invention. The compositions of the invention may include erythropoietin. For example, a suitable tissue protective cytokine of the invention may be an EPO molecule, which may exist in a number of forms, e.g.  $\alpha$ ,  $\beta$ , asialo and others. The  $\alpha$  and  $\beta$  forms have the same potency, biological activity, and molecular weight, but differ slightly in the



carbohydrate components, while the asialo form is an  $\alpha$  or  $\beta$  form with the terminal sialic acids removed from the carbohydrate components.

Also, any tissue protective cytokine capable of treating, preventing, delaying the onset of, and/or reducing the effect of sepsis, sepsis-related conditions, and general inflammatory conditions is contemplated as well. As used herein, the term "tissue protective cytokines" refer to any cytokine that is a derivative of erythropoietin that possesses the tissue protective activity of erythropoietin. Preferably the tissue protective cytokine lacks at least one or more of erythropoietin's erythropoietic effects. Most preferably, the tissue protective cytokine lacks all of the erythropoietic effects of erythropoietin. For example, this may be accomplished by modifying erythropoietin through chemical or mutational processes that affect its pharmacological attributes (reduction in half-life) or structural ability to bind to the erythropoietin receptor homodimer. Non-limiting examples of suitable tissue protective cytokines for use with the present invention include the tissue protective cytokines disclosed in International Publication No. WO/02053580 and U.S. Patent Publication Nos. 2002/0086816 and 2003/0072737, which are incorporated by reference herein in their entirety.

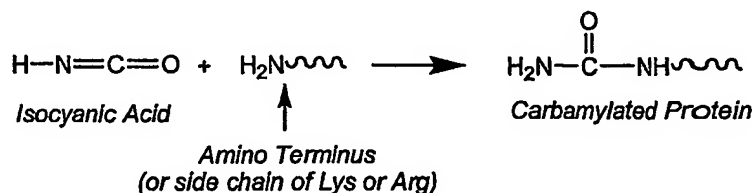
In addition, the tissue protective cytokines for use with the present invention may include EPO molecules with a modification of at least one arginine, lysine, tyrosine, tryptophan, or cysteine residue or carboxyl groups are also contemplated for use as tissue protective cytokines according to the present invention. These residues may be chemically modified by guanidination, amidination, carbamylation, trinitrophenylation, acylation (acetylation or succinylation), nitration, or mixtures thereof, as disclosed in International Publication No. WO/02053580.

Thus, the tissue protective cytokine of the present invention may be carbamylated EPO. As discussed in the background of the invention, rhu-EPO has been researched in connection with treatment of acute renal failure, which is a possible complication of septicemia. However, because rhu-EPO has erythropoietic activity, *i.e.*, the ability to maintain hematocrit levels in the body and hyperactivation of platelets, red blood cells are increased and platelets become hyperactive upon administration thereof resulting in the blood thickening and an increased risk of thrombosis. Thus, the use of rhu-EPO would likely exacerbate the widespread clotting that occurs as a result of sepsis.

Unlike rhu-EPO and selected other modified EPO molecules, carbamylated EPO does not retain erythropoietic activity and fails to bind with the classic homodimer erythropoietin receptor as is noted in PCT application no. PCT/US04/013099, filed April 26, 2004, hereby

incorporated in its entirety. Carbamylated EPO, however, does advantageously maintain the tissue protective functionality of endogenous EPO. It is believed that the retained tissue protective function of carbamylated EPO is mediated through its interaction with a tissue protective receptor complex as disclosed in PCT application no. PCT/US04/013099. Thus, carbamylated EPO may be used to treat, prevent, delay the onset, and/or reduce the effects of pro-inflammatory cytokines such as TNF within conditions including, but not limited to, sepsis, adhesions, wound healing, chronic diseases and general inflammatory conditions without posing the risk of further clotting associated with the administration of erythropoietin. In addition, because the carbamylated EPO molecules of the present invention are effective in protecting against necrosis, the carbamylated EPO molecules of the present invention are particularly beneficial in treating, preventing, delaying the onset, and/or reducing the effects of sepsis, adhesions, and general inflammatory conditions in patients susceptible to stroke, myocardial infarction, deterioration of mental faculties, and age-related conditions.

Therefore, the tissue protective cytokine of the invention may be a modified EPO with alteration of at least one or more lysine residues or the N-terminal group of the EPO molecule, which for purposes of this application, may also be referred to as "sites". The modifications may result from the reaction of the lysine residue or N-terminal amino group with an amino-group modifying agent. For example, the generic reaction scheme below is representative of one method to carbamylate proteins, such as EPO:



In another embodiment, one or more lysine residues on an EPO molecule may be carbamylated by virtue of reaction with a cyanate ion. For example, one or more lysine residues may be modified by incubation with 4-sulfohenylisothiocyanate. In yet another embodiment, one or more lysine residues on the EPO molecule are alkyl-carbamylated, aryl-carbamylated, or aryl-thiocarbamylated with an alkyl isocyanate, an aryl isocyanate, or an aryl-thioisocyanate, respectively. In still another embodiment, one or more lysine residues are alkylated by a reactive alkylcarboxylic or arylcarboxylic acid derivative, e.g., acetic

anhydride, succinic anhydride, or phthalic anhydride. The modified lysine residue may also be chemically reduced.

One or more lysine residues may also be carbamylated by reacting the residue(s) with trinitrobenzenesulfonic acid, or a salt thereof. In yet another embodiment, one or more lysine  
5 residues may be modified by reaction with a glyoxal or a glyoxal derivative, *e.g.*, methylglyoxal or 3-deoxyglucosone, to form the corresponding alpha-carboxyalkyl derivatives.

Other methods of carbamylation may be used in accordance with the present invention. For example, the method disclosed in Plapp *et al.*, J. BIOL. CHEM., 246: 939-945  
10 (1971) is a suitable way of making the carbamylated EPO according to the present invention. Another example of a method of carbamylation is discussed in Satake *et al.*, 1990, *Biochim. Biophys. Acta* 1038:125-9, where six of the lysine residues in erythropoietin were carbamylated.

And, as mentioned above, any of the forms of EPO may be used according to the  
15 present invention. Thus, as an example: in one embodiment, the EPO molecule subject to carbamylation is in  $\alpha$  form; in another embodiment, the EPO molecule subject to carbamylation is in  $\beta$  form; and in yet another embodiment, the EPO molecule subject to carbamylation is asialic.

The carbamylation process preferably occurs for a period of time sufficient to  
20 substantively reduce or completely eliminate erythropoietic activity. In one embodiment, the carbamylation process is performed for a sufficient time period to remove at least about 90 percent of the sites. In another embodiment, the carbamylation process is performed for a sufficient time period to remove at least about 95 percent of the sites. In still another embodiment, the carbamylation process is performed for a sufficient time period to remove  
25 100 percent of the sites. Alternatively, this may be viewed as carbamylating erythropoietin for a period of time sufficient to carbamylate at least six lysine residues in one embodiment, at least seven lysines in another embodiment, and at least eight lysine residues in another embodiment. The time required for sufficient carbamylation to occur may vary. For instance, sufficient carbamylation may occur over a period up to about 6 to 24 hours, up to  
30 about 10 to 20 hours, or up to about 16 hours.

\* The tissue protective cytokines for use with the present invention may also be obtained by limited proteolysis, removal of amino groups, and/or mutational substitution of arginine, lysine, tyrosine, tryptophan, or cysteine residues by molecular biological techniques as disclosed in Satake *et al.*, 1990, *Biochim. Biophys. Acta* 1038:125-9, which is incorporated

by reference herein in its entirety. For example, suitable tissue protective cytokines include at least one or more mutated EPOs having a site mutation at C7S, R10I, V11S, L12A, E13A, R14A, R14B, R14E, R14Q, Y15A, Y15F, Y15I, K20A, K20E, E21A, C29S, C29Y, C33S, C33Y, P42N, T44I, K45A, K45D, V46A, N47A, F48A, F48I, Y49A, Y49S, W51F, W51N, Q59N, E62T, L67S, L70A, D96R, K97D, S100R, S100E, S100A, S100T, G101A, G101I, L102A, R103A, S104A, S104I, L105A, T106A, T106I, T107A, T107L, L108K, L108A, S126A, F142I, R143A, S146A, N147K, N147A, F148Y, L149A, R150A, G151A, K152A, L153A, L155A, C160S, I6A, C7A, B13A, N24K, A30N, H32T, N38K, N83K, P42A, D43A, K52A, K97A, K116A, T132A, I133A, T134A, K140A, P148A, R150B, G151A, K152W, K154A, G158A, C161A, and/or R162A. Examples of the above-referenced modifications are described in co-pending U.S. Patent Publication Nos. 2003/0104988, 2002/0086816 and 2003/0072737, which are incorporated by reference herein in their entirety. In the mutein nomenclature used herein, the changed amino acid is depicted with the native amino acid's one letter code first, followed by its position in the EPO molecule, followed by the replacement amino acid one letter code. For example, S100E refers to a human EPO molecule in which, at amino acid 100, the serine has been changed to a glutamic acid.

In another embodiment, the tissue protective cytokine may include one or more of the above site mutations, providing that the site mutations do not include I6A, C7A, K20A, P42A, D43A, K45D, K45A, F48A, Y49A, K52A, K49A, S100B, R103A, K116A, T132A, I133A, K140A, N147K, N147A, R150A, R150E, G151A, K152A, K154A, G158A, C161A, or R162A.

In still another embodiment, the tissue protective cytokines may include combinations of site mutations, such as K45D/S100E, K97D/S100E, A30N/H32T, K45D/R150E, R103E/L108S, K140A/K52A, K140A/K52A/K45A, K97A/K152A, K97A/K152A/K45A, K97A/K152A/K45A/K52A, K97A/K152A/K45A/K52A/K140A, K97A/K152A/K45A/K52A/K140A/K154A, N24K/N38K/N83K, and N24K/Y15A. In yet another embodiment, the tissue protective cytokines do not include any of the above combinations. In another embodiment, the tissue protective cytokines may include any of the above-referenced site mutations providing that the site mutations do not include any of the following combinations of substitutions: N24K/N38K/N83K and/or A30N/H32T.

Certain modifications or combinations of modifications may affect the flexibility of the mutein's ability to bind with its receptor, such as an EPO receptor or secondary receptor. Examples of such modifications or combinations of modifications include, but are not limited to, K152W, R14A/Y15A, I6A, C7A, D43A, P42A, F48A, Y49A, T132A, I133A, T134A,

N147A, P148A, R150A, G151A, G158A, C161A, and R162A. Corresponding mutations are known to those of ordinary skill in the art to be detrimental in human growth hormone. Thus, in one embodiment, the tissue protective cytokine does not include one or more of the modifications or combinations of modifications that may affect the flexibility of the mutein's ability to bind with its receptor. Further discussion of such tissue protective cytokines is included in co-pending U.S. Patent Application No. 10/612,665, attorney docket no. 10165-022-999, filed July 1, 2003, entitled "Recombinant Tissue Protective Cytokines and Encoding Nucleic Acids Thereof for Protection, Restoration, and Enhancement of Responsive Cells, Tissues, and Organs," the entire disclosure of which is incorporated by reference herein

Moreover, suitable tissue protective cytokines for use with the present invention includes the long acting chemically modified EPO molecules disclosed in International Application No. US03/028073, filed under attorney docket no. 20528.0006 on September 9, 2003, entitled "Long Acting Erythropoietins that Maintain Tissue Protective Activity of Endogeneous Erythropoietin", which is incorporated in its entirety by reference herein. For example, suitable tissue protective cytokines for use with the present invention includes EPO that has undergone at least one chemical modification to at least one of the N-linked oligosaccharide chains or the O-linked oligosaccharide chain, wherein the chemical modification includes oxidation, sulfation, phosphorylation, PEGylation, or a combination thereof. In one embodiment, the EPO molecule subject to chemical modification is in  $\alpha$  form. In another embodiment, the EPO molecule subject to chemical modification is in  $\beta$  form. In yet another embodiment, the EPO molecule subject to chemical modification is asialic. In yet another embodiment, the EPO molecule subject to chemical modification may be ARANESP (Amgen, Thousand Oaks, CA) or CERA (Hoffmann-La Roche Inc., Nutley, NJ).

A variety of host-expression vector systems may be utilized to produce the tissue protective cytokines of the present invention. For example, when the tissue protective cytokine is based on an EPO molecule, various host-expression systems may be used. Such host-expression systems represent vehicles by which EPO may be produced and subsequently purified, but also represent cells that may, when transformed or transfected with the appropriate nucleotide coding sequences, exhibit the modified erythropoietin gene product *in situ*. These include but are not limited to, bacteria, insect, plant, mammalian, including human host systems, such as, but not limited to, insect cell systems infected with recombinant virus expression vectors (e.g., baculovirus) containing EPO coding sequences; plant cell systems infected with recombinant virus expression vectors (e.g., cauliflower mosaic virus,

CaMV; tobacco mosaic virus, TMV) or transformed with recombinant plasmid expression vectors (*e.g.*, Ti plasmid) containing erythropoietin-related molecule coding sequences; or mammalian cell systems, including human cell systems, *e.g.*, HT1080, COS, CHO, BHK, 293, 3T3, harboring recombinant expression constructs containing promoters derived from the genome of mammalian cells, *e.g.*, metallothionein promoter, or from mammalian viruses, *e.g.*, the adenovirus late promoter; the vaccinia virus 7.5K promoter.

In addition, a host cell strain may be chosen that modulates the expression of the inserted sequences, or modifies and processes the gene product in the specific fashion desired. Such modifications and processing of protein products may be important for the function of the protein. As known to those of ordinary skill in the art, different host cells have specific mechanisms for the post-translational processing and modification of proteins and gene products. Appropriate cell lines or host systems can be chosen to ensure the correct modification and processing of the foreign protein expressed. To this end, eukaryotic host cells that possess the cellular machinery for proper processing of the primary transcript, glycosylation, and phosphorylation of the gene product may be used. Such mammalian host cells, including human host cells, include but are not limited to HT1080, CHO, VERO, BHK, HeLa, COS, MDCK, 293, 3T3, and WI38.

For long-term, high-yield production of recombinant proteins, stable expression is preferred. For example, cell lines that stably express the recombinant tissue protective cytokine-related molecule gene product may be engineered. Rather than using expression vectors that contain viral origins of replication, host cells can be transformed with DNA controlled by appropriate expression control elements, *e.g.*, promoter, enhancer, sequences, transcription terminators, polyadenylation sites, and the like, and a selectable marker. Following the introduction of the foreign DNA, engineered cells may be allowed to grow for 1-2 days in an enriched media, and then are switched to a selective media. The selectable marker in the recombinant plasmid confers resistance to the selection and allows cells to stably integrate the plasmid into their chromosomes and grow to form foci that in turn can be cloned and expanded into cell lines. This method may advantageously be used to engineer cell lines that express the EPO mutein-related molecule gene product. Such engineered cell lines may be particularly useful in screening and evaluation of compounds that affect the functionality of the EPO-related molecule gene product.

Alternatively, the expression characteristic of an endogenous EPO mutein gene within a cell line or microorganism may be modified by inserting a heterologous DNA regulatory element into the genome of a stable cell line or cloned microorganism such that the inserted

regulatory element is operatively linked with the endogenous erythropoietin mutein gene. For example, an endogenous EPO mutein gene that is normally "transcriptionally silent", *i.e.*, an EPO gene that is normally not expressed, or is expressed only at very low levels in a cell line, may be activated by inserting a regulatory element that is capable of promoting the expression of an expressed gene product in that cell line or microorganism. Alternatively, a transcriptionally silent, endogenous EPO gene may be activated by insertion of a promiscuous regulatory element that works across cell types.

A heterologous regulatory element may be inserted into a stable cell line or cloned microorganism, such it is operatively linked with an endogenous erythropoietin gene, using techniques, such as targeted homologous recombination, which are well known to those of skill in the art, and also described French Patent No. 2646438, U.S. Patent Nos. 4,215,051 and 5,578,461, and International Publication Nos. WO93/09222 and WO91/06667, the entire disclosures of which are incorporated by reference herein.

#### **Pharmaceutical Compositions**

The present invention also relates to pharmaceutical compositions including the tissue protective cytokines of the present invention. Because the tissue protective cytokines of the present invention advantageously have the ability to ameliorate the effects of proinflammatory cytokines, such as TNF, as well as the ability to protect tissues from cell death, the cytokines are contemplated for the treatment of sepsis, adhesions, wounds, chronic disease and inflammatory conditions in individuals also at risk for various tissue injuries, such as stroke and myocardial infarction.

In addition, the tissue protective cytokines of the present invention are contemplated for treatment of sepsis, adhesions, wounds and general inflammatory conditions in individuals also experiencing deterioration of mental faculties, such as Alzheimer's, Parkinson's and the like.

The pharmaceutical compositions of the invention contain a therapeutically effective amount of the tissue protective cytokine of the present invention, preferably in purified form. As used herein, the term "therapeutically effective amount" means an amount of tissue protective cytokine that is nontoxic but sufficient to provide the desired effect and performance at a reasonable benefit / risk ratio attending any medical treatment.

The formulation should suit the mode of administration. In other words, the pharmaceutical compositions of the invention include an amount of the tissue protective cytokine(s) of the invention such that the targeted effects of proinflammatory cytokines, *i.e.*,



fever, wasting, lethargy, anemia, edema, ischemia, organ failure, and insulin resistance, or conditions related to proinflammatory cytokines, *i.e.*, sepsis, adhesions, wound healing, chronic disease or an inflammatory condition, is treatable provided the proper dose and strategy is employed. And, as discussed in more detail below, the pharmaceutical

5 composition should be delivered in a non-toxic dosage amount.

In one embodiment, a chemically modified or mutated erythropoietin is included in the pharmaceutical composition of the invention. In another embodiment the chemically modified erythropoietin is a carbamylated EPO. The carbamylated EPO may be an EPO molecule with at least one or more modified lysine residues or a modified N-terminal group.

10 In another embodiment, the mutated erythropoietin may be S100E. In addition, the present invention contemplates the use of a mixture of tissue protective cytokines produced by any of the methods of the present invention described above in the pharmaceutical compositions of the invention. For example, the pharmaceutical composition of the invention may include at least one carbamylated EPO that is a result of modifying one or more lysine residues and at  
15 least one mutated EPO that is the result of modifying an amino group within erythropoietin, such as S100E.

The pharmaceutical compositions of the invention may include a therapeutically effective amount of the tissue protective cytokine and a suitable amount of a pharmaceutically acceptable carrier so as to provide the form for proper administration to the  
20 patient. In a specific embodiment, the term "pharmaceutically acceptable" means approved by a regulatory agency of the Federal or a state government or listed in the U.S. Pharmacopeia or other generally recognized foreign pharmacopeia for use in animals, and more particularly in humans. The term "carrier" refers to a diluent, adjuvant, excipient, or vehicle with which the therapeutic is administered.

25 Such pharmaceutical carriers can be sterile liquids, such as saline solutions in water and oils, including those of petroleum, animal, vegetable or synthetic origin, such as peanut oil, soybean oil, mineral oil, sesame oil and the like. A saline solution is a preferred carrier when the pharmaceutical composition is administered intravenously. Saline solutions and aqueous dextrose and glycerol solutions can also be employed as liquid carriers, particularly  
30 for injectable solutions. Suitable pharmaceutical excipients include starch, glucose, lactose, sucrose, gelatin, malt, rice, flour, chalk, silica gel, sodium stearate, glycerol monostearate, talc, sodium chloride, dried skim milk, glycerol, propylene, glycol, water, ethanol and the like.

The pharmaceutical compositions of the invention may also contain minor amounts of wetting or emulsifying agents, or pH buffering agents. These compositions can take the form of solutions, suspensions, emulsion, tablets, pills, capsules, powders, sustained-release formulations and the like.

5       The compounds of the invention can be formulated as neutral or salt forms. Pharmaceutically acceptable salts include those formed with free amino groups such as those derived from hydrochloric, phosphoric, acetic, oxalic, tartaric acids, etc., and those formed with free carboxyl groups such as those derived from sodium, potassium, ammonium, calcium, ferric hydroxides, isopropylamine, triethylamine, 2-ethylamino ethanol, histidine, procaine, etc.

#### Treatment and Administration Methods

The aforementioned tissue protective cytokines and pharmaceutical compositions including the tissue protective cytokines are intended for the therapeutic or prophylactic treatment, prevention, delay, and reduction of the effects of proinflammatory cytokines, such as TNF. These effects include fever, wasting, lethargy, anemia, edema, ischemia, organ failure and insulin resistance. For example, as demonstrated below in Example 4, the tissue protective cytokines of the present invention reduced the fever, elevation of the body's core temperature above the body's normal core temperature, associated with the release of proinflammatory cytokines. As is demonstrated in Figure 6, the administration of a tissue protective cytokine, carbamylated erythropoietin, resulted in a greater than 50% reduction in the fever experienced as a result of subjecting a rat to LPS. The tissue protective cytokines may be administered to treat, prevent, delay or reduce conditions related to proinflammatory cytokines such as sepsis and sepsis-related conditions such as adhesions.

15       In addition, the tissue protective cytokines of the present invention are also contemplated for the treatment and prevention of inflammatory conditions in one or more organ(s) or tissue(s). The organs include, but are not limited to, the airways and lung, the kidney and urinary tract system, and the prostate. As used herein, the term "inflammatory condition" refers to a condition in which mechanisms such as the reaction of specific T lymphocytes or antibody with antigen causes the recruitment of inflammatory cells and endogenous mediator chemicals. In some cases, the normal function of the organ or tissue will be altered by an increase in vascular permeability and/or by contraction of visceral smooth muscle.

Thus, the tissue protective cytokines of the present invention may be used to treat and/or prevent inflammatory conditions wherein the normal function of the organ(s) or tissue(s) is altered. These conditions may include ischemia-related conditions, as well as non-ischemia-related conditions, such as allergy, rheumatic diseases, and infection including viral, fungal, and bacterial infection. Furthermore, the injury or infection may be acute or chronic. In one embodiment, the tissue protective cytokines of the invention are contemplated for use in treating and/or preventing inflammatory conditions under non-ischemia conditions, *i.e.*, conditions where there is a substantially normal blood supply to the organ(s) and/or tissue(s) in question.

Furthermore, the tissue protective cytokines of the present invention may be used to enhance the healing of wounds. This may be accomplished by reducing the time needed to heal, reducing the appearance of or completely eliminate scarring, reducing the risk of complications, or otherwise improving the quality of healing. For example, scarring from an incision may be dramatically reduced, if not completely avoided, when the tissue protective cytokines of the present invention are employed prior to, during, or after the incision occurs. In addition to surgical procedures the tissue protective cytokines of the present invention are useful in addressing wounds resulting from conditions including but not limited to trauma (blunt force and cuts), pressure (bed sores), burns, and diseases, such as diabetes or vascular insufficiencies.

Moreover, the tissue protective cytokines and pharmaceutical compositions of the present invention may be used to address the effects of proinflammatory cytokines, such as TNF. As demonstrated in Figures 7a and 7b, the tissue protective cytokines of the present invention can reduce the upregulation of proinflammatory cytokines, IL-6 and TNF respectively, in response to an injury or infective agent. The tissue protective cytokines of the present invention may be administered in therapeutic doses to treat, prevent, reduce, or eliminate effects of proinflammatory cytokines such as fever, wasting, lethargy, anemia, edema, ischemia, organ failure and insulin resistance. Given that the tissue protective cytokines interfere with the upregulation of proinflammatory cytokines, the tissue protective cytokines of the present invention may be able to restore endogenous functions interrupted by the proinflammatory cytokines without directly affecting those endogenous functions.

Additionally, the tissue protective cytokines of the present invention may be administered in conjunction with other known therapeutic treatments for conditions related to proinflammatory cytokines to provide a synergistic effect. For example, a treatment for the anemia associated with cancer or other chronic diseases may involve the administration of a

typical therapeutic dose of recombinant erythropoietin to restore the patient's hematocrit and a therapeutic dose of the tissue protective cytokines of the present invention to counteract the effects of proinflammatory cytokines. This would permit the use of lower doses of recombinant erythropoietin in such chronic disease thereby greatly reducing the risk of thrombotic events.

The tissue protective cytokines of the present invention may be used for systematic or chronic administration, acute treatment, and/or intermittent administration. In one embodiment, the pharmaceutical compositions of the invention are administered chronically to protect or enhance the target cells, tissue or organ. In another embodiment, the pharmaceutical compositions of the invention may be administered acutely, *i.e.*, for a single treatment during injury. In yet another embodiment, the pharmaceutical compositions of the invention are administered in a cyclic nature.

The compositions of the invention may be administered prior to injury. As such, the tissue protective cytokines of the present invention may be administered prior to a surgical procedure to prevent sepsis, delay the onset of sepsis, and/or reduce complications from sepsis. For example, the tissue protective cytokines of the present invention may be given to a patient prior to abdominal surgery. And, as briefly mentioned above, administering the tissue protective cytokines of the present invention prior to surgery may not only have an effect with regard to sepsis, adhesions, and general inflammatory conditions, but they may also reduce the appearance of, or completely eliminate scarring from the surgery.

In addition, the compositions of the invention may be administered at the time of injury or shortly thereafter. Thus, a patient undergoing major abdominal surgery may be given the tissue protective cytokines of the present invention at the time of, or shortly thereafter, the surgical procedure in order to prevent, delay the onset of, or reduce complications stemming from sepsis, adhesions, or general inflammatory conditions. The tissue protective cytokines of the present invention may also reduce the appearance of, or completely eliminate scarring from the surgery if administered during or after injury.

For example, the tissue protective cytokines of the present invention may be used for irrigation purposes, *e.g.*, while cleaning the wound, a saline solution including the tissue protective cytokine of the present invention may be administered to treat, prevent, delay the onset of, or reduce complications stemming from sepsis, adhesions, or general inflammatory conditions. Furthermore, the tissue protective cytokines of the present invention may be given to a pregnant woman following a cesarean section in order to prevent, delay the onset of, and/or reduce complications from sepsis, adhesions, and/or general inflammatory

conditions. As another example, the tissue protective cytokines of the present invention may be given to a patient during chemotherapy to stave off sepsis, adhesions, or general inflammatory conditions.

In one embodiment, the tissue protective cytokines of the present invention are administered intravenously at the time of injury and subcutaneously for a predetermined period of time thereafter in order to prevent, delay the onset of, or reduce complications stemming from sepsis, adhesions, or general inflammatory conditions. For example, the compositions of the invention may be administered in an amount of about 10  $\mu\text{g}/\text{kg}$  intravenously at the time of injury followed by 10  $\mu\text{g}/\text{kg}$  subcutaneously for an allotted time.

In cases of a positive sepsis diagnosis, the compositions of the invention may be administered daily to treat sepsis, stabilize the patient, and prevent the sepsis condition from progressing to a more serious stage, *e.g.*, severe sepsis or septic shock. In addition, the tissue protective cytokines of the present invention may be administered with known antibiotics, anti-fungals, anti-virals, and the like, including those listed within International Publication No. WO 2004/004656, hereby incorporated by reference in its entirety.

The administration of the composition may be parenteral, *i.e.*, by a method other than the via the digestive tract. For example, parenteral administration may include intravenous injection, intraperitoneal injection, intra-arterial, intramuscular, intradermal, or subcutaneous administration. The composition may also be administered via inhalation or transmucosally, *e.g.*, orally, nasally, rectally, intravaginally, sublingually, submucosally, and transdermally. In addition, the tissue protective cytokines of the present invention may be administered locally to the area in need of treatment, such as by the use of a perfusate; topical application, *e.g.*, in conjunction with a wound dressing after surgery; by injection; by means of a catheter; by means of a suppository; or by means of an implant, said implant being of a porous, non-porous, or gelatinous material, including membranes, such as silastic membranes, or fibers. Combinations of the administration methods discussed above are contemplated by the present invention.

In one embodiment, the administration of the pharmaceutical composition of the invention is parenteral. Such administration may be performed in a dose amount of about 0.01 pg to about 5 mg, preferably about 1 pg to about 5 mg. In one embodiment, the dose amount is about 500 pg to about 5 mg. In another embodiment, the dose amount is about 1 ng to about 5 mg. In yet another embodiment, the dose amount is about 500 ng to about 5 mg. In still another embodiment, the dose amount is about 1  $\mu\text{g}$  to about 5 mg. For example, the dose amount may be about 500  $\mu\text{g}$  to about 5 mg. In another embodiment, the dose

amount may be about 1 mg to about 5 mg. Such compositions may include aqueous and non-aqueous sterile injectable solutions or suspensions, which may contain antioxidants, buffers, bacteriostats and solutes that render the compositions substantially isotonic with the blood of an intended recipient. In this aspect of the invention, the pharmaceutical compositions may  
5 also include water, alcohols, polyols, glycerine, vegetable oils, and mixtures thereof.

Pharmaceutical compositions adapted for parenteral administration may be presented in unit-dose or multi-dose containers, for example sealed ampules and vials, and may be stored in a lyophilized (freeze-dried) condition requiring only the addition of a sterile liquid carrier, *e.g.*, sterile saline solution for injections, immediately prior to use. Extemporaneous  
10 injection solutions and suspensions may be prepared from sterile powders, granules and tablets. In one embodiment, an autoinjector comprising an injectable solution of a long acting EPO of the invention may be provided for emergency use by ambulances, emergency rooms, and battlefield situations.

#### 15 Intravenous Administration

In one embodiment, the pharmaceutical composition of the invention is formulated in accordance with routine procedures as a pharmaceutical composition adapted for intravenous administration to human beings. For example, the pharmaceutical composition may be in the form of a solution in sterile isotonic aqueous buffer. Where necessary, the pharmaceutical  
20 composition may also include a solubilizing agent and/or a local anesthetic such as lidocaine to ease pain at the site of the injection. The ingredients may be supplied either separately or mixed together in unit dosage form, for example, as a dry lyophilized powder or water-free concentrate in a hermetically-sealed container such as an ampule or sachette indicating the quantity of active agent. When the pharmaceutical compositions of the invention are to be  
25 administered by infusion, an infusion bottle with sterile pharmaceutical grade water or saline may be used for dispensing the composition. And, when the pharmaceutical composition are to be administered by injection, an ampule of sterile saline may be provided to mix the ingredients may be mixed prior to administration.

#### 30 Oral Administration

One of ordinary skill in the art will recognize the pharmaceutical compositions of the present invention may be adapted for oral administration as capsules or tablets; powders or granules; solutions, syrups or suspensions (in aqueous or non-aqueous liquids); edible foams or whips; emulsions; or combinations thereof. The oral formulation may include about 10  
35

percent to about 95 percent by weight active ingredient. In one embodiment, the active ingredient is included in the oral formulation in an amount of about 20 percent to about 80 percent by weight. In still another embodiment, the oral formulation includes about 25 percent to about 75 percent by weight of the active ingredient.

5        Tablets or hard gelatine capsules may include lactose, starch or derivatives thereof, magnesium stearate, sodium saccharine, cellulose, magnesium carbonate, stearic acid or salts thereof. Soft gelatine capsules may include vegetable oils, waxes, fats, semi-solid, liquid polyols, or mixtures thereof. Solutions and syrups may include water, polyols, sugars, or mixtures thereof.

10        Moreover, an active agent intended for oral administration may be coated with or admixed with a material that delays disintegration and/or absorption of the active agent in the gastrointestinal tract. For example, the active agent may admixed or coated with glyceryl monostearate, glyceryl distearate, or a combination thereof. Thus, the sustained release of an active agent may be achieved over many hours and, if necessary, the active agent can be  
15        protected from being degraded within the stomach. Pharmaceutical compositions for oral administration may also be formulated to facilitate release of an active agent at a particular gastrointestinal location due to specific pH or enzymatic conditions.

#### Transdermal Administration

20        Pharmaceutical compositions adapted for transdermal administration may be provided as discrete patches intended to remain in intimate contact with the epidermis of the recipient for a prolonged period of time. In addition, pharmaceutical compositions adapted for topical administration may be provided as ointments, creams, suspensions, lotions, powders, solutions, pastes, gels, sprays, aerosols, oils, eye drops, lozenges, pastilles, and mouthwashes  
25        and combinations thereof. When the topical administration is intended for the skin, mouth, eye, or other external tissues, a topical ointment or cream is preferably used. And, when formulated in an ointment, the active ingredient, i.e., the long acting EPO, may be employed with either a paraffinic or a water-miscible ointment base. Alternatively, the active ingredient may be formulated in a cream with an oil-in-water base or a water-in-oil base.  
30        When the topical administration is in the form of eye drops, the pharmaceutical compositions of the invention preferably include the active ingredient, which is dissolved or suspended in a suitable carrier, e.g., in an aqueous solvent.

#### Nasal and Pulmonary Administration



Pharmaceutical compositions adapted for nasal and pulmonary administration may include solid carriers such as powders (preferably having a particle size of about 20 microns to about 500 microns). Powders may be administered by rapid inhalation through the nose from a container of powder held close to the nose. In an alternate embodiment,

5 pharmaceutical compositions intended for nasal administration according to the present invention may include liquid carriers, e.g., nasal sprays or nasal drops. Preferably, the pharmaceutical compositions of the invention are administered into the nasal cavity directly.

Direct lung inhalation may be accomplished by deep inhalation through a mouthpiece into the oropharynx and other specially adapted devices including, but not limited to, 0 pressurized aerosols, nebulizers or insufflators, which can be constructed so as to provide predetermined dosages of the active ingredient. Pharmaceutical compositions intended for lung inhalation may include aqueous or oil solutions of the active ingredient. Preferably, the pharmaceutical compositions of the invention are administered via deep inhalation directly into the oropharynx.

#### Rectal and Vaginal Administration

Pharmaceutical compositions adapted for rectal administration may be provided as suppositories or enemas. In one embodiment, the suppositories of the invention includes about 0.5 percent to 10 percent by weight of active ingredient. In another embodiment, the 0 suppository includes about 1 percent to about 8 percent by weight active ingredient. In still another embodiment, the active ingredient is present in the suppository in an amount of about 2 percent to about 6 percent by weight. In this aspect of the invention, the pharmaceutical compositions of the invention may include traditional binders and carrier, such as triglycerides.

5 Pharmaceutical compositions adapted for vaginal administration may be provided as pessaries, tampons, creams, gels, pastes, foams or spray formulations.

#### Perfusion Administration

The pharmaceutical compositions of the invention may also be administered by use of 0 a perfusate, i.e., pumping a liquid into an organ or tissue (especially by way of blood vessels). In such embodiments, the pharmaceutical composition preferably has about 0.01 pM to about 30 pM, preferably about 15 pM to about 30 nM, of the tissue protective cytokine of the present invention. In one embodiment, the perfusion solution is the University of Wisconsin (UW) solution (with a pH of about 7.4 to about 7.5 and an osmolality of about 320 mOSm/l),

which contains about 1 U(10ng)/ml to about 25 U(250ng)/ml of an EPO compound of the present invention; 5 percent hydroxyethyl starch (preferably having a molecular weight from about 200,000 to about 300,000 and substantially free of ethylene glycol, ethylene chlorohydrin, sodium chloride, and acetone), 25 mM  $\text{KH}_2\text{PO}_4$ , 3 mM glutathione; 5 mM adenosine; 10 mM glucose; 10 mM HEPES buffer; 5 mM magnesium gluconate; 1.5mM  $\text{CaCl}_2$ ; 105 mM sodium gluconate; 200,000 units penicillin; 40 units insulin; 16 mg dexamethasone; and 12 mg phenol red. The UW solution is discussed in detail in U.S. Patent No. 4,798,824, which is incorporated in its entirety by reference herein.

#### 10 Local Administration

It may be desirable to administer the pharmaceutical compositions of the invention locally to the area in need of treatment. Such administration may be achieved by local infusion during surgery; topical application, *e.g.*, in conjunction with a wound dressing after surgery; by injection; by means of a catheter; by means of a suppository; or by means of an implant, said implant being of a porous, non-porous, or gelatinous material, including  
15 membranes, such as silastic membranes, or fibers.

#### Controlled-Release Systems

In addition, as briefly discussed above with respect to transdermal administration, the tissue protective cytokines of the present invention may be delivered in a controlled-release system. For example, the tissue protective cytokine may be administered using intravenous infusion, an implantable osmotic pump, a transdermal patch, liposomes, or other modes of administration. Such controlled release systems may be placed in proximity of the therapeutic target, *i.e.*, the target cells, tissue or organ, thus requiring only a fraction of the  
15 systemic dose.

#### Dosing

Selection of the preferred effective and non-toxic dose for the administration methods above will be determined by a skilled artisan based upon factors known to one of ordinary skill in the art. Examples of these factors include the particular form of tissue protective cytokine; the pharmacokinetic parameters of the tissue protective cytokine, such as bioavailability, metabolism, half-life, etc. (provided to the skilled artisan); the condition to be treated; the benefit to be achieved in a normal individual; the body mass of the patient; the method of administration; the frequency of administration, *i.e.*, chronic, acute, intermittent;

concomitant medications; and other factors well known to affect the efficacy of administered pharmaceutical agents. Thus the precise dosage should be decided according to the judgment of the practitioner and the circumstances of the particular patient.

5 Treatment Kits

The invention also provides a pharmaceutical pack or kit that include one or more containers filled with one or more of the ingredients of the pharmaceutical compositions of the invention. In one embodiment, the effective amount of the tissue protective cytokine and a pharmaceutically acceptable carrier may be packaged in a single dose vial or other  
0 container.

When the pharmaceutical composition of the invention is adapted for parenteral administration, for example, the composition may be stored in a lyophilized condition. Thus, the kit may include the lyophilized composition, a sterile liquid carrier, and a syringe for injections.

5 In one embodiment, the kit includes an ampule containing enough lyophilized material for several treatments such that the administrator would weigh out a specific amount of material and add a specific amount of carrier for each treatment session. In another embodiment the kit may contain a plurality of ampules each containing specific amounts of the lyophilized material and a plurality of containers each containing specific amounts of  
0 carrier, such that the administrator need only mix the contents of one ampule and one carrier container for each treatment session without measuring or weighing. In yet another embodiment, the kit contains an autoinjector including an injectable solution of the tissue protective cytokine(s) of the invention. In still another embodiment, the kit contains at least one ampule with the lyophilized composition, at least one container of carrier solution, at  
5 least one container with a local anesthetic, and at least one syringe (or the like). The ampules and containers are preferably hermetically-sealed.

When the pharmaceutical compositions of the invention are to be administered by infusion, the kit preferably includes at least one ampule with the pharmaceutical composition and at least one infusion bottle with sterile pharmaceutical grade water or saline.

0 A kit according to the present invention may also include at least one mouthpiece or specially adapted devices for direct lung inhalation such as pressurized aerosols, nebulizers, or insufflators. In this aspect of the invention, the kit may include the device for direct lung  
10 inhalation, which contains the pharmaceutical composition, or the device and at least one

ampule of aqueous or oil solutions of the tissue protective cytokine(s) of the present invention.

When the tissue protective cytokine(s) of the invention is adapted for oral, transdermal, rectal, vaginal, or nasal, the kit preferably includes at least one ampule containing the active ingredient and at least one administration aid. Examples of administration aids include, but are not limited to, measuring spoons (for oral administration), sterile cleaning pads (for transdermal administration, and nasal aspirators (for nasal administration). Such kits may include a single dose of the tissue protective cytokine (acute treatment) or a plurality of doses (prolonged treatment).

In addition, the kit may be outfitted with one or more types of solutions. For example, the tissue protective cytokines of the invention may be made in an albumin solution and a polysorbate solution. If the kit includes the polysorbate solution, the words "Albumin free" preferably appear on the container labels as well as the kit main panels.

Moreover, the kit may also include a notice in the form prescribed by a governmental agency regulating the manufacture, use or sale of pharmaceuticals or biological products, which notice reflects approval by the agency of manufacture, use or sale for human administration.

#### **Assays to Determine Sepsis / Inflammation Treatability**

The present invention also contemplates assays to determine whether a tissue protective cytokine is able to effectively treat, prevent, delay the onset of, or reduce complications of sepsis, adhesions, and inflammation resulting from infection. Any assay that includes laboratory controlled sepsis induction, adhesion induction, or inflammatory response induction is contemplated for the present invention.

For example, a suitable assay according to the invention may include a blind study where the cecum of Sprague Dawley rats are exposed and ligated just distally to the ileocecal valve to avoid intestinal obstruction. The cecum is then be punctured and squeezed gently to force out a small amount of feces, and then returned to the abdominal cavity. The release of feces into the organ induces infection which, in turn, induces sepsis, adhesions, inflammation, or a combination thereof. The abdomen is then sutured. The rats are preferably separated into groups with at least one group receiving saline and another group receiving the tissue protective cytokine to be tested. At the time of ligation, the various groups of animals are given a predetermined amount of saline or the tissue protective cytokine, preferably intravenously. Subcutaneous administration of the selected treatment, *i.e.*, saline or the

tissue protective cytokine, may be undertaken for a predetermined time following the ligation procedure. In addition, the study may include a group of rats that have been opened, but not subjected to infection.

The animals may then be monitored for adhesions and illness scores. Table 1 provides a method of scoring an animal based on the formation of adhesions.

TABLE 1. CUMULATIVE ADHESION SCORING SCALE		
Points	0	No adhesions
	+ 1	One adhesive band from the omentum to the target organ
	+ 1	One adhesive band from the omentum to the scar
	+ 1	One adhesive band from the omentum to the another place
	+ 1	One adhesive band from adnexa / epididymal fat bodies to the target organ
	+ 1	One adhesive band from adnexa / epididymal fat bodies to scar
	+ 1	One adhesive band from adnexa / epididymal fat bodies to another place
	+ 1	Any adhesive band other than described above (e.g., liver to scar)
	+ 1	Target organ adherent to abdominal wall
	+ 1	Target organ adherent to abdominal scar
	+ 1	Target organ adherent to bowel
	+ 1	Target organ adherent to liver or spleen
	+ 1	Any other organ adherent
Total Score		

One point is given for each adhesion and a cumulative adhesion score is calculated.

In one embodiment, the cumulative adhesion score is preferably 8 or less. In another embodiment, the cumulative adhesion score is about 5 or less. In still another embodiment, the cumulative adhesion score is about 3 or less.

An illness score may also be calculated for each animal based on a variety of factors. Factors used for this score include, but are not limited to, behavioral factors such as walking posture, rope hanging ability, investigatory behavior regarding surroundings, climbing foam pad up a wall, body responses such as erectness of hair, and oxygenation, and the number of adhesions formed. For example, when a rat is ill, the animal will hunch while walking and will not investigate his/her surroundings. In addition, the pulse rate of an ill rat is inaccurate, while a healthy rat typically has a pulse rate of about 300 beats/minute. Table 2 provides a method of scoring each animal with regard to illness in order to assess the effectiveness of the tissue protective cytokine being used for treatment

TABLE 2. CUMULATIVE ILLNESS SCORE	
<i>Behavioral Tests</i>	
+ 1	piloerection (hairs stand to erect)
+ 1	immobility
+ 1	Loss of Beam Balance
+ 1	unable to hold or climb
+ 1	Not using claws
+ 1	Becoming hunchbacked
+ 1	Abnormal walking
+ 1	No exploration of surroundings
+ 1	Not grasping a string within 30 seconds
+ 1	reduced reflexes
+ 1	Lack of appetite (food and drink)
+ 1	Loss of body weight
+ 1	moribund
+ 1	Abnormal Heart Rate (< or > 50% normal)
+ 1	Spontaneous Hemorrhage
+ 1	Decreased Oxygen Saturation
Total Score	

On a continuum, a cumulative illness score of 14 or above signifies the death of the animal, while a much lower score indicates that the animal is relatively healthy. In one embodiment, a sepsis-induced animal has an illness score of about 5 or less after 8 days of treatment with at least one tissue protective cytokine of the invention. In another embodiment, an animal has an illness score of about 4 or less after treatment. In yet another embodiment, an animal has an illness score of about 2 or less after treatment. In still another embodiment, an animal has an illness score of about 1 or less after treatment.

## 10 **EXAMPLES**

The following non-limiting examples are merely illustrative of the preferred embodiments of the present invention, and are not to be construed as limiting the invention, the scope of which is defined by the appended claims. Parts are by weight unless otherwise indicated.

### 15 **Example 1: Blind Study Using Rat Abdominal Sepsis Model**

20 The cecum of Sprague Dawley rats was exposed, ligated just distally to the ileocecal valve to avoid intestinal obstruction, punctured twice with a 18-gauge needle, squeezed gently to force out a small amount of feces, and then returned to the abdominal cavity (feces

introduced in peritoneum, which induced infection). The abdomen was closed with 3-0 silk sutures.

The animals were allocated to two groups:

Group 1: Sepsis induced, treated with saline (n = 8). At time of ligation, animals in Group 1 were given 100  $\mu$ l saline intravenously. Daily subcutaneous saline administration (100  $\mu$ l) followed for 8 days or until death.

Group 2: Sepsis induced, treated with carbamylated EPO (n = 8). At time of ligation, animals were given 10  $\mu$ g/kg carbamylated EPO (prepared so that erythropoietic activity is effectively eliminated) intravenously in 100  $\mu$ l of saline. Daily subcutaneous treatment followed for 8 days (or until death) at a dosage amount of 10  $\mu$ g/kg in 100  $\mu$ l saline.

#### Morbidity and Mortality

In Group 1, less than about 50 percent of the animals survived after 8 days. In Group 2, however, the survival rate was greater than about 50 percent, as illustrated graphically in FIG. 1. In particular, one day following the treatment there was about a 60 percent survival rate for animals in Group 1 compared to about a 80 percent survival rate for animals in Group 2. After 3 days, however, the survival rate of Group 1 dropped significantly to about 25 percent survival rate, whereas the survival rate of Group 2 animals was greater than about 60 percent. Thus, the animals receiving the carbamylated EPO of the present invention had a much higher survival rate than animals receiving saline.

#### Cumulative Adhesion Score

Specimens were taken from the peritoneal fluid and abscesses for aerobic and anaerobic culture. For aerobic culture, samples were incubated on blood on EMB agar for 24 hours at 37°C. For anaerobic culture, samples were layered on anaerobic blood agar and incubated in a Gas-Pak jar for 24 hours at 37°C. Growing colonies were identified with standard bacteriologic techniques.

Dead animals were autopsied within 4 hours and the causes of death were recorded. Using Table 1 described earlier in the application, a cumulative adhesion score was calculated for each animal 24 hours post-injury and then averaged for the group (shown graphically in FIG. 2). In particular, the average total score of Group 1 was about 10, whereas the average total score of Group 2 was about 6. In sum, the animals receiving the carbamylated EPO of the present invention had less adhesions than animals receiving saline.



### Illness Score

An illness score was calculated as described earlier in the application in Table 2 and the results are illustrated graphically in FIG. 3. In particular, one day following the treatment, the average illness score of Group 1 animals was about 9 compared to an average  
5 illness score of Group 2 animals of about 3. After 5 days, the Group 1 animals had an average illness score of about 12, whereas the Group 2 animals had an average illness score of about 5 or less.

### Scarring

10 The rats were also visually examined for scarring from the incisions. Group 2 rats had less scarring than Group 1 rats.

### Example 2: Blind Study Using Rat Abdominal Sepsis Model

The cecum of Sprague Dawley rats was exposed, ligated just distally to the ileocecal  
15 valve to avoid intestinal obstruction, punctured twice with a 18-gauge needle, squeezed gently to force out a small amount of feces, and then returned to the abdominal cavity (feces introduced in peritoneum, which induced infection). The abdomen was closed with 3-0 silk sutures.

The animals were allocated to three groups:

20 Group 1: Opened as described above, but no sepsis induced (n = 6).

Group 2: Sepsis induced, treated with saline (n = 8). At time of ligation, animals in Group 2 were given 100  $\mu$ l saline intravenously. Daily subcutaneous saline administration (100  $\mu$ l) followed for 8 days (or until death).

Group 3: Sepsis induced, treated with carbamylated EPO (n = 8). At time of ligation,  
25 animals were given 10  $\mu$ g/kg carbamylated EPO in 100  $\mu$ l saline intravenously. Daily subcutaneous treatment followed for 8 days (or until death) at a dosage amount of 10  $\mu$ g/kg in 100  $\mu$ l saline.

### Cumulative Adhesion Score

30 Specimens were taken from the peritoneal fluid and abscesses for aerobic and  
anaerobic culture. For aerobic culture, samples were incubated on blood on EMB agar for 24 hours at 37°C. For anaerobic culture, samples were layered on anaerobic blood agar and incubated in a Gas-Pak jar for 24 hours at 37°C. Growing colonies were identified with standard bacteriologic techniques.

Dead animals were autopsied within 4 hours and the causes of death were recorded. Using Table 1 described earlier in the application, a cumulative adhesion score was calculated for each animal 24 hours post-injury and then averaged for the group (shown graphically in FIG. 4). In particular, the average total score of Groups 1, 2, and 3 were less than about 2, about 10 and about 6, respectively. Thus, the animals receiving the carbamylated EPO of the present invention had less adhesions than animals receiving saline.

#### Tumor Necrosis Factor Study

The level of tumor necrosis factor (TNF) present in the blood of animals after a period of time was examined using an ELISA from R&D Systems (#RTA00) capable of detecting rat TNF-alpha for each group in an effort to determine a mechanism behind carbamylated EPO's ability to decrease adhesions. As shown in FIG. 5, the difference in the amount of TNF after 24 hours is not significantly different between the three groups. After three hours (peak inflammation), the amount of TNF in the system decreased for all three groups. These results suggest that the accepted mechanism behind adhesions, *i.e.*, an inflammatory response, may not be the accurate mechanism. In fact, the TNF study suggests that the mechanism behind adhesion may be due to cell death and, because the carbamylated EPO of the present invention has a tissue protective function, the adhesions may decrease upon administration because of decreased cell necrosis.

#### Scarring

Upon visual examination, the rats in Group 3 had substantially less scarring than Groups 1 and 2.

#### Example 3: Blind Study Using Abdominal Sepsis Model

The cecum of Sprague Dawley rats was exposed, ligated just distally to the ileocecal valve to avoid intestinal obstruction, punctured twice with a 18-gauge needle, squeezed gently to force out a small amount of feces, and then returned to the abdominal cavity (feces introduced in peritoneum, which induced infection). The abdomen was closed with 3-0 silk sutures.

The animals were allocated to four groups:

Group 1: Opened as described above, but no sepsis induced (n = 6).

Group 2: Sepsis induced, treated with saline (n = 8). At time of ligation, animals in Group 2 were given 100  $\mu$ l saline intravenously. Daily subcutaneous saline administration (100  $\mu$ l) followed for 8 days (or until death).

Group 3: Sepsis induced, treated with rhu-EPO (n=8). At time of ligation, animals were given 10  $\mu$ g/kg rhu-EPO intravenously in 100  $\mu$ l saline. Daily subcutaneous treatment followed for 8 days (or until death) at a dosage amount of 10  $\mu$ g/kg in 100  $\mu$ l of saline.

Group 4: Sepsis induced, treated with carbamylated EPO (n = 8). At time of ligation, animals were given 10  $\mu$ g/kg carbamylated EPO intravenously in 100  $\mu$ l saline. Daily subcutaneous treatment followed for 8 days (or until death) at a dosage amount of 10  $\mu$ g/kg in 100  $\mu$ l saline

#### Morbidity and Mortality

One day following ligation, all of the animals in Group 1 (sham) survived, whereas none of the animals in Group 2 survived. Only 2 of the animals in Group 3 (rhu-EPO) survived compared to 5 animals in Group 4. Thus, the animals receiving the carbamylated EPO of the present invention had a much higher survival rate than animals receiving saline or rhu-EPO.

#### Scarring

Upon visual examination, the rats in Group 4 had substantially less scarring than Groups 1-3.

#### Example 4: Lipopolysaccharide induced response in Rats

The purpose of this example was to determine the effectiveness of carbamylated erythropoietin on sepsis-like symptoms induced by lipopolysaccharide (LPS). LPS is an endotoxin present on the surface of bacteria which induces sepsis-like response (core temperature increase and cytokine induction) in animals. Male Sprague/Dawley rats (300-350g) were administered 240  $\mu$ g/kg, i.p. The animals were then treated with saline (n=6) or carbamylated erythropoietin (n=6) at 10  $\mu$ g/kg, i.v. The concentration dependent effects of LPS on core body temperature were then determined. Alternatively, the direct intraventricular application (Seeley et al, (1996) *Horm Metab Res.* 28:664-8.) of carbamylated erythropoietin (5  $\mu$ g/kg in 2  $\mu$ l) was administered to determine if the route of application alters the core temperature differentially. Core temperature will be monitored

during the first 24 hrs. In some cases, blood was removed for subsequent cytokine (e.g., TNF, IL-6) analysis. Seeley et al, (1996) *Horm Metab Res.* 28:664-8.

#### Core Temperature.

As part of the sepsis-like conditions induced by LPS, the animals administered LPS experience a biphasic fever. The first phase of the fever is characterized by a precise increase in temperature accompanied by an increase in blood pressure and wakefulness of the afflicted individual. Whereas the second phase of the fever is less precise, and is accompanied by either normotension or hypotension as well as lethargy and sleepiness. It is theorized that the phases of the fever represent a transition in the strategy that the body utilizes to combat the sickness. (Romanovsky *et al.*, *Am. J. Physiol.*, 271: R244-R253, 1996) In the present example, the administration of carbamylated erythropoietin to LPS treated animals resulted in a reduction in both phases of the fever as demonstrated by Figure 6.

#### Serum levels of TNF and IL-6.

Carbamylated erythropoietin's ability to mediate the fever response to LPS was further correlated by its ability to suppress the presence of pyrogenic cytokines such as TNF and IL-6, as demonstrated in Figure 7(a) and Figure 7(b). ELISA was used to determine the presence of TNF and IL-6 within the serum sampled from the rats. Both Figures 7(a) and 7(b) demonstrate that the treatment with carbamylated erythropoietin significantly reduced the presence of pro-inflammatory cytokines, IL-6 and TNF.

#### Peripheral v. Central Administration of Carbamylated Erythropoietin.

In order to rule out the direct effect of carbamylated erythropoietin upon the hypothalamus, the carbamylated erythropoietin was administered intraventricularly in the manner noted above. As Figure 8(a) and Figure 8(b) demonstrate, there was no correlation in the reduction of core temperature between the peripherally and centrally administered carbamylated erythropoietin. In light of these results as well as carbamylated erythropoietin's effects on the pyrogenic cytokines, it appears that carbamylated erythropoietin effects the core temperature through the suppression of the pyrogenic cytokines. This suggests that tissue protective cytokines, such as carbamylated erythropoietin, are useful in mediating, ameliorating or preventing the effects of these cytokines in chronic illnesses (wasting, lethargy, anemia, etc.).

**Example 5: Effect of Erythropoietin analogues on Ischemic Skin Flap Injury in Rats**

An ischemic wound flap model was performed to determine the effect of carbamylated erythropoietin on ischemic skin flap wound recovery. Male Sprague/Dawley rats (300-350g) were anesthetized using isoflurane. A skin flap 9 cm long and 3 cm wide was then cut in the back of the rat. The flap included skin, subcutaneous layer and panniculus carnosus. Following incision, the flap was raised and then immediately re-sutured in its bed, as described (Buemi, M., et al., (2002) *Acta Derm. Venereol.* 82:411-417; Sarau, A., et al., (2003) *Laryngoscope.* 113:85-89). Animals were dosed with an erythropoietin analogue, carbamylated EPO, (0.3 µg/kg, s.c.) immediately following surgery, day 1, day 2 and then bi-weekly during analysis. Animals were weighed and the wound photographed weekly. Buemi, M., et al., (2002) *Acta Derm. Venereol.* 82:411-417. The area of the wound healed was then quantified based on photographs of the animals taken 34 days following the procedure. As is demonstrated in Figure 9, the rats that received carbamylated erythropoietin had a greater percentage of the wound healed than those treated with saline for the same time period.

The invention described and claimed herein is not to be limited in scope by the specific embodiments herein disclosed, since these embodiments are intended as illustrations of several aspects of the invention. In particular, one of ordinary skill in the art will recognize that although the above examples were performed using carbamylated EPO, similar results would be expected of any of the tissue protective cytokines of the present invention. Any equivalent embodiments are intended to be within the scope of this invention. Indeed, various modifications of the invention in addition to those shown and described herein will become apparent to those skilled in the art from the foregoing description. Such modifications are also intended to fall within the scope of the appended claims. All patents and patent applications cited in the foregoing text are expressly incorporate herein by reference in their entirety.

CLAIMS

What is claimed is:

1. A method of treating, preventing, delaying the onset of, or reducing the effects of  
5 proinflammatory cytokines in a mammal comprising the steps of administering a  
therapeutically effective amount of at least one tissue protective cytokine in a pharmaceutical  
carrier.
2. The method of claim 1, wherein the at least one tissue protective cytokine comprises a  
10 chemically modified erythropoietin or mutated erythropoietin.
3. The method of claim 2, wherein the the chemically modified erythropoietin is selected  
from the group consisting of i) an erythropoietin that lacks sialic acid moieties, ii) an  
erythropoietin having at least no sialic acid moieties; iii) an erythropoietin having at least  
15 no N-linked or no O-linked carbohydrates; iv) an erythropoietin having at least a reduced  
carbohydrate content by virtue of treatment of native erythropoietin with at least one  
glycosidase; v) an erythropoietin having at least one or more oxidized carbohydrates; vi)  
an erythropoietin having at least one or more oxidized carbohydrates and is chemically  
reduced; vii) an erythropoietin having at least one or more modified arginine residues;  
20 viii) an erythropoietin having at least one or more modified lysine residues or a  
modification of the N-terminal amino group of the erythropoietin molecule; ix) an  
erythropoietin having at least a modified tyrosine residue; x) an erythropoietin having at  
least a modified aspartic acid or a glutamic acid residue; xi) an erythropoietin having at  
least a modified tryptophan residue; xii) an erythropoietin having at least one amino  
25 group removed; xiii) an erythropoietin having at least an opening of at least one of the  
cystine linkages in the erythropoietin molecule; or xiv) a truncated erythropoietin.
4. The method of claim 3, wherein the chemically modified erythropoietin lacks

erythropoietin's erythropoietic effects.

5. The method of claim 4, wherein the chemically modified erythropoietin comprises carbamylated erythropoietin.

5

6. The method of claim 2, wherein the mutated erythropoietin is selected from the group consisting of one or more of the following mutations C7S, R10I, V11S, L12A, E13A, R14A, R14B, R14E, R14Q, Y15A, Y15F, Y15I, K20A, K20E, E21A, C29S, C29Y, C33S, C33Y, P42N, T44I, K45A, K45D, V46A, N47A, F48A, F48I, Y49A, Y49S, W51F, W51N, Q59N, E62T, L67S, L70A, D96R, K97D, S100R, S100E, S100A, S100T, G101A, G101I, L102A, R103A, S104A, S104I, L105A, T106A, T106I, T107A, T107L, L108K, L108A, S126A, F142I, R143A, S146A, N147K, N147A, F148Y, L149A, R150A, G151A, K152A, L153A, L155A, C160S, I6A, C7A, B13A, N24K, A30N, H32T, N38K, N83K, P42A, D43A, K52A, K97A, K116A, T132A, I133A, T134A, K140A, P148A, R150B, G151A, K152W, K154A, G158A, C161A, and/or R162A.

7. The method of claim 6, wherein the mutated erythropoietin lacks erythropoietin's erythropoietic effects.

8. The method of claim 1 wherein the proinflammatory cytokine comprises an Interleukin or TNF.

9. The method of claim 8 wherein the proinflammatory cytokine is TNF.

10. The method of claim 1 wherein the effect of the proinflammatory cytokine comprises fever, wasting, lethargy, anemia, edema, ischemia, organ failure and insulin resistance.

11. A method of treating, preventing, delaying the onset of a condition associated with an effect of proinflammatory cytokines in a mammal comprising the steps of administering a therapeutically effective amount of at least one tissue protective cytokine in a pharmaceutical carrier.



12. The method of claim 11, wherein the at least one tissue protective cytokine comprises a chemically modified erythropoietin or mutated erythropoietin.

13. The method of claim 12, wherein the the chemically modified erythropoietin is

5 selected from the group consisting of i) an erythropoietin that lacks sialic acid moieties, ii) an erythropoietin having at least no sialic acid moieties; iii) an erythropoietin having at least no N-linked or no O-linked carbohydrates; iv) an erythropoietin having at least a reduced carbohydrate content by virtue of treatment of native erythropoietin with at least one glycosidase; v) an erythropoietin having at least one or more oxidized carbohydrates; 10 vi) an erythropoietin having at least one or more oxidized carbohydrates and is chemically reduced; vii) an erythropoietin having at least one or more modified arginine residues; viii) an erythropoietin having at least one or more modified lysine residues or a modification of the N-terminal amino group of the erythropoietin molecule; ix) an erythropoietin having at least a modified tyrosine residue; x) an erythropoietin having at 15 least a modified aspartic acid or a glutamic acid residue; xi) an erythropoietin having at least a modified tryptophan residue; xii) an erythropoietin having at least one amino group removed; xiii) an erythropoietin having at least an opening of at least one of the cystine linkages in the erythropoietin molecule; or xiv) a truncated erythropoietin.

20 14. The method of claim 13, wherein the chemically modified erythropoietin lacks erythropoietin's erythropoietic effects.

15. The method of claim 14, wherein the chemically modified erythropoietin comprises carbamylated erythropoietin.

25

\* 16. The method of claim 12, wherein the mutated erythropoietin is selected from the group consisting of one or more of the following mutations C7S, R10L, V11S, L12A, E13A, R14A, R14B, R14E, R14Q, Y15A, Y15F, Y15I, K20A, K20E, E21A, C29S, C29Y, C33S,

C33Y, P42N, T44I, K45A, K45D, V46A, N47A, F48A, F48I, Y49A, Y49S, W51F, W51N, Q59N, E62T, L67S, L70A, D96R, K97D, S100R, S100E, S100A, S100T, G101A, G101I, L102A, R103A, S104A, S104I, L105A, T106A, T106I, T107A, T107L, L108K, L108A, S126A, F142I, R143A, S146A, N147K, N147A, F148Y, L149A, R150A, G151A, K152A,  
5 L153A, L155A, C160S, I6A, C7A, B13A, N24K, A30N, H32T, N38K, N83K, P42A, D43A, K52A, K97A, K116A, T132A, I133A, T134A, K140A, P148A, R150B, G151A, K152W, K154A, G158A, C161A, and/or R162A.

17. The method of claim 16, wherein the mutated erythropoietin lacks erythropoietin's  
10 erythropoietic effects.

18. The method of claim 11, wherein the condition associated with the effects of proinflammatory cytokines comprises sepsis, adhesions, wounds, inflammation or chronic disease.

15 19. A pharmaceutical composition comprising an amount of at least one tissue protective cytokine effective in treating, preventing, delaying the onset of, or reducing the effects of proinflammatory cytokines in a mammal.

20 20. The pharmaceutical composition of claim 19, wherein the at least one tissue protective cytokine comprises a chemically modified erythropoietin or mutated erythropoietin.

21. The pharmaceutical composition of claim 20, wherein the the chemically modified  
25 erythropoietin is selected from the group consisting of i) an erythropoietin that lacks sialic acid moieties; ii) an erythropoietin having at least no sialic acid moieties; iii) an erythropoietin having at least no N-linked or no O-linked carbohydrates; iv) an erythropoietin having at least a reduced carbohydrate content by virtue of treatment of  
30 native erythropoietin with at least one glycosidase; v) an erythropoietin having at least one or more oxidized carbohydrates; vi) an erythropoietin having at least one or more oxidized carbohydrates and is chemically reduced; vii) an erythropoietin having at least

one or more modified arginine residues; viii) an erythropoietin having at least one or more modified lysine residues or a modification of the N-terminal amino group of the erythropoietin molecule; ix) an erythropoietin having at least a modified tyrosine residue; x) an erythropoietin having at least a modified aspartic acid or a glutamic acid residue; xi) an erythropoietin having at least a modified tryptophan residue; xii) an erythropoietin having at least one amino group removed; xiii) an erythropoietin having at least an opening of at least one of the cystine linkages in the erythropoietin molecule; or xiv) a truncated erythropoietin.

22. The pharmaceutical composition of claim 21, wherein the chemically modified erythropoietin lacks erythropoietin's erythropoietic effects.

23. The pharmaceutical composition of claim 22, wherein the chemically modified erythropoietin comprises carbamylated erythropoietin.

15

24. The pharmaceutical composition of claim 20, wherein the mutated erythropoietin is selected from the group consisting of one or more of the following mutations C7S, R10I, V11S, L12A, E13A, R14A, R14B, R14E, R14Q, Y15A, Y15F, Y15I, K20A, K20E, E21A, C29S, C29Y, C33S, C33Y, P42N, T44I, K45A, K45D, V46A, N47A, F48A, F48I, Y49A, Y49S, W51F, W51N, Q59N, E62T, L67S, L70A, D96R, K97D, S100R, S100E, S100A, S100T, G101A, G101I, L102A, R103A, S104A, S104I, L105A, T106A, T106I, T107A, T107L, L108K, L108A, S126A, F142I, R143A, S146A, N147K, N147A, F148Y, L149A, R150A, G151A, K152A, L153A, L155A, C160S, I6A, C7A, B13A, N24K, A30N, H32T, N38K, N83K, P42A, D43A, K52A, K97A, K116A, T132A, I133A, T134A, K140A, P148A, R150B, G151A, K152W, K154A, G158A, C161A, and/or R162A.

15

25. The pharmaceutical composition of claim 24, wherein the mutated erythropoietin lacks erythropoietin's erythropoietic effects.

15

26. The pharmaceutical composition of claim 19 wherein the proinflammatory cytokine comprises an Interleukin or TNF.

27. The pharmaceutical composition of claim 26 wherein the proinflammatory cytokine is  
5 TNF.

28. The pharmaceutical composition of claim 19 wherein the effect of the proinflammatory cytokine comprises fever, wasting, lethargy, anemia, edema, ischemia, organ failure and insulin resistance.

10

29. A pharmaceutical composition comprised of an amount of at least one tissue protective cytokine effective in treating, preventing, delaying the onset of a condition associated with proinflammatory cytokines in a mammal.

15 30. The pharmaceutical composition claim 29, wherein the at least one tissue protective cytokine comprises a chemically modified erythropoietin or mutated erythropoietin.

31. The pharmaceutical composition claim 30, wherein the the chemically modified erythropoietin is selected from the group consisting of i) an erythropoietin that lacks sialic  
20 acid moieties, ii) an erythropoietin having at least no sialic acid moieties; iii) an erythropoietin having at least no N-linked or no O-linked carbohydrates; iv) an erythropoietin having at least a reduced carbohydrate content by virtue of treatment of native erythropoietin with at least one glycosidase; v) an erythropoietin having at least one or more oxidized carbohydrates; vi) an erythropoietin having at least one or more  
25 oxidized carbohydrates and is chemically reduced; vii) an erythropoietin having at least one or more modified arginine residues; viii) an erythropoietin having at least one or more modified lysine residues or a modification of the N-terminal amino group of the erythropoietin molecule; ix) an erythropoietin having at least a modified tyrosine residue;  
30 x) an erythropoietin having at least a modified aspartic acid or a glutamic acid residue; xi) an erythropoietin having at least a modified tryptophan residue; xii) an erythropoietin

having at least one amino group removed; xiii) an erythropoietin having at least an opening of at least one of the cystine linkages in the erythropoietin molecule; or xiv) a truncated erythropoietin.

5 32. The pharmaceutical composition of claim 31, wherein the chemically modified erythropoietin lacks erythropoietin's erythropoietic effects.

33. The pharmaceutical composition of claim 32, wherein the chemically modified erythropoietin comprises carbamylated erythropoietin.

10

34. The pharmaceutical composition of claim 30, wherein the mutated erythropoietin is selected from the group consisting of one or more of the following mutations C7S, R10I, V11S, L12A, E13A, R14A, R14B, R14E, R14Q, Y15A, Y15F, Y15I, K20A, K20E, E21A, C29S, C29Y, C33S, C33Y, P42N, T44I, K45A, K45D, V46A, N47A, F48A, F48I, Y49A, 15 Y49S, W51F, W51N, Q59N, E62T, L67S, L70A, D96R, K97D, S100R, S100E, S100A, S100T, G101A, G101I, L102A, R103A, S104A, S104I, L105A, T106A, T106I, T107A, T107L, L108K, L108A, S126A, F142I, R143A, S146A, N147K, N147A, F148Y, L149A, R150A, G151A, K152A, L153A, L155A, C160S, I6A, C7A, B13A, N24K, A30N, H32T, N38K, N83K, P42A, D43A, K52A, K97A, K116A, T132A, I133A, T134A, K140A, P148A, 20 R150B, G151A, K152W, K154A, G158A, C161A, and/or R162A.

35. The pharmaceutical composition of claim 34, wherein the mutated erythropoietin lacks erythropoietin's erythropoietic effects.

25 36. The pharmaceutical composition of claim 29, wherein the condition associated with the effects of proinflammatory cytokines comprises sepsis, adhesions, wounds, inflammation or chronic disease.

pi

30

1/9

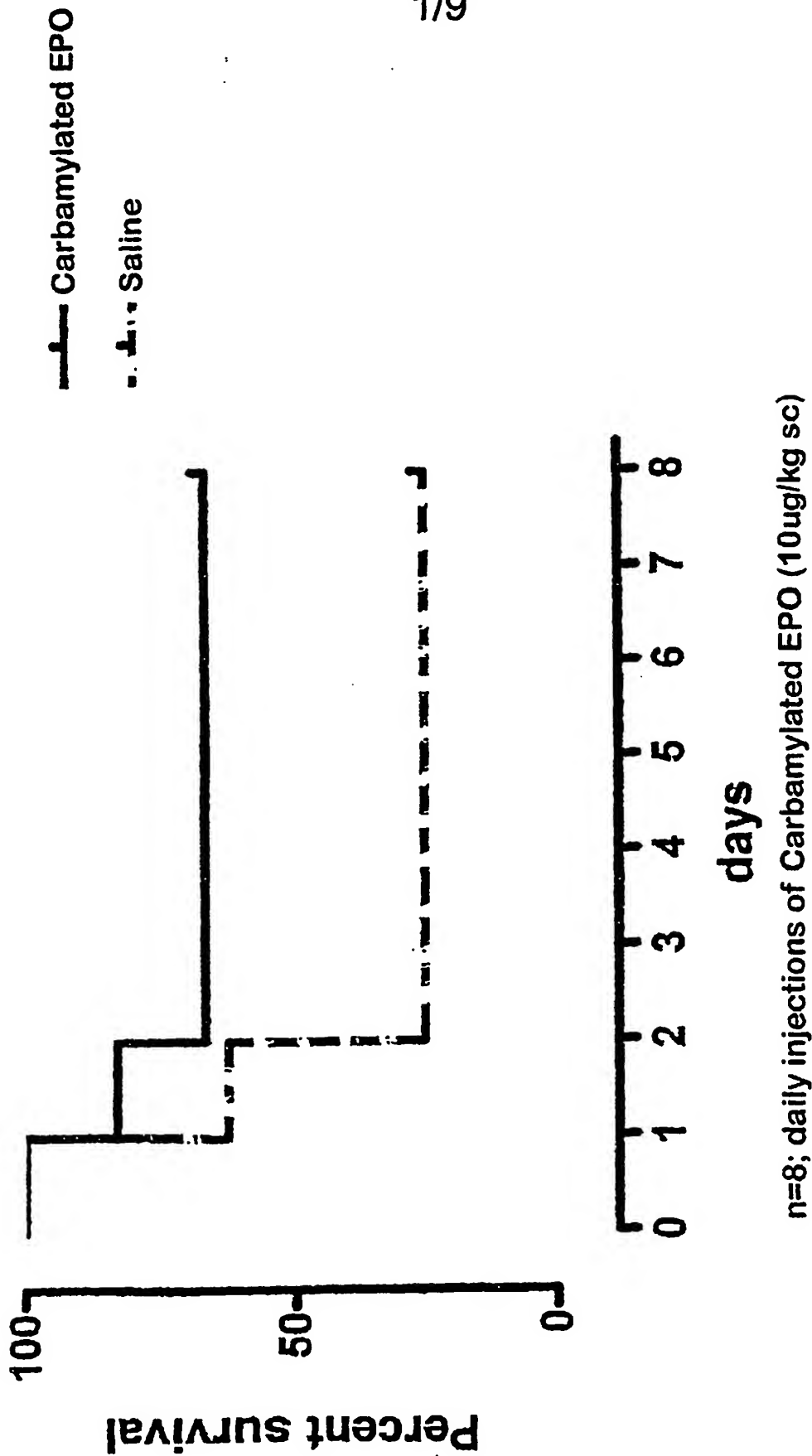


Fig. 1

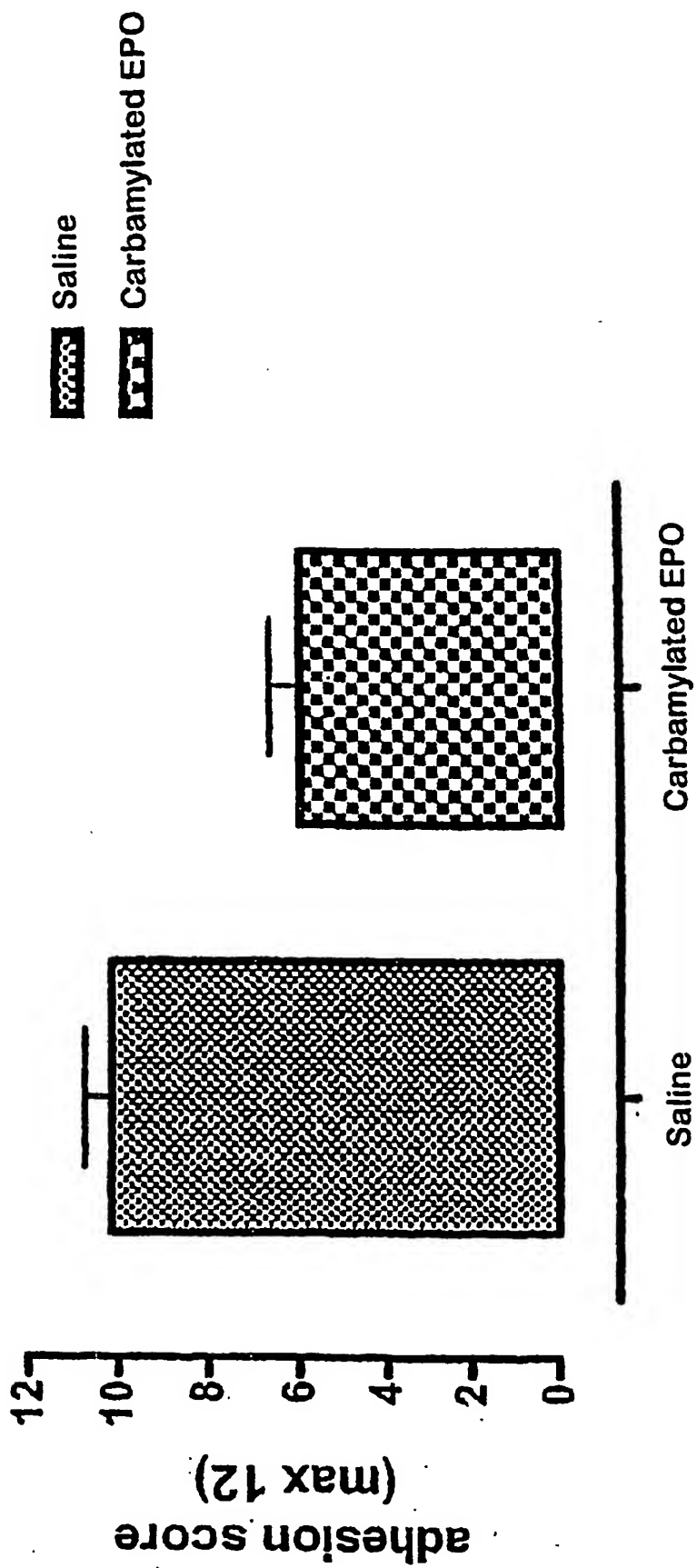


Fig. 2



# cecal perforation model

n = 8 each group

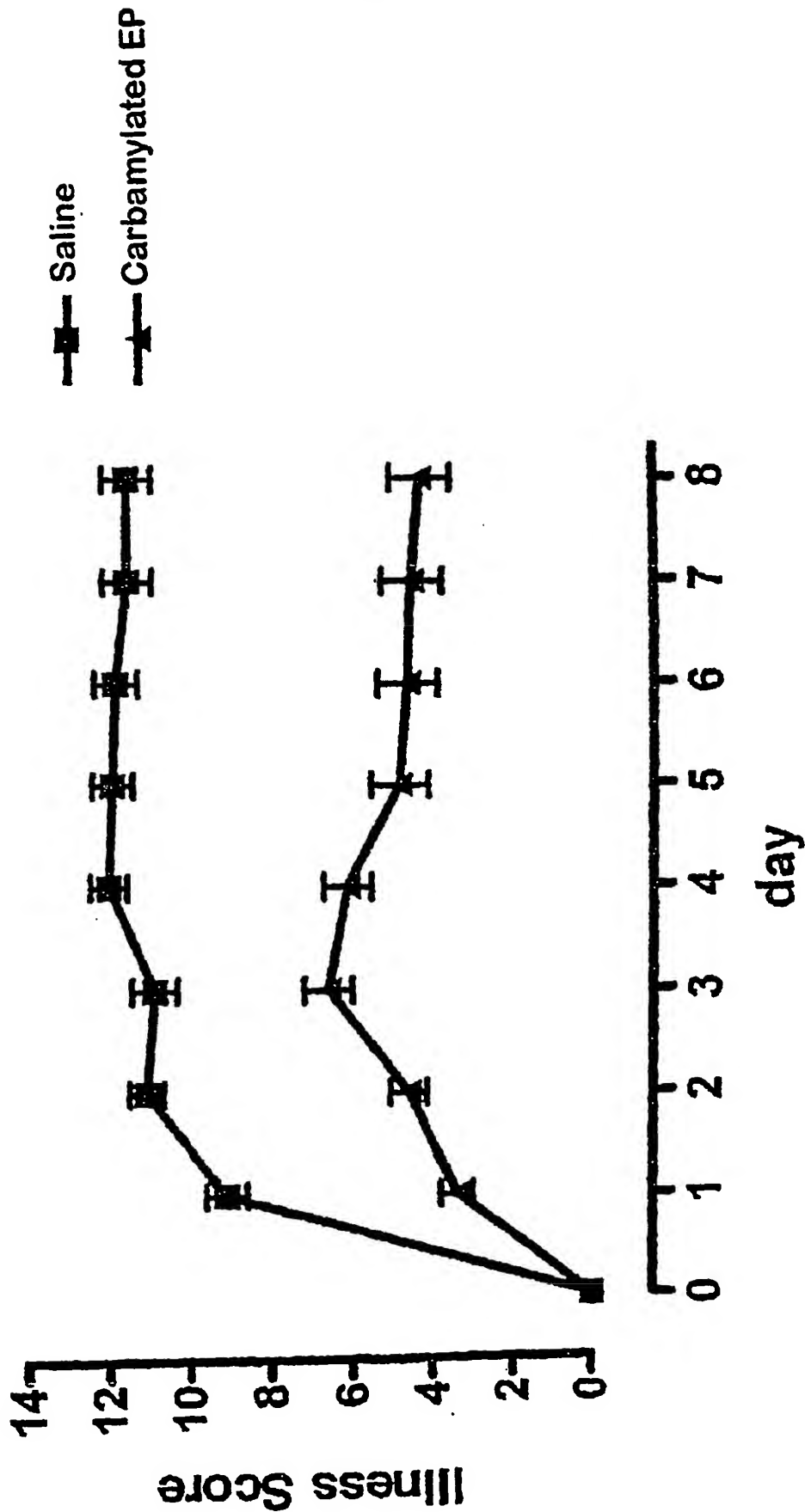


Fig. 3

# ADHESION SCORE AFTER 24 hrs

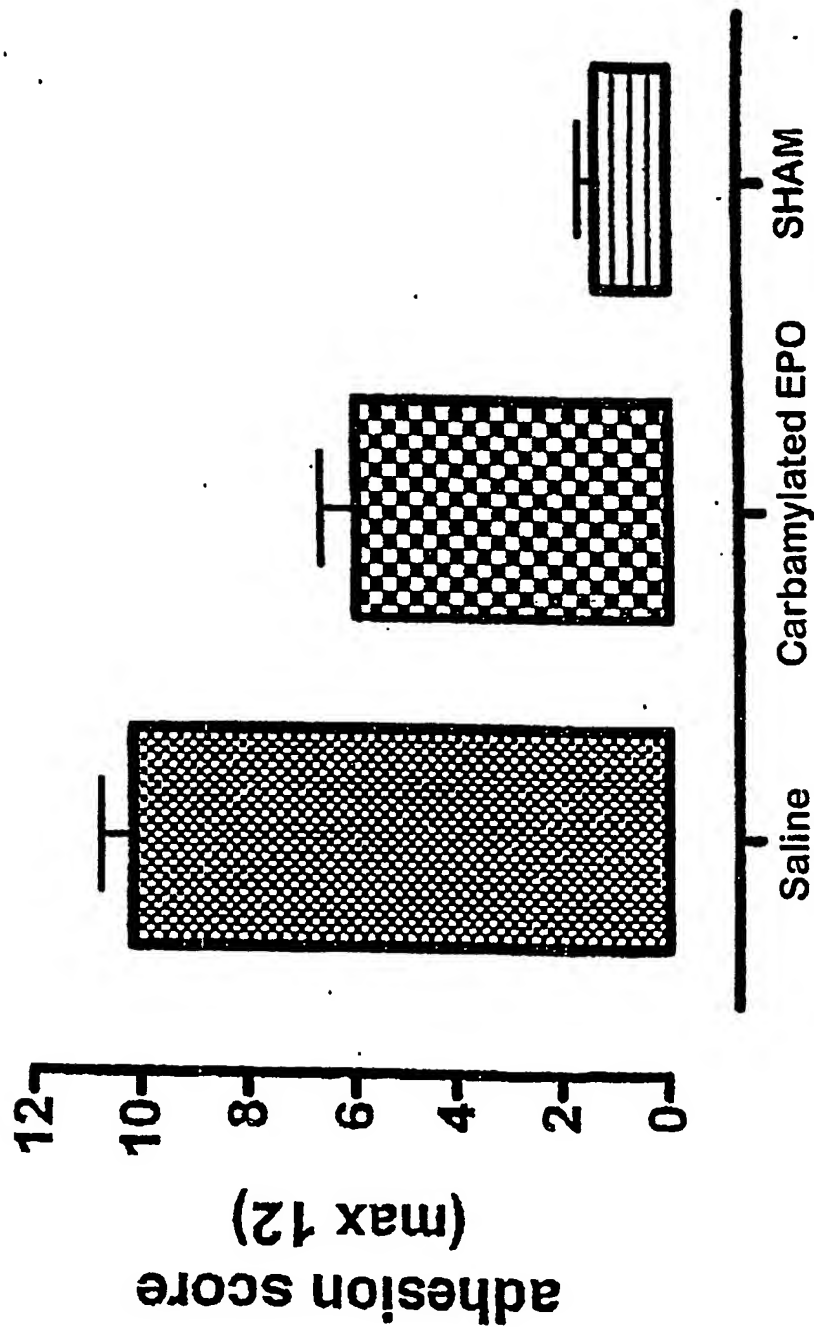


Fig. 4

5/9

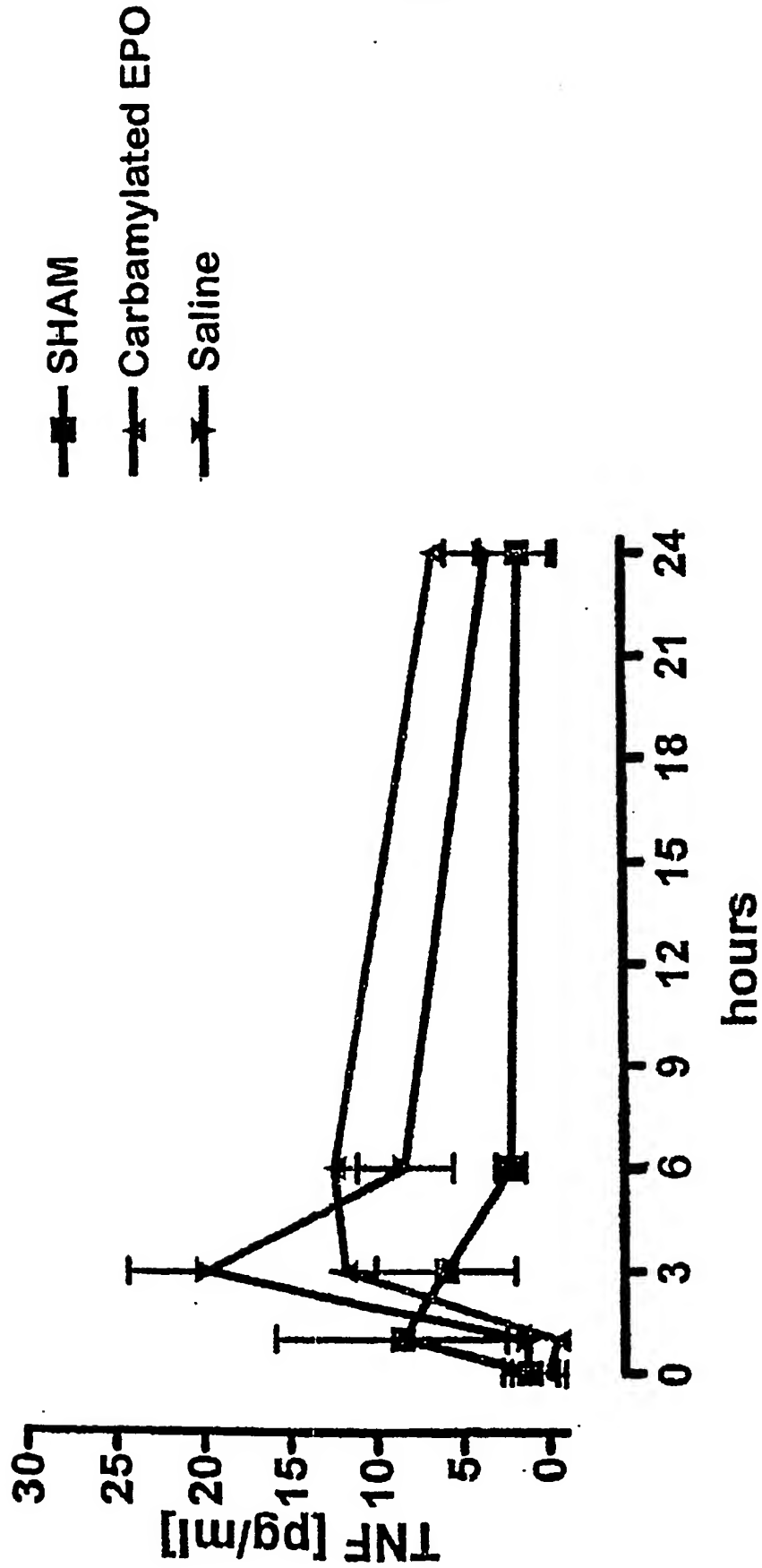


Fig. 5

# 240 ug LPS with blood sampling

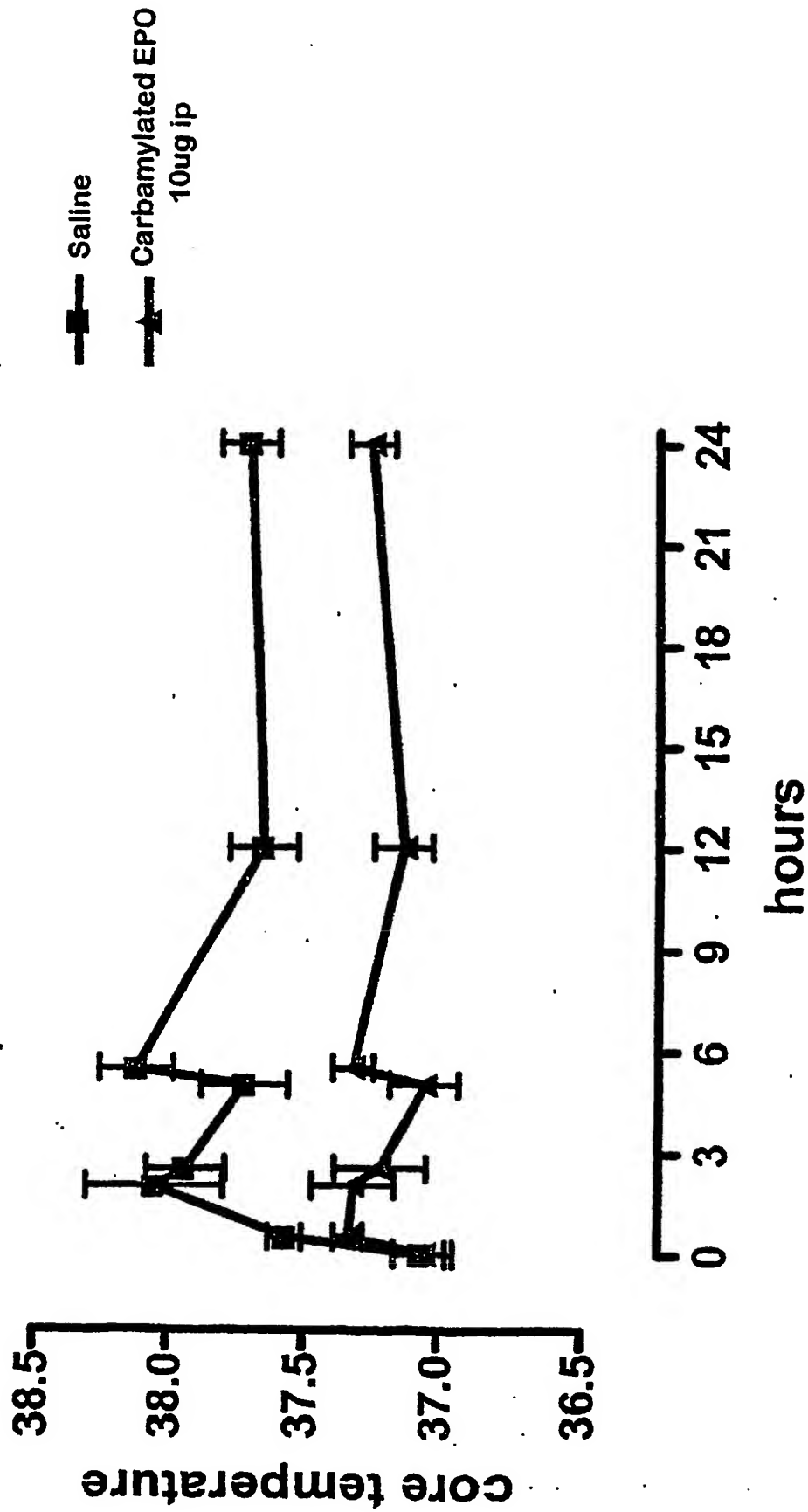
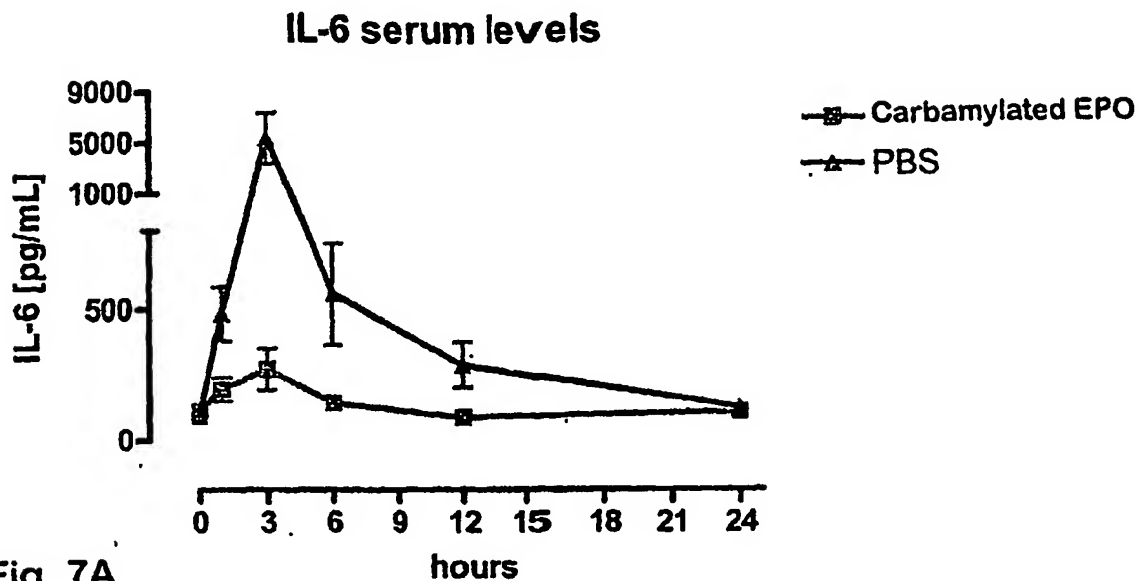
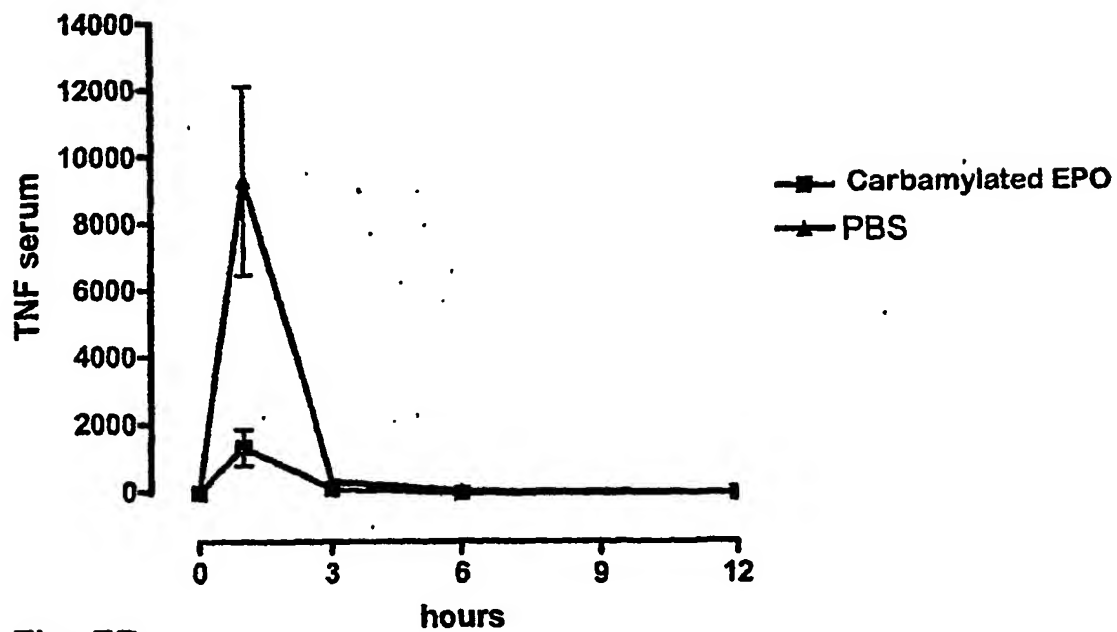


Fig. 6

**serum concentrations following 240 ug LPS****Fig. 7A****Fig. 7B**

### Peripheral Carbamylated EPO vs Central

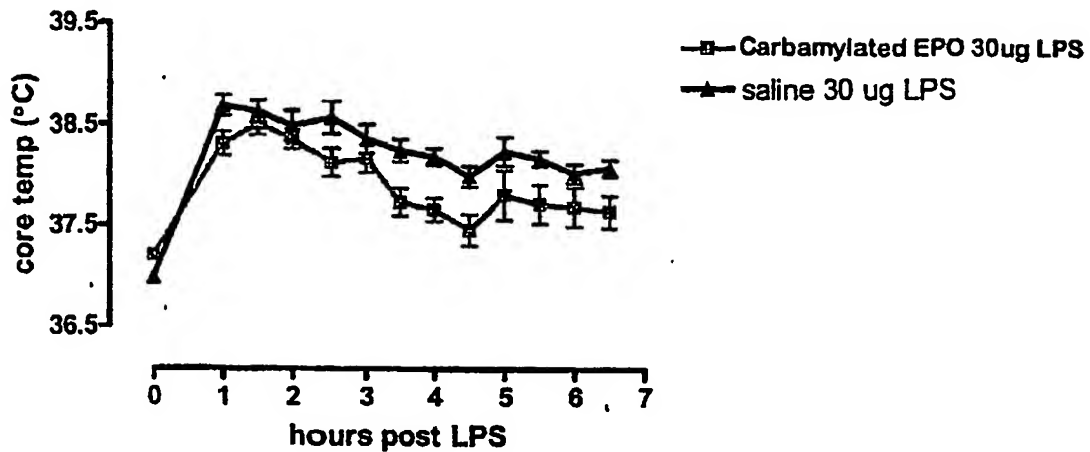


Fig. 8A

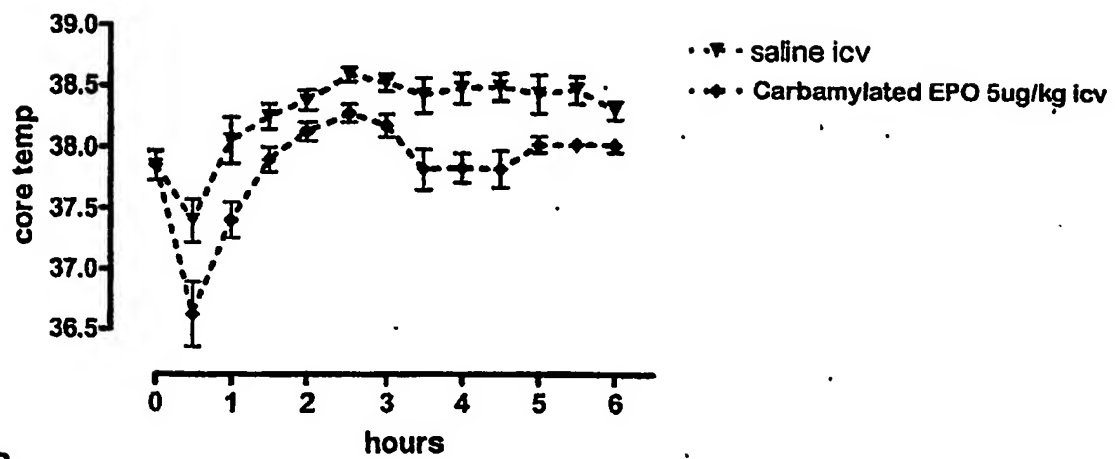


Fig. 8B

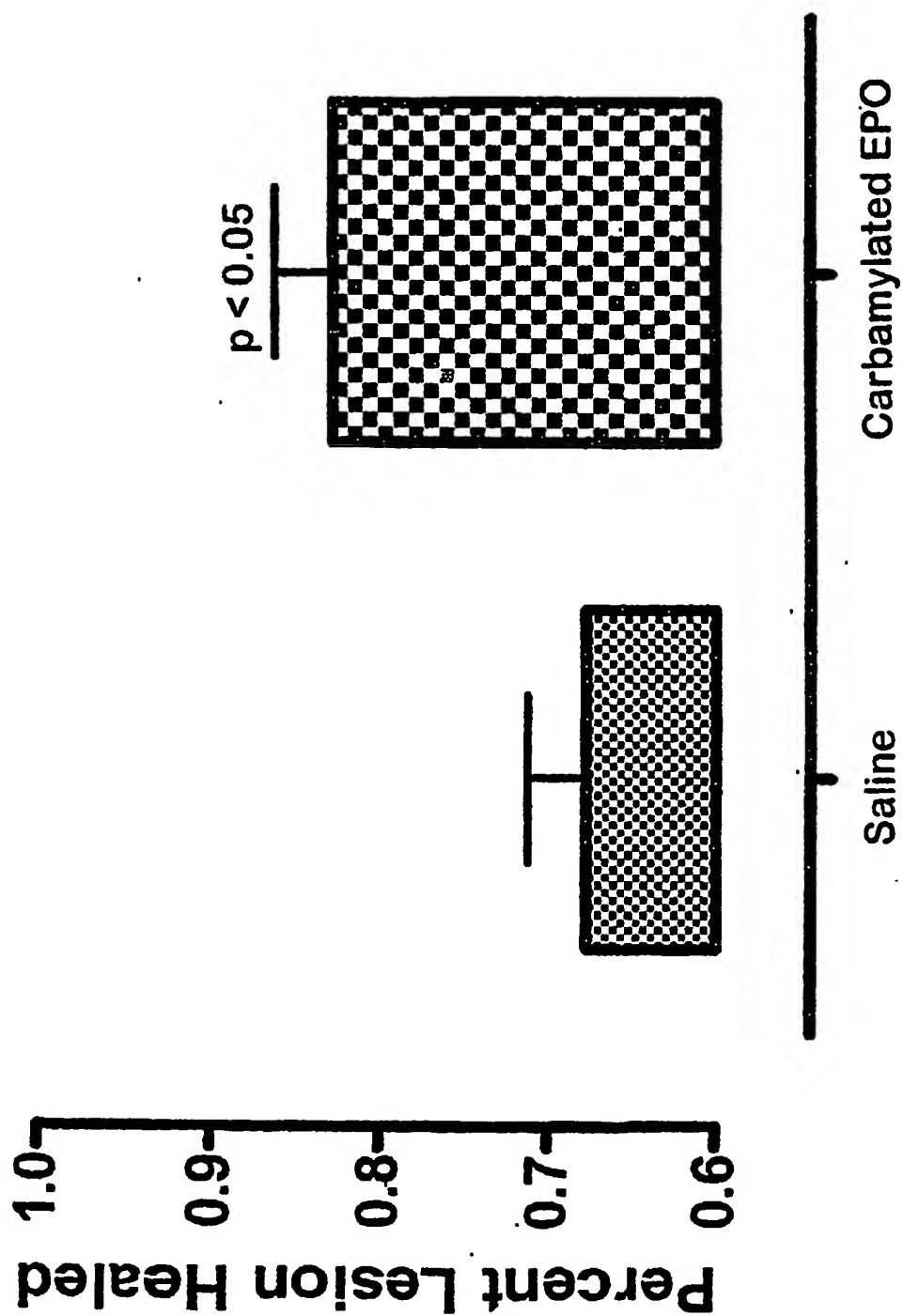


Fig. 9

## Vascular Injury During Elevated Glucose can be Mitigated by Erythropoietin and Wnt Signaling

Zhao Zhong Chong<sup>1</sup>, Yan Chen Shang<sup>1</sup> and Kenneth Maiese<sup>1,2,\*</sup>

<sup>1</sup>Division of Cellular and Molecular Cerebral Ischemia, <sup>2</sup>Departments of Neurology and Anatomy & Cell Biology,

<sup>3</sup>Center for Molecular Medicine and Genetics and <sup>4</sup>Institute of Environmental Health Sciences, Wayne State University School of Medicine, Detroit, Michigan 48201, USA

**Abstract:** Impacting a significant portion of the world's population with increasing incidence in minorities, the young, and the physically active, diabetes mellitus (DM) and its complications affect approximately 20 million individuals in the United States and over 100 million individuals worldwide. In particular, vascular disease from DM may lead to some of the most serious complications that can extend into both the cardiac and nervous systems. Unique strategies that can prevent endothelial cell (EC) demise and elucidate novel cellular mechanisms for vascular cytoprotection become vital for the prevention and treatment of vascular DM complications. Here, we demonstrate that erythropoietin (EPO), an agent that has recently been shown to extend cell viability in a number of systems extending beyond hematopoietic cells, prevents EC injury and apoptotic nuclear DNA degradation during elevated glucose exposure. More importantly, EPO employs Wnt1, a cysteine-rich glycosylated protein involved in gene expression, cell differentiation, and cell apoptosis, to confer EC cytoprotection and maintains the integrity of Wnt1 expression during elevated glucose exposure. In addition, application of anti-Wnt1 neutralizing antibody abrogates the protective capacity of both EPO and Wnt1, illustrating that Wnt1 is an important component in the cytoprotection of ECs during elevated glucose exposure. Intimately linked to this cytoprotection is the downstream Wnt1 pathway of glycogen synthase kinase (GSK-3 $\beta$ ) that requires phosphorylation of GSK-3 $\beta$  and inhibition of its activity by EPO. Interestingly, inhibition of GSK-3 $\beta$  activity during elevated glucose leads to enhanced EC survival, but does not synergistically improve protection by EPO or Wnt1, suggesting that EPO and Wnt1 are closely tied to the blockade of GSK-3 $\beta$  activity. Our work exemplifies an exciting potential application for EPO in regards to the treatment of DM vascular disease complications and highlights a previously unrecognized role for Wnt1 and the modulation of the downstream pathway of GSK-3 $\beta$  to promote vascular cell viability during DM.

**Key Words:** Apoptosis, diabetes, endothelial cells, erythropoietin, glucose, growth factors, GSK-3 $\beta$ , oxidative stress, SB21, vascular disease, wingless, Wnt, Wnt1 antibody.

### INTRODUCTION

Affecting close to 20 million individuals in the United States and over 100 million individuals worldwide, diabetes mellitus (DM) is recognized with increasing incidence in minorities, the young, and the physically active (Maiese, *et al.*, 2007b, Quinn, 2001). Of these individuals, Type 1 DM accounts for approximately 10% of all diabetics that represents a highly significant health concern, since this disorder begins early in life and leads to cardiovascular, renal, and nervous system disease. Type 2 DM represents at least 80 percent of all diabetics and is rapidly increasing in incidence as a result of changes in human behavior and increased body mass index (Laakso, 2001). Both Type 1 and type 2 DM represent important health concerns whether they begin early or later in life (Maiese, *et al.*, 2007a), since each can result in long-term complications throughout the body (Daneman, 2006). In regards to the vascular and nervous systems, patients with DM can develop severe neurological and vascular

disease that can lead to an increased risk for cognitive decline especially from vascular disease (Chong, *et al.*, 2005b, Li, *et al.*, 2006a, Schneider Beerl, *et al.*, 2004).

Individuals with DM can suffer from either increased as well as depressed serum glucose levels as a result of poor control or unrecognized disease progression (Saydah, *et al.*, 2004). These clinical observations are directly relevant to processes that occur at the cellular level in vascular cells during DM. Recent work has shown that cerebral endothelial cells (ECs) are susceptible to advanced glycation end products that can occur during DM (Niiya, *et al.*, 2006). In experimental models of DM with elevated glucose levels, cerebral endothelial cell dysfunction may lead to blood-brain barrier permeability (Huber, *et al.*, 2006).

Given that EC injury can occur during elevated glucose (Maiese, *et al.*, 2007b), agents that reduce cellular loss may be highly successful for the treatment of complications arising from DM. Erythropoietin (EPO) may be an agent that closely fits this desired profile since protection by EPO can be quite robust for a number of disorders (Li, *et al.*, 2004, Maiese, *et al.*, 2004, Maiese, *et al.*, 2005c, Mikati, *et al.*, 2007, Santhanam and Katusic, 2006). EPO is approved by the Food and Drug Administration for the treatment of

\*Address correspondence to this author at the Department of Neurology, 8C-1 UHC, Wayne State University School of Medicine, 4201 St. Antoine, Detroit, MI 48201, USA; Tel: 313-966-0833; Fax: 313-966-0486; E-mail: kmaiese@med.wayne.edu, aa2088@wayne.edu

Received: February 15, 07, Revised: April 18, 07, Accepted: May 2, 07



anemia, but a body of recent work has revealed that EPO is not only required for erythropoiesis, but also functions in other organs and tissues outside of the liver and the kidney, such as the brain, heart, and vascular system (Chong, *et al.*, 2003b, Chong, *et al.*, 2002, Chong and Maiese, 2007, Mikati, *et al.*, 2007, Moon, *et al.*, 2006, Um, *et al.*, 2007). EPO can be detected in the breath of healthy individuals (Schumann, *et al.*, 2006) suggesting its ubiquitous presence and has been correlated with increased Mental Development Index scores (Bierer, *et al.*, 2006). In clinical studies with DM, plasma EPO is often low in diabetic patients with (Mojiminiyi, *et al.*, 2006) or without anemia (Symeonidis, *et al.*, 2006). Furthermore, the failure to produce erythropoietin in response to a declining hemoglobin level suggests an impaired EPO response in diabetic patients (Thomas, *et al.*, 2005). Yet, increased EPO secretion during diabetic pregnancies may represent the body's endogenous protection mechanisms against DM complications (Teramo, *et al.*, 2004). Similar to the potential protective role of insulin (Duarte, *et al.*, 2006), EPO has been shown in diabetics and non-diabetics with severe, resistant congestive heart failure have shown to decrease fatigue, increase left ventricular ejection fraction, and significantly decrease the number of hospitalization days (Silverberg, *et al.*, 2006).

Unfortunately, agents such as EPO may not be tolerated by all individuals, especially those with co-morbid conditions such as congestive heart failure (van der Meer, *et al.*, 2004), hypertension (Maiese, *et al.*, 2005c), and neoplasms (Henry, *et al.*, 2004, Maiese, *et al.*, 2005b). For these reasons, it is vital to elucidate novel pathways that may influence cellular toxicity during DM (Berent-Spillion and Russell, 2007, Li, *et al.*, 2006a, Maiese, *et al.*, 2005a). In this instance, it is the cellular mechanisms controlled by EPO that can specifically target DM vascular complications that garner particular interest. One novel pathway for EPO to block cellular injury during elevated glucose involves Wnt1. Wnt proteins, derived from the *Drosophila Wingless* (Wg) and the mouse *Int-1* genes, are secreted cysteine-rich glycosylated proteins that play a role in a variety of cellular functions that involve gene expression, gene replication, cell differentiation, and cell apoptosis (Abe and Takeichi, 2007, Chong and Maiese, 2004, Cohen, *et al.*, 2006, Jozwiak, *et al.*, 2007, Li, *et al.*, 2005, Li, *et al.*, 2006c, Wang and MacNaughton, 2005). Variations in genes in the Wnt signaling pathway, such as transcription factor 7-like 2 gene, may impart increased risk for Type 2 DM in some populations (Grant, *et al.*, 2006) as well as have increased association with obesity (Guo, *et al.*, 2006). In addition, experimental work in mice suggest that some Wnt family members may offer glucose tolerance and insulin sensitivity (Wright, *et al.*, 2007). Additional studies have described the expression of Wnt5b in adipose tissue, the pancreas, and the liver in diabetic patients with a suggested function for the regulation of adipose cell function (Kanzawa, *et al.*, 2004) as well as the ability of Wnt4 or Wnt5a to protect glomerular mesangial cells from elevated glucose induced apoptosis (Lin, *et al.*, 2006). Interestingly, Wnt1 which is considered to be one of the best characterized members of the Wnt family has been closely linked to the control of apoptotic cellular injury. Loss of Wnt1 expression (He, *et al.*, 2005, You, *et al.*, 2004) leads to apoptosis while the presence of Wnt1 can promote cell

survival during insults such as serum deprivation (Bourrat, *et al.*, 2000) or amyloid toxicity (Chong, *et al.*, 2007a).

A downstream pathway to consider that can involve both EPO and Wnt1 cytoprotection during DM is glycogen synthase kinase (GSK-3 $\beta$ ). Wnt-1 can inhibit GSK-3 $\beta$  to prevent the phosphorylation and degradation of  $\beta$ -catenin to allow  $\beta$ -catenin to translocate to the nucleus to allow the Wnt pathway to block cell injury (Chong, *et al.*, 2005c, Rhee, *et al.*, 2002). Inhibition of GSK-3 $\beta$  activity can influence cell survival and inflammation (Chong, *et al.*, 2007b) and, as a result, GSK-3 $\beta$  is considered to be a therapeutic target for a number of disorders (Balaraman, *et al.*, 2006, Chong, *et al.*, 2005b, Nurni, *et al.*, 2006). In regards to DM, inactivation of GSK-3 $\beta$  by small molecule inhibitors or RNA interference prevents toxicity from high concentrations of glucose and increases rat beta cell replication (Muusmann, *et al.*, 2007) while cardioprotective agents during experimental DM have been linked to the inactivation of GSK-3 $\beta$  (Yus, *et al.*, 2005). Furthermore, pharmacologic inhibition of GSK-3 $\beta$  by recombinant Wnt5a or other agents prevents high glucose-mediated apoptosis in glomerular mesangial cells (Lin, *et al.*, 2006). In clinical studies, physical exercise is one of the important lifestyle interventions for DM to promote glycemic control (Maionara, *et al.*, 2002) and at the cellular level, physical exercise has been shown to phosphorylate and inhibit GSK-3 $\beta$  activity (Howlett, *et al.*, 2006). We demonstrate that EC protection by EPO during elevated glucose relies upon the activation of the Wnt1 pathway, since EPO promotes the expression of Wnt1 and EC protection is abolished by co-treatment with an anti-Wnt1 neutralizing antibody. Additionally, inhibition of GSK-3 $\beta$  activity during elevated glucose leads to enhanced EC survival, but does not synergistically improve protection by EPO or Wnt1, illustrating that the pathways of EPO and Wnt1 are intimately linked to the blockade of GSK-3 $\beta$  activity.

## MATERIALS AND METHODS

### Cerebral Microvascular Endothelial Cell Cultures

Per our prior protocols, vascular ECs were isolated from male Sprague-Dawley adult rat brain cerebra by using a modified collagenase/dispase-based digestion protocol (Chong, *et al.*, 2003a, Chong, *et al.*, 2002, Chong and Maiese, 2007). Briefly, ECs were cultured in endothelial growth media consisting of M199E (M199 with Eagle's salt) with 20% heat-inactivated fetal bovine serum, 2 mmol/l L-glutamine, 90  $\mu$ g/ml heparin, and 20  $\mu$ g/ml EC growth supplement (ICN Biomedicals, Aurora, OH). Cells from the third passage were identified by positive direct immunocytochemistry for factor VIII-related antigen (Chong, *et al.*, 2003a, Chong, *et al.*, 2002, Chong and Maiese, 2007) and possessed characteristic spindle-shaped morphology with antigenic properties shown to resemble brain endothelium *in vivo* (Abbott, *et al.*, 1992).

### Experimental Treatments

Elevated glucose concentrations in ECs was performed by replacing the media with serum-free M199E media with 2 mmol/l L-glutamine and 90  $\mu$ g/ml heparin containing 25 mM D-glucose and then incubated at 37°C for 48 hours. In this

injury paradigm for elevated glucose, hyperosmolarity did not play a significant role in cell toxicity. A mannitol concentration of 25 mM resulted in similar and not significantly different survival rates than untreated control ECs with survival equal to approximately 90% (data not shown), suggesting that hyperosmolarity was not a significant factor in cell injury. Furthermore, we performed additional studies with the biologically inactive agent L-glucose plus 5.6 mM D-glucose and have observed that L-glucose in concentrations of 25 mM did not significantly alter cell survival (data not shown).

For treatments applied 1 hour prior to elevated glucose concentrations, application of erythropoietin (EPO) (R&D Systems, Minneapolis, MN), human recombinant Wnt1 protein (R&D Systems, Minneapolis, MN), a mouse monoclonal anti body against Wnt1 (R&D Systems, Minneapolis, MN), or the glycogen synthase kinase (GSK)-3 $\beta$  inhibitor SB216763 [3-(2,4-Dichlorophenyl)-4-(1-methyl-1H-indol-3-yl)-1H-pyrrole-2,5-dione] (SB21) (Tocris, Ellisville, MO) were continuous.

#### Cell Survival and DNA Fragmentation

EC injury was determined by bright field microscopy using a 0.4% trypan blue dye exclusion method 48 hours per our previous protocols (Chong and Maiese, 2007) following elevated glucose. Genomic DNA fragmentation was determined by the terminal deoxynucleotidyl transferase nick end labeling (TUNEL) assay (Chong, *et al.*, 2003a, Chong, *et al.*, 2003b, Chong, *et al.*, 2002) with the 3'-hydroxy ends of cut DNA labeled with biotinylated dUTP using the enzyme terminal deoxynucleotidyl transferase (Promega, Madison, WI) followed by streptavidin-peroxidase and visualized with 3,3'-diaminobenzidine (Vector Laboratories, Burlingame, CA).

#### Expression of Wnt1 and Phosphorylated Glycogen Synthase Kinase

Cells were homogenized and following protein determination, each sample (50  $\mu$ g/lane) was then subjected to 12.5% SDS-polyacrylamide gel electrophoresis. After transfer, the membranes were incubated with a rabbit polyclonal antibody against Wnt1 (1:1000, R&D Systems, Minneapolis, MN) or a rabbit antibody against phosphorylated GSK-3 $\beta$  (p-GSK-3 $\beta$ , Ser<sup>9</sup>) (Cell Signaling, Beverly, MA). Following washing, the membranes were incubated with a horseradish peroxidase (HRP) conjugated secondary antibody (goat anti-mouse IgG, 1:1000 (Wnt1) or goat anti-rabbit IgG, 1:10000 (p-GSK-3 $\beta$ )). The antibody-reactive bands were revealed by chemiluminescence (Amersham Pharmacia Biotech, Piscataway, NJ) and band density was performed using the public domain NIH Image program (developed at the U.S. National Institutes of Health and available at <http://rsb.info.nih.gov/nih-image/>).

#### Statistical Analysis

For each experiment, the mean and standard error were determined. Statistical differences between groups were assessed by means of analysis of variance (ANOVA) from 6 replicate experiments with the post-hoc Student's t-test. Statistical significance was considered at  $p < 0.05$ .

## RESULTS

### Elevated Glucose Leads to EC Injury

Primary cultures of microvascular ECs were exposed to elevated D-glucose (25 mM) and cell survival was determined 48 hours later by the trypan blue exclusion method. As shown in Fig. (1A), representative pictures demonstrate that elevated glucose treatment results in a loss of membrane integrity and staining in a significant number of ECs cells with trypan blue. The quantitative results demonstrate that EC survival was significantly decreased from  $90 \pm 2\%$  to  $46 \pm 2\%$  48 hours following administration of D-glucose (Fig. 1B).

We next assessed genomic DNA fragmentation in primary cultures of microvascular ECs 48 hours following administration of elevated D-glucose (25 mM) with TUNEL. Representative pictures in Fig. (1C) demonstrate significant apoptosis with chromatin condensation and nuclear fragmentation in ECs during elevated D-glucose. As shown in Fig. (1D), percent DNA fragmentation was significantly increased from  $9 \pm 3\%$  of control cells to  $57 \pm 5\%$  48 hours following administration of D-glucose.

### Wnt1 Provides Necessary Cellular Protection Against High Glucose in ECs

Application of recombinant human Wnt1 protein (100 ng/ml) in EC cultures 1 hour prior to elevated D-glucose (25 mM) exposure significantly reduced trypan blue uptake in ECs when assessed 48 hours later following elevated D-glucose application (Fig. 2A). In Fig. (2B, EC) survival was significantly reduced to  $46 \pm 4\%$  following exposure to elevated D-glucose when compared with untreated control cultures ( $93 \pm 2\%$ ,  $p < 0.01$ ). Yet, application of Wnt1 of 100 ng/ml 1 hour prior to elevated D-glucose significantly reduces trypan blue uptake in ECs resulting in an EC survival of  $69 \pm 5\%$  ( $p < 0.01$ ).

Administration of an antibody to Wnt1 (Wnt1Ab, 1  $\mu$ g/ml) alone did not significantly alter EC survival when compared to untreated control cultures (data not shown). In studies with exposure to elevated D-glucose (25 mM), application of the Wnt1Ab, 1  $\mu$ g/ml slightly decreased EC survival when compared to cultures treated with elevated glucose alone, suggesting that endogenous Wnt1 may offer a minimum level of protection to ECs (Fig. 2B).

We next examined whether specific antagonism against exogenous Wnt1 application with the Wnt1Ab could neutralize the protective capacity of Wnt1 during elevated glucose exposure. In the presence of the Wnt1Ab (1  $\mu$ g/ml), the protective capacity of Wnt1 was significantly reduced yielding EC survivals of  $46 \pm 5\%$  ( $p < 0.01$ ) when compared to a survival of  $69 \pm 5\%$  in ECs with Wnt1 only treatment 48 hours following administration of D-glucose (Fig. 2B).

Similarly, application of Wnt1 protein (100 ng/ml) to EC cultures 1 hour prior to administration of elevated D-glucose at the concentration of 25 mM significantly reduced apoptotic chromatin condensation and nuclear fragmentation determined 48 hours later by TUNEL (Figs. 2C, 2D). Yet, co-application of the Wnt1Ab (1  $\mu$ g/ml) with Wnt1 resulted in an increase in percent DNA fragmentation in ECs during

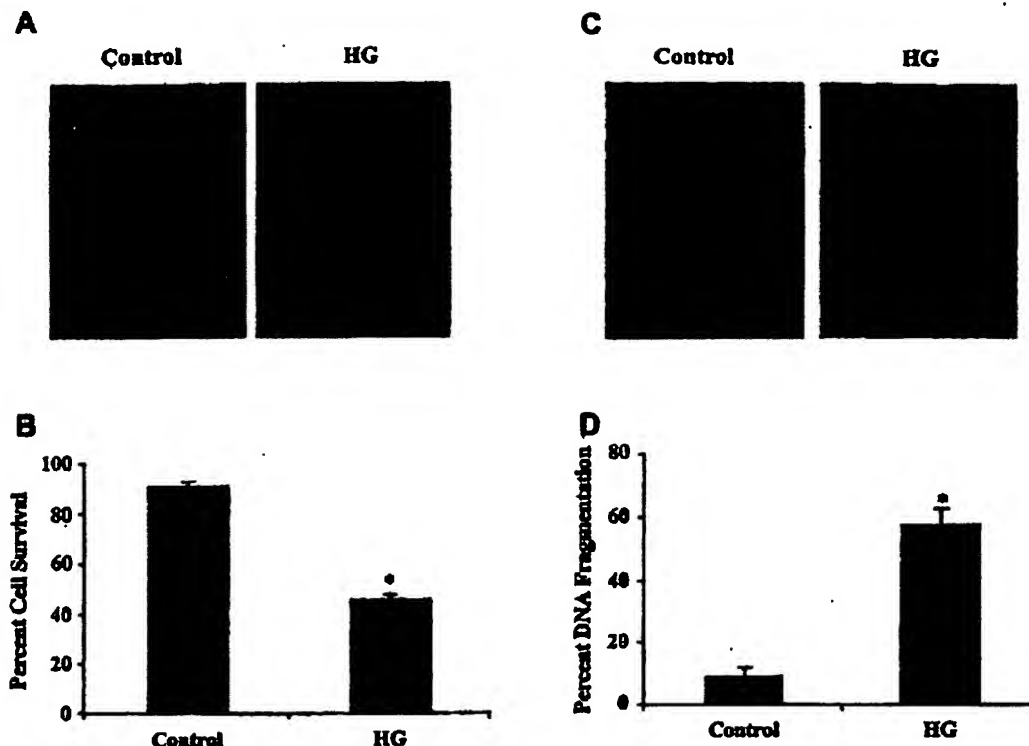


**Fig. (1).** Elevated glucose decreases primary EC survival and increases apoptotic demise. (A) Primary ECs were exposed to elevated D-glucose (HG) at the concentration of 25 mM and EC survival was determined 48 hours later. Representative images illustrate increased trypan blue staining during elevated glucose. (B) EC survival was significantly decreased from  $90 \pm 2\%$  to  $46 \pm 2\%$  48 hours following administration of D-glucose ( $*p < 0.01$  vs. Control). (C) Primary ECs were exposed to elevated D-glucose (HG) (25 mM) and EC nuclear DNA degradation was determined 48 hours later. Representative images illustrate increased TUNEL staining during elevated glucose. (D) EC apoptotic nuclear DNA degradation was significantly increased from  $9 \pm 3\%$  to  $57 \pm 5\%$  48 hours following administration of D-glucose ( $*p < 0.01$  vs. Control). In all cases, each data point represents the mean and SEM and control = untreated EC cultures.

elevated glucose treatment, illustrating the necessity of the Wnt1 pathway for cytoprotection (Figs. 2C, 2D).

#### EPO Prevents EC Injury and Apoptotic Loss Through Wnt1

To investigate the ability of EPO to offer cytoprotection during elevated glucose treatment, EPO (10 ng/ml) was applied to ECs 1 hour prior to the administration of D-glucose at the concentration of 25 mM. Cell survival was determined by trypan blue dye exclusion 48 hours following administration of D-glucose. EPO significantly reduced trypan blue uptake in ECs during elevated glucose (Fig. 3A). Interestingly, application of the Wnt1 antibody (Wnt1Ab, 1  $\mu$ g/ml) 30 min prior to EPO administration abolished the cytoprotective capacity of EPO resulting in a significant increase in trypan blue staining in ECs. Quantitation of these results in Fig. (3B) illustrates that EC survival was significantly increased with EPO administration from  $46 \pm 4\%$  during elevated D-glucose to  $71 \pm 4\%$  ( $p < 0.01$ ). Yet, co-application of Wnt1Ab (1  $\mu$ g/ml) with EPO blocked cytoprotection by EPO to reduce cell survival to  $53 \pm 4\%$  (Fig. 3B).

Furthermore, application of EPO (10 ng/ml) to EC cultures 1 hour prior to administration of D-glucose at the concentration of 25 mM significantly reduced apoptotic chromatin condensation and nuclear DNA fragmentation when assessed 48 hours later by TUNEL (Figs. 3C, 3D). In contrast, co-application of Wnt1Ab (1  $\mu$ g/ml) with EPO led to a significant increase in percent DNA fragmentation in ECs during high glucose treatment from  $26 \pm 2\%$  with EPO only administration to  $53 \pm 6\%$  ( $p < 0.01$ ) during EPO and Wnt1Ab application.

#### EPO Prevents the Loss of Wnt1 Expression and Inhibits GSK-3 $\beta$ Activity During Elevated Glucose Exposure

Western blot assay was performed for Wnt1 expression (Fig. 4A) and phosphorylated GSK-3 $\beta$  (p-GSK-3 $\beta$ , Ser<sup>9</sup>) expression (Fig. 4C) at 6, 24, and 48 hours following exposure to elevated D-glucose (25 mM). In Fig. (4A), elevated D-glucose initially increased the expression of Wnt1 at 6 and 24 hours when compared to EC control cultures. After 24 hours post elevated glucose exposure, expression of Wnt1 was lost and approached control levels (Figs. 4A, 4B). In

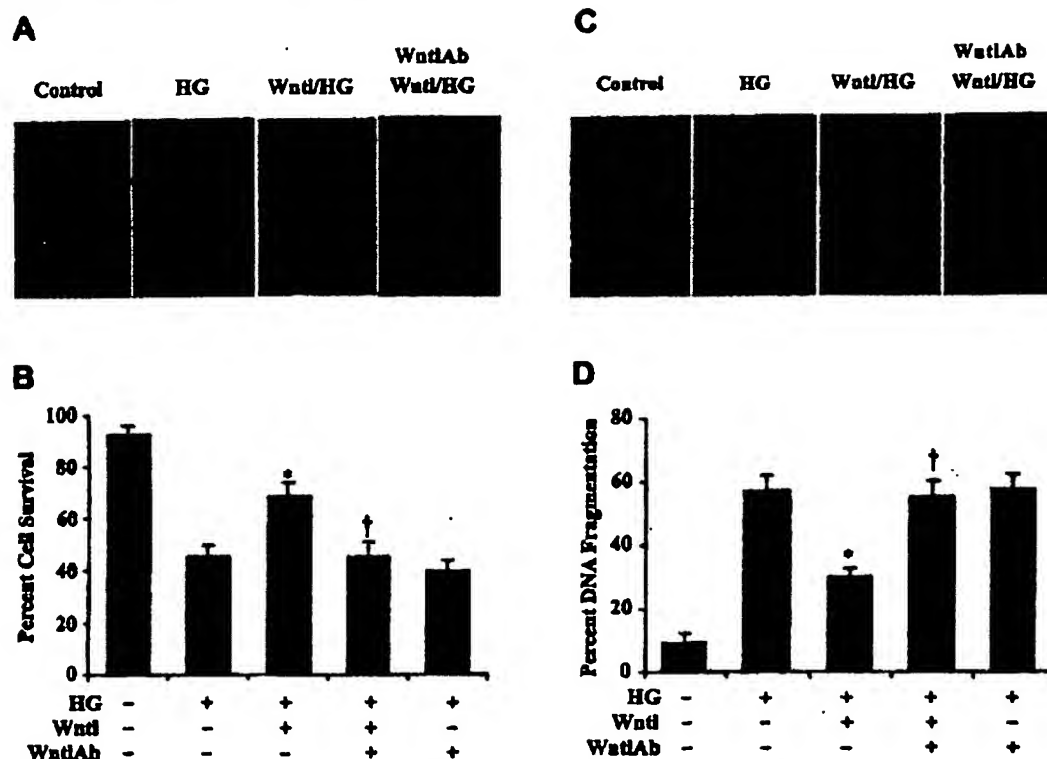


**Fig. (2).** Wnt1 fosters necessary cellular protection against elevated glucose in primary ECs. (A) Recombinant human Wnt1 protein (100 ng/ml) was applied to EC cultures 1 hour prior to the exposure of D-glucose (25 mM) (HG) and cell survival was determined 48 hours later. Representative images illustrate increased trypan blue staining during elevated glucose, but administration of Wnt1 significantly decreased trypan blue uptake by ECs. In contrast, application of Wnt1 antibody (Wnt1Ab, 1  $\mu$ g/ml) 30 min prior to the administration of Wnt1 protein antagonized the ability of Wnt1 to significantly reduce trypan blue uptake in ECs during elevated glucose exposure. (B) Wnt1 (100 ng/ml) administration significantly increased EC survival when compared with cultures exposed to elevated glucose alone (\* $p$ <0.01 vs. HG). In contrast, application of Wnt1 antibody (Wnt1Ab, 1  $\mu$ g/ml) 30 min prior to the administration of Wnt1 protein blocked Wnt1 cytoprotection in ECs during elevated glucose (\* $p$ <0.01 vs. Wnt1/HG). (C) Recombinant human Wnt1 protein (100 ng/ml) was administered to EC cultures 1 hour prior to the exposure of D-glucose (25 mM) (HG) and nuclear DNA fragmentation with TUNEL was determined 48 hours later. Representative images illustrate increased TUNEL staining during elevated glucose, but administration of Wnt1 significantly decreased TUNEL labeling in ECs. In contrast, application of Wnt1 antibody (Wnt1Ab, 1  $\mu$ g/ml) 30 min prior to the administration of Wnt1 protein antagonized the ability of Wnt1 to significantly reduce TUNEL labeling in ECs during elevated glucose exposure. (D) Wnt1 (100 ng/ml) administration significantly decreased EC nuclear DNA degradation when compared with cultures exposed to elevated glucose alone (\* $p$ <0.01 vs. HG). In contrast, application of Wnt1 antibody (Wnt1Ab, 1  $\mu$ g/ml) 30 min prior to the administration of Wnt1 protein prevented Wnt1 from reducing nuclear DNA degradation in ECs during elevated glucose (\* $p$ <0.01 vs. Wnt1/HG). In all cases, each data point represents the mean and SEM and control = untreated EC cultures.

contrast, EPO (10 ng/ml) during elevated D-glucose exposure significantly maintained the expression of Wnt1 over a 48 hour course, suggesting that EPO can prevent the degradation of Wnt1 during elevated glucose exposure (Fig. 4B).

EPO also modulated the expression of p-GSK-3 $\beta$  at the conserved regulatory residue of Ser<sup>9</sup> (Eldor-Finkelman, *et al.*, 1996). Elevated D-glucose also initially increased the expression of p-GSK-3 $\beta$  at 6 and 24 hours when compared to EC control cultures. After 24 hours post elevated glucose exposure, expression of p-GSK-3 $\beta$  was lost suggesting that p-GSK-3 $\beta$  activity was no longer inhibited (Figs. 4C, 4D). Yet, EPO (10 ng/ml) during elevated D-glucose exposure was able to maintain the inhibition of GSK-3 $\beta$  and signifi-

cantly promote the expression of p-GSK-3 $\beta$  over a 48 hour course (Fig. 4D).

#### Glycogen Synthase Kinase-3 $\beta$ (GSK-3 $\beta$ ) Activity Inhibition Confers Cytoprotection to ECs and Parallels Protection with EPO Application

Exposure to elevated D-glucose (25 mM) leads to EC injury 48 hours late (Figs. 5A, 5B). In contrast, application of the GSK-3 $\beta$  inhibitor (SB216763, SB21), 5  $\mu$ M 1 hour prior to elevated D-glucose exposure (25 mM) in concentrations consistent with the current literature (Yoshimura, *et al.*, 2005) increases EC survival. Furthermore, inhibition of GSK-3 $\beta$  activity alone or in combination with the applica-

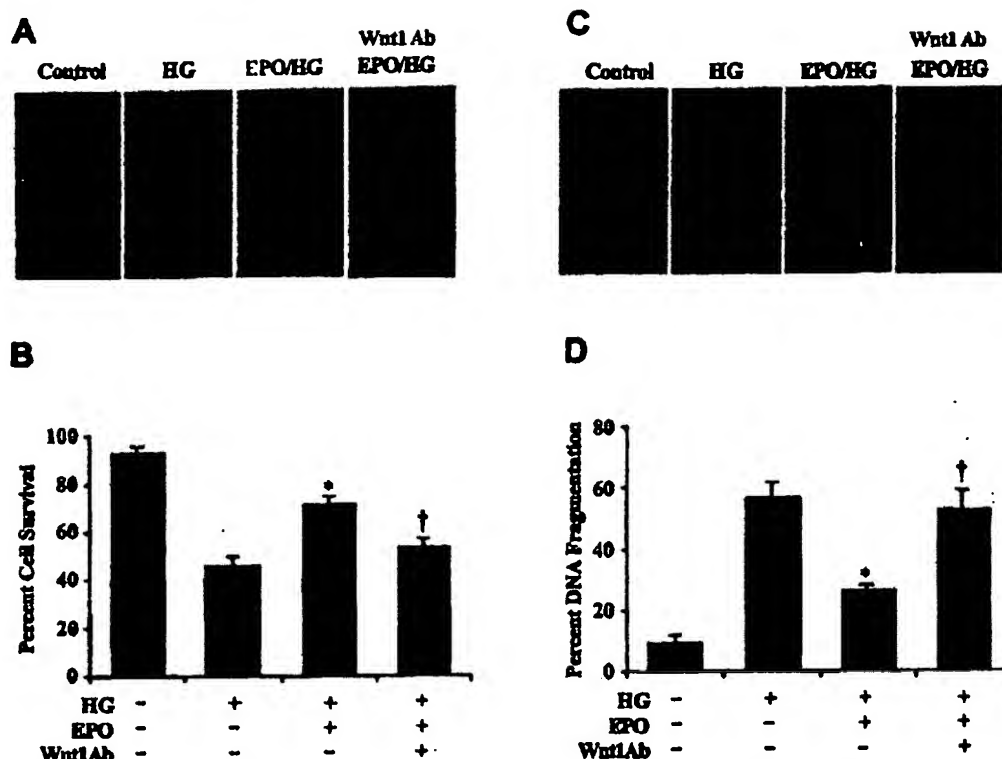


**Fig. (3).** Cytoprotection in ECs by EPO requires Wnt1 during elevated glucose exposure. (A) EPO (10 ng/ml) was applied to EC cultures 1 hour prior to the exposure of D-glucose (25 mM) (HG) and cell survival was determined 48 hours later. Representative images illustrate increased trypan blue staining during elevated glucose, but administration of EPO significantly decreased trypan blue uptake by ECs. In contrast, application of Wnt1 antibody (Wnt1Ab, 1 µg/ml) 30 min prior to the administration of EPO antagonized the ability of EPO to prevent trypan blue uptake in ECs during elevated glucose exposure. (B) EPO (10 ng/ml) application significantly increased EC survival when compared with cultures exposed to elevated glucose alone (\* $p < 0.01$  vs. HG). In contrast, application of Wnt1 antibody (Wnt1Ab, 1 µg/ml) 30 min prior to the EPO treatment blocked Wnt1 cytoprotection in ECs during elevated glucose ( $\dagger p < 0.01$  vs. EPO/HG). (C) EPO (10 ng/ml) was applied to EC cultures 1 hour prior to the exposure of D-glucose (25 mM) (HG) and nuclear DNA fragmentation with TUNEL was determined 48 hours later. Representative images illustrate increased TUNEL staining during elevated glucose, but administration of EPO significantly decreased nuclear DNA fragmentation as demonstrated by reduced TUNEL labeling in ECs. In contrast, application of Wnt1 antibody (Wnt1Ab, 1 µg/ml) 30 min prior to the administration of EPO prevented EPO from significantly reducing TUNEL labeling in ECs during elevated glucose exposure. (D) EPO (10 ng/ml) administration significantly decreased EC nuclear DNA degradation when compared with cultures exposed to elevated glucose alone (\* $p < 0.01$  vs. HG). In contrast, application of Wnt1 antibody (Wnt1Ab, 1 µg/ml) 30 min prior to EPO application prevented EPO from reducing nuclear DNA degradation in ECs during elevated glucose ( $\dagger p < 0.01$  vs. EPO/HG). In all cases, each data point represents the mean and SEM and control = untreated EC cultures.

tion of EPO (10 ng/ml) administered 1 hour prior to elevated D-glucose significantly increases EC survival during application of EPO alone or during co-administration with EPO, suggesting that EPO relies upon the inhibition of GSK-3 $\beta$  activity to provide EC cytoprotection. Increased EC survival during inhibition of GSK-3 $\beta$  activity was not altered by co-application of the Wnt1Ab, indicating that modulation of the GSK-3 $\beta$  activity to preserve EC survival occurs downstream from the initial activation of Wnt1 (Fig. 5A).

Similarly, application of the GSK-3 $\beta$  inhibitor (SB216763, (SB21), 5 µM 1 hour prior to elevated D-glucose exposure (25 mM) prevented EC apoptotic DNA fragmentation (Fig. 5C) assessed by TUNEL without evidence of a synergistic increase in protection against DNA fragmentation during co-

administration of EPO (10 ng/ml) (Fig. 5D), further supporting the premise that EPO utilizes inhibition of GSK-3 $\beta$  activity to prevent EC injury and apoptotic demise. In addition, EC apoptotic injury during inhibition of GSK-3 $\beta$  activity was not altered by co-application of the Wnt1Ab (Fig. 5D).

## DISCUSSION

EPO has been identified as a possible candidate for a number of disease entities that involve cardiac, nervous, and vascular system diseases (Maiese, *et al.*, 2004, Maiese, *et al.*, 2005c). In particular, EPO may have significant relevance for the treatment of vascular complications in DM in light of prior clinical studies illustrating that EPO can decrease fatigue and enhance cardiac output in patients with DM

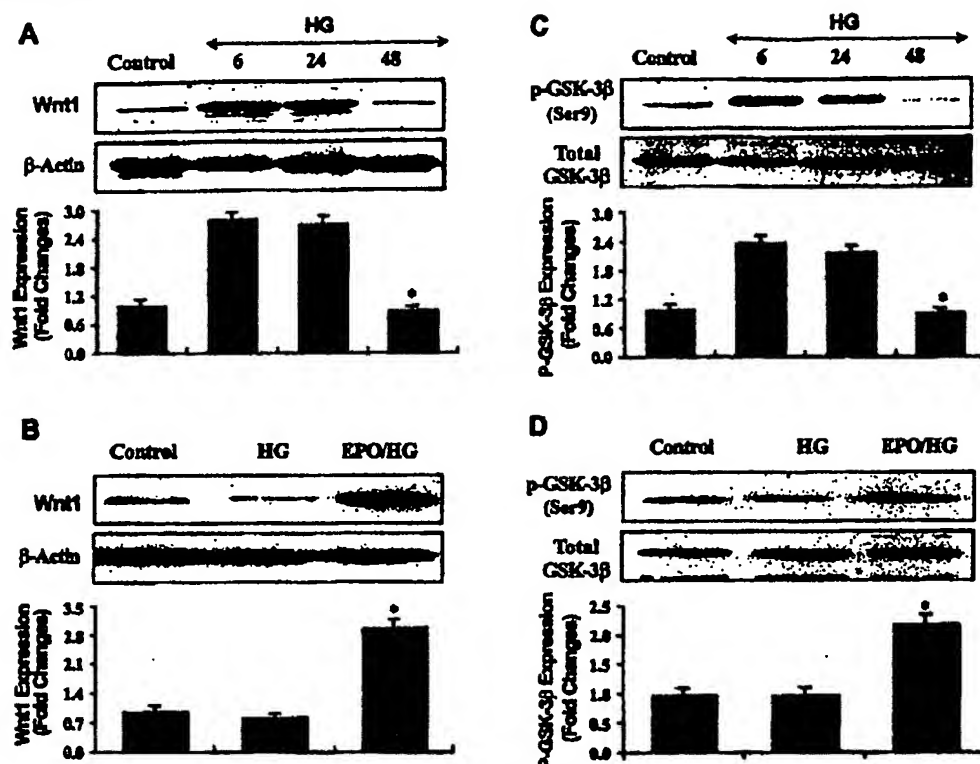


**Fig (4).** EPO modulates the expression of Wnt1 and phosphorylated glycogen synthase kinase-3 $\beta$  during elevated glucose exposure. EC protein extracts (50  $\mu$ g/lane) were immunoblotted with anti-Wnt1 (A and B), anti-phosphorylated glycogen synthase kinase-3 $\beta$  (anti-p-GSK-3 $\beta$ ) (C and D). Representative images of Western blot detection for Wnt1 (A) and p-GSK-3 $\beta$  (C) were performed at 6, 24, and 48 hour time intervals following administration of elevated D-glucose (25 mM) (HG). Wnt1 and p-GSK-3 $\beta$  expression increased at 6 and 24 hours following exposure to high glucose, but expression of these proteins was lost 48 hours following elevated glucose (\* $p$  < 0.01 vs. 6 hours or 24 hours HG). Application of EPO (10 ng/ml) 1 hour prior to the administration of elevated glucose significantly increased Wnt1 (B) (\* $p$  < 0.01 vs. HG) and p-GSK-3 $\beta$  (D) (\* $p$  < 0.01 vs. HG) expression 48 hours following elevated glucose treatment. In all cases, each data point represents the mean and SEM and control = untreated EC cultures.

(Silverberg, *et al.*, 2003). Protection by EPO in vascular cells may directly prevent cell toxicity during elevated glucose or modulate inflammatory pathways that ultimately lead to cellular disposal. For example, EPO not only can preserve microglial integrity (Li, *et al.*, 2006b), but it also can prevent microglial cell activation and proliferation to block phagocytosis of injured cells through pathways that involve early apoptotic cellular membrane phosphatidylserine exposure (Maiese, *et al.*, 2004, Maiese, *et al.*, 2005c).

Employing an elevated glucose model for ECs, we illustrate that a final glucose concentration of 25 mM over a 48 hour course leads to a significant loss in cell survival and correspondingly a significant increase in genomic DNA degradation when compared to control ECs. Our work also demonstrates that primary cerebral ECs are extremely sensitive to elevations in D-glucose that are similar to clinical glucose concentrations not only during poorly controlled diabetes (Pagano, *et al.*, 1994), but also during early clinical onset diabetes (Ryan, *et al.*, 2004) and during expected diurnal variations with diabetes (Troisi, *et al.*, 2000) known to

occur in a range from 15 mM-25 mM (270 mg/dl - 450 mg/dl). In addition, the application of the biologically inactive agent L-glucose (25 mM) as well as factors related to hyperosmolarity were not responsible for the observed neuronal injury (data not shown).

In regards to the ability of EPO to offer direct EC cell protection during elevated glucose of 25 mM, we demonstrate that EPO alone is not toxic to EC in a concentration of 10 ng/ml. Administration of EPO (10 ng/ml) with a 1 hour pre-treatment significantly enhanced EC survival during elevated glucose. EPO also blocked apoptotic DNA degradation in ECs during elevated glucose similar to alternate models of oxidative stress in cardiac and vascular cell models (Avasarala and Konduru, 2005, Chong, *et al.*, 2003a, Chong, *et al.*, 2002, Chong and Maiese, 2007, Moon, *et al.*, 2006). The concentration of EPO of 10 ng/ml that achieved cytoprotection in ECs during elevated glucose is similar to serum levels of EPO in patients with cardiac or renal disease that have been associated with potential EPO cellular protection (Mason-Garcia, *et al.*, 1990, Namiuchi, *et al.*, 2005) and

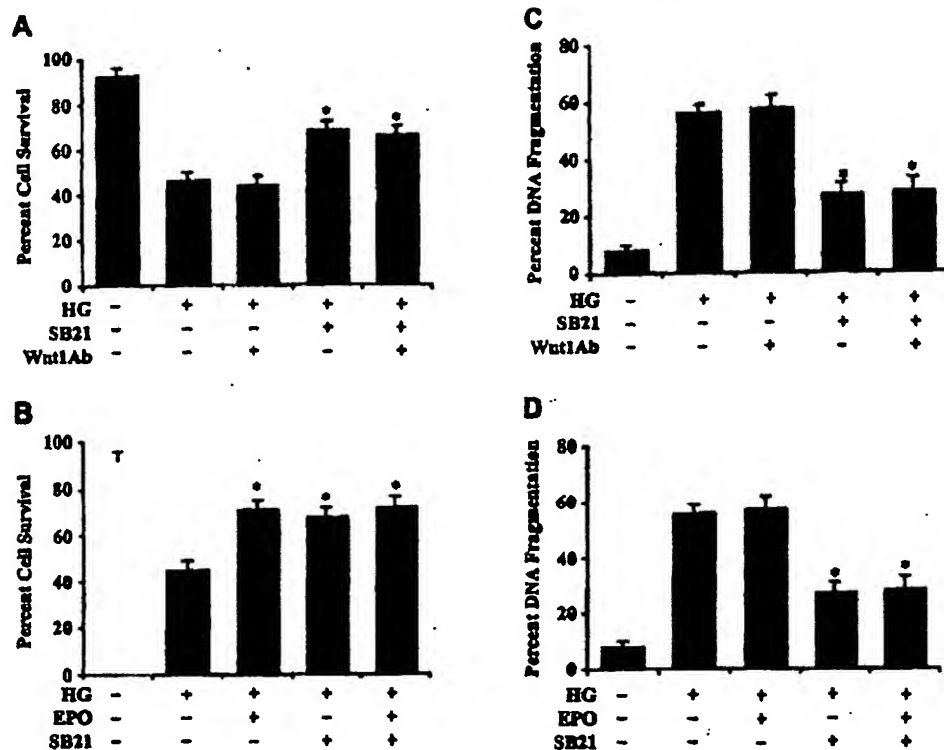


**Fig. (5).** EPO protects ECs during elevated glucose exposure by inhibiting glycogen synthase kinase-3 $\beta$  (GSK-3 $\beta$ ) activity. Primary ECs were exposed to elevated D-glucose (25 mM) (HG) and EC survival or nuclear DNA fragmentation were determined 48 hours following elevated glucose exposure. (A and C) Elevated glucose resulted in a significant decrease EC survival and a significant increase in nuclear DNA fragmentation in ECs. Application of the GSK-3 $\beta$  inhibitor SB21 (5  $\mu$ M) 1 hour prior to administration of elevated D-glucose significantly increased cell survival and decreased nuclear DNA fragmentation 48 hours following elevated glucose treatment (\* $p$ <0.01 vs. HG). Co-application of Wnt1 antibody (Wnt1Ab) did not alter the ability of SB21 to protect ECs during elevated glucose treatment (\* $p$ <0.01 vs. HG). (B and D) EPO (10 ng/ml) administered 1 hour prior to elevated D-glucose (25 mM) application significantly increased cell survival and decreased nuclear DNA fragmentation in ECs 48 hours following elevated glucose treatment (\* $p$ <0.01 vs. HG). Co-application of GSK-3 $\beta$  inhibitor SB21 with EPO significantly increased survival and decreased apoptotic nuclear DNA degradation during elevated glucose exposure, but lead to similar survival levels and DNA degradation during EPO administration alone with elevated glucose without a synergistic increase, suggesting that EPO requires the inhibition of GSK-3 $\beta$  activity for cytoprotection in ECs (\* $p$ <0.01 vs. HG alone). In all cases, each data point represents the mean and SEM and control = untreated EC cultures.

clinical protocols with EPO administration have been shown to significantly increase plasma EPO levels well above the 1.0 ng/ml range similar to experimental *in vitro* work and confer beneficial results (Bierer, *et al.*, 2006; Sohmiya, *et al.*, 1998).

EPO modulates a variety of signal transduction pathways for cytoprotection that can involve protein kinase B, signal transducer and activator of transcription pathways, forkhead transcription factors, caspases, and nuclear factor  $\kappa$ B (Bahlmann, *et al.*, 2004; Chong, *et al.*, 2003a; Chong, *et al.*, 2005a; Chong and Maiese, 2007; Menon, *et al.*, 2006; Urao, *et al.*, 2006), but pathways of EPO protection especially in the vascular system that rely upon Wnt signaling have not been previously described. Although clinical trials in patients with DM have suggested that EPO may improve cardiac function (Silverberg, *et al.*, 2003) or offer protection against complications in woman with diabetic pregnancies suggests

(Teramo, *et al.*, 2004), the cellular pathways responsible for EPO cytoprotection during DM are unknown. Prior work has suggested that Wnt family members may regulate glucose tolerance (Wright, *et al.*, 2007), adipose cell function (Kanazawa, *et al.*, 2004), and glomerular mesangial cells protection during elevated glucose (Lin, *et al.*, 2006). We show that endogenous activation of Wnt1 may offer a minimum level of protection during elevated glucose exposure, since application of the Wnt1Ab resulted in a slight increase in EC injury. Furthermore, administration of exogenous Wnt1 protein significantly increased EC survival and prevented apoptotic EC degeneration during elevated glucose exposure. More importantly, administration of the Wnt1Ab could neutralize the protective capacity of Wnt1, illustrating that Wnt1 is an important component in the cytoprotection of ECs during elevated glucose exposure. Interestingly, EPO cytoprotection in ECs during elevated glucose exposure also



relies upon Wnt1. EPO maintains the expression of Wnt1 over a 48 hour course during elevated glucose exposure and prevents loss of Wnt1 expression that would occur in the absence of EPO during elevated glucose. In addition, loss of EC protection with EPO during the administration of the Wnt1Ab demonstrates that Wnt1 is critical for EPO to protect against EC injury and apoptosis during elevated glucose.

EPO recently has been shown to block the activation of GSK-3 $\beta$  and employ this pathway to maintain microglial cell integrity during oxidative stress (Li, *et al.*, 2006b). Given that the GSK-3 $\beta$  pathway is a significant regulatory component during Wnt signaling (Chong, *et al.*, 2007a, Chong, *et al.*, 2005d, Maiese, *et al.*, 2007a) and that GSK-3 $\beta$  may influence beta cell survival (Mussmann, *et al.*, 2007) and cardioprotection (Yue, *et al.*, 2005) during DM, we examined whether the GSK-3 $\beta$  pathway played a role in EC injury and EPO cytoprotection during elevated glucose exposure. We demonstrate that GSK-3 $\beta$  becomes phosphorylated over a 24 hour course elevated glucose exposure, but that EPO in the presence of elevated glucose significantly maintains the inhibitory phosphorylation of GSK-3 $\beta$  over a 48 hour period following the initial exposure of elevated glucose. This inhibition of GSK-3 $\beta$  activity is closely linked to EC survival, since inhibition of GSK-3 $\beta$  activity during administration of the GSK-3 $\beta$  antagonist SB216763 (SB21) prevents EC injury and apoptotic cell loss during elevated glucose. Increased EC survival during inhibition of GSK-3 $\beta$  activity was not altered by the co-application of Wnt1Ab, suggesting that prevention of the GSK-3 $\beta$  activity to preserve EC survival occurs downstream from the initial activation of Wnt1. Finally, inhibition of GSK-3 $\beta$  activity during co-administration of EPO results in similar survival levels without a synergistic increase, also illustrating that EPO relies upon blockade of GSK-3 $\beta$  activity to offer cytoprotection in ECs during elevated glucose.

## ACKNOWLEDGEMENTS

This research was supported by the following grants (KM): American Diabetes Association, American Heart Association (National), Bugher Foundation Award, Janssen Neuroscience Award, LEARN Foundation Award, MI Life Sciences Challenge Award, Nelson Foundation Award, NIH NIEHS (P30 ES06639), and NIH NINDS/NIA.

## REFERENCES

- Abbott, NI, Hughes, CC, Revest, PA, Greenwood, J. (1992) Development and characterization of a rat brain capillary endothelial culture: towards an *in vitro* blood-brain barrier. *J Cell Sci* 103(Pt 1): 23-37.
- Abe, K, Takeichi, M. (2007) NMDA-receptor activation induces calpain-mediated beta-catenin cleavages for triggering gene expression. *Neuron* 53: 387-97.
- Avasthi, JR, Konduru, SS. (2005) Recombinant erythropoietin down-regulates IL-6 and CXCR4 genes in TNF-alpha-treated primary cultures of human microvascular endothelial cells: implications for multiple sclerosis. *J Mol Neurosci* 25: 183-9.
- Bahlmann, FH, Song, R, Boehm, SM, Mengel, M, von Wasielowski, R, Lindschau, C, Kinch, T, de Groot, K, Lande, R, Niemczyk, E, Guler, F, Maenn, J, Haller, H, Fliser, D. (2004) Low-dose therapy with the long-acting erythropoietin analogue darbepoetin alpha persistently activates endothelial Akt and attenuates progressive organ failure. *Circulation* 110: 1006-12.
- Balaraman, Y, Litaye, AR, Lovey, AL, Srinivasan, S. (2006) Glycogen synthase kinase 3beta and Alzheimer's disease: pathophysiological and therapeutic significance. *Cell Mol Life Sci* 63: 1226-35.
- Berent-Spillion, A, Russell, JW. (2007) Metabotropic glutamate receptor 3 protects neurons from glucose-induced oxidative injury by increasing intracellular glutathione concentration. *J Neurochem* 101: 342-54.
- Bierer, R, Peceny, MC, Hartenberger, CH, Ohls, RK. (2006) Erythropoietin concentrations and neurodevelopmental outcome in preterm infants. *Pediatrics* 118: e635-40.
- Bourat, JC, Brown, AM, Soler, AP. (2000) Wnt-1 dependent activation of the survival factor NF-kappaB in PC12 cells. *J Neurosci Res* 61: 21-32.
- Chong, ZZ, Kang, JQ, Maiese, K. (2003a) Apaf-1, Bcl-xL, cytochrome c, and caspase-9 form the critical elements for cerebral vascular protection by erythropoietin. *J Cereb Blood Flow Metab* 23: 320-30.
- Chong, ZZ, Kang, JQ, Maiese, K. (2003b) Erythropoietin fosters both intrinsic and extrinsic neuronal protection through modulation of microglia, Akt1, Bad, and caspase-mediated pathways. *Br J Pharmacol* 138: 1107-1118.
- Chong, ZZ, Kang, JQ, Maiese, K. (2002) Erythropoietin is a novel vascular protectant through activation of Akt1 and mitochondrial modulation of cysteine proteases. *Circulation* 106: 2973-9.
- Chong, ZZ, Li, F, Maiese, K. (2007a) Cellular demise and inflammatory microglial activation during beta-amyloid toxicity are governed by Wnt1 and canonical signaling pathways. *Cell Signal* 19: 1150-62.
- Chong, ZZ, Li, F, Maiese, K. (2005a) Erythropoietin requires NF-kappaB and its nuclear translocation to prevent early and late apoptotic neuronal injury during beta-amyloid toxicity. *Curr Neurovasc Res* 2: 387-99.
- Chong, ZZ, Li, F, Maiese, K. (2005b) Oxidative stress in the brain: Novel cellular targets that govern survival during neurodegenerative disease. *Prog Neurobiol* 75: 207-46.
- Chong, ZZ, Li, F, Maiese, K. (2005c) Stress in the brain: novel cellular mechanisms of injury linked to Alzheimer's disease. *Brain Res Brain Res Rev* 49: 1-21.
- Chong, ZZ, Li, F, Maiese, K. (2007b) The pro-survival pathways of mTOR and protein kinase B target glycogen synthase kinase-3beta and nuclear factor-kappaB to foster endogenous microglial cell protection. *Int J Mol Med* 19: 263-72.
- Chong, ZZ, Li, FQ, Maiese, K. (2005d) Employing new cellular therapeutic targets for Alzheimer's disease: A change for the better? *Curr Neurovasc Res* 2: 55-72.
- Chong, ZZ, Maiese, K. (2007) Erythropoietin involves the phosphatidylinositol 3-kinase pathway, 14-3-3 protein and FOXO3a nuclear trafficking to preserve endothelial cell integrity. *Br J Pharmacol* 150: 839-50.
- Chong, ZZ, Maiese, K. (2004) Targeting WNT, protein kinase B, and mitochondrial membrane integrity to foster cellular survival in the nervous system. *Histol Histopathol* 19: 495-504.
- Cohen, SM, Furey, TS, Doggett, NA, Kaufman, DG. (2006) Genome-wide sequence and functional analysis of early replicating DNA in normal human fibroblasts. *BMC Genomics* 7: 301.
- Daneman, D. (2006) Type 1 diabetes. *Lancet* 367: 847-58.
- Duarte, AI, Proenca, T, Oliveira, CR, Santos, MS, Rego, AC. (2006) Insulin restores metabolic function in cultured cortical neurons subjected to oxidative stress. *Diabetes* 55: 2863-70.
- Eldar-Finkels, H, Argant, GM, Foord, O, Fischer, EH, Krebs, EG. (1996) Expression and characterization of glycogen synthase kinase-3 mutants and their effect on glycogen synthase activity in intact cells. *Proc Natl Acad Sci USA* 93: 10223-33.
- Grant, SF, Thorleifsson, O, Reynisdottir, I, Benediktsson, R, Manolescu, A, Sainz, J, Helgason, A, Stefansson, H, Emilsson, V, Helgadóttir, A, Styrtisdóttir, U, Magnusson, KP, Walters, GB, Paladóttir, B, Jónsdóttir, T, Gudmundsdóttir, T, Olfsson, A, Saemundsdóttir, J, Wilensky, RL, Reilly, MP, Rader, DJ, Bagger, Y, Christensen, C, Gudason, V, Sigurdsson, O, Thorsteinsdóttir, U, Gulcher, JR, Kong, A, Stefansson, K. (2006) Variant of transcription factor 7-like 2 (TCF7L2) gene confers risk of type 2 diabetes. *Nat Genet* 38: 320-3.
- Guo, YF, Xiang, DH, Shen, H, Zhao, LJ, Xiao, P, Qiao, Y, Wang, W, Yang, TL, Recker, RR, Deng, HW. (2006) Polymorphisms of the low-density lipoprotein receptor-related protein 5 (LRP5) gene are associated with obesity phenotypes in a large family-based association study. *J Med Genet* 43: 791-803.
- Ha, B, Reguart, N, You, L, Mazzetta, J, Xu, Z, Lee, AY, Mikami, I, McCormick, F, Jablons, DM. (2005) Blockade of Wnt-1 signaling induces apoptosis in human colorectal cancer cells containing downstream mutations. *Oncogene* 24: 3054-8.
- Henry, DH, Bowers, P, Romano, MT, Provenzano, R. (2004) Epoetin alfa. Clinical evolution of a pleiotropic cytokine. *Arch Intern Med* 164: 262-76.
- Howlett, KP, Sakamoto, K, Yu, H, Goodyear, LJ, Hargreaves, M. (2006) Insulin-stimulated insulin receptor substrate-2-associated phosphatidy-



## Erythropoietin, Hypertension, and Wnt

- inositol 3-kinase activity is enhanced in human skeletal muscle after exercise. *Metabolism* 55: 1046-52.
- Huber, JD, VanGilder, RL, Houser, KA. (2006) Streptozotocin-induced diabetes progressively increases blood-brain barrier permeability in specific brain regions in rats. *Am J Physiol Heart Circ Physiol* 291: H2660-8.
- Jozwiak, J, Kotulska, K, Grzjokowska, W, Jozwiak, S, Zalewski, W, Oldak, M, Lejek, M, Rainko, K, Maksym, R, Lazarczyk, M, Skopinski, P, Wlodarski, P. (2007) Upregulation of the WNT pathway in tuberous sclerosis-associated subependymal giant cell astrocytomas. *Brain Dev* 29: 273-80.
- Kanazawa, A, Tsukada, S, Sekine, A, Tsunoda, T, Takahashi, A, Kashiwagi, A, Tanaka, Y, Babazono, T, Matsuda, M, Kaku, K, Iwamoto, Y, Kawamori, R, Kikawa, R, Nakamura, Y, Maeda, S. (2004) Association of the gene encoding wingless-type mammary tumor virus integration-site family member 5B (WNT5B) with type 2 diabetes. *Am J Hum Genet* 75: 832-43.
- Laakso, M. (2001) Cardiovascular disease in type 2 diabetes: challenges for treatment and prevention. *J Intern Med* 249: 225-33.
- Li, F, Chong, ZZ, Maiese, K. (2006a) Cell Life Versus Cell Longevity: The Mysteries Surrounding the NAD(+) Precursor Nicotinamide. *Curr Med Chem* 13: 883-95.
- Li, F, Chong, ZZ, Maiese, K. (2004) Erythropoietin on a Tightrope: Balancing Neuronal and Vascular Protection between Intrinsic and Extrinsic Pathways. *Neuroscience* 13: 265-89.
- Li, F, Chong, ZZ, Maiese, K. (2006b) Microglial integrity is maintained by erythropoietin through integration of Akt and its substrates of glycogen synthase kinase-3beta, beta-catenin, and nuclear factor-kappaB. *Curr Neurovasc Res* 3: 187-201.
- Li, F, Chong, ZZ, Maiese, K. (2005) Vital elements of the wnt-5zid signaling pathway in the nervous system. *Curr Neurovasc Res* 2: 331-40.
- Li, F, Chong, ZZ, Maiese, K. (2006c) Winding through the WNT pathway during cellular development and demise. *Histol Histopathol* 21: 103-24.
- Lin, CL, Wang, JY, Huang, YT, Kuo, YH, Surendran, K, Wang, FS. (2006) Wnt/beta-catenin signaling modulates survival of high glucose-stressed mesangial cells. *J Am Soc Nephrol* 17: 2812-20.
- Maiese, K, Chong, ZZ, Li, F. (2005a) Driving cellular plasticity and survival through the signal transduction pathways of metabotropic glutamate receptors. *Curr Neurovasc Res* 2: 425-46.
- Maiese, K, Chong, ZZ, Shang, YC. (2007a) Mechanistic insights into diabetes mellitus and oxidative stress. *Curr Med Chem* 14: 1689-1699.
- Maiese, K, Li, F, Chong, ZZ. (2005b) Erythropoietin and cancer. *JAMA* 293: 1858-1859.
- Maiese, K, Li, F, Chong, ZZ. (2004) Erythropoietin in the brain: can the promise to protect be fulfilled? *Trends Pharmacol Sci* 25: 577-583.
- Maiese, K, Li, F, Chong, ZZ. (2005c) New avenues of exploration for erythropoietin. *JAMA* 293: 90-3.
- Maiese, K, Morhan, SD, Chong, ZZ. (2007b) Oxidative stress biology and cell injury during type 1 and type 2 diabetes mellitus. *Curr Neurovasc Res* 4: 63-71.
- Malorana, A, O'Driscoll, G, Goodman, C, Taylor, R, Green, D. (2002) Combined aerobic and resistance exercise improves glycaemic control and fitness in type 2 diabetes. *Diabetes Res Clin Pract* 56: 115-23.
- Mason-Garcia, M, Beckman, BS, Brookins, JW, Powell, JS, Lanham, W, Blaisdell, S, Keay, L, Li, SC, Fisher, JW. (1990) Development of a new radioimmunoassay for erythropoietin using recombinant erythropoietin. *Kidney Int* 38: 969-75.
- Menon, MP, Karur, V, Bogachava, O, Bogachov, O, Cusum, B, Wojchowski, DM. (2006) Signals for stress erythropoiesis are integrated via an erythropoietin receptor-phosphotyrosine-343-Stat5 axis. *J Clin Invest* 116: 683-94.
- Mikati, MA, Hokeney, JA, Sabban, ME. (2007) Effects of a single dose of erythropoietin on subsequent seizure susceptibility in rats exposed to acute hypoxia at p10. *Epilepsia* 48: 175-81.
- Mojumilly, OA, Abdella, NA, Zaki, MY, El Gebely, SA, Mohamedi, HM, Aldhahi, WA. (2006) Prevalence and associations of low plasma erythropoietin in patients with type 2 diabetes mellitus. *Diabet Med* 23: 839-44.
- Moon, C, Krawczyk, M, Paik, D, Coleman, T, Brines, M, Juhászová, M, Sollett, SJ, Lakatta, EG, Talan, MI. (2006) Erythropoietin, modified to not stimulate red blood cell production, retains its cardioprotective properties. *J Pharmacol Exp Ther* 316: 999-1005.
- Musmann, R, Geese, M, Harder, F, Kegel, S, Andag, U, Lomow, A, Burk, U, Onitschek, D, Dohrmann, C, Austen, M. (2007) Inhibition of glycogen synthase kinase (GSK) 3 promotes replication and survival of pancreatic beta cells. *J Biol Chem* 282: 12030-7.
- Namuchi, S, Kagaya, Y, Ohta, J, Shiba, N, Sugi, M, Oikawa, M, Kunii, H, Yamao, H, Komatsu, N, Yui, M, Tada, H, Sakuma, M, Watanabe, J, Ichihara, T, Shirato, K. (2005) High serum erythropoietin level is associated with smaller infarct size in patients with acute myocardial infarction who undergo successful primary percutaneous coronary intervention. *J Am Coll Cardiol* 45: 1406-12.
- Niwa, Y, Abumiya, T, Shichinohe, H, Kuroda, S, Kikuchi, S, Ieko, M, Yamagishi, S, Takeuchi, M, Sato, T, Iwasaki, Y. (2006) Susceptibility of brain microvascular endothelial cells to advanced glycation end products-induced tissue factor upregulation is associated with intracellular reactive oxygen species. *Brain Res* 1100: 179-87.
- Nurmi, A, Goldstein, G, Narvainen, J, Pihlaja, R, Ahtola, T, Grohn, O, Koistinen, J. (2006) Antioxidant pyrrolidine dithiocarbamate activates Akt-GSK signaling and is neuroprotective in neonatal hypoxia-ischemia. *Free Radic Biol Med* 40: 1776-84.
- Pagano, G, Barger, G, Vuolo, A, Bruno, G. (1994) Prevalence and clinical features of known type 2 diabetes in the elderly: a population-based study. *Diabet Med* 11: 475-9.
- Quina, L. (2001) Type 2 diabetes: epidemiology, pathophysiology, and diagnosis. *Nurs Clin North Am* 36: 175-92, v.
- Rhee, CS, Sen, M, Lu, D, Wu, C, Leoni, L, Rubin, J, Cori, M, Carson, DA. (2002) Wnt and frizzled receptors as potential targets for immunotherapy in head and neck squamous cell carcinomas. *Oncogene* 21: 6598-605.
- Ryan, EA, Innes, S, Wallace, C. (2004) Short-term intensive insulin therapy in newly diagnosed type 2 diabetes. *Diabetes Care* 27: 1028-32.
- Santhanam, AV, Katske, ZS. (2006) Erythropoietin and cerebral vascular protection: role of nitric oxide. *Acta Pharmacol Sin* 27: 1389-94.
- Saydah, SH, Pradkin, J, Cowie, CC. (2004) Poor control of risk factors for vascular disease among adults with previously diagnosed diabetes. *JAMA* 291: 335-42.
- Schneider, Boeri, M, Goldbourt, U, Silverman, JM, Noy, S, Schneider, J, Ravona-Springer, R, Sverdluk, A, Davidson, M. (2004) Diabetes mellitus in midlife and the risk of dementia three decades later. *Neurology* 63: 1902-7.
- Schumann, C, Triantafyllou, K, Krueger, S, Hombach, V, Triantafyllou, M, Becher, G, Lepper, PM. (2006) Detection of erythropoietin in exhaled breath condensate of normoxic subjects using a multiplex bead array. *Mediators Inflamm* 2006: 18061.
- Silverberg, DS, Wexler, D, Blum, M, Tchobiner, JZ, Sheps, D, Koren, G, Schwartz, D, Baruch, R, Yachnia, T, Shaked, M, Schwartz, I, Steinbruch, S, Iaina, A. (2003) The effect of correction of anemia in diabetics and non-diabetics with severe resistant congestive heart failure and chronic renal failure by subcutaneous erythropoietin and intravenous iron. *Nephrol Dial Transplant* 18: 141-6.
- Silverberg, DS, Wexler, D, Iaina, A, Steinbruch, S, Wellman, Y, Schwartz, D. (2006) Anemia, chronic renal disease and congestive heart failure—the cardio renal anemia syndrome: the need for cooperation between cardiologists and nephrologists. *Int Urol Nephrol* 38: 295-310.
- Sohniya, M, Kakiba, T, Kato, Y. (1998) Therapeutic use of continuous subcutaneous infusion of recombinant human erythropoietin in malnourished predialysis anemic patients with diabetic nephropathy. *Eur J Endocrinol* 139: 367-70.
- Symeonidis, A, Kourkili-Symeonidis, A, Paboyiannis, A, Leontiadis, M, Kyriazopoulou, V, Vasiliakos, P, Vaganakis, A, Zourabos, N. (2006) Inappropriately low erythropoietin response for the degree of anemia in patients with noninsulin-dependent diabetes mellitus. *Ann Hematol* 85: 79-85.
- Teramo, K, Karl, MA, Eronen, M, Markkanen, H, Hillemaa, V. (2004) High amniotic fluid erythropoietin levels are associated with an increased frequency of fetal and neonatal morbidity in type 1 diabetic pregnancies. *Diabetologia* 47: 1695-703.
- Thomas, MC, Cooper, ME, Tsalamandris, C, Meacham, R, Jerrome, G. (2005) Anemia with impaired erythropoietin response in diabetic patients. *Arch Intern Med* 165: 466-9.
- Troisi, RJ, Cowie, CC, Harris, MI. (2000) Diurnal variation in fasting plasma glucose: implications for diagnosis of diabetes in patients examined in the afternoon. *JAMA* 284: 3157-9.
- Um, M, Gross, AW, Lodish, HF. (2007) A "classical" homodimeric erythropoietin receptor is essential for the antiproliferative effects of erythropoietin on differentiated neuroblastoma SH-SY5Y and pheochromocytoma PC-12 cells. *Cell Signal* 19: 634-43.
- Urso, N, Ohiguchi, M, Yamada, H, Adachi, Y, Matsuno, K, Matsui, A, Matsumaga, S, Tazaihi, K, Nomura, T, Takahashi, T, Tsumi, T, Ma-

- trubars, H. (2006) Erythropoietin-mobilized endothelial progenitors enhance reendothelialization via Akt-endothelial nitric oxide synthase activation and prevent neointimal hyperplasia. *Circ Res* 98: 1405-13.
- van der Meer, P, Voorz, AA, Lipsic, E, Smilde, TD, van Gilst, WH, van Veldhuisen, DJ. (2004) Prognostic value of plasma erythropoietin on mortality in patients with chronic heart failure. *J Am Coll Cardiol* 44: 63-7.
- Wang, H, MacNaughton, WK. (2005) Overexpressed beta-catenin blocks nitric oxide-induced apoptosis in colonic cancer cells. *Cancer Res* 65: 8604-7.
- Wright, WS, Longo, KA, Dollinsky, VW, Gerin, I, Kang, S, Bennett, CN, Chiang, SH, Prestwich, TC, Gress, C, Burant, CF, Sasulic, VS, McDougald, OA. (2007) Wnt10b inhibits Obesity in ob/ob and Agouti Mice. *Diabetes* 56: 295-303.
- Yoshimura, T, Kawano, Y, Arimura, N, Kawabata, S, Kikuchi, A, Kaibuchi, K. (2005) GSK-3beta regulates phosphorylation of CRMP-2 and neuronal polarity. *Cell* 120: 137-49.
- You, L, Ha, B, Uematsu, K, Xu, Z, Mazieres, J, Lee, A, McCormick, F, Jablon, DM. (2004) Inhibition of Wnt-1 signaling induces apoptosis in beta-catenin-deficient mesothelioma cells. *Cancer Res* 64: 3474-8.
- Yue, TL, Bao, W, Gu, JL, Cui, J, Tao, L, Ma, XL, Ohlstein, EH, Jucker, BM. (2005) Rosiglitazone treatment in Zucker diabetic Fatty rats is associated with ameliorated cardiac insulin resistance and protection from ischemia/reperfusion-induced myocardial injury. *Diabetes* 54: 554-62.

# Current Neurovascular Research

Volume 4, Number 3, August 2007

## Contents

- Exciting News from the Messenger 152  
*K. Malese*

### ORIGINAL ARTICLES

- Safety Analysis and Improved Cardiac Function Following Local Autologous Transplantation of CD133<sup>+</sup> Enriched Bone Marrow Cells After Myocardial Infarction 153  
*H. Ahmadi, H. Baharvand, S.K. Ashtiani, M. Soleimani, H. Sadeghian, J.M. Ardekani, N.Z. Mehrjerdi, A. Kouhkan, M. Namiri, M. Madani-Civi, F. Fattahi, A. Shahverdi and A.V. Dizaji*
- Cerebral Aneurysm Formation in Nitric Oxide Synthase-3 Knockout Mice 161  
*T. Abruzzo, A. Kendler, R. Apkarian, M. Workman, J.C. Khoury and H.J. Cloft*
- Neurohormonal Activation in Ischemic Stroke: Effects of Acute Phase Disturbances on Long-Term Mortality 170  
*M. Anne, K. Juha, M. Timo, T. Mikko, V. Olli, S. Kyösti, H. Heikki and M. Vilho*
- A Non-Steroidal Anti-Inflammatory Agent Provides Significant Protection During Focal Ischemic Stroke with Decreased Expression of Matrix Metalloproteinases 176  
*Y. Wang, X.-L. Deng, X.-H. Xiao and B.-X. Yuan*
- Effects of Thyroid Hormones on Memory and on Na<sup>+</sup>, K<sup>+</sup>-ATPase Activity in Rat Brain 184  
*E.A. dos Reis-Lunardelli, C.C. Castro, C. Bavaresco, A.S. Coitinho, L.S.S. da Trindade, M.F. Perrenoud, R. Roesler, J.J.F. Sarkis, A.T. de Souza Wyse and I. Izquierdo*
- Vascular Injury During Elevated Glucose can be Mitigated by Erythropoietin and Wnt Signaling 194  
*Z.Z. Chong, Y.C. Shang and K. Malese*

### REVIEW ARTICLES

- Physiology and Pathophysiology of Na<sup>+</sup>/H<sup>+</sup> Exchange Isoform 1 in Central the Nervous System 205  
*J. Luo and D. Sun*
- The Response of the Aged Brain to Stroke: Too Much, Too Soon? 216  
*A. Popa-Wagner, S.T. Carmichael, Z. Kokata, C. Kessler and L.C. Walker*

This is to acknowledge that the cover image was graciously supplied by Hossein Baharvand and colleagues. The image is a representation of a myocardial perfusion scan in a patient with transplanted autologous CD133<sup>+</sup> bone marrow cells six months following coronary artery bypass grafting.

## Aims and Scope

**Current Neurovascular Research (CNR)** provides a cross platform for the publication of scientifically rigorous research that addresses disease mechanisms of both neuronal and vascular origins in neuroscience. The journal serves as an international forum for the publication of novel and pioneering original work as well as timely neuroscience research reviews in the disciplines of cell developmental disorders, plasticity, and degeneration that bridge the gap between basic science research and clinical discovery. CNR emphasizes the elucidation of disease mechanisms, both cellular and molecular, that can impact the development of unique therapeutic strategies for neuronal and vascular disorders.

---

### *Journal Instructions for Authors*

For the journal Instructions for Authors please refer either to the first published issue of each year or the journal's website at [www.bentham.org](http://www.bentham.org)

### *Multiple Journal Subscriptions & Global Online Licenses*

For multiple journal subscriptions, possible discounts and global online licenses please contact our special sales department at E-mail: [subscriptions@bentham.org](mailto:subscriptions@bentham.org)

### *Advertising*

To place an advertisement in this journal please contact the advertising department at E-mail: [ads@bentham.org](mailto:ads@bentham.org)

### *Journal Sample Copies*

A free online sample issue can be viewed at the journal's internet homepage. Alternatively a free print sample issue may be requested, please send your request to E-mail: [sample.copy@bentham.org](mailto:sample.copy@bentham.org)

Copyright © 2007 Bentham Science Publishers Ltd.

It is a condition of this publication that manuscripts submitted to this journal have not been published and will not be simultaneously submitted or published elsewhere. By submitting a manuscript, the authors agree that the copyright for their article is transferred to the Publisher if and when the article is accepted for publication. The copyright covers the exclusive rights to reproduce and distribute the article, including reprints, photographic reproductions, microform or any other reproduction of similar nature, and translations. All rights reserved: no part of this publication may be reproduced, stored in a retrieval system, or transmitted in any form or by any means, on-line, mechanical, photocopying, recording or otherwise, without the prior written permission of the Publisher.

### *Photocopying Information for Users in the USA*

Authorization to photocopy items for internal or personal use, or the internal or personal use of specific clients, is granted by Bentham Science Publishers Ltd. for libraries and other users registered with the Copyright Clearance Center (CCC) Transactional Reporting Services, provided that the appropriate fee of US\$ 50.00 per copy per article is paid directly to Copyright Clearance Center, 222 Rosewood Drive, Danvers MA 01923, USA. Refer also to [www.copyright.com](http://www.copyright.com)

### *Photocopying Information for Users Outside the USA*

Bentham Science Publishers Ltd. grants authorization for individuals to photocopy copyright material for private research use, on the sole basis that requests for such use are referred directly to the requestor's local Reproduction Rights Organization (RRO). The copyright fee is US\$ 50.00 per copy per article exclusive of any charge or fee levied. In order to contact your local RRO, please contact the International Federation of Reproduction Rights Organizations (IFRRO), Rue du Prince Royal 87, B-1050 Brussels, Belgium; Tel: +32 2 551 08 99; Fax: +32 2 551 08 95; E-mail: [secretariat@ifrro.be](mailto:secretariat@ifrro.be) This authorization does not extend to any other kind of copying by any means, in any form, and for any purpose other than private research use.

The Item-Fee Code for this publication is: 1567-2026/07 \$50.00 + .00

### *Online Articles*

This publication is available online from IngentaConnect at [www.ingentaconnect.com](http://www.ingentaconnect.com) Individual articles are also available for sale online via Infotrieve at [www.infotrieve.com](http://www.infotrieve.com) or from Ingenta at [www.ingentaconnect.com](http://www.ingentaconnect.com)

### *Permission for Other Use*

The Publisher's consent does not extend to copying for general distribution, for promotion, for creating new works, or for resale. Specific permission must be obtained from the Publisher for such copying. Requests must be sent to the permissions department at E-mail: [permission@bentham.org](mailto:permission@bentham.org)

### *Disclaimer*

No responsibility is assumed by Bentham Science Publishers Ltd., its staff or members of the editorial board for any injury and/or damage to persons or property as a matter of products liability, negligence or otherwise, or from any use or operation of any methods, products instruction, advertisements or ideas contained in this publication/journal. Any dispute will be governed exclusively by the laws of the U.A.E. and will be settled exclusively by the competent Court at the city of Dubai, U.A.E.

**Claudio Contaldo, Christoph Meier, Ahmed Elsherbiny, Yves Harder, Otmar Trentz, Michael D. Menger and Guido A. Wanner**

*Am J Physiol Heart Circ Physiol* 293:274-283, 2007. First published Mar 2, 2007;  
doi:10.1152/ajpheart.01031.2006

**You might find this additional information useful...**

This article cites 40 articles, 19 of which you can access free at:

<http://ajpheart.physiology.org/cgi/content/full/293/1/H274#BIBL>

Updated information and services including high-resolution figures, can be found at:

<http://ajpheart.physiology.org/cgi/content/full/293/1/H274>

Additional material and information about *AJP - Heart and Circulatory Physiology* can be found at:

<http://www.the-aps.org/publications/ajpheart>

This information is current as of February 14, 2008 .

Downloaded from ajpheart.physiology.org on February 14, 2008

*AJP - Heart and Circulatory Physiology* publishes original investigations on the physiology of the heart, blood vessels, and lymphatics, including experimental and theoretical studies of cardiovascular function at all levels of organization ranging from the intact animal to the cellular, subcellular, and molecular levels. It is published 12 times a year (monthly) by the American Physiological Society, 9650 Rockville Pike, Bethesda MD 20814-3991. Copyright © 2005 by the American Physiological Society. ISSN: 0363-6135, ESN: 1522-1539. Visit our website at <http://www.the-aps.org/>.

## Human recombinant erythropoietin protects the striated muscle microcirculation of the dorsal skinfold from postischemic injury in mice

Claudio Contaldo,<sup>1,2</sup> Christoph Meier,<sup>2</sup> Ahmed Elsherbiny,<sup>2</sup> Yves Harder,<sup>1</sup> Otmar Trentz,<sup>2</sup> Michael D. Menger,<sup>1</sup> and Guido A. Wanner<sup>2</sup>

<sup>1</sup>Institute for Clinical and Experimental Surgery, University of Saarland, Hamburg/Saar, Germany; and <sup>2</sup>Division of Trauma Surgery, University Hospital Zurich, Zurich, Switzerland

Submitted 20 September 2006; accepted in final form 28 February 2007

Contaldo C, Meier C, Elsherbiny A, Harder Y, Trentz O, Menger MD, Wanner GA. Human recombinant erythropoietin protects the striated muscle microcirculation of the dorsal skinfold from postischemic injury in mice. *Am J Physiol Heart Circ Physiol* 293: H274–H283, 2007. First published March 2, 2007; doi:10.1152/ajpheart.01031.2006.—Erythropoietin (EPO) has been proposed as a novel cytoprotectant in ischemia-reperfusion (I/R) injury of the brain, heart, and kidney. However, whether EPO exerts its protection by prevention of postischemic microcirculatory deterioration is unknown. We have investigated the effect of EPO on I/R-induced microcirculatory dysfunctions. We used the mouse dorsal skinfold chamber preparation to study nutritive microcirculation and leukocyte-endothelial cell interaction in striated muscle of the dorsal skinfold by in vivo fluorescence microscopy before 3 h of ischemia and during 5 days of reperfusion. Animals were pretreated with EPO (5,000 U/kg body wt) 1 or 24 h before ischemia. Vehicle-treated I/R-injured animals served as controls. Additional animals underwent sham operation only or were pretreated with EPO but not subjected to I/R. I/R significantly ( $P < 0.05$ ) reduced functional capillary density, increased microvascular permeability, and enhanced venular leukocyte-endothelial cell interaction during early reperfusion. These findings were associated with pronounced ( $P < 0.05$ ) arteriolar constriction and diminution of blood flow during late reperfusion. Pretreatment with EPO induced EPO receptor and endothelial nitric oxide synthase expression at 6 h of reperfusion ( $P < 0.05$ ). In parallel, EPO significantly ( $P < 0.05$ ) reduced capillary perfusion failure and microvascular hyperpermeability during early reperfusion and arteriolar constriction and flow during late reperfusion. EPO pretreatment substantially ( $P < 0.05$ ) diminished I/R-induced leukocytic inflammation by reducing the number of rolling and firmly adhering leukocytes in postcapillary venules. EPO applied 1 h before ischemia induced angiogenic budding and sprouting at 1 and 3 days of reperfusion and formation of new capillary networks at 5 days of reperfusion. Thus our study demonstrates for the first time that EPO effectively attenuates I/R injury by preserving nutritive perfusion, reducing leukocytic inflammation, and inducing new vessel formation.

ischemia-reperfusion; microcirculation; leukocyte-endothelial cell interaction; microvascular permeability; intravital microscopy; angiogenesis; neovascularization

ISCHEMIA-REPERFUSION (I/R) injury represents a major challenge in cardiovascular medicine and also in trauma and vascular and plastic and reconstructive surgery. The deleterious effects of I/R injury are mediated by microcirculatory dysfunctions, including breakdown of capillary perfusion (27, 28), chemotactic accumulation and venular wall adhesion of activated leukocytes (23, 26, 37), and loss of the integrity of the microvascular

endothelial lining (20, 26). In trauma and reconstructive surgery, as well as in transplantation medicine, elective surgical procedures involve prolonged periods of ischemia, which additionally enhance tissue injury during postischemic reperfusion. Although experimental studies have provided evidence that a variety of compounds, such as oxygen radical scavengers and anti-inflammatory drugs (15), reduce I/R injury, pharmacological treatment of reperfusion injury has not been successfully established in clinical practice.

Erythropoietin (EPO) is well known for its stimulatory function on erythrocytic progenitors. However, when administered exogenously, EPO represents a viability and growth factor that exerts neuroprotective (16), cardioprotective (1, 33, 38), and vascular actions (12). Accordingly, it is intensively investigated for its nonhematopoietic pleiotropic actions, which may be responsible for tissue protection (7).

EPO is a renal glycoprotein that is released in response to hypoxia and exerts its effect through its interaction with EPO receptors. Besides an increase of intracellular calcium, the main signaling pathways of hematopoietic cells involve 1) expression of the antiapoptotic protein Bcl-x, 2) activation of MAPK and phosphatidylinositol 3-kinase (PI3K/Akt), and 3) activation of transcription factor 5 for survival, proliferation, and migration of stimulated cells (2, 11, 25, 31).

The effect of EPO on the vascular endothelium is poorly understood. There is some evidence derived from isolated human vessel preparations that EPO modifies endothelial nitric oxide (NO) synthase (eNOS) expression and vascular functions, because it stimulated NO-mediated endothelium-dependent relaxation of arterial vessels (32). EPO may induce endothelial cell responses by EPO receptor and eNOS expression as well as NO release, in particular under hypoxic conditions (6). On the other hand, EPO may have a deleterious effect within the microvasculature, because it mediates prothrombotic mechanisms, such as endothelin-1 (10) and plasminogen activator inhibitor-1 induction (29).

Previous studies have reported that EPO effectively reduces I/R injury in the brain (34), heart (9), and kidney (35). However, whether EPO exerts its protection in I/R injury by preventing postischemic microcirculatory deterioration is unknown. Because it is well known that microcirculatory dysfunction plays a pivotal role in the manifestation of I/R injury (15, 27), we have investigated whether EPO affects I/R-induced microcirculatory deterioration, including capillary perfusion failure, leukocyte-endothelial cell interac-

Address for reprint requests and other correspondence: C. Contaldo, Division of Plastic, Reconstructive and Aesthetic Surgery, Univ. Hospital Zurich, CH-8091 Zurich, Switzerland (e-mail: claudio.contaldo@usz.ch).

The costs of publication of this article were defrayed in part by the payment of page charges. The article must therefore be hereby marked "advertisement" in accordance with 18 U.S.C. Section 1734 solely to indicate this fact.

Table 1. Hemoglobin, hematocrit, and RBC count after EPO pretreatment and in vehicle-treated controls

	Control		EPO-Control	
	Baseline	5 Days	Baseline	5 Days
Body wt, g	20.7 ± 1.0	20.6 ± 1.6	21.3 ± 1.1	21.5 ± 1.3
Hemoglobin, g/dl	15.6 ± 1.0	15.2 ± 1.3	15.4 ± 0.9	17.1 ± 1.8
Hematocrit, %	48.5 ± 3.5	47.5 ± 3.5	47.6 ± 3.2	51.5 ± 5.7
RBC count, 10 <sup>6</sup> /μl	9.4 ± 0.8	9.5 ± 0.6	9.6 ± 0.9	10.1 ± 0.9

Values are means ± SD; *n* = 6. A single dose of erythropoietin (EPO) did not significantly increase hemoglobin, hematocrit, and red blood cell (RBC) count.

tions, microvascular hyperpermeability, and neovascularization.

## MATERIALS AND METHODS

**Animals.** Experiments were performed according to the guiding principles for research involving animals and the German legislation on protection of animals. The experiments were approved by the local governmental animal care committee. A total of 55 C57BL/6J mice (12–24 wk of age, 24–26 g body wt; Charles River Laboratories, Sulzfeld, Germany) were housed in single cages at 22°C and 60–65% relative humidity with a 12:12-h light-dark cycle. The animals were allowed free access to tap water and standard laboratory chow (Altromin, Lage, Germany).

**Experimental model.** The dorsal skinfold chamber in mice was used for intravital microscopy, as previously described in detail (24). Briefly, mice were anesthetized intraperitoneally with a mixture of ketamine hydrochloride (90 mg/kg body wt; Ketavet, Parke Davis, Freiburg, Germany) and xylazine hydrochloride (25 mg/kg body wt; Rompun, Bayer, Leverkusen, Germany), and two symmetrical titanium frames were implanted to sandwich the extended double layer of the skin. One layer was removed in a 15-mm-diameter circular area. The remaining layer, consisting of epidermis, subcutaneous tissue, and striated skin muscle, was covered with a glass coverslip incorporated in one of the titanium frames. Animals tolerated the chamber well and showed no signs of discomfort or changes in sleeping and feeding habits. A recovery period of 3 days was allowed before the experiment was started.

**I/R.** A silicone pad and an adjustable screw were used to apply ~40-mmHg pressure and, thereby, establish a 3-h period of pressure-induced ischemia in a group of 18 animals (36). The pressure was just sufficient to occlude the feeding arterioles and, thus, induce complete

cessation of blood flow. In another group of 12 animals, the chamber tissue was not exposed to ischemia; these animals served as nonischemic sham or EPO controls. An additional group of 12 animals were used for blood sampling to monitor potential effects of EPO on hematocrit and hemoglobin levels.

**Intravital fluorescence microscopy.** For *in vivo* microscopic analysis of the microcirculation, the anesthetized mice were placed in the left lateral position on a Plexiglas stage. A modified multifluorescence microscope with a 100-W mercury lamp (Axiotech, Zeiss, Jena, Germany) was attached to a system of ultraviolet (330- to 390-nm excitation and >430-nm emission), blue (450- to 490-nm excitation and >520-nm emission), and green (530- to 560-nm excitation and >580-nm emission) filters. An epi-illumination technique was used to analyze the striated muscle microcirculation within the chamber tissue. Microscopic images were recorded by a charge-coupled device video camera (model FK 6990, COHU, Pieper, Schwerte, Germany), transferred to a video system (S-VHS Panasonic AG 7350, Matsushita, Tokyo, Japan), and recorded on videotape for subsequent offline evaluation. We injected 0.05 ml of FITC-dextran (150,000 mol wt, 50 mg/ml saline; Sigma Chemical, St. Louis, MO) for intravascular contrast enhancement and 0.05 ml of rhodamine 6G (0.1 mg/ml saline; Sigma Chemical) for leukocyte staining *in vivo* into the tail vein. For quantitative analysis of microvascular perfusion, leukocyte-endothelial cell interaction, and macromolecular extravasation and angiogenic neovascularization, we used long-distance objectives (×4 magnification, 0.16 NA; ×10 magnification, 0.30 NA; ×20 magnification, 0.32 NA; Zeiss) (2).

**Quantitative microcirculation analysis.** The chamber was scanned for random selection of distinct observation areas, which included four to six second- and third-order arterioles, nine nutritive capillary fields, and four to six draining postcapillary venules. Video printouts were made during videography and initially marked to indicate the exact location for measurements of vessel diameter and RBC velocity. Diameters were measured in micrometers perpendicularly to the vessel path. The line-shift method (Capimage, Zeintl Software, Heidelberg, Germany) with computer assistance was used to analyze centerline RBC velocity. Volumetric blood flow (*Q*) was calculated from diameter (*d*) and RBC velocity (*v*) as follows:  $Q = \pi \cdot (d/2)^2 \cdot v/1.6$  (pl/s), where 1.6 represents the Baker-Wayland factor, which corrects for the parabolic velocity profile in >20-μm microvessels (5). The number of permanent adherent leukocytes (i.e., cells that adhered to the venular vessel wall over a 30-s period) was evaluated as the number of cells per square millimeter of endothelial surface (calculated from diameter and length of the vessel segment and with the assumption that the vessel is cylindrical). Rolling leukocytes, defined as cells moving with a velocity less than two-fifths of the

Table 2. Baseline data of microcirculation and leukocyte-endothelial cell interaction

	Sham	EPO-Control	I/R	I/R + EPO 1 h	I/R + EPO 24 h
<b>Arterioles</b>					
Diameter, μm	44.3 ± 12.2	34.0 ± 2.1	49.6 ± 3.4	39.9 ± 4.0	39.9 ± 4.0
RBC velocity, mm/s	1.41 ± 0.44	1.37 ± 0.52	1.49 ± 0.11	1.44 ± 0.37	1.39 ± 0.27
Blood flow, pl/s	23.6 ± 15.2	14.2 ± 1.45	25.5 ± 10.8	36.1 ± 21.9	18.3 ± 5.8
<b>Venules</b>					
Diameter, μm	37 ± 8.8	35 ± 5.2	44.4 ± 5.6	34.9 ± 7.6	35.3 ± 1.9
RBC velocity, mm/s	0.50 ± 0.24	0.47 ± 0.13	0.51 ± 0.18	0.35 ± 0.21	0.39 ± 0.06
Blood flow, pl/s	6.9 ± 2.5	6.9 ± 2.5	8.3 ± 2.8	4.5 ± 2.1	3.7 ± 1.1
<b>Capillaries</b>					
Functional capillary density, cm <sup>-1</sup>	207 ± 17	221 ± 21	252 ± 31	236 ± 25	245 ± 26
<b>Leukocyte-endothelial cell interaction</b>					
Rolling, cells/min	3.8 ± 0.8	1.6 ± 0.9	2.6 ± 0.7	3.1 ± 0.5	2.4 ± 1.1
Adherence, cells/mm <sup>2</sup>	113 ± 28	104 ± 12	126 ± 23	109 ± 09	116 ± 18

Values are means ± SD. Sham, chamber preparation without ischemia-reperfusion (I/R) and EPO; EPO-control, EPO treatment (5,000 U/kg body wt ip) 1 h before measurements without I/R; I/R, I/R and treatment with equivalent volume of vehicle (saline); I/R + EPO 1 h and I/R + EPO 24 h, I/R and EPO treatment 1 h and 24 h before induction of ischemia, respectively. Note no significant differences between groups at baseline.

centerline velocity, are expressed as the number of cells per minute passing a reference point within the microvessel (26).

Macromolecular extravasation was determined as an indicator of microvascular permeability and, thus, endothelial integrity and was assessed by densitometric measurement of gray levels in the tissue directly adjacent to the venular vessel wall ( $E_1$ ), as well as within the marginal cell-free plasma layer of the vessel ( $E_2$ ). Macromolecular extravasation was then calculated as the ratio of  $E_1$  to  $E_2$  (26).

**Experimental protocol.** Sham animals ( $n = 6$ ) underwent chamber preparation without I/R induction and EPO treatment. EPO-control animals ( $n = 6$ ) received recombinant human EPO (5,000 U/kg body wt ip; Roche, Basel, Switzerland) 1 h before intravital microscopic baseline measurements but were not subjected to I/R. The I/R + EPO 1h group ( $n = 6$ ) was subjected to I/R and treated with EPO (5,000 U/kg body wt ip) 1 h before induction of ischemia. The I/R + EPO 24h group ( $n = 6$ ) was subjected to I/R and treated with EPO (5,000 U/kg body wt ip) 24 h before induction of ischemia. I/R animals ( $n = 6$ ) were subjected to I/R but treated with equivalent volumes of the vehicle (saline). Repetitive intravital microscopic observations in the anesthetized animal were performed at baseline (before I/R) and 2 and 6 h, as well as 1, 3, and 5 days, after onset of reperfusion. Sham and EPO-control animals were studied at corresponding time points. At the end of the experiments, the animals were euthanized by injection of an overdose of the anesthetic. In another group of 12 animals, hematocrit and hemoglobin concentration were assessed and RBCs were counted 5 days after systemic administration of EPO (5,000 U/kg body wt,  $n = 6$ ) or vehicle ( $n = 6$ ). One additional animal of each group was killed 6 h after onset of reperfusion and used for immunohistochemical study of EPO receptor and eNOS expression in small arterioles. Four additional animals from the I/R and I/R + EPO 1h groups were used for semiquantitative study of the EPO receptor and eNOS expression pattern.

**Immunohistochemical detection and evaluation of EPO receptor and eNOS.** For analysis of the pattern and cell type-specific expression of EPO receptor and eNOS, activity of endogenous peroxidase was blocked by incubation of 4- $\mu$ m sections of the tissue in 0.3%  $H_2O_2$ -methanol, and the slides were exposed to cross-reacting polyclonal rabbit anti-rat EPO receptor (1:50 dilution; StressGen Biotechnologies, Victoria, BC, Canada) or eNOS (1:25 dilution; BD Biosciences, Germany) antibody at 37°C for 2 h. A horseradish peroxidase-conjugated goat anti-rabbit antibody was used as secondary antibody (1:500 dilution; Amersham Biosciences, Freiburg, Germany), and 3,3'-diaminobenzidine was used as chromogen. Slides were counterstained with hematoxylin and examined by light microscopy (model BX 60F, Olympus Optical, Tokyo, Japan). As a negative control, additional sections from each specimen were exposed to appropriate IgG isotype-matched antibody (Sigma Aldrich Chemie), instead of the primary antibodies, under the same conditions to determine the specificity of antibody binding. All the control stains were found to be negative. The intensity of the staining reactions in arterioles was evaluated using a semiquantitative score.

**Statistical analysis.** Values are means  $\pm$  SD. For comparison between individual time points, ANOVA for repeated measures was followed by the appropriate post hoc test, including correction of the alpha error according to Bonferroni's probabilities. For comparison between the groups, ANOVA for comparison of multiple groups was followed by Student-Newman-Keuls test for appropriate post hoc analysis (SigmaStat, Jandel, San Rafael, CA).  $P < 0.05$  was taken to indicate statistically significant differences.

## RESULTS

Hematocrit and hemoglobin concentrations, as well as RBC counts, slightly increased 5 days after treatment with EPO (5,000 U/kg body wt), but these values were not significantly different from vehicle-treated control values (Table 1).

**Postischemic arteriolar perfusion.** Analysis of arteriolar diameters, RBC velocity, and blood flow revealed comparable values at baseline in all groups (Table 2). I/R provoked arteriolar constriction, which was most pronounced ( $P < 0.05$ ) during the late-reperfusion phase (Fig. 1A). Analysis of arteriolar RBC velocity and arteriolar blood flow showed a reactive hyperemia during the first 6 h of reperfusion followed by a significant decrease ( $P < 0.05$ ) during the late-reperfusion phase (Fig. 1, B and C). Pretreatment with EPO 1 or 24 h before ischemia completely prevented arteriolar constriction

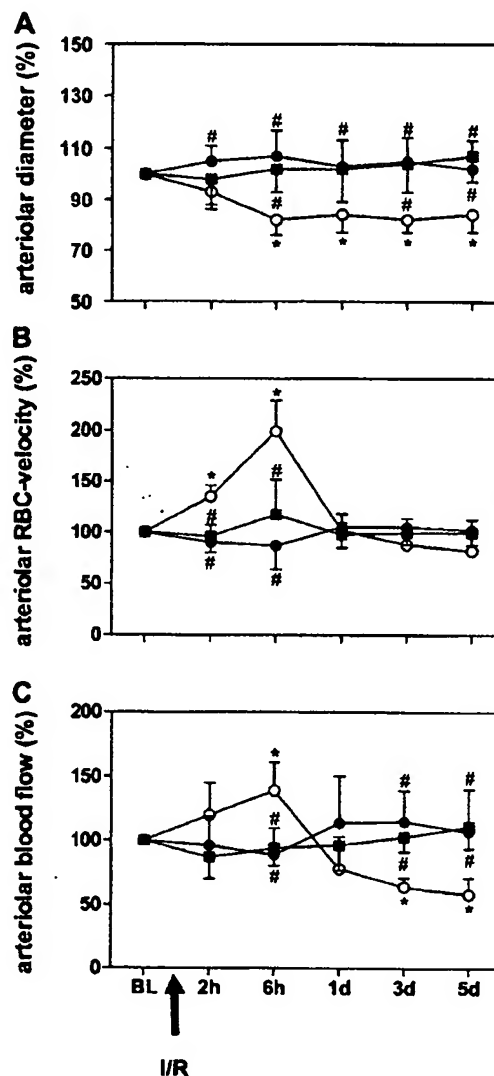


Fig. 1. Arteriolar diameters (A), RBC velocity (B), and blood flow (C), expressed as percentage of baseline (BL), in vehicle-treated animals subjected to ischemia-reperfusion (I/R) injury (C) and I/R animals pretreated with erythropoietin (EPO) 1 h (●) or 24 h (■) before induction of ischemia. Arrow indicates induction of 3 h of ischemia and onset of reperfusion (I/R). Note arteriolar constriction and reduction of arteriolar blood flow after I/R and prevention of postischemic deterioration of arteriolar blood perfusion after EPO pretreatment. Values are means  $\pm$  SD. \* $P < 0.05$  vs. BL. # $P < 0.05$  vs. vehicle-treated I/R animals at corresponding time points.



(Fig. 1A) and effectively abrogated ( $P < 0.05$ ) the decrease of postischemic arteriolar perfusion during the late-reperfusion phase (Fig. 1, B and C).

**Postischemic capillary perfusion.** Analysis of functional capillary density, as well as capillary diameters, RBC velocity, and blood flow, revealed comparable values at baseline in all groups (Table 2). I/R induced a significant decrease ( $P < 0.05$ ) in functional capillary density to 40% of baseline during early reperfusion that did not completely recover after the 5-day reperfusion period (Fig. 2A). This was associated with a hyperemic capillary perfusion of the remaining patent capillaries during early reperfusion followed by a significant ( $P < 0.05$ ) capillary narrowing and blood flow reduction during the late-reperfusion phase (Fig. 2, B–D). Pretreatment with EPO 1 or 24 h before ischemia significantly ( $P < 0.05$ ) attenuated the I/R-induced decrease of functional capillary density (Fig. 2A). EPO was able to completely abrogate the decrease of capillary blood flow during the late-reperfusion period and also induced capillary hyperperfusion ( $P < 0.05$ ), mainly by widening luminal diameter (Figs. 2, B–D).

**Postischemic venular perfusion.** Analysis of venular diameters, RBC velocity, and blood flow revealed comparable values at baseline in all groups (Table 2). I/R did not significantly affect diameters and flow conditions throughout the reperfusion phase (data not shown). Also, EPO pretreatment 1 h or 24 h before ischemia did not significantly change venular flow conditions during postischemic reperfusion (data not shown).

**Postischemic leukocyte-endothelial cell interaction.** Analysis of venular leukocyte rolling and adherence revealed comparable values at baseline in all groups (Table 2). The I/R-induced 5- to 10-fold increase ( $P < 0.05$ ) of leukocyte rolling and firm adherence during the initial postischemic reperfusion period did not completely recover during the 5-day observation period (Fig. 3). Pretreatment with EPO 1 or 24 h before ischemia significantly ( $P < 0.05$ ) attenuated leukocyte rolling (Fig. 3A) and also reduced leukocyte firm adherence, resulting in numbers of cells per endothelial surface comparable to that observed at baseline (Fig. 3B).

**Postischemic microvascular permeability.** Analysis of macromolecular extravasation from postcapillary venules, as an indicator of microvascular permeability, revealed comparable values at baseline in all groups (Table 2). The I/R-induced significant increase ( $P < 0.05$ ) of macromolecular extravasation during the early postischemic reperfusion period did not recover after the 5-day observation period (Fig. 4). Pretreatment with EPO 1 or 24 h before ischemia significantly ( $P < 0.05$ ) attenuated I/R-induced microvascular hyperpermeability. At 5 days after reperfusion, permeability in animals treated with EPO 1 h before ischemia was comparable to that at baseline (Fig. 4) and in sham-operated controls (Fig. 5).

**Microcirculation and inflammation in sham-operated and nonischemic EPO-control animals.** In animals that were subjected to only sham operation or treated with EPO without I/R, no significant changes were observed in arteriolar, capillary,

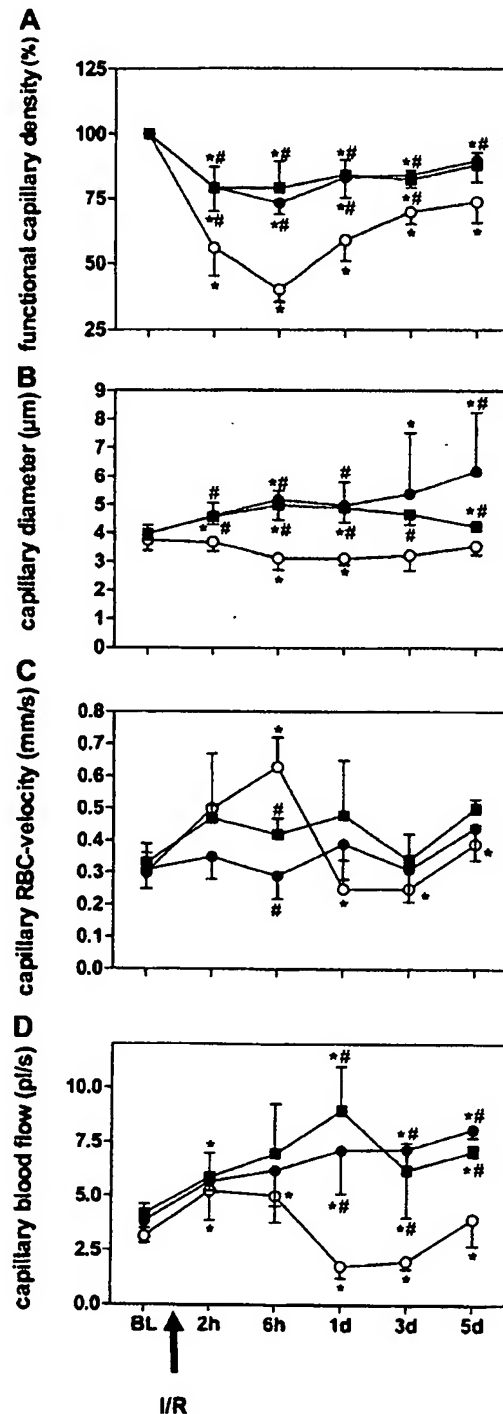


Fig. 2. Functional capillary density (A), capillary diameters (B), RBC velocity (C), and blood flow (D) of perfused capillaries, expressed as percentage of baseline, in vehicle-treated I/R animals (○) and I/R animals pretreated with EPO 1 h (●) or 24 h (■) before induction of ischemia. Arrow indicates induction of 3 h of ischemia and onset of reperfusion (I/R). Note significant derangement of capillary perfusion after I/R and protection of functional capillary density with capillary hyperperfusion after EPO pretreatment. Values are means  $\pm$  SD. \* $P < 0.05$  vs. BL. # $P < 0.05$  vs. vehicle-treated I/R animals at corresponding time points.

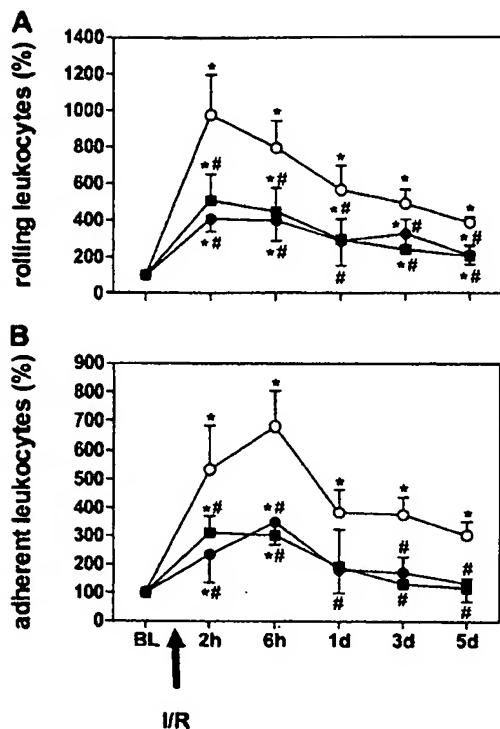


Fig. 3. Leukocyte rolling (A) and leukocyte firm adherence (B), expressed as percentage of baseline, in vehicle-treated I/R animals (○) and I/R animals pretreated with EPO 1 h (●) or 24 h (■) before induction of ischemia. Arrow indicates induction of 3 h of ischemia and onset of reperfusion (I/R). Note massive induction of leukocyte rolling and adherence by I/R and significant attenuation of this leukocytic inflammatory response after EPO pretreatment. Values are means  $\pm$  SD. \* $P < 0.05$  vs. BL. # $P < 0.05$  vs. vehicle-treated I/R animals at corresponding time points.

and venular perfusion over the 5-day period (Fig. 5, A–C). No leukocytic inflammatory responses or changes in macromolecular extravasation were noted in these animals (Fig. 5, D–F).

**Postischemic angiogenesis and neovascularization.** Despite the reduction of arteriolar and capillary perfusion during the postischemic reperfusion period, I/R was not associated with an angiogenic response and neovascularization (Fig. 6). In contrast, pretreatment with EPO, in particular 1 h before ischemia, resulted in capillary budding and sprouting 1 and 3 days after onset of reperfusion and formation of new capillary networks with perfused microvessels at the end of the 5-day observation period (Fig. 6).

**Postischemic EPO receptor and eNOS expression.** EPO receptor and eNOS expression was markedly enhanced 6 h after reperfusion in animals pretreated with EPO compared with sham-control animals (Fig. 7). Expression of eNOS was distinct in the endoluminal aspects of endothelial cells in sham animals and I/R controls; after EPO pretreatment, however, the entire cytoplasm showed substantial eNOS expression ( $P < 0.05$ ). The staining was observed in endothelial, but not smooth muscle, cells. EPO receptor expression was distinct in all endothelial cells in sham animals. In vehicle-treated I/R controls, a marked expression of EPO receptor was observed compared with sham ( $P < 0.05$ ); after EPO pretreatment, this

effect was more pronounced (not significant compared with I/R controls). In smooth muscle cells, marked expression of EPO receptor was observed after EPO treatment (Fig. 8).

## DISCUSSION

In the present study, we demonstrate for the first time that EPO pretreatment can attenuate I/R-induced microcirculatory dysfunction and leukocyte-endothelial cell interaction in postischemic striated muscle. Our study strongly suggests that, in the presence of hypoxia, EPO pretreatment may exert its protection through an enhanced eNOS expression and may stimulate the proliferation of endothelial cells in critically reperfused striated muscle.

There is insufficient information about the dose of EPO that should be used to achieve nonhematopoietic effects. The first investigators who described nonhematopoietic beneficial actions of EPO used single, high doses of 5,000 U/kg, which have been shown to reduce infarct size in the heart by preventing apoptosis. This effect was achieved when EPO was injected immediately after myocardial ischemia without increasing the risk of thrombosis. At lower doses, EPO has been shown to be somehow effective, but higher doses extended the therapeutic window. Accordingly, for our study of the effect of EPO on microcirculatory dysfunction in I/R, we used the high dose (5,000 U/kg). In future studies, it is necessary to define the relationship between EPO dose and the various effects of EPO, including the antiapoptotic, proangiogenic, vasculoprotective, and anti-inflammatory actions.

Three hours of ischemia caused a classic hyperemic response during initial reperfusion, with enhancement of arteriolar RBC velocity and, thus, volumetric blood flow. This, however, was followed by a severe arteriolar constriction 6 h after the onset of reperfusion that persisted over the entire 5-day observation period. This arteriolar constriction was functionally significant, as indicated by a reduced volumetric blood flow within the striated muscle tissue. EPO pretreatment completely abrogated the I/R-induced arteriolar constriction and,

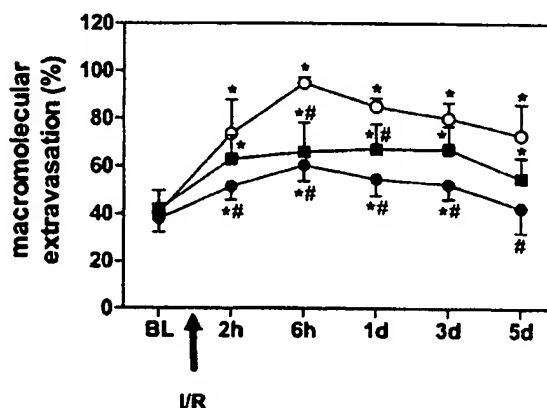


Fig. 4. Macromolecular extravasation, an indicator for microvascular permeability, in vehicle-treated I/R animals (○) and I/R animals pretreated with EPO 1 h (●) or 24 h (■) before induction of ischemia. Arrow indicates induction of 3 h of ischemia and onset of reperfusion (I/R). Note increase of microvascular permeability during postischemic reperfusion, which is significantly attenuated after EPO pretreatment. Values are means  $\pm$  SD. \* $P < 0.05$  vs. BL. # $P < 0.05$  vs. vehicle-treated I/R animals at corresponding time points.

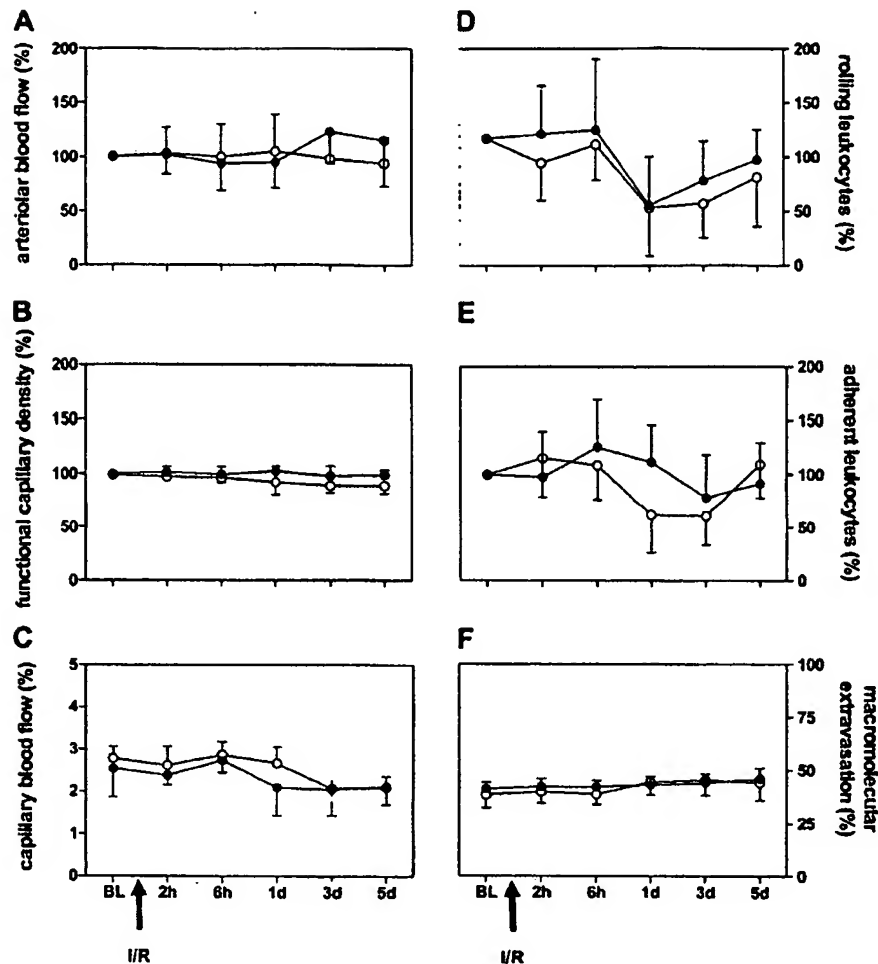


Fig. 5. Arteriolar blood flow, functional capillary density, capillary blood flow, leukocyte rolling, leukocyte adherence, and macromolecular extravasation in sham-operated animals (○) and EPO-controls without I/R (●). Arrow indicates induction of 3 h of ischemia and onset of reperfusion (I/R). Sham operation and EPO treatment did not significantly affect microcirculatory and inflammatory parameters. Values are means  $\pm$  SD.

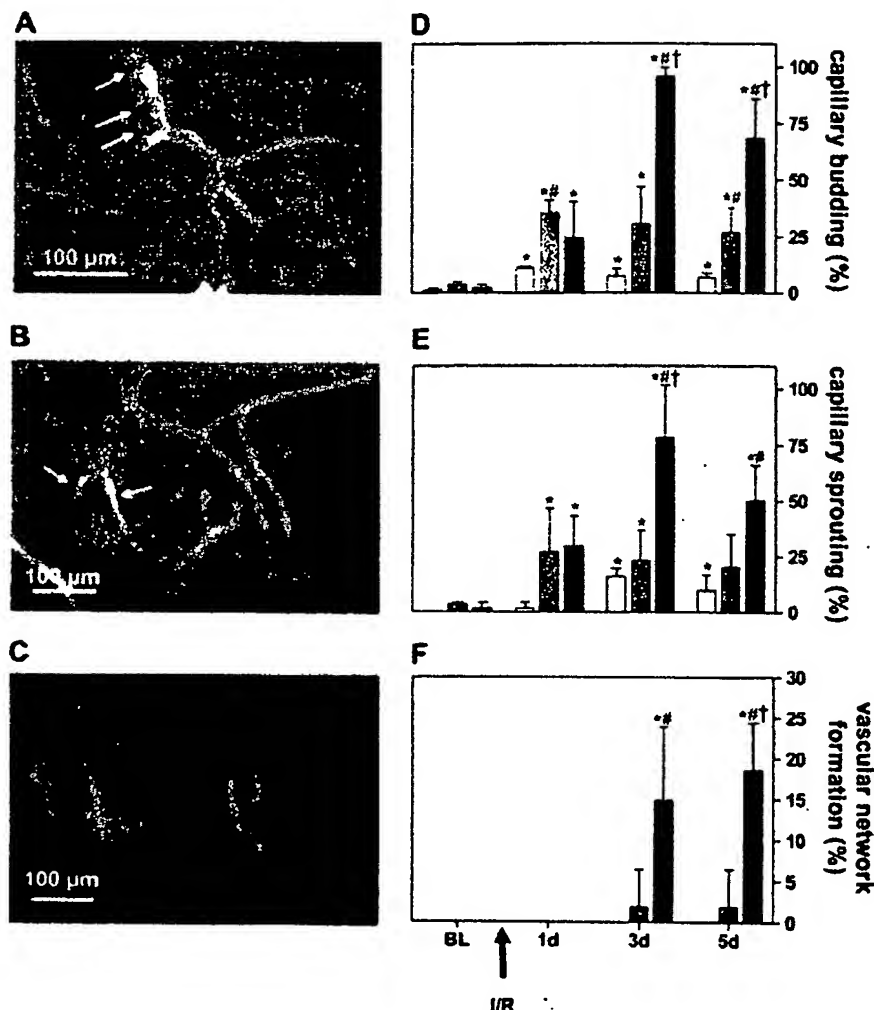
thus, blood flow reduction. This action of EPO may be caused by the EPO-associated attenuation of venular leukocyte adherence. The I/R-induced leukocyte accumulation in venules may act in a paracrine manner on the vasomotor control of the feeding arterioles, because the second- and third-order arterioles are running in parallel to the postcapillary and collecting venules. This view is based on observations of a previous study in which abrogation of CD18-dependent leukocyte adherence in postcapillary venules was shown to successfully blunt arteriolar constriction during postischemic reperfusion (40).

These findings are not inconsistent with the assumption that some beneficial effect of EPO is related to NO synthase, because vascular endothelial dysfunctions in reperfused striated muscle have been shown to be associated with decreased NO concentrations and reduced eNOS activity (17). Accordingly, we observed in the present study that EPO pretreatment increased eNOS expression, and this may be responsible for the abrogation of the I/R-induced arteriolar constriction. Consistent with this observation, a recent study, showing that postischemic inflammation depends on eNOS phosphorylation, supports the view that eNOS is involved in EPO-mediated

microcirculatory protection bifunctionally: by increasing the NO availability and through an anti-inflammatory effect (21).

In parallel to the reduction of the arteriolar blood flow, I/R induced significant capillary no-reflow, as indicated by a massive diminution of postischemic functional capillary density. It has been suggested that the postischemic capillary no-reflow in striated muscle is caused by an increased extramural tissue pressure due to the I/R-induced venular leukocytic inflammation, the increase in microvascular permeability, and the formation of interstitial edema (18). Indeed, abrogation of venular leukocyte adherence by monoclonal antibodies directed against CD11/CD18 has been shown to reduce postischemic microvascular permeability and, consequently, capillary perfusion failure (18). This ideally parallels the observations in the present study after EPO pretreatment. Thus the protective action of EPO on postischemic microcirculatory dysfunction seems to be primarily based on targeting of the inflammatory leukocytic response in the postcapillary venules. The attenuation of leukocyte-endothelial cell interactions by EPO may be caused by the increased expression of eNOS during postischemic reperfusion, because NO has been

Fig. 6. A–C: postischemic intravital fluorescence microscopy [contrast enhancement by 5% FITC-dextran (150,000 mol wt)] of angiogenic budding (A, arrows), sprouting (B, arrow), and microvascular network formation (C) in animals pretreated with EPO 1 h before induction of ischemia. D–F: quantitative analysis of capillary budding, capillary sprouting, and microvascular network formation in vehicle-treated I/R animals (open bars) and I/R animals pretreated with EPO 1 h (solid bars) or 24 h (shaded bars) before induction of ischemia. Arrow indicates induction of 3 h of ischemia and onset of reperfusion (I/R). Note lack of angiogenesis and neovascularization after I/R and capillary budding, capillary sprouting, and microvascular network formation after EPO pretreatment, in particular when EPO was given 1 h before ischemia. Values (percent “angiogenesis-positive” fields of all fields analyzed) are means  $\pm$  SD. \* $P$  < 0.05 vs. BL. # $P$  < 0.05 vs. vehicle-treated I/R animals at corresponding time points. † $P$  < 0.05 vs. EPO at 24 h.



shown to be protective in limiting leukocyte adherence in I/R injury (19).

In the present I/R model, hypoxia-inducible factors (HIFs) may have been upregulated and vascular endothelial growth factor (VEGF) may have been induced, and both may have contributed to the angiogenesis. Theoretically, VEGF as the vascular permeability factor may also have contributed to the increased microvascular permeability. However, because microvascular permeability was increased most after I/R in vehicle controls, whereas angiogenesis was observed only in EPO-treated animals, which showed a significantly reduced microvascular permeability compared with the vehicle-treated controls, it is highly unlikely that the postischemic increase in microvascular permeability is induced in the present model by the action of HIFs and VEGF. In contrast, it is most probable that the increased microvascular permeability is due to the ischemia- and reoxygenation-mediated inflammatory injury (26) and that this injury is reduced after EPO treatment because of anti-inflammatory potentials of EPO.

I/R induced a reactive hyperemia during the initial postischemic reperfusion period but was associated with luminal

narrowing and reduction of blood flow in the still-patent capillaries during the late-reperfusion phase. EPO pretreatment, in particular 1 h before ischemia, resulted in a widening of the capillary lumen, which was associated with capillary hyperperfusion. Although we are not aware whether the capillary widening was passive in nature or actively mediated by EPO, others demonstrated in hepatic tissue that I/R is associated with a reduction of capillary (sinusoidal) diameters due to pericyte constriction, which is triggered by an imbalance between endothelin-1 and NO, and that widening of sinusoids can be achieved by modulating the balance in favor of NO (30). Accordingly, the postischemic capillary widening observed after EPO pretreatment in the present study may be caused by the increased release of NO due to the pronounced eNOS expression.

Thus our study provides evidence that EPO can have a direct action on the endothelium *in vivo* that increases NO bioavailability by upregulation of eNOS under hypoxic conditions. Binding studies with radio-ionated EPO demonstrated ~27,000 receptors per endothelial cell on the intraluminal surface (3). Our results suggest that hypoxia increases the

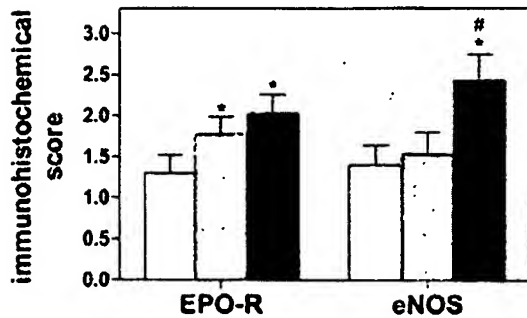


Fig. 7. Staining intensity of EPO receptor (EPO-R) and endothelial nitric oxide synthase (eNOS) in vascular endothelial cells of mouse striated muscle after 3 h of ischemia and 6 h of reperfusion in sham-operated animals (open bars), vehicle-treated I/R animals (shaded bars), and I/R animals pretreated with EPO 1 h before induction of ischemia (solid bars) determined by a semiquantitative score (0 = no, 1 = weak, 2 = moderate, 3 = strong staining). Values are means  $\pm$  SD ( $n = 5$  per group). \* $P < 0.05$  vs. sham. # $P < 0.05$  vs. vehicle-treated I/R animals at corresponding time points.

capacity of the endothelial cell to produce NO in response to EPO pretreatment by induction of EPO receptors and eNOS. These results are consistent with the findings of a recent study in which it was shown that endothelial responses may require an increased exposure to EPO combined with upregulation of EPO receptors (6). Without induction of EPO receptors, only a minimal EPO response is achieved, as demonstrated in the present study in EPO-control animals, which revealed negligible changes in microhemodynamics after EPO pretreatment.

Angiogenesis, involving capillary sprouting from preexisting blood vessels, comprises a series of events including degradation of extracellular matrix components, proliferation and migration of endothelial cells, and tube formation. Therapeutic angiogenesis describes the induction and stimulation of

neovascularization for treatment or prevention of pathological clinical situations characterized by local hypovascularity, such as postischemic conditions of critically reperfused striated muscle. In the present study, we observed capillary budding and sprouting from small postcapillary venules, in particular when EPO was given 1 h before ischemia, but no angiogenic response in vehicle-treated animals. This suggests that the ischemic stimulus and EPO pretreatment are necessary for effective induction of angiogenesis.

A recent study demonstrated that ischemic tissue viability can be improved by systemic EPO administration. However, the underlying mechanisms remained unclear, although enhanced angiogenesis was assumed (8). EPO has been shown to induce therapeutic angiogenesis with an effectiveness equal to that of VEGF. Compared with the plethora of data from other angiogenic factors such as VEGF or those of the fibroblast growth factor family, data on the angiogenic properties of EPO are rather rare. The angiogenic activity of EPO has been described in vitro and in the rat aortic ring model (10), in estrogen-dependent uterine angiogenesis (39), and in immortalized human umbilical vein endothelial cells (31). In vivo studies in the chicken embryo chorioallantoic membrane assay (13) demonstrated that EPO induces endothelial cell proliferation and migration and stimulates angiogenesis following an intussusceptive microvascular growth mechanism. In a recent study, accelerated wound healing after experimental thermal injury and EPO treatment was associated with substantial neovascularization in traumatized tissue (14). Promising studies have further indicated that EPO might play a role in endothelial progenitor cell recruitment, promoting repair of the endothelium in the setting of tissue injury (4). Here, we have demonstrated for the first time that EPO can induce angiogenesis and functionally intact microvascular networks in I/R injury.

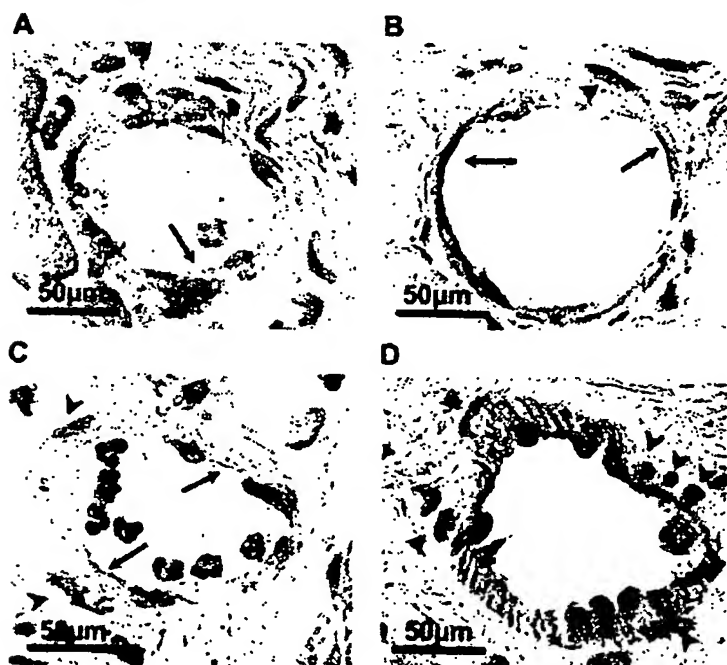


Fig. 8. Immunohistological demonstration of EPO receptor (A and B) and eNOS (C and D) expression (brown staining) of endothelial cells (arrows) and smooth muscle cells (arrowheads) in cross sections of mouse striated muscle arterioles after 3 h of ischemia and 6 h of reperfusion. Normal expression of eNOS and EPO receptors in sham-operated animals is shown in A and C. Note strong expression of EPO-receptor in endothelial cells and smooth muscle cells (B) and eNOS in endothelial cells (D) after EPO pretreatment 1 h before ischemia.

In conclusion, our data demonstrate that EPO administration in a single dose before onset of postischemic reperfusion offers significant protection against I/R injury in striated muscle by reducing capillary no-reflow and leukocytic inflammation during early reperfusion and by modulating arteriolar vasomotor response and inducing angiogenesis in the later postischemic period.

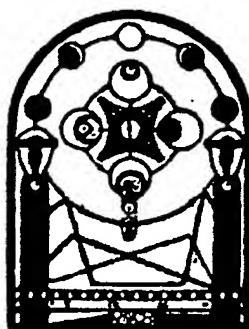
#### GRANTS

This research was supported by the "Arbeitsgemeinschaft Osteosynthese" Grant 02-W80.

#### REFERENCES

- Abdelrahman M, Sharples EJ, McDonald MC, Collin M, Patel NS, Yaqoob MM, Thiemermann C. Erythropoietin attenuates the tissue injury associated with hemorrhagic shock and myocardial ischemia. *Shock* 22: 63–69, 2004.
- Amon M, Menger MD, Vollmar B. Heme oxygenase and nitric oxide synthase mediate cooling-associated protection against TNF- $\alpha$ -induced microcirculatory dysfunction and apoptotic cell death. *FASEB J* 17: 175–185, 2003.
- Anagnostou A, Lee ES, Kessimian N, Levinson R, Steiner M. Erythropoietin has a mitogenic and positive chemotactic effect on endothelial cells. *Proc Natl Acad Sci USA* 87: 5978–5982, 1990.
- Bahlmann FH, De Groot K, Spandau JM, Landry AL, Hertel B, Duckert T, Boehm SM, Menne J, Haller H, Fliser D. Erythropoietin regulates endothelial progenitor cells. *Blood* 103: 921–926, 2004.
- Baker M, Wayland H. On-line volume flow rate and velocity profile measurement for blood in microvessels. *Microvasc Res* 7: 131–143, 1974.
- Beleslin-Cokic BB, Cokic VP, Yu X, Weksler BB, Schechter AN, Noguchi CT. Erythropoietin and hypoxia stimulate erythropoietin receptor and nitric oxide production by endothelial cells. *Blood* 104: 2073–2080, 2004.
- Brines M, Cerami A. Discovering erythropoietin's extra-hematopoietic functions: biology and clinical promise. *Kidney Int* 70: 246–250, 2006.
- Buemi M, Vaccaro M, Sturiale A, Galeano MR, Sansotta C, Cavallari V, Floccari F, D'Amico D, Torre V, Calapai G, Frisina N, Guarneri F, Vermiglio G. Recombinant human erythropoietin influences revascularization and healing in a rat model of random ischemic flaps. *Acta Derm Venereol* 82: 411–417, 2002.
- Bullard AJ, Govewalla P, Yellow DM. Erythropoietin protects the myocardium against reperfusion injury in vitro and in vivo. *Basic Res Cardiol* 100: 397–403, 2005.
- Carlini RG, Gupta A, Liapis H, Rothstein M. Endothelin-1 release by erythropoietin involves calcium signaling in endothelial cells. *J Cardiovasc Pharmacol* 26: 889–892, 1995.
- Carlini RG, Reyes AA, Rothstein M. Recombinant human erythropoietin stimulates angiogenesis in vitro. *Kidney Int* 47: 740–745, 1995.
- Chong ZZ, Kang JQ, Maiese K. Erythropoietin is a novel vascular protectant through activation of Akt1 and mitochondrial modulation of cysteine proteases. *Circulation* 106: 2973–2979, 2002.
- Crivellato E, Nico B, Vacca A, Djonov V, Presta M, Ribatti D. Recombinant human erythropoietin induces intussusceptive microvascular growth in vivo. *Leukemia* 18: 331–336, 2004.
- Galeano M, Altavilla D, Bitto A, Minutoli L, Calo M, Lo Cascio P, Polito F, Giugliano G, Squadrone G, Mioni C, Giuliani D, Venuti FS, Squadrone F. Recombinant human erythropoietin improves angiogenesis and wound healing in experimental burn wounds. *Crit Care Med* 34: 1139–1146, 2006.
- Granger DN, Kubes P. The microcirculation and inflammation: modulation of leukocyte-endothelial cell adhesion. *J Leukoc Biol* 55: 662–675, 1994.
- Grasso G, Sfacteria A, Cerami A, Brines M. Erythropoietin as a tissue-protective cytokine in brain injury: what do we know and where do we go? *Neuroscientist* 10: 93–98, 2004.
- Hallstrom S, Gasser H, Neumayer C, Fugl A, Nanobashvili J, Jakubowski A, Huk I, Schlag G, Malinski T. S-nitroso human serum albumin treatment reduces ischemia/reperfusion injury in skeletal muscle via nitric oxide release. *Circulation* 105: 3032–3038, 2002.
- Jerome SN, Smith CW, Korthuis RJ. CD18-dependent adherence reactions play an important role in the development of the no-reflow phenomenon. *Am J Physiol Heart Circ Physiol* 264: H479–H483, 1993.
- Kanwar S, Kubes P. Nitric oxide is an antiadhesive molecule for leukocytes. *New Horiz* 3: 93–104, 1995.
- Kubes P, Ibbotson G, Russell J, Wallace JL, Granger DN. Role of platelet-activating factor in ischemia/reperfusion-induced leukocyte adherence. *Am J Physiol Gastrointest Liver Physiol* 259: G300–G305, 1990.
- Kupatt C, Hinkel R, Vachenaue R, Horstkotte J, Raake P, Sandner T, Kreuzpointner R, Muller F, Dimmeler S, Feron O, Beck H, Buning H, Boekstegers P. VEGF165 transfection decreases postischemic NF- $\kappa$ B-dependent myocardial reperfusion injury in vivo: role of eNOS phosphorylation. *FASEB J* 17: 705–707, 2003.
- Kupatt C, Horstkotte J, Vlastos GA, Plosser A, Lebberz C, Semisch M, Thalott M, Buttner K, Browarzyk C, Mages J, Hoffmann R, Deten A, Lamparter M, Muller F, Beck H, Buning H, Boekstegers P, Hatzopoulos AK. Embryonic endothelial progenitor cells expressing a broad range of proangiogenic and remodeling factors enhance vascularization and tissue recovery in acute and chronic ischemia. *FASEB J* 19: 1576–1578, 2005.
- Lefer A, Weyrich AS, Buerke M. Role of selectins, a new family of adhesion molecules, in ischemia-reperfusion injury. *Cardiovasc Res* 28: 289–294, 1994.
- Lehr HA, Leunig M, Menger MD, Nolte D, Messmer K. Dorsal skinfold chamber technique for intravital microscopy in nude mice. *Am J Pathol* 143: 1055–1062, 1993.
- Mahmud DL, Amlak GM, Deb DK, Platanias LC, Uddin S, Wickrema A. Phosphorylation of forkhead transcription factors by erythropoietin and stem cell factor prevents acetylation and their interaction with coactivator p300 in erythroid progenitor cells. *Oncogene* 21: 1556–1562, 2002.
- Menger MD, Pellikan S, Steiner D. Microvascular ischemia/reperfusion injury in striated muscle: significance of "reflow-paradox." *Am J Physiol Heart Circ Physiol* 263: H1901–H1906, 1992.
- Menger MD, Rucker M, Vollmar B. Capillary dysfunction in striated muscle ischemia/reperfusion: on the mechanisms of capillary "no-reflow." *Shock* 8: 2–7, 1997.
- Menger MD, Steiner D, Messmer K. Microvascular ischemia-reperfusion injury in striated muscle: significance of "no-reflow." *Am J Physiol Heart Circ Physiol* 263: H1892–H1899, 1992.
- Nagai T, Akizawa T, Kohjiro S, Koiwa F, Nabeshima K, Niihara K, Kino K, Kanamori N, Kinugasa E, Ideura T. rHuEPO enhances the production of plasminogen activator inhibitor-1 in cultured endothelial cells. *Kidney Int* 50: 102–107, 1996.
- Pannen BH, Al-Adili F, Bauer M, Clemens MG, Gelger KK. Role of endothelins and nitric oxide in hepatic reperfusion injury in the rat. *Hepatology* 27: 755–764, 1998.
- Ribatti D, Presta M, Vacca A, Ria R, Giullani R, Dell'Era P, Nico B, Roncalli L, Dammacco F. Human erythropoietin induces a pro-angiogenic phenotype in cultured endothelial cells and stimulates neovascularization in vivo. *Blood* 93: 2627–2636, 1999.
- Ruschitzka FT, Wenger RH, Stallmach T, Quaschnig T, de Wit C, Wagner K, Labugger R, Kelm M, Noll G, Rulicke T, Shaw S, Lindberg RL, Rodenwaldt B, Lutz H, Bauer C, Luscher TF, Gassmann M. Nitric oxide prevents cardiovascular disease and determines survival in polyglobulic mice overexpressing erythropoietin. *Proc Natl Acad Sci USA* 97: 11609–11613, 2000.
- Shi Y, Rafiee P, Su J, Pritchard KA Jr, Tweddell JS, Baker JE. Acute cardioprotective effects of erythropoietin in infant rabbits are mediated by activation of protein kinases and potassium channels. *Basic Res Cardiol* 99: 173–182, 2004.
- Solaroglu I, Solaroglu A, Kaptanoglu E, Dede S, Haberal A, Beskonakli E, Kilinc K. Erythropoietin prevents ischemia-reperfusion from inducing oxidative damage in fetal rat brain. *Childs Nerv Syst* 19: 19–22, 2003.
- Spandou E, Tsouchnikas I, Karkavelas G, Dounousi E, Simeonidou C, Guiba-Tziampiri O, Tsakiris D. Erythropoietin attenuates renal injury in experimental acute renal failure ischemic/reperfusion model. *Nephrol Dial Transplant* 21: 330–336, 2006.
- Vollmar B, Westermann S, Menger MD. Microvascular response to compartment syndrome-like external pressure elevation: an in vivo fluorescence microscopic study in the hamster striated muscle. *J Trauma* 46: 91–96, 1999.
- Welbourn CR, Goldman G, Paterson IS, Valeri CR, Shepro D, Hechtman HB. Pathophysiology of ischemia-reperfusion injury: central role of the neutrophil. *Br J Surg* 78: 651–655, 1991.

38. Wright GL, Hanlon P, Amin K, Steenbergen C, Murphy E, Arcasoy MO. Erythropoietin receptor expression in adult rat cardiomyocytes is associated with an acute cardioprotective effect for recombinant erythropoietin during ischemia-reperfusion injury. *FASEB J* 18: 1031-1033, 2004.
39. Yasuda Y, Masuda S, Chikuma M, Inoue K, Nagao M, Sasaki R. Estrogen-dependent production of erythropoietin in uterus and its implication in uterine angiogenesis. *J Biol Chem* 273: 25381-25387, 1998.
40. Zamboni WA, Stephenson LL, Roth AC, Suchy H, Russell RC. Ischemia-reperfusion injury in skeletal muscle: CD18-dependent neutrophil-endothelial adhesion and arteriolar vasoconstriction. *Plast Reconstr Surg* 99: 2002-2007, 1997.



# Erythropoietin Protects the Intestine Against Ischemia/Reperfusion Injury in Rats

Ensari Guneli,<sup>1</sup> Zahide Cavdar,<sup>2</sup> Huray Islekel,<sup>2</sup> Sulen Sarioglu,<sup>3</sup> Serhat Erbayraktar,<sup>4</sup> Muge Kiray,<sup>5</sup> Selman Sokmen,<sup>6</sup> Osman Yilmaz,<sup>1</sup> and Necati Gokmen<sup>7</sup>

<sup>1</sup>Department of Laboratory Animal Sciences, Health Sciences Institute, Dokuz Eylul University, Izmir, Turkey; <sup>2</sup>Department of Biochemistry, Health Sciences Institute, Dokuz Eylul University, Izmir, Turkey; <sup>3</sup>Department of Pathology, Faculty of Medicine, Dokuz Eylul University, Izmir, Turkey; <sup>4</sup>Department of Neurosurgery, Faculty of Medicine, Dokuz Eylul University, Izmir, Turkey; <sup>5</sup>Department of Histology and Embryology, Faculty of Medicine, Dokuz Eylul University, Izmir, Turkey; <sup>6</sup>Department of Surgery, Faculty of Medicine, Dokuz Eylul University, Izmir, Turkey; <sup>7</sup>Department of Anesthesiology and Reanimation, Faculty of Medicine, Dokuz Eylul University, Izmir, Turkey

Previous studies have shown that erythropoietin (EPO) has protective effects against ischemia/reperfusion (I/R) injury in several tissues. The aim of this study was to determine whether EPO could prevent intestinal tissue injury induced by I/R. Wistar rats were subjected to intestinal ischemia (30 min) and reperfusion (60 min). A single dose of EPO (5000 U/kg) was administered intraperitoneally at two different time points: either at five minutes before the onset of ischemia or at the onset of reperfusion. At the end of the reperfusion period, jejunum was removed for examinations. Myeloperoxidase (MPO), malondialdehyde (MDA), and antioxidant defense system were assessed by biochemical analyses. Histological evaluation was performed according to the Chiu scoring method. Endothelial nitric oxide synthase (eNOS) was demonstrated by immunohistochemistry. Apoptotic cells were determined by TUNEL staining. Compared with the sham, I/R caused intestinal tissue injury (Chiu score,  $3 \pm 0.36$  vs  $0.4 \pm 0.24$ ,  $P < 0.01$ ) and was accompanied by increases in MDA levels ( $0.747 \pm 0.076$  vs  $0.492 \pm 0.033$ ,  $P < 0.05$ ), MPO activity ( $10.51 \pm 1.87$  vs  $4.3 \pm 0.45$ ,  $P < 0.05$ ), intensity of eNOS immunolabelling ( $3 \pm 0.4$  vs  $1.3 \pm 0.33$ ,  $P < 0.05$ ), the number of TUNEL-positive cells ( $20.4 \pm 2.6$  vs  $4.6 \pm 1.2$ ,  $P < 0.001$ ), and a decrease in catalase activity ( $16.83 \pm 2.6$  vs  $43.15 \pm 4.7$ ,  $P < 0.01$ ). Compared with the vehicle-treated I/R, EPO improved tissue injury; decreased the intensity of eNOS immunolabelling ( $1.6 \pm 0.24$  vs  $3 \pm 0.4$ ,  $P < 0.05$ ), the number of TUNEL-positive cells ( $9.2 \pm 2.7$  vs  $20.4 \pm 2.6$ ,  $P < 0.01$ ), and the high histological scores ( $1 \pm 0.51$  vs  $3 \pm 0.36$ ,  $P < 0.01$ ), and increased catalase activity ( $42.85 \pm 6$  vs  $16.83 \pm 2.6$ ,  $P < 0.01$ ) when given before ischemia, while it was found to have decreased the levels of MDA ( $0.483 \pm 0.025$  vs  $0.747 \pm 0.076$ ,  $P < 0.05$ ) and MPO activity ( $3.86 \pm 0.76$  vs  $10.51 \pm 1.87$ ,  $P < 0.05$ ), intensity of eNOS immunolabelling ( $1.4 \pm 0.24$  vs  $3 \pm 0.4$ ,  $P < 0.01$ ), the number of TUNEL-positive cells ( $9.1 \pm 3$  vs  $20.4 \pm 2.6$ ,  $P < 0.01$ ), and the number of high histological scores ( $1.16 \pm 0.4$  vs  $3 \pm 0.36$ ,  $P < 0.05$ ) when given at the onset of reperfusion. These results demonstrate that EPO protects against intestinal I/R injury in rats by reducing oxidative stress and apoptosis. We attributed this beneficial effect to the antioxidative properties of EPO.

Online address: <http://www.molmed.org>

doi: 10.2119/2007-00032.Guneli

## INTRODUCTION

The restoration of blood flow to an ischemic region leads to tissue injury at a greater rate than the original ischemic insult, an event called reperfusion injury. Among the abdominal organs, the small intestine is probably the most sensitive to ischemia/reperfusion (I/R) induced injury (1). It occurs frequently in a variety of clinical conditions, including mesenteric artery occlusion, abdominal aneurism surgery, trauma, shock, and

small intestinal transplantation, and is associated with high morbidity and mortality (2). Although the exact mechanisms involved in the pathogenesis of intestinal I/R injury have not been fully elucidated, it is generally believed that oxidative stress mediators such as reactive oxygen species (ROS), polymorphonuclear neutrophils, and nitric oxide (NO) play an important role (3).

Erythropoietin (EPO) is a glycoprotein cytokine produced primarily by the kid-

ney in the regulation of red blood cell production. In addition to this well-known and widely recognized effect, many studies have shown that EPO also acts as a tissue protecting factor (4–7). The favorable effects of the EPO-related changes are not fully understood, although its antiapoptotic, antioxidative, and antiinflammatory properties as well as its angiogenic potential seem to be related to the EPO-mediated protective effect (5,8,9). The protective effects of EPO are mediated through the tissue-protective EPO receptor, consisting of a heteromeric complex containing an EPO receptor and a  $\beta$  common receptor subunit (10). However, little is known about the presence and protective role of EPO and its recep-

Address correspondence and reprint requests to Serhat Erbayraktar, Department of Neurosurgery, Faculty of Medicine, Dokuz Eylul University, Inciralti, Izmir 35340, Turkey. Phone: +90 232 4123333; Fax: +90 232 2590541; E-mail: [s.erbayraktar@deu.edu.tr](mailto:s.erbayraktar@deu.edu.tr). Submitted April 20, 2007; Accepted for publication August 17, 2007.



tor in the intestine. Juul SE et al (1999) have demonstrated that EPO receptors are expressed on the intestinal tissue in rodents and humans (11). EPO was found to have a beneficial effect on intestinal damage such as colitis (12), necrotizing enterocolitis, (13) and anastomosis (14) in animal models. Previous studies have shown that EPO exhibits protective effects on tissue injury associated with I/R in many tissues such as cardiac (15), kidney (16), liver (17), lung (18), brain (19), and retina (20). However, it is not known whether EPO has a protective effect in the intestinal injury associated with I/R. Under the light of these data, the aim of the present study therefore was to determine whether recombinant human erythropoietin (rHuEPO) has a protective effect on intestinal I/R injury in rats.

## MATERIALS AND METHODS

### Animals

Male albino Wistar rats (200–250 g) were used in the present study. All the animals were kept under optimum conditions ( $21 \pm 1^\circ \text{C}$ , 40 to 70 percent humidity, 12/12 darkness-lightness cycle) at Dokuz Eylül University's Laboratory Animal Unit and were fed ad libitum with standard pellet diet and water. The experimental protocol was approved by Dokuz Eylül University's Ethic Committee for Animal Research.

### Experimental Groups

The rats were randomly divided into four groups as described: (a) Sham group: All the surgical steps were performed, except that intestinal I/R was not induced. Animals were kept under anesthesia for the duration of the intestinal I/R method. The sham group served as control of I/R group; (b) I/R group: Intestinal I/R was performed and served as control of rHuEPO-administered groups; (c) EPO + I/R group: Intestinal I/R was performed and rHuEPO was administered five minutes before the onset of ischemia; (d) I + EPO + R group: Intestinal I/R was performed and rHuEPO was administered at the onset of reperfusion.

A single dose of rHuEPO (5000 U/kg) was injected via i.p. route. rHuEPO (NeoRecormon, Roche, Germany) were purchased commercially.

### Technique of Intestinal I/R

Feeding of the animals was stopped 12 h prior to the start of the intestinal I/R procedure and they received only water. The rats were anesthetized with urethane (1500 mg/kg, i.p.) and their temperature was regulated by means of a lamp light bulb during the test. Intestinal I/R was induced as follows: The rats were placed in the supine position and secured in the dissection tray. The abdominal region was shaved and cleaned with antiseptic solutions. The intestinal region was reached by means of midline laparotomy. Superior mesenteric artery (SMA) was subjected with care and occluded with an atraumatic microvascular clamp, thus intestinal ischemia was created in 30 min. Ischemia was recognized by the existence of pulseless or pale color of the intestine. The abdominal region was then closed. Following ischemia, the clamp was removed and 60 min reperfusion was induced. The return of the pulses and the reestablishment of the pink color were assumed to be the reperfusion of the intestine. At the end of reperfusion, the jejunal segment was taken out, and the animals were killed by exsanguination.

### Tissue Preparation for Biochemical Analysis

All tissues were washed two times with cold saline solution and homogenized using a glass Teflon homogenizer (B. Braun, Germany) in buffer at a ratio of 1/10 (50 mM potassium phosphate buffer pH: 7.8, containing 0.5 mmol/L PMSF, 10  $\mu\text{g}/\text{mL}$  aprotinin) after cutting the tissue into small pieces with scissors and centrifuged at 2500g. Malondialdehyde (MDA) analyses were measured at this homogenate stage. The homogenate was then centrifuged at 45 000g for 30 min. The supernatant was used for colorimetric determination of superoxide dismutase (SOD), catalase (CAT), and glutathione peroxidase (GSH-Px) enzyme activities. For glutathione (GSH) and myeloperoxi-

dase (MPO) assay, tissue preparation details were mentioned in the analysis section. All preparation procedures were performed at  $+4^\circ \text{C}$ . All homogenates were stored at  $-80^\circ \text{C}$  prior to testing.

### MDA Assay

The MDA assay was based on the condensation of one molecule of malondialdehyde with two molecules of thiobarbituric acid (TBA) in the presence of reduced agents. The TBA + MDA complex was analyzed by HPLC system as described by Tatum et al. (21). Briefly, the HPLC system (Shimadzu VP Class, Shimadzu Corporation, Japan) consisted of a LC-10 ADVP pump system (Shimadzu VP) equipped with an automatic injector (SIL-10 ADVP), RF-10XL fluorescence detector and a personal computer using Class VP 6.1 Software. Aliquots of TBA + MDA samples were injected on a C18 column (Nucleosil 100-5, 150-4.6 mm; Macherey-Nagel Incorporation, Bethlehem, PA, USA) maintained at  $30^\circ \text{C}$ , followed by fluorimetric detection at 550 nm after excitation at 340 nm. Serial concentrations (0.75  $\mu\text{M}$  – 50  $\mu\text{M}$ ) of 1, 1, 3, 3-tetraethoxypropane (TEP) were used as standard. Measurements were expressed in terms of MDA normalized to the tissue protein content.

Thiobarbituric acid (TBA), 1,1,3,3-Tetraethoxypropane (TEP), butylated hydroxytoluen (BHT), potassium monobasic phosphate ( $\text{KH}_2\text{PO}_4$ ), potassium dibasic phosphate ( $\text{K}_2\text{HPO}_4$ ), sodium hydroxide (NaOH), sodium dodecylsulfate (SDS), ethanol, pyridine, n-butanol, and HPLC grade methanol were obtained from Sigma Chemicals, Germany.

### Determination of MPO Activity

MPO activity was measured in tissues with commercially available ELISA kit (Bioxtech MPO-EIA, Oxis Research, Portland, OR, USA). Briefly, tissue samples were homogenized in 50 mM potassium phosphate buffer, pH: 7.8, containing 0.5 mmol/L PMSF, 10  $\mu\text{g}/\text{mL}$  aprotinin, five percent 0.5 percent hexadecyltrimethylammonium bromide

(HETAB), and centrifuged at 40,000g for 15 min at +4° C. Then, the supernatant was assayed according to the manufacturer's instructions. The absorbance was read at 405 nm using Multi-Detection MicroPlate Reader (Synergy HT, BioTek Instruments, Inc., Winooski, VT, USA). Quantifications were achieved by the construction of standard curve using known concentrations of MPO. Results were expressed as ng/mg protein.

#### Determination of SOD Activity

For determination of SOD activity, the colorimetric assay (Bioxytech SOD-525, Oxis Research) was used. This method is based on the SOD-mediated increase in the rate of autooxidation of tetrahydrobenzofluorene in an aqueous alkaline solution to yield a chromophore with maximum absorbance at 525 nm. This absorbance was measured by spectrophotometer (Varian, Carry 50 UV-Visible, Australia). Results were expressed as U/mg protein.

#### Determination of CAT Activity

CAT activity was determined by means of commercially available colorimetric assay (Bioxytech, Catalase 520, Oxis Research) and performed according to the manufacturer's instructions. One unit of enzyme activity was defined as the amount of catalase that is available causing a change in absorbance at 520 nm for ten minutes. CAT activity was expressed as U/mg protein.

#### Measurement of Glutathione Peroxidase (GSH-Px) Activity

GSH-Px activity was measured by automated spectrophotometric method (Hitachi Modular Analytics, Roche Diagnostics Inc., Tokyo, Japan). The enzymatic reaction was initiated by the addition of cumene hydroperoxide (CuOOH) to the reaction mixture containing GSH, NADPH, EDTA, NaNO<sub>2</sub>, and glutathione reductase. The change in the absorbance at 340 nm was monitored.

#### \* Measurement of GSH Levels

Colorimetric assay for assessment of reduced glutathione concentration

(Bioxytech, GSH-400, Oxis Research) was used. Firstly, the tissue was homogenized in precipitation reagent (Bioxytech GSH-420, Oxis Research) and homogenate was centrifuged at 3000g for ten minutes at +4° C and upper aqueous layer was used for assay. Then, the level of reduced glutathione was measured at 412 nm by spectrophotometer (Varian, Carry 50 UV-Visible, Australia). Results were expressed as  $\mu$ mole/mg protein.

#### Protein Determination

The protein content in each tissue sample was determined using the bicinchoninic acid protein assay (BCA) (Sigma Chemicals, Germany). Bovine serum albumin was used as a standard (22).

#### Histological Analysis

Serial sections were taken from ten percent formalin fixed paraffin embedded tissue blocks of intestinal tissues and stained with Hematoxylin & Eosin (H&E). Tissue injury in the intestinal mucosa was evaluated using light microscopy according to the criteria described by Chiu et al (1970) and graded from 0 to 5 (23). The grades are: *Grade 0*: Normal mucosa; *Grade 1*: Formation of subepithelial detachments at the tip of the villi with capillary congestion; *Grade 2*: Subepithelial detachments exerted a moderate amount of upward push on the mucosa epithelium; *Grade 3*: Large subepithelial detachments exerted a massive amount of upward push on the mucosa epithelium along the villi and few denuded villus tips were observed; *Grade 4*: The villi were denuded to the level of lamina propria and dilated capillaries; *Grade 5*: Presence of ulceration, disintegration of lamina propria, and hemorrhage.

#### Detection of Apoptosis by TUNEL Method

Four-micrometer-thick sections were collected on poly-L-lysine-coated glass slides. The nuclear DNA fragmentation of the apoptotic cell was labeled in situ by the terminal deoxynucleotidyl treat-

ments with xylene and rehydration with progressively decreasing alcohol concentrations followed by phosphate-buffered saline (PBS), each section was treated with 20  $\mu$ g/mL proteinase K (Sigma) in 0.1 mol/L Tris/HCL buffer (pH 7.4) for 15 min. After rinsing with PBS, endogenous peroxidase activity was blocked with three percent hydrogen peroxide (H<sub>2</sub>O<sub>2</sub>) for five minutes. After rinsing with PBS, they were incubated with 0.5 U/ $\mu$ L terminal deoxynucleotidyl transferase (Boehringer Mannheim, Germany) and 0.05 nmol/ $\mu$ L biotinylated deoxyuridine triphosphate in terminal deoxynucleotidyl transferase buffer (Boehringer Mannheim) for 60 min in a humidified chamber at 37° C. Each slide was then observed with a microscope to check the staining quality before image acquisition. For each animal, five sections were analyzed by counting apoptotic bodies in five randomly chosen fields.

#### Immunohistochemistry

Immunohistochemical staining was used to locate eNOS expression in jejunal tissue. Sections were incubated at 60° C overnight, and then deparaffinized in xylene for 30 min. After rehydrating through a graded ethanol series, sections were treated with two percent trypsin at 37° C for 15 min. Sections were then incubated in a solution of three percent H<sub>2</sub>O<sub>2</sub> for 15 min to inhibit endogenous peroxidase activity. Next, the sections were incubated overnight with anti-eNOS antibody (GeneTex, Inc, San Antonio, TX, USA) and then for another 30 min with the biotinylated mouse secondary antibody. The bound secondary antibody was then amplified with Vector Elite ABC kit (Vectastain, Vector Laboratories, Burlingame, CA, USA). The antibody-biotin-avidin-peroxidase complexes were visualized using 0.02 percent DAB and nuclei were counterstained with Harris hematoxylin. The sections were finally mounted onto lysine-coated slides. The images were analyzed using a computer-assisted image analyzer system consisting of a microscope (Olympus BX-50, Tokyo, Japan) equipped with a

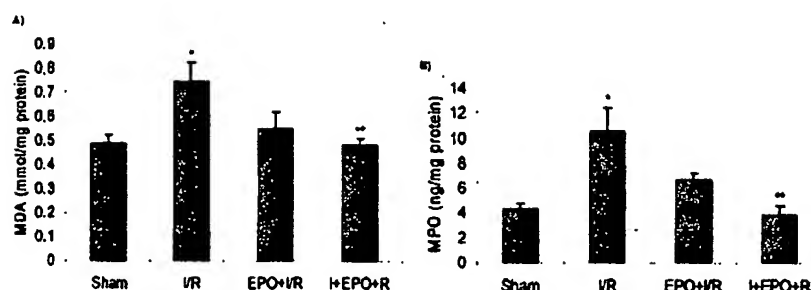


**Figure 1.** Jejunal tissue levels of malondialdehyde (MDA) and myeloperoxidase (MPO) in sham-operated animals, vehicle-treated I/R animals, and I/R animals treated with EPO five minutes before ischemia and at the onset of reperfusion. Data are mean  $\pm$  S.E.M. ( $n = 5-7$  per group). \* $P < 0.05$  vs sham; \*\* $P < 0.05$  vs vehicle-treated I/R animals (one-way ANOVA followed by Tukey's post-test). Note that there is a significant decrease in the MDA and MPO levels in the I + EPO + R group compared with the I/R group. Sham; intestinal I/R was not induced. I/R; intestinal I/R, EPO + I/R; rHuEPO administered five minutes before ischemia, I + EPO + R; rHuEPO administered onset of reperfusion.

high-resolution video camera (JVC TK-890E, Japan). This analysis was performed in at least ten areas per jejunal section, in two sections from each animal at  $\times 40$  magnification. The immunolabelling scores were evaluated blindly. Immunolabelling intensity was graded as mild (1), moderate (2), strong (3), and very strong (4).

#### Statistical Analysis

SPSS statistical package was used for data analysis (version 11.0, SPSS Inc., Chicago, IL, USA). The difference among groups was assessed with one-way ANOVA and Tukey HSD test was used to examine the difference between two groups. Statistical significance was accepted for the  $P$  values lower than 0.05; the arithmetic mean  $\pm$  S.E.M. was used to define distribution.

#### RESULTS

##### Effects of rHuEPO on MDA Levels and MPO Activity in the Intestinal Tissue Subjected to I/R in Rats

MDA levels examined as an indicator of lipid peroxidation are shown in Figure 1A. Compared with the sham group, MDA levels in the jejunal tissue in the I/R group were found to have increased ( $0.747 \pm 0.076$

vs  $0.492 \pm 0.033$  mmol/mg protein,  $P < 0.05$ ). As for the rHuEPO-administered groups, a significant decrease in the MDA levels was observed in the I + EPO + R group ( $0.483 \pm 0.025$  vs  $0.747 \pm 0.076$  mmol/mg protein,  $P < 0.05$ ), while there was a decrease in the EPO + I/R group but the difference was not significant when compared with I/R group ( $P > 0.05$ ).

MPO activity examined as an indicator of neutrophil accumulation is shown in Figure 1B. Compared with the sham

group, MPO activity in the jejunal tissue in the I/R group were found to have increased ( $10.51 \pm 1.87$  vs  $4.3 \pm 0.45$  ng/mg protein,  $P < 0.05$ ). As for the rHuEPO-administered groups, a significant decrease in the MPO activities was observed in the I + EPO + R group ( $3.86 \pm 0.76$  vs  $10.51 \pm 1.87$  ng/mg protein,  $P < 0.05$ ) while there was a decrease in the EPO + I/R group, but the difference was not significant when compared with the I/R group ( $P > 0.05$ ).

##### Effects of rHuEPO on Antioxidant Activity in the Intestinal Tissue Subjected to I/R in Rats

The levels of enzymatic activity (SOD, CAT, and GSH-Px) and non-enzymatic levels (GSH) in the jejunal tissue are shown in Table 1. Compared with the sham group, the I/R group exhibited slight changes in the enzymatic activity of SOD and GSH-Px and also in the levels of GSH, but these differences were not significant ( $P > 0.05$ ); however, a significant decrease was determined in the level of CAT activity ( $16.83 \pm 2.6$  vs  $43.15 \pm 4.7$  U/mg protein,  $P < 0.01$ ). As for the rHuEPO-administered groups, only the EPO + I/R group was found to have an increased CAT activity ( $42.85 \pm 6$  vs  $16.83 \pm 2.6$  U/mg protein,  $P < 0.01$ ) when compared with the I/R group.

**Table 1.** Jejunal tissue levels of antioxidant system elements (superoxide dismutase (SOD), catalase (CAT) and glutathione peroxidase (GSH-Px) and glutathione (GSH)) in sham-operated animals, vehicle-treated I/R animals, and I/R animals treated with EPO five minutes before ischemia and at the onset of reperfusion.

	Enzymatic antioxidants		Non-enzymatic antioxidant	
	SOD (U/mg/protein)	CAT (U/mg/protein)	GSH-Px (U/mg/protein)	GSH ( $\mu$ mol/mg/protein)
Sham	$4.94 \pm 1.24$	$43.15 \pm 4.7$	$0.036 \pm 0.007$	$0.381 \pm 0.079$
I/R	$6.18 \pm 0.43$	$16.83 \pm 2.6^a$	$0.035 \pm 0.010$	$0.275 \pm 0.025$
EPO + I/R	$5.34 \pm 0.66$	$42.85 \pm 6^b$	$0.034 \pm 0.013$	$0.262 \pm 0.022$
I + EPO + R	$5.15 \pm 0.88$	$29.31 \pm 4.6$	$0.032 \pm 0.008$	$0.280 \pm 0.028$

<sup>a</sup> $P < 0.01$  vs sham.

<sup>b</sup> $P < 0.01$  vs vehicle-treated I/R animals.

Data are mean  $\pm$  S.E.M. ( $n = 5-7$  per group). Note that there is a significant increase in the CAT levels in the EPO + I/R group compared with the I/R group. Sham; intestinal I/R was not induced. I/R; intestinal I/R, EPO + I/R; rHuEPO administered five minutes before ischemia, I + EPO + R; rHuEPO administered onset of reperfusion.

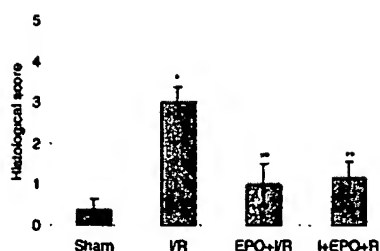


**Figure 2.** Intestinal mucosal injury evaluated by Chiu scoring system in sham-operated animals, vehicle-treated I/R animals, and I/R animals treated with EPO five minutes before ischemia and at the onset of reperfusion. Grading as (0 = normal mucosa, 1 = slight-, 2 = moderate-, 3 = massive subepithelial detachments, 4 = denudes villi, 5 = ulceration). Data are mean  $\pm$  S.E.M. (n = 5–7 per group). \* $P < 0.01$  vs sham; \*\* $P < 0.05$  vs vehicle-treated I/R animals (one-way ANOVA followed by Tukey's post-test). Note that there is a significant decrease in the intestinal injury score after treatment with EPO compared with the vehicle treated I/R animals. Sham; intestinal I/R was not induced, I/R; intestinal I/R, EPO + I/R; rHuEPO administered five minutes before ischemia, I + EPO + R; rHuEPO administered onset of reperfusion.

#### Effects of rHuEPO on Histological Changes in the Intestinal Tissue Subjected to I/R in Rats

H&E staining was carried out to determine the histological changes in the jejunal tissue. Histological evaluation was performed according to the Chiu scoring method. Data related to scoring obtained by means of H&E staining as well as the microphotographs are shown in Figure 2 and Figure 3. As expected, no mucosal injury was observed in the sham group. According to the Chiu scoring system, the injury in the I/R group was found to have increased compared with the sham group ( $3 \pm 0.36$  vs  $0.4 \pm 0.24$ ,  $P < 0.01$ ). It was determined that rHuEPO administered both before ischemia and at the onset of reperfusion significantly prevented the mucosal injury caused by I/R (EPO + I/R  $1 \pm 0.51$ ,  $P < 0.01$  and I + EPO + R  $1.16 \pm 0.4$  vs I/R  $3 \pm 0.36$ ,  $P < 0.05$ , respectively).

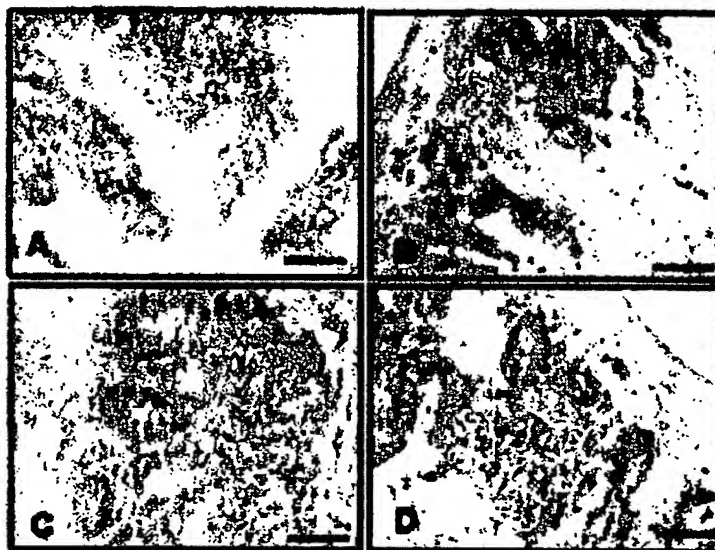


**Figure 3.** Photomicrographs of the jejunal tissue stained by the hematoxylin and eosin in sham-operated animals, vehicle-treated I/R animals, and I/R animals treated with EPO five minutes before ischemia and at the onset of reperfusion. (A) Sham: Histological features of normal jejunal tissue were observed. (B) I/R: The villi are denuded to the level of the lamina propria and dilated capillaries. (C) EPO + I/R: The villi are preserved (D) I + EPO + R: Erosion of the surface epithelium while the architecture of the villi are preserved. Sham; intestinal I/R was not induced, I/R; intestinal I/R, EPO + I/R; rHuEPO administered five minutes before ischemia, I + EPO + R; rHuEPO administered onset of reperfusion (40 $\times$ ).

#### Effects of rHuEPO on the Apoptotic Changes in the Intestinal Tissue Subjected to I/R in Rats

Localization of apoptotic cells in the jejunal tissue was made using the TUNEL staining method. The number of apoptotic cells (TUNEL-positive cells) is shown in Figure 4. Microphotographs of apoptotic cells stained by the TUNEL method are shown in Figure 5. Fewer TUNEL-positive cells were observed in the sham group ( $4.6 \pm 1.2$ ). Compared with the sham, the numbers of TUNEL-positive cell were found to have increased in the I/R group ( $20.4 \pm 2.6$  vs  $4.6 \pm 1.2$ ,  $P < 0.001$ ). However, a decrease in the numbers of TUNEL-positive cell was observed in rHuEPO administered in groups both before ischemia and at the onset of reperfusion groups (EPO + I/R  $9.2 \pm 2.7$  and I + EPO + R  $9.1 \pm 3$  vs I/R  $20.4 \pm 2.6$ ,  $P < 0.01$ ).

#### Effects of rHuEPO on the eNOS Expression in the Intestinal Tissue Subjected to I/R in Rats

We used immunohistochemical staining to localize eNOS expression. Immunohistochemical staining was scored in a semiquantitative manner to determine the differences between the groups in the distribution patterns of intensity of eNOS immunolabelling of the intestinal tissue (Figure 6). The intensity of the staining was recorded as mild (1), moderate (2), strong (3), and very strong (4). Microphotographs of eNOS immunoreactivity in the jejunal tissue are shown in Figure 7. According to the scoring system, the intensity of eNOS immunolabelling in the I/R group was also found to have increased compared with the sham group ( $3 \pm 0.4$  vs  $1.3 \pm 0.33$ ,  $P < 0.05$ ). However, it was determined that rHuEPO administered both before ischemia and at the onset of reperfusion sig-

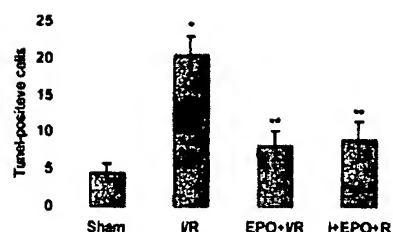


**Figure 4.** The number of apoptotic cells in the jejunal tissue determined by TUNEL staining in sham-operated animals, vehicle-treated I/R animals, and I/R animals treated with EPO five minutes before ischemia and at the onset of reperfusion. Results are expressed as mean TUNEL positive nuclei/observed field  $\pm$  S.E.M. ( $n = 5-7$  per group). \* $P < 0.001$  vs sham; \*\* $P < 0.01$  vs vehicle-treated I/R animals (one-way ANOVA followed by Tukey's post-test). Note that there is a significant decrease in the TUNEL-positive cells in EPO treated I/R animals compared with the vehicle treated I/R animals. Sham; Intestinal I/R was not induced, I/R; Intestinal I/R, EPO + I/R; rHuEPO administered five minutes before ischemia, I + EPO + R; rHuEPO administered onset of reperfusion.

nificantly decreased (EPO + I/R  $1.6 \pm 0.24$ ,  $P < 0.05$  and I + EPO + R  $1.4 \pm 0.24$  vs I/R  $3 \pm 0.4$ ,  $P < 0.01$ , respectively).

## DISCUSSION

Given the fact that histological assessment made using a microscopic scoring system has been accepted as a good standard in the evaluation of I/R injury in the intestinal tissue (23,24), the present study has established that a high single dose of rHuEPO administered both before ischemia and at the onset of reperfusion protected the intestinal tissue against I/R injury in rats. Data from the present study demonstrate that anti-apoptotic, antioxidative, and antiinflammatory properties seem to be related to the EPO-mediated protective effect against intestinal I/R injury. The present study, to the best of our information, is the first study demonstrating the effects of rHuEPO in preventing the I/R-induced intestinal injury.

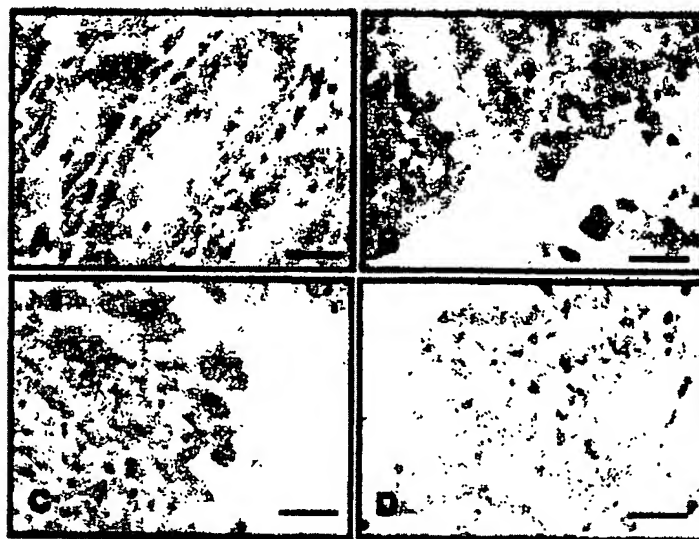


**Figure 5.** Photomicrographs of apoptotic cells in the jejunal tissue stained by the TUNEL method in sham-operated animals, vehicle-treated I/R animals, and I/R animals treated with EPO five minutes before ischemia and at the onset of reperfusion. The dark brown dots correspond to representative TUNEL-positive nuclei. (A) Sham: Intestinal I/R was not induced. (B) I/R: Intestinal I/R. (C) EPO + I/R: rHuEPO administered five minutes before ischemia. (D) I + EPO + R: rHuEPO administered onset of reperfusion (200 $\times$ ).

Oxidative stress plays an important role in the intestinal I/R injury. In the intestinal tissue subjected to I/R, activated neutrophils induce tissue injury through the production and release of ROS and cytotoxic proteins (for example, proteases, MPO, lactoferrin) into the extracellular fluid, constituting the inflammatory cascades that trigger the radical-induced I/R injury (3,25,26). MPO activity is commonly used to measure the extent of inflammation in intestinal tissues subjected to I/R injury (3). In the present study, intestinal I/R caused an elevation in tissue MPO activity, indicating the presence of enhanced leukocyte recruitment in the inflamed tissue, while the increased intestinal MDA level, an indicator of lipid peroxidation, verified the oxidative damage in the intestinal tissue.

Some researchers reported the antiinflammatory properties of EPO against I/R induced tissue injury (9,19,27). The present study determined that the MPO activity decreased with the application of rHuEPO, but a significant decrease was

observed in the group in which rHuEPO was administered at the onset of reperfusion. The inhibition of neutrophil recruitment into the tissue is reflected by the partial capacity of rHuEPO to reverse the neutropenia observed during reperfusion.

ROS are potent oxidizing agents, the damage of cellular membranes by lipid peroxidation being a major consequence. Previous studies established that EPO inhibits lipid peroxidation in the oxidative damage induced by in vitro (28,29) and in vivo (17,30,31) models. These studies also established that EPO inhibited lipid peroxidation induced by strong hydroxyl radicals ( $\cdot\text{OH}$ ) formed by iron-mediated Fenton reaction. In the present study, it was found that rHuEPO administered at the onset of both ischemia and reperfusion caused a decrease in MDA levels, but a really significant decrease was observed in the group in which rHuEPO was administered at the onset of reperfusion. The present study as well as a number of other previously conducted

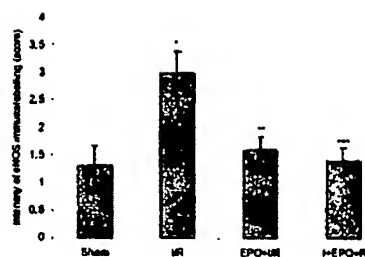


**Figure 6.** The intensity of eNOS Immunolabelling evaluated by scoring system in sham-operated animals, vehicle-treated I/R animals, and I/R animals treated with EPO five minutes before ischemia and at the onset of reperfusion. Grades of score: mild (1), moderate (2), strong (3), and very strong (4). Data are mean  $\pm$  S.E.M. ( $n = 3-5$  per group). \* $P < 0.05$  vs sham; \*\* $P < 0.05$  vs vehicle-treated I/R animals; \*\*\* $P < 0.01$  vs vehicle-treated I/R animals (one-way ANOVA followed by Tukey's post-test). Note that there is a significant decrease in EPO groups compared with the I/R group. Sham: Intestinal I/R was not induced, I/R: Intestinal I/R, EPO + I/R: rHuEPO administered five minutes before ischemia, I + EPO + R: rHuEPO administered onset of reperfusion.

researches demonstrated that EPO had a direct antioxidant function by scavenging ROS from the environment. EPO is a glycoprotein hormone containing approximately 30 percent carbohydrate, 11 percent sialic acid, 11 percent total hexose, and 8 percent *N*-acetylglucosamine. Cross et al (1984) has shown that small glycopolypeptides are powerful  $\cdot\text{OH}$  scavengers (32). Such scavenging action, as they have pointed out, is to be expected from the high sugar content of the glycopolypeptides. Thus, protection by EPO may be mediated through the scavenging action of its sugar moiety. Mechanistic studies suggest that Bcl-2 might be mediated in the antioxidant activity of EPO (33).

There are many studies revealing the association of EPO with the antioxidant system. These studies showed that EPO increased the activity of antioxidant enzymes, such as SOD, CAT, and GSH-Px (28,29,34-37). In the present study, it also was found that rHuEPO administered

prior to ischemia significantly elevated the level of CAT activity when compared with the I/R group. In conformity with the results obtained from previous studies on the antioxidant system, we found that EPO might be capable of increasing the activity of CAT or restoring this enzyme, which decreases due to I/R in the intestinal tissue. Findings obtained from the present study and a handful of previously conducted studies have verified that EPO might be capable of acting as a direct antioxidant as well by activating antioxidant defense mechanisms.

Apoptosis, known as programmed cell death, is a form of cell death that serves to eliminate dying cells in proliferating or differentiating cell populations (38). However, activation of apoptosis in pathologic states results in rapid and extensive cell death with consequent tissue dysfunction. Previous studies reported that apoptosis is a major mode of cell death in the intestinal damage induced

by I/R (39,40). In the present study, the number of TUNEL-positive cells as an indicator of apoptosis increased significantly after 30 min ischemia followed by 60 min reperfusion in the jejunal tissue. In previous studies dealing with I/R injury, EPO enhanced functional and morphologic tissue recovery, mainly through its antiapoptotic action. For example, rHuEPO was found to be effective in reducing the number of TUNEL-positive cells in I/R-induced injury in the heart (41). Sharples et al (2004) determined that rHuEPO reduced the number of TUNEL-positive cells prior to both ischemia and reperfusion in renal I/R injury (16). In the present study, an increased number of TUNEL-positive cells in the jejunal tissue subjected to I/R was also reduced by rHuEPO. Despite well-characterized reductions in apoptosis after EPO treatment, the mechanisms mediating the effects of EPO are not yet fully understood. It was reported that

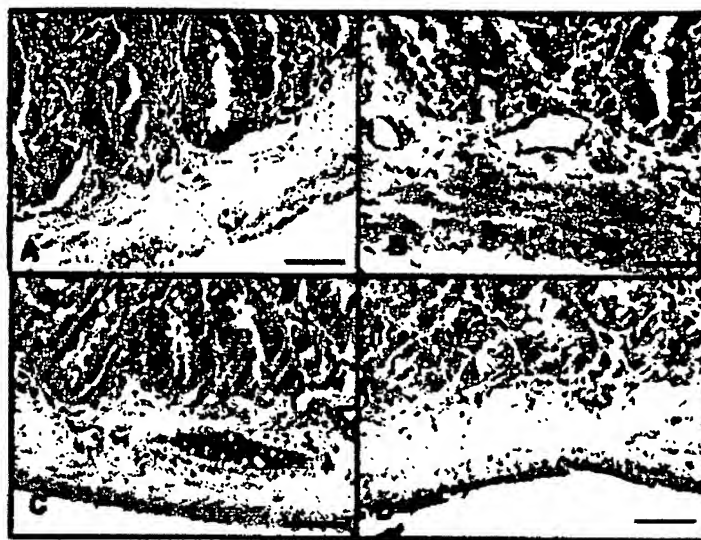


**Figure 7.** Immunolabelling of endothelial nitric oxide synthase (eNOS) in the jejunal tissue in sham-operated animals, vehicle-treated I/R animals, and I/R animals treated with EPO five minutes before ischemia and at the onset of reperfusion. Note that mild immunolabelling of eNOS is detected in jejunal specimens from sham animals, strong immunoreactivity is detected in I/R animals and moderate immunoreactivity is detected in rHuEPO administered groups. (A) Sham: Intestinal I/R was not induced, (B) I/R: Intestinal I/R, (C) EPO + I/R: rHuEPO administered five minutes before ischemia, (D) I + EPO + R: rHuEPO administered onset of reperfusion (40 $\times$ ).



Jak2-STAT-Bcl-2 pathway are involved in mediating the antiapoptotic effect of EPO (42).

Oxidative stress is known to induce apoptosis by damaging DNA, oxidizing membrane lipids, and/or directly activating the expression of the genes/proteins responsible for apoptosis (43–45). Kojima et al (2003) have reported that oxidative stress after I/R plays an important role in induction of apoptosis in the intestinal mucosa (46). In the present study, increased oxidative stress in intestinal I/R may be responsible for apoptosis. Therefore, the inhibitory effect of EPO on the I/R-induced ROS production may be the underlying mechanism for its protective effect against apoptosis.

Although NO is an important signaling molecule in physiological processes, its protective or detrimental role in intestinal I/R injury is still controversial. It has been reported that endothelial nitric oxide synthase (eNOS)-derived NO may have a protective role at the onset of I/R of the small intestine (47). However, evidence also suggests that eNOS can become "dysfunctional" during oxidative stress. It has been demonstrated that superoxide anions may react with NO released by eNOS and thereby turn into cytotoxic oxidant peroxynitrite (48). Therefore, an altered function of eNOS may play a role in intestinal I/R. In the present study, the 30 min ischemia followed by 60 min reperfusion increased eNOS expression in the jejunal tissue. These results show that intestinal I/R injury may be related to increased NO production associated with eNOS, producing peroxynitrite. However, our study showed that increased eNOS expression induced by I/R decreased with rHuEPO treatment, thus it might be reducing peroxynitrite, and causing enhanced intestinal I/R injury. These results demonstrate that inhibitory effect of EPO on the eNOS-mediated NO overproduction may be the underlying mechanism for its protective effect against intestinal I/R injury. However, these results contradict a recent study which has demonstrated that EPO increases eNOS expression in car-

diomyocyte in both in vitro and in vivo models of I/R (49). On the other hand, previous studies in cultured endothelial cells indicated that EPO had little or no effect on increasing eNOS activity (50,51). Wang and Waziri (1999) reported that 24 h incubation of human coronary artery endothelial cells with EPO-inhibited NO production and eNOS expression (52). Calapai et al (2000) showed that increase of NO production in the hippocampus, as observed after ischemia, was reduced in animals treated with rHuEPO (53). Briefly, as reviewed by Li et al (2002), effects of EPO on eNOS expression are still controversial (54). Nevertheless, elucidation of the role of NO pathway in intestinal protection of EPO will need further investigations.

In conclusion, a single dose of EPO protects the intestinal tissue against I/R injury in rats, demonstrating antioxidant, anti-inflammatory, and antiapoptotic effects. Future experiments will be needed to precisely explore the EPO signaling pathways in the intestine to delineate the benefits of EPO therapy and incorporate its potential use into clinical practice in the future.

#### ACKNOWLEDGMENTS

This research was supported by grants from Dokuz Eylul University Research Foundation (Project 2005. KB. SAG.031).

#### REFERENCES

- Granger DN, Korthuis RJ. (1995) Physiologic mechanisms of postischemic tissue injury. *Annu. Rev. Physiol.* 57:311–32.
- Brandt, JL. (2003) Mesenteric vascular disease. Current Diagnosis and Treatment in Gastroenterology. New York: Section 1.9.
- Mallick LH, Yang W, Winslet WC, Seifalian AM. (2004) Ischemia-Reperfusion Injury of the Intestine and Protective Strategies Against Injury. *Dig. Dis. Sci.* 49:1359–77.
- Erbayraktar S et al. (2006) Carbamylated erythropoietin reduces radiosurgically-induced brain injury. *Mol. Med.* 12:74–80.
- Siren AL, Ehrenreich H. (2001) Erythropoietin—a novel concept for neuroprotection. *Eur. Arch. Psychiatry Clin. Neurosci.* 25:179–84.
- Celik M et al. (2002) Erythropoietin prevents motor neuron apoptosis and neurologic disability in experimental spinal cord ischemic injury. *Proc. Natl. Acad. Sci.* 99:2258–63.
- Erbayraktar S et al. (2003) Asialoerythropoietin is a nonerythropoietic cytokine with broad neuroprotective activity in vivo. *Proc. Natl. Acad. Sci.* 100:6741–6746.
- Erbayraktar S, Yilmaz O, Cokmen N, Brines M. (2003) Erythropoietin is a multifunctional tissue-protective cytokine. *Curr. Hematol. Rep.* 2:465–470.
- Contaldo C et al. (2007) Human recombinant erythropoietin protects the striated muscle microcirculation of the dorsal skinfold from postischemic injury in mice. *Am. J. Physiol. Heart. Circ. Physiol.* 293:274–283.
- Brines M et al. (2004) Erythropoietin mediates tissue protection through an erythropoietin and common beta-subunit heteroreceptor. *Proc. Natl. Acad. Sci.* 101:14907–12.
- Juul SE et al. (1999) Why is erythropoietin present in human milk? Studies of erythropoietin receptors on enterocytes of human and rat neonates. *Pediatr. Res.* 46: 263–8.
- Cuzzocrea S et al. (2004) Erythropoietin reduces the development of experimental inflammatory bowel disease. *J. Pharmacol. Exp. Ther.* 311:1272–80.
- Ledbetter DJ, Juul SE. (2000) Erythropoietin and the incidence of necrotizing enterocolitis in infants with very low birth weight. *J. Pediatr. Surg.* 35:178–82.
- Fatourus M et al. (1999) Alterations in body weight, breaking strength, and wound healing in wistar rats treated pre- and postoperatively with erythropoietin or granulocyte macrophage-colony stimulating factor: Evidence of a previously unknown anabolic effect of erythropoietin? *J. Lab. Clin. Med.* 133:253–9.
- Lipsic E et al. (2004) Timing of erythropoietin treatment for cardioprotection in ischemia-reperfusion. *J. Cardiovasc. Pharmacol.* 44:473–9.
- Sharples EL et al. (2004) Erythropoietin protects the kidney against the injury and dysfunction caused by ischemia-reperfusion. *J. Am. Soc. Nephrol.* 15:2115–24.
- Solaroglu A, Dede FS, Okutan E, Bayrak A, Haberal A, Kilinc K. (2004) A single dose of erythropoietin attenuates lipid peroxidation in experimental liver ischemia-reperfusion injury in the rat fetus. *J. Matern. Fetal. Neonatal. Med.* 16:231–4.
- Wu H et al. (2006) Pretreatment with recombinant human erythropoietin attenuates ischemia-reperfusion-induced lung injury in rats. *Eur. J. Cardiothorac. Surg.* 29:902–7.
- Villa P et al. (2003) Erythropoietin selectively attenuates cytokine production and inflammation in cerebral ischemia by targeting neuronal apoptosis. *J. Exp. Med.* 198:971–5.
- Junk AK et al. (2002) Erythropoietin administration protects retinal neurons from acute ischemia-reperfusion injury. *Proc. Natl. Acad. Sci.* 99:10659–64.
- Tatum VL, Changchit C, Chow CK. (1990) Measurement of malonaldehyde by HPLC with fluorescence detection. *Lipids* 25:226–9.
- Wiechelman KJ, Braun RD, Fitzpatrick JD. (1988) Investigation of the bichinchoninic acid protein

- assay: identification of the groups responsible for color formation. *Anal. Biochem.* 175:231-7.
23. Chiu CJ, McArdle AH, Brown R, Scott HJ, Gurd FN. (1970) Intestinal mucosal lesion in low-flow states. I. A morphologic, hemodynamic and metabolic reappraisal. *Arch. Surg.* 101:478.
  24. Park PO, Haglund U, Bulkley GB, Falt K. (1990) The sequence of development of intestinal tissue injury following strangulation ischemia and reperfusion. *Surgery.* 107:574.
  25. Zimmerman BJ, Granger DN. (1994) Mechanisms of reperfusion injury. *Am. J. Med. Sci.* 307:284-92.
  26. Kettle AJ, Winterbourn CC. (1997) Myeloperoxidase: a key regulator of neutrophil oxidant production. *Redox. Rep.* 3:3-15.
  27. Liu X et al. (2006) Mechanism of the cardioprotection of rEPO pretreatment on suppressing the inflammatory response in ischemia-reperfusion. *Life Sci.* 78:2255-64.
  28. Chattopadhyay T, Das C, Bandyopadhyay D, Datta AG. (2000) Protective effect of erythropoietin on the oxidative damage of erythrocyte membrane by hydroxyl radical. *Biochem. Pharmacol.* 59:419-25.
  29. Chakraborty M, Ghosal J, Biswas T, Datta AG. (1988) Effect of erythropoietin on membrane lipid peroxidation, superoxide dismutase, catalase, and glutathione peroxidase of rat RBC. *Biochem. Med. Metab. Biol.* 40:8-18.
  30. Akisu M, Kullahcioglu GF, Baka M, Husseyinov A, Kultursay N. (2001a) The role of recombinant human erythropoietin in lipid peroxidation and platelet-activating factor generation in a rat model of necrotizing enterocolitis. *Eur. J. Pediatr. Surg.* 11:167-72.
  31. Akisu M, Tuzun S, Arslanoglu S, Yalaz M, Kultursay N. (2001b) Effect of recombinant human erythropoietin administration on lipid peroxidation and antioxidant enzyme(s) activities in pre-term infants. *Acta. Med. Okayama.* 55:357-62.
  32. Cross CE, Halliwell B, Allen A. (1984) Antioxidant protection: A function of tracheobronchial and gastrointestinal mucus. *Lancet.* 1:1328-30.
  33. Digicaylioglu M, Lipton SA. (2001) Erythropoietin-mediated neuroprotection involves cross-talk between Jak2 and NF- $\kappa$ B signaling cascades. *Nature.* 412:641-7.
  34. Genc S, Akhisaroglu M, Kuralay F, Genc K. (2002) Erythropoietin restores glutathione peroxidase activity in 1-methyl-4-phenyl-1,2,5,6-tetrahydropyridine-induced neurotoxicity in C57BL mice and stimulates murine astroglial glutathione peroxidase production in vitro. *Neurosci. Lett.* 321:73-76.
  35. Kumral A et al. (2005) Protective effects of erythropoietin against ethanol-induced apoptotic neurodegeneration and oxidative stress in the developing C57BL/6 mouse brain. *Brain Res. Dev. Brain Res.* 160:146-56.
  36. Sakanaka M et al. (1998) In vivo evidence that erythropoietin protects neurons from ischemic damage. *Proc. Natl. Acad. Sci.* 95:4635-40.
  37. Turi S, Nemeth I, Varga I, Bodrogi T, Matkovics B. (1992) The effect of erythropoietin on the cellular defense mechanism of red blood cells in children with chronic renal failure. *Pediatr. Nephrol.* 6:536-41.
  38. Kerr JF, Wyllie AH, Currie AR. (1972) Apoptosis: a basic biological phenomenon with wide-ranging implications in tissue kinetics. *Br. J. Cancer.* 26:239-57.
  39. Ikeda H et al. (1998) Apoptosis is a major mode of cell death caused by ischemia and ischemia/reperfusion injury to the rat intestinal epithelium. *Gut.* 42:530-7.
  40. Noda T, Iwakiri R, Fujimoto K, Matsuo S, Aw TY. (1998) Programmed cell death induced by ischemia-reperfusion in rat intestinal mucosa. *Am. J. Physiol.* 274:270-6.
  41. Parsa CJ et al. (2004) Cardioprotective effects of erythropoietin in the reperfused ischemic heart: a potential role for cardiac fibroblasts. *J. Biol. Chem.* 279:20655-62.
  42. Brines M and Cerami A. (2006) Discovering erythropoietin's extra-hematopoietic functions: biology and clinical promise. *Kidney Int.* 70:246-50.
  43. Bai J, Cederbaum AI. (2001) Mitochondrial catalase and oxidative injury. *Biol. Signals Recept.* 10:189-99.
  44. Buttke TM, Sandstrom PA. (1994) Oxidative stress as a mediator of apoptosis. *Immunol. Today.* 15:7-10.
  45. Curtin JF, Donovan M, Cotter TG. (2002) Regulation and measurement of oxidative stress in apoptosis. *J. Immunol. Methods.* 265:49-72.
  46. Kojima M et al. (2003) Effects of antioxidative agents on apoptosis induced by ischemia-reperfusion in rat intestinal mucosa. *Aliment Pharmacol. Ther.* 1:139-45.
  47. Rovietto F et al. (2007) Protective role of PI3-kinase-Akt-eNOS signaling pathway in intestinal injury associated with splanchnic artery occlusion shock. *Br. J. Pharmacol.* 151:377-83.
  48. Munzel T, Daiber A, Ullrich V, Mulsch A. (2005) Vascular consequences of endothelial nitric oxide synthase uncoupling for the activity and expression of the soluble guanylyl cyclase and the cGMP-dependent protein kinase. *Arterioscl. Thromb. Vasc. Biol.* 25:1551-7.
  49. Rui T et al. (2005) Erythropoietin prevents the acute myocardial inflammatory response induced by ischemia/reperfusion via induction of AP-1. *Cardiovasc. Res.* 65:719-27.
  50. Lopez Ongil SL, Saura M, Lamas S, Rodriguez Puyol M, Rodriguez Puyol D. (1996) Recombinant human erythropoietin does not regulate the expression of endothelin-1 and constitutive nitric oxide synthase in vascular endothelial cells. *Exp. Nephrol.* 4:37-42.
  51. Banerjee D, Rodriguez M, Nag M, Adamson JW. (2000) Exposure of endothelial cells to recombinant human erythropoietin induces nitric oxide synthase activity. *Kidney Int.* 57:1895-904.
  52. Wang XQ, Vaziri ND. (1999) Erythropoietin depresses nitric oxide synthase expression by human endothelial cells. *Hypertension.* 33:894-9.
  53. Calapai MC et al. (2000) Erythropoietin protects against brain ischemia injury by inhibition of nitric oxide formation. *Eur. J. Pharmacol.* 401:349-356.
  54. Li H, Wallerath T, Münzel T, Förstermann U. (2002) Regulation of endothelial-type NO synthase expression in pathophysiology and in response to drugs. *Nitric Oxide.* 7:149-64.



## Erythropoietin (EPO) — EPO-receptor signaling improves early endochondral ossification and mechanical strength in fracture healing

Joerg H. Holstein<sup>a,b,\*</sup>, Michael D. Menger<sup>b</sup>, Claudia Scheuer<sup>b</sup>, Christoph Meier<sup>b,c</sup>,  
Ulf Culemann<sup>a</sup>, Rainer J. Wirbel<sup>a</sup>, Patric Garcia<sup>a,b</sup>, Tim Pohlemann<sup>a</sup>

<sup>a</sup> Department of Trauma-, Hand- and Reconstructive Surgery, University of Saarland, Homburg/Saar, Germany

<sup>b</sup> Institute for Clinical and Experimental Surgery, University of Saarland, Homburg/Saar, Germany

<sup>c</sup> Division of Trauma Surgery, University Hospital Zurich, Switzerland

Received 27 May 2006; accepted 8 November 2006

### Abstract

Beyond its role in the regulation of red blood cell proliferation, the glycoprotein erythropoietin (EPO) has been shown to promote cell regeneration and angiogenesis in a variety of different tissues. In addition, EPO has been indicated to share significant functional and structural homologies with the vascular endothelial growth factor (VEGF), a cytokine essential in the process of fracture healing. However, there is complete lack of information on the action of EPO in bone repair and fracture healing. Therefore, we investigated the effect of EPO treatment on bone healing in a murine closed femur fracture model using radiological, histomorphometric, immunohistochemical, biomechanical and protein biochemical analysis. Thirty-six SKH1-hr mice were treated with daily i.p. injections of 5000 U/kg EPO from day 1 before fracture until day 4 after fracture. Controls received equivalent amounts of the vehicle. After 2 weeks of fracture healing, we could demonstrate expression of the EPO-receptor (EPOR) in terminally differentiating chondrocytes within the callus. At this time point EPO-treated animals showed a higher torsional stiffness (biomechanical analysis:  $39.6 \pm 19.4\%$  of the contralateral unfractured femur) and an increased callus density (X-ray analysis (callus density/spongiosa density):  $110.5 \pm 7.1\%$ ) when compared to vehicle-treated controls ( $14.3 \pm 8.2\%$  and  $105.9 \pm 6.6\%$ ;  $p < 0.05$ ). Accordingly, the histomorphometric examination revealed an increased fraction of mineralized bone and osteoid ( $33.0 \pm 3.0\%$  versus  $28.5 \pm 3.6\%$ ;  $p < 0.05$ ). Of interest, this early effect of the initial 6-day EPO treatment had vanished at 5 weeks after fracture. We conclude that EPO–EPOR signaling is involved in the process of early endochondral ossification, enhancing the transition of soft callus to hard callus.

© 2006 Elsevier Inc. All rights reserved.

**Keywords:** EPO; EPOR; Endochondral ossification; Fracture healing; Mice

### Introduction

In the United States, each year approximately 6 million people sustain bone fractures (Praemer et al., 1992). In spite of an appropriate orthopedic management some of these fractures heal poorly or even result in non-union. In these cases the reason for inadequate bone healing mostly remains unclear, and, therefore, therapy options are limited.

Fracture healing is a complex physiological process that occurs in a sequentially orchestrated manner: inflammation, mesenchymal cell condensation, chondrogenesis, angiogenesis, and osteogenesis. Directly after trauma, inflammatory cells, macrophages and platelets can be detected at the fracture site. Amongst others, cytokines like platelet-derived growth factor (PDGF) and transforming growth factor (TGF- $\beta$ ) lead to a proliferation of mesenchymal cells in the periosteum. Further, mesenchymal cells differentiate to chondrocytes, which form a cartilaginous callus (soft callus). During ossification the hypertrophic chondrocytes terminally differentiate and undergo apoptosis (Miclau and Helms, 2000). The cartilage calcifies before being replaced by newly formed woven bone (hard callus)

\* Corresponding author. Department of Trauma-, Hand- and Reconstructive Surgery, University of Saarland, D-66421 Homburg/Saar, Germany. Tel.: +49 6841 16 31501; fax: +49 6841 16 31503.

E-mail address: [chjhol@uniklinikum-saarland.de](mailto:chjhol@uniklinikum-saarland.de) (J.H. Holstein).

(Barnes et al., 1999). Simultaneously, new blood vessels invade the callus, which seems to play a critical role in the process of osteogenesis (Gerber et al., 1999). One of the key molecules promoting angiogenesis during fracture healing is the vascular endothelial growth factor (VEGF) (Ferguson et al., 1999). In addition, VEGF is expressed in terminally differentiating chondrocytes, suggesting an important role of VEGF in the degradation of hypertrophic cartilage matrix (Neufeld et al., 1999). In fact, recent studies report that osteogenesis can be stimulated by the application of VEGF (Geiger et al., 2005).

The glycoprotein erythropoietin (EPO) regulates the production of red blood cells by its specific interaction with the cell-surface receptor EPOR (Krantz, 1991). Additionally, EPOR is expressed in several non-hematopoietic cell types (D'Andrea et al., 1989). For instance, in the brain EPO–EPOR signalling is associated with the response to neuronal injury (Brines et al., 2000). In the kidney, the intestine, and skeletal muscle, EPO has been shown to induce cell proliferation (Westenfelder et al., 1999; Ogilvie et al., 2000; Juul et al., 2001). EPOR has been also detected in several types of vascular endothelial cells (Anagnostou et al., 1994), and EPO has further been demonstrated to promote angiogenesis (Anagnostou et al., 1990).

The cytokine VEGF shares significant homology with EPO. The expression of both EPO and VEGF is stimulated by hypoxia through an analogical pathway (Goldberg et al., 1988; Steinbrech et al., 2000). Simultaneously, hypoxia and oxygen tension play a crucial role in the process of fracture healing (Brighton and Krebs, 1972). As mentioned above, EPO and VEGF have also been shown to promote angiogenesis and cell proliferation (Anagnostou et al., 1990; Westenfelder et al., 1999; Hoeben et al., 2004). In addition, the VEGF gene and the EPO gene have substantial similarities in terms of structure and enhancer elements (Steinbrech et al., 2000). Thus, it seems of major interest to investigate whether the positive effects of VEGF on bone healing and especially on osteogenesis can also be produced by EPO treatment. Because there is no information on the action of EPO in fracture healing, we herein studied for the first time the effect of high dose peritrauma application of EPO on bone healing using a closed femur fracture model in mice.

## Materials and methods

### Experimental groups

Thirty-six SKH-1Ha mice (30–40 g bw) were treated with EPO for 6 days. Therefore, 5000 U/kg bodyweight (bw) EPO was applied daily by an intraperitoneal injection from day 1 before fracture until day 4 after fracture. The dose of 5000 U/kg was chosen according to other studies analyzing non-hematopoietic actions of EPO in myocardial tissue (Li et al., 2006; Nishiya et al., 2006). Two or five weeks after surgery, animals were killed and bone healing was analyzed radiologically ( $n=17$  at 2 weeks;  $n=16$  at 5 weeks), biomechanically ( $n=2 \times 8$ ), and histomorphometrically ( $n=2 \times 7$ ). At 2 weeks additional animals were studied by immunohistochemical ( $n=4$ ) and protein biochemical techniques ( $n=4$ ). An additional 44 mice, which received the vehicle only, served as controls.

Analyses in controls were similar to those of EPO-treated animals.

### Surgical procedure

All experiments were performed in adherence to the National Institute of Health guidelines for the use of experimental animals and were approved by the German legislation on the protection of animals. The mice were anesthetized by an intraperitoneal injection of 25 mg/kg bw xylazine and 75 mg/kg bw ketamine. Under sterile conditions a 4 mm medial parapatellar incision was performed at the right knee, and the patella was dislocated laterally. A hole ( $\varnothing=0.5$  mm) was drilled into the intracondylar notch, and a tungsten guide wire ( $\varnothing=0.1$  mm) was inserted retrogradely into the intramedullary canal. Using a 3-point bending device (Schmidmaier et al., 2004) a standardized closed midshaft fracture (according to AO-classification: A2–A3) was produced. Subsequently, a locking femur nail ( $\varnothing=0.5$  mm) was implanted over the guide wire to stabilize the fracture (Holstein et al., in press). Fracture configuration and implant position were controlled by X-rays (Inside IP-21 high resolution dental films, Kodak, Rochester, NY, USA). After 2 or 5 weeks, animals were killed with an overdose of barbiturates. The healed bones were X-rayed again and prepared for further biomechanical, histological and protein biochemical evaluation.

### Hemoglobin concentration

To consider the effect of EPO on erythropoiesis, hemoglobin concentration was determined in EPO-treated animals as well as in untreated controls (Coulter diff AC T, Coulter Beckman, Fullerton, CA, USA).

### Radiological analysis

Dorso-ventral X-rays of the healed femora were digitized and evaluated using the Cap Image Analysis System (Zeintl, Heidelberg, Germany). Because of possible variabilities in the properties of the X-rays, all parameters were calculated in a relative manner as follows: (i) total (hard) callus area/femoral bone diameter at the fracture site [Cl.Ar/B.Dm (mm)] and (ii) radiological callus density/radiological spongiosa density [Cl.Dn/Sn.Dn (%)].

In addition, callus maturity was analyzed according to the classification of Goldberg et al. (1985) with stage 1 indicating radiological non-union; stage 2, possible union; and stage 3, radiological union.

### Biomechanical analysis

After sacrifice of the animals, the right and the left femora were resected carefully and freed from soft tissue. After the implant was removed, callus strength (right femur) was measured by a torsional testing device (Holstein et al., in press). To account for differences in bone strength of the individual animals, the unfractured left femora were also analyzed, serving as an internal control. Therefore, all values of the fractured femora are given in

percent of the corresponding unfractured femora. To guarantee standardized measuring conditions, a working gauge length (Manigrasso and O'Connor, 2004) of 4 mm was determined. Applying a gradually increasing torque, biomechanical parameters were calculated as follows: (i) peak torque at failure (Nmm), (ii) peak rotation angle at failure ( $^{\circ}$ ), and (iii) torsional stiffness (Nmm/ $^{\circ}$ ).

#### *Histomorphometric analysis*

After resection of the healed femora and removal of the implants, bones were fixed in 4% phosphate buffered formalin for 24 h, decalcified in 10% EDTA solution for 5 weeks, and embedded in paraffin.

For histomorphometric studies, longitudinal sections of 5  $\mu$ m thickness were stained according to the trichrome method. At a magnification of 1.25 $\times$  (Olympus BX60 Microscope, Olympus, Tokyo, Japan; Zeiss Axio Cam and Axio Vision 3.1, Carl Zeiss, Oberkochen, Germany; ImageJ Analysis System, NIH, Bethesda, MD, USA) structural indices were calculated according to the nomenclature and units recommended by the American Society of Bone and Mineral Research (ASBMR) (Parfitt et al., 1987): (i) total callus area (bone [mineralized bone, osteoid and bone marrow], cartilaginous, and fibrous callus area)/femoral bone diameter (cortical width plus marrow diameter) at the fracture gap [Cl.Ar/B.Dm (mm)], (ii) bone callus area (mineralized bone, osteoid and bone marrow)/total callus area [B.Cl.Ar/Cl.Ar (%)], (iii) cartilaginous callus area/total callus area [Cg.Cl.Ar/Cl.Ar (%)], (iv) fibrous callus area/total callus area [Fb.Cl.Ar/Cl.Ar (%)], and (v) mineralized callus area plus osteoid callus area (bone without bone marrow)/total callus area [(Md.Cl.Ar+O.Cl.Ar)/Cl.Ar (%)].

#### *Immunohistochemical analysis*

To evaluate cell proliferation and apoptosis within the fracture callus, immunohistochemical staining for proliferating cell nuclear antigen (PCNA) and caspase-3 was performed. In addition, the expression of EPOR was examined immunohistochemically. Therefore, tissue sections were deparaffinized in xylene and rehydrated in a descending, graded series of alcohol. Endogenous peroxidase was blocked by 3% H<sub>2</sub>O<sub>2</sub> (10 min). Antigen retrieval was achieved by microwaving (10 min; 700 W) specimens in citrate buffer (pH 6.0). After blocking of unspecific binding sites with PBS and goat normal serum (30 min; room temperature), sections were incubated overnight with mouse monoclonal anti-PCNA (1:50 PBS; PC10, Dako, Glostrup, Denmark), rabbit polyclonal anti-caspase-3 (1:50 PBS; ASP175, Cell Signaling, Beverly, MA, USA) or rabbit polyclonal anti-EPOR antibody (1:50 PBS; M-20, Santa Cruz Biotechnology, Santa Cruz, CA, USA) at room temperature. Peroxidase-conjugated sheep anti-rabbit (1:100; Dianova, Hamburg, Germany) and goat anti-mouse (1:100; Amersham Biosciences, Buckinghamshire, UK) were used as secondary antibodies (incubation for 1 h at room temperature). Diaminobenzidine (DAB; Dako) served as the chromogen and Mayer's hemalum as the counterstain.

PCNA and EPOR expression were also quantified. Within the callus, PCNA-positive staining was found only in periosteal cells and osteoblasts. For quantification, the number of PCNA-positive cells was counted and is given in percent of all osteoblasts and periosteal cells visible. EPOR-positive staining was found only in chondrocytes. For quantification, the number of EPOR-positive cells was counted and is given in percent of all chondrocytes visible.

#### *Western blot analysis*

In addition to immunohistochemical staining, Western blot analyses for PCNA and EPOR were performed after 2 weeks of fracture healing. Therefore, the callus tissue was frozen and stored at  $-80^{\circ}\text{C}$  until required. Specimens were homogenized and extracted in lysis buffer consisting of 10 mM Tris pH 7.5, 10 mM NaCl, 0.1 mM EDTA, 0.5% Triton-X 100, 0.02% NaN<sub>3</sub>, 0.2 mM PMSF and protease inhibitor cocktail (1:100; Sigma, Taufkirchen, Germany). Proteins were separated and transferred to membranes by standard protocols and probed using anti-PCNA (Dako) and the M-20 EPOR antibody (Santa Cruz Biotechnology), respectively.

To identify specific binding, an additional analysis was performed, in which samples were treated with a distinct peptide (provided by Santa Cruz Biotechnology) that blocks the specific binding site of the M-20 EPOR antibody. When this was done, the characteristic bands for EPOR vanished.

Western blot analyses were performed only after 2 weeks but not after 5 weeks of fracture healing, because after the later time period the callus in both groups did not show any remaining cartilaginous tissue.

Protein expression was visualized by means of luminol-enhanced chemiluminescence (ECL, Amersham Biosciences) after exposure of the membrane to a blue-light-sensitive autoradiography film (Hyperfilm ECL, Amersham Biosciences). Signals were densitometrically assessed (Geldoc, Quantity one software; BioRad, Hercules, CA, USA) and normalized to the  $\beta$ -actin signals (mouse monoclonal anti- $\beta$ -actin antibody, 1:5000; Sigma) to correct for unequal loading.

#### *Statistics*

All data are given as means  $\pm$  standard deviation (SD). After proving the assumption of normality and equal variance, comparison between the experimental groups was performed by one-way ANOVA followed by Student–Newman–Keuls-test, which includes a correction of the alpha-error to compensate for multiple comparisons. Statistics were performed using the SigmaStat software package (Jandel, San Rafael, CA, USA). A  $p$  value  $< 0.05$  was considered to indicate significant differences.

#### *Results*

##### *Hemoglobin concentration*

EPO-treated animals showed a slight, but not significant elevation of the hemoglobin concentration after 6 days treatment compared to controls ( $13.7 \pm 0.7$  g/dl vs.  $13.1 \pm 0.7$  g/dl;  $p = 0.11$ ).

### Radiological analysis

Radiological non-union was observed in two animals after 2 weeks of fracture healing (one EPO-treated animal, one control) and in one EPO-treated animal at 5 weeks. According to the classification of Goldberg et al. (1985), callus maturity revealed no significant differences between experimental and control animals. The relative callus size decreased at 5 weeks compared to that at 2 weeks without significant differences between EPO-treated animals and controls. In contrast, at 2 weeks the callus density in relation to the density of the spongiosa was slightly but significantly higher in the EPO group, whereas this difference could no longer be detected at 5 weeks (Table 1 and Fig. 1).

### Biomechanical analysis

Although the peak torque at failure of the bone was only slightly higher after 2 weeks of fracture healing, the peak rotation angle was significantly decreased in EPO-treated animals when compared to vehicle-treated controls. Correspondingly, the torsional stiffness was significantly increased after EPO treatment. After 5 weeks, no significant differences in torque, rotation angle and stiffness could be detected between the EPO and the control group (Table 2).

### Histomorphometric analysis

All samples demonstrated a typical pattern of secondary fracture healing with callus formation as well as intramembraneous and endochondral ossification. Two weeks after fracture, the callus consisted of cartilaginous, fibrous, and osseous tissue. The osseous tissue was composed of old cortical bone and new woven bone. At 5 weeks cartilaginous and fibrous tissue disappeared in almost all samples and soft callus was completely replaced by woven bone undergoing extensive remodeling. Therefore, a distinction between new maturing bone and old surrounding bone was not possible at this time point.

The histomorphometric analysis revealed a maximum relative callus size at 2 weeks without significant differences

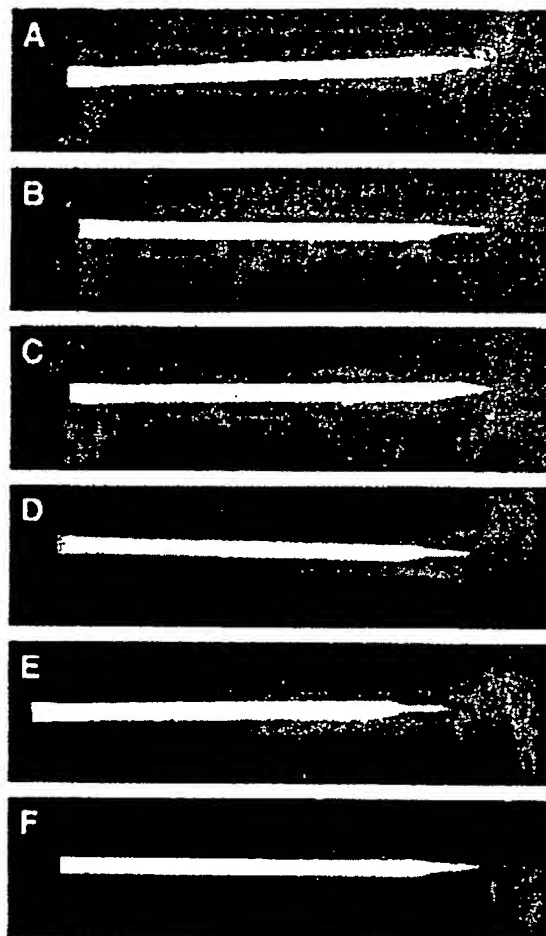


Fig. 1. X-rays of 6 different femora immediately after fracture (A and D), as well as at 2 (B and E) and 5 (C and F) weeks of fracture healing. Figures A–C represent femora of EPO-treated animals, figures D–F those of controls.

between the two groups. Callus size was found decreased after 5 weeks of fracture healing. Although the composition of the callus with cartilaginous, fibrous and osseous tissue did not

Table 1  
Radiological analysis of the callus of EPO-treated animals and vehicle-treated controls after 2 weeks and 5 weeks of fracture healing

	2 weeks			5 weeks		
	EPO	Controls	P	EPO	Controls	P
Cl.Ar/B.Dm [mm]	9.0±1.5	9.3±2.0	0.65	6.9±2.5	5.0±1.5	0.07
Cl.Dn/Sn.Dn [%]	110.6±7.1	105.9±6.6	0.04	107.1±8.3	106.9±11.9	0.97
Goldberg stage [stage]	2.5±0.6	2.5±0.6	0.88	2.8±0.6	2.9±0.3	0.80

Data are given as means±SD. Cl.Ar/B.Dm: callus area in relation to the diameter of the femur at the fracture site; Cl.Dn/Sn.Dn: callus density in relation to spongiosa density; Goldberg: classification for callus maturity according to Goldberg (stage 1: radiological non-union; stage 2: possible union; stage 3: radiological union).

Table 2  
Biomechanical analysis of the callus of EPO-treated animals and vehicle-treated controls after 2 weeks and 5 weeks of fracture healing

	2 weeks			5 weeks		
	EPO	Controls	P	EPO	Controls	P
Peak torque [%]	27.9±5.3	24.9±6.2	0.35	69.0±15.1	67.4±6.9	0.80
Peak rotation angle [%]	91.6±48.1	205.9±63.5	0.01	76.3±16.2	76.8±16.8	0.96
Torsional stiffness [%]	39.6±19.4	14.3±8.2	0.01	94.7±33.3	93.1±28.1	0.92

Data are given as means±SD. Peak torque, peak rotation angle and torsional stiffness of the fractured site are given in percent of the unfractured bone of the contralateral site.

**Table 3**  
Histomorphometric analysis of the callus of EPO-treated animals and vehicle-treated controls after 2 weeks and 5 weeks of fracture healing

	2 weeks			5 weeks		
	EPO	Controls	P	EPO	Controls	P
Cl.Ar/B.Dm [mm]	10.3±2.3	11.5±1.7	0.33	6.0±1.6	5.0±1.2	0.24
B.Cl.Ar/Cl.Ar [%]	58.1±6.6	54.1±8.1	0.36	76.8±4.9	73.0±1.7	0.11
Cg.Cl.Ar/Cl.Ar [%]	5.8±2.7	5.2±4.8	0.79	0.0±0.0	0.0±0.0	1.00
Fb.Cl.Ar/Cl.Ar [%]	6.8±2.9	7.2±5.7	0.89	0.7±1.2	0.0±0.0	0.20
(Md.Cl.Ar+O.Cl.Ar)/Cl.Ar [%]	33.0±3.0	28.5±3.6	0.04	39.0±6.1	29.3±13.5	0.12

Data are given as means ± SD. Cl.Ar/B.Dm: callus area in relation to the diameter of the femur at the fracture site; B.Cl.Ar/Cl.Ar: bone callus area (mineralized bone, osteoid and bone marrow) in relation to total callus area; Cg.Cl.Ar/Cl.Ar: cartilaginous callus area in relation to total callus area; Fb.Cl.Ar/Cl.Ar: fibrous callus area in relation to total callus area; (Md.Cl.Ar+O.Cl.Ar)/Cl.Ar: fraction of mineralized bone and osteoid in relation to the total callus.

differ between EPO-treated animals and controls, the fraction of osteoid and mineralized bone (bone without bone marrow) was significantly higher after EPO treatment at 2 weeks. After 5 weeks this fraction was still elevated in the EPO group. However, the difference did not prove significant due to a high variability of data in control animals (Table 3 and Fig. 2).

### Immunohistochemical analysis

In both groups the immunohistochemical analysis of the proteinase caspase-3 as a marker for cell apoptosis indicated only weak signaling in the periosteum and the bone marrow at 2 as well as at 5 weeks. There was no staining in the range of woven bone or cartilage (data not shown).

In contrast, intense staining of PCNA in periosteal cells and osteoblasts within the newly woven bone could be observed. However, the number of PCNA-positive periosteal cells ( $14.7 \pm 6.4$ ) and osteoblasts ( $31.2 \pm 6.2$ ) after EPO treatment did not differ significantly from that in vehicle-treated controls ( $12.9 \pm 7.1$  and  $30.5 \pm 11.4$ ). Additionally, numerous proliferating cells inside the bone marrow showed positive PCNA staining (Fig. 3). At 5 weeks, PCNA within the woven bone disappeared and only bone marrow was stained positively.

Of interest, there was a strong staining for EPOR in hypertrophic chondrocytes after 2 weeks of fracture healing in both groups. The staining was detected primarily in the cytoplasm, demonstrating a spoke wheel pattern within the perinuclear space (Fig. 4). The quantitative analysis revealed higher values in vehicle-treated controls ( $63.8 \pm 6.7$ ) compared to EPO-treated animals ( $54.0 \pm 6.9$ ), however, this difference did not prove statistically significant ( $p=0.13$ ). In addition, bone marrow also showed some faintly EPOR-stained cells, which could be observed at both 2 weeks and 5 weeks of fracture healing.

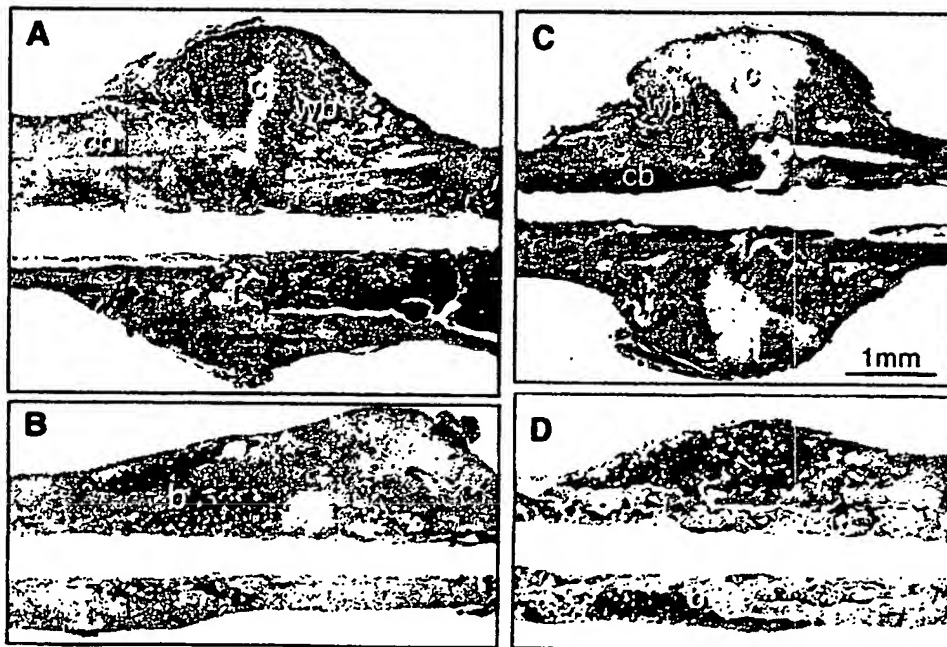


**Fig. 2.** Longitudinal sections (5  $\mu$ m thickness, magnification of 1.25 $\times$ ) of the callus of femora at 2 (A and C) and 5 (B and D) weeks of fracture healing stained according to the trichrome method. A and B show the callus of EPO-treated animals, C and D that of controls. At 2 weeks after fracture, callus consisted of cartilaginous (c) and fibrous (f) tissue as well as of cortical (cb) and newly woven bone (wb). Note that the callus is dominated by the newly woven bone, in particular after EPO treatment. At 5 weeks of fracture healing cartilaginous and fibrous tissue disappeared completely. A distinction between newly maturing bone and old surrounding bone is no longer possible at this time point.



Fig. 3. Immunohistochemical analysis of cell proliferation as indicated by PCNA expression within the callus of an EPO-treated animal after 2 weeks of fracture healing (A) (c: cartilage, cb: cortical bone, wb: newly woven bone). Higher magnification (B and C) reveals within the newly woven bone intense PCNA staining in periosteal cells (B, double arrow) and osteoblasts (B and C, arrows). Additionally, numerous cells of the bone marrow (C, arrow head) showed positive PCNA staining.



Fig. 4. Immunohistochemical analysis of EPOR expression within the callus of an EPO-treated animal after 2 weeks of fracture healing (A) (c: cartilage, cb: cortical bone, wb: woven bone). Higher magnification (B) reveals the strong staining of EPOR in hypertrophic chondrocytes (arrow and double arrow). The staining was detected primarily in the cytoplasm, demonstrating a spoke wheel pattern within the perinuclear space (double arrow).

#### Western blot analysis

Consistent with the findings from the immunohistochemical analysis, all samples showed characteristic bands according to the molecular weight of PCNA at 2 weeks. Furthermore,

Table 4  
Western blot analysis of PCNA and EPOR expression in callus of EPO-treated animals and vehicle-treated controls after 2 weeks of fracture healing

	2 weeks		P
	EPO	Controls	
PCNA [OD * mm <sup>2</sup> ]	14.2±1.3	13.8±1.1	0.67
EPOR [OD * mm <sup>2</sup> ]	21.5±6.0	36.1±5.7	0.01

Data are given as means±SD.



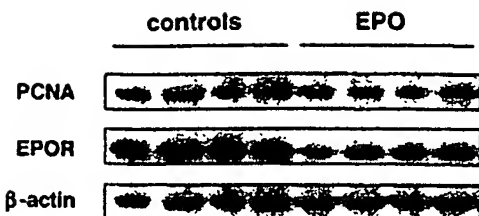


Fig. 5. Western blot analysis of PCNA and EPOR expression within the callus after 2 weeks of fracture healing. Note the higher expression of EPOR in vehicle-treated controls when compared with that of EPO-treated animals.  $\beta$ -actin was used as loading control.

Western blot analysis confirmed EPOR expression. Of interest, the quantitative analysis revealed significantly higher values in vehicle-treated controls compared to EPO-treated animals (Table 4 and Fig. 5).

## Discussion

To the best of our knowledge, we report for the first time on EPO-receptor expression in bone repair. The fact that EPOR expression was restricted to hypertrophic chondrocytes during the initial 2 weeks of fracture healing indicates that EPO plays a critical role in the process of endochondral ossification. This process includes the different stages of (i) terminal chondrocyte differentiation and apoptosis, (ii) extracellular matrix degradation and calcification, as well as (iii) angiogenesis and osteogenesis (Miclau and Helms, 2000). Beside EPO, also VEGF has been reported to be expressed in terminally differentiating chondrocytes, coincidentally with the onset of vascularization and subsequent ossification of the callus (Ferguson et al., 1999). It is known that hypertrophic chondrocytes release calcium and phosphatases, promoting the calcification of the extracellular matrix, as well as proteolytic enzymes, inducing the degradation of the matrix (Brighton and Hunt, 1986; Einhorn et al., 1989). Several studies could show that the expression of VEGF is essential for angiogenesis and osteogenesis during initial fracture healing (Geiger et al., 2005). The strong genetic and functional homologies between EPO and VEGF and the fact that EPO just like VEGF induces angiogenesis in other tissues indicate similar roles of both cytokines also in the process of fracture healing.

Beside its role as a direct angiogenic and mitotic factor, EPO has also been shown to act by VEGF- and nitric oxide (NO)-dependent pathways. Galeano et al. (2006) could demonstrate that EPO treatment significantly accelerates burn wound re-epithelialization by promoting angiogenesis and maturation of the extracellular matrix. Moreover, they found a twofold increase of VEGF and endothelial nitric oxide synthase (eNOS) content in the wound after EPO treatment. Of interest, not only VEGF, but also eNOS has been detected during the middle stages (day 7–14) of fracture healing in pericytes and chondrocytes, contributing to endochondral ossification (Zhu et al., 2002). These data suggest that EPO

might promote also endochondral ossification by VEGF- and NO-dependent pathways.

EPO treatment was associated with a reduction of EPOR expression, as indicated by Western blot analysis. This finding is in line with the results of other reports, demonstrating a downregulation of the EPO-receptor on HCD33 and HCD57 cells upon EPO challenge (Krantz, 1991).

Of interest, neither the radiological nor the histological analysis revealed a significant difference in callus size between EPO-treated animals and vehicle-treated controls. However, EPO had a significant impact on the radiological callus density during the first 2 weeks of fracture healing. This may be due to a higher grade of mineralization and a major fraction of bone. This view is supported by the histological analysis of the callus, which revealed an increased proportion of mineralized bone and osteoid in the EPO group during initial fracture healing.

As an indication of cell proliferation, in all groups, numerous cells of the bone marrow were stained positive for PCNA. Furthermore, at the “endochondral ossification front”, which is between hard and soft callus, PCNA positively stained cells were found at 2 weeks after fracture. The positive cells in these so called “mixed spicules” (Iwaki et al., 1997) are considered premature osteoblasts. At the periphery of the callus some weakly stained osteoblasts and several strongly stained periosteal cells could be detected. At 5 weeks, PCNA-positive cells disappeared in both groups, except for a few cells located within the bone marrow. These results are in line with those of Iwaki et al. (1997) and suggest a high cell activity during the process of endochondral ossification.

Because there is evidence for programmed cell death of hypertrophic chondrocytes during endochondral ossification (Lee et al., 1998), we additionally examined the expression of caspase-3 as a marker for cell apoptosis. Of interest, apart from some cells in the bone marrow, no positive staining within the fracture callus was observed. These findings indicate that caspase-3 as an executor caspase is not involved in the process of endochondral ossification.

The effect of EPO on fracture healing became most apparent in the biomechanical analysis during the initial 2 weeks of fracture healing. Torsional testing revealed a significantly higher stiffness of the callus in EPO-treated animals compared to controls. Correspondingly, peak angle at fracture was twice as much in controls, suggesting a softer consistency of the callus and, thus, a major fraction of soft callus. These results match with the higher radiological density as well as the increased amount of mineralized bone and osteoid found in EPO-treated animals at 2 weeks after fracture.

Of interest, this early protective effect of EPO treatment could no longer be observed at 5 weeks after fracture. This is probably due to the fact that EPO treatment was applied only during the initial 6 days before and after fracture. However, because our data indicate that EPOR is expressed only during the early time period after fracture and that therefore the action of EPO is most evident during the process of endochondral ossification to accelerate bone repair, a prolonged therapy may not further benefit fracture healing.

## Conclusion

Taken together, our data show that during the first 2 weeks after fracture high dose EPO treatment is capable of increasing torsional stiffness of the callus. Because during this time period hypertrophic chondrocytes express EPOR, this beneficial effect is most probably induced by EPO–EPOR signaling-mediated acceleration of endochondral ossification.

## Acknowledgements

We greatly appreciate M. Hannig and F. Al Marrawi, Dental Medicine, University of Saarland, for their help with the X-ray analysis. We thank Janine Becker for the excellent technical assistance.

## References

- Anagnostou, A., Lee, E.S., Kessimian, N., Levinson, R., Steiner, M., 1990. Erythropoietin has a mitogenic and positive chemotactic effect on endothelial cells. *Proceedings of the National Academy of Sciences of the United States of America* 87 (15), 5978–5982.
- Anagnostou, A., Liu, Z., Steiner, M., Chin, K., Lee, E.S., Kessimian, N., Noguchi, C.T., 1994. Erythropoietin receptor mRNA expression in human endothelial cells. *Proceedings of the National Academy of Sciences of the United States of America* 91 (9), 3974–3978.
- Barnes, G.L., Kostenuik, P.J., Gerstenfeld, L.C., Einhorn, T.A., 1999. Growth factor regulation of fracture repair. *Journal of Bone and Mineral Research* 14 (11), 1805–1815.
- Brighton, C.T., Hunt, R.M., 1986. Histochemical localization of calcium in the fracture callus with potassium pyroantimonate. Possible role of chondrocyte mitochondrial calcium in callus calcification. *Journal of Bone and Joint Surgery* 68A (5), 703–715.
- Brighton, C.T., Krebs, A.G., 1972. Oxygen tension of healing fractures in the rabbit. *Journal of Bone and Joint Surgery* 54A (2), 323–332.
- Brines, M.L., Ghezzi, P., Keenan, S., Agnello, D., de Lanerolle, N.C., Cerami, C., Itri, L.M., Cerami, A., 2000. Erythropoietin crosses the blood–brain barrier to protect against experimental brain injury. *Proceedings of the National Academy of Sciences of the United States of America* 97 (19), 10526–10531.
- D'Andrea, A.D., Lodish, H.F., Wong, G.G., 1989. Expression cloning of the murine erythropoietin receptor. *Cell* 57 (2), 277–285.
- Einhorn, T.A., Hirschman, A., Kaplan, C., Nashed, R., Devlin, V.J., Warman, J., 1989. Neutral protein-degrading enzymes in experimental fracture callus: a preliminary report. *Journal of Orthopaedic Research* 7 (6), 792–805.
- Ferguson, C., Alper, E., Miclau, T., Helms, J.A., 1999. Does adult fracture repair recapitulate embryonic skeletal formation? *Mechanisms of Development* 87 (1–2), 57–66.
- Galeano, M., Altavilla, D., Bitto, A., Minutoli, L., Calo, M., Lo Cascio, P., Polito, F., Giugliano, G., Squadrito, G., Mioni, C., Giuliani, D., Venuti, F.S., Squadrito, F., 2006. Recombinant human erythropoietin improves angiogenesis and wound healing in experimental burn wounds. *Critical Care Medicine* 34 (4), 1139–1146.
- Geiger, F., Bertram, H., Berger, I., Lorenz, H., Wall, O., Eckhardt, C., Simank, H.G., Richter, W., 2005. Vascular endothelial growth factor gene-activated matrix (VEGF(165)-GAM) enhances osteogenesis and angiogenesis in large segmental bone defects. *Journal of Bone and Mineral Research* 20 (11), 2028–2035.
- Gerber, H.P., Vu, T.H., Ryan, A.M., Kowalski, J., Werb, Z., Ferrara, N., 1999. VEGF couples hypertrophic cartilage remodeling, ossification and angiogenesis during endochondral bone formation. *Nature Medicine* 5 (6), 623–628.
- Goldberg, V., Powell, A., Shaffer, J., Zika, J., Bos, G., Heiple, K., 1985. Bone grafting: role of histocompatibility in transplantation. *Journal of Orthopaedic Research* 3 (4), 389–404.
- Goldberg, M.A., Dunning, S.P., Bunn, H.F., 1988. Regulation of the erythropoietin gene: evidence that the oxygen sensor is a heme protein. *Science* 242 (4884), 1412–1415.
- Hoeben, A., Landuyt, B., Highley, M.S., Wildiers, H., van Oosterom, A.T., De Bruijn, E.A., 2004. Vascular endothelial growth factor and angiogenesis. *Pharmacological Reviews* 56 (4), 549–580.
- Holstein, J.H., Menger, M.D., Meier, C., Culemann, U., Pohlemann, T., in press. Development of a locking femur nail for mice. *Journal of Biomechanics*.
- Iwaki, A., Jingushi, S., Oda, Y., Izumi, T., Shida, J.I., Tsuneyoshi, M., Sugioka, Y., 1997. Localization and quantification of proliferating cells during rat fracture repair: detection of proliferating cell nuclear antigen by immunohistochemistry. *Journal of Bone and Mineral Research* 12 (1), 96–102.
- Juul, S.E., Ledbetter, D.J., Joyce, A.E., Dame, C., Christensen, R.D., Zhao, Y., DeMarco, V., 2001. Erythropoietin acts as a trophic factor in neonatal rat intestine. *Gut* 49 (2), 182–189.
- Krantz, S.B., 1991. Erythropoietin. *Blood* 77 (3), 419–434.
- Lee, F.Y., Choi, Y.W., Behrens, F.F., De Fouw, D.O., Einhorn, T.A., 1998. Programmed removal of chondrocytes during endochondral fracture healing. *Journal of Orthopaedic Research* 16 (1), 144–150.
- Li, L., Takemura, G., Li, Y., Miyata, S., Esaki, M., Okada, H., Kanamori, H., Khai, N.C., Maruyama, R., Ogino, A., Minatoguchi, S., Fujiwara, T., Fujiwara, H., 2006. Preventive effect of erythropoietin on cardiac dysfunction in doxorubicin-induced cardiomyopathy. *Circulation* 113 (4), 535–543.
- Manigrasso, M.B., O'Connor, P.J., 2004. Characterization of a closed femur fracture model in mice. *Journal of Orthopaedic Trauma* 18 (10), 687–695.
- Miclau, T., Helms, J.A., 2000. Molecular aspects of fracture healing. *Current Opinion in Orthopaedics* 11 (5), 367–371.
- Neufeld, G., Cohen, T., Gengrinovitch, S., Poltorak, Z., 1999. Vascular endothelial growth factor (VEGF) and its receptors. *Federation of American Societies for Experimental Biology Journal* 13 (1), 9–23.
- Nishiya, D., Omura, T., Shimada, K., Matsumoto, R., Kusuyama, T., Enomoto, S., Iwao, H., Takeuchi, K., Yoshikawa, J., Yoshiyama, M., 2006. Effects of erythropoietin on cardiac remodeling after myocardial infarction. *Journal of Pharmacological Sciences* 101 (1), 31–39.
- Ogilvie, M., Yu, X., Nicolas-Metral, V., Pulido, S.M., Liu, C., Ruegg, U.T., Noguchi, C.T., 2000. Erythropoietin stimulates proliferation and interferes with differentiation of myoblasts. *Journal of Biological Chemistry* 275 (50), 39754–39761.
- Parfitt, A.M., Drezner, M.K., Glorieux, F.H., Kanis, J.A., Malluche, H., Meunier, P.J., Ott, S.M., Recker, R.R., 1987. Bone histomorphometry: standardization of nomenclature, symbols, and units. Report of the ASBMR Histomorphometry Nomenclature Committee. *Journal of Bone and Mineral Research* 2 (6), 595–610.
- Praemer, A., Furrer, S., Price, O.P., 1992. Musculoskeletal Conditions in the United States. American Academy of Orthopedic Surgeons, Rosemont, IL, pp. 85–91.
- Schmidmaier, G., Wildemann, B., Melis, B., Krummrey, G., Einhorn, T.A., Haas, N.P., Raschke, M., 2004. Development and characterization of a standard closed tibial fracture model in the rat. *European Journal of Trauma* 30 (1), 35–42.
- Steinbrech, D.S., Mehrara, B.J., Saadeh, P.B., Greenwald, J.A., Spector, J.A., Gittes, G.K., Longaker, M.T., 2000. VEGF expression in an osteoblast-like cell line is regulated by a hypoxia response mechanism. *American Journal of Physiology. Cell Physiology* 278 (4), C853–C860.
- Westenfelder, C., Biddle, D.L., Baranowski, R.L., 1999. Human, rat, and mouse kidney cells express functional erythropoietin receptors. *Kidney International* 55 (3), 808–820.
- Zhu, W., Murrell, G.A., Lin, J., Gardiner, E.M., Diwan, A.D., 2002. Localization of nitric oxide synthases during fracture healing. *Journal of Bone and Mineral Research* 17 (8), 1470–1477.



*Original Article*

# Nonerythropoietic derivative of erythropoietin protects against tubulointerstitial injury in a unilateral ureteral obstruction model

Harumi Kitamura<sup>1</sup>, Yoshitaka Isaka<sup>1,2</sup>, Yoshitsugu Takabatake<sup>1</sup>, Ryoichi Imamura<sup>3</sup>, Chigure Suzuki<sup>1</sup>, Shiro Takahara<sup>2</sup> and Enyu Imai<sup>1</sup>

<sup>1</sup>Department of Nephrology, <sup>2</sup>Department of Advanced Technology for Transplantation, and <sup>3</sup>Department of Urology, Osaka University Graduate School of Medicine, Osaka, Japan

## Abstract

**Background.** Erythropoietin (EPO), a member of the cytokine type I superfamily, acts to increase circulating erythrocytes primarily by preventing apoptosis of erythroid progenitors, is known to protect tissues and can raise haemoglobin (Hb) concentrations. Recently, a second receptor for EPO comprising the EPO receptor and  $\beta$ -common receptor has been reported to mediate EPO-induced tissue protection. EPO modified by carbamylation (CEPO) only signals through this second receptor. Accordingly, we hypothesized that treatment with CEPO, which would not increase Hb concentrations, would protect against tubular damage and thereby inhibit tubulointerstitial injuries.

**Methods.** We evaluated therapeutic effects of CEPO using a rat unilateral ureteral obstruction model.

**Results.** CEPO decreased tubular apoptosis and  $\alpha$ -smooth muscle actin ( $\alpha$ SMA) expression in the absence of polycythaemia, while the untreated obstructed kidneys exhibited increased tubular apoptosis with expanded ( $\alpha$ SMA) expression. While EPO treatment similarly inhibited tubular apoptosis and  $\alpha$ SMA expression, EPO treatment increased Hb concentrations and induced a wedge-shaped infarction.

**Conclusion.** We established a therapeutic approach using CEPO to protect against tubulointerstitial injury. The therapeutic value of this approach warrants further attention and preclinical studies.

**Keywords:** apoptosis; carbamylated erythropoietin; tubulointerstitial injury; ureteral obstruction

## Introduction

Tubulointerstitial inflammation is a common pathological feature of progressive renal diseases [1–3] that leads to

fibrosis via tubular atrophy, myofibroblast proliferation, macrophage infiltration and interstitial matrix accumulation [4–7]. Unilateral ureteral obstruction (UUO), a representative model of tubulointerstitial renal fibrosis, has numerous quantifiable cellular and molecular events, such as apoptosis and phenotypic alteration [5]. In progressive obstructive nephropathy, the tubules dilate and the renal tubular epithelial cells undergo apoptosis, leading to tubular atrophy.

Preliminary knowledge of the biology of erythropoietin (EPO)-mediated tissue protection was largely developed from studies of the nervous system [8,9], which is susceptible to ischaemic injury due to its high basal metabolic rate. As the normal kidney, like the nervous system, is characterized by regions in which energy substrates are limited, findings derived from nervous system studies are applicable to the kidney. Although chronic renal hypoxia with subsequent tubulointerstitial injury commonly leads to end-stage renal failure [10], early treatment with EPO slows the progression of renal failure [11]. On the other hand, EPO administration to rats with chronic renal failure was shown to accelerate the progression of chronic renal disease, especially in relation to the increased blood pressure [12].

A potential role for the non-haematopoietic activities of EPO in the kidney was suggested by the identification of the EPO receptor (EpoR) protein expression throughout the kidney, including both proximal and distal tubular cells [13]. As the affinity of these receptors ( $\sim 1$  nM) is well below the normal plasma EPO concentrations ( $\sim 1$ – $10$  pM), the cytoprotective effects of EPO may require higher doses than those used to treat anaemia. However, recent clinical trials have suggested that higher doses of EPO are likely to be associated with adverse effects [14–17].

Recently, a second receptor that mediates EPO-induced tissue protection for EPO comprising the EpoR and the  $\beta$ -common (CD131) receptor (BCR) has been identified [18]. EPO modified by carbamylation, carbamylated EPO (CEPO), is reported to signal only through this receptor, not through the homodimeric EpoR [17]. It has been shown that CEPO does not stimulate erythropoiesis, but that it prevents tissue injury in spinal cord neurons [17,19] and

Correspondence and offprint requests to: Yoshitaka Isaka, Department of Advanced Technology for Transplantation, Osaka University Graduate School of Medicine, Suita, Osaka, 565-0871 Japan. Tel: +81-6-6879-3746; Fax: +81-6-6879-3749; E-mail: isaka@att.med.osaka-u.ac.jp

cardiomyocytes [18,20]. The results that membrane proteins prepared from the rat kidney were greatly enriched in the EpoR covalently bound in a complex with  $\beta$ cR suggest that the EpoR physically interacts with  $\beta$ cR in the kidney [18]. In this study, we examined whether treatment with CEPO is able to protect the kidney from the tubular apoptosis that typically occurs after unilateral obstruction injury, thereby inhibiting subsequent tubulointerstitial fibrosis.

## Materials and methods

### Experimental design

CEPO was synthesized from human EPO (Epoetin alfa; Kirin Corp., Tokyo, Japan) as described earlier [19]. Briefly, one volume of EPO ( $\sim 1$  mg/ml) was mixed with one volume of 1 M Na-borate (pH  $\sim 8.8$ ) and recrystallized KOCN was added to a final concentration of 1 M. After incubation, samples were immediately dialysed against milli-Q water, and subsequently against 20 mM sodium citrate in 0.1 M NaCl, pH 6.0. After dialysis, the samples were concentrated to  $\sim 2$  mg/ml.

The therapeutic effects of CEPO on interstitial fibrosis were examined using a UUO model [5]. All procedures were handled in a humane fashion in accordance with the guidelines of the Animal Committee of Osaka University. Six-week-old male Sprague Dawley (SD, SLC Inc., Hamamatsu, Japan) rats were anaesthetized by intraperitoneal injection of pentobarbital (50 mg/kg), the left kidney and ureter were surgically exposed using a mid-line incision and the left proximal ureter was ligated with silk thread. Rats were randomly divided into three groups: (1) the saline-treatment group (control group;  $n = 9$ ); (2) the EPO-treatment group (EPO group) and (3) the CEPO-treatment group (CEPO group). Rats with sham operation served as normal control (sham ope group). Control, EPO and CEPO group rats received subcutaneous injections of 0.5 ml of saline, 500 IU/kg (low dose;  $n = 6$ ) or 1000 IU/kg (high dose;  $n = 11$ ) recombinant human Epoetin alfa (Kirin Corp., Tokyo, Japan) in 0.5 ml of saline, or 500 IU/kg (low dose;  $n = 6$ ) or 1000 IU/kg (high dose;  $n = 11$ ) CEPO in 0.5 ml of saline [17], respectively, every 2 days after disease induction. In order to examine the effect of EPO or CEPO (high dose) treatment on blood pressure, three rats from each group were selected and blood pressures were monitored 1 day before the disease induction and 1 day before the harvest using a tail cuff and a pneumatic pulse transducer (BP-98 A; Softron, Tokyo, Japan). On day 7, kidneys were perfused with cold autoclaved PBS and samples of the cortex were taken for RNA preparation and histology. Tissues for RNA extraction were frozen using liquid nitrogen and homogenized with acid-guanidium thiocyanate-phenol-chloroform. Tissues for light microscopy were fixed with 4% paraformaldehyde overnight, dehydrated through a graded ethanol series and embedded in paraffin. Histological sections (2  $\mu$ m) of the kidneys were stained using Masson's trichrome method. The fibrotic area in the interstitium, stained blue by Masson's Trichrome, was highlighted on digitized images using a computer-aided manipulator. The fibrotic area relative to the total area of the field was

calculated as a percentage. The scores of 10 fields per kidney were averaged, after which the mean scores from animals in each group were averaged.

### Antibodies

Anti-human  $\alpha$ -smooth muscle actin ( $\alpha$ SMA) antibody (EPOS System: Dako, Hamburg, Germany) was used to identify myofibroblasts. Pathways that protect the kidneys were detected using the following antibodies in immunohistochemical testing or western blotting: polyclonal EpoR antibody (1:1000, Santa Cruz), polyclonal IL-3/IL-5/GM-CSFR $\beta$  antibody (1:1000, Santa Cruz), polyclonal Ki-67 antibody (1:50, Dako), polyclonal phospho-Akt (Ser473) antibody (1:1000, Cell Signaling Technology, Beverly, MA, USA) and polyclonal Akt antibody (1:1000, Cell Signaling). We normalized protein levels using polyclonal  $\beta$ -actin antibody (1:1000, Cell Signaling).

### Morphology and immunohistochemical staining

Tissue samples were fixed in 4% (wt/vol) buffered paraformaldehyde (PFA) for 16 h and then embedded in paraffin. Tissue sections (4  $\mu$ m) were mounted on silane (2% 3-aminopropyltriethoxysilane)-coated slides (Muto Pure Chemicals, Tokyo, Japan), deparaffinized with xylene and stained with periodic acid-Schiff (PAS). Immunohistochemical staining was carried out using the Envision system (Dako), according to the manufacturer's instructions. To examine the expression of  $\alpha$ SMA or Ki-67, endogenous peroxidase activities were blocked with 3%  $H_2O_2$  for 10 min and then incubated with anti- $\alpha$ SMA and anti-Ki-67 antibodies for 60 min at room temperature. After labelling, the endogenous peroxidase activity in tissue sections was blocked by incubating in methanol with 0.3% hydroxyoxidase for 30 min. The sections were then processed using an avidin-biotinylated peroxidase complex method (Vectastain ABC kit, Vector Laboratories, Inc., Burlingame, CA, USA) with diaminobenzidine as the chromogen. All histological slides were examined by light microscopy using a Nikon Eclipse 80 i (Nikon, Tokyo, Japan), and pictures were taken with Nikon ACT-1 version 2.63.

The  $\alpha$ SMA-positive area relative to the total field area was calculated as a percentage using a computer-aided manipulator. The mean score for 15 fields per kidney was determined, and the mean scores for kidneys in each group were then averaged. For Ki-67 staining, the number of positive cell nuclei counted in 15 random areas was averaged.

### Terminal deoxynucleotidyltransferase-mediated dUTP nick end-labeling (TUNEL) staining

TUNEL staining was performed using the *in situ* Apoptosis Detection Kit (Takara Bio, Otsu, Japan), according to the manufacturer's instructions. Briefly, sections were deparaffinized and subjected to antigen retrieval in preheated 10 mmol/l sodium citrate (pH 7) using a microwave. They were then incubated with 3%  $H_2O_2$  for 10 min, followed by incubation with a TdT enzyme solution for 90 min at 37°C. The reaction was terminated by incubation in stop/wash

buffer for 30 min at 37°C. The number of TUNEL-positive cell nuclei was counted in 15 random areas and averaged.

#### Western blot analysis

Kidney tissues were homogenized in Cell Lysis Buffer (Cell Signaling) with protease inhibitor cocktail tablets (Roche, Basel, Switzerland). Homogenates were centrifuged ( $12000 \times g$  for 10 min at 4°C), and supernatant total protein was measured by the Lowry protein assay (Bio-Rad, Hercules, CA). Total protein lysate (15  $\mu$ g) containing 1:1 denaturing sample buffer was boiled for 5 min and resolved on 6.0–8.0% SDS-polyacrylamide gels, and electrophoretically transferred onto an immobilon PVDF membrane (Millipore, Bedford, MA, USA). The filter was blocked with 5% (wt/vol) nonfat milk in 10 mM Tris-buffered saline with 0.1% Tween-20 (TBS-T), followed by overnight incubation at 4°C with diluted primary antibodies (EpoR antibody, polyclonal IL-3/IL-5/GM-CSFR $\beta$  antibody, polyclonal phospho-Akt antibody and polyclonal Akt antibody as the above concentration) in TBS-T containing 5% BSA. After washing three times in TBS-T, the filter was incubated with secondary antibody (1:1000) (Cell Signaling) in TBS-T for 45 min at room temperature and developed to detect specific protein bands using ECL reagents (Amersham Bioscience Corp., Piscataway, NJ, USA).

#### Statistical analysis

Data are expressed as means  $\pm$  SD. Statistical significance, defined as  $P < 0.01$  or  $< 0.05$ , was evaluated using one-way ANOVA.

## Results

#### Effects on erythropoiesis

Compared to saline-treated (control group) rats, both high dose and low dose of EPO treatment (EPO group) significantly increased Hb (saline,  $14.3 \pm 0.4$  g/dl, median 14.2 g/dl, range 13.7–14.8 g/dl, first to third quartile 14.0–14.7 g/dl; high dose of EPO,  $16.1 \pm 0.9$  g/dl, median 16.3 g/dl, range 14.3–16.9 g/dl, first to third quartile 15.7–16.8 g/dl,  $P < 0.01$  versus saline group; low dose of EPO,  $16.0 \pm 0.29$  g/dl, median 16.0 g/dl, range 15.8–16.1 g/dl, first to third quartile 15.8–16.1 g/dl,  $P < 0.05$  versus saline group), Ht (saline,  $43.2 \pm 5.5\%$ , median 45.6%, range 33.4–46.4%, first to third quartile 39.0–46.3% versus EPO,  $58.0 \pm 2.5\%$ , median 59.2%, range 53.4–60.1%, first to third quartile 55.8–59.9%,  $P < 0.01$ ) and reticulocyte concentrations (saline,  $40.6 \pm 5.2\%$ , median 40%, range 35–49%, first to third quartile 36.5–45.0%; high dose of EPO,  $116.8 \pm 2.6\%$ , median 117.5%, range 113–119%, first to third quartile 114–118.8%,  $P < 0.05$  versus saline group; low dose of EPO,  $95.5 \pm 9.2\%$ , median 95.5%, range 89–102%, first to third quartile 89–102%,  $P < 0.05$  versus saline group) as shown in Figure 1. On the other hand, the high dose of CEPO treatment (CEPO group) neither enhanced nor reduced Hb, Ht and reticulo-

cyte counts ( $13.9 \pm 0.4$  g/dl, median 13.8 g/dl, range 13.4–14.3 g/dl, first to third quartile 13.5–14.2 g/dl,  $P < 0.01$  versus EPO group,  $43.5 \pm 1.5\%$ , median 43.5%, range 41.4–46.3%, first to third quartile 42.3–43.9%,  $P < 0.01$  versus EPO group and  $37.5 \pm 3.7\%$ , median 37%, range 34–42%, first to third quartile 34.3–41.3%, respectively,  $P < 0.05$  versus EPO group), suggesting that CEPO, unlike EPO, does not stimulate erythropoiesis.

We also examined the effect of EPO or CEPO treatment on serum creatinine, which reflects the renal function of the contralateral right kidney, because obstructed kidneys are non-functioning kidneys. The serum creatinine level was increased in saline-treated disease control rats ( $0.35 \pm 0.07$  mg/dl), compared with the normal rats with sham operation (sham op group) ( $0.22 \pm 0.01$  g/dl). Treatment with a high dose of EPO or CEPO did not significantly affect the creatinine levels ( $0.30 \pm 0.03$  g/dl and  $0.31 \pm 0.03$  g/dl, respectively, Figure 1c), suggesting that EPO or CEPO has no significant effect on the contralateral glomerular filtration rate.

We then checked the effect of EPO or CEPO treatment on the blood pressure, because treatment with EPO was reported to worsen systemic blood pressure [12]. Treatment with EPO ( $139.4 \pm 25.5$  mmHg;  $n = 3$ ) or CEPO ( $119.2 \pm 6.9$  mmHg;  $n = 3$ ) did not significantly increase the systolic blood pressure compared with untreated rats ( $126.4 \pm 9.1$  mmHg;  $n = 3$ , Figure 1d). One of three rats treated with EPO, however, showed markedly elevated blood pressure (173/133 mmHg). Of interest is that this rat exhibited a wedge-shaped infarction in the kidney.

#### Effects on tubular apoptosis and proliferation in UUO kidney

Quantification of the number of apoptotic cells by TUNEL immunostaining on EPO- or CEPO-treated obstructed kidneys showed an increase in TUNEL-positive, apoptotic cells among tubular epithelial cells at 1 week (average of TUNEL-positive cell number per 15 fields,  $55 \pm 16$ ) in the control group (Figure 2a, d). Apoptotic cells were significantly decreased in the high dose of EPO ( $35 \pm 14$ ,  $P < 0.05$ , Figure 2b, d) and CEPO ( $35 \pm 10$ ,  $P < 0.05$ , Figure 2c, d) groups (no significance between the EPO and CEPO groups). In addition, the low dose of EPO or CEPO also had a significant effect on the number of TUNEL-positive apoptotic cells ( $31 \pm 5$  and  $24 \pm 8$ , respectively, Figure 2d), suggesting that both EPO and CEPO have similar anti-apoptotic actions.

The Ki-67 antigen is a large nuclear protein that is preferentially expressed during the active phase of the cell cycle ( $G_1$ ,  $S$ ,  $G_2$  and  $M$  phases), but is absent in resting cells ( $G_0$ ). To assess the regeneration of tubular epithelial cells, cortical Ki-67-positive tubular cells were counted at  $\times 400$  magnification in a minimum of 15 fields. The mean number of positive cell nuclei per field did not significantly differ among the three groups (control group,  $13 \pm 2$ , high dose of the EPO group,  $15 \pm 4$ , high dose of the CEPO group,  $17 \pm 4$ ), but EPO and CEPO showed a tendency to promote tubular cell proliferation.

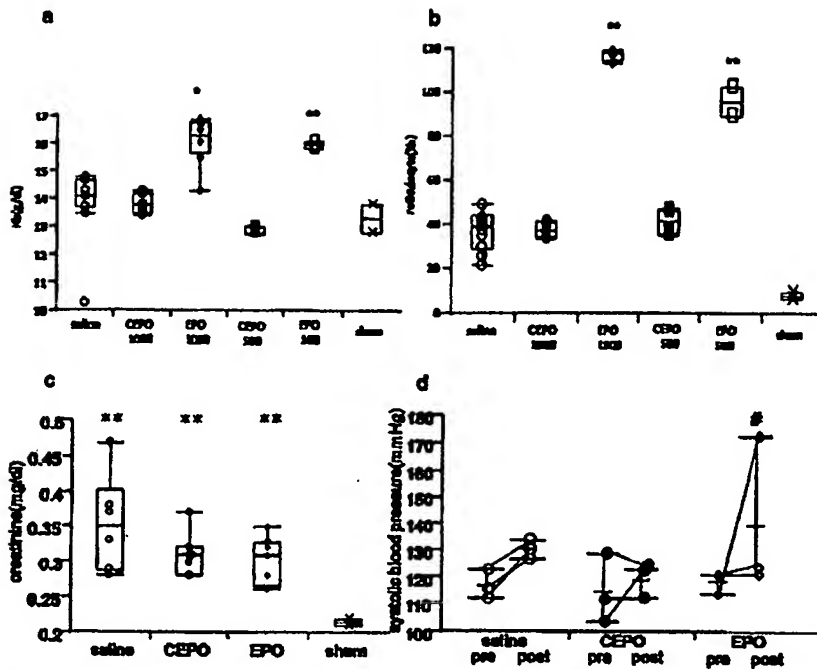


Fig. 1. Effects on erythropoiesis, renal function and blood pressure. Box plots show the changes in Hb (a), reticulocyte concentrations (b) and serum creatinine (c). Shown are the mean (black line), range (vertical bars) and first to third quartile (box). Both high dose and low dose of EPO treatment ( $n = 11$ ) significantly increased Hb and reticulocyte concentrations ( $^*P < 0.01$  versus saline group and CEPO group,  $^{**}P < 0.05$  versus saline group and CEPO group). In contrast, CEPO treatment ( $n = 11$ ) did not enhance Hb or reticulocyte count. EPO or CEPO treatment did not significantly affect the serum creatinine levels compared to control groups (c,  $^*P < 0.05$  versus sham ope group). Changes in the systolic blood pressure are shown (d). Treatment with EPO or CEPO had no significant effect on the systolic blood pressure, but one of three rats (#) treated with EPO showed markedly elevated blood pressure (173/133 mmHg).

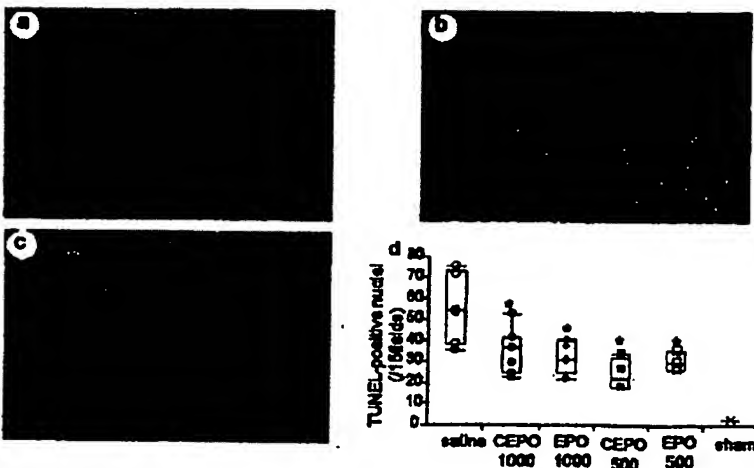


Fig. 2. Effects on tubular apoptosis. Representative TUNEL immunostaining in control group (a), high dose of EPO group (b) and high dose of CEPO group (c) are shown. The dark brown dots correspond to representative TUNEL-positive nuclei. Box plots demonstrate that EPO or CEPO [both high dose ( $n = 11$ ) and low dose ( $n = 6$ )] treatment significantly decreased TUNEL-positive, apoptotic cells (d,  $^*P < 0.05$  versus control group). Shown are the mean (black line), range (vertical bars) and first to third quartile (box) (magnification,  $\times 400$ ).

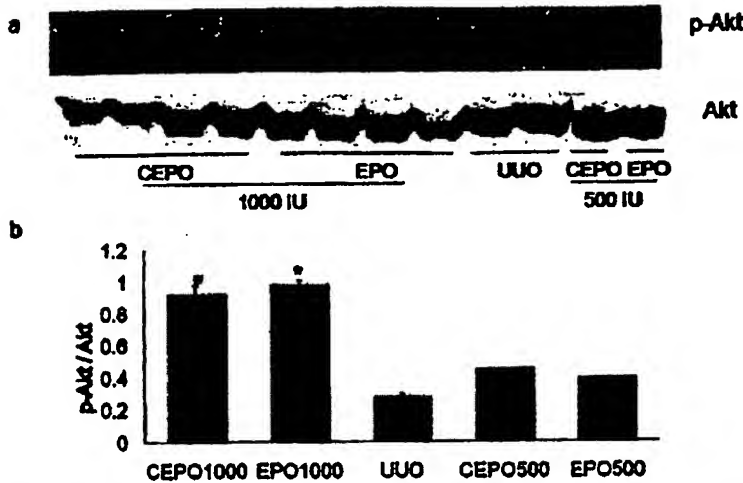


Fig. 3. Effects of EPO or CEPO treatment on Akt activation. Western blot analysis demonstrated that the expression of EpoR and  $\beta$ cR were low in control UUO kidneys, while the EpoR was upregulated in EPO and CEPO groups. In addition, the expression of  $\beta$ cR was strongly activated in CEPO group (a). Treatment with 1000 IU EPO or CEPO significantly increased phosphorylation of Akt at 1 week, but that 500 IU EPO or CEPO had a weak effect on activation of Akt (b). The band density of p-Akt expressed as the mean  $\pm$  S.D. is illustrated (c, \* $P < 0.05$  versus control group).

#### Effects on cell signaling

Working on the assumption that tissue protection is mediated via the EpoR and  $\beta$ cR heteroreceptors, we first examined the expression of EpoR and  $\beta$ cR (Figure 3a). Western blot analysis demonstrated that the expression of EpoR and  $\beta$ cR were low in control group obstructed kidneys, while the EpoR was upregulated in the EPO and CEPO groups. In addition, the expression of  $\beta$ cR was slightly increased in the EPO group, but strongly activated in the CEPO group.

Intracellular EPO signaling, which is implicated in tubular protection, was examined through the activation of Akt (Figure 3b, c). Western blot analysis demonstrated that treatment with 1000 IU of EPO or CEPO significantly increased phosphorylation of Akt at 1 week (no significance between the EPO and CEPO groups). Compared with the anti-apoptotic effects (Figure 2d), treatment with 500 IU EPO or CEPO had a weak effect on activation of Akt, suggesting that a high dose of EPO or CEPO is necessary to protect the kidneys through activation of Akt.

#### Effects on interstitial phenotypic changes in the UUO kidney

One of the most important events associated with interstitial fibrosis, enhanced expression of  $\alpha$ SMA, which is a marker of interstitial phenotypic changes, was assessed by immunohistochemistry and was shown to be strong in the interstitial area of control group obstructed kidneys (Figure 4a). However, immunostaining for  $\alpha$ SMA was weak in the high dose of the EPO (Figure 4b, d) or CEPO (Figure 4c, d) group obstructed kidneys (no significance between the EPO and CEPO groups). In contrast, treatment with 500 IU EPO or CEPO had no significant effect on inhibiting  $\alpha$ SMA expression (Figure 4d).

In order to determine the effects on interstitial fibrotic changes in obstructed kidneys, histological analysis was performed using Masson's trichrome staining. The area of the fibrotic lesion of the cortical interstitium was determined in the sections stained light blue. Saline-treated obstructed kidneys exhibited increased tubular dilation, with a marked expansion of the interstitium (Figure 5a). In contrast, the high dose of the EPO or CEPO group obstructed kidneys showed lower interstitial expansion, although they exhibited the same extent of tubular dilation (Figure 5b, c). However, a wedge-shaped infarction (Figure 5d, arrow) was observed in 4 of 11 EPO group kidneys, while no kidneys in the CEPO group showed infarctions. The Hb level in the EPO group with infarction was not higher than that in the EPO group without infarction ( $15.9 \pm 1.4$  g/dl versus  $16.2 \pm 0.5$  g/dl, respectively).

On morphometric analysis, fibrotic areas of the interstitium were significantly increased in control group obstructed kidneys ( $5.87 \pm 2.20\%$ ). However, fibrotic areas in the EPO ( $4.01 \pm 1.86$  and  $3.45 \pm 0.22\%$  in high dose and low dose, respectively) or CEPO ( $3.91 \pm 1.16$  and  $3.69 \pm 0.76\%$  in high dose and low dose, respectively) group of obstructed kidneys were significantly smaller when compared with control group kidneys (Figure 5e) (no significance between the EPO and CEPO groups).

#### Discussion

In this paper, we examined whether EPO or CEPO has therapeutic effects on tubulointerstitial injury in a rat UUO model. Based on our results, both high doses of EPO and CEPO appear to have similar protective functions against tubulointerstitial injury. Previous studies have also shown that EPO and CEPO have a similar efficacy for tissue

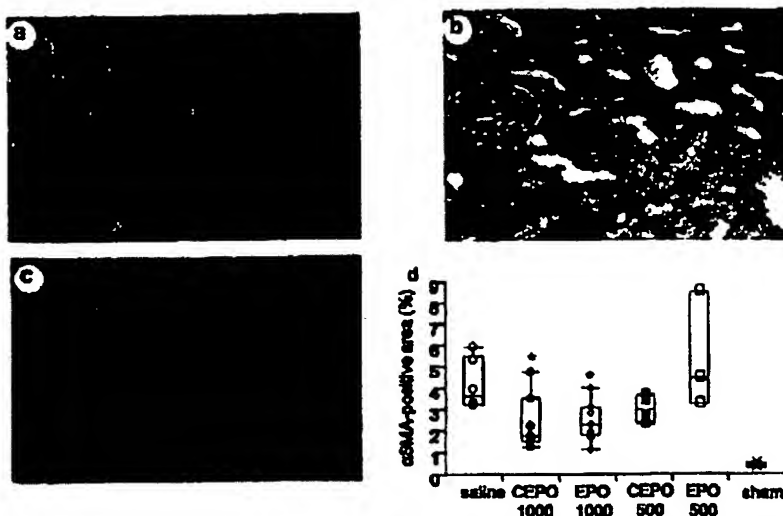


Fig. 4. Effects of EPO or CEPO on phenotypic changes. Interstitial phenotypic changes were assessed by immunohistochemical staining for  $\alpha$ SMA in the control group (a), high dose of EPO group (b) and high dose of CEPO group (c). Quantification (%) of the  $\alpha$ SMA-positive areas is shown (d). Shown are the mean (black line), range (vertical bars) and first to third quartile (box). While the high dose of EPO ( $n = 11$ ) and CEPO ( $n = 11$ ) significantly suppressed  $\alpha$ SMA expression, the low doses of EPO ( $n = 6$ ) and CEPO ( $n = 6$ ) did not ( $^*P < 0.05$  versus control group) (magnification,  $\times 400$ ).

protection. When delivered in a single dose ( $10 \mu\text{g/kg} = 2000 \text{ IU/kg}$ ), the potency of CEPO and EPO seems to be comparable in rat models of stroke and spinal cord compression [19]. However, when multiple doses are administered, CEPO is more potent than EPO in the spinal cord compression model [19]. Detailed dose-response studies remain to be carried out to compare the performance of CEPO with EPO; however, CEPO may be more useful than EPO.

The key findings that support this conclusion are as follows: (1) fewer TUNEL-positive, apoptotic cells were present among the tubular epithelial cells in both 1000 IU EPO- and CEPO-treated kidneys than in saline-treated kidneys, but this effect was also observed in 500 IU EPO- or CEPO-treated kidneys; (2) treatment with 1000 IU EPO or CEPO increased phosphorylation of Akt at 1 week, while 500 IU EPO or CEPO had a weak effect on activation of Akt; (3) both high dose and low dose of EPO treatment significantly increased Hb, Ht and reticulocyte concentrations, while CEPO treatment neither enhanced nor reduced Hb, Ht and reticulocyte counts; (4) a wedge-shaped infarction was observed in 4 of 11 EPO-treated kidneys, while no kidneys in CEPO-treated rats showed infarctions; (5) Hb levels in EPO-treated rats with infarction were not higher than those in EPO-treated rats without infarction, while one of three rats treated with EPO showed markedly elevated blood pressure.

We demonstrated that high dose of EPO and CEPO treatments markedly suppressed obstruction-induced tubular epithelial apoptosis and interstitial phenotypic alteration as assessed by  $\alpha$ SMA expression. Renal tubular apoptosis in UUO has been suggested to be related to renal tissue loss and dysfunction [21]. Western blot analysis demonstrated the increase of phosphorylated Akt by EPO and CEPO treatment as previously reported [22]; activation of Akt may be

one possible signal transduction pathway by which tubular apoptosis, as well as later interstitial phenotypic changes, is suppressed. Once activated, Akt activates multiple targets with anti-apoptotic effects, including phosphorylation of Bad, Bax, caspase-9 and GSK-3 $\beta$ , maintenance of mitochondrial membrane potential and preservation of glycolysis and ATP synthesis [23]. However, this activation of Akt was weak in kidneys with EPO or CEPO treatment at 500 IU. This observation could be related to the fact that the affinity of the EpoR in tubular epithelial cells is well below normal plasma EPO concentrations [13].

Kashii *et al.* [24] reported that phosphatidylinositol-3 kinase (PI3K) is activated by EPO in the EPO-dependent UT-7 leukaemia cell line, where it recruits Akt. The PI3K-Akt pathway also leads to the upregulation of Bcl-xL and the inhibition of apoptosis in Baf-3 cells [25]. Furthermore, using the EPO-dependent human erythroid progenitor cell line, Silva *et al.* [26] showed that EPO treatment maintains cell viability by repressing apoptosis through the upregulation of Bcl-xL, an anti-apoptotic gene of the Bcl-2 family. These results suggest that the upregulation of the PI3K-Akt pathway in EPO- or CEPO-treated kidneys suppresses tubular epithelial apoptosis, likely due to the induction of anti-apoptotic genes of the Bcl-2 family.

In this study, we found that EpoR and  $\beta$ cR levels were significantly higher in CEPO-treated kidneys than in control group obstructed kidneys. Recently, it was reported that membrane proteins prepared from the rat brain, heart, liver or kidney were greatly enriched in the EpoR covalently bound in a complex with  $\beta$ cR and that knockout of the  $\beta$ cR fully abolished tissue protective properties of EPO or CEPO in the nervous system and heart [18]. Although the precise protein interactions of the EpoR and  $\beta$ cR have not been determined, CEPO-mediated upregulation of EpoR and  $\beta$ cR

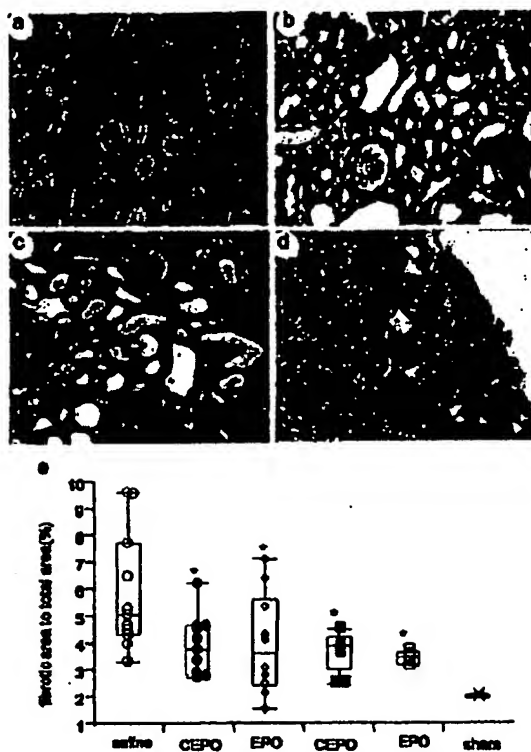


Fig. 5. Effects of EPO or CEPO on interstitial fibrotic changes. Interstitial fibrosis was assessed by Masson's trichrome staining in the control group (a), high dose of EPO group (b) and low dose of CEPO group (c) (magnification,  $\times 200$ ). Representative wedge-shaped infarction (arrow) in EPO-treated kidneys is shown (magnification,  $\times 4$ ) (d). Quantification (%) of the fibrotic area is shown by box plots (e,  $^*P < 0.05$  versus control group). Shown are the mean (black line), range (vertical bars), and first to third quartile (box).

levels may contribute to the dimerization of the EpoR and  $\beta$ cR, and thereby lead to tissue protection.

A number of important factors must be considered prior to clinical application of EPO for cytoprotection. Recently, the Food and Drug Administration (FDA) issued a public health advisory outlining new safety information, including revised product labeling about erythropoiesis-stimulating agents (ESAs). This issue arises from the findings of several important studies: (1) an increased number of deaths and of non-fatal heart attacks, strokes, heart failure and blood clots when ESAs were adjusted to maintain higher RBC levels in patients with chronic kidney failure [16,17]; (2) faster tumour growth when ESAs were adjusted to maintain Hb levels above 12 g/dl in patients with head and neck cancer undergoing radiation therapy [14,27]; (3) earlier deaths and did not have fewer blood transfusions when ESAs were given according to the dosing recommendations for cancer patients receiving chemotherapy in cancer patients not receiving chemotherapy [28]; (4) more blood clots in patients scheduled for orthopaedic surgery who received ESAs to

reduce blood transfusions during and after surgery than those not given an ESA.

We also demonstrated that high dose of EPO treatment increased Hb concentration, thereby inducing wedge-shaped infarction in 4 of 11 rats. However, Hb levels in EPO-treated rats with infarction were not higher than those in EPO-treated rats without infarction. In addition, low dose of EPO treatment developed similar increments of Hb as high dose of EPO, although we observed no infarcted lesion in low dose of EPO-treated kidney. As EPO administration to rats with chronic renal failure was shown to accelerate the progression of chronic renal disease, especially in relation to the increased blood pressure [12], we also examined the effect of high dose of EPO or CEPO treatment on blood pressure. One of three rats treated with EPO showed markedly elevated blood pressure concomitantly with a wedge-shaped infarction in the kidney. Therefore, elevated blood pressure due to EPO administration may contribute to the infarction. In addition, it is known that EPO is pro-thrombotic in a dose-dependent manner, which is partly mediated by augmented expression of P- and E-selectins [29]. In addition, EPO induces the production of young, hyper-reactive platelets [30], which is particularly problematic for chronic administration of EPO and for the high doses that would be required for renoprotection [13,31]. Clinical studies indicate that patients with chronic kidney diseases [16,17] and patients with cancer [28] are at a higher risk of adverse events with EPO. Furthermore, the frequency and severity of adverse effects increased when larger doses of EPO were used to target higher haematocrit levels that were still within the normal range [32].

Compared to EPO, CEPO showed similar renoprotective effects on tubulointerstitial injury in the absence of polycythaemia. Recently, we also reported the therapeutic effects of EPO and CEPO on ischaemia-reperfusion injury, which is a transient insult on renal tubular epithelial cells. In the previous paper, single administration of EPO or CEPO (100 IU/kg) is sufficient to prevent ischaemia-reperfusion injury, while a high dose of EPO or CEPO is necessary to prevent the kidney from ureteral obstruction in this paper. In the previous study, we did not observe a wedge-shaped infarction in EPO-treated kidneys, probably due to the administration of a low dose of EPO. The likely situation to require a high dose of EPO may couple with the dose-dependent adverse effects of EPO, especially thrombosis or hypertension. In this case, the engineered non-erythropoietic tissue-protective EPO, such as CEPO, may be promising. Thus, CEPO may be able to protect the kidneys from tubulointerstitial injury. Further research is required concerning dose-ranging and pharmacodynamic properties after CEPO administration and related adverse effects using preclinical models appropriate for supporting potential clinical studies, but the therapeutic use of CEPO warrants further attention and preclinical studies.

*Conflict of interest statement.* None declared.

## References

1. Nath KA. *Am J Kidney Dis* 1992; 20: 1-17
2. Phillips AO, Steadman R. *Histol Histopathol* 2002; 17: 247-252

3. Uchiyama-Tanaka Y, Mori Y, Kimura T et al. *Am J Kidney Dis* 2004; 43: e18-e25
4. Eddy AA. *J Am Soc Nephrol* 1996; 7: 2495-2508
5. Klahr S, Morrissey J. *Am J Physiol Renal Physiol* 2002; 283: F861-F875
6. Klahr S, Schreiner G, Ichikawa I. *N Engl J Med* 1988; 318: 1657-1666
7. Sharma AK, Maurer SM, Kim Y et al. *Kidney Int* 1993; 44: 774-788
8. Sakanaka M, Wen TC, Matsuda S et al. *Proc Natl Acad Sci USA* 1998; 95: 4635-4640
9. Siren AL, Fratelli M, Brines M et al. *Proc Natl Acad Sci USA* 2001; 98: 4044-4049
10. Nangaku M. *J Am Soc Nephrol* 2006; 17: 17-25
11. Kuriyama S, Tomonari H, Yoshida H et al. *Nephron* 1997; 77: 176-185
12. Garcia DL, Anderson S, Renuke HG et al. *Proc Natl Acad Sci USA* 1988; 85: 6142-6146
13. Westenfelder C, Biddle DL, Baranowski RL. *Kidney Int* 1999; 55: 808-820
14. Henke M, Laszig R, Rube C et al. *Lancet* 2003; 362: 1255-1260
15. Phrommintikul A, Haas SJ, Elsak M et al. *Lancet* 2007; 369: 381-388
16. Drueke TB, Locatelli F, Clyne N et al. *N Engl J Med* 2006; 355: 2071-2084
17. Singh AK, Szczec L, Tang KL et al. *N Engl J Med* 2006; 355: 2085-2098
18. Brines M, Grasso G, Fiordaliso P et al. *Proc Natl Acad Sci USA* 2004; 101: 14907-14912
19. Leist M, Ghezzi P, Grasso G et al. *Science* 2004; 305: 239-242
20. Savino C, Pedotti R, Baggi F et al. *J Neuroimmunol* 2006; 172: 27-37
21. Truong LD, Petrussevska G, Yang G et al. *Kidney Int* 1996; 50: 200-207
22. Imamura R, Isaka Y, Ichimaru N et al. *Biochem Biophys Res Commun* 2007; 353: 786-792
23. Cantley LC. *Science* 2002; 296: 1655-1657
24. Kashii Y, Uchida M, Kirito K et al. *Blood* 2000; 96: 941-949
25. Chavakis T, Kanse SM, Lupu F et al. *Blood* 2000; 96: 514-522
26. Silva M, Grillot D, Benito A et al. *Blood* 1996; 88: 1576-1582
27. Henke M, Mattern D, Pepe M et al. *J Clin Oncol* 2006; 24: 4708-4713
28. Wright JR, Ung YC, Julian JA et al. *J Clin Oncol* 2007; 25: 1027-1032
29. Stohlawetz PJ, Dzirlo L, Hergovich N et al. *Blood* 2000; 95: 2983-2989
30. Wolf RF, Peng J, Friess P et al. *Thromb Haemost* 1997; 78: 1505-1509
31. Brines M, Cerami A. *Kidney Int* 2006; 70: 246-250
32. Peterson L. FDA oncologic drugs advisory committee (ODAC) meeting on the safety of erythropoietin in oncology. *Trends Med* 2004; 1-4

Received for publication: 18.5.07

Accepted in revised form: 29.10.07



# The Effect of Erythropoietin on Gentamicin-Induced Auditory Hair Cell Loss

Arianne Monge, MD; Ivana Nagy, PhD; Sharouz Bonabi, MD; Stephan Schmid, MD;  
Max Gassmann, DVM, PhD; Daniel Bodmer, MD, PhD

**Objective/Hypothesis:** Mammalian auditory hair cells that are unable to regenerate and various agents, including gentamicin, can irreversibly damage the hair cells. Erythropoietin, known as the primary regulator of erythropoiesis, exerts also neuroprotective effects by binding to its receptor. We tested whether erythropoietin can protect the hair cells from gentamicin-induced damage. **Study Design:** This study localized the erythropoietin receptor in the cochlea and analyzed the effect of erythropoietin on gentamicin-damaged hair cells in vitro. **Methods:** Expression of erythropoietin receptor in the rat cochlea was analyzed by reverse transcriptase-polymerase chain reaction (RT-PCR) and immunohistochemistry. Protection of auditory hair cells from gentamicin was tested in vitro by exposing cultured rat organs of Corti with increasing concentrations of erythropoietin (0.1 U/mL, 1 U/mL, and 10 U/mL). **Results:** We detected erythropoietin and erythropoietin receptor mRNA expression in the organ of Corti, spiral ganglion, and stria vascularis by RT-PCR. Immunohistochemistry revealed that the erythropoietin receptor localizes to the outer and inner hair cells and supporting cells of the organ of Corti, as well as to the spiral ganglion cells and the stria vascularis. Significantly less hair cell loss occurred in the organs of Corti that were pretreated with 0.1 U/mL erythropoietin as compared with samples treated with gentamicin only. **Conclusion:** Decreased hair cell loss in erythropoietin-treated organs of Corti that had been exposed to gentamicin provides evidence for a protective effect of erythropoietin in aminoglycoside-induced hair cell death. **Key Words:** Apoptosis, erythropoietin receptor, inner ear, organ of Corti, protection.

*Laryngoscope*, 116:312-316, 2006

From the Department of Otolaryngology, Head & Neck Surgery (A.M., I.N., S.B., S.S., D.B.), University Hospital Zurich, Zurich, Switzerland; and the Institute of Veterinary Physiology (A.M., M.G.), Veterinary Faculty and Zurich Center for Integrative Human Physiology (ZIH), Zurich, Switzerland.

Editor's Note: This Manuscript was accepted for publication November 22, 2005.

Funding for this study provided by the Olga Mayenfisch and Hartmann Müller Foundation.

Send Correspondence to Dr. Daniel Bodmer, University Hospital Zurich, Department of Otolaryngology, Head & Neck Surgery, Frauenklinikstrasse 24, CH-8091 Zurich, Switzerland. E-mail: daniel.bodmer@usz.ch

DOI: 10.1097/01.mlg.0000199400.08650.3f

## INTRODUCTION

Sensorineural hearing loss (HL) results from a variety of causes, including genetic disorders, infectious diseases, overexposure to intense sound, and certain drugs such as gentamicin. Gentamicin, a widely used aminoglycoside antibiotic, causes damage to the sensory hair cells of the organ of Corti (OC) in the inner ear. After prolonged exposure to gentamicin, hair cells undergo apoptotic cell death.<sup>1</sup> Because auditory hair cells of mammals, unlike of fish or birds, do not regenerate, damage to them leads to progressive and irreversible HL. Thus, it is of utmost interest to identify new substances that are able to protect the hair cells and prevent HL after exposure to different factors of cellular stress. The aim of this study was to investigate a possible protective effect of erythropoietin (Epo) on gentamicin-induced hair cell loss. Epo, a glycoprotein hormone that is produced in the fetal liver and adult kidney, promotes survival, proliferation, and differentiation of erythroid progenitor cells.<sup>2</sup> Binding of Epo to the Epo receptor (EpoR), expressed on erythroid progenitor cells, represses apoptosis and allows the final maturation of erythroid progenitor cells to erythrocytes.<sup>2</sup> It has been shown that Epo and its receptor are expressed also in other organs and tissues, including the inner ear, central nervous system, lung, heart, kidney, gastrointestinal and reproductive tracts.<sup>3-6</sup> In addition, Epo was documented to inhibit cellular apoptosis in different in vitro studies and to be protective in vivo in various animal models such as for brain, spinal cord, retina, heart, kidney, and intestine pathology.<sup>4,6</sup> Moreover the Gottingen EPO-Stroke-Trial, a pilot study in patients who had sustained stroke, revealed an enhanced outcome of the EPO-treated patients regarding their clinical progress and brain infarct size.<sup>7</sup> Based on the widespread protective functions of Epo, we tested whether Epo is able to protect the auditory hair cells from gentamicin-induced apoptotic cell death in vitro.

## MATERIALS AND METHODS

### Tissue Culture

All animal procedures were carried out according to an approved animal research protocol (Kantonales Veterinäramt, Zurich, Switzerland). In this study, 27 newborn and four adult

Sprague-Dawley (SD) rats were used. For tissue culture, 5- to 6-day-old SD rat pups were used. The rats were killed, and cochlear microdissections were performed under a light microscope to isolate the OC, spiral ganglion, and stria vascularis. After isolation, all OCs were transferred to cell culture plates and maintained on 0.4-mm culture plate inserts (Millipore) in Dulbecco Modified Eagle Medium with 25 mol/L HEPES supplemented with 10% fetal calf serum (all Invitrogen) and 30 U/mL penicillin (Sigma). To induce hair cell damage, OCs were cultured with 3.3 mol/L gentamicin (Invitrogen) in cell culture medium for 24 hours.<sup>7</sup> OCs were pretreated for 24 hours with increasing amounts of recombinant, human Epo (Roche, Basel, Switzerland) at the final concentration of 0.1 U/mL, 1 U/mL or 10 U/mL in the cell culture medium.<sup>8</sup> After this pretreatment, OCs were exposed to both gentamicin and Epo for 24 hours.

### Reverse Transcriptase-Polymerase Chain Reaction

After culturing five OCs, ganglions, and stria vascularis from three SD rat pups, RNA was isolated as described previously.<sup>9</sup> Total RNA was used and the reverse transcriptase-polymerase chain reaction (RT-PCR) reaction was performed using the RT-PCR Kit with Platinum Taq (Invitrogen) following supplied instructions. Reactions were performed in the Eppendorf Mastercycler under the following conditions: 30 minutes at 50°C, 15 minutes at 94°C, 35 cycles of PCR (1 min at 94°C, 1 min at 50°C, 1 min at 72°C), and 10 minutes at 72°C. Aliquots of the reaction mixture were used as template for PCR amplification of Epo and EpoR complementary DNA (cDNA). The following primer sets were used: Epo primers 5'-ATTTGCGACA GTCGGTTCT-3' (sense) and 5'-GTATCCGCTTGAAGTGTTCG-3' (antisense) of the rat Epo gene and EpoR primers 5'-CTATGGCTGTTGCAACGCGA-3' (sense) and 5'-CCGAGGG CACAGAGCTTAG-3' (antisense) of the rat EpoR gene. The Epo RT-PCR product was 395 base pairs long and the EpoR RT-PCR product was 402 base pairs long, respectively. Negative control reactions were performed in the absence of RNA. Products were separated by agarose gel electrophoresis (2%) and visualized by ethidium bromide staining.

### Immunohistochemistry

Three newborn, 6-day-old and four adult, 2-month-old SD rats were anesthetized and perfusions were performed as described previously.<sup>10</sup> For decalcification, the fixed cochleae of adult mice were incubated in 10% EDTA containing phosphate-buffered saline (PBS) for 4 weeks. After deparaffinization of the inner ear tissue slices, the endogenous peroxidase activity was blocked by incubating the samples for 10 minutes in 3% H<sub>2</sub>O<sub>2</sub>/methanol. Nonspecific background staining was blocked by incubation for 30 minutes in goat serum in 0.15% BSA/PBS and 0.5% Triton-X (Sigma) followed by overnight incubation at 4°C with the primary antibody rabbit anti EpoR (sc-69, Santa Cruz Biotechnology, Inc., Santa Cruz, CA) diluted 1:100 in 0.15% BSA/PBS. In the negative controls, the primary antibody was omitted. Slices were washed three times in PBS, and detection was performed by incubation with goat antirabbit-biotinylated secondary antibody (sc-2040 Santa Cruz Biotechnology) for 30 minutes at room temperature, followed by 30 minutes incubation with avidin-biotin-HRP complex (ABC-Kit, Vectastain; Vector Laboratories). Visualization was performed with 3,3'-diaminobenzidine tetra hydrochloride tablets (Sigma) following the supplier's protocol. Slices from the same cochlea were stained with hematoxylin-eosin (HE) and used as controls.

### Hair Cell Counts

For each condition, six to seven OCs obtained from three to four 5- to 6-day-old SD rats were fixed in 4% paraformaldehyde

containing PBS stained with phalloidin after the culturing period. The OCs were fixed in 4% paraformaldehyde containing PBS and permeabilized with 6% Triton X-100 in PBS containing 10% fetal calf serum. The OCs were incubated with a 1:300 dilution of Texas Red X-phalloidin (Molecular Probes) for 1 hour at room temperature. Visualization was performed using a fluorescence microscope (Olympus DX71) and photographed with an AxioCam (Zeiss). Surviving outer hair cells (OHCs) were counted in a section corresponding to 20 inner hair cells at three different sites located on the basal and middle turns of each OC.

### Statistical Analysis

Results obtained in the hair cell counting were analyzed by unpaired *t*-test using GraphPad Prism 3.03 software (GraphPad Software, Inc., San Diego, CA). The unpaired *t*-test compares the means of two groups, assuming the data are sampled from Gaussian populations. Differences between groups were considered statistically significant when the *P* value was less than .05. Data are presented as mean  $\pm$  standard error of mean (SEM).

## RESULTS

### Expression of Erythropoietin and Erythropoietin Receptor mRNA in the Cochlea

To investigate expression of Epo and EpoR in the cochlea, we performed RT-PCR analysis with isolated RNA from OC, ganglions, and stria vascularis from newborn rats. Epo and EpoR mRNA were detected in the OC, ganglion, and stria vascularis (Fig. 1). Total RNA from rat kidney served as positive control for Epo and EpoR.<sup>11</sup> In the negative control, reaction mixtures without RNA were used.

### Localization of the Erythropoietin Receptor in the Cochlea

Immunohistochemistry was performed to localize the EpoR. Horizontal tissue sections were stained with an anti EpoR antibody. The positive staining control shows the presence of EpoR in tubule cells in the kidney of an

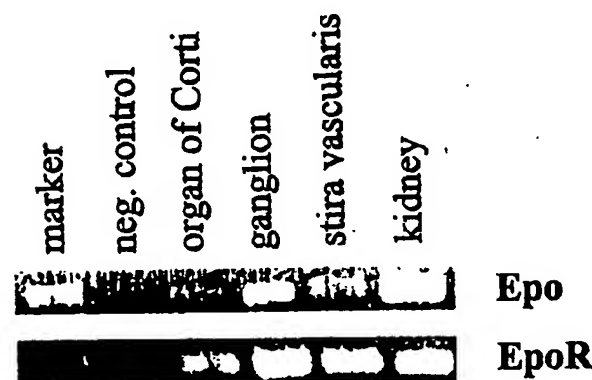


Fig. 1. Expression of erythropoietin (Epo) and erythropoietin receptor (EpoR) mRNA in the cochlea. Detection of Epo and EpoR mRNA by reverse transcriptase-polymerase chain reaction (RT-PCR) in the organ of Corti, ganglion, and stria vascularis of newborn rats. The Epo RT-PCR product is 395 base pairs long and the EpoR RT-PCR product is 402 base pairs long, respectively. The marker corresponds to a length of 396 base pairs. Reaction mixture without RNA (negative controls) and kidney total RNA (positive controls) were used.

adult rat (Fig. 2A).<sup>5</sup> Positive EpoR staining was found in the OC in the outer hair cells, the inner hair cells, and the supporting cells of newborn (Fig. 2B) and adult (Fig. 2C) rats. The expression of the EpoR does not appear to change during the development from newborn to adult rats. The spiral ganglion cells of newborn (data not shown) and adult rats (Fig. 2D) also stained positive for EpoR. Furthermore, the EpoR could be found also in the stria vascularis of newborn (data not shown) and adult rats (Fig. 2E).

#### **Effect of Erythropoietin on Gentamicin-Induced Hair Cell Damage**

To exclude a toxic effect of Epo, the OCs were cultured with the highest dosage of Epo used in this study (10

U/mL) for 48 hours and 96 hours, and the number of OHCs was compared with the number of OHCs in untreated OCs. Because no difference was found (data not shown), a toxic effect of Epo was excluded.

Untreated control OCs showed three orderly rows of OHCs and a single row of inner hair cells (IHCs) (Fig. 3A). Cultured OCs were exposed to 3.3 mol/L gentamicin for 24 hours to damage the hair cells. This treatment led to a pronounced loss of OHCs (Fig. 3A). After exposure with gentamicin, a mean of  $26.1 \pm 4.3$  surviving OHCs were found compared with  $59.4 \pm 0.2$  OHCs in untreated OCs (Fig. 3B), representing a significant loss of 56.1% of OHCs in gentamicin-damaged OCs.

We tested the effect of Epo on gentamicin-induced hair cell damage by pretreating the OCs for 24 hours with

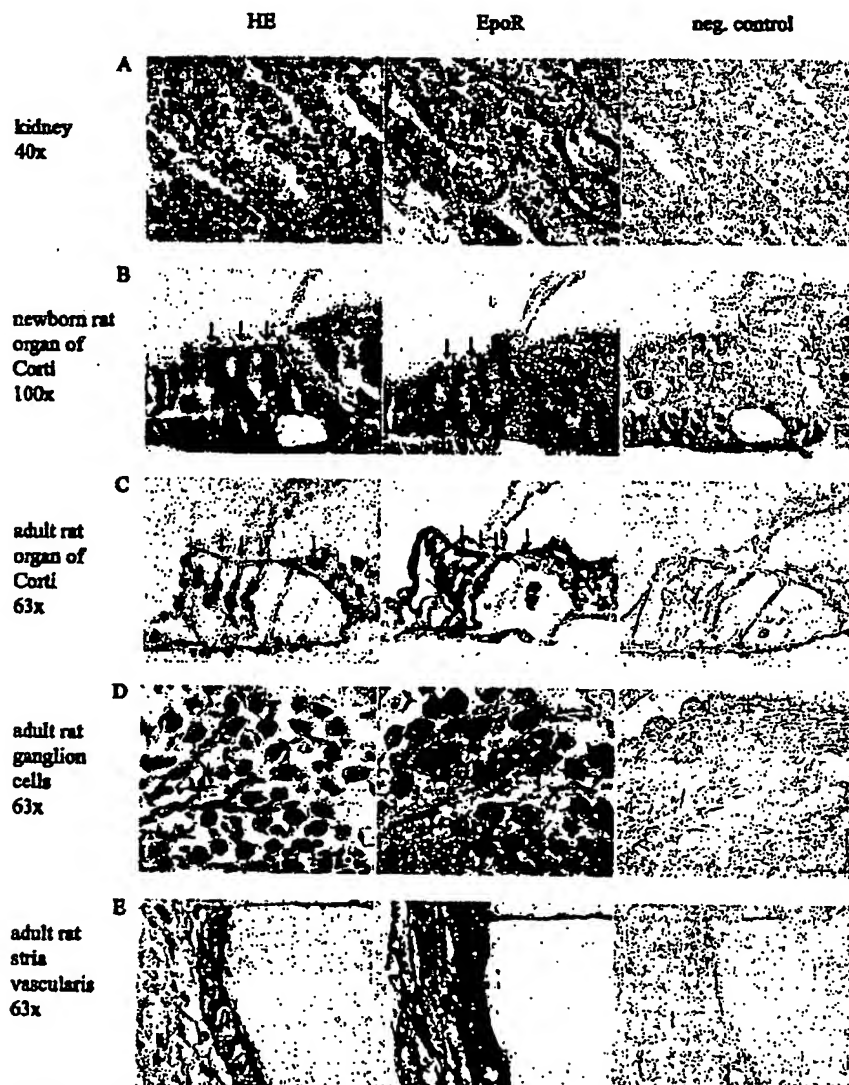


Fig. 2. Localization of the erythropoietin receptor (EpoR) in the cochlea. Horizontal tissue sections showing hematoxylin-eosin staining (on the left), EpoR (in the middle), and the negative control for immunohistochemistry (on the right). Kidney sections were used as a positive staining control (A). The EpoR was found in the outer hair cells (black arrows), inner hair cells (green arrows), and supporting cells of the organ of Corti of newborn (B) and adult (C) rats, in ganglion cells (D), and in the stria vascularis (E).

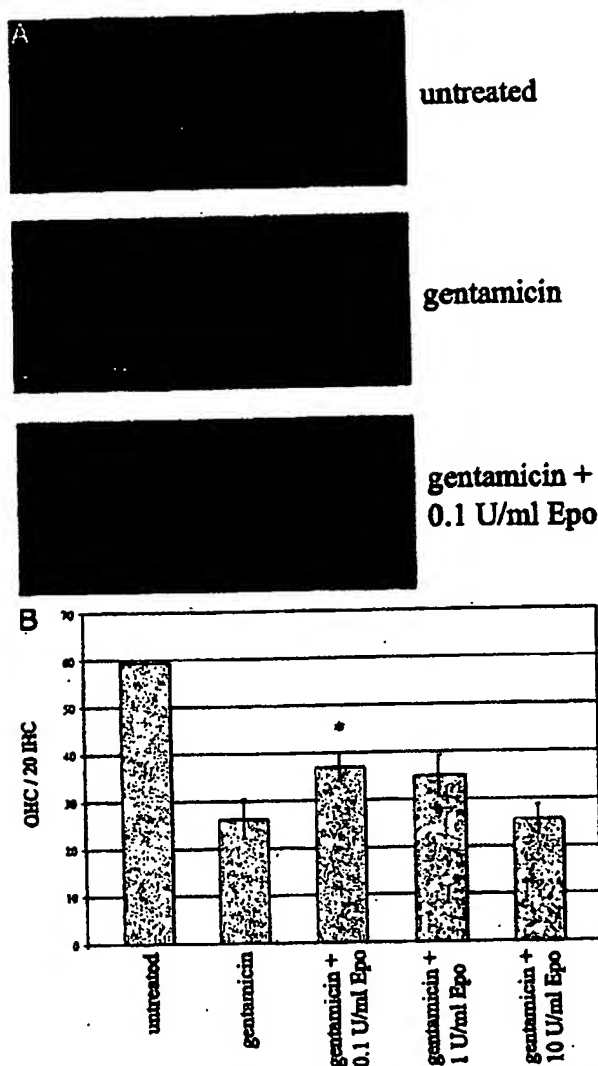


Fig. 3. Effect of erythropoietin (Epo) on gentamicin-induced hair cell damage. (A) Photograph of phalloidin-labeled organs of Corti (OCs). Untreated OCs demonstrate three orderly rows of outer hair cells (OHCs) and a single row of inner hair cells. OCs cultured with gentamicin showed significant loss of hair cells. Treatment with 0.1 U/mL of Epo in addition to gentamicin resulted in significant decrease in hair cells loss compared with gentamicin treatment only. (B) Quantitative analysis of surviving OHCs. Histogram and bars represent mean  $\pm$  standard error of mean. Asterisk shows a statistically significant increase of surviving OHCs in the group treated with Epo in addition to gentamicin compared with gentamicin treatment only.

increasing concentrations of Epo (0.1 U/mL, 1 U/mL, and 10 U/mL) and exposing them for additional 24 hours to gentamicin and Epo. OCs incubated with 0.1 U/mL Epo in addition to gentamicin showed decreased OHC loss (Fig. 3A); quantification revealed a mean of surviving OHCs of  $36.9 \pm 3.0$  (Fig 3B). A *t*-test showed significantly ( $P = .0315$ ) decreased OHC loss when compared with OHC number in OCs that were exposed to gentamicin only. However, incubation with 0.1 U/mL Epo did not lead to

complete protection against gentamicin-induced hair cell death, and a reduction in the number of surviving OHCs could still be observed when compared with the untreated control (Fig. 3A, B). After incubation with 1 U/mL of Epo, the mean was  $34.9 \pm 4.4$  surviving OHCs, but this increase was not statistically significant compared with gentamicin treatment only. OCs treated with 10 U/mL of Epo (mean  $25.5 \pm 3.1$  surviving OHCs) did not differ in the number of surviving OHCs compared with gentamicin-treated OCs.

## DISCUSSION

In the present study, we show that Epo and EpoR mRNA are expressed in the cochlea. The EpoR was localized in the OHCs, IHCs, and supporting cells of the OC, the ganglion cells, and the stria vascularis. We report for the first time a dose-dependent protective effect of Epo on gentamicin-damaged hair cells *in vitro*.

A crucial factor for an effect of Epo is the presence of the EpoR, because Epo acts by binding to its receptor. Recently, EpoR was reported to be expressed in several cell types of the inner ear (i.e., supporting cells of the OC) of 2-month-old guinea pigs, but EpoR expression could not be detected in the OHCs of the OC.<sup>9</sup> In the present study, we show the expression of EpoR also in the OHCs and IHCs of the OC of newborn and adult rats. These different EpoR localizations may be the result of a species-specific distribution of the EpoR in the cochlea. Furthermore, in human brain, a change of EpoR distribution with development was reported.<sup>10</sup> Therefore, we examined the localization of EpoR in the cochlea of newborn and adult rats. However, we did not observe a different distribution of EpoR between newborn and adult rat cochleas.

In this study, Epo mRNA could be detected in the OC, ganglion, and stria vascularis of newborn rats. However, another study demonstrated Epo protein expression in spiral ganglion neurons, but not in the OC or stria vascularis.<sup>9</sup> This could be explained by the fact that Epo is not produced locally or the production was too low to be detected. These previous findings supported our hypothesis that externally applied Epo could have an effect in the cochlea, because the EpoR is expressed in the hair cells of the OC, but Epo is not present in a constant high level.

At present, very little is known about the effects of Epo related to the auditory system. Interestingly, there are reports demonstrating improved hearing capacity after administration of Epo to patients with uremic deafness,<sup>12,13</sup> but it is not clear whether these findings reflect better tissue oxygenation through improved oxygen supply or a direct effect of Epo on the auditory system. Until now, there are no reports about a direct effect of Epo on auditory hair cells. Therefore, we analyzed whether Epo can protect the hair cells from gentamicin-induced damage *in vitro*. We excluded a toxic effect of Epo by itself on auditory hair cells. Treatment with 0.1 U/mL of Epo in addition to gentamicin led to a significant decrease in OHC loss compared with the gentamicin-treated group. Increased survival of OHCs was observed also for 1 U/mL Epo; however, the increase was not statistically significant. Treatment with 10 U/mL Epo did not reduce hair cells loss. These findings suggest a tight therapeutic range

for Epo. That is in agreement with the literature; studies in neurons reported a concentration-dependent protection of Epo, whereas higher Epo concentrations were ineffective; also, a toxic effect of Epo itself was excluded.<sup>8</sup> Our results suggest that 0.1 U/mL of Epo may be the optimal dose for promoting survival of gentamicin-induced hair cells loss in vitro. Although Epo enhanced hair cell survival, it did not provide complete protection against gentamicin-induced ototoxicity. Future work is required to clarify whether concentrations lower than 0.1 U/mL of Epo, or shorter pretreatments with Epo, might provide higher protection against gentamicin-induced hair cell loss. As such, it has been reported that neuronal survival against NO toxicity increased when Epo pretreatment was shortened.<sup>9</sup>

Our in vitro data are limited to 5- to 6-day-old rats, because only OC from newborn animals can be used for tissue culture. However, we localized the EpoR also in OHCs and IHCs in the OC of adult rats. This finding suggests that Epo might have a protective effect on auditory hair cells also in the adult. In vivo experiments with adult animals will be required to test this hypothesis in the future. It will be interesting to investigate also whether Epo can protect the auditory hair cells from other types of damage such as exposure to different drugs, noise, or aging.

Our results provide evidence for a protective effect of Epo against gentamicin-induced hair cell loss in vitro.

#### Acknowledgments

The authors thank Verena Hoffmann and Stephan Keller for excellent technical assistance.

#### BIBLIOGRAPHY

- Huang T, Cheng AG, Stupak H, et al. Oxidative stress-induced apoptosis of cochlear sensory cells: otoprotective strategies. *Int J Dev Neurosci* 2000;18:259-270.
- Jelkmann W. Erythropoietin: structure, control of production, and function. *Physiol Rev* 1992;72:449-489.
- Caye-Thomasen P, Wagner N, Lidgaard Frederiksen B, Asai K, Thomsen J. Erythropoietin and erythropoietin receptor expression in the guinea pig inner ear. *Hear Res* 2005;203:21-27.
- Gassmann M, Heinicke K, Soliz J et al. Non-erythroid functions of erythropoietin. *Adv Exp Med Biol* 2003;543:323-330.
- Lewis LD. Preclinical and clinical studies: a preview of potential future applications of erythropoietic agents. *Semin Hematol* 2004;41:17-25.
- Ghezzi P, Brines M. Erythropoietin as an antiapoptotic, tissue-protective cytokine. *Cell Death Differ* 2004;11:37-44.
- Ehrenreich H, Hasselblatt M, Dembowski C, et al. Erythropoietin therapy for acute stroke is both safe and beneficial. *Mol Med* 2002;8:496-505.
- Corbaccella E, Lanzoni I, Ding D, Prevati M, Salvi R. Minocycline attenuates gentamicin induced hair cell loss in neonatal cochlear cultures. *Hear Res* 2004;197:11-18.
- Chong ZZ, Kang JQ, Maiese K. Erythropoietin fosters both intrinsic and extrinsic neuronal protection through modulation of microglia, Akt1, Bad, and caspase-mediated pathways. *Br J Pharmacol* 2003;138:1107-1118.
- Nagy I, Bodmer M, Brors D, Bodmer D. Early gene expression in the organ of Corti exposed to gentamicin. *Hear Res* 2004;195:1-8.
- Nagy I, Bodmer M, Schmid S, Bodmer D. Promyelocytic leukemia zinc finger protein localizes to the cochlear outer hair cells and interacts with prestin, the outer hair cell motor protein. *Hear Res* 2005;204:216-222.
- Westenfelder C, Biddle DL, Baranowski RL. Human, rat, and mouse kidney cells express functional erythropoietin receptors. *Kidney Int* 1999;55:808-820.
- Juul SE, Yachnis AT, Rojiani AM, Christensen RD. Immunohistochemical localization of erythropoietin and its receptor in the developing human brain. *Pediatr Dev Pathol* 1999;2:148-158.
- Shaheen FA, Mansuri NA al-ShaikhAM, et al. Reversible uremic deafness: is it correlated with the degree of anemia? *Ann Otol Rhinol Laryngol* 1997;106:391-393.
- Markowski J, Gierak T, Wiecek A, Klimak D, Chudak J. Assessment of hearing organ ability in high-frequency auditory in patients suffering from chronic renal failure treated by haemodialysis and human recombinant erythropoietin (rhEPO). *Otolaryngol Pol* 2002;56:589-596.

# THE Laryngoscope

FOUNDED IN 1896

VOLUME 116

NUMBER 2

FEBRUARY 2006

[www.laryngoscope.com](http://www.laryngoscope.com)

## Contents

 Denotes supplementary material on Web site

 Denotes online only article

### Triological Society Papers

- 165 **Assessment of Intraoperative Safety in Transoral Robotic Surgery**  
Neil G. Hockstein, MD; Bert W. O'Malley, Jr., MD; Gregory S. Weinstein, MD

### Independent Papers

- 169 **Primary Treatment of Ranula With Intracystic Injection of OK-432**  
Jong-Lyel Roh, MD, PhD
- 173 **Morbidity After Flap Reconstruction of Hypopharyngeal Defects**  
Jonathan R. Clark, BSc(Med), MBBS, FRACS; Ralph Gilbert, MD, FRCS(C);  
Jonathan Irish, MD, FRCS(C); Dale Brown, MB, BCh, FRCS(C);  
Peter Neligan, MD, FRCS(C); Patrick J. Gullane, MD, FRCS(C), FACS
- 182 **The Edwin Smith Papyrus: The Birth of Analytical Thinking in Medicine and Otolaryngology**  
Marc Stiefel, MD; Arlene Shaner, MA, MLS; Steven D. Schaefer, MD

This journal is listed in *Index Medicus/MEDLINE*, *Current Contents/Clinical Medicine*, *Biological Abstracts*, *Chemical Abstracts*, *Excerpta Medica*, and *Science Citation Index*.

The *Laryngoscope* (ISSN 0023-852X), a peer reviewed journal, is a program of The American Laryngological, Rhinological and Otolological Society, Inc. and is published monthly by Lippincott, Williams & Wilkins, 16522 Hunters Green Parkway, Hagerstown, MD, 21740-2116. Business offices are located at 351 West Camden Street, Baltimore, MD 21201. Periodical postage paid at Hagerstown, MD, and at additional mailing offices. Copyright © 2006 by The American Laryngological, Rhinological and Otolological Society, Inc., d/b/a *Laryngoscope* Journal.

Postmaster: Send address changes to *The Laryngoscope*, P.O. Box 1550, Hagerstown, MD 21740.

Annual Subscription Rates: *United States* - \$245.00 Individual, \$462.00 Institution, \$98.00 In-training. *Rest of World* - \$271.00 Individual, \$462.00 Institution, \$94.00 In-training. Single copy rate \$40.00. All prices include a handling charge. Subscriptions outside of North America must add \$21.00 for airfreight delivery. United States residents of AL, CO, DC, FL, GA, HI, IA, ID, IN, KS, KY, LA, MD, MO, ND, NM, NV, PR, RI, SC, SD, UT, VT, WA, WV add state sales tax. The GST tax of 7% must be added to all orders shipped to Canada (Lippincott Williams & Wilkins' GST Identification #895524239, Publications Mail Agreement #1170775). Subscription prices outside the United States must be prepaid. Prices subject to change without notice. Visit us online at [www.lww.com](http://www.lww.com).

Individual and in-training subscription rates include print and access to the online version. Institutional rates are for print only; online subscriptions are available via Ovid. Institutions can choose to purchase a print and online subscription together for a discounted rate. Institutions that wish to purchase a print subscription, please contact Lippincott Williams & Wilkins, 16522 Hunters Green Parkway, Hagerstown, MD 21740-2116; phone 800-638-3030 (outside the United States 301-223-2300); fax 301-223-2400. Institutions that wish to purchase an online subscription or online with print, please contact the Ovid Regional Sales Office near you or visit [www.ovid.com/site/index.jsp](http://www.ovid.com/site/index.jsp) and select Contact and Locations.

Address for non-member subscription information, orders, or change of address: Lippincott Williams & Wilkins, P.O. Box 1580, Hagerstown, MD 21741-1580; phone 800-638-3030 (outside the United States 301-223-2300); fax 301-223-2400. In Japan, contact LWW Igaku-Shoin Ltd., 3-23-14 Hongo, Bunkyo-ku, Tokyo 113-0033; phone 81-3-5689-5400; fax 81-3-5689-5402. In Bangladesh, India, Nepal, Sri Lanka, and Pakistan, contact Globe Publications Pvt. B-13 3<sup>rd</sup> Floor, A Block, Shopping Complex, Naraina Vihar, Ring Road, New Delhi, 110028; phone 91-11-579-3211; fax 91-11-579-8876.

Address for member subscription information, orders, or change of address: *The Laryngoscope* is a benefit of membership to the American Laryngological, Rhinological and Otolological Society, Inc. To become a member or provide a change of address, please contact the American Laryngological, Rhinological and Otolological Society, Inc., 555 N. 30th St., Omaha, NE 68131; phone 402-346-5500; fax 402-346-5300. For all other membership inquiries, contact Lippincott Williams & Wilkins Customer Service Department, P.O. Box 1580, Hagerstown, MD 21741-1580; phone 800-638-3030 (outside the United States 301-223-2300); fax 301-223-2400; e-mail [memberservice@lww.com](mailto:memberservice@lww.com).



## Erythropoietin, Modified to Not Stimulate Red Blood Cell Production, Retains Its Cardioprotective Properties

Chanil Moon, Melissa Krawczyk, Doojin Paik, Thomas Coleman, Michael Brines, Magdalena Juhaszova, Steven J. Sollott, Edward G. Lakatta, and Mark I. Talan

Laboratory of Cardiovascular Sciences, Gerontology Research Center, National Institute on Aging, Baltimore, Maryland (C.M., M.K., M.J., S.J.S., E.G.L., M.I.T.); Department of Anatomy and Cell Biology, Hanyang University, Seoul, Korea (D.P.); and Kenneth S. Warren Institute and Warren Pharmaceuticals, Ossining, New York (T.C., M.B.)

Received August 29, 2005; accepted November 21, 2005

### ABSTRACT

Erythropoietin (EPO), a hematopoietic cytokine, possesses strong antiapoptotic, tissue-protective properties. For clinical applications, it is desirable to separate the hematopoietic and tissue-protective properties. Recently introduced carbamylated erythropoietin (CEPO) does not stimulate the erythropoiesis but retains the antiapoptotic and neuroprotective effects. We tested the ability of CEPO to protect cardiac tissue from toxin-induced and oxidative stress in vitro and ischemic damage in vivo and compared these effects with the effects of EPO. CEPO reduced by 50% the extent of staurosporine-induced apoptosis in isolated rats' cardiomyocytes and increased by 25% the reactive oxygen species threshold for induction of the mitochondrial permeability transition. In an experimental model of myocardial infarction induced by permanent ligation of a coronary artery in rats, similarly to EPO, a single bolus injection of 30

$\mu\text{g/kg}$  b.wt. of CEPO immediately after coronary ligation reduced apoptosis in the myocardial area at risk, examined 24 h later, by 50%. Left ventricular remodeling (ventricular dilation) and functional decline (fall in ejection fraction) assessed by repeated echocardiography were significantly and similarly attenuated in CEPO- and EPO-treated rats. Four weeks after coronary ligation, the myocardial infarction (MI) size in CEPO- and EPO-treated rats was half of that in untreated coronary-ligated animals. Unlike EPO, CEPO had no effect on hematocrit. The antiapoptotic cardioprotective effects of CEPO, shown by its ability to limit both post-MI left ventricular remodeling and the extent of the myocardial scar in the model of permanent coronary artery ligation in rats, demonstrate comparable potency to that of native (nonmodified) EPO.

Erythropoietin (EPO) is a well known hematopoietic cytokine produced by the kidney in response to hypoxia (Yousoufian et al., 1993). Recombinant human EPO (rhEPO) is widely used to treat the anemia related to surgery, cancer, and kidney failure (Jelkmann, 1994). However, EPO possesses much broader salutary effects than merely stimulation of red blood cell production. EPO receptors, originally thought to be confined only to hematopoietic tissue in adults, were also found in other tissues, for example, neural tissue (for review, see Masuda et al., 1999). Many recent studies have demonstrated the neuroprotective effects of rhEPO in different animal models (Sadamoto et al., 1998; Bernaudin et

al., 1999; Brines et al., 2000) and in a phase II clinical trial in cerebral ischemia (Ehrenreich et al., 2002).

In several recent studies, the effects of systemic administration of rhEPO have been extended to include cardioprotection from ischemia. The antiapoptotic effects of rhEPO on cardiomyocytes have been reported in tissue culture and in vivo animal models of ischemia-reperfusion injury (for review, see Smith et al., 2003; Bogoyevitch, 2004). The recent discovery of EPO receptors in cardiomyocytes of adult rat solidified these findings (Wright et al., 2004).

In a rat model of myocardial ischemia using permanent ligation of a coronary artery, we have shown that in comparison with untreated animals, a single systemic injection of 30  $\mu\text{g/kg}$  b.wt. of rhEPO immediately after coronary artery ligation reduced apoptosis in the myocardial area at risk 24 h later by 50%. Left ventricular remodeling was suppressed in rhEPO-treated rats, and 8 weeks after coronary ligation, the

This research was supported by the Intramural Research Program of the National Institutes of Health, National Institute on Aging.

Article, publication date, and citation information can be found at <http://jpet.aspetjournals.org>.  
doi:10.1124/jpet.105.094854.

**ABBREVIATIONS:** EPO, erythropoietin; rhEPO, recombinant human erythropoietin; MI, myocardial infarction; STAT, signal transducer and activator of transcription; PI3K, phosphatidylinositol 3 kinase; MPT, mitochondrial permeability transition; CEPO, carbamylated erythropoietin; LV, left ventricle; ROS, reactive oxygen species; TMRM, tetramethylrhodamine methyl ester; SH, sham (S); EDV, end-diastolic volume; ESV, end-systolic volume; EF, ejection fraction; TUNEL, terminal deoxynucleotidyltransferase-mediated dUTP nick-end labeling; ANOVA, analysis of variance.

myocardial infarct (MI) scar was 4-fold smaller than in untreated coronary artery-ligated animals (Moon et al., 2003).

A number of signaling pathways reportedly have been involved in the mechanism of EPO-induced cardioprotection. Jak-2/STAT signaling was implicated as well as PI3K signaling (Parsa et al., 2003), protein kinase C, p38, and p42/44 mitogen-activated protein kinase activation, affecting sarcolemmal and mitochondrial potassium channels,  $K_{ATP}$  (Shi et al., 2004), and Akt signaling (Calvillo et al., 2003; Parsa et al., 2003). We have recently reported that the end effector of cardioprotection by rhEPO is the permeability transition pore complex: rhEPO limits the induction of mitochondrial permeability transition (MPT) in cardiomyocytes and, thus, promotes their survival during adverse conditions (Juhászova et al., 2004).

Thus, a number of convincing preclinical experiments suggest that systemic administration of rhEPO presents a new therapeutic approach to limit myocardial damage and subsequent heart remodeling after ischemia (Maiese et al., 2005). However, the classic property of EPO to activate production of red blood cells and thrombocytes is the weakness of such therapy, limiting it to a single application and, even as such, might be contraindicated in some patients. The attendant elevation of hematocrit associated with repeated rhEPO treatment may have an adverse effect on the outcome of MI (Spiess, 1999).

A modification of EPO by subjecting it to carbamylation has recently been introduced for tissue protection (Leist et al., 2004). This carbamylated EPO (CEPO) completely lacks bioactivity in hematopoiesis bioassays and in vivo animal testing with repeated high-dose injection but effectively protects isolated neural cells from induced apoptosis. Moreover, in in vivo experiments, CEPO does not bind to EPO receptors (Leist et al., 2004). Further experiments established that CEPO's pharmacodynamic parameters are similar to that of rhEPO, and it mimics rhEPO efficacy in experimental models of brain ischemia, spinal cord and nerve damage, and autoimmune encephalomyelitis (Leist et al., 2004). In a temporary coronary ligation (ischemia-reperfusion model) in the rat (Fiordaliso et al., 2005), CEPO was shown to be cardioprotective in preventing increases in LV end-diastolic pressure, LV wall stress in systole and diastole, and improving the LV response to dobutamine. Protection against staurosporine-induced cardiomyocyte apoptosis in vitro was also observed.

The objective of this study is to establish the relationship between the efficacy of CEPO as a cardioprotective compound in vitro and in vivo and the mechanism of protection operating through induction of the MPT independently of its effects on hematopoiesis. We hypothesized that CEPO would demonstrate antiapoptotic properties in isolated cardiomyocytes undergoing hypoxia/reoxygenation stress and enhance their survival by limiting induction of the MPT. We also hypothesized that similar to EPO, systemic administration of a single dose of CEPO immediately after coronary ligation in rats would 1) reduce apoptosis in the area of myocardium at risk [area at risk (AAR)] 24 h later, 2) would attenuate the ensuing left ventricular remodeling and functional decline in the following weeks, and 3) would result in a smaller MI size at the end of 4 weeks of observation.

## Materials and Methods

### Materials

CEPO was produced by Warren Pharmaceuticals, Inc. (Ossining, NY) by subjecting rhEPO (Dragon Pharmaceutical, Vancouver, BC, Canada) to carbamylation—the process by which all lysines were transformed to homocitrulline (Leist et al., 2004). The dosages of CEPO used in the in vivo experiments were equivalent to EPO in terms of weight; i.e., 3000 IU/kg b.wt. EPO and 30  $\mu$ g/kg b.wt. CEPO.

### In Vitro Protocols

**Left Ventricular Myocytes Isolation for Experiments on Cell Culture.** Left ventricular cardiomyocytes were isolated from adult Sprague-Dawley rats (250–300 g; Taconic Farms, Germantown, NY) in a perfusion chamber using Adumyts (Cellutron, Highland Park, NJ) proprietary buffers. Twenty minutes before sacrifice, animals were given 5000 U/kg heparin (Sigma-Aldrich, St. Louis, MO). Hearts were isolated rapidly, perfused through the aorta, and gassed with 85%  $O_2$  and 15%  $N_2$  at 37°C. Myocytes were then isolated by mechanical dissociation, separated by differential centrifugation, and plated on laminin (Sigma-Aldrich)-coated dishes (Calvillo et al., 2003). After 1 h, the medium was changed, and CEPO or EPO (100 ng/ml) or control buffer was added to the myocytes 30 min before induction of apoptosis by staurosporine (0.1  $\mu$ M; Sigma-Aldrich). After 16-h incubation, myocytes were washed with ice-cold Hanks' solution (Invitrogen, Carlsbad, CA), fixed for 20 min in 10% MeOH-free formaldehyde (Polysciences, Warrington, PA) at 4°C, washed in ice-cold Hanks' solution, stored in –20°C 70% EtOH overnight, and processed for in situ terminal deoxynucleotidyl transferase assay (Roche, Minneapolis, MN) for detection of apoptosis.

**Left Ventricular Myocytes Isolation for Mitochondrial Permeability Transition Experiments.** Single ventricular myocytes were isolated via a previously described technique with minor modifications (Capogrossi et al., 1986). Briefly, 2- to 4-month-old Sprague-Dawley rats were anesthetized with sodium pentobarbital, and hearts were rapidly excised and perfused with 40 ml of nominally  $Ca^{2+}$ -free bicarbonate buffer gassed with 95%  $O_2$  to 5%  $CO_2$  at 37°C. The composition of buffer was the following: 116.4 mM NaCl, 5.4 mM KCl, 1.2 mM  $MgSO_4$ , 1.2 mM  $NaH_2PO_4$ , 5.6 mM glucose, and 26.2 mM  $NaHCO_3$ , pH 7.4. Hearts were continuously perfused with bicarbonate buffer containing 0.1% collagenase type B, 0.04 mg/ml protease XVI, and 0.1% bovine serum albumin type V for 4 min, and 50  $\mu$ M  $Ca^{2+}$  was added. After 10-min perfusion, the left ventricle was minced and incubated in bicarbonate buffer containing 100  $\mu$ M  $Ca^{2+}$  for 10 min at 37°C. Myocytes were then resuspended in HEPES buffer with gradually increasing  $Ca^{2+}$  concentration up to 1 mM and kept at room temperature until use. The composition of the HEPES buffer was the following: 137 mM NaCl, 4.9 mM KCl, 1.2 mM  $MgSO_4$ , 1.2 mM  $NaH_2PO_4$ , 15 mM glucose, 20 mM HEPES, and 1.0 mM  $CaCl_2$  (adjusted pH to 7.4). Cardiac myocytes viability was typically 70 to 80%.

**Confocal Microscopy and Determination of MPT-ROS Threshold.** Experiments were conducted as described previously (Juhászova et al., 2004), using a method to quantify the ROS susceptibility for the induction of MPT in individual mitochondria within cardiac myocytes (Zorov et al., 2000). Briefly, isolated cardiac myocytes were exposed in vitro to conditions that mimic oxidative stress by repetitive laser scanning of a row of mitochondria in a myocyte loaded with tetramethylrhodamine methyl ester (TMRM; see Fig. 2). This results in incremental, additive exposure of only the laser-exposed area to the photodynamic production of ROS and consequent MPT induction. The occurrence of MPT is clearly identified by the immediate dissipation of  $\Delta\psi$ . Myocytes were loaded with 125 nM TMRM for at least 1 h at room temperature and imaged with an LSM-510 inverted confocal microscope (Carl Zeiss Inc., Jena, Germany) (Fig. 2A). Line scan images at 2 Hz were recorded from mitochondria arrayed along individual myofibrils with excitation at



568 nm and collecting emission at >560 nm, using a Zeiss Plan-Apochromat 63×/1.4 numerical aperture oil immersion objective, and the confocal pinhole was set to obtain spatial resolutions of 0.4  $\mu$ m in the horizontal plane and 1  $\mu$ m in the axial dimension. Images were processed by MetaMorph software (Universal Imaging, Downingtown, PA). The ROS threshold for MPT induction ( $t_{MPT}$ ) was measured as the average time necessary to induce MPT in a row consisting of ~25 mitochondria (Fig. 2B). Experiments were carried out at 23°C. The cardioprotective action of insulin, which normally results in an enhancement of the MPT-ROS threshold by ~35 to 40% (Juhászova et al., 2004), was used as a positive control in the present experiments. In parallel experiments, cells were exposed to CEPO (10, 100, or 250 ng/ml for 20 min prior to  $t_{MPT}$  measurements). Wortmannin (50  $\mu$ M) was also applied in certain protocols.

## II. In Vivo Experiments

**Animals and Experimental Design.** Eighty male Sprague-Dawley rats, 2 months of age, were housed and studied in conformance with the National Institutes of Health Guide for the Care and Use of Laboratory Animals, Manual 3040-2 (1999), with institutional Animal Care and Use Committee approval. After baseline echocardiography, animals were randomly divided into coronary artery-ligated (MI;  $n = 54$ ) or sham (SH;  $n = 16$ ) groups and, under inhalation anesthesia by isoflurane, subjected to ligation of the left anterior descending coronary artery to induce myocardial infarction (MI) or to a sham operation, as previously described (Moon et al., 2003). Animals in the MI group were either treated with a single systemic injection of CEPO ( $n = 18$ ) or EPO ( $n = 18$ ) or remained untreated ( $n = 18$ ). Both CEPO and EPO, 30  $\mu$ g/kg b.wt., were given i.v. in 0.3 ml of saline immediately (<5 min) after surgery. Untreated animals received a single i.v. injection of 0.3 ml of saline at the same time. SH animals were either injected with CEPO ( $n = 8$ ), or with saline ( $n = 8$ ) in a dose and manner similar to MI animals. Therefore, the experimental design consisted of five groups of rats: sham, not treated (SH-SALINE); sham, treated with CEPO (SH-CEPO); MI, not treated (MI-SALINE); and MI, treated with CEPO (MI-CEPO), and MI, treated with EPO (MI-EPO). Six animals from each of the MI-CEPO, MI-EPO, and the MI-SALINE groups were killed 24 h after surgery, and their hearts were harvested for appropriate immunohistochemical staining to assess the early effect of CEPO treatment on the extent of post-MI apoptosis. In the remainder of the operated animals, LV function was assessed by echocardiography 1 and 4 weeks after surgery, at which time all animals were killed using a bolus injection of 4 ml of 0.5 M KCl under general anesthesia with sodium pentobarbital (50 mg/kg b.wt., i.p.), and their hearts were harvested for histological analyses.

**Echocardiography.** Cardiac function was assessed by echocardiography (HP Sonos 5500 equipped with a 12-MHz phase array linear transducer, S12, allowing a 150-mm/s maximal sweep rate; Hewlett Packard, Palo Alto, CA) under general anesthesia with pentobarbital sodium (30 mg/kg b.wt., i.p.) as described previously (Moon et al., 2003). Briefly, parasternal long-axis views were obtained and recorded, ensuring that the mitral and aortic valves and the apex were visualized. Endocardial area tracings using the leading-edge method were performed in the two-dimensional mode (short- and long-axis views) from digital images captured on cine-loop. LV end-diastolic volume (EDV) and LV end-systolic volume (ESV) were calculated by a modified Simpson's method from the long-axis view. LV ejection fraction (EF %) was derived as  $EF = (EDV - ESV)/EDV \times 100$ . All measurements were made by one observer who was blinded with respect to the identity of the tracings. All measurements were averaged over three to five consecutive cardiac cycles. The reproducibility of measurements was assessed at baselines by two sets of measurements in 10 randomly selected rats. The repeated measure variability did not exceed  $\pm 5\%$ .

**Infarct Size Measurement.** Hearts were excised and placed in 10% phosphate-buffered formalin. The fixed tissue was then embedded in paraffin and serially cut from the apex to the level just below

the coronary artery ligation site; transverse 6- $\mu$ m-thick sections were cut at 600- $\mu$ m distances such that 10 to 12 sections were obtained from each heart. Sections were stained with hematoxylin/eosin and azan, and morphological analysis was performed by computerized video imaging using an Axioplan microscope (Zeiss) and NIH IMAGE software (Bethesda, MD). The myocardial infarct size of each section was calculated as the ratio of infarction area to the area of total LV section (area method) and as the average of ratios of the outer infarction length to the outer LV circumference and the inner infarction length to the inner LV circumference (perimeter method). The infarct size of all sections for both area and perimeter methods was averaged and expressed as the percentage of LV for each heart.

**LV Posterior Wall Thickness Measurement.** The thickness of LV posterior wall was measured and averaged in each LV section where the myocardial infarct size was measured.

**Assessment of Apoptosis in Hearts.** Twenty-four hours after coronary artery ligation or sham operation, under general anesthesia with pentobarbital sodium (50 mg/kg b.wt., i.p.), 2 ml of 5% Evans blue was injected into the right ventricular chamber via the right jugular vein. The rats were killed immediately by a bolus injection of 4 ml of 0.5 M KCl, and the hearts were removed, rapidly rinsed in phosphate-buffered saline, and snap-frozen in liquid nitrogen. Serial, 6- $\mu$ m-thick cryostat sections were prepared. Processing of subsequent sections alternated between tetrazolium chloride and terminal deoxynucleotidyltransferase-mediated dUTP nick-end labeling (TUNEL) staining. The parts unstained by Evans blue containing a combination of dead tissue and underperfused but viable myocardium (AAR) were incubated for 20 min in tetrazolium chloride and then transferred into 4% paraformaldehyde. In all resulting sections, the AAR of myocardial tissue was stained in red, whereas dead tissue remained white (Bialik et al., 1997). The AAR on every other section was further subjected to TUNEL staining for detection of apoptotic cells by the nick-end labeling method using a commercially available kit (Roche) as directed by the manufacturer. Slides were examined by light microscopy. In each section, the number of cardiomyocytes and the number of TUNEL-positive cardiomyocyte nuclei were counted and totaled in 10 randomly selected fields of the AAR at  $\times 400$  amplification. Only nuclei that were clearly located in cardiomyocytes were counted.

**Statistical Analyses.** Sonographic indices of morphometric and functional assessment at each time point were expressed as a percentage of change from the baseline (measurements taken before surgery). All values were corrected for body mass. Statistical significance of differences among groups with regard to changes of these indices over time was determined using ANOVA for repeated measurements, specifically noting group  $\times$  time interactions. A post hoc pair comparison between MI-SALINE, MI-CEPO, and MI-EPO groups was conducted for the 4<sup>th</sup>-week data. Statistical significance of differences between groups with regard to infarct size and apoptosis was determined using a one-way ANOVA following by a post hoc pair comparison. The same approach was used in vitro experiments. Statistical significance was assumed at  $p < 0.05$ .

## Results

### In Vitro Experiments

**Apoptosis in Isolated Cardiomyocytes.** After 16 h of staurosporine exposure, 78% of untreated myocytes were apoptotic. In the presence of 100 ng/ml rhEPO or CEPO, the number of apoptotic myocytes was reduced by 77 and 87%, respectively (Fig. 1).

**Assessment of MPT-ROS Threshold.** Figure 2C presents the cardioprotective effects of CEPO in isolated cardiac myocytes as indexed by the ROS threshold for MPT induction ( $t_{MPT}$ ). CEPO exposure at 10, 100, and 250 ng/ml resulted in increased MPT-ROS threshold by 20 to 25% above the un-

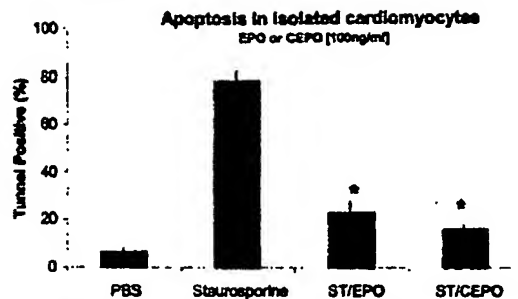


Fig. 1. The antiapoptotic effect of rEPO and CEPO on isolated rat cardiomyocytes. After a 30-min in vitro exposure of isolated rat ventricular cardiomyocytes to 100 ng/ml CEPO or EPO, apoptosis was induced by staurosporine. After 16-h incubation, myocytes were processed for in situ terminal deoxynucleotidyl transferase assay for detection of apoptosis. PBS, phosphate-buffered saline. \*,  $p < 0.05$  versus staurosporine (post hoc comparison).

treated control. This protective effect was completely blocked by 50 nM wortmannin. For comparison, insulin, used as a positive control, increased  $t_{MPT}$  by 35%.

#### In Vivo Experiments

**Mortality and Final Number of Animals.** Three animals died among coronary artery-ligated CEPO-treated animals, four among coronary artery-ligated EPO-treated animals, and two among untreated rats. One animal died in the sham-operated group. No mortality was registered after the first 24 h. Thus, the final number of animals per group in 24-h study was: MI-SALINE, six; MI-CEPO, six; and MI-EPO, six. The final number of animals per group in 4-week study was SH-SALINE, seven; SH-CEPO, eight; MI-SALINE, 10; MI-CEPO, nine; and MI-EPO, eight.

**The Effect of CEPO and EPO on Hematocrit.** One week after MI induction, the hematocrit values increased on

average by 5.1% in EPO-treated rats ( $p < 0.05$ ) but did not change in CEPO-treated animals ( $-0.7\%$ ,  $p > 0.05$ ).

**Echocardiography.** At baseline, before coronary artery ligation or sham operation, echocardiographic indices of LV volumes and EF are presented in Table 1. There were no statistical differences at baseline among coronary artery-ligated or sham-operated animals untreated or treated with CEPO or EPO in EDV, ESV, or EF. Average changes of these parameters from baseline during 4 weeks of observation are illustrated in Fig. 3. Treatment of sham-operated animals with CEPO (S-CEPO) did not affect the direction or magnitude of changes during the 4 weeks after surgery relative to untreated animals (S-SALINE). In nontreated ligated animals (MI-SALINE), there was a gradual enlargement of LV over time; by week 4, this averaged a 26% and approximately 140% increase of baseline LV volumes at end-diastole and end-systole, respectively. The EF in MI-SALINE animals fell by more than 50% by week 4. The magnitude and pattern of changes of all indices in MI-SALINE group were significantly different from those of both sham-operated groups (the ANOVA-derived group  $\times$  time interaction,  $p < 0.05$ ).

The pattern and magnitude of changes reflecting the extent of LV remodeling and functional decline were less pronounced in both the MI-CEPO and MI-EPO groups than in MI-SALINE group. In fact, contrary to the MI-SALINE group, the evaluation of LV remodeling (ANOVA-derived group  $\times$  time interaction) showed that there were no statistical differences between MI-CEPO or MI-EPO and sham groups for all three presented indices. Moreover, EF and ESV were significantly different between either MI-CEPO or MI-EPO and MI-SALINE. Post hoc paired comparisons also revealed that both MI-CEPO and MI-EPO groups statistically differed at week 4 from MI-SALINE group with respect to EF and ESV: ESV at week 4 was significantly smaller and EF was significantly higher in both MI-CEPO and MI-EPO

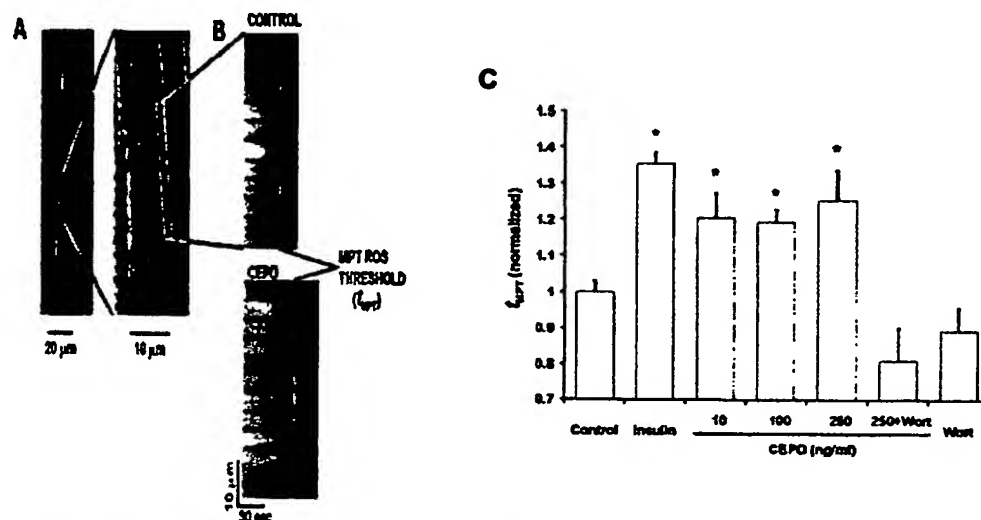


Fig. 2. Cellular mechanism of cardioprotection. A and B, methodology used to determine the ROS threshold of MPT induction, the index of cardioprotection. Mitochondria in isolated rat cardiac myocytes stained with TMRM (A) were laser line-scanned until MPT induction (B). The average time required for the standardized photoproduction of ROS to cause MPT induction ( $t_{MPT}$ ) is taken as the index of the ROS threshold in that cell (see text and references, Zorov et al., 2000; Juhaszova et al., 2004). C, CEPO reduces the MPT susceptibility to ROS ( $t_{MPT}$ ) via PI3K-dependent signaling in cardiac myocytes. Isolated cells were exposed to 30 nM insulin (as the positive control) or to 10, 100, or 250 ng/ml CEPO for 20 min prior to  $t_{MPT}$  measurement (see text). Wortmannin (50 nM) was used to inhibit PI3K. \*,  $p < 0.01$  versus control.

TABLE 1  
Baseline (week 0) echocardiographic indices of LV volumes and EF (mean  $\pm$  S.E.)

	SH-SALINE (n = 7)	SH-CEPO (n = 8)	MI-SALINE (n = 10)	MI-CEPO (n = 9)	MI-EPO (n = 8)
EDV (ml)	0.35 $\pm$ 0.02	0.34 $\pm$ 0.01	0.35 $\pm$ 0.01	0.33 $\pm$ 0.01	0.33 $\pm$ 0.01
ESV (ml)	0.14 $\pm$ 0.004	0.14 $\pm$ 0.008	0.14 $\pm$ 0.006	0.13 $\pm$ 0.004	0.13 $\pm$ 0.006
EF (%)	59.5 $\pm$ 0.9	58.5 $\pm$ 1.2	60.6 $\pm$ 0.8	61.4 $\pm$ 0.4	60.0 $\pm$ 1.3

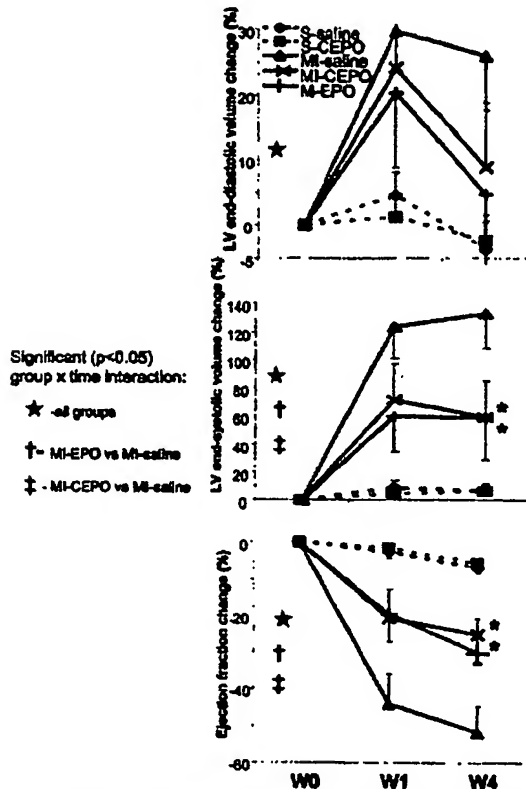


Fig. 3. Changes in echocardiographic indices of LV volume and function (ejection fraction) during 4 weeks after coronary artery ligation (MI) or sham (S) operation in CEPO-, EPO-, and saline-treated (SALINE) rats. All indices are derived from images obtained from the long-axis view in two-dimensional mode echo, adjusted for body mass, and expressed as the percentage of change from the baseline values (see Table 1). Statistically significant ( $p < 0.05$ ) group  $\times$  time interactions (ANOVA for repeated measurements) are indicated by the following: \*, among all groups; †, MI-SALINE versus MI-CEPO; and ‡, MI-SALINE versus MI-EPO. \*, significantly different ( $p < 0.05$ ) in post hoc comparison between MI-SALINE and MI-CEPO (or MI-EPO) groups at week 4.

groups in comparison with MI-SALINE. In any of presented indices, the MI-CEPO and MI-EPO groups did not differ from each other either in the pattern of changes over time or at any specific time point.

**Infarct Size.** The average infarct size, expressed as a percentage of LV, in MI-SALINE, MI-CEPO, and MI-EPO group is presented in Fig. 4. Regardless of the technique used to estimate the MI size, perimeter, or area calculation, the average MI size in either MI-CEPO or MI-EPO groups was half of that in MI-SALINE group ( $p < 0.05$ ).

**Posterior Wall Thickness.** The thickness of LV posterior wall measured histologically at the same sections the MI size was measured was similar in MI-EPO and MI-CEPO groups

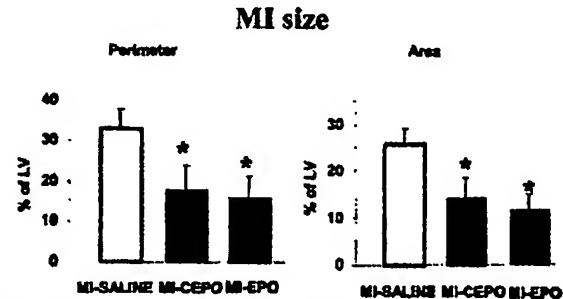


Fig. 4. MI size 4 weeks after ligation of a coronary artery in untreated rats and rats treated with CEPO or EPO. \*,  $p < 0.05$  post hoc comparison.

( $0.89 \pm 0.03$  mm) and not different from that in MI-SALINE group ( $0.84 \pm 0.02$  mm,  $p > 0.05$ ).

**Determination of Extent of Apoptosis within the Area at Risk.** Figure 5, A and B, illustrates the TUNEL staining at 24 h after coronary artery ligation in representative histological slides of comparable AARs in hearts from MI-SALINE and MI-CEPO groups, respectively. More apoptotic nuclei are clearly observed in the untreated heart (Fig. 5A). Figure 5C shows the average number of apoptotic nuclei in comparison with a total number of counted nuclei in the AAR of untreated hearts and hearts treated with EPO or CEPO. Only  $17 \pm 1.2\%$  of nuclei were TUNEL-positive in the MI-CEPO group and  $15.3 \pm 1.2\%$  in the MI-EPO group, compared with  $33.6 \pm 0.8\%$  in MI-SALINE group ( $p < 0.01$ ) (Fig. 5D).

## Discussion

CEPO is a recently introduced, engineered cytokine that was designed to retain the tissue-protective (antiapoptotic) characteristics of EPO but not trigger erythropoiesis (Leist et al., 2004). CEPO's pharmacokinetic parameters are very similar to those of EPO, but even injected daily for 4 weeks in doses as high as  $200 \mu\text{g/kg}$  b.wt. it fails to increase hematocrit in mice (Leist et al., 2004). However, CEPO's pharmacodynamics is remarkably different from that of EPO, because CEPO does not signal the classic EPO receptor (Leist et al., 2004). Nevertheless, extensive testing demonstrated strong neuroprotective properties of CEPO that are comparable with that of EPO. Antiapoptotic effects of CEPO have been shown in vitro on isolated neural cells and in vivo in cerebral infarct and spinal injury models in rats (Leist et al., 2004). Similar tissue protective properties of EPO and CEPO and the lack of hemopoietic properties of CEPO led to the recent suggestion that the tissue protection by EPO is mediated through a heteroreceptor complex comprising both the EPO receptor and a common  $\beta$  receptor subunit, also known as CD131 (Brines et al., 2004).

We (Moon et al., 2003) and others (see review in Bogoyevitch, 2004) have reported the cardioprotective properties of EPO in different experimental models of myocardial

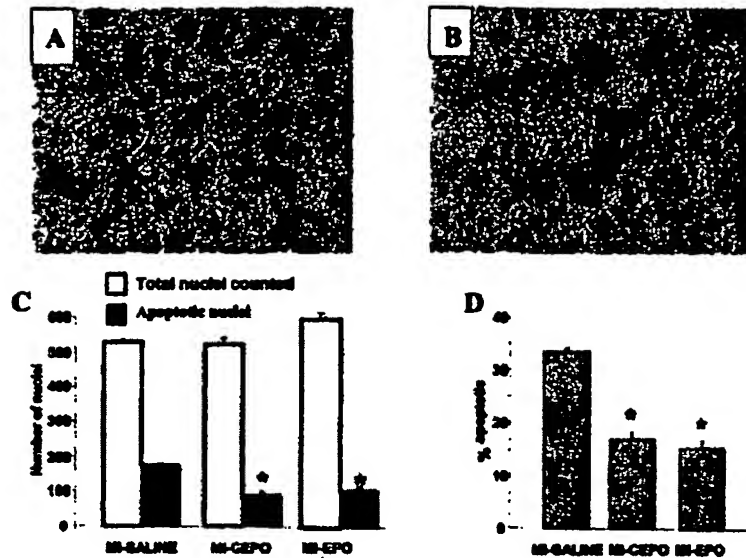


Fig. 5. Representative examples of TUNEL staining in the AAR of myocardium 24 h after coronary artery ligation in untreated rats (A) and in rats treated with CEPO (B) (magnification  $\times 400$ ). C, the average number of counted and TUNEL-positive nuclei in the area at risk in untreated MI rats and rats treated with CEPO or EPO. D, the percentage of TUNEL-positive nuclei in the AAR of the hearts from coronary-ligated rats. \*,  $p < 0.05$  versus MI-SALINE.

ischemia. Our experiments have shown that a single 3000 IU/kg systemic injection of EPO after permanent ligation of a coronary artery in rat resulted 24 h later in a 50% reduction of apoptosis in the myocardial area at risk. LV remodeling at 8 weeks was significantly attenuated in treated animals, and the MI size was only 15 to 25% of that in untreated animals (Moon et al., 2003). Recently, using a temporary ligation model of myocardial ischemia, cardioprotection using CEPO was also demonstrated (Fiordaliso et al., 2005). In the present study, we showed in a permanent ligation model that, as in an experiment with EPO (Moon et al., 2003), a single dose of CEPO (30  $\mu\text{g/kg}$  b.wt. i.v.) immediately after permanent coronary artery ligation in rat reduced the apoptosis in the AAR 24 h later by 50%. During 4 weeks of post-MI observation, the LV remodeling and functional decline were similarly and significantly attenuated in both CEPO- and EPO-treated animals. The MI scar at the end of 4 weeks was significantly smaller in EPO- or CEPO-treated rats than in untreated animals. The LV posterior wall thickness was not different from that of untreated animals. However, with such a significant LV dilation and obvious posterior wall thinning in untreated animals, and with such a remarkable reduction in LV and MI size in treated animals, one would expect the posterior wall would be significantly thicker in treated animals. The lack of such thickness either suggests the possibility that both EPO and CEPO therapy suppress the myocardial hypertrophy or that 4-week observation is not sufficient to reveal the difference in posterior wall thickness.

The results of *in vitro* experiments on the culture of isolated cardiomyocytes also were similar for CEPO and EPO: CEPO added to culture protected the myocytes from apoptosis induced by staurosporine, and the effect was comparable with the effect of EPO. This experiment confirms a direct effect of CEPO on cardiomyocytes rather than an indirect effect, which could not be ruled out in the *in vivo* experiments. The remarkable similarities of outcomes of experiments in which permanent coronary ligation in rats followed by a single injection of EPO or CEPO suggest that both

compounds probably engage the same mechanism of cardioprotection, which is, at least in part, antiapoptotic. This conclusion is supported by experiments with TUNEL staining in cardiomyocyte cultures or in myocardial tissue 24 h after coronary ligation as well as by experiments measuring the MRT-ROS threshold of single cardiomyocytes—a final common pathway for antiapoptotic signaling. The particular signaling pathway involved in EPO-CEPO-induced cardioprotection remains less certain. In different studies of EPO effects, many possible antiapoptotic signaling pathways have been reported: Jak-2/STAT, PI3K, protein kinase C, p38, p42/44 mitogen-activated protein kinase activation,  $K_{ATP}$ , and Akt (Brines et al., 2000; Calvillo et al., 2003; Parsa et al., 2003; Ghezzi and Brines, 2004; Shi et al., 2004). Introduction of CEPO allowed us to narrow the possibilities. Because CEPO does not bind to classic EPO receptors (Leist et al., 2004) its effects would not necessarily involve transcription factors STAT-5 or Jak2, a downstream kinase directly activated upon ligand binding to EPO receptors. On the other hand, the finding that the PI3-kinase inhibitor wortmannin completely blocked the beneficial effect of CEPO on MPT-ROS threshold suggests that the PI3-kinase signaling pathway is definitely involved in CEPO-mediated protection against ischemia, similar to that observed with rhEPO (Juhászova et al., 2004). The very effect of CEPO on MPT-ROS threshold gives additional weight to the idea that both EPO and CEPO exert their tissue-protective properties not through affinity to classic homodimeric EPO receptors but rather to heteromeric receptor complexes containing at least one EPO receptor subunit (Brines et al., 2004; Leist et al., 2004).

In summary, the demonstration of strong antiapoptotic effects of CEPO on ischemic myocardium, comparable with that of EPO, in conjunction with CEPO's lack of hematopoietic activity suggests the possibility of its use in treatment of myocardial infarction or myocardial ischemia in situations when repeated dosing is clinically desirable or the use of EPO is prohibitive due to its procoagulant and prothrombotic effects (Stohlawetz et al., 2000). Moreover, since death of car-

diac myocytes due to apoptosis is now considered a major causative factor in evolution of chronic heart failure to end-stage dilated cardiomyopathy (Wencker et al., 2003), CEPO might be suitable for a long-term treatment of the late LV remodeling.

## References

- Bernaudo M, Marti HH, Roussel S, Divoux D, Nouvelot A, MacKenzie ET, and Petit E (1999) A potential role for erythropoietin in focal permanent cerebral ischemia in mice. *J Cereb Blood Flow Metab* 19:643-651.
- Bialik S, Geenan DL, Sasson IE, Cheng R, Horner JW, Evans SM, Lord EM, Koch CJ, and Kitais RN (1997) Myocyte apoptosis during acute myocardial infarction in the mouse localizes to hypoxic regions but occurs independently of p53. *J Clin Invest* 100:1363-1372.
- Brines ML, Ghezzi P, Keenan S, Agnello D, de Lanerolle NC, Cerami C, Itri LM, and Cerami A (2000) Erythropoietin crosses the blood-brain barrier to protect against experimental brain injury. *Proc Natl Acad Sci USA* 97:10526-10531.
- Brines M, Grasso G, Fiordaliso F, Sfracteria A, Ghezzi P, Fratelli M, Latini R, Xie QW, Smart J, Su-Rick CJ, et al. (2004) Erythropoietin mediates tissue protection through an erythropoietin and common beta-subunit heteroreceptor. *Proc Natl Acad Sci USA* 101:14907-14912.
- Bogoyevitch MA (2004) An update on the cardiac effects of erythropoietin cardioprotection by erythropoietin and the lessons learnt from studies in neuroprotection. *Cardiovasc Res* 63:208-216.
- Calvillo L, Latini R, Kajstura J, Leri A, Anversa P, Ghezzi P, Salio M, Cerami A, and Brines M (2003) Recombinant human erythropoietin protects the myocardium from ischemia-reperfusion injury and promotes beneficial remodeling. *Proc Natl Acad Sci USA* 100:4802-4816.
- Capogrossi MC, Kort AA, Spurrison HA, and Lakatta EG (1986) Single adult rabbit and rat cardiac myocytes retain the Ca<sup>2+</sup>- and species-dependent systolic and diastolic contractile properties of intact muscle. *J Gen Physiol* 88:589-613.
- Ehrenreich H, Hasselblatt M, Dombrowski C, Cepek L, Lewczuk P, Stiefel M, Rustenbeck HH, Breiter N, Jacob S, Knerlich F, et al. (2002) Erythropoietin therapy for acute stroke is both safe and beneficial. *Mol Med* 8:495-505.
- Fiordaliso F, Chimenti S, Staszewsky L, Bai A, Carlo E, Cucovillo I, Doni M, Mengozzi M, Tonelli R, Ghezzi P, et al. (2005) A nonerythropoietic derivative of erythropoietin protects the myocardium from ischemia-reperfusion injury. *Proc Natl Acad Sci USA* 102:2046-2051.
- Ghezzi P and Brines M (2004) Erythropoietin as an antiapoptotic, tissue-protective cytokine. *Cell Death Differ* 11 (Suppl 1):S37-S44.
- Jelkmann W (1994) Biology of erythropoietin. *Clin Invest* 72:53-510.
- Juhászova M, Zorov DB, Kim SH, Pepe S, Fu Q, Fishbein KW, Ziman BD, Wang S, Vitellius K, Antos CL, et al. (2004) Glycogen synthase kinase-3 $\beta$  mediates convergence of protection signaling to inhibit the mitochondrial permeability transition pore. *J Clin Invest* 113:1535-1549.
- Leist M, Ghezzi P, Grasso G, Bianchi R, Villa P, Fratelli M, Savino C, Bianchi M, Nielsen J, Gerwien J, et al. (2004) Derivatives of erythropoietin that are tissue protective but not erythropoietic. *Science (Wash DC)* 306:239-242.
- Maiese K, Li F, and Chong ZZ (2005) New avenues of exploration for erythropoietin. *J Am Med Assoc* 293:90-96.
- Masuda S, Nagao M, and Sasaki R (1999) Erythropoietic, neurotrophic and angiogenic functions of erythropoietin and regulation of erythropoietin production. *Int J Hematol* 70:1-6.
- Moon C, Krawczyk M, Ahn D, Ahmet I, Paik D, Lakatta EG, and Talan MI (2003) Erythropoietin reduces myocardial infarction and left ventricular functional decline after coronary artery ligation in rats. *Proc Natl Acad Sci USA* 100:11612-11617.
- Parse CJ, Matsumoto A, Kim J, Riel RU, Pascal LS, Walton GB, Thompson RB, Petroficki JA, Annex BH, Stamler JS, and Koch WJ (2003) A novel protective effect of erythropoietin in the infarcted heart. *J Clin Invest* 112:999-1007.
- Sadamoto Y, Igase K, Sakanaka M, Sato K, Otsuka H, Sakaki S, Masuda S, and Sasaki R (1998) Erythropoietin prevents platelet aggregation and cortical infarction in rats with permanent occlusion of the middle cerebral artery. *Biochem Biophys Res Commun* 253:26-32.
- Shi Y, Rafiee P, Su J, Pritchard KA Jr, Tweddell JS, and Baker JE (2004) Acute cardioprotective effects of erythropoietin in infant rabbits are mediated by activation of protein kinases and potassium channels. *Basic Res Cardiol* 99:173-182.
- Smith KJ, Bleyer AJ, Little WC, and Sane DC (2003) The cardiovascular effects of erythropoietin. *Cardiovasc Res* 59:533-548.
- Spice BD (1999) Is a high hematocrit value an independent risk factor for adverse outcome after coronary artery bypass grafting? *J Thorac Cardiovasc Surg* 118:765-766.
- Stohlawetz PJ, Dzirio L, Hargovich N, Lackner E, Mensik C, Eichler HQ, Kabra E, Geissler K, and Jilma B (2000) Effects of erythropoietin on platelet reactivity and thrombopoiesis in humans. *Blood* 95:2983-2989.
- Wencker D, Chandra M, Nguyen K, Miao W, Garantziotis S, Factor SM, Shirani J, Armstrong RC, and Kitais RN (2003) A mechanistic role for cardiac myocyte apoptosis in heart failure. *J Clin Invest* 111:1497-1504.
- Wright GL, Hanken P, Amin K, Stoenbergen C, Murphy E, and Arcasey MO (2004) Erythropoietin receptor expression in adult rat cardiomyocytes is associated with an acute cardioprotective effect for recombinant erythropoietin during ischemia-reperfusion injury. *FASEB J* 18:1031-1033.
- Youssefian H, Lemmas G, Neumann D, Yoshimura A, and Lodish HF (1993) Structure, function and activation of the erythropoietin receptor. *Blood* 81:2223-2236.
- Zorov DB, Filburn CR, Klots LO, Zweier JL, and Sollott SJ (2000) Reactive oxygen species (ROS)-induced ROS release: a new phenomenon accompanying induction of the mitochondrial permeability transition in cardiac myocytes. *J Exp Med* 192:1001-1014.

Address correspondence to: Dr. Mark Talan, Senior Investigator, Head, Cardiovascular Gene Therapy Unit, Laboratory of Cardiovascular Sciences, Intramural Research Program, National Institute on Aging, 5600 Nathan Shock Drive, Baltimore, MD 21224-6825. E-mail: talanm@grc.nia.nih.gov

## Delayed administration of erythropoietin and its non-erythropoietic derivatives ameliorates chronic murine autoimmune encephalomyelitis

Costanza Savino<sup>a</sup>, Rosetta Pedotti<sup>b</sup>, Fulvio Baggi<sup>b</sup>, Federica Ubiali<sup>b</sup>, Barbara Gallo<sup>b</sup>, Sara Nava<sup>b</sup>, Paolo Bigini<sup>a</sup>, Sara Barbera<sup>a</sup>, Elena Fumagalli<sup>a</sup>, Tiziana Mennini<sup>a</sup>, Annamaria Vezzani<sup>a</sup>, Massimo Rizzi<sup>a</sup>, Thomas Coleman<sup>c</sup>, Anthony Cerami<sup>c</sup>, Michael Brines<sup>c</sup>, Pietro Ghezzi<sup>a,c,\*</sup>, Roberto Bianchi<sup>a</sup>

<sup>a</sup> "Mario Negri" Institute for Pharmacological Research, 20157, Milan, Italy

<sup>b</sup> National Neurological Institute "Carlo Besta", 20133 Milan, Italy

<sup>c</sup> The Kenneth S. Warren Institute, Kitchawan, NY 10562-1118, USA

Received 4 August 2005; accepted 26 October 2005

### Abstract

Erythropoietin (EPO) mediates a wide range of neuroprotective activities, including amelioration of disease and neuroinflammation in rat models of EAE. However, optimum dosing parameters are currently unknown. In the present study, we used a chronic EAE model induced in mice by immunization with the myelin oligodendrocyte glycoprotein peptide (MOG<sub>35–55</sub>) to compare the effect of EPO given with different treatment schedules. EPO was administered intraperitoneally at 0.5, 5.0 or 50 µg/kg three times weekly starting from day 3 after immunization (preventive schedule), at the onset of clinical disease (therapeutic schedule) or 15 days after the onset of symptoms (late therapeutic schedule). The results show that EPO is effective even when given after the appearance of clinical signs of EAE, but with a reduced efficacy compared to the preventative schedule. To determine whether this effect requires the homodimeric EPO receptor (EPOR<sub>2</sub>)-mediated hematopoietic effect of EPO, we studied the effect of carbamylated EPO (CEPO) that does not bind EPOR<sub>2</sub>. CEPO, ameliorated EAE without changing the hemoglobin concentration. Another non-erythropoietic derivative, asialoEPO was also effective. Both EPO and CEPO equivalently decreased the EAE-associated production of TNF-α, IL-1β and IL-1Ra in the spinal cord, and IFN-γ by peripheral lymphocytes, indicating that their action involves targeting neuroinflammation. The lowest dosage tested appeared fully effective. The possibility to dissociate the anti-neuroinflammatory action of EPO from its hematopoietic action, which may cause undesired side effects in non-anemic patients, present new avenues to the therapy of multiple sclerosis.

© 2005 Elsevier B.V. All rights reserved.

**Keywords:** EAE; Erythropoietin; Carbamylated erythropoietin; Asialoerythropoietin; Inflammation; Multiple sclerosis; Cytokine; Spinal cord

**Abbreviations.** MOG<sub>35–55</sub>, myelin oligodendrocyte glycoprotein peptide 35–55; EAE, experimental autoimmune encephalomyelitis; ConA, concanavalin A; EPO, erythropoietin; asialoEPO, desialylated EPO; CEPO, carbamylated EPO; EPOR, EPO receptor; IFN-γ, interferon-gamma; IL-, interleukin; IL-1Ra, IL-1 receptor antagonist; TNF, tumor necrosis factor; GFAP, glial fibrillary acidic protein; GM-CSF, granulocyte-macrophage colony-stimulating factor; VEGF, vascular endothelial growth factor; HIF-1, hypoxia inducible factor-1; BBB, blood-brain barrier; MS, multiple sclerosis.

\* Corresponding author. "Mario Negri" Institute for Pharmacological Research, 20157, Milan, Italy. Tel.: +39 02 39014486; fax: +39 02 3546277.

E-mail address: pietro.ghezzi@libero.it (P. Ghezzi).

### 1. Introduction

In addition to its hemopoietic effects, erythropoietin (EPO) possesses neuroprotective and neurotrophic properties (Brines and Cerami, 2005; Ghezzi and Brines, 2004; Jelkmann and Wagner, 2004; Juul, 2004). Our observations (Brines et al., 2000) and those of others (Juul et al., 2004) have shown that EPO crosses the intact blood brain barrier to provide protection from injury. The systemic administration of EPO mediates a wide range of neuroprotective actions in animal models of brain traumatic injury (Brines et

al., 2000), cerebral ischemia (Chang et al., 2005; Villa et al., 2003; Wang et al., 2004), of spinal cord injury and ischemia (Celik et al., 2002; Gorio et al., 2002), and diabetic neuropathy (Bianchi et al., 2004). Using a rat model of cerebral ischemia, we observed that the neuroprotective action is paralleled by a marked anti-neuroinflammatory effect, with inhibition of cytokine production and glial activation/proliferation (Villa et al., 2003).

Multiple sclerosis (MS) is a chronic autoimmune disease of the central nervous system (CNS) associated with demyelination, inflammation and loss of axons. Several cytokines have shown some efficacy in reducing the severity of experimental autoimmune encephalomyelitis (EAE), an animal model for MS, including anti-inflammatory cytokines and inhibitors of IL-1, TNF, or IFN- $\gamma$  (reviewed in Martino et al., 2002; Steinman, 2003; Steinman, 2004), but none have so far proven clinically effective.

The observation that EPO is effective in models of diseases possessing common neuroinflammatory components prompted us to study its effectiveness in an acute EAE model in Lewis rats, induced by immunization against myelin basic protein and we observed a reduction of inflammation and amelioration of clinical signs with EPO (Agnello et al., 2002; Brines et al., 2000). Others have confirmed these findings in different EAE models including optic neuritis (Dien et al., 2005; Li et al., 2004; Sattler et al., 2004). Since optimum dosing, particularly whether EPO is effective only when given before the development of clinical symptoms (i.e., a preventive schedule) is unknown, we evaluated the potential utility of administration after the development of clinical disease.

The present study examines the effects of EPO in a chronic model of EAE using C57BL/6 mice immunized with MOG<sub>35–55</sub> (Amor et al., 1996; Furlan et al., 2001). This model, unlike the Lewis rat model where the disease is acute and lasts only a few days, allows a comparison of the effectiveness of EPO when it is given 3 days after immunization, before disease onset, as we have done in the acute model (Agnello et al., 2002; Brines et al., 2000), or beginning late after its onset, to mimic clinically relevant settings.

In this model, we also studied the effect of EPO on spinal cord inflammation by use of immunohistochemical markers such as CD11b, GFAP, and TNF- $\alpha$ . We also measured expression of TNF- $\alpha$ , IL-1, and IL-1Ra in the spinal cord, and studied the antigen-specific or concanavalin A-induced T cell proliferation, and production of IFN- $\gamma$  by peripheral lymphocytes using ELISPOT and ELISA assays.

A major issue in the use of EPO as neuroprotective, anti-neuroinflammatory drug, is represented by its erythrodifferentiating action that represent a potential cause of several side effects, including vascular perfusion defects (Natali et al., 2005). In mice the increase in hematocrit induced by EPO causes vasoconstriction and cardiac dysfunction due to NO depletion and endothelin activation (Quaschnig et al., 2003; Ruschitzka et al., 2000). In animals and humans, EPO

can lead to hypertension (Group, 1991; Lim, 1991; Varet et al., 1990) or thrombosis (reviewed in Bokemeyer et al., 2004).

We have successfully identified derivatives of EPO, including asialoEPO (Erbayraktar et al., 2003) and carbamylated EPO (CEPO) (Leist et al., 2004), which do not increase the hematocrit but retain neuroprotective actions in animal models of cerebral ischemia, spinal cord injury, and diabetic neuropathy. We studied their effect in EAE not only because these could represent drugs that lack the undesired effects of EPO but also to investigate whether protection by EPO is associated with an increase in red blood cells.

Furthermore, since others have hypothesized that the neuroprotective effects of EPO are mediated through a mechanism implicating dimerization of the classical EPO receptor (EPOR) (Maiese et al., 2005), we have studied the effects on the clinical expression and CNS pathology of EAE of CEPO, a tissue-protective cytokine which we have previously shown does not bind the classical, dimeric EPOR (Leist et al., 2004).

Since both EPO and its non-erythropoietic derivatives are effective in ameliorating EAE when administered using either a preventive or a therapeutic treatment schedule, this effect cannot be associated with an increase in hematocrit. Decreased production of inflammatory cytokines in the spinal cord and lymphocytes suggest that inflammation is a primary target of tissue-protective cytokines.

## 2. Materials and methods

### 2.1. EAE induction

EAE was induced in C57BL/6 female mice (6–8 weeks of age). Mice were obtained from Charles River (Calco, Italy) and housed in specific pathogen-free conditions, allowing access to food and water ad libitum. Procedures involving animals and their care were conducted in conformity with the institutional guidelines in compliance with national (D.L. n. 116, G.U., suppl. 40, Feb. 18, 1992) and international laws and policies (EU Council Directive 86/609, OJ L 358, 1, Dec. 12, 1987; Guide for the Care and Use of Laboratory Animals, U.S. National Research Council, 1996). The protocols for the proposed investigation were reviewed and approved by the Animal Care and Use Committees (IACUC) of the Istituto di Ricerche Farmacologiche “Mario Negri”. EAE was induced by subcutaneous immunization in the flanks with a total of 200  $\mu$ g of MOG<sub>35–55</sub> (Multiple Peptide Systems, San Diego, CA, USA) in incomplete Freund's adjuvant (Sigma, St. Louis, MO, USA) supplemented with 8 mg/ml of *Mycobacterium tuberculosis* (strain H37RA; Difco, Detroit, MI, USA). Mice received 500 ng of pertussin toxin (Sigma) i.v. at the time of immunization and 48 h later. Weight and clinical score were recorded daily (0=healthy, 1=flaccid tail, 2=ataxia, and/or hind-limbs paresis, or slow righting reflex,



3=paralysis of hind limb and/or paresis of forelimbs, 4=paraparesis of fore limb, 5=moribund or death). The food pellets and the drinking water were placed on Petri plates on the floor of the cage to enable sick mice to eat and drink.

## 2.2. Experimental design and treatments

EPO (recombinant human EPO) was obtained from Dragon Pharmaceuticals, Vancouver, BC, Canada. AsiaEPO and CEPO were prepared as described (Erbayraktar et al., 2003; Leist et al., 2004) and kindly supplied by Warren Pharmaceuticals and H. Lundbeck A/S, Copenhagen. For the preventive schedule, mice were treated intraperitoneally (i.p.) with EPO or its derivatives at the indicated dose, three times a week starting on day 3 after immunization. In the therapeutic treatment schedule, treatment was started at the exordium of EAE (normally between days 10 and 12 after immunization). In some experiments, we also administered the drug using a late therapeutic schedule beginning 15 days after the onset of disease. The experimental schedule is schematized in Fig. 1.

## 2.3. Hematocrit

Blood was collected in heparinized capillary tubes and centrifuged at  $2500 \times g$  for 20 min at  $4^\circ\text{C}$  and hematocrit was determined.

## 2.4. Immunohistochemistry

Mice were anesthetized with Equithesin (1% phenobarbital/4% (vol./vol.) chloral hydrate,  $30 \mu\text{l}/10 \text{ g}$ , i.p.) and transcardially perfused with 100 ml saline followed by 250 ml of sodium phosphate buffered 4% paraformaldehyde solution. Spinal cords were rapidly removed, fixed in sodium phosphate-buffered 4% paraformaldehyde solution for 2 h, transferred to 20% sucrose solution in PBS overnight, then in 30% sucrose solution until they sank and finally frozen in 2-methylbutane at  $-45^\circ\text{C}$ . Sections ( $30 \mu\text{m}$ ) were cut on a cryostat at  $-20^\circ\text{C}$  in the transverse plane through the lumbar spinal cord and every

fifth section selected for histochemistry against different antigens or hematoxylin–eosin staining. Free floating sections were processed for immunoreactivity both with anti-GFAP mouse monoclonal antibody (1:250; Immunological Sciences) and with anti-CD11b (MRC OX-42) mouse monoclonal antibody (1:50; Serotec, UK), or anti-TNF (1:50; HyCult Biotechnology b.v, Uden, The Netherlands) according to the protocols described, respectively, by Houser et al. (1984) and the manufacturer's protocol. All sections were mounted for light microscopy in saline on coated slides, dehydrated through graded alcohol, fixed in xylene and cover-slipped using DPX mountant (BDH, Poole, UK). Adjacent sections were stained with hematoxylin and eosin as described (Gill et al., 1974). Slides were analyzed under light microscopy in a blinded fashion.

## 2.5. Cytokine expression in the spinal cord

Total RNA was isolated from tissue samples according to the acid guanidium–phenol–chloroform method (Chomczynski and Sacchi, 1987). The samples were digested by a denaturing solution containing 4 M guanidium thiocyanate, 25 mM sodium citrate, 0.5% sarcosyl, 0.1 M 2-mercaptoethanol, pH 7.0. The lysate was extracted with a mixture of 0.1 M sodium acetate, pH 4.0/phenol/chloroform (1:10:2) and isoamyl alcohol (49:1), and nucleic acids were precipitated with equal volumes of isopropyl alcohol. Total RNA was quantified by spectrophotometer and an aliquot was loaded onto 1% agarose gel to visually assess for RNA integrity. Before performing RNA reverse transcription to cDNA, an aliquot of each sample (1–2  $\mu\text{g}$ ) was treated with 1–2 U/ $\mu\text{l}$  of DNase I (Invitrogen, S. Giuliano Milanese, Italy) to eliminate genomic DNA contaminants. DNase-treated total RNA (1–2  $\mu\text{g}$ ) from each sample was used as a substrate for single-stranded cDNA synthesis using murine leukemia virus reverse transcriptase (MMLV-RT, 50 U/ $\mu\text{l}$ ; Perkin-Elmer, Emeryville, CA, USA), random hexamers (2.5  $\mu\text{M}$ ), and deoxyNTP mix (1.25 mM each) in a final volume of 20  $\mu\text{l}$ . The mixture was incubated at room temperature for 10 min, then incubation was performed in a thermocycler (Omn-E; Hybaid, Ashford, UK) at  $42^\circ\text{C}$  for

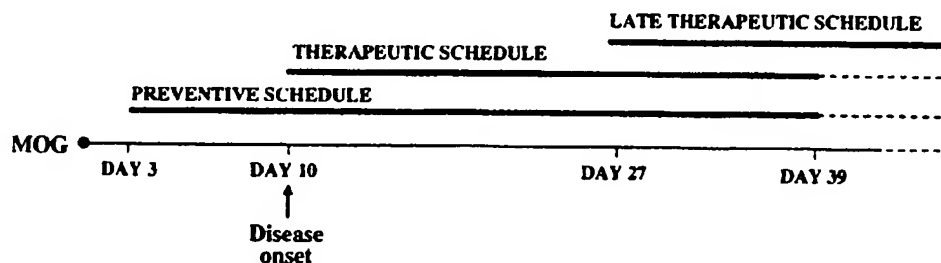


Fig. 1. Treatment schedules. EAE was induced by immunization with MOG on day 0. EPO or CEPO were administered intraperitoneally three times a week at the doses indicated within the text. Length of treatment is indicated by the thick, solid line. On day 39, treatment was discontinued in order to evaluate the persistence of the pharmacological activity.



15 min, at 99 °C for 5 min, and at 5 °C for 5 min. Real-time quantitative PCR was carried out using the 5700 SDS (Applied Biosystems, Monza, Italy), exploiting SYBR GREEN as fluorescent dye. The primers used were the following: IL-1 $\beta$ , forward primer, TAACCTGCTGGTGTG-TGACGTT; IL-1 $\beta$ , reverse primer, CCGAGCCTGTAGT-GCAGTTGT; IL-1Ra, forward primer, TGGGAAAAGA-CCCTGCAAGA; IL-1Ra, reverse primer, AAGGTCAATA-GGCACCATGTCTATC; TNF- $\alpha$ , forward primer, ATGCT-GGGACAGTGACCTGG; TNF- $\alpha$ , reverse primer, CCTTGATGGTGGTGCATGAG;  $\beta$ -actin, forward primer, TGTCCACCTTCCAGCAGATGT;  $\beta$ -actin, reverse primer, CGGACTCGTCATACTCCTGCTT.

## 2.6. Cytokine production from spleen cells

Mononuclear cell suspensions were prepared from spleens removed from mice treated with EPO, CEPO and controls, and cultured at  $3.5 \times 10^6$  cells/ml in a 24-well plates with different concentration of MOG (1, 3, and 10  $\mu$ M) or with 4  $\mu$ g/ml of Concanavalin A (Sigma-Aldrich, Italy). Culture media consisted of RPMI-1640 containing 1% penicillin–streptomycin, 1% L-glutamine, 1% sodium pyruvate, 1% nonessential amino acids (all from Euroclone Celbio, Milan, Italy),  $2 \times 10^{-5}$  M 2-Mercaptoethanol (2-ME, BDH, Milan Italy) and 10% FCS (Sigma-Aldrich, Milan, Italy). Supernatants were collected at different time points for measurements of cytokine levels: 24 h for IL-2, 48 h for IFN- $\gamma$ , and 96 h for IL-4 and IL-10. Cytokine concentrations were determined in supernatants by using specific enzyme-linked immunosorbent assay (ELISA) with capture and detection antibodies for the specific cytokines according to the manufacturer's protocols (BD OptEIA ELISA Set, Pharmingen, San Diego, CA, USA). Standard curves for each cytokines were generated with recombinant mouse cytokines and cytokine levels in supernatants were determined by interpolation with the appropriate standard curve. Detection limits for the different cytokines were: 31.3 pg/ml for IFN- $\gamma$  and IL-10, 7.8 pg/ml for IL-4 and 3.1 pg/ml for IL-2. Means and standard error mean (S.E.M.) were determined using data from individual animals tested in duplicates.

## 2.7. Cytokine production in spleen cells by ELISPOT

IFN- $\gamma$  and IL-10 production in response to MOG<sub>35–55</sub> peptide or Concanavalin A (ConA, positive control) was assessed by ELISPOT assays. Mononuclear cell suspension were prepared from spleens aseptically removed from vehicle and EPO- or CEPO-treated mice. IFN- $\gamma$  and IL-10 ELISPOT kits (from R&D Systems, Space Import/Export, Milan, Italy) were used following manufacturer's instruction. Briefly, quadruplicate cultures of  $3 \times 10^5$  cells were seeded with antigens (10  $\mu$ M MOG<sub>35–55</sub> and 4  $\mu$ g/ml ConA) in RPMI-1640 medium containing 1% penicillin–streptomycin, 1% L-glutamine, 1% sodium pyruvate, 1%

nonessential amino acids (all from Euroclone Celbio, Milan, Italy),  $2 \times 10^{-5}$  M 2-mercaptoethanol (2-ME, BDH, Milan Italy) and 10% FCS (Sigma-Aldrich, Milan, Italy). Cells were incubated at 37 °C in 5% CO<sub>2</sub>, and harvested after 24 h for IFN- $\gamma$  detection and 48 h for IL-10 detection. After several washes, biotinylated secondary antibodies specific for mouse IFN- $\gamma$  or IL-10 were added to the wells; after overnight incubation, alkaline-phosphatase conjugated to streptavidin was added for 2 h, and revealed by substrate solution (BCIP/NBT). The number of specific spots, representing an individual cluster of cytokine-secreting cells, was determined using an automated ELISPOT reader (AID, Strassberg, Germany) with set parameters for size, intensity and gradient. Background mean values (cells cultured in medium alone) were subtracted from ConA on MOG induced mean spot numbers for each mouse.

## 2.8. Statistical analysis

EAE weight and scores and PCR results were compared using the Mann–Whitney nonparametric test or Student's *t* test for unpaired data or by covariance analysis according to the indications in table and figure legends.

## 3. Results

### 3.1. EPO treatment ameliorates EAE pathology

Mice were injected intraperitoneally with EPO (50  $\mu$ g/kg bw) either at day 3 post-immunization (preventive schedule) or at the onset of clinical disease (therapeutic schedule) as outlined in Fig. 1. As shown in Fig. 2, EPO effectively prevented and/or ameliorated the disease both in terms of disease severity (Fig. 2A) and of reduced body weight loss (Fig. 2B). In addition, EPO administered according to the preventive schedule significantly delayed the disease onset ( $14.7 \pm 1.5$  vs.  $11.7 \pm 0.4$  of vehicle-treated mice,  $P < 0.05$ ). In the experiments shown in Fig. 2, we discontinued EPO treatment on day 39 and monitored the mice for a further period of 20 days. The cumulative scores at day 39 were  $68.1 \pm 6.0$ ,  $27.7 \pm 6.2$  and  $53.4 \pm 2.3$  for vehicle treated, EPO preventive and EPO therapeutic groups, respectively and both schedule of treatment were statistically significantly different from vehicle-treated mice. On day 60, mice treated with EPO, both according to the preventive and the therapeutic schedule still showed a lower disease score when compared to vehicle-treated mice (vehicle =  $3.00 \pm 0.2$ , EPO preventive =  $1.17 \pm 0.3$ , and EPO therapeutic =  $1.56 \pm 0.06$ ). This indicates that protection persisted for at least 20 days after the discontinuation of EPO. The clinical parameters of EAE in these experiments are summarized in Table 1.

In untreated mice, on day 39 after immunization, the hematocrit was  $47.3 \pm 2.2\%$  (range = 42.2–49.2), while in

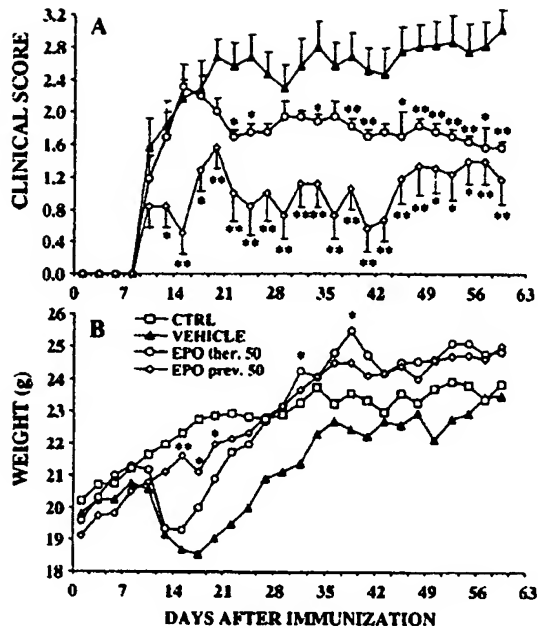


Fig. 2. Preventive or therapeutic EPO treatment ameliorates EAE. Mice were immunized with MOG and injected with vehicle or EPO (50  $\mu\text{g/kg}$  i.p.) starting at day 3 following EAE induction (preventive schedule) or at symptom onset (therapeutic schedule). In panel A, disease score is reported only from day of onset. Data are the mean  $\pm$  S.E.M., number of animals per group was: vehicle=9; EPO preventive=9; EPO therapeutic=8. \* $P<0.05$ , \*\* $P<0.01$  by Mann–Whitney test.

EPO-treated mice it was  $38.1 \pm 11.4\%$  (range=21.5–52.6) and  $60.0 \pm 6.4\%$  (range=49.0–69.2) for preventive and therapeutic schedule, respectively. It must be noted that mice treated according to the preventive schedule received EPO for a period of 39 days, while in those treated using the therapeutic schedule EPO was given for a total of 29 days, and the more prolonged treatment resulted in a decrease in

Table 1  
Clinical EAE parameters in mice treated with EPO starting at day 3 after immunization (preventive schedule) or EPO and CEPO starting at symptom onset (therapeutic schedule)

Treatment	Mean maximum score	AUC (days 11–60)	No. of mice with score $\geq 2$	No. of mice with score $\geq 3$
Vehicle	$3.2 \pm 0.3$	$123.1 \pm 10.9$	7/9	6/9
EPO 50.0 $\mu\text{g/kg}$ preventive	$1.8 \pm 0.2^a$	$50.9 \pm 10.4^b$	3/9	0/9
EPO 50.0 $\mu\text{g/kg}$ therapeutic	$2.5 \pm 0.2^c$	$88.0 \pm 2.8^d$	1/8	0/8
CEPO 5.0 $\mu\text{g/kg}$	$2.3 \pm 0.2^c$	$75.3 \pm 11.8^b$	3/9	0/9
CEPO 50.0 $\mu\text{g/kg}$	$2.4 \pm 0.2$	$76.0 \pm 10.7^d$	3/7	0/7

Data are mean  $\pm$  S.E.M. Values are calculated at day 60.

<sup>a</sup>  $P<0.01$  vs. EAE vehicle-treated mice, by Mann–Whitney test.

<sup>b</sup>  $P<0.01$  vs. vehicle by ANOVA.

<sup>c</sup>  $P<0.05$  vs. EAE vehicle-treated mice, by Mann–Whitney test.

<sup>d</sup>  $P<0.05$  vs. vehicle by ANOVA.

the hematocrit in some of the mice, due to the formation of neutralizing autoantibodies against human recombinant EPO. By day 60 the hematocrit in EPO-treated mice was  $40.0 \pm 10.3\%$  (range=23.8–50.4) and  $48.1 \pm 3.1\%$  (range=42.6–50.7) for preventive and therapeutic schedule, respectively. Again, it can be seen that the longer treatment in the preventive schedule resulted in a paradoxical decrease in the hematocrit. We did not, however, observe a significant correlation between the hematocrit and the EAE score (not shown).

Finally, we tested EPO using a late therapeutic treatment schedule, where EPO was administered from day 27 after immunization, i.e. about 15 days after disease onset. The results are shown in Fig. 3. Although the disease score did not significantly differ when comparing untreated and EPO-treated mice, using the Mann–Whitney test to compare the two curves, the overall status of the animals was improved in the EPO group, as it is evident from the body weight curves reported in Fig. 3B, where at the end of the experiment, on day 46, the body weight loss was significantly less in mice treated with 50.0  $\mu\text{g/kg}$  of EPO (untreated EAE mice weighted 52% of healthy controls; EPO-treated EAE mice weighted 78% of controls).

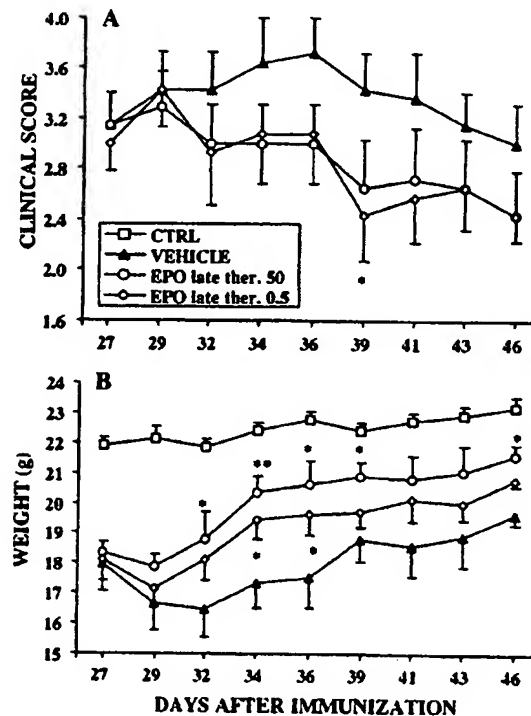


Fig. 3. Therapeutic efficacy of late EPO treatment on disease score (A) and body weight (B). Mice were immunized with MOG and injected with vehicle or EPO (50  $\mu\text{g/kg}$  i.p.) starting at day 27 following EAE induction (late therapeutic schedule). Data are the mean  $\pm$  S.E.M.,  $n=7$  ( $n=5$  in the case of healthy mice). \* $P<0.05$  vs. respective vehicle-treated group by Student's *t*-test.

In vehicle-treated EAE mice, at sacrifice, the hematocrit was  $53.4 \pm 3.5\%$  (range=46.3–57.1), while it was  $70.6 \pm 4.2\%$  (range=65.6–74.4) and  $53.5 \pm 4.0\%$  (range=49.4–60.5) in EPO-treated mice for 50.0 and 0.5  $\mu\text{g}/\text{kg}$  doses, respectively.

### 3.2. Non-erythropoietic EPO derivatives are effective in EAE

We first tested CEPO using the therapeutic schedule (administration starting at the onset of the disease) at two doses (50 and 5  $\mu\text{g}/\text{kg}$  bw). As shown in Fig. 4A, CEPO, at both doses, significantly improved the course of the disease. As previously observed for EPO, the effect of CEPO was also evident on the body weight of the animals (Fig. 4B). Also in the case of CEPO, the therapeutic effect was maintained for at least 20 days after treatment was interrupted at day 39. Table 1 summarizes the clinical features of the disease in the experiments reported in Fig. 4.

In EAE-untreated mice, at day 39 the hematocrit was  $47.3 \pm 2.2\%$  (range=42.2–49.2), while it was  $49.2 \pm 4.5\%$  (range=44.4–53.2), and  $44.9 \pm 2.6\%$  (range=42.2–47.5) in CEPO-treated mice for 50.0 and 5.0  $\mu\text{g}/\text{kg}$ , respectively. By day 60, after treatment discontinuation, the hematocrit was  $48.7 \pm 4.7\%$  (range=39.6–52.1) and  $47.1 \pm 1.8\%$  (range=43.9–49.6) in CEPO-treated mice for 50 and 5  $\mu\text{g}/\text{kg}$  bw, respectively.

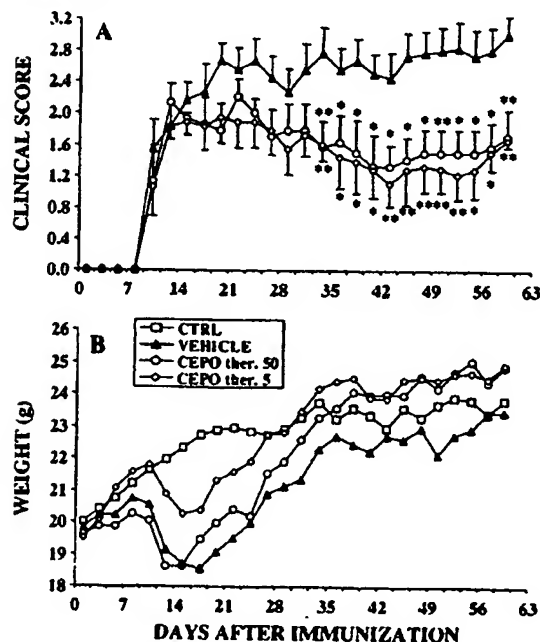


Fig. 4. Preventive or therapeutic CEPO treatment ameliorates EAE. Mice were immunized with MOG and injected with vehicle or CEPO (5.0 or 50.0  $\mu\text{g}/\text{kg}$  i.p.) starting at symptoms onset (therapeutic schedule). In panel A, disease score is reported only from day of onset. Data are the mean  $\pm$  S.E.M., number of animals per group was: vehicle=9; CEPO 50.0  $\mu\text{g}/\text{kg}$ =7; CEPO 5.0  $\mu\text{g}/\text{kg}$ =9. \* $P < 0.05$ , \*\* $P < 0.01$  by Mann-Whitney test.

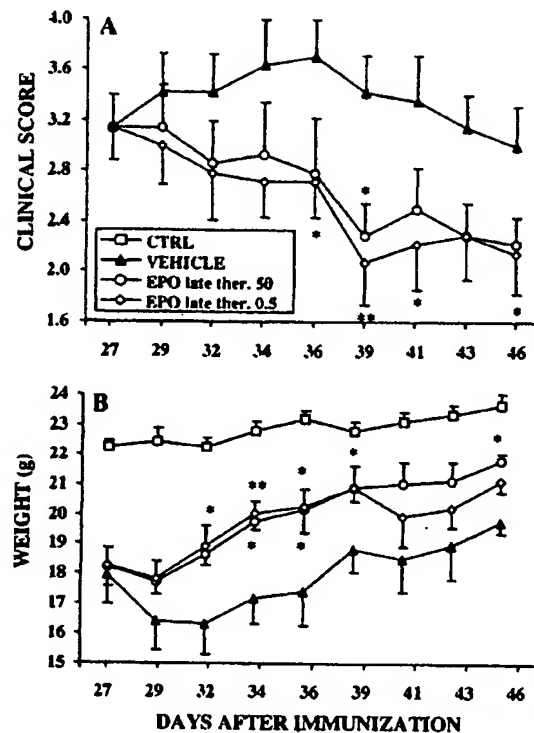


Fig. 5. Therapeutic efficacy of late CEPO treatment on disease score (A) and body weight (B). Mice were immunized with MOG<sub>33–35</sub> and injected with vehicle or CEPO (50.0 or 0.5  $\mu\text{g}/\text{kg}$  i.p.) starting at day 27 following EAE induction (late therapeutic schedule). Data are the mean  $\pm$  S.E.M.,  $n = 7$  ( $n = 5$  in the case of healthy mice). \* $P > 0.05$  vs. respective vehicle-treated group by Student's  $t$ -test.

When CEPO treatment was started late after disease onset (day 27), the clinical score was improved (Fig. 5A), an effect which was reflected by a significantly reduced body weight loss (Fig. 5B). The clinical parameters of EAE mice treated with CEPO (Fig. 5) or EPO (Fig. 2) according to this late treatment schedule are reported in Table 2. It can be seen that, as observed in the experiments from Table 1, the effect of CEPO was more prominent in terms of reducing the number of mice with the most severe ( $> 3$ ) clinical score.

Table 2

Clinical EAE parameters in mice treated with EPO or CEPO starting 15 days after onset (late therapeutic schedule)

Treatment	Score at sacrifice (day 46)	AUC (days 27–46)	Day of maximal score	No. of mice with score $\geq 2$	No. of mice with score $\geq 3$
Vehicle	$3.0 \pm 0.8$	$36.6 \pm 2.3$	36	7/7	5/7
EPO 0.5 $\mu\text{g}/\text{kg}$	$2.4 \pm 0.5$	$22.6 \pm 2.5$	29	5/7	3/7
EPO 50.0 $\mu\text{g}/\text{kg}$	$2.4 \pm 0.9$	$22.7 \pm 2.6$	29	7/7	3/7
CEPO 0.5 $\mu\text{g}/\text{kg}$	$2.1 \pm 0.8$	$19.9 \pm 2.4^{**}$	27	6/7	1/7
CEPO 50.0 $\mu\text{g}/\text{kg}$	$2.2 \pm 0.6$	$21.0 \pm 2.4^*$	27	5/7	2/7

Data are mean  $\pm$  S.E.M. of the data shown in Figs. 1A and 5A.

\*  $P < 0.05$  vs. vehicle by ANOVA.

\*\*  $P < 0.01$  vs. vehicle by ANOVA.

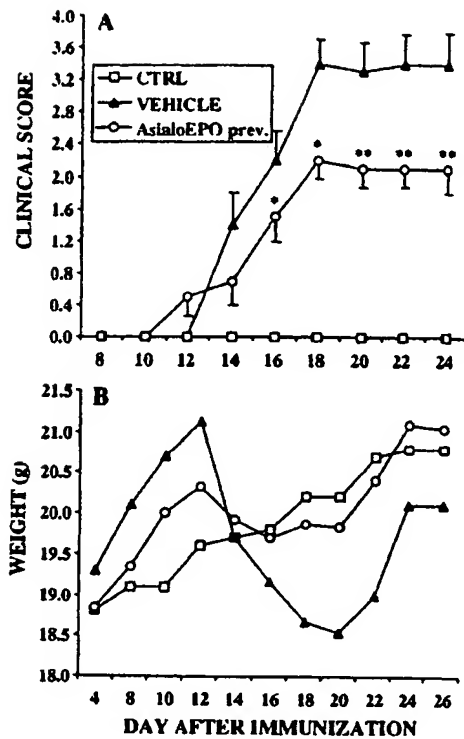


Fig. 6. Efficacy of asialoEPO on disease score (A) and body weight (B). Mice were immunized with MOG<sub>35–55</sub> and injected with vehicle or asialoEPO (50 µg/kg bw i.p.) starting at day 3 following EAE induction and continuing three times weekly (preventive schedule). In panel A, disease score is reported only from day of onset. Data are the mean ± S.E.M.,  $n = 10$ . \* $P < 0.05$ , \*\* $P < 0.01$  by Mann–Whitney test.

In this experiment, in untreated EAE mice, the hematocrit at sacrifice was  $53.4 \pm 3.5\%$  (range = 46.3–57.1), while it was  $56.0 \pm 2.5\%$  (range = 52.6–59.5) and  $53.1 \pm 2.4\%$  (range = 49.7–56.7) in CEPO-treated mice for 50.0 and 0.5 µg/kg, respectively.

We also tested the effect of asialoEPO using the preventive treatment schedule and the same dose used for most of the experiments described above (50 µg/kg bw,

i.p., starting from day 3 after immunization). As shown in Fig. 6, asialoEPO significantly protected from EAE, reducing the disease severity, delaying its onset and reducing body weight loss, in a way comparable to EPO. In these experiments, the hematocrit was determined at sacrifice, on day 24, and found not to be altered by asialoEPO (vehicle:  $43.2 \pm 3.8$ , range = 37.4–48.8; asialoEPO:  $41.8 \pm 4.9$ , range = 37.2–50.9).

### 3.3. EPO and CEPO administration reduces IFN-γ production by MOG-stimulated spleen cells

For these experiments, mice were treated with EPO or CEPO at the doses of 0.5 or 50.0 µg/kg i.p. starting from day 27 after immunization ("late therapeutic" schedule), and treatment was continued until day 60, when mice (4 animals per group) were sacrificed. Splenocytes were prepared and stimulated with different concentrations of MOG<sub>35–55</sub> or ConA and cytokines were measured in supernatants at the times indicated in Materials and methods. Although there was a trend towards a reduced IFN-γ production in splenocytes, this was not statistically significant.

We therefore evaluated IFN-γ and IL-10 production in the same cultures by ELISPOT. As shown in Table 3, using the late therapeutic schedule, all treatments of EPO and CEPO significantly reduced the number of IFN-γ-secreting cells, both in ConA- and MOG-stimulated cells. However the reduction was more evident in MOG-stimulated cells (mean change = −67.3%) than in ConA-stimulated cells (mean change = −19.3%). On the contrary, a statistically significant reduction in the number of IL-10-secreting cells was observed only in MOG<sub>35–55</sub>-stimulated cells. The same table shows that healthy, non-EAE mice, had a normal response to ConA but did not respond to the antigen.

### 3.4. EPO diminishes the inflammatory response

Immunohistochemical analysis of the lumbar spinal cord sections were done in untreated healthy mice and in EAE mice treated with vehicle or EPO using the preventive treatment schedule. Anti-GFAP- and anti-CD11b-stained

Table 3  
Cytokine production from spleen cells: ELISPOT measurement

Treatment	IFN-γ-secreting cells		IL-10-secreting cells	
	ConA	MOG	ConA	MOG
Vehicle	654.6 ± 12.1	162.1 ± 19.9	196.6 ± 16.2	117.1 ± 11.6
EPO 0.5 µg/kg	553.4 ± 36.2***	45.4 ± 11.7**	143.4 ± 24.8	53.1 ± 23.9**
EPO 50.0 µg/kg	533.8 ± 42.1*	61.4 ± 5.4**	145.1 ± 39.3	84.6 ± 24.4
CEPO 0.5 µg/kg	499.7 ± 27.3*	50.3 ± 4.8**	204.3 ± 21.9	36.8 ± 20.6*
CEPO 50.0 µg/kg	526.1 ± 41.1*	54.8 ± 14.8**	159.6 ± 28.1	49.8 ± 18.4***
Non-EAE controls	519.2 ± 10.1	3.8 ± 1.1	162.5 ± 24.2	24.5 ± 8.5

Data are mean ± S.E.M.

\*  $P < 0.02$  by Student's *t*-test vs. vehicle.

\*\*  $P < 0.0001$  by Student's *t*-test vs. vehicle.

\*\*\*  $P < 0.05$  by Student's *t*-test vs. vehicle.



Fig. 7. EPO decreases EAE-induced TNF- $\alpha$  immunostaining in the spinal cord. Mice were treated with or without EPO (50  $\mu\text{g}/\text{kg}$  i.p. three times weekly from day 3) and sacrificed on day 29. Representative sections obtained from the lumbar spinal cord from healthy mice (A, E), EAE mice treated with PBS (B, F), EAE mice treated with EPO (C, G) and EAE mice treated with CEPO (D, H). Upper panels (A–D), scale bar = 500  $\mu\text{m}$ ; lower panels (E–H), scale bar = 125  $\mu\text{m}$ .

sections of lumbar spinal cord showed a weak increase in glial immunoreactivity that was not affected by EPO (not shown). A well-defined immunoreactivity for TNF- $\alpha$  can be seen in EAE mice, almost exclusively in the anterior horn neurons (Fig. 7). Treatment with EPO and, to a lesser extent, with CEPO reduced both the number of TNF- $\alpha$ -positive neurones, and their immunoreactivity.

We also measured the mRNA expression for IL-1 $\beta$ , IL-1Ra and TNF- $\alpha$  in the spinal cord of mice receiving EPO or CEPO according to the preventive schedule and at two different doses (50.0 and 0.5  $\mu\text{g}/\text{kg}$ ). As shown in Table 4, expression of all three cytokines was greatly induced by EAE, compared to naive mice. Both EPO and CEPO diminished cytokine expression, and this effect was greater at the highest doses tested.

#### 4. Discussion

The present study shows that: 1) EPO is effective in a chronic model of EAE; 2) A protective effect, although diminished compared to the preventative schedule is observed also when the drug is given late after the induction of the disease and lasts for at least 3 weeks after interruption of treatment; 3) The EPO effect is independent of an increase in hematocrit, as non-erythropoietic variants asialoEPO and CEPO are also active; 4) this effect is also observed with CEPO that does not bind the classical EPOR; 5) Action of EPO and CEPO is associated with a decrease in

the production of inflammatory cytokines in the spinal cord and peripheral lymphocytes.

It is important to note that in most experiments, treatment with EPO or CEPO for periods longer than one month induced anaemia in ~50% of the animals (data not shown) because administration of human proteins to mice induces formation of neutralizing antibodies recognizing also endogenous EPO, a well-known phenomenon with EPO (Casadevall et al., 2002). Moreover, this effect was more pronounced with mice treated according to the preventive schedule, since they received EPO for 24 days longer than with the late therapeutic schedule, and 10 days longer than with the therapeutic schedule. In spite of this, the preventative schedule provided superior protection from EAE.

A main finding of this study is that non-erythropoietic variants of EPO that do not increase the hematocrit are active in this model of EAE. The two EPO derivatives used are representative of two different strategies to dissociate erythropoietic and neuroprotective action. AsialoEPO, like EPO, binds dimeric EPOR and induces erythroid differentiation *in vitro* (Erbayraktar et al., 2003); its activity at the molecular level is therefore identical to EPO and it lacks an effect on the hematocrit *in vivo* due to its very short half-life (Erbayraktar et al., 2003; Fukuda et al., 1989; Imai et al., 1990).

On the other hand, CEPO lacks the ability to bind EPOR, both on soluble Fc-EPOR fusion constructs and on haematopoietic cells and does not activate classical EPOR-mediated signalling mechanisms (Leist et al., 2004). It can therefore be safely assumed that CEPO, and possibly EPO, act through different receptor systems. For instance, we have recently shown that CEPO requires the common  $\beta$ -receptor (CD131), the signalling subunit of the receptors for IL-3, IL-5 and GM-CSF to be effective in models of spinal cord injury (Brines et al., 2004).

In fact, EPOR-mediated neuroprotection, in terms of protection from neuronal apoptosis *in vitro*, was suggested to proceed through activation of NF- $\kappa\text{B}$  (Digicaylioglu and Lipton, 2001). This cannot be the case in EAE, as NF- $\kappa\text{B}$  induces transcription of inflammatory genes, including

Table 4  
Effect of EPO or CEPO on spinal cord cytokine mRNA in EAE mice

EAE treatment group	IL-1 $\beta$	IL-1Ra	TNF- $\alpha$
Non-EAE controls	198 $\pm$ 75	98 $\pm$ 33	175 $\pm$ 44
Vehicle	797 $\pm$ 93	1047 $\pm$ 325	563 $\pm$ 125
EPO 0.5 $\mu\text{g}/\text{kg}$	626 $\pm$ 266	463 $\pm$ 220	350 $\pm$ 121
EPO 50.0 $\mu\text{g}/\text{kg}$	286 $\pm$ 112*	189 $\pm$ 78*	141 $\pm$ 37*
CEPO 0.5 $\mu\text{g}/\text{kg}$	600 $\pm$ 211	697 $\pm$ 421	541 $\pm$ 159
CEPO 50.0 $\mu\text{g}/\text{kg}$	344 $\pm$ 83*	220 $\pm$ 74*	340 $\pm$ 93

PCR data (arbitrary units normalized to housekeeping gene, as described in Materials and methods): S.E.M. ( $n = 3-4$ ).

\*  $P < 0.05$  vs. vehicle.

TNF- $\alpha$ , rather than decreasing them as we observed in this and other (Agnello et al., 2002) EAE models, as well as in cerebral ischemia (Villa et al., 2003). In fact, inhibition of NF- $\kappa$ B, using knock-out mice (Hilliard et al., 1999, 2002) or using chemical (Pahan and Schmid, 2000) or peptide (Dasgupta et al., 2004) inhibitors of NF- $\kappa$ B activation, is protective in EAE.

Clearly, the complexity of EAE makes it difficult identify a single mechanism of action for CEPO. However, inflammation is clearly a common pathogenic component of the chronic (EAE, diabetic neuropathy) and acute (spinal cord injury, cerebral ischemia) models where CEPO has shown efficacy (Leist et al., 2004). As shown here, EPO reduced the spinal cord expression of TNF- $\alpha$ , a key molecule in the development of this disease (reviewed in Steinman, *J Exp Med* 2003). Expression of IL-1 $\beta$  was also reduced by EPO or CEPO treatments, and peripheral lymphocytes from mice treated with EPO or CEPO produced less IFN- $\gamma$  and more IL-10, an important suppressor cytokine and a major regulatory agent in inflammatory response. On the other hand, unlike IFN- $\beta$  (Nicoletti et al., 1996), EPO does not increase spinal cord expression of IL-1Ra whose induction, in this context, probably reflects a response to the inflammatory process. Taken together, these results indicate that EPO importantly reduces the inflammatory milieu in EAE.

Another possible mechanism of action of these compounds is via promotion of repair mechanisms. Neurorepair, including remyelination, is an important physiological process and a therapeutic strategy (Martino, 2004), as indicated by the effectiveness of stem cell therapy in EAE (Pluchino et al., 2003). EPO has been reported to promote angiogenesis, neurogenesis as well as differentiation of oligodendrocytes (Shingo et al., 2001; Sugawa et al., 2002; Wang et al., 2004). This could be an important effect of EPO in the chronic model of EAE used here. In fact, a recent report has indicated that EPO increases oligodendrocyte progenitor cell proliferation in a different model of EAE, induced in SJL/J mice by immunization with myelin proteolipid protein peptide 139–151 (Zhang et al., 2005) and augments BDNF expression in the CNS in this and other experimental conditions (Viviani et al., 2005; Zhang et al., 2005). On the other hand, it should be noted that, while an augmented oligodendrogenesis might be important in chronic EAE models, this can hardly contribute to the effect of EPO in acute EAE, as in Lewis rats the disease recovers very rapidly (Agnello et al., 2002). Since EPO has neurotrophic activity (Ghezzi and Brines, 2004), it is important to note that other growth factors, including nerve growth factor (Micera et al., 2000), ciliary neurotrophic factor (Linker et al., 2002), insulin-like growth factor-I (Yao et al., 1995), and granulocyte colony-stimulating factor (Lock et al., 2002), are effective in models of EAE. In a previous work, we noted that CEPO lacks its tissue-protective activity in the absence of the common  $\beta$ -receptor, the signal-transducing subunit shared by the granulocyte–macrophage colony-

stimulating factor (GM-CSF), and the IL-3 and IL-5 receptors. However, GM-CSF was reported to worsen, rather than protecting from, EAE (Marusic et al., 2002; McQualter et al., 2001), indicating that the mere engagement of this common  $\beta$ -chain does not explain the protective action of CEPO.

Finally, it is important to consider EPO in the context of the pathogenesis of MS. EPO transcription is regulated by the hypoxia inducible factor-1 (HIF-1) and a hypoxia-like metabolic injury occurs in MS (Lassmann, 2003). More recently it was shown that up-regulation of neuroprotective pathways against hypoxia are activated in MS brains (Graumann et al., 2003). (It should also be pointed out that cytokines are known to stimulate HIF directly in normoxic cells, which presumably plays a role in inflammatory injuries.) It is therefore interesting that a HIF-1 target gene product has protective effects in animal models of MS. The other major HIF-1 target gene, vascular endothelial growth factor (VEGF), which was also shown to be induced in MS patients (Graumann et al., 2003; Proescholdt et al., 2002) and in a model of EAE in rats and guinea pigs (Proescholdt et al., 2002; Kirk and Karlik, 2003), seems not to share the protective action of EPO and was suggested, on the contrary, to be implicated in the inflammatory component of EAE (Kirk and Karlik, 2003). In fact, intracerebral infusion of VEGF in a rat model of EAE exacerbated the inflammatory response by inducing BBB damage (Proescholdt et al., 2002). The different behaviour of EPO and VEGF might be related, among other things, to the fact that, while VEGF is known to reduce tight junction proteins allowing leakage from within the capillary into the brain parenchyma via increased permeability of the blood–brain barrier (BBB), EPO counteracts this effect (Martinez-Estrada et al., 2003). In support, BBB disruption takes place in EAE and EPO was shown to diminish BBB leakage in EAE (Li et al., 2004). Since leakage contributes to the inflammatory process and, vice versa, may be a consequence of inflammation (de Vries et al., 1997), this mechanism could be part of the overall anti-neuroinflammatory action of EPO in EAE.

Translation of effectiveness of EPO in animal models of cerebral ischemia to human disease has already been validated in a proof-of-concept clinical trial showing that administration of EPO in patients with cerebral ischemia is both safe and beneficial (Fehrenreich et al., 2002). Hopefully, a successful translation from EAE to multiple sclerosis or other demyelinating diseases will also occur. Antagonism of inflammation by CEPO and related tissue-protective cytokines with reduced EPO adverse effects may thus provide a new avenue for the therapy of MS.

#### Acknowledgements

We are indebted Dr. Roberto Furlan, Milano, for teaching us the mouse EAE model and for helping us analyze the

data. Supported in part by MIUR, Rome, Italy (Fondo per gli Investimenti della Ricerca di Base RBAU01ARSJ, by Fondo Integrativo Speciale per la Ricerca, Neurobiotecnologie), by Ministero della Sanità-Ricerca Finalizzata, by Fondazione Italiana Sclerosi Multipla (FISM 2002/R/41) and by a grant from the Kenneth S. Warren Institute. C.S. was the recipient of a fellowship from the Fondazione Italiana Sclerosi Multipla (FISM) and P.B. is recipient of a fellowship from Fondazione Monzino.

## References

- Agnello, D., Bigini, P., Villa, P., Mennini, T., Cerami, A., Brines, M.L., Ghezzi, P., 2002. Erythropoietin exerts an anti-inflammatory effect on the CNS in a model of experimental autoimmune encephalomyelitis. *Brain Res.* 952, 128–134.
- Amor, S., O'Neill, J.K., Morris, M.M., Smith, R.M., Wraith, D.C., Groome, N., Travers, P.J., Baker, D., 1996. Encephalitogenic epitopes of myelin basic protein, proteolipid protein, myelin oligodendrocyte glycoprotein for experimental allergic encephalomyelitis induction in Biozzi ABH (H-2Ag7) mice share an amino acid motif. *J. Immunol.* 156, 3000–3008.
- Bianchi, R., Buyukakilli, B., Brines, M., Savino, C., Cavaletti, G., Oggioni, N., Lauria, G., Borgna, M., Lombardi, R., Cimen, B., Comelekoglu, U., Kanik, A., Tataroglu, C., Cerami, A., Ghezzi, P., 2004. Erythropoietin both protects from and reverses experimental diabetic neuropathy. *Proc. Natl. Acad. Sci. U. S. A.* 101, 823–828.
- Bokemeyer, C., Aapro, M.S., Courdi, A., Foubert, J., Link, H., Osterborg, A., Repetto, L., Soubeyran, P., 2004. EORTC guidelines for the use of erythropoietic proteins in anemic patients with cancer. *Eur. J. Cancer* 40, 2201–2216.
- Brines, M., Cerami, A., 2005. Emerging biological roles for erythropoietin in the nervous system. *Nat. Rev. Neurosci.* 6, 484–494.
- Brines, M.L., Ghezzi, P., Keenan, S., Agnello, D., de Lanerolle, N.C., Cerami, C., Itri, L.M., Cerami, A., 2000. Erythropoietin crosses the blood–brain barrier to protect against experimental brain injury. *Proc. Natl. Acad. Sci. U. S. A.* 97, 10526–10531.
- Brines, M., Grasso, G., Fiordaliso, F., Sfacteria, A., Ghezzi, P., Fratelli, M., Latini, R., Xie, Q.W., Smart, J., Su-Rick, C.J., Pobre, E., Diaz, D., Gomez, D., Hand, C., Coleman, T., Cerami, A., 2004. Erythropoietin mediates tissue protection through an erythropoietin and common beta-subunit heteroreceptor. *Proc. Natl. Acad. Sci. U. S. A.* 101, 14907–14912.
- Casadevall, N., Nataf, J., Viron, B., Kolta, A., Kiladjian, J.J., Martin-Dupont, P., Michaud, P., Papo, T., Ugo, V., Teyssandier, I., Varet, B., Mayeux, P., 2002. Pure red-cell aplasia and antierythropoietin antibodies in patients treated with recombinant erythropoietin. *N. Engl. J. Med.* 346, 469–475.
- Celik, M., Gokmen, N., Erbayraktar, S., Akhisaroglu, M., Konak, S., Ulukus, C., Genc, S., Genc, K., Sagiroglu, E., Cerami, A., Brines, M., 2002. Erythropoietin prevents motor neuron apoptosis and neurologic disability in experimental spinal cord ischemic injury. *Proc. Natl. Acad. Sci. U. S. A.* 99, 2258–2263.
- Chang, Y.S., Mu, D., Wendland, M., Sheldon, R.A., Vexler, Z.S., McQuillen, P.S., Ferrero, D.M., 2005. Erythropoietin improves functional and histological outcome in neonatal stroke. *Pediatr. Res.* 58, 106–111.
- Chomczynski, P., Sacchi, N., 1987. Single-step method of RNA isolation by acid guanidinium thiocyanate–phenol–chloroform extraction. *Anal. Biochem.* 162, 156–159.
- Dasgupta, S., Jana, M., Zhou, Y., Fung, Y.K., Ghosh, S., Pahan, K., 2004. Antineuroinflammatory effect of NF-kappaB essential modifier-binding domain peptides in the adoptive transfer model of experimental allergic encephalomyelitis. *J. Immunol.* 173, 1344–1354.
- de Vries, H.E., Kuiper, J., de Boer, A.G., Van Berkel, T.J., Breimer, D.D., 1997. The blood–brain barrier in neuroinflammatory diseases. *Pharmacol. Rev.* 49, 143–155.
- Diem, R., Sattler, M.B., Merkler, D., Demmer, I., Maier, K., Stadelmann, C., Ehrenreich, H., Bahr, M., 2005. Combined therapy with methylprednisolone and erythropoietin in a model of multiple sclerosis. *Brain* 128, 375–385.
- Digicaylioglu, M., Lipton, S.A., 2001. Erythropoietin-mediated neuroprotection involves cross-talk between Jak2 and NF-kappaB signalling cascades. *Nature* 412, 641–647.
- Ehrenreich, H., Hasselblatt, M., Dembowski, C., Cepek, L., Lewczuk, P., Stiefel, M., Rustenbeck, H.H., Breiter, N., Jacob, S., Knerlich, F., Bohn, M., Poser, W., Ruther, E., Kochen, M., Gefeller, O., Gleiter, C., Wessel, T.C., De Ryck, M., Itri, L., Prange, H., Cerami, A., Brines, M., Siren, A.L., 2002. Erythropoietin therapy for acute stroke is both safe and beneficial. *Mol. Med.* 8, 495–505.
- Erbayraktar, S., Grasso, G., Sfacteria, A., Xie, Q.W., Coleman, T., Kreilgaard, M., Torup, L., Sager, T., Erbayraktar, Z., Gokmen, N., Yilmaz, O., Ghezzi, P., Villa, P., Fratelli, M., Casagrande, S., Leist, M., Helboe, L., Gerwein, J., Christensen, S., Geist, M.A., Pedersen, L.O., Cerami-Hand, C., Wuerth, J.P., Cerami, A., Brines, M., 2003. Asialoerythropoietin is a nonerythropoietic cytokine with broad neuroprotective activity in vivo. *Proc. Natl. Acad. Sci. U. S. A.* 100, 6741–6746.
- Fukuda, M.N., Sasaki, H., Lopez, L., Fukuda, M., 1989. Survival of recombinant erythropoietin in the circulation: the role of carbohydrates. *Blood* 73, 84–89.
- Furlan, R., Brumbilla, E., Ruffini, F., Poliani, P.L., Bergami, A., Marconi, P.C., Franciotta, D.M., Penna, G., Comi, G., Adorini, L., Martino, G., 2001. Intrathecal delivery of IFN-gamma protects C57BL/6 mice from chronic progressive experimental autoimmune encephalomyelitis by increasing apoptosis of central nervous system-infiltrating lymphocytes. *J. Immunol.* 167, 1821–1829.
- Ghezzi, P., Brines, M., 2004. Erythropoietin as an antiapoptotic, tissue-protective cytokine. *Cell Death Differ.* 11, S37–S44.
- Gill, G.W., Frost, J.K., Miller, K.A., 1974. A new formula for a half-oxidized hematoxylin solution that neither overstains nor requires differentiation. *Acta Cytol.* 18, 300–311.
- Gorio, A., Gokmen, N., Erbayraktar, S., Yilmaz, O., Madaschi, L., Cichetti, C., Di Giulio, A.M., Vardar, E., Cerami, A., Brines, M., 2002. Recombinant human erythropoietin counteracts secondary injury and markedly enhances neurological recovery from experimental spinal cord trauma. *Proc. Natl. Acad. Sci. U. S. A.* 99, 9450–9455.
- Graumann, U., Reynolds, R., Steck, A.J., Schaeren-Wiemers, N., 2003. Molecular changes in normal appearing white matter in multiple sclerosis are characteristic of neuroprotective mechanisms against hypoxic insult. *Brain Pathol.* 13, 554–573.
- Group, T.U.R.H.E.P.S., 1991. Double-blind, placebo-controlled study of the therapeutic use of recombinant human erythropoietin for anemia associated with chronic renal failure in predialysis patients. The US Recombinant Human Erythropoietin Predialysis Study Group. *Am. J. Kidney Dis.* 18, 50–59.
- Hilliard, B., Samoilova, E.B., Liu, T.S., Rostami, A., Chen, Y., 1999. Experimental autoimmune encephalomyelitis in NF-kappa B-deficient mice: roles of NF-kappa B in the activation and differentiation of autoreactive T cells. *J. Immunol.* 163, 2937–2943.
- Hilliard, B.A., Mason, N., Xu, L., Sun, J., Lamhamedi-Cherradi, S.E., Liou, H.C., Hunter, C., Chen, Y.H., 2002. Critical roles of c-Rel in autoimmune inflammation and helper T cell differentiation. *J. Clin. Invest.* 110, 843–850.
- Huuser, C.R., Barber, R.P., Crawford, G.D., Matthews, D.A., Phelps, P.E., Salvaterra, P.M., Vaughn, J.E., 1984. Species-specific second antibodies reduce spurious staining in immunocytochemistry. *J. Histochem. Cytochem.* 32, 395–402.
- Imai, N., Higuchi, M., Kawamura, A., Tomonoh, K., Oh-Eda, M., Fujiwara, M., Shimonaka, Y., Ochi, N., 1990. Physicochemical and biological characterization of asialoerythropoietin. Suppressive effects of sialic



- acid in the expression of biological activity of human erythropoietin in vitro. *Eur. J. Biochem* 194, 457–462.
- Jelkmann, W., Wagner, K., 2004. Beneficial and ominous aspects of the pleiotropic action of erythropoietin. *Ann. Hematol.* 83, 673–686.
- Juul, S., 2004. Recombinant erythropoietin as a neuroprotective treatment: in vitro and in vivo models. *Clin. Perinatol.* 31, 129–142.
- Juul, S.E., McPherson, R.J., Farrell, F.X., Jolliffe, L., Ness, D.J., Gleason, C.A., 2004. Erythropoietin concentrations in cerebrospinal fluid of nonhuman primates and fetal sheep following high-dose recombinant erythropoietin. *Biol. Neonate* 85, 138–144.
- Kirk, S.L., Karlik, S.J., 2003. VEGF and vascular changes in chronic neuroinflammation. *J. Autoimmun.* 21, 353–363.
- Lassmann, H., 2003. Hypoxia-like tissue injury as a component of multiple sclerosis lesions. *J. Neurol. Sci.* 206, 187–191.
- Leist, M., Ghezzi, P., Grasso, G., Bianchi, R., Villa, P., Fratelli, M., Savino, C., Bianchi, M., Nielsen, J., Gerwien, J., Kallunki, P., Larsen, A.K., Helboe, L., Christensen, S., Pedersen, L.O., Nielsen, M., Torup, L., Sager, T., Sfacteria, A., Erbayraktar, S., Erbayraktar, Z., Gokmen, N., Yilmaz, O., Cerami-Hand, C., Xie, Q.-w., Coleman, T., Cerami, A., Brines, M., 2004. Derivatives of erythropoietin that are tissue protective but not erythropoietic. *Science* 305, 239–242.
- Li, W., Maeda, Y., Yuan, R.R., Elkabes, S., Cook, S., Dowling, P., 2004. Beneficial effect of erythropoietin on experimental allergic encephalomyelitis. *Ann. Neurol.* 56, 767–777.
- Lim, V.S., 1991. Recombinant human erythropoietin in predialysis patients. *Am. J. Kidney Dis.* 18, 34–37.
- Lunker, R.A., Maurer, M., Gaupp, S., Martini, R., Holtmann, B., Giess, R., Rieckmann, P., Lassmann, H., Toyka, K.V., Sendtner, M., Gold, R., 2002. CNTF is a major protective factor in demyelinating CNS disease: a neurotrophic cytokine as modulator in neuroinflammation. *Nat. Med.* 8, 620–624.
- Lock, C., Hemmans, G., Pedutti, R., Brendolan, A., Schadt, E., Garren, H., Langer-Gould, A., Strober, S., Cannella, B., Allard, J., Klonowski, P., Austin, A., Lad, N., Kaminski, N., Galli, S.J., Oksenberg, J.R., Raine, C.S., Heller, R., Steinman, L., 2002. Gene-microarray analysis of multiple sclerosis lesions yields new targets validated in autoimmune encephalomyelitis. *Nat. Med.* 8, 500–508.
- Maiese, K., Li, F., Chong, Z.Z., 2005. New avenues of exploration for erythropoietin. *JAMA* 293, 90–95.
- Martinez-Estrada, O.M., Rodriguez-Millan, E., Gonzalez-De Vicente, E., Reina, M., Vilaro, S., Fabre, M., 2003. Erythropoietin protects the in vitro blood brain barrier against VEGF-induced permeability. *Eur. J. Neurosci.* 18, 2538–2544.
- Martino, G., 2004. How the brain repairs itself: new therapeutic strategies in inflammatory and degenerative CNS disorders. *Lancet Neurol.* 3, 372–378.
- Martino, G., Adorini, L., Rieckmann, P., Hillert, J., Kallmann, B., Comi, G., Filippi, M., 2002. Inflammation in multiple sclerosis: the good, the bad, and the complex. *Lancet Neurol.* 1, 499–509.
- Marusic, S., Miyashiro, J.S., Douhan III, J., Konz, R.F., Xuan, D., Pelker, J.W., Ling, V., Lennard, J.P., Jacobs, K.A., 2002. Local delivery of granulocyte macrophage colony-stimulating factor by retrovirally transduced antigen-specific T cells leads to severe, chronic experimental autoimmune encephalomyelitis in mice. *Neurosci. Lett.* 332, 185–189.
- McQuarrie, J.L., Darwiche, R., Ewing, C., Onuki, M., Kay, T.W., Hamilton, J.A., Reid, H.H., Bernard, C.C., 2001. Granulocyte macrophage colony-stimulating factor: a new putative therapeutic target in multiple sclerosis. *J. Exp. Med.* 194, 873–882.
- Micera, A., Properzi, F., Triaca, V., Aloe, L., 2000. Nerve growth factor antibody exacerbates neuropathological signs of experimental allergic encephalomyelitis in adult Lewis rats. *J. Neuroimmunol.* 104, 116–123.
- Natali, A., Toschi, E., Baldeweg, S., Casularo, A., Baldi, S., Sironi, A.M., Yudkin, J.S., Ferrannini, E., 2005. Haematocrit, type 2 diabetes, and endothelium-dependent vasodilatation of resistance vessels. *Eur. Heart J.* 26, 464–471.
- Nicoletti, F., Patti, F., DiMarco, R., Zacccone, P., Nicoletti, A., Meroni, P., Reggio, A., 1996. Circulating serum levels of IL-1Ra in patients with relapsing remitting multiple sclerosis are normal during remission phases but significantly increased either during exacerbations or in response to IFN-beta treatment. *Cytokine* 8, 395–400.
- Pahan, K., Schmid, M., 2000. Activation of nuclear factor- $\kappa$ B in the spinal cord of experimental allergic encephalomyelitis. *Neurosci. Lett.* 287, 17–20.
- Puchino, S., Quattrini, A., Brambilla, E., Gritti, A., Salani, G., Dma, G., Galli, R., Del Carro, U., Amadio, S., Bergami, A., Furlan, R., Comi, G., Vecchi, A.L., Martino, G., 2003. Injection of adult neurospheres induces recovery in a chronic model of multiple sclerosis. *Nature* 422, 688–694.
- Proescholdt, M.A., Jacobson, S., Tresser, N., Oldfield, E.H., Merrill, M.J., 2002. Vascular endothelial growth factor is expressed in multiple sclerosis plaques and can induce inflammatory lesions in experimental allergic encephalomyelitis rats. *J. Neuropathol. Exp. Neurol.* 61, 914–925.
- Quaschnig, T., Ruschitzka, F., Stallmach, T., Shaw, S., Morawietz, H., Goetsch, W., Hermann, M., Slowinski, T., Theuring, F., Hoehner, B., Luscher, T.F., Gassmann, M., 2003. Erythropoietin-induced excessive erythrocytosis activates the tissue endothelin system in mice. *FASEB J.* 17, 259–261.
- Ruschitzka, F.T., Wenger, R.H., Stallmach, T., Quaschnig, T., de Wit, C., Wagner, K., Labugger, R., Kelm, M., Noll, G., Rulicke, T., Shaw, S., Lindberg, R.L., Rodenwaldt, B., Lutz, H., Bauer, C., Luscher, T.F., Gassmann, M., 2000. Nitric oxide prevents cardiovascular disease and determines survival in polyglobulic mice overexpressing erythropoietin. *Proc. Natl. Acad. Sci. U. S. A.* 97, 11609–11613.
- Santler, M.B., Merkler, D., Maier, K., Stadelmann, C., Ehrenreich, H., Bahr, M., Diem, R., 2004. Neuroprotective effects and intracellular signaling pathways of erythropoietin in a rat model of multiple sclerosis. *Cell Death Differ.* 11 (Suppl 2), S181–S192.
- Shingo, T., Sorokan, S.T., Shimazaki, T., Weiss, S., 2001. Erythropoietin regulates the in vitro and in vivo production of neuronal progenitors by mammalian forebrain neural stem cells. *J. Neurosci.* 21, 9733–9743.
- Steinman, L., 2003. Optic neuritis, a new variant of experimental encephalomyelitis, a durable model for all seasons, now in its seventieth year. *J. Exp. Med.* 197, 1065–1071.
- Steinman, L., 2004. Immune therapy for autoimmune diseases. *Science* 305, 212–216.
- Sugawa, M., Sakurai, Y., Ishikawa-Ieda, Y., Suzuki, H., Asou, H., 2002. Effects of erythropoietin on glial cell development; oligodendrocyte maturation and astrocyte proliferation. *Neurosci. Res.* 44, 391–403.
- Varet, B., Casadevall, N., Lacombe, C., Naveaux, P., 1990. Erythropoietin: physiology and clinical experience. *Semin. Hematol.* 27, 25–31.
- Villa, P., Digini, P., Mennini, T., Agnello, D., Laragione, T., Cagnotto, A., Viviani, B., Marinovich, M., Cerami, A., Coleman, T.R., Brines, M., Ghezzi, P., 2003. Erythropoietin selectively attenuates cytokine production and inflammation in cerebral ischemia by targeting neuronal apoptosis. *J. Exp. Med.* 198, 971–975.
- Viviani, B., Bartsaghi, S., Corsini, E., Villa, P., Ghezzi, P., Garau, A., Galli, C.L., Marinovich, M., 2005. Erythropoietin protects primary hippocampal neurons increasing the expression of brain-derived neurotrophic factor. *J. Neurochem.* 93, 412–421.
- Wang, L., Zhang, Z., Wang, Y., Zhang, R., Chopp, M., 2004. Treatment of stroke with erythropoietin enhances neurogenesis and angiogenesis and improves neurological function in rats. *Stroke* 35, 1732–1737.
- Yao, D.L., Liu, X., Hudson, L.D., Webster, H.D., 1995. Insulin-like growth factor I treatment reduces demyelination and up-regulates gene expression of myelin-related proteins in experimental autoimmune encephalomyelitis. *Proc. Natl. Acad. Sci. U. S. A.* 92, 6190–6194.
- Zhang, J., Li, Y., Cui, Y., Chen, J., Lu, M., Elias, S.B., Chopp, M., 2005. Erythropoietin treatment improves neurological functional recovery in EAE mice. *Brain Res.* 1034, 34–39.



## BASIC RESEARCH

# Protective effects of erythropoietin against acute lung injury in a rat model of acute necrotizing pancreatitis

Oge Tascilar, Güldeniz Karadeniz Cakmak, Ishak Ozel Tekin, Ali Ugur Emre, Bulent Hamdi Ucan, Burak Bahadır, Serefden Acikgoz, Oktay Irkorucu, Kemal Karakaya, Hakan Balbaloglu, Gürkan Kertis, Handan Ankarali, Mustafa Comert

Oge Tascilar, Güldeniz Karadeniz Cakmak, Ali Ugur Emre, Bulent Hamdi Ucan, Oktay Irkorucu, Kemal Karakaya, Hakan Balbaloglu, Mustafa Comert, Department of Surgery, Zonguldak Karaelmas University, School of Medicine, Kozlu-Zonguldak 67600, Turkey

Ishak Ozel Tekin, Department of Immunology, Zonguldak Karaelmas University, School of Medicine, Kozlu-Zonguldak 67600, Turkey

Burak Bahadır, Gürkan Kertis, Department of Pathology, Zonguldak Karaelmas University, The School of Medicine, Kozlu-Zonguldak 67600, Turkey

Serefden Acikgoz, Department of Biochemistry, Zonguldak Karaelmas University, School of Medicine, Kozlu-Zonguldak 67600, Turkey

Handan Ankarali, Department of Biostatistics, Zonguldak Karaelmas University, School of Medicine, Kozlu-Zonguldak 67600, Turkey

Correspondence to: Dr. Güldeniz Karadeniz Cakmak, Zonguldak Karaelmas Universitesi, Arastirma ve Uygulama Hastanesi Bashekimligi, Kozlu-Zonguldak 67600, Turkey. [gkkaradeniz@yahoo.com](mailto:gkkaradeniz@yahoo.com)

Telephone: +90-372-2610169 Fax: +90-372-2610155

Received: August 1, 2007 Revised: September 16, 2007

**RESULTS:** The mean pleural effusion volume, calculated LW/BW ratio, serum IL-6 and lung tissue MDA levels were significantly lower in EPO groups than in ANP groups. No statistically significant difference was observed in either serum or tissue values of IL-2 among the groups. The level of tumor necrosis factor- $\alpha$  (TNF- $\alpha$ ) and IL-6 and accumulation of ox-LDL were evident in the lung tissues of ANP groups when compared to EPO groups, particularly at 72 h. Histopathological evaluation confirmed the improvement in lung injury parameters after exogenous EPO administration, particularly at 48 h and 72 h.

**CONCLUSION:** EPO administration leads to a significant decrease in ALI parameters by inhibiting polymorphonuclear leukocyte (PMNL) accumulation, decreasing the levels of proinflammatory cytokines in circulation, preserving microvascular endothelial cell integrity and reducing oxidative stress-associated lipid peroxidation and therefore, can be regarded as a cytoprotective agent in ANP-induced ALI.

© 2007 WJG. All rights reserved.

## Abstract

**AIM:** To investigate the effect of exogenous erythropoietin (EPO) administration on acute lung injury (ALI) in an experimental model of sodium taurodeoxycholate-induced acute necrotizing pancreatitis (ANP).

**METHODS:** Forty-seven male Wistar albino rats were randomly divided into 7 groups: sham group ( $n = 5$ ), 3 ANP groups ( $n = 7$  each) and 3 EPO groups ( $n = 7$  each). ANP was induced by retrograde infusion of 5% sodium taurodeoxycholate into the common bile duct. Rats in EPO groups received 1000 U/kg intramuscular EPO immediately after induction of ANP. Rats in ANP groups were given 1 mL normal saline instead. All animals were sacrificed at postoperative 24 h, 48 h and 72 h. Serum amylase, IL-2, IL-6 and lung tissue malondialdehyde (MDA) were measured. Pleural effusion volume and lung/body weight (LW/BW) ratios were calculated. Tissue levels of TNF- $\alpha$ , IL-2 and IL-6 were screened immunohistochemically. Additionally, ox-LDL accumulation was assessed with immune-fluorescent staining. Histopathological alterations in the lungs were also scored.

**Key words:** Erythropoietin; Acute pancreatitis; Acute lung injury; Acute respiratory distress syndrome; Cytokine

Tascilar O, Cakmak GK, Tekin IO, Emre AU, Ucan BH, Bahadır B, Acikgoz S, Irkorucu O, Karakaya K, Balbaloglu H, Kertis G, Ankarali H, Comert M. Protective effects of erythropoietin against acute lung injury in a rat model of acute necrotizing pancreatitis. *World J Gastroenterol* 2007; 13(46): 6172-6182

<http://www.wjgnet.com/1007-9327/13/6172.asp>

## INTRODUCTION

Acute pancreatitis (AP) is a life-threatening necro-inflammatory disease with significant morbidity and mortality rates, especially when complicated by systemic inflammatory response syndrome (SIRS) and multiple organ failure (MODS)<sup>[1,2]</sup>. Death occurs in 60% of the patients within the first 6 d of disease onset and pulmonary complications including acute lung injury (ALI) and acute respiratory distress syndrome (ARDS)

account for a significant number of these deaths<sup>[14]</sup>. The exact mechanisms by which diverse etiological factors induce an attack are indefinite, but once the disease process is initiated, common inflammatory and repair pathways are invoked. Within the first few days following the onset of AP, lung injury occurs as a consequence of AP, whereas sepsis is a dominant cause for lung injury and mortality in the later phase of the disease process<sup>[14]</sup>. Despite improved understanding of the pathogenesis of ARDS, pharmacological modalities are ineffective in decreasing its mortality. None of the randomized clinical trials using novel therapeutic agents has demonstrated an improvement in patient outcome. Consequently, effective therapeutic interventions are thus called for.

Erythropoietin (EPO), a 30.4-kDa glycoprotein and a member of the type I cytokine superfamily, was first introduced as a hormone that regulates erythroid progenitors within the bone marrow to mature into erythrocytes, through binding to its specific cell surface receptors<sup>[15]</sup>. Hence, EPO is approved for the treatment of anemia as a consequence of a variety of disorders. In the current era, the premise that EPO is essential only for erythropoiesis has been changed according to the researches demonstrating the existence of EPO and its receptor in other organs and tissues outside of liver and kidney, such as brain, heart, pancreas, as well as vascular, gastrointestinal and reproductive systems<sup>[16,17]</sup>. Beyond its hematopoietic properties, EPO modulates a broad array of vital cellular processes including progenitor stem cell development, cellular integrity, and angiogenesis<sup>[18,19]</sup>. Additionally, in various tissues, EPO inhibits the apoptotic mechanisms of injury, including preservation of cellular membrane asymmetry to prevent inflammation<sup>[10,12]</sup>. Experimental evidence supports a vigorous cytoprotective effect and EPO is now considered to have applicability in a variety of disorders, such as cerebral ischemia, myocardial infarction, and chronic congestive heart failure<sup>[12,15]</sup>. Wu *et al.*<sup>[10]</sup> demonstrated that pretreatment with EPO appears to attenuate ischemia-reperfusion-induced lung injury. This function is partly related with the ability of EPO to inhibit the accumulation of polymorphonuclear leukocytes (PMNL) in lung tissue and decrease the systematic expression of tumor necrosis factor- $\alpha$  (TNF- $\alpha$ ). In addition to these studies, it has been reported that EPO can attenuate different kinds of lung injuries, showing that rats exposed to hyperoxia exhibit well-maintained alveolar structure and enhanced vascularity when treated with EPO<sup>[17]</sup>. Importantly, EPO can protect the ultrastructure of tracheobronchial epithelia and pulmonary type II epithelia of rats during traumatic brain injury<sup>[16,19]</sup>.

AP associated lung injury is a multifactorial phenomenon with various phases. In the light of the above-mentioned findings, the present study was to evaluate the hypothesis that EPO administration offers pulmonary protective effect against pancreatitis induced lung injury in rats.

## MATERIALS AND METHODS

### Animals

Forty-seven male Wistar albino rats weighing 250-300 g

were housed under constant temperature (22°C) and humidity in a 12-h dark/light cycle.

### Experimental design

The experiments were conducted following the Ethic Committee Faculty of Medicine, University of Zonguldak Karaelmas guiding principles for the care and use of laboratory animals. The animals were randomized into seven experimental groups as follows: sham group in which rats received sham operation ( $n = 5$ ), 3 ANP groups in which acute necrotizing pancreatitis (ANP) was induced by retrograde infusion of sodium taurodeoxycholate and 1 mL normal saline (0.9% NaCl) was given intramuscularly immediately after induction of AP ( $n = 7$  each), 3 EPO groups in which AP was induced by the same way and 1000 U/kg EPO (Eprex, Epoetin alfa, Janssen-Cilag AG, Sweden) was injected intramuscularly immediately after induction of AP. All animals in the ANP and EPO groups were sacrificed at postoperative 24 h, 48 h and 72 h, respectively. Histopathological, biochemical and immunohistochemical evaluations were performed.

### Induction of acute pancreatitis

Anesthesia was induce by injecting ketamine HCL at 100 mg/kg im and laparotomy was performed under strict sterile conditions. An upper midline abdominal incision was made to identify the common pancreaticobiliary duct. The duodenal wall was punctured at its antimesenteric aspect with a 24-gauge IV catheter (Novacath, Medipro A.Ş., Istanbul, Turkey). The catheter was advanced 5 mm into the common duct through the papilla of Vater. ANP was induced by retrograde infusion of 0.2 mL 5% sodium taurodeoxycholate (Sigma, St.Louis, MO, USA) over 3 min using an infusion pump as previously described<sup>[20]</sup> and the pancreaticobiliary duct was clamped near the liver hilum throughout the intraductal infusion in all groups, except for sham group. Animals in sham group were subjected to anesthesia, laparotomy and duodenal manipulation, but not to biliopancreatic duct cannulation. The midline incision was closed in two layers with 4/0 silk suture (Ethicon, Edinburg, UK). Rats were allowed to recover from anesthetic and returned to their cages with free access to water and food after surgery.

### Sampling procedures

All the rats were sacrificed by aortic puncture method. The abdominal and thoracic cavities were entered to obtain blood and lung samples. Blood samples were centrifuged at  $1800 \times g$  for 15 min at 4°C to obtain plasma and stored at -80°C for biochemical analysis. Then, the rats were killed with the lung removed immediately. Random cross-sections of the lung tissue were fixed in 10% neutral phosphate-buffered formalin and embedded in paraffin wax for histopathological examination. Samples of lung tissue were weighed and stored at -85°C for subsequent biochemical and immunohistochemical measurements.

### Assessment of pulmonary effusion

The thorax was opened to collect pleural effusion (PE) by suction which was measured volumetrically. Care was also taken to eliminate blood contamination with PE. The

lungs were then removed and all surrounding tissues were dissected and weighed with an analytical balance. The volume of PE (mL) and the lung weight/body weight (LW/BW) ratios were calculated and considered as an index of pulmonary edema.

#### Biochemical analysis

**Serum amylase, IL-2 and IL-6 assay:** Serum amylase levels were measured by a Beckman Coulter LX-20<sup>®</sup> system analyzer (Fullerton, CA, USA) using Beckman kits (Fullerton, CA, USA), following the manufacturer's instructions. IL-2 and IL-6 levels in the serum were measured with commercially available kits (Biosource International, Commercial ELISA Kit, California, USA).

**Lung tissue malondialdehyde (MDA) assay:** MDA levels in the lung tissue were measured in tissue homogenate. In brief, tissue was homogenized with cold 1.15% KCl to make a 10% homogenates, and 0.2 mL of 8.1% SDS, 1.5 mL of 20% acetic acid solution adjusted to pH 3.5 with NaOH and 1.5 mL of 0.8% aqueous solution of thiobarbituric acid were added to 0.2 mL of 10% tissue homogenates. The mixture was made up to 4.0 mL with distilled water and heated in an oil bath at 95°C for 60 min. After cooling with tap water, 1.0 mL of distilled water and 5.0 mL of the mixture of n-butanol and pyridine (15:1, v/v) were added and the solution was shaken vigorously. After centrifugation at 4000 r/min for 10 min, the organic layer was taken with its absorbance measured at 532 nm on a Shimadzu UV 1601 spectrophotometer. As a standard, 1,1,3,3-tetraethoxypropane was used. MDA concentration per gram tissue was calculated (nmol/gr tissue).

**Immunohistochemical method for screening IL-2, IL-6 and TNF- $\alpha$  in the lung tissue:** Cryostat sections of lung tissue (7  $\mu$ m) were fixed with absolute ethanol and stained with avidin biotin complex based immunohistochemical method. Immunohistochemistry was performed to observe peroxidase diaminobenzidine reaction. Cytokine staining was performed with biotinylated mouse anti-rat IL-2, IL-6, TNF- $\alpha$  antibodies (Biosource International, California, USA). Streptavidin-peroxidase (HRP) and diaminobenzidine (DAB) were purchased from DAKOCytomation (Denmark). Ethanol-fixed tissue sections were treated with biotinylated mouse anti-rat IL-2, IL-6 and TNF- $\alpha$  for 30 min, washed three times with PBS, incubated for an additional 30 min with streptavidin-HRP and washed three times with PBS. The sections were then treated with 0.03% 3, 3'-diaminobenzidine tetrahydrochloride plus 0.01% hydrogen peroxide in 50 mmol/L Tris-HCl buffer (pH 7.4) for 10 min. All incubations were performed at room temperature. The sections were examined under a light microscope by an independent observer, blind to the study.

**Immune-fluorescent staining method for screening ox-LDL in the pancreas and lung tissues:** Rat lung and pancreas were obtained and stored at -85°C. Slides were prepared from the 7  $\mu$ m-thick frozen lung biopsy sections. Slides were further divided into two pieces: one for the test and the other for the negative control. Thirty  $\mu$ L human

polyclonal anti-ox-LDL IgG solution as primary antibody was added only on the test slides and the control slides were manipulated with phosphate-buffered solution (PBS) as the same amount of primary antibody. After a 30-min incubation in a humid chamber at room temperature, both the control and test slides were washed with phosphate-buffered saline and 30  $\mu$ L fluorescent isothiocyanate (FITC)-labeled anti human IgG was administered as a conjugate substance. The slides were incubated for a further 30 min at room temperature and washed with the standard PBS solution. After drying, the slides were covered with a mounting medium and examined under a fluorescent microscope (LEICA DMRX, Germany).

#### Histopathologic analysis

The lung tissue samples were fixed in 10% formalin immediately after removal, embedded in paraffin, sectioned at 5  $\mu$ m intervals, stained with hematoxylin and eosin, and examined under a light microscope. Histopathological evaluation and scoring of the parameters were performed by a single pathologist unaware of the treatment groups. Morphometric analysis of histological sections was accomplished with the point counting technique. For this purpose, we used an optical microscope provided with an integrating eyepiece containing 100 points and 50 lines. The following parameters were evaluated as previously described<sup>[21,22]</sup>.

**Alveolar distension and collapse index:** At a magnification of  $\times 100$ , we analyzed 10 randomly selected fields of the proximal and 10 fields of the distal sections. We designated grades 0, 1, 2, and 3 to microscopic fields respectively as 0%, 25%, 50%, and over 50% of the area with either alveolar distension or alveolar collapse.

**Alveolar edema index:** At a magnification of  $\times 400$ , we analyzed 10 randomly selected fields of the proximal and 10 fields of the distal sections. The relationship between the number of points of the eyepiece falling on alveolar edema and the number of points falling on the whole alveolar lumen was determined.

**Alveolar cellularity index:** We analyzed 10 microscopic fields from each lung slide at a magnification of  $\times 1000$ . The alveolar cellularity index was obtained by the relationship between the lines of the integrating eyepiece crossing a nucleus and the lines crossing alveolar septa.

**Polymorphonuclear cell (PMNL) index:** We analyzed 10 microscopic fields from each lung slide at a magnification of  $\times 1000$ . PMNL index was obtained by the relationship between the lines of the integrating eyepiece crossing a nucleus and the lines crossing alveolar septa.

#### Statistical analysis

Statistical analysis was performed using SPSS version 11.5 for Windows XP. The results were expressed as mean  $\pm$  standard deviation (SD). The differences in serum amylase, IL-2 and IL-6 were assessed by Welch test and *post hoc* Games-Howell test or one way ANOVA and *post hoc* Tukey

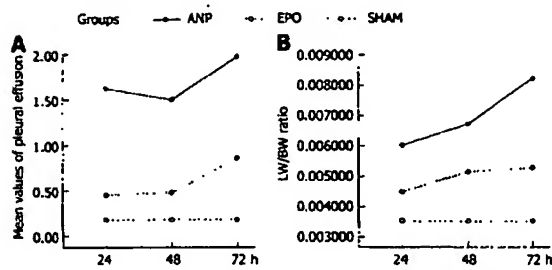


Figure 1 Values of pleural effusion volumes (A) and calculated LW/BW ratios (B) (mean  $\pm$  SD).

HSD test where appropriate. The differences between groups (ANP, EPO, sham), time course (three different hours) and its interaction in terms of tissue MDA levels, pulmonary effusion volume, calculated LW/BW ratio, and mean histopathological scores, were analyzed by factorial analysis of variance with a single control.  $P < 0.05$  was considered statistically significant.

## RESULTS

### Pleural effusion and LW/BW ratio

The mean pleural effusion volume (mL) and the calculated LW/BW ratio were significantly increased in ANP groups when compared to EPO groups ( $P < 0.0001$ ). The mean  $\pm$  SD volume of pleural effusion measured was  $1.62 \pm 1.08$  mL,  $1.5 \pm 0.33$  mL and  $1.97 \pm 0.39$  mL in 3 ANP groups and  $0.45 \pm 0.37$  mL,  $0.48 \pm 0.38$  mL and  $0.85 \pm 0.13$  mL in 3 EPO groups, respectively. No statistically significant difference was detected between sham and EPO groups ( $0.18 \pm 0.08$  mL *vs*  $0.45 \pm 0.37$  mL,  $0.48 \pm 0.38$  mL and  $0.85 \pm 0.13$  mL,  $P > 0.05$  for each). The volume of pleural effusion was statistically significant higher in ANP groups than in sham group ( $0.18 \pm 0.08$  mL *vs*  $1.62 \pm 1.08$  mL,  $1.5 \pm 0.33$  mL and  $1.97 \pm 0.39$  mL,  $P < 0.001$  for each). The time course of pleural effusion volume in 3 ANP groups is shown in Figure 1A. In terms of LW/BW ratio, a statistically significant difference was seen from 24 h to 72 both in 3 ANP groups ( $0.006 \pm 0.0022$  *vs*  $0.008 \pm 0.0019$ ,  $P < 0.05$ ) and in 3 EPO groups ( $0.004 \pm 0.0008$  *vs*  $0.005 \pm 0.0011$ ,  $P < 0.05$ ) and the mean calculated ratio was higher at 72 h for each. In comparison to sham group, no statistically significant difference was found in EPO groups ( $0.003 \pm 0.0004$  *vs*  $0.004 \pm 0.0008$ ,  $0.005 \pm 0.0009$  and  $0.005 \pm 0.0011$ ,  $P > 0.05$ ), where as ANP resulted in a significant increase in calculated LW/BW ratio at 24 h, 48 h, and 72 h ( $0.003 \pm 0.0004$  *vs*  $0.006 \pm 0.0022$ ,  $0.007 \pm 0.0016$ , and  $0.008 \pm 0.0019$ ,  $P < 0.05$  for each) (Figure 1B). The pleural effusion values and LW/BW ratio are listed in Table 1.

### Biochemical analysis

**Serum amylase, IL-2 and IL-6 assay:** A statistically significant increase was detected in the mean  $\pm$  SD serum levels of amylase in 3 ANP groups when compared to sham group ( $534 \pm 124$  u/L *vs*  $3502 \pm 1830$  u/L,  $3759 \pm 1505$  u/L and  $5056 \pm 1872$  u/L,  $P < 0.05$  for each). The

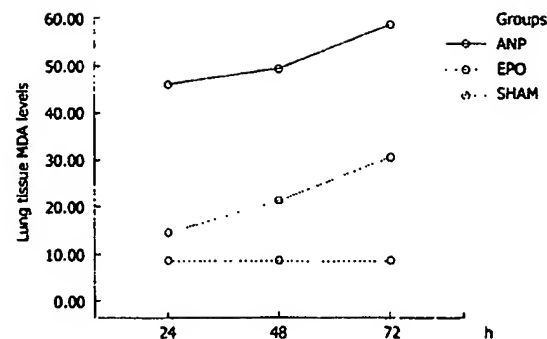


Figure 2 Values of MDA in lung tissue (mean  $\pm$  SD).

mean  $\pm$  SD value of serum amylase was  $3502 \pm 1830$  u/L,  $3759 \pm 1505$  u/L and  $5056 \pm 1872$  u/L in 3 ANP groups and  $1523 \pm 514$  u/L,  $2317 \pm 311$  u/L and  $735 \pm 454$  u/L in 3 EPO groups, respectively. On the other hand, no statistically significant difference was found between the ANP and EPO groups with respect to the time intervals ( $P > 0.05$ ). The serum levels of IL-6 were significantly lower in 3 EPO groups than in 3 ANP groups ( $P = 0.001$  for each). The IL-6 value (mean  $\pm$  SD) was  $24.4 \pm 3.26$  pg/mL,  $27.7 \pm 3.74$  pg/mL and  $33.2 \pm 2.1$  pg/mL respectively in 3 ANP groups, and  $12.2 \pm 2.15$  pg/mL,  $12.8 \pm 1.89$  pg/mL and  $13.8 \pm 3.24$  pg/mL respectively in 3 EPO groups. We did not observe any statistically significant difference in IL-2 values among these groups ( $7.4 \pm 2.88$  pg/mL *vs*  $7.7 \pm 3.17$  pg/mL,  $9.3 \pm 2.74$  pg/mL,  $7.2 \pm 3.1$  pg/mL,  $6.9 \pm 2.04$  pg/mL,  $7.7 \pm 2.93$  g/mL and  $10.6 \pm 3.9$  pg/mL,  $P > 0.005$  for each). The mean  $\pm$  SD values of serum amylase, IL-2, IL-6 and tissue MDA are listed in Table 2.

**Lung tissue MDA assay:** Pulmonary injury in ANP groups was characterized by an increase in lung tissue MDA levels, an indicator of lipid peroxidation. The lung tissue MDA levels were significantly reduced in EPO groups at 24 h, 48 h, and 72 h, when compared to ANP groups ( $P < 0.0001$ ). The MDA value (mean  $\pm$  SD) was  $45.9 \pm 6.8$  nmol/gr tissue,  $49.3 \pm 9.5$  nmol/gr tissue, and  $58.8 \pm 9$  nmol/gr tissue respectively in 3 ANP groups and  $14.7 \pm 2.1$  nmol/gr tissue,  $21.2 \pm 2.7$  nmol/gr tissue, and  $30.4 \pm 2.1$  nmol/gr tissue respectively in 3 EPO groups. A statistically significant increase in MDA values was noted at 24 h-72 h ( $45.9 \pm 6.8$  nmol/gr tissue *vs*  $58.8 \pm 9$  nmol/gr tissue, and  $14.7 \pm 2.1$  nmol/gr tissue *vs*  $30.4 \pm 2.1$  nmol/gr tissue,  $P < 0.0001$ ) and 48 h to 72 h ( $49.3 \pm 9.5$  nmol/gr tissue *vs*  $58.8 \pm 9$  nmol/gr tissue and  $21.2 \pm 2.7$  nmol/gr tissue *vs*  $30.4 \pm 2.1$  nmol/gr tissue,  $P = 0.001$ ) in either ANP or EPO groups. The mean MDA value was higher at 72 h. In comparison with sham group, the MDA levels were significantly higher in all the other groups ( $8.5 \pm 3.1$  nmol/gr tissue *vs*  $45.9 \pm 6.8$  nmol/gr tissue,  $49.3 \pm 9.5$  nmol/gr tissue,  $58.8 \pm 9$  nmol/gr tissue,  $21.2 \pm 2.7$  nmol/gr tissue, and  $30.4 \pm 2.1$  nmol/gr tissue,  $P < 0.001$  for each) except for EPO groups at 24 h ( $8.5 \pm 3.1$  nmol/gr tissue *vs*  $14.7 \pm 2.1$  nmol/gr tissue,  $P = 0.224$ ) (Figure 2).

Groups	Sham	ANP1	ANP2	ANP3	EPO1	EPO2	EPO3
Pleural effusion (mL)	0.18 ± 0.08	1.62 ± 1.08	1.5 ± 0.33	1.97 ± 0.39	0.45 ± 0.37	0.48 ± 0.38	0.85 ± 0.13
LW/BW ratio	0.003 ± 0.0004	0.006 ± 0.0022	0.007 ± 0.0016	0.008 ± 0.0019	0.004 ± 0.0008	0.005 ± 0.0009	0.005 ± 0.0011

Groups	Sham	ANP1	ANP2	ANP3	EPO1	EPO2	EPO3
Amylase (U/L)	534 ± 124	3502 ± 1830	3759 ± 1505	5056 ± 1872	1523 ± 514	2317 ± 311	735 ± 454
IL-6 (pg/mL)	4.7 ± 2.01	24.4 ± 3.26	27.7 ± 3.74	33.2 ± 2.1	12.2 ± 2.15	12.8 ± 1.89	13.8 ± 3.24
IL-2 (pg/mL)	7.4 ± 2.88	7.7 ± 3.17	9.3 ± 2.74	7.2 ± 3.1	6.9 ± 2.04	7.7 ± 2.93	10.6 ± 3.9
MDA (nmol/gr tissue)	8.5 ± 3.1	45.9 ± 6.8	49.3 ± 9.5	58.8 ± 9	14.7 ± 2.1	21.2 ± 2.7	30.4 ± 2.1

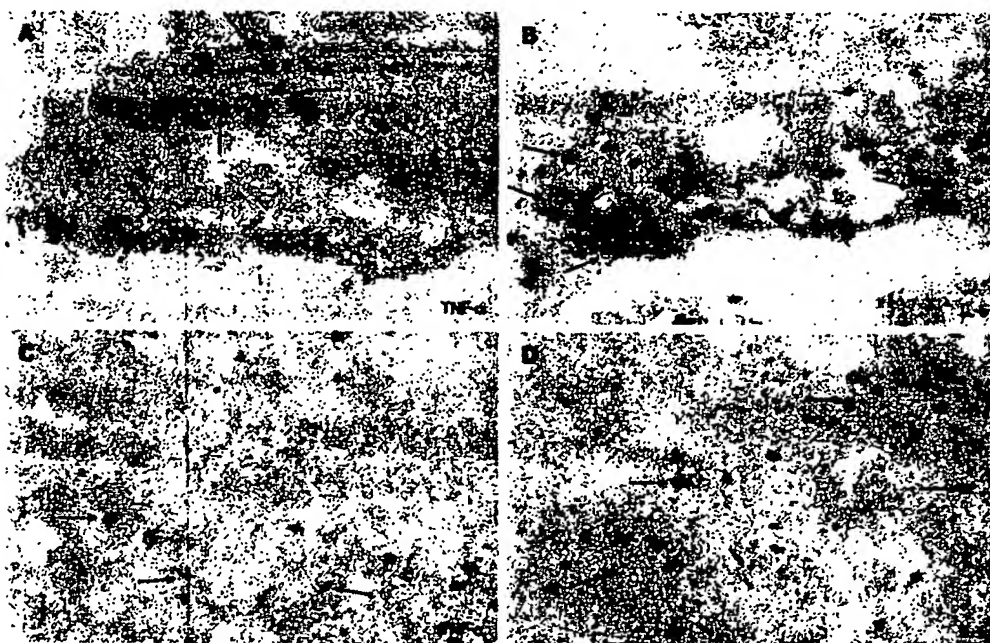


Figure 3 Light microscopic view of immunohistochemical staining for intracellular accumulations of TNF- $\alpha$  and IL-6 in the lung sections of ANP groups (A and B) and EPO groups (C and D) at 72 h. Arrows indicate the significantly positive staining in ANP groups (A and B) and less intensive immunohistochemical staining in EPO groups (C and D).

**Immunohistochemical screening:** The intracellular accumulation of TNF- $\alpha$  and IL-6 was evident in the lung tissues of ANP groups (Figure 3A and B) when compared to EPO groups, particularly at 72 h (Figure 3C and D). No significant difference in IL-2 accumulation was detected among the groups.

**Immune-fluorescent screening of ox-LDL:** As we did not observe any positive immunofluorescent staining either in pancreas or in lung tissue of sham and EPO groups, a significant positive staining for ox-LDL was determined in ANP groups, which became much evident at 72 h (Figure 4A and B).

#### Histopathologic analysis

**Alveolar distention and collapse:** Alveolar distention and collapse were significantly intense in ANP groups at 24 h, 48 h and 72 h when compared to EPO groups ( $P < 0.0001$ ). The alveolar distention and collapse scores (mean  $\pm$  SD) for ANP and EPO groups calculated at 24 h, 48 h and 72 h were  $0.85 \pm 0.69$ ,  $1.57 \pm 0.78$ , and  $1.71 \pm 0.75$  vs  $0.71 \pm 0.75$ ,  $1 \pm 0.57$  and  $0.42 \pm 0.53$  respectively. Only ANP groups demonstrated a significant difference at 72 h in comparison with sham ( $1.71 \pm 0.75$  vs  $0.4 \pm 0.54$ ,  $P = 0.03$ ) (Figure 5A).

**Alveolar edema index:** Alveolar edema index was

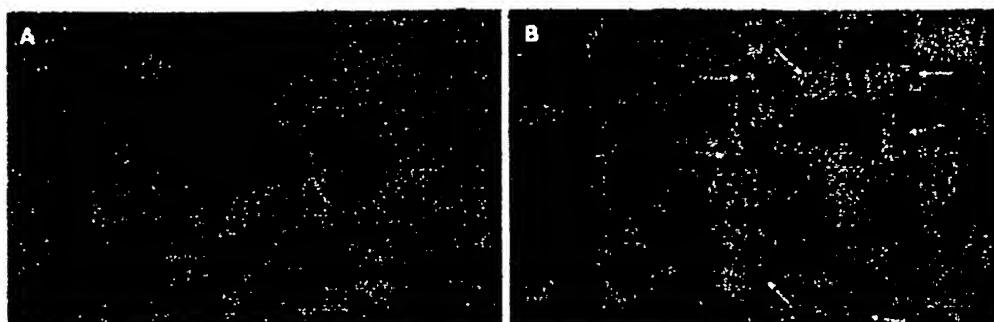


Figure 4 Lung tissue sections from EPO groups and ANP groups showing no fluorescent staining (A) and positive fluorescent staining (B) at 72 h. Arrows indicate the accumulation areas of ox-LDL in the lung.

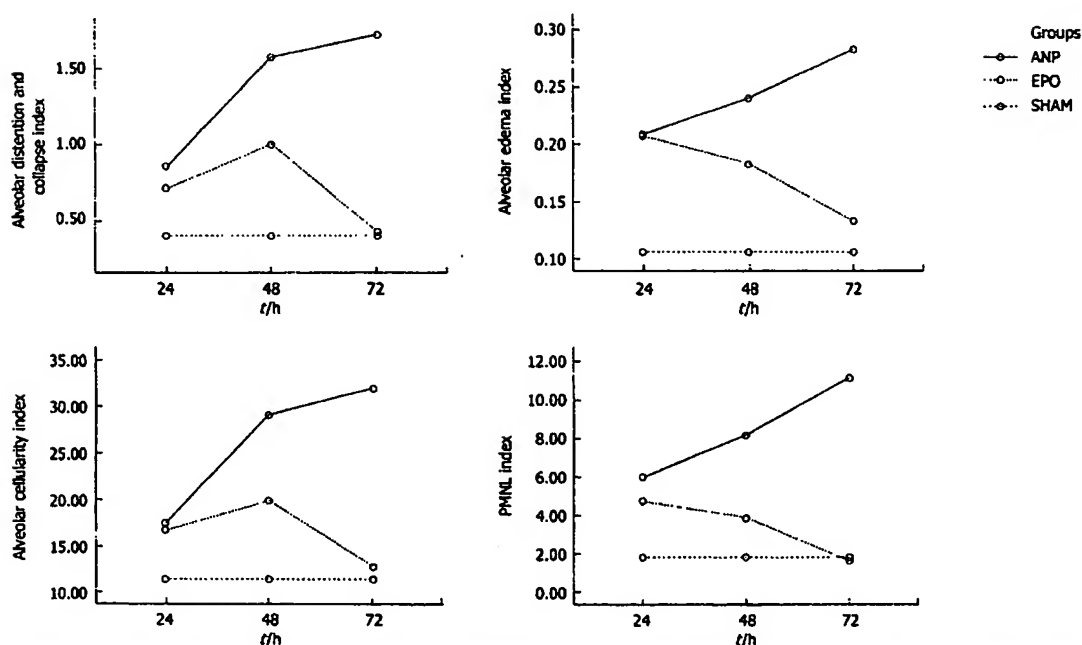


Figure 5 Mean values of alveolar distention and collapse index (A), alveolar edema index (percentage of the alveolar lumen filled with edema) (B), alveolar cellularity index (C) and polymorphonuclear cell index (D) obtained in the seven groups.

significantly different both in ANP groups and in EPO groups depending on the time course ( $P = 0.002$ ). Alveolar edema was more intense in ANP groups at 48 h and 72 h, when compared to EPO groups ( $0.24 \pm 0.05$  vs  $0.18 \pm 0.03$ ,  $P < 0.05$  and  $0.28 \pm 0.03$  vs  $0.13 \pm 0.04$ ,  $P < 0.01$ ). Moreover, at 72 h the mean alveolar edema index determined was the highest in ANP groups and the lowest in EPO groups ( $0.28 \pm 0.03$  vs  $0.13 \pm 0.04$ ). In comparison with sham group, ANP groups had a significantly increased mean alveolar edema index at 24 h, 48 h and 72 h ( $0.1 \pm 0.02$  vs  $0.2 \pm 0.08$ ,  $P = 0.019$ ;  $0.1 \pm 0.02$  vs  $0.24 \pm 0.05$ ,  $P = 0.001$ ; and  $0.1 \pm 0.02$  vs  $0.28 \pm 0.03$ ,  $P = 0.0001$ ; respectively). On the other hand, no statistically significant difference was detected between sham group and EPO groups at 48 h and 72 h ( $0.1 \pm 0.02$  vs  $0.18 \pm 0.03$ ,  $P = 0.149$  and  $0.1 \pm 0.02$

vs  $0.13 \pm 0.04$ ,  $P = 0.968$ ), which might propose that EPO treatment could decrease alveolar edema index at 48 h and 72 h (Figure 5B).

**Alveolar cellularity index:** Alveolar cellularity index was significantly different in either ANP groups or in EPO groups depending on the time course ( $P = 0.011$ ). There was no significant difference in alveolar cellularity index between ANP and EPO groups at 24 h ( $17.42 \pm 9.16$  vs  $16.71 \pm 8.61$ ,  $P > 0.05$ ), whereas the mean value for ANP groups was significantly increased at 48 h and 72 h ( $29.14 \pm 8.39$  vs  $19.85 \pm 5.89$ ,  $P < 0.05$  and  $32 \pm 6.42$  vs  $12.71 \pm 7.11$ ,  $P < 0.01$ ). Additionally, the mean alveolar cellularity index at 72 h was the highest in ANP groups and the lowest in EPO groups ( $32 \pm 6.42$  vs  $12.71 \pm 7.11$ ).



Groups	Sham	ANP1	ANP2	ANP3	EPO1	EPO2	EPO3
Alveolar distention collapse	0.4 ± 0.54	0.85 ± 0.69	1.57 ± 0.78	1.71 ± 0.75	0.71 ± 0.75	1 ± 0.57	0.42 ± 0.53
Alveolar edema index	0.1 ± 0.02	0.2 ± 0.08	0.24 ± 0.05	0.28 ± 0.03	0.2 ± 0.04	0.18 ± 0.03	0.13 ± 0.04
Alveolar cellularity index	11.4 ± 8.14	17.42 ± 9.16	29.14 ± 8.39	32 ± 6.42	16.71 ± 8.61	19.85 ± 5.89	12.71 ± 7.11
PMNL cell index	1.8 ± 1.78	6 ± 3.51	8.14 ± 3.48	11.14 ± 5.55	4.71 ± 2.36	3.85 ± 2.19	1.57 ± 1.61

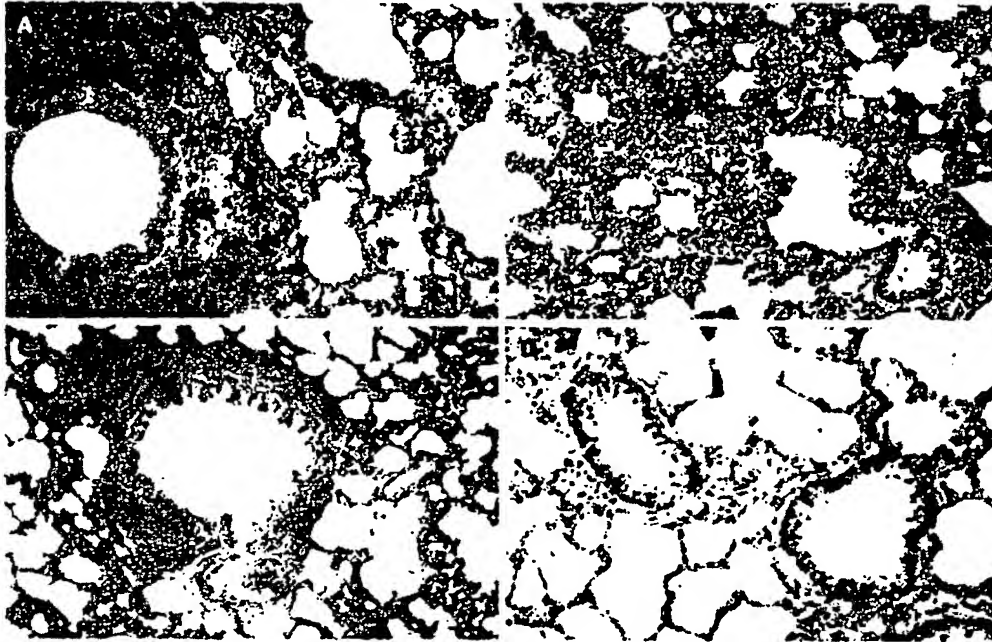


Figure 6 Light microscopy revealing significant lung injury-associated alveolar septal thickening, interstitial edema, infiltration of inflammatory cells, destruction of alveolar wall (emphysema), and microabscess formation in ANP groups at 48 h (A) and 72 h (B), and attenuation of inflammatory reaction, edema and emphysema in EPO groups at 48 h (C) and 72 h (D).

Compared with sham group, alveolar cellularity index was significantly increased in only ANP groups at 48 h and 72 h ( $11.4 \pm 8.14$  vs  $29.14 \pm 8.39$ ,  $P = 0.006$  and  $11.4 \pm 8.14$  vs  $32 \pm 6.42$ ,  $P = 0.001$ ). This might suggest that EPO administration following ANP could decrease alveolar cellularity index at 48 h and 72 h (Figure 5C).

**PMNL index:** A statistically significant difference was observed in PMNL index between ANP and EPO groups with respect to the time intervals ( $P = 0.009$ ). PMNL index was similar either in ANP groups or in EPO groups at 24 h ( $6 \pm 3.51$  vs  $4.71 \pm 2.36$ ,  $P > 0.05$ ). However, EPO treatment significantly decreased the mean PMNL index at 48 h and 72 h ( $8.14 \pm 3.48$  vs  $3.85 \pm 2.19$ ,  $P < 0.05$  and  $11.14 \pm 5.55$  vs  $1.57 \pm 1.61$ ,  $P < 0.01$ ). The mean  $\pm$  SD value at 72 h was the greatest in ANP groups and the lowest in EPO groups ( $11.14 \pm 5.55$  vs  $1.57 \pm 1.61$ ). There was no statistically significant difference in PMNL index at 24 h, 48 h and 72 h between ANP and EPO groups ( $1.8 \pm 1.78$  vs  $4.71 \pm 2.36$ ,  $P = 0.315$ ;  $1.8 \pm 1.78$  vs  $3.85 \pm 2.19$ ,  $P = 0.930$ ; and  $1.8 \pm 1.78$  vs  $1.57 \pm 1.61$ ,  $P =$

1.00, respectively), whereas ANP induction resulted in an increased PMNL index at 48 h and 72 h ( $1.8 \pm 1.78$  vs  $8.14 \pm 3.48$ ,  $P = 0.028$  and  $1.8 \pm 1.78$  vs  $11.14 \pm 5.55$ ,  $P = 0.0001$ , respectively) but not at 24 h ( $1.8 \pm 1.78$  vs  $6 \pm 3.51$ ,  $P = 0.725$ ). This might be explained as EPO administration could decrease PMNL index at 48 h and 72 h (Figure 5D). The histopathological indexes of lung injury (mean  $\pm$  SD) are listed in Table 3. The representative light microscopic views of lung injury at 48 h and 72 h, and necrotizing pancreatitis with severe fatty necrosis in ANP and EPO groups are shown in Figures 6 and 7. According to the above-mentioned criteria, it might be speculated that EPO administration could alleviate pulmonary injury by decreasing alveolar edema, alveolar cellularity and PMNL indexes at 48 h and 72 h following taurocolic acid-induced pancreatitis. The effect of EPO on alveolar distention and collapse was restricted at 72 h.

## DISCUSSION

ANP is an inflammatory disorder with various systemic

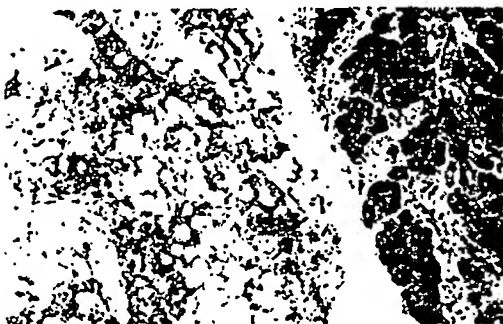


Figure 7 Light microscopic view of pancreatitis with severe fatty necrosis.

complications. ALI and ARDS are the most dreadful complications of ANP and impending catastrophe which is difficult to deal with clinically. Various medications directed at key stages of the pathophysiology are not clinically efficacious as indicated in the preceding experimental trials<sup>[23]</sup>. Therefore, therapies for preventing or reversing lung injury would be ideal for the treatment of AP<sup>[1,2,3,24-26]</sup>.

Randomized studies of AP in the clinical setting do have limitations. In this regard, reliable AP animal models are of paramount importance. Taurocholate infusion model is a well-established ANP rat model that induces multiple organ failure involving the lung<sup>[27]</sup>. Moreover, Milani *et al.*<sup>[28]</sup> found that mechanical and morphologic alterations in pancreatitis-associated pulmonary injury in rats are similar to those observed in humans.

The pathophysiology of ALI/ARDS and most of other pulmonary complications is multifactorial in ANP. The major pathway is the induction of a strong inflammatory response both in experimental models and in patients<sup>[29]</sup>. Regardless of the priming process, the disease progression can be viewed as three phases in continuum: local inflammation of the pancreas (a generalized inflammation stage and SIRS), and the final stage of multiorgan dysfunction<sup>[24,25]</sup>. The first sign of MODS is often the impaired lung function that manifests itself clinically as ARDS<sup>[1,2,24,25,29]</sup>. SIRS is one of the crucial reasons for pancreatitis-associated lung injury and PMNL plays a central role with various inflammatory cytokines and reactive oxygen species (ROS)<sup>[2,29,31]</sup>. Many researchers have focused their efforts on preventing AP-induced lung injury by pharmacologic interventions. Attractively, recent works have discovered the potential role of EPO as a multifunctional endogenous mediator offering cytoprotective effect against injury in various tissues including lung<sup>[16-19]</sup>. In multiple species including humans, many tissues injured by ischemia, mechanical trauma, excitotoxins, and other stressors are significantly improved by administration of EPO following injury<sup>[3,2]</sup>. The presence of a therapeutic window dictates specific time constraints for efficacious administration of exogenous EPO as a cytoprotectant<sup>[9]</sup>. According to this hypothesis we administered EPO immediately following the induction of pancreatitis and evaluated its effect in three different time courses.

The principle mechanism by which EPO confers tissue protection involves the modulation of cellular apoptosis. EPO inhibits the apoptotic mechanisms of injury, including preservation of cellular membrane asymmetry to prevent inflammation, can therefore be regarded as a general tissue-protective cytokine<sup>[11,12,14]</sup>. Agents that can prevent apoptosis can be effective long after the occurrence of injury<sup>[3]</sup>. This phenomenon might describe the long protective effect of EPO on lung injury in our study, particularly at 48 h and 72 h. We would also like to emphasize that, in patients with a severe attack, the effects of distant organ damage including lung injury, are often not fully established and become apparent only after the following 48 h. There is thus a therapeutic window between hospital presentation and development of distant organ dysfunction. As an obvious time window existed in this process, therapeutic approach should focus on it during this period. From this assumption, the animals were sacrificed on postoperative hours 24, 48 and 72 for histopathological and biochemical evaluations in our study.

Another crucial determinant for observing the cytoprotective effect of EPO is the serum concentration. The serum concentration of EPO required for tissue protection is higher than that required for erythropoiesis. Preclinical data suggest that the minimum therapeutic level needed for protection against tissue injury appears to be 300-500 mIU/kg body weight (intravenously or intraperitoneally) for the organs to be adequately investigated. EPO administration (100-1000 U/kg body weight) achieves possible systemic protective effects whereas high doses of EPO (3000-5000 U/kg body weight) are necessary for cardioprotection and neuroprotection<sup>[33]</sup>. According to this, we administered EPO at the dose of 1000 mIU/kg body weight to observe the cytoprotective effects.

EPO plays a dual role in vascular protection by preserving endothelial cell integrity<sup>[6,8,9]</sup>, thus playing a role in maintaining the integrity of microvasculature<sup>[11]</sup>. One of the major factors for the development of alveolar edema in ANP is the increased microvascular permeability. The experimental protocol we performed let us to measure the amount of edema within alveoli. We used alveolar edema index and alveolar distension and collapse index as markers of ALI according to the previous observations suggesting that histologic evidence of pulmonary tissue injury can appear before the development of clinically relevant respiratory mechanical changes<sup>[23]</sup>. We prefer three different time courses, since pulmonary injury indexes are quite intense in taurocolic acid induced acute pancreatitis on d 1 and 3, some of which persist through d 8<sup>[22]</sup>. In the present study, pulmonary edema, alveolar cellularity index and PMNL index (pulmonary injury index) were significantly reduced in EPO groups at 48 h and 72 h, suggesting that EPO can preserve endothelial cell integrity.

Oxidative stress has been implicated as a crucial landmark by increasing endothelial permeability in ARDS<sup>[1]</sup>. ROS scavengers possess protective effect against local acute pancreatitis-associated with lung injury<sup>[31,34,35]</sup>. In addition to other effects, EPO has been demonstrated in various tissues to be an antioxidant as it can decrease

the plasma iron concentration and increase the ability of plasma to inhibit lipid peroxidation<sup>[16,17]</sup>. In the present study, we determined the tissue levels of thiobarbituric acid reactant MDA, which is considered a good indicator of lipid peroxidation, and found a significant decrease in EPO group when compared to ANP groups in all three time courses. This might be attributed to the antioxidant effect of EPO. Furthermore, the tissue damage induced by ANP was associated with a significant ox-LDL accumulation either in pancreas samples or in lung tissue specimens. Ox-LDL is an early product of lipid peroxidation and ox-LDL accumulation in pancreatitis is associated with lung injury.

At present, the role of inflammatory mediators in the pathogenesis of ARDS has become a hot issue in the research field. EPO has been demonstrated to prevent cellular inflammation by inhibiting several proinflammatory cytokines, such as IL-6, TNF- $\alpha$ , and monocyte chemoattractant protein<sup>[17,18]</sup>. Attractively, these effects of EPO can be mediated by both hormonal and paracrine modalities<sup>[18]</sup>. There is mounting evidence that proinflammatory cytokines are the agents behind the systemic complications of AP<sup>[1,2]</sup>. It was reported that systemic inflammation plays a role in development of ALI triggered by pancreatitis<sup>[14]</sup>. The critical players of this process include proinflammatory cytokines including IL-1 $\beta$ , TNF- $\alpha$ , IL-6, IL-8, and platelet activating factor (PAF)<sup>[20]</sup>. Among these, the serum and/or tissue levels of TNF- $\alpha$ , IL-2 and IL-6 were analyzed in this study. Regardless of the model of acute pancreatitis, inhibition of the potent cytokine TNF- $\alpha$  might decrease organ injury and improve survival<sup>[19]</sup>. The tissue levels of TNF- $\alpha$  in the lungs were analyzed with immunohistochemical staining. Since no quantitative analysis was possible unavailable techniques, we evaluated this parameter not statistically but morphologically. IL-6 is another proinflammatory cytokine, and its high circulating level has been shown to be an excellent predictor of the severity of ARDS with different etiologies, including AP<sup>[14]</sup>. Moreover, IL-6 has been proposed to be one of the best prognostic parameters for pulmonary failure in human AP<sup>[30,31]</sup>. Mayer *et al*<sup>[31]</sup> have confirmed the important role of soluble IL-2 receptors (a lymphocyte activation marker), as a marker for severe AP, especially when complicated by lung or kidney failure or sepsis during lethal course of the disease<sup>[31]</sup>. In the present study, pulmonary injury in ANP groups was characterized by the increased serum or tissue IL-6 and TNF- $\alpha$  level. EPO treatment significantly decreased IL-6 and TNF- $\alpha$  level which might be due to the antiinflammatory properties of its molecule. However, we did not determine a statistically significant difference in the IL-2 level among the groups. This result might reflect the ineffectiveness of EPO on lymphocyte activity.

In conclusion, EPO administration plays a crucial role in preventing histological changes of ALI induced by experimental ANP. Moreover, it can significantly reduce the circulating and tissue levels of proinflammatory cytokines which have been considered the key factors for ALI. Additionally, oxidative stress markers are decreased particularly at 72 h following the induction of pancreatitis that might be attributed to the long-lasting

antioxidant effect of EPO. All these findings show that EPO can attenuate ANP-induced lung injury by inhibiting PMNL accumulation, decreasing the circulating levels of proinflammatory cytokines, preserving microvascular endothelial cell integrity and reducing oxidative stress-associated lipid peroxidation. Years of clinical application in patients with anemia and chronic renal disease indicate that EPO is safe and well tolerated and can act as an ideal cytoprotective agent<sup>[7,12,33]</sup>. Nevertheless, the issue which should also be taken into consideration is that EPO is not an absolutely innocent agent with subsequent clinical toxic effects. Therefore, it would be of value to investigate its pharmacodynamics, pharmacokinetics, side-effects, administration routes and doses before used as a potential candidate for the treatment of ANP-associated ALI in routine clinical practice. In other words, this is a preliminary study and more experiments are necessary for the efficacy and potentially cytoprotective mechanisms of EPO action.

## COMMENTS

### Background

Pulmonary complication is the major cause for mortality in acute necrotizing pancreatitis (ANP). Since no absolutely effective treatment is available at present, therapies for preventing or reversing lung injury would be ideal for the treatment of AP.

### Research frontiers

Erythropoietin (EPO) has long been known as a glycoprotein hormone that regulates erythropoiesis in mammals. Beyond its hematopoietic properties, EPO modulates a broad array of vital cellular processes including progenitor stem cell development, cellular integrity, and angiogenesis. EPO has recently been demonstrated to play a role in prolonging cell survival by acting as an antiapoptotic agent. EPO inhibits the apoptotic mechanisms of injury including preservation of cellular membrane asymmetry to prevent inflammation, and can therefore be regarded as a general tissue-protective cytokine. Additionally, experimental evidence supports a vigorous cytoprotective effect of EPO, which is now considered to have applicability in a variety of disorders, such as cerebral ischemia, myocardial infarction, and chronic congestive heart failure.

### Related publications

The present study was an experimental study addressing the beneficial effects of EPO on lung injury. We cited several articles from other investigators reporting researches of EPO action on various tissues including lungs.

### Innovations and breakthroughs

Recent works have discovered the potential role of EPO as a multifunctional endogenous mediator offering cytoprotective effect against injury in various tissues including the lungs. Pretreatment with EPO appears to attenuate ischemia-reperfusion-induced lung injury and hyperoxic lung injury in neonatal rats. From this point of view we evaluated the potential protecting effects of EPO against acute lung injury in a rat model of ANP. Our data show that EPO administration can alleviate pulmonary injury parameters in experimental pancreatitis.

### Applications

The impending catastrophe in ANP is generally preceded by acute lung injury. Despite improved understanding of the pathogenesis of ARDS, pharmacological modalities are ineffective in decreasing its mortality. None of the randomized clinical trials using novel therapeutic agents has demonstrated an improvement in patient outcome. The verification of cytoprotective effects of EPO on acute lung injury in a model of experimental pancreatitis might shed some valuable light on the novel effective therapeutic interventions.

### Terminology

Erythropoietin (EPO), a 30.4-kDa glycoprotein and a member of the type I

cytokine superfamily, was first introduced as a hormone that regulates erythroid progenitors within the bone marrow to mature into erythrocytes, through binding to its specific cell surface receptors. Acute necrotizing pancreatitis (ANP) is a life-threatening necroinflammatory disease of pancreas with significant morbidity and mortality rates. Acute lung injury (ALI) is one of the most dreadful complications of AP which might be described as the continuum of pathological responses to pulmonary parenchymal injury. Acute respiratory distress syndrome (ARDS) is a severe form of ALI and acute pulmonary inflammation syndrome and resultant increased capillary endothelial permeability with clinical features of severe dyspnea and extreme hypoxemia refractory to a high inspired oxygen concentration.

### Peer review

This is a well-designed and interesting study about the beneficial effects of EPO on lung injury in an experimental model of ANP. Since this is a preliminary study as discussed by the authors, more comprehensive experiments should be carried out to reveal the underlying cellular mechanisms of EPO's cytoprotective action against lung injury.

### REFERENCES

- Bhatia M, Mochhala S. Role of inflammatory mediators in the pathophysiology of acute respiratory distress syndrome. *J Pathol* 2004; 202: 145-156
- Bhatia M, Wong FL, Cao Y, Lau HY, Huang J, Puneet P, Chevali L. Pathophysiology of acute pancreatitis. *Pancreatol* 2005; 5: 132-144
- Makhija R, Kingsnorth AN. Cytokine storm in acute pancreatitis. *J Hepatobiliary Pancreat Surg* 2002; 9: 401-410
- Pastor CM, Matthay MA, Frossard JL. Pancreatitis-associated acute lung injury: new insights. *Chest* 2003; 124: 2341-2351
- Coleman T, Brines M. Science review: recombinant human erythropoietin in critical illness: a role beyond anemia? *Crit Care* 2004; 8: 337-341
- Chong ZZ, Kang JQ, Maiese K. Angiogenesis and plasticity: role of erythropoietin in vascular systems. *J Hematother Stem Cell Res* 2002; 11: 863-871
- Genc S, Koroglu TF, Genc K. Erythropoietin as a novel neuroprotectant. *Res Neural Neurosci* 2004; 22: 105-119
- Chong ZZ, Kang JQ, Maiese K. Erythropoietin is a novel vascular protectant through activation of Akt1 and mitochondrial modulation of cysteine proteases. *Circulation* 2002; 106: 2973-2979
- Chong ZZ, Kang JQ, Maiese K. Apaf-1, Bcl-xL, cytochrome c, and caspase-9 form the critical elements for cerebral vascular protection by erythropoietin. *J Cereb Blood Flow Metab* 2003; 23: 320-330
- Chong ZZ, Li F, Maiese K. Activating Akt and the brain's resources to drive cellular survival and prevent inflammatory injury. *Histol Histopathol* 2005; 20: 299-315
- Ghezzi P, Brines M. Erythropoietin as an antiapoptotic, tissue-protective cytokine. *Cell Death Differ* 2004; 11 Suppl 1: S37-S44
- Maiese K, Li F, Chong ZZ. New avenues of exploration for erythropoietin. *JAMA* 2005; 293: 90-95
- Kumral A, Uysal N, Tugyan K, Sonmez A, Yilmaz O, Gokmen N, Kiray M, Genc S, Duman N, Koroglu TF, Ozkan H, Genc K. Erythropoietin improves long-term spatial memory deficits and brain injury following neonatal hypoxia-ischemia in rats. *Behav Brain Res* 2004; 153: 77-86
- Savino R, Ciliberto G. A paradigm shift for erythropoietin: no longer a specialized growth factor, but rather an all-purpose tissue-protective agent. *Cell Death Differ* 2004; 11 Suppl 1: S2-S4
- Mancini DM, Katz SD, Lang CC, LaManca J, Hudaihed A, Androne AS. Effect of erythropoietin on exercise capacity in patients with moderate to severe chronic heart failure. *Circulation* 2003; 107: 294-299
- Wu H, Ren B, Zhu J, Dong G, Xu B, Wang C, Zheng X, Jing H. Pretreatment with recombinant human erythropoietin attenuates ischemia-reperfusion-induced lung injury in rats. *Eur J Cardiothorac Surg* 2006; 29: 902-907
- Ozer EA, Kumral A, Ozer E, Yilmaz O, Duman N, Ozkal S, Koroglu T, Ozkan H. Effects of erythropoietin on hyperoxic lung injury in neonatal rats. *Pediatr Res* 2005; 58: 38-41
- Yildirim E, Ozisik K, Solaroglu I, Kaptanoglu E, Beskonakli E, Sargon MF, Kilinc K, Sakinci U. Protective effect of erythropoietin on type II pneumocyte cells after traumatic brain injury in rats. *J Trauma* 2005; 58: 1252-1258
- Yildirim E, Solaroglu I, Okutan O, Ozisik K, Kaptanoglu E, Sargon MF, Sakinci U. Ultrastructural changes in tracheobronchial epithella following experimental traumatic brain injury in rats: protective effect of erythropoietin. *J Heart Lung Transplant* 2004; 23: 1423-1429
- Chen CC, Wang SS, Tsay SH, Lee FY, Lu RH, Chang FY, Lee SD. Effects of gabexate mesilate on serum inflammatory cytokines in rats with acute necrotizing pancreatitis. *Cytokine* 2006; 33: 95-99
- Leme AS, Lichtenstein A, Arantes-Costa FM, Landucci EC, Martins MA. Acute lung injury in experimental pancreatitis in rats: pulmonary protective effects of crotafotin and N-acetylcysteine. *Shock* 2002; 18: 428-433
- Lichtenstein A, Milani R Jr, Fermezian SM, Leme AS, Capelozzi VL, Martins MA. Acute lung injury in two experimental models of acute pancreatitis: infusion of saline or sodium taurocholate into the pancreatic duct. *Crit Care Med* 2000; 28: 1497-1502
- Udobi KF, Childs E, Touijer K. Acute respiratory distress syndrome. *Am Fam Physician* 2003; 67: 315-322
- Bhatia M, Brady M, Shokuh S, Christmas S, Neoptolemos JP, Slavin J. Inflammatory mediators in acute pancreatitis. *J Pathol* 2000; 190: 117-125
- Bhatia M. Novel therapeutic targets for acute pancreatitis and associated multiple organ dysfunction syndrome. *Curr Drug Targets Inflamm Allergy* 2002; 1: 343-351
- Puneet P, Mochhala S, Bhatia M. Chemokines in acute respiratory distress syndrome. *Am J Physiol Lung Cell Mol Physiol* 2005; 288: L3-L15
- Chan YC, Leung PS. Acute pancreatitis: animal models and recent advances in basic research. *Pancreas* 2007; 34: 1-14
- Milani Junior R, Pereira PM, Dolhnikoff M, Saldiva PH, Martins MA. Respiratory mechanics and lung morphometry in severe pancreatitis-associated acute lung injury in rats. *Crit Care Med* 1995; 23: 1882-1889
- Granger J, Remick D. Acute pancreatitis: models, markers, and mediators. *Shock* 2005; 24 Suppl 1: 45-51
- Takala A, Jousela I, Takkunen O, Kautiainen H, Jansson SE, Orpana A, Karonen SL, Repo H. A prospective study of inflammation markers in patients at risk of indirect acute lung injury. *Shock* 2002; 17: 252-257
- Browne GW, Pitchumoni CS. Pathophysiology of pulmonary complications of acute pancreatitis. *World J Gastroenterol* 2006; 12: 7087-7096
- Erbayraktar S, Grasso G, Sfacteria A, Xie QW, Coleman T, Kreilgaard M, Torup L, Sager T, Erbayraktar Z, Gokmen N, Yilmaz O, Ghezzi P, Villa P, Fratelli M, Casagrande S, Leist M, Helboe L, Gerwein J, Christensen S, Geist MA, Pedersen LO, Cerami-Hand C, Wuerth JP, Cerami A, Brines M. Asialoerythropoietin is a nonerythropoietic cytokine with broad neuroprotective activity in vivo. *Proc Natl Acad Sci USA* 2003; 100: 6741-6746
- Bogoyevitch MA. An update on the cardiac effects of erythropoietin cardioprotection by erythropoietin and the lessons learnt from studies in neuroprotection. *Cardiovasc Res* 2004; 63: 208-216
- Demols A, Van Laethem JL, Quertinmont E, Legros F, Louis H, Le Moine O, Deviere J. N-acetylcysteine decreases severity of acute pancreatitis in mice. *Pancreas* 2000; 20: 161-169
- Esefoglul M, Gul M, Ates B, Yilmaz I. Ultrastructural clues for the protective effect of ascorbic acid and N-acetylcysteine against oxidative damage on caerulein-induced pancreatitis. *Pancreatol* 2006; 6: 477-485
- Bany-Mohammed FM, Slivka S, Hallman M. Recombinant human erythropoietin: possible role as an antioxidant in premature rabbits. *Pediatr Res* 1996; 40: 381-387
- Kaptanoglu E, Solaroglu I, Okutan O, Surucu HS, Akbiyik F,

- Beskonakli E. Erythropoietin exerts neuroprotection after acute spinal cord injury in rats: effect on lipid peroxidation and early ultrastructural findings. *Neurosurg Rev* 2004; 27: 113-120
- 38 Chong ZZ, Kang JQ, Maiese K. Hematopoietic factor erythropoietin fosters neuroprotection through novel signal transduction cascades. *J Cereb Blood Flow Metab* 2002; 22: 503-514
- 39 Denham W, Yang J, Wang H, Botchkina G, Tracey KJ, Norman J. Inhibition of p38 mitogen activate kinase attenuates the severity of pancreatitis-induced adult respiratory distress syndrome. *Crit Care Med* 2000; 28: 2567-2572
- 40 Remick DG, Bolgos GR, Siddiqui J, Shin J, Nemzek JA. Six at six: interleukin-6 measured 6 h after the initiation of sepsis predicts mortality over 3 days. *Shock* 2002; 17: 463-467
- 41 Mayer J, Rau B, Gansauge F, Beger HG. Inflammatory mediators in human acute pancreatitis: clinical and pathophysiological implications. *Gut* 2000; 47: 546-552
- 42 Maiese K, Li F, Chong ZZ. Erythropoietin in the brain: can the promise to protect be fulfilled? *Trends Pharmacol Sci* 2004; 25: 577-583
- 43 Jelkmann W, Wagner K. Beneficial and ominous aspects of the pleiotropic action of erythropoietin. *Ann Hematol* 2004; 83: 673-686

S- Editor Liu Y L- Editor Wang XL E- Editor Ma WH



## RESEARCH PAPER

# Post-ischemic treatment with erythropoietin or carbamylated erythropoietin reduces infarction and improves neurological outcome in a rat model of focal cerebral ischemia

Y Wang<sup>1</sup>, ZG Zhang<sup>1</sup>, K Rhodes<sup>2</sup>, M Renzi<sup>2</sup>, RL Zhang<sup>1</sup>, A Kapke<sup>3</sup>, M Lu<sup>3</sup>, C Pool<sup>4</sup>, G Heavner<sup>4</sup> and M Chopp<sup>1,5</sup>

<sup>1</sup>Department of Neurology, Henry Ford Health Science Center, Detroit, MI, USA; <sup>2</sup>CNS Research Team, Johnson & Johnson Pharmaceutical Research & Development, Spring House, PA, USA; <sup>3</sup>Department of Biostatistics and Research Epidemiology, Henry Ford Health Science Center, Detroit, MI, USA; <sup>4</sup>Protein Design, Centocor, Radnor, PA, USA and <sup>5</sup>Department of Physics, Oakland University, Rochester, MI, USA

**Background and purpose:** Recombinant human erythropoietin (rhEPO; Epoetin- $\alpha$ ; PROCIT<sup>™</sup>) has been shown to exert neuroprotective and restorative effects in a variety of CNS injury models. However, limited information is available regarding the dose levels required for these beneficial effects or the neuronal responses that may underlie them. Here we have investigated the dose-response to rhEPO and compared the effects of rhEPO with those of carbamylated rhEPO (CEPO) in a model of cerebral stroke in rats.

**Experimental approach:** Rats subjected to embolic middle cerebral artery occlusion (MCAo) were treated with rhEPO or CEPO, starting at 6 h and repeated at 24 and 48 h, after MCAo. Cerebral infarct volumes were assessed at 28 days and neurological impairment at 7, 14, 21 and 28 days, post-MCAo.

**Key results:** rhEPO at dose levels of 500, 1150 or 5000 IU kg<sup>-1</sup> or CEPO at a dose level of 50  $\mu$ g kg<sup>-1</sup> significantly reduced cortical infarct volume and reduced neurologic impairment. All doses of rhEPO, but not CEPO, produced a transient increase in haematocrit, while rhEPO and CEPO substantially reduced the number of apoptotic cells and activated microglia in the ischemic boundary region.

**Conclusions and implications:** These data indicate that rhEPO and CEPO have anti-inflammatory and anti-apoptotic effects, even with administration at 6 h following embolic MCAo in rats. Taken together, these actions of rhEPO and CEPO are likely to contribute to their reduction of neurologic impairment following cerebral ischemia.

*British Journal of Pharmacology* (2007) 151, 1377–1384; doi:10.1038/sj.bjp.0707285; published online 2 July 2007

**Keywords:** MCAo; EPO; CEPO; microglia; infarct volume; neurobehavioural outcome

**Abbreviations:** CEPO, carbamylated EPO; EPOR, EPO receptor; MCAo, middle cerebral artery occlusion; rhEPO, recombinant human erythropoietin

## Introduction

Erythropoietin (EPO) is a naturally occurring cytokine most widely recognized for its role in stimulating the maturation, differentiation and survival of haematopoietic progenitor cells (Naranda *et al.*, 1999; Wojchowski *et al.*, 1999). Recently, however, a more general cytoprotective role for EPO has been described. In the central nervous system

(CNS), for example, expression of EPO and the EPO receptor (EPOR) is greatly increased in neurons, neuronal progenitor cells, glia and cerebrovascular endothelial cells in response to many different types of cell injury (Anagnostou *et al.*, 1990; Masuda *et al.*, 1994; Bernaudin *et al.*, 1999; Marti, 2004; Wang *et al.*, 2004; Tsai *et al.*, 2006). Inhibition of EPO activity by administration of soluble EPOR worsens the severity of injury (Sakanaka *et al.*, 1998), suggesting that endogenously produced EPO is directly involved in an intrinsic neuronal repair pathway. In the best-studied experimental neuronal injury paradigm, hypoxic–ischaemic brain injury, an up-regulation of neuronal, endothelial and glial EPO and EPOR expression occurs following cerebral ischaemia (Lewczuk

Correspondence: Professor M Chopp, Department of Neurology, Henry Ford Health Science Center, Ed. & Res. Bldg., Rm 3056, 2799 West Grand Boulevard, Detroit, MI 48202, USA.

E-mail: choppm@neuro.hfh.edu

Received 9 January 2007; revised 2 March 2007; accepted 14 March 2007; published online 2 July 2007

*et al.*, 2000; Sinor and Greenberg, 2000; Siren *et al.*, 2001; Marti, 2004; Maiese *et al.*, 2005). Administration of exogenous recombinant human EPO (rhEPO) after focal or global cerebral ischaemia (Sadamoto *et al.*, 1998; Sakanaka *et al.*, 1998; Brines *et al.*, 2004; Leist *et al.*, 2004), augments the cytoprotective and restorative EPO response pathway leading to a substantial improvement in neurobehavioural outcome. The neuroprotective and restorative activity of exogenous EPO in rodent ischaemia models has been documented in studies published by several independent laboratories and has also translated into the human clinical setting where evidence for a clinical benefit of rhEPO in patients suffering middle cerebral artery (MCA) territory stroke has been reported (Ehrenreich *et al.*, 2002).

Carbamylated EPO (CEPO) has been observed in patients suffering from end-stage renal disease (Mun and Golper, 2000; Park *et al.*, 2004). CEPO does not show any binding to the classical EPOR *in vitro* or stimulate an haematopoietic response *in vivo*, but nevertheless has been shown to exert neuroprotective effects when administered following cerebral ischaemia or other types of neuronal injury (Leist *et al.*, 2004). Although the specific cellular mechanisms responsible for the cytoprotective activity of CEPO, and the relationships between signalling pathways that mediate the beneficial effects of rhEPO and CEPO remain to be fully elucidated, the protective effects of CEPO may involve signalling through the common  $\beta$ -receptor (CD 131) (Brines *et al.*, 2004).

Although the beneficial effects of exogenous rhEPO and CEPO have been demonstrated in a range of cerebral ischaemia models, investigators frequently use high doses of rhEPO (typically 5000 IU kg<sup>-1</sup>) in these studies. As this dose of rhEPO is far greater than that required to evoke haematopoietic response, there remains a need for a systematic investigation of the dose levels, treatment window and treatment interval that are required for efficacy in these models. Moreover, the levels of peripherally administered EPO or CEPO that reach brain tissue in models of cerebral ischaemia have not been reported, highlighting the need to establish a link between peripheral intravenous dose and brain levels of drug. In the present study, we examined the dose-response to EPO and CEPO in an embolic model of MCA occlusion (MCAo) stroke, using a repeated dosing protocol that parallels the dosing regimen reported to show clinical benefit in human stroke patients (Ehrenreich *et al.*, 2002). We examined the effects of rhEPO or CEPO treatment on neurobehavioural outcome and volume of infarction, when the treatment was initiated 6 h after MCAo.

## Methods

All experimental procedures were approved by the Henry Ford Hospital Committee for the Care of Experimental Animals.

### Model of embolic MCAo

Male Wistar rats (The Jackson Laboratory, Bar Harbor, ME, USA) weighing 350–400 g were employed in the present study. The MCA was occluded by placement of an embolus at the origin of the MCA, as described previously (Zhang *et al.*, 1997). This model frequently exhibits spontaneous clot lysis

and reperfusion within 24–48 h following MCAo (Zhang *et al.*, 1997; Jiang *et al.*, 1998).

### ELISA measurements of rhEPO and CEPO levels

Brain homogenate supernatant, plasma and cerebrospinal fluid (CSF) samples were used for measurement of rhEPO or CEPO levels using a human EPO Quantikine Cytokine IVD enzyme-linked immunosorbent assay (ELISA) kit (R&D Systems, Minneapolis, MN, USA). As the antibodies used in this kit show reduced affinity for CEPO, a standard curve was generated using CEPO as the target antigen and a correction factor was calculated to adjust the ELISA results to account for the reduced antibody sensitivity. The lower limit of detection in the EPO ELISA was 2.5 mIU ml<sup>-1</sup>.

### Neurological and behavioural assessment

To detect sensorimotor impairments, an array of behavioural tests including foot-fault and the modified neurological severity score (mNSS) were performed before MCAo and at 1, 3, 7, 14, 21 and 28 days after MCAo by an investigator not aware of the treatments. These tests are sensitive and reliable indices of sensorimotor impairments after ischaemic stroke and have been applied extensively in our laboratory to assess neurological outcome following MCAo in rats (Chen *et al.*, 2003; Wang *et al.*, 2004; Zhang *et al.*, 2005).

### Infarct volume

Rats were killed 28 days after MCAo and infarct volume was measured on seven equally spaced (2 mm) haematoxylin and eosin-stained coronal sections, which covers the entire territory supplied by the MCA (Bregma; 4.7 to –7.3 mm), including the ischaemic core, were used for each rat using a Global Lab Image analysis program (Data Translation, Marlboro, MA, USA), as described previously (Paxinos and Watson, 1986; Zhang *et al.*, 1997). Briefly, the area of both hemispheres and the area containing the ischaemic neuronal damage (mm<sup>2</sup>) were calculated by tracing the area on the computer screen. The lesion volume (mm<sup>3</sup>) was determined by multiplying the appropriate area by the section interval thickness. To reduce errors associated with processing of tissue for histological analysis, the ischaemic volume is presented as the percentage of infarct volume of the contralateral hemisphere (indirect volume calculation).

### Histology and terminal deoxynucleotidyl transferase-mediated biotinylated UTP nick end labelling

To examine the effect of EPO on microglial response, deparaffinized coronal sections were histochemically stained with peroxidase-labeled isolectin-B<sub>4</sub> from *Griffonia simplicifolia* seeds (GSAI-B<sub>4</sub>-HRP; Sigma, St Louis, MO, USA; Zhang *et al.*, 1997c). Briefly, the sections were incubated with isolectin (20 mg ml<sup>-1</sup>) in phosphate-buffered saline (PBS) containing divalent cations at room temperature for 3 h and then overnight at 4 °C. Sections were then reacted with diaminobenzidine and H<sub>2</sub>O<sub>2</sub> to generate orange-brown reaction product at sites of isolectin-B<sub>4</sub> binding. Eight fields



of view within the ischaemic boundary, defined as an area 0.35 mm away from the infarct rim, were acquired from each coronal section. Four coronal sections from Bregma (0.7 to -1.3 mm), which cover the ischaemic core were used for each rat (Paxinos and Watson, 1986; Zhang *et al.*, 1997). Data are presented as percentage of pixels with isolectin-B4 within the field of view. To measure the number of apoptotic cells, deoxynucleotidyl transferase-mediated biotinylated UTP nick end labelling (TUNEL) was performed using the Apoptosis Detection Kit (ApopTag; Chemicon International, Temecula, CA, USA) according to the manufacturer's protocol. Total number of TUNEL-positive cells in the ischaemic boundary region was counted on four coronal sections per rat. Data are presented as the number of TUNEL-positive cells.

#### Haematocrit

To determine each animal's haematocrit, a blood sample (100  $\mu$ l) was drawn via a tail vein immediately before the initial drug dose treatment and again once per week up to 28 days after MCAo. Haematocrit was measured in microcapillary tubes using standard procedures (Readacrit Centrifuge, Clay Adams, Parsippany, NJ, USA).

#### Experimental protocols

- (1) To determine brain levels of EPO and CEPO: MCAo rats were treated (intravenous) with a bolus dose rhEPO of 1000, 2500, 5000 and 10000 IU kg<sup>-1</sup> or CEPO of 5 and 50  $\mu$ g kg<sup>-1</sup> administered 6 h after MCAo. MCAo rats treated with the same volume of saline were used as a control group. Thirty minutes after administration of rhEPO or CEPO, plasma (400–500  $\mu$ l) and CSF (250–300  $\mu$ l) samples were obtained via tail vein bleed or cisterna magna puncture, respectively. Immediately following blood and CSF collection, animals were perfused with ice-cold saline, and their brains were removed, separated into left and right hemispheres and stored frozen on dry ice. Brains were subsequently thawed, homogenized in 1 ml ice-cold PBS containing a protease inhibitor cocktail (Sigma-Aldrich, St Louis, MO, USA) and centrifuged at 1000 g for 15 min at 4°C to pellet nuclei and cellular debris.
- (2) To examine the dose response of EPO and CEPO on infarct volume and functional outcome, following embolization animals were randomly divided into treatment groups ( $n=10$  per group) and were treated (intravenous, tail vein) with rhEPO at a dose level of 50, 500, 1150 or 5000 IU kg<sup>-1</sup>, CEPO at a dose of 50  $\mu$ g kg<sup>-1</sup> or vehicle (vehicle was PROCrit™ formulation: 2.5 mg human serum albumin, 5.6 mg sodium citrate, 5.6 mg NaCl, 0.06 mg citric acid in 100 ml sterile water (pH 6.9)). Treatment was initiated 6 h after embolization. For each dose level, an intravenous bolus dose of rhEPO, CEPO or vehicle was given 6, 24 and 48 h after MCAo. The injection volume was 0.32–0.37 ml per rat based on 0.1 ml 100 g<sup>-1</sup> animal body weight. Activity units of rhEPO can be converted to mass units based on the formula 120 IU = 1  $\mu$ g protein. Therefore, 500 IU kg<sup>-1</sup> = 4.16  $\mu$ g kg<sup>-1</sup>; 1000 IU kg<sup>-1</sup> = 8.32  $\mu$ g kg<sup>-1</sup>; 2500 IU kg<sup>-1</sup> = 20.8  $\mu$ g kg<sup>-1</sup>; 5000 IU kg<sup>-1</sup> = 41.6  $\mu$ g kg<sup>-1</sup>.

#### Statistics

Data were evaluated for normality and data were not normally distributed. The Generalized Estimating Equation (GEE) approach, considered to have less restriction on data distribution, was employed. Analysis of variance was used to study the effects of treatment, dose and time to first dose on functional recovery. An analysis was performed for each treatment group (rhEPO or CEPO) in comparison to the vehicle control group, respectively. Analysis began testing the treatment/dose by administration time interaction, followed by testing the main effect if no interaction was detected at  $P<0.05$  level, or a pair-wise comparisons, if otherwise. All data are presented as means  $\pm$  s.e. Statistical significance was set at  $P<0.05$ .

#### Drugs

In this paper, rhEPO refers specifically to Epoetin-Alfa (PROCrit; distributed by Ortho Biotech Product, LP, Bridgewater, NJ, USA as the finished commercial product (10000 IU ml<sup>-1</sup>). Doses used in these studies were drawn by syringe directly from the commercial drug vial. All other reagents were obtained from standard commercial vendors except where noted otherwise.

Carbamylated rhEPO (CEPO) was prepared from 50 ml of rhEPO (2.0 mg ml<sup>-1</sup>), obtained from Ortho Biologics Inc. (Manati Puerto Rico). Stock rhEPO was diluted with 50 ml of 1 M borate buffer (pH 8.8). To this solution was added 8.1 g of potassium cyanate, recrystallized from ethanol. The reaction mixture was incubated at 37°C for 24 h and then dialysed twice against 3.5 l of water, and five additional times against 3.5 l of sodium citrate (20 mM, 0.1 M NaCl (pH 6.0)). The resulting solution was concentrated using a Centricon centrifugal concentrator to a final volume of 28 ml. The concentration was determined to be 3.47 mg ml<sup>-1</sup> using an extinction coefficient of  $\epsilon_{0.1\%} = 1.345$ . This concentrated material was analysed by size exclusion high-performance liquid chromatography, polyacrylamide gel electrophoresis gel electrophoresis (4–12% gel), and surface-enhanced laser desorption ionization mass spectrometry (SELDI-MS). The protein was de-glycosylated for mass spectrometry studies as follows: 10  $\mu$ l Rapigest (Waters Corp., Milford, MA, USA) (2 mg ml<sup>-1</sup> in PBS), 3  $\mu$ l NP-40 detergent (15%), 4  $\mu$ l ethanol, 4  $\mu$ l each of PNGase, sialidase and O-glycanase (all from Prozyme Inc., San Leandro, CA, USA) were added to 10  $\mu$ l of CEPO or an EPO control sample and incubated for 72 h at 37°C. Both de-glycosylated and glycosylated samples were analysed by SELDI-MS. The mass spectrum of de-glycosylated, carbamylated EPO showed an increase of 368 AMU over de-glycosylated EPO, corresponding to an average of 8.6 carbamoyl groups per molecule (EPO has eight lysines and a free N terminus). Trinitrobenzene sulphonic acid analysis was unable to detect any free amino groups.

#### Results

##### *Intravenous rhEPO and CEPO cross the blood–brain barrier following MCAo*

As the antibodies used in the ELISA assay to quantitate rhEPO in this study are specific for human EPO, endogenous

rat EPO does not contribute to the observed drug levels and therefore neither CEPO nor EPO was detected in plasma or brain of rats treated with saline. High levels of rhEPO and CEPO were detected in plasma, and measurable levels of the corresponding protein were observed in CSF and brain parenchyma 30 min after an intravenous bolus dose given 6 h after MCAo (Table 1). At the lower dose levels, the levels of EPO achieved in CSF and brain parenchyma were at the low end of the sensitivity range for our ELISA assay and there was considerable variability in the data. Interestingly, there was not a statistically significant difference in rhEPO or CEPO levels in the ipsilateral (that is, MCA occluded) hemisphere versus the contralateral non-ischaemic hemisphere. Nevertheless, these data demonstrate that across a fairly wide dose range, peripherally administered rhEPO and CEPO crossed the blood-brain barrier (BBB) and entered the brain parenchyma and CSF compartments.

#### Drug effects on haematocrit

Administration of three equal intravenous bolus doses of rhEPO (50, 500, 1150 or 5000 IU kg<sup>-1</sup>) at 6, 24 and 48 h following MCAo produced significant ( $P < 0.05$ ) but transient rise in haematocrit, with the peak response occurring at day 14 after the initial dose (Figure 1). Thereafter, haematocrit levels decreased, approaching pre-treatment levels at day 28. Consistent with previous reports (Leist *et al.*, 2004), administration of three equal intravenous bolus doses of CEPO (50 µg kg<sup>-1</sup>) at 6, 24 and 48 h following MCAo did not alter haematocrit at any time point.

#### Delayed (6 h) treatment with EPO or CEPO reduces infarct volume

To examine the long-term neuroprotective effects of CEPO and rhEPO, ischaemic rats were treated 6 h after MCAo with different dose levels of CEPO or rhEPO and killed 28 days after MCAo. We first measured the entire infarct volume including the cortex and the subcortex. Treatment with rhEPO at doses of 500 and 5000 IU kg<sup>-1</sup> or CEPO at a dose of 50 µg kg<sup>-1</sup>, significantly ( $P < 0.05$ ) reduced mean infarct volume compared with the mean infarct volume in animals treated with vehicle (Figure 2). The rhEPO 5000 IU kg<sup>-1</sup> group exhibited 28% reduction of mean infarct volume, an effect that is indistinguishable with the outcome observed in animals treated with 50 µg kg<sup>-1</sup> CEPO (27%). The rhEPO 500 IU kg<sup>-1</sup> dose group showed 17% reduction of infarct

volume (Figure 2). There was no effect on infarct volume in the rhEPO 50 IU kg<sup>-1</sup> group (Figure 2).

Administration of rhEPO or CEPO 6 h after MCAo could protect against subsequent neuronal damage in the cerebral cortex. We then separately measured infarct volume in the cortex and the subcortex. Treatment with rhEPO at doses of 500 and 1150 IU kg<sup>-1</sup> or CEPO at a dose of 50 µg kg<sup>-1</sup> significantly reduced cortical (26 and 30% for rhEPO 500 and 1150 IU kg<sup>-1</sup>, respectively, 36% for CEPO) but not subcortical infarct volume (Figure 2). Remarkably, rhEPO at a dose of 5000 IU kg<sup>-1</sup> significantly reduced infarct volume in both the cortex (22%) and subcortex (36%, Figure 2).

To examine whether treatment with rhEPO or CEPO improves neurobehavioural outcome, we performed a battery of behavioural tests that are sensitive to sensorimotor impairment in rodents (Li *et al.*, 2000; Chen *et al.*, 2003; Zhang *et al.*, 2003, 2004, 2005; Wang *et al.*, 2004). All rats subjected to embolic MCAo and treated with vehicle exhibited severe neurological deficits. However, rats treated 6 h after MCAo with rhEPO at doses of 500, 1150 and 5000 IU kg<sup>-1</sup> or CEPO at a dose of 50 µg kg<sup>-1</sup>, showed significantly ( $P < 0.05$ ) improved neurological outcome. The separation between vehicle and treated animals began 7–21 days after MCAo, and the reduction of sensorimotor impairment versus vehicle control persisted to the end of the study, 28 days after MCAo (Figure 3). Improvement of behavioural outcome was better ( $P < 0.01$ ) in rats treated

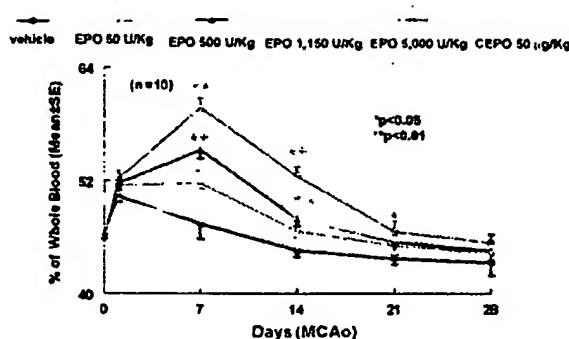
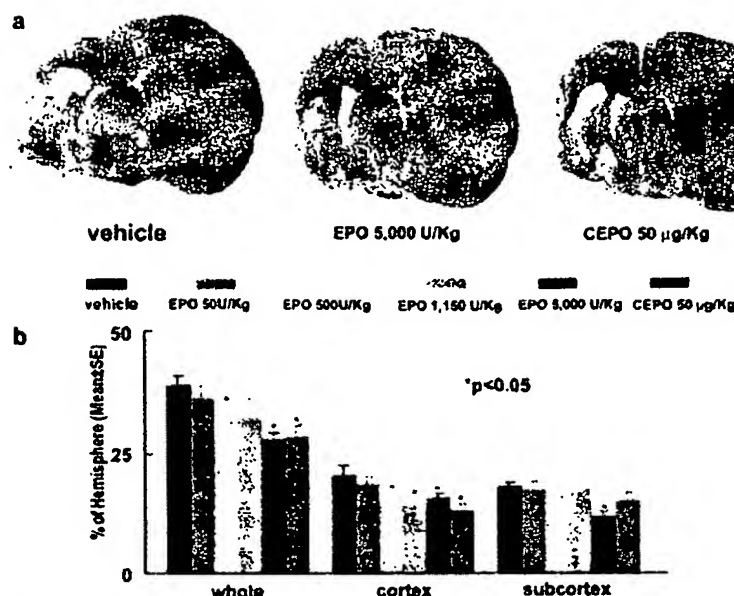


Figure 1 Changes in haematocrit before, during and after treatment with rhEPO and CEPO. Zero and 1 day time points represent prior to MCA occlusion and CEPO or rhEPO treatment, respectively. \* $P < 0.05$  and \*\* $P < 0.01$  vs the vehicle group.  $N = 10$  rats per group. CEPO, carbamylated rhEPO; MCA, middle cerebral artery; rhEPO, recombinant human erythropoietin.

Table 1 CEPO and EPO levels measured 30 min after CEPO or rhEPO administration

Groups	rhEPO (IU kg <sup>-1</sup> )				CEPO (µg kg <sup>-1</sup> )	
	1000 (ng mL <sup>-1</sup> , n = 3)	2500 (ng mL <sup>-1</sup> , n = 4)	5000 (ng mL <sup>-1</sup> , n = 3)	10 000 (ng mL <sup>-1</sup> , n = 3)	5 (ng mL <sup>-1</sup> , n = 3)	50 (ng mL <sup>-1</sup> , n = 3)
CSF	17.8 ± 11.7	2.6 ± 2.0	3.0 ± 0.7	28.9 ± 3.2	2.0 ± 0.4	16.5 ± 5.7
Plasma	476 ± 313	329 ± 137	969 ± 60	11574 ± 766	177 ± 5.3	504 ± 1006
Ipsilateral	0.22 ± 0.11	0.20 ± 0.18	1.03 ± 0.11	7.37 ± 1.09	0.4 ± 0.01	1.2 ± 0.2
Contralateral	0.2 ± 0.1	0.1 ± 0.04	0.8 ± 0.2	5.8 ± 1.4	0.4 ± 0.03	0.7 ± 0.04

Abbreviations: CEPO, carbamylated rhEPO; CSF, cerebrospinal fluid; EPO, erythropoietin; rhEPO, recombinant human erythropoietin. Values are mean ± s.e.



**Figure 2** Infarct volumes 28 days after embolic MCA occlusion. Panel a shows infarction on a coronal section stained with H&E of a representative rat from vehicle, rhEPO 5000 IU kg<sup>-1</sup> and CEPO 50 µg kg<sup>-1</sup> groups. Panel b shows quantitative analysis revealing that delayed (6 h) treatment with CEPO or rhEPO reduced infarct volume. Infarct volumes were measured as a whole hemisphere (Whole), cortex and subcortex. *N* = 12 rats for control, rhEPO 500 IU kg<sup>-1</sup>, and rhEPO 5000 IU kg<sup>-1</sup> groups. *N* = 6 rats for rhEPO 50 IU kg<sup>-1</sup>, rhEPO 1150 IU kg<sup>-1</sup>, and CEPO 50 µg kg<sup>-1</sup> groups. \**P* < 0.05 vs the vehicle group. CEPO, carbamylated rhEPO; H&E, haematoxylin and eosin; MCA, middle cerebral artery; rhEPO, recombinant human erythropoietin.

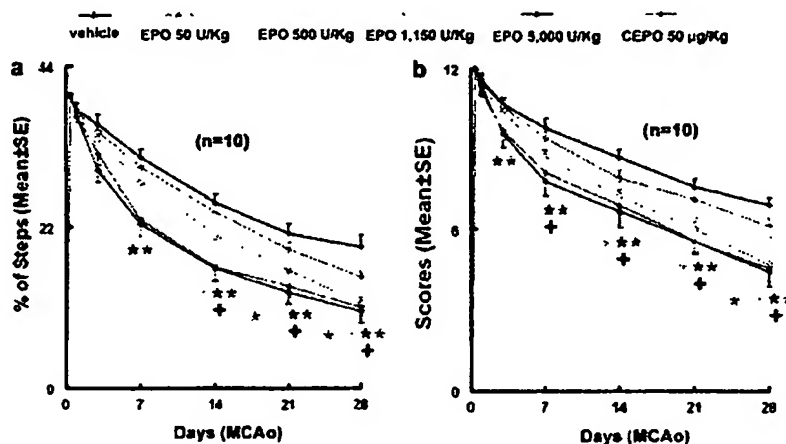


**Figure 3** The effects of CEPO and rhEPO on neurological function. Delayed (6 h) treatment with CEPO or rhEPO improves neurological function measured by foot-fault test (a) and mNSS (b) compared with the vehicle group. \**P* < 0.05 vs the vehicle group and ~*P* < 0.05 vs rhEPO 500 and 1150 IU kg<sup>-1</sup> groups. *N* = 10 rats per group. CEPO, carbamylated rhEPO; mNSS, modified neurological severity score; rhEPO, recombinant human erythropoietin.

with 5000 IU kg<sup>-1</sup> rhEPO when compared to rats treated with rhEPO at doses of 500 or 1150 IU kg<sup>-1</sup> (Figure 3). Surprisingly, treatment with rhEPO 50 IU kg<sup>-1</sup> beginning at 6 h post-MCAo also slightly but significantly improved neurological outcome when assessed 28 days after MCAo (*P* = 0.03, Figure 3).

#### Delayed treatment with rhEPO or CEPO reduces apoptosis and microglial activation

Previous studies have reported that acute treatment with rhEPO prevents neuronal apoptosis and reduces activation of inflammatory cells within the CNS (Siren *et al.*, 2001; Ghezzi and Brines, 2004). To examine whether delayed treatment

with rhEPO reduced apoptosis and microglial activation, we measured the number of apoptotic cells and activated microglia in the ischaemic boundary region 28 days following MCAo (Zhang *et al.*, 1997c). Treatment of rhEPO at a dose of  $5000 \text{ IU kg}^{-1}$  or CEPO ( $50 \mu\text{g kg}^{-1}$ ) significantly reduced the number of TUNEL-positive cells (31% for rhEPO and 35% for CEPO) and activated microglial cells (36% for rhEPO and

CEPO) compared with the number in the vehicle group 28 days after MCA occlusion (Figure 4).

## Discussion

The results of the present study demonstrated that rhEPO at doses of 500, 1150 and  $5000 \text{ IU kg}^{-1}$  or CEPO at  $50 \mu\text{g kg}^{-1}$ , administered 6 h following embolic MCAo significantly reduced infarct volume and improved neurological outcome compared with rats treated with vehicle. Moreover, our results indicate that measurable concentrations of rhEPO and CEPO are achieved in CSF and brain parenchyma following peripheral intravenous bolus dosing and that the concentrations achieved at the higher dose levels are consistent with those required for activity using *in vitro* models of neuronal injury. In these models,  $1 \text{ IU ml}^{-1}$  EPO ( $1 \text{ IU ml}^{-1}$  EPO =  $8 \text{ ng ml}^{-1}$  EPO) protected P19 cells from injury induced by serum withdrawal (Siren *et al.*, 2001).

The neuroprotective effects of rhEPO have been demonstrated in several experimental models of stroke (Siren *et al.*, 2001; Grasso *et al.*, 2004; Leist *et al.*, 2004; Villa *et al.*, 2006). In a model of transient cortical ischaemia, rhEPO at doses of 500 to  $5000 \text{ IU kg}^{-1}$  has been shown to reduce infarct volume (Brines *et al.*, 2000, 2004; Siren *et al.*, 2001). In the present study, we used a model of embolic MCAo that mimics malignant MCA infarction and severe neurological impairment of human stroke (Hacke *et al.*, 1996; Zhang *et al.*, 1997; Carmichael, 2005). Our data show that delayed (6 h) treatment with rhEPO at doses of 500, 1150 and 5000 but not  $50 \text{ IU kg}^{-1}$  significantly reduced infarct volume 28 days after stroke. rhEPO at a dose of  $5000 \text{ IU kg}^{-1}$  was more effective in reducing the entire infarct volume (28%) compared with a dose of  $500 \text{ IU kg}^{-1}$  (17%). These data suggest that delayed treatment with rhEPO is effective even for malignant stroke and that the neuroprotective effects of EPO are dose-dependent.

There are two major differences between those earlier studies and the present work. First, earlier studies used either a permanent focal MCAo model in which there is little or no reperfusion of the ischaemic tissue or a model of cortical infarction in which a distal branch of the MCA was occluded (Sadamoto *et al.*, 1998; Brines *et al.*, 2000; Leist *et al.*, 2004). The embolic MCAo model used here frequently exhibits spontaneous clot lysis and reperfusion within 24–48 h following MCAo, which closely mimics human stroke (Zhang *et al.*, 1997; Jiang *et al.*, 1998). Second, and perhaps most importantly, earlier reports demonstrating activity of rhEPO in rodent stroke models used a single intravenous bolus drug infusion. In the present study, we used a multiple-dose paradigm in which three equal doses of drug were administered, with the initial dose given 6 h and additional doses given 24 and 48 h after the initial dose. This dosing paradigm was used to match as closely as possible the dosing paradigm used in a small but positive clinical study using rhEPO and stroke (Ehrenreich *et al.*, 2002).

As expected, all doses of rhEPO used in the present study produced a significant but transient elevation in haematocrit. This effect on haematocrit is consistent with the effects produced by other haematopoietic agents studied in preclinical stroke models (Belayev *et al.*, 2005). Consistent

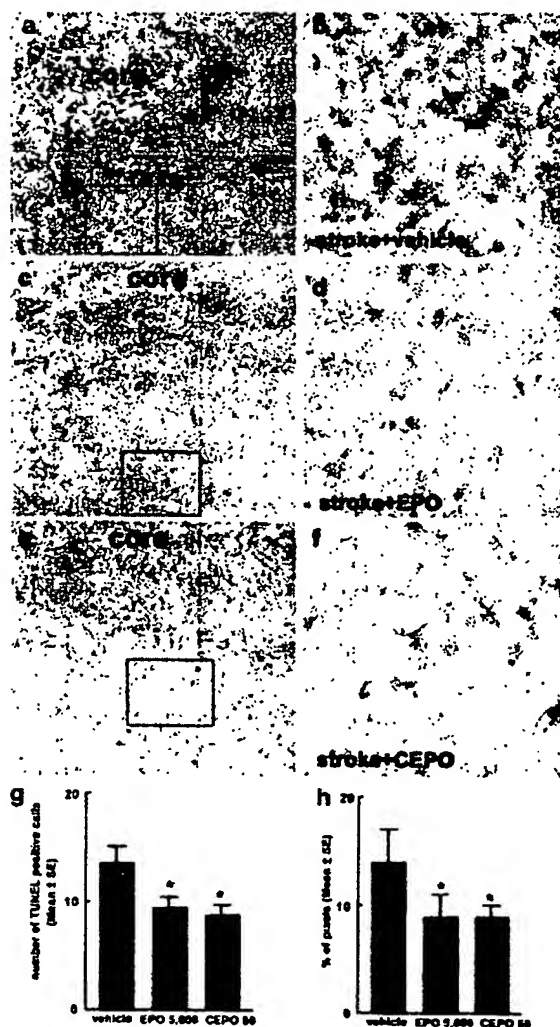


**Figure 4** The effect of CEPO and EPO on apoptosis and microglial responses. Panels a–f are images of activated microglial cells identified by IBA4-positive cells in the cortical boundary region from representative rats treated with vehicle (a and b), rhEPO  $5000 \text{ IU kg}^{-1}$  (c and d) or CEPO  $50 \mu\text{g kg}^{-1}$  (e and f). Panels b, d and f are high magnification images from the box area in panels a, c and e, respectively. (g and h) Quantitative data of TUNEL-positive cells and activated microglial cells, respectively, in the ischaemic boundary region. Core in the panels a, c and e indicates the ischaemic core. Bar =  $80 \mu\text{m}$  for panels a, c and e; Bar =  $20 \mu\text{m}$  for panels b, d, and f. CEPO, carbamylated rhEPO; EPO, erythropoietin; rhEPO, recombinant human erythropoietin; TUNEL, deoxynucleotidyl transferase-mediated biotinylated UTP nick end labelling model. \* $P < 0.05$  vs the vehicle group.

with earlier reports, CEPO which does not bind to the classical EPOR did not elevate haematocrit (Leist *et al.*, 2004). The present study extends previous findings by demonstrating that, as for rhEPO, delayed (6 h) treatment with CEPO significantly reduced infarct volume and improved functional outcome 28 days after embolic MCAo. Although the cellular mechanisms responsible for the neuroprotective effects of CEPO have not been fully elucidated, CEPO may evoke a protective response by signalling through the common  $\beta$ -receptor subunit, perhaps in a heteromeric complex with the EPOR (Brines *et al.*, 2004). Here, we showed that CEPO and rhEPO, administered intravenously, crossed the BBB, consistent with previous reports (Brines *et al.*, 2000; Juul *et al.*, 2004; Leist *et al.*, 2004).

The present study showed that the neuroprotective effect of delayed treatment with CEPO and rhEPO was primarily localized to the cerebral cortex. In this model of embolic stroke, we demonstrated previously that impairment of cerebral microvascular circulation in the cortex develops within 6 h after the onset of MCAo and the majority of ischaemic damage to neurons in the cortex are reversible (Garcia *et al.*, 1993; Zhang *et al.*, 2001). Thus, this 6 h window in the cortex could provide an access for rhEPO and CEPO to reach cerebral microvessels and pass the BBB rescuing potentially viable neurons in the ischaemic boundary region. Antiapoptotic and anti-inflammatory effects have been proposed as likely mechanisms contributing to the neuroprotective activity of rhEPO and CEPO (Siren *et al.*, 2001; Agnello *et al.*, 2002; Brines *et al.*, 2004; Maiese *et al.*, 2004). We found that delayed treatment with rhEPO and CEPO substantially reduced apoptosis and production of activated microglial cells in the ischaemic boundary region 28 days after the onset of MCAo. However, it remains to be determined whether these beneficial effects of rhEPO and CEPO are generated either by direct or by indirect anti-inflammatory and antiapoptotic effects.

In summary, delayed (6 h) treatment with CEPO and rhEPO reduces infarct volume and improves functional outcome following embolic MCAo. The long treatment window described here, coupled with the use of a multiple dose paradigm, suggests a viable therapeutic window for the use of these agents in the treatment of human stroke.

## Acknowledgements

This work was supported by NINDS Grants nos. PO1 NS23393, PO1 NS42345, RO1NS43324 and RO1HL 64766 and by the Johnson & Johnson Stroke Management Group, Warren, NJ, USA.

## Conflict of interest

At the time this work was completed, K Rhodes and M Renzi were employees of Johnson & Johnson Pharmaceutical Research and Development, LLC. G Heavner and C Pool were employees of Centocor Inc., a Johnson & Johnson company. These employees do not derive any financial gain from the publication of this manuscript and hence there is no inherent conflict of interest.

## References

- Agnello D, Biglioni P, Villa P, Mennini T, Cerami A, Brines ML *et al.* (2002). Erythropoietin exerts an anti-inflammatory effect on the CNS in a model of experimental autoimmune encephalomyelitis. *Brain Res* 952: 128–134.
- Anagnostou A, Lee ES, Kessimian N, Levinson R, Steiner M (1990). Erythropoietin has a mitogenic and positive chemotactic effect on endothelial cells. *Proc Natl Acad Sci USA* 87: 5978–5982.
- Belayev L, Khoutorova L, Zhao W, Vigdorchik A, Belayev A, Busto R *et al.* (2005). Neuroprotective effect of darbepoetin alfa, a novel recombinant erythropoietic protein, in focal cerebral ischemia in rats. *Stroke* 36: 1071–1076.
- Bernaudin M, Marti HH, Roussel S, Divoux D, Nouvelot A, MacKenzie ET *et al.* (1999). A potential role for erythropoietin in focal permanent cerebral ischemia in mice. *J Cereb Blood Flow Metab* 19: 643–651.
- Brines M, Grasso G, Fiordaliso F, Sfacteria A, Ghezzi P, Fratelli M *et al.* (2004). Erythropoietin mediates tissue protection through an erythropoietin and common beta-subunit heteroreceptor. *Proc Natl Acad Sci USA* 101: 14907–14912.
- Brines ML, Ghezzi P, Keenan S, Agnello D, de Lanerolle NC, Cerami C *et al.* (2000). Erythropoietin crosses the blood-brain barrier to protect against experimental brain injury. *Proc Natl Acad Sci USA* 97: 10526–10531.
- Carmichael ST (2005). Rodent models of focal stroke: size, mechanism, and purpose. *NeuroRx* 2: 396–409.
- Chen J, Zhang ZG, Li Y, Wang Y, Wang L, Jiang H *et al.* (2003). Statins induce angiogenesis, neurogenesis, and synaptogenesis after stroke. *Ann Neurol* 53: 743–751.
- Ehrenreich H, Hasselblatt M, Dembowski C, Cepek L, Lewczuk P, Stiefel M *et al.* (2002). Erythropoietin therapy for acute stroke is both safe and beneficial. *Mol Med* 8: 495–505.
- Garcia JH, Yoshida Y, Chen H, Li Y, Zhang ZG, Lian J *et al.* (1993). Progression from ischemic injury to infarct following middle cerebral artery occlusion in the rat. *Am J Pathol* 42: 623–635.
- Ghezzi P, Brines M (2004). Erythropoietin as an antiapoptotic, tissue-protective cytokine. *Cell Death Differ* 11 (Suppl 1): S37–S44.
- Grasso G, Sfacteria A, Cerami A, Brines M (2004). Erythropoietin as a tissue-protective cytokine in brain injury: what do we know and where do we go? *Neuroscientist* 10: 93–98.
- Hacke W, Schwab S, Horn M, Spranger M, De Georgis M, von Kummer R (1996). Malignant middle cerebral artery territory infarction: clinical course and prognostic signs. *Arch Neurol* 53: 309–315.
- Jiang Q, Zhang RL, Zhang ZG, Ewing JR, Divine GW, Chopp M (1998). Diffusion-, T2-, and perfusion-weighted nuclear magnetic resonance imaging of middle cerebral artery embolic stroke and recombinant tissue plasminogen activator intervention in the rat. *J Cereb Blood Flow Metab* 18: 758–767.
- Juul SE, McPherson RJ, Farrell FX, Jolliffe L, Ness DJ, Gleason CA (2004). Erythropoietin concentrations in cerebrospinal fluid of nonhuman primates and fetal sheep following high-dose recombinant erythropoietin. *Biol Neonate* 85: 138–144.
- Leist M, Ghezzi P, Grasso G, Bianchi R, Villa P, Fratelli M *et al.* (2004). Derivatives of erythropoietin that are tissue protective but not erythropoietic. *Science* 305: 239–242.
- Lewczuk P, Hasselblatt M, Kamrowski-Kruck H, Heyer A, Unzicker C, Siren AL *et al.* (2000). Survival of hippocampal neurons in culture upon hypoxia: effect of erythropoietin. *Neuroreport* 11: 3485–3488.
- Li Y, Chopp M, Chen J, Wang L, Gautam SC, Zhang Z (2000). Intrastriatal transplantation of bone marrow nonhematopoietic cells improves functional recovery after stroke in adult mice. *J Cereb Blood Flow Metab* 20: 1311–1319.
- Maiese K, Li F, Chong ZZ (2005). New avenues of exploration for erythropoietin. *JAMA* 293: 90–95.
- Maiese K, Li F, Chong ZZ (2004). Erythropoietin in the brain: can the promise to protect be fulfilled? *Trends Pharmacol Sci* 25: 577–583.
- Marti HH (2004). Erythropoietin and the hypoxic brain. *J Exp Biol* 207: 3233–3242.
- Masuda S, Okano M, Yamagishi K, Nagao M, Ueda M, Sasaki R (1994). A novel site of erythropoietin production. Oxygen-dependent production in cultured rat astrocytes. *J Biol Chem* 269: 19488–19493.

- Mun KC, Golper TA (2000). Impaired biological activity of erythropoietin by cyanate carbamylation. *Blood Purif* 18: 13–17.
- Naranda T, Wong K, Kaufman RI, Goldstein A, Olsson L (1999). Activation of erythropoietin receptor in the absence of hormone by a peptide that binds to a domain different from the hormone binding site. *Proc Natl Acad Sci USA* 96: 7569–7574.
- Park KD, Mun KC, Chang EJ, Park SB, Kim HC (2004). Inhibition of erythropoietin activity by cyanate. *Scand J Urol Nephrol* 38: 69–72.
- Paxinos G, Watson C (1986). *The Rat Brain in Stereotaxic Coordinates*, 2nd edn. Academic Press Inc.: New York, NY, p viii.
- Sadamoto Y, Igase K, Sakanaka M, Sato K, Otsuka H, Sakaki S et al. (1998). Erythropoietin prevents place navigation disability and cortical infarction in rats with permanent occlusion of the middle cerebral artery. *Biochem Biophys Res Commun* 253: 26–32.
- Sakanaka M, Wen TC, Matsuda S, Masuda S, Morishita E, Nagao M et al. (1998). *In vivo* evidence that erythropoietin protects neurons from ischemic damage. *Proc Natl Acad Sci USA* 95: 4635–4640.
- Sinor AD, Greenberg DA (2000). Erythropoietin protects cultured cortical neurons, but not astroglia, from hypoxia and AMPA toxicity. *Neurosci Lett* 290: 213–215.
- Siren AL, Fratelli M, Brines M, Goemans C, Casagrande S, Lewczuk P et al. (2001). Erythropoietin prevents neuronal apoptosis after cerebral ischemia and metabolic stress. *Proc Natl Acad Sci USA* 98: 4044–4049.
- Tsai PT, Ohab JJ, Kertesz N, Groszer M, Matter C, Gao J et al. (2006). A critical role of erythropoietin receptor in neurogenesis and post-stroke recovery. *J Neurosci* 26: 1269–1274.
- Villa P, van Beek J, Larsen AK, Gerwien J, Christensen S, Cerami A et al. (2006). Reduced functional deficits, neuroinflammation, and secondary tissue damage after treatment of stroke by non-erythropoietic erythropoietin derivatives. *J Cereb Blood Flow Metab* 27: 552–563.
- Wang L, Zhang Z, Wang Y, Zhang R, Chopp M (2004). Treatment of stroke with erythropoietin enhances neurogenesis and angiogenesis and improves neurological function in rats. *Stroke* 35: 1732–1737.
- Wojchowski DM, Gregory RC, Miller CP, Pandit AK, Pircher TJ (1999). Signal transduction in the erythropoietin receptor system. *Exp Cell Res* 253: 143–156.
- Zhang L, Zhang ZG, Ding GL, Jiang Q, Liu X, Meng H et al. (2005). Multitargeted effects of statin-enhanced thrombolytic therapy for stroke with recombinant human tissue-type plasminogen activator in the rat. *Circulation* 112: 3486–3494.
- Zhang L, Zhang ZG, Zhang C, Zhang RL, Chopp M (2004). Intravenous administration of a GPIIb/IIIa receptor antagonist extends the therapeutic window of intra-arterial tenecteplase-tissue plasminogen activator in a rat stroke model. *Stroke* 35: 2890–2895.
- Zhang L, Zhang ZG, Zhang R, Morris D, Lu M, Collier BS et al. (2003). Adjuvant treatment with a glycoprotein IIb/IIIa receptor inhibitor increases the therapeutic window for low-dose tissue plasminogen activator administration in a rat model of embolic stroke. *Circulation* 107: 2837–2843.
- Zhang RL, Chopp M, Zhang ZG, Jiang Q, Ewing JR (1997). A rat model of focal embolic cerebral ischemia. *Brain Res* 766: 83–92.
- Zhang Z, Chopp M, Powers C (1997c). Temporal profile of microglial response following transient (2h) middle cerebral artery occlusion. *Brain Res* 744: 189–198.
- Zhang ZG, Zhang L, Tsang W, Goussev A, Powers C, Ho K et al. (2001). Dynamic platelet accumulation at the site of the occluded middle cerebral artery and in downstream microvessels is associated with loss of microvascular integrity after embolic middle cerebral artery occlusion. *Brain Res* 912: 181–194.

## Erythropoietin attenuates hydrogen peroxide-induced damage of hepatocytes

Hepatositlerde oluşturulan hidrojen peroksit toksisitesinde eritropoietin'in koruyucu rolü

Nuray YAZIHAN<sup>1,2</sup>, Haluk ATAÖĞLU<sup>2,3</sup>, Burcu YENER<sup>3</sup>, Cengiz AYDIN<sup>4</sup>

Departments of <sup>1</sup>Pathophysiology and <sup>2</sup>Microbiology and <sup>3</sup>Molecular Biology Research and Development Unit, Ankara University, Faculty of Medicine, Ankara

<sup>4</sup>Clinical Biochemistry Laboratory, Yüksek İhtisas Research and Training Hospital, Ankara

**Background/aims:** High levels of hydrogen peroxide (H<sub>2</sub>O<sub>2</sub>) are observed during inflammatory and ischemic states of the liver and usually lead to cellular dysfunction and cytotoxicity. Recently, it has been reported that erythropoietin and mitochondrial K (ATP) channel openers have a protective effect via a pharmacological preconditioning action during ischemia reperfusion injury of the liver and heart. However, it remains unclear as to whether K (ATP) channel blockers can reduce the protective effect of erythropoietin in the H<sub>2</sub>O<sub>2</sub>-induced injury of hepatocytes. **Methods:** To determine whether erythropoietin treatment decreases H<sub>2</sub>O<sub>2</sub>-induced toxicity, we used human hepatocyte cell line Hep3B for assays. Cells were pretreated with different dosages of erythropoietin (0.1-1-10-50 IU/ml) 2 h before H<sub>2</sub>O<sub>2</sub> application. For determination of effects of blockage of mitochondrial K (ATP) channels during erythropoietin treatment, glibenclamide treatment was applied to the medium 2 h before H<sub>2</sub>O<sub>2</sub> toxicity. Cell number, lactate dehydrogenase and caspase-3 levels were measured in erythropoietin, glibenclamide and/or H<sub>2</sub>O<sub>2</sub>-treated groups. **Results:** Erythropoietin treatment significantly increased cell number at the 24<sup>th</sup> and 48<sup>th</sup> h compared to the control group. H<sub>2</sub>O<sub>2</sub> application induced apoptosis and lactate dehydrogenase release from Hep3B cells and decreased cell number. Erythropoietin prevents H<sub>2</sub>O<sub>2</sub> toxicity in hepatocytes. The K channel inhibitor glibenclamide decreased the cytoprotective and cytoprotective effect of erythropoietin during H<sub>2</sub>O<sub>2</sub> toxicity of Hep3B cells. **Conclusions:** Erythropoietin treatment may be considered as a therapeutic agent during oxidative injuries of hepatocytes and its cytoprotective effect is abolished by glibenclamide.

**Key words:** ATP dependent K channel, caspase-3, erythropoietin (EPO), glibenclamide, hepatocyte, hydrogen peroxide (H<sub>2</sub>O<sub>2</sub>) toxicity, lactate dehydrogenase (LDH)

### INTRODUCTION

In liver injury, hepatocytes are subjected to oxidative stress from both reactive oxidative species (ROS) generated intracellularly in response to

**Amaç:** Karaciğerin enflamatuvar ve iskemik hasarlarında yüksek düzeyde H<sub>2</sub>O<sub>2</sub> açığa çıkmakta ve genellikle hücresel disfonksiyona ve sitotoksositeye neden olmaktadır. Son dönemlerde, eritropoietin ve mitokondrial K (ATP) kanal açıcılarının karaciğer ve kalbin iskemi reperfüzyon hasarı sırasında farmakolojik önartlanma oluşturarak koruyucu etkiye sahip olduğu gösterilmiştir. Bununla beraber; K (ATP) kanal blokörlerinin, eritropoietinin karaciğerde oluşturulan H<sub>2</sub>O<sub>2</sub> toksisitesine karşı koruyucu etkisini azaltıp azaltamayacağı henüz bilinmemektedir. **Yöntem:** Eritropoietinin H<sub>2</sub>O<sub>2</sub> ile oluşturulan toksisitesindeki etkisini araştırmak amacıyla çalışmamızda insan hepatosit hücre dizisi Hep3B kullanılmıştır. Hücreler H<sub>2</sub>O<sub>2</sub> uygulamasından 2 saat önce eritropoietinin farklı dozlarıyla (0.1-1-10-50 IU/ml) ön tedavi edilmiştir. Eritropoietinin uygulaması sırasında mitokondrial K (ATP) kanal blokajının etkisini görmek amacıyla glibenklamid ortamına H<sub>2</sub>O<sub>2</sub> toksisitesinden 2 saat önce eritropoietin ile eşzamanlı olarak eklenmiştir. Hücre sayısı, laktat dehidrogenaz ve kaspaz-3 düzeyleri eritropoietin, glibenklamid ve/veya H<sub>2</sub>O<sub>2</sub> ile muamele edilmiş hücrelerde ölçülmüştür. **Bulgular:** Eritropoietin uygulaması hücre sayısını kontrol grubuna göre 24 ve 48. saatlerde belirgin bir şekilde arttırmıştır. H<sub>2</sub>O<sub>2</sub> eklenmesi; hücrelerde apoptosis, hücre ölümlü ve laktat dehidrogenaz salınımını arttırmıştır. Eritropoietin tedavisi; hepatositleri H<sub>2</sub>O<sub>2</sub> toksisitesinden korumuştur. K kanal inhibitörü glibenklamid Hep3B lere H<sub>2</sub>O<sub>2</sub> toksisitesi sırasındaki sitoproliferatif ve sitoprotektif etkisini azaltmıştır. **Sonuç:** Eritropoietin uygulaması hepatositlerin oksidatif hasarı sırasında törapetik bir ajan olarak önerilebilir ve eritropoietinin sitoprotektif etkisi glibenklamid ile azalmaktadır.

**Anahtar kelimeler:** ATP bağımlı K kanalı, kaspaz-3, eritropoietin (EPO), glibenklamid, hepatosit, hidrojen peroksit (H<sub>2</sub>O<sub>2</sub>) toksisitesi, laktat dehidrogenaz (LDH)

cytokines and hepatotoxins and ROS produced extracellularly by inflammatory cells. Peroxisomal oxidases and microsomal cytochrome P450 enzy-

Address for correspondence: Nuray YAZIHAN  
Department of Pathophysiology, Ankara University, Faculty of Medicine, Ankara, Turkey  
Phone: +90 312 310 30 10-372 • Fax: +90 312 310 63 70

Manuscript received: 26.04.2007 Accepted: 13.09.2007



mes are the most important sources of ROS, jointly accounting for the production of 80% of the hydrogen peroxide ( $\text{H}_2\text{O}_2$ ) in the liver under normal physiological conditions (1). Both exogenously exposed and endogenously produced ROS are known to act as intermediates in apoptotic signaling.  $\text{H}_2\text{O}_2$  is involved in numerous types of cell and tissue injury. High levels of  $\text{H}_2\text{O}_2$  are observed during inflammatory states and usually lead to cellular dysfunction and cytotoxicity. Especially during alcohol-induced hepatotoxicity, induction of microsomal cytochrome P450 enzymes occurs (2). During infections and inflammation, neutrophils trigger a long-lasting oxidant stress through NADPH oxidase. Superoxide generated by NADPH oxidase dismutates to oxygen and  $\text{H}_2\text{O}_2$ , which is a highly diffusible oxidant. In addition, myeloperoxidase released from the neutrophils' azurophilic granules can generate hypochlorous acid (3). The hydroxyl and superoxide radicals generated by  $\text{H}_2\text{O}_2$  can lead to necrotic cell injury through damaging interactions with cellular DNA, protein, or lipids, which disrupts critical cellular macromolecules and energy production (1,4).

Erythropoietin (EPO) is a hematopoietic cytokine. Decreased oxygen delivery, most often due to anemic hypoxemia, is the primary stimulus to EPO release. Typical for cytokines, EPO has multiple functions besides bone marrow. Previous studies showed that it has strong antiapoptotic and antioxidant properties (5,6). EPO activates different protein kinase signalling pathways and can increase resistance to ischemia and oxidative stress. Before ischemia reperfusion (I/R) injuries, administration of mitochondrial ATP dependent K channel opener protects neurons from oxidative damage and apoptosis (7,8). The same results were seen after a liver I/R model (9). EPO treatment during I/R damage mimics preconditioning (10). It has been shown that ATP dependent K channel activation is involved in cardioprotective effects of EPO during cardiac I/R damage (11). Previous studies demonstrated the sizeable beneficial effects of EPO in several clinical *in vivo* models of I/R injury (9), shock (12) and laparoscopy (10) induced damage of the liver, but direct effect of EPO treatment during  $\text{H}_2\text{O}_2$  toxicity in hepatocytes is not yet known. In this study, we aimed to investigate whether EPO treatment is protective during  $\text{H}_2\text{O}_2$  toxicity and its relationship with ATP dependent K channel activation.

## MATERIALS AND METHODS

### Cell lines, chemicals and materials:

Human hepatoma cell line Hep3B cells were obtained from the ATCC. Cells were cultured in RPMI-1640 medium (PAA, Austria), supplemented with fetal calf serum (FCS) (PAA, Austria), L-glutamine (Sigma, USA), streptomycin (Sigma, USA) and penicillin (Sigma, USA). Effect of EPO (rHuEPO – recombinant human erythropoietin- Eprex 4000 IU/0.4 ml flacon, Janssen-Cilag) treatment during  $\text{H}_2\text{O}_2$  (Sigma, USA) toxicity was studied. Cell counts were tested by 3-[4,5-dimethylthiazol-2-yl]-2,5 diphenyltetrazolium bromide (MTT, Sigma, USA). For evaluation of apoptosis, caspase-3 levels were measured by a fluorometric kit (Biotium, USA). Lactate dehydrogenase (LDH) level was measured with a kit using an automatic multianalyzer (Roche; P800).

Effects of glibenclamide (Sigma, USA) during  $\text{H}_2\text{O}_2$  toxicity were evaluated.

### Cell culture and experimental protocol:

The human hepatoma cell line Hep3B was cultured in RPMI-1640 medium, supplemented with 10% v/v FCS, 2 mM L-glutamine, streptomycin (100  $\mu\text{g}/\text{ml}$ ) and penicillin (100 IU/ml) in a humidified atmosphere containing 5%  $\text{CO}_2$  at 37°C. One day before the experiments, cells were seeded on 96-well microtiter plates (Nunc, Denmark) as  $2 \times 10^5$  cells/ml.

Depending on the groups, different concentrations of EPO (0.1-1-10-50 IU/ml), glibenclamide (10  $\mu\text{M}$ ) and/or  $\text{H}_2\text{O}_2$  (100  $\mu\text{M}$ ) were added to medium. Before induction of cell death by  $\text{H}_2\text{O}_2$ , cells were pretreated with different dosages of EPO for 2 h, then  $\text{H}_2\text{O}_2$  was applied for 2 h. Then medium was changed according to group protocols. Glibenclamide treatment was applied to medium 2 h before  $\text{H}_2\text{O}_2$  toxicity. For determination of effects of glibenclamide during EPO treatment, we used EPO at a concentration of 50 IU/ml in the experiment.

LDH and caspase-3 levels were measured from EPO, glibenclamide and/or  $\text{H}_2\text{O}_2$  treated groups at the 48<sup>th</sup> h. After supernatants were removed, cell surface was washed with sterile phosphate buffered saline (PBS) and cells were harvested with lysis solution, and caspase-3 levels of groups were measured from cell lysates. LDH measurement was done from both the supernatant and cell lysate.

### Evaluation of cellular proliferation:

The MTT, a colorimetric assay based upon the ability of living cells to reduce 3-[4,5-dimethylthiazol-2-yl]-2,5 diphenyltetrazolium bromide into formazan, was used for evaluation of the effects of H<sub>2</sub>O<sub>2</sub>, EPO and glibenclamide on cellular death or proliferation (2<sup>nd</sup>, 24<sup>th</sup> and 48<sup>th</sup> h).

### Biochemical Determination of Cell Death

Hep3B cells were plated in 96 multi-well culture plates as 3X10<sup>5</sup> cells/ml. LDH is normally present in the cytosol of hepatocytes. In response to cell damage, LDH is released from the cells. Therefore, to determine cell death, we measured secreted and intracellular LDH levels and we calculated % released LDH at the 48<sup>th</sup> h of each group. To do this, the medium was collected to measure enzyme activities. The adherent cells were lysed. Both medium and cell lysates were used for quantitative determination of LDH activity (IU/L), which was performed with an automatic multianalyzer (Roche) using kit (Roche). Released enzyme fractions for each sample were calculated as the ratio of enzyme present in the medium vs. the sum of the levels of the same enzyme in the supernatant and in the cells.

### Measurement of apoptosis:

#### Caspase-3 levels:

The presence of apoptosis was determined by caspase-3 levels. Equal numbers of cells were used for caspase-3 level measurements. Cells were lysed with assay buffer (50 mM HEPES, pH 7.4, 100 mM NaCl, 0.1% CHAPS, 10 mM DTT, 2 mM EDTA, 2 mM EGTA, Triton X-100, 0.1%). Caspase-3 levels were measured by DEVD-R110 Fluorometric HTS Assay Kit from cell lysates. The fluorogenic substrate (Ac-DEVD)<sub>2</sub>-R110 was used for this assay. It is completely hydrolyzed by the enzyme in two successive steps. Cleavage of the first DEVD peptide results in the monopeptide Ac-DEVD-R110 intermediate, which has absorption and emission wavelengths similar to those of R110 ( $\lambda_{\text{abs}}/\lambda_{\text{em}}=496/520$  nm), but has only about 10% the fluorescence of the latter. Hydrolysis of the second DEVD peptide releases the dye R110, leading to a substantial fluorescence increase.

Equal volumes of sample and caspase-3 detection buffer were added to assay plate, then incubated at 37°C for 1 h. Results were read with a fluorometer at 470 nm excitation filter and 520 nm emission

on filter. R110 was used for generating a standard curve to calculate amount of substrate conversion.

### Statistical Analysis

Results of the experiments were analyzed by one way ANOVA, followed by a multiple comparison test using SPSS 10.0.  $p < 0.05$  was accepted as statistically significant. Results are given as mean  $\pm$  SEM.

## RESULTS

### Cell proliferation and toxicity:

H<sub>2</sub>O<sub>2</sub> exposure decreased living cell number immediately at the 2<sup>nd</sup> h compared to control and EPO treatment groups ( $p < 0.05$ ). At the end of the experiment (48<sup>th</sup> h), cell numbers in the H<sub>2</sub>O<sub>2</sub>-treated group were decreased significantly compared to the other groups ( $p < 0.001$ ). At the 48<sup>th</sup> h of EPO treatment, hepatocyte number was increased compared to H<sub>2</sub>O<sub>2</sub> and control groups ( $p < 0.001$ ). There was no significant difference between cytoprotective effects of the different dosages of EPO treatment during H<sub>2</sub>O<sub>2</sub> toxicity (Figure 1).

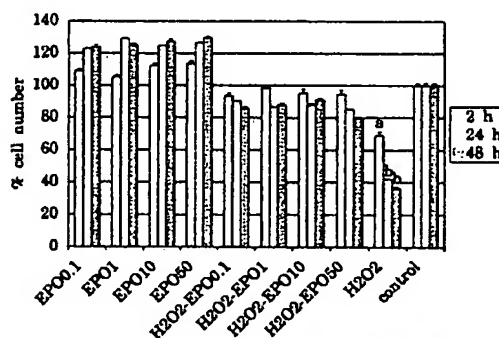


**Figure 1.** % Cell death was determined at 2<sup>nd</sup>, 24<sup>th</sup> and 48<sup>th</sup> h by 3-(4,5-dimethylthiazol-2-yl)-2,5-diphenyltetrazolium bromide (MTT) assay. H<sub>2</sub>O<sub>2</sub> exposure induced prominent cell death in Hep3B hepatocytes. Data are from six independent experiments for each condition. Data are given as mean  $\pm$  SEM.  $P < 0.05$  was accepted as statistically significant.

\*represents  $p < 0.05$ , \*\*represents  $p < 0.001$  difference between H<sub>2</sub>O<sub>2</sub>-exposed cells and the control group.

Glibenclamide diminished the proliferative and cytoprotective effect of EPO treatment ( $p < 0.05$ ) (Figure 2).

Cellular cytotoxicity of H<sub>2</sub>O<sub>2</sub> was also determined by LDH release percentages at the 48<sup>th</sup> h. H<sub>2</sub>O<sub>2</sub> ex-

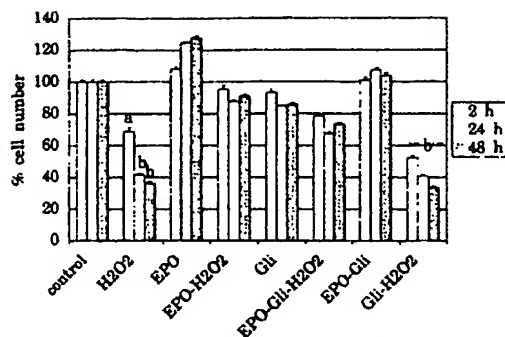


**Figure 2.** ATP dependent K channel blockage with glibenclamide inhibited the cytoproliferative effect of EPO. Data are given as mean $\pm$ SEM.  $P < 0.05$  was accepted as statistically significant. \*represents  $p < 0.05$ , \*represents  $p < 0.001$  difference between H<sub>2</sub>O<sub>2</sub>-exposed cells and the control group.

posure caused increased LDH release from Hep3B cells. EPO treatment protected hepatocytes from toxic effects of H<sub>2</sub>O<sub>2</sub> (Figure 3).

#### Determination of apoptosis:

Caspase-3 level was used for the determination of the apoptotic effect of H<sub>2</sub>O<sub>2</sub>. At the 48<sup>th</sup> h, H<sub>2</sub>O<sub>2</sub> caused apoptosis in Hep3B cells ( $p < 0.001$ ). EPO treatment was protective against H<sub>2</sub>O<sub>2</sub> by decreasing apoptosis as measured by caspase-3 levels (Figure 4). Similar results were seen from the apoptosis assay like MTT and LDH leakage. Glibenclamide abolished the antiapoptotic effect of EPO treatment at the 48<sup>th</sup> h. Glibenclamide alone slightly increased apoptosis in Hep3B cells but it was not statistically significant (Figure 5).

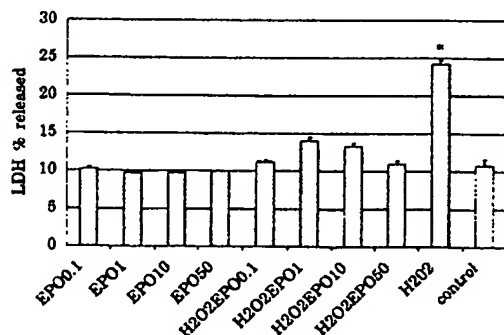


**Figure 3.** H<sub>2</sub>O<sub>2</sub> induced cytotoxicity at the 48<sup>th</sup> h of the experiment determined by LDH % released to medium. H<sub>2</sub>O<sub>2</sub> induced two-fold LDH release from hepatocytes at the end of the 48<sup>th</sup> h ( $p < 0.01$ ). Data are given as mean $\pm$ SEM. \*represents difference between control and H<sub>2</sub>O<sub>2</sub> groups.

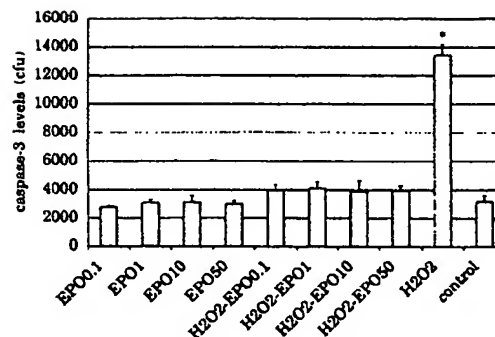


**Figure 4.** Caspase-3 levels: H<sub>2</sub>O<sub>2</sub> toxicity caused prominent apoptosis at the 48<sup>th</sup> h ( $p < 0.001$ ). EPO treatment during H<sub>2</sub>O<sub>2</sub> toxicity decreased apoptosis. Data are given as mean $\pm$ SEM. \*represents difference between control and H<sub>2</sub>O<sub>2</sub> toxicity groups ( $p < 0.001$ ).

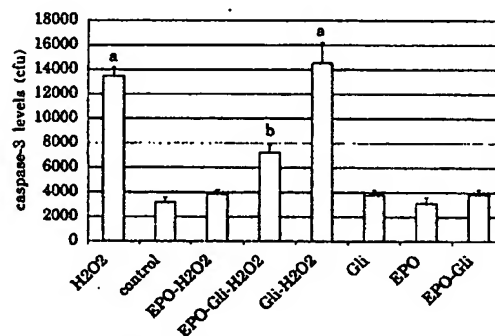


**Figure 5.** Caspase-3 levels: Glibenclamide, EPO, EPO+glibenclamide treatment did not cause any increase in caspase-3 levels of the hepatocytes at the 48<sup>th</sup> h. H<sub>2</sub>O<sub>2</sub> toxicity increased caspase-3 levels compared to control ( $p < 0.001$ ). EPO treatment during toxicity decreased H<sub>2</sub>O<sub>2</sub>-induced damage ( $p < 0.01$ ). \*represents difference between H<sub>2</sub>O<sub>2</sub>, glibenclamide-H<sub>2</sub>O<sub>2</sub> and control groups ( $p < 0.001$ ). \*represents difference between EPO-glibenclamide-H<sub>2</sub>O<sub>2</sub> and control groups ( $p < 0.01$ ).

#### DISCUSSION

In liver diseases, ROS are involved in cell death and liver injury. During oxidative stress or ischemia, mitochondrial damage occurs; cytochrome c releases and activates downstream caspases leading to apoptosis. Application of H<sub>2</sub>O<sub>2</sub> induced apoptosis and cell death in hepatocytes (1). We found increased caspase-3 level in this group. LDH is an enzyme that is normally present in the cytosol of hepatocytes. In response to cell damage (necrosis or late-stage apoptosis), LDH is released from the cells (13). Therefore, to determine cell death, we measured secreted and intracellular LDH

levels. Cell number of the H<sub>2</sub>O<sub>2</sub> toxicity group was lower at the 48<sup>th</sup> h compared to 2<sup>nd</sup> and 24<sup>th</sup> h. We calculated % released LDH at the 48<sup>th</sup> h of each group. As a result of increased cellular damage, increased LDH leakage occurs from cells to the medium, as we found in the H<sub>2</sub>O<sub>2</sub> toxicity group.

We applied EPO treatment before H<sub>2</sub>O<sub>2</sub> toxicity. Application of EPO decreased peroxide-triggered apoptosis, LDH leakage, and cell death. Caspase-3 levels were decreased in the EPO treatment group. We found that EPO treatment has antiapoptotic and proliferative effect on hepatocytes, and this effect was independent of the dosages selected in the experimental design. EPO had a hepatoprotective effect against H<sub>2</sub>O<sub>2</sub> toxicity and the nonspecific ATP dependent K channel blocker, glibenclamide, abolished this effect. Direct acute protective effects of EPO have been shown to implicate these channels. Previous studies have shown that systemic application of single-dose EPO treatment inhibits nitric oxide mediated free-radical formation in the rat liver, and reduces oxidative stress, caspase-3 levels and liver enzymes in the serum of rats after I/R injury (9-12). Our study supported these findings and we found that EPO has a direct cytoprotective and cytoproliferative effect on hepatocytes.

Information related to the role of K channels in hepatocytes is limited. The ATP-sensitive K<sup>+</sup> channels in both sarcolemmal and mitochondrial inner membrane are the critical mediators in cellular protection of ischemic preconditioning. Activation of mitochondrial ATP dependent K<sup>+</sup> channels plays a significant role in the reduction of

apoptosis (13,14). ATP dependent K<sup>+</sup> channels have significant roles in liver growth control as indicated by stimulation of DNA synthesis. It was shown that K ATP channel blockers quinidine and glibenclamide inhibited DNA synthesis both with and without hepatic growth factor stimulation in hepatocytes (15).

Opening of these channels has been related to protein kinase C activation, calcium-mediated signals and through mitogen-activated protein kinases (MAPK) activation (16,17). It is known that EPO activates protein kinase receptors and MAPK. Activation of protein kinases induces mitogenic activity in cells (18). The cytoproliferative effect of EPO is also mediated by these kinases and these effects were blocked by ATP dependent K channel blockage (19). Although we did not evaluate intracellular pathways and kinases, blockage of the cytoprotective and proliferative effects of EPO treatment by K channel blockage might be due to blockage of protein kinases.

In conclusion, these results suggest that the protective role of EPO against hepatic H<sub>2</sub>O<sub>2</sub> toxicity correlated with activation of ATP dependent K channel activation.

EPO is a therapeutic drug for different liver injury models. However, further investigations are required to clarify this role, because the hepatic protective mechanisms associated with EPO and subtypes of K ATP channels are not yet clearly defined.

#### Acknowledgement

This study was supported by TUBITAK - project no: SBAG-2812-104S32.

#### REFERENCES

1. Jaeschke H, Gores GJ, Cederbaum AI, et al. Mechanisms of hepatotoxicity. *Toxicol Sci* 2002; 65(2): 166-76.
2. Yeldandi AV, Rao MS, Reddy JK. Hydrogen peroxide generation in peroxisome proliferator-induced oncogenesis. *Mutat Res* 2000; 448(2): 159-77.
3. Jaeschke H. Mechanisms of liver injury. II. Mechanisms of neutrophil-induced liver cell injury during hepatic ischemia-reperfusion and other acute inflammatory conditions. *Am J Physiol Gastrointest Liver Physiol* 2006; 290(6): G1083-8.
4. Schwabe RF, Brenner DA. Mechanisms of liver injury. I. TNF-alpha-induced liver injury: role of IKK, JNK, and ROS pathways. *Am J Physiol Gastrointest Liver Physiol* 2006; 290(4): G583-9.
5. Ghezzi P, Brines M. Erythropoietin as an antiapoptotic, tissue-protective cytokine. *Cell Death Differ* 2004; 11 (Suppl 1): S37-44.
6. Fliser D, Bahlmann FH, Haller H. EPO: renoprotection beyond anemia correction. *Pediatr Nephrol* 2006; 21(12): 1785-9.
7. Wei L, Yu SP, Gottron F, et al. Potassium channel blockers attenuate hypoxia- and ischemia-induced neuronal death in vitro and in vivo. *Stroke* 2003; 34(5): 1281-6.
8. Chai Y, Niu L, Sun XL, et al. Iptakalim protects PC12 cell against H<sub>2</sub>O<sub>2</sub>-induced oxidative injury via opening mitochondrial ATP-sensitive potassium channel. *Biochem Biophys Res Commun* 2006; 350(2): 307-14.
9. Hai S, Takemura S, Minamiyama Y, et al. Mitochondrial K(ATP) channel opener prevents ischemia-reperfusion injury in rat liver. *Transplant Proc* 2005; 37(1): 428-31.
10. Ates E, Yilmaz S, Ihtiyar E, et al. Preconditioning-like amelioration of erythropoietin against laparoscopy-induced oxidative injury. *Surg Endosc* 2006; 20(5): 815-9.
11. Joyeux-Faure M, Ramond A, Beguin PC, et al. Early pharmacological preconditioning by erythropoietin mediated by inducible NOS and mitochondrial ATP-dependent potassium channels in the rat heart. *Fundam Clin Pharmacol* 2006; 20(1): 51-6.

12. Cuzzocrea S, Di Paola R, Mazzon E, et al. Erythropoietin reduces the development of nonseptic shock induced by zymosan in mice. *Crit Care Med.* 2006; 34(4): 1168-77.
13. Peltenburg HG, Hermens WT, Willems GM, et al. Estimation of the fractional catabolic rate constants for the elimination of cytosolic liver enzymes from plasma. *Hepatology* 1989; 10(5): 833-9.
14. Liu D, Slevin JR, Lu C, et al. Involvement of mitochondrial K<sup>+</sup> release and cellular efflux in ischemic and apoptotic neuronal death. *J Neurochem* 2003; 86(4): 966-79.
15. Takashi E, Wang Y, Ashraf M. Activation of mitochondrial K(ATP) channel elicits late preconditioning against myocardial infarction via protein kinase C signaling pathway. *Circ Res* 1999; 85(12): 1146-53.
16. Malhi H, Irani AN, Rajvanshi P, et al. KATP channels regulate mitogenically induced proliferation in primary rat hepatocytes and human liver cell lines. Implications for liver growth control and potential therapeutic targeting. *J Biol Chem* 2000; 275(34): 26050-7.
17. Huang Q, Bu S, Yu Y, et al. Diazoxide prevents diabetes through inhibiting pancreatic beta-cells from apoptosis via Bcl-2/Bax rate and p38-beta mitogen-activated protein kinase. *Endocrinology* 2007; 148(1): 81-91.
18. Ahmad N, Wang Y, Haider KH, et al. Cardiac protection by mitoKATP channels is dependent on Akt translocation from cytosol to mitochondria during late preconditioning. *Am J Physiol Heart Circ Physiol* 2006; 290(6): H2402-8.
19. Hanlon PR, Fu P, Wright GL, et al. Mechanisms of erythropoietin-mediated cardioprotection during ischemia-reperfusion injury: role of protein kinase C and phosphatidylinositol 3-kinase signaling. *FASEB J* 2005; 19(10): 1323-5.